Schomburg · Schomburg
Editors

SPRINGER

Handbook of Enzymes

Second Edition

SUPPLEMENT VOLUME S10

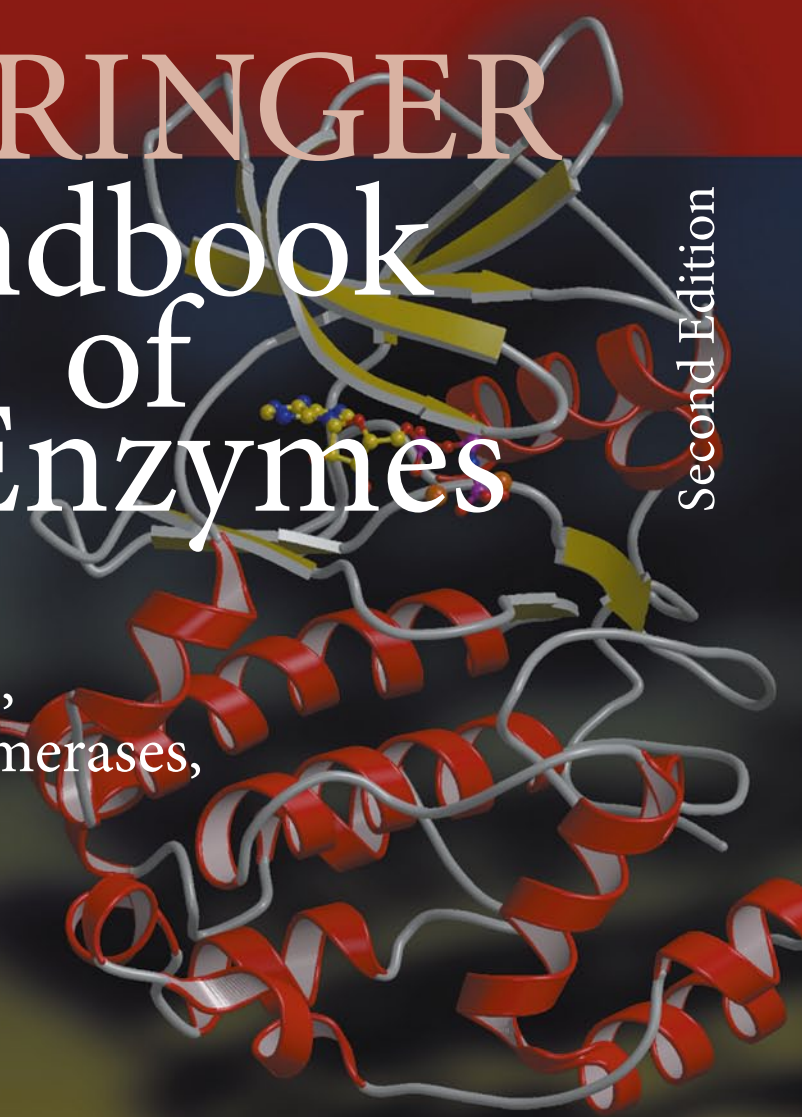

CLASS 3.4–6

Hydrolases, Lyases, Isomerases, Ligases

EC 3.4–6

Springer

Springer Handbook of Enzymes
Supplement Volume S10

Dietmar Schomburg and
Ida Schomburg (Eds.)

Springer Handbook of Enzymes

Supplement Volume S10
Class 3.4–6
Hydrolases, Lyases, Isomerases, Ligases
EC 3.4–6

coedited by Antje Chang

Second Edition

Springer

Professor Dietmar Schomburg
e-mail: d.schomburg@tu-bs.de

Dr. Ida Schomburg
e-mail: i.schomburg@tu-bs.de

Dr. Antje Chang
e-mail: a.chang@tu-bs.de

Technical University Braunschweig
Bioinformatics & Systems Biology
Langer Kamp 19b
38106 Braunschweig
Germany

Library of Congress Control Number: 2013933109

ISBN 978-3-642-36259-0 ISBN (eBook) 978-3-642-36260-6

2nd Edition Springer Berlin Heidelberg New York

The first edition was published as the "Enzyme Handbook, edited by D. and I. Schomburg".

Springer is a part of Springer Science+Business Media
springer.com

Printed in Germany

Cover design: Erich Kirchner, Heidelberg
Typesetting: medionet Publishing Services Ltd., Berlin

Printed on acid-free paper 2/3141m-5 4 3 2 1 0

Preface

Today, as the full information about the genome is becoming available for a rapidly increasing number of organisms and transcriptome and proteome analyses are beginning to provide us with a much wider image of protein regulation and function, it is obvious that there are limitations to our ability to access functional data for the gene products – the proteins and, in particular, for enzymes. Those data are inherently very difficult to collect, interpret and standardize as they are widely distributed among journals from different fields and are often subject to experimental conditions. Nevertheless a systematic collection is essential for our interpretation of genome information and more so for applications of this knowledge in the fields of medicine, agriculture, etc. Progress on enzyme immobilisation, enzyme production, enzyme inhibition, coenzyme regeneration and enzyme engineering has opened up fascinating new fields for the potential application of enzymes in a wide range of different areas.

The development of the enzyme data information system BRENDA was started in 1987 at the German National Research Centre for Biotechnology in Braunschweig (GBF), continued at the University of Cologne from 1996 to 2007, and then returned to Braunschweig, to the Technical University, Institute of Bioinformatics & Systems Biology. The present book "Springer Handbook of Enzymes" represents the printed version of this data bank. The information system has been developed into a full metabolic database.

The enzymes in this Handbook are arranged according to the Enzyme Commission list of enzymes. Some 5,000 "different" enzymes are covered. Frequently enzymes with very different properties are included under the same EC-number. Although we intend to give a representative overview on the characteristics and variability of each enzyme, the Handbook is not a compendium. The reader will have to go to the primary literature for more detailed information. Naturally it is not possible to cover all the numerous literature references for each enzyme (for some enzymes up to 40,000) if the data representation is to be concise as is intended.

It should be mentioned here that the data have been extracted from the literature and critically evaluated by qualified scientists. On the other hand, the original authors' nomenclature for enzyme forms and subunits is retained. In order to keep the tables concise, redundant information is avoided as far as possible (e.g. if K_m values are measured in the presence of an obvious cosubstrate, only the name of the cosubstrate is given in parentheses as a commentary without reference to its specific role).

The authors are grateful to the following biologists and chemists for invaluable help in the compilation of data: Cornelia Munaretto and Dr. Antje Chang.

Braunschweig
Autumn 2012

Dietmar Schomburg, Ida Schomburg

List of Abbreviations

A	adenine
Ac	acetyl
ADP	adenosine 5'-diphosphate
Ala	alanine
All	allose
Alt	altrose
AMP	adenosine 5'-monophosphate
Ara	arabinose
Arg	arginine
Asn	asparagine
Asp	aspartic acid
ATP	adenosine 5'-triphosphate
Bicine	N,N'-bis(2-hydroxyethyl)glycine
C	cytosine
cal	calorie
CDP	cytidine 5'-diphosphate
CDTA	trans-1,2-diaminocyclohexane-N,N,N,N-tetraacetic acid
CMP	cytidine 5'-monophosphate
CoA	coenzyme A
CTP	cytidine 5'-triphosphate
Cys	cysteine
d	deoxy-
D-	(and L-) prefixes indicating configuration
DFP	diisopropyl fluorophosphate
DNA	deoxyribonucleic acid
DPN	diphosphopyridinium nucleotide (now NAD^+)
DTNB	5,5'-dithiobis(2-nitrobenzoate)
DTT	dithiothreitol (i.e. Cleland's reagent)
EC	number of enzyme in Enzyme Commission's system
E. coli	Escherichia coli
EDTA	ethylene diaminetetraacetate
EGTA	ethylene glycol bis(-aminoethyl ether) tetraacetate
ER	endoplasmic reticulum
Et	ethyl
EXAFS	extended X-ray absorption fine structure
FAD	flavin-adenine dinucleotide
FMN	flavin mononucleotide (riboflavin 5'-monophosphate)
Fru	fructose
Fuc	fucose
G	guanine
Gal	galactose

GDP	guanosine 5'-diphosphate
Glc	glucose
GlcN	glucosamine
GlcNAc	N-acetylglucosamine
Gln	glutamine
Glu	glutamic acid
Gly	glycine
GMP	guanosine 5'-monophosphate
GSH	glutathione
GSSG	oxidized glutathione
GTP	guanosine 5'-triphosphate
Gul	gulose
h	hour
H4	tetrahydro
HEPES	4-(2-hydroxyethyl)-1-piperazineethane sulfonic acid
His	histidine
HPLC	high performance liquid chromatography
Hyl	hydroxylysine
Hyp	hydroxyproline
IAA	iodoacetamide
IC 50	50% inhibitory concentration
Ig	immunoglobulin
Ile	isoleucine
Ido	idose
IDP	inosine 5'-diphosphate
IMP	inosine 5'-monophosphate
ITP	inosine 5'-triphosphate
K_m	Michaelis constant
L-	(and D-) prefixes indicating configuration
Leu	leucine
Lys	lysine
Lyx	lyxose
M	mol/l
mM	millimol/l
m-	*meta*-
Man	mannose
MES	2-(N-morpholino)ethane sulfonate
Met	methionine
min	minute
MOPS	3-(N-morpholino)propane sulfonate
Mur	muramic acid
MW	molecular weight
NAD^+	nicotinamide-adenine dinucleotide
NADH	reduced NAD
$NADP^+$	NAD phosphate
NADPH	reduced NADP
NAD(P)H	indicates either NADH or NADPH

NBS	N-bromosuccinimide
NDP	nucleoside 5'-diphosphate
NEM	N-ethylmaleimide
Neu	neuraminic acid
NMN	nicotinamide mononucleotide
NMP	nucleoside 5'-monophosphate
NTP	nucleoside 5'-triphosphate
o-	*ortho*-
Orn	ornithine
p-	*para*-
PBS	phosphate-buffered saline
PCMB	*p*-chloromercuribenzoate
PEP	phosphoenolpyruvate
pH	-log10[H^+]
Ph	phenyl
Phe	phenylalanine
PHMB	*p*-hydroxymercuribenzoate
PIXE	proton-induced X-ray emission
PMSF	phenylmethane-sulfonylfluoride
p-NPP	*p*-nitrophenyl phosphate
Pro	proline
Q_{10}	factor for the change in reaction rate for a 10°C temperature increase
Rha	rhamnose
Rib	ribose
RNA	ribonucleic acid
mRNA	messenger RNA
rRNA	ribosomal RNA
tRNA	transfer RNA
Sar	N-methylglycine (sarcosine)
SDS-PAGE	sodium dodecyl sulfate polyacrylamide gel electrophoresis
Ser	serine
T	thymine
t_H	time for half-completion of reaction
Tal	talose
TDP	thymidine 5'-diphosphate
TEA	triethanolamine
Thr	threonine
TLCK	N^{α}-*p*-tosyl-L-lysine chloromethyl ketone
T_m	melting temperature
TMP	thymidine 5'-monophosphate
Tos-	tosyl- (*p*-toluenesulfonyl-)
TPN	triphosphopyridinium nucleotide (now $NADP^+$)
Tris	tris(hydroxymethyl)-aminomethane
Trp	tryptophan
TTP	thymidine 5'-triphosphate
Tyr	tyrosine
U	uridine

U/mg	μmol/(mg*min)
UDP	uridine 5'-diphosphate
UMP	uridine 5'-monophosphate
UTP	uridine 5'-triphosphate
Val	valine
Xaa	symbol for an amino acid of unknown constitution in peptide formula
XAS	X-ray absorption spectroscopy
Xyl	xylose

Index of Recommended Enzyme Names

Description of Data Fields

All information except the nomenclature of the enzymes (which is based on the recommendations of the Nomenclature Committee of IUBMB (**I**nternational **U**nion of **B**iochemistry and **M**olecular **B**iology) and IUPAC (**I**nternational **U**nion of **P**ure and **A**pplied **C**hemistry) is extracted from original literature (or reviews for very well characterized enzymes). The quality and reliability of the data depends on the method of determination, and for older literature on the techniques available at that time. This is especially true for the fields *Molecular Weight* and *Subunits*.
The general structure of the fields is: **Information – Organism – Commentary – Literature**
The information can be found in the form of numerical values (temperature, pH, K_m etc.) or as text (cofactors, inhibitors etc.).
Sometimes data are classified as *Additional Information*. Here you may find data that cannot be recalculated to the units required for a field or also general information being valid for all values. For example, for *Inhibitors*, *Additional Information* may contain a list of compounds that are not inhibitory.
The detailed structure and contents of each field is described below. If one of these fields is missing for a particular enzyme, this means that for this field, no data are available.

1 Nomenclature

EC number
The number is as given by the IUBMB, classes of enzymes and subclasses defined according to the reaction catalyzed.

Systematic name
This is the name as given by the IUBMB/IUPAC Nomenclature Committee

Recommended name
This is the name as given by the IUBMB/IUPAC Nomenclature Committee

Synonyms
Synonyms which are found in other databases or in the literature, abbreviations, names of commercially available products. If identical names are frequently used for different enzymes, these will be mentioned here, cross references are given. If another EC number has been included in this entry, it is mentioned here.

CAS registry number
The majority of enzymes have a single chemical abstract (CAS) number. Some have no number at all, some have two or more numbers. Sometimes

two enzymes share a common number. When this occurs, it is mentioned in the commentary.

2 Source Organism

In this data field the organism in which the enzymes has been detected are listed. The systematic names according to the NCBI Taxonomy are preferred. If the scientific name is missing, the synonym or the names from the respective literature references are used. In addition, organism are listed for which a specific protein sequence or nucleotide sequence has been allocated. The accession number and the respective data source, e.g, UNIPROT is given in the commentary.

3 Reaction and Specificity

Catalyzed reaction
The reaction as defined by the IUBMB. The commentary gives information on the mechanism, the stereochemistry, or on thermodynamic data of the reaction.

Reaction type
According to the enzyme class a type can be attributed. These can be oxidation, reduction, elimination, addition, or a name (e.g. Knorr reaction)

Natural substrates and products
These are substrates and products which are metabolized in vivo. A natural substrate is only given if it is mentioned in the literature. The commentary gives information on the pathways for which this enzyme is important. If the enzyme is induced by a specific compound or growth conditions, this will be included in the commentary. In *Additional information* you will find comments on the metabolic role, sometimes only assumptions can be found in the references or the natural substrates are unknown.
In the listings, each natural substrate (indicated by a bold **S**) is followed by its respective product (indicated by a bold **P**). Products are given with organisms and references included only if the respective authors were able to demonstrate the formation of the specific product. If only the disappearance of the substrate was observed, the product is included without organisms of references. In cases with unclear product formation only a **?** as a dummy is given.

Substrates and products
All natural or synthetic substrates are listed (not in stoichiometric quantities). The commentary gives information on the reversibility of the reaction, on isomers accepted as substrates and it compares the efficiency of substrates. If a specific substrate is accepted by only one of several isozymes, this will be stated here.

The field *Additional Information* summarizes compounds that are not accepted as substrates or general comments which are valid for all substrates. In the listings, each substrate (indicated by a bold **S**) is followed by its respective product (indicated by a bold **P**). Products are given with organisms and references included if the respective authors demonstrated the formation of the specific product. If only the disappearance of the substrate was observed, the product will be included without organisms or references. In cases with unclear product formation only a **?** as a dummy is given.

Inhibitors

Compounds found to be inhibitory are listed. The commentary may explain experimental conditions, the concentration yielding a specific degree of inhibition or the inhibition constant. If a substance is activating at a specific concentration but inhibiting at a higher or lower value, the commentary will explain this.

Cofactors, prosthetic groups

This field contains cofactors which participate in the reaction but are not bound to the enzyme, and prosthetic groups being tightly bound. The commentary explains the function or, if known, the stereochemistry, or whether the cofactor can be replaced by a similar compound with higher or lower efficiency.

Activating Compounds

This field lists compounds with a positive effect on the activity. The enzyme may be inactive in the absence of certain compounds or may require activating molecules like sulfhydryl compounds, chelating agents, or lipids. If a substance is activating at a specific concentration but inhibiting at a higher or lower value, the commentary will explain this.

Metals, ions

This field lists all metals or ions that have activating effects. The commentary explains the role each of the cited metal has, being either bound e.g. as Fe-S centers or being required in solution. If an ion plays a dual role, activating at a certain concentration but inhibiting at a higher or lower concentration, this will be given in the commentary.

Turnover number (s^{-1})

The k_{cat} is given in the unit s^{-1}. The commentary lists the names of the substrates, sometimes with information on the reaction conditions or the type of reaction if the enzyme is capable of catalyzing different reactions with a single substrate. For cases where it is impossible to give the turnover number in the defined unit (e.g., substrates without a defined molecular weight, or an undefined amount of protein) this is summarized in *Additional Information*.

Specific activity (U/mg)

The unit is micromol/minute/milligram of protein. The commentary may contain information on specific assay conditions or if another than the natur-

al substrate was used in the assay. Entries in *Additional Information* are included if the units of the activity are missing in the literature or are not calculable to the obligatory unit. Information on literature with a detailed description of the assay method may also be found.

K_m-Value (mM)
The unit is mM. Each value is connected to a substrate name. The commentary gives, if available, information on specific reaction condition, isozymes or presence of activators. The references for values which cannot be expressed in mM (e.g. for macromolecular, not precisely defined substrates) are given in *Additional Information*. In this field we also cite literature with detailed kinetic analyses.

K_i-Value (mM)
The unit of the inhibition constant is mM. Each value is connected to an inhibitor name. The commentary gives, if available, the type of inhibition (e.g. competitive, non-competitive) and the reaction conditions (pH-value and the temperature). Values which cannot be expressed in the requested unit and references for detailed inhibition studies are summerized under *Additional information*.

pH-Optimum
The value is given to one decimal place. The commentary may contain information on specific assay conditions, such as temperature, presence of activators or if this optimum is valid for only one of several isozymes. If the enzyme has a second optimum, this will be mentioned here.

pH-Range
Mostly given as a range e.g. 4.0–7.0 with an added commentary explaining the activity in this range. Sometimes, not a range but a single value indicating the upper or lower limit of enzyme activity is given. In this case, the commentary is obligatory.

pI-Value
The isoelectric point (IEP) of an enzyme is the pH-value at which the protein molecule has no net electric charge, carrying the equal number of positively and negatively ions. In the commentary the method of determination is given, if it is provided by the literature.

Temperature optimum (°C)
Sometimes, if no temperature optimum is found in the literature, the temperature of the assay is given instead. This is always mentioned in the commentary.

Temperature range (°C)
This is the range over which the enzyme is active. The commentary may give the percentage of activity at the outer limits. Also commentaries on specific assay conditions, additives etc.

4 Enzyme Structure

Molecular weight
This field gives the molecular weight of the holoenzyme. For monomeric enzymes it is identical to the value given for subunits. As the accuracy depends on the method of determination this is given in the commentary if provided in the literature. Some enzymes are only active as multienzyme complexes for which the names and/or EC numbers of all participating enzymes are given in the commentary.

Subunits
The tertiary structure of the active species is described. The enzyme can be active as a monomer a dimer, trimer and so on. The stoichiometry of subunit composition is given. Some enzymes can be active in more than one state of complexation with differing effectivities. The analytical method is included.

Posttranslational modifications
The main entries in this field may be proteolytic modification, or side-chain modification, or no modification. The commentary will give details of the modifications e.g.:
- proteolytic modification <1> (<1>, propeptide Name) [1];
- side-chain modification <2> (<2>, N-glycosylated, 12% mannose) [2];
- no modification [3]

5 Isolation / Preparation / Mutation / Application

Source / tissue
For multicellular organisms, the tissue used for isolation of the enzyme or the tissue in which the enzyme is present is given. Cell-lines may also be a source of enzymes.

Localization
The subcellular localization is described. Typical entries are: cytoplasm, nucleus, extracellular, membrane.

Purification
The field consists of an organism and a reference. Only references with a detailed description of the purification procedure are cited.

Renaturation
Commentary on denaturant or renaturation procedure.

Crystallization
The literature is cited which describes the procedure of crystallization, or the X-ray structure.

Cloning
Lists of organisms and references, sometimes a commentary about expression or gene structure.

Engineering
The properties of modified proteins are described.

Application
Actual or possible applications in the fields of pharmacology, medicine, synthesis, analysis, agriculture, nutrition are described.

6 Stability

pH-Stability
This field can either give a range in which the enzyme is stable or a single value. In the latter case the commentary is obligatory and explains the conditions and stability at this value.

Temperature stability
This field can either give a range in which the enzyme is stable or a single value. In the latter case the commentary is obligatory and explains the conditions and stability at this value.

Oxidation stability
Stability in the presence of oxidizing agents, e.g. O_2, H_2O_2, especially important for enzymes which are only active under anaerobic conditions.

Organic solvent stability
The stability in the presence of organic solvents is described.

General stability information
This field summarizes general information on stability, e.g., increased stability of immobilized enzymes, stabilization by SH-reagents, detergents, glycerol or albumins etc.

Storage stability
Storage conditions and reported stability or loss of activity during storage.

References
Authors, Title, Journal, Volume, Pages, Year.

aminopeptidase S 3.4.11.24

1 Nomenclature

EC number
3.4.11.24

Recommended name
aminopeptidase S

Synonyms
AP <3,6> [2,7]
APCo-II <2> [19,24]
AmpS <1> [21]
M28.003 <3,5,6> (<3,5,6> Merops-ID [1,2,3,4,5,6,7,8,9,10,11]) [1,2,3,4,5,6,7,8,9,10,11]
S9 aminopeptidase <9> [27,29]
S9AP-St <9> [27,29]
SAP <3> [23]
SGAP <3,6,7> [1,2,9,10,11,12,13,16,18,20,22,25,26,30]
SGAPase <3> [8]
SSAP <8> [15,16]
Streptomyces aminopeptidase <4> [17]
Streptomyces dinuclear aminopeptidase <4> [17]
Streptomyces griseus aminopeptidase <3> [10,12,13,20]
Streptomyces griseus leucine aminopeptidase <7> [22]
aminolysin-S <9> [28]
aminopeptidase S <1> [21]
aminopeptidase yscCo-II <2> [19,24]
bacterial leucine aminopeptidase <3> [14]
dinuclear aminopeptidase <3> [23,25,30]
dizinc aminopeptidase <3> [25]
double-zinc aminopeptidase <3> [18,26]
leucine aminopeptidase <7,8> [15,22]
transaminopeptidase <9> [28]

CAS registry number
124404-20-2
9031-94-1

D. Schomburg and I. Schomburg (eds.), *Class 3.4–6 Hydrolases, Lyases, Isomerases, Ligases: EC 3.4–6*, Springer Handbook of Enzymes S10, DOI 10.1007/978-3-642-36260-6_1,

2 Source Organism

<1> *Staphylococcus aureus* [21]
<2> *Saccharomyces cerevisiae* [19,24]
<3> *Streptomyces griseus* [1,3,5,7,8,9,10,11,12,13,14,16,18,20,23,25,26,30]
<4> *Streptomyces sp.* [17]
<5> *Sulfolobus solfataricus* [6]
<6> *Streptomyces griseus* (UNIPROT accession number: P80561) [2,4]
<7> *Streptomyces griseus* (UNIPROT accession number: Q5WA30) [22]
<8> *Streptomyces septatus* (UNIPROT accession number: Q75V72) [15,16]
<9> *Streptomyces thermocyaneoviolaceus* [27,28,29]

3 Reaction and Specificity

Catalyzed reaction

release of an N-terminal amino acid with a preference for large hydrophobic amino-terminus residues (<3> catalytic mechanism, Asp160, Met161, Gly201, Arg202, and Phe219 are involved, active site structure, modeling of enzyme-substrate complex [1]; <3> catalytic mechanism, high preference towards large hydrophobic amino terminus residues, active site structure, Glu131 is involved in the catalytic mechanism, enzyme-substrate and enzyme-product complex modeling [11]; <6> hydrolyses peptide bonds formed by terminal hydrophobic amino acids such as leucine, methionine, and phenylalanine [4]; <3> M161 is involved in substrate binding at the active site cleft [9]; <3> preference for hydrophobic residues at the ultimate and the penultimate positions, D-amino acids at these positions reduce the activity, activity is not restricted by the length of substrate chains [7]; <3> catalytic pathway and reaction mechanism, catalytic residues are Glu131 and Tyr246, Tyr246 is involved in stabilization of the reaction transition state intermediate, also residue Glu151 is involved [18]; <3> raction mechanism, catalytic residues are Glu131 and Tyr246, residues Arg202 and Asp160 stabilize the reaction intermediate together with Glu131 [12]; <3> structure and reaction mechanism [20]; <3> the enzyme prefers large hydrophobic aminoterminal residues, Glu131, Asp160, and Arg202 are involved in binding of the N-terminal substrate amino acid, substrate binding and reaction mechanism, tetrahedral reaction intermediate, modelling of the enzyme-substrate and enzyme-product complexes [13]; <3> catalytic reaction mechanism, a single proton transfer is involved in catalysis at pH 8.0, whereas two proton transfers are implicated at pH 6.5, involvement of a zinc-bound hydroxide as the reaction nucleophile, Tyr246 polarizes the carbonyl carbon and stabilizes the transition state, enzyme-substrate interaction, overview [26])

Reaction type

hydrolysis
hydrolysis of peptide bond

Natural substrates and products

- **S** peptide + H_2O <3,5,6> (Reversibility: ?) [1,2,3,4,5,6,7,8,9,10,11]
- **P** ? <3,5,6> [1,2,3,4,5,6,7,8,9,10,11]
- **S** Additional information <3> (<3> aminopeptidases are involved in peptides processing and degradation, and are important in uptake of nutrients, regulation, overview [14]) (Reversibility: ?) [14]
- **P** ?

Substrates and products

- **S** 4-nitrophenyl phenylphosphonate + H_2O <4> (Reversibility: ?) [17]
- **P** 4-nitrophenol + phenylphosphonate
- **S** 4-nitrophenyl-L-leucine + H_2O <3> (Reversibility: ?) [20]
- **P** 4-nitrophenol + L-leucine
- **S** Ala-4-nitroanilide + H_2O <3> (Reversibility: ?) [25]
- **P** Ala + 4-nitroaniline
- **S** Arg-4-nitroanilide + H_2O <2> (<2> 105.2% of the activity with Lys-4-nitroanilide [24]) (Reversibility: ?) [19,24]
- **P** Arg + 4-nitroaniline
- **S** D-Arg-OMe + L-Pro-OBzl <9> (Reversibility: ?) [27]
- **P** L-Pro-D-Arg-OMe + benzyl alcohol
- **S** D-Arg-OMe + L-Pro-OBzl <9> (Reversibility: ?) [27]
- **P** c(L-Pro-D-Arg) + benzyl alcohol + methanol
- **S** D-Leu-OBzl + D-Leu-OBzl <9> (Reversibility: ?) [27]
- **P** D-Leu-D-Leu-OBzl + benzyl alcohol
- **S** D-Leu-OMe + D-Leu-OMe <9> (Reversibility: ?) [27]
- **P** D-Leu-D-Leu-OMe + MeOH
- **S** D-Leu-OMe + D-Pro-OBzl <9> (Reversibility: ?) [27]
- **P** D-Pro-D-Leu-OMe + benzyl alcohol
- **S** D-Leu-OMe + L-Pro-OBzl <9> (Reversibility: ?) [27]
- **P** L-Pro-D-Leu-OMe + benzyl alcohol
- **S** D-Phe-OMe + D-Pro-OBzl <9> (Reversibility: ?) [27]
- **P** D-Pro-D-Phe-OMe + benzyl alcohol
- **S** D-Phe-OMe + L-Pro-OBzl <9> (Reversibility: ?) [27]
- **P** L-Pro-D-Phe-OMe + benzyl alcohol
- **S** D-Trp-OMe + D-Pro-OBzl <9> (Reversibility: ?) [27]
- **P** D-Pro-D-Trp-OMe + benzyl alcohol
- **S** D-Trp-OMe + L-Pro-OBzl <9> (Reversibility: ?) [27]
- **P** L-Pro-D-Trp-OMe + benzyl alcohol
- **S** D-Tyr-OMe + D-Pro-OBzl <9> (Reversibility: ?) [27]
- **P** D-Pro-D-Tyr-OMe + benzyl alcohol
- **S** D-Tyr-OMe + L-Pro-OBzl <9> (Reversibility: ?) [27]
- **P** L-Pro-D-Tyr-OMe + benzyl alcohol
- **S** D-Val-OBzl + D-Val-OBzl <9> (Reversibility: ?) [27]
- **P** D-Val-D-Val-OBzl + benzyl alcohol
- **S** D-Val-OMe + L-Pro-OBzl <9> (Reversibility: ?) [27]
- **P** L-Pro-D-Val-OMe + benzyl alcohol

S Glu-4-nitroanilide + H_2O <2> (<2> 5.4% of the activity with Lys-4-nitroanilide [24]) (Reversibility: ?) [24]
P Glu + 4-nitroaniline
S Gly-4-nitroanilide + H_2O <3> (Reversibility: ?) [25]
P Gly + 4-nitroaniline
S Gly-Leu-Gly + H_2O <3> (Reversibility: ?) [7]
P ? <3> [7]
S hemoglobin + H_2O <3> (<3> human hemoglobin [20]) (Reversibility: ?) [20]
P ?
S L-Ala-4-nitroanilide + H_2O <8> (<8> very low activity [16]) (Reversibility: ?) [16]
P L-Ala + 4-nitroaniline
S L-Ala-OMe + L-Pro-OBzl <9> (Reversibility: ?) [27]
P L-Pro-L-Ala-OMe + benzyl alcohol
S L-Arg-4-nitroanilide + H_2O <8> (<8> low activity [16]) (Reversibility: ?) [16]
P L-Arg + 4-nitroaniline
S L-Arg-OMe + L-Pro-OBzl <9> (Reversibility: ?) [27]
P L-Pro-L-Arg-OMe + benzyl alcohol
S L-Arg-OMe + L-Pro-OBzl <9> (Reversibility: ?) [27]
P c(L-Pro-L-Arg) + benzyl alcohol + methanol
S L-Arg-OMe + β-Ala-OBzl <9> (Reversibility: ?) [29]
P β-Ala-L-Arg-OMe + benzyl alcohol
S L-Asn-OMe + β-Ala-OBzl <9> (Reversibility: ?) [29]
P β-Ala-L-Asn-OMe + benzyl alcohol
S L-Asp-OMe + L-Pro-OBzl <9> (Reversibility: ?) [27]
P L-Pro-L-Asp-OMe + benzyl alcohol
S L-Glu-OMe + L-Pro-OBzl <9> (Reversibility: ?) [27]
P L-Pro-L-Glu-OMe + benzyl alcohol
S L-His-OMe + D-Pro-OBzl <9> (Reversibility: ?) [27]
P D-Pro-L-His-OMe + benzyl alcohol
S L-His-OMe + D-Pro-OBzl <9> (Reversibility: ?) [27]
P c(D-Pro-L-His) + benzyl alcohol + methanol
S L-His-OMe + L-Pro-OBzl <9> (Reversibility: ?) [27]
P L-Pro-L-His-OMe + benzyl alcohol
S L-His-OMe + L-Pro-OBzl <9> (Reversibility: ?) [27]
P c(L-Pro-L-His) + benzyl alcohol + methanol
S L-His-OMe + β-Ala-OBzl <9> (Reversibility: ?) [29]
P β-Ala-L-His-OMe + benzyl alcohol
S L-Ile-OMe + D-Pro-OBzl <9> (Reversibility: ?) [27]
P D-Pro-L-Ile-OMe + benzyl alcohol
S L-Ile-OMe + L-Pro-OBzl <9> (Reversibility: ?) [27]
P L-Pro-L-Ile-OMe + benzyl alcohol
S L-Ile-OMe + β-Ala-OBzl <9> (Reversibility: ?) [29]
P β-Ala-L-Ile-OMe + benzyl alcohol
S L-Leu-4-nitroanilide + H_2O <7> (Reversibility: ?) [22]

P L-leucine + 4-nitroaniline
S L-Leu-4-nitroanilide + H_2O <3,8> (<3,8> best substrate [16]; <8> preferred substrate of the wild-type enzyme [15]) (Reversibility: ?) [15,16]
P L-Leu + 4-nitroaniline
S L-Leu-NH_2 + H_2O <8> (Reversibility: ?) [15]
P L-Leu + NH_3
S L-Leu-O-methyl ester + H_2O <8> (Reversibility: ?) [15]
P L-Leu + methanol
S L-Leu-OEt + D-Pro-OBzl <9> (Reversibility: ?) [27]
P D-Pro-L-Leu-OEt + benzyl alcohol
S L-Leu-OEt + L-Pro-OBzl <9> (Reversibility: ?) [27]
P L-Pro-L-Leu-OEt + benzyl alcohol
S L-Leu-OEt + β-Ala-OBzl <9> (Reversibility: ?) [29]
P β-Ala-L-Leu-OEt + benzyl alcohol
S L-Leu-OEt + β-Ala-OBzl + β-Ala-OBzl <9> (Reversibility: ?) [29]
P β-Ala-L-Leu-β-Ala-OBzl + benzyl alcohol + ethanol
S L-Lys-4-nitroanilide + H_2O <3,8> (<3,8> low activity [16]) (Reversibility: ?) [16]
P L-Lys + 4-nitroaniline
S L-Lys-OMe + L-Pro-OBzl <9> (Reversibility: ?) [27]
P L-Pro-L-Lys-OMe + benzyl alcohol
S L-Lys-OMe + β-Ala-OBzl <9> (Reversibility: ?) [29]
P β-Ala-L-Lys-OMe + benzyl alcohol
S L-Met-4-nitroanilide + H_2O <3,8> (<3,8> low activity [16]) (Reversibility: ?) [16]
P L-Met + 4-nitroaniline
S L-Met-OMe + D-Pro-OBzl <9> (Reversibility: ?) [27]
P D-Pro-L-Met-OMe + benzyl alcohol
S L-Met-OMe + L-Met-OMe + β-Ala-OBzl <9> (Reversibility: ?) [29]
P β-Ala-L-Met-L-Met-OMe + benzyl alcohol + methanol
S L-Met-OMe + L-Pro-OBzl <9> (Reversibility: ?) [27]
P L-Pro-L-Met-OMe + benzyl alcohol
S L-Met-OMe + β-Ala-OBzl <9> (Reversibility: ?) [29]
P β-Ala-L-Met-OMe + benzyl alcohol
S L-Met-OMe + β-Ala-OBzl + β-Ala-OBzl <9> (Reversibility: ?) [29]
P (β-Ala)2-L-Met-OMe + benzyl alcohol +
S L-Met-OMe + β-Ala-OBzl + β-Ala-OBzl <9> (Reversibility: ?) [29]
P β-Ala-L-Met-β-Ala-OBzl + benzyl alcohol + methanol
S L-Phe-4-nitroanilide + H_2O <3,8> (<3,8> low activity [16]) (Reversibility: ?) [15,16]
P L-Phe + 4-nitroaniline
S L-Phe-NH_2 + H_2O <8> (Reversibility: ?) [15]
P L-Phe + NH_3
S L-Phe-O-methyl ester + H_2O <8> (Reversibility: ?) [15]
P L-Phe + methanol
S L-Phe-OEt + D-Pro-OBzl <9> (Reversibility: ?) [27]
P D-Pro-L-Phe-OEt + benzyl alcohol

S L-Phe-OEt + L-Phe-OEt + β-Ala-OBzl <9> (Reversibility: ?) [29]
P β-Ala-L-Phe-L-Phe-OMe + benzyl alcohol + ethanol
S L-Phe-OEt + L-Pro-OBzl <9> (Reversibility: ?) [27]
P L-Pro-L-Phe-OEt + benzyl alcohol
S L-Phe-OEt + β-Ala-OBzl <9> (Reversibility: ?) [29]
P β-Ala-L-Phe-OEt + benzyl alcohol
S L-Phe-OEt + β-Ala-OBzl + β-Ala-OBzl <9> (Reversibility: ?) [29]
P β-Ala-L-Phe-β-Ala-OBzl + benzyl alcohol + ethanol
S L-Pro-4-nitroanilide + H_2O <8> (<8> very low activity [16]) (Reversibility: ?) [16]
P L-Pro + 4-nitroaniline
S L-Pro-OMe + β-Ala-OBzl <9> (Reversibility: ?) [29]
P L-Pro-β-Ala-OBzl + methanol
S L-Pro-OMe + β-Ala-OBzl + β-Ala-OBzl <9> (Reversibility: ?) [29]
P L-Pro-$(\beta\text{-Ala})_2$-OBzl + methanol + benzyl alcohol
S L-Ser-OMe + L-Pro-OBzl <9> (Reversibility: ?) [27]
P L-Pro-L-Ser-OMe + benzyl alcohol
S L-Thr-OMe + L-Pro-OBzl <9> (Reversibility: ?) [27]
P L-Pro-L-Thr-OMe + benzyl alcohol
S L-Thr-OMe + L-Thr-OMe <9> (Reversibility: ?) [27]
P L-Thr-L-Thr-OMe + methanol
S L-Thr-OMe + L-Thr-OMe <9> (Reversibility: ?) [29]
P $(\text{L-Thr})_2$-OMe + methanol
S L-Thr-OMe + β-Ala-OBzl <9> (Reversibility: ?) [29]
P β-Ala-L-Thr-OMe + benzyl alcohol
S L-Trp-OMe + D-Pro-OBzl <9> (Reversibility: ?) [27]
P D-Pro-L-Trp-OMe + benzyl alcohol
S L-Trp-OMe + L-Pro-OBzl <9> (Reversibility: ?) [27]
P L-Pro-L-Trp-OMe + benzyl alcohol
S L-Trp-OMe + β-Ala-OBzl <9> (Reversibility: ?) [29]
P β-Ala-L-Trp-OMe + benzyl alcohol
S L-Tyr-OMe + D-Pro-OBzl <9> (Reversibility: ?) [27]
P D-Pro-L-Tyr-OMe + benzyl alcohol
S L-Tyr-OMe + L-Pro-OBzl <9> (Reversibility: ?) [27]
P L-Pro-L-Tyr-OMe + benzyl alcohol
S L-Tyr-OMe + L-Tyr-OMe + β-Ala-OBzl <9> (Reversibility: ?) [29]
P β-Ala-L-Tyr-L-Tyr-OMe + benzyl alcohol + methanol
S L-Tyr-OMe + β-Ala-OBzl <9> (Reversibility: ?) [29]
P β-Ala-L-Tyr-OMe + benzyl alcohol
S L-Tyr-OMe + β-Ala-OBzl + β-Ala-OBzl <9> (Reversibility: ?) [29]
P $(\beta\text{-Ala})_2$-L-Tyr-OMe + benzyl alcohol
S L-Val-OBzl + L-Val-OBzl <9> (Reversibility: ?) [27]
P L-Val-L-Val-OBzl + benzyl alcohol
S L-Val-OMe + D-Pro-OBzl <9> (Reversibility: ?) [27]
P D-Pro-L-Val-OMe + benzyl alcohol
S L-Val-OMe + L-Pro-OBzl <9> (Reversibility: ?) [27]
P L-Pro-L-Val-OMe + benzyl alcohol

S L-Val-OMe + β-Ala-OBzl <9> (Reversibility: ?) [29]
P β-Ala-L-Val-OMe + benzyl alcohol
S L-Val-OMe + β-Ala-OBzl + β-Ala-OBzl <9> (Reversibility: ?) [29]
P (β-Ala)2-L-Val-OMe + benzyl alcohol
S L-alanine-4-nitroanilide + H_2O <9> (Reversibility: ?) [28]
P L-Ala + 4-nitroaniline
S L-alanine-4-nitroanilide + H_2O <3> (<3> good substrate [3]) (Reversibility: ?) [3,5]
P L-alanine + 4-nitroaniline <3> [3,5]
S L-leucine-4-nitroanilide + H_2O <3,5,6> (<3> best of the amino acid 4-nitroanilide substrates [3,5]) (Reversibility: ?) [2,3,5,6,7,10]
P L-leucine + 4-nitroaniline <3,5,6> [2,3,5,6,7,10]
S L-lysine-4-nitroanilide + H_2O <3> (<3> good substrate [3]) (Reversibility: ?) [3]
P L-lysine + 4-nitroaniline <3> [3]
S L-methionine-4-nitroanilide + H_2O <3> (<3> very good substrate [3]) (Reversibility: ?) [3]
P L-methionine + 4-nitroaniline <3> [3]
S L-phenylalanine ethyl ester + L-phenylalanine + H_2O <9> (<9> assay at 50°C [28]) (Reversibility: ?) [28]
P L-Phe-L-Phe + cyclo(L-phenylalanine-L-phenylalanine) + L-Phe-L-Phe ethyl ester
S L-phenylalanine-4-nitroanilide + H_2O <9> (Reversibility: ?) [28]
P L-Phe + 4-nitroaniline
S L-phenylalanine-4-nitroanilide + H_2O <3> (<3> very good substrate [3]) (Reversibility: ?) [3]
P L-phenylalanine + 4-nitroaniline <3> [3]
S L-proline-4-nitroanilide + H_2O <3> (<3> good substrate [3]) (Reversibility: ?) [3]
P L-proline + 4-nitroaniline <3> [3]
S L-proline-*p*-nitroanilide + H_2O <9> (Reversibility: ?) [28]
P L-Pro + 4-nitroaniline
S L-valine-4-nitroanilide + H_2O <3> (<3> good substrate [3]) (Reversibility: ?) [3,5]
P L-valine + 4-nitroaniline <3> [3,5]
S Leu-4-nitroanilide + H_2O <2,3> (<2> 12.2% of the activity with Lys-4-nitroanilide [24]; <3> assay at pH 8.0, 30°C [30]) (Reversibility: ?) [24,25,30]
P Leu + 4-nitroaniline
S Leu-4-nitroaniline + H_2O <3> (Reversibility: ?) [26]
P Leu + 4-nitroaniline
S Leu-Gly-Gly + H_2O <3> (Reversibility: ?) [7]
P Leu + Gly-Gly <3> [7]
S Lys-4-nitroanilide + H_2O <2,3> (Reversibility: ?) [19,24,25]
P Lys + 4-nitroaniline
S Met-4-nitroanilide + H_2O <3> (Reversibility: ?) [25]
P Met + 4-nitroaniline

S Met-enkephalin + H_2O <1> (<1> substrate is a pentapeptide with sequence Tyr-Gly-Gly-Phe-Met, stepwise degradation from the N-terminus [21]) (Reversibility: ?) [21]
P ?
S Pro-4-nitroanilide + H_2O <2> (<2> 11.7% of the activity with Lys-4-nitroanilide [24]) (Reversibility: ?) [24]
P Pro + 4-nitroaniline
S Val-4-nitroanilide + H_2O <3> (Reversibility: ?) [25]
P Val + 4-nitroaniline
S β-Ala-OBzl + β-Ala-OBzl <9> (Reversibility: ?) [29]
P (β-Ala)$_2$-OBzl + benzyl alcohol
S bis(4-nitrophenyl) phosphate + H_2O <4> (Reversibility: ?) [17]
P 4-nitrophenol + phosphate
S bis(4-nitrophenyl) phosphate + H_2O <3> (<3> assay at pH 8.0, 30°C [30]) (Reversibility: ?) [30]
P ?
S bis(p-nitrophenyl)phosphate + H_2O <3> (Reversibility: ?) [25]
P ?
S casein + H_2O <3> (Reversibility: ?) [10]
P ?
S human hemoglobin α-chain + H_2O <3> (<3> hydrolysis of the first few residues to proline at the 4th position [7]) (Reversibility: ?) [7]
P ? <3> [7]
S human hemoglobin β-chain + H_2O <3> (<3> hydrolysis of the first few residues to proline at the 5th position [7]) (Reversibility: ?) [7]
P ? <3> [7]
S peptide + H_2O <3,5,6> (<3> substrate specificity [7]; <3> high preference towards large hydrophobic amino terminus residues [11]) (Reversibility: ?) [1,2,3,4,5,6,7,8,9,10,11]
P ? <3,5,6> [1,2,3,4,5,6,7,8,9,10,11]
S Additional information <3,8> (<3> no activity with Gly-Pro-4-nitroanilide and Ala-Pro-4-nitroanilide, no acitivity with Xaa-Pro N-terminal sequences, glycine-4-nitroanilide and acidic amino acid 4-nitroanilide are very poor substrates [3]; <3> substrates with blocked amino groups are partially hydrolyzed, poor activity with Val-Gly, Val-Leu, and Trp-Leu, Gly-Gly-Gly and D-leucine-D-leucine are no substrates [7]; <3> aminopeptidases are involved in peptides processing and degradation, and are important in uptake of nutrients, regulation, overview [14]; <8> no activity with L-Glu-4-nitroanilide, D-Phe-4-nitroanilide, and D-Leu-4-nitroanilide [16]; <3> no activity with L-Glu-4-nitroanilide, L-Arg-4-nitroanilide, D-Phe-4-nitroanilide, and D-Leu-4-nitroanilide, L-Ala-4-nitroanilide and L-Pro-4-nitroanilide are poor substrates [16]; <8> substrate specificities of recombinant wild-type and F221 mutant enzymes, overview [15]; <3> the enzyme is active on a wide variety of peptides substrates, no activity with D-Leu-D-Leu, no prolidase activity, but release of N-terminal prolyl residues [20]; <3> the enzyme shows broad substrate specificity preferring N-terminal Leu or Met and Phe, but is not able to hydrolyse peptide

substrates bonds with formed by acidic amino acids in the P1 position or proline in the P1 or P1 position [14]; <3> the enzyme is active toward various peptides with different N-terminal side chains and specific toward hydrophobic ones, the enzyme also exhibits a significant activity toward the hydrolysis of the phosphodiester bis(*p*-nitrophenyl)phosphate, overview, active site structure involves the three auxiliary amino acid side chains of Tyr246, Glu131, and Arg202 that are involved in catalysis, modeling of substrate binding using the crystal structure of the enzyme, overview, the activity shows proton inventory and viscosity dependence, overview [25]; <3> the thermostable enzyme prefers large hydrophobic N-terminal residues in its peptide and protein substrates, a single proton transfer is involved in catalysis at pH 8.0, whereas two proton transfers are implicated at pH 6.5 [26]) (Reversibility: ?) [3,7,14,15,16,20,25,26]

P ? <3> [3,7]

Inhibitors

1,10-phenanthroline <2,3,6> (<2> 1 mM, complete inhibition [19]; <2> 1 mM, 91% inhibition [24]; <6> 50% inhibition at pI 4.9 [2]) [2,3,19,24]
4-iodo-L-phenylalanine <3> (<3> weak inhibition, binds at the active site via the two zinc ions displacing the metal ions, binding structure analysis [12]) [12]
Ca^{2+} <3,8> (<8> slight inhibition at 1 mM [16]) [16]
Cd^{2+} <3,8> [16]
chloroquine <2> (<2> 5 mM, 79% inhibition [24]) [24]
Cr^{2+} <2> [19]
$CrCl_2$ <2> (<2> 1 mM, 83% inhibition in presence of 1 mM $CoCl_2$ [24]) [24]
Cu^{2+} <2,3,8> [16,19]
$CuCl_2$ <2> (<2> 1 mM, 96% inhibition in presence of 1 mM $CoCl_2$ [24]) [24]
D-phenylalanine <3> [5]
EDTA <2,3,5,6> (<2> 5 mM, 90% inhibition [24]; <5> aminopeptidase I and II [6]; <6> complete inhibition, activity cannot be completely restored by addition of 1 mM $CaCl_2$ alone but together with 0.0001 mM $ZnCl_2$ by 90% [2]; <3> complete inhibition at 10 mM, reactivation by divalent metal ions [20]) [2,6,20,24]
EGTA <6> (<6> complete inhibition, activity can be completely restored by addition of 1 mM $CaCl_2$ [2]) [2]
Fe^{2+} <3,8> [16]
$HgCl_2$ <2> (<2> 5 mM, 98% inhibition in presence of 1 mM $CoCl_2$ [24]) [24]
L-alanine <3> [5]
L-arginine <3> [5]
L-aspartate <3> [5]
L-histidine <7> [22]
L-leucine <3> (<3> binding mechanism and structure [11]; <3> very low product inhibition [16]) [5,11,16]
L-leucine chloromethyl ketone <3> [5]
L-methionine <3> (<3> binding mechanism and structure [11]) [5,11]
L-phenylalanine <3> (<3> binding mechanism and structure [11]) [5,11]

L-phenylalanine chloromethyl ketone <3> [5]
L-serine <7> [22]
L-tryptophan <3> (<3> weak inhibition, binds at the active site via the two zinc ions displacing the metal ions, binding structure analysis [12]) [12]
Leu-hydroxamate <2> (<2> 1 mM, 73% inhibition [24]) [24]
Lys-hydroxamate <2> (<2> 1 mM, 80% inhibition [19]; <2> 1 mM, 81% inhibition [24]) [19,24]
Mg^{2+} <3,8> (<8> slight inhibition at 0.1-1 mM [16]) [16]
$MgSO_4$ <2> (<2> 1 mM, 24% inhibition in presence of 1 mM $CoCl_2$ [24]) [24]
Mn^{2+} <3,8> [16]
$MnSO_4$ <2> (<2> 1 mM, 26% inhibition in presence of 1 mM $CoCl_2$ [24]) [24]
Ni^{2+} <2,3,8> [16,19]
$NiSO_4$ <2> (<2> 1 mM, 40% inhibition in presence of 1 mM $CoCl_2$ [24]) [24]
PMSF <2> (<2> 1 mM, complete inhibition [19]) [19]
Zn^{2+} <2,3,8> [16,19]
$ZnCl_2$ <2> (<2> 1 mM, 70% inhibition in presence of 1 mM $CoCl_2$ [24]) [24]
amastatin <3,8> [5,16]
antipain <2> (<2> 0.01 mg/ml, 93% inhibition [24]) [24]
bestatin <2,3,5,8> (<5> aminopeptidase I and II [6]; <2> 0.004 mg/ml, 94% inhibition [24]; <2> 0.004 mg/ml, complete inhibition [19]) [5,6,16,19,24]
diisopropylphosphofluoridate <3> (<3> pretreatment, complete inhibition [7]) [7]
fluoride <3> (<3> noncompetitive inhibitor at pH 5.9-8.0, fluoride ion interacts equally with the free enzyme as with the enzyme-substrate complex [26]; <3> uncompetitive inhibitor toward peptide hydrolysis [25]) [25,26,30]
free amino acids <3> (<3> competitive inhibition, highest inhibition by L-histidine [20]) [20]
leucine <3> (<3> weak inhibitor, binding structure, overview [13]; <3> product inhibition occurs in peptide hydrolysis [25]) [13,25]
leupeptin <2> (<2> 0.01 mg/ml, 51% inhibition [24]) [24]
methionine <3> (<3> weak inhibitor, binding structure, overview [13]) [13]
nitrilotriacetic acid <2> (<2> 5 mM, 95% inhibition [24]) [24]
o-phenanthroline <5> (<5> aminopeptidase I and II [6]) [6]
p-(chloromercuri)benzene sulfonate <5> (<5> aminopeptidase II [6]) [6]
p-hydroxymercuribenzoate <2> (<2> 5 mM, 90% inhibition [24]) [24]
phenylalanine <3> (<3> weak inhibitor, binding structure, overview [13]) [13]
phenylmethylsulfonyl fluoride <2> (<2> 1 mM, 95% inhibition [24]) [24]
phosphate <3> (<3> noncompetitive inhibitor with peptide substrates, the enzyme-substrate-inhibitor ternary complex is inactive, but phosphate is a competitive inhibitor toward bis(*p*-nitrophenyl)phosphate hydrolysis, with K_i ranging from 2.31 to 315 mM at pH 5.0-9.0 [25]) [25,26]
tosyl-lysine chloromethyl ketone <2> (<2> 2 mM, 80% inhibition [19]; <2> 5 mM, 94% inhibition [24]) [19,24]
tosyl-phenylalanine chloromethyl ketone <5> (<5> slight inhibition [6]) [6]
Additional information <1,3,5,8> (<5> aminopeptidase II is not affected by PMSF, pepstatin, tosyl-lysine chloromethyl ketone, tosyl-phenylalanine chlor-

omethyl ketone, leupeptin, and phosphoramidon, aminopeptidase I is not affected by PMSF, *p*-(chloromercuri)benzene sulfonate, pepstatin, tosyl-lysine chloromethyl ketoneleupeptin, and phosphoramidon [6]; <3> nonchelating 1,7-phenanthroline has little effect on the activity [3]; <1> the enzyme activity is completely abolished by metal chelating agents, but can be restored by addition of zinc or cobalt [21]; <8> very low product inhibition by L-leucine [16]) [3,6,16,21]

Activating compounds

Additional information <5> (<5> aminopeptidase II is not affected by PMSF, pepstatin, tosyl-lysine chloromethyl ketone, tosyl-phenylalanine chloromethyl ketone, leupeptin, and phosphoramidon, aminopeptidase I is not affected by PMSF, *p*-(chloromercuri)benzene sulfonate, pepstatin, tosyl-lysine chloromethyl ketoneleupeptin, and phosphoramidon [6]) [6]

Metals, ions

Ca^{2+} <3,6,7> (<3> activates [25,26]; <6> activation [4]; <6> activates about 6fold, non-cooperative binding [2]; <3> activates, binds to the enzyme, activation level with different enzyme substrates, overview [3]; <3> activates, enhances stability of the enzyme, modulates the enzyme activity and affinity towards substrates and inhibitors in a structure-dependent manner, binding structure [5]; <3> location of binding site is in about 25 A distance from the zinc binding site, determination of structural environment [9]; <7> activates and stabilizes, influences substrate specificity, Asp173 and Asp174 are key residues in Ca^{2+} binding and important for enzyme activity, residues Asp3, Ile4, Asp262, and Asp266 are also involved in calcium binding but are important for enzyme stabilization, overview, binding capacity of recombinant wild-type and mutant enzymes, overview [22]; <3> activates the enzyme with some substrates, about 3fold with L-Leu-4-nitroanilide, and affects substrate specificity, e.g. decreases the activity with Lys-4-nitroanilide [16]; <3> activates, has complex effects on the enzyme, stabilizes the enzyme [20]; <3> affects metal binding, inhibition, and entropy of activation of the enzyme [23]; <3> modulating the enzyme activity [13]) [2,3,4,5,9,13,16,18,20,22,23,25,26]

Cd^{2+} <3,4> (<4> dinuclear metal-enzyme derivative, structure [17]; <3> metal binding modelling using titration, kinetic, and thermodynamic data, dinuclear metal enzyme, sequential binding to two metal binding sites, affected by Ca^{2+} [23]) [17,23]

Co^{2+} <1,2,3,4> (<3> activates [20]; <2> activity is strictly dependent on, maximal activity at 0.5 mM $CoCl_2$ [24]; <4> dinuclear metal-enzyme derivative, structure [17]; <2> metalloenzyme containing Co^{2+} in its structure [19]; <3> slightly activating at 0.1-1 mM [16]; <1> the enzyme contains two metal ions with high occupancy and a third metal ion with low occupancy at the active site of the enzyme molecule, Glu319 and a water molecule are bridging, Glu253, His348, His381, Tyr355, and Asp383 are involved in metal binding, structure analysis [21]) [16,17,19,20,21,24]

Mn^{2+} <4> (<4> dinuclear metal-enzyme derivative, structure [17]) [17]

Ni^{2+} <4> (<4> dinuclear metal-enzyme derivative, structure [17]) [17]

Zn^{2+} <1,3,6,7> (<3> 2 mol zinc per mol of enzyme, binding structure [1,5]; <3> 2 mol zinc per mol of enzyme, tightly bound at the active site in a distance of 3.6 A of each other, determination of structural environment [9]; <6> 2 mol/mol of protein, tightly bound, zinc coordination amino acid residues are conserved in similar enzymes [4]; <3> double-zinc exopeptidase [11]; <3,6> metalloprotease, dependent on [2,3]; <3> zinc-metallo-exoprotease [10]; <1> the enzyme contains two metal ions with high occupancy and a third metal ion with low occupancy at the active site of the enzyme molecule, Glu319 and a water molecule are bridging, Glu253, His348, His381, Tyr355, and Asp383 are involved in metal binding, structure analysis [21]; <3> the enzyme is a double-zinc aminopeptidase [18]; <7> the enzyme is a double-zinc aminopeptidase, metal ions are bound at the active site [22]; <3> the enzyme is a double-zinc aminopeptidase, the metal ions are bound at the active site, binding structure analysis [12]; <3> the enzyme is a double-zinc exopeptidase, binding structure, overview [13]; <3> the enzyme is a zinc-metalloenzyme containing 2 mol zinc per mol of enzyme, stabilizes the enzyme [20]; <3> dizinc enzyme [25]; <3> double-zinc aminopeptidase [26]) [1,2,3,4,5,9,10,11,12,13,18,20,21,22,25,26]
Additional information <1,3,4,8> (<3> substitution of the Zn^{2+} ion by Mn^{2+} or Co^{2+} results in altered substrate specificity, e.g. the Co^{2+} containing enzyme highly prefers L-alanine-4-nitroanilide [3]; <8> Ca^{2+} and Co^{2+} do not affect the enzymes substrate specificity at 0.1-1 mM [16]; <1> determination of metal ion identity [21]; <3> the enzyme depends on metals [20]; <4> the enzyme possesses dinuclear metal cluster [17]) [3,16,17,20,21]

Turnover number (s^{-1})

0.0033 <4> (4-nitrophenyl phenylphosphonate, <4> pH 8.0, 50°C, Ni^{2+}-enzyme [17]) [17]
0.0064 <3> (bis(4-nitrophenyl) phosphate, <3> in presence of Mn-Ni-heterodinuclear aminopeptidase [30]) [30]
0.01 <4> (4-nitrophenyl phenylphosphonate, <4> pH 8.0, 50°C, Mn^{2+}-enzyme [17]) [17]
0.01 <3,4> (bis(4-nitrophenyl) phosphate, <4> pH 8.0, 30°C, Ni^{2+}-enzyme [17]; <3> in presence of Ni-Ni-homo-dinuclear aminopeptidase [30]) [17,30]
0.014 <4> (4-nitrophenyl phenylphosphonate, <4> pH 8.0, 50°C, Zn^{2+}-enzyme [17]) [17]
0.016 <3> (bis(4-nitrophenyl) phosphate, <3> in presence of Mn-Cd-heterodinuclear aminopeptidase [30]) [30]
0.017 <4> (4-nitrophenyl phenylphosphonate, <4> pH 8.0, 50°C, Cd^{2+}-enzyme [17]) [17]
0.022 <4> (4-nitrophenyl phenylphosphonate, <4> pH 8.0, 50°C, Co^{2+}-enzyme [17]) [17]
0.043 <3,4> (bis(4-nitrophenyl) phosphate, <4> pH 8.0, 30°C, Cd^{2+}-enzyme [17]; <3> in presence of Cd-Cd-homo-dinuclear aminopeptidase [30]) [17,30]
0.0433 <3> (Leu-4-nitroanilide, <3> in presence of Ni-Ni-homo-dinuclear aminopeptidase [30]) [30]

0.0505 <3> (Leu-4-nitroanilide, <3> in presence of Mn-Ni-hetero-dinuclear aminopeptidase [30]) [30]
0.081 <3> (bis(4-nitrophenyl) phosphate, <3> in presence of Mn-Mn-homo-dinuclear aminopeptidase [30]) [30]
0.087 <3> (bis(4-nitrophenyl) phosphate, <3> in presence of Mn-Co-hetero-dinuclear aminopeptidase [30]) [30]
0.1 <3> (bis(4-nitrophenyl) phosphate, <3> in presence of Mn-Zn-hetero-dinuclear aminopeptidase [30]) [30]
0.13 <3> (L-valine-4-nitroanilide, <3> pH 8.0, 30°C, in absence of Ca^{2+} [5]) [5]
0.191 <3> (L-Val-4-nitroanilide, <3> pH 8.0, 30°C [3]) [3]
0.21 <4> (bis(4-nitrophenyl) phosphate, <4> pH 8.0, 30°C, Mn^{2+}-enzyme [17]) [17]
0.26 <3> (L-valine-4-nitroanilide, <3> pH 8.0, 30°C, in presence of Ca^{2+} [5]) [5]
0.28 <3> (Val-4-nitroanilide, <3> pH 8.0, 30°C [25]) [25]
0.42 <3> (Bis(*p*-nitrophenyl)phosphate, <3> pH 8.0, 30°C [25]) [25]
0.45 <3,4> (bis(4-nitrophenyl) phosphate, <4> pH 8.0, 30°C, Zn^{2+}-enzyme [17]; <3> in presence of Zn-Zn-homo-dinuclear aminopeptidase [30]) [17,30]
0.47 <3> (L-alanine-4-nitroanilide, <3> pH 8.0, 30°C, in absence of Ca^{2+} [5]) [5]
0.49 <7> (L-Leu-4-nitroanilide, <7> pH 8.0, 37°C, recombinant mutant E196A, in presence of Ca^{2+} [22]) [22]
0.55 <7> (L-Leu-4-nitroanilide, <7> pH 8.0, 37°C, recombinant mutant E196A, in absence of Ca^{2+} [22]) [22]
0.64 <8> (L-Phe-O-methyl ester, <8> pH 8.0, 37°C, recombinant wild-type enzyme [15]) [15]
0.74 <3,4> (bis(4-nitrophenyl) phosphate, <4> pH 8.0, 30°C, Co^{2+}-enzyme [17]; <3> in presence of Co-Co-homo-dinuclear aminopeptidase [30]) [17,30]
0.97 <7> (L-Leu-4-nitroanilide, <7> pH 8.0, 37°C, recombinant wild-type enzyme, in presence of Ca^{2+} [22]) [22]
1.08 <7> (L-Leu-4-nitroanilide, <7> pH 8.0, 37°C, recombinant mutant D3A/D262G, in presence of Ca^{2+} [22]) [22]
1.1 <3> (Gly-4-nitroanilide, <3> pH 8.0, 30°C [25]) [25]
1.31 <3> (L-leucine-4-nitroanilide, <3> pH 8.0, 30°C, in absence of Ca^{2+} [5]) [5]
1.5 <3> (Leu-4-nitroanilide, <3> in presence of Mn-Cd-hetero-dinuclear aminopeptidase [30]) [30]
1.68 <3> (Leu-4-nitroanilide, <3> in presence of Cd-Cd-homo-dinuclear aminopeptidase [30]) [30]
1.71 <3> (L-Ala-4-nitroanilide, <3> pH 8.0, 30°C [3]) [3]
1.81 <3> (L-alanine-4-nitroanilide, <3> pH 8.0, 30°C, in presence of Ca^{2+} [5]) [5]
2.12 <7> (L-Leu-4-nitroanilide, <7> pH 8.0, 37°C, recombinant wild-type enzyme, in absence of Ca^{2+} [22]) [22]
2.71 <7> (L-Leu-4-nitroanilide, <7> pH 8.0, 37°C, recombinant mutant D3A/D262G, in absence of Ca^{2+} [22]) [22]
2.8 <3> (Lys-4-nitroanilide, <3> pH 8.0, 30°C [25]) [25]

2.94 <3> (L-Ala-4-nitroanilide, <3> pH 8.0, 30°C [3]) [3]
2.94 <3> (L-alanine-4-nitroanilide, <3> pH 8.0, 30°C, in presence of Ca^{2+} [5]) [5]
3-6 <7> (L-Leu-4-nitroanilide, <7> pH 8.0, 37°C, recombinant mutant D3A/D262G, in absence of Ca^{2+} [22]) [22]
4.72 <7> (L-Leu-4-nitroanilide, <7> pH 8.0, 37°C, recombinant chimeric mutant, in presence of Ca^{2+} [22]) [22]
4.9 <3> (Ala-4-nitroanilide, <3> pH 8.0, 30°C [25]) [25]
5.2 <7> (L-Leu-4-nitroanilide, <7> pH 8.0, 37°C, recombinant chimeric mutant, in absence of Ca^{2+} [22]) [22]
10.7 <8> (L-Phe-NH_2, <8> pH 8.0, 37°C, recombinant mutant F221I [15]) [15]
17.6 <8> (L-Phe-4-nitroanilide, <8> pH 8.0, 37°C, recombinant wild-type enzyme [15]) [15]
19.3 <8> (L-Phe-4-nitroanilide, <8> pH 8.0, 37°C, recombinant mutant F221I [15]) [15]
27.5 <3> (Leu-4-nitroanilide, <3> in presence of Mn-Mn-homo-dinuclear aminopeptidase [30]) [30]
31.7 <8> (L-Leu-NH_2, <8> pH 8.0, 37°C, recombinant mutant F221A [15]) [15]
34 <8> (L-Leu-4-nitroanilide, <8> pH 8.0, 37°C, recombinant mutant F221A [15]) [15]
37.4 <3> (Leu-4-nitroanilide, <3> in presence of Mn-Co-hetero-dinuclear aminopeptidase [30]) [30]
41 <3> (Leu-4-nitroanilide, <3> in presence of Co-Co-homo-dinuclear aminopeptidase [30]) [30]
41.5 <8> (L-Leu-4-nitroanilide, <8> pH 8.0, 37°C, recombinant enzyme, in absence of Ca^{2+} [16]) [16]
42.1 <8> (L-Leu-4-nitroanilide, <8> pH 8.0, 37°C, recombinant enzyme, in presence of Ca^{2+} [16]) [16]
43.3 <3> (Met-4-nitroanilide, <3> pH 8.0, 30°C [25]) [25]
43.8 <8> (L-Phe-NH_2, <8> pH 8.0, 37°C, recombinant wild-type enzyme [15]) [15]
54.3 <8> (L-Phe-O-methyl ester, <8> pH 8.0, 37°C, recombinant wild-type enzyme [15]) [15]
64.2 <8> (L-Leu-O-methyl ester, <8> pH 8.0, 37°C, recombinant wild-type enzyme [15]) [15]
65.9 <8> (L-Leu-4-nitroanilide, <8> pH 8.0, 37°C, recombinant wild-type enzyme [15]) [15]
75 <3> (L-leucine-4-nitroanilide, <3> pH 8.0, 22°C, acetylated aminopeptidases 2 [7]) [7]
75.3 <3> (L-Leu-4-nitroanilide, <3> pH 8.0, 37°C, recombinant enzyme, in absence of Ca^{2+} [16]) [16]
92.8 <3> (Leu-4-nitroanilide, <3> in presence of Mn-Zn-hetero-dinuclear aminopeptidase [30]) [30]
101 <3> (Leu-4-nitroanilide, <3> in presence of Zn-Zn-homo-dinuclear aminopeptidase [30]) [30]

104 <8> (L-Leu-NH_2, <8> pH 8.0, 37°C, recombinant wild-type enzyme [15]) [15]
108 <8> (L-Leu-4-nitroanilide, <8> pH 8.0, 37°C, recombinant mutant F221I [15]) [15]
111 <3> (L-leucine-4-nitroanilide, <3> pH 8.0, 22°C, native aminopeptidases 2 [7]) [7]
115 <8> (L-Phe-NH_2, <8> pH 8.0, 37°C, recombinant mutant F221A [15]) [15]
116 <3> (L-leucine-4-nitroanilide, <3> pH 8.0, 22°C, acetylated aminopeptidases 1 [7]) [7]
142 <8> (L-Leu-O-methyl ester, <8> pH 8.0, 37°C, recombinant wild-type enzyme [15]) [15]
153 <3> (L-leucine-4-nitroanilide, <3> pH 8.0, 22°C, native aminopeptidases 1 [7]) [7]
155 <8> (L-Leu-NH_2, <8> pH 8.0, 37°C, recombinant mutant F221I [15]) [15]
169 <8> (L-Leu-O-methyl ester, <8> pH 8.0, 37°C, recombinant mutant F221I [15]) [15]
223 <3> (L-Leu-4-nitroanilide, <3> pH 8.0, 37°C, recombinant enzyme, in presence of Ca^{2+} [16]) [16]
224 <8> (L-Phe-O-methyl ester, <8> pH 8.0, 37°C, recombinant mutant F221A [15]) [15]
229 <8> (L-Phe-4-nitroanilide, <8> pH 8.0, 37°C, recombinant mutant F221A [15]) [15]
391 <3> (L-Leu-4-nitroanilide, <3> pH 8.0, 30°C [3]) [3]
657 <3> (Leu-4-nitroanilide, <3> pH 8.0, 30°C [25]) [25]

Specific activity (U/mg)

0.0016 <4> (<4> Ni^{2+}-enzyme, substrate 4-nitrophenyl phenylphosphonate [17]; <4> Ni^{2+}-enzyme, substrate bis(4-nitrophenyl) phosphate [17]) [17]
0.0017 <4> (<4> Zn^{2+}-enzyme, substrate 4-nitrophenyl phenylphosphonate [17]) [17]
0.0033 <4> (<4> Mn^{2+}-enzyme, substrate 4-nitrophenyl phenylphosphonate [17]) [17]
0.0048 <4> (<4> Co^{2+}-enzyme, substrate 4-nitrophenyl phenylphosphonate [17]) [17]
0.0078 <4> (<4> Cd^{2+}-enzyme, substrate bis(4-nitrophenyl) phosphate [17]) [17]
0.0097 <4> (<4> Cd^{2+}-enzyme, substrate 4-nitrophenyl phenylphosphonate [17]) [17]
0.02 <9> (<9> substrate β-Ala-4-nitroanilide [29]) [29]
0.031 <4> (<4> Mn^{2+}-enzyme, substrate bis(4-nitrophenyl) phosphate [17]) [17]
0.103 <5> (<5> crude cell extract, cells grown on glucose, exponential phase [6]) [6]
0.116 <5> (<5> crude cell extract, cells grown on yeast extract, exponential phase [6]) [6]

0.122 <5> (<5> crude cell extract, cells grown on glucose, stationary phase [6]) [6]
0.136 <4> (<4> Co^{2+}-enzyme, substrate bis(4-nitrophenyl) phosphate [17]) [17]
0.139 <5> (<5> crude cell extract, cells grown on yeast extract, stationary phase [6]) [6]
0.158 <4> (<4> Zn^{2+}-enzyme, substrate bis(4-nitrophenyl) phosphate [17]) [17]
4.05 <2> [24]
5.13 <9> (<9> substrate L-Pro-4-nitroanilide [29]) [29]
38.4 <9> (<9> substrate L-Phe-4-nitroanilide [29]) [29]
306 <6> (<6> purified API [2]) [2]
317 <6> (<6> purified APII [2]) [2]
461 <6> (<6> purified API in presence of 1 mM $CaCl_2$ [2]) [2]
625.1 <3> (<3> purified enzyme [10]; <3> purified recombinant enzyme [10]) [10]
830 <3> (<3> purified recombinant wild-type enzyme [18]) [18]
1244 <9> (<9> substrate L-Ala-4-nitroanilide [29]) [29]
Additional information <3,7,8> (<7> recombinant wild-type and mutant enzymes, overview [22]) [5,15,22,25]

K_m-Value (mM)

0.00229 <3> (Leu-4-nitroanilide, <3> in presence of Ni-Ni-homo-dinuclear aminopeptidase [30]) [30]
0.00242 <3> (Leu-4-nitroanilide, <3> in presence of Mn-Ni-hetero-dinuclear aminopeptidase [30]) [30]
0.093 <3> (Leu-4-nitroanilide, <3> in presence of Co-Co-homo-dinuclear aminopeptidase [30]) [30]
0.15 <3> (Leu-4-nitroanilide, <3> in presence of Mn-Co-hetero-dinuclear aminopeptidase [30]) [30]
0.16 <2> (Arg-4-nitroanilide, <2> 37°C, 0.5 mM $CoCl_2$ [24]) [19,24]
0.16 <2> (Lys-4-nitroanilide, <2> 37°C, 0.5 mM $CoCl_2$ [24]) [19,24]
0.18 <3> (Val-4-nitroanilide, <3> pH 8.0, 30°C [25]) [25]
0.19 <3> (Leu-4-nitroanilide, <3> in presence of Mn-Cd-hetero-dinuclear aminopeptidase [30]) [30]
0.213 <3> (Leu-4-nitroanilide, <3> in presence of Cd-Cd-homo-dinuclear aminopeptidase [30]) [30]
0.25 <8> (L-Leu-4-nitroanilide, <8> pH 8.0, 37°C, recombinant mutant F221I [15]) [15]
0.33 <8> (L-Leu-4-nitroanilide, <8> pH 8.0, 37°C, recombinant enzyme, in absence of Ca^{2+} [16]) [16]
0.34 <8> (L-Leu-4-nitroanilide, <8> pH 8.0, 37°C, recombinant enzyme, in presence of Ca^{2+} [16]) [16]
0.34 <8> (L-Phe-4-nitroanilide, <8> pH 8.0, 37°C, recombinant wild-type enzyme [15]) [15]
0.36 <8> (L-Leu-4-nitroanilide, <8> pH 8.0, 37°C, recombinant wild-type enzyme [15]) [15]

0.44 <8> (L-Phe-4-nitroanilide, <8> pH 8.0, 37°C, recombinant mutant F221A [15]) [15]
0.45 <3> (Leu-4-nitroanilide, <3> pH 8.0, 30°C [25]) [25]
0.53 <3> (L-Val-4-nitroanilide, <3> pH 8.0, 30°C [3]) [3]
0.55 <3> (L-leucine-4-nitroanilide, <3> pH 8.0, 30°C, in presence of Ca^{2+} [5]) [5]
0.58 <3> (L-Leu-4-nitroanilide, <3> pH 8.0, 30°C [3]) [3]
0.58 <3> (Met-4-nitroanilide, <3> pH 8.0, 30°C [25]) [25]
0.65 <3> (L-Leu-4-nitroanilide, <3> pH 8.0, 37°C, recombinant enzyme, in presence of Ca^{2+} [16]) [16]
0.67 <3> (L-leucine-4-nitroanilide, <3> pH 8.0, 22°C, native aminopeptidases 1 and 2 [7]) [7]
0.68 <8> (L-Leu-4-nitroanilide, <8> pH 8.0, 37°C, recombinant mutant F221A [15]) [15]
0.72 <3> (L-leucine-4-nitroanilide, <3> pH 8.0, 22°C, acetylated aminopeptidases 1 and 2 [7]) [7]
0.79 <3> (L-valine-4-nitroanilide, <3> pH 8.0, 30°C, in presence of Ca^{2+} [5]) [5]
0.88 <3> (Leu-4-nitroanilide, <3> in presence of Mn-Mn-homo-dinuclear aminopeptidase [30]) [30]
1.4 <3> (Gly-4-nitroanilide, <3> pH 8.0, 30°C [25]) [25]
1.85 <8> (L-Phe-4-nitroanilide, <8> pH 8.0, 37°C, recombinant mutant F221I [15]) [15]
2.15 <3> (L-valine-4-nitroanilide, <3> pH 8.0, 30°C, in absence of Ca^{2+} [5]) [5]
2.3 <3> (L-Leu-4-nitroanilide, <3> pH 8.0, 37°C, recombinant enzyme, in absence of Ca^{2+} [16]) [16]
2.4 <4> (4-nitrophenyl phenylphosphonate, <4> pH 8.0, 50°C, Cd^{2+}-enzyme [17]) [17]
2.54 <7> (L-Leu-4-nitroanilide, <7> pH 8.0, 37°C, recombinant mutant D3A/D262G, in absence of Ca^{2+} [22]) [22]
2.61 <7> (L-Leu-4-nitroanilide, <7> pH 8.0, 37°C, recombinant wild-type enzyme, in absence of Ca^{2+} [22]) [22]
2.97 <3> (L-leucine-4-nitroanilide, <3> pH 8.0, 30°C, in absence of Ca^{2+} [5]) [5]
3 <4> (4-nitrophenyl phenylphosphonate, <4> pH 8.0, 50°C, Ni^{2+}-enzyme [17]) [17]
3.27 <3> (Leu-4-nitroanilide, <3> in presence of Zn-Zn-homo-dinuclear aminopeptidase [30]) [30]
3.31 <3> (Leu-4-nitroanilide, <3> in presence of Mn-Zn-hetero-dinuclear aminopeptidase [30]) [30]
3.4 <3> (bis(*p*-nitrophenyl)phosphate, <3> pH 8.0, 30°C [25]) [25]
3.47 <7> (L-Leu-4-nitroanilide, <7> pH 8.0, 37°C, recombinant mutant E196A, in presence of Ca^{2+} [22]) [22]
3.79 <7> (L-Leu-4-nitroanilide, <7> pH 8.0, 37°C, recombinant mutant E196A, in absence of Ca^{2+} [22]) [22]

3.8 <3> (bis(4-nitrophenyl) phosphate, <3> in presence of Mn-Zn-hetero-dinuclear aminopeptidase [30]) [30]
3.84 <3> (L-alanine-4-nitroanilide, <3> pH 8.0, 30°C, in presence of Ca^{2+} [5]) [5]
3.9 <3> (bis(4-nitrophenyl) phosphate, <3> in presence of Mn-Co-hetero-dinuclear aminopeptidase [30]) [30]
3.91 <7> (L-Leu-4-nitroanilide, <7> pH 8.0, 37°C, recombinant chimeric mutant, in presence of Ca^{2+} [22]) [22]
4.02 <7> (L-Leu-4-nitroanilide, <7> pH 8.0, 37°C, recombinant chimeric mutant, in absence of Ca^{2+} [22]; <7> pH 8.0, 37°C, recombinant wild-type enzyme, in presence of Ca^{2+} [22]) [22]
4.07 <7> (L-Leu-4-nitroanilide, <7> pH 8.0, 37°C, recombinant mutant D3A/D262G, in presence of Ca^{2+} [22]) [22]
4.08 <3> (L-Ala-4-nitroanilide, <3> pH 8.0, 30°C [3]) [3]
4.5 <3,4> (bis(4-nitrophenyl) phosphate, <4> pH 8.0, 30°C, Zn^{2+}-enzyme [17]; <3> in presence of Zn-Zn-homo-dinuclear aminopeptidase [30]) [17,30]
4.81 <3> (L-alanine-4-nitroanilide, <3> pH 8.0, 30°C, in absence of Ca^{2+} [5]) [5]
4.9 <4> (4-nitrophenyl phenylphosphonate, <4> pH 8.0, 50°C, Mn^{2+}-enzyme [17]) [17]
5 <3> (Lys-4-nitroanilide, <3> pH 8.0, 30°C [25]) [25]
6.9 <8> (L-Phe-O-methyl ester, <8> pH 8.0, 37°C, recombinant wild-type enzyme [15]) [15]
6.98 <8> (L-Phe-NH_2, <8> pH 8.0, 37°C, recombinant wild-type enzyme [15]) [15]
7.68 <8> (L-Phe-NH_2, <8> pH 8.0, 37°C, recombinant mutant F221A [15]) [15]
7.8 <3> (Ala-4-nitroanilide, <3> pH 8.0, 30°C [25]) [25]
7.9 <4> (4-nitrophenyl phenylphosphonate, <4> pH 8.0, 50°C, Co^{2+}-enzyme [17]) [17]
8.31 <8> (L-Leu-NH_2, <8> pH 8.0, 37°C, recombinant mutant F221I [15]) [15]
9.5 <3,4> (bis(4-nitrophenyl) phosphate, <4> pH 8.0, 30°C, Co^{2+}-enzyme [17]; <3> in presence of Co-Co-homo-dinuclear aminopeptidase [30]) [17,30]
9.7 <3,4> (bis(4-nitrophenyl) phosphate, <4> pH 8.0, 30°C, Cd^{2+}-enzyme [17]; <3> in presence of Cd-Cd-homo-dinuclear aminopeptidase [30]) [17,30]
10.6 <3,4> (bis(4-nitrophenyl) phosphate, <4> pH 8.0, 30°C, Ni^{2+}-enzyme [17]; <3> in presence of Ni-Ni-homo-dinuclear aminopeptidase [30]) [17,30]
11 <3> (bis(4-nitrophenyl) phosphate, <3> in presence of Mn-Cd-hetero-dinuclear aminopeptidase [30]) [30]
12 <4> (bis(4-nitrophenyl) phosphate, <4> pH 8.0, 30°C, Mn^{2+}-enzyme [17]) [17]
12.3 <3> (bis(4-nitrophenyl) phosphate, <3> in presence of Mn-Mn-homo-dinuclear aminopeptidase [30]) [30]
12.8 <8> (L-Phe-O-methyl ester, <8> pH 8.0, 37°C, recombinant mutant F221A [15]) [15]

12.8 <3> (bis(4-nitrophenyl) phosphate, <3> in presence of Mn-Ni-heterodinuclear aminopeptidase [30]) [30]
14.9 <4> (4-nitrophenyl phenylphosphonate, <4> pH 8.0, 50°C, Zn^{2+}-enzyme [17]) [17]
15.6 <8> (L-Leu-NH_2, <8> pH 8.0, 37°C, recombinant wild-type enzyme [15]) [15]
15.8 <8> (L-Leu-O-methyl ester, <8> pH 8.0, 37°C, recombinant wild-type enzyme [15]) [15]
16.1 <8> (L-Leu-O-methyl ester, <8> pH 8.0, 37°C, recombinant mutant F221I [15]) [15]
24.2 <8> (L-Phe-NH_2, <8> pH 8.0, 37°C, recombinant mutant F221I [15]) [15]
42.7 <8> (L-Leu-NH_2, <8> pH 8.0, 37°C, recombinant mutant F221A [15]) [15]
Additional information <3,8> (<3> kinetics [3,5]; <3> kinetics and thermodynamics [23]; <8> kinetics of recombinant wild-type and F221 mutant enzymes [15]; <3> kinetic analysis, effects of pH, solvent isotope effects, overview [25]; <3> kinetics,enzyme-substrate interaction, overview [26]) [3,5,15,23,25,26]

K_i-Value (mM)

1.1e-005 <3> (amastatin, <3> pH 8.0, 37°C, recombinant enzyme [16]) [16]
1.6e-005 <3> (amastatin, <3> pH 8.0, 30°C, in presence of Ca^{2+} [5]) [5]
0.0005 <3> (L-leucine chloromethyl ketone, <3> pH 8.0, 30°C, in presence of Ca^{2+} [5]) [5]
0.00055 <3> (amastatin, <3> pH 8.0, 30°C, in absence of Ca^{2+} [5]) [5]
0.00079 <8> (amastatin, <8> pH 8.0, 37°C, recombinant enzyme [16]) [16]
0.0019 <3> (L-phenylalanine chloromethyl ketone, <3> pH 8.0, 30°C, in presence of Ca^{2+} [5]) [5]
0.0026 <3> (bestatin, <3> pH 8.0, 30°C, in presence of Ca^{2+} [5]) [5]
0.0039 <3> (bestatin, <3> pH 8.0, 37°C, recombinant enzyme [16]) [16]
0.0053 <3> (L-phenylalanine chloromethyl ketone, <3> pH 8.0, 30°C, in absence of Ca^{2+} [5]) [5]
0.0054 <3> (bestatin, <3> pH 8.0, 30°C, in absence of Ca^{2+} [5]) [5]
0.0055 <3> (L-leucine chloromethyl ketone, <3> pH 8.0, 30°C, in absence of Ca^{2+} [5]) [5]
0.065 <8> (bestatin, <8> pH 8.0, 37°C, recombinant enzyme [16]) [16]
1.1 <3> (fluoride, <3> substrate Leu-4-nitroanilide, in presence of Mn-Mn-homo-dinuclear aminopeptidase [30]) [30]
2.31 <3> (bis(*p*-nitrophenyl)phosphate, <3> pH 5.0, 30°C [25]) [25]
8.7 <3> (L-methionine, <3> pH 8.0, 30°C, in presence of Ca^{2+} [5]) [5]
9.1 <3> (L-methionine, <3> pH 6.5, 30°C, in presence of Ca^{2+} [5]) [5]
10.3 <3> (leucine, <3> pH 8.0, 30°C [25]) [25]
11.4 <3> (fluoride, <3> pH 8.0 [26]) [26]
12.4 <3> (L-leucine, <3> pH 8.0, 30°C, in presence of Ca^{2+} [5]) [5]
12.7 <3> (L-phenylalanine, <3> pH 8.0, 30°C, in presence of Ca^{2+} [5]) [5]
12.8 <3> (L-leucine, <3> pH 6.5, 30°C, in presence of Ca^{2+} [5]) [5]

17 <3> (fluoride, <3> substrate Leu-4-nitroanilide, in presence of Mn-Co-hetero-dinuclear aminopeptidase [30]) [30]
28 <3> (fluoride, <3> substrate Leu-4-nitroanilide, in presence of Co-Co-homo-dinuclear aminopeptidase [30]) [30]
29 <3> (L-leucine, <3> above, pH 8.0, 37°C, recombinant enzyme [16]) [16]
36.6 <3> (D-phenylalanine, <3> pH 8.0, 30°C, in presence of Ca^{2+} [5]) [5]
70 <3> (fluoride, <3> substrate Leu-4-nitroanilide, in presence of Mn-Zn-hetero-dinuclear aminopeptidase [30]) [30]
75 <3> (fluoride, <3> substrate Leu-4-nitroanilide, in presence of Mn-Ni-hetero-dinuclear aminopeptidase [30]) [30]
82 <3> (fluoride, <3> substrate Leu-4-nitroanilide, in presence of Ni-Ni-homo-dinuclear aminopeptidase [30]) [30]
100 <8> (L-leucine, <8> above, pH 8.0, 37°C, recombinant enzyme [16]) [16]
108 <3> (fluoride, <3> substrate Leu-4-nitroanilide, in presence of Zn-Zn-homo-dinuclear aminopeptidase [30]) [30]
Additional information <3> (<3> inhibition kinetics [25]) [25]

pH-Optimum

6.5-8 <3> (<3> assay at [26]) [26]
7 <2,5> (<5> assay at [6]) [6,19,24]
7.8 <3> (<3> assay at [10]) [10]
8 <3,4,6,7,8> (<3,4,6,7,8> assay at [2,3,7,10,15,17,18,22,25]) [2,3,7,10,15,17,18,22,25]
8.4 <3> (<3> about [11]) [11]
8.5 <3,8> [16]
9 <3> [30]

pH-Range

4-10 <3> (<3> bell-shaped pH-profile [25]) [25]
6-8 <2> (<2> pH 6: about 55% of maximal activity, pH 11: about 35% of maximal activity [24]) [24]
6.3-9.5 <3> (<3> at 50 mM Ca^{2+} [20]) [20]
6.3-11.5 <3> (<3> at 0.05 mM Ca^{2+} [20]) [20]
Additional information <3,8> (<3,8> pH profile [16]; <3> pH-dependent activity is altered by Ca^{2+} concentration [20]; <3> a single proton transfer is involved in catalysis at pH 8.0, whereas two proton transfers are implicated at pH 6.5 [26]) [16,20,26]

pi-Value

5.2 <3> (<3> isoelectric focusing [10]; <3> recombinant enzyme, isoelectric focusing and amino acid sequence calculation [10]) [10]

Temperature optimum (°C)

22 <3> (<3> assay at [7]) [7]
24 <3> (<3> assay at [10]) [10]
25 <6> (<6> assay at [2]) [2]
30 <3,4> (<3> assay at [3,18,25,30]; <4> assay at, substrate bis(4-nitrophenyl) phosphate [17]) [3,17,18,25,30]
37 <1,3,7,8> (<1,3,7,8> assay at [10,15,21,22]) [10,15,21,22]

50 <4> (<4> assay at, substrate 4-nitrophenyl phenylphosphonate [17]) [17]
65 <3> (<3> in absence of Ca^{2+} [16]) [16]
70 <5> (<5> assay at [6]) [6]
75 <3,8> (<3> in presence of Ca^{2+} [16]) [16]

Temperature range (°C)
19-56 <3> [26]
20-60 <3> [25]
30-75 <3> (<3> in absence of Ca^{2+} [16]) [16]
30-90 <3,8> (<3> in presence of Ca^{2+} [16]) [16]

4 Enzyme Structure

Molecular weight
21000 <6> (<6> API, gel filtration [2]) [2]
22500 <6> (<6> APII, gel filtration [2]) [2]
26800 <3> (<3> recombinant enzyme, gel filtration [10]) [10]
29000-29730 <3> (<3> native PAGE and mass spectrometry [5]) [5]
29720 <6> (<6> amino acid sequence determination [4]) [4]
30000 <3> (<3> crystal structure determination [8]) [8]
170000 <5> (<5> aminopeptidase II, gel filtration [6]) [6]
290000 <2> (<2> gel filtration [24]) [19,24]
450000 <5> (<5> above, aminopeptidase I, gel filtration [6]) [6]
Additional information <3,6> (<6> enzymes are retarded on the Superose gel [2]; <3> extracellular enzymes show a low MW of 20-30 kDa [14]) [2,14]

Subunits
dimer <1> (<1> the enzyme forms an inactive dimer in the crystal with a large internal cavity with the active sites located at the opposing ends of the cavity essentially inaccessible from the outside [21]) [21]
hexamer <2> (<2> 6 * 48000, SDS-PAGE [24]; <2> 6 * 48000 [19]) [19,24]
monomer <3,6> (<3> 1 * 30000 [13,26]; <6> 1 * 29723, amino acid sequence determination [4]; <3> 1 * 29728-29731, mass spectrometry [5]; <3> 1 * 30000, crystal structure determination [8]; <3> 1 * 30800, recombinant enzyme, SDS-PAGE [10]; <6> 1 * 33000, API, SDS-PAGE, 1 * 34000, APII, SDS-PAGE [2]) [2,4,5,8,10,13,26]

5 Isolation/Preparation/Mutation/Application

Source/tissue
commercial preparation <3,6> (<3> pronase preparation, containing no prolidase acivity [7]; <3,6> protease type XIV i.e. pronase E, a protease mixture form Streptomyces griseus [2,3,5,8]) [2,3,5,7,8]
commercial product <3,6> (<3,6> protease type XIV i.e. pronase E, a protease mixture form Streptomyces griseus [4,9]) [4,9]

Additional information <3> (<3> the enzyme is contained in the pronase enzyme mixture from strain K-1 [20]) [20]

Localization

extracellular <3> (<3> excretion [8]) [1,8,10,14,20]
intracellular <3> [14]

Purification

<1> (recombinant His-tagged enzyme from Escherichia coli strain BL21(DE3) by nickel affinity chromatography, and gel filtration) [21]
<2> [19,24]
<3> (DEAE Sephacel column) [30]
<3> (from commercial product) [5,8]
<3> (from commercial product, 2 peaks API and APII, endopeptidase is eliminated) [2]
<3> (from commercial product, purification of the acetylated enzyme derivatives by DEAE cellulose chromatography) [7]
<3> (recombinant enzyme from Streptomyces lividans cells by diafiltration, hydrophobic interaction chromatography, and gel filtration to homogeneity) [10]
<3> (recombinant from Streptomyces lividans cell culture medium, high purity, 19% recovery) [10]
<3> (recombinant soluble wild-type and mutant enzymes 28fold from Escherichia coli strain BL21(DE3) by heat treatment for 20 min at 50°C and anion exchange chromatography) [18]
<3> (to homogeneity from strain K-1 pronase) [20]
<5> (partial) [6]
<8> (native enzyme by ion exchange chromatography, ammonium sulfate fractionation, and gel filtration, recombinant enzyme from Escherichia coli strain BL21(DE3) culture supernatant by ion exchange chromatography) [16]
<8> (recombinant wild-type and mutant enzymes from Escherichia coli strain Bl21(DE3)) [15]
<9> [29]

Crystallization

<1> (purified recombinant enzyme, sitting drop vapour diffusion method, the reservoir solution contains 0.1 M HEPES/NaOH, pH 7.6, 2.0 M ammonium sulfate, and 2% PEG 400, 4 weeks, X-ray diffraction structure determination and analysis at 1.8 A resolution) [21]
<3> (hanging drop vapour diffusion method, 18-25 mg/ml purified enzyme in 10 mM Tris-HCl, pH 8.0, 20 mM NaCl, 1 mM $CaCl_2$, plus an equal volume of sodium acetate buffer at pH 5.0 to 6.0, 16-20% w/v polyethylene glycol 4000, suspended over 1 ml reservoir solution of sodium acetate, pH 5.0-6.0, 16-20% PEG 4000, 3-4 weeks, X-ray diffraction structure determination at 47.2 to 1.9 A resolution and analysis) [8]
<3> (protein with or without bound Zn^{2+} or replaced with Hg^{2+}, hanging drop vapour diffusion method, 20 mg/ml purified enzyme in 10 mM Tris-HCl, pH 8.0, 20 mM NaCl, 1 mM $CaCl_2$, plus an equal volume of sodium acet-

ate buffer at pH 5.0 to 6.0, 16-20% w/v polyethylene glycol 4000, suspended over 1 ml reservoir solution of sodium acetate, pH 5.0-6.0, 16-20% PEG 4000, 4-5 weeks to full size crystals, X-ray diffraction structure determination at 2.1 to 1.75 A resolution and analysis) [9]
<3> (purified enzyme complexed with L-methionine, L-phenylalanine, or L-leucine, hanging-drop vapour diffusion method, protein solution: 18 mg/ml protein, 10 mM Tris-HCl, pH 8.0, 20 mM NaCl, 6 mM $CaCl_2$, 100 mM L-methionine or 200 mM L-leucine, plus equal volume of precipitant solution: 24% w/v PEG 4000, 0.1 M ammonium sulfate, equilibrated against 1 ml of reservoir precipitant solution, 3-4 days, cyrstals of enzyme complexed with L-Phe were precipitated with 0.1 M acetate buffer, pH 5.5 instead in the same procedure within 8-10 weeks, X-ray complex structure determination at 1.6 A resolution and analysis) [11]
<3> (purified enzyme complexed with methionine, hanging-drop vapour diffusion method, protein solution: 18 mg/ml protein, 10 mM Tris-HCl, pH 8.0, 20 mM NaCl, 6 mM $CaCl_2$, 0.1 M methionine, plus equal volume of precipitant solution: 24% w/v PEG 4000, 0.1 M ammonium sulfate, equilibrated against 1 ml reservoir of the precipitant solution, 3-4 days, X-ray diffraction structure determination at 1.53 A high resolution and analysis) [1]
<3> (purified enzyme in complex with tryptophan or 4-iodo-L-phenylalanine, hanging drop vapour diffusion method, 18 mg/ml protein in 10 mM Tris-HCl, pH 8.0, 20 mM NaCl, 6 mM $CaCl_2$, and 100 mM tryptophan or 2 mM 4-iodo-L-phenylalanine, equal volumes of protein and reservoir solution are mixed, the latter containing 18% w/v PEG 4000 and 0.1 M sodium acetate, pH 5.5, equilibration against 1 ml reservoir solution for 1 day, microseeding, 3-4 days, X-ray diffraction structure determination and analysis at 1.3 A resolution) [12]
<3> (purified native enzyme in complex with product analogous weak inhibiting amino acids phenylalanine, leucine, and methionine, hanging drop vapour diffusion method, 18 mg/ml protein in 10 mM Tris-HCl, pH 8.0, 20 mM NaCl, 6 mM $CaCl_2$, and 100 mM L-methionine or 200 mM L-leucine, the precipitant solution contains 24% w/v PEG 4000 and 0.1 M ammonium sulfate, equilibration against 1 ml reservoir solution, microseeding, 3-4 days, with phenylalanine a protein solution containing 18 mg/ml protein, 10 mM Tris-HCl, pH 8.0, 20 mM NaCl, 6 mM $CaCl_2$, and 100 mM Phe is mixed with a reservoir solution containing 18% w/v PEG 4000, and 0.1 M acetate buffer, pH 5.5, microseeding, 3-4 days, X-ray diffraction structure determination and analysis at 1.8 A, 1.7 A, and 1.53 A resolution, respectively, structure modelling) [13]
<3> (structure determination and analysis) [20]

Cloning

<1> (expression of the His-tagged enzyme in Escherichia coli strain BL21(DE3)) [21]
<3> (DNA and amino acid sequence determination and analysis) [20]
<3> (DNA and amino acid sequence determination, subcloning and expression of the recombinant enzyme possessing a Asp70 and Asp184 residues in

Escherichia coli strain BL21(DE3), the soluble enzyme is inducible by growth on 1 M sorbitol, optimization of the expression method) [18]
<3> (expression in Streptomyces lividans by insertional cloning and protoplast transformation, the expression system contains the constitutive Streptomyces fradiae aph promoter) [10]
<3> (gene SGAP, standard protoplast transformation and expression in Streptomyces lividans, excretion to the medium) [10]
<3> (gene Sgap, DNA and amino acid sequence determination and analysis, overexpression as secreted enzyme in Escherichia coli) [16]
<7> (gene Sgap, screening of 21 strains with strain NBRC12875 showing the highest activity) [22]
<8> (expression of wild-type and mutant enzymes in Escherichia coli strain BL21(DE3)) [15]
<8> (gene Ssap, genomic library screening, DNA and amino acid sequence determination and analysis, overexpression as secreted enzyme in Escherichia coli strain BL21(DE3)) [16]
<9> (expression in Escherichia coli BL21) [27,29]

Engineering

D3A/D262G <7> (<7> site-directed mutagenesis, the mutant shows increased activity compared to the wild-type enzyme [22]) [22]
E131 <3> (<3> site-directed mutagenesis, the mutant enzyme shows reduced activity compared to the wild-type enzyme [18]) [18]
E131D <3> (<3> a general acid-base mutant, thermodynamic parameters for the reaction are similar to the wild-type enzyme, but the k_{cat} of the mutant is 4fold reduced, while the activation energy is elevated compared to the wild-type enzyme [26]) [26]
E196A <7> (<7> site-directed mutagenesis, the mutant shows reduced activity compared to the wild-type enzyme [22]) [22]
F221A <8> (<8> site-directed mutagenesis, the mutant shows altered substrate specificity compared to the wild-type enzyme [15]) [15]
F221G <8> (<8> site-directed mutagenesis, the mutant shows altered substrate specificity compared to the wild-type enzyme [15]) [15]
F221S <8> (<8> site-directed mutagenesis, the mutant shows altered substrate specificity compared to the wild-type enzyme [15]) [15]
S502C <9> (<9> mutant without aminopeptidase activity but with peptide synthesis activity [28]) [28]
Y246 <3> (<3> site-directed mutagenesis, the mutant enzyme shows highly reduced activity compared to the wild-type enzyme [18]) [18]
Additional information <7,8> (<8> alteration of leucine aminopeptidase to phenylalanine aminopeptidase by site-directed mutagenesis [15]; <7> construction of chimeric enzymes from the enzymes of Streptomyces griseus and Streptomyces septatus by DNA in vivo shuffling and site-directed mutagenesis for calcium activation and binding studies, overview [22]) [15,22]

Application

analysis <7> (<7> the enzyme is clinically important as a model for understanding the structure and mechanism of action of other metallopeptidases [22]) [22]
biotechnology <3> (<3> enzyme is attractive for diverse applications, e.g. the processing of recombinant DNA proteins and fusion protein production due to its heat stability, high activity, and small size [11]; <3> the enzyme is useful in many biotechnological applications e.g. in processing of recombinant DNA, proteins, and fusion protein products [13]) [11,13]

6 Stability

Temperature stability

40-60 <8> (<8> 30 min, recombinant enzyme, stable [16]) [16]
50 <3> (<3> 20 min, stable [18]) [18]
69 <3,6> (<3> recombinant enzyme, stable at for at least 1 h [10]; <6> stable during heating for 5 h at 69°C as part of the purification process [2]) [2,10]
70 <3> (<3> stable at [5]; <3> 30 min, 50% loss of activity, in absence of Ca^{2+} [16]; <3> stable at pH 6.0-10.5 [20]) [5,16,20]
75 <3> (<3> rate constant for inactivation Kin is 0.00028/s in absence of Ca^{2+}, and 0.000025/s in presence of Ca^{2+} [5]) [5]
78 <8> (<8> 30 min, recombinant enzyme, 50% loss of activity [16]) [16]
80 <3> (<3> 30 min, 50% loss of activity, in presence of Ca^{2+} [16]) [16]
90 <5> (<5> stable at for 15 min, pH 7.0 [6]) [6]
95 <9> (<9> enzyme inactivation after 30 min at 95°C [28]) [28]
Additional information <3,8> (<3> the enzyme is heat-stable [13]) [13,16]

General stability information

<3>, Ca^{2+} stabilizes [5]

Storage stability

<2>, 4°C, 50% loss of activity after 4 days, 80% loss of activity after 8 days. Remains active for 2 months, when concentrated and kept in a suspension with 4 M ammonium sulfate in 20 mM MOPS/Tris, pH 7 [24]
<3>, -20°C, liquid and freeze-dried, stable for at least 8 weeks, no loss of activity [10]

References

[1] Gilboa, R.; Greenblatt, H.M.; Perach, M.; Spungin-Bialik, A.; Lessel, U.; Wohlfahrt, G.; Schomburg, D.; Blumberg, S.; Shoham, G.: Interactions of Streptomyces griseus aminopeptidase with a methionine product analogue: a structural study at 1.53 A resolution. Acta Crystallogr. Sect. D, **56**, 551-558 (2000)

[2] Spungin, A.; Blumberg, S.: Streptomyces griseus aminopeptidase is a calcium-activated zinc metalloprotein. Purification and properties of the enzyme. Eur. J. Biochem., **183**, 471-477 (1989)
[3] Ben-Meir, D.; Spungin, A.; Ashkenazi, R.; Blumberg, S.: Specificity of Streptomyces griseus aminopeptidase and modulation of activity by divalent metal ion binding and substitution. Eur. J. Biochem., **212**, 107-112 (1993)
[4] Maras, B.; Greenblatt, H.M.; Shoham, G.; Spungin-Bialik, A.; Blumberg, S.; Barra, D.: Aminopeptidase from Streptomyces griseus: primary structure and comparison with other zinc-containing aminopeptidases. Eur. J. Biochem., **236**, 843-846 (1996)
[5] Papir, G.; Spungin-Bialik, A.; Ben-Meir, D.; Fudim, E.; Gilboa, R.; Greenblatt, H.M.; Shoham, G.; Lessel, U.; Schomburg, D.; Ashkenazi, R.; Blumberg, S.: Inhibition of Streptomyces griseus aminopeptidase and effects of calcium ions on catalysis and binding–comparisons with the homologous enzyme Aeromonas proteolytica aminopeptidase. Eur. J. Biochem., **258**, 313-319 (1998)
[6] Fusi, P.; Villa, M.; Burlini, N.; Tortora, P.; Guerritore, A.: Intracellular proteases from the extremely thermophilic archaebacterium Sulfolobus solfataricus. Experientia, **47**, 1057-1060 (1991)
[7] Vosbeck, K.D.; Greenberg, B.D.; Awad, W.M., Jr.: The proteolytic enzymes of the K-1 strain of Streptomyces griseus obtained from a commercial preparation (Pronase). Specificity and immobilization of aminopeptidase. J. Biol. Chem., **250**, 3981-3987 (1975)
[8] Almog, O.; Greenblatt, H.M.; Spungin, A.; Ben-Meir, D.; Blumberg, S.; Shoham, G.: Crystallization and preliminary crystallographic analysis of Streptomyces griseus aminopeptidase. J. Mol. Biol., **230**, 342-344 (1993)
[9] Greenblatt, H.M.; Almog, O.; Maras, B.; Spungin-Bialik, A.; Barra, D.; Blumberg, S.; Shoham, G.: Streptomyces griseus aminopeptidase: X-ray crystallographic structure at 1.75 A resolution. J. Mol. Biol., **265**, 620-636 (1997)
[10] Ni, S.X.; Cossar, D.; Man, A.; Norek, K.; Miller, D.; Kearse, C.; Tsvetnitsky, V.: Purification and characterization of recombinant Streptomyces griseus aminopeptidase. Protein Expr. Purif., **30**, 62-68 (2003)
[11] Gilboa, R.; Spungin-Bialik, A.; Wohlfahrt, G.; Schomburg, D.; Blumberg, S.; Shoham, G.: Interactions of Streptomyces griseus aminopeptidase with amino acid reaction products and their implications toward a catalytic mechanism. Proteins, **44**, 490-504 (2001)
[12] Reiland, V.; Gilboa, R.; Spungin-Bialik, A.; Schomburg, D.; Shoham, Y.; Blumberg, S.; Shoham, G.: Binding of inhibitory aromatic amino acids to Streptomyces griseus aminopeptidase. Acta Crystallogr. Sect. D, **60**, 1738-1746 (2004)
[13] Gilboa, R.; Greenblatt, H.M.; Perach, M.; Spungin-Bialik, A.; Lessel, U.; Wohlfahrt, G.; Schomburg, D.; Blumberg, S.; Shoham, G.: Interactions of Streptomyces griseus aminopeptidase with a methionine product analogue: a structural study at 1.53 A resolution. Acta Crystallogr. Sect. D, **D56**, 551-558 (2000)
[14] Jankiewicz, U.; Bielawski, W.: The properties and functions of bacterial aminopeptidases. Acta Microbiol. Pol., **52**, 217-231 (2003)

[15] Arima, J.; Uesugi, Y.; Iwabuchi, M.; Hatanaka, T.: Alteration of leucine aminopeptidase from Streptomyces septatus TH-2 to phenylalanine aminopeptidase by site-directed mutagenesis. Appl. Environ. Microbiol., **71**, 7229-7235 (2005)
[16] Arima, J.; Iwabuchi, M.; Hatanaka, T.: Gene cloning and overproduction of an aminopeptidase from Streptomyces septatus TH-2, and comparison with a calcium-activated enzyme from Streptomyces griseus. Biochem. Biophys. Res. Commun., **317**, 531-538 (2004)
[17] Ercan, A.; Park, H.I.; Ming, L.J.: Remarkable enhancement of the hydrolyses of phosphoesters by dinuclear centers: Streptomyces aminopeptidase as a 'natural model system'. Chem. Commun., **1**, 2501-2502 (2000)
[18] Fundoiano-Hershcovitz, Y.; Rabinovitch, L.; Langut, Y.; Reiland, V.; Shoham, G.; Shoham, Y.: Identification of the catalytic residues in the double-zinc aminopeptidase from Streptomyces griseus. FEBS Lett., **571**, 192-196 (2004)
[19] Herrera-Camacho, I.; Lopez-Garcia, A.; Millan-Perez-Pena, L.: Aminopeptidase yscCO-II. Handbook of proteolytic enzymes (Barrett, A.J., Rawlings, N.D., Woessner, J.F., eds.) Academic Press, **1**, 1016-1017 (2004)
[20] Awad, W.M., Jr.: Streptomyces griseus aminopeptidase. Handbook of Proteolytic Enzymes (Barrett, A.J.; Rowlings, N.D.; Woessner, J.F., eds.), **1**, 957-959 (2004)
[21] Odintsov, S.G.; Sabala, I.; Bourenkov, G.; Rybin, V.; Bochtler, M.: Staphylococcus aureus aminopeptidase S is a founding member of a new peptidase clan. J. Biol. Chem., **280**, 27792-27799 (2005)
[22] Arima, J.; Uesugi, Y.; Uraji, M.; Yatsushiro, S.; Tsuboi, S.; Iwabuchi, M.; Hatanaka, T.: Modulation of Streptomyces leucine aminopeptidase by calcium: identification and functional analysis of key residues in activation and stabilization by calcium. J. Biol. Chem., **281**, 5885-5894 (2006)
[23] Hasselgren, C.; Park, H.I.; Ming, L.J.: Metal ion binding and activation of Streptomyces griseus dinuclear aminopeptidase: cadmium(II) binding as a model. J. Biol. Inorg. Chem., **6**, 120-127 (2001)
[24] Herrera-Camacho, I.; Morales-Monterrosas, R.; Quiroz-Alvarez, R.: Aminopeptidase yscCo-II: a new cobalt-dependent aminopeptidase from yeast-purification and biochemical characterization. Yeast, **16**, 219-229 (2000)
[25] Ercan, A.; Park, H.I.; Ming, L.-J.: A moonlighting dizinc aminopeptidase from Streptomyces griseus: mechanisms for peptide hydrolysis and the 4 x 1010-fold acceleration of the alternative phosphodiester hydrolysis. Biochemistry, **45**, 13779-13793 (2006)
[26] Hershcovitz, Y.F.; Gilboa2, R.; Reiland, V.; Shoham, G.; Shoham, Y.: Catalytic mechanism of SGAP, a double-zinc aminopeptidase from Streptomyces griseus. FEBS J., **274**, 3864-3876 (2007)
[27] Arima, J.; Morimoto, M.; Usuki, H.; Mori, N.; Hatanaka, T.: The aminolysis reaction of streptomyces S9 aminopeptidase promotes the synthesis of diverse prolyl dipeptides. Appl. Environ. Microbiol., **76**, 4109-4112 (2010)
[28] Usuki, H.; Uesugi, Y.; Arima, J.; Yamamoto, Y.; Iwabuchi, M.; Hatanaka, T.: Engineered transaminopeptidase, aminolysin-S for catalysis of peptide

bond formation to give linear and cyclic dipeptides by one-pot reaction. Chem. Commun. (Camb.), **46**, 580-582 (2010)
[29] Arima, J.; Morimoto, M.; Usuki, H.; Mori, N.; Hatanaka, T.: β-alanyl peptide synthesis by Streptomyces S9 aminopeptidase. J. Biotechnol., **147**, 52-58 (2010)
[30] Ercan, A.; Tay, W.M.; Grossman, S.H.; Ming, L.J.: Mechanistic role of each metal ion in Streptomyces dinuclear aminopeptidase: PEPTIDE hydrolysis and 7x10(10)-fold rate enhancement of phosphodiester hydrolysis. J. Inorg. Biochem., **104**, 19-29 (2010)

angiotensin-converting enzyme 2 3.4.17.23

1 Nomenclature

EC number
3.4.17.23

Recommended name
angiotensin-converting enzyme 2

Synonyms
ACE <4> [12]
ACE 2 <10,12,13> [74]
ACE-2 <2,3,4,9> [38,68]
ACE-related carboxypeptidase <9> [3]
ACE2 <1,2,3,4,5,6,9,10,11,12,13> [1,2,3,5,6,9,14,15,16,17,19,20,22,25,26,30,37,39,40,41,42,43,44,45,46,47,48,49,50,51,52,53,54,55,56,57,58,59,60,61,62,63,65,66,67,68,69,70,71,72,73,75,76,77,78,79,80,81,82,83,84,85,86,87,88,89,90,91,92,93,94,95,96,97]
ACE2 homologue <2> [41]
ACEH <9> [7]
Ang converting enzyme 2 <10,12,13> [74]
angiotensin II converting enzyme 2 <3> [81]
angiotensin converting enzyme 2 <2,3,4,6,9,10,11,12,13> (<3> functions as a carboxypeptidase [41]) [14,41,43,46,47,51,55,57,58,60,63,74,78,84]
angiotensin converting enzyme II <9> [95]
angiotensin converting enzyme-2 <2,3,4> [38]
angiotensin-converting enzyme <4,9> [22]
angiotensin-converting enzyme 2 <4,8,9,10,12,13> [10,19,67,68,70,76]
angiotensin-converting enzyme homolog <9> [7]
angiotensin-converting enzyme homologue <9> [6]
angiotensin-converting enzyme type 2 <13> [79]
angiotensin-converting enzyme-2 <3,4> [37,53,97]
angiotensin-converting enzyme-like protein <9> [7]
angiotensin-converting enzyme-related carboxypeptidase <9> [1,6]
angiotensinase <9> [4]
hACE2 <3,10,13> [36,67,74]

CAS registry number
328404-18-8

D. Schomburg and I. Schomburg (eds.), *Class 3.4–6 Hydrolases, Lyases, Isomerases, Ligases: EC 3.4–6*, Springer Handbook of Enzymes S10, DOI 10.1007/978-3-642-36260-6_2,

2 Source Organism

<1> *Cricetulus griseus* [83]
<2> *Mus musculus* [26,33,34,38,41,44,45,47,50,51,56,83,86,89,93]
<3> *Homo sapiens* [15,16,17,21,24,26,28,29,30,31,32,35,36,38,40,41,42,49,52,53,58,61,81,84,85,91,92,94]
<4> *Rattus norvegicus* [5,12,13,14,19,20,22,23,25,27,37,38,39,44,46,54,55,59,62,82,87,88,90,93,96,97]
<5> *Sus scrofa* [75]
<6> *Oryctolagus cuniculus* [48,60,90]
<7> *Chlorocebus aethiops* [18]
<8> *Rhipicephalus microplus* (UNIPROT accession number: Q17248) [10]
<9> *Homo sapiens* (UNIPROT accession number: Q9BYF1) [1,2,3,4,6,7,8,9,11,22,43,63,68,69,72,77,80,95]
<10> *Mus musculus* (UNIPROT accession number: Q8R0I0) [57,63,67,74]
<11> *Felis silvestris* (UNIPROT accession number: Q56H28) [63]
<12> *Rattus norvegicus* (UNIPROT accession number: Q5EGZ1) [63,65,66,70,71,74,77]
<13> *Homo sapiens* (UNIPROT accession number: Q9FYF1) [64,72,73,74,76,78,79]

3 Reaction and Specificity

Catalyzed reaction

angiotensin II + H_2O = angiotensin-(1-7) + L-phenylalanine (<3> a transmembrane glycoprotein with an extracellular catalytic domain. ACE2 functions as a carboxypeptidase, cleaving a single C-terminal residue from a distinct range of substrates [41]; <9> ACE2 catalytic efficiency is 400-fold higher with angiotensin II (1-8) as a substrate than with angiotensin I (1-10). ACE2 also efficiently hydrolyzes des-Arg9-bradykinin, but it does not hydrolyze bradykinin [8])

Reaction type

hydrolysis of peptide bond

Natural substrates and products

S angiotensin I + H_2O <9> (Reversibility: ?) [95]
P angiotensin(1-9) + L-Phe
S angiotensin I + H_2O <4,8,9> (<4> ACE2 contributes to the production of angiotensin(1-7) from angiotensin I in proximal straight tubule [14]) (Reversibility: ?) [1,2,3,5,6,7,8,9,10,11,14]
P angiotensin-(1-9) + Leu
S angiotensin II + H_2O <2,3,4,6,9> (<3> ACE2, a homologue of ACE, EC 3.4.15.1, converts angiotensin II into Ang(1-7). Ang(1-7) shows vasoprotective effects, serum autoantibodies to ACE2 predispose patients with connective tissue diseases to constrictive vasculopathy, pulmonary arter-

ial hypertension, or persistent digital ischemia [85]; <2,4> angiotensin II has many adverse cardiovascular effects when acting through the AT1 receptor [93]; <4> high levels of angiotensin II induces pulmonary arterial hypertension [97]) (Reversibility: ?) [85,86,87,88,89,90,91,93,95,96,97]

P angiotensin(1-7) + L-Phe (<2> Ang(1-7) is a vasodilator peptide [89]; <9> Ang-(1-7) is a potential endogenous inhibitor of the classical renin-angiotensin system cascade [95])

S angiotensin II + H_2O <3> (<3> the enzyme is involved in the renin angiotensin system [81]) (Reversibility: ?) [81]

P angiotensin-(1-7) + L-Phe

S angiotensin II + H_2O <3,4,12,13> (<4> ACE2 is highly regulated at transcription. ACE2 plays a critical role in regulating the balance between vasoconstrictor and vasodilator effects within the RAS cascade. Angiotensin II may be a stimulus determining cardiac ACE2 gene expression, because either reduction in its levels or prevention of angiotensin II binding to the AT1 receptor increases ACE2 mRNA. ACE2 serves as the cellular entry point for severe acute respiratory syndrome (SARS) virus [27]; <3> the uteroplacental location of angiotensin (1-7) and ACE2 in pregnancy suggests an autocrine function of angiotensin(1-7) in the vasoactive regulation that characterizes placentation and establishes pregnancy [35]; <12> hepatic production of Ang-(1-7) is catalysed by ACE2 [65]; <13> the major role of ACE2 in Ang peptides metabolism is the production of Ang-(1-7). ACE2 also participates in the metabolism of other peptides non related to the renin-angiotensin system: apelin-13, neurotensin, kinetensin, dynorphin, [des-Arg9]-bradykinin, and [Lys-des-Arg9]-bradykinin [74]) (Reversibility: ?) [27,35,65,74]

P angiotensin-(1-7) + Phe

S Additional information <2,3,4,7,9,10,12,13> (<2> ACE2 is a crucial SARS-CoV receptor. SARS-CoV infections and the Spike protein of the SARS-CoV reduce ACE2 expression. Injection of SARS-CoV Spike into mice worsens acute lung failure in vivo that can be attenuated by blocking the renin-angiotensin pathway [33]; <7> angiotensin-converting enzyme 2: a functional receptor for SARS coronavirus [18]; <3> presence of ACE2 alone is not sufficient for maintaining viral infection. Other virus receptors or coreceptors may be required in different tissues [32]; <3> the enzyme has a function in blood pressure regulation, blood flow and fluid regulation. Loss of ACE2 impairs heart function [17]; <3> the enzyme is involved in diesease condition including hypertension, diabetes and cardiac function. ACE2 is the SARS virus receptor [16]; <9> ACE2 ectodomain shedding and/or sheddase(s) activation regulated by calmodulin is independent from the phorbol ester-induced shedding [68]; <13> ACE2 is down-regulated and ACE is up-regulated in hypertensive nephropathy. Ang II, once released, can act to up-regulate ACE but down-regulate ACE2 via the AT1 receptor-mediated mechanism. Activation of the ERK1/2 and p38 MAP kinase pathway may represent a key mechanism by which Ang II down-regulates ACE2 [64]; <9> ACE2 is involved in the regulation of heart function, ACE 2 is a functional receptor for the coro-

navirus that causes the severe acute respiratory syndrome [72]; <12> ACE2 plays a crucial role in liver fibrogenesis [71]; <13> ACE2 plays a key role in pulmonary, cardiovascular and hypertensive and diabetic kidney diseases. ACE2 plays a pivotal role in maintaining a balanced status of the RAS synergistically with ACE by exerting counter-regulatory effects [78]; <10> ACE2 plays a pivotal role in the central regulation of blood pressure and volume homeostasis [67]; <13> ACE2 plays a protective role in organs directly related to hypertension and associated diseases [73]; <13> the affinity for Ang-I is poor in comparison with ACE, therefore the conversion of Ang-I to Ang-(1-9) is not of physiological importance, except maybe under conditions in which ACE activity is inhibited [74]; <2,4> ACE2 activation promotes antithrombotic activity. ACE2 is an ACE, EC 3.4.15.1, homologue [93]; <3> ACE2 is a terminal carboxypeptidase and the receptor for the SARS and NL63 coronaviruses. Soluble sACE2 acts as receptor binding SARS-CoV glycoprotein S pseudo-typed FIV virus and blocks virus infection of target cells [84]) (Reversibility: ?) [16,17,18,32,33,64,67,68,71,72,73,74,78,84,93]

P ?

Substrates and products

S (7-methoxycoumarin-4-yl)-YVADAPK-(2,4-dinitrophenyl)-OH + H_2O <4> (Reversibility: ?) [38]

P (7-methoxycoumarin-4-yl)-YVADAP + N^6-(2,4-dinitrophenyl)-L-lysine

S (7-methoxycoumarin-4-yl)-acetyl-APK(2,4-dinitrophenyl) + H_2O <3> (Reversibility: ?) [49,53]

P (7-methoxycoumarin-4-yl)-acetyl-AP + N^6-(2,4-dinitrophenyl)-L-Lys

S (7-methoxycoumarin-4-yl)-acetyl-APK(2,4-dinitrophenyl)-OH + H_2O <4> (Reversibility: ?) [39]

P (7-methoxycoumarin-4-yl)-acetyl-AP + N^6-(2,4-dinitrophenyl)-L-Lys

S (7-methoxycoumarin-4-yl)-acetyl-Ala-Pro-Lys(2,4-dinitrophenyl) + H_2O <3> (Reversibility: ?) [52]

P (7-methoxycoumarin-4-yl)-acetyl-Ala-Pro + N^6-(2,4-dinitrophenyl)-L-Lys

S (7-methoxycoumarin-4-yl)-acetyl-Tyr-Val-Ala-Asp-Ala-Pro-Lys(2,4-dinitrophenyl)-OH + H_2O <3> (Reversibility: ?) [42]

P (7-methoxycoumarin-4-yl)-acetyl-Tyr-Val-Ala-Asp-Ala-Pro + N^6-(2,4-dinitrophenyl)-L-Lys

S (7-methoxycoumarin-4-yl)-acetyl-YVADAPK-(2,4-dinitrophenyl)-OH + H_2O <2,3> (Reversibility: ?) [38]

P (7-methoxycoumarin-4-yl)-acetyl-YVADAP + N^6-(2,4-dinitrophenyl)-L-Lys

S (7-methoxycoumarin-4-yl)acetyl-APK(2,4-dinitrophenyl) + H_2O <3,4,9> (Reversibility: ?) [22,58]

P (7-methoxycoumarin-4-yl)acetyl-AP + N^6-(2,4-dinitrophenyl)-L-lysine

S (7-methoxycoumarin-4-yl)acetyl-APK(2,4-dinitrophenyl)-OH + H_2O <9> (<9> synthetic fluorogenic substrate [2,8]) (Reversibility: ?) [2,8]

P (7-methoxycoumarin-4-yl)acetyl-AP + N^6-(2,4-dinitrophenyl)-L-lysine

S (7-methoxycoumarin-4-yl)acetyl-APK-(2,4-dinitrophenyl)-OH + H_2O <3> (Reversibility: ?) [85]
P ?
S (7-methoxycoumarin-4-yl)acetyl-APK-2,4-dinitrophenyl + H_2O <3> (Reversibility: ?) [24]
P (7-methoxycoumarin-4-yl)acetyl-AP + N^6-(2,4-dinitrophenyl)-L-lysine
S (7-methoxycoumarin-4-yl)acetyl-Ala-Pro-Lys(2,4-dinitrophenyl) + H_2O <3> (Reversibility: ?) [30,36]
P (7-methoxycoumarin-4-yl)acetyl-Ala-Pro + N^6-(2,4-dinitrophenyl)-L-lysine
S (7-methoxycoumarin-4-yl)acetyl-YVADAPK(2,4-dinitrophenyl)-OH + H_2O <9> (<9> synthetic fluorogenic caspase-1 substrate [8,9]) (Reversibility: ?) [8,9]
P (7-methoxycoumarin-4-yl)acetyl-YVADAP + N^6-(2,4-dinitrophenyl)-L-lysine
S (des-Arg9)-bradykinin + H_2O <3> (Reversibility: ?) [41]
P ?
S 7-methoxycoumarin-4-acetyl-Ala-Pro-Lys-(2,4-dinitrophenyl)-OH + H_2O <4> (Reversibility: ?) [82]
P ?
S 7-methoxycoumarin-4-acetyl-Arg-Pro-Pro-Gly-Phe-Ser-Ala-Phe-Lys-(2,4-dinitrophenyl)-OH + H_2O <2,4> (Reversibility: ?) [93]
P ?
S 7-methoxycoumarin-4-acetyl-Tyr-Val-Ala-Asp-Ala-Pro-Lys-(2,4-dinitrophenyl)-OH + H_2O <2,4> (Reversibility: ?) [93]
P ?
S KRPPGSPF + H_2O <9> (<9> i.e. Lys-des-Arg-bradykinin [8]) (Reversibility: ir) [8]
P KRPPGSP + Phe
S Lys-des-Arg9 bradykinin + H_2O <3> (Reversibility: ?) [16,17]
P KRPPGFSP + Phe
S Lys-des-Arg9-bradykinin + H_2O <2,4> (Reversibility: ?) [44]
P ?
S RPPGSPF + H_2O <9> (<9> i.e. des-Arg-bradykinin [1,8]) (Reversibility: ir) [1,8]
P RPPGSP + Phe (<9> i.e. des-Arg-bradykinin-(1-7) [1,8])
S SARS-coronavirus S_1 protein + H_2O <9,10,11,12> (Reversibility: ?) [63]
P ?
S TBC5046 + H_2O <9> (<9> synthetic fluorogenic peptide, i.e. des-Arg-bradykinin with N-terminal *o*-aminobenzoic acid and a 3-nitrophenylalanine instead of Phe at the C-terminus [1]) (Reversibility: ir) [1]
P *o*-aminobenzoic acid-des-Arg-bradykinin-(1-7) + 3-nitrophenylalanine
S YPVEPFI + H_2O <9> (<9> i.e. β-casomorphin [8]) (Reversibility: ir) [8]
P YPVEPF + Ile
S angiotensin I + H_2O <9> (Reversibility: ?) [95]
P angiotensin(1-9) + L-Phe

S angiotensin I + H_2O <2,3,4,8,9,10,13> (<9> C-terminal bond between His-Leu is cleaved [6]; <9> no angiotensin-converting activity, i.e. no conversion of the decapeptide angiotensin I to the octapeptide angiotensin II [3]; <9> wild-type and truncated mutant [7]; <4> ACE2 contributes to the production of angiotensin(1-7) from angiotensin I in proximal straight tubule [14]; <3> poor affinity [41]; <13> the affinity for Ang-I is poor in comparison with ACE, therefore the conversion of Ang-I to Ang-(1-9) is not of physiological importance, except maybe under conditions in which ACE activity is inhibited [74]) (Reversibility: ?) [1,2,3,4,5,6,7,8,9,10,11,14,15,16,17,41,43,44,45,46,50,53,57,69,74,78]

P angiotensin-(1-9) + Leu

S angiotensin II + H_2O <2,3,4,6,9> (<2,4> i.e. Asp-Arg-Val-Tyr-Ile-His-Pro-Phe [87,93]; <3> ACE2, a homologue of ACE, EC 3.4.15.1, converts angiotensin II into Ang(1-7). Ang(1-7) shows vasoprotective effects, serum autoantibodies to ACE2 predispose patients with connective tissue diseases to constrictive vasculopathy, pulmonary arterial hypertension, or persistent digital ischemia [85]; <2,4> angiotensin II has many adverse cardiovascular effects when acting through the AT1 receptor [93]; <4> high levels of angiotensin II induces pulmonary arterial hypertension [97]; <4> i.e. Asp-Arg-Val-Tyr-Ile-His-Pro-Phe, detection of myocardial ACE2 activity by surface enhanced laser desorption lionization time of flight mass spectroscopy, SELDI-TOF-MS [88]) (Reversibility: ?) [85,86,87,88,89,90,91,93,95,96,97]

P angiotensin(1-7) + L-Phe (<2> Ang(1-7) is a vasodilator peptide [89]; <9> Ang-(1-7) is a potential endogenous inhibitor of the classical renin-angiotensin system cascade [95]; <2,4> i.e. Asp-Arg-Val-Tyr-Ile-His-Pro [87,88,93])

S angiotensin II + H_2O <3> (<3> the enzyme is involved in the renin angiotensin system [81]) (Reversibility: ?) [81]

P angiotensin-(1-7) + L-Phe

S angiotensin II + H_2O <2,3,4,9,10,12,13> (<9> preferred substrate [4]; <3> efficient cleavage [41]; <9> 400fold higher activity than with angiotensin I [8]; <9> wild-type and truncated mutant [7]; <4> ACE2 is highly regulated at transcription. ACE2 plays a critical role in regulating the balance between vasoconstrictor and vasodilator effects within the RAS cascade. Angiotensin II may be a stimulus determining cardiac ACE2 gene expression, because either reduction in its levels or prevention of angiotensin II binding to the AT1 receptor increases ACE2 mRNA. ACE2 serves as the cellular entry point for severe acute respiratory syndrome (SARS) virus [27]; <3> the uteroplacental location of angiotensin (1-7) and ACE2 in pregnancy suggests an autocrine function of angiotensin(1-7) in the vasoactive regulation that characterizes placentation and establishes pregnancy [35]; <10> primary substrate [57]; <12> hepatic production of Ang-(1-7) is catalysed by ACE2 [65]; <13> the major role of ACE2 in Ang peptides metabolism is the production of Ang-(1-7). ACE2 also participates in the metabolism of other peptides non related to the renin-angiotensin system: apelin-13, neurotensin, kinetensin, dynorphin, [des-

Arg9]-bradykinin, and [Lys-des-Arg9]-bradykinin [74]; <13> ACE2 has approximately a 400fold greater affinity for Ang-II than Ang-I [74]) (Reversibility: ?) [2,4,7,8,15,16,17,22,26,27,35,37,38,39,40,41,42,43,44,45,46,47,49,50,51,52,53,54,55,56,57,58,59,61,62,65,69,74,78]

P angiotensin-(1-7) + Phe
S angiotensin IV + H_2O <3> (Reversibility: ?) [16]
P VYIHP + Phe
S angiotensin-(3-8) + H_2O <9> (Reversibility: ir) [2]
P angiotensin-(3-7) + Phe
S angiotensin-(4-8) + H_2O <9> (Reversibility: ir) [2]
P angiotensin-(4-7) + Phe
S angiotensin-(5-8) + H_2O <9> (Reversibility: ir) [2]
P angiotensin-(5-7) + Phe
S apelin-13 + H_2O <3,4> (Reversibility: ?) [16,17,46]
P QRPRLSHKGPMP + Phe
S apelin-13 + H_2O <9> (Reversibility: ?) [8]
P apelin-12 + Phe
S apelin-13 + H_2O <2,3,4> (<2,4> high catalytic efficiency [44]) (Reversibility: ?) [41,44]
P ?
S apelin-36 + H_2O <4,9> (Reversibility: ?) [8,46]
P apelin-35 + Phe
S apelin-36 + H_2O <2,3,4> (<2,4> high catalytic efficiency [44]) (Reversibility: ?) [16,17,44]
P ?
S β-casomorphin + H_2O <3> (Reversibility: ?) [16,17]
P YPFVEP + Ile
S β-casomorphin + H_2O <2,4> (Reversibility: ?) [44]
P ?
S casomorphin + H_2O <4> (Reversibility: ?) [46]
P ?
S des-Arg10-Lys-bradykinin + H_2O <4> (Reversibility: ?) [46]
P KRPPGFSP + Phe
S des-Arg9-bradykinin + H_2O <3> (Reversibility: ?) [16,17]
P RPPGFSP + Phe
S des-Arg9-bradykinin + H_2O <2,4> (Reversibility: ?) [44]
P ?
S des-Arg9-bradykinin + H_2O <4> (Reversibility: ?) [46]
P bradykinin (1-7) + Phe
S dynorphin A + H_2O <2,4> (Reversibility: ?) [44,46]
P ?
S dynorphin A 1-13 + H_2O <9> (Reversibility: ir) [8]
P dynorphin A 1-12 + Lys
S dynorphin A(1-13) + H_2O <3> (Reversibility: ?) [16,17]
P YGGFLRRIRPKL + Lys
S ghrelin + H_2O <3> (Reversibility: ?) [16]
P ?

S ghrelin + H_2O <9> (Reversibility: ir) [8]
P ghrelin minus C-terminal amino acid + arginine
S kinetensin + H_2O <4> (Reversibility: ?) [46]
P ?
S neocasomorphin + H_2O <9> (Reversibility: ir) [8]
P neocasomorphin minus C-terminal amino acid + isoleucine
S neurotensin + H_2O <2,4> (Reversibility: ?) [44]
P ?
S neurotensin 1-13 + H_2O <4> (Reversibility: ?) [46]
P ?
S neurotensin(1-11) + H_2O <3> (Reversibility: ?) [16]
P pELYENKPRRP + Tyr
S neurotensin(1-8) + H_2O <3> (Reversibility: ?) [16]
P pELYENKP + Arg
S neurotensin-(1-8) + H_2O <9> (Reversibility: ir) [8]
P neurotensin-(1-7) + arginine
S Additional information <2,3,4,7,9,10,12,13> (<2> ACE2 is a crucial SARS-CoV receptor. SARS-CoV infections and the Spike protein of the SARS-CoV reduce ACE2 expression. Injection of SARS-CoV Spike into mice worsens acute lung failure in vivo that can be attenuated by blocking the renin-angiotensin pathway [33]; <7> angiotensin-converting enzyme 2: a functional receptor for SARS coronavirus [18]; <3> presence of ACE2 alone is not sufficient for maintaining viral infection. Other virus receptors or coreceptors may be required in different tissues [32]; <3> the enzyme has a function in blood pressure regulation, blood flow and fluid regulation. Loss of ACE2 impairs heart function [17]; <3> the enzyme is involved in diesease condition including hypertension, diabetes and cardiac function. ACE2 is the SARS virus receptor [16]; <3> angiotensin I is not a good substrate for recombinant human ACE2 [26]; <3> no activity with angiotensin (1-9) and angiotensin(1-7) [15]; <3> no hydrolysis of angiotensin (1-9), angiotensin (1-7), bradikinin, bradykinin(1-7), neurotensin(1-13) [16]; <2,4> ACE2 functions as a carboxymonopeptidase with a preference for C-terminal Leu or Phe, ACE2 counterbalances the enzymatic actions of ACE, ACE2 does not metabolize bradykinin [44]; <3> the ACE2 ectodomain can be cleaved from the cell membrane and released into the extracellular milieu by stimulation of phorbol esters and ADAM17, calmodulin inhibits shedding of the ACE2 ectodomain from the membrane [53]; <9> ACE2 ectodomain shedding and/or sheddase(s) activation regulated by calmodulin is independent from the phorbol ester-induced shedding [68]; <13> ACE2 is down-regulated and ACE is up-regulated in hypertensive nephropathy. Ang II, once released, can act to up-regulate ACE but down-regulate ACE2 via the AT1 receptor-mediated mechanism. Activation of the ERK1/2 and p38 MAP kinase pathway may represent a key mechanism by which Ang II down-regulates ACE2 [64]; <9> ACE2 is involved in the regulation of heart function, ACE 2 is a functional receptor for the coronavirus that causes the severe acute respiratory syndrome [72]; <12> ACE2 plays a crucial role in liver fibrogenesis [71];

<13> ACE2 plays a key role in pulmonary, cardiovascular and hypertensive and diabetic kidney diseases. ACE2 plays a pivotal role in maintaining a balanced status of the RAS synergistically with ACE by exerting counter-regulatory effects [78]; <10> ACE2 plays a pivotal role in the central regulation of blood pressure and volume homeostasis [67]; <13> ACE2 plays a protective role in organs directly related to hypertension and associated diseases [73]; <13> the affinity for Ang-I is poor in comparison with ACE, therefore the conversion of Ang-I to Ang-(1-9) is not of physiological importance, except maybe under conditions in which ACE activity is inhibited [74]; <13> ACE2 functions predominantly as a carboxymonopeptidase with a substrate preference for hydrolysis between proline and a hydrophobic or basic C-terminal residue [78]; <13> hydrolyses its substrates by removing a single amino acid from their respective C-terminal [74]; <2,4> ACE2 activation promotes antithrombotic activity. ACE2 is an ACE, EC 3.4.15.1, homologue [93]; <3> ACE2 is a terminal carboxypeptidase and the receptor for the SARS and NL63 coronaviruses. Soluble sACE2 acts as receptor binding SARS-CoV glycoprotein S pseudotyped FIV virus and blocks virus infection of target cells [84]) (Reversibility: ?) [15,16,17,18,26,32,33,44,53,64,67,68,71,72,73,74,78,84,93]

P ?

Inhibitors

(2S)-3-(biphenyl-4-yl)-2-((3S)-2-mercapto-3-methylpentanamido)propanoic acid <3> [42]
(2S)-3-biphenyl-4-yl-2-[(2-methyl-2-sulfanylpropanoyl)amino]propanoic acid <3> [42]
(2S)-3-biphenyl-4-yl-2-[(2-sulfanylpropanoyl)amino]propanoic acid <3> [42]
(2S)-3-biphenyl-4-yl-2-[(sulfanylacetyl)amino]propanoic acid <3> [42]
(2S)-3-biphenyl-4-yl-2-[[(2R)-2-sulfanylbutanoyl]amino]propanoic acid <3> [42]
(2S)-3-biphenyl-4-yl-2-[[(2R)-3-methyl-2-sulfanylbutanoyl]amino]propanoic acid <3> [42]
(2S)-3-biphenyl-4-yl-2-[[(2R)-3-phenyl-2-sulfanylpropanoyl]amino]propanoic acid <3> [42]
(2S)-3-biphenyl-4-yl-2-[[(2S)-2-phenyl-2-sulfanylacetyl]amino]propanoic acid <3> [42]
(2S)-3-biphenyl-4-yl-2-[[(2S)-2-sulfanylhexanoyl]amino]propanoic acid <3> [42]
(2S)-3-biphenyl-4-yl-2-[[(2S)-3-phenyl-2-sulfanylpropanoyl]amino]propanoic acid <3> [42]
(2S)-3-biphenyl-4-yl-2-[[cyclobutyl(sulfanyl)acetyl]amino]propanoic acid <3> [42]
(S)-3-(biphenyl-4-yl)-2-((2R,3R)-2-mercapto-3-methylpentanamido)propanoic acid <3> [42]
(S)-3-(biphenyl-4-yl)-2-((R)-2-cyclohexyl-2-mercaptoacetamido)propanoic acid <3> [42]

(S)-3-(biphenyl-4-yl)-2-((R)-2-cyclopentyl-2-mercaptoacetamido)propanoic acid <3> [42]
(S)-3-(biphenyl-4-yl)-2-((R)-2-mercapto-3-(naphthalen-2-yl)propanamido)propanoic acid <3> [42]
(S)-3-(biphenyl-4-yl)-2-((R)-2-mercapto-4,4-dimethylpentanamido)propanoic acid <3> [42]
(S)-3-(biphenyl-4-yl)-2-((R)-2-mercapto-4-methylpentanamido)propanoic acid <3> [42]
(S)-3-(biphenyl-4-yl)-2-((R)-2-mercapto-4-phenylbutanamido)propanoic acid <3> [42]
(S)-3-(biphenyl-4-yl)-2-((R)-3-cyclohexyl-2-mercaptopropanamido)propanoic acid <3> [42]
(S,S)-2-[1-carboxy-2-[3-(3,5-dichlorobenzyl)-3H-imidazol-4-yl]-ethylamino]-4-methylpentanoic acid <3> (<3> MLN-4760 [41]) [41]
(S,S)-2-{1-carboxy-2-[3-(3,5-dichlorobenzyl)-3H-imidazol-4-yl]-ethylamino}-4-methylpentanoic acid <13> (<13> i.e MLN-4760 [72]) [72]
1,3,8-trihydroxy-6-methylanthraquinone <3> (<3> 1,3,8-trihydroxy-6-methylanthraquinone (emodin) blocks interaction between the SARS corona virus spike protein and its receptor angiotensin-converting enzyme 2, 94.12% inhibition at 0.05 mM [40]) [40]
1,4-bis-(1-anthraquinonylamino)-anthraquinone <3> (<3> slight inhibition [40]) [40]
1,8,dihydroxy-3-carboxyl-9,10-anthraquinone <3> (<3> 1,8,dihydroxy-3-carboxyl-9,10-anthraquinone (rhein) exhibits slight inhibition [40]) [40]
1N-08795 <3> (<3> 90% inhibition at 0.2 mM [58]) [58]
1N-26923 <3> (<3> 93% inhibition at 0.2 mM [58]) [58]
1N-27714 <3> (<3> 89% inhibition at 0.2 mM [58]) [58]
1N-28616 <3> (<3> 93% inhibition at 0.2 mM [58]) [58]
1S-90995 <3> (<3> 11% inhibition at 0.2 mM [58]) [58]
1S-91206 <3> (<3> 75% inhibition at 0.2 mM [58]) [58]
2-[(2-carboxy-3-phenyl-propyl)-hydroxy-phosphinoyl]-pyrrolidine-1-carboxylic acid benzyl ester <3> [61]
2-[(2-carboxy-4-methyl-pentyl)-hydroxy-phosphinoyl]-pyrrolidine-1-carboxylic acid benzyl ester <3> [61]
2-[(2-carboxy-propyl)-hydroxy-phosphinoyl]-pyrrolidine-1-carboxylic acid benzyl ester <3> [61]
2-benzyl-3-(hydroxy-pyrrolidin-2-yl-phosphinoyl)-propionic acid <3> [61]
2-benzyl-3-[(1-benzyloxycarbonylamino-2-phenyl-ethyl)-hydroxy-phosphinoyl]-propionic acid <3> [61]
2-benzyl-3-[(1-benzyloxycarbonylamino-3-methyl-butyl)-hydroxy-phosphinoyl]-propionic acid <3> [61]
2-benzyl-3-[(1-benzyloxycarbonylamino-ethyl)-hydroxy-phosphinoyl]-propionic acid <3> [61]
2-methylphenyl-benzylsuccinic acid <9> [6]
3,4-dimethylphenyl-benzylsuccinic acid <9> [6]
3,5-dichloro-benzylsuccinate <9> [6]
3,5-dimethylphenyl-benzylsuccinic acid <9> [6]

3-([1-[2-acetylamino-3-(1H-imidazol-4-yl)-propionyl]-pyrrolidin-2-yl]-hydroxy-phosphinoyl)-2-(3-phenyl-isoxazol-5-ylmethyl)-propionic acid <3> [61]
3-([1-[2-acetylamino-3-(1H-imidazol-4-yl)-propionyl]-pyrrolidin-2-yl]-hydroxy-phosphinoyl)-2-benzyl-propionic acid <3> [61]
3-([1-[2-acetylamino-3-(1H-imidazol-4-yl)-propionylamino]-3-methyl-butyl]-hydroxy-phosphinoyl)-2-(3-phenyl-isoxazol-5-ylmethyl)-propionic acid <3> [61]
3-([1-[2-acetylamino-3-(1H-imidazol-4-yl)-propionylamino]-3-methyl-butyl]-hydroxy-phosphinoyl)-2-benzyl-propionic acid <3> [61]
3-([1-[2-acetylamino-3-(4-hydroxy-phenyl)-propionyl]-pyrrolidin-2-yl]-hydroxy-phosphinoyl)-2-benzyl-propionic acid <3> [61]
3-[(1-amino-2-phenyl-ethyl)-hydroxy-phosphinoyl]-2-benzylpropionic acid <3> [61]
3-[(1-amino-3-methyl-butyl)-hydroxy-phosphinoyl]-2-benzylpropionic acid <3> [61]
3-[(1-amino-ethyl)-hydroxy-phosphinoyl]-2-benzyl-propionic acid <3> [61]
3-[[1-(2-acetylamino-3-methyl-butyryl)-pyrrolidin-2-yl]-hydroxy-phosphinoyl]-2-benzyl-propionic acid <3> [61]
3-[[1-(2-acetylamino-3-phenyl-propionyl)-pyrrolidin-2-yl]-hydroxy-phosphinoyl]-2-benzyl-propionic acid <3> [61]
3-[[1-(2-acetylamino-4-methyl-pentanoyl)-pyrrolidin-2-yl]-hydroxy-phosphinoyl]-2-(3-phenyl-isoxazol-5-ylmethyl)-propionic acid <3> [61]
3-[[1-(2-acetylamino-4-methyl-pentanoyl)-pyrrolidin-2-yl]-hydroxy-phosphinoyl]-2-benzyl-propionic acid <3> [61]
3-[[1-(2-acetylamino-4-methyl-pentanoylamino)-2-phenylethyl]-hydroxy-phosphinoyl]-2-benzyl-propionic acid <3> [61]
3-[[1-(2-acetylamino-6-amino-hexanoyl)-pyrrolidin-2-yl]-hydroxy-phosphinoyl]-2-benzyl-propionic acid <3> [61]
3-[[1-(2-acetylamino-propionyl)-pyrrolidin-2-yl]-hydroxyphosphinoyl]-2-benzyl-propionic acid <3> [61]
3-methylphenyl-benzylsuccinic acid <9> [6]
3S-95223 <3> (<3> 40% inhibition at 0.2 mM [58]) [58]
4-acetylamino-5-[2-[(2-carboxy-3-phenyl-propyl)-hydroxyphosphinoyl]-pyrrolidin-1-yl]-5-oxo-pentanoic acid <3> [61]
4-methylphenyl-benzylsuccinic acid <9> [6]
4-nitrophenyl-benzylsuccinic acid <9> [6]
4S-14713 <3> (<3> 70% inhibition at 0.2 mM [58]) [58]
4S-16659 <3> (<3> 76% inhibition at 0.2 mM [58]) [58]
5,7-dihydroxyflavone <3> (<3> 5,7-dihydroxyflavone (chrysin) is a weak inhibitor [40]) [40]
5115980 <3> (<3> 1% inhibition at 0.2 mM [58]) [58]
7490938 <3> (<3> 20% inhibition at 0.2 mM [58]) [58]
7850455 <3> (<3> 20% inhibition at 0.2 mM [58]) [58]
7857351 <3> (<3> 27% inhibition at 0.2 mM [58]) [58]
7870029 <3> (<3> 11% inhibition at 0.2 mM [58]) [58]
Ac-GDYSHCSPLRYYPWWKCTYPDPEGGG-NH_2 <9> (<9> strong inhibition, most potent inhibitory peptide, i.e. DX600 [9]) [9]

Ac-GDYSHCSPLRYYPWWPDPEGGG-NH_2 <3> (<3> i.e. DX600 [91]) [91]
Cl^- <9> (<9> inhibition is substrate dependent, inhibitory with substrate angiotensin II [2]; <9> ACE2 activity is regulated by chloride ions. The presence of chloride increases the hydrolysis of angiotensin I by ACE2, but inhibits cleavage of the vasoconstrictor angiotensin II [69]) [2,69]
Cu^{2+} <3> (<3> 69% inhibition at 0.01 mM [52]) [52]
DX600 <2,3,4> (<2> 0.01 mM, 99% inhibition [51]; <3> IC50: 10 nM [16]; <2,3,4> competitive inhibitor, 0.1 mM [38]; <2> a decrease in thrombus ACE2 activity is associated with increased thrombus formation in nude mice [93]; <4> a decrease in thrombus ACE2 activity is associated with increased thrombus formation in spontaneously hypertensive rats [93]) [16,38,41,44,51,93,97]
EDTA <2,9> (<2> complete inhibition at 10 mM [51]; <9> no inhibition by benzylsuccinate, no inhibition by lisinopril, no inhibition by captopril, no inhibition by enalaprilat [7]) [7,51]
Ile-Pro-Pro <5> (<5> inhibits EC 3.4.15.1 at one-thousandth of the concentration needed to inhibit ACE2 [75]) [75]
Leu-Pro-Pro <5> (<5> inhibits EC 3.4.15.1 at one-thousandth of the concentration needed to inhibit ACE2 [75]) [75]
MLN 4760 <2,3> (<2,3> IC50: 3 nM [26]) [26]
MLN-4760 <2,3,4,9> (<3> 0.01 mM [49]; <4> 0.001 mM [37]; <3> 0.0001 mM [52]; <3> i.e. (SS) 2-[(1)-carboxy-2-[3-(3,5-dichlorobenzyl)-3H-imidazol-4-yl]ethylamino]-4-methyl-pentanoic acid, IC50: 0.44 nM [16]; <4> specific inhibitor, 1 mM [39]; <2> total inhibition at 0.01 mM [50]; <9> ACE2-specific inhibitor. Inhibition of wild-type ACE2 was sensitive to chloride concentration [69]; <9> i.e. ((S,S)-2-[1-carboxy-2-[3-(3,5-dichlorobenzyl)-3H-imidazol4-yl]-ethylamino]-4-methylpentanoic acid) [72]) [16,37,39,49,50,52,56,59,69,72,82]
MLN4760 <3> [30]
N-[(1S)-1-carboxy-3-methylbutyl]-3-(3,5-dichlorobenzyl)-L-histidine <9> (<9> enzyme-specific inhibitor [4]) [4]
N-[(1S)-1-carboxy-3-methylbutyl]-3-(3,5-dichlorophenyl)-L-histidine <1> (<1> i.e. C_{16}, a ACE2 specific inhibitor [83]) [83]
Pro-Phe <3> (<3> IC50: 0.15 mM [16]) [16,41]
T0507-4963 <3> (<3> 41% inhibition at 0.2 mM [58]) [58]
T0513-5544 <3> (<3> 4% inhibition at 0.2 mM [58]) [58]
T0515-3007 <3> (<3> 13% inhibition at 0.2 mM [58]) [58]
Val-Pro-Pro <5> (<5> inhibits EC 3.4.15.1 at one-thousandth of the concentration needed to inhibit ACE2 [75]) [75]
angiotensin I <3,9> [6,16]
angiotensin II C-terminal analogs <3> (<3> screening of a library of angiotensin II C-terminal analogs identifies a number of tetrapeptides with increased ACE2 inhibition, and identifies residues critical to the binding of angiotensin II to the active site of ACE2 [81]) [81]
anthraquinone <3> (<3> slight inhibition [40]) [40]
benzylsuccinate <2> (<2> essentially abolishes the formation of Ang(1-9) by ACE2 [50]) [50]
benzylsuccinic acid <9> [6]

cyclohexyl-benzylsuccinic acid <9> [6]
dicyclohexyl-benzylsuccinic acid <9> [6]
phenylbenzylsuccinic acid <9> [6]
telmisartan <2> (<2> specific angiotensin II type 1 receptor blocker [56]) [56]
Additional information <2,3,4,9> (<9> no inhibition by captopril [3]; <9> construction of 6 constrained peptide libraries, selected from peptide libraries displayed on phage, peptides, 21-27 amino acids, with inhibitory effects on the enzyme, specificity and stability, selection of inhibitory sequence motifs, best CXPXRXXPWXXC, overview [9]; <9> no inhibition by enalaprilat [4]; <9> no inhibition by lisinopril [2]; <9> no inhibition by lisinopril, no inhibition by captopril, no inhibition by enalaprilat [6]; <4> rampiril does not influence the mRNA content in renal tubules [5]; <3> carboxylalkyl compounds cilazaprilat, indolaprilat, perindoprilat, quinaprilat and spiraprilat, the thiol compounds rentiapril and zofenapril, and the phosphoryl compounds ceranopril and fosinoprilat fail to inhibit the hydrolysis of either angiotensin I or angiotensin II by ACE2 at concentrations that abolished activity of EC 3.4.15.1 [15]; <2,3,4> ACE-2 mRNA and activity are severely downregulated in lung fibrosis [38]; <3> GM6001 does not have any effect on the activity of ACE2 and little effect on basal shedding of ACE2 [53]; <3> not inhibited by Ca^{2+}, Cd^{2+}, Co^{2+}, Mg^{2+}, Mn^{2+}, and Zn^{2+} [52]; <3> not inhibited by captopri and lisinopril [41]; <2> not inhibited by captopril and benzyloxycarbonyl-Pro-Pro [51]; <3> not inhibited by rentiapril, ceranopril, indolaprilat, zofenoprilat, spiraprilat, quinaprilat, perindoprilat, fosinoprilat, cilazaprilat, captopril, lisinopril, and enalaprilat [58]; <2> the Spike protein of the SARS-coronavirus reduces ACE2 expression [47]; <4> ACE2 is insensitive to ACE inhibitors [87]; <2> central angiotensin II type 1 receptors reduce ACE2 expression/activity in hypertensive mice [89]; <4> chronic cigarette smoke administration causes an reduction in ACE2 activity and increases angiotensin II levels in the lung [97]) [2,3,4,5,6,9,15,38,41,47,51,52,53,58,87,89,97]

Activating compounds

8-[[2-(dimethylamino)ethyl]amino]-5-(hydroxymethyl <12> (<12> enhances ACE2 activity in a dose-dependent manner and causes considerable reductions in blood pressure and a striking reversal of cardiac and renal fibrosis in the spontaneously hypertensive rat model of hypertension [70]) [70]
XNT <2,4> (<2> activates ACE2, reduces platelet attachment to injured vessels, reduces thrombus size, and prolonges the time for complete vessel occlusion in mice. Thrombus area is reduced by 60%, whereas time for thrombus formation is prolonged by 45% in XNT-treated mice [93]; <4> treatment at 10 mg/kg resultes in a 30% attenuation of thrombus formation in the SHR [93]) [93]
all-trans retinoic acid <6> [48]
losartan <2,4> (<4> a specific angiotensin II receptor antagonist, is a well-known antihypertensive drug with a potential role in positively regulating ACE2 in the lung [97]; <2> an angiotensin II type 1 receptor blocker, in-

creases central ACE2 activity. Losartan also restores brain ACE2 activity in transgenic RA mice, overview [89]) [89,97]
resorcinolnaphthalein <12> (<12> enhances ACE2 activity in a dose-dependent manner [70]) [70]
Additional information <2> (<2> no activation by PD123319, an angiotensin II type 2 antagonist [89]) [89]

Metals, ions

Cl^- <9> (<9> binding ligands are Tyr207 and Arg514, possible model for chloride activation, effect is substrate dependent: activation with angiotensin I and (7-methoxycoumarin-4-yl)acetyl-APK(2,4-dinitrophenyl)-OH, inhibition with angiotensin II [2]; <9> enhances activity by about 10fold [8]; <9> required, highest activity at 1.5 M NaCl [1]; <9> ACE2 activity is regulated by chloride ions. The presence of chloride increases the hydrolysis of angiotensin I by ACE2, but inhibits cleavage of the vasoconstrictor angiotensin II [69]) [1,2,8,69]
F^- <9> (<9> enhances activity by about 10fold [8]) [8]
Zinc <3> (<3> zinc carboxypeptidase [81]) [81]
Zn^{2+} <2,3,4,9,10,12,13> (<10,12,13> metallopeptidase [74]; <9,12> zinc metalloprotease [77]; <3> dependent [41]; <9> contains zinc-binding consensus sequence HEXXH, amino acids 374-378, zinc-binding protease [6]; <9> zinc-binding motif HEXXH and third zinc ligand glutamate402, contains zinc-binding consensus sequence HEXXH, amino acids 374-378, zinc-binding protease [7]; <9> zinc-binding motif HEXXH and third zinc ligand glutamate402, zinc-binding protease [2]) [2,6,7,41,74,77,82,93]
Additional information <9> (<9> metalloprotease [3]; <9> no effect of Br^- [8]) [3,8]

Turnover number (s^{-1})

2 <9> (angiotensin I, <9> pH 6.5, room temperature [6,8]) [6,8]
2.9 <3> (angiotensin I, <3> 37°C, pH 7.4 [15]) [15]
12.8 <3> (angiotensin II, <3> 37°C, pH 7.4 [15]) [15]
84 <9> (angiotensin 4-8, <9> pH 7.4, 37°C [2]) [2]
162 <9> (angiotensin 3-8, <9> pH 7.4, 37°C [2]) [2]
1110 <9> (angiotensin II, <9> pH 7.4, 37°C [2]) [2]
1518 <9> (angiotensin 5-8, <9> pH 7.4, 37°C [2]) [2]
6840 <9> ((7-methoxycoumarin-4-yl)acetyl-APK(2,4-dinitrophenyl)-OH, <9> pH 6.5, room temperature [8]) [8]

K_m-Value (mM)

0.005 <9> (angiotensin II, <9> pH 7.4, 37°C [2]) [2]
0.0057 <3> (angiotensin II, <3> 37°C, pH 7.4 [15]) [15]
0.0069 <9> (angiotensin I) [6]
0.0091 <9> (angiotensin 3-8, <9> pH 7.4, 37°C [2]) [2]
0.0126 <9> (angiotensin 4-8, <9> pH 7.4, 37°C [2]) [2]
0.0245 <9> (angiotensin 5-8, <9> pH 7.4, 37°C [2]) [2]
0.053 <9> (angiotensin II, <9> pH 7.4, 37°C, mutant enzyme R514Q [69]) [69]

0.0586 <9> (angiotensin II, <9> pH 7.4, 37°C, wild-type enzyme [69]) [69]
0.0868 <3> (angiotensin I, <3> 37°C, pH 7.4 [15]) [15]
0.147 <9> ((7-methoxycoumarin-4-yl)acetyl-APK(2,4-dinitrophenyl)-OH, <9> pH 6.5, room temperature [8]) [8]

K_i-Value (mM)

0.00000035 <3> (3-[[1-(2-acetylamino-3-methyl-butyryl)-pyrrolidin-2-yl]-hydroxy-phosphinoyl]-2-benzyl-propionic acid) [61]
0.0000004 <3> (3-([1-[2-acetylamino-3-(1H-imidazol-4-yl)-propionyl]-pyrrolidin-2-yl]-hydroxy-phosphinoyl)-2-(3-phenyl-isoxazol-5-ylmethyl)-propionic acid) [61]
0.00000125 <3> (3-[[1-(2-acetylamino-4-methyl-pentanoyl)-pyrrolidin-2-yl]-hydroxy-phosphinoyl]-2-(3-phenyl-isoxazol-5-ylmethyl)-propionic acid) [61]
0.0000014 <3> ((2S)-3-biphenyl-4-yl-2-[[(2R)-2-sulfanylbutanoyl]amino]propanoic acid, <3> apparent value, in (7-methoxycoumarin-4-yl)-acetyl-Tyr-Val-Ala-Asp-Ala-Pro-Lys(2,4-dinitrophenyl)-OH as substrate in 0.001 mM $Zn(OAc)_2$, 0.1 mM TCEP, 50 mM HEPES, 0.3 mM CHAPS, and 300 mM NaCl, at pH 7.5 [42]) [42]
0.0000014 <3> ((S)-3-(biphenyl-4-yl)-2-((R)-2-mercapto-4-methylpentanamido)propanoic acid, <3> apparent value, in (7-methoxycoumarin-4-yl)-acetyl-Tyr-Val-Ala-Asp-Ala-Pro-Lys(2,4-dinitrophenyl)-OH as substrate in 0.001 mM $Zn(OAc)_2$, 0.1 mM TCEP, 50 mM HEPES, 0.3 mM CHAPS, and 300 mM NaCl, at pH 7.5 [42]) [42]
0.0000015 <3> ((2S)-3-(biphenyl-4-yl)-2-((3S)-2-mercapto-3-methylpentanamido)propanoic acid, <3> apparent value, in (7-methoxycoumarin-4-yl)-acetyl-Tyr-Val-Ala-Asp-Ala-Pro-Lys(2,4-dinitrophenyl)-OH as substrate in 0.001 mM $Zn(OAc)_2$, 0.1 mM TCEP, 50 mM HEPES, 0.3 mM CHAPS, and 300 mM NaCl, at pH 7.5 [42]) [42]
0.0000015 <3> ((2S)-3-biphenyl-4-yl-2-[[(2R)-3-methyl-2-sulfanylbutanoyl]amino]propanoic acid, <3> apparent value, in (7-methoxycoumarin-4-yl)-acetyl-Tyr-Val-Ala-Asp-Ala-Pro-Lys(2,4-dinitrophenyl)-OH as substrate in 0.001 mM $Zn(OAc)_2$, 0.1 mM TCEP, 50 mM HEPES, 0.3 mM CHAPS, and 300 mM NaCl, at pH 7.5 [42]) [42]
0.0000016 <3> ((S)-3-(biphenyl-4-yl)-2-((2R,3R)-2-mercapto-3-methylpentanamido)propanoic acid, <3> apparent value, in (7-methoxycoumarin-4-yl)-acetyl-Tyr-Val-Ala-Asp-Ala-Pro-Lys(2,4-dinitrophenyl)-OH as substrate in 0.001 mM $Zn(OAc)_2$, 0.1 mM TCEP, 50 mM HEPES, 0.3 mM CHAPS, and 300 mM NaCl, at pH 7.5 [42]) [42]
0.0000018 <3> ((2S)-3-biphenyl-4-yl-2-[[(2S)-2-sulfanylhexanoyl]amino]propanoic acid, <3> apparent value, in (7-methoxycoumarin-4-yl)-acetyl-Tyr-Val-Ala-Asp-Ala-Pro-Lys(2,4-dinitrophenyl)-OH as substrate in 0.001 mM $Zn(OAc)_2$, 0.1 mM TCEP, 50 mM HEPES, 0.3 mM CHAPS, and 300 mM NaCl, at pH 7.5 [42]) [42]
0.0000018 <3> ((S)-3-(biphenyl-4-yl)-2-((R)-2-cyclopentyl-2-mercaptoacetamido)propanoic acid, <3> apparent value, in (7-methoxycoumarin-4-yl)-acetyl-Tyr-Val-Ala-Asp-Ala-Pro-Lys(2,4-dinitrophenyl)-OH as substrate in

0.001 mM $Zn(OAc)_2$, 0.1 mM TCEP, 50 mM HEPES, 0.3 mM CHAPS, and 300 mM NaCl, at pH 7.5 [42]) [42]
0.0000021 <3> (3-([1-[2-acetylamino-3-(1H-imidazol-4-yl)-propionyl]-pyrrolidin-2-yl]-hydroxy-phosphinoyl)-2-benzyl-propionic acid) [61]
0.0000024 <3> ((2S)-3-biphenyl-4-yl-2-[[cyclobutyl(sulfanyl)acetyl]amino]-propanoic acid, <3> apparent value, in (7-methoxycoumarin-4-yl)-acetyl-Tyr-Val-Ala-Asp-Ala-Pro-Lys(2,4-dinitrophenyl)-OH as substrate in 0.001 mM $Zn(OAc)_2$, 0.1 mM TCEP, 50 mM HEPES, 0.3 mM CHAPS, and 300 mM NaCl, at pH 7.5 [42]) [42]
0.0000028 <3> (DX600) [16]
0.0000052 <3> (3-([1-[2-acetylamino-3-(4-hydroxy-phenyl)-propionyl]-pyrrolidin-2-yl]-hydroxy-phosphinoyl)-2-benzyl-propionic acid) [61]
0.0000052 <3> (3-[[1-(2-acetylamino-3-phenyl-propionyl)-pyrrolidin-2-yl]-hydroxy-phosphinoyl]-2-benzyl-propionic acid) [61]
0.0000065 <3> (3-[[1-(2-acetylamino-6-amino-hexanoyl)-pyrrolidin-2-yl]-hydroxy-phosphinoyl]-2-benzyl-propionic acid) [61]
0.0000066 <3> (3-[[1-(2-acetylamino-4-methyl-pentanoyl)-pyrrolidin-2-yl]-hydroxy-phosphinoyl]-2-benzyl-propionic acid) [61]
0.0000069 <3> ((2S)-3-biphenyl-4-yl-2-[(2-sulfanylpropanoyl)amino]propanoic acid, <3> apparent value, in (7-methoxycoumarin-4-yl)-acetyl-Tyr-Val-Ala-Asp-Ala-Pro-Lys(2,4-dinitrophenyl)-OH as substrate in 0.001 mM $Zn(OAc)_2$, 0.1 mM TCEP, 50 mM HEPES, 0.3 mM CHAPS, and 300 mM NaCl, at pH 7.5 [42]) [42]
0.000007 <3> (4-acetylamino-5-[2-[(2-carboxy-3-phenyl-propyl)-hydroxy-phosphinoyl]-pyrrolidin-1-yl]-5-oxo-pentanoic acid) [61]
0.0000071 <3> ((S)-3-(biphenyl-4-yl)-2-((R)-2-mercapto-4,4-dimethylpentanamido)propanoic acid, <3> apparent value, in (7-methoxycoumarin-4-yl)-acetyl-Tyr-Val-Ala-Asp-Ala-Pro-Lys(2,4-dinitrophenyl)-OH as substrate in 0.001 mM $Zn(OAc)_2$, 0.1 mM TCEP, 50 mM HEPES, 0.3 mM CHAPS, and 300 mM NaCl, at pH 7.5 [42]) [42]
0.0000075 <3> (3-[[1-(2-acetylamino-propionyl)-pyrrolidin-2-yl]-hydroxy-phosphinoyl]-2-benzyl-propionic acid) [61]
0.000044 <3> ((S,S)-2-[1-carboxy-2-[3-(3,5-dichlorobenzyl)-^{3}H-inidazol-4-yl]-ethylamino]-4-methylpentanoic acid) [41]
0.000065 <3> ((S)-3-(biphenyl-4-yl)-2-((R)-2-cyclohexyl-2-mercaptoacetamido)propanoic acid, <3> apparent value, in (7-methoxycoumarin-4-yl)-acetyl-Tyr-Val-Ala-Asp-Ala-Pro-Lys(2,4-dinitrophenyl)-OH as substrate in 0.001 mM $Zn(OAc)_2$, 0.1 mM TCEP, 50 mM HEPES, 0.3 mM CHAPS, and 300 mM NaCl, at pH 7.5 [42]) [42]
0.000084 <3> ((2S)-3-biphenyl-4-yl-2-[[(2S)-2-phenyl-2-sulfanylacetyl]amino]propanoic acid, <3> apparent value, in (7-methoxycoumarin-4-yl)-acetyl-Tyr-Val-Ala-Asp-Ala-Pro-Lys(2,4-dinitrophenyl)-OH as substrate in 0.001 mM $Zn(OAc)_2$, 0.1 mM TCEP, 50 mM HEPES, 0.3 mM CHAPS, and 300 mM NaCl, at pH 7.5 [42]) [42]
0.000086 <3> ((2S)-3-biphenyl-4-yl-2-[[(2R)-3-phenyl-2-sulfanylpropanoyl]amino]propanoic acid, <3> apparent value, in (7-methoxycoumarin-4-yl)-acetyl-Tyr-Val-Ala-Asp-Ala-Pro-Lys(2,4-dinitrophenyl)-OH as substrate in

0.001 mM $Zn(OAc)_2$, 0.1 mM TCEP, 50 mM HEPES, 0.3 mM CHAPS, and 300 mM NaCl, at pH 7.5 [42]) [42]
0.00022 <3> (3-([1-[2-acetylamino-3-(1H-imidazol-4-yl)-propionylamino]-3-methyl-butyl]-hydroxy-phosphinoyl)-2-(3-phenyl-isoxazol-5-ylmethyl)-propionic acid) [61]
0.0003 <3> (2-[(2-carboxy-3-phenyl-propyl)-hydroxy-phosphinoyl]-pyrrolidine-1-carboxylic acid benzyl ester) [61]
0.00032 <3> ((2S)-3-biphenyl-4-yl-2-[(sulfanylacetyl)amino]propanoic acid, <3> apparent value, in (7-methoxycoumarin-4-yl)-acetyl-Tyr-Val-Ala-Asp-Ala-Pro-Lys(2,4-dinitrophenyl)-OH as substrate in 0.001 mM $Zn(OAc)_2$, 0.1 mM TCEP, 50 mM HEPES, 0.3 mM CHAPS, and 300 mM NaCl, at pH 7.5 [42]) [42]
0.00042 <3> ((S)-3-(biphenyl-4-yl)-2-((R)-3-cyclohexyl-2-mercaptopropanamido)propanoic acid, <3> apparent value, in (7-methoxycoumarin-4-yl)-acetyl-Tyr-Val-Ala-Asp-Ala-Pro-Lys(2,4-dinitrophenyl)-OH as substrate in 0.001 mM $Zn(OAc)_2$, 0.1 mM TCEP, 50 mM HEPES, 0.3 mM CHAPS, and 300 mM NaCl, at pH 7.5 [42]) [42]
0.00055 <3> ((S)-3-(biphenyl-4-yl)-2-((R)-2-mercapto-3-(naphthalen-2-yl)-propanamido)propanoic acid, <3> apparent value, in (7-methoxycoumarin-4-yl)-acetyl-Tyr-Val-Ala-Asp-Ala-Pro-Lys(2,4-dinitrophenyl)-OH as substrate in 0.001 mM $Zn(OAc)_2$, 0.1 mM TCEP, 50 mM HEPES, 0.3 mM CHAPS, and 300 mM NaCl, at pH 7.5 [42]) [42]
0.0008 <3> (3-([1-[2-acetylamino-3-(1H-imidazol-4-yl)-propionylamino]-3-methyl-butyl]-hydroxy-phosphinoyl)-2-benzyl-propionic acid) [61]
0.00086 <3> ((S)-3-(biphenyl-4-yl)-2-((R)-2-mercapto-4-phenylbutanamido)-propanoic acid, <3> apparent value, in (7-methoxycoumarin-4-yl)-acetyl-Tyr-Val-Ala-Asp-Ala-Pro-Lys(2,4-dinitrophenyl)-OH as substrate in 0.001 mM $Zn(OAc)_2$, 0.1 mM TCEP, 50 mM HEPES, 0.3 mM CHAPS, and 300 mM NaCl, at pH 7.5 [42]) [42]
0.00092 <3> (3-[[1-(2-acetylamino-4-methyl-pentanoylamino)-2-phenylethyl]-hydroxy-phosphinoyl]-2-benzyl-propionic acid) [61]
0.0014 <3> ((2S)-3-biphenyl-4-yl-2-[[(2S)-3-phenyl-2-sulfanylpropanoyl]amino]propanoic acid, <3> apparent value, in (7-methoxycoumarin-4-yl)-acetyl-Tyr-Val-Ala-Asp-Ala-Pro-Lys(2,4-dinitrophenyl)-OH as substrate in 0.001 mM $Zn(OAc)_2$, 0.1 mM TCEP, 50 mM HEPES, 0.3 mM CHAPS, and 300 mM NaCl, at pH 7.5 [42]) [42]
0.0022 <3,9> (angiotensin I) [6,16]
0.0023 <3> ((2S)-3-biphenyl-4-yl-2-[(2-methyl-2-sulfanylpropanoyl)amino]-propanoic acid, <3> apparent value, in (7-methoxycoumarin-4-yl)-acetyl-Tyr-Val-Ala-Asp-Ala-Pro-Lys(2,4-dinitrophenyl)-OH as substrate in 0.001 mM $Zn(OAc)_2$, 0.1 mM TCEP, 50 mM HEPES, 0.3 mM CHAPS, and 300 mM NaCl, at pH 7.5 [42]) [42]
0.0028 <9> (Ac-GDYSHCSPLRYYPWWKCTYPDPEGGG-NH_2, <9> pH 8.0, room temperature with substrate angiotensin I, pH 7.4, room temperature with substrate (7-methoxycoumarin-4-yl)acetyl-YVADAPK(2,4-dinitrophenyl)-OH [9]) [9]

0.003 <3> (2-[(2-carboxy-4-methyl-pentyl)-hydroxy-phosphinoyl]-pyrrolidine-1-carboxylic acid benzyl ester) [61]
0.003 <3> (2-[(2-carboxy-propyl)-hydroxy-phosphinoyl]-pyrrolidine-1-carboxylic acid benzyl ester) [61]
0.008 <3> (2-benzyl-3-[(1-benzyloxycarbonylamino-3-methyl-butyl)-hydroxy-phosphinoyl]-propionic acid) [61]
0.01 <3> (2-benzyl-3-(hydroxy-pyrrolidin-2-yl-phosphinoyl)-propionic acid, <3> K_i above 0.01 mM [61]) [61]
0.01 <3> (2-benzyl-3-[(1-benzyloxycarbonylamino-2-phenyl-ethyl)-hydroxy-phosphinoyl]-propionic acid, <3> Ki above 0.01 mM [61]) [61]
0.01 <3> (2-benzyl-3-[(1-benzyloxycarbonylamino-ethyl)-hydroxy-phosphinoyl]-propionic acid, <3> K_i above 0.01 mM [61]) [61]
0.01 <3> (3-[(1-amino-2-phenyl-ethyl)-hydroxy-phosphinoyl]-2-benzylpropionic acid, <3> K_i above 0.01 mM [61]) [61]
0.01 <3> (3-[(1-amino-3-methyl-butyl)-hydroxy-phosphinoyl]-2-benzylpropionic acid, <3> K_i above 0.01 mM [61]) [61]
0.01 <3> (3-[(1-amino-ethyl)-hydroxy-phosphinoyl]-2-benzyl-propionic acid, <3> K_i above 0.01 mM [61]) [61]
Additional information <9> (<9> K_i values of peptides from constrained peptide libraries [9]) [9]

pH-Optimum

6.5 <9> [8]
7 <4,9> (<4> assay at [82]) [1,82]
7.4 <1,9> (<1,9> assay at [7,83]) [7,83]
7.5 <2,4> (<2,4> assay at [93]) [93]
8 <9> (<9> assay at [9]) [9]

pH-Range

4.5-8 <9> (<9> activity drops sharply at pH 8.0, substantial activity at pH 4.5-6.5, inactive at pH 9.0 [1]) [1]

Temperature optimum (°C)

22 <9> (<9> room temperature, assay at [8]) [8]
37 <1,9> (<1,9> assay at [1,2,7,83]) [1,2,7,83]
42 <4> (<4> assay at [82]) [82]

4 Enzyme Structure

Molecular weight

27000 <2> (<2> SDS-PAGE [41]) [41]
42000 <11> (<11> His-tagged ACE219-367, SDS-PAGE [63]) [63]
80000 <4> (<4> SDS-PAGE [37]) [37]
89600 <9> (<9> recombinant enzyme, MALDI-TOF mass spectrometry [8]) [8]
90000 <9> (<9> recombinant His-tagged enzyme, SDS-PAGE [43]) [43]
92000 <4> (<4> SDS-PAGE [54]) [54]
92460 <9> (<9> DNA sequence determination [7]) [7]

Subunits

Additional information <1,2,3> (<2> ACE2 is a type I membrane-anchored protein with a catalytically active ectodomain, that undergoes shedding involving tumor necrosis factor α-converting enzyme, TACE [83]; <1> ACE2 is a type I membrane-anchored protein with a catalytically active ectodomain, that undergoes shedding resulting in the smaller soluble enzyme form and involving tumor necrosis factor α-converting enzyme, TACE, mechanism, overview [83]; <3> the membraneous enzyme contains an ectodomain which is cleaved in the shedding process resulting in the stille active soluble enzyme form, regulation, overview [84]) [83,84]

Posttranslational modification

glycoprotein <1,3,4,9> (<9> 7 potential N-glycosylation sites [7]; <1> the lager membraneous and smaller soluble enzyme forms are glycosylated [83]) [7,30,46,83]

proteolytic modification <3> (<3> ACE2 is is shed from human airway epithelia, constitutive generation of soluble ACE2 is inhibited by ADAM17 inhibitor DPC 333, i.e. (2R)-2-[(3R)-3-amino-3(4-[2-methyl-(4-quinolinyl) methoxy] phenyl)-2-oxopyrrolidinyl]-N-hydroxy-4-methylpentanamide, but not by while ADAM10 inhibitor GI254023, while phorbol ester, ionomycin, endotoxin, and IL-1β and TNFα acutely induce ACE2 release, thus, the regulation of ACE2 cleavage involves a disintegrin and metalloprotease 17, ADAM17, and ADAM10, overview. The ACE2 ectodomain regulates its release and residue L584 might be part of a putative sheddase recognition motif [84]) [84]

5 Isolation/Preparation/Mutation/Application

Source/tissue

A-549 cell <3> [94]
Calu-3 cell <3> [84]
HEK-293 cell <3> [24]
HK-2 cell <13> [64]
HT-1080 cell <3> [84]
Leydig cell <4,9> (<4,9> ACE2 may participate in the control of the testicular function [22]) [22]
Sertoli cell <9> [22]
adipose tissue <4,12> (<4> epididymal adipose tissue [96]) [77,96]
adrenal gland <4> (<4> low ACE mRNA expression [25]) [25]
alveolar cell <3> [32]
aorta thoracica <4> (<4> chronic treatment with the AT1R antagonist almesartan induces a fivefold increase in ACE2 mRNA in the aorta which leads to a significant increase in aortic angiotensin(1-7) protein expression [12]) [12]
artery <13> (<13> non-diseased mammary arteries and atherosclerotic carotid arteries. Total vessel wall expression of ACE and ACE2 is similar during all stages of atherosclerosis. The observed ACE2 protein is enzymatically ac-

tive and activity is lower in the stable advanced atherosclerotic lesions, compared to early and ruptured atherosclerotic lesions [76]) [76]
astrocyte <4> (<4> transcriptional regulation of ACE2 mRNA in astrocytes is dependent on the relative concentrations of both angiotensin II and angiotensin(1-7) as well as on interaction with their respective receptors [13]) [13]
atherosclerotic plaque <6> (<6> cells in atherosclerotic plaques co-express ACE2, Oct-4, and CD34 [48]) [48,60]
bile duct <12> [65]
blood <3> (<3> coronary sinus blood, evidence against a major role for angiotensin converting enzyme-related carboxypeptidase in angiotensin peptide metabolism in the human coronary circulation [31]) [31]
blood plasma <2,3,4> (<3> no or very low ACE2 in healthy individuals. ACE2 may be upregulated in subjects with cardiovascular disease [28]; <3> ACE2 circulates in human plasma, but its activity is suppressed by the presence of an endogenous inhibitor [52]) [28,51,52,59]
blood vessel <2,3,4> (<3> cardiac blood vessel [17]) [17,88,93]
brain <2,3,4,10,12,13> (<4> fetal, low ACE mRNA expression [25]; <4> transcriptional regulation of ACE2 mRNA in astrocytes is dependent on the relative concentrations of both angiotensin II and angiotensin(1-7) as well as on interaction with their respective receptors [13]; <13> ACE2 is widespread throughout the brain, present in nuclei involved in the central regulation of cardiovascular function like the cardio-respiratory neurons of the brainstem, as well as in non-cardiovascular areas such as the motor cortex and raphe [74]; <10> overexpression to the forebrain, essentially the subfornical organ, inhibits both pressor and drinking responses resulting from intracerebroventricular administration of Ang-II [67]; <10> predominantly in neurons [74]) [13,25,51,67,74,77,89,92]
brain stem <2,4> (<4> about 20% of the ACE2 gene expression in kidney cortex [27]) [27,51]
bronchoalveolar lavage fluid <3> [84]
cardiofibroblast <9> [95]
cardiomyocyte <3,4> [49,82]
cardiovascular regulatory neuron <4> [54]
carotid atherosclerotic plaque <13> (<13> ACE2 mRNA is expressed in early and advanced human carotid atherosclerotic lesions [76]) [76]
cell culture <4,6> [90,97]
cerebellum <4> (<4> low ACE mRNA expression [25]) [25]
cerebral cortex <2,4> (<4> about 10% of the ACE2 gene expression in kidney cortex [27]) [27,51]
ciliary body <5> [75]
colon <3,9> (<9> only moderate levels [7]) [6,7,41,77]
connective tissue <3,4> [85,87]
coronary artery <4> (<4> vascular walls and endothelium [88]) [88]
endothelial cell <3> (<3> expressed ACE2 to a high level, has not been shown to be infected by SARS-CoV. Presence of ACE2 alone is not sufficient for maintaining viral infection. Other virus receptors or coreceptors may be required in different tissues [32]) [32]

endothelium <4,6> (<6> the enzyme is present in endothelia overlying neointima formation and atherosclerotic plaques, but not in endothelial layer overlying normal vessel wall [60]; <4> and vascular walls of coronary arteries [88]) [60,88]
enterocyte <3> (<3> surface enterocytes of the small intestine [32]) [32]
epithelium <3,9> (<9> of coronary and intrarenal vessels and renal tubuls [3]; <3> from airway, apical surface [84]) [3,84,92]
eye <5> (<5> vitreous body, retina and ciliary body. Counterbalancing interaction of ACE1 (EC 3.4.15.1) and ACE2 in physiological regulation of ocular circulation and pressure and possible protective role in certain ophthalmic disorders such as glaucoma and diabetic retinopathy [75]) [75]
glomerulus <2,4> [46,56]
heart <2,3,4,6,9,13> (<4> 12-day administration of agents that either inhibit the synthesis of circulating angiotensin II or block the activity of angiotensin II at the AT1 receptor induce an increase in cardiac ACE2 mRNA, accompanied by increases in cardiac membrane ACE2 activity in rats medicated with either losartan or both losartan and lisinopril [19]; <4> about 35% of the ACE2 gene expression in kidney cortex [27]; <13> the endothelium-bound carboxypeptidase is expressed in the heart and kidney [78]; <3> the enzyme is upregulated in cardiovascular disease [81]) [7,17,19,23,25,27,30,37,41,44,49,50,54,55,77,78,81,82,86,88,90,95]
heart ventricle <9> [3,6]
hepatic stellate cell <4> [87]
hippocampus <2> [51]
hypothalamus <2,4> (<4> about 15% of the ACE2 gene expression in kidney cortex [27]; <4> low ACE mRNA expression [25]; <2> brain ACE2 activity is highest in hypothalamus [51]) [25,27,51]
intestine <4> (<4> highest ACE2 mRNA expression in intestine epithelium [25]) [25,59]
kidney <2,3,4,9,10,12,13> (<4> diabetic rats, 50% reduced enzyme content in renal tubules [5]; <4> ACE2 mRNA is widely expressed, with relatively high levels in proximal straight tubule. ACE2 protein is present in tubular segments, glomeruli and endothelial cells. No activity in medullary thick ascending limb of henles loop [14]; <4> cortex and medulla, about 50% of the ACE2 gene expression in kidney cortex [27]; <3> tubular epithelium [17]; <2> ACE and ACE2 co-localized strongly in the apical brush border of the proximal tubule [56]; <4> predominantly expressed in the proximal tubule [46]; <12> in salt-sensitive Sabra hypertensive (SBH/y) rats, ACE2 mRNA and protein expression are lower than that in salt-resistant Sabra normotensive (SBN/y) rats [74]; <9> localization of ACE2 in the podocytes early in the development of diabetes indicates that it may protect against podocyte loss, thus preventing the worsening glomerular injury [77]; <13> the endothelium-bound carboxypeptidases is expressed in the heart and kidney. ACE2 is expressed in renal tubular epithelium, vascular smooth muscle cells of the intrarenal arteries and in the glomeruli [78]) [5,6,7,14,17,25,26,27,30,39,41,44,46,51,56,57,59,66,74,77,78,89,96]

liver <3,4,12> (<12> ACE2 plays a crucial role in liver fibrogenesis [71]; <3> the enzyme is upregulated in fibrotic liver [81]) [59,71,77,81,87]
lung <2,3,4,11,12> (<2> ACE2 and the AT2 receptor protect against lung injury. Exogenous recombinant human ACE2 attenuates acute lung failure in Ace knockout as well as in wild-type mice. Acute lung injury results in a marked downregulation of ACE2. Loss of ACE2 expression in acute lung injury leads to leaky pulmonary blood vessels through AT1 receptor stimulation [34]; <4> ECE2 and ACE activities are increased in the same portions in the lungs of FR30 rats (adult 4-months-old offspring from 70% food-restricted dams throughout gestation) [25]) [25,34,41,45,47,59,63,77,92,97]
lung epithelium <10> [57]
macrophage <4,6> [48,60,88]
myocardium <4> [88,90]
myocyte <4,6> [88,90]
non-small cell lung cancer cell <3> (<3> decreased ACE2 expression, expression profile in relation to clinicopathological factors, e.g. smoking, overview [94]) [94]
ovary <9> (<9> only moderate levels [7]) [7,77]
pancreas <4,9,12> (<4> low ACE mRNA expression [25]; <12> ACE-mediated inhibition of TGF-β expression may prevent islet fibrosis and loss of islet function [77]; <9> non-malignant tissues surrounding invasive pancreatic ductal adenocarcinoma [80]) [25,77,80]
pancreatic invasive ductal adenocarcinoma cell <9> [80]
pituitary gland <2,4> (<4> low ACE mRNA expression [25]) [25,51]
placenta <3,4,9,12> (<3> expression of ACE2 is similar in samples obtained from normal term or preeclamptic pregnancies, except for increased expression of ACE2 in umbilical arterial endothelium in preeclampsia. The uteroplacental location of angiotensin (1-7) and ACE2 in pregnancy suggests an autocrine function of angiotensin(1-7) in the vasoactive regulation that characterizes placentation and establishes pregnancy [35]; <12> during pregnancy, the placenta and the uterus, constitute important sources of ACE2, in addition to its normal production in the kidney, leading to an estimated twofold increase in total ACE2 activity [66]) [25,35,66,77]
podocyte <2> [56]
pulmonary artery smooth muscle cell <4> (<4> primary cell culture [97]) [97]
renal cortex <4> [39]
renal medulla <4> [39]
renal tubule <4> (<4> predominantly in proximal tubules, diabetic rats, 30% reduced enzyme content [5]) [5]
retina <4,5,9,12> (<4> ACE2 is localized predominantly to the inner nuclear layer but also to photoreceptors, in the diabetic retina ACE2 is increased, ramipril treatment has no influence [20]) [20,75,77]
rostral ventrolateral medulla <4> [54]
serum <3> [85]
skin <2,3,4> [91,93]

small intestine <3,9> (<9> only moderate levels [7]; <3> surface enterocytes [32]) [6,7,32,77]
smooth muscle cell <6> [48,60]
stomach <4> (<4> low ACE mRNA expression [25]) [25]
testis <3,4,9> (<4,9> ACE2 may participate in the control of the testicular function [22]) [3,6,7,22,41,77]
urine <3> [29,30]
uterine endometrium <13> [79]
uterus <12> (<12> during pregnancy the placenta and the uterus, constitute important sources of ACE2, in addition to its normal production in the kidney, leading to an estimated twofold increase in total ACE2 activity [66]) [66]
vein <13> (<13> total vessel wall expression of ACE and ACE2 is similar during all stages of atherosclerosis. The observed ACE2 protein is enzymatically active and activity is lower in the stable advanced atherosclerotic lesions, compared to early and ruptured atherosclerotic lesions [76]) [76]
vena cava <2,4> (<2> induced thrombus [93]; <4> induced thrombus. No differences between spontaneously hypertensive rats and Wistar Kyoto rats in ACE2 protein and ACE activity in the thrombi [93]) [93]
Additional information <1,2,3,4> (<2> no activity in plasma [26]; <4> weak or no ACE2 mRNA expression in: hippocampus, skeletal muscle, liver, spleen, testis, uterus and mammary gland [25]; <3> no detectable enzyme levels in vascular smooth muscle cell or vascular endothelium [49]; <1> no activity in CHO cell [83]; <2> no activity in EC cells [83]) [25,26,49,83]

Localization

cell membrane <4> [88]
cell surface <3> [84]
cytoplasm <3,9> (<9> ACE2 exists as bothmembrane bound and soluble forms, the latter being generated by proteolytic cleavage of the ectodomain by the tumor necrosis factor convertase ADAM17 [77]) [77,94]
membrane <1,2,3,4,9> (<9> integral membrane protein [72]; <2,3> transmembrane enzyme [41]; <9> enzyme possesses a transmembrane domain, posttranslational cleavage for secretion of the protein in vivo and in cell culture [3]; <3> ACE2 also undergoes phorbol-12-myristate-13-acetate-inducible ectodomain shedding from the membrane [49]; <9> ACE2 exists as bothmembrane bound and soluble forms, the latter being generated by proteolytic cleavage of the ectodomain by the tumor necrosis factor convertase ADAM17 [77]; <3> ACE 2 is shedded [84]; <2> ACE2 is a type I membrane-anchored protein with a catalytically active ectodomain, that undergoes shedding [83]; <1> the larger form of ACE2 is a type I membrane-anchored protein with a catalytically active ectodomain, that undergoes shedding resulting in the smaller soluble enzyme form [83]) [3,4,7,41,46,49,50,52,56,72,77,83,84,94]
plasma membrane <3> (<3> evenly distributed to detergent-soluble regions of the plasma membrane in non-polarized CHO cells, in polarized Madin-Darby canine kidney epithelial cells ACE is localized predominantly to the apical surface (92%) where it is proteolytically cleaved within the ectodomain to release a soluble form, recombinantly expressed enzymes [30]; <3> the

ACE2 ectodomain can be cleaved from the cell membrane and released into the extracellular milieu [53]) [30,53]
soluble <1,3> (<3> ACE 2 is shedded [84]; <1> smaller enzyme form without ectodomain [83]) [83,84]
Additional information <9> (<9> transmembrane domain [6]) [6]

Purification

<3> (Ni^{3+}-charged nitrilotriacetic acid-linked resin chromatography and anti-Flag column chromatography) [52]
<9> (recombinant from CHO K1 cells) [3]
<9> (recombinant from Sf21 cells as mIgG-tagged protein) [1]
<9> (recombinant from Sf9 cells, to near homogeneity) [8]
<9> (recombinant truncated extracellular form of human ACE2 (residues 1-740)) [72]
<9> (recombinant wild-type and extracellular domain as FLAG-tagged proteins from Sf9 cells) [9]
<11> (nickel-nitrilotriacetic acid agarose affinity chromatography) [63]
<13> (recombinant) [72]

Crystallization

<9> (hanging drop vapor diffusion at 16-18°C, crystal structures of the native and inhibitor(MLN-4760)-bound forms of the ACE2 extracellular domains are solved to 2.2 and 3.0 A resolution, respectively) [72]
<13> (hanging drop vapor diffusion at 16-18°C, crystal structures of the native and inhibitor-bound forms of the ACE2 extracellular domains are solved to 2.2 A and 3.0 A resolution) [72]

Cloning

<1> (expression in CHO cells) [83]
<2> (expression in E4 cells) [83]
<3> (cloning and expression of a constitutively secreted form of ACE2, WKY rats are transduced with lentiviral vector containing shACE2. The plasma ACE2 levels could be increased by lentivector-mediated shACE2 gene transfer. This provides a tool to investigate the role of this enzyme in the development of the cardiovascular disease both through the role of hyperactivity of the RAS and through infectious agents) [36]
<3> (expressed in HEK 293-T cells) [52]
<3> (expressed in HEK-ACE2 cells) [53]
<3> (expression in CHO cells and polarized Madin-Darby canine kidney epithelial cells) [30]
<3> (expression of wild-type and utant L584A ACE2 in HEK-293 cells) [84]
<4> (ACE2 expression analysis by RT-PCR) [87]
<4> (cloning of the enzyme utilizing the murine cytωlovirus immediate early gene promoter, MCMV Pr, in an adenoviral vector for ACE2 overexpression in rats as a gene therapy model. overview) [88]
<4> (expressed in CHO cells) [62]

<4> (overexpression of ACE2, by usage of a recombinant adeno-associated virus 6 delivery system, in myocardium of stroke-prone spontaneously hypertensive rats, gene expression profiling, overview) [90]
<9> (ACE2 expressed in Chinese hamster ovary cells specifically binds to glutathione-S-transferase-calmodulin, but not glutathione-S-transferase alone) [68]
<9> (ACE2 expression analysis) [95]
<9> (DNA and amino acid sequence determination, gene maps to choromosomal location Xp22, expression in CHO cells of the wild-type and of the soluble truncated mutant, the latter as c-Myc- and His-tagged protein) [7]
<9> (Sf21 cells via infection with baculovirus, mIgG-tagged protein) [1]
<9> (expressed in the endothelial cell line Eahy926) [43]
<9> (expression in HEK-293 cells) [69]
<9> (expression in Spodoptera frugiperda Sf9 cells via infection with baculovirus) [8]
<9> (expression of extracellular domain and wild-type, both as FLAG-tagged proteins, in Spodotera frugiperda Sf9 cells via baculovirus infection) [9]
<9> (expression of recombinant ACE2 in P-selectin-transfected Chinese hamster ovary cells) [22]
<9> (expression of the mutant enzyme in CHO cells) [2]
<9> (gene ACE2, DNA sequence determination and analysis, expression in CHO K1 cells, secretion of the active enzyme from transfected cells by cleavage N-terminal to the transmembrane domain) [3]
<11> (expressed in Escherichia coli BL21(DE3) cells) [63]
<13> (development of a transgenic mouse model (syn-hACE2) where the full open reading frame of the human ACE2 gene is under the control of a synapsin promoter, allowing the hACE2 protein to be expressed specifically in neurons) [74]

Engineering

H345A <3> (<3> no activity with (7-methoxycoumarin-4-yl)acetyl-APK-2,4-dinitrophenyl [24]) [24]
H345L <3> (<3> no activity with (7-methoxycoumarin-4-yl)acetyl-APK-2,4-dinitrophenyl [24]) [24]
H505A <3> (<3> 1.5% of wild-type activity with (7-methoxycoumarin-4-yl)acetyl-APK-2,4-dinitrophenyl as substrate [24]) [24]
H505L <3> (<3> no activity with (7-methoxycoumarin-4-yl)acetyl-APK-2,4-dinitrophenyl [24]) [24]
K481Q <9> (<9> angiotensin I cleavage activity is 21% of wild-type activity, angiotensin II cleavage activity is 71.8% of wild-type activity [69]) [69]
L584A <3> (<3> the point mutation in the ACE2 ectodomain markedly attenuates shedding. The resultant ACE2-L584A mutant trafficks to the cell membrane and facilitates SARS-CoV entry into target cells [84]) [84]
N580A <3> (<3> the mutation in the ectodomain has no effect on sACE2 release [84]) [84]
P583A <3> (<3> the mutation in the ectodomain has no effect on sACE2 release [84]) [84]

R169Q <3,9> (<3> as active as wild-type enzyme with (7-methoxycoumarin-4-yl)acetyl-APK-2,4-dinitrophenyl as substrate [24]; <9> angiotensin I cleavage activity is 5.2% of wild-type activity, angiotensin II cleavage activity is 1.1% of wild-type activity. The mutant enzyme does not show any activity with angiotensin I in the absence of chloride ions [69]) [24,69]
R169QK481QR514Q <9> (<9> angiotensin I cleavage activity is 53.2% of wild-type activity, angiotensin II cleavage activity is 203.4% of wild-type activity [69]) [69]
R273K <3> (<3> no activity with (7-methoxycoumarin-4-yl)acetyl-APK-2,4-dinitrophenyl [24]) [24]
R273Q <3> (<3> no activity with (7-methoxycoumarin-4-yl)acetyl-APK-2,4-dinitrophenyl [24]) [24]
R514Q <3,9> (<3> about 10% of wild-type activity with (7-methoxycoumarin-4-yl)acetyl-APK-2,4-dinitrophenyl as substrate [24]; <9> angiotensin I cleavage activity is 52% of wild-type activity, angiotensin II cleavage activity is 179.3% of wild-type activity, enhancement of angiotensin II cleavage is a result of a 2.5-fold increase in V_{max} compared with the wild-type [69]) [24,69]
R582A <3> (<3> the mutation in the ectodomain has no effect on sACE2 release [84]) [84]
V581A <3> (<3> the mutation in the ectodomain has no effect on sACE2 release [84]) [84]
V604A <3> (<3> the mutation in the ectodomain has no effect on sACE2 release [84]) [84]
W271A <9> (<9> angiotensin I cleavage activity is 5.3% of wild-type activity, angiotensin II cleavage activity is 0.9% of wild-type activity. Lacks any significant chloride sensitivity with the substrate angiotensin I [69]) [69]
Additional information <1,2,3,4,6,9> (<9> construction of a soluble truncated mutant enzyme lacking the transmembrane and cytosolic domains [2,7]; <6> ACE2 overexpression leads to markedly increased myocyte volume, assessed in primary rabbit myocytes [90]; <3> construction of cytoplasmic tail deletion mutants by introduction of a stop codon at position amino acid 763. Construction of chimeric proteins containing portions of human ACE2 and portions of human CD4 or human β-defensin-2, both showing loss of domain shedding [84]; <3> construction of several transgenic linages with differential virological and immunological outcome of severe acute respiratory syndrome coronavirus infection in susceptible and resistant transgenic mice expressing human ACE2, overview. Transgenic lineages AC70 and AC22, representing those susceptible and resistant to the lethal SARS-CoV infection, respectively, are both permissive to SARS-CoV infection, causing elevated secretion of many inflammatory mediators within the lungs and brains, viral infection appears to be more intense in AC70 than in AC_{22} mice, especially in the brain, differential SARS-CoV-induced morbidity and mortality between AC70 and AC22 mice, overview [92]; <2> generation of triple-transgenic-model mice with brain ACE2 overexpression on a chronically hypertensive, AngII-increased background. The transgenic mice show dramatically decreased baseline spontaneous baroreflex sensitivity and brain ACE2 activity compared with nontransgenic mice, whereas peripheral

ACE2 activity/expression remains unaffected [89]; <1> M2-mutant CHO cells, mutated in tumor necrosis factor α-converting enzyme, TACE, show reduced shedding of the ectodomain of ACE2 and increased release of the larger soluble enzyme form, compared to the smaller one, overview. Tandem mutation in the juxtamembrane region also causes a decreaee in the small soluble enzyme form [83]; <3> overexpression of ACE 2 might have a protective effect by inhibiting cell growth and vascular endothelial growth factor a production in vitro [94]; <4> overexpression of ACE2 favorably affects the pathological process of left ventricular remodeling after myocardial infarction by inhibiting ACE activity, reducing AngII levels and upregulating Ang(1-7) expression [88]; <4> overexpression of ACE2, by usage of a recombinant adeno-associated virus 6 delivery system, in myocardium of stroke-prone spontaneously hypertensive rats mediates onset of experimental severe cardiac fibrosis [90]) [2,7,83,84,88,89,90,92,94]

Application

analysis <2,3> (<2,3> mass spectrometric assay for angiotensin-converting enzyme 2 using angiotensin II as substrate will have applications in drug screening, antagonist development, and clinical investigations [26]) [26]

medicine <2,3,4,7,9,10,12,13> (<9> potential important target in cardio-renal disease [2]; <3> ACE2 protects against acute lung injury in several animal models of acute respiratory distress syndrome. Increasing ACE2 activity might be a novel approach for the treatment of acute lung failure in several diseases [21]; <4> angiotensin-converting enzyme 2 is a target for gene therapy for hypertension disorders [23]; <4> chronic treatment with the AT1R antagonist almesartan induces a fivefold increase in ACE2 mRNA in the aorta which leads to a significant increase in aortic angiotensin(1-7) protein expression. These effects are associated with significant decreases in aortic medial thickness and may represent an important protective mechanism in the prevention of cardiovascular events in hypertensive subjects [12]; <7> identification of ACE2 as a receptor for SARS-CoV will contribute to the development of antivirals and vaccines [18]; <2> recombinant ACE2 can protect mice from severe acute lung injury [34]; <2,3,4> ACE-2 protects against lung fibrogenesis by limiting the local accumulation of the profibrotic peptide angiotensin II [38]; <3> ACE2 is a functional receptor for the causative agent of severe acute repiratory syndrome, the SARS coronavirus, ACE2 also plays a role in the development of liver fibrosis and subsequent cirrhosis [41]; <2> ACE2 is a key factor for protection from ARDS/acute lung injury and it functions as a critical SARS receptor in vivo, recombinant ACE2 protein might not only be a treatment to block spreading of SARS but also to protect SARS patients from developing lung failure [45]; <2> ACE2 may be a target for therapeutic interventions that aim to reduce albuminuria and glomerular injury [56]; <2> ACE2 protects murine lungs from acute respiratory distress syndrome [47]; <13> ACE2 activators are a reliable approach which could lead to the development of a novel class of antihypertensive and cardioprotective drugs [73]; <10> ACE2 offers a new target for the treatment of hypertension and other cardiovascular diseases [67]; <12> administration of ACE2

activators may be a valid strategy for antihypertensive therapy [70]; <13> differential regulation of ACE2 activity during the progression of atherosclerosis suggest that this novel molecule of the renin-angiotensin system may play a role in the pathogenesis of atherosclerosis [76]; <13> enhancing ACE2 action may serve to provide additional therapeutic benefits patients with cardiovascular and diabetic kidney disease. Increased ACE2 activity by the use of human recombinant ACE2 and/or a small molecule activator(-xanthenone) of ACE2 may represent potential new therapies for lung, cardiovascular and kidney diseases by providing dual beneficial effects by antagonizing angiotensin II action while generating angiotensin-(1-7) [78]; <9> reduction of ACE2 expression by RNA interference promotes the proliferation of cultured pancreatic cancer cells. ACE2 may have clinical potential as a novel molecular target for the treatment of pancreatic ductal adenocarcinoma [80]) [2,12,18,21,23,34,38,41,45,47,56,67,70,73,76,78,80]
pharmacology <3,4,9> (<9> design and synthesis of first potent and selective enzyme inhibitors may be useful as pharmacological tools to help understanding the biological relevance and potantial role of the enzyme in human disease [6]; <4> ACE2 is a potential therapeutic target in the treatment of heart failure [88]; <3> ACE2 might be a target for treatment of non-small cell lung cancer [94]) [6,88,94]

6 Stability

Temperature stability

22 <9> (<9> recombinant enzyme, at room temperature, stable for 6 h [8]) [8]

General stability information

<9>, Zn^{2+} stabilizes [8]

References

[1] Yan, Z.H.; Ren, K.J.; Wang, Y.; Chen, S.; Brock, T.A.; Rege, A.A.: Development of intramolecularly quenched fluorescent peptides as substrates of angiotensin-converting enzyme 2. Anal. Biochem., **312**, 141-147 (2003)
[2] Guy, J.L.; Jackson, R.M.; Acharya, K.R.; Sturrock, E.D.; Hooper, N.M.; Turner, A.J.: Angiotensin-converting enzyme-2 (ACE2): comparative modeling of the active site, specificity requirements, and chloride dependence. Biochemistry, **42**, 13185-13192 (2003)
[3] Donoghue, M.; Hsieh, F.; Baronas, E.; Godbout, K.; Gosselin, M.; Stagliano, N.; Donovan, M.; Woolf, B.; Robison, K.; Jeyaseelan, R.; Breitbart, R.E.; Acton, S.: A novel angiotensin-converting enzyme-related carboxypeptidase (ACE2) converts angiotensin I to angiotensin 1-9. Circ. Res., **87**, E1-9 (2000)
[4] Zisman, L.S.; Keller, R.S.; Weaver, B.; Lin, Q.; Speth, R.; Bristow, M.R.; Canver, C.C.: Increased angiotensin-(1-7)-forming activity in failing human

heart ventricles: evidence for upregulation of the angiotensin-converting enzyme homologue ACE2. Circulation, **108**, 1707-1712 (2003)
[5] Tikellis, C.; Johnston, C.I.; Forbes, J.M.; Burns, W.C.; Burrell, L.M.; Risvanis, J.; Cooper, M.E.: Characterization of renal angiotensin-converting enzyme 2 in diabetic nephropathy. Hypertension, **41**, 392-397 (2003)
[6] Dales, N.A.; Gould, A.E.; Brown, J.A.; Calderwood, E.F.; Guan, B.; Minor, C.A.; Gavin, J.M.; Hales, P.; Kaushik, V.K.; Stewart, M.; Tummino, P.J.; Vickers, C.S.; Ocain, T.D.; Patane, M.A.: Substrate-based design of the first class of angiotensin-converting enzyme-related carboxypeptidase (ACE2) inhibitors. J. Am. Chem. Soc., **124**, 11852-11853 (2002)
[7] Tipnis, S.R.; Hooper, N.M.; Hyde, R.J.; Christie, G.; Karran, E.; Turner, A.J.: A humen homolog of angiotensin converting enzyme - cloning and functional expression as a captopril-insensitive carboxypeptidase. J. Biol. Chem., **275**, 33238-33243 (2000)
[8] Vickers, C.; Hales, P.; Kaushik, V.; Dick, L.; Gavin, J.; Tang, J.; Godbout, K.; Parsons, T.; Baronas, E.; Hsieh, F.; Acton, S.; Patane, M.; Nichols, A.; Tummino, P.: Hydrolysis of biological peptides by human angiotensin-converting enzyme-related carboxypeptidase. J. Biol. Chem., **277**, 14838-14843 (2002)
[9] Huang, L.; Sexton, D.J.; Skogerson, K.; Devlin, M.; Smith, R.; Sanyal, I.; Parry, T.; Kent, R.; Enright, J.; Wu, Q.L.; Conley, G.; DeOliveira, D.; Morganelli, L.; Ducar, M.; Wescott, C.R.; Ladner, R.C.: Novel peptide inhibitors of angiotensin-converting enzyme 2. J. Biol. Chem., **278**, 15532-15540 (2003)
[10] Stoesser, G.; Baker, W.; van den Broek, A.; Garcia-Pastor, M.; Kanz, C.; Kulikova, T.; Leinonen, R.; Lin Q.; Lombard, V.; Lopez, R.; Mancuso, R.; Nardone, F.; Stoehr, P.; Tuli, M.A.; Tzouvara, K.; Vaughan, R.: The EMBL Nucleotide Sequence Database: major new developments. Nucleic Acids Res., **31**, 17-22 (2003)
[11] Benson, D.A.; Karsch-Mizrachi, I.; Lipman, D.J.; Ostell, J.; Wheeler, D.L.: GenBank: update. Nucleic Acids Res., **32**, D23-D26 (2004)
[12] Dantas, A.P.; Sandberg, K.: Regulation of ACE2 and ANG-(1-7) in the aorta: New insights into the renin-angiotensin system in the control of vascular function. Am. J. Physiol., **289**, H980-H981 (2005)
[13] Gallagher, P.E.; Chappell, M.C.; Ferrario, C.M.; Tallant, E.A.: Distinct roles for ANG II and ANG-(1-7) in the regulation of angiotensin-converting enzyme 2 in rat astrocytes. Am. J. Physiol., **290**, C420-C426 (2006)
[14] Li, N.; Zimpelmann, J.; Cheng, K.; Wilkins, J.A.; Burns, K.D.: The role of angiotensin converting enzyme 2 in the generation of angiotensin 1-7 by rat proximal tubules. Am. J. Physiol. Renal Physiol., **288**, F353-F362 (2005)
[15] Rice, G.I.; Thomas, D.A.; Grant, P.J.; Turner, A.J.; Hooper, N.M.: Evaluation of angiotensin-converting enzyme (ACE), its homologue ACE2 and neprilysin in angiotensin peptide metabolism. Biochem. J., **383**, 45-51 (2004)
[16] Warner, F.J.; Smith, A.I.; Hooper, N.M.; Turner, A.J.: Angiotensin-converting enzyme-2: a molecular and cellular perspective. Cell. Mol. Life Sci., **61**, 2704-2713 (2004)

[17] Danilczyk, U.; Eriksson, U.; Oudit, G.Y.; Penninger, J.M.: Physiological roles of angiotensin-converting enzyme 2. Cell. Mol. Life Sci., **61**, 2714-2719 (2004)
[18] Kuhn, J.H.; Li, W.; Choe, H.; Farzan, M.: Angiotensin-converting enzyme 2: a functional receptor for SARS coronavirus. Cell. Mol. Life Sci., **61**, 2738-2743 (2004)
[19] Ferrario, C.M.; Jessup, J.; Chappell, M.C.; Averill, D.B.; Brosnihan, K.B.; Tallant, E.A.; Diz, D.I.; Gallagher, P.E.: Effect of angiotensin-converting enzyme inhibition and angiotensin II receptor blockers on cardiac angiotensin-converting enzyme 2. Circulation, **111**, 2605-2610 (2005)
[20] Tikellis, C.; Johnston, C.I.; Forbes, J.M.; Burns, W.C.; Thomas, M.C.; Lew, R.A.; Yarski, M.; Smith, A.I.; Cooper, M.E.: Identification of angiotensin converting enzyme 2 in the rodent retina. Curr. Eye Res., **29**, 419-427 (2004)
[21] Kuba, K.; Imai, Y.; Penninger, J.M.: Angiotensin-converting enzyme 2 in lung diseases. Curr. Opin. Pharmacol., **6**, 271-276 (2006)
[22] Douglas, G.C.; OBryan, M.K.; Hedger, M.P.; Lee, D.K.; Yarski, M.A.; Smith, A.I.; Lew, R.A.: The novel angiotensin-converting enzyme (ACE) homolog, ACE2, is selectively expressed by adult Leydig cells of the testis. Endocrinology, **145**, 4703-4711 (2004)
[23] Katovich, M.J.; Grobe, J.L.; Huentelman, M.; Raizada, M.K.: Angiotensin-converting enzyme 2 as a novel target for gene therapy for hypertension. Exp. Physiol., **90**, 299-305 (2005)
[24] Guy, J.L.; Jackson, R.M.; Jensen, H.A.; Hooper, N.M.; Turner, A.J.: Identification of critical active-site residues in angiotensin-converting enzyme-2 (ACE2) by site-directed mutagenesis. FEBS J., **272**, 3512-3520 (2005)
[25] Riviere, G.; Michaud, A.; Breton, C.; VanCamp, G.; Laborie, C.; Enache, M.; Lesage, J.; Deloof, S.; Corvol, P.; Vieau, D.: Angiotensin-converting enzyme 2 (ACE2) and ACE activities display tissue-specific sensitivity to undernutrition-programmed hypertension in the adult rat. Hypertension, **46**, 1169-1174 (2005)
[26] Elased, K.M.; Cunha, T.S.; Gurley, S.B.; Coffman, T.M.; Morris, M.: New mass spectrometric assay for angiotensin-converting enzyme 2 activity. Hypertension, **47**, 1010-1017 (2006)
[27] Ferrario, C.M.: Angiotensin-converting enzyme 2 and angiotensin-(1-7): an evolving story in cardiovascular regulation. Hypertension, **47**, 515-521 (2006)
[28] Rice, G.I.; Jones, A.L.; Grant, P.J.; Carter, A.M.; Turner, A.J.; Hooper, N.M.: Circulating activities of angiotensin-converting enzyme, its homolog, angiotensin-converting enzyme 2, and neprilysin in a family study. Hypertension, **48**, 914-920 (2006)
[29] Lew, R.A.; Warner, F.J.; Hanchapola, I.; Smith, A.I.: Characterization of angiotensin converting enzyme-2 (ACE2) in human urine. Int. J. Pept. Res. Ther., **12**, 283-289 (2006)
[30] Warner, F.J.; Lew, R.A.; Smith, A.I.; Lambert, D.W.; Hooper, N.M.; Turner, A.J.: Angiotensin-converting enzyme 2 (ACE2), but not ACE, is preferentially localized to the apical surface of polarized kidney cells. J. Biol. Chem., **280**, 39353-39362 (2005)

[31] Campbell, D.J.; Zeitz, C.J.; Esler, M.D.; Horowitz, J.D.: Evidence against a major role for angiotensin converting enzyme-related carboxypeptidase (ACE2) in angiotensin peptide metabolism in the human coronary circulation. J. Hypertens., **22**, 1971-1976 (2004)
[32] To, K.F.; Lo, A.W.: Exploring the pathogenesis of severe acute respiratory syndrome (SARS): the tissue distribution of the coronavirus (SARS-CoV) and its putative receptor, angiotensin-converting enzyme 2 (ACE2). J. Pathol., **203**, 740-743 (2004)
[33] Kuba, K.; Imai, Y.; Rao, S.; Gao, H.; Guo, F.; Guan, B.; Huan, Y.; Yang, P.; Zhang, Y.; Deng, W.; Bao, L.; Zhang, B.; Liu, G.; Wang, Z.; Chappell, M.; Liu, Y.; Zheng, D.; Leibbrandt, A.; Wada, T.; Slutsky, A.S.; Liu, D.; Qin, C.; Jiang, C.; Penninger, J.M.: A crucial role of angiotensin converting enzyme 2 (ACE2) in SARS coronavirus-induced lung injury. Nat. Med., **11**, 875-879 (2005)
[34] Imai, Y.; Kuba, K.; Rao, S.; Huan, Y.; Guo, F.; Guan, B.; Yang, P.; Sarao, R.; Wada, T.; Leong-Poi, H.; Crackower, M.A.; Fukamizu, A.; Hui, C.C.; Hein, L.; Uhlig, S.; Slutsky, A.S.; Jiang, C.; Penninger, J.M.: Angiotensin-converting enzyme 2 protects from severe acute lung failure. Nature, **436**, 112-116 (2005)
[35] Valdes, G.; Neves, L.A.; Anton, L.; Corthorn, J.; Chacon, C.; Germain, A.M.; Merrill, D.C.; Ferrario, C.M.; Sarao, R.; Penninger, J.; Brosnihan, K.B.: Distribution of angiotensin-(1-7) and ACE2 in human placentas of normal and pathological pregnancies. Placenta, **27**, 200-207 (2006)
[36] Huentelman, M.J.; Zubcevic, J.; Katovich, M.J.; Raizada, M.K.: Cloning and characterization of a secreted form of angiotensin-converting enzyme 2. Regul. Pept., **122**, 61-67 (2004)
[37] Trask, A.J.; Averill, D.B.; Ganten, D.; Chappell, M.C.; Ferrario, C.M.: Primary role of angiotensin-converting enzyme-2 in cardiac production of angiotensin-(1-7) in transgenic Ren-2 hypertensive rats. Am. J. Physiol. Heart Circ. Physiol., **292**, H3019-H3024 (2007)
[38] Li, X.; Molina-Molina, M.; Abdul-Hafez, A.; Uhal, V.; Xaubet, A.; Uhal, B.D.: Angiotensin converting enzyme-2 is protective but downregulated in human and experimental lung fibrosis. Am. J. Physiol. Lung Cell Mol. Physiol., **295**, L178-185 (2008)
[39] Joyner, J.; Neves, L.A.; Granger, J.P.; Alexander, B.T.; Merrill, D.C.; Chappell, M.C.; Ferrario, C.M.; Davis, W.P.; Brosnihan, K.B.: Temporal-spatial expression of AN^{g}-(1-7) and angiotensin-converting enzyme 2 in the kidney of normal and hypertensive pregnant rats. Am. J. Physiol. Regul. Integr. Comp. Physiol., **293**, R169-R177 (2007)
[40] Ho, T.Y.; Wu, S.L.; Chen, J.C.; Li, C.C.; Hsiang, C.Y.: Emodin blocks the SARS coronavirus spike protein and angiotensin-converting enzyme 2 interaction. Antiviral Res., **74**, 92-101 (2007)
[41] Lambert, D.W.; Hooper, N.M.; Turner, A.J.: Angiotensin-converting enzyme 2 and new insights into the renin-angiotensin system. Biochem. Pharmacol., **75**, 781-786 (2008)
[42] Deaton, D.N.; Gao, E.N.; Graham, K.P.; Gross, J.W.; Miller, A.B.; Strelow, J.M.: Thiol-based angiotensin-converting enzyme 2 inhibitors: P1 modifica-

tions for the exploration of the S1 subsite. Bioorg. Med. Chem. Lett., **18**, 732-737 (2008)
[43] Zhong, J.C.; Yu, X.Y.; Lin, Q.X.; Li, X.H.; Huang, X.Z.; Xiao, D.Z.; Lin, S.G.: Enhanced angiotensin converting enzyme 2 regulates the insulin/Akt signalling pathway by blockade of macrophage migration inhibitory factor expression. Br. J. Pharmacol., **153**, 66-74 (2008)
[44] Keidar, S.; Kaplan, M.; Gamliel-Lazarovich, A.: ACE2 of the heart: From angiotensin I to angiotensin (1-7). Cardiovasc. Res., **73**, 463-469 (2007)
[45] Imai, Y.; Kuba, K.; Penninger, J.M.: Angiotensin-converting enzyme 2 in acute respiratory distress syndrome. Cell. Mol. Life Sci., **64**, 2006-2012 (2007)
[46] Koitka, A.; Cooper, M.E.; Thomas, M.C.; Tikellis, C.: Angiotensin converting enzyme 2 in the kidney. Clin. Exp. Pharmacol. Physiol., **35**, 420-425 (2008)
[47] Imai, Y.; Kuba, K.; Penninger, J.M.: The discovery of angiotensin-converting enzyme 2 and its role in acute lung injury in mice. Exp. Physiol., **93**, 543-548 (2008)
[48] Zulli, A.; Rai, S.; Buxton, B.F.; Burrell, L.M.; Hare, D.L.: Co-localization of angiotensin-converting enzyme 2-, octomer-4- and CD34-positive cells in rabbit atherosclerotic plaques. Exp. Physiol., **93**, 564-569 (2008)
[49] Guy, J.L.; Lambert, D.W.; Turner, A.J.; Porter, K.E.: Functional angiotensin-converting enzyme 2 is expressed in human cardiac myofibroblasts. Exp. Physiol., **93**, 579-588 (2008)
[50] Garabelli, P.J.; Modrall, J.G.; Penninger, J.M.; Ferrario, C.M.; Chappell, M.C.: Distinct roles for angiotensin-converting enzyme 2 and carboxypeptidase A in the processing of angiotensins within the murine heart. Exp. Physiol., **93**, 613-621 (2008)
[51] Elased, K.M.; Cunha, T.S.; Marcondes, F.K.; Morris, M.: Brain angiotensin-converting enzymes: role of angiotensin-converting enzyme 2 in processing angiotensin II in mice. Exp. Physiol., **93**, 665-675 (2008)
[52] Lew, R.A.; Warner, F.J.; Hanchapola, I.; Yarski, M.A.; Manohar, J.; Burrell, L.M.; Smith, A.I.: Angiotensin-converting enzyme 2 catalytic activity in human plasma is masked by an endogenous inhibitor. Exp. Physiol., **93**, 685-693 (2008)
[53] Lambert, D.W.; Clarke, N.E.; Hooper, N.M.; Turner, A.J.: Calmodulin interacts with angiotensin-converting enzyme-2 (ACE2) and inhibits shedding of its ectodomain. FEBS Lett., **582**, 385-390 (2008)
[54] Yamazato, M.; Yamazato, Y.; Sun, C.; Diez-Freire, C.; Raizada, M.K.: Overexpression of angiotensin-converting enzyme 2 in the rostral ventrolateral medulla causes long-term decrease in blood pressure in the spontaneously hypertensive rats. Hypertension, **49**, 926-931 (2007)
[55] Der Sarkissian, S.; Grobe, J.L.; Yuan, L.; Narielwala, D.R.; Walter, G.A.; Katovich, M.J.; Raizada, M.K.: Cardiac overexpression of angiotensin converting enzyme 2 protects the heart from ischemia-induced pathophysiology. Hypertension, **51**, 712-718 (2008)
[56] Ye, M.; Wysocki, J.; William, J.; Soler, M.J.; Cokic, I.; Batlle, D.: Glomerular localization and expression of angiotensin-converting enzyme 2 and angio-

tensin-converting enzyme: implications for albuminuria in diabetes. J. Am. Soc. Nephrol., **17**, 3067-3075 (2006)
[57] Wiener, R.S.; Cao, Y.X.; Hinds, A.; Ramirez, M.I.; Williams, M.C.: Angiotensin converting enzyme 2 is primarily epithelial and is developmentally regulated in the mouse lung. J. Cell. Biochem., **101**, 1278-1291 (2007)
[58] Rella, M.; Rushworth, C.A.; Guy, J.L.; Turner, A.J.; Langer, T.; Jackson, R.M.: Structure-based pharmacophore design and virtual screening for novel angiotensin converting enzyme 2 inhibitors. J. Chem. Inf. Model., **46**, 708-716 (2006)
[59] Herath, C.B.; Warner, F.J.; Lubel, J.S.; Dean, R.G.; Jia, Z.; Lew, R.A.; Smith, A.I.; Burrell, L.M.; Angus, P.W.: Upregulation of hepatic angiotensin-converting enzyme 2 (ACE2) and angiotensin-(1-7) levels in experimental biliary fibrosis. J. Hepatol., **47**, 387-395 (2007)
[60] Zulli, A.; Burrell, L.M.; Widdop, R.E.; Black, M.J.; Buxton, B.F.; Hare, D.L.: Immunolocalization of ACE2 and AT2 receptors in rabbit atherosclerotic plaques. J. Histochem. Cytochem., **54**, 147-150 (2006)
[61] Mores, A.; Matziari, M.; Beau, F.; Cuniasse, P.; Yiotakis, A.; Dive, V.: Development of potent and selective phosphinic peptide inhibitors of angiotensin-converting enzyme 2. J. Med. Chem., **51**, 2216-2226 (2008)
[62] Fukushi, S.; Mizutani, T.; Sakai, K.; Saijo, M.; Taguchi, F.; Yokoyama, M.; Kurane, I.; Morikawa, S.: Amino acid substitutions in the s2 region enhance severe acute respiratory syndrome coronavirus infectivity in rat angiotensin-converting enzyme 2-expressing cells. J. Virol., **81**, 10831-10834 (2007)
[63] Guo, H.; Guo, A.; Wang, C.; Yan, B.; Lu, H.; Chen, H.: Expression of feline angiotensin converting enzyme 2 and its interaction with SARS-CoV S1 protein. Res. Vet. Sci., **84**, 494-496 (2008)
[64] Koka, V.; Huang, X.R.; Chung, A.C.; Wang, W.; Truong, L.D.; Lan, H.Y.: Angiotensin II up-regulates angiotensin I¯converting enzyme (ACE), but down-regulates ACE2 via the AT1-ERK/p38 MAP kinase pathway. Am. J. Pathol., **172**, 1174-1183 (2008)
[65] Herath. C.B.; Lubel, J.S.; Jia, Z.; Velkoska, E.; Casley, D.; Brown, L.; Tikellis, C.; Burrell, L.M.; Angus, P.W.: Portal pressure responses and angiotensin peptide production in rat liver are determined by relative activity of angiotensin converting enzyme (ACE) and ACE2. Am. J. Physiol. Gastrointest. Liver Physiol., **297**, G98-G106 (2009)
[66] Levy, A.; Yagil, Y.; Bursztyn, M.; Barkalifa, R.; Scharf, S.; Yagil, C.: ACE2 expression and activity are enhanced during pregnancy. Am. J. Physiol. Regul. Integr. Comp. Physiol., **295**, R1953-R1961 (2008)
[67] Feng, Y.; Yue, X.; Xia, H.; Bindom, S.M.; Hickman, P.J.; Filipeanu, C.M.; Wu, G.; Lazartigues, E.: Angiotensin-converting enzyme 2 overexpression in the subfornical organ prevents the angiotensin II-mediated pressor and drinking responses and is associated with angiotensin II type 1 receptor downregulation. Circ. Res., **102**, 729-736 (2008)
[68] Lai, Z.W.; Lew, R.A.; Yarski, M.A.; Mu, F.T.; Andrews, R.K.; Smith, A.I.: The identification of a calmodulin-binding domain within the cytoplasmic tail of angiotensin-converting enzyme-2. Endocrinology, **150**, 2376-2381 (2009)

[69] Rushworth, C.A.; Guy, J.L.; Turner, A.J.: Residues affecting the chloride regulation and substrate selectivity of the angiotensin-converting enzymes (ACE and ACE2) identified by site-directed mutagenesis. FEBS J., **275**, 6033-6042 (2008)
[70] Hernandez Prada, J.A.; Ferreira, A.J.; Katovich, M.J.; Shenoy, V.; Qi, Y.; Santos, R.A.; Castellano, R.K.; Lampkins, A.J.; Gubala, V.; Ostrov, D.A.; Raizada, M.K.: Structure-based identification of small-molecule angiotensin-converting enzyme 2 activators as novel antihypertensive agents. Hypertension, **51**, 1312-1317 (2008)
[71] Huang, Q.; Xie, Q.; Shi, C.C.; Xiang, X.G.; Lin, L.Y.; Gong, B.D.; Zhao, G.D.; Wang, H.; Jia, NN.: Expression of angiotensin-converting enzyme 2 in CCL4-induced rat liver fibrosis. Int. J. Mol. Med., **23**, 717-723 (2009)
[72] Towler, P.; Staker, B.; Prasad, S.G.; Menon, S.; Tang, J.; Parsons,T.; Ryan, D.; Fisher, M.; Williams, D.; Dales, N.A.; Patane, M.A.; Pantoliano, M.W.: ACE2 X-ray structures reveal a large hinge-bending motion important for inhibitor binding and catalysis. J. Biol. Chem., **279**, 17996-18007 (2004)
[73] Ferreira. A.J.; Raizada, M.K.: Are we poised to target ACE2 for the next generation of antihypertensives?. J. Mol. Med., **86**, 685-690 (2008)
[74] Xia, H.; Lazartigues, E.: Angiotensin-converting enzyme 2 in the brain: properties and future directions. J. Neurochem., **107**, 1482-1494 (2008)
[75] Luhtala, S.; Vaajanen, A.; Oksala, O.; Valjakka, J.; Vapaatalo, H.: Activities of angiotensin-converting enzymes ACE1 and ACE2 and inhibition by bioactive peptides in porcine ocular tissues. J. Ocul. Pharmacol. Ther., **25**, 23-28 (2009)
[76] Sluimer, J.C.; Gasc, J.M.; Hamming, I.; van Goor, H.; Michaud, A.; van den Akker, L.H.; Juetten, B.; Cleutjens, J.; Bijnens, A.P.; Corvol, P.; Daemen, M.J.; Heeneman, S.: Angiotensin-converting enzyme 2 (ACE2) expression and activity in human carotid atherosclerotic lesions. J. Pathol., **215**, 273-279 (2008)
[77] Bindom, S.M.; Lazartigues, E.: The sweeter side of ACE2: physiological evidence for a role in diabetes. Mol. Cell. Endocrinol., **302**, 193-202 (2009)
[78] Oudit, G.Y.; Imai, Y.; Kuba, K.; Scholey, J.W.; Penninger, J.M.: The role of ACE2 in pulmonary diseases - relevance for the nephrologist.. Nephrol. Dial. Transplant., **24**, 1362-1365 (2009)
[79] Vaz-Silva, J.; Carneiro, M.M.; Ferreira, M.C.; Pinheiro, S.V.; Silva, D.A.; Silva-Filho, A.L.; Witz, C.A.; Reis, A.M.; Santos, R.A.; Reis, F.M.: The vasoactive peptide angiotensin-(1-7), its receptor Mas and the angiotensin-converting enzyme type 2 are expressed in the human endometrium. Reprod. Sci., **16**, 247-256 (2009)
[80] Zhou, L.; Zhang, R.; Yao, W.; Wang, J.; Qian, A.; Qiao, M.; Zhang, Y.; Yuan, Y.: Decreased expression of Angiotensin-converting enzyme 2 in pancreatic ductal adenocarcinoma is associated with tumor progression. Tohoku J. Exp. Med., **217**, 123-131 (2009)
[81] Clayton, D.; Hanchapola, I.; Perlmutter, P.; Smith, A.I.; Aguilar, M.I.: The active site specificity of angiotensin II converting enzyme 2 investigated through single and multiple residue changes and β-amino acid substrate analogs. Adv. Exp. Med. Biol., **611**, 559-560 (2009)

[82] Trask, A.J.; Groban, L.; Westwood, B.M.; Varagic, J.; Ganten, D.; Gallagher, P.E.; Chappell, M.C.; Ferrario, C.M.: Inhibition of angiotensin-converting enzyme 2 exacerbates cardiac hypertrophy and fibrosis in Ren-2 hypertensive rats. Am. J. Hypertens., **23**, 687-693 (2010)
[83] Iwata, M.; Silva Enciso, J.E.; Greenberg, B.H.: Selective and specific regulation of ectodomain shedding of angiotensin-converting enzyme 2 by tumor necrosis factor α-converting enzyme. Am. J. Physiol. Cell Physiol., **297**, C1318-C1329 (2009)
[84] Jia, H.P.; Look, D.C.; Tan, P.; Shi, L.; Hickey, M.; Gakhar, L.; Chappell, M.C.; Wohlford-Lenane, C.; McCray, P.B.: Ectodomain shedding of angiotensin converting enzyme 2 in human airway epithelia. Am. J. Physiol. Lung Cell Mol. Physiol., **297**, L84-L96 (2009)
[85] Takahashi, Y.; Haga, S.; Ishizaka, Y.; Mimori, A.: Autoantibodies to angiotensin-converting enzyme 2 in patients with connective tissue diseases. Arthritis Res. Ther., **12**, R85 (2010)
[86] Kassiri, Z.; Zhong, J.; Guo, D.; Basu, R.; Wang, X.; Liu, P.P.; Scholey, J.W.; Penninger, J.M.; Oudit, G.Y.: Loss of angiotensin-converting enzyme 2 accelerates maladaptive left ventricular remodeling in response to myocardial infarction. Circ. Heart Fail., **2**, 446-455 (2009)
[87] Huang, M.L.; Li, X.; Meng, Y.; Xiao, B.; Ma, Q.; Ying, S.S.; Wu, P.S.; Zhang, Z.S.: Upregulation of angiotensin-converting enzyme (ACE) 2 in hepatic fibrosis by ACE inhibitors. Clin. Exp. Pharmacol. Physiol., **37**, e1-e6 (2010)
[88] Zhao, Y.; Yin, H.Q.; Yu, Q.T.; Qiao, Y.; Dai, H.Y.; Zhang, M.X.; Zhang, L.; Liu, Y.F.; Wang, L.C.; Liu, D.S.; Deng, B.P.; Zhang, Y.H.; Pang, C.M.; Song, H.D.; Qu, X.; Jiang, H.; Liu, C.X.; Lu, X.T.; Liu, B.; Gao, F.; Dong, B.: ACE2 overexpression improves left ventricular remodeling and function in rats with myocardial infarction. Hum. Gene Ther., **21**, 1545-1554 (2010)
[89] Xia, H.; Feng, Y.; Obr, T.D.; Hickman, P.J.; Lazartigues, E.: Angiotensin II type 1 receptor-mediated reduction of angiotensin-converting enzyme 2 activity in the brain impairs baroreflex function in hypertensive mice. Hypertension, **53**, 210-216 (2009)
[90] Masson, R.; Nicklin, S.A.; Craig, M.A.; McBride, M.; Gilday, K.; Gregorevic, P.; Allen, J.M.; Chamberlain, J.S.; Smith, G.; Graham, D.; Dominiczak, A.F.; Napoli, C.; Baker, A.H.: Onset of experimental severe cardiac fibrosis is mediated by overexpression of angiotensin-converting enzyme 2. Hypertension, **53**, 694-700 (2009)
[91] Stewart, J.M.; Ocon, A.J.; Clarke, D.; Taneja, I.; Medow, M.S.: Defects in cutaneous angiotensin-converting enzyme 2 and angiotensin-(1-7) production in postural tachycardia syndrome. Hypertension, **53**, 767-774 (2009)
[92] Yoshikawa, N.; Yoshikawa, T.; Hill, T.; Huang, C.; Watts, D.M.; Makino, S.; Milligan, G.; Chan, T.; Peters, C.J.; Tseng, C.T.: Differential virological and immunological outcome of severe acute respiratory syndrome coronavirus infection in susceptible and resistant transgenic mice expressing human angiotensin-converting enzyme 2. J. Virol., **83**, 5451-5465 (2009)
[93] Fraga-Silva, R.A.; Sorg, B.S.; Wankhede, M.; Dedeugd, C.; Jun, J.Y.; Baker, M.B.; Li, Y.; Castellano, R.K.; Katovich, M.J.; Raizada, M.K.; Ferreira, A.J.:

ACE2 activation promotes antithrombotic activity. Mol. Med., **16**, 210-215 (2010)
[94] Feng, Y.; Wan, H.; Liu, J.; Zhang, R.; Ma, Q.; Han, B.; Xiang, Y.; Che, J.; Cao, H.; Fei, X.; Qiu, W.: The angiotensin-converting enzyme 2 in tumor growth and tumor-associated angiogenesis in non-small cell lung cancer. Oncol. Rep., **23**, 941-948 (2010)
[95] Lin, C.S.; Pan, C.H.; Wen, C.H.; Yang, T.H.; Kuan, T.C.: Regulation of angiotensin converting enzyme II by angiotensin peptides in human cardiofibroblasts. Peptides, **31**, 1334-1340 (2010)
[96] Coelho, M.S.; Lopes, K.L.; Freitas, R.d.e.A.; de Oliveira-Sales, E.B.; Bergasmaschi, C.T.; Campos, R.R.; Casarini, D.E.; Carmona, A.K.; Araujo, M.d.a..S.; Heimann, J.C.; Dolnikoff, M.S.: High sucrose intake in rats is associated with increased ACE2 and angiotensin-(1-7) levels in the adipose tissue. Regul. Pept., **162**, 61-67 (2010)
[97] Han, S.X.; He, G.M.; Wang, T.; Chen, L.; Ning, Y.Y.; Luo, F.; An, J.; Yang, T.; Dong, J.J.; Liao, Z.L.; Xu, D.; Wen, F.Q.: Losartan attenuates chronic cigarette smoke exposure-induced pulmonary arterial hypertension in rats: possible involvement of angiotensin-converting enzyme-2. Toxicol. Appl. Pharmacol., **245**, 100-107 (2010)

SARS coronavirus main proteinase 3.4.22.69

1 Nomenclature

EC number
3.4.22.69

Recommended name
SARS coronavirus main proteinase

Synonyms
3C-like protease <2,3> [9,16,38,49,51]
3CL protease <2> [14,48]
3cLpro <1,2,3> [7,11,13,16,19,28,38,49,51]
C30.004 (Merops-ID)
Mpro
SARS 3C-like protease <2> [17]
SARS 3C-like proteinase <2> [15,18,27]
SARS 3CL protease <2> [31]
SARS 3CLpro <2> [49]
SARS CoV main proteinase <2> [1,2,4,5]
SARS CoVMpro <2> [33]
SARS Mpro <2> [25]
SARS coronavirus 3C-like protease <2> [48]
SARS coronavirus 3C-like proteinase <2> [50]
SARS coronavirus 3CL protease <2> [20]
SARS coronavirus main peptidase <2> [23]
SARS coronavirus main protease <2> [25]
SARS coronavirus main proteinase <2> [5,33]
SARS main protease <2> [12,25]
SARS-3CL protease <2> [48]
SARS-3CLpro <2> [29,50]
SARS-CoV 3C-like peptidase <2> [24]
SARS-CoV 3C-like protease <1> [19]
SARS-CoV 3CL protease <2> [22,30,44,46]
SARS-CoV 3CLpro <2> [32,36,38,44,45]
SARS-CoV 3CLpro enzyme <2> [11]
SARS-CoV Mpro <2> [21,40]
SARS-CoV main protease <2> [21,26,43]
SARS-coronavirus 3CL protease <2> [8]
SARS-coronavirus main protease <2> [47]
TGEV Mpro
coronavirus 3C-like protease <1> [19]

D. Schomburg and I. Schomburg (eds.), *Class 3.4–6 Hydrolases, Lyases, Isomerases, Ligases: EC 3.4–6*, Springer Handbook of Enzymes S10, DOI 10.1007/978-3-642-36260-6_3,

porcine transmissible gastroenteritis virus Mpro
severe acute respiratory syndrome coronavirus 3C-like protease <2> [41,42]
severe acute respiratory syndrome coronavirus main protease <2> [21]
severe acute respiratory syndrome coronavirus main proteinase <2> [33]

CAS registry number
218925-73-6
37353-41-6

2 Source Organism

<1> *alphacoronavirus* [19]
<2> *SARS coronavirus* [1,2,3,4,5,6,7,8,9,10,11,12,13,14,15,16,17,18,20,21,22,23,24,25,26,27,28,29,30,31,32,33,34,35,36,37,38,39,40,41,42,43,44,45,46,47,48,49,50]
<3> *SARS coronavirus Tor2* (UNIPROT accession number: P0C6U8) [51]

3 Reaction and Specificity

Catalyzed reaction
TSAVLQ-/-SGFRK-NH_2 and SGVTFQ-/-GKFKK the two peptides corresponding to the two self-cleavage sites of the SARS 3C-like proteinase are the two most reactive peptide substrates. The enzyme exhibits a strong preference for substrates containing Gln at P1 position and Leu at P2 position.

Reaction type
hydrolysis of peptide bond

Natural substrates and products
S coronavirus polyprotein + H_2O <2> (<2> 3CLpro processes the translated polyproteins to functional viral proteins [28]) (Reversibility: ?) [28]
P ?
S Additional information <2> (<2> SARS-CoV 3CLpro mediates extensive proteolytic processing of two overlapping replicase polyproteins, pp1a (486000 Da) and pp1ab (790000 Da), to yield the corresponding functional polypeptides that are essential for SARSCoV replication and transcription processes [42]; <2> the genomic RNA produces two large proteins with overlapping sequences, polyproteins 1a and 1ab, which are autocatalytically cleaved by two or three viral proteases to yield functional polypeptides. The key enzyme in this processing is SARS 3CL protease [31]; <2> 3CLpro cleaves the replicase polyproteins at 11 sites with the conserved Gln-(Ser, Ala, Gly) sequences [49]) (Reversibility: ?) [31,42,49]
P ?

Substrates and products

- **S** (Ala-Arg-Leu-Gln-NH)$_2$-rhodamine <2> (Reversibility: ?) [3]
- **P** rhodamine 110 + (Ala-Arg-Leu-Gln-NH)-rhodamine
- **S** (CAL fluor red 610)-TSAVLQSGFRK(BHQ1) + H_2O <2> (Reversibility: ?) [8]
- **P** (CAL fluor red 610)-TSAVLQ + SGFRK(BHQ1)
- **S** 2-aminobenzoyl-SVTLQSG-Tyr(NO_2)Arg + H_2O <2> (Reversibility: ?) [28]
- **P** ?
- **S** 2-aminobenzoyl-TSAVLQSGFRK-2,4-dinitrophenyl amide + H_2O <2> (Reversibility: ?) [26]
- **P** 2-aminobenzoyl-TSAVLQ + SGFRK-2,4-dinitrophenyl amide
- **S** AAVLQSGF$^-NH_2$ + H_2O <2> (Reversibility: ?) [15]
- **P** AAVLQ + SGF-NH_2
- **S** ATVRLQAGNAT + H_2O <2> (Reversibility: ?) [15,27]
- **P** ATVRLQ + AGNAT
- **S** AVLQS-NH_2 + H_2O <2> (Reversibility: ?) [15]
- **P** AVLQ + L-serinamide
- **S** AVLQSE-NH_2 + H_2O <2> (Reversibility: ?) [15]
- **P** AVLQ + Ser-Glu-NH_2
- **S** AVLQSGF-NH_2 + H_2O <2> (Reversibility: ?) [15]
- **P** AVLQ + SGF-NH_2
- **S** DABCYL-Lys-Asn-Ser-Thr-Leu-Gln-Ser-Gly-Leu-Arg-Lys-Glu-EDANS + H_2O <2> (Reversibility: ?) [45]
- **P** DABCYL-Lys-Asn-Ser-Thr-Leu-Gln + Ser-Gly-Leu-Arg-Lys-Glu-EDANS
- **S** DABCYL-Lys-Thr-Ser-Ala-Val-Leu-Gln-Ser-Gly-Phe-Arg-Lys-Met-Glu-EDANS + H_2O <2> (Reversibility: ?) [44]
- **P** DABCYL-Lys-Thr-Ser-Ala-Val-Leu-Gln + Ser-Gly-Phe-Arg-Lys-Met-Glu-EDANDS
- **S** DABCYL-Lys-Thr-Ser-Ala-Val-Leu-Gln-Ser-Gly-Phe-Arg-Lys-Met-Glu-EDANS + H_2O <2> (Reversibility: ?) [46,49]
- **P** DABCYL-Lys-Thr-Ser-Ala-Val-Leu-Gln + Ser-Gly-Phe-Arg-Lys-Met-Glu-EDANS
- **S** Dabcyl-KNSTLQSGLRKE-EDANS + H_2O <2> (Reversibility: ?) [35]
- **P** Dabcyl-KNSTLQ + SGLRKE-EDANS
- **S** Dabcyl-KTSAVLQSGFRKME-EDANS + H_2O <2> (Reversibility: ?) [36,38]
- **P** Dabcyl-KTSAVLQ + SGFRKME-EDANS
- **S** Dabcyl-KTSAVLQSGFRKMQ-EDANS + H_2O <2> (Reversibility: ?) [34]
- **P** Dabcyl-KTSAVLQ + SGFRKMQ-EDANS
- **S** EDANS-VNSTLQSGLRK-(Dabcyl)-M + H_2O <2> (Reversibility: ?) [37]
- **P** EDANS-VNSTLQ + SGLRK-(Dabcyl)-M
- **S** FYPKLQASQAW + H_2O <2> (Reversibility: ?) [15,27]
- **P** FYPKLQ + ASQAW
- **S** GPFVDRQTAQAAGTDT-NH_2 + H_2O <2> (<2> 1% of the activity with TSAVLQSGFRK-NH_2 [31]) (Reversibility: ?) [31]
- **P** ?
- **S** KVATVQSKMSD + H_2O <2> (Reversibility: ?) [15]
- **P** KVATVQ+ SKMSD

S KVATVQSKMSD + H_2O <2> (<2> weak activity [27]) (Reversibility: ?) [27]
P KVATVQ + SKMSD
S KVATVQSKMSD-NH_2 <2> (<2> undecapeptide containing the non-canonical P3/P4 cleavage site of 3CL protease, 6% of the activity with TSAVLQSGFRK-NH_2 [31]) (Reversibility: ?) [31]
P ?
S L-Thr-L-Ser-L-Ala-L-Val-L-Leu-L-Gln-4-nitroanilide + H_2O <2> (Reversibility: ?) [48]
P L-Thr-L-Ser-L-Ala-L-Val-L-Leu-L-Gln + 4-nitroaniline
S LAVLQSGF-NH_2 + H_2O <2> (Reversibility: ?) [15]
P LAVLQ + SGF-NH_2
S LQSG-NH_2 + H_2O <2> (Reversibility: ?) [15]
P Leu-Gln + Ser-Gly-NH_2
S MCAAVLQSGFR-Lys(Dnp)-Lys-NH_2 + H_2O <2> (Reversibility: ?) [40]
P MCAAVLQ + Ser-Gly-Phe-Arg-Lys(Dnp)-Lys-NH_2
S NRATLQAIASE + H_2O <2> (<2> weak activity [27]) (Reversibility: ?) [15,27]
P NRATLQ + AIASE
S NVATLQAENVT + H_2O <2> (<2> weak activity [27]) (Reversibility: ?) [15,27]
P NVATLQ + AENVT
S PATVLQAVGAC + H_2O <2> (Reversibility: ?) [15]
P PATVLQ + AVGAC
S PHTVLQAVGAC + H_2O <2> (Reversibility: ?) [27]
P PHTVLQ + AVGAC
S REPLMQSADAS + H_2O <2> (<2> weak activity [27]) (Reversibility: ?) [15,27]
P REPLMQ + SADAS
S SAALQSGF-NH_2 + H_2O <2> (Reversibility: ?) [15]
P SAALQ + SGF-NH_2
S SAKLQSGF-NH_2 + H_2O <2> (Reversibility: ?) [15]
P SAKLQ + SGF-NH_2
S SALLQSGF-NH_2 + H_2O <2> (Reversibility: ?) [15]
P SALLQ + SGF-NH_2
S SATLQSGF-NH_2 + H_2O <2> (Reversibility: ?) [15]
P SATLQ + SGF-NH_2
S SAVAQSGF-NH_2 + H_2O <2> (Reversibility: ?) [15]
P SAVAQ + SGF-NH_2
S SAVFQSGF-NH_2 + H_2O <2> (Reversibility: ?) [15]
P SAVMQ + SGF-NH_2
S SAVIQSGF-NH_2 + H_2O <2> (Reversibility: ?) [15]
P SAVIQ + SGF-NH_2
S SAVKLQNNELS + H_2O <2> (<2> weak activity [27]) (Reversibility: ?) [15,27]
P SAVKLQ + NNELS
S SAVLESGF-NH_2 + H_2O <2> (Reversibility: ?) [15]

P SAVLE + SGF-NH_2
S SAVLKSGF-NH_2 + H_2O <2> (Reversibility: ?) [15]
P SAVLK + SGF-NH_2
S SAVLNSGF-NH_2 + H_2O <2> (Reversibility: ?) [15]
P SAVLN + SGF-NH_2
S SAVLQAGF-NH_2 + H_2O <2> (Reversibility: ?) [15]
P SAVLQ + AGF-NH_2
S SAVLQEGFRK + H_2O <2> (<2> the cleavage rate of the mutant enzyme T25G is remarkably higher compared to the wild type enzyme [49]) (Reversibility: ?) [49]
P SAVLQ + EGFRK
S SAVLQFGFRK + H_2O <2> (<2> the cleavage rate of the mutant enzyme T25G is remarkably higher compared to the wild type enzyme [49]) (Reversibility: ?) [49]
P SAVLQ + FGFRK
S SAVLQGGF-NH_2 + H_2O <2> (Reversibility: ?) [15]
P SAVLQ + GGF-NH_2
S SAVLQGGFRK + H_2O <2> (<2> the cleavage rate of the mutant enzyme T25G is similar to the wild type enzyme [49]) (Reversibility: ?) [49]
P SAVLQ + GGFRK
S SAVLQHGFRK + H_2O <2> (<2> low activity [49]) (Reversibility: ?) [49]
P SAVLQ + HGFRK
S SAVLQKGFRK + H_2O <2> (<2> low activity [49]) (Reversibility: ?) [49]
P SAVLQ + KGFRK
S SAVLQLGF-NH_2 + H_2O <2> (Reversibility: ?) [15]
P SAVLQ + LGF-NH_2
S SAVLQLGFRK + H_2O <2> (<2> the cleavage rate of the mutant enzyme T25G is remarkably higher compared to the wild type enzyme [49]) (Reversibility: ?) [49]
P SAVLQ + LGFRK
S SAVLQMGFRK + H_2O <2> (<2> the cleavage rate of the mutant enzyme T25G is remarkably higher compared to the wild type enzyme [49]) (Reversibility: ?) [49]
P SAVLQ + MGFRK
S SAVLQSGF-NH_2 + H_2O <2> (Reversibility: ?) [15]
P SAVLQ + SGF-NH_2
S SAVLQSGFRK + H_2O <2> (<2> best substrate for both, wild type and mutant enzyme T25G [49]) (Reversibility: ?) [38,49]
P SAVLQ + SGFRK
S SAVLQWGFRK + H_2O <2> (<2> low activity [49]) (Reversibility: ?) [49]
P SAVLQ + WGFRK
S SAVMQSGF-NH_2 + H_2O <2> (Reversibility: ?) [15]
P SAVMQ + SGF-NH_2
S SAVRQSGF-NH_2 + H_2O <2> (Reversibility: ?) [15]
P SAVRQ + SGF-NH_2
S SAVVQSGF-NH_2 + H_2O <2> (Reversibility: ?) [15]
P SAVVQ + SGF-NH_2

S SGVTFQGKFKK + H_2O <2> (<2> highest cleavage efficiency. The two peptides corresponding to the two self-cleavage sites of the SARS 3C-like proteinase are the two most reactive ones [27]) (Reversibility: ?) [15,27]
P SGVTFQ + GKFKK
S SITSAVLQ-*p*-nitroanilide + H_2O <2> (Reversibility: ?) [7]
P ?
S SITSAVLQ-*p*-nitrophenyl ester + H_2O <2> (Reversibility: ?) [7]
P ?
S SITSAVLQSGFRKMA + H_2O <2> (Reversibility: ?) [7]
P ?
S SLVLQSGF-NH_2 + H_2O <2> (Reversibility: ?) [15]
P SLVLQ + SGF-NH_2
S STVLQSGF-NH_2 + H_2O <2> (Reversibility: ?) [15]
P STVLQ + SGF-NH_2
S SVVLQSGF-NH_2 + H_2O <2> (Reversibility: ?) [15]
P SVVLQ + SGF-NH_2
S SWTSAVLQSGFRKWA + H_2O <2> (Reversibility: ?) [4]
P ?
S Ser-Ala-Val-Leu-Gln-Leu-Gly-Phe-Arg-Lys + H_2O <2> (<2> substrate for T25G mutant protein [49]) (Reversibility: ?) [49]
P Ser-Ala-Val-Leu-Gln + Leu-Gly-Phe-Arg-Lys
S Ser-Ala-Val-Leu-Gln-Met-Gly-Phe-Arg-Lys + H_2O <2> (Reversibility: ?) [49]
P Ser-Ala-Val-Leu-Gln + Met-Gly-Phe-Arg-Lys
S Ser-Ala-Val-Leu-Gln-Ser-Gly-Phe-Arg-Lys + H_2O <2> (Reversibility: ?) [49]
P Ser-Ala-Val-Leu-Gln + Ser-Gly-Phe-Arg-Lys
S TAVLQSGF-NH_2 + H_2O <2> (Reversibility: ?) [15]
P TAVLQ + SGF-NH_2
S TFTRLQSLENV + H_2O <2> (Reversibility: ?) [15,27]
P TFTRLQ + SLENV
S TSAVLQSGFRK-NH_2 + H_2O <2> (<2> highest cleavage efficiency. The two peptides corresponding to the two self-cleavage sites of the SARS 3C-like proteinase are the two most reactive ones [27]; <2> peptide containing the P1/P2 cleavage site, the N-terminal self-cleavage site of the protease, most suitable substrate [31]) (Reversibility: ?) [15,27,31]
P TSAVLQ + SGFRK-NH_2
S TVILQAGF + H_2O <2> (Reversibility: ?) [33]
P TVILQ + Ala-Gly-Phe
S TVKLQAGF + H_2O <2> (Reversibility: ?) [33]
P TVKLQ + Ala-Gly-Phe
S TVKLQAGF-NH_2 + H_2O <2> (Reversibility: ?) [15]
P TVKLQ + AGF-NH_2
S TVRLQAGF + H_2O <2> (Reversibility: ?) [33]
P TVRLQ + Ala-Gly-Phe
S TVTLQSGF-NH_2 + H_2O <2> (Reversibility: ?) [15]
P TVTLQ + SGF-NH_2

S TVVLQSGF-NH_2 + H_2O <2> (Reversibility: ?) [15]
P TVVLQ + SGF-NH_2
S Thr-Ser-Ala-Val-Leu-Gln-*p*-nitroanilide + H_2O <2> (Reversibility: ?) [47,48,50]
P Thr-Ser-Ala-Val-Leu-Gln + *p*-nitroaniline
S VLQS-NH_2 + H_2O <2> (Reversibility: ?) [15]
P VLQ + L-serinamide
S VLQSG-NH_2 + H_2O <2> (Reversibility: ?) [15]
P VLQ + Ser-Gly-NH2
S VVTLQSGF¯NH_2 + H_2O <2> (Reversibility: ?) [15]
P VVTLQ + SGF-NH_2
S [4-(4-dimethylaminophenylazo)benzoic acid]-KNSTLQSGLRKE-[5-[2'-(aminoethyl)amino]-naphthalenesulfonic acid] + H_2O <2> (Reversibility: ?) [9]
P ?
S [4-(4-dimethylaminophenylazo)benzoic acid]-KTSAVLQSGF RKME-[5-[2'-(aminoethyl)amino]-naphthalenesulfonic acid] + H_2O <2> (Reversibility: ?) [17]
P ?
S [4-(4-dimethylaminophenylazo)benzoic acid]-KTSAVLQSGFRKME-[5-[2'-(aminoethyl)amino]-naphthalenesulfonic acid] + H_2O <2> (Reversibility: ?) [7,13]
P ?
S [4-(4-dimethylaminophenylazo)benzoic acid]-VNSTLQSGLRK-[5-[2'-(aminoethyl)amino]-naphthalenesulfonic acid]-M + H_2O <1> (Reversibility: ?) [19]
P ?
S acetyl-TSAVLH-7-amido-4-carbamoyl-coumarin + H_2O <2> (<2> SARS-CoV 3Clpro prefers Gln over His in P1 position. Unlike SARS-CoV 3Clpro, His is strongly preferred in the P1 position by 3C-like proteases from infectious bronchitis virus murine hepatitis virus [6]) (Reversibility: ?) [6]
P acetyl-TSAVLH + 7-amino-4-carbamoyl-coumarin
S acetyl-TSTKLQ-7-amido-4-carbamoyl-coumarin + H_2O <2> (<2> optimized fluorogenic peptide substrate. The enzyme exhibits a strong preference for P1 Gln containing substrates and P2 Leu containing substrates [6]) (Reversibility: ?) [6]
P acetyl-TSTKLQ + 7-amino-4-carbamoyl-coumarin
S coronavirus polyprotein + H_2O <2> (<2> 3CLpro processes the translated polyproteins to functional viral proteins [28]) (Reversibility: ?) [28]
P ?
S dabcyl-KTSAVLQSGFRKME-EDANS + H_2O <2> (Reversibility: ?) [49]
P ?
S *o*-aminobenzoyl-TSAVLQSGFRY(3-NO2)G + H_2O <2> (Reversibility: ?) [8]
P *o*-aminobenzoyl-TSAVLQ + SGFRY(3-NO_2)G
S Additional information <2> (<2> a 3CLpro mechanism utilizes an electrostatic trigger to initiate the acylation reaction, a cysteine-histidine catalytic dyad ion pair, an enzyme-facilitated release of P1, and a general

base catalyzed deacylation reaction [7]; <2> complete description of the tetrapeptide substrate specificity of 3Clpro using fully degenerate peptide libraries consisting of all 160 000 possible naturally occurring tetrapeptides. P1-Gln P2-Leu specificity and elucidate a novel preference for P1-His containing substrates equal to the expected preference for P1-Gln [6]; <2> SARS-CoV 3CLpro mediates extensive proteolytic processing of two overlapping replicase polyproteins, pp1a (486000 Da) and pp1ab (790000 Da), to yield the corresponding functional polypeptides that are essential for SARSCoV replication and transcription processes [42]; <2> the genomic RNA produces two large proteins with overlapping sequences, polyproteins 1a and 1ab, which are autocatalytically cleaved by two or three viral proteases to yield functional polypeptides. The key enzyme in this processing is SARS 3CL protease [31]; <2> a complete description of the tetrapeptide substrate specificity of 3Clpro using fully degenerate peptide libraries consisting of all 160000 possible naturally occurring tetrapeptides. The enzyme exhibits a strong preference for P1 Gln containing substrates and P2 Leu containing substrates. The enzyme also shows a strong preference for P1 histidine containing substrates. 3Clpro has extended substrate specificity at P5 and P6 preferring hydrophobic amino acids such as Leu [6]; <2> comprehensive overview of SARS-CoV 3CLpro substrate specificity. The hydrophobic pocket in the P2 position at the protease cleavage site is crucial to SARS-CoV 3CLpro-specific binding, which is limited to substitution by hydrophobic residue. The binding interface of SARS-CoV 3CLpro that is facing the P1 position is suggested to be occupied by acidic amino acids, thus the P1 position is intolerant to acidic residue substitution, owing to electrostatic repulsion. Steric hindrance caused by some bulky or branching amino acids in P3 and P2 positions may also hinder the binding of SARS-CoV 3CLpro. In addition to the conserved Gln residue in the P1 position at the SARS-CoV 3CLpro cleavage site, the P2 position, which is exclusively occupied by Leu residue, also serves as another important determinant of substrate specificity. Peptide substrate with Phe replacement in the P2 position is also favorable for SARSCoV 3CLpro cleavage. Ile is intolerant in the P2 position. P1 position, which is frequently occupied by Ser residue, also contributes to the substrate specificity of SARS-CoV 3CLpro considerably. The P1 position is highly unfavorable to the substitution by Pro, Asp, and Glu residues. The substrate specificity of SARS-CoV 3CLpro is less dependent on the P2 and P3 positions at the cleavage site. The peptide cleavage results show that the P3 and P4 positions have no effect on determining the substrate specificity preferences of SARS-CoV 3CLpro [42]; <2> cuts the 11 peptides covering all of the 11 cleavage sites on the viral polyprotein with different efficiency [27]; <2> the S3 subsite of the SARS CoVMpro has a negative character. The electrostatic interactions between Glu47 and P3Lys play a key role in specific binding. These observations are very important and provide further information for structural-based drug design against SARS virus [33]; <2> 3CLpro cleaves the replicase polyproteins at 11 sites

with the conserved Gln-(Ser, Ala, Gly) sequences [49]; <2> no cleavage of SAVLQPGFRK [49]) (Reversibility: ?) [6,7,27,31,33,42,49]

P ?

Inhibitors

(S)-2-((2S,3R)-2-((S)-2-acetamido-3-methylbutanamido)-3-(benzyloxy)butanamido)-4-methyl-N-((S)-4-(5-nitro-1,4-dioxo-3,4-dihydrophthalazin-2(1H)-yl)-3-oxo-1-((S)-2-oxopyrrolidin-3-yl)butan-2-yl)pentanamide <2> [15]
1,1'-sulfonylbis(4-nitrobenzene) <2> [21]
1-(1-benzothiophen-2-ylmethyl)-5-iodo-1H-indole-2,3-dione <2> [15,16]
1-(2-naphthlmethyl)isatin-5-carboxamide <2> [50]
1-(2-naphthylmethyl)-2,3-dioxoindoline-5-carboxamide <2> [15]
1-[(1H-benzimidazol-5-ylcarbonyl)oxy]-1H-1,2,3-benzotriazole <2> (<2> inhibition and irreversible mechanism-based inactivators, no irreversible inactivation with the C_{14}5A mutant enzyme [13]) [13]
1-[(1H-indol-2-ylcarbonyl)oxy]-1H-1,2,3-benzotriazole <2> (<2> inhibition and irreversible mechanism-based inactivators, no irreversible inactivation with the C145A mutant enzyme [13]) [13]
1-[(1H-indol-5-ylcarbonyl)oxy]-1H-1,2,3-benzotriazole <2> (<2> inhibition and irreversible mechanism-based inactivators, no irreversible inactivation with the C145A mutant enzyme [13]) [13]
1-[(1H-indol-5-ylcarbonyl)oxy]-1H-benzotriazole <2> [32]
1-[(4-chlorophenyl)sulfonyl]-2-nitro-4-(trifluoromethyl)benzene <2> [21]
1-[[(5-fluoro-1H-indol-2-yl)carbonyl]oxy]-1H-1,2,3-benzotriazole <2> (<2> inhibition and irreversible mechanism-based inactivators, no irreversible inactivation with the C145A mutant enzyme [13]) [13]
1-[bis(4-chlorophenyl)methyl]-3-[2-[(2,4-dichlorobenzyl)oxy]-2-(2,4-dichlorophenyl)ethyl]-1H-imidazol-3-ium <2> [15]
1-butyl-N-[4-(3,5-diphenyl-4,5-dihydro-1H-pyrazol-1-yl)benzyl]-1H-benzimidazol-2-amine <2> [36]
1-hydroxypyridine-2-thione zinc <2> [16]
2',5'-dimethyl-3-(methylthio)-4'-nitro-5-(2-thienyl)-2'H-1,3'-bipyrazole-4-carbonitrile <2> [21]
2,2-difluoro-2-(pyridin-3-yl)-1-(thiophen-2-yl)ethanone <2> (<2> 0.1 mM, 38% inhibition [28]) [28]
2,4-dichloro-5-methylphenyl 2,6-dinitro-4-(trifluoromethyl)phenyl sulfone <2> [21]
2,5-bis[[(benzyloxy)carbonyl]amino]-1,2,5,6-tetradeoxy-1,6-di-1H-indol-3-yl-L-iditol <2> [14]
2-(3',4'-dihydroxyphenyl)-3-β-D-galactosyl-4H-chromen-4-one <2> (<2> 0.05 mM, 30.1% inhibition [9]) [9]
2-(3',4'-dihydroxyphenyl)-5,7-dihydroxy-3-β-D-arobinosyl-4H-chromen-4-one <2> (<2> 0.05 mM, 49.4% inhibition [9]) [9]
2-(3',4'-dihydroxyphenyl)-5,7-dihydroxy-3-β-D-galactosyl-4H-chromen-4-one <2> (<2> 0.05 mM, 41.8% inhibition [9]) [9]
2-(3',4'-dihydroxyphenyl)-5,7-dihydroxy-3-β-D-glucosyl-4H-chromen-4-one <2> (<2> 0.05 mM, 57.5% inhibition [9]) [9]

2-(3',4'-dihydroxyphenyl)-5,7-dihydroxy-3-β-L-fucosyl-4H-chromen-4-one <2> (<2> 0.05 mM, 57.4% inhibition [9]) [9]
2-(3',4'-dihydroxyphenyl)-5-hydroxy-3,7-di(β-D-galactosyl)-4H-chromen-4-one <2> (<2> 0.05 mM, 53.0% inhibition [9]) [9]
2-(3-chlorophenyl)-2,2-difluoro-1-(furan-2-yl)ethanone <2> (<2> 0.1 mM, 13% inhibition [28]) [28]
2-(3-chlorophenyl)-2-fluoro-1-(furan-2-yl)ethanone <2> (<2> 0.1 mM, 15% inhibition [28]) [28]
2-(4,5-dihydro-1,3-thiazol-2-yl)-1-(1,3-thiazol-2-yl)ethanone <2> [21]
2-(4-aminophenyl)-6-methyl-1H-benzimidazole-7-sulfonic acid <2> [15,16]
2-(5-bromopyridin-3-yl)-2,2-difluoro-1-(furan-2-yl)ethanone <2> (<2> 0.1 mM, 21% inhibition [28]) [28]
2-(5-chloropyridin-3-yl)-2,2-difluoro-1-(furan-2-yl)ethanone <2> (<2> 0.1 mM, 27% inhibition [28]) [28]
2-(5-chloropyridin-3-yl)-2-fluoro-1-(furan-2-yl)ethanone <2> (<2> 0.1 mM, 14% inhibition [28]) [28]
2-([N-[(benzyloxy)carbonyl]-L-alanyl-L-valyl]amino)-5-[[(2S,5S)-5-[[(benzyloxy)carbonyl]amino]-2-(1-methylethyl)-4-oxohexanoyl]amino]-1,2,5,6-tetradeoxy-1,6-diphenyl-L-iditol <2> [15]
2-(benzylsulfanyl)-4-(3-chlorophenyl)-6-oxo-1,6-dihydropyrimidine-5-carbonitrile <2> [46]
2-(benzylsulfanyl)-4-(4-methoxyphenyl)-6-oxo-1,6-dihydropyrimidine-5-carbonitrile <2> [46]
2-(benzylsulfanyl)-4-(4-methylphenyl)-6-oxo-1,6-dihydropyrimidine-5-carbonitrile <2> [46]
2-(benzylsulfanyl)-6-oxo-4-phenyl-1,6-dihydropyrimidine-5-carbonitrile <2> [46]
2-[(1H-1,2,3-benzotriazol-1-yloxy)carbonyl]aniline <2> (<2> inhibition and irreversible mechanism-based inactivators, no irreversible inactivation with the C145A mutant enzyme [13]) [13]
2-[(2-acetylphenyl)sulfonyl]benzoic acid <2> [21]
2-[(2-cyclohexylquinazolin-4-yl)sulfanyl]-N-(furan-2-ylmethyl)acetamide <2> (<2> 0.01 mM, 30% inhibition [29]) [29]
2-[(4-chlorophenyl)sulfonyl]-5-nitropyridine 1-oxide <2> [21]
2-[(4-nitrobenzyl)sulfanyl]-4-(3-nitrophenyl)-6-oxo-1,6-dihydropyrimidine-5-carbonitrile <2> [46]
2-[(4-nitrobenzyl)sulfanyl]-6-oxo-4-phenyl-1,6-dihydropyrimidine-5-carbonitrile <2> [46]
2-acetyl-3-(3-iodophenyl)-7-methoxy-3,3a,4,5-tetrahydro-2H-benzo[g]indazole <2> [36]
2-benzyl-2H-isoindole-4,7-dione <2> [36]
2-fluoro-2-(pyridin-3-yl)-1-(thiophen-2-yl)ethanone <2> (<2> 0.1 mM, 10% inhibition [28]) [28]
2-phenyl-5,7-dihydroxy-3-β-D-galactosyl-4H-chromen-4-one <2> (<2> 0.05 mM, 18.7% inhibition [9]) [9]
2-phenylethyl 2-methyl-4-(2-nitrophenyl)-5-oxo-1,4,5,6,7,8-hexahydroquinoline-3-carboxylate <2> [15]

3,4-dichloro-5-[2-(5-chloro-3-methyl-1-benzothien-2-yl)-2-oxoethyl]furan-2(5H)-one <2> [15,16]
3,4-dichloro-5-[2-(5-chloro-3-methyl-1-benzothiophen-2-yl)-2-oxoethyl]furan-2(5H)-one <2> [16]
3-(4-bromophenyl)-5-(4-chlorophenyl)-1-(3,4-dichlorophenyl)-4-(1H-imidazol-1-yl)-4,5-dihydro-1H-pyrazole <2> [36]
3-(N-L-γ-Glu-L-Ala)-1,1,1-trifluoropropan-2-one <2> [30]
3-[(2-furylmethyl)amino]-6,6-dimethyl-4-oxo-4,5,6,7-tetrahydro-2-benzothiophene-1-carbonitrile <2> [21]
3-[N-(N-benzyloxycarbonyl-L-Leu)]-4-phenyl-1,1,1-trifluorobutan-2-one <2> [30]
3-[N-(N-benzyloxycarbonyl-L-Phe)]-4-phenyl-1,1,1-trifluorobutan-2-one <2> [30]
3-[N-(N-tert-butoxycarbonyl)-L-Leu]-1,1,1-trifluorobutan-2-one <2> [30]
3-[N-[N-benzyloxycarbonyl-L-Ala-L-Val-L-Leu]]-4-phenyl-1,1,1-trifluorobutan-2-one <2> [30]
3-[N-[N-decanoyl-L-Leu]]-4-phenyl-1,1,1-trifluorobutan-2-one <2> [30]
3-benzyl-1-[(6,7-dimethyl-2-oxo-1,2-dihydroquinolin-3-yl)methyl]-1-[2-(2-methylphenyl)ethyl]urea <2> (<2> 0.01 mM, 40% inhibition [29]) [29]
3-{N-[N-tert-butoxycarbonyl-L-γ-Glu(OtBu)-L-Ala]}-1,1,1-trifluoropropan-2-one <2> [30]
4,5-anhydro-2-([N-[(benzyloxy)carbonyl]-L-phenylalanyl]amino)-1,2-dideoxy-D-erythro-pent-3-ulose <2> [6]
4,6-dimethyl-2-[(4-methylphenyl)sulfonyl]-5-nitronicotinonitrile <2> [21]
4,6-dimethyl-5-nitro-2-(phenylsulfonyl)nicotinonitrile <2> [21]
4-(3-nitrophenyl)-6-oxo-2-[(2-phenylethyl)sulfanyl]-1,6-dihydropyrimidine-5-carbonitrile <2> [46]
4-(4-chlorophenyl)-2-[(4-nitrobenzyl)sulfanyl]-6-oxo-1,6-dihydropyrimidine-5-carbonitrile <2> [46]
4-(4-chlorophenyl)-6-oxo-2-[(2-phenylethyl)sulfanyl]-1,6-dihydropyrimidine-5-carbonitrile <2> [46]
4-(4-methoxyphenyl)-2-[(4-nitrobenzyl)sulfanyl]-6-oxo-1,6-dihydropyrimidine-5-carbonitrile <2> [46]
4-(4-methoxyphenyl)-6-oxo-2-[(2-phenylethyl)sulfanyl]-1,6-dihydropyrimidine-5-carbonitrile <2> [46]
4-(4-methylphenyl)-2-[(4-nitrobenzyl)sulfanyl]-6-oxo-1,6-dihydropyrimidine-5-carbonitrile <2> [46]
4-(4-methylphenyl)-6-oxo-2-[(2-phenylethyl)sulfanyl]-1,6-dihydropyrimidine-5-carbonitrile <2> [46]
4-(5-chloro-2-thienyl)-2-[(2-thienylsulfonyl)methyl]-1,3-thiazole <2> [21]
4-[(1H-1,2,3-benzotriazol-1-yloxy)carbonyl]-N,N-diethylaniline <2> (<2> inhibition and irreversible mechanism-based inactivators, no irreversible inactivation with the C145A mutant enzyme [13]) [13]
4-[(1H-1,2,3-benzotriazol-1-yloxy)carbonyl]-N,N-dimethylaniline <2> (<2> inhibition and irreversible mechanism-based inactivators, no irreversible inactivation with the C145A mutant enzyme [13]) [13]

4-[(1H-1,2,3-benzotriazol-1-yloxy)carbonyl]-N-methylaniline <2> (<2> inhibition and irreversible mechanism-based inactivators, no irreversible inactivation with the C_{14}5A mutant enzyme [13]) [13]
4-[(3,5-dibromo-4-hydroxyphenyl)sulfonyl]benzoic acid <2> [21]
4-[(E)-[(2-methoxyphenyl)imino]methyl]-2-phenyl-1,3-oxazol-5-yl acetate <2> [36]
4-[2-(2-benzyloxycarbonylamino-3-methyl-butyrylamino)-3-phenyl-propionylamino]-5-(2-oxo-pyrrolidin-3-yl)-pent-2-enoic acid ethyl ester <2> [20]
4-[2-(2-benzyloxycarbonylamino-3-methyl-butyrylamino)-4-methyl-pentanoylamino]-5-(2-oxo-pyrrolidin-3-yl)-pent-2-enoic acid ethyl ester <2> [20]
4-[2-(2-benzyloxycarbonylamino-3-tert-butoxy-butyrylamino)-4-methyl-pentanoylamino]-5-(2-oxo-pyrrolidin-3-yl)-pent-2-enoic acid ethyl ester <2> [20]
4-methoxy-6-[([1,3]thiazolo[5,4-b]pyridin-2-ylsulfinyl)methyl]-2H-pyran-2-one <2> [36]
5,7-dichloro-4-hydroxy-3-[[1-(4-hydroxyphenyl)-1H-tetrazol-5-yl]sulfanyl]-quinolin-2(1H)-one <2> [36]
5-(1,3-dimethyl-1H-pyrazol-5-yl)-N-(3-methyl-4-nitroisoxazol-5-yl)thiophene-2-carboxamide <2> [21]
5-[(4-chlorophenyl)sulfonyl]pyrimidine-2,4-diamine <2> [21]
5-chloropyridin-3-yl (3S)-2-acetyl-1,2,3,4-tetrahydroisoquinoline-3-carboxylate <2> [32]
5-chloropyridin-3-yl 1-[(3-nitrophenyl)sulfonyl]-1H-indole-5-carboxylate <2> [32]
5-chloropyridin-3-yl 1-[(4-methylphenyl)sulfonyl]-1H-indole-5-carboxylate <2> [32]
5-chloropyridin-3-yl 1-acetyl-1H-indole-4-carboxylate <2> [32]
5-chloropyridin-3-yl 1-acetyl-1H-indole-5-carboxylate <2> [32]
5-chloropyridin-3-yl 1-naphthoate <2> [10]
5-chloropyridin-3-yl 1H-indole-4-carboxylate <2> [32]
5-chloropyridin-3-yl 1H-indole-5-carboxylate <2> [32]
5-chloropyridin-3-yl 1H-indole-6-carboxylate <2> [32]
5-chloropyridin-3-yl 1H-indole-7-carboxylate <2> [32]
5-chloropyridin-3-yl 2-nitrobenzoate <2> [10]
5-chloropyridin-3-yl 2-oxo-2H-chromene-3-carboxylate <2> [10]
5-chloropyridin-3-yl 3-nitrobenzoate <2> [10]
5-chloropyridin-3-yl 4-chlorobenzoate <2> [10]
5-chloropyridin-3-yl 5-(2-nitrophenyl)-2-furoate <2> [10]
5-chloropyridin-3-yl 5-(3-nitrophenyl)-2-furoate <2> [10]
5-chloropyridin-3-yl 5-(4-chloro-2-nitrophenyl)-2-furoate <2> [10]
5-chloropyridin-3-yl 5-(4-chlorophenyl)-2-furoate <2> [10]
5-chloropyridin-3-yl 5-(4-nitrophenyl)-2-furoate <2> [10]
5-chloropyridin-3-yl isonicotinate <2> [10]
5-chloropyridin-3-yl nicotinate <2> [10]
5-chloropyridin-3-yl thiophene-2-carboxylate <2> [15,16]
6-oxo-4-phenyl-2-[(2-phenylethyl)sulfanyl]-1,6-dihydropyrimidine-5-carbonitrile <2> [46]

DTT <2> (<2> 80% of enzyme activity inhibited in the presence of 2.5 mM DTT [3]) [3]
Hg^{2+} <2> [16]
N-(2,2'-bithien-5-ylmethyl)-1,3-dimethyl-4-nitro-1H-pyrazol-5-amine <2> [21]
N-(2-allylthiophenyl)cinnamide <2> [35]
N-(2-benzylthiophenyl)cinnamide <2> [35]
N-(2-carbomethoxyethylthiophenyl)cinnamide <2> [35]
N-(2-chloro-4-nitrophenyl)-N^{α}-[[4-(dimethylamino)phenyl]carbonyl]phenylalaninamide <2> [15,16]
N-(2-cinnamoylthiophenyl)cinnamide <2> [35]
N-[(5-methyl-4,5-dihydro-1H-pyrazol-3-yl)carbonyl]-L-valyl-N-[(1S,2E)-4-ethoxy-1-[[(3S)-3-methyl-2-oxopyrrolidin-3-yl]methyl]-4-oxobut-2-en-1-yl]-L-leucinamide <2> [11]
N-[(5-methyl-4,5-dihydro-1H-pyrazol-3-yl)carbonyl]-L-valyl-N-[(1S,2E)-4-ethoxy-1-[[(3S)-3-methyl-2-oxopyrrolidin-3-yl]methyl]-4-oxobut-2-en-1-yl]-L-phenylalaninamide <2> [11]
N-[(benzyloxy)carbonyl]-3-[(2,2-dimethylpropanoyl)amino]-L-alanyl-N-[(1S,2E)-4-oxo-1-[[(3S)-2-oxopyrrolidin-3-yl]methyl]pent-2-en-1-yl]-L-leucinamide <2> (<2> inhibits the viral protease, thus preventing CVB3 genome replication [38]) [38]
N-[(benzyloxy)carbonyl]-L-alanyl-L-valyl-N-[(3S)-6-(dipropylamino)-1,1,1-trifluoro-2,6-dioxohexan-3-yl]-L-leucinamide <2> [44]
N-[(benzyloxy)carbonyl]-L-alanyl-L-valyl-N-[(3S)-6-amino-1,1,1-trifluoro-2,6-dioxohexan-3-yl]-L-leucinamide <2> [44]
N-[(benzyloxy)carbonyl]-L-valyl-N-[(2S)-1,5-dioxo-1,5-di(1,3-thiazol-2-yl)pentan-2-yl]-L-leucinamide <2> [44]
N-[(benzyloxy)carbonyl]-L-valyl-N-[(2S)-1-oxo-3-[(3S)-2-oxopyrrolidin-3-yl]-1-(1,3-thiazol-2-yl)propan-2-yl]-L-leucinamide <2> [44]
N-[(benzyloxy)carbonyl]-L-valyl-N-[(2S)-5-(morpholin-4-yl)-1,5-dioxo-1-(1,3-thiazol-2-yl)pentan-2-yl]-L-leucinamide <2> [44]
N-[(benzyloxy)carbonyl]-L-valyl-N-[(3S)-1,1,1-trifluoro-6-(morpholin-4-yl)-2,6-dioxohexan-3-yl]-L-leucinamide <2> [44]
N-[(benzyloxy)carbonyl]-L-valyl-N-[(3S)-5-carboxy-1,1,1-trifluoro-2-oxopentan-3-yl]-L-leucinamide <2> [44]
N-[(benzyloxy)carbonyl]-L-valyl-N-[(3S)-6-(dipropylamino)-1,1,1-trifluoro-2,6-dioxohexan-3-yl]-L-leucinamide <2> [44]
N-[(benzyloxy)carbonyl]-L-valyl-N-[(3S)-6-[benzyl(methyl)amino]-1,1,1-trifluoro-2,6-dioxohexan-3-yl]-L-leucinamide <2> [44]
N-[(benzyloxy)carbonyl]-O-tert-butylthreonyl-N-[(1S)-1-formyl-2-[(3S)-2-oxopyrrolidin-3-yl]ethyl]-L-phenylalaninamide <2> (<2> inhibits the viral protease, thus preventing CVB3 genome replication [38]) [38]
N-[(benzyloxy)carbonyl]-O-tert-butylthreonyl-N-[(1S,2E)-4-cyclopropyl-4-oxo-1-[[(3S)-2-oxopyrrolidin-3-yl]methyl]but-2-en-1-yl]-L-leucinamide <2> [38]
N-[(benzyloxy)carbonyl]-O-tert-butylthreonyl-N-[(1S,2E)-4-ethoxy-4-oxo-1-[[(3S)-2-oxopyrrolidin-3-yl]methyl]but-2-en-1-yl]-L-leucinamide <2> [38]
N-[2-(2-cyanocinnamoylthio)phenyl]-2-cyanocinnamide <2> [35]

N-[2-(2-pyridylmethylthio)phenyl]cinnamide <2> [35]
N-[2-(3-dimethylaminopropylthio)phenyl]-2-cyanocinnamide <2> [35]
N-[2-(3-pyridylmethylthio)phenyl]cinnamide <2> [35]
N-[3-(5-tert-butyl-2-methyl-3-furyl)-1H-pyrazol-5-yl]thiophene-2-sulfonamide <2> [21]
N-[4-(3,5-diphenyl-4,5-dihydro-1H-pyrazol-1-yl)benzyl]-1-ethyl-1H-benzimidazol-2-amine <2> [36]
N-[4-(3,5-diphenyl-4,5-dihydro-1H-pyrazol-1-yl)benzyl]-1-propyl-1H-benzimidazol-2-amine <2> [36]
N-[4-[(4-chlorophenyl)sulfonyl]-3-(methylthio)-1H-pyrazol-5-yl]thiophene-2-carboxamide <2> [21]
N-ethyl-N-phenyldithiocarbamic acid zinc <2> [16]
N-tert-butyl-L-seryl-L-valyl-N-[(1S,2E)-4-ethoxy-1-[[(3S)-3-methyl-2-oxopyrrolidin-3-yl]methyl]-4-oxobut-2-en-1-yl]-L-phenylalaninamide <2> [11]
N-tert-butyl-L-seryl-L-valyl-N-[(1S,2E)-4-ethoxy-4-oxo-1-[2-(2-oxopyrrolidin-3-yl)ethyl]but-2-en-1-yl]-L-leucinamide <2> [11]
N^2-[(benzyloxy)carbonyl]-N-[(3S)-6-(dipropylamino)-1,1,1-trifluoro-2,6-dioxohexan-3-yl]-L-leucinamide <2> [44]
NP-40 <2> (<2> 80% of enzyme activity inhibited in the presence of 0.1% NP-40 [3]) [3]
NaCl <2> (<2> 80% of enzyme activity inhibited in the presence of 100 mM NaCl [3]) [3]
S-[5-(trichloromethyl)-4H-1,2,4-triazol-3-yl] 5-(phenylethynyl)furan-2-carbothioate <2> [21]
TG-0203770 <2> [38]
TG-0204998 <2> [38]
TG-0205221 <2> [38]
TG-0205486 <2> [38]
Zn^{2+} <2> [16]
[3-([[3-(dihydroxyboranyl)benzyl]oxy]carbonyl)-5-nitrophenyl]boronic acid <2> [16]
[benzene-1,2-diylbis[methanediylcarbamoyl(5-nitrobenzene-3,1-diyl)]]diboronic acid <2> [16]
[benzene-1,2-diylbis[methanediyloxycarbonyl(5-nitrobenzene-3,1-diyl)]]diboronic acid <2> [16]
[benzene-1,3-diylbis[oxycarbonyl(5-nitrobenzene-3,1-diyl)]]diboronic acid <2> [16]
[benzene-1,4-diylbis[carbamoyl(5-nitrobenzene-3,1-diyl)]]diboronic acid <2> [15]
[benzene-1,4-diylbis[oxycarbonyl(5-nitrobenzene-3,1-diyl)]]diboronic acid <2> [16]
acetyl-Ala-Val-Leu-NHCH($CH_2CH_2CON(CH_3)_2$)-CHO <2> [31]
acetyl-Ser-Ala-Val-Leu-NHCH($CH_2CH_2CON(CH_3)_2$)-CHO <2> [31]
acetyl-Thr-Ser-Ala-Val-Leu-NHCH($CH_2CH_2CON(CH_3)_2$)-CHO <2> [31]
acetyl-Val-Leu-NHCH($CH_2CH_2CON(CH_3)_2$)-CHO <2> [31]
acetyl-leucylalanyl-alanyl-ketomethyl(cycloglutamine)-phthalhydrazide <2> [24]

acetyl-valyl-(O-benzyloxy)threonyl-leucyl-ketomethyl(cycloglutamine)-phthalhydrazide <2> [24]
benzyl (2S,3S)-3-tert-butoxy-1-((S)-3-cyclohexyl-1-oxo-1-((S)-1-oxo-3-((S)-2-oxopyrrolidin-3-yl)propan-2-ylamino)propan-2-ylamino)-1-oxobutan-2-ylcarbamate <2> [20]
benzyl [(1S)-1-benzyl-3-chloro-2-oxopropyl]carbamate <2> (<2> potent and selective inhibitor [34]) [34]
benzyl [(1S)-3-chloro-1-(4-fluorobenzyl)-2-oxopropyl]carbamate <2> (<2> potent and selective inhibitor [34]) [34]
benzyl [(1S)-3-chloro-1-(naphthalen-2-ylmethyl)-2-oxopropyl]carbamate <2> (<2> potent and selective inhibitor [34]) [34]
benzyl [(1S,4S,7S,8R,9R,10S,13S,16S)-7,10-dibenzyl-8,9-dihydroxy-1,16-dimethyl-4,13-bis(1-methylethyl)-2,5,12,15,18-pentaoxo-20-phenyl-19-oxa-3,6,11,14,17-pentaazaicos-1-yl]carbamate <2> [16]
benzyl [(2S)-1-[[(2S)-1-(1,3-benzothiazol-2-yl)-5-(diethylamino)-1,5-dioxopentan-2-yl]amino]-3-methyl-1-oxobutan-2-yl]carbamate <2> [44]
benzyl [(2S)-1-[[(2S)-1-[[(2S)-1-(1,3-benzothiazol-2-yl)-5-(diethylamino)-1,5-dioxopentan-2-yl]amino]-4-methyl-1-oxopentan-2-yl]amino]-3-methyl-1-oxobutan-2-yl]carbamate <2> [44]
benzyl [(2S)-1-[[(2S)-1-[[(2S)-5-(diethylamino)-1,5-dioxo-1-(1,3-thiazol-2-yl)-pentan-2-yl]amino]-4-methyl-1-oxopentan-2-yl]amino]-3-methyl-1-oxobutan-2-yl]carbamate <2> [44]
benzyl [(2S)-1-[[(2S)-5-(diethylamino)-1,5-dioxo-1-(1,3-thiazol-2-yl)pentan-2-yl]amino]-3-methyl-1-oxobutan-2-yl]carbamate <2> [44]
benzyl [(2S)-1-[[(2S)-5-(diethylamino)-1,5-dioxo-1-(1,3-thiazol-2-yl)pentan-2-yl]amino]-4-methyl-1-oxopentan-2-yl]carbamate <2> [44]
benzyl [(7S,8R,9R,10S)-8,9-dihydroxy-7,10-bis(1H-indol-3-ylmethyl)-1,16-dimethyl-4,13-bis(1-methylethyl)-2,5,12,15,18-pentaoxo-20-phenyl-19-oxa-3,6,11,14,17-pentaazaicos-1-yl]carbamate <2> (<2> highly selective for the 3CL protease and that no inhibitionis observed against HIV protease at 0.1 mM [14]) [14]
betulinic acid <2> (<2> competitive [22]) [22]
bis[1,3]thiazolo[4,5-b:5',4'-e]pyridine-2,6-diamine <2> [15,16]
celastrol <2> (<2> competitive inhibitor [45]) [45]
cinaserin <2> [15,35]
curcumin <2> [22,45]
diethyl (2E,2'E)-3,3'-[sulfonylbis(benzene-4,1-diylimino)]bis(2-cyanoprop-2-enoate) <2> [21]
dihydrocelastrol <2> [45]
esculetin-4-carboxylic acid ethyl ester <2> (<2> a novel class of anti-SARS agents from the tropical marine sponge Axinella corrugata [8]) [8]
ethyl (2E)-4-[(N-[(2E)-3-[4-(dimethylamino)phenyl]prop-2-enoyl]-L-phenylalanyl)amino]-5-phenylpent-2-enoate <2> [16]
ethyl (2E,4S)-4-[[(2R,5S)-2-benzyl-6-methyl-5-[[(5-methylisoxazol-3-yl)carbonyl]amino]-4-oxoheptanoyl]amino]-5-[(3S)-3-methyl-2-oxopyrrolidin-3-yl]-pent-2-enoate <2> [11]

ethyl (2E,4S)-4-[[(2R,5S)-5-[(N-tert-butyl-L-seryl)amino]-6-methyl-2-(3-methylbut-2-en-1-yl)-4-oxoheptanoyl]amino]-5-[(3S)-3-methyl-2-oxopyrrolidin-3-yl]-pent-2-enoate <2> [11]
ethyl (2E,4S)-4-[[(2R,5S)-6-methyl-2-(3-methylbut-2-en-1-yl)-5-[[(5-methylisoxazol-3-yl)carbonyl]amino]-4-oxoheptanoyl]amino]-5-[(3S)-3-methyl-2-oxopyrrolidin-3-yl]pent-2-enoate <2> [11]
extracts of Rheum palmatum <2> [48]
hexachlorophene <2> [15,16]
iguesterin <2> (<2> competitive inhibitor [45]) [45]
methyl 3-([N-[(benzyloxy)carbonyl]-L-valyl]amino)-5-fluoro-4-oxopentanoate <2> (<2> potent and selective inhibitor [34]) [34]
methyl 4-hydroxy-6-(trifluoromethyl)furo[2,3-b]pyridine-2-carboxylate <2> [15,16]
niclosamide <2> [22]
phenylmercuric acetate <2> [16]
phenylmercuric nitrate <2> [16]
pristimerin <2> (<2> competitive inhibitor [45]) [45]
savinin <2> (<2> competitive [22]) [22]
sulfonyldi-4,1-phenylene bis(2,3,3-trichloroacrylate) <2> [21]
tert-butyl (3S)-3-[[(benzyloxy)carbonyl]amino]-5-bromo-4-oxopentanoate <2> (<2> potent and selective inhibitor [34]) [34]
tetraethyl 2,2'-[sulfonylbis(benzene-4,1-diyliminomethylylidene)]dipropanedioate <2> [21]
thimerosal <2> [16]
tingenone <2> (<2> competitive inhibitor [45]) [45]
toluene-3,4-dithiolato zinc <2> [16]
zinc N-ethyl-N-phenyldithiocarbamate <2> [38]
Additional information <2> (<2> molecular docking identifies the binding of 3-chloropyridine moieties specifically to the S_1 pocket of SARS-CoV Mpro [10]; <2> based on the X-ray structure of 3CLPro co-crystallized with a trans-α,β-unsaturated ethyl ester, a set of QM/QM and QM/MM calculations are performed, yielding three models with increasingly higher the number of atoms. It is suggested 3CLPro inhibitors need small polar groups to decrease the energy barrier for alkylation reaction. The results can be useful for the development of new compounds against SARS [39]; <2> extracts from Rheum palmatum have a high level of inhibitory activity against 3CL protease with IC50 of 0.01376 mg/ml and an inhibition rate of up to 96% [48]) [10,39,48]

Turnover number (s^{-1})

0.00004 <2> (*o*-aminobenzoyl-TSAVLQSGFRK-2,4-dinitrophenyl amide, <2> mutant enzyme Δ(297-306) [26]) [26]
0.00021 <2> (*o*-aminobenzoyl-TSAVLQSGFRK-2,4-dinitrophenyl amide, <2> mutant enzyme R298A/Q299A [26]) [26]
0.0006 <2> (*o*-aminobenzoyl-TSAVLQSGFRK-2,4-dinitrophenyl amide, <2> mutant enzyme Δ(298-306) [26]) [26]

0.0007 <2> (*o*-aminobenzoyl-TSAVLQSGFRK-2,4-dinitrophenyl amide, <2> mutant enzyme Q299A [26]) [26]
0.001 <2> (*o*-aminobenzoyl-TSAVLQSGFRK-2,4-dinitrophenyl amide, <2> mutant enzyme Δ(299-306) [26]) [26]
0.0017 <2> (*o*-aminobenzoyl-TSAVLQSGFRK-2,4-dinitrophenyl amide, <2> mutant enzyme Q299N [26]) [26]
0.0021 <2> (*o*-aminobenzoyl-TSAVLQSGFRK-2,4-dinitrophenyl amide, <2> mutant enzyme Q299K [26]) [26]
0.0022 <2> (*o*-aminobenzoyl-TSAVLQSGFRK-2,4-dinitrophenyl amide, <2> mutant enzyme Q200E [26]) [26]
0.0034 <2> (*o*-aminobenzoyl-TSAVLQSGFRK-2,4-dinitrophenyl amide, <2> mutant enzyme R298A [26]) [26]
0.0048 <2> (*o*-aminobenzoyl-TSAVLQSGFRK-2,4-dinitrophenyl amide, <2> mutant enzyme R298L [26]; <2> mutant enzyme S139A/Q299A [26]) [26]
0.0069 <2> (*o*-aminobenzoyl-TSAVLQSGFRK-2,4-dinitrophenyl amide, <2> mutant enzyme S123a/R298A [26]) [26]
0.0153 <2> ((Ala-Arg-Leu-Gln-NH)$_2$-rhodamine, <2> rate of hydrolysis measured by change in absorbance at 496 nm [3]) [3]
0.017 <2> (*o*-aminobenzoyl-TSAVLQSGFRK-2,4-dinitrophenyl amide, <2> mutant enzyme Δ(300-306) [26]; <2> mutant enzyme R298K [26]) [26]
0.022 <2> (*o*-aminobenzoyl-TSAVLQSGFRK-2,4-dinitrophenyl amide, <2> mutant enzyme Δ(303-306) [26]) [26]
0.025 <2> (*o*-aminobenzoyl-TSAVLQSGFRK-2,4-dinitrophenyl amide, <2> mutant enzyme Δ(301-306) [26]) [26]
0.027 <2> (Ser-Ala-Val-Leu-Gln-Met-Gly-Phe-Arg-Lys, <2> wild-type protein [49]) [49]
0.027 <2> (*o*-aminobenzoyl-TSAVLQSGFRK-2,4-dinitrophenyl amide, <2> mutant enzyme Δ(304-306) [26]) [26]
0.03 <2> (*o*-aminobenzoyl-TSAVLQSGFRK-2,4-dinitrophenyl amide, <2> mutant enzyme Δ(302-306) [26]) [26]
0.032 <2> (*o*-aminobenzoyl-TSAVLQSGFRK-2,4-dinitrophenyl amide, <2> wild-type enzyme [26]) [26]
0.033 <2> (*o*-aminobenzoyl-TSAVLQSGFRK-2,4-dinitrophenyl amide, <2> mutant enzyme S123A [26]; <2> mutant enzyme S139A [26]) [26]
0.035 <2> (*o*-aminobenzoyl-TSAVLQSGFRK-2,4-dinitrophenyl amide, <2> mutant enzyme S123C [26]) [26]
0.039 <2> (*o*-aminobenzoyl-TSAVLQSGFRK-2,4-dinitrophenyl amide, <2> mutant enzyme Δ(305-306) [26]) [26]
0.1 <2> (Thr-Ser-Ala-Val-Leu-Gln-*p*-nitroanilide, <2> R298A mutant protein [47]) [47]
0.14 <2> ([4-(4-dimethylaminophenylazo)benzoic acid]-KNSTLQSGLRKE-[5-[2'-(aminoethyl)amino]-naphthalenesulfonic acid], <2> mutant enzyme Q189A [9]) [9]
0.16 <2> ([4-(4-dimethylaminophenylazo)benzoic acid]-KNSTLQSGLRKE-[5-[2'-(aminoethyl)amino]-naphthalenesulfonic acid], <2> wild-type enzyme [9]) [9]

0.27 <2> (Ser-Ala-Val-Leu-Gln-Met-Gly-Phe-Arg-Lys, <2> T25G mutant protein [49]) [49]
0.31 <2> (Thr-Ser-Ala-Val-Leu-Gln-*p*-nitroanilide, <2> E166A mutant protein [47]) [47]
0.38 <2> (*o*-aminobenzoyl-TSAVLQSGFRY(NO2)G) [8]
0.48 <2> (Thr-Ser-Ala-Val-Leu-Gln-*p*-nitroanilide, <2> R298L mutant protein [47]) [47]
0.6 <2> (SITSAVLQ-*p*-nitrophenyl ester) [7]
0.63 <2> (Thr-Ser-Ala-Val-Leu-Gln-*p*-nitroanilide, <2> wild-type protein [47]) [47]
0.847 <2> (TFTRLQSLENV, <2> pH 7.3, room temperature [27]) [27]
0.86 <2> (SITSAVLQ-*p*-nitroanilide) [7]
1.5 <2> ([4-(4-dimethylaminophenylazo)benzoic acid]-KTSAVLQSGFRKME-5-[2'-(aminoethyl)amino]-naphthalenesulfonic acid) [7]
1.57 <2> (FYPKLQASQAW, <2> pH 7.3, room temperature [27]) [27]
1.6 <2> (SAVLQMGFRK, <2> wild type enzyme, at 37°C [49]) [49]
1.68 <2> (PHTVLQAVGAC, <2> pH 7.3, room temperature [27]) [27]
2.55 <2> (SGVTFQGKFKK, <2> pH 7.3, room temperature [27]) [27]
3.29 <2> (ATVRLQAGNAT, <2> pH 7.3, room temperature [27]) [27]
8.5 <2> (SITSAVLQSGFRKMA) [7]
12.2 <2> (TSAVLQSGFRK-NH_2, <2> pH 7.3, room temperature [27]) [27]
16.2 <2> (SAVLQMGFRK, <2> mutant enzyme T25G, at 37°C [49]) [49]
76 <2> (GPFVDRQTAQAAGTDT-NH_2, <2> pH 7.5, 37°C, mutant enzyme R188I [31]) [31]
455 <2> (KVATVQSKMSD-NH_2, <2> pH 7.5, 37°C, mutant enzyme R188I [31]) [31]
4753 <2> (TSAVLQSGFRK-NH_2, <2> pH 7.5, 37°C, mutant enzyme R188I [31]) [31]
Additional information <2> (<2> steady-state analysis of the solvent isotope effects on k_{cat} [7]) [7]

K_m-Value (mM)

0.004 <2> (*o*-aminobenzoyl-TSAVLQSGFRK-2,4-dinitrophenyl amide, <2> mutant enzyme Δ(303-306) [26]) [26]
0.005 <2> (*o*-aminobenzoyl-TSAVLQSGFRK-2,4-dinitrophenyl amide, <2> mutant enzyme Q200E [26]; <2> mutant enzyme Q299N [26]) [26]
0.006 <2> (*o*-aminobenzoyl-TSAVLQSGFRK-2,4-dinitrophenyl amide, <2> mutant enzyme Δ(304-306) [26]) [26]
0.01 <2> (*o*-aminobenzoyl-TSAVLQSGFRK-2,4-dinitrophenyl amide, <2> mutant enzyme R298A/Q299A [26]; <2> mutant enzyme S139A [26]) [26]
0.011 <2> (*o*-aminobenzoyl-TSAVLQSGFRK-2,4-dinitrophenyl amide, <2> wild-type enzyme [26]; <2> mutant enzyme R298A [26]) [26]
0.012 <2> (*o*-aminobenzoyl-TSAVLQSGFRK-2,4-dinitrophenyl amide, <2> mutant enzyme S123a/R298A [26]) [26]
0.013 <2> (*o*-aminobenzoyl-TSAVLQSGFRK-2,4-dinitrophenyl amide, <2> mutant enzyme Δ(299-306) [26]; <2> mutant enzyme R298L [26]; <2> mutant enzyme S123A [26]; <2> mutant enzyme S123C [26]) [26]

0.014 <2> (*o*-aminobenzoyl-TSAVLQSGFRK-2,4-dinitrophenyl amide, <2> mutant enzyme Δ(305-306) [26]) [26]
0.015 <2> (*o*-aminobenzoyl-TSAVLQSGFRK-2,4-dinitrophenyl amide, <2> mutant enzyme Δ(300-306) [26]) [26]
0.016 <2> (*o*-aminobenzoyl-TSAVLQSGFRK-2,4-dinitrophenyl amide, <2> mutant enzyme R298K [26]) [26]
0.018 <2> (*o*-aminobenzoyl-TSAVLQSGFRK-2,4-dinitrophenyl amide, <2> mutant enzyme Q299A [26]) [26]
0.0186 <2> (SAVLQMGFRK, <2> mutant enzyme T25G, at 37°C [49]) [49]
0.0186 <2> (Ser-Ala-Val-Leu-Gln-Met-Gly-Phe-Arg-Lys, <2> T25G mutant protein [49]) [49]
0.021 <2> (*o*-aminobenzoyl-TSAVLQSGFRK-2,4-dinitrophenyl amide, <2> mutant enzyme Δ(297-306) [26]; <2> mutant enzyme S139A/Q299A [26]) [26]
0.022 <2> (*o*-aminobenzoyl-TSAVLQSGFRK-2,4-dinitrophenyl amide, <2> mutant enzyme Δ(302-306) [26]) [26]
0.03 <2> (*o*-aminobenzoyl-TSAVLQSGFRK-2,4-dinitrophenyl amide, <2> mutant enzyme Δ(298-306) [26]; <2> mutant enzyme Δ(301-306) [26]) [26]
0.0338 <2> (TSAVLQSGFRK-NH_2, <2> pH 7.5, 37°C, mutant enzyme R188I [31]) [31]
0.037 <2> (*o*-aminobenzoyl-TSAVLQSGFRK-2,4-dinitrophenyl amide, <2> mutant enzyme Q299K [26]) [26]
0.03817 <2> ([4-(4-dimethylaminophenylazo)benzoic acid]-KNSTLQSGLRKE-[5-[2'-(aminoethyl)amino]-naphthalenesulfonic acid], <2> mutant enzyme Q189A [9]) [9]
0.045 <2> ([4-(4-dimethylaminophenylazo)benzoic acid]-KTSAVLQSGFRKME-5-['-(aminoethyl)amino]-naphthalenesulfonic acid) [7]
0.046 <2> (GPFVDRQTAQAAGTDT-NH_2, <2> pH 7.5, 37°C, mutant enzyme R188I [31]) [31]
0.04938 <2> ([4-(4-dimethylaminophenylazo)benzoic acid]-KNSTLQSGLRKE-[5-[2'-(aminoethyl)amino]-naphthalenesulfonic acid], <2> wild-type enzyme [9]) [9]
0.051 <2> (KVATVQSKMSD-NH_2, <2> pH 7.5, 37°C, mutant enzyme R188I [31]) [31]
0.073 <2> (SITSAVLQ-*p*-nitrophenyl ester) [7]
0.0766 <2> (SAVLQMGFRK, <2> wild type enzyme, at 37°C [49]) [49]
0.0766 <2> (Ser-Ala-Val-Leu-Gln-Met-Gly-Phe-Arg-Lys, <2> wild-type protein [49]) [49]
0.146 <2> (*o*-aminobenzoyl-TSAVLQSGFRY(NO2)G) [8]
0.18 <2> (SITSAVLQ-*p*-nitroanilide) [7]
0.2226 <2> (Thr-Ser-Ala-Val-Leu-Gln-*p*-nitroanilide, <2> wild-type protein [47]) [47]
0.286 <2> (TFTRLQSLENV, <2> pH 7.3, room temperature [27]) [27]
0.306 <2> ((Ala-Arg-Leu-Gln-$NH)_2$-rhodamine, <2> rate of hydrolysis measured by change in absorbance at 496 nm [3]) [3]
0.3534 <2> (Thr-Ser-Ala-Val-Leu-Gln-*p*-nitroanilide, <2> E166A mutant protein [47]) [47]

0.549 <2> (FYPKLQASQAW, <2> pH 7.3, room temperature [27]) [27]
0.583 <2> (SGVTFQGKFKK, <2> pH 7.3, room temperature [27]) [27]
0.6 <2> (SITSAVLQSGFRKMA) [7]
1.15 <2> (TSAVLQSGFRK-NH_2, <2> pH 7.3, room temperature [27]) [27]
1.44 <2> (ATVRLQAGNAT, <2> pH 7.3, room temperature [27]) [27]
1.94 <2> (PHTVLQAVGAC, <2> pH 7.3, room temperature [27]) [27]
61.9 <2> (SWTSAVLQSGFRKWA, <2> HPLC-based cleavage assay, measurement of fluorescence emission at 353 nm [4]) [4]
Additional information <2> (<2> steady-state analysis of the solvent isotope effects on K_M-value [7]) [7]

K_i-Value (mM)

6e-018 <2> ($C_{17}H_{20}N_2S$, promazine, <2> in silico binding studies [2]) [2]
8.7e-017 <2> ($C_{37}H_{48}N_4O_5$, lopinavir, <2> in silico binding studies [2]) [2]
2.1e-016 <2> ($C_{17}H_{19}ClN_2O_2S$, UC2, <2> in silico binding studies [2]) [2]
0.0000075 <2> (1-[(1H-indol-5-ylcarbonyl)oxy]-1H-1,2,3-benzotriazole) [13]
0.0000111 <2> (4-[(1H-1,2,3-benzotriazol-1-yloxy)carbonyl]-N,N-diethylaniline) [13]
0.0000121 <2> (4-[(1H-1,2,3-benzotriazol-1-yloxy)carbonyl]-N-methylaniline) [13]
0.0000123 <2> (1-[(1H-indol-2-ylcarbonyl)oxy]-1H-1,2,3-benzotriazole) [13]
0.0000138 <2> (1-[[(5-fluoro-1H-indol-2-yl)carbonyl]oxy]-1H-1,2,3-benzotriazole) [13]
0.0000174 <2> (4-[(1H-1,2,3-benzotriazol-1-yloxy)carbonyl]-N,N-dimethylaniline) [13]
0.0000195 <2> (2-[(1H-1,2,3-benzotriazol-1-yloxy)carbonyl]aniline) [13]
0.0000229 <2> (1-[(1H-benzimidazol-5-ylcarbonyl)oxy]-1H-1,2,3-benzotriazole) [13]
0.00003 <2> (N-(2-chloro-4-nitrophenyl)-N^{α}-[[4-(dimethylamino)phenyl]carbonyl]phenylalaninamide) [15,16]
0.000038 <2> (N-[(benzyloxy)carbonyl]-3-[(2,2-dimethylpropanoyl)amino]-L-alanyl-N-[(1S,2E)-4-oxo-1-[[(3S)-2-oxopyrrolidin-3-yl]methyl]pent-2-en-1-yl]-L-leucinamide) [38]
0.000038 <2> (TG-0204998, <2> in 10 mM MES, pH 6.5, and 25°C [38]) [38]
4e-005 <2> ([benzene-1,2-diylbis[methanediylcarbamoyl(5-nitrobenzene-3,1-diyl)]]diboronic acid) [16]
0.00004 <2> ([benzene-1,4-diylbis[carbamoyl(5-nitrobenzene-3,1-diyl)]]diboronic acid) [15]
0.000053 <2> (benzyl (2S,3S)-3-tert-butoxy-1-((S)-3-cyclohexyl-1-oxo-1-((S)-1-oxo-3-((S)-2-oxopyrrolidin-3-yl)propan-2-ylamino)propan-2-ylamino)-1-oxobutan-2-ylcarbamate) [20]
0.000054 <2> (N-[(benzyloxy)carbonyl]-O-tert-butylthreonyl-N-[(1S)-1-formyl-2-[(3S)-2-oxopyrrolidin-3-yl]ethyl]-L-phenylalaninamide) [38]
0.000054 <2> (TG-0205221, <2> in 10 mM MES, pH 6.5, and 25°C [38]) [38]
0.000058 <2> (4-[2-(2-benzyloxycarbonylamino-3-tert-butoxy-butyrylamino)-4-methyl-pentanoylamino]-5-(2-oxo-pyrrolidin-3-yl)-pent-2-enoic acid ethyl ester) [20]

0.000058 <2> (N-[(benzyloxy)carbonyl]-O-tert-butylthreonyl-N-[(1S,2E)-4-ethoxy-4-oxo-1-[[(3S)-2-oxopyrrolidin-3-yl]methyl]but-2-en-1-yl]-L-leucinamide) [38]
0.000058 <2> (TG-0203770, <2> in 10 mM MES, pH 6.5, and 25°C [38]) [38]
0.000073 <2> (benzyl [(7S,8R,9R,10S)-8,9-dihydroxy-7,10-bis(1H-indol-3-ylmethyl)-1,16-dimethyl-4,13-bis(1-methylethyl)-2,5,12,15,18-pentaoxo-20-phenyl-19-oxa-3,6,11,14,17-pentaazaicos-1-yl]carbamate) [14]
0.000099 <2> (N-[(benzyloxy)carbonyl]-O-tert-butylthreonyl-N-[(1S,2E)-4-cyclopropyl-4-oxo-1-[[(3S)-2-oxopyrrolidin-3-yl]methyl]but-2-en-1-yl]-L-leucinamide) [38]
0.000099 <2> (TG-0205486, <2> in 10 mM MES, pH 6.5, and 25°C [38]) [38]
0.00017 <2> (1-hydroxypyridine-2-thione zinc) [16]
0.0003 <2> (phenylmercuric nitrate) [16]
0.000306 <2> (benzyl [(1S)-1-benzyl-3-chloro-2-oxopropyl]carbamate) [34]
0.00034 <2> (2,5-bis[[(benzyloxy)carbonyl]amino]-1,2,5,6-tetradeoxy-1,6-di-1H-indol-3-yl-L-iditol) [14]
0.000371 <2> (benzyl [(1S)-3-chloro-1-(naphthalen-2-ylmethyl)-2-oxopropyl]carbamate) [34]
0.00038 <2> (benzyl [(1S)-3-chloro-1-(4-fluorobenzyl)-2-oxopropyl]carbamate) [34]
0.0004 <2> (tert-butyl (3S)-3-[[(benzyloxy)carbonyl]amino]-5-bromo-4-oxopentanoate) [34]
0.0005 <2> (Hg^{2+}) [16]
0.0005 <2> (ethyl (2E)-4-[(N-[(2E)-3-[4-(dimethylamino)phenyl]prop-2-enoyl]-L-phenylalanyl)amino]-5-phenylpent-2-enoate) [16]
0.000512 <2> (methyl 3-([N-[(benzyloxy)carbonyl]-L-valyl]amino)-5-fluoro-4-oxopentanoate) [34]
0.0006 <2> (2-([N-[(benzyloxy)carbonyl]-L-alanyl-L-valyl]amino)-5-[[(2S,5S)-5-[[(benzyloxy)carbonyl]amino]-2-(1-methylethyl)-4-oxohexanoyl]amino]-1,2,5,6-tetradeoxy-1,6-diphenyl-L-iditol) [15]
0.0006 <2> (benzyl (2S,3S)-3-tert-butoxy-1-((S)-3-cyclohexyl-1-oxo-1-((S)-1-oxo-3-((S)-2-oxopyrrolidin-3-yl)propan-2-ylamino)propan-2-ylamino)-1-oxobutan-2-ylcarbamate) [20]
0.0006 <2> (benzyl [(1S,4S,7S,8R,9R,10S,13S,16S)-7,10-dibenzyl-8,9-dihydroxy-1,16-dimethyl-4,13-bis(1-methylethyl)-2,5,12,15,18-pentaoxo-20-phenyl-19-oxa-3,6,11,14,17-pentaazaicos-1-yl]carbamate) [16]
0.00066 <2> (4-[2-(2-benzyloxycarbonylamino-3-methyl-butyrylamino)-4-methyl-pentanoylamino]-5-(2-oxo-pyrrolidin-3-yl)-pent-2-enoic acid ethyl ester) [20]
0.0007 <2> (phenylmercuric acetate) [16]
0.0008 <2> (iguesterin) [45]
0.001 <2> (N-ethyl-N-phenyldithiocarbamic acid zinc) [16]
0.0011 <2> (Zn^{2+}) [16]
0.0014 <2> (toluene-3,4-dithiolato zinc) [16]
0.0022 <2> (4,5-anhydro-2-([N-[(benzyloxy)carbonyl]-L-phenylalanyl]amino)-1,2-dideoxy-D-erythro-pent-3-ulose) [6]

0.0022 <2> (N-[(benzyloxy)carbonyl]-L-valyl-N-[(2S)-1-oxo-3-[(3S)-2-oxo-pyrrolidin-3-yl]-1-(1,3-thiazol-2-yl)propan-2-yl]-L-leucinamide) [44]
0.00226 <2> (4-[2-(2-benzyloxycarbonylamino-3-methyl-butyrylamino)-3-phenyl-propionylamino]-5-(2-oxo-pyrrolidin-3-yl)-pent-2-enoic acid ethyl ester) [20]
0.0024 <2> (thimerosal) [16]
0.0031 <2> (pristimerin) [45]
0.004 <2> (tingenone) [45]
0.0042 <2> (celastrol) [45]
0.0045 <2> ([benzene-1,4-diylbis[oxycarbonyl(5-nitrobenzene-3,1-diyl)]]diboronic acid) [16]
0.006 <2> ([benzene-1,2-diylbis[methanediyloxycarbonyl(5-nitrobenzene-3,1-diyl)]]diboronic acid) [16]
0.006 <2> ([benzene-1,3-diylbis[oxycarbonyl(5-nitrobenzene-3,1-diyl)]]diboronic acid) [16]
0.0082 <2> (betulinic acid) [22]
0.0091 <2> (savinin) [22]
0.0137 <2> (hexachlorophene) [15,16]
0.016 <2> ([3-([[3-(dihydroxyboranyl)benzyl]oxy]carbonyl)-5-nitrophenyl]-boronic acid) [16]
0.021 <2> (N-[(benzyloxy)carbonyl]-L-valyl-N-[(3S)-1,1,1-trifluoro-6-(morpholin-4-yl)-2,6-dioxohexan-3-yl]-L-leucinamide) [44]
0.0341 <2> (N-[(benzyloxy)carbonyl]-L-valyl-N-[(3S)-6-[benzyl(methyl)amino]-1,1,1-trifluoro-2,6-dioxohexan-3-yl]-L-leucinamide) [44]
0.0452 <2> (N-[(benzyloxy)carbonyl]-L-valyl-N-[(2S)-1,5-dioxo-1,5-di(1,3-thiazol-2-yl)pentan-2-yl]-L-leucinamide) [44]
0.0493 <2> (benzyl [(2S)-1-[[(2S)-1-[[(2S)-1-(1,3-benzothiazol-2-yl)-5-(diethylamino)-1,5-dioxopentan-2-yl]amino]-4-methyl-1-oxopentan-2-yl]amino]-3-methyl-1-oxobutan-2-yl]carbamate) [44]
0.061 <2> (1-[bis(4-chlorophenyl)methyl]-3-[2-[(2,4-dichlorobenzyl)oxy]-2-(2,4-dichlorophenyl)ethyl]-1H-imidazol-3-ium) [15]
0.112 <2> (benzyl [(2S)-1-[[(2S)-1-[[(2S)-5-(diethylamino)-1,5-dioxo-1-(1,3-thiazol-2-yl)pentan-2-yl]amino]-4-methyl-1-oxopentan-2-yl]amino]-3-methyl-1-oxobutan-2-yl]carbamate) [44]
0.116 <2> (N-[(benzyloxy)carbonyl]-L-valyl-N-[(3S)-5-carboxy-1,1,1-trifluoro-2-oxopentan-3-yl]-L-leucinamide) [44]
0.135 <2> (N-[(benzyloxy)carbonyl]-L-alanyl-L-valyl-N-[(3S)-6-amino-1,1,1-trifluoro-2,6-dioxohexan-3-yl]-L-leucinamide) [44]
0.159 <2> (benzyl [(2S)-1-[[(2S)-1-(1,3-benzothiazol-2-yl)-5-(diethylamino)-1,5-dioxopentan-2-yl]amino]-3-methyl-1-oxobutan-2-yl]carbamate) [44]
0.297 <2> (N-[(benzyloxy)carbonyl]-L-alanyl-L-valyl-N-[(3S)-6-(dipropylamino)-1,1,1-trifluoro-2,6-dioxohexan-3-yl]-L-leucinamide) [44]
0.363 <2> (N-[(benzyloxy)carbonyl]-L-valyl-N-[(3S)-6-(dipropylamino)-1,1,1-trifluoro-2,6-dioxohexan-3-yl]-L-leucinamide) [44]
0.462 <2> (benzyl [(2S)-1-[[(2S)-5-(diethylamino)-1,5-dioxo-1-(1,3-thiazol-2-yl)pentan-2-yl]amino]-4-methyl-1-oxopentan-2-yl]carbamate) [44]

0.478 <2> (N-[(benzyloxy)carbonyl]-L-valyl-N-[(2S)-5-(morpholin-4-yl)-1,5-dioxo-1-(1,3-thiazol-2-yl)pentan-2-yl]-L-leucinamide) [44]
0.584 <2> (N^2-[(benzyloxy)carbonyl]-N-[(3S)-6-(dipropylamino)-1,1,1-trifluoro-2,6-dioxohexan-3-yl]-L-leucinamide) [44]
0.614 <2> (benzyl [(2S)-1-[[(2S)-5-(diethylamino)-1,5-dioxo-1-(1,3-thiazol-2-yl)pentan-2-yl]amino]-3-methyl-1-oxobutan-2-yl]carbamate) [44]

pH-Optimum

7 <2> (<2> substrate: TSAVLQSGFRK-NH_2 [27]) [4,27]
7.4 <2> (<2> wild-type enzyme [15]) [15]
7.6 <2> (<2> mutant enzyme C145S [15]) [15]
8 <2> [3]

pH-Range

6-9 <2> (<2> pH 6: about 50% of maximal activity, pH 9: about 65% of maximal activity, substrate: TSAVLQSGFRK-NH_2 [27]) [27]
6.3-8.7 <2> (<2> pH 6.3: about 55% of maximal activity, pH 8.7: about 45% of maximal activity, wild-type enzyme [15]) [15]
6.3-9.3 <2> (<2> pH 6.3: about 55% of maximal activity, pH 9.3: about 45% of maximal activity, mutant enzyme C145S [15]) [15]

pi-Value

6.24 <2> (<2> mutant enzyme R188I, calculated from sequence [31]) [31]

Temperature optimum (°C)

42 <2> [3]

4 Enzyme Structure

Molecular weight

33760 <2> (<2> determined by MALDI [3]) [3]

Subunits

dimer <2> (<2> one monomer per asymmetric unit, dimer is generated through the crystallographic twofold [1]; <2> by comparing molecular dynamics simulation of dimer and monomer, the indirect reasons for the inactivation of the monomer are found, that is the conformational variations of the active site in the monomer relative to dimer [25]; <2> dimerization is important for enzyme activity and only one active protomer in the dimer is enough for the catalysis [18]; <2> the enzyme exists as a mixture of monomer and dimer at a higher protein concentration (4 mg/ml) and exclusively as a monomer at a lower protein concentration [16]; <2> the SARS coronavirus main proteinase is a homodimer. Investigation of the monomer-dimer equilibrium [5]; <2> a mixture of monomer and dimer at a protein concentration of 4 mg/ml and mostly monomer at 0.2 mg/ml. The dimer may be the biological functional form of the protein [27]; <2> in solution the wild type protease exhibits both forms of monomer and dimer and the amount of the monomer is almost equal to that of the dimeric form [37]; <2> is only enzy-

matically active as a homodimer. Arg298 serves as a key component for maintaining dimerization, and consequently, its mutation will trigger a cooperative switch from a dimer to a monomer. The monomeric enzyme is irreversibly inactivated because its catalytic machinery is frozen in the collapsed state, characteristic of the formation of a short 310-helix from an active-site loop. Dimerization appears to be coupled to catalysis in 3CLpro through the use of overlapped residues for two networks, one for dimerization and another for the catalysis [41]; <2> SARS-CoV Mpro exists in solution as an equilibrium of both monomeric and dimeric forms, and the dimeric form is the enzymatically active form [40]; <2> wild type and Δ(300-306) proteases exist with dimer as the major form. The major form becomes monomeric in Δ(299-306), Δ(298-306) and Δ(297-306) [26]) [1,5,16,18,25,26,27,37,40,41]
homodimer <2,3> (<2> X-ray crystallography [38]; <2> analytical ultracentrifugation, gel filtration [47]; <3> only the dimeric enzyme is active [51]; <2> tendency of substrate induced dimer formation, gel filtration, analytic ultracentrifugation [50]) [38,47,50,51]
monomer <2> (<2> by comparing molecular dynamics simulation of dimer and monomer, the indirect reasons for the inactivation of the monomer are found, that is the conformational variations of the active site in the monomer relative to dimer [25]; <2> the enzyme exists as a mixture of monomer and dimer at a higher protein concentration (4 mg/ml) and exclusively as a monomer at a lower protein concentration [16]; <2> a mixture of monomer and dimer at a protein concentration of 4 mg/ml and mostly monomer at 0.2 mg/ml. The dimer may be the biological functional form of the protein [27]; <2> in solution the wild type protease exhibits both forms of monomer and dimer and the amount of the monomer is almost equal to that of the dimeric form [37]; <2> wild type and Δ(300-306) proteases exist with dimer as the major form. The major form becomes monomeric in Δ(299-306), Δ(298-306) and Δ(297-306) [26]) [16,25,26,27,37]

5 Isolation/Preparation/Mutation/Application

Purification
<1> [19]
<2> [6,20,21,24,27,37]
<2> (E166A mutant protein: immobilized metal ion affinity chromatography (Ni^{2+})) [47]
<2> (Ni-NTA column chromatography) [49]
<2> (ammonium sulfate precipitation and anion-exchange column chromatography) [48]
<2> (ammonium sulfate precipitation, anion-exchange chromatography) [48]
<2> (commercial preparation) [45]
<2> (fused to maltose-binding protein, removing the maltose-binding protein by cleavage with factor Xa, purification by Phenyl Sepharose column chromatography) [1]

<2> (glutathione S-transferase column chromatography and HiTrap 26/10 QFF column chroamtography) [38]
<2> (immobilized metal ion affinity chromatography (Ni^{2+})) [49]
<2> (purification of proteolysis-resistant mutant R188I of the SARS 3CL protease) [31]
<2> (recombinant His-tagged SARS-CoV 3CL protease) [8]
<2> (recombinant enzyme) [34]
<2> (strong cation column chromatography connected in series to a strong anion column chromatography) [3]
<2> (wild-type enzyme and C-terminally truncated proteases) [26]
<3> (glutathione Sepharose column chromatography and Superdex 75 gel filtration) [51]

Renaturation

<2> (reversible unfolding of SARS-CoV main protease in guanidine-HCl. In the presence of 6 M of guanidine-HCl, the enzyme is completely unfolded in 10 min. The unfolding is completely reversible. A 10fold dilution induces refolding of the enzyme to a yield of 92-95%) [12]

Crystallization

<1> (crystal structure of monomeric mutant enzyme G11A) [19]
<2> [21]
<2> (1.8 A X-ray crystal structure of 3Clpro bound to an irreversible inhibitor, an α,β-epoxyketone) [6]
<2> (SARS 3CLpro bound to two phthalhydrazide-charged peptidyl inhibitors, acetyl-valyl-(O-benzyloxy)threonyl-leucyl-ketomethyl(cycloglutamine)-phthalhydrazide and acetyl-leucylalanyl-alanyl-ketomethyl(cycloglutamine)-phthalhydrazide. The inhibitors are covalently attached to SARS 3CLpro in crystals) [24]
<2> (X-ray, resolution of 2.0 A for tetragonal crystals, 2.14 A for monoclinic crystals and 2.8 A for orthorhombic crystals, pH-dependent change of structure) [4]
<2> (complexed with inhibitors TG-0204998 and TG-0205486, sitting drop vapor diffusion method, using 3-6% (w/v) PEG 6000, 4-6% (v/v) DMSO or methyl-2,4-pentanediol, 1 mM dithiothreitol, 0.1 M MES, pH 6.5) [38]
<2> (crystal structures of 3Cpro from CVB3 and 3CLpro from CoV-229E and SARS-CoV in complex with inhibitors are solved) [38]
<2> (crystals grown in hanging-drop vapour-diffusion method) [1]
<2> (enzyme-inhibitor complex, hanging-drop method) [34]
<2> (hanging-drop vapor-diffusion method. Crystal structure of the enzyme at a resolution of 1.82 A, in space group P21 at pH 6.0. Two crystal structures of Mpro having an additional Ala at the N terminus of each protomer (M+A(-1)pro), both at a resolution of 2.00 A, in space group P43212: one unbound and one bound by a substrate-like aza-peptide epoxide) [23]
<2> (monomeric crystal structure of the SARS-CoV 3CLpro mutant R298A at a resolution of 1.75 A, hanging drop method) [41]
<2> (sitting drop diffusion method, crystallization of SARS 3CLpro-inhibitor complexes) [20]

<2> (structures of monomeric and dimeric forms of the C-terminal domain of Mpro (Mpro-C). Mpro-C monomer maintains the same fold as that in the crystal structure of Mpro. On the other hand, the Mpro-C dimer has a novel structure characterized by 3D domain-swapping, which provides the structural basis for the dimer stability) [43]
<3> (hanging drop vapor diffusion method, crystals of S139A mutant are grown from the mother liquor containing 0.1 M MES pH 6.0, 10% (w/v) PEG 6000, 1 mM dithiohtreitol, and 5% (v/v) DMSO, crystals of F140A are grown at three pH values in 0.1 M MES pH 6.0/0.1 M MES pH 6.5/0.1 M Tris pH 7.6, with 10% (w/v) PEG 6000, 1 mM dithiothreitol, and 5% (v/v) DMSO) [51]

Cloning

<1> (mutant enzyme G11A and wild-type enzyme are expressed in Escherichia coli) [19]
<2> [6,20,37]
<2> (E166A mutant protein expressed in Escherichia coli BL21(DE3)) [47]
<2> (His-tagged SARS-CoV 3CL protease expressed in Escherichia coli) [8]
<2> (His-tagged artificial polyprotein (cyan fluorescent protein-SARS-CoV 3CLpro-yellow fluorescent protein) expressed in Escherichia coli) [50]
<2> (R298A protease is expressed in Escherichia coli strain BL21(DE3)) [41]
<2> (expressed in E. coli BL21) [3]
<2> (expressed in Escherichia coli) [48,49]
<2> (expressed in Escherichia coli BL21 cells) [38]
<2> (expression in Escherichia coli) [24,27]
<2> (fused to maltose-binding protein and expressed in Escherichia coli BL21) [1]
<2> (high level of expression of of proteolysis-resistant mutant R188I in Escherichia coli) [31]
<2> (wild type and His-tagged T25G mutant are expressed in Escherichia coli cells) [49]
<2> (wild-type and mutant glutathione S-transferase-fusion constructs are transformed into Escherichia coli BL21 cell strain for overexpression) [17]
<2> (wild-type enzyme and C-terminally truncated proteases, expression in Escherichia coli) [26]
<3> (expressed in Escherichia coli BL21(DE3) cells) [51]

Engineering

C145A <2> (<2> no irreversible inactivation by benzotriazole esters [13]) [13]
C300A <2> (<2> mutant enzyme shows more than 30% of wild-type activity [17]) [17]
E14A <2> (<2> the ratio of dimer to monomer in solution is 0.36, compared to 1 for the wild-type enzyme [37]) [37]
E166A <2> (<2> involved in connecting the substrate binding site with the dimer interface, dimerization influenced by substrate binding [47]) [47]
E166A/R298A <2> (<2> monomer [47]) [47]

E288A <2> (<2> mutant enzyme retains less than 10% of the wild-type activity [17]) [17]
F140A <2,3> (<2> the ratio of dimer to monomer in solution is 0.63, compared to 1 for the wild-type enzyme [37]; <3> mutant F140A is a dimer with the most collapsed active pocket discovered so far, well-reflecting the stabilizing role of this residue, the mutant enzyme is completely inactive [51]) [37,51]
F291A <2> (<2> activity is higher than that of wild-type enzyme [17]) [17]
F3A <2> (<2> the ratio of dimer to monomer in solution is 0.93, compared to 1 for the wild-type enzyme [37]) [37]
G11A <1> (<1> mutation entirely abolishes activity [19]) [19]
G283A <2> (<2> no significant activity differences from the wild-type protease [17]) [17]
I286A <2> (<2> activity is higher than that of wild-type enzyme [17]) [17]
L282A <2> (<2> mutant enzyme shows more than 30% of wild-type activity [17]) [17]
N214A <2> (<2> mutant enzyme shows more than 30% of wild-type activity [17]) [17]
N289A <2> (<2> mutant enzyme retains less than 10% of the wild-type activity [17]) [17]
Q189A <2> (<2> k_{cat} for the substrate [4-(4-dimethylaminophenylazo)benzoic acid]-KNSTLQSGLRKE-[5-[2-(aminoethyl)amino]-naphthalenesulfonic acid] is 1.14 fold lower than wild-type value, K_m-value for the substrate [4-(4-dimethylaminophenylazo)benzoic acid]-KNSTLQSGLRKE-[5-[2-(aminoethyl)amino]-naphthalenesulfonic acid] is 1.3fold lower than the wild-type value [9]) [9]
Q290A <2> (<2> mutant enzyme retains less than 10% of the wild-type activity [17]) [17]
Q299A <2> (<2> mutant enzyme retains less than 10% of the wild-type activity [17]; <2> the quaternary structures of exists in a mixture of monomeric and dimeric forms [26]) [17,26]
Q299E <2> (<2> more than 90% loss of activity [26]) [26]
Q299K <2> (<2> more than 90% loss of activity [26]) [26]
Q299N <2> (<2> more than 90% loss of activity [26]) [26]
R188I <2> (<2> replacing Arg with Ile at position 188 renders the protease resistant to proteolysis. The catalytic ability of 3CL-R188I protease was found to be extreme as compared to that of a mature 3CL protease containing a C-terminal His tag. The k_{cat} values is 0.0203 per sec for mature 3CL protease and 4753 per sec for the 3CL-R188I [31]) [31]
R298A <2> (<2> mutant enzyme retains less than 10% of the wild-type activity [17]; <2> monomeric mutant [41]; <2> the quaternary structures of exists in a mixture of monomeric and dimeric forms [26]; <2> induce dimer dissociation (influenced by substrate binding), about 10fold decrease in activty [47]) [17,26,41,47]
R298A/Q299A <2> (<2> mutant is present almost exclusively in the monomeric form [26]; <2> monomer, no activity detected [47]) [26,47]
R298K <2> (<2> mutation has no significant effect on activity [26]) [26]

R298L <2> (<2> mutation destroys 85% of the enzyme activity [26]; <2> induce dimer dissociation (influenced by substrate binding), about 10fold decrease in activty [47]) [26,47]
R4A <2> (<2> the ratio of dimer to monomer in solution is 0.45, compared to 1 for the wild-type enzyme [37]) [37]
S10A <2> (<2> the ratio of dimer to monomer in solution is 0.66, compared to 1 for the wild-type enzyme [37]) [37]
S123A <2> (<2> mutation does not destroy the enzyme activity, the dimeric structure remains intact [26]) [26]
S123C <2> (<2> mutation does not destroy the enzyme activity, the dimeric structure remains intact [26]) [26]
S139A <2,3> (<2> mutation can destroy neither the enzyme activity nor the dimeric structure [26]; <2> mutation does not destroy the enzyme activity, the dimeric structure remains intact [26]; <2> the ratio of dimer to monomer in solution is 0.81, compared to 1 for the wild-type enzyme [37]; <3> mutant S139A is a monomer that still retains a small fraction of dimer in solution, which may account for its remaining activity [51]) [26,37,51]
S1A <2> (<2> the ratio of dimer to monomer in solution is 1.08, compared to 1 for the wild-type enzyme [37]) [37]
S284A <2> (<2> activity is higher than that of wild-type enzyme [17]) [17]
S284A/T285A/I286A <2> (<2> activity is 3.7fold higher than wild-type activity [17]) [17]
S301A <2> (<2> no significant activity differences from the wild-type protease [17]) [17]
T25G <2> (<2> activity like wild-type (substrate DABCYL-Lys-Thr-Ser-Ala-Val-Leu-Gln-Ser-Gly-Phe-Arg-Lys-Met-Glu-EDANS), higher specific activity than wild-type protein for substrate Ser-Ala-Val-Leu-Gln-Met-Gly-Phe-Arg-Lys [49]; <2> the mutant enzyme has an expanded S1 space that demonstrates 43.5-fold better k_{cat}/K_m compared with wild type in cleaving substrates with a larger Met at P1, mutant enzyme T25G shows a 12fold and 8fold higher activity against the substrates with Met and Leu at P1, respectively [49]) [49]
T25S <2> (<2> almost complete loss of activity [49]) [49]
T280A <2> (<2> no significant activity differences from the wild-type protease [17]) [17]
T285A <2> (<2> activity is higher than that of wild-type enzyme [17]) [17]
Additional information <2> (<2> truncation of C-terminus from 306 to 300 has no appreciable effect on the quaternary structure, and the enzyme remains catalytically active. Further deletion of Gln299 or Arg298 drastically decreases the enzyme activity to 1-2% of wild type, and the major form is a monomeric one. The catalytic constant and specificity constant (k_{cat}/K_m) of the proteases are significantly decreased in the Δ(299-306), Δ(298-306), and Δ(297-306) mutants. Wild type and Δ(300-306) proteases exist with dimer as the major form. The major form becomes monomeric in Δ(299-306), Δ(298-306) and Δ(297-306) [26]; <2> without the N-finger, SARS-CoV Mpro can no longer retain the active dimer structure. It can form a new type of dimer which is inactive. Therefore, the N-finger of SARS-CoV Mpro is not only cri-

tical for its dimerization but also essential for the enzyme to form the enzymatically active dimer [40]) [26,40]

Application

analysis <2> (<2> developing a novel red-shifted fluorescence-based assay for 3CLpro and its application for identifying small-molecule anti-SARS agents from marine organisms [8]) [8]

medicine <2> (<2> SARS-3CLpro is a viral cysteine protease critical to the life cycle of the pathogen and hence a therapeutic target of importance [29]; <2> this enzyme is a target for the design of potential anti-SARS drugs [28]) [28,29]

6 Stability

Temperature stability

61 <2> (<2> Tm-value, sigmoid denaturation curve [27]) [27]

Organic solvent stability

guanidine-HCl <2> (<2> dimeric enzyme dissociates at guanidinium chloride concentration of less than 0.4 M, at which the enzymatic activity loss showes close correlation with the subunit dissociation. Further increase in guanidinium chloride induces a reversible biphasic unfolding of the enzyme. The unfolding of the C-terminal domain-truncated enzyme follows a monophasic unfolding curve. Unfolding curves of mutants of the full-length protease W31 and W207/W218 are monophasic but correspond to the first and second phases of the protease, respectively. The unfolding intermediate of the protease represents a folded C-terminal domain but an unfolded N-terminal domain, which is enzymatically inactive due to loss of regulatory properties [12]) [12]

General stability information

<2>, replacing Arg with Ile at position 188 renders the protease resistant to proteolysis [31]

References

[1] Xu, T.; Ooi, A.; Lee, H.C.; Wilmouth, R.; Liu, D.X.; Lescar, J.: Structure of the SARS coronavirus main proteinase as an active C2 crystallographic dimer. Acta Crystallogr. Sect. F, **61**, 964-966 (2005)

[2] Zhang, X.W.; Yap, Y.L.: Old drugs as lead compounds for a new disease? Binding analysis of SARS coronavirus main proteinase with HIV, psychotic and parasite drugs. Bioorg. Med. Chem., **12**, 2517-2521 (2004)

[3] Graziano, V.; McGrath, W.J.; DeGruccio, A.M.; Dunn, J.J.; Mangel, W.F.: Enzymatic activity of the SARS coronavirus main proteinase dimer. FEBS Lett., **580**, 2577-2583 (2006)

[4] Tan, J.; Verschueren, K.H.; Anand, K.; Shen, J.; Yang, M.; Xu, Y.; Rao, Z.; Bigalke, J.; Heisen, B.; Mesters, J.R.; Chen, K.; Shen, X.; Jiang, H.; Hilgenfeld, R.: pH-dependent conformational flexibility of the SARS-CoV main proteinase (M(pro)) dimer: molecular dynamics simulations and multiple X-ray structure analyses. J. Mol. Biol., **354**, 25-40 (2005)
[5] Graziano, V.; McGrath, W.J.; Yang, L.; Mangel, W.F.: SARS CoV main proteinase: The monomer-dimer equilibrium dissociation constant. Biochemistry, **45**, 14632-14641 (2006)
[6] Goetz, D.H.; Choe, Y.; Hansell, E.; Chen, Y.T.; McDowell, M.; Jonsson, C.B.; Roush, B.C.; McKerrow, J.; Craik, C.S.: Substrate specificity profiling and identification of a new class of inhibitor for the major protease of the SARS coronavirus. Biochemistry, **46**, 8744-8752 (2007)
[7] Solowiej, J.; Thomson, J.A.; Ryan, K.; Luo, C.; He, M.; Lou, J.; Murray, B.W.: Steady-state and pre-steady-state kinetic evaluation of severe acute respiratory syndrome coronavirus (SARS-CoV) 3CLpro cysteine protease: development of an ion-pair model for catalysis. Biochemistry, **47**, 2617-2630 (2008)
[8] Hamill, P.; Hudson, D.; Kao, R.Y.; Chow, P.; Raj, M.; Xu, H.; Richer, M.J.; Jean, F.: Development of a red-shifted fluorescence-based assay for SARS-coronavirus 3CL protease: identification of a novel class of anti-SARS agents from the tropical marine sponge Axinella corrugata. Biol. Chem., **387**, 1063-1074 (2006)
[9] Chen, L.; Li, J.; Luo, C.; Liu, H.; Xu, W.; Chen, G.; Liew, O.W.; Zhu, W.; Puah, C.M.; Shen, X.; Jiang, H.: Binding interaction of quercetin-3-β -galactoside and its synthetic derivatives with SARS-CoV 3CLpro: Structure-activity relationship studies reveal salient pharmacophore features. Bioorg. Med. Chem., **14**, 8295-8306 (2006)
[10] Niu, C.; Yin, J.; Zhang, J.; Vederas, J.C.; James, M.N.: Molecular docking identifies the binding of 3-chloropyridine moieties specifically to the S_1 pocket of SARS-CoV Mpro. Bioorg. Med. Chem., **16**, 293-302 (2008)
[11] Ghosh, A.K.; Xi, K.; Grum-Tokars, V.; Xu, X.; Ratia, K.; Fu, W.; Houser, K.V.; Baker, S.C.; Johnson, M.E.; Mesecar, A.D.: Structure-based design, synthesis, and biological evaluation of peptidomimetic SARS-CoV 3CLpro inhibitors. Bioorg. Med. Chem. Lett., **17**, 5876-5880 (2007)
[12] Chang, H.; Chou, C.; Chang, G.: Reversible unfolding of the severe acute respiratory syndrome coronavirus main protease in guanidinium chloride. Biophys. J., **92**, 1374-1383 (2007)
[13] Wu, C.; King, K.; Kuo, C.; Fang, J.; Wu, Y.; Ho, M.; Liao, C.; Shie, J.; Liang, P.; Wong, C.: Stable benzotriazole esters as mechanism-based inactivators of the severe acute respiratory syndrome 3CL protease. Chem. Biol., **13**, 261-268 (2006)
[14] Shao, Y.; Yang, W.; Peng, H.; Hsu, M.; Tsai, K.; Kuo, T.; Wang, A.H.; Liang, P.; Lin, C.; Yang, A.; Wong, C.: Structure-based design and synthesis of highly potent SARS-CoV 3CL protease inhibitors. Chembiochem, **8**, 1654-1657 (2007)
[15] Lai, L.; Han, X.; Chen, H.; Wei, P.; Huang, C.; Liu, S.; Fan, K.; Zhou, L.; Liu, Z.; Pei, J.; Liu, Y.: Quaternary structure, substrate selectivity and inhibitor

design for SARS 3C-like proteinase. Curr. Pharm. Des., **12**, 4555-4564 (2006)
[16] Liang, P.: Characterization and inhibition of SARS-coronavirus main protease. Curr. Top. Med. Chem., **6**, 361-376 (2006)
[17] Shi, J.; Song, J.: The catalysis of the SARS 3C-like protease is under extensive regulation by its extra domain. FEBS J., **273**, 1035-1045 (2006)
[18] Chen, H.; Wei, P.; Huang, C.; Tan, L.; Liu, Y.; Lai, L.: Only one protomer is active in the dimer of SARS 3C-like proteinase. J. Biol. Chem., **281**, 13894-13898 (2006)
[19] Chen, S.; Hu, T.; Zhang, J.; Chen, J.; Chen, K.; Ding, J.; Jiang, H.; Shen, X.: Mutation of Gly-11 on the dimer interface results in the complete crystallographic dimer dissociation of severe acute respiratory syndrome coronavirus 3C-like protease. Crystal structure with molecular dynamics simulations. J. Biol. Chem., **283**, 554-564 (2008)
[20] Yang, S.; Chen, S.; Hsu, M.; Wu, J.; Tseng, C.K.; Liu, Y.; Chen, H.; Kuo, C.; Wu, C.; Chang, L.; Chen, W.; Liao, S.; Chang, T.; Hung, H.; Shr, H.; Liu, C.; Huang, Y.; Chang, L.; Hsu, J.; Peters, C.J.; Wang, A.H.; Hsu, M.: Synthesis, crystal structure, structure-activity relationships, and antiviral activity of a potent SARS coronavirus 3CL protease inhibitor. J. Med. Chem., **49**, 4971-4980 (2006)
[21] Lu, I.; Mahindroo, N.; Liang, P.; Peng, Y.; Kuo, C.; Tsai, K.; Hsieh, H.; Chao, Y.; Wu, S.: Structure-based drug design and structural biology study of novel nonpeptide inhibitors of severe acute respiratory syndrome coronavirus main protease. J. Med. Chem., **49**, 5154-5161 (2006)
[22] Wen, C.; Kuo, Y.; Jan, J.; Liang, P.; Wang, S.; Liu, H.; Lee, C.; Chang, S.; Kuo, C.; Lee, S.; Hou, C.; Hsiao, P.; Chien, S.; Shyur, L.; Yang, N.: Specific plant terpenoids and lignoids possess potent antiviral activities against severe acute respiratory syndrome coronavirus. J. Med. Chem., **50**, 4087-4095 (2007)
[23] Lee, T.; Cherney, M.M.; Liu, J.; James, K.E.; Powers, J.C.; Eltis, L.D.; James, M.N.: Crystal structures reveal an induced-fit binding of a substrate-like aza-peptide epoxide to SARS coronavirus main peptidase. J. Mol. Biol., **366**, 916-932 (2007)
[24] Yin, J.; Niu, C.; Cherney, M.M.; Zhang, J.; Huitema, C.; Eltis, L.D.; Vederas, J.C.; James, M.N.: A mechanistic view of enzyme inhibition and peptide hydrolysis in the active site of the SARS-CoV 3C-like peptidase. J. Mol. Biol., **371**, 1060-1074 (2007)
[25] Zheng, K.; Ma, G.; Zhou, J.; Min, Z.; Zhao, W.; Jiang, Y.; Yu, Q.; Feng, J.: Insight into the activity of SARS main protease: molecular dynamics study of dimeric and monomeric form of enzyme. Proteins Struct. Funct. Bioinform., **66**, 467-479 (2007)
[26] Lin, P.Y.; Chou, C.Y.; Chang, H.C.; Hsu, W.C.; Chang, G.G.: Correlation between dissociation and catalysis of SARS-CoV main protease. Arch. Biochem. Biophys., **472**, 34-42 (2008)
[27] Fan, K.; Wei, P.; Feng, Q.; Chen, S.; Huang, C.; Ma, L.; Lai, B.; Pei, J.; Liu, Y.; Chen, J.; Lai, L.J.: Biosynthesis, purification, and substrate specificity of se-

vere acute respiratory syndrome coronavirus 3C-like proteinase. Biol. Chem., **279**, 1637-1642 (2004)
[28] Zhang, J.; Huitema, C.; Niu, C.; Yin, J.; James, M.N.; Eltis, L.D.; Vederas, J.C.: Aryl methylene ketones and fluorinated methylene ketones as reversible inhibitors for severe acute respiratory syndrome (SARS) 3C-like proteinase. Bioorg. Chem., **36**, 229-240 (2008)
[29] Mukherjee, P.; Desai, P.; Ross, L.; White, E.L.; Avery, M.A.: Structure-based virtual screening against SARS-3CL(pro) to identify novel non-peptidic hits. Bioorg. Med. Chem., **16**, 4138-4149 (2008)
[30] Shao, Y.M.; Yang, W.B.; Kuo, T.H.; Tsai, K.C.; Lin, C.H.; Yang, A.S.; Liang, P.H.; Wong, C.H.: Design, synthesis, and evaluation of trifluoromethyl ketones as inhibitors of SARS-CoV 3CL protease. Bioorg. Med. Chem., **16**, 4652-4660 (2008)
[31] Akaji, K.; Konno, H.; Onozuka, M.; Makino, A.; Saito, H.; Nosaka, K.: Evaluation of peptide-aldehyde inhibitors using R188I mutant of SARS 3CL protease as a proteolysis-resistant mutant. Bioorg. Med. Chem., **16**, 9400-9408 (2008)
[32] Ghosh, A.K.; Gong, G.; Grum-Tokars, V.; Mulhearn, D.C.; Baker, S.C.; Coughlin, M.; Prabhakar, B.S.; Sleeman, K.; Johnson, M.E.; Mesecar, A.D.: Design, synthesis and antiviral efficacy of a series of potent chloropyridyl ester-derived SARS-CoV 3CLpro inhibitors. Bioorg. Med. Chem. Lett., **18**, 5684-5688 (2008)
[33] Phakthanakanok, K.; Ratanakhanokchai, K.; Kyu, K.L.; Sompornpisut, P.; Watts, A.; Pinitglang, S.: A computational analysis of SARS cysteine proteinase-octapeptide substrate interaction: implication for structure and active site binding mechanism. BMC Bioinformatics, **10 Suppl 1**, S48 (2009)
[34] Bacha, U.; Barrila, J.; Gabelli, S.B.; Kiso, Y.; Mario Amzel, L.; Freire, E.: Development of broad-spectrum halomethyl ketone inhibitors against coronavirus main protease 3CL(pro). Chem. Biol. Drug Des., **72**, 34-49 (2008)
[35] Yang, Q.; Chen, L.; He, X.; Gao, Z.; Shen, X.; Bai, D.: Design and synthesis of cinanserin analogs as severe acute respiratory syndrome coronavirus 3CL protease inhibitors. Chem. Pharm. Bull., **56**, 1400-1405 (2008)
[36] Kuo, C.J.; Liu, H.G.; Lo, Y.K.; Seong, C.M.; Lee, K.I.; Jung, Y.S.; Liang, P.H.: Individual and common inhibitors of coronavirus and picornavirus main proteases. FEBS Lett., **583**, 549-555 (2009)
[37] Chen, S.; Zhang, J.; Hu, T.; Chen, K.; Jiang, H.; Shen, X.: Residues on the dimer interface of SARS coronavirus 3C-like protease: dimer stability characterization and enzyme catalytic activity analysis. J. Biochem., **143**, 525-536 (2008)
[38] Lee, C.C.; Kuo, C.J.; Ko, T.P.; Hsu, M.F.; Tsui, Y.C.; Chang, S.C.; Yang, S.; Chen, S.J.; Chen, H.C.; Hsu, M.C.; Shih, S.R.; Liang, P.H.; Wang, A.H.: Structural basis of inhibition specificities of 3C and 3C-like proteases by zinc-coordinating and peptidomimetic Compounds. J. Biol. Chem., **284**, 7646-7655 (2009)
[39] Taranto, A.G.; Carvalho, P.; Avery, M.A.: QM/QM studies for Michael reaction in coronavirus main protease (3CL Pro). J. Mol. Graph. Model., **27**, 275-285 (2008)

[40] Zhong, N.; Zhang, S.; Zou, P.; Chen, J.; Kang, X.; Li, Z.; Liang, C.; Jin, C.; Xia, B.: Without its N-finger, the main protease of severe acute respiratory syndrome coronavirus can form a novel dimer through its C-terminal domain. J. Virol., **82**, 4227-4234 (2008)
[41] Shi, J.; Sivaraman, J.; Song, J.: Mechanism for controlling the dimer-monomer switch and coupling dimerization to catalysis of the severe acute respiratory syndrome coronavirus 3C-like protease. J. Virol., **82**, 4620-4629 (2008)
[42] Chu, L.H.; Choy, W.Y.; Tsai, S.N.; Rao, Z.; Ngai, S.M.: Rapid peptide-based screening on the substrate specificity of severe acute respiratory syndrome (SARS) coronavirus 3C-like protease by matrix-assisted laser desorption/ionization time-of-flight mass spectrometry. Protein Sci., **15**, 699-709 (2006)
[43] Zhong, N.; Zhang, S.; Xue, F.; Kang, X.; Zou, P.; Chen, J.; Liang, C.; Rao, Z.; Jin, C.; Lou, Z.; Xia, B.: C-terminal domain of SARS-CoV main protease can form a 3D domain-swapped dimer. Protein Sci., **18**, 839-844 (2009)
[44] Regnier, T.; Sarma, D.; Hidaka, K.; Bacha, U.; Freire, E.; Hayashi, Y.; Kiso, Y.: New developments for the design, synthesis and biological evaluation of potent SARS-CoV 3CL(pro) inhibitors. Bioorg. Med. Chem. Lett., **19**, 2722-2727 (2009)
[45] Ryu, Y.B.; Park, S.J.; Kim, Y.M.; Lee, J.Y.; Seo, W.D.; Chang, J.S.; Park, K.H.; Rho, M.C.; Lee, W.S.: SARS-CoV 3CLpro inhibitory effects of quinone-methide triterpenes from Tripterygium regelii. Bioorg. Med. Chem. Lett., **20**, 1873-1876 (2010)
[46] Ramajayam, R.; Tan, K.P.; Liu, H.G.; Liang, P.H.: Synthesis, docking studies, and evaluation of pyrimidines as inhibitors of SARS-CoV 3CL protease. Bioorg. Med. Chem. Lett., **20**, 3569-3572 (2010)
[47] Cheng, S.C.; Chang, G.G.; Chou, C.Y.: Mutation of Glu-166 blocks the substrate-induced dimerization of SARS coronavirus main protease. Biophys. J., **98**, 1327-1336 (2010)
[48] Luo, W.; Su, X.; Gong, S.; Qin, Y.; Liu, W.; Li, J.; Yu, H.; Xu, Q.: Anti-SARS coronavirus 3C-like protease effects of Rheum palmatum L. extracts. Biosci. Trends, **3**, 124-126 (2009)
[49] Kuo, C.J.; Shih, Y.P.; Kan, D.; Liang, P.H.: Engineering a novel endopeptidase based on SARS 3CL(pro). Biotechniques, **47**, 1029-1032 (2009)
[50] Li, C.; Qi, Y.; Teng, X.; Yang, Z.; Wei, P.; Zhang, C.; Tan, L.; Zhou, L.; Liu, Y.; Lai, L.: Maturation mechanism of severe acute respiratory syndrome (SARS) coronavirus 3C-like proteinase. J. Biol. Chem., **285**, 28134-28140 (2010)
[51] Hu, T.; Zhang, Y.; Li, L.; Wang, K.; Chen, S.; Chen, J.; Ding, J.; Jiang, H.; Shen, X.: Two adjacent mutations on the dimer interface of SARS coronavirus 3C-like protease cause different conformational changes in crystal structure. Virology, **388**, 324-334 (2009)

sortase A 3.4.22.70

1 Nomenclature

EC number
3.4.22.70

Recommended name
sortase A

Synonyms
C60.001 (Merops-ID)
SrtA <1,2,3,5,7,8,9,11,12,14,15> [10,11,16,19,25,26,27,28,29,30,31,32,34,36,38,39,40,41,42,43,44,45,47,48,49,51,52,53,54,55,56,57,58,59]
SrtA protein
SrtA sortase <4> [17]
sortase A transpeptidase <1> [22]
sortase SrtA <1> [46]
sortase transpeptidase <1> [26]

CAS registry number
9033-39-0

2 Source Organism

<1> *Staphylococcus aureus* [2,3,4,5,6,7,8,9,10,11,12,13,14,15,16,19,20,21,22,23,26,29,30,31,32,33,34,35,36,37,38,39,40,41,46,47,51,52,53,54,57]
<2> *Enterococcus faecalis* [49,56]
<3> *Streptococcus pneumoniae* [27,42,48,55]
<4> *Streptococcus agalactiae* [17]
<5> *Streptococcus sanguinis* [43]
<6> *Corynebacterium diphtheriae* [24]
<7> *Listeria monocytogenes* [25]
<8> *Streptococcus gordonii* [44]
<9> *Bacillus anthracis* [18,28,38,58]
<10> *Staphylococcus aureus* (UNIPROT accession number: Q9S446) [1]
<11> *Streptococcus suis* [45]
<12> *Streptococcus pneumoniae* D39 [55]
<13> *Streptococcus pyogenes* (UNIPROT accession number: Q99ZN4) [50]
<14> *Streptococcus pneumoniae* TIGR4 [55]
<15> *Streptococcus uberis* 0140J (UNIPROT accession number: B9DS55) [59]

D. Schomburg and I. Schomburg (eds.), *Class 3.4–6 Hydrolases, Lyases, Isomerases, Ligases: EC 3.4–6*, Springer Handbook of Enzymes S10, DOI 10.1007/978-3-642-36260-6_4,

3 Reaction and Specificity

Catalyzed reaction

The enzyme catalyses a cell wall sorting reaction in which a surface protein with a sorting signal containing a LPXTG motif is cleaved between the Thr and Gly residue. The resulting threonine carboxyl end of the protein is covalently attached to a pentaglycine cross-bridge of peptidoglycan.

Reaction type

hydrolysis of peptide bond

Natural substrates and products

S Additional information <1,2,3,4,6,8,10,11> (<1> transpeptidase activity: the enzyme catalyzes a cell wall sorting reaction in which a surface protein with a sorting signal containing a LPXT-/-G motif is cleaved between the Thr and Gly residue. The resulting threonine carboxyl end of the protein is covalently attached to a pentaglycine cross-bridge of peptidoglycan. When a nucleophile is not available, sortase slowly hydrolyzes the LPETG peptide at the same site. Ping-pong mechanism in which a common acyl-enzyme intermediate is formed in transpeptidation and hydrolysis. The nucleophile binding site of the enzyme is specific for diglycine [2]; <10> the enzyme anchors surface proteins to the bacterial cells wall [1]; <1> the enzyme cleaves surface proteins of Staphylococcus aureus at the LPXT-/-G motif, catalyzes surface protein anchoring by means of a transpeptidation reaction that captures cleaved polypeptides as thioester enzyme intermediates [5]; <1> the enzyme cleaves surface proteins at the LPXTG motif and catalyzes the formation of an amide bond between the carboxyl group of Thr and the amino group of cell-wall crossbridges [3]; <1> gram-positive pathogenic bacteria display proteins on their surface that play important roles during infection. In Staphylococcus aureus theses surface proteins are anchored to the cell wall by two sortase, sortase A and sortaseB that recognize specific surface protein sorting signals. Sortase A is an essential virulence factor for establishment of septic arthritis [9]; <1> primary role of the SrtA isoform in Staphylococcus aureus adhesion and host colonization [12]; <4> SrtA sortase of Streptococcus agalactiae is required for cell wall anchoring of proteins containing the LPXTG motif, for adhesion to epithelial cells, and for colonization of the mouse intestine [17]; <1> the transpeptidase required for cell wall protein anchoring and virulence in Staphylococcus aureus [19]; <6> two elements of Spa pilin precursor, the pilin motif and the sorting signal, are together sufficient to promote the polymerization of an otherwise secreted protein by a process requiring the function of the sortase A [24]; <8> in addition to its role in processing LPXTG containing adhesins, sortase A has the function of contributing to transcriptional regulation of adhesin gene expression [44]; <3> role of srtA in adherence in vitro is dependent on capsule expression, the role of SrtA in adherence to human cells only being apparent in the absence of the pneumococcal capsule [42]; <2> sortase

localization is facilitated by a positive charge that is necessary for efficient pilus biogenesis [49]; <3> SrtA is dispensable for pilus assembly and localization to the cell wall [48]; <11> SrtA is involved in the virulence manifestation of streptococcal toxic shock syndrome [45]) (Reversibility: ?) [1,2,3,5,9,12,17,19,24,42,44,45,48,49]

P ?

Substrates and products

S 2-aminobenzoyl-LPATG-diaminopropionic acid + H_2O <9> (<9> efficient cleavage [28]) (Reversibility: ?) [28]

P 2-aminobenzoyl-LPAT + glycyl-diaminopropionic acid

S 2-aminobenzoyl-LPETG-diaminopropionic acid + <1> (Reversibility: ?) [21]

P ?

S 2-aminobenzoyl-LPETG-diaminopropionic acid + Gly5 <1> (Reversibility: ?) [13]

P ?

S 2-aminobenzoyl-LPETG-diaminopropionic acid + H_2O <1> (<1> evidence for a reverse protonation catalytic mechanism [13]) (Reversibility: ?) [13]

P ?

S 2-aminobenzoyl-LPETG-diaminopropionic acid + H_2O <9> (<9> cleavage between the threonine and the glycine residues, efficient cleavage [28]) (Reversibility: ?) [28]

P 2-aminobenzoyl-LPET + glycyl-diaminopropionic acid

S 2-aminobenzoyl-LPNTA-diaminopropionic acid + H_2O <9> (<9> small amount of cleavage [28]) (Reversibility: ?) [28]

P 2-aminobenzoyl-LPNT + alanyl-diaminopropionic acid

S 4-([4-(dimethylamino)phenyl]-azo)-benzoyl-QALPETGEE-((2-aminoethyl)-amino)naphthalene-1-sulfonic acid + H_2O <1> (<1> a catalytically important and conserved binding surface is formed by residues A118, T180 and I182. R197 is also required for catalysis [16]) (Reversibility: ?) [16]

P ?

S 4-[[4'-(dimethylamino)phenyl]azo]-benzoyl-Gln-Ala-Leu-Pro-Glu-Thr-Gly-Glu-Glu-5-[(2'-aminoethyl)-amino]naphthalenesulfonic acid + H_2O <1> (Reversibility: ?) [4,5,6]

P 4-[[4'-(dimethylamino)phenyl]azo]-benzoyl-Gln-Ala-Leu-Pro-Glu-Thr + Gly-Glu-Glu-5-[(2'-aminoethyl)-amino]naphthalenesulfonic acid

S 4-[[4'-(dimethylamino)phenyl]azo]-benzoyl-Leu-Pro-Glu-Thr-Gly-5-[(2'-aminoethyl)-amino]naphthalenesulfonic acid + H_2O <1> (Reversibility: ?) [3]

P 4-[[4'-(dimethylamino)phenyl]azo]-benzoyl-Leu-Pro-Glu-Thr + Gly-5-[(2'-aminoethyl)-amino]naphthalenesulfonic acid

S AHLPKTGLR + 5-aminopentan-1-ol <1> (Reversibility: ?) [53]

P ?

S AHLPKTGLR + 6-aminohexyl 4-O-β-D-galactopyranosyl-β-D-glucopyranoside <1> (Reversibility: ?) [53]

P ?

S AHLPKTGLR + N-(2-(2-ethoxyethoxy)ethanamine)biotin amide <1> (Reversibility: ?) [53]
P ?
S AHLPKTGLR + N-hexylbiotin amide <1> (Reversibility: ?) [53]
P ?
S AHLPKTGLR-NH_2 + triglycine <1> (Reversibility: ?) [53]
P ?
S Abz-LPETG-Dap(Dnp)-NH_2 + Gly5 <1> (Reversibility: ?) [10,12]
P Abz-LPETGGGGG-OH + Gly-Dap(Dnp)-NH_2
S Abz-LPETG-Dap(Dnp)-NH_2 + Gly5 <1> (<1> transpeptidation of LPXTG-containing peptides to the cell-wall precursor mimic NH_2-Ala2 [46]) (Reversibility: ?) [46]
P ?
S Abz-LPETGG-Dap(Dnp)-NH_2 + Ala-Ala <13> (<13> transpeptidation of LPXTG-containing peptides to the cell-wall precursor mimic AlaAla [50]) (Reversibility: ?) [50]
P Abz-LPETAA + GG-Dap(Dnp)-NH_2
S Dnp-AQALPETGEE-NH_2 + Gly5 <1> (Reversibility: ?) [12]
P ?
S [4-(4-dimethylaminophenylazo)benzoic acid]-QALPETGEE-[5-[2'-(aminoethyl)amino]-naphthalenesulfonic acid] + H_2O <1> (Reversibility: ?) [35]
P ?
S acetyl-ooocctcttacctcagttacaoooLPKTGGR-NH_2 + H-GGGKLALKLALK ALKAALKLA-NH_2 <1> (Reversibility: ?) [51]
P acetyl-ooocctcttacctcagttacaoooLPKTGGGKLALKLALKALKAALKLA-NH_2 + H-GGR-NH_2
S Abz-KVENPQTNAGT-Dap(Dnp)-NH_2 + GGGGG <1> (Reversibility: ?) [39]
P ?
S Abz-LPETG-Dap + GGGGG <1> (Reversibility: ?) [26]
P Abz-LPETGGGGG + glycyl-diaminopropionic acid
S Abz-LPETG-Dap + H_2O <1> (Reversibility: ?) [26]
P Abz-LPET + glycyl-diaminopropionic acid
S Abz-LPETG-Dap(Dnp)-NH_2 + Gly-Gly-Gly-Gly-Gly <1> (Reversibility: ?) [32]
P ?
S Abz-LPETG-Dap(Dnp)-NH_2 + GGGGG <1> (Reversibility: ?) [30]
P ?
S Abz-LPETG-dinitrophenyl ester + Gly-Gly-Gly <1> (<1> HPLC results provide direct evidence for the formation of the kinetically competent acyl enzyme intermediate [29]) (Reversibility: ?) [29]
P aminobenzoyl-LPETGGG + Gly-dinitrophenyl ester
S Abz-LPETGG-Dap(Dnp)-NH_2 + NH_2-GGGGG-OH <1> (Reversibility: ?) [40]
P ?
S *o*-aminobenzoyl-LPETG-2,4-dinitrophenyl + H_2O <9> (Reversibility: ?) [58]
P *o*-aminobenzoyl-LPETG + 2,4-dinitrophenol
S *o*-aminobenzoyl-LPETG-2,4-dinitrophenyl ester + H_2O <1> (Reversibility: ?) [22]

P ?
S Abz-LPETG-Dap(Dnp)-NH_2 acid + H_2O <1> (Reversibility: ?) [54]
P ?
S *o*-aminobenzoyl-Leu-Pro-Glu-Thr-Gly-2,4-dinitrophenyl ester + Gly-Gly-Gly <1> (<1> ping-pong mechanism in which a common acyl-enzyme intermediate is formed in transpeptidation and hydrolysis. The nucleophile binding site of the enzyme is specific for diglycine. The S_1 and S2 sites of the sortase both prefer a glycine residue, the S_1 site is exclusively selective for glycine [2]) (Reversibility: ?) [2]
P *o*-aminobenzoyl-Leu-Pro-Glu-Thr-Gly-Gly-Gly + Gly-2,4-dinitrophenol
S *o*-aminobenzoyl-Leu-Pro-Glu-Thr-Gly-2,4-dinitrophenol + H_2O <1> (<1> ping-pong mechanism in which a common acyl-enzyme intermediate is formed in transpeptidation and hydrolysis. The nucleophile binding site of the enzyme is specific for diglycine. The S1 and S2 sites of the sortase both prefer a glycine residue, the S1 site is exclusively selective for glycine [2]) (Reversibility: ?) [2]
P *o*-aminobenzoyl-Leu-Pro-Glu-Thr + Gly-2,4-dinitrophenyl ester
S recombinant Helicobacter pylori R1,3-fucosyltransferase + triglycine <1> (Reversibility: ?) [53]
P ?
S recombinant human β1,4-galactosyltransferase + N-(2-(2-ethoxyethoxy)ethanamine)biotin amide <1> (Reversibility: ?) [53]
P ?
S recombinant human β1,4-galactosyltransferase + N-hexylbiotin amide <1> (Reversibility: ?) [53]
P ?
S Additional information <1,2,3,4,5,6,7,8,9,10,11,15> (<10> the enzyme anchors surface proteins to the bacterial cell wall [1]; <1> the enzyme cleaves surface proteins of Staphylococcus aureus at the LPXT-/-G motif [5,6]; <1> transpeptidase activity. The enzyme catalyzes a cell wall sorting reaction in which a surface protein with a sorting signal containing a LPXT-/-G motif is cleaved between the Thr and Gly residue. The resulting threonine carboxyl end of the protein is covalently attached to a pentaglycine cross-bridge of peptidoglycan. When a nucleophile is not available, sortase slowly hydrolyzes the LPET-/-G peptide at the same site. Ping-pong mechanism in which a common acyl-enzyme intermediate is formed in transpeptidation and hydrolysis. The nucleophile binding site of the enzyme is specific for diglycine. The S1 and S2 sites of the sortase both prefer a glycine residue, the S1 site is exclusively selective for glycine [2]; <1> transpeptidase activity: the enzyme catalyzes a cell wall sorting reaction in which a surface protein with a sorting signal containing a LPXT-/-G motif is cleaved between the Thr and Gly residue. The resulting threonine carboxyl end of the protein is covalently attached to a pentaglycine cross-bridge of peptidoglycan. When a nucleophile is not available, sortase slowly hydrolyzes the LPETG peptide at the same site. Ping-pong mechanism in which a common acyl-enzyme intermediate is formed in transpeptidation and hydrolysis. The nucleophile binding site of the en-

zyme is specific for diglycine [2]; <10> the enzyme anchors surface proteins to the bacterial cells wall [1]; <1> the enzyme cleaves surface proteins of Staphylococcus aureus at the LPXT-/-G motif, catalyzes surface protein anchoring by means of a transpeptidation reaction that captures cleaved polypeptides as thioester enzyme intermediates [5]; <1> the enzyme cleaves surface proteins at the LPXTG motif and catalyzes the formation of an amide bond between the carboxyl group of Thr and the amino group of cell-wall crossbridges [3]; <1> gram-positive pathogenic bacteria display proteins on their surface that play important roles during infection. In Staphylococcus aureus theses surface proteins are anchored to the cell wall by two sortase, sortase A and sortaseB that recognize specific surface protein sorting signals. Sortase A is an essential virulence factor for establishment of septic arthritis [9]; <1> primary role of the SrtA isoform in Staphylococcus aureus adhesion and host colonization [12]; <4> SrtA sortase of Streptococcus agalactiae is required for cell wall anchoring of proteins containing the LPXTG motif, for adhesion to epithelial cells, and for colonization of the mouse intestine [17]; <1> the transpeptidase required for cell wall protein anchoring and virulence in Staphylococcus aureus [19]; <6> two elements of Spa pilin precursor, the pilin motif and the sorting signal, are together sufficient to promote the polymerization of an otherwise secreted protein by a process requiring the function of the sortase A [24]; <7> non-gel proteomics is a powerful technique to rapidly identify sortase substrates and to gain insights on potential sorting motifs. LPXTG-containing proteins were identified exclusively in strains having a functional SrtA [25]; <9> sortase A may be critical in the early stage of inhaltation anthrax [18]; <1> sortase A plays a role in the establishment of infections [20]; <9> no cleavage of 2-aminobenzoyl-NPKTG-diaminopropionic acid and 2-aminobenzoyl-LGATG-diaminopropionic acid [28]; <8> in addition to its role in processing LPXTG containing adhesins, sortase A has the function of contributing to transcriptional regulation of adhesin gene expression [44]; <3> role of srtA in adherence in vitro is dependent on capsule expression, the role of SrtA in adherence to human cells only being apparent in the absence of the pneumococcal capsule [42]; <1> sortase can transfer peptide substrates to oligosaccharides appended with a 6-deoxy-6-aminohexose moiety in a selective manner as that of an oligoglycine sequence [37]; <5> SrtA contributes to antiopsonization in Streptococci. SrtA anchors surface adhesins as well as some proteins that function as antiopsonic molecules as a means of evading the human immune system. SrtA of Streptococcus sanguinis plays important roles in bacterial colonization [43]; <2> sortase localization is facilitated by a positive charge that is necessary for efficient pilus biogenesis [49]; <3> SrtA is dispensable for pilus assembly and localization to the cell wall [48]; <11> SrtA is involved in the virulence manifestation of streptococcal toxic shock syndrome [45]; <15> sortase A anchors the following proteins in the cell wall of Streptococcus uberis strain 0140J: putative fructan β-fructosidase precursor, putative lactoferrin binding protein, putative collagen-like surface anchored protein, putative C5a peptidase

precursor, and putative zinc-carboxypeptidase. Alternate cell wall anchoring motifs are either LPXTXD/E or LPXXXD [59]; <1> SrtA cleaves proteins at LPXTG-motif between threonine and glycine, and subsequently transfers the acyl-fragment to a N-terminal oligoglycine [51]; <1> SrtA recognizes LPXTG near the C-terminus of a target protein. The Cys184 of SrtA performs a nucleophilic attack at the peptide bond between T and G in LPXTG, resulting in a thioester intermediate with the carboxyl group of the C-terminal T linked to Cys184. This reactive intermediate reacts with the cross-bridge N-terminus of a cell-wall proteoglycan to anchor the target protein to the cell-wall peptidoglycan. SrtA accepts various peptide/protein substrates, so long as they bear the sorting signal LPXTG, and a range of amino nucleophiles [57]; <9> SrtA recognizes the LPXTG-sorting signal through a lock-in-key mechanism [58]; <1> the enzyme cleaves the LPXTG sequence at the amide bond between the threonine and the glycine to form an acyl-enzyme complex. Nucleophilic attack by the amino group of the tri-glycine on the intermediate results in the formation of an LPXTGGG bond and the liberation of the free enzyme [53]) (Reversibility: ?) [1,2,3,5,6,9,12,17,18,19,20,24,25,28,37,42,43,44,45,48,49,51,53,57,58,59]

P ?

Inhibitors

(1E)-N'-[(1E)-(4-[(E)-[(diaminomethylene)hydrazono]methyl]phenyl)methylene]ethanehydrazonamide <1> [35]

(2-(trimethylammonium)ethyl)methanethiosulfonate <9> (<9> inibition at 5 mM, inhibition is relieved by supplementing the reaction with 10 mM dithiothreitol [28]) [28]

(2-sulfonatoethyl)methanethiosulfonate <1> [7]

(2E)-2,3-bis(4-methoxyphenyl)acrylamide <1> (<1> IC50: 0.476 mM [23]) [23]

(2E)-2,3-bis(4-methoxyphenyl)acrylonitrile <1> (<1> IC50: 0.187 mM [23]) [23]

(2E)-2-(2-furoyl)-3-[(methyl[4-[(5-nitropyridin-2-yl)oxy]phenyl]oxido-l4-sulfanylidene)amino]acrylonitrile <1> [35]

(2E)-3-(2-furyl)-N-[3-(hydroxymethyl)-4-morpholin-4-ylphenyl]acrylamide <1> [35]

(2E)-3-[(methyl[4-[(5-nitropyridin-2-yl)oxy]phenyl]oxido-l4-sulfanylidene)amino]-2-(2-thienylcarbonyl)acrylonitrile <1> [35]

(2E)-4-([4-[(2-hydroxybenzoyl)amino]phenyl]amino)-4-oxobut-2-enoic acid <1> [35]

(2E)-N-(3-formyl-4-morpholin-4-ylphenyl)-3-(2-furyl)acrylamide <1> [35]

(2E)-N-(3-formyl-4-morpholin-4-ylphenyl)-3-(2-thienyl)acrylamide <1> [35]

(2E)-N-[3-(hydroxymethyl)-4-morpholin-4-ylphenyl]-3-(2-thienyl)acrylamide <1> [35]

(2Z)-2,3-bis(4-methoxyphenyl)acrylonitrile <1> (<1> IC50: 0.0279mM [23]) [23]

(2Z)-3-(2,5-dimethoxyphenyl)-2-(4-methoxyphenyl)acrylonitrile <1> (<1> IC50: 0.009244 mM [23]) [23]

(2Z)-3-(2-methoxyphenyl)-2-(4-methoxyphenyl)acrylonitrile <1> (<1> IC50: 0.0362 mM [23]) [23]
(2Z)-3-(3,4-dimethoxyphenyl)-2-(4-methoxyphenyl)acrylonitrile <1> (<1> IC50: 0.02296 mM [23]) [23]
(2Z)-3-(3,5-dimethoxyphenyl)-2-(4-methoxyphenyl)acrylonitrile <1> (<1> IC50: 0.025463 mM [23]) [23]
(2Z)-3-(3-methoxyphenyl)-2-(4-methoxyphenyl)acrylonitrile <1> (<1> IC50: 0.0174 mM [23]) [23]
(4E)-5-methyl-4-[[(4-nitrophenyl)amino]methylidene]-2-phenyl-2,4-dihydro-^{3}H-pyrazole-3-thione <1> [54]
(5R)-3,5-bis(6-bromo-1H-indol-3-yl)-5,6-dihydropyrazin-2(1H)-one <1> (<1> IC50: 68.98 mg/L [15]) [15]
(5Z)-3-(2,4-dimethylphenyl)-5-(3-nitrobenzylidene)-2-thioxo-1,3-thiazolidin-4-one <1> [54]
(5Z)-3-(3-chlorophenyl)-5-(4-methyl-3-nitrobenzylidene)-2-thioxo-1,3-thiazolidin-4-one <1> [54]
(5Z)-3-benzyl-5-benzylidene-2-thioxo-1,3-thiazolidin-4-one <1> [54]
(5Z)-3-ethyl-5-(2-nitrobenzylidene)-2-thioxo-1,3-thiazolidin-4-one <1> [54]
(5Z)-5-(3-bromo-2-hydroxy-5-nitrobenzylidene)-3-(2,4-dimethylphenyl)-2-thioxo-1,3-thiazolidin-4-one <1> [54]
(5Z)-5-(3-bromo-2-hydroxy-5-nitrobenzylidene)-3-(3-chlorophenyl)-2-thioxo-1,3-thiazolidin-4-one <1> [54]
(5Z)-5-(3-bromo-2-hydroxy-5-nitrobenzylidene)-3-(3-methylphenyl)-2-thioxo-1,3-thiazolidin-4-one <1> [54]
(5Z)-5-(3-bromo-2-hydroxy-5-nitrobenzylidene)-3-(4-nitrophenyl)-2-thioxo-1,3-thiazolidin-4-one <1> [54]
(5Z)-5-(3-bromo-2-hydroxy-5-nitrobenzylidene)-3-phenyl-2-thioxo-1,3-thiazolidin-4-one <1> [54]
(5Z)-5-(3-bromo-4-hydroxy-5-nitrobenzylidene)-3-(2,4-dimethylphenyl)-2-thioxo-1,3-thiazolidin-4-one <1> [54]
(5Z)-5-(3-chlorobenzylidene)-3-ethyl-2-thioxo-1,3-thiazolidin-4-one <1> [54]
(5Z)-5-benzylidene-3-(prop-2-en-1-yl)-2-thioxo-1,3-thiazolidin-4-one <1> [54]
(5Z)-5-benzylidene-3-methyl-2-thioxo-1,3-thiazolidin-4-one <1> [54]
(5Z)-5-benzylidene-3-propyl-2-thioxo-1,3-thiazolidin-4-one <1> [54]
(6-methyl-1H-inden-3-yl)[4-(6-methyl-1H-indol-3-yl)-1H-imidazol-2-yl]-methanone <1> (<1> IC50: 15.67 mg/Ll [15]) [15]
(6R)-3,6-bis(6-bromo-1H-indol-3-yl)-5,6-dihydropyrazin-2(1H)-one <1> (<1> IC50: 86.34 mg/L [15]) [15]
(6R)-6-(6-bromo-1H-indol-3-yl)-3-(1H-indol-3-yl)-5,6-dihydropyrazin-2(1H)-one <1> (<1> IC50: 34.04 mg/L [15]) [15]
(Z)-3-(2,5-dimethoxyphenyl)-2-(4-methoxyphenyl) acrylonitrile <1> (<1> potential of this inhibitor for the treatment of Staphylococcus aureus infections [11]) [11]
1-(3,4-dichlorophenyl)-3-(dimethylamino)propan-1-one <1> [38]
1-(4-bromophenyl)-3-(3-methylpiperidin-1-yl)propan-1-one <1> [38]
1-(4-chlorophenyl)-3-morpholin-4-ylpropan-1-one <1> [38]
1-(4-fluorophenyl)-3-morpholin-4-ylpropan-1-one <1> [38]

1-(4-methylphenyl)-3-morpholin-4-ylpropan-1-one <1> [38]
1-[4-(2-aminopyrimidin-4-yl)phenyl]-3-(4-chlorophenyl)urea <1> [35]
2-(3,5-dichlorophenyl)-4-(ethylsulfanyl)-5-sulfanylpyridazin-3(2H)-one <1> [54]
2-(3,5-dichlorophenyl)-5-ethoxy-4-sulfanylpyridazin-3(2H)-one <1> [54]
2-(3-bromophenyl)-4,5-dichloropyridazin-3(2H)-one <1> [54]
2-(3-bromophenyl)-4-(ethylsulfanyl)-5-sulfanylpyridazin-3(2H)-one <1> [54]
2-(3-bromophenyl)-4-chloro-5-ethoxypyridazin-3(2H)-one <1> [54]
2-(3-bromophenyl)-5-chloro-4-ethoxypyridazin-3(2H)-one <1> [54]
2-(3-bromophenyl)-5-chloro-4-methoxypyridazin-3(2H)-one <1> [54]
2-(3-chlorophenyl)-4-methoxy-5-sulfanylpyridazin-3(2H)-one <1> [54]
2-(4-nitrophenyl)-4,5-dichloropyridazin-3-one <1> [54]
2-cyclohexyl-4-(ethylsulfanyl)-5-sulfanylpyridazin-3(2H)-one <1> [54]
2-ethyl-4-hydroxy-5-(methylsulfanyl)pyridazin-3(2H)-one <1> [54]
2-hydroxy-N-[4-[([[(4-methylphenyl)sulfonyl]amino]carbonyl)amino]phenyl]benzamide <1> [35]
2-morpholin-4-yl-5-[[(2E)-3-(2-thienyl)prop-2-enoyl]amino]benzamide <1> [35]
2-phenyl-4,5-dichloro-pyridazin-3-one <1> [54]
3,3,3-trifluoro-1-(phenylsulfonyl)-1-propene <1> (<1> IC50: 0.19 mM, irreversible [19]) [19]
3,5-bis[[2-(4-nitrophenyl)-2-oxoethyl]thio]isothiazole-4-carbonitrile <1> [35]
3-(dimethylamino)-1-(2-thienyl)propan-1-one <1> [38]
3-(dimethylamino)-1-(3-nitrophenyl)propan-1-one <1> [38]
3-anilino-1-(3-nitrophenyl)propan-1-one <1> [38]
4,5-dichloro-2-(3,5-dichlorophenyl)pyridazin-3(2H)-one <1> [54]
4,5-dichloro-2-(3-fluorophenyl)pyridazin-3(2H)-one <1> [54]
4,5-dichloro-2-(3-methylphenyl)pyridazin-3(2H)-one <1> [54]
4,5-dichloro-2-cyclohexylpyridazin-3(2H)-one <1> [54]
4-(benzyloxy)-5-hydroxy-2-phenylpyridazin-3(2H)-one <1> [54]
4-(ethylsulfanyl)-2-(3-fluorophenyl)-5-sulfanylpyridazin-3(2H)-one <1> [54]
4-(ethylsulfanyl)-2-(3-methylphenyl)-5-sulfanylpyridazin-3(2H)-one <1> [54]
4-(ethylsulfanyl)-2-(4-nitrophenyl)-5-sulfanylpyridazin-3(2H)-one <1> [54]
4-(ethylsulfanyl)-2-phenyl-5-sulfanylpyridazin-3(2H)-one <1> [54]
4-(ethylsulfanyl)-5-hydroxy-2-phenylpyridazin-3(2H)-one <1> [54]
4-chloro-2-(3,5-dichlorophenyl)-5-ethoxypyridazin-3(2H)-one <1> [54]
4-chloro-2-cyclohexyl-5-ethoxypyridazin-3(2H)-one <1> [54]
4-chloro-5-(methylsulfanyl)-2-phenylpyridazin-3(2H)-one <1> [54]
4-chloro-5-ethoxy-2-(3-fluorophenyl)pyridazin-3(2H)-one <1> [54]
4-chloro-5-ethoxy-2-(3-methylphenyl)pyridazin-3(2H)-one <1> [54]
4-chloro-5-ethoxy-2-(4-nitrophenyl)pyridazin-3(2H)-one <1> [54]
4-chloro-5-ethoxy-2-phenylpyridazin-3-one <1> [54]
4-ethoxy-2-phenyl-5-sulfanylpyridazin-3(2H)-one <1> [54]
4-ethoxy-5-(2-pyridyldithio)-2-phenylpyridazin-3-one <1> [54]
4-ethoxy-5-(methyldithio)-2-phenylpyridazin-3-one <1> [54]
4-ethoxy-5-mercapto-2-phenylpyridazin-3-one <1> [54]
4-hydroxy-5-(methylsulfanyl)-2-phenylpyridazin-3(2H)-one <1> [54]

5-[[(2E)-3-(2-furyl)prop-2-enoyl]amino]-2-morpholin-4-ylbenzoic acid <1> [35]
5-chloro-2-(3,5-dichlorophenyl)-4-ethoxypyridazin-3(2H)-one <1> [54]
5-chloro-2-(3,5-dichlorophenyl)-4-methoxypyridazin-3(2H)-one <1> [54]
5-chloro-2-(3-fluorophenyl)-4-methoxypyridazin-3(2H)-one <1> [54]
5-chloro-2-cyclohexyl-4-ethoxypyridazin-3(2H)-one <1> [54]
5-chloro-2-cyclohexyl-4-methoxypyridazin-3(2H)-one <1> [54]
5-chloro-4-ethoxy-2-(3-fluorophenyl)pyridazin-3(2H)-one <1> [54]
5-chloro-4-ethoxy-2-(3-methylphenyl)pyridazin-3(2H)-one <1> [54]
5-chloro-4-ethoxy-2-(4-nitrophenyl)pyridazin-3(2H)-one <1> [54]
5-chloro-4-ethoxy-2-phenylpyridazin-3-one <1> [54]
5-chloro-4-methoxy-2-(3-methylphenyl)pyridazin-3(2H)-one <1> [54]
5-chloro-4-methoxy-2-phenylpyridazin-3(2H)-one <1> [54]
5-ethoxy-2-(3-fluorophenyl)-4-sulfanylpyridazin-3(2H)-one <1> [54]
5-ethoxy-2-(3-methylphenyl)-4-sulfanylpyridazin-3(2H)-one <1> [54]
5-ethoxy-2-phenyl-4-sulfanylpyridazin-3(2H)-one <1> [54]
5-hydroxy-4-methoxy-2-phenylpyridazin-3(2H)-one <1> [54]
5-methoxy-2-phenyl-4-sulfanylpyridazin-3(2H)-one <1> [54]
Aaptamine <1> [34]
NH_2-YALPE-AlaPsi(PO2H-CH_2)Gly-EE-NH_2 <1> (<1> nonhydrolyzable phosphinic peptidomimetic inhibitor of SrtA derived from the LPXTG substrate sequence, simple reversible competitive inhibitor [26]) [26]
[2-(trimethylammonium)ethyl]methanethiosulfonate <1> (<1> the inhibitor interferes with the cleavage of sorting signals at the LPXTG motif [7]) [7]
[4-(6-bromo-1H-indol-3-yl)-1H-imidazol-2-yl](1H-indol-3-yl)methanone <1> (<1> IC50: 19.44 mg/L [15]) [15]
[4-(6-bromo-1H-indol-3-yl)-1H-imidazol-2-yl](6-hydroxy-1H-indol-3-yl)methanone <1> (<1> IC50: 16.7 mg/L [15]) [15]
benzyloxycarbonyl-Leu-Pro-Ala-Thr-CH_2Cl <1> (<1> irreversible inhibitor of recombinant enzyme [4]) [4]
benzyloxycarbonyl-Leu-Pro-Ala-Thr-CHN_2 <1> (<1> irreversible inhibitor of recombinant enzyme [4]) [4]
berberine chloride <1> (<1> potential of this inhibitor for the treatment of Staphylococcus aureus infections [11]) [11,34]
β-sitosterol-3-O-glucopyranoside <1> (<1> IC50: 18.3 mg/L [15]; <1> potential of this inhibitor for the treatment of Staphylococcus aureus infections [11]) [11,14,15]
bis(4-ethoxy-2-phenyl-5-pyridazyl)disulfide <1> [54]
cis-1,2-bis(phenylsulfonyl)ethylene <1> (<1> IC50: 0.00113 mM, irreversible [19]) [19]
demethylaaptamine <1> [34]
demethyloxyaaptamine <1> [34]
divinyl sulfone <1> (<1> IC50: 0.00106 mM, irreversible [19]) [19]
ethyl 4-[3-(4-bromophenyl)-3-oxopropyl]piperazine-1-carboxylate <1> [38]
ethyl vinyl sulfone <1> (<1> IC50: 0.00471 mM, irreversible [19]) [19]
galangin <1> (<1> IC50 for recombinant SrtA(Δ24): 0.123 mM, no antibacterial activity against Staphylococcus aureus [14]) [14]

galangin-3-methyl ether <1> (<1> IC50 for recombinant SrtA(Δ24): 0.1179 mM, no antibacterial activity against Staphylococcus aureus [14]) [14]
isoaaptamine <1> (<1> the suppression of fibronectin-binding activity by isoaaptamine highlights its potential for the treatment of Staphylococcus aureus infections via inhibition of SrtA activity [34]) [34]
isorhamnetin <1> (<1> IC50 for recombinant SrtA(Δ24): 0.05886 mM, no antibacterial activity against Staphylococcus aureus [14]) [14]
kaempferol <1> (<1> IC50 for recombinant SrtA(Δ24): 0.07794 mM, no antibacterial activity against Staphylococcus aureus [14]) [14]
methyl (2E)-2,3-bis(4-methoxyphenyl)acrylate <1> (<1> IC50: 0.231 mM [23]) [23]
methyl (2S,3S,7aS)-2-ethenesulfonyl-5-oxo-3-phenyltetrahydropyrrolizine-7a-carboxylate <1> [46]
methyl (2S,3S,7aS)-2-ethenesulfonyl-5-oxo-3-pyridin-3-yl-tetrahydropyrrolizine-7a-carboxylate <1> [46]
methyl (2S,3S,7aS)-3-(3,4-dimethoxyphenyl)-2-ethenesulfonyl-5-oxotetrahydropyrrolizine-7a-carboxylate <1> [46]
methyl (2S,4S,5S)-4-ethenesulfonyl-2-(2-methoxycarbonylethyl)-5-pyridin-3-yl-pyrrolidine-2-carboxylate <1> [46]
methyl (2Z)-2,3-bis(4-methoxyphenyl)acrylate <1> (<1> IC50: 0.909 mM [23]) [23]
methyl (4S,5S)-4-(ethenylsulfonyl)-5-(2-fluorophenyl)-L-prolinate <1> [46]
methyl (4S,5S)-4-(ethenylsulfonyl)-5-(3-fluorophenyl)-L-prolinate <1> [46]
methyl (4S,5S)-4-(ethenylsulfonyl)-5-phenyl-L-prolinate <1> [46]
methyl 2-morpholin-4-yl-5-[[(2E)-3-(2-thienyl)prop-2-enoyl]amino]benzoate <1> [35]
methyl 4-[3-(dimethylamino)propanoyl]benzenesulfinate <1> [38]
methyl 5-[[(2E)-3-(2-furyl)prop-2-enoyl]amino]-2-morpholin-4-ylbenzoate <1> [35]
methyl vinyl sulfone <1> (<1> IC50: 0.00624 mM, irreversible [19]) [19]
morin <1> (<1> IC50 for recombinant SrtA(Δ24): 0.03739 mM, no antibacterial activity against Staphylococcus aureus [14]) [14]
myricetin <1> (<1> IC50 for recombinant SrtA(Δ24): 0.04403 mM, no antibacterial activity against Staphylococcus aureus [14]) [14]
p-hydroxymercuribenzoate <1> [7]
phenyl vinyl sulfone <1> (<1> IC50: 0.736 mM, irreversible [19]) [19]
psammaplin A1 <1> (<1> potential of this inhibitor for the treatment of Staphylococcus aureus infections [11]) [11]
quercetin <1> (<1> IC50 for recombinant SrtA(Δ24): 0.0527 mM, no antibacterial activity against Staphylococcus aureus [14]) [14]
quercetin-3,3'-dimethyl ether <1> (<1> IC50 for recombinant SrtA(Δ24): 0.05361 mM, no antibacterial activity against Staphylococcus aureus [14]) [14]
Additional information <1,9> (<1> no inhibition by (3R,6S)-3,6-bis(6-bromo-1H-indol-3-yl)piperazin-2-one and (3R,6S)-3,6-bis(6-bromo-1H-indol-3-yl)piperazin-2-one [15]; <1> no inhibition by phenyl trans-styryl sulfone [19]; <1> no inhibition by trans-stilbene [23]; <1> SrtA activity is a prime

target for inhibition of Staphylococcus aureus colonization [12]; <1,9> aryl (β-amino)ethyl ketones inhibit sortase enzymes. Inhibition of sortases occurs through an irreversible, covalent modification of their active site cysteine. Sortases specifically activate this class of molecules via β-elimination, generating a reactive olefin intermediate that covalently modifies the cysteine thiol [38]; <1> anti-SrtA serum inhibits Staphylococcus aureus biofilm formation [52]) [12,15,19,23,38,52]

Metals, ions

Ca^{2+} <1> (<1> 2 mM, 8fold stimulation of activity, binding near the active site stimulates catalysis possibly by altering the conformation of a surface loop that recognizes newly translocated polypeptides [3]; <1> a single Ca^{2+} bound to an ordered pocket on SrtA allosterically activates catalysis by modulating both the structure and dynamics of a large active site loop [22]) [3,22]
Mg^{2+} <1> (<1> can substitute in part for Ca^{2+} [3]) [3]
Mn^{2+} <1> (<1> can substitute in part for Ca^{2+} [3]) [3]

Turnover number (s^{-1})

0.0000067 <9> (*o*-aminobenzoyl-LPETG-2,4-dinitrophenyl, <9> sortase A Δ56 (residues Asp-57-Lys210), in 20 mM HEPES, pH 7.5 [58]) [58]
0.0000083 <9> (*o*-aminobenzoyl-LPETG-2,4-dinitrophenyl, <9> sortase A Δ64 (residues Asp65-Lys210), in 20 mM HEPES, pH 7.5 [58]) [58]
0.000019 <1> (aminobenzoyl-LPETG-diaminopropionyl(dinitrophenyl)-NH_2, <1> mutant enzyme [30]) [30]
0.00019 <1> (2-aminobenzoyl-LPETG-diaminopropionic acid, <1> 37°C, pH 7.5, mutant enzyme R197K [21]) [21]
0.00021 <1> (2-aminobenzoyl-LPETG-diaminopropionic acid, <1> 37°C, pH 7.5, mutant enzyme R197A [21]) [21]
0.0003 <1> (aminobenzoyl-LPETG-diaminopropionyl(dinitrophenyl)-NH_2, <1> mutant enzyme [30]) [30]
0.00046 <1> (aminobenzoyl-LPETG-diaminopropionyl(dinitrophenyl)-NH_2, <1> mutant enzyme [30]) [30]
0.0006 <1> (aminobenzoyl-LPETG-diaminopropionyl(dinitrophenyl)-NH_2, <1> mutant enzyme [30]) [30]
0.000628 <1> (aminobenzoyl-LPETGG-diaminopropionic acid(dinitrophenyl)-NH_2, <1> 37°C, pH 7.5, mutant enzyme R197A [40]) [40]
0.00098 <1> (2-aminobenzoyl-LPETG-diaminopropionic acid, <1> 37°C, pH 7.5, mutant enzyme R197H [21]) [21]
0.0019 <1> (aminobenzoyl-LPETGG-diaminopropionic acid(dinitrophenyl)-NH_2, <1> 37°C, pH 7.5, mutant enzyme R197K [40]) [40]
0.0123 <1> (aminobenzoyl-LPETGG-diaminopropionic acid(dinitrophenyl)-NH_2, <1> 37°C, pH 7.5, mutant enzyme L169A [40]) [40]
0.013 <1> (Dnp-AQALPETGEE-NH2) [12]
0.15 <1> (aminobenzoyl-LPETGG-diaminopropionic acid(dinitrophenyl)-NH_2, <1> 37°C, pH 7.5, mutant enzyme V168A [40]) [40]
0.16 <1> (aminobenzoyl-LPETGG-diaminopropionic acid(dinitrophenyl)-NH_2, <1> 37°C, pH 7.5, mutant enzyme E171A [40]) [40]
0.18 <1> (Gly-Gly-Gly) [29]

0.27 <1> (Abz-LPETG-Dap(Dnp)-NH_2, <1> 37°C, pH 7.5 [10]) [10,12]
0.29 <1> (2-aminobenzoyl-LPETG-diaminopropionic acid, <1> 37°C, pH 7.5, mutant enzyme N98A [21]) [21]
0.29 <1> (aminobenzoyl-LPETGG-diaminopropionic acid(dinitrophenyl)-NH_2, <1> 37°C, pH 7.5, mutant enzyme R197Cit [40]) [40]
0.3 <1> (2-aminobenzoyl-LPETG-diaminopropionic acid, <1> 37°C, pH 7.5, wild-type enzyme [21]) [21]
0.37 <1> (2-aminobenzoyl-LPETG-diaminopropionic acid, <1> 37°C, pH 7.5, mutant enzyme N98Q [21]) [21]
0.69 <1> (aminobenzoyl-LPETG-diaminopropionyl(dinitrophenyl)-NH_2, <1> wild-type enzyme [30]) [30]
0.72 <1> (aminobenzoyl-LPETG-diaminopropionyl(dinitrophenyl)-NH_2, <1> mutant enzyme [30]) [30]
0.78 <1> (aminobenzoyl-LPETG-diaminopropionyl(dinitrophenyl)-NH_2, <1> mutant enzyme [30]) [30]
1.09 <1> (aminobenzoyl-LPETGG-diaminopropionic acid(dinitrophenyl)-NH_2, <1> 37°C, pH 7.5, mutant enzyme D170A [40]) [40]
1.1 <1> (aminobenzoyl-LPETGG-diaminopropionic acid(dinitrophenyl)-NH_2, <1> 37°C, pH 7.5, wild-type enzyme [40]) [40]
1.13 <1> (aminobenzoyl-LPETGG-diaminopropionic acid(dinitrophenyl)-NH_2, <1> 37°C, pH 7.5, mutant enzyme G167A [40]; <1> 37°C, pH 7.5, mutant enzyme Q172A [40]) [40]
Additional information <1> [6]

Specific activity (U/mg)

0.0255 <1> [12]

K_m-Value (mM)

0.00013 <1> (*o*-aminobenzoyl-LPETG-2,4-dinitrophenyl ester, <1> mutant enzyme E108A [22]) [22]
0.0018 <1> (*o*-aminobenzoyl-LPETG-2,4-dinitrophenyl ester, <1> mutant enzyme E171A [22]) [22]
0.00824 <1> (2-aminobenzoyl-LPETG-diaminopropionic acid, <1> 37°C, pH 7.5, wild-type enzyme [21]) [21]
0.0085 <1> (*o*-aminobenzoyl-LPETG-2,4-dinitrophenyl ester, <1> wild-type enzyme [22]) [22]
0.0087 <1> (*o*-aminobenzoyl-LPETG-2,4-dinitrophenyl ester, <1> mutant enzyme D170A [22]) [22]
0.00932 <1> (2-aminobenzoyl-LPETG-diaminopropionic acid, <1> 37°C, pH 7.5, mutant enzyme N98Q [21]) [21]
0.0097 <1> (2-aminobenzoyl-LPETG-diaminopropionic acid, <1> 37°C, pH 7.5, mutant enzyme N98A [21]) [21]
0.01391 <1> (2-aminobenzoyl-LPETG-diaminopropionic acid, <1> 37°C, pH 7.5, mutant enzyme R197K [21]) [21]
0.01597 <1> (2-aminobenzoyl-LPETG-diaminopropionic acid, <1> 37°C, pH 7.5, mutant enzyme R197A [21]) [21]
0.0168 <1> (2-aminobenzoyl-LPETG-diaminopropionic acid, <1> 37°C, pH 7.5, mutant enzyme R197H [21]) [21]

0.02 <1> (*o*-aminobenzoyl-Leu-Pro-Glu-Thr-Gly-2,4-dinitrophenol, <1> hydrolysis reaction [2]) [2]
0.035 <9> (*o*-aminobenzoyl-LPETG-2,4-dinitrophenyl, <9> sortase A Δ64 (residues Asp65-Lys210), in 20 mM HEPES, pH 7.5 [58]) [58]
0.038 <9> (*o*-aminobenzoyl-LPETG-2,4-dinitrophenyl, <9> sortase A Δ56 (residues Asp-57-Lys210), in 20 mM HEPES, pH 7.5 [58]) [58]
0.041 <1> (Gly-Gly-Gly, <1> pH 7.5, transpeptidation with *o*-aminobenzoyl-Leu-Pro-Glu-Thr-Gly-2,4-dinitrophenol [2]) [2]
0.117 <1> (*o*-aminobenzoyl-Leu-Pro-Glu-Thr-Gly-2,4-dinitrophenol, <1> pH 7.5, transpeptidation with Gly-Gly-Gly [2]) [2]
0.137 <1> (Gly) [12]
0.14 <1> (Gly5, <1> 37°C, pH 7.5 [10]) [10]
0.2 <1> (Gly-Gly-Gly) [29]
0.79 <1> (aminobenzoyl-LPETG-diaminopropionyl(dinitrophenyl)-NH2, <1> mutant enzyme [30]) [30]
3.8 <1> (aminobenzoyl-LPETG-diaminopropionyl(dinitrophenyl)-NH2, <1> mutant enzyme [30]) [30]
4.69 <1> (aminobenzoyl-LPETGG-diaminopropionyl(dinitrophenol)-NH_2, <1> 37°C, pH 7.5, mutant enzyme R197A [40]) [40]
4.7 <1> (aminobenzoyl-LPETG-diaminopropionyl(dinitrophenyl)-NH_2, <1> mutant enzyme [30]) [30]
5.5 <1> (Abz-LPETG-Dap(Dnp)-NH_2, <1> 37°C, pH 7.5 [10]) [10,12]
5.6 <1> (Dnp-AQALPETGEE-NH_2) [12]
6.56 <1> (aminobenzoyl-LPETGG-diaminopropionyl(dinitrophenol)-NH_2, <1> 37°C, pH 7.5, mutant enzyme V168A [40]) [40]
6.7 <1> (aminobenzoyl-LPETG-diaminopropionyl(dinitrophenyl)-NH_2, <1> mutant enzyme [30]) [30]
6.74 <1> (aminobenzoyl-LPETGG-diaminopropionyl(dinitrophenol)-NH_2, <1> 37°C, pH 7.5, mutant enzyme E171A [40]) [40]
8.13 <1> (aminobenzoyl-LPETGG-diaminopropionyl(dinitrophenol)-NH_2, <1> 37°C, pH 7.5, mutant enzyme D170A [40]) [40]
8.5 <1> (aminobenzoyl-LPETG-diaminopropionyl(dinitrophenyl)-NH_2, <1> mutant enzyme [30]) [30]
8.7 <1> (aminobenzoyl-LPETGG-diaminopropionyl(dinitrophenol)-NH_2, <1> 37°C, pH 7.5, mutant enzyme G167A [40]) [40]
8.76 <1> (aminobenzoyl-LPETGG-diaminopropionyl(dinitrophenol)-NH_2, <1> 37°C, pH 7.5, wild-type enzyme [40]) [40]
9.14 <1> (aminobenzoyl-LPETGG-diaminopropionyl(dinitrophenol)-NH_2, <1> 37°C, pH 7.5, mutant enzyme L169A [40]) [40]
10.4 <1> (aminobenzoyl-LPETGG-diaminopropionyl(dinitrophenol)-NH_2, <1> 37°C, pH 7.5, mutant enzyme R197K [40]) [40]
10.6 <1> (aminobenzoyl-LPETG-diaminopropionyl(dinitrophenyl)-NH_2, <1> wild-type enzyme [30]) [30]
11.2 <1> (aminobenzoyl-LPETG-diaminopropionyl(dinitrophenyl)-NH_2, <1> mutant enzyme [30]) [30]
12.7 <1> (aminobenzoyl-LPETGG-diaminopropionyl(dinitrophenol)-NH_2, <1> 37°C, pH 7.5, mutant enzyme Q172A [40]) [40]

13.7 <1> (aminobenzoyl-LPETGG-diaminopropionyl(dinitrophenol)-NH_2, <1> 37°C, pH 7.5, mutant enzyme R197Cit [40]) [40]
Additional information <1> [6]

K_i-Value (mM)

0.00000021 <1> (benzyloxycarbonyl-Leu-Pro-Ala-Thr-CH_2Cl, <1> pH 7.5, 37°C [4]) [4]
0.00000022 <1> (benzyloxycarbonyl-Leu-Pro-Ala-Thr-CHN_2, <1> pH 7.5, 37°C [4]) [4]
0.00003 <1> (4-ethoxy-5-(2-pyridyldithio)-2-phenylpyridazin-3-one, <1> in 20 mM HEPES, 5 mM $CaCl_2$, 0.05% (v/v) Tween-20, pH 7.5, at 25°C [54]) [54]
0.0004 <1> (4-ethoxy-5-(methyldithio)-2-phenylpyridazin-3-one, <1> in 20 mM HEPES, 5 mM $CaCl_2$, 0.05% (v/v) Tween-20, pH 7.5, at 25°C [54]) [54]

4 Enzyme Structure

Molecular weight

17800 <1> (<1> SDS-PAGE [53]) [53]
23000 <9> (<9> SDS-PAGE, immune-reactive species [28]) [28]
24810 <3,12,14> (<3,12,14> calculated from amino acid sequence [55]) [55]
Additional information <1> (<1> signal peptide, membrane anchor and a shorter linker domain of sortase enzymes display no amino acid conservation. The core residue, SrtA residues 60-206, is present in all sortase homologs examined, suggesting that this domain may comprise the catalytically active domain [3]) [3]

Subunits

? <1> (<1> x * 16595, SrtΔN59, electrospray ionization mass spectrometry [3]) [3]
dimer <1> (<1> the dimeric form of SrtA is more active than the monomeric enzyme [31]) [31,32]
monomer <1> (<1> the dimeric form of SrtA is more active than the monomeric enzyme [31]) [31]

5 Isolation/Preparation/Mutation/Application

Source/tissue

Additional information <1> (<1> kidney of Mus musculus infected with Staphylococcus aureus. mRNA levels of sortase A decrease over time, from day 3 of infection to day 14. The transcript number of srtA decreases faster in septic mice than in mice with a non-septic disease [41]) [41]

Localization

membrane <1,2> (<1> class A sortases adopt a type II membrane topology (N terminus inside and C terminus outside the cytoplasm), class B enzymes represent type I membrane proteins (N terminus outside, C terminus inside)

[3]; <2> sortase A (SrtA) colocalizes with SecA at single foci in the enterococcus. Proteins that localize to single foci in Enterococcus faecalis share a positively charged domain flanking a transmembrane helix. Positively charged domain can act as a localization retention signal for the focal compartmentalization of the membrane protein [49]) [3,49]

Purification

<1> [5,8,22,30,40]
<1> (His6-SrtA) [36]
<1> (HisTrapHP column chromatography, gel filtration) [53]
<1> (N-terminally His6-tagged SrtAΔN24 expressed in Escherichia coli BL21) [39]
<1> (of SrtAΔN59 and mutant proteins) [32]
<1> (purification of SrtAΔN59 and SrtA wild-type proteins) [31]
<1> (recombinant) [13]
<1> (recombinant SrtA lacking the amino-terminal 24 amino acids) [46]
<1> (recombinant SrtAΔN24 in a His6-tagged form) [12]
<1> (recombinant sortase A-GST fusion protein) [47]
<3> (His-Trap column chromatography) [55]
<4> [17]
<9> (Talon His-affinity resin column chromatography and Sephacryl-100 gel filtration) [58]
<9> (by Ni-NTA affinity chromatography) [28]
<12> (His-Trap column chromatography) [55]
<13> (recombinant enzyme, SrtA residues Val82-Thr249 (catalytic domain)) [50]
<14> (His-Trap column chromatography) [55]

Crystallization

<1> (crystals are grown by the hanging-drop technique with a protein concentration of 50 mg/ml in 25 mM MES buffer, pH 6.35. The crystallization conditions include 3.2 M ammonium sulfate, 0.1 M NaCl, and trace amounts of ethylene glycol. Crystal structure of native SrtA, of an active-site mutant of SrtA, and of the mutant SrtA complexed with its substrate LPETG peptide) [8]
<13> (hanging drop method of vapor diffusion at 20°C, SrtA residues Val82-Thr249 (catalytic domain)) [50]

Cloning

<1> (N-terminally His6-tagged SrtA lacking the amino-terminal 24 amino acids is expressed in BL21(DE3) cells containing the plasmid pET15bSrtADN24) [46]
<1> (N-terminally His6-tagged SrtAΔN24 is expressed in Escherichia coli BL21) [39]
<1> (SrtAΔ24 is expressed in Escherichia coli) [14]
<1> (expressed in Escherichia coli BL21(DE3) cells) [53]
<1> (expression in Escherichia coli) [4,31,32,36]
<1> (expression of SrtAΔN24 in a His6-tagged form) [12]

<1> (mutant enzymes expressed in Escherichia coli) [40]
<1> (overexpression in Escherichia coli) [13]
<1> (recombinant mature sortase A (without the N-terminal signal peptide) is produced as GST fusion in Escherichia coli) [47]
<1> (wild-type and variant SrtA proteins) [30]
<3> (expressed in Escherichia coli BL21(DE3) cells) [55]
<9> (cloned into the plasmid vector pQE30) [28]
<9> (expressed in Escherichia coli BL21(DE3) cells) [58]
<12> (expressed in Escherichia coli BL21(DE3) cells) [55]
<13> (DNA sequence encoding SrtA residues Val82-Thr249, expression in Escherichia coli BL21) [50]
<14> (expressed in Escherichia coli BL21(DE3) cells) [55]

Engineering

C184A <1> (<1> mutant enzyme can not cleave the LPXTG motif [5]) [5]
C184S <1> (<1> 2700fold decrease in k_{cat}/K_m compared to wild-type value [30]) [30]
D170A <1> (<1> turnover-number for *o*-aminobenzoyl-LPETG-2,4-dinitrophenyl is nearly identical to wild-type value [22]; <1> T_m is 1.7°C higher than the Tm-value of wild-type enzyme. No change in k_{cat}/K_m compared to wild-type value [40]) [22,40]
D185A 1.3 <1> (<1> fold decrease in k_{cat}/K_m compared to wild-type value [30]) [30]
D186A <1> (<1> 1.8fold decrease in k_{cat}/K_m compared to wild-type value [30]) [30]
ΔN59 <1> (<1> trucation of N-terminal 59 amino acids does not affect the activity of the enzyme [3,8]; <1> enhanced solubility of the mutant helps the crystallization [8]) [3,8]
E108A <1> (<1> turnover-number for *o*-aminobenzoyl-LPETG-2,4-dinitrophenyl is 43.8fold lower than wild-type value [22]) [22]
E171A <1> (<1> turnover-number for *o*-aminobenzoyl-LPETG-2,4-dinitrophenyl is 4.7fold lower than wild-type value [22]; <1> T_m is 1.8°C lower than the Tm-value of wild-type enzyme. k_{cat}/K_m is 5.4fold lower than wild-type value [40]) [22,40]
G167A <1> (<1> T_m is 0.5°C lower than the T_m-value of wild-type enzyme. No change in k_{cat}/K_M compared to wild-type enzyme [40]) [40]
H120A <1> (<1> 96000fold decrease in k_{cat}/K_m compared to wild-type value [30]) [30]
H120Q <1> (<1> 36000fold decrease in k_{cat}/K_m compared to wild-type value [30]) [30]
H126A <9> (<9> inactive [58]) [58]
I123G <1> (<1> mutant is generated by using wild type truncated protein SrtAΔN59 as a template. Mutation reduces dimerization [32]) [32]
I182A <1> (<1> mutation produces modest decreases in SrtA activity and leds to substrate inhibition. 28fold decrease in k_{cat}/K_m compared to wild-type value [30]) [30]

I182S <1> (<1> 74fold decrease in k_{cat}/K_m compared to wild-type value [30]) [30]
K137A <1> (<1> mutant is generated by using wild type truncated protein SrtAΔN59 as a template. Mutation completely disrupts dimerization [32]) [32]
K152A <1> (<1> mutant is generated by using wild type truncated protein SrtAΔN59 as a template. Mutation increases dimerization [32]) [32]
K62A <1> (<1> mutant is generated by using wild type truncated protein SrtAΔN59 as a template [32]) [32]
L169A <1> (<1> T_m is 1.8°C lower than the T_m-value of wild-type enzyme. k_{cat}/K_m is 93fold lower than wild-type value [40]) [40]
L181A <1> (<1> mutation produces modest decreases in SrtA activity and leds to substrate inhibition. 7.6fold decrease in k_{cat}/K_m compared to wild-type value [30]) [30]
N132A <1> (<1> mutant is generated by using wild type truncated protein SrtAΔN59 as a template. Mutation completely disrupts dimerization [32]) [32]
N98A <1> (<1> k_{cat}/K_m is 1.2fold lower than wild-type value [21]) [21]
N98Q <1> (<1> k_{cat}/K_m is 1.1fold higher than wild-type value [21]) [21]
P126G <1> (<1> mutant is generated by using wild type truncated protein SrtAΔN59 as a template. Mutation reduces dimerization [32]) [32]
Q172A <1> (<1> T_m is 1.2°C lower than the T_m-value of wild-type enzyme. k_{cat}/K_m is 1.4fold lower than wild-type value [40]) [40]
R197A <1> (<1> k_{cat}/K_m is 2769fold lower than wild-type value [21]; <1> 540fold decrease in k_{cat}/K_m compared to wild-type value [30]; <1> T_m is 2.9°C lower than the T_m-value of wild-type enzyme. k_{cat}/K_m is 960fold lower than wild-type value [40]) [21,30,40]
R197Cit <1> (<1> generation of a semi-synthetic SrtA in which Arg197 is replaced with citrulline, a nonionizable analog. This change results in less than a 3fold decrease in k_{cat}/K_M, indicating that Arg197 utilizes a hydrogen bond, rather than an electrostatic interaction. T_m is 0.3°C higher than the T_m-value of wild-type enzyme [40]; <1> k_{cat}/K_m is 5.9fold lower than wild-type value [40]) [40]
R197H <1> (<1> k_{cat}/K_m is 610fold lower than wild-type value [21]) [21]
R197K <1> (<1> k_{cat}/K_m is 2571fold lower than wild-type value [21]; <1> 1000fold decrease in k_{cat}/K_m compared to wild-type value [30]; <1> T_m is 2°C lower than the T_m-value of wild-type enzyme. k_{cat}/K_m is 690fold lower than wild-type value [40]) [21,30,40]
T180A <1> (<1> mutation produces modest decreases in SrtA activity and leds to substrate inhibition. 14fold decrease in k_{cat}/K_m compared to wild-type value [30]) [30]
T183A <1> (<1> 1200fold decrease in k_{cat}/K_m compared to wild-type value [30]) [30]
V168A <1> (<1> T_m is 1.7°C lower than the T_m-value of wild-type enzyme. k_{cat}/K_m is 5.5fold lower than wild-type value [40]) [40]

Y143A <1> (<1> mutant is generated by using wild type truncated protein SrtAΔN59 as a template. Mutation completely disrupts dimerization [32]) [32]
Additional information <1,3,9> (<9> srtA mutants AHG263 (srtA gene deleted by allelic replacement with ermC marker) and AHG188 [28]; <3> srtA-deficient mutant, colonizes the nasopharynx at a significantly lower level than the D39 parent strain during the second and third week of the carriage, and was eliminated from the nasopharynx one week earlier than the D39 pneumococci [27]; <1> marked changes in the specificity profile of SrtA are obtained by replacing the β_6/β_7 loop in SrtA with the corresponding domain from SrtB. The chimeric β_6/β_7 loop swap enzyme (SrtLS) conferrs the ability to acylate NPQTN-containing substrates, with a k_{cat}/K_{mapp} of 0.0062 /M * s. This enzyme is unable to perform the transpeptidation stage of the reaction, suggesting that additional domains are required for transpeptidation to occur. The overall catalytic specificity profile (k_{cat}/K_{mapp} (NPQTN)/k_{cat}/K_{mapp} (LPETG)) of SrtLS is altered 700000fold from SrtA. These results indicate that the β_6/β_7 loop is an important site for substrate recognition in sortases [39]) [27,28,39]

Application

analysis <1> (<1> development of a reverse-phase HPLC assay to identify and characterize sortase reaction intermediates [29]) [29]
medicine <1,3,9,10> (<1> substrate-derived irreversible inhibitors of SrtA that might find application in delineating the role of the cysteine protease-transpeptidase in cell surface protein sorting and adherence of Gram-positive organisms [4]; <10> in principle the purified SrtA protein can be used to screen for compounds that inhibit cell wall sorting, a strategy that may lead to new therapies for human infections caused by Gram-positive bacteria [1]; <1> potential of inhibitors for the treatment of Staphylococcus aureus infections: (Z)-3-(2,5-dimethoxyphenyl)-2-(4-methoxyphenyl) acrylonitrile, β-sitosterol-3-O-glucopyranoside, berberine chloride and psammaplin A1 [11]; <1> SrtA activity is a prime target for inhibition of Staphylococcus aureus colonization [12]; <9> Bacillus anthracis SrtA anchors surface proteins bearing LPXTG motif sorting signals to the cell wall envelope of vegetative bacilli, srtA gene of Bacillus anthracis is not required for the development of acute anthrax disease in A/J mice [28]; <3> SrtA contributes to pneumococcal nasopharyngeal colonization in the chinchilla model [27]; <1> 4-vinylsulfonyl 5-phenyl prolinates inhibit Staphylococcus aureus sortase SrtA irreversibly by modification of the enzyme Cys184 and could be used as hits for the development of antibacterials and antivirulence agents [46]) [1,4,11,12,27,28,46]
molecular biology <1> (<1> a general strategy for the site-specific modification of cell surface proteins with synthetic molecules by using sortase, a transpeptidase from Staphylococcus aureus. The short peptide tag LPETGG is genetically introduced to the C terminus of the target protein, expressed on the cell surface. Subsequent addition of sortase and an N-terminal triglycine-containing probe results in the site-specific labeling of the tagged protein. C-terminal-specific labeling of osteoclast differentiation factor with a biotin- or

fluorophore-containing short peptide on the living cell surface. The labeling reaction occurrs efficiently in serum-containing medium, as well as serum-free medium or PBS. The labeled products are detected after incubation for 5 min. In addition, site-specific protein-protein conjugation is successfully demonstrated on a living cell surface by the Sortase-catalyzed reaction. This strategy provides a powerful tool for cell biology and cell surface engineering [36]; <1> method for immobilizing ligand proteins onto Biacore sensor chips using the transpeptidase activity of Staphylococcus aureus sortase A. This method provides a robust and gentle approach for the site-directed, covalent coupling of proteins to biosensor chips. The high specificity of the sortase allows immobilization of proteins from less than pure protein samples allowing short cuts in protein purification protocols [47]) [36,47]
synthesis <1> (<1> in vitro applications of sortase A to protein conjugation. Application of recombinant Staphylococcus aureus sortase A to attach a tagged model protein substrate (green fluorescent protein) to polystyrene beads chemically modified with either alkylamine or the in vivo sortase A ligand, Gly-Gly-Gly, on their surfaces. Sortase A can be used to sequence-specifically ligate eGFP to amino-terminated poly(ethylene glycol) and to generate protein oligomers and cyclized monomers using suitably tagged eGFP An alkylamine can substitute for the natural Gly3 substrate, which suggests the possibility of using the enzyme in materials applications. The highly specific and mild sortase A-catalyzed reaction, based on small recognition tags unlikely to interfere with protein expression represents a useful addition to the protein immobilization and modification tool kit [33]) [33]

References

[1] Mazmanian, S.K.; Liu, G.; Ton-That, H.; Schneewind, O.: Staphylococcus aureus sortase, an enzyme that anchors surface proteins to the cell wall. Science, **285**, 760-763 (1999)
[2] Huang, X.; Aulabaugh, A.; Ding, W.; Kapoor, B.; Alksne, L.; Tabei, K.; Ellestad, G.: Kinetic mechanism of Staphylococcus aureus sortase SrtA. Biochemistry, **42**, 11307-11315 (2003)
[3] Ilangovan, U.; Ton-That, H.; Iwahara, J.; Schneewind, O.; Clubb, R.T.: Structure of sortase, the transpeptidase that anchors proteins to the cell wall of Staphylococcus aureus. Proc. Natl. Acad. Sci. USA, **98**, 6056-6061 (2001)
[4] Scott, C.J.; McDowell, A.; Martin, S.L.; Lynas, J.F.; Vandenbroeck, K.; Walker, B.: Irreversible inhibition of the bacterial cysteine protease-transpeptidase sortase (SrtA) by substrate-derived affinity labels. Biochem. J., **366**, 953-958 (2002)
[5] Ton-That, H.; Liu, G.; Mazmanian, S.K.; Faull, K.F.; Schneewind, O.: Purification and characterization of sortase, the transpeptidase that cleaves surface proteins of Staphylococcus aureus at the LPXTG motif. Proc. Natl. Acad. Sci. USA, **96**, 12424-12429 (1999)
[6] Ton-That, H.; Mazmanian, S.K.; Faull, K.F.; Schneewind, O.: Anchoring of surface proteins to the cell wall of Staphylococcus aureus. Sortase catalyzed

in vitro transpeptidation reaction using LPXTG peptide and NH_2-Gly_3 substrates. J. Biol. Chem., **275**, 9876-9881 (2000)
[7] Ton-That, H.; Schneewind, O.: Anchor structure of staphylococcal surface proteins. IV. Inhibitors of the cell wall sorting reaction. J. Biol. Chem., **274**, 24316-24320 (1999)
[8] Zong, Y.; Bice, T.W.; Ton-That, H.; Schneewind, O.; Narayana, S.V.L.: Crystal structures of Staphylococcus aureus sortase A and its substrate somplex. J. Biol. Chem., **279**, 31383-31389 (2004)
[9] Jonsson, I.M.; Mazmanian, S.K.; Schneewind, O.; Bremell, T.; Tarkowski, A.: The role of Staphylococcus aureus sortase A and sortase B in murine arthritis. Microbes Infect., **5**, 775-780 (2003)
[10] Kruger, R.G.; Dostal, P.; McCafferty, D.G.: Development of a high-performance liquid chromatography assay and revision of kinetic parameters for the Staphylococcus aureus sortase transpeptidase SrtA. Anal. Biochem., **326**, 42-48 (2004)
[11] Oh, K.B.; Oh, M.N.; Kim, J.G.; Shin, D.S.; Shin, J.: Inhibition of sortase-mediated Staphylococcus aureus adhesion to fibronectin via fibronectin-binding protein by sortase inhibitors. Appl. Microbiol. Biotechnol., **70**, 102-106 (2006)
[12] Kruger, R.G.; Otvos, B.; Frankel, B.A.; Bentley, M.; Dostal, P.; McCafferty, D.G.: Analysis of the substrate specificity of the Staphylococcus aureus sortase transpeptidase SrtA. Biochemistry, **43**, 1541-1551 (2004)
[13] Frankel, B.A.; Kruger, R.G.; Robinson, D.E.; Kelleher, N.L.; McCafferty, D.G.: Staphylococcus aureus sortase transpeptidase SrtA: insight into the kinetic mechanism and evidence for a reverse protonation catalytic mechanism. Biochemistry, **44**, 11188-11200 (2005)
[14] Kang, S.S.; Kim, J.G.; Lee, T.H.; Oh, K.B.: Flavonols inhibit sortases and sortase-mediated Staphylococcus aureus clumping to fibrinogen. Biol. Pharm. Bull., **29**, 1751-1755 (2006)
[15] Oh, K.B.; Mar, W.; Kim, S.; Kim, J.Y.; Oh, M.N.; Kim, J.G.; Shin, D.; Sim, C.J.; Shin, J.: Bis(indole) alkaloids as sortase A inhibitors from the sponge Spongosorites sp. Bioorg. Med. Chem. Lett., **15**, 4927-4931 (2005)
[16] Liew, C.K.; Smith, B.T.; Pilpa, R.; Suree, N.; Ilangovan, U.; Connolly, K.M.; Jung, M.E.; Clubb, R.T.: Localization and mutagenesis of the sorting signal binding site on sortase A from Staphylococcus aureus. FEBS Lett., **571**, 221-226 (2004)
[17] Lalioui, L.; Pellegrini, E.; Dramsi, S.; Baptista, M.; Bourgeois, N.; Doucet-Populaire, F.; Rusniok, C.; Zouine, M.; Glaser, P.; Kunst, F.; Poyart, C.; Trieu-Cuot, P.: The SrtA sortase of Streptococcus agalactiae is required for cell wall anchoring of proteins containing the LPXTG motif, for adhesion to epithelial cells, and for colonization of the mouse intestine. Infect. Immun., **73**, 3342-3350 (2005)
[18] Zink, S.D.; Burns, D.L.: Importance of srtA and srtB for growth of Bacillus anthracis in macrophages. Infect. Immun., **73**, 5222-5228 (2005)
[19] Frankel, B.A.; Bentley, M.; Kruger, R.G.; McCafferty, D.G.: Vinyl sulfones: inhibitors of SrtA, a transpeptidase required for cell wall protein anchoring

and virulence in Staphylococcus aureus. J. Am. Chem. Soc., **126**, 3404-3405 (2004)
[20] Weiss, W.J.; Lenoy, E.; Murphy, T.; Tardio, L.; Burgio, P.; Projan, S.J.; Schneewind, O.; Alksne, L.: Effect of srtA and srtB gene expression on the virulence of Staphylococcus aureus in animal models of infection. J. Antimicrob. Chemother., **53**, 480-486 (2004)
[21] Marraffini, L.A.; Ton-That, H.; Zong, Y.; Narayana, S.V.; Schneewind, O.: Anchoring of surface proteins to the cell wall of Staphylococcus aureus. A conserved arginine residue is required for efficient catalysis of sortase A. J. Biol. Chem., **279**, 37763-37770 (2004)
[22] Naik, M.T.; Suree, N.; Ilangovan, U.; Liew, C.K.; Thieu, W.; Campbell, D.O.; Clemens, J.J.; Jung, M.E.; Clubb, R.T.: Staphylococcus aureus sortase A transpeptidase. Calcium promotes sorting signal binding by altering the mobility and structure of an active site loop. J. Biol. Chem., **281**, 1817-1826 (2006)
[23] Oh, K.; Kim, S.; Lee, J.; Cho, W.; Lee, T.; Kim, S.: Discovery of diarylacrylonitriles as a novel series of small molecule sortase A inhibitors. J. Med. Chem., **47**, 2418-2421 (2004)
[24] Ton-That, H.; Marraffini, L.A.; Schneewind, O.: Sortases and pilin elements involved in pilus assembly of Corynebacterium diphtheriae. Mol. Microbiol., **53**, 251-261 (2004)
[25] Pucciarelli, M.G.; Calvo, E.; Sabet, C.; Bierne, H.; Cossart, P.; Garcia-del Portillo, F.: Identification of substrates of the Listeria monocytogenes sortases A and B by a non-gel proteomic analysis. Proteomics, **5**, 4808-4817 (2005)
[26] Kruger, R.G.; Barkallah, S.; Frankel, B.A.; McCafferty, D.G.: Inhibition of the Staphylococcus aureus sortase transpeptidase SrtA by phosphinic peptidomimetics. Bioorg. Med. Chem., **12**, 3723-3729 (2004)
[27] Chen, S.; Paterson, G.K.; Tong, H.H.; Mitchell, T.J.; DeMaria, T.F.: Sortase A contributes to pneumococcal nasopharyngeal colonization in the chinchilla model. FEMS Microbiol. Lett., **253**, 151-154 (2005)
[28] Gaspar, A.H.; Marraffini, L.A.; Glass, E.M.; Debord, K.L.; Ton-That, H.; Schneewind, O.: Bacillus anthracis sortase A (SrtA) anchors LPXTG motif-containing surface proteins to the cell wall envelope. J. Bacteriol., **187**, 4646-4655 (2005)
[29] Aulabaugh, A.; Ding, W.; Kapoor, B.; Tabei, K.; Alksne, L.; Dushin, R.; Zatz, T.; Ellestad, G.; Huang, X.: Development of an HPLC assay for Staphylococcus aureus sortase: evidence for the formation of the kinetically competent acyl enzyme intermediate. Anal. Biochem., **360**, 14-22 (2007)
[30] Frankel, B.A.; Tong, Y.; Bentley, M.L.; Fitzgerald, M.C.; McCafferty, D.G.: Mutational analysis of active site residues in the Staphylococcus aureus transpeptidase SrtA. Biochemistry, **46**, 7269-7278 (2007)
[31] Lu, C.; Zhu, J.; Wang, Y.; Umeda, A.; Cowmeadow, R.B.; Lai, E.; Moreno, G.N.; Person, M.D.; Zhang, Z.: Staphylococcus aureus sortase A exists as a dimeric protein in vitro. Biochemistry, **46**, 9346-9354 (2007)
[32] Zhu, J.; Lu, C.; Standland, M.; Lai, E.; Moreno, G.N.; Umeda, A.; Jia, X.; Zhang, Z.: Single mutation on the surface of Staphylococcus aureus sortase A can disrupt its dimerization. Biochemistry, **47**, 1667-1674 (2008)

[33] Parthasarathy, R.; Subramanian, S.; Boder, E.T.: Sortase A as a novel molecular "stapler" for sequence-specific protein conjugation. Bioconjugate Chem., **18**, 469-476 (2007)
[34] Jang, K.H.; Chung, S.C.; Shin, J.; Lee, S.H.; Kim, T.I.; Lee, H.S.; Oh, K.B.: Aaptamines as sortase A inhibitors from the tropical sponge Aaptos aaptos. Bioorg. Med. Chem. Lett., **17**, 5366-5369 (2007)
[35] Chenna, B.C.; Shinkre, B.A.; King, J.R.; Lucius, A.L.; Narayana, S.V.; Velu, S.E.: Identification of novel inhibitors of bacterial surface enzyme Staphylococcus aureus sortase A. Bioorg. Med. Chem. Lett., **18**, 380-385 (2008)
[36] Tanaka, T.; Yamamoto, T.; Tsukiji, S.; Nagamune, T.: Site-specific protein modification on living cells catalyzed by Sortase. Chembiochem, **9**, 802-807 (2008)
[37] Samantaray, S.; Marathe, U.; Dasgupta, S.; Nandicoori, V.K.; Roy, R.P.: Peptide-sugar ligation catalyzed by transpeptidase sortase: A facile approach to neoglycoconjugate synthesis. J. Am. Chem. Soc., **130**, 2132-2133 (2008)
[38] Maresso, A.W.; Wu, R.; Kern, J.W.; Zhang, R.; Janik, D.; Missiakas, D.M.; Duban, M.; Joachimiak, A.; Schneewind, O.: Activation of inhibitors by sortase triggers irreversible modification of the active site. J. Biol. Chem., **282**, 23129-23139 (2007)
[39] Bentley, M.L.; Gaweska, H.; Kielec, J.M.; McCafferty, D.G.: Engineering the substrate specificity of Staphylococcus aureus sortase A. The $\beta_6/\beta 7$ loop from SrtB confers NPQTN recognition to SrtA. J. Biol. Chem., **282**, 6571-6581 (2007)
[40] Bentley, M.L.; Lamb, E.C.; McCafferty, D.G.: Mutagenesis studies of substrate recognition and catalysis in the sortase A transpeptidase from Staphylococcus aureus. J. Biol. Chem., **283**, 14762-14771 (2008)
[41] Josefsson, E.; Kubica, M.; Mydel, P.; Potempa, J.; Tarkowski, A.: In vivo sortase A and clumping factor A mRNA expression during Staphylococcus aureus infection. Microb. Pathog., **44**, 103-110 (2008)
[42] Paterson, G.K.; Mitchell, T.J.: The role of Streptococcus pneumoniae sortase A in colonization and pathogenesis. Microbes Infect., **8**, 145-153 (2006)
[43] Yamaguchi, M.; Terao, Y.; Ogawa, T.; Takahashi, T.; Hamada, S.; Kawabata, S.: Role of Streptococcus sanguinis sortase A in bacterial colonization. Microbes Infect., **8**, 2791-2796 (2006)
[44] Nobbs, A.H.; Vajna, R.M.; Johnson, J.R.; Zhang, Y.; Erlandsen, S.L.; Oli, M.W.; Kreth, J.; Brady, L.J.; Herzberg, M.C.: Consequences of a sortase A mutation in Streptococcus gordonii. Microbiology, **153**, 4088-4097 (2007)
[45] Wang, C.; Li, M.; Feng, Y.; Zheng, F.; Dong, Y.; Pan, X.; Cheng, G.; Dong, R.; Hu, D.; Feng, X.; Ge, J.; Liu, D.; Wang, J.; Cao, M.; Hu, F.; Tang, J.: The involvement of sortase A in high virulence of STSS-causing Streptococcus suis serotype 2. Arch. Microbiol., **191**, 23-33 (2009)
[46] Kudryavtsev, K.V.; Bentley, M.L.; McCafferty, D.G.: Probing of the cis-5-phenyl proline scaffold as a platform for the synthesis of mechanism-based inhibitors of the Staphylococcus aureus sortase SrtA isoform. Bioorg. Med. Chem., **17**, 2886-2893 (2009)

[47] Clow, F.; Fraser, J.D.; Proft, T.: Immobilization of proteins to biacore sensor chips using Staphylococcus aureus sortase A. Biotechnol. Lett., **30**, 1603-1607 (2008)
[48] LeMieux, J.; Woody, S.; Camilli, A.: Roles of the sortases of Streptococcus pneumoniae in assembly of the RlrA pilus. J. Bacteriol., **190**, 6002-6013 (2008)
[49] Kline, K.A.; Kau, A.L.; Chen, S.L.; Lim, A.; Pinkner, J.S.; Rosch, J.; Nallapareddy, S.R.; Murray, B.E.; Henriques-Normark, B.; Beatty, W.; Caparon, M.G.; Hultgren, S.J.: Mechanism for sortase localization and role in efficient pilus assembly in Enterococcus faecalis. J. Bacteriol., **191**, 3237-3247 (2009)
[50] Race, P.R.; Bentley, M.L.; Melvin, J.A.; Crow, A.; Hughes, R.K.; Smith, W.D.; Sessions, R.B.; Kehoe, M.A.; McCafferty, D.G.; Banfield, M.J.: Crystal structure of Streptococcus pyogenes sortase A: implications for sortase mechanism. J. Biol. Chem., **284**, 6924-6933 (2009)
[51] Pritz, S.; Wolf, Y.; Kraetke, O.; Klose, J.; Bienert, M.; Beyermann, M.: Enzymatic ligation of peptides, peptide nucleic acids and proteins by means of sortase A. Adv. Exp. Med. Biol., **611**, 107-108 (2009)
[52] Xiong, N.; Hu, C.; Zhang, Y.; Chen, S.: Interaction of sortase A and lipase 2 in the inhibition of Staphylococcus aureus biofilm formation. Arch. Microbiol., **191**, 879-884 (2009)
[53] Ito, T.; Sadamoto, R.; Naruchi, K.; Togame, H.; Takemoto, H.; Kondo, H.; Nishimura, S.: Highly oriented recombinant glycosyltransferases: site-specific immobilization of unstable membrane proteins by using Staphylococcus aureus sortase A. Biochemistry, **49**, 2604-2614 (2010)
[54] Suree, N.; Yi, S.W.; Thieu, W.; Marohn, M.; Damoiseaux, R.; Chan, A.; Jung, M.E.; Clubb, R.T.: Discovery and structure-activity relationship analysis of Staphylococcus aureus sortase A inhibitors. Bioorg. Med. Chem., **17**, 7174-7185 (2009)
[55] Gianfaldoni, C.; Maccari, S.; Pancotto, L.; Rossi, G.; Hilleringmann, M.; Pansegrau, W.; Sinisi, A.; Moschioni, M.; Masignani, V.; Rappuoli, R.; Del Giudice, G.; Ruggiero, P.: Sortase A confers protection against Streptococcus pneumoniae in mice. Infect. Immun., **77**, 2957-2961 (2009)
[56] Guiton, P.S.; Hung, C.S.; Kline, K.A.; Roth, R.; Kau, A.L.; Hayes, E.; Heuser, J.; Dodson, K.W.; Caparon, M.G.; Hultgren, S.J.: Contribution of autolysin and sortase A during Enterococcus faecalis DNA-dependent biofilm development. Infect. Immun., **77**, 3626-3638 (2009)
[57] Wu, Z.; Guo, X.; Wang, Q.; Swarts, B.M.; Guo, Z.: Sortase A-catalyzed transpeptidation of glycosylphosphatidylinositol derivatives for chemoenzymatic synthesis of GPI-anchored proteins. J. Am. Chem. Soc., **132**, 1567-1571 (2010)
[58] Weiner, E.M.; Robson, S.A.; Marohn, M.; Clubb, R.T.: The sortase A enzyme that attaches proteins to the cell wall of Bacillus anthracis contains an unusual active site architecture. J. Biol. Chem., **285**, 23433-23443 (2010)
[59] Egan, S.A.; Kurian, D.; Ward, P.N.; Hunt, L.; Leigh, J.A.: Identification of sortase A (SrtA) substrates in Streptococcus uberis: evidence for an additional hexapeptide (LPXXXD) sorting motif. J. Proteome Res., **9**, 1088-1095 (2010)

sortase B 3.4.22.71

1 Nomenclature

EC number
3.4.22.71

Recommended name
sortase B

Synonyms
SrtB <1,2,3> [4,9,12]
StrB <2> [14]
sortase B <1> [15]

CAS registry number
9033-39-0

2 Source Organism

<1> *Staphylococcus aureus* [1,2,4,5,7,10,13,15]
<2> *Listeria monocytogenes* [3,8,9,14]
<3> *Bacillus anthracis* [6,10,11,12]

3 Reaction and Specificity

Catalyzed reaction
The enzyme catalyses a cell wall sorting reaction in which a surface protein with a sorting signal containing a NXTN motif is cleaved. The resulting threonine carboxyl end of the protein is covalently attached to a pentaglycine cross-bridge of peptidoglycan.

Reaction type
hydrolysis of peptide bond

Natural substrates and products
S IsdC + H_2O <1> (<1> the enzyme cleaves the C-terminal sorting signal of IsdC at the NPQTN motif and rethers the polypeptide to the pentaglycine cell wall cross-bridge. During catalysis, the active site cysteine of sortase and the cleaved substrate form an acyl intermediate, which is then resolved by the amino group of pentaglycine cross-bridges [2]; <1> the enzyme anchors the IsdC precursor with a C-terminal NPQTN motif sorting

D. Schomburg and I. Schomburg (eds.), *Class 3.4–6 Hydrolases, Lyases, Isomerases, Ligases: EC 3.4–6*, Springer Handbook of Enzymes S10, DOI 10.1007/978-3-642-36260-6_5,

sognal, to the cell wall envelope. The sorting signal of IsdC is cleaved between threonine and asparagine of the NPQTN motif, and the carboxyl group of the thrteonine is amide-linked to the amino group of pentaglycine cross-bridges [7]) (Reversibility: ?) [2,7]

P ?

S SvpA + H_2O <2> (<2> anchoring of SvpA to the bacterial cell wall is specifically mediated by SrzB [3]) (Reversibility: ?) [3]

P ?

S Additional information <1,2,3> (<1> Gram-positive pathogenic bacteria display proteins on their surface that play important roles during infection. In Staphylococcus aureus these surface proteins are anchored to the cell wall by two sortases, sortase A and sortaseB that recognize specific surface protein sorting signals. Sortase B plays a contributing role during the pathogenesis of staphylococcal infections [1]; <2> anchoring of SvpA to the bacterial cell wall is specifically mediated by SrzB. The enzyme is involved in the attachment of a subset of proteins to the cell wall, most likely by recognizing an NXZTN sorting motif. SrtB-mediated anchoring can be required to anchor surface proteins involved in the adaption of this microorganism to different environmental conditions [3]; <2> the svpA-srtB locus is regulated by iron availability, mediated by Fur [8]; <3> surface protein IsdC and sortase B are required for heme-iron scavenging of Bacillus anthracis [11]) (Reversibility: ?) [1,3,8,11]

P ?

Substrates and products

S IsdC + H_2O <1> (<1> the enzyme cleaves the C-terminal sorting signal of IsdC at the NPQTN motif and rethers the polypeptide to the pentaglycine cell wall cross-bridge. During catalysis, the active site cysteine of sortase and the cleaved substrate form an acyl intermediate, which is then resolved by the amino group of pentaglycine cross-bridges [2]; <1> the enzyme anchors the IsdC precursor with a C-terminal NPQTN motif sorting sognal, to the cell wall envelope. The sorting signal of IsdC is cleaved between threonine and asparagine of the NPQTN motif, and the carboxyl group of the thrteonine is amide-linked to the amino group of pentaglycine cross-bridges [7]) (Reversibility: ?) [2,7]

P ?

S Lmo2185 + H_2O <2> (Reversibility: ?) [14]

P ?

S Lmo2186 + H_2O <2> (<2> NPKSS is a sorting motif of Lmo2186. Recognition of NPKSS by SrtB, even when placed in the context of the heterologous sorting signal of Lmo2185. Proline at position 2, and not lysine at position 3, is essential for the recognition of NPKSS by SrtB [14]) (Reversibility: ?) [14]

P ?

S SvpA + H_2O <2> (<2> anchoring of SvpA to the bacterial cell wall is specifically mediated by SrzB [3]) (Reversibility: ?) [3]

P ?

S Additional information <1,2,3> (<1> gram-positive pathogenic bacteria display proteins on their surface that play important roles during infection. In Staphylococcus aureus these surface proteins are anchored to the cell wall by two sortases, sortase A and sortaseB that recognize specific surface protein sorting signals. Sortase B plays a contributing role during the pathogenesis of staphylococcal infections [1]; <2> anchoring of SvpA to the bacterial cell wall is specifically mediated by SrzB. The enzyme is involved in the attachment of a subset of proteins to the cell wall, most likely by recognizing an NXZTN sorting motif. SrtB-mediated anchoring can be required to anchor surface proteins involved in the adaption of this microorganism to different environmental conditions [3]; <2> the svpA-srtB locus is regulated by iron availability, mediated by Fur [8]; <2> non-gel proteomics is a powerful technique to rapidly identify sortase substrates and to gain insights on potential sorting motifs. Two surface proteins, Lmo2185 and Lmo2186 are identified only when SrtB is active. The analysis of the peptides identified in these proteins suggests that SrtB of Listeria monocytogenes may recognize two different sorting motifs, NXZTN and NPKXZ [9]; <3> sortase B may be critical in the early stage of inhaltation anthrax [6]; <3> surface protein IsdC and sortase B are required for heme-iron scavenging of Bacillus anthracis [11]) (Reversibility: ?) [1,3,6,8,9,11]

P ?

Inhibitors

(Z)-3-(2,5-dimethoxyphenyl)-2-(4-methoxyphenyl) acrylonitrile <1> (<1> potential of this inhibitor for the treatment of Staphylococcus aureus infections [4]; <1> 50% inhibition with 0.0101 mg/ml [15]) [4,15]

berberine chloride <1> (<1> potential of this inhibitor for the treatment of Staphylococcus aureus infections [4]) [4]

β-sitosterol-3-O-glucopyranoside <1> (<1> potential of this inhibitor for the treatment of Staphylococcus aureus infections [4]) [4]

galangin <1> (<1> IC50 for recombinant $SrtB_{\Delta 30}$: 0.03837 mM, no antibacterial activity against Staphylococcus aureus [5]) [5]

galangin-3-methyl ether <1> (<1> IC50 for recombinant $SrtB_{\Delta 30}$: 0.1136 mM, no antibacterial activity against Staphylococcus aureus [5]) [5]

isorhamnetin <1> (<1> IC50 for recombinant $SrtB_{\Delta 30}$: 0.04335 mM, no antibacterial activity against Staphylococcus aureus [5]) [5]

kaempferol <1> (<1> IC50 for recombinant $SrtB_{\Delta 30}$: 0.02455 mM, no antibacterial activity against Staphylococcus aureus [5]) [5]

morin <1> (<1> IC50 for recombinant $SrtB_{\Delta 30}$: 0.00854 mM, no antibacterial activity against Staphylococcus aureus [5]) [5]

myricetin <1> (<1> IC50 for recombinant $SrtB_{\Delta 30}$: 0.03689 mM, no antibacterial activity against Staphylococcus aureus [5]) [5]

psammaplin A1 <1> (<1> potential of this inhibitor for the treatment of Staphylococcus aureus infections [4]) [4]

quercetin <1> (<1> IC50 for recombinant $SrtB_{\Delta 30}$: 0.03328 mM, no antibacterial activity against Staphylococcus aureus [5]) [5]

quercetin-3,3'-dimethyl ether <1> (<1> IC50 for recombinant $SrtB_{\Delta 30}$: 0.0603 mM, no antibacterial activity against Staphylococcus aureus [5]) [5]
Additional information <3> (<3> aryl (β-amino)ethyl ketones inhibit sortase enzymes. Inhibition of sortases occurs through an irreversible, covalent modification of their active site cysteine. Sortases specifically activate this class of molecules via β-elimination, generating a reactive olefin intermediate that covalently modifies the cysteine thiol [12]) [12]

5 Isolation/Preparation/Mutation/Application

Purification

<1> [10]
<3> [10,11]

Crystallization

<1> (2.0 A resolution. Space group P2(1)2(1)2(1) with cell dimension of a = 71.208 A, b = 104.367 A, c = 58.087 A, $\alpha = \beta = \gamma = 90^\circ$) [10]
<1> (hanging-drop vapor diffusion method. Crystal structure of SrtB-Δ-N30 in complex with two active site inhibitors E64 and MTSET, and with the cell wall substrate analog tripleglycine) [2]
<3> (1.6 A resolution. Space group P2(1) with cell dimension of a = 40.47 A, b = 64.6 A, c = 42.96 A, $\alpha = 105.77^\circ$, $\beta = 105.77^\circ$, $\gamma = 90^\circ$) [10]
<3> (SrtB in complex with aryl (β-amino)ethyl ketone inhibitors. Analysis of the three-dimensional structure ofBacillusanthracissortaseBwithandwithoutinhibitorprovidesinsights into the mechanism of inhibition) [12]

Cloning

<1> ($SrtB_{\Delta 24}$ is expressed in Escherichia coli) [5]
<3> (expression in Escherichia coli) [11]

Engineering

Additional information <1> (<1> marked changes in the specificity profile of SrtA are obtained by replacing the β_6/β_7 loop in SrtA with the corresponding domain from SrtB [13]) [13]

Application

medicine <1> (<1> potential to be used as inhibitors for the treatment of Staphylococcus aureus infections: (Z)-3-(2,5-dimethoxyphenyl)-2-(4-methoxyphenyl) acrylonitrile, β-sitosterol-3-O-glucopyranoside, berberine chloride and psammaplin A1 [4]) [4]

References

[1] Jonsson, I.M.; Mazmanian, S.K.; Schneewind, O.; Bremell, T.; Tarkowski, A.: The role of Staphylococcus aureus sortase A and sortase B in murine arthritis. Microbes Infect., **5**, 775-780 (2003)

[2] Zong, Y.; Mazmanian, S.K.; Schneewind, O.; Narayana, S.V.L.: The structure of sortase B, a cysteine transpeptidase that tethers surface protein to the Staphylococcus aureus cell wall. Structure, **12**, 105-112 (2004)
[3] Bierne, H.; Garandeau, C.; Pucciarelli, M.G.; Sabet, C.; Newton, S.; Garcia-del Portillo, F.; Cossart, P.; Charbit, A.: Sortase B, a new class of sortase in Listeria monocytogenes. J. Bacteriol., **186**, 1972-1982 (2004)
[4] Oh, K.B.; Oh, M.N.; Kim, J.G.; Shin, D.S.; Shin, J.: Inhibition of sortase-mediated Staphylococcus aureus adhesion to fibronectin via fibronectin-binding protein by sortase inhibitors. Appl. Microbiol. Biotechnol., **70**, 102-106 (2006)
[5] Kang, S.S.; Kim, J.G.; Lee, T.H.; Oh, K.B.: Flavonols inhibit sortases and sortase-mediated Staphylococcus aureus clumping to fibrinogen. Biol. Pharm. Bull., **29**, 1751-1755 (2006)
[6] Zink, S.D.; Burns, D.L.: Importance of srtA and srtB for growth of Bacillus anthracis in macrophages. Infect. Immun., **73**, 5222-5228 (2005)
[7] Marraffini, L.A.; Schneewind, O.: Anchor structure of staphylococcal surface proteins. V. Anchor structure of the sortase B substrate IsdC. J. Biol. Chem., **280**, 16263-16271 (2005)
[8] Newton, S.M.; Klebba, P.E.; Raynaud, C.; Shao, Y.; Jiang, X.; Dubail, I.; Archer, C.; Frehel, C.; Charbit, A.: The svpA-srtB locus of Listeria monocytogenes: fur-mediated iron regulation and effect on virulence. Mol. Microbiol., **55**, 927-940 (2005)
[9] Pucciarelli, M.G.; Calvo, E.; Sabet, C.; Bierne, H.; Cossart, P.; Garcia-del Portillo, F.: Identification of substrates of the Listeria monocytogenes sortases A and B by a non-gel proteomic analysis. Proteomics, **5**, 4808-4817 (2005)
[10] Zhang, R.; Wu, R.; Joachimiak, G.; Mazmanian, S.K.; Missiakas, D.M.; Gornicki, P.; Schneewind, O.; Joachimiak, A.: Structures of sortase B from Staphylococcus aureus and Bacillus anthracis reveal catalytic amino acid triad in the active site. Structure, **12**, 1147-1156 (2004)
[11] Maresso, A.W.; Chapa, T.J.; Schneewind, O.: Surface protein IsdC and sortase B are required for heme-iron scavenging of Bacillus anthracis. J. Bacteriol., **188**, 8145-8152 (2006)
[12] Maresso, A.W.; Wu, R.; Kern, J.W.; Zhang, R.; Janik, D.; Missiakas, D.M.; Duban, M.; Joachimiak, A.; Schneewind, O.: Activation of inhibitors by sortase triggers irreversible modification of the active site. J. Biol. Chem., **282**, 23129-23139 (2007)
[13] Bentley, M.L.; Gaweska, H.; Kielec, J.M.; McCafferty, D.G.: Engineering the substrate specificity of Staphylococcus aureus sortase A. The β_6/β_7 loop from SrtB confers NPQTN recognition to SrtA. J. Biol. Chem., **282**, 6571-6581 (2007)
[14] Mariscotti, J.F.; Garcia-del Portillo, F.; Pucciarelli, M.G.: The Listeria monocytogenes sortase-B recognizes varied amino acids at position 2 of the sorting motif. J. Biol. Chem., **284**, 6140-6146 (2009)
[15] Oh, K.B.; Nam, K.W.; Ahn, H.; Shin, J.; Kim, S.; Mar, W.: Therapeutic effect of (Z)-3-(2,5-dimethoxyphenyl)-2-(4-methoxyphenyl) acrylonitrile (DMMA) against Staphylococcus aureus infection in a murine model. Biochem. Biophys. Res. Commun., **396**, 440-444 (2010)

human endogenous retrovirus K endopeptidase 3.4.23.50

1 Nomenclature

EC number
3.4.23.50

Recommended name
human endogenous retrovirus K endopeptidase

Synonyms
HERV K10 endopeptidase
HERV K10 retropepsin <1> [6]
HERV-K PR
HERV-K protease <1> [8]
HERV-K113 protease <1> [9]
endogenous retrovirus HERV-K10 putative protease
human endogenous retrovirus K retropepsin
human endogenous retrovirus K113 protease <1> [9]
human retrovirus K10 retropepsin <1> [6]
Additional information <1> (<1> the enzyme belongs to the human endogenous retrovirus family HERV-K/HML-5 [7]) [7]

CAS registry number
144114-21-6

2 Source Organism

<1> *Homo sapiens* [2,3,4,5,6,7,8,9]
<2> *Homo sapiens* (UNIPROT accession number: P10265) [1]

3 Reaction and Specificity

Catalyzed reaction
Processing at the authentic HIV-1 PR recognition site and release of the mature p17 matrix and the p24 capsid protein, as a result of the cleavage of the -SQNY-/-PIVQ- cleavage site. (<1> the enzyme contains the aspartic protease triad Asp-Thr-Gly in the catalytic site [6])

Reaction type
hydrolysis of peptide bond

D. Schomburg and I. Schomburg (eds.), *Class 3.4–6 Hydrolases, Lyases, Isomerases, Ligases: EC 3.4–6*, Springer Handbook of Enzymes S10, DOI 10.1007/978-3-642-36260-6_6,

Natural substrates and products

S Gag polyprotein + H_2O <1> (<1> the enzyme is synthesized as part of the Gag polyprotein or the Gag-Pol polyprotein and autolytically processed to the mature dimer [6]) (Reversibility: ?) [6]
P ?
S Gag-Pol polyprotein + H_2O <1> (<1> the enzyme is synthesized as part of the Gag polyprotein or the Gag-Pol polyprotein and autolytically processed to the mature dimer [6]) (Reversibility: ?) [6]
P ?
S Additional information <1> (<1> the results do not exclude the possibility that the HERV-K PR could complement an HIV-1 PR whoses function is impaired due to drugs or drug-resistant mutations, they clearly demomstrate that the HERV-K PR cannot substitute for the function of the wild-type HIV-1 PR [4]; <1> the enzyme probably functions in the processing of Gag precursor protein [5]) (Reversibility: ?) [4,5]
P ?

Substrates and products

S 2-aminobenzoyl-ATHQVY-(4-nitro)FVRKA + H_2O <1> (Reversibility: ?) [6]
P 2-aminobenzoyl-ATHQVY + (4-nitro)FVRKA
S 2-aminobenzoyl-Ala-Thr-His-Gln-Val-Tyr-Phe(NO_2)-Val-Arg-Lys-Ala + H_2O <1> (Reversibility: ?) [3]
P ?
S Gag polyprotein + H_2O <1> (<1> the enzyme is synthesized as part of the Gag polyprotein or the Gag-Pol polyprotein and autolytically processed to the mature dimer [6]) (Reversibility: ?) [6]
P ?
S Gag-Pol polyprotein + H_2O <1> (<1> the enzyme is synthesized as part of the Gag polyprotein or the Gag-Pol polyprotein and autolytically processed to the mature dimer [6]) (Reversibility: ?) [6]
P ?
S HERV-K Gag polyprotein + H_2O <1> (Reversibility: ?) [3]
P ?
S HIV-1 matrix-capsid polyprotein + H_2O <1> (<1> processing at the authentic HIV-1 PR recognition site [2]; <1> cleavage also in presence of HIV-1 PR inhibitor [4]) (Reversibility: ?) [2,4]
P ?
S KARVY-(4-nitro)FEA-Nle-NH_2 + H_2O <1> (Reversibility: ?) [6]
P KARVY + (4-nitro)FEA-Nle-NH_2
S Lys-Ala-Arg-Val-Tyr-Phe(NO_2)-Glu-Ala-Nle-NH_2 + H_2O <1> (Reversibility: ?) [2]
P ?
S Additional information <1> (<1> the results do not exclude the possibility that the HERV-K PR could complement an HIV-1 PR whoses function is impaired due to drugs or drug-resistant mutations, they clearly demomstrate that the HERV-K PR cannot substitute for the function of the

wild-type HIV-1 PR [4]; <1> the enzyme probably functions in the processing of Gag precursor protein [5]; <1> the C-terminal 13-amino-acid extension of the enzyme might play a regulatory role [6]) (Reversibility: ?) [4,5,6]

P ?

Inhibitors

ABT538 <1> [2]
KNI227 <1> [2]
KNI272 <1> [2]
L735,524 <1> [2]
Q8467 <1> [3]
Ro31-8624 <1> [2]
Ro31-8959 <1> [2]
SD145 <1> [3]
SD146 <1> (<1> efficiently blocks HERV-K Gag processing in vitro and in cells [3]) [3]
SD152 <1> [3]
XK234 <1> [3]
XM412 <1> [3]
XV638 <1> [3]
XV643 <1> [3]
XV644 <1> [3]
XV648 <1> [3]
XV651 <1> [3]
XV652 <1> [3]
XW805 <1> [3]
indinavir <1> (<1> weak inhibition [6]) [3,6]
pepstatin <1> (<1> weak inhibition [6]) [3,6]
pepstatin A <1> (<1> 1 mM, complete inactivation [5]) [2,5]
ritonavir <1> (<1> weak inhibition [6]) [3,6]
saquinavir <1> (<1> weak inhibition [6]) [3,6]
Additional information <1> (<1> the enzyme is highly resistant to all the HIV-1 PR inhibitors tested, including L-735,524, Ro31-8959, and ABT 538 [2]) [2]

Activating compounds

Additional information <1> (<1> high ionic strength activates the enzyme [6]) [6]

Metals, ions

NaCl <1> (<1> 1 M, activates [6]) [6]

Turnover number (s^{-1})

0.13 <1> (2-aminobenzoyl-Ala-Thr-His-Gln-Val-Tyr-Phe(NO_2)-Val-Arg-Lys-Ala, <1> pH 5.0, 25°C, 13000 Da C-terminally truncated enzyme form [3]) [3]
0.8 <1> (Lys-Ala-Arg-Val-Tyr-Phe(NO_2)-Glu-Ala-Nle-NH_2, <1> pH 4.5, 18200 Da enzyme form [2]) [2]

1.37 <1> (2-aminobenzoyl-Ala-Thr-His-Gln-Val-Tyr-Phe(NO_2)-Val-Arg-Lys-Ala, <1> pH 5.0, 25°C, 18000 Da enzyme form [3]) [3]
2.1 <1> (Lys-Ala-Arg-Val-Tyr-Phe(NO_2)-Glu-Ala-Nle-NH_2, <1> pH 4.5, 11600 Da core domain [2]) [2]

K_m-Value (mM)

0.001 <1> (Lys-Ala-Arg-Val-Tyr-Phe(NO_2)-Glu-Ala-Nle-NH_2, <1> pH 4.5, 11600 Da core domain [2]) [2]
0.002 <1> (2-aminobenzoyl-Ala-Thr-His-Gln-Val-Tyr-Phe(NO_2)-Val-Arg-Lys-Ala, <1> pH 5.0, 25°C, 13000 Da C-terminally truncated enzyme form [3]) [3]
0.0103 <1> (Lys-Ala-Arg-Val-Tyr-Phe(NO_2)-Glu-Ala-Nle-NH_2, <1> pH 4.5, 18200 Da enzyme form [2]) [2]
0.041 <1> (2-aminobenzoyl-Ala-Thr-His-Gln-Val-Tyr-Phe(NO_2)-Val-Arg-Lys-Ala, <1> pH 5.0, 25°C, 18000 Da enzyme form [3]) [3]

K_i-Value (mM)

0.0000001 <1> (XV648, <1> pH 5.0, 25°C, 13000 Da C-terminally truncated enzyme form [3]) [3]
0.00000015 <1> (SD146, <1> pH 5.0, 25°C, 13000 Da C-terminally truncated enzyme form [3]) [3]
0.00000017 <1> (XV643, <1> pH 5.0, 25°C, 13000 Da C-terminally truncated enzyme form [3]) [3]
0.00000022 <1> (XV644, <1> pH 5.0, 25°C, 13000 Da C-terminally truncated enzyme form [3]) [3]
0.00000052 <1> (XV652, <1> pH 5.0, 25°C, 13000 Da C-terminally truncated enzyme form [3]) [3]
0.0000022 <1> (XV638, <1> pH 5.0, 25°C, 13000 Da C-terminally truncated enzyme form [3]) [3]
0.0000023 <1> (XV648, <1> pH 5.0, 25°C, 18000 Da enzyme form [3]) [3]
0.0000029 <1> (XV644, <1> pH 5.0, 25°C, 18000 Da enzyme form [3]) [3]
0.0000032 <1> (XV651, <1> pH 5.0, 25°C, 13000 Da C-terminally truncated enzyme form [3]) [3]
0.0000033 <1> (XV652, <1> pH 5.0, 25°C, 18000 Da enzyme form [3]) [3]
0.0000036 <1> (XW805, <1> pH 5.0, 25°C, 13000 Da C-terminally truncated enzyme form [3]) [3]
0.0000039 <1> (XV643, <1> pH 5.0, 25°C, 18000 Da enzyme form [3]) [3]
0.0000043 <1> (SD146, <1> pH 5.0, 25°C, 18000 Da enzyme form [3]) [3]
0.0000046 <1> (KNI227, <1> pH 4.5, 11600 Da core domain [2]) [2]
0.0000059 <1> (SD145, <1> pH 5.0, 25°C, 13000 Da C-terminally truncated enzyme form [3]) [3]
0.0000079 <1> (SD152, <1> pH 5.0, 25°C, 13000 Da enzyme form [3]) [3]
0.000015 <1> (KNI227, <1> pH 4.5, 18200 Da enzyme form [2]) [2]
0.0000162 <1> (Q8467, <1> pH 5.0, 25°C, 13000 Da C-terminally truncated enzyme form [3]) [3]
0.00002 <1> (XV638, <1> pH 5.0, 25°C, 18000 Da enzyme form [3]) [3]
0.000027 <1> (SD152, <1> pH 5.0, 25°C, 18000 Da enzyme form [3]) [3]
0.00003 <1> (SD145, <1> pH 5.0, 25°C, 13000 Da enzyme form [3]) [3]
0.000031 <1> (XW805, <1> pH 5.0, 25°C, 18000 Da enzyme form [3]) [3]

0.000043 <1> (XV651, <1> pH 5.0, 25°C, 18000 Da enzyme form [3]) [3]
0.00006 <1> (ABT538, <1> pH 4.5, 11600 Da core domain [2]) [2]
0.000061 <1> (Q8467, <1> pH 5.0, 25°C, 18000 Da enzyme form [3]) [3]
0.000091 <1> (XM412, <1> pH 5.0, 25°C, 13000 Da C-terminally truncated enzyme form [3]) [3]
0.00012 <1> (KNI272, <1> pH 4.5, 11600 Da core domain [2]) [2]
0.00034 <1> (KNI272, <1> pH 4.5, 18200 Da enzyme form [2]) [2]
0.00039 <1> (XM412, <1> pH 5.0, 25°C, 18000 Da enzyme form [3]) [3]
0.00061 <1> (indinavir, <1> pH 5.0, 25°C, 13000 Da C-terminally truncated enzyme form [3]) [3]
0.00067 <1> (XK234, <1> pH 5.0, 25°C, 13000 Da C-terminally truncated enzyme form [3]) [3]
0.00094 <1> (indinavir, <1> pH 5.0, 25°C, 18000 Da enzyme form [3]) [3]
0.00113 <1> (ritonavir, <1> pH 5.0, 25°C, 13000 Da C-terminally truncated enzyme form [3]) [3]
0.00121 <1> (ritonavir, <1> pH 5.0, 25°C, 18000 Da enzyme form [3]) [3]
0.00187 <1> (XK234, <1> pH 5.0, 25°C, 18000 Da enzyme form [3]) [3]
0.00257 <1> (pepstatin, <1> pH 5.0, 25°C, 13000 Da C-terminally truncated enzyme form [3]) [3]
0.00258 <1> (saquinavir, <1> pH 5.0, 25°C, 13000 Da C-terminally truncated enzyme form [3]) [3]
0.0049 <1> (pepstatin, <1> pH 5.0, 25°C, 18000 Da enzyme form [3]) [3]
0.00574 <1> (saquinavir, <1> pH 5.0, 25°C, 18000 Da enzyme form [3]) [3]
Additional information <1> [2]

pH-Optimum

4-5 <1> (<1> 11600 Da core domain [2]) [2]
4.5 <1> (<1> C-terminally truncated mutant enzyme, substrate KAR-VYF^{-}NO$_2^{-}$EA-Nle-NH$_2$ [6]) [6]
6.5 <1> [5]

4 Enzyme Structure

Molecular weight

16470 <1> (<1> avarage molecular weight under near physiological conditions, sedimentation equilibrium analysis [2]) [2]
43000 <1> (<1> SDS-PAGE [9]) [9]

Subunits

dimer <1> (<1> 2 * 17500, the enzyme is synthesized as monomeric part of the Gag polyprotein or the Gag-Pol polyprotein and autolytically processed to the mature protein dimer, structure overview [6]) [6]
Additional information <1> (<1> the 11600 Da core domain exists as a dimer at pH 7.0 [2]) [2]

Posttranslational modification

proteolytic modification <1> (<1> the enzyme is synthesized as monomeric part of the Gag polyprotein or the Gag-Pol polyprotein and autolytically processed to the mature protein dimer, autoprocessing at the N-terminal sequence Lys-Ala-Ala-Tyr-Trp-Ala-Ser-Gln [6]) [6]

5 Isolation/Preparation/Mutation/Application

Purification

<1> (18200 Da enzyme form and 11600 Da core domain) [2]
<1> (full-length and C-terminally truncated enzyme in Escherichia coli) [3]
<1> (recombinant wild-type and C-terminally truncated mutant enzymes from Escherichia coli by ammonium sulfate fractionation, cation and anion exchange chromatography, and hydrophobic interaction chromatography, or recombinant C-terminally truncated mutant enzyme from inclusion bodies by dialysis and pepstatin A affinity chromatography followed by autoprocession to active, soluble enzme) [6]

Cloning

<1> (213 amino acids of the 3'-end of the HERV-K protease open reading frame are expressed in Escherichia coli. Autocatalytic cleavage of the expressed polypeptide results in a catalytically active 18200 Da protein) [2]
<1> (expression of a full-length and C-terminally truncated enzyme in Escherichia coli) [3]
<1> (nucleotide sequence determination and analysis, detailed phylogenetic analysis of virus from primates and humans, and structural analysis of 100 HERV-K(HML-5) provirus sequences, reconstruction of a coding-competent HML-5 provirus, overview) [7]
<1> (sequence determination and analysis, expression of wild-type and C-terminally truncated mutant enzymes in Escherichia coli) [6]
<1> (targeting of the HERV-K PR to protease-deficient HIV-1 virions by expressing it as a Vpr fusion partner. The Vpr fusion proteins are sucessfully delivered to the HIV-1 virions, where the HERV-K PR not only autoprocesses itself to ist mature form, but also cleaves a number of HIV-1 polyproteins) [4]
<1> (the HERV-K113 sequence is cloned into a small plasmid vector. It is shown that based on a substantial LTR-promoter activity, full length messenger RNA and spliced env-, rec- and 1.5 kb (hel)-transcripts are produced. Envelope protein of HERV-K113 is synthesized as an 85 kDa precursor that is found partially processed. The accessory Rec protein is highly expressed and accumulates in the nucleus. Expression analysis reveals synthesis of the Gag precursor and the protease in lysates of transfected HEK-293T cells. The cloned HERV-K113 provirus is not replication competent) [9]
<1> (the enzyme is expressed either as a full-length native protein or as truncated protein in Escherichia coli) [5]

Engineering

Additional information <1> (<1> a C-terminally truncated mutant enzyme shows increased affinity for the peptide substrates and increased sensitivity to peptidomimetic inhibitors compared to the wild-type enzyme [6]) [6]

Application

medicine <1> (<1> in the present study HIV-1 and HCV-1-positive plasma samples are screened for the presence of HERV-K(HML-2) RNA in an RT-PCR using HERV-K pol specific primers. Type 1 and type 2 HERV-K(HML-2) viral RNA genomes are found to coexist in the same plasma of HIV-1 patients suggesting that HERV-K(HML-2) viral particles are induced in HIV-1-infected individuals [8]) [8]

6 Stability

pH-Stability

3-9 <1> (<1> room temperature, prolonged incubation, 60% remaining activity in presence or absence of 1 M NaCl, no autolysis [6]) [6]

References

[1] Ono M.; Yasunaga T.; Miyata T.; Ushikubo H.: Nucleotide sequence of human endogenous retrovirus genome related to the mouse mammary tumor virus genome. J. Virol., **60**, 589-598 (1986)

[2] Towler, E.M.; Gulnik, S.V.; Bhat, T.N.; Xie, D.; Gustschina, E.; Sumpter, T.R.; Robertson, N.; Jones, C.; Sauter, M.; Mueller-Lantzsch, N.; Debouck, C.; Erickson, J.W.: Functional characterization of the protease of human endogenous retrovirus, K10: can it complement HIV-1 protease?. Biochemistry, **37**, 17137-17144 (1998)

[3] Kuhelj, R.; Rizzo, C.J.; Chang, C.H.; Jadhav, P.K.; Towler, E.M.; Korant, B.D.: Inhibition of human endogenous retrovirus-K10 protease in cell-free and cell-based assays. J. Biol. Chem., **276**, 16674-16682 (2001)

[4] Padow, M.; Lai, L.; Fisher, R.J.; Zhou, Y.C.; Wu, X.; Kappes, J.C.; Towler, E.M.: Analysis of human immunodeficiency virus type 1 containing HERV-K protease. AIDS Res. Hum. Retroviruses, **16**, 1973-1980 (2000)

[5] Schommer, S.; Sauter, M.; Krausslich, H.G.; Best, B.; Mueller-Lantzsch, N.: Characterization of the human endogenous retrovirus K proteinase. J. Gen. Virol., **77**, 375-379 (1996)

[6] Strisovsky, K.; Kraeusslich, H.: Human retrovirus K10 retropepsin. Handbook of Proteolytic Enzymes (Barrett, J.; Rawlings, N.D.; Woessner, J.F., eds.), **1**, 182-184 (2004)

[7] Lavie, L.; Medstrand, P.; Schempp, W.; Meese, E.; Mayer, J.: Human endogenous retrovirus family HERV-K(HML-5): status, evolution, and reconstruction of an ancient βretrovirus in the human genome. J. Virol., **78**, 8788-8798 (2004)

[8] Contreras-Galindo, R.; Kaplan, M.H.; Markovitz, D.M.; Lorenzo, E.; Yamamura, Y.: Detection of HERV-K(HML-2) Viral RNA in Plasma of HIV Type 1-Infected Individuals. AIDS Res. Hum. Retroviruses, **22**, 979-984 (2006)
[9] Beimforde, N.; Hanke, K.; Ammar, I.; Kurth, R.; Bannert, N.: Molecular cloning and functional characterization of the human endogenous retrovirus K113. Virology, **371**, 216-225 (2008)

HycI peptidase 3.4.23.51

1 Nomenclature

EC number
3.4.23.51

Recommended name
HycI peptidase

Synonyms
HYCI <1> [1,2,3,4,7]
HycE processing protein <1> [7]
HycI endopeptidase <2> [8]

2 Source Organism

<1> *Escherichia coli* (UNIPROT accession number: P0AEV9) [1,2,3,4,5,6,7]
<2> *Escherichia coli* K-12 (UNIPROT accession number: P0AEV9) [8]

3 Reaction and Specificity

Catalyzed reaction
This enzyme specifically removes a 32-amino acid peptide from the C-terminus of the precursor of the large subunit of hydrogenase 3 in Escherichia coli by cleavage at the C-terminal side of Arg537.

Natural substrates and products
S precursor of the large subunit of hydrogenase 3 + H_2O <1> (<1> i.e. HycE [7]; <1> HycI involved in the C-terminal processing of HycE, the large subunit of the hydrogenase 3 from Escherichia coli [1]; <1> HycI is an endopeptidase that is responsible for the C-terminal cleavage of the large subunit of hydrogenase 3 in Escherichia coli (UniProt: A1AER2) [3]; <1> the final step of maturation of [NiFe]-hydrogenases involves the activity of an endopeptidase which removes an oligopeptide from the C-terminus of the large subunit. The proteolytic maturation is followed by a conformational change, closing of the metal centre, its assembly with the small hydrogenase subunit and finally in the appearance of enzyme activity. HycI is specific for hydrogenase 3 maturation [4]) (Reversibility: ?) [1,3,4,5,7]
P ?

D. Schomburg and I. Schomburg (eds.), *Class 3.4–6 Hydrolases, Lyases, Isomerases, Ligases: EC 3.4–6*, Springer Handbook of Enzymes S10, DOI 10.1007/978-3-642-36260-6_7,

Substrates and products

S precursor of the large subunit of hydrogenase 3 + H_2O <1,2> (<1> i.e. HycE [7]; <1> HycI involved in the C-terminal processing of HycE, the large subunit of the hydrogenase 3 from Escherichia coli [1]; <1> HycI is an endopeptidase that is responsible for the C-terminal cleavage of the large subunit of hydrogenase 3 in Escherichia coli (UniProt: A1AER2) [3]; <1> the final step of maturation of [NiFe]-hydrogenases involves the activity of an endopeptidase which removes an oligopeptide from the C-terminus of the large subunit. The proteolytic maturation is followed by a conformational change, closing of the metal centre, its assembly with the small hydrogenase subunit and finally in the appearance of enzyme activity. HycI is specific for hydrogenase 3 maturation [4]; <1> cleavage occurrs at the C-terminal side of the Arg537 (removal of a 32-amino acid peptide from the C-terminus). Nickel incorporation into the HYCE precursor is a prerequisite for processing [6]; <1> HycI involved in the C-terminal processing of HycE (UniProt: A1AER2), the large subunit of the hydrogenase 3 from Escherichia coli. Mutational alteration of the amino acid residues neighbouring the cleavage site shows that proteolysis still occurrs when chemically similar amino acids are exchanged. Processing is blocked in a variant in which the methionine at the C-terminal side is replaced by a glutamate residue. Truncation of the precursor from the C-terminal end renders variants amenable to maturation even when two-thirds of the extension are removed but abolishes proteolysis upon further deletion of a cluster of six basic amino acids. A construct in which the C-terminal extension from the large subunit of the hydrogenase 2 is fused to the mature part of the large subunit of hydrogenase 3 is neither processed by HycI nor by HybD, the endopeptidase specific for the large subunit of hydrogenase 2 [1]; <1> HycI is specific for hydrogenase 3 maturation [2,4]; <1> i.e. HycE (UniProt: A1AER2). Cleavage of HycE is specific in that the maturation of the large subunits of hydrogenases 1 and 2 is not affected in strains lacking hycl [7]; <1> i.e. hycE. Once the metallocenter [NiMeL] is formed in the HycE precursor, processing by HycI and assembly with the other Hyc subunits takes place [5]; <2> the HycI endopeptidase is involved in the C-terminal processing of the large subunit of hydrogenase 3 (HycE) [8]) (Reversibility: ?) [1,2,3,4,5,6,7,8]

P ?

Inhibitors

Additional information <1> (<1> not inhibited by phenylmethylsulfonyl fluoride, benzamidine or EDTA [7]) [7]

Metals, ions

Cd^{2+} <1> (<1> conserved amino-acid residues involved in cadmium ligation in the crystal are essential for the endoproteolytic activity in HycI [2]) [2]

Ni^{2+} <1> (<1> HycI shows an open conformation at the putative nickel-binding site. Ni^{2+} has lower binding affinity with HycI than that of Cd^{2+}, which is likely required for HycI to dissociate from HycE after the C-terminal processing [3]; <1> the reaction requires nickel to be bound to the precursor and

the protease does not have a function in nickel delivery to the substrate. Radioactive labelling of cells with 63Ni, devoid of endopeptidase, resolves several forms of the precursor which are possibly intermediates in the maturation pathway. The endopeptidase uses the metal in the large subunit of [NiFe]-hydrogenases as a recognition motif [2]) [2,3]

pi-Value

3.7 <2> (<2> calculated from amino acid sequence [8]) [8]

4 Enzyme Structure

Molecular weight

17000 <1,2> (<1> gel filtration [7]) [7,8]

Subunits

monomer <1,2> (<1> 1 * 17000 [4]; <2> 1 * 17000, HycI exists as a monomer in solution, X-ray crystallography [8]) [4,8]

5 Isolation/Preparation/Mutation/Application

Purification

<1> [7]
<1> (partial) [6]
<1> (purified endopeptidases HycI is devoid of metal) [2]
<2> (HisTrap HP5 column chromatography, HiPrep column chromatography, and Superdex 200 gel filtration) [8]

Crystallization

<1> (solution structure of Escherichia coli HycI determined by high resolution nuclear magnetic resonance spectroscopy. The overall structure is similar to the crystal structure of holo-HybD in the same family. HycI shows an open conformation at the putative nickel-binding site, whereas HybD adopts a closed conformation) [3]
<2> (sitting drop vapor diffusion method, using 28% (w/v) polyethylene glycol 400, 0.2 M $CaCl_2$, and 0.1 M Na-HEPES (pH 7.5), at 20°C) [8]

Cloning

<1> [3]
<2> [8]

Engineering

D16N <1> (<1> no processing activity [2]) [2]
D62M <1> (<1> no processing activity [2]) [2]
D62N <1> (<1> no processing activity [2]) [2]
H90Q <1> (<1> some minor processing activity [2]) [2]

References

[1] Theodoratou, E.; Paschos, A.; Mintz-Weber, S.; Bock, A.: Analysis of the cleavage site specificity of the endopeptidase involved in the maturation of the large subunit of hydrogenase 3 from Escherichia coli. Arch. Microbiol., **173**, 110-116 (2000)
[2] Theodoratou, E.; Paschos, A.; Magalon, A.; Fritsche, E.; Huber, R.; Bock, A.: Nickel serves as a substrate recognition motif for the endopeptidase involved in hydrogenase maturation. Eur. J. Biochem., **267**, 1995-1999 (2000)
[3] Yang, F.; Hu, W.; Xu, H.; Li, C.; Xia, B.; Jin, C.: Solution structure and backbone dynamics of an endopeptidase HycI from Escherichia coli: implications for mechanism of the [NiFe] hydrogenase maturation. J. Biol. Chem., **282**, 3856-3863 (2007)
[4] Theodoratou, E.; Huber, R.; Böck A.: [NiFe]-Hydrogenase maturation endopeptidase: structure and function. Biochem. Soc. Trans., **33**, 108-111 (2005)
[5] Maier, T.; Böck, A.: Generation of active [NiFe] hydrogenase in vitro from a nickel-free precursor form. Biochemistry, **35**, 10089-10093 (1996)
[6] Rossmann, R.M.; Sauter, M.; Lottspeich, F.; Böck, A.: Maturation of the large subunit (HYCE) of Escherichia coli hydrogenase 3 requires nickel incorporation followed by C-terminal processing at Arg537. Eur. J. Biochem., **220**, 377-384 (1994)
[7] Rossmann, R.; Maier, T.; Lottspeich, F.; Boeck, A.: Characterization of a protease from Escherichia coli involved in hydrogenase maturation. Eur. J. Biochem., **227**, 545-550 (1995)
[8] Kumarevel, T.; Tanaka, T.; Bessho, Y.; Shinkai, A.; Yokoyama, S.: Crystal structure of hydrogenase maturating endopeptidase HycI from Escherichia coli. Biochem. Biophys. Res. Commun., **389**, 310-314 (2009)

ADAMTS13 endopeptidase 3.4.24.87

1 Nomenclature

EC number
3.4.24.87

Recommended name
ADAMTS13 endopeptidase

Synonyms
ADAMTS 13 <3> [59,90]
ADAMTS VWF cleaving metalloprotease <3> [3]
ADAMTS-13 <2,3,4> (<3> i.e. a disintegrin and metalloprotease with a thrombospondin type 1 motifs 13 [75]) [1,4,5,25,26,30,40,42,43,44,45,47,69,75,79,91]
ADAMTS13 <1,2,3,4,5,6,7,8,9,10> (<3> i.e. a disintegrin and metalloprotease with thrombospondin repeats [6,12]; <3> ADAMTS13 belongs to the ADAMTS or a disintegrin-like and metalloproteinase with thrombospondin type-1 motif family [97]; <3> ADAMTS13 is a member of the a disintegrin and metalloprotease with thrombospondin type 1 repeats, i.e. ADAMTS, family [63]; <3> i.e a disintegrin and metalloprotease with thrombospondin 13 [92]; <2> i.e. a disintegrin and metalloprotease with thrombospondin domain 13 [76]; <3> i.e. a disintegrin and metalloprotease with thrombospondin motif [78]; <3> i.e. a disintegrin and metalloprotease with thrombospondin motifs-13 [68]; <2,3> i.e. a disintegrin-like and metalloprotease with trombospondin type-1 repeats 13 [67,101,102]; <3> i.e. disintegrin-like domain and Metalloprotease with ThromboSpondin type I motif 13 [99]) [2,3,6,10,11,12,13,16,21,22,28,31,32,33,34,35,36,37,38,39,41,46,48,49,50,52,53,-54,55,56,57,58,60,61,62,63,64,65,66,67,68,70,71,72,73,74,76,77,78,80,81,82,83,8-5,86,87,88,89,92,93,94,95,96,97,98,99,100,101,102,103,104,105,106]
ADAMTS13 metalloprotease <3> [60,66]
M12.241 <3,9> (<3,9> Merops-ID [1,2,3,4,5,6,7,8,9,10,11,12,13]) [1,2,3,4,5,6,7,8,9,10,11,12,13]
Upshaw factor <3> [1]
VWF cleaving metalloprotease <3> [3]
VWF cleaving protease <3> [1,33,39,49,57]
VWF-CP <3> [4,13,39]
VWF-cleaving metalloprotease <3> [83]
VWFCP <9> [10]
a disintegrin and metalloprotease with thrombospondin motifs 13 <3> [38]
a disintegrin and metalloprotease with thrombospondin-13 <4> [25]

D. Schomburg and I. Schomburg (eds.), *Class 3.4–6 Hydrolases, Lyases, Isomerases, Ligases: EC 3.4–6*, Springer Handbook of Enzymes S10, DOI 10.1007/978-3-642-36260-6_8,

a disintegrin and metalloproteinase with a thrombonspondin type 1 motif member 13 <3> [44]
a disintegrin-like and metalloprotease with thrombospondin type I repeats - 13 <10> [53]
a disintegrin-like and metalloprotease with thrombospondin type-1 motifs 13 <3> [94]
a disintegrin-like and metalloproteinase domain with thrombospondin type I motifs 13 <3> [83]
a disintegrin-like domain and metalloprotease with thrombospondin type I motif <3> [48]
metalloprotease ADAMTS-13 <3> [59]
plasma metalloprotease ADAMTS13 <1,2,3,4,5,6,7,8> [89]
plasma von Willebrand factor cleaving activity <3> [37]
vWF protease <3> [9]
vWF-cleaving protease <3> [8,13,42,43,56,94,99,103]
vWF-degrading protease <3> [7]
van Willebrand factor processing activity <3> [1]
von Willebrand cleavage protease <3> [95]
von Willebrand factor cleaving protease <3> [1,33,49,57,94]
von Willebrand factor-cleaving metalloprotease <3> [83]
von Willebrand factor-cleaving protease <2,3,9> [2,4,5,9,10,13,14,31,39,42,43, 48,67,94,103]
von Willebrand factor-cleaving proteinase <9> [55]
von-Willebrand factor cleaving protease <3> [11,12]
von-Willebrand factor degrading protease <3> [7]
von-Willebrand-factor-cleaving protease <3> [28]
xWF-CP <3> [14]
Additional information <3,9> (<3> a disintegrin and metalloprotease with thrombospondin type 1 motif, member 13 [35]; <3> a disintegrin and metalloprotease with trombonspondin motif 13 [37]; <3> ADAMTS13 belongs to the family of a disintegrin-like and metalloprotease domains with repeated thrombospondin domains [104]; <3> ADAMTS13 is a member of a disintegrin and metalloprotease with thrombospondin type 1 repeats, ADAMTS, family [73]; <3> ADAMTS13 is a member of the ADAMTS, a disintegrin and metalloproteinase with thrombospondin motifs, family of proteins [95]; <9> ADAMTS13 is a reprolysin-type metalloproteinase belonging to the ADAMTS, i.e. a disintegrin and metalloproteinase with thrombospondin type 1 motif, family [55]) [35,37,55,73,95,104]

CAS registry number

334869-10-2

2 Source Organism

<1> *Cavia porcellus* [89]
<2> *Mus musculus* [24,34,41,61,62,67,72,76,89,91]

<3> *Homo sapiens* [1,3,4,5,6,7,8,9,11,12,13,14,15,16,17,18,19,21,22,23,26,27,28,29,30,31,32,33,35,36,37,38,39,40,41,42,43,44,45,46,47,48,49,56,57,58,59,60,63,64,65,66,67,68,69,70,71,73,74,75,77,78,79,80,81,82,83,84,85,86,87,88,89,90,92,94,95,96,97,98,99,100,101,102,103,104,]
<4> *Rattus norvegicus* [25,89]
<5> *Sus scrofa* [89]
<6> *Oryctolagus cuniculus* [89]
<7> *Canis lupus familiaris* [89]
<8> *Macaca fascicularis* (gene pepQ [89]) [89]
<9> *Homo sapiens* (UNIPROT accession number: Q76LX8, ADAMTS-13 precursor) [2,10,20,50,51,52,54,55,93]
<10> *Mus musculus* (UNIPROT accession number: Q769J6) [53]

3 Reaction and Specificity

Catalyzed reaction

The enzyme cleaves the von Willebrand factor at bond Tyr842-/-Met843 within the A2 domain (<3> active site sequence HEIGHSFGLEHE 150 amino acid residues from the N-terminus of the protein [8]; <9> active site sequence HEXXHXXGXXHD [10]; <3> enzyme is a hemostatic factor [5]; <3> the cysteine-rich/spacer domains are essential for the proteolytic activity [4]; <3> the spacer region is essential, while the C-terminal thrombospondin type 1 motif and the CUB domain are dispensable in vitro [11])

Reaction type

hydrolysis of peptide bond

Natural substrates and products

S more | <3> (<3> ADAMTS13 binds to CD36, a transmembrane protein of endothelial cells and platelets, i.e. glycoprotein IV, not diminishing the proteolytic activity of ADAMTS13, but providing an anchor for ADAMTS13 on the surface of endothelial cells and platelets [104]) (Reversibility: ?) [104]
P ?
S proteins + H_2O <3,9> (<9> enzyme is involved in thrombotic thrombocytopenic purpura [10]) (Reversibility: ?) [1,2,3,4,5,6,7,8,9,10,11,12,13]
P peptides <3,9> [1,2,3,4,5,6,7,8,9,10,11,12,13]
S von Willebrand factor + H_2O <1,2,3,4,5,6,7,8> (<3> ADAMTS-13 cleavage of von Willebrand factor strings secreted from stimulated and unstimulated HUVECs occurs at the position 1605-6 of the von Willebrand factor A2 domain [69]; <3> ADAMTS-13 cleaves the Tyr1605-Met1606 bond in the VWF A2 domain, mechanisms of VWF recognition, cleavage analysis and kinetics under static and flow conditions, overview [66]; <3> ADAMTS-13 cleaves von Willebrand factor (VWF) exclusively at the Tyr1605-Met1606 peptide bond in the A2 domain [79]; <1,2,3,4,5,6,7,8> ADAMTS13 cleaves von Willebrand factor at the Tyr1605-Met1606 bond within the central A2 domain [89]) (Reversibility: ?) [63,66,69,79,89]

P von Willebrand factor 140-kD fragment + von Willebrand factor 176-kD fragment
S von Willebrand factor + H_2O <2,3> (<3> ADAMTS13 cleaves von Willebrand factor at the Tyr1605-Met1606 bond [73]; <2,3> ADAMTS13 cleaves von Willebrand factor to smaller less-active forms [67]; <3> ADAMTS13 specifically cleaves von Willebrand factor multimers at the site of the Tyr1605-Met1606 bond of the VWF-A2 domain [84]; <3> cleavage at the Tyr1605-Met1606 bond within the van Willebrand factor A2 domain [96]; <3> cleavage can also occur at the surface of endothelial cells. ADAMTS13 that is prebound to endothelial cells exhibits increased proteolysis of VWF as compared with ADAMTS13 present only in solution. Thus, cleavage of VWF occurs mainly at the endothelial cell surface [85]; <3> cleavage of ultra large von Willebrand multimers into smaller fragments [90]; <3> specific cleavage of the long strings of ultra-large von Willebrand factor multimers [104]) (Reversibility: ?) [67,73,77,84,85,90,96,104]
P von Willebrand factor fragments
S von Willebrand factor + H_2O <3> (<3> cleavage of peptide bond Tyr842-Met843 [8]) (Reversibility: ?) [8]
P 2 peptides of 140 kD and 65 kD <3> [8]
S von Willebrand factor + H_2O <3> (<3> cleavage of the peptide bond Tyr842-Met843 within the A2 domain, enzyme deficiency causes lethal thrombotic thrombocytopenic purpura [4]; <3> either congenital or acquired defects of the enzyme lead to thrombotic thromcytopenic purpura, cleavage of the peptide bond bond Tyr842-Met843 within the A2 domain, i.e. Tyr1605-Met1606 in von Willebrand factor UniProt Id P04275 [5]; <3> large multimeric substrate, cleavage of the peptide bond Tyr842-Met843 within the A2 domain [12]; <3> protein from plasma of patients suffering type I von Willebrand disease is more susceptible to proteolysis by the enzyme due to amino acid polymorphism heterozygous at position Tyr/Cys1584, phenotypic parameters, cleavage of the peptide bond Tyr842-Met843 within the A2 domain [6]) (Reversibility: ?) [4,5,6,12]
P 2 peptides of 140 kDa and 176 kDa <3> [4,5,6,12]
S von Willebrand factor + H_2O <3> (<3> rapid physiological process that occurs on endothelial surfaces, activity is reduced by 87-100% in patients with thrombotic thrombocytopenic pupura [3]) (Reversibility: ?) [3]
P 2 peptides of 176 kDa and 140 kDa <3> [3]
S von Willebrand factor + H_2O <3> (<3> rapid physiological process that occurs on endothelial surfaces, reduced activity results in thrombotic thrombocytopenic pupura [13]) (Reversibility: ?) [13]
P 2 peptides <3> [13]
S von Willebrand factor + H_2O <2,3,4,9> (<3> specific for [97]; <3> cleavage of peptide bond Tyr842-Met843, large hemostatically active multimers ar cleaved to smaller less active forms, increased proteolytic degradation in patients suffering from von Willebrand disease typ 2A [7]; <9> cleavage of peptide bond Tyr842-Met843, rapid degradation of multimers to smaller fragments, decreased activity results in bone marrow transplant-associated thrombotic microangiopathy and thrombotic thrombo-

cytopenic pupura [2]; <3> decrease of the multimeric pattern of enzyme and decreased activity results in bone marrow transplant-associated thrombotid microangiopathy [9]; <3> enzyme deficiency causes lethal thrombotic thrombocytopenic purpura, cleavage of peptide bond Tyr1605-Met1606 resulting in limited platelet accumulation in microvascular thrombi (Tyr842-Met843 within the A2 domain, i.e. Tyr1605-Met1606 in von Willebrand factor UniProt Id P04275) [11]; <3> the cleavage site is exposed to the enzyme by conformational changes due to shear stress in the plasma, decrease of the multimeric pattern of enzyme and decreased activity results in bone marrow transplant-associated thrombotic microangiopathy, cleavage of peptide bond Tyr842-Met843, large hemostatically active multimers are cleaved to smaller less active forms, increased proteolytic degradation in patients suffering von Willebrand disease typ 2A [1]; <3> cleavage of Tyr842-Met843 within the A2 domain, i.e. Tyr1605-Met1606 in von Willebrand factor UniProt Id P04275 [21]; <3> ADAMTS13 cleaves at the peptide bond Tyr842-Met843 within the A2 domain, i.e. Tyr1605-Met1606 in von Willebrand factor UniProt Id P04275 [41]; <3> ADAMTS13 cleaves the bond Tyr842-Met843 within the A2 domain, i.e. Tyr1605-Met1606 in von Willebrand factor UniProt Id P04275 [33]; <3> amino acid position C1584 is necessary for enhanced von Willebrand factor proteolysis by ADAMTS13 [38]; <9> ADAMTS13 efficiently cleaves only the Tyr842-Met843 bond within the central A2 domain of multimeric von Willebrand factor (i.e. Tyr1605-Met1606 in von Willebrand factor UniProt Id P04275) [50]; <3> a catalysis-deficient ADAMTS13 P475S mutant does not show VWF-induced changes in conformation [95]; <3> ADAMTS13 cleaves ultra-large von Willebrand factor multimers [105]; <3> cleavage of ultra-large multimers [80]; <3> force-induced von Willebrand factor A2 domain unfolding of the substrate facilitates cleavage, using single VWF A1A2A3 tridomain polypeptides, structural destabilization of A1A2A3 was induced by 5- to 80-pN forces [75]; <3> persistently elevated levels of von Willebrand factor in plasma during and after liver transplantation, while plasma levels of ADAMTS13 dropp during transplantation [56]; <3> specific cleavage of ultra-large von Willebrand factor multimers [60,83,99]; <2> von Willebrand factor is also susceptible to cleavage by ADAMTS13 when incorporated in a thrombus [76]) (Reversibility: ?) [1,2,7,9,10,11,21,22,25,32,33,34,35,37,38,39,40,41,42,43,44,45,46,47,48,49,50,55,56,57,58,59,60,61,62,64,65,68,70,71,72,74,75,76,78,80,83,86,91,92,93,94,95,97,99,100,101,103,105]

P ? <3,9> [1,2,7,9,10,11]

S Additional information <3,9,10> (<10> important role for ADAMTS13 in preventing excessive spontaneous Weibel-Palade body secretion, and in the regulation of leukocyte adhesion and extravasation during inflammation [53]; <3> ADAMTS13 contains eight thrombospondin type 1 repeats and binds to CD36, a transmembrane protein present on endothelial cells and platelets. CD36 also binds to thrombospondin-2 via three thrombospondin type 1 repeats in a manner competitive to ADAMTS13, overview [105]; <3> MDTCS domain modelling and substrate recognition mode

analysis, overview [97]; <3> proteolysis can occur only once VWF has been unraveled from its globular conformation, either by high fluid shear stress in vivo or in the presence of denaturants in vitro, conditions that are able to promote the exposure of the VWF scissile bond [66]; <3> removal of newly released ultralarge-von Willebrand factor strings or bundles anchored on endothelial cells by ADAMTS13 occurs rapidly and efficiently in the presence and in the absence of fluid shear stress, suggesting that the cell-bound ultra large-von Willebrand factor polymers may be preferred substrates for ADAMTS13 [73]; <9> thrombospondin1 and ADAMTS13 form complexes together in cells and in direct protein binding assays [93]) (Reversibility: ?) [53,66,73,93,97,105]

P ?

Substrates and products

S collagen + H_2O <3> (Reversibility: ?) [33,35]

P ?

S DREQAPNLVYMVTGNPASDEIKRLPGDIQVVPIGVGPNANVQELER-IGWPNAPILIQDFETLPREAPDLVLQRA + H_2O <3> (<3> i.e. VWF74 peptide, a pseudo-wild-type peptide von Willebrand factor 74, VWF74, encompassing the von Willebrand factor, VWF, A2 domain sequence 1596-1669 [79]) (Reversibility: ?) [79]

P ?

S FRET-VWF115 peptide + H_2O <3> (<3> von Willebrand factor-derived peptide substrate comprising residues 1554-1668 [60]) (Reversibility: ?) [60]

P ?

S FRET-VWF73 + H_2O <2> (<2> fluorogenic von Willebrand factor-derived peptide substrate. The distal C-terminal domains of ADAMTS13 are not necessary for the cleavage of the VWF73-based peptide substrate [62]) (Reversibility: ?) [62]

P ?

S FRETS-VWF73 peptide + h2O <3> (<3> fluorogenic von Willebrand factor-derived peptide substrate [97]) (Reversibility: ?) [97]

P ?

S FRETS-vWF73 + H_2O <3> (<3> a fluorogenic von Willebrand factor-derived peptide substrate [70]) (Reversibility: ?) [70]

P ?

S FRETS-von Willebrand factor 73 + H_2O <3> (Reversibility: ?) [22]

P ?

S FRETSVWF73 + H_2O <3> (<3> a von Willebrand factor-derived fluorescein-labeled peptide substrate [68]) (Reversibility: ?) [68]

P ?

S FRETSVWF73 peptide + H_2O <3> (<3> a von Willebrand factor-derived fluorescein-labeled peptide substrate [65]) (Reversibility: ?) [65]

P ?

S GST-VWF73 + H_2O <2,3> (<3> labeled von Willebrand factor-derived peptide substrate [92]; <2> labeled von Willebrand factor-derived peptide

substrate. The distal C-terminal domains of ADAMTS13 are not necessary for the cleavage of the VWF73-based peptide substrate [62]) (Reversibility: ?) [62,92]
P ?
S GST-von Willebrand factor 73 + H_2O <3> (<3> contains residues Asp1596-Arg1668 from von Willebrand factor domain A2 [46]) (Reversibility: ?) [46]
P ?
S HRPH-A2-B <3> (<3> HRPH-A2-B is a derivative of von Willebrand factor 73, consisting of a HRP conjugate of a biotinylated von Willebrand factor 78 sequence [45]) (Reversibility: ?) [45]
P ? (<3> cleavage of Tyr842-Met843 within the A2 domain, i.e. Tyr1605-Met1606 in von Willebrand factor UniProt Id P04275 [45])
S VWF115 + H_2O <3> (<3> VWFA2 domain fragment, spanning von Willebrand factor residues 1554-1668, generation of 2 cleavage products of 10 kDa and 7 kDa [64]) (Reversibility: ?) [64]
P 10 kDa VWF115 fragment + 7 kDa VWF115 fragment
S VWF115 + H_2O <3> (<3> a von Willebrand factor-derived peptide substrate, comprising amino acid residues 1554-1668 of von Willebrand factor [63]) (Reversibility: ?) [63]
P ?
S VWF115 D1614A mutant + H_2O <3> (<3> Asp1614 VWFA2 domain fragment, spanning von Willebrand factor residues 1554-1668, generation of 2 cleavage products of 10 kDa and 7 kDa [64]) (Reversibility: ?) [64]
P 10 kDa VWF115 fragment + 7 kDa VWF115 fragment
S VWF73 peptide + H_2O <3> (<3> von Willebrand factor-derived peptide substrate [73]) (Reversibility: ?) [73]
P ?
S VWF73 region of von Willebrand factor + H_2O <3> (<3> with this minimal substrate urea is not required for cleavage, minimal substrate for ADAMTS-13 [5]) (Reversibility: ?) [5]
P ? <3> [5]
S VWFA2 peptide + H_2O <3> (<3> A2 domain fragment of von Willebrand factor, cleavage of oxidized or nonoxidized VWFA2 peptide by ADAMTS13, cleavage of the Tyr1605-Met(O)1606 peptide bond by ADAMTS13, overview [77]) (Reversibility: ?) [77]
P VWFA2 peptide fragments
S fluorescence resonance energy transfer substrate-von Willebrand factor 73 + H_2O <3> (Reversibility: ?) [39]
P ?
S fluorescent resonance energy transfer-von Willebrand factor 73 + H_2O <4> (Reversibility: ?) [25]
P ?
S large von Willebrand factor multimer + H_2O <3> (Reversibility: ?) [47]
P ?
S more | <3> (<3> ADAMTS13 binds to CD36, a transmembrane protein of endothelial cells and platelets, i.e. glycoprotein IV, not diminishing the

proteolytic activity of ADAMTS13, but providing an anchor for ADAMTS13 on the surface of endothelial cells and platelets [104]) (Reversibility: ?) [104]

P ?

S proteins + H_2O <3,9> (<3,9> enzyme is involved in thrombotic thrombocytopenic purpura [1,10]) (Reversibility: ?) [1,2,3,4,5,6,7,8,9,10,11,12,13]

P peptides <3,9> [1,2,3,4,5,6,7,8,9,10,11,12,13]

S ultra-large von Willebrand factor + H_2O <3> (Reversibility: ?) [41,42]

P ?

S ultra-large von Willebrand factor multimer + H_2O <3> (Reversibility: ?) [47]

P ?

S von Willebrand factor + H_2O <1,2,3,4,5,6,7,8> (<3> ADAMTS-13 cleavage of von Willebrand factor strings secreted from stimulated and unstimulated HUVECs occurs at the position 1605-6 of the von Willebrand factor A2 domain [69]; <3> ADAMTS-13 cleaves the Tyr1605-Met1606 bond in the VWF A2 domain, mechanisms of VWF recognition, cleavage analysis and kinetics under static and flow conditions, overview [66]; <3> ADAMTS-13 cleaves von Willebrand factor (VWF) exclusively at the Tyr1605-Met1606 peptide bond in the A2 domain [79]; <1,2,3,4,5,6,7,8> ADAMTS13 cleaves von Willebrand factor at the Tyr1605-Met1606 bond within the central A2 domain [89]; <3> ADAMTS-13 cleavage of HUVEC-secreted von Willebrand factor strings at Y1605-6M sites of the von Willebrand factor A2 domain [69]; <3> ADAMTS-13 cleaves the Tyr1605-Met1606 bond in the VWF A2 domain, mechanisms of VWF recognition. One ADAMTS13 binding site of VWF is located in the region of VWF spanning residues 1874 to 2813, which includes the VWF D4 domain, interacts with the C-terminal domains of ADAMTS13, interaction occurs even when VWF is in static conditions, globular and with the VWF A2 domain hidden. The binding site may participate as the initial step of a multistep interaction ultimately leading to proteolysis of VWF byADAMTS13 [66]; <8> ADAMTS13 cleaves von Willebrand factor at the Tyr1605-Met1606 bond within the central A2 domain. Activity with the recombinant human substrate in vitro, comparison to other mammal enzymes, overview [89]; <3> ADAMTS13 cleaves von Willebrand factor at the Tyr1605-Met1606 bond within the central A2 domain. Comparison of the activity with human recombinan substrate in vitro with enzymes from other mammal enzymes, overview [89]; <1> ADAMTS13 cleaves von Willebrand factor at the Tyr1605-Met1606 bond within the central A2 domain. The guinea pig ADAMTS13 shows no activity with the recombinant human substrate in vitro, comparison to other mammal enzymes, overview [89]; <6> ADAMTS13 cleaves von Willebrand factor at the Tyr1605-Met1606 bond within the central A2 domain. The rabbit ADAMTS13 shows activity similar to the human ADAMTS13 with the recombinant human substrate in vitro, comparison to other mammal enzymes, overview [89]; <4> ADAMTS13 cleaves von Willebrand factor at the Tyr1605-Met1606 bond within the central A2 domain. The rat ADAMTS13 shows

no activity with the recombinant human substrate in vitro, comparison to other mammal enzymes, overview [89]; <2> ADAMTS13 cleaves von Willebrand factor at the Tyr1605-Met1606 bond within the central A2 domain. The wild-type mouse ADAMTS13 shows no activity with the recombinant human substrate in vitro, comparison to other mammal enzymes, overview [89]; <5,7> ADAMTS13 cleaves von Willebrand factor at the Tyr1605-Met1606 bond within the central A2 domain. Very low activity with recombinant human substrate in vitro, comparison to other mammal enzymes, overview [89]; <3> binding of all the proximal noncatalytic domains of ADAMTS13 to von Willebrand factor is necessary to position the active site of ADAMTS13 to the scissile bond, Tyr1605-Met1606, on von Willebrand factor, resulting in productive cleavage. The metalloprotease domain of ADAMTS13 alone is ineffective in cleaving von Willebrand factor, linear relationship between the domains of ADAMTS13 and von Willebrand factor proteolysis. All the proximal noncatalytic domains of ADAMTS13 are required for productive engagement with von Willebrand factor-A2 domain at least under static/denaturing conditions [63]) (Reversibility: ?) [63,66,69,79,89]

P von Willebrand factor 140-kDa fragment + von Willebrand factor 176-kDa fragment (<3> LC-MS product identification [79])

S von Willebrand factor + H_2O <2,3> (<3> ADAMTS13 cleaves von Willebrand factor at the Tyr1605-Met1606 bond [73]; <2,3> ADAMTS13 cleaves von Willebrand factor to smaller less-active forms [67]; <3> ADAMTS13 specifically cleaves von Willebrand factor multimers at the site of the Tyr1605-Met1606 bond of the VWF-A2 domain [84]; <3> cleavage at the Tyr1605-Met1606 bond within the van Willebrand factor A2 domain [96]; <3> cleavage can also occur at the surface of endothelial cells. ADAMTS13 that is prebound to endothelial cells exhibits increased proteolysis of VWF as compared with ADAMTS13 present only in solution. Thus, cleavage of VWF occurs mainly at the endothelial cell surface [85]; <3> cleavage of ultra large von Willebrand multimers into smaller fragments [90]; <3> specific cleavage of the long strings of ultra-large von Willebrand factor multimers [104]; <3> ADAMTS13 cleaves von Willebrand factor at the Tyr1605-Met1606 bond. The ADAMTS13 spacer domain is required for cleavage of von Willebrand factor, role of the amino acid residues Arg659, Arg660, and Tyr661 of theADAMTS13 spacer domain in substrate recognition, sequence comparisons and kinetics, detailed overview [73]; <3> cleavage of the Tyr1605-Met(O)1606 peptide bond by ADAMTS13 [77]; <3> specific cleavage of the long strings of ultra-large von Willebrand factor multimers. The specificity of ADAMTS13 for proteolysis of von Willebrand factor is facilitated by multiple cooperative contacts that bind ADAMTS13 to von Willebrand factor [104]) (Reversibility: ?) [67,73,77,84,85,90,96,104]

P von Willebrand factor fragments

S von Willebrand factor + H_2O <3> (<3> cleavage of peptide bond Tyr842-Met843 [7]; <3> cleavage site is located in the A2 domain of the substrate, cleavage of peptide bond Tyr842-Met843 [1]; <3> large multimeric com-

plexes are reduced to smaller ones, cleavage of peptide bond Tyr842-Met843 [13]; <3> rapid physiological process that occurs on endothelial surfaces, reduced activity results in thrombotic thrombocytopenic pupura [13]) (Reversibility: ?) [1,7,13]

P 2 peptides <3> [1,7,13]

S von Willebrand factor + H_2O <3> (<3> cleavage of peptide bond Tyr842-Met843 [8]) (Reversibility: ?) [8]

P 2 peptides of 140 kD and 65 kD <3> [8]

S von Willebrand factor + H_2O <3> (<3> cleavage of the peptide bond Tyr842-Met843 within the A2 domain [4,6,12]; <3> specific cleavage of the peptide bond Tyr842-Met843 within the A2 domain, i.e. Tyr1605-Met1606 in von Willebrand factor UniProt Id P04275 [5]; <3> cleavage of the peptide bond Tyr842-Met843 within the A2 domain, enzyme deficiency causes lethal thrombotic thrombocytopenic purpura [4]; <3> either congenital or acquired defects of the enzyme lead to thrombotic thromcytopenic purpura, cleavage of the peptide bond bond Tyr842-Met843 within the A2 domain, i.e. Tyr1605-Met1606 in von Willebrand factor UniProt Id P04275 [5]; <3> large multimeric substrate, cleavage of the peptide bond Tyr842-Met843 within the A2 domain [12]; <3> protein from plasma of patients suffering type I von Willebrand disease is more susceptible to proteolysis by the enzyme due to amino acid polymorphism heterozygous at position Tyr/Cys1584, phenotypic parameters, cleavage of the peptide bond Tyr842-Met843 within the A2 domain [6]; <3> complete proteolysis is observed at 37°C in the presence of $BaCl_2$ while about 25% von Willebrand factor still binds to collagen when $BaCl_2$ supplementation is omitted. Proteolysis kinetics at 22°C and 4°C is slower but complete [17]) (Reversibility: ?) [4,5,6,12,17]

P 2 peptides of 140 kDa and 176 kDa <3> [4,5,6,12]

S von Willebrand factor + H_2O <3> (<3> large multimeric complexes are reduced to smaller ones, cleavage of peptide bond Tyr842-Met843 in the vWFdomain A2 [3,11]; <3> rapid physiological process that occurs on endothelial surfaces, activity is reduced by 87-100% in patients with thrombotic thrombocytopenic pupura [3]) (Reversibility: ?) [3,11]

P 2 peptides of 176 kD and 140 kD <3> [3,11]

S von Willebrand factor + H_2O <2,3,4,9> (<3> specific for [97]; <9> cleavage of peptide bond Tyr842-Met843, native and recombinant enzyme [2]; <3> cleavage of peptide bond Tyr842-Met843, large hemostatically active multimers are cleaved to smaller less active forms, increased proteolytic degradation in patients suffering from von Willebrand disease typ 2A [7]; <9> cleavage of peptide bond Tyr842-Met843, rapid degradation of multimers to smaller fragments, decreased activity results in bone marrow transplant-associated thrombotic microangiopathy and thrombotic thrombocytopenic pupura [2]; <3> decrease of the multimeric pattern of enzyme and decreased activity results in bone marrow transplant-associated thrombotid microangiopathy [9]; <3> enzyme deficiency causes lethal thrombotic thrombocytopenic purpura, cleavage of peptide bond Tyr1605-Met1606 resulting in limited platelet accumulation in microvas-

cular thrombi (Tyr842-Met843 within the A2 domain, i.e. Tyr1605-Met1606 in von Willebrand factor UniProt Id P04275) [11]; <3> the cleavage site is exposed to the enzyme by conformational changes due to shear stress in the plasma, decrease of the multimeric pattern of enzyme and decreased activity results in bone marrow transplant-associated thrombotic microangiopathy, cleavage of peptide bond Tyr842-Met843, large hemostatically active multimers are cleaved to smaller less active forms, increased proteolytic degradation in patients suffering von Willebrand disease typ 2A [1]; <3> cleavage of Tyr842-Met843 within the A2 domain, i.e. Tyr1605-Met1606 in von Willebrand factor UniProt Id P04275 [21,26]; <3> important role for Asp1614 and surrounding charged residues in the binding and cleavage of the von Willebrand factor A2 domain [21]; <3> VWF73, a region from D1596 to R1668 of von Willebrand factor, provides a minimal substrate for ADAMTS-13 [5]; <3> ADAMTS13 cleaves at the peptide bond Tyr842-Met843 within the A2 domain, i.e. Tyr1605-Met1606 in von Willebrand factor UniProt Id P04275 [41]; <3> ADAMTS13 cleaves the bond Tyr842-Met843 within the A2 domain, i.e. Tyr1605-Met1606 in von Willebrand factor UniProt Id P04275 [33]; <3> amino acid position C1584 is necessary for enhanced von Willebrand factor proteolysis by ADAMTS13 [38]; <9> ADAMTS13 efficiently cleaves only the Tyr842-Met843 bond within the central A2 domain of multimeric von Willebrand factor (i.e. Tyr1605-Met1606 in von Willebrand factor UniProt Id P04275) [50]; <9> ADAMTS13 efficiently cleaves only the Tyr842-Met843 bond within the central A2 domain of multimeric von Willebrand factor (i.e. Tyr1605-Met1606 in von Willebrand factor UniProt Id P04275). This specificity depends in part on binding of the noncatalytic ADAMTS13 spacer domain to the C-terminal α-helix of von Willebrand factor domain A2. By kinetic analysis of recombinant ADAMTS13 constructs, it is shown that the first thrombospondin-1, Cys-rich, and spacer domains of ADAMTS13 interact with segments of von Willebrand factor domain A2 between Gln1624 and Arg1668 (in von Willebrand factor UniProt Id P04275), and together these exosite interactions increase the rate of substrate cleavage by at least approximately 300fold. Specific recognition of von Willebrand factor depends on cooperative, modular contacts between several ADAMTS13 domains and discrete segments of von Willebrand factor domain A2. Specification of the cleavage site depends on sequences flanking the scissile bond between positions P9 (Arg1597) and P18 (Ile1623) [50]; <9> all alterations examined in the Y1605-M1606 cleavage site greatly reduce the cleavability of von Willebrand factor by ADAMTS13. Greatest cleavage resistance is observed in Y1605A/M1606A. Y1605H and M1606L show a loss of cleavability in the recombinant full-length von Willebrand factor assay, suggesting that an aromatic ring at 1605 is critical for ADAMTS13 recognition. The G1643S polymorphism shows increased cleavage, suggesting a type 2A von Willebrand factor phenotype, while D1472H, Q1571H and P1601T show slightly decreased ADAMTS13 cleavage. A-domain changes in von Willebrand factor alter ADAMTS13-mediated proteolysis [52]; <3> a catalysis-deficient

ADAMTS13 P475S mutant does not show VWF-induced changes in conformation [95]; <3> ADAMTS13 cleaves ultra-large von Willebrand factor multimers [105]; <3> cleavage of ultra-large multimers [80]; <3> force-induced von Willebrand factor A2 domain unfolding of the substrate facilitates cleavage, using single VWF A1A2A3 tridomain polypeptides, structural destabilization of A1A2A3 was induced by 5- to 80-pN forces [75]; <3> persistently elevated levels of von Willebrand factor in plasma during and after liver transplantation, while plasma levels of ADAMTS13 dropp during transplantation [56]; <2,3> specific cleavage of ultra-large von Willebrand factor multimers [60,62,83,99]; <2> von Willebrand factor is also susceptible to cleavage by ADAMTS13 when incorporated in a thrombus [76]; <3> cleaving of ultra-large multimers between residues Tyr842 and Met843 in the central A2 domain, the TSP-1 domain of ADAMTS13 is required for interaction with the extracellular matrix and the substrate, as well as the CUB domains, that are also essential for intracellular trafficking [78]; <3> i.e. VWF, a large glycoprotein secreted by vascular endothelial cells as multimers [95]; <3> identification of ADAMTS13 peptide sequences binding to von Willebrand factor, overview [58]; <3> recombinant substrate stably expressed in HEK293 cells, the ADAMTS13 metalloprotease domain cleaves the von Willebrand factor A2 domain at the Y1605-M1606 scissile bond [71]; <3> substrate is FRET-VWF73 [94]; <2> substrate of human origin [61]; <3> the S119-W262 H-bond in the ADAMTS13 metalloprotease domain is crucial for maximal turnover [68]; <3> wild-type plasma-derived substrate of human origin, and substrate modified by α2-3,6,8,9-neuraminidase from Arthrobacter ureafaciens removing α2-3- and α_2-6-linked sialic acid, and treatment with PNGase F to remove complex N-linked glycan structures. α2-6-linked sialic acid increases von Willebrand factor proteolysis by ADAMTS13 through a conformational mechanism, overview [74]) (Reversibility: ?) [1,2,5,7,9,10,11,20,21,22,25,26,31,32,33,34,35,37,38,39,40,41,42,43,44,45,46,47,48,49,50,52,55,56,57,58,59,60,61,62,64,65,68,70,71,72,74,75,76,78,80,83,86,91,92,93,94,95,97,99,100,101,103,105]

P ? <3,9> [1,2,7,9,10,11]

S von Willebrand factor 115 (1554-1668) + H_2O <3> (<3> A2 domain fragment [21]) (Reversibility: ?) [21]

P ?

S von Willebrand factor 115-A3 (1554-1874) + H_2O <3> (<3> A2 domain fragment [21]) (Reversibility: ?) [21]

P ?

S von Willebrand factor 73 + H_2O <3> (Reversibility: ?) [36]

P 7722 Da peptide + ?

S von Willebrand factor 73 + H_2O <3> (<3> minimal substrate cleavable by ADAMTS-13 [45]) (Reversibility: ?) [45]

P ?

S von Willebrand factor 76 (1593-1668) + H_2O <3> (<3> A2 domain fragment [21]) (Reversibility: ?) [21]

P ?

S Additional information <1,2,3,4,5,6,7,8,9,10> (<3> no activity with human fibrinogen, bovine serum albumin, and calf skin collagen [7]; <3> pro-von Willebrand factor is cleaved by pro-ADAMTS13 and by ADAMTS13 [12]; <3> does not cleave GST-von Willebrand factor 64 which lacks 9 aa residues (E1660APDLVLQR1668) [46]; <3> PNGase-treated von Willebrand factor is more succeptible to proteolysis by ADAMTS13 and binds with increased affinity [33]; <10> important role for ADAMTS13 in preventing excessive spontaneous Weibel-Palade body secretion, and in the regulation of leukocyte adhesion and extravasation during inflammation [53]; <3> ADAMTS13 contains eight thrombospondin type 1 repeats and binds to CD36, a transmembrane protein present on endothelial cells and platelets. CD36 also binds to thrombospondin-2 via three thrombospondin type 1 repeats in a manner competitive to ADAMTS13, overview [105]; <3> MDTCS domain modelling and substrate recognition mode analysis, overview [97]; <3> proteolysis can occur only once VWF has been unraveled from its globular conformation, either by high fluid shear stress in vivo or in the presence of denaturants in vitro, conditions that are able to promote the exposure of the VWF scissile bond [66]; <3> removal of newly released ultralarge-von Willebrand factor strings or bundles anchored on endothelial cells by ADAMTS13 occurs rapidly and efficiently in the presence and in the absence of fluid shear stress, suggesting that the cell-bound ultra large-von Willebrand factor polymers may be preferred substrates for ADAMTS13 [73]; <9> thrombospondin1 and ADAMTS13 form complexes together in cells and in direct protein binding assays [93]; <3> ADAMTS 13 activity measurement using a collagen binding assay [90]; <2> assay on the fluorogenic substrate FRETS-vWF73 [61]; <3> binding specificities of wild-type ADAMTS13 and ADAMTS13-RYY to von Willebrand factor115, von Willebrand factor106, and full-length von Willebrand factor, overview [71]; <3> construction of substrate peptides VWF Asp1596-Ala1669, i.e. VWF74, VWF Asp1596-Ala1669 containing nitrotyrosine, i.e. VWF74-NT, or methionine sulfoxide, i.e. VWF74-MetSO, at position 1605 or 1606, respectively. VWF74 oxidized by peroxynitrite undergoes a severe impairment of its hydrolysis. Likewise, VWF74-MetSO is minimally hydrolyzed, whereas VWF74-NT is hydrolyzed only slightly more efficiently than VWF74, overview [79]; <1,3,4,5,6,7,8> differences in susceptibility to cleavage of recombinant von Willebrand factor by different species need to be considered when interpreting the physiology of human recombinant von Willebrand factor from results of tests in animal models [89]; <3> molecular modeling of ADAMTS13 metalloprotease domain using its sequence homology to adamalysin II and the crystal structure [60]; <2> no activity in von Willebrand factor-deficient or ADAMTS13-deficient mice with the recombinant substrate of human origin. Differences in susceptibility to cleavage of recombinant von Willebrand factor by different species need to be considered when interpreting the physiology of human recombinant von Willebrand factor from results of tests in animal models [89]; <3> proteolysis can occur only once VWF has been unraveled from its globu-

lar conformation, either by high fluid shear stress in vivo or in the presence of denaturants in vitro, conditions that are able to promote the exposure of the VWF scissile bond. The ADAMTS13 C-terminal distal domains (TSP5-CUB) bind to a novel binding site in the C-terminal region of VWF, spanning residues 1874-2813 and including the VWF D4 domain, which, critically, is constitutively exposed on the surface of VWF in solution without flow. C-terminal VWF fragments, as well as an antibody specifically directed toward the VWF D4 domain, inhibit VWF proteolysis by ADAMTS13 under shear conditions [66]; <3> role for ADAMTS13 disintegrin-like domains in substrate recognition and proteolysis, homology modeling, overview. Residues Arg349, Leu350, and Val352 are predicted to form a cluster on the surface of the ADAMTS13 disintegrin-like domain immediately adjacent to the active-site cleft [64]; <3> structure-function analysis, overview [58]; <3> the positively charged Arg349 on ADAMTS13 appears to directly interact with the negatively charged Asp1614 on the von Willebrand factor-A2 domain. This seemingly weak interaction between the disintegrin and VWF-A2 appears to be essential for efficient catalysis of von Willebrand factor under static/denaturing conditions. Molecular modeling of the involvement of the disintegrin domain of ADAMTS13 in von Willebrand factor processing, overview [63]) (Reversibility: ?) [7,12,33,46,53,58,60,61,63,64,66,71,73,79,89,90,93,97,105]

P ? <3> [7,12]

Inhibitors

1,10-phenanthroline <3> (<3> activity can be restored by Ca^{2+} [1]) [1]

Cl^- <3> (<3> Chloride ions inhibit von Willebrand factor hydrolysis by ADAMTS-13 of the A1-A2-A3 and A1-A2 domains in the presence of either urea or high shear stress, whereas this effect is either absent or negligible when using A2 and A2-A3 domains [40]) [40]

$CoCl_2$ <3> (<3> an increasing concentration of $CoCl_2$ inhibits ADAMTS13 activity [22]) [22]

EDTA <2,3,4> (<3> complete inhibition [7]; <3,4> complete inhibition at 10 mM [25,79]; <3> activity can be restored by Ca^{2+}, complete inhibition [1]; <3> no activity in the presence of EDTA [42]; <3> potent inhibitor of the metalloprotease ADAMTS13 [80]) [1,7,9,24,25,42,60,79,80]

EGTA <3> (<3> complete inhibition [7]; <3> activity can be restored by Ca^{2+}, complete inhibition [1]) [1,7]

HOCl <3> (<3> HOCl can oxidize methionine to methionine sulfoxide and tyrosine to chlorotyrosine, oxidation of VWF A2 peptide, at Met1606 and Tyr1605, markedly impairs ADAMTS13 cleavage. Oxidative modification by myeloperoxidase/H_2O_2 is similar to that produced by HOCl [77]) [77]

$MnSO_4$ <3> (<3> an increasing concentration of $MnSO_4$ inhibits ADAMTS13 activity [22]) [22]

N-ethylmaleimide <3> (<3> slow and weak inhibition [7]) [7]

$NiSO_4$ <3> (<3> an increasing concentration of $NiSO_4$ inhibits ADAMTS13 activity [22]) [22]

Pro-1645-Lys-1668 fragment of von Willebrand factor 73 <3> [45]

Trypsin <3> (<3> inhibits ADAMTS13 activity through inhibition of enzyme binding to endothelial cell surfaces, overview [85]) [85]
VWFA2 domain <3> (<3> a C-terminal 32 kDa fragment of VWF, soluble VWFA2 domain effectively inhibits the binding of ADAMTS13 to immobilized VWFA2, and completely inhibits the interaction between ADAMTS13 and immobilized 64 kDa VWFA1A2A3 fragment [66]) [66]
W688X6-1 <3> (<3> the monoclonal antibody W688X6-1 shows dose-dependent inhibitory activity toward ADAMTS13-mediated hydrolysis [39]) [39]
WH2-22-1A <3> (<3> the monoclonal antibody WH2-22-1A shows dose-dependent inhibitory activity toward ADAMTS13-mediated hydrolysis [39]) [39]
Z-Phe-Phe-CHN_2 <3> (<3> best peptidyl diazomethyl ketone inhibitor [7]) [7]
Zn^{2+} <3> (<3> ADAMTS13 activity is undetectable at concentrations of zinc ions above 3 mM Zn^{2+} [22]) [22]
citrate <3> (<3> weak [7]) [7]
heparin <3> (<3> inhibits ADAMTS13 activity through inhibition of enzyme binding to endothelial cell surfaces, overview [85]) [85]
peroxynitrite <3> (<3> formation of methionine sulfoxide by peroxynitrite at position 1606 of von Willebrand factor inhibits its cleavage by ADAMTS-13 a prothrombotic mechanism in diseases associated with oxidative stress, overview. Oxidation by peroxynitrite of purified VWF multimers inhibits ADAMTS-13 hydrolysis, but does not alter their electrophoretic pattern nor their ability to induce platelet agglutination by ristocetin. In vitro treatment of ADAMTS-13 with peroxynitrite over a concentration ranging from 0.050 to 0.250 mM causes a complete inhibition of the protease activity of the enzyme [79]) [79]
plasma from patients with thrombotic thrombocytopenic purpurea <2> [24]
Additional information <2,3,4,9> (<9> enzyme is inhibited by plasma from an individuum with acquired thrombotic thrombocytopenic pupura [2]; <3> inhibition by autoantibodies from patients with acquired thrombotic thrombocytopenic purpura [5]; <3> inhibition of the enzyme by IgG from a patient with idiopathic thrombotic thrombocytopenic pupura [11]; <3> inhibitory autoantibodies from plasma of 3 patients with acquired thrombotic thrombocytopenic purpura, epitope mapping [4]; <3> no inhibition by iodoacetamide, leupeptin, and serine protease inhibitors DFP, PMSF, aprotinin [1]; <3> no inhibition by iodoacetamide, leupeptin, and serine protease inhibitorsDFP, PMSF, aprotinin [7]; <4> CCl4 at concentration of 6.5 mM does not directly inhibit the activity of ADAMTS-13 [25]; <3> increasing concentrations of $BaCl_2$ (up to 5 mM) have little effect on the activity of ADAMTS13 at pH 7.4, $Mg(SO_4)$ and $Cu(SO_4)$ have little effect on the activity of ADAMTS13 at pH 7.4 [22]; <3> proteolysis of ADAMTS-13 by thrombin leads to a 8fold reduction in affinity for von Willebrand factor [44]; <2> ADAMTS-13 activity is evaluated in a model of sepsis induced by cecum ligature and puncture in wild-type and Vwf-/- mice. In wild-type mice, cecum ligature and puncture-induced sepsis elicits a significant ADAMTS-13 decrease, and a strong negative correlation exists between von Willebrand factor, VWF, and ADAMTS-13. In Vwf-/- mice, cecum ligature and puncture also induces severe sepsis, but ADAMTS-13 is not significantly diminished [91]; <3> an en-

dogenous ADAMTS13 inhibitor can cause enzyme deficiency [86]; <3> autoantibodies against ADAMTS13 lead to ADAMTS13 deficiency, which causes e.g. thrombotic thrombocytopenic purpurea, overview [78]; <3> C-terminal VWF fragments, as well as an antibody specifically directed toward the VWF D4 domain, inhibit VWF proteolysis by ADAMTS13 under shear conditions [66]; <3> construction and screening of an epitope peptide library, e.g. of epitope-A, i.e. a C-terminus of spacer domain from Arg670 to Gln684, and epitope-B, i.e. Pro618 to Glu641 in the middle of spacer domain. Synthetic epitope-B peptide inhibits the cleavage of VWF by ADAMTS13, while the synthetic epitope-A peptide does inhibit not as efficiently as epitope-B. Elimination of four amino acids from either sides of epitope-B terminus markedly reduces the inhibitory effect [58]; <3> infection with Plasmodium falciparum inhibits ADAMTS13. ADAMTS13 activity in normal plasma is reduced by approximately 60% after pooled normal plasma is incubated in a 3:1 mix with malarial plasma for 30 min [96]; <3> influenza A infection is sufficient to trigger thrombotic thrombocytopenic purpura by producing the anti-ADAMTS13 IgG inhibitor, overview [84]; <3> inhibitory anti-ADAMTS 13 antibodies, measurement and clinical application, overview [59]; <3> malaria patients possess high ADAMTS13 autoantibodies levels as well as endogenous ADAMTS13 inhibitors compared to healthy controls [57]; <3> specific blockade of von Willebrand factor string cleavage by antibody to ADAMTS-13, overview [69]; <3> substrate modified by treatment with PNGase F to remove complex N-linked glycan structures results in increased ADAMTS13 activity [74]) [1,2,4,5,7,11,22,25,44,57,58,59,66,69,74,78,84,86,91,96]

Activating compounds

urea <3> (<3> required [5]; <3> activates at 1 M [12]; <3> activation, substrate is degraded at 1 M [7,8]) [5,7,8,12]

ristocetin <3> (<3> activates [6]) [6]

rituximab <3> (<3> a monoclonal anti-CD 20 antibody, Rituximab leads to a prompt reduction in IgG antibody levels, followed by an increase in ADAMTS 13 activity increases. However, in patients receiving Rituximab electively, normalisation of ADAMTS 13 enzyme activity may be delayed for up to 3 months [59]) [59]

Additional information <3,4> (<3> low salt concentrations activate the proteolytic activity [7]; <4> CCl4 at concentration of 6.5 mM does not directly enhance the activity of ADAMTS-13 [25]; <3> cleavage of von Willebrand factor A2 requires the force-induced A2 unfolding [75]; <3> inhibition of ADAMTS13 by auto-antibodies is reversed by rituximab, overview [98]; <3> mild denaturation of fluid shear stress increase the hydrolysis of von Willebrand factor [78]; <3> substrate modified by α2-3,6,8,9-neuraminidase from Arthrobacter ureafaciens removing α2-3- and α2-6-linked sialic acid results in reduced ADAMTS13 activity [74]) [7,25,74,75,78,98]

Metals, ions

Ba^{2+} <1,2,3,4,5,6,7,8,9> (<1,2,3,4,5,6,7,8> activates [3,60,61,77,89]; <9> activates, metalloprotease [2]; <3> best activating metal ion [1,7]; <3> complete proteolysis is observed at 37°C in the presence of $BaCl_2$ while about 25% von

Willebrand factor still binds to collagen when $BaCl_2$ supplementation is omitted [17]; <3> barium ions stimulate ADAMTS13 activity in citrated plasma but not in citrate-free plasma, cleavage of von Willebrand factor by recombinant ADAMTS13 is activated up to 200fold by barium ions [22]) [1,2,3,7,17,22,47,60,61,77,89]
Ca^{2+} <2,3,9> (<3> required [64,65,66,69,71,73,78,97]; <2> activates [61]; <3> dependent on [8]; <3> dependent [42]; <3> activating [7]; <3> Ca^{2+} binding site with coordinates Asp173, Cys281, Asp284, and Met249, activating [1]; <9> metalloprotease, conserved binding site using Glu83, Asp173, Cys281, Asp284 [10]; <3> cooperative role for Ca^{2+} and Zn^{2+} in supporting ADAMTS13 activity [22]; <3> ADAMTS13 has a predicted calcium-binding site [37]; <3> in citrate-anticoagulated plasma activity is enhanced about 3fold by calcium ions (up to 5 mM), cleavage of von Willebrand factor by recombinant ADAMTS13 is activated up to 200fold by calcium ions [22]; <3> highly dependent on, Ca^{2+} induces a conformational change in ADAMTS13, but only under low-ionic-strength conditions, which is abolished in mutants E83A and D173A. The Ca^{2+}-binding site in proximity to the ADAMTS13 active site comprises Glu184, Asp187, and Glu212, identified by homology modelling. Mutagenesis of these residues within this site to alanine dramatically attenuates the K_{Dapp} for Ca^{2+} of ADAMTS13, and for D187A and E212A also reduces the V_{max} to approximately 25% of wild-type. The major influence of Ca^{2+} on ADAMTS13 function is mediated through binding to a high affinity site adjacent to its active site cleft. The short sequence spanning residues 162 to 168 of the metalloprotease domain is not a Ca^{2+} binding site [60]) [1,7,8,10,22,37,42,60,61,64,65,66,69,71,73,78,97]
Cu^{2+} <3> (<3> activates [60]) [60]
Mg^{2+} <3> (<3> activates [60]; <3> slightly activating [1,7]) [1,7,60]
Mn^{2+} <3> (<3> activates [60]) [60]
Ni^{2+} <3> (<3> activates [60]) [60]
Sr^{2+} <3> (<3> activating [1,7]) [1,7]
Urea <3> (<3> activates [3]) [3]
Zn^{2+} <3,9> (<3> required [69,77,78,79,80]; <3> dependent on [60]; <3> metalloprotease [68]; <3> zinc metalloprotease [95]; <3> dependent [42]; <9> metalloprotease, conserved binding site [10]; <3> cooperative role for Ca^{2+} and Zn^{2+} in supporting ADAMTS13 activity [22]; <3> ADAMTS13 has a putative zinc catalytic site [37]; <3> in citrate-anticoagulated plasma activity is enhanced about 2fold by zinc ions (1 mM), cleavage of von Willebrand factor by recombinant ADAMTS13 is activated up to 200fold by zinc ions [22]; <3> metalloprotease ADAMTS-13 [59]; <3> required, metalloprotease [64]; <3> required, three active sites His and catalytic residues Glu coordinate a catalytic Zn^{2+} ion [63]) [10,22,37,42,59,60,63,64,68,69,77,78,79,80,95]
guanidine <3> (<3> activates [3]) [3]
Additional information <3> (<3> divalent metal ion-dependent [11]; <3> enzyme is a member of the ADAMTS metalloprotease family, disintegrin and metalloproteinase with thrombospondin type I motif [8]; <3> metalloprotease, contains an essential Zn^{2+} binding site, no activtion by Zn^{2+} and Mn^{2+} [1]; <3> no activtion by Zn^{2+}, Cu^{2+}, Cd^{2+}, Ni^{2+}, Co^{2+}, Mn^{2+} [7]; <3>

Ca^{2+} is the most potent activating divalent cation out of Ca^{2+}, Ba^{2+}, Mg^{2+}, Mn^{2+}, Ni^{2+}, and Cu^{2+} [60]) [1,7,8,11,60]

Turnover number (s^{-1})

0.0019 <3> (VWF115, <3> pH 7.8, 37°C, recombinant wild-type enzyme [64]) [64]
0.0062 <3> (VWF115, <3> pH 7.8, 37°C, recombinant mutant R349A [64]) [64]
0.008 <3> (VWF115 D1614A mutant, <3> pH 7.8, 37°C, recombinant wild-type enzyme [64]) [64]
0.00875 <3> (VWF115 D1614A mutant, <3> pH 7.8, 37°C, recombinant mutant R349A [64]) [64]
0.14 <3> (von Willebrand factor 115, <3> recombinant enzyme, at 37°C [21]) [21]
0.31 <3> (FRET-VWF115 peptide, <3> pH 7.8, 37°C, recombinant mutant D187A [60]) [60]
0.67 <3> (HRPH-A2-B) [45]
0.72 <3> (DREQAPNLVYMVTGNPASDEIKRLPGDIQVVPIGVGPNANVQELERIGWPNAPILIQDFETLPREAPDLVLQRA, <3> pH 7.5, 25°C, recombinant enzyme [79]) [79]
0.76 <3> (VWF73 peptide, <3> pH 6.0, 37°C, recombinant Y661A mutant ADAMTS13 [73]) [73]
1.09 <3> (VWF73 peptide, <3> pH 6.0, 37°C, recombinant R660A mutant ADAMTS13 [73]) [73]
1.31 <3> (FRET-VWF115 peptide, <3> pH 7.8, 37°C, recombinant wild-type enzyme [60]) [60]
1.32 <3> (VWF73 peptide, <3> pH 6.0, 37°C, recombinant wild-type ADAMTS13 [73]) [73]
1.43 <3> (VWF73 peptide, <3> pH 6.0, 37°C, recombinant R659A mutant ADAMTS13 [73]) [73]
1.55 <3> (VWF73 peptide, <3> pH 6.0, 37°C, recombinant E663A mutant ADAMTS13 [73]) [73]
1.56 <3> (VWF73 peptide, <3> pH 6.0, 37°C, recombinant ADAMTS13 6-amino-acid-deletion mutant [73]) [73]
1.63 <3> (VWF73 peptide, <3> pH 6.0, 37°C, recombinant E664A mutant ADAMTS13 [73]) [73]
2.05 <3> (VWF73 peptide, <3> pH 6.0, 37°C, recombinant G662A mutant ADAMTS13 [73]) [73]
4.43 <3> (FRETSVWF73 peptide, <3> pH 7.5, 37°C, recombinant ADAMTS13 [65]) [65]
Additional information <3> (<3> k_{cat}: 0.83 per min for FRETS-VWF73, a fluorescent synthetic peptide, corresponding to residues Asp1596-Arg1668 of von Willebrand factor domain A2 and containing the Tyr1605-Met1606 bond cleaved by ADAMTS13 [22]) [22]

Specific activity (U/mg)

Additional information <2,3> (<2> determination of ADAMTS13 antigen and proteolytic activity in murine plasma, overview [61]; <3> intracellular

and secreted forms of ADAMTS13 show comparable proteolytic activity [95]; <3> more ADAMTS-13-mediated cleavage of the relatively few von Willebrand factor strings secreted at a slow rate from unstimulated HUVECs, and less ADAMTS-13 cleavage of the many von Willebrand factor strings secreted rapidly in response to cell stimulation [69]) [61,69,95]

K_m-Value (mM)

0.00025 <3> (HRPH-A2-B) [45]
0.00129 <3> (FRET-VWF115 peptide, <3> pH 7.8, 37°C, recombinant wild-type enzyme [60]) [60]
0.00161 <3> (von Willebrand factor 115, <3> recombinant enzyme, at 37°C [21]) [21]
0.0017 <3> (VWF73 peptide, <3> pH 6.0, 37°C, recombinant Y661A mutant ADAMTS13 [73]) [73]
0.0018 <3> (VWF73 peptide, <3> pH 6.0, 37°C, recombinant wild-type ADAMTS13 [73]) [73]
0.0032 <3> (FRETS-von Willebrand factor 73, <3> apparent value, pH 7.4 [22]) [22]
0.0034 <3> (VWF73 peptide, <3> pH 6.0, 37°C, recombinant E664A mutant ADAMTS13 [73]) [73]
0.0035 <3> (VWF73 peptide, <3> pH 6.0, 37°C, recombinant E663A mutant ADAMTS13 [73]) [73]
0.00432 <3> (FRET-VWF115 peptide, <3> pH 7.8, 37°C, recombinant mutant D187A [60]) [60]
0.0049 <3> (VWF73 peptide, <3> pH 6.0, 37°C, recombinant G662A mutant ADAMTS13 [73]) [73]
0.005 <3> (VWF73 peptide, <3> pH 6.0, 37°C, recombinant R660A mutant ADAMTS13 [73]) [73]
0.0058 <3> (FRETSVWF73 peptide, <3> pH 7.5, 37°C, recombinant ADAMTS13 [65]) [65]
0.00662 <3> (DREQAPNLVYMVTGNPASDEIKRLPGDIQVVPIGVGPNANV QELERIGWPNAPILIQDFETLPREAPDLVLQRA, <3> pH 7.5, 25°C, recombinant enzyme [79]) [79]
0.01 <3> (VWF73 peptide, <3> pH 6.0, 37°C, recombinant R659A mutant ADAMTS13 [73]) [73]
0.022 <3> (VWF73 peptide, <3> pH 6.0, 37°C, recombinant ADAMTS13 6-amino-acid-deletion mutant [73]) [73]
0.09 <3> (VWF115, <3> pH 7.8, 37°C, recombinant mutant R349A [64]) [64]
0.37 <3> (VWF115 D1614A mutant, <3> pH 7.8, 37°C, recombinant wild-type enzyme [64]) [64]
0.47 <3> (VWF115 D1614A mutant, <3> pH 7.8, 37°C, recombinant mutant R349A [64]) [64]
0.59 <3> (VWF115, <3> pH 7.8, 37°C, recombinant wild-type enzyme [64]) [64]
Additional information <3> (<3> K_m: 0.0032 mM for FRETS-VWF73, a fluorescent synthetic peptide, corresponding to residues Asp1596-Arg1668 of von Willebrand factor domain A_2 and containing the Tyr1605-Met1606 bond

cleaved by ADAMTS13 [22]; <3> Ca^{2+} binding kinetics of wild-type and mutant enzymes, overview [60]; <3> kinetic analysis of ADAMTS13 disintegrin-like domain mutants [64]; <3> kinetics of ADAMTS13 disintegrin domain mutants with substrate VWF115, overview [63]; <3> Michaelis-Menten ADAMTS-13/A1A2A3 binding kinetics, overview [75]; <3> Michaelis-Menten steady-state kinetics, overview [79]) [22,60,63,64,75,79]

K_i-Value (mM)

0.000028 <3> (VWFA2 domain, <3> pH 7.8, 37°C [66]) [66]
0.012 <3> (Pro-1645-Lys-1668 fragment of von Willebrand factor 73) [45]
Additional information <3> (<3> C-terminal fragments competitive inhibition binding, kinetics, overview [66]) [66]

pH-Optimum

6 <3> (<3> peptide substrates [73]) [73]
7.4 <3> (<3> assay at [69,74,77,97]) [69,74,77,97]
7.5 <3> (<3> assay at [65,79,85]) [65,79,85]
7.5-8 <2,3> (<2> assay at [61]; <3> multimeric substrate [73]) [61,73]
7.8 <3> (<3> assay at [60,64,66,71]) [60,64,66,71]
8 <1,2,3,4,5,6,7,8,9> (<1,2,3,4,5,6,7,8,9> assay at [2,4,6,12,89]; <3> assay at [8]; <3> in presence of Ba^{2+} [7]) [2,4,6,7,8,12,89]
8-9 <3> [3]
8.15 <3> (<3> assay at [75]) [75]
9-10 <3> (<3> in presence of Ca^{2+} [7]) [7]
Additional information <3> (<3> no activity at neutral pH at low salt concentration [7]) [7]

Temperature optimum (°C)

22 <3> (<3> room temperature, assay at [12]) [12]
25 <3> (<3> assay at [79]) [79]
37 <1,2,3,4,5,6,7,8,9> (<1,2,3,4,5,6,7,8,9> assay at [2,4,6,7,8,60,61,64,65,66,69,71,73,74,77,85,89,96]) [2,4,6,7,8,60,61,64,65,66,69,71,73,74,77,85,89,96]

4 Enzyme Structure

Molecular weight

150000 <3> (<3> full-length form, SDS-PAGE [39]) [39]
150000-190000 <3> (<3> gel filtration [8]) [8]
170000 <3> (<3> SDS-PAGE [42]; <3> about 170000 Da, full-length enzyme, SDS-PAGE [40]) [40,42]
195000 <4> (<4> SDS-PAGE [25]) [25]
300000 <3> (<3> gel filtration [7]) [7]

Subunits

? <3,9> (<3> x * 200000-230000, SDS-PAGE [13]; <3> x * 150000, SDS-PAGE, x * 190000, non-reducing PAGE [94]; <3> x * 190000, recombinant wild-type enzyme, SDS-PAGE [64]; <9> x * 45000, recombinant His-tagged ADAMTS13 ancillary domains, ADAMTS13-DTCS, SDS-PAGE [55]) [13,55,64,94]

monomer <3> (<3> 1 * 150000, SDS-PAGE [8]; <3> 1 x 300000, nonreducing SDS-PAGE [7]; <3> ADAMTS13 is a multidomain glycoprotein. It consists of numerous domains including a metalloprotease domain, a disintegrin domain, first thrombospondin type 1 repeat, i.e. TSP1, a cysteine-rich domain, and a spacer domain, schematic domain structure model of ADAMTS13, overview [63]) [7,8,63]
Additional information <3,9> (<3> structure [1]; <9> ADAMTS13 is a multidomain enzyme. In addition to the N-terminal metalloproteinase domain, the ancillary domains, including a disintegrin-like domain, a thrombospondin-1 type 1 repeat, a Cys-rich domain and a spacer domain, are required for von Willebrand factor recognition and cleavage [55]; <3> ADAMTS13 is a multidomain protein [95]; <3> ADAMTS13 protease consists of a signal peptide, a short propeptide, the metalloprotease domain, a disintegrin-like domain, a thrombospondin-1 repeat, a Cys-rich domain, a spacer domain, seven additional thrombospondin-1 repeats, and two CUB domains [94]; <3> ADAMTS13-DTCS, residues 287-685, an exosite-containing ADAMTS13 fragment, structures reveal folding similarities between the disintegrin-like domain and the N-terminal portion of the cysteine-rich domain. The spacer domain forms a globular functional unit with a 10-stranded-sandwich fold that has multiple interaction sites with the cysteine-rich domain. The MDTCS domains are conserved among ADAMTS family proteins [97]; <3> epitope mapping of anti-ADAMTS13 immunoglobulin G from patients with thrombotic thrombocytopenic purpura and sequence alignment of the ADAMTS13 spacer domains of human, mouse, and zebrafish [73]; <3> the metalloprotease domain is required for activity but not sufficient, the spacer domain is indispensable for activity, and the Cys-rich domain is also involved in activity. Also an intracellular disulfide bond is essential for catalytic activity. ADAMTS13 multidomain structure, overview [78]; <3> the multidomain ADAMTS13 contains the metalloprotease, the disintegrin, the TSP1-1, the cysteine-rich, the spacer, the TSP1-2, TSP1-3, TSP1-5, TSP1-6, TSP1-7, TSP1-8, CUB-1, and CUB-2 domains [82]) [1,55,73,78,82,94,95,97]

Posttranslational modification

glycoprotein <3,9> (<3> N-glycosylation [13]; <9> binding site for α-mannosyl residue, 10 potential N-glycosylation sites, Asn-Xaa-Thr/Ser [10]; <3> enzym contains 10 potential N-glycosylation sites [12]; <9> N-glycosylation is necessary for efficient secretion of ADAMTS13, while conversion of the N-glycans from oligomannose to complex type in the Golgi complex enhances the proteolytic activity of the protease toward von Willebrand factor multimers. After its secretion, ADAMTS13 does not require N-glycans for its von Willebrand factor cleaving activity [51]; <3> ADAMTS13 is a multidomain glycoprotein [63]; <9> the ADAMTS13 ancillary domains, ADAMTS13-DTCS, contain four potential N-glycosylation sites [55]) [10,12,13,51,55,63]
proteolytic modification <3,9> (<9> made as a zymogen, requires proteolytic activation, possibly intracellularly by furin, cleavage of residues 1-74 [10]; <3> propeptide is very short and poorly conserved, dispensable for protein folding, is cleaved off by furin after export from the endoplasmic reticulum,

the pro-enzyme form is fully active [12]; <3> the pro-peptide is removed during self-activation, which is not required for full enzyme activity [78]) [10,12,78]

5 Isolation/Preparation/Mutation/Application

Source/tissue

A-498 cell <3> (<3> a renal carcinoma cell line [94]) [94]
HUAEC cell <3> [42]
HUVEC cell <3> [42]
adrenal gland <3> [37]
astrocyte <9> (<9> in cerebral corpora amylacea, that occur in aging brains and in patients with neurodegenerative conditions [93]) [93]
blood <3> (<3> cord blood. Neonates and children have a percentage ADANTS-13 activity similar to adults. 28/38 newborns have percentage activity within the normal range of healthy adults, 10 have significantly lower percentage activity that normalizes by day 2-3 [23]) [8,23,38,75]
blood plasma <2,3,9> (<3> platelet-poor [17]; <3> ADAMTS-13 activity in type 1, 2A, and 2B von Willebrand disease is higher than in healthy controls, but lower than in type 3 von Willebrand disease [30]; <3> ADAMTS13 activity decreases in a time-dependent manner during systemic inflammation [28]; <3> no severe ADAMTS13 deficiency is detected in patients with sickle cell disease [15]; <3> of normal non-pregnant woman, pregnant and post-delivery women. Between the non-pregant state and the 6-11 week period of pregnancy, there is no statistical difference in the levels of ADAMTS13 activity. Starting from the 12-16 week, group differences become significant. the late postpartum shows the highest level of protease activity, including in the non-pregant state. In non-pregnant women, protease activity is significantly lower in nulliparous compared to parous women. In pregant and psot-delivery women, mean ADAMTS13 actrivity is slightly lower in primigravidae than in multigravidae [27]; <3> von Willebrand factor-cleaving protease activity remains at the intermediate level in thrombotic thrombocytopenic purpura [14]; <9> levels of ADAMTS13 are lower and levels of von Willebrand Factor are higher in young patients with cardiovascular disease compared to healthy individuals [54]) [5,14,15,17,22,27,28,29,30,31,32,33,34,35,36,37,39,40,41,43,44,45,48,49,54]
blood platelet <3,9> (<3> ADAMTS13 associates to the platelet surface via binding of membrane-integrated CD36 [105]; <9> synthesizes and secreted ADAMTS13 [93]) [37,93,105]
brain <2,3,9> (<9> enzyme expression [2]) [2,37,72,93]
cerebral artery <2> [72]
corpus amylaceum <9> (<9> in astrocytes of aging brains and patients with neurodegenerative conditions. Corporae amylaceae include glycosylated material, ubiquitin, and an assortment of proteins derived from neuronal cytoplasm. Many of these proteins are not specifically localized to neurons or astrocytes, some components of corpora amylacea, such as complement proteins, are most abundantly expressed outside the central nervous system.

Corporae amylaceae can result from a conglomeration of interacting proteins from degenerating neurons and from extravasated blood elements released after transient breakdown of the blood-brain barrier [93]) [93]
endothelial cell <3> (<3> ADAMTS13 associates to the cell surface via binding of membrane-integrated CD36 [105]; <3> at the surface of endothelial cells [85]; <3> obtained from collagenase-digested human umbilical veins, ADAMTS-13 is released directly from the Golgi to the cell exterior without an organelle storage site, e.g. a cytoplasmic granule [69]) [37,42,57,69,85,101,105]
epithelial cell <3> (<3> primary renal cortical cell cultures, real-time PCR and immunohistochemic analysis, overview [94]) [94]
heart <3,9> (<9> enzyme expression [2]) [2,37]
hepatic stellate cell <3,4> (<4> the dramatically increased ADAMTS-13 protein and proteolytic activity in the activated hepatic stellate cells in vitro and in vivo may be important part of functions of activated hepatic stellate cells, perhaps by modulating the processes of liver regeneration or formation of liver fibrosis after various insults [25]; <3> ADAMTS13 is secreted by almost all tissues but primarily by hepatic stellate cells [95]; <3> retinoid enriched, i.e. lipocyte, secretes the enzyme [78]) [25,37,78,95]
hepatocyte <3> (<3> ADAMTS13 and von Willebrand factor contents, overview [100]) [100]
hepatoma cell <3> (<3> ADAMTS13 and von Willebrand factor contents, overview [100]) [100]
kidney <3,9> (<9> enzyme expression [2]; <3> in the renal cortex [94]) [2,9,37,94]
liver <2,3,9> (<9> enzyme expression, adult and fetal [2]; <3> expression at [13]; <2> high expression of Adamts-13 [24]; <2> primary site of ADAMTS13 synthesis, the enzyme is secreted [62]; <3> secretes the enzyme, ADAMTS13 activity in hepatic carcinoma, liver cirrhosis due to viral infection, primary biliary cirrhosis, cholestasis, and biliary atresia, overview [100]; <9> synthesizes and secreted ADAMTS13 [93]) [2,10,13,24,62,93,100]
lung <2,3> (<2> medium expression of Adamts-13 [24]) [24,37]
muscle <9> (<9> enzyme expression [2]) [2]
neuronal cell <9> (<9> thrombospondin1 and ADAMTS13 form complexes together in cells and in direct protein binding assays [93]) [93]
ovary <3> [37]
pancreas <3> [37]
placenta <3,9> (<9> enzyme expression [2]) [2,37]
plasma <1,2,3,4,5,6,7,8,9> (<3> from patiens with type I von Willebrand disease, i.e. VWD [6]; <3> ADAMTS13 circulates in plasma [94]; <3> from paroxysmal and chronic atrial fibrillation patients and healthy controls, ADAMTS13 contents and activities, overview [99]; <3> persistently elevated levels of von Willebrand factor in plasma during and after liver transplantation, while plasma levels of ADAMTS13 dropp during transplantation [56]; <9> the enzyme circulates in the blood [93]) [1,2,3,4,6,7,8,9,10,11,12,13,55,56,57,60,61,62,63,64,65,67,68,69,70,73,74,75,76,77,78,79,80,81,82,83,84,85,86,87,89,90,91,92,93,94,95,96,97,98,99,100,101,103,104,105]
podocyte <3> (<3> secretes the enzyme [78]) [78]

prostate <3> [37]
renal tubule <3> (<3> in both proximal and distal in healthy persons and in patients with renal disorders, e.g. tubulopathy [94]) [94]
serum <3> [7]
skeletal muscle <2> (<2> low expression of ADAMTS-13 [24]) [24]
spleen <2> (<2> medium expression of ADAMTS-13 [24]) [24]
testis <9> (<9> enzyme expression [2]) [2]
umbilical vein endothelial cell <3> (<3> at the surface of endothelial cells [85]) [85]
urine <3> (<3> only in urine from patients with renal disorder tubulopathy [94]) [94]
uterus <3> [37]
Additional information <2,3> (<3> not in platelet [7]; <2> activity is undetectable in heart, brain, kidney and testis [24]; <3> ADAMTS-13 levels in healthy controls and patients with disseminated intravascular coagulation [101]; <3> wide tissue distribution of ADAMTS13 expression [94]) [7,24,94,101]

Localization

Golgi apparatus <3> (<3> homogeneous distribution of wild-type ADAMTS13 in cis-Golgi and endoplasmic reticulum compartments. Reduction of ADAMTS13(Val88Met) in both compartments. ADAMTS13(Gly1239-Val) fails to reach the cis-Golgi compartment and remains in the endoplasmic reticulum [19]) [19]
cell surface <3> (<3> ADAMTS13 binds to endothelial cells in a specific, reversible, and time-dependent manner with a K_d of 58 nM. Binding requires the COOH-terminal thrombospondin type 1 repeats of the protease. Binding is inhibited in the presence of heparin and by trypsin treatment of the cells [85]) [85,105]
endoplasmic reticulum <3> (<3> homogeneous distribution of wild-type ADAMTS13 in cis-Golgi and endoplasmic reticulum compartments. Reduction of ADAMTS13(Val88Met) in both compartments. ADAMTS13(Gly1239-Val) fails to reach the cis-Golgi compartment and remains in the endoplasmic reticulum [19]) [19]
extracellular <1,2,3,4,5,6,7,8,9> (<3,9> plasma [1,2,3,4,5,6,7,8,9,10,11,12,13]; <3> the enzyme is secreted [80,94]; <2,9> secreted enzyme [62,93]; <3> ADAMTS-13 is released directly from the Golgi to the cell exterior without an organelle storage site, e.g. a cytoplasmic granule [69]; <3> secrete enzyme [100]) [1,2,3,4,5,6,7,8,9,10,11,12,13,55,56,57,60,61,62,63,64,65,67,68,69,70,73,74,75,76,77,78,79,80,81,82,83,84,85,86,87,89,90,91,92,93,94,95,96,97,98,99,100,101,103,104,105]
intracellular <3> [101]

Purification

<3> [33,40,44]
<3> (HiLoad Superdex 200 gel filtration) [39]
<3> (Sephadex 26/10 gel filtration) [21]
<3> (about 10000fold) [7]

<3> (from commercial factor VIII/vWF concentrate) [8]
<3> (recombinant ADAMTS-13 from HEK293 cells by Zn^{2+}-agarose affinity and anion exchange chromatography to homogeneity) [79]
<3> (recombinant His-tagged ADAMTS13 by nickel affinity chromatography) [85]
<3> (recombinant His-tagged ADAMTS13 from HEK-293 cells by anion exchange chromatography, Ni affinity chromatography, and gel filtration) [65]
<3> (recombinant structure-based mutants of ADAMTS13-MDTCS residues 75-685 fragment with a C-terminal tobacco etch virus proteinase cleavage site followed by tandem His-tag sequences from CHO Lec 3.2.8.1 cells by nickel affinity chromatography and gel filtration) [97]
<3> (recombinant tagged deletion mutants) [5]
<3> (recombinant wild-type ADAMTS13 with a C-terminal Myc/His tag from HEK293 cells, and recombinant His-tagged truncated DAMTS13 mutants MP-Dis and MP by nickel affinity chromatography and gel filtration) [64]
<3> (recombinant wild-type and mutant ADAMTS13 from HEK-293 cells by nickel affinity chromatography) [71]
<3> (recombinant wild-type and mutant ADAMTS13s with a C-terminal Myc/His tag expressed from HEK-293 cells by nickel affinity chromatography) [60]
<3> (to homogeneity) [1]
<9> (recombinant His-tagged ADAMTS13 ancillary domains, ADAMTS13-DTCS, consisting of residues 287-685, from CHO Lec cells by nickel affinity and cation exchange chromatography) [55]

Crystallization

<3> (purified recombinant detagged ADAMTS13-DTCS, residues 287-685, an non-catalytic von Willebrand factor-exosite-containing ADAMTS13 fragment, sitting drop vapor diffusion method, mixing of 500 nl of protein solution and 500 nl reservoir solution containing 26% w/v PEG1500, 100 mM MES, pH 6.0, supplemented with 200 nl of 40% w/w pentaerythritol ethoxylate, equilibration for several days at 20°C. Os-derivative crystals by soaking native crystals in reservoir solution supplemented with 1 mM OsCl3 and 20% glycerol for several hours, X-ray diffraction structure determination and analysis at 2.6 A and 2.8 A resolution resulting in two crystal structures) [97]
<9> (recombinant His-tagged ADAMTS13 ancillary domains, residues 287-685, sitting-drop vapour-diffusion method, mixing of 100 nl protein solution, containing about 20 mg/ml protein, with an equal amount of reservoir solution, containing 26% w/v PEG 1500, 100 mM MES, pH 6.0, equilibration against 0.1 ml of reservoir solution, at 20°C, for 24 h, crystals are soaked in a solution containing 20% glycerol, 26% PEG 1500, 100 mM MES, pH 6.0, for cryoprotection, X-ray diffraction structure determination and analysis at 2.6-2.8 A resolution, labeling with heavy-atom derivatives) [55]

Cloning

<2> (expression of the murine Adamts-13 cDNA in HEK 293 cells) [24]
<2> (expression of wild-type and mutant enzyme forms in HEK-293 cells and CHO cells) [67]

<2> (gene Adamts13, DNA and amino acid sequence determination and analysis, expression of truncated ADAMTS13 in 129/Sv transgenic mice) [62]
<2> (gene Adamts13, DNA and amino acid sequence determination, construction of self-inactivated lentiviral vector, and expression of functional His-tagged ADAMTS13 cDNA in COS-7 cells) [61]
<3> [16,21,22,26,40,47]
<3> (ADAMTS13 DNA and amino acid sequence determination and analysis of wild-type and mutant enzymes, genotyping and expression analysis in HEK-293 cells, overview) [81]
<3> (ADAMTS13 genotyping, overview) [82]
<3> (DNA and amino acid sequence determination and analysis, genotyping) [102]
<3> (DNA sequence determination and analysis) [10]
<3> (DNA sequence determination and analysis, transient expression of wild-type and mutants as FLAG-tagged enzymes in HeLa cells) [13]
<3> (DNA sequence determination of natural genetic variants, heterozygous polymorphism at Tyr/Cys1584 and other, overview) [6]
<3> (construction of ADAMTS13 epitope library) [58]
<3> (expressed in HEK-293 cells) [33,35,39,44]
<3> (expressed in HeLa cells) [43]
<3> (expressed in T-REx 293 cells) [46]
<3> (expression of ADAMTS13 in HEK-293 cells) [79,103]
<3> (expression of His-tagged ADAMTS13) [85]
<3> (expression of a series of partial deletions in the A2 domain flanked with N- and C-terminal tags in Escherichia coli) [5]
<3> (expression of structure-based mutants of ADAMTS13-MDTCS residues 75-685 fragment with a C-terminal tobacco etch virus proteinase cleavage site followed by tandem His-tag sequences in CHO Lec 3.2.8.1 cells. Transient expression of His-tagged mutant ADAMTS13-MDTCS domains using a cytomegalovirus promoter-driven expression vector in HeLa cells) [97]
<3> (expression of wild-type ADAMTS13 with a C-terminal Myc/His tag in HEK293 cells, transient expression of His-tagged truncated DAMTS13 mutants MP-Dis and MP and point mutants in HEK-293T cells) [64]
<3> (expression of wild-type and mutant ADAMTS13 in HEK-293 cells) [71]
<3> (expression of wild-type and mutant ADAMTS13s with a C-terminal Myc/His tag expressed in HEK-293 cells) [60]
<3> (expression of wild-type and mutant enzymes in HEK 293 and COS-7 cells) [19]
<3> (gene ADAMTS13, location of chromosome 9q34) [1]
<3> (gene ADMTS13 and mutant variant truncated after the spacer domain, MDTCS, expression in transgenic mice) [92]
<3> (stable expression in HEK-293 cells) [74]
<3> (stable expression of His-tagged ADAMTS13 in HEK-293 cells) [65]
<3> (transient expression in HEK293 cells) [2]
<3> (transient expression in HeLa cells, in HepG2 cells, in RFL6 cells, and in COS-1 cells, highest expression level is obtained in HeLa cells) [12]

<3> (transient expression of C-terminally tagged enzyme in COS-7 cells or expression in a Sf9 cells/baculovirus expression system, tagged with His6 or V5 epitopes) [11]
<3> (transient expression of wild-type and mutants in HeLa cells as FLAG-tagged proteins) [4]
<9> (expression of FLAG-tagged ADAMTS13 in HEK-293 cells, co-expression with thrombospondin1) [93]
<9> (stable expression of His-tagged ADAMTS13 ancillary domains, ADAMTS13-DTCS, consisting of residues 287-685, in CHO Lec cells) [55]

Engineering

A1033T <3> (<3> naturally occuring mutation of ADAMTS13 [82]) [82]
A250V <3> (<3> naturally occuring mutation of ADAMTS13 [82]) [82]
A596V <3> (<3> naturally occuring mutation of ADAMTS13 [82]) [82]
A606P <3> (<3> naturally occuring mutation of ADAMTS13 [82]) [82]
A732V <3> (<3> naturally occuring mutation of ADAMTS13 [82]) [82]
A900V <3> (<3> naturally occuring C2699T polymorphism in patients with coronary artery disease and preserved left ventricular function [102]; <3> naturally occuring mutation of ADAMTS13 [82]) [82,102]
C1024G <3> (<3> naturally occuring mutation of ADAMTS13 [82]) [82]
C1213Y <3> (<3> naturally occuring mutation of ADAMTS13 [82]) [82]
C311Y <3> (<3> naturally occuring mutation of ADAMTS13 [82]) [82]
C347S <3> (<3> naturally occuring mutation of ADAMTS13 [82]) [82]
C508Y <3> (<3> naturally occuring mutant, no secretion of the enzyme to the plasma, possible defects in secretion pathway, or protein folding and stability [13]; <3> naturally occuring mutation of ADAMTS13 [82]) [13,82]
C758R <3> (<3> naturally occuring mutation of ADAMTS13 [82]) [82]
C908S <3> (<3> naturally occuring mutation of ADAMTS13 [82]) [82]
C908Y <3> (<3> naturally occuring mutation of ADAMTS13 [82]) [82]
C951G <3> (<3> naturally occuring mutation of ADAMTS13 [82]) [82]
C977W <3> (<3> deletion of 6 nucleotides GTGCCC at position 2930-2935, i.e. c.2930935del GTGCCC, in exon 23, leading to the replacement of Cys977 residue by a Trp [81]) [81]
D187A <3> (<3> site-directed mutagenesis of a Ca^{2+} binding site residue, the kinetic dissociation constant of ADAMTS13 for Ca^{2+} is dramatically reduced compared to the wild-type enzyme, V_{max} of the mutant is also reduced by 75%, and Kcat/K_m 13fold, compared to the wild-type [60]) [60]
D235H <3> (<3> naturally occuring mutation of ADAMTS13 [82]) [82]
D330A <3> (<3> site-directed mutagenesis, the mutant shows activity similar to the wild-type enzyme [64]) [64]
D340A <3> (<3> site-directed mutagenesis, the mutant shows slightly reduced activity compared to the wild-type enzyme [64]) [64]
D343A <3> (<3> site-directed mutagenesis, the mutant shows slightly reduced activity compared to the wild-type enzyme [64]) [64]
D500E <3> (<3> point mutation in the RGD cysteine-rich domain, unaltered activity compared to the wild-type enzyme [4]) [4]

E184A <3> (<3> site-directed mutagenesis of a Ca^{2+} binding site residue, the kinetic dissociation constant of ADAMTS13 for Ca^{2+} is dramatically reduced compared to the wild-type enzyme [60]) [60]
E212A <3> (<3> site-directed mutagenesis of a Ca^{2+} binding site residue, the kinetic dissociation constant of ADAMTS13 for Ca^{2+} is dramatically reduced compared to the wild-type enzyme, V_{max} of the mutant is also reduced by 75% compared to the wild-type [60]) [60]
E627X <3> (<3> naturally occuring mutation of ADAMTS13 [82]) [82]
E634K <3> (<3> naturally occuring mutation of ADAMTS13 [82]) [82]
E663A <3> (<3> site-directed mutagenesis [71]; <3> site-directed mutagenesis, the mutant shows activity similar to the wild-type enzyme with substrate VWF73 peptide [73]) [71,73]
E664A <3> (<3> site-directed mutagenesis [71]; <3> site-directed mutagenesis, the mutant shows activity similar to the wild-type enzyme with substrate VWF73 peptide [73]) [71,73]
E740K <3> (<3> naturally occuring mutation of ADAMTS13 [82]) [82]
G1239V <3> (<3> mutation leads to a secretion defect causing intracellular accumulation of the protease [19]; <3> naturally occuring mutation of ADAMTS13 [82]) [19,82]
G525D <3> (<3> naturally occuring mutation of ADAMTS13 [82]) [82]
G662A <3> (<3> site-directed mutagenesis [71]; <3> site-directed mutagenesis, the mutant shows activity similar to the wild-type enzyme with substrate VWF73 peptide [73]) [71,73]
G982R <3> (<3> naturally occuring mutation of ADAMTS13 [82]) [82]
H234Q <3> (<3> naturally occuring mutation of ADAMTS13 [82]) [82]
H96D <3> (<3> naturally occuring mutation of ADAMTS13 [82]) [82]
I1217T <3> (<3> naturally occuring mutation of ADAMTS13 [82]) [82]
I178T <3> (<3> naturally occuring mutation of ADAMTS13 [82]) [82]
I673F <3> (<3> naturally occuring mutation of ADAMTS13 [82]) [82]
I79M <3> (<3> naturally occuring mutation of ADAMTS13 [82]) [82]
L232Q <3> (<3> naturally occuring mutation of ADAMTS13 [82]) [82]
L350G <3> (<3> site-directed mutagenesis, the mutant shows highly reduced activity compared to the wild-type enzyme [64]) [64]
L351G <3> (<3> site-directed mutagenesis, the mutant shows slightly reduced activity compared to the wild-type enzyme [64]) [64]
N146Q <9> (<9> decreased secretion and von Willebrand factor cleaving activity [51]) [51]
N552Q <9> (<9> decreased secretion [51]) [51]
N828Q <9> (<9> decreased secretion and von Willebrand factor cleaving activity [51]) [51]
P353L <3> (<3> naturally occuring mutation of ADAMTS13 [82]) [82]
P457L <3> (<3> naturally occuring mutation of ADAMTS13 [82]) [82]
P475S <3> (<3> low activity [37]; <3> naturally occuring mutant, efficient secretion, reduced activity [13]; <3> naturally occuring mutation of ADAMTS13 [82]; <3> the ADAMTS13 mutant shows similar expression but reduced activity compared to the wild-type enzyme, and minimal von Willebrand factor-induced changes in conformation [95]; <3> the common natu-

rally occuring polymorphsim is not involved in ADAMTS13 inhibition in malaria patients [57]) [13,37,57,82,95]
P618A <3> (<3> naturally occuring C1852G polymorphism in patients with coronary artery disease and preserved left ventricular function [102]; <3> naturally occuring mutation of ADAMTS13 [82]; <3> naturally occuring mutation of ADAMTS13 involved in inherited thrombotic thrombocytopenic purpura [81]) [81,82,102]
P618A/A732V <3> (<3> mutation induces secretion deficiency [37]) [37]
P671L <3> (<3> naturally occuring mutation of ADAMTS13 [82]) [82]
Q1302X <3> (<3> naturally occuring mutation of ADAMTS13 [82]) [82]
Q333A <3> (<3> site-directed mutagenesis, the mutant shows activity similar to the wild-type enzyme [64]) [64]
Q448E <3> (<3> naturally occuring mutant, efficient secretion, fully active [13]; <3> mutation has no significant effect on ADAMTS13 secretion [37]; <3> naturally occuring C1342G polymorphism in patients with coronary artery disease and preserved left ventricular function [102]; <3> naturally occuring mutation of ADAMTS13 [82]; <3> naturally occuring mutation of ADAMTS13 involved in inherited thrombotic thrombocytopenic purpura [81]) [13,37,81,82,102]
Q449X <3> (<3> naturally occuring mutation of ADAMTS13 [82]) [82]
Q44X <3> (<3> naturally occuring mutation of ADAMTS13 [82]) [82]
Q456H <3> (<3> naturally occuring mutation of ADAMTS13 [82]) [82]
Q929X <3> (<3> naturally occuring mutation of ADAMTS13 [82]) [82]
R102C <3> (<3> naturally occuring mutation of ADAMTS13 [82]) [82]
R1034X <3> (<3> naturally occuring mutation of ADAMTS13 [82]) [82]
R1060W <3> (<3> naturally occuring mutation of ADAMTS13 [82]) [82]
R1096H <3> (<3> naturally occuring mutation of ADAMTS13 [82]) [82]
R1123C <3> (<3> naturally occuring mutation of ADAMTS13 [82]) [82]
R1206X <3> (<3> naturally occuring mutation of ADAMTS13 [82]) [82]
R1219W <3> (<3> naturally occuring mutation of ADAMTS13 [82]) [82]
R1336 <3> (<3> mutation induces secretion deficiency [37]) [37]
R1336W <3> (<3> naturally occuring mutation of ADAMTS13 [82]) [82]
R193W <3> (<3> naturally occuring mutation of ADAMTS13 [82]) [82]
R268P <3> (<3> naturally occuring mutant, no secretion of the enzyme to the plasma, possible defects in secretion pathway, or protein folding and stability [13]; <3> naturally occuring mutation of ADAMTS13 [82]) [13,82]
R349A <3> (<3> site-directed mutagenesis, the mutant shows highly reduced activity compared to the wild-type enzyme, the mutant enzyme shows increased activity with the mutant D1614A von Willebrand factor115 substrate compared to the wild-type enzyme [64]) [64]
R349C <3> (<3> naturally occuring mutation of ADAMTS13 [82]) [82]
R398H <3> (<3> naturally occuring mutation of ADAMTS13 [82]) [82]
R484K <3> (<3> naturally occuring mutation of ADAMTS13 [82]) [82]
R507Q <3> (<3> naturally occuring mutation of ADAMTS13 [82]) [82]
R528G <3> (<3> naturally occuring mutation of ADAMTS13 [82]) [82]
R625H <3> (<3> naturally occuring mutation of ADAMTS13 [82]) [82]

R659A <3> (<3> site-directed mutagenesis [71]; <3> site-directed mutagenesis, the mutant shows altered activity compared to the wild-type enzyme with substrate VWF73 peptide [73]) [71,73]
R660A <3> (<3> site-directed mutagenesis [71]; <3> site-directed mutagenesis, the mutant shows altered activity compared to the wild-type enzyme with substrate VWF73 peptide [73]) [71,73]
R660A/Y661A <3> (<3> site-directed mutagenesis [71]) [71]
R660A/Y661A/Y665A <3> (<3> site-directed mutagenesis, the ADAMTS13 variant, i.e. ADAMTS13-RYY, shows a 12fold reduced catalytic efficiency arising from over 25fold reduced substrate binding [71]) [71]
R660A/Y665A <3> (<3> site-directed mutagenesis [71]) [71]
R692C <3> (<3> naturally occuring mutation of ADAMTS13 [82]) [82]
R7W <3> (<3> mutation has no significant effect on ADAMTS13 secretion [37]; <3> naturally occuring mutation of ADAMTS13 [82]; <3> naturally occuring mutation of ADAMTS13 involved in inherited thrombotic thrombocytopenic purpura [81]) [37,81,82]
R910X <3> (<3> naturally occuring mutation of ADAMTS13 [82]) [82]
S119A <3> (<3> site-directed mutagensis, mutant S119A has properties similar to natural mutant S119F [68]) [68]
S119F <3> (<3> a naturally occuring mutation in the ADAMTS13 metalloprotease domain that leads to distorted kinetics and to the loss of the H-bond with conserved residue W262, the mutation is involved in development of hereditary thrombotic thrombocytopenic purpura due to reduced ADAMTS13 activity, overview. Secreted S119F is active toward multimeric von Willebrand factor and FRETSVWF73 but with abnormal kinetics. The mutant is expressed normally, but shows markedly impaired secretion [68]; <3> naturally occuring mutation of ADAMTS13 [82]) [68,82]
S119F/Q448E <3> (<3> naturally occuring mutation in the ADAMTS13 metalloprotease domain. The mutant is expressed normally, but shows markedly impaired secretion [68]) [68]
S203P <3> (<3> naturally occuring mutation of ADAMTS13 [82]) [82]
S263C <3> (<3> naturally occuring mutation of ADAMTS13 [82]) [82]
S903L <3> (<3> naturally occuring mutation of ADAMTS13 [82]) [82]
T1226I <3> (<3> naturally occuring mutation of ADAMTS13 [82]) [82]
T196I <3> (<3> naturally occuring mutation of ADAMTS13 [82]) [82]
T339R <3> (<3> naturally occuring mutation of ADAMTS13 [82]) [82]
V352G <3> (<3> site-directed mutagenesis, the mutant shows reduced activity compared to the wild-type enzyme [64]) [64]
V604I <3> (<3> naturally occuring mutation of ADAMTS13 [82]) [82]
V832M <3> (<3> naturally occuring mutation of ADAMTS13 [82]) [82]
V88M <3> (<3> mutation leads to a defect of secretion of the protease associated with a reduction of enzymatic activity [19]; <3> naturally occuring mutation of ADAMTS13 [82]) [19,82]
W1016X <3> (<3> naturally occuring mutation of ADAMTS13 [82]) [82]
W1245X <3> (<3> naturally occuring mutation of ADAMTS13 [82]) [82]
W390C <3> (<3> naturally occuring mutation of ADAMTS13 [82]) [82]
W390X <3> (<3> naturally occuring mutation of ADAMTS13 [82]) [82]

Y304C <3> (<3> naturally occuring mutation of ADAMTS13 [82]) [82]
Y658A <3> (<3> site-directed mutagenesis [71]) [71]
Y661A <3> (<3> site-directed mutagenesis [71]; <3> site-directed mutagenesis, the mutant shows altered activity compared to the wild-type enzyme with substrate VWF73 peptide [73]) [71,73]
Y661A/Y665A <3> (<3> site-directed mutagenesis [71]) [71]
Y665A <3> (<3> site-directed mutagenesis [71]) [71]
delQ1624-R1641 <9> (<9> mutation minimally affects the rate of cleavage [50]) [50]
Additional information <2,3,9> (<3> construction of 13 sequential C-terminal truncated mutants, mutants lacking the the cysteine-rich and spacer domain show dramatically reduced or no activity, the other mutants retain their activity, overview [4]; <3> construction of an enzyme truncated after the metalloprotease domain, which is inactive, addition of the spacer region can restore activity, overview [11]; <3> natural mutant is cleaved at peptide bond Tyr1605-Met1606 [1]; <3> Q449stop mutant is efficiently secreted, has a MW of 54 kDa, and shows no activity, detection of naturally occuring mutations in a Japanese family with thrombotic thrombocytopenic pupura, overview [13]; <3> introduction of polymorphisms R7W, Q448E, and A732V have no or only minor effects on ADAMTS13 secretion. In contrast, P618A, R1336W, and the A732V/P618A combination strongly reduce ADAMTS13-specific activity and antigen levels. R7W and Q448E are positive modifiers of ADAMTS13 secretion in the context of P618A and A732V but neither can rescue the severely reduced specific activity conferred by P618A. In the context of R133W, polymorphisms R7W and Q448E enhance the detrimental effect of the missense mutation and lead to undetectable enzyme activity [16]; <3> deletion mutation C365DEL and a point mutation R1060W severely impair ADAMTS-13 synthesis and decrease of von Willebrand cleaving activity [43]; <3> ability of systemically administered adenovirus encoding human ADAMTS13 to restore the deficient protein in the circulation of Adamts13-/- mice, derived from B/129 wild-type mice. Injection of the adenovirus efficiently transduces the liver, kidney, lung, heart and spleen, resulting in the secretion of ADAMTS13 into plasma, especially from lung and liver, not from brain, overview [80]; <3> analysis of ADAMTS13 mutations and polymorphisms in congenital thrombotic thrombocytopenic purpura, wide spectrum of clinical phenotype in congenital thrombotic thrombocytopenic purpura, overview [82]; <3> construction of a self-inactivating lentiviral vector encoding human full-length ADAMTS13 and a variant truncated after the spacer domain, MDTCS. In utero gene transfer of lentiviral vector encoding ADAMTS13 genes by injection at embryonic days 8 and 14 resulting in detectable plasma proteolytic activity. The mice expressing ADAMTS13 and MDTCS exhibit reduced sizes of von Willebrand factor compared to the Adamts13-/- mice, they show increased survival rates and functional enzyme activity in plasma, overview. The expressed human ADAMTS13 and MDTCS offer systemic protection against arterial thrombosis [92]; <3> construction of ADAMTS13 truncated mutants, MDTCS and del(TSP5-CUB), and analysis of their binding with different C-terminal domain VWF fragments, overview

[66]; <3> construction of disintegrin domain mutants by site-directed mutagenesis, that exhibit dramatically reduced activity toward the von Willebrand factor fragment VWF115, comprising amino acid residues 1554-1668 of von Willebrand factor. The isolated metalloprotease domain of ADAMTS13 alone is ineffective in cleaving, but if the various noncatalytic domains are incrementally added back, proteolytic activity is gradually restored [63]; <3> construction of truncated DAMTS13 mutants MP-Dis and MP, which have a molecular weight of 30 kDa and 40 kDa, respectively [64]; <3> deletion of amino acid residues Arg659-Glu664 from the ADAMTS13 spacer domain by site-directed mutagenesis results in dramatically reduced proteolytic activity toward von Willebrand factor73 peptides, guanidine-HCl denatured von Willebrand factor, and native von Willebrand factor under fluid shear stress, as well as ultralarge von Willebrand factor on endothelial cells [73]; <2> generation of a congenic mouse model expressing the C-terminally truncated form of ADAMTS13 on 129/Sv genetic background, presence of IAP insertion in the Adamts13 gene of the congenic Adamts13S/S mice by PCR, and detection an IAP chimeric transcript by Northern blotting of RNA from liver, overview. The distal C-terminally truncated form of mouseADAMTS13 does not completely lose the activity. In vivo thrombus growth is accelerated in Adamts13S/S mice, overview [62]; <3> generation of structure-based mutants of ADAMTS13-MDTCS residues 75-685 fragment. The MDTCS domains are conserved among ADAMTS family proteins [97]; <3> identification of a deletion of two amino acids Ala978 and Arg979, i.e. p.C977W+p.A978_R979del, in the TSP1-6 repeat domain of ADAMTS13 in a family with inherited thrombotic thrombocytopenic purpura. Three common ADAMTS13 intragenic SNPs p.R7W, p.Q448E and p.P618A are also identified in heterozygous state in paternal alleles (I:2) and also in II:5 and II:8. [81]; <2> plasma ADAMTS13 proteolytic activity on average can be restored in Adamts13-/- mice to approximately 25% of wild-type level by autologous transplantation of hematopoietic progenitor cells transduced ex vivo with a self-inactivating lentiviral vector encoding a full-length murine Adamts13 and an enhanced GFP reporter gene [61]; <9> replacement of signal sequence and prosequence with the mouse Nid1 signal sequence dramatically increases the secretion of ADAMTS13-DTCS into the medium [55]) [1,4,11,13,16,43,55,61,62,63,64,66, 73,80,81,82,92,97]

Application

diagnostics <3> (<3> ADAMTS-13 may serve as a diagnostic and prognostic marker of disseminated intravascular coagulation. Patients with a low activity of ADAMTS-13 have a poor survival rate compared to patients with a high activity of ADAMTS-13 [101]; <3> Potential role of ADAMTS13 as a diagnostic and prognostic marker of disseminated intravascular coagulopathy. ADAMTS13 and the activity of von Willebrand factor are also a marker for development of multiple organ dysfucntion in infectious and non-infectious systemic inflammatory response syndrome [78]; <3> role for clinical testing of plasma ADAMTS13 activity and inhibitors in care of thrombotic thrombocytopenic purpura patients, overview [70]; <3> role of ADAMTS 13 assays in

diagnosis and prognosis of thrombotic thrombocytopenic purpura, TTP, overview [59]; <3> value of ADAMTS13 activity and inhibitor in the post-mortem diagnosis of thrombotic thrombocytopenic purpura, overview [86]) [59,70,78,86,101]
drug development <3> (<3> inhibitory anti-ADAMTS 13 antibodies, measurement and clinical application, overview [59]) [59]
medicine <2,3,9> (<3> analysis of vWF protease and vWF multimeric distribution are valuable tools in making the distinction between bone marrow transplant-associated thrombotid microangiopathy and thrombotic thrombocytopenic pupura [9]; <3> ADAMTS-13 is deficient in congenital thrombotic thrombocytopenic purpura and inhibited in aquired thrombotic thrombocytopenic purpura. The availability of recombinant ADAMTS-13 raises the prospect of developing a recombinant substitution therapy to improve thrombotic thrombocytopenic purpura treatment and allows present diagnostic assays to be simplified [26]; <3> assay using recombinant or synthetic substrates (high-throughput methods) will contribute significantly to the accurate diagnosis of microangiopathies, ultimately leading to improved treatment of these diseases. These assays may also help clarify the role of ADAMTS13 in thrombotic disorders including disseminated intravascular coagulation, stroke, and myocardial infarction [18]; <3> description of a simple procedure to analyse the kinetics of von Willebrand factor proteolysis that is suitable for routine diagnostic use [17]; <9> in order to develop new strategies for improving the diagnosis and treatment of thrombotic thrombocytopenic purpura, this study systemically analyzed a series of ADAMTS13 mutant proteins to identify variant forms that are proteolytically active and yet resistant to suppression by inhibitory antibodies. A deficiency of ADAMTS13, due to mutations in the ADAMTS13 gene or the presence of antibodies that inhibit the activity of the protease,causes thrombotic thrombocytopenic purpura. Plasma therapy, the conventional therapy for TTP, may cause serious adverse reactions and is ineffective in some patients [20]; <3> VWF73, a region from D1596 to R1668 of von Willebrand factor, provides a minimal substrate for ADAMTS-13. VWF73 could be a powerful tool to establish clinical enzymatic assays. It may contribute to improve the prognosis and prevention of thrombotic thrombocytopenic purpurea [5]; <3> ADAMTS13 deficiency and the resultant increase in von Willebrand factor adhesion activity may be clinically significant for association with the severity of thrombocytopenia and clinical prognosis in sepsis, sickle cell disease, and and increased risk for stroke [37]; <3> ADAMTS13 deficiency is linked to thrombotic thrombocytopenic purpura [35]; <9> levels of ADAMTS13 are lower and levels of Von Willebrand Factor are higher in young patients with cardiovascular disease compared to healthy individuals. Individuals with low levels of ADAMTS13 had five times more risk on cardiovascular disease than subjects with normal levels of ADAMTS13. The relationship is strongest in the subgroup of patients with coronary heart disease. This may be of importance for identifying individuals who are prone to have a cardiovascular event [54]; <2> ADAMTS13 may be a useful therapeutic agent for stroke in humans [72]; <3> correction of ADAMTS13 deficiency by in utero gene transfer of

lentiviral vector encoding ADAMTS13 genes [92]; <3> infusion of a high dose of recombinant human ADAMTS13 into a wild-type mouse immediately before reperfusion reduces infarct volume and improves functional outcome without producing cerebral hemorrhage. Thus, recombinant ADAMTS13 can be considered as a therapeutic agent for prevention and/or treatment of stroke. Recombinant ADAMTS13 does not enhance bleeding in a hemorrhagic stroke model [67]) [5,9,17,18,20,26,35,37,54,67,72,92]

6 Stability

Temperature stability

22 <3> (<3> stable for several days during purification at room temperature [7]) [7]

General stability information

<3>, ADAMTS-13 is highly stable in plasma that is stored frozen at -80°C [29]

References

[1] Chung, D.W.; Fujikawa, K.: Processing of von Willebrand Factor by ADAMTS-13. Biochemistry, **41**, 11065-11070 (2002)
[2] Plaimauer, B.; Zimmermann, K.; Volkel, D.; Antoine, G.; Kerschbaumer, R.; Jenab, P.; Furlan, M.; Gerritsen, H.; Lammle, B.; Schwarz, H.P.; Scheiflinger, F.: Cloning, expression, and functional characterization of the von Willebrand factor-cleaving protease (ADAMTS13). Blood, **100**, 3626-3632 (2002)
[3] Dong, J.F.; Moake, J.L.; Nolasco, L.; Bernardo, A.; Arceneaux, W.; Shrimpton, C.N.; Schade, A.J.; McIntire, L.V.; Fujikawa, K.; Lopez, J.A.: ADAMTS-13 rapidly cleaves newly secreted ultralarge von Willebrand factor multimers on the endothelial surface under flowing conditions. Blood, **100**, 4033-4039 (2002)
[4] Soejima, K.; Matsumoto, M.; Kokame, K.; Yagi, H.; Ishizashi, H.; Maeda, H.; Nozaki, C.; Miyata, T.; Fujimura, Y.; Nakagaki, T.: ADAMTS-13 cysteine-rich/spacer domains are functionally essential for von Willebrand factor cleavage. Blood, **102**, 3232-3237 (2003)
[5] Kokame, K.; Matsumoto, M.; Fujimura, Y.; Miyata, T.: VWF73, a region from D1596 to R1668 of von Willebrand factor, provides a minimal substrate for ADAMTS-13. Blood, **103**, 607-612 (2003)
[6] Bowen, D.J.; Collins, P.W.: An amino acid polymorphism in von Willebrand factor correlates with increased susceptibility to proteolysis by ADAMTS13. Blood, **103**, 941-947 (2003)
[7] Furlan, M.; Robles, R.; Lamie, B.: Partial purification and characterization of a protease from human plasma cleaving von Willebrand factor to fragments produced by in vivo proteolysis. Blood, **87**, 4223-4234 (1996)

[8] Fujikawa, K.; Suzuki, H.; McMullen, B.; Chung, D.: Purification of human von Willebrand factor-cleaving protease and its identification as a new member of the metalloproteinase family. Blood, **98**, 1662-1666 (2001)
[9] Arai, S.; Allan, C.; Streiff, M.; Hutchins, G.M.; Vogelsang, G.B.; Tsai, H.M.: Von Willebrand factor-cleaving protease activity and proteolysis of von Willebrand factor in bone marrow transplant-associated thrombotic microangiopathy. Hematol. J., **2**, 292-299 (2001)
[10] Zheng, X.; Chung, D.; Takayama, T.K.; Majerus, E.M.; Sadler, J.E.; Fujikawa, K.: Structure of von Willebrand factor-cleaving protease (ADAMTS13), a metalloprotease involved in thrombotic thrombocytopenic purpura. J. Biol. Chem., **276**, 41059-41063 (2001)
[11] Zheng, X.; Nishio, K.; Majerus, E.M.; Sadler, J.E.: Cleavage of von Willebrand factor requires the spacer domain of the metalloprotease ADAMTS13. J. Biol. Chem., **278**, 30136-30141 (2003)
[12] Majerus, E.M.; Zheng, X.; Tuley, E.A.; Sadler, J.E.: Cleavage of the ADAMTS13 propeptide is not required for protease activity. J. Biol. Chem., **278**, 46643-46648 (2003)
[13] Kokame, K.; Matsumoto, M.; Soejima, K.; Yagi, H.; Ishizashi, H.; Funato, M.; Tamai, H.; Konno, M.; Kamide, K.; Kawano, Y.; Miyata, T.; Fujimura, Y.: Mutations and common polymorphisms in ADAMTS13 gene responsible for von Willebrand factor-cleaving protease activity. Proc. Natl. Acad. Sci. USA, **99**, 11902-11907 (2002)
[14] Sugimoto, T.; Saigo, K.; Shin, T.; Kaneda, Y.; Manabe, N.; Narita, H.; Wakuya, J.; Imoto, S.; Murayama, T.; Matsumoto, M.; Fujimura, Y.; Nishimura, R.; Koizumi, T.; Kumagai, S.: von Willebrand factor-cleaving protease activity remains at the intermediate level in thrombotic thrombocytopenic purpura. Acta Haematol., **113**, 198-203 (2005)
[15] Schnog, J.J.; Hovinga, J.A.; Krieg, S.; Akin, S.; Laemmle, B.; Brandjes, D.P.; Mac Gillavry, M.R.; Muskiet, F.D.; Duits, A.J.; Duits, A.J.: ADAMTS13 activity in sickle cell disease. Am. J. Hematol., **81**, 492-498 (2006)
[16] Plaimauer, B.; Fuhrmann, J.; Mohr, G.; Wernhart, W.; Bruno, K.; Ferrari, S.; Konetschny, C.; Antoine, G.; Rieger, M.; Scheiflinger, F.: Modulation of ADAMTS13 secretion and specific activity by a combination of common amino acid polymorphisms and a missense mutation. Blood, **107**, 118-125 (2006)
[17] Perutelli, P.; Amato, S.; Molinari, A.C.: Cleavage of von Willebrand factor by ADAMTS-13 in vitro: effect of temperature and barium ions on the proteolysis kinetics. Blood Coagul. Fibrinolysis, **16**, 607-611 (2005)
[18] Miyata, T.; Kokame, K.; Banno, F.: Measurement of ADAMTS13 activity and inhibitors. Curr. Opin. Hematol., **12**, 384-389 (2005)
[19] Peyvandi, F.; Lavoretano, S.; Palla, R.; Valsecchi, C.; Merati, G.; De Cristofaro, R.; Rossi, E.; Mannuccio Mannucci, P.: Mechanisms of the interaction between two ADAMTS13 gene mutations leading to severe deficiency of enzymatic activity. Hum. Mutat., **27**, 330-336 (2006)
[20] Zhou, W.; Dong, L.; Ginsburg, D.; Bouhassira, E.E.; Tsai, H.M.: Enzymatically active ADAMTS13 variants are not inhibited by anti-ADAMTS13

autoantibodies: a novel therapeutic strategy?. J. Biol. Chem., **280**, 39934-39941 (2005)
[21] Zanardelli, S.; Crawley, J.T.; Chion, C.K.; Lam, J.K.; Preston, R.J.; Lane, D.A.: ADAMTS13 substrate recognition of von Willebrand factor A2 domain. J. Biol. Chem., **281**, 1555-1563 (2006)
[22] Anderson, P.J.; Kokame, K.; Sadler, J.E.: Zinc and calcium ions cooperatively modulate ADAMTS13 activity. J. Biol. Chem., **281**, 850-857 (2006)
[23] Schmugge, M.; Dunn, M.S.; Amankwah, K.S.; Blanchette, V.S.; Freedman, J.; Rand, M.L.: The activity of the von Willebrand factor cleaving protease ADAMTS-13 in newborn infants. J. Thromb. Haemost., **2**, 228-233 (2004)
[24] Bruno, K.; Voelkel, D.; Plaimauer, B.; Antoine, G.; Pable, S.; Motto, D.G.; Lemmerhirt, H.L.; Dorner, F.; Zimmermann, K.; Scheiflinger, F.: Cloning, expression and functional characterization of the full-length murine ADAMTS13. J. Thromb. Haemost., **3**, 1064-1073 (2005)
[25] Niiya, M.; Uemura, M.; Zheng, X.W.; Pollak, E.S.; Dockal, M.; Scheiflinger, F.; Wells, R.G.; Zheng, X.L.: Increased ADAMTS-13 proteolytic activity in rat hepatic stellate cells upon activation in vitro and in vivo. J. Thromb. Haemost., **4**, 1063-1070 (2006)
[26] Plaimauer, B.; Scheiflinger, F.: Expression and characterization of recombinant human ADAMTS-13. Semin. Hematol., **41**, 24-33 (2004)
[27] Sanchez-Luceros, A.; Farias, C.E.; Amaral, M.M.; Kempfer, A.C.; Votta, R.; Marchese, C.; Salviu, M.J.; Woods, A.I.; Meschengieser, S.S.; Lazzari, M.A.: von Willebrand factor-cleaving protease (ADAMTS13) activity in normal non-pregnant women, pregnant and post-delivery women. Thromb. Haemost., **92**, 1320-1326 (2004)
[28] Reiter, R.A.; Varadi, K.; Turecek, P.L.; Jilma, B.; Knoebl, P.: Changes in ADAMTS13 (von-Willebrand-factor-cleaving protease) activity after induced release of von Willebrand factor during acute systemic inflammation. Thromb. Haemost., **93**, 554-558 (2005)
[29] Perutelli, P.; Amato, S.; Calevo, M.G.; Molinari, A.C.: Von Willerbrand factor cleaving protease (ADAMTS-13) activity is stable in a set of plasma samples after prolonged storage at -80 Deg. Thromb. Res., **116**, 443-445 (2005)
[30] Perutelli, P.; Amato, S.; Molinari, A.C.: ADAMTS-13 activity in von Willebrand disease. Thromb. Res., **117**, 685-688 (2006)
[31] Matsukawa, M.; Kaikita, K.; Soejima, K.; Fuchigami, S.; Nakamura, Y.; Honda, T.; Tsujita, K.; Nagayoshi, Y.; Kojima, S.; Shimomura, H.; Sugiyama, S.; Fujimoto, K.; Yoshimura, M.; Nakagaki, T.; Ogawa, H.: Serial changes in von Willebrand factor-cleaving protease (ADAMTS13) and prognosis after acute myocardial infarction. Am. J. Cardiol., **100**, 758-763 (2007)
[32] Shida, Y.; Nishio, K.; Sugimoto, M.; Mizuno, T.; Hamada, M.; Kato, S.; Matsumoto, M.; Okuchi, K.; Fujimura, Y.; Yoshioka, A.: Functional imaging of shear-dependent activity of ADAMTS13 in regulating mural thrombus growth under whole blood flow conditions. Blood, **111**, 1295-1298 (2008)

[33] McKinnon, T.A.; Chion, A.C.; Millington, A.J.; Lane, D.A.; Laffan, M.A.: N-linked glycosylation of VWF modulates its interaction with ADAMTS13. Blood, **111**, 3042-3049 (2008)
[34] Chauhan, A.K.; Walsh, M.T.; Zhu, G.; Ginsburg, D.; Wagner, D.D.; Motto, D.G.: The combined roles of ADAMTS13 and VWF in murine models of TTP, endotoxemia, and thrombosis. Blood, **111**, 3452-3457 (2008)
[35] Starke, R.; Machin, S.; Scully, M.; Purdy, G.; Mackie, I.: The clinical utility of ADAMTS13 activity, antigen and autoantibody assays in thrombotic thrombocytopenic purpura. Br. J. Haematol., **136**, 649-655 (2007)
[36] Jin, M.; Casper, T.C.; Cataland, S.R.; Kennedy, M.S.; Lin, S.; Li, Y.J.; Wu, H.M.: Relationship between ADAMTS13 activity in clinical remission and the risk of TTP relapse. Br. J. Haematol., **141**, 651-658 (2008)
[37] Dong, J.F.: Structural and functional correlation of ADAMTS13. Curr. Opin. Hematol., **14**, 270-276 (2007)
[38] Keeney, S.; Grundy, P.; Collins, P.W.; Bowen, D.J.: C1584 in von Willebrand factor is necessary for enhanced proteolysis by ADAMTS13 in vitro. Haemophilia, **13**, 405-408 (2007)
[39] Soejima, K.; Nakamura, H.; Hirashima, M.; Morikawa, W.; Nozaki, C.; Nakagaki, T.: Analysis on the molecular species and concentration of circulating ADAMTS13 in blood. J. Biochem., **139**, 147-154 (2006)
[40] De Cristofaro, R.; Peyvandi, F.; Baronciani, L.; Palla, R.; Lavoretano, S.; Lombardi, R.; Di Stasio, E.; Federici, A.B.; Mannucci, P.M.: Molecular mapping of the chloride-binding site in von Willebrand factor (VWF): energetics and conformational effects on the VWF/ADAMTS-13 interaction. J. Biol. Chem., **281**, 30400-30411 (2006)
[41] Chung, M.C.; Popova, T.G.; Jorgensen, S.C.; Dong, L.; Chandhoke, V.; Bailey, C.L.; Popov, S.G.: Degradation of circulating von Willebrand factor and its regulator ADAMTS13 implicates secreted Bacillus anthracis metalloproteases in anthrax consumptive coagulopathy. J. Biol. Chem., **283**, 9531-9542 (2008)
[42] Turner, N.; Nolasco, L.; Tao, Z.; Dong, J.F.; Moake, J.: Human endothelial cells synthesize and release ADAMTS-13. J. Thromb. Haemost., **4**, 1396-1404 (2006)
[43] Tao, Z.; Anthony, K.; Peng, Y.; Choi, H.; Nolasco, L.; Rice, L.; Moake, J.L.; Dong, J.F.: Novel ADAMTS-13 mutations in an adult with delayed onset thrombotic thrombocytopenic purpura. J. Thromb. Haemost., **4**, 1931-1935 (2006)
[44] Lam, J.K.; Chion, C.K.; Zanardelli, S.; Lane, D.A.; Crawley, J.T.: Further characterization of ADAMTS-13 inactivation by thrombin. J. Thromb. Haemost., **5**, 1010-1018 (2007)
[45] Wu, J.J.; Fujikawa, K.; McMullen, B.A.; Chung, D.W.: Characterization of a core binding site for ADAMTS-13 in the A_2 domain of von Willebrand factor. Proc. Natl. Acad. Sci. USA, **103**, 18470-18474 (2006)
[46] Gao, W.; Anderson, P.J.; Majerus, E.M.; Tuley, E.A.; Sadler, J.E.: Exosite interactions contribute to tension-induced cleavage of von Willebrand factor by the antithrombotic ADAMTS13 metalloprotease. Proc. Natl. Acad. Sci. USA, **103**, 19099-19104 (2006)

[47] Shenkman, B.; Budde, U.; Angerhaus, D.; Lubetsky, A.; Savion, N.; Seligsohn, U.; Varon, D.: ADAMTS-13 regulates platelet adhesion under flow. A new method for differentiation between inherited and acquired thrombotic thrombocytopenic purpura. Thromb. Haemost., **96**, 160-166 (2006)
[48] Fuchigami, S.; Kaikita, K.; Soejima, K.; Matsukawa, M.; Honda, T.; Tsujita, K.; Nagayoshi, Y.; Kojima, S.; Nakagaki, T.; Sugiyama, S.; Ogawa, H.: Changes in plasma von Willebrand factor-cleaving protease (ADAMTS13) levels in patients with unstable angina. Thromb. Res., **122**, 618-623 (2008)
[49] Gunther, K.; Garizio, D.; Nesara, P.: ADAMTS13 activity and the presence of acquired inhibitors in human immunodeficiency virus-related thrombotic thrombocytopenic purpura. Transfusion, **47**, 1710-1716 (2007)
[50] Gao, W.; Anderson, P.J.; Sadler, J.E.: Extensive contacts between ADAMTS13 exosites and von Willebrand factor domain A2 contribute to substrate specificity. Blood, **112**, 1713-1719 (2008)
[51] Zhou, W.; Tsai, H.M.: N-Glycans of ADAMTS13 modulate its secretion and von Willebrand factor cleaving activity. Blood, **113**, 929-935 (2009)
[52] Pruss, C.M.; Notley, C.R.; Hegadorn, C.A.; OBrien, L.A.; Lillicrap, D.: ADAMTS13 cleavage efficiency is altered by mutagenic and, to a lesser extent, polymorphic sequence changes in the A1 and A2 domains of von Willebrand factor. Br. J. Haematol., **143**, 552-558 (2008)
[53] Chauhan, A.K.; Kisucka, J.; Brill, A.; Walsh, M.T.; Scheiflinger, F.; Wagner, D.D.: ADAMTS13: a new link between thrombosis and inflammation. J. Exp. Med., **205**, 2065-2074 (2008)
[54] Bongers, T.N.; de Bruijne, E.L.; Dippel, D.W.; de Jong, A.J.; Deckers, J.W.; Poldermans, D.; de Maat, M.P.; Leebeek, F.W.: Lower levels of ADAMTS13 are associated with cardiovascular disease in young patients. Atherosclerosis, **207**, 250-254 (2009)
[55] Akiyama, M.; Takeda, S.; Kokame, K.; Takagi, J.; Miyata, T.: Production, crystallization and preliminary crystallographic analysis of an exosite-containing fragment of human von Willebrand factor-cleaving proteinase ADAMTS13. Acta Crystallogr. Sect. F, **65**, 739-742 (2009)
[56] Pereboom, I.T.; Adelmeijer, J.; van Leeuwen, Y.; Hendriks, H.G.; Porte, R.J.; Lisman, T.: Development of a severe von Willebrand factor/ADAMTS13 dysbalance during orthotopic liver transplantation. Am. J. Transplant., **9**, 1189-1196 (2009)
[57] de Mast, Q.; Groot, E.; Asih, P.B.; Syafruddin, D.; Oosting, M.; Sebastian, S.; Ferwerda, B.; Netea, M.G.; de Groot, P.G.; van der Ven, A.J.; Fijnheer, R.: ADAMTS13 deficiency with elevated levels of ultra-large and active von Willebrand factor in P. falciparum and P. vivax malaria. Am. J. Trop. Med. Hyg., **80**, 492-498 (2009)
[58] Moriki, T.; Maruyama, I.N.; Igari, A.; Ikeda, Y.; Murata, M.: Identification of ADAMTS13 peptide sequences binding to von Willebrand factor. Biochem. Biophys. Res. Commun., **391**, 783-788 (2010)
[59] Scully, M.: Inhibitory anti-ADAMTS 13 antibodies: measurement and clinical application. Blood Rev., **24**, 11-16 (2010)

[60] Gardner, M.; Chion, C.; Groot, R.; Shah, A.; Crawley, J.; Lane, D.: A functional calcium-binding site in the metalloprotease domain of ADAMTS13. Blood, **113**, 1149-1157 (2009)
[61] Laje, P.; Shang, D.; Cao, W.; Niiya, M.; Endo, M.; Radu, A.; DeRogatis, N.; Scheiflinger, F.; Zoltick, P.W.; Flake, A.W.; Zheng, X.L.: Correction of murine ADAMTS13 deficiency by hematopoietic progenitor cell-mediated gene therapy. Blood, **113**, 2172-2180 (2009)
[62] Banno, F.; Chauhan, A.; Kokame, K.; Yang, J.; Miyata, S.; Wagner, D.; Miyata, T.: The distal carboxyl-terminal domains of ADAMTS13 are required for regulation of in vivo thrombus formation. Blood, **113**, 5323-5329 (2009)
[63] Zheng, X.: A team player: The disintegrin domain of ADAMTS13. Blood, **113**, 5373-5374 (2009)
[64] de Groot, R.; Bardhan, A.; Ramroop, N.; Lane, D.A.; Crawley, J.T.: Essential role of the disintegrin-like domain in ADAMTS13 function. Blood, **113**, 5609-5616 (2009)
[65] Raife, T.J.; Cao, W.; Atkinson, B.S.; Bedell, B.; Montgomery, R.R.; Lentz, S.R.; Johnson, G.F.; Zheng, X.L.: Leukocyte proteases cleave von Willebrand factor at or near the ADAMTS13 cleavage site. Blood, **114**, 1666-1674 (2009)
[66] Zanardelli, S.; Chion, A.C.; Groot, E.; Lenting, P.J.; McKinnon, T.A.; Laffan, M.A.; Tseng, M.; Lane, D.A.: A novel binding site for ADAMTS13 constitutively exposed on the surface of globular VWF. Blood, **114**, 2819-2828 (2009)
[67] Zhao, B.Q.; Chauhan, A.K.; Canault, M.; Patten, I.S.; Yang, J.J.; Dockal, M.; Scheiflinger, F.; Wagner, D.D.: von Willebrand factor-cleaving protease ADAMTS13 reduces ischemic brain injury in experimental stroke. Blood, **114**, 3329-3334 (2009)
[68] Feys, H.B.; Pareyn, I.; Vancraenenbroeck, R.; De Maeyer, M.; Deckmyn, H.; Van Geet, C.; Vanhoorelbeke, K.: Mutation of the H-bond acceptor S119 in the ADAMTS13 metalloprotease domain reduces secretion and substrate turnover in a patient with congenital thrombotic thrombocytopenic purpura. Blood, **114**, 4749-4752 (2009)
[69] Turner, N.A.; Nolasco, L.; Ruggeri, Z.M.; Moake, J.L.: Endothelial cell ADAMTS-13 and VWF: production, release, and VWF string cleavage. Blood, **114**, 5102-5111 (2009)
[70] Zheng, X.: ADAMTS13 testing: Why bother?. Blood, **115**, 1475-1476 (2010)
[71] Pos, W.; Crawley, J.T.; Fijnheer, R.; Voorberg, J.; Lane, D.A.; Luken, B.M.: An autoantibody epitope comprising residues R660, Y661, and Y665 in the ADAMTS13 spacer domain identifies a binding site for the A_2 domain of VWF. Blood, **115**, 1640-1649 (2010)
[72] Fujioka, M.; Hayakawa, K.; Mishima, K.; Kunizawa, A.; Irie, K.; Higuchi, S.; Nakano, T.; Muroi, C.; Fukushima, H.; Sugimoto, M.; Banno, F.; Kokame, K.; Miyata, T.; Fujiwara, M.; Okuchi, K.; Nishio, K.: ADAMTS13 gene deletion aggravates ischemic brain damage: a possible neuroprotective role of ADAMTS13 by ameliorating postischemic hypoperfusion. Blood, **115**, 1650-1653 (2010)

[73] Jin, S.Y.; Skipwith, C.G.; Zheng, X.L.: Amino acid residues Arg(659), Arg(660), and Tyr(661) in the spacer domain of ADAMTS13 are critical for cleavage of von Willebrand factor. Blood, **115**, 2300-2310 (2010)
[74] McGrath, R.T.; McKinnon, T.A.; Byrne, B.; OKennedy, R.; Terraube, V.; McRae, E.; Preston, R.J.; Laffan, M.A.; ODonnell, J.S.: Expression of terminal α2-6-linked sialic acid on von Willebrand factor specifically enhances proteolysis by ADAMTS13. Blood, **115**, 2666-2673 (2010)
[75] Wu, T.; Lin, J.; Cruz, M.A.; Dong, J.F.; Zhu, C.: Force-induced cleavage of single VWFA1A2A3 tridomains by ADAMTS-13. Blood, **115**, 370-378 (2010)
[76] Rayes, J.; Hollestelle, M.J.; Legendre, P.; Marx, I.; de Groot, P.G.; Christophe, O.D.; Lenting, P.J.; Denis, C.V.: Mutation and ADAMTS13-dependent modulation of disease severity in a mouse model for von Willebrand disease type 2B. Blood, **115**, 4870-4877 (2010)
[77] Chen, J.; Fu, X.; Wang, Y.; Ling, M.; McMullen, B.; Kulman, J.; Chung, D.W.; Lopez, J.A.: Oxidative modification of von Willebrand factor by neutrophil oxidants inhibits its cleavage by ADAMTS13. Blood, **115**, 706-712 (2010)
[78] Claus, R.A.; Bockmeyer, C.L.; Sossdorf, M.; Loesche, W.: The balance between von-Willebrand factor and its cleaving protease ADAMTS13: biomarker in systemic inflammation and development of organ failure?. Curr. Mol. Med., **10**, 236-248 (2010)
[79] Lancellotti, S.; De Filippis, V.; Pozzi, N.; Peyvandi, F.; Palla, R.; Rocca, B.; Rutella, S.; Pitocco, D.; Mannucci, P.M.; De Cristofaro, R.: Formation of methionine sulfoxide by peroxynitrite at position 1606 of von Willebrand factor inhibits its cleavage by ADAMTS-13: a new prothrombotic mechanism in diseases associated with oxidative stress. Free Radic. Biol. Med., **48**, 446-456 (2010)
[80] Trionfini, P.; Tomasoni, S.; Galbusera, M.; Motto, D.; Longaretti, L.; Corna, D.; Remuzzi, G.; Benigni, A.: Adenoviral-mediated gene transfer restores plasma ADAMTS13 antigen and activity in ADAMTS13 knockout mice. Gene Ther., **16**, 1373-1379 (2009)
[81] Palla, R.; Lavoretano, S.; Lombardi, R.; Garagiola, I.; Karimi, M.; Afrasiabi, A.; Ramzi, M.; De Cristofaro, R.; Peyvandi, F.: The first deletion mutation in the TSP1-6 repeat domain of ADAMTS13 in a family with inherited thrombotic thrombocytopenic purpura. Haematologica, **94**, 289-293 (2009)
[82] Lotta, L.A.; Garagiola, I.; Palla, R.; Cairo, A.; Peyvandi, F.: ADAMTS13 mutations and polymorphisms in congenital thrombotic thrombocytopenic purpura. Hum. Mutat., **31**, 11-19 (2010)
[83] Kato, R.; Shinohara, A.; Sato, J.: ADAMTS13 deficiency, an important cause of thrombocytopenia during pregnancy. Int. J. Obstet. Anesth., **18**, 73-77 (2009)
[84] Kosugi, N.; Tsurutani, Y.; Isonishi, A.; Hori, Y.; Matsumoto, M.; Fujimura, Y.: Influenza A infection triggers thrombotic thrombocytopenic purpura by producing the anti-ADAMTS13 IgG inhibitor. Intern. Med., **49**, 689-693 (2010)

[85] Vomund, A.N.; Majerus, E.M.: ADAMTS13 bound to endothelial cells exhibits enhanced cleavage of von Willebrand factor. J. Biol. Chem., **284**, 30925-30932 (2009)
[86] Dwyre, D.M.; Dursteler, B.; Nashelsky, M.; Friedman, K.D.; Raife, T.J.: Value of ADAMTS13 activity and inhibitor in the postmortem diagnosis of thrombotic thrombocytopenic purpura. J. Clin. Apher., **24**, 106-110 (2009)
[87] Park, Y.A.; Hay, S.N.; King, K.E.; Matevosyan, K.; Poisson, J.; Powers, A.; Sarode, R.; Shaz, B.; Brecher, M.E.: Is it quinine TTP/HUS or quinine TMA? ADAMTS13 levels and implications for therapy. J. Clin. Apher., **24**, 115-119 (2009)
[88] Park, Y.A.; Hay, S.N.; Brecher, M.E.: ADAMTS13 activity levels in patients with human immunodeficiency virus-associated thrombotic microangiopathy and profound CD_4 deficiency. J. Clin. Apher., **24**, 32-36 (2009)
[89] Varadi, K.; Rottensteiner, H.; Vejda, S.; Weber, A.; Muchitsch, E.M.; Turecek, P.L.; Ehrlich, H.J.; Scheiflinger, F.; Schwarz, H.P.: Species-dependent variability of ADAMTS13-mediated proteolysis of human recombinant von Willebrand factor. J. Thromb. Haemost., **7**, 1134-1142 (2009)
[90] Hughes, C.; McEwan, J.R.; Longair, I.; Hughes, S.; Cohen, H.; Machin, S.; Scully, M.: Cardiac involvement in acute thrombotic thrombocytopenic purpura: association with troponin T and IgG antibodies to ADAMTS 13. J. Thromb. Haemost., **7**, 529-536 (2009)
[91] Lerolle, N.; Dunois-Larde, C.; Badirou, I.; Motto, D.G.; Hill, G.; Bruneval, P.; Diehl, J.L.; Denis, C.V.; Baruch, D.: von Willebrand factor is a major determinant of ADAMTS-13 decrease during mouse sepsis induced by cecum ligation and puncture. J. Thromb. Haemost., **7**, 843-850 (2009)
[92] Niiya, M.; Endo, M.; Shang, D.; Zoltick, P.; Muvarak, N.; Cao, W.; Jin, S.; Skipwith, C.; Motto, D.; Flake, A.; Zheng, X.: Correction of ADAMTS13 deficiency by in utero gene transfer of lentiviral vector encoding ADAMTS13 genes. Mol. Ther., **17**, 34-41 (2009)
[93] Meng, H.; Zhang, X.; Blaivas, M.; Wang, M.M.: Localization of blood proteins thrombospondin1 and ADAMTS13 to cerebral corpora amylacea. Neuropathology, **29**, 664-671 (2009)
[94] Manea, M.; Tati, R.; Karlsson, J.; Bekassy, Z.; Karpman, D.: Biologically active ADAMTS13 is expressed in renal tubular epithelial cells. Pediatr. Nephrol., **25**, 87-96 (2010)
[95] Sauna, Z.E.; Okunji, C.; Hunt, R.C.; Gupta, T.; Allen, C.E.; Plum, E.; Blaisdell, A.; Grigoryan, V.; Geetha, S.; Fathke, R.; Soejima, K.; Kimchi-Sarfaty, C.: Characterization of conformation-sensitive antibodies to ADAMTS13, the von Willebrand cleavage protease. PLoS ONE, **4**, e6506 (2009)
[96] Larkin, D.; de Laat, B.; Jenkins, P.V.; Bunn, J.; Craig, A.G.; Terraube, V.; Preston, R.J.; Donkor, C.; Grau, G.E.; van Mourik, J.A.; ODonnell, J.S.: Severe Plasmodium falciparum malaria is associated with circulating ultralarge von Willebrand multimers and ADAMTS13 inhibition. PLoS Pathog., **5**, e1000349 (2009)
[97] Akiyama, M.; Takeda, S.; Kokame, K.; Takagi, J.; Miyata, T.: Crystal structures of the noncatalytic domains of ADAMTS13 reveal multiple discon-

tinuous exosites for von Willebrand factor. Proc. Natl. Acad. Sci. USA, **106**, 19274-19279 (2009)
[98] Bresin, E.; Gastoldi, S.; Daina, E.; Belotti, D.; Pogliani, E.; Perseghin, P.; Scalzulli, P.R.; Paolini, R.; Marceno, R.; Remuzzi, G.; Galbusera, M.: Rituximab as pre-emptive treatment in patients with thrombotic thrombocytopenic purpura and evidence of anti-ADAMTS13 autoantibodies. Thromb. Haemost., **101**, 233-238 (2009)
[99] Uemura, T.; Kaikita, K.; Yamabe, H.; Soejima, K.; Matsukawa, M.; Fuchigami, S.; Tanaka, Y.; Morihisa, K.; Enomoto, K.; Sumida, H.; Sugiyama, S.; Ogawa, H.: Changes in plasma von Willebrand factor and ADAMTS13 levels associated with left atrial remodeling in atrial fibrillation. Thromb. Res., **124**, 28-32 (2009)
[100] Kobayashi, T.; Wada, H.; Usui, M.; Sakurai, H.; Matsumoto, T.; Nobori, T.; Katayama, N.; Uemoto, S.; Ishizashi, H.; Matsumoto, M.; Fujimura, Y.; Isaji, S.: Decreased ADAMTS13 levels in patients after living donor liver transplantation. Thromb. Res., **124**, 541-545 (2009)
[101] Hyun, J.; Kim, H.K.; Kim, J.E.; Lim, M.G.; Jung, J.S.; Park, S.; Cho, H.I.: Correlation between plasma activity of ADAMTS-13 and coagulopathy, and prognosis in disseminated intravascular coagulation. Thromb. Res., **124**, 75-79 (2009)
[102] Schettert, I.T.; Pereira, A.C.; Lopes, N.H.; Hueb, W.A.; Krieger, J.E.: Association between ADAMTS13 polymorphisms and risk of cardiovascular events in chronic coronary disease. Thromb. Res., **125**, 61-66 (2010)
[103] Taniguchi, S.; Hashiguchi, T.; Ono, T.; Takenouchi, K.; Nakayama, K.; Kawano, T.; Kato, K.; Matsushita, R.; Nagatomo, M.; Nakamura, S.; Nakashima, T.; Maruyama, I.: Association between reduced ADAMTS13 and diabetic nephropathy. Thromb. Res., **125**, e310-e316 (2010)
[104] George, J.: ADAMTS13: What it does, how it works, and why its important. Transfusion, **49**, 196-198 (2009)
[105] Davis, A.K.; Makar, R.S.; Stowell, C.P.; Kuter, D.J.; Dzik, W.H.: ADAMTS13 binds to CD36: a potential mechanism for platelet and endothelial localization of ADAMTS13. Transfusion, **49**, 206-213 (2009)
[106] Rossi, F.C.; Angerami, R.N.; de Paula, E.V.; Orsi, F.L.; Shang, D.; del Guercio, V.M.; Resende, M.R.; Annichino-Bizzacchi, J.M.; da Silva, L.J.; Zheng, X.L.; Castro, V.: A novel association of acquired ADAMTS13 inhibitor and acute dengue virus infection. Transfusion, **50**, 208-212 (2010)

HslU-HslV peptidase 3.4.25.2

1 Nomenclature

EC number
3.4.25.2

Recommended name
HslU-HslV peptidase

Synonyms
AAA+ HslUV protease <4> [36]
ATP-dependent protease <4> [49]
ATP-dependent protease hslV
ClpQ
ClpYQ <1,2,4> [32,36,43,47]
ClpYQ complex <4> [49]
ClpYQ protease <4> [35,47]
CodW <3> [41]
CodW-CodX <3> [31]
HslU ATPase <4> [33]
HslU chaperone <4> [37]
HslUV <2,4> [33,34,36,43,45,47]
HslUV complex <4> [37,49]
HslUV protease <4> [35,45,47]
HslUV protease-chaperone complex <2> [34]
HslV peptidase <4> [33,37]
HslV protease <2,4,6> [37,40,48]
HslV-HslU <4> [31]
HslVU ATP-dependent protease <4> [48]
HslVU protease <4> [39]
PfHslUV <5> [44]
T01.006 (Merops-ID)
heat shock protein hslV
hslVU <4> (<4> ATP-dependent protease consisting of two heat shock proteins, the HslU ATPase and HslV peptidase [38,46]) [38,42,46]

CAS registry number
178303-43-0

D. Schomburg and I. Schomburg (eds.), *Class 3.4–6 Hydrolases, Lyases, Isomerases, Ligases: EC 3.4–6*, Springer Handbook of Enzymes S10, DOI 10.1007/978-3-642-36260-6_9,

2 Source Organism

<1> *Staphylococcus aureus* [32]
<2> *Haemophilus influenzae* [28,29,34,40,43]
<3> *Bacillus subtilis* [31,41]
<4> *Escherichia coli* [10,11,12,13,14,15,16,17,18,19,20,21,22,23,24,25,26,27,31,33,35,36,37,38,39,40,42,43,45,46,47,48,49]
<5> *Plasmodium falciparum* [44]
<6> *Thermotoga maritima* [40]
<7> *Shigella flexneri* [30]
<8> *Escherichia coli* (UNIPROT accession number: P0A7B8) (subunit p110 [3,8]) [3,6,7,8,9]
<9> *Escherichia coli* (UNIPROT accession number: Q8FBC0) [21]
<10> *Shigella flexneri* (UNIPROT accession number: P0A7C1) [2]
<11> *Escherichia coli* (UNIPROT accession number: P0A7C0) [4,5]
<12> *Escherichia coli* (UNIPROT accession number: P0A7B9) [1]

3 Reaction and Specificity

Catalyzed reaction
ATP-dependent cleavage of peptide bonds with broad specificity. (<4> model for a proteolytic cycle by HslVU protease, overview [48])

Reaction type
hydrolysis of peptide bond

Natural substrates and products
S DnaA204-protein + H_2O <4> (<4> the degradation of the DnaA204 protein contributes to the temperature sensitivity of the dna204 strain [19]) (Reversibility: ?) [19]
P ?
S RcsA + H_2O <4> (<4> specific substrate degradation, the enzyme is involved in regulation of RcsA, a capsule synthesis activator, the ClpYQ protease acts as a secondary protease in degrading the Lon protease substrate RscA [35]) (Reversibility: ?) [35]
P ?
S SulA + H_2O <2,4> (<4> degradation [48]; <2,4> specific substrate degradation [33,34,35]) (Reversibility: ?) [33,34,35,48]
P ?
S SulA + H_2O <4> (<4> hslVU in addition to Lon plays an important role in regulation of cell division through degradation of SulA [20]) (Reversibility: ?) [17,20]
P Additional information <4> (<4> the enzyme produces 58 peptides with various sizes, 3-31 residues [17]) [17]
S TraJ + H_2O <4> (<4> TraJ appears to be a substrate for HslVU throughout the growth cycle, but is protected or modified by a factor encoded by

the F transfer region in the absence of stress. Activation of the Cpx regulon destabilizes the F plasmid transfer activator, TraJ, via the HslVU protease [39]) (Reversibility: ?) [39]

P ?

S puromycylpolypeptide + H_2O <4> (<4> HslV and HslU interact and participate in the degradation of misfolded puromycylpolypeptides [24]) (Reversibility: ?) [24]

P ?

S Additional information <1,4,5,8> (<8> hslV and hslU are coregulated. It is possible that ATPase HslU and protease HslV are involved in an ATP/GTP-dependent protein metabolism [8]; <1> ClpYQ plays a minor role in stress survival and is required for growth at high temperature of 45°C [32]; <4> the GYVG motif of HslU is important in unfolding of natively folded proteins as well as in translocation of unfolded proteins for degradation by HslV in its inner chamber [33]; <5> the HslUV complex is an assembly of heat shock locus gene products U and V. The formation of the complete complex is essential for the proteasome to carry out its biochemical and physiological role in the parasite, namely to degrade specific target proteins in an ATP-dependent chaperone assisted manner [44]; <4> ClpQ and ClpY are two heat shock proteins [49]; <4> in vivo, ClpYQ targets SulA, RcsA, RpoH, and TraJ molecules, identification of the molecular determinants required for the binding of its natural protein substrates by yeast two-hybrid analysis. Domain I of ClpY contains the residues, amino acids 137-150 of loop 1 and 175-209 of loop 2, double loops in domain I of ClpY, that are responsible for recognition of its natural substrates, while domain C is necessary to engage ClpQ, overview [47]) (Reversibility: ?) [8,32,33,44,47,49]

P ?

Substrates and products

S ATP + H_2O <4> (Reversibility: ?) [33]

P ADP + phosphate

S Arc + H_2O <4> (<4> degradation [48]; <4> repressor protein, specific degradation, especially at heat shock temperatures, recognition of sequences near the N-terminus of Arc and strong binding requiring Mg^{2+} and ATP for degradation [36]) (Reversibility: ?) [36,48]

P ?

S Arc mutant I137A + H_2O <4> (<4> monomeric mutant, degradation [48]) (Reversibility: ?) [48]

P ?

S Arc-MYL-st11 + H_2O <4> (<4> recombinant Arc fusion protein [36]) (Reversibility: ?) [36]

P ?

S Arc-MYL-st11 plus + H_2O <4> (<4> recombinant Arc fusion protein [36]) (Reversibility: ?) [36]

P ?

S Arc1-53-st11-titin-ssrA + H_2O <4> (<4> recombinant truncated Arc fusion protein [36]) (Reversibility: ?) [36]
P ?
S DnaA204-protein + H_2O <4> (<4> the degradation of the DnaA204 protein contributes to the temperature sensitivity of the dna204 strain [19]) (Reversibility: ?) [19]
P ?
S Insulin B-chain + H_2O <4> (<4> HslVU degrades insulin B-chain even more rapidly in the presence of ATPγS than with ATP [11]) (Reversibility: ?) [11,27]
P ?
S N-carbobenzyloxy-Gly-Gly-Leu-7-amido-4-methylcoumarin + H_2O <4> (Reversibility: ?) [33,37]
P N-carbobenzyloxy-Gly-Gly-Leu + 7-amino-4-methylcoumarin
S RcsA + H_2O <4> (<4> positive regulator of capsule transcription, RcsA [15]; <4> specific substrate degradation, the enzyme is involved in regulation of RcsA, a capsule synthesis activator, the ClpYQ protease acts as a secondary protease in degrading the Lon protease substrate RscA [35]; <4> specific substrate degradation, the enzyme is involved in regulation of RcsA, a capsule synthesis activator [35]) (Reversibility: ?) [15,35]
P ?
S RpoH + H_2O <4> (<4> RpoH is a heat shock sigma transcription factor [15]) (Reversibility: ?) [15]
P ?
S SulA + H_2O <2,4> (<4> degradation [48]; <2,4> specific substrate degradation [33,34,35]; <2> specific substrate degradation, activities with SulA mutant protein substrates F10A, I37V, and P8L [34]; <4> specific substrate degradation, the substrate is a cell division inhibitor [35]; <4> recombinant substrate, produced as maltose-binding fusion protein and cleaved by factorXa [48]) (Reversibility: ?) [33,34,35,48]
P ?
S SulA + H_2O <4,9> (<4> the central and the C-terminal regions are preferentially cleaved. Major cleavage sites: Ala80-Ser81, Ala150-Ser151, Leu54-Gln55, Ile163-His164, Leu67-Thr68, Leu49-Leu50, Leu65-Trp66. No cleavage in absence of ATP [17]; <4> cell division inhibitor SulA, the internal region of SulA is necessary for interactions with ClpY, the N-terminal amino acid residues of SulA are not necessary [15]; <4> hslVU in addition to Lon plays an important role in regulation of cell division through degradation of SulA [20]) (Reversibility: ?) [15,16,17,20,21]
P Additional information <4> (<4> the enzyme produces 58 peptides with various sizes, 3-31 residues [17]) [17]
S SulA-maltose binding protein-fusion protein + H_2O <4> (<4> recombinant substrate, formation of a ternary complex of HslV-HslU-substrate during reaction, molecular interaction study, interaction via HslU, not HslV [37]; <4> recombinant substrate, specific substrate degradation requires the flexibility provided by glycine residues and aromatic ring structures of the first 91 amino acids [33]) (Reversibility: ?) [33,37]

P ?
S TraJ + H_2O <4> (<4> TraJ appears to be a substrate for HslVU throughout the growth cycle, but is protected or modified by a factor encoded by the F transfer region in the absence of stress. Activation of the Cpx regulon destabilizes the F plasmid transfer activator, TraJ, via the HslVU protease [39]) (Reversibility: ?) [39]
P ?
S α-casein + H_2O <4> (<4> degradation [48]; <4> interaction via HslV intact active site [37]; <4> the structural features of the GYVG motif increase degrading activity [33]) (Reversibility: ?) [33,37,48]
P ?
S barnase-DHFR fusion proteins + H_2O <2,4> (Reversibility: ?) [43]
P ?
S benzyloxycarbonyl-GGL-7-amido-4-methylcoumarin + H_2O <2,4,8,9> (<4> HslV alone cleaves to a much lesser extent than in presence of HslU [10]) (Reversibility: ?) [9,10,11,14,16,18,21,27,28,29]
P benzyloxycarbonyl-GGL + 7-amino-4-methylcoumarin
S benzyloxycarbonyl-Gly-Gly-Leu-7-amido-4-methylcoumarin + H_2O <4> (<4> the N-terminal Thr active sites of HslV are involved in the communication between HslV and HslU in addition to its role in the catalysis of peptide bond cleavage [42]) (Reversibility: ?) [42]
P ?
S benzyloxycarbonyl-Gly-Gly-Leu-7-amido-4-methylcoumarin + H_2O <4> (Reversibility: ?) [45]
P ?
S carboxymethylated lactalbumin + H_2O <4> (Reversibility: ?) [27]
P ?
S casein + H_2O <2,4,9> (Reversibility: ?) [14,16,21,26,27,28]
P ?
S fusion protein of SulA and maltose-binding protein + H_2O <4> (Reversibility: ?) [20]
P ?
S gt1 + H_2O <4> (<4> substrate of HslU [36]) (Reversibility: ?) [36]
P ?
S puromycylpolypeptide + H_2O <4> (<4> HslV and HslU interact and participate in the degradation of misfolded puromycylpolypeptides [24]) (Reversibility: ?) [24]
P ?
S succinyl-LLVY-7-amido-4-methylcoumarin + H_2O <4> (Reversibility: ?) [10]
P succinyl-LLVY + 7-amino-4-methylcoumarin
S unfolded lactalbumin + H_2O <4> (<4> HslV alone can efficiently degrade certain unfolded proteins, such as unfolded lactalbumin and lysozyme prepared by complete reduction of disulfide bonds, but not their native forms. HslV alone cleaves a lactalbumin fragment sandwiched by two thioredoxin molecules, indicating that it can hydrolyze the internal peptide bonds of lactalbumin. Uncomplexed HslV is inactive under normal

conditions, but can degrade unfolded proteins when the ATP level is low, as it is during carbon starvation [38]) (Reversibility: ?) [38]

P ?

S unfolded lysozyme + H_2O <4> (<4> HslV alone can efficiently degrade certain unfolded proteins, such as unfolded lactalbumin and lysozyme prepared by complete reduction of disulfide bonds, but not their native forms. HslV alone cleaved a lactalbumin fragment sandwiched by two thioredoxin molecules, indicating that it can hydrolyze the internal peptide bonds of lactalbumin. Uncomplexed HslV is inactive under normal conditions, but can degrade unfolded proteins when the ATP level is low, as it is during carbon starvation [38]) (Reversibility: ?) [38]

P ?

S Additional information <1,2,4,5,8> (<4> no hydrolysis of γ-globulin, lysozyme and bovine serum albumin [27]; <4> HslV and HslU can function together as a novel ATP-dependent protease, the HslVU protease. Pure HslV is a weak peptidase degrading certain hydrophobic peptides. HslU dramatically stimulates peptide hydrolysis by HslV when ATP is present. With a 1:4 molar ratio of HslV to HslU, approximately a 200fold increase in peptide hydrolysis is observed. HslV stimulates the ATPase activity of HslU 2-4fold. CTP and dATP are slowly hydrolyzed by HslU and allow some peptide hydrolysis [10]; <4> ATP-binding, but not its hydrolysis, is essential for assembly and proteolytic activity of HslVU [11]; <4> less than 1% of the activity with benzyloxycarbonyl-GGL-7-amido-4-methylcoumarin is observed with succinyl-AAF$^-$7-amido-4-methylcoumarin and succinyl-LLVY-7-amido-4-methylcoumarin. No activity with benzoyl-RGFFL-4-methoxy-β-naphthylamide, glutaryl-AAA-4-methoxy-β-naphthylamide, benzyloxycarbonyl-LLE-4-methoxy-β-naphthylamide, succinyl-FLF-β-naphthylamide, succinyl-LY-7-amido-4-methylcoumarin, benzoyl-GP-7-amido-4-methylcoumarin, acetyl-YVAA-7-amido-4-methylcoumarin, tert-butyloxycarbonyl-LRR-7-amido-4-methylcoumarin, t-butyloxycarbonyl-FVR-7-amido-4-methylcoumarin, benzoyl-GGR-7-amido-4-methylcoumarin, benzoyl-Arg-7-amido-4-methylcoumarin [18]; <8> hslV and hslU are coregulated. It is possible that ATPase HslU and protease HslV are involved in an ATP/GTP-dependent protein metabolism [8]; <1> ClpYQ plays a minor role in stress survival and is required for growth at high temperature of 45°C [32]; <4> the GYVG motif of HslU is important in unfolding of natively folded proteins as well as in translocation of unfolded proteins for degradation by HslV in its inner chamber [33]; <4> analysis of interaction of free and inhibited HslV with HslU showing moderate affinity, scheme of substrate-induced HslUV assemblage, overview [37]; <4> substrate binding, ATP-dependent protein degradation, and reaction mechanism, substrate engagement must occur after ATP-binding before HslUV unfolds the proteins, overview [36]; <2> the enzyme degrades only the SulA moiety of recombinant fusion proteins, the fused proteins, e.g. the green fluorescent protein, are not hydrolyzed [34]; <5> the HslUV complex is an assembly of heat shock locus gene products U and V. The formation of the complete complex is essential for the proteasome to carry out its bio-

chemical and physiological role in the parasite, namely to degrade specific target proteins in an ATP-dependent chaperone assisted manner [44]; <2,4> degradation of proteins in an ATP-dependent and tag-specific manner. For degradation from the N-terminus, HslUV has the strongest unfolding ability of all the bacterial proteases (unfolding abilities of the 26S proteasome), whereas for degradation from the C-terminus, HslUV is one of the weaker unfoldases. HslUV unfolds proteins more effectively when degrading from the N- towards the C-terminus than in the opposite direction [43]; <4> HslVU is an ATP-dependent protease consisting of two heat shock proteins, the HslU ATPase and HslV peptidase. In the reconstituted enzyme, HslU stimulates the proteolytic activity of HslV by one to two orders of magnitude, while HslV increases the rate of ATP hydrolysis by HslU several-fold. HslV alone can efficiently degrade certain unfolded proteins, such as unfolded lactalbumin and lysozyme prepared by complete reduction of disulfide bonds, but not their native forms. HslV alone cleaves a lactalbumin fragment sandwiched by two thioredoxin molecules, indicating that it can hydrolyze the internal peptide bonds of lactalbumin. Uncomplexed HslV is inactive under normal conditions, but can degrade unfolded proteins when the ATP level is low, as it is during carbon starvation [46]; <4> ClpQ and ClpY are two heat shock proteins [49]; <4> in vivo, ClpYQ targets SulA, RcsA, RpoH, and TraJ molecules, identification of the molecular determinants required for the binding of its natural protein substrates by yeast two-hybrid analysis. Domain I of ClpY contains the residues, amino acids 137-150 of loop 1 and 175-209 of loop 2, double loops in domain I of ClpY, that are responsible for recognition of its natural substrates, while domain C is necessary to engage ClpQ, overview [47]; <4> ClpYQ is a two-component ATP-dependent protease in which ClpQ is the peptidase subunit and ClpY is the ATPase and the substrate-binding subunit. The ATP-dependent proteolysis is mediated by substrate recognition in the ClpYQ complex [47]; <4> HslVU is a bacterial ATP-dependent protease consisting of hexameric HslU ATPase and dodecameric HslV protease. HslV uses the N-terminal threonine as the active site residue. HslV has 12 active sites among the 14β-subunits that can potentially contribute to proteolytic activity, but only 6 active sites are sufficient to support full catalytic activity. Substrate-mediated stabilization of the HslV-HslU interaction [48]) (Reversibility: ?) [8,10,11,18,27,32,33,34,36,37, 43,44,46,47,48,49]

P ?

Inhibitors

3,4-dichloroisocoumarin <4> (<4> 0.2 mM, 50% inhibition [18]) [18]

ADP <4> (<4> when added together with ATP [18]) [18]

ATP <4> (<4> inhibits the degradation of unfolded proteins by HslV [38]; <4> inhibits the degradation of unfolded proteins by HslV. This inhibitory effect of ATP is markedly diminished by substitution of the Arg86 residue located in the apical pore of HslV with Gly, suggesting that interaction of ATP with the Arg residue blocks access of unfolded proteins to the proteolytic chamber of HslV [46]) [38,46]

N-acetyl-Leu-Leu-norleucinal <4> (<4> i.e. calpain inhibitor-I, inhibits HslV [37]) [37]
NEM <4> (<4> 0.1 mM, 62% inhibition [18]; <4> preincubation with followed by inactivation of dithiothreitol causes inhibition of peptide hydrolysis [10]) [10,18]
NLVS <4> (<4> in the presence of ATP, the proteasome inhibitor markedly increases the interaction between HslV and HslU and causes the activation of the HslU ATPase [48]) [48]
acety-Leu-Leu-norleucinal <4> (<4> 0.01 mM, 90% inhibition [18]) [18]
benzyloxycarbonyl-Ile-Glu(tert-butyl)-Ala-Leu-al <4> (<4> 0.001 mM, almost complete inhibition of peptidase activity, no inhibition of hydrolysis of insulin B-chain or other polypeptide substrates [27]) [27]
benzyloxycarbonyl-Leu-Leu-norleucinal <4> (<4> 0.01 mM, 97% inhibition [18]) [18]
benzyloxycarbonyl-Leu-Leu-norvalinal <4> (<4> 0.004 mM, inhibits hydrolysis of both benzyloxycarbonyl-GGL-7-amido-4-methylcoumarin and insulin B-chain to a similar extent [27]) [27]
diisopropyl fluorophosphate <4> (<4> 10 mM, about 70% inhibition [10]) [10]
dithiothreitol <4> [10]
lactacystin <4> (<4> 0.1 mM, 24% inhibition [18]; <4> irreversible, much greater inhibition of the degradation of insulin B-chain than on peptide hydrolysis [27]; <4> in the presence of ATP, the proteasome inhibitor markedly increases the interaction between HslV and HslU and causes the activation of the HslU ATPase [48]) [18,27,48]
phenylmethylsulfonyl fluoride <4> (<4> 1 mM, 10% inhibition [18]; <4> 2 mM, about 70% inhibition [10]) [10,17,18]
Additional information <4> (<4> the I125-labeled nitrophenyl derivative 125iodo-NIP-Leu-Leu-Leu vinyl sulfone covalently modifies and inhibits HslV, but only in presence of HslU and ATP [13]) [13]

Cofactors/prosthetic groups

5'-adenylyl β,γ-imidotriphosphate <4> (<4> the enzyme degrades SulA and the fusion protein of SulA and maltose-binding protein in presence of ATP but not with ATPγS [20]; <4> can support peptide hydrolysis, but only after an initial time lag not seen with ATP. This delay decreases at higher temperatures and with higher HslV or HslU concentrations and is eliminated by preincubation of HslV and HslU together [14]; <4> can support peptide hydrolysis, but only after an initial time lag not seen with ATP. This delay decreases at higher temperatures and with higher HslV or HslU concentrations and is eliminated by preincubation of HslV and HslU together. Supports hydrolysis of casein and other polypeptides only 20% as well as ATP. But in presence of K^+, Cs^+ or NH_4^+, activation of casein degradation is even better than that by ATP, although it is not hydrolyzed [14]) [14,20]
ATP <2,4> (<2,4> dependent on [34,37,47,48,49]; <4> ATP-binding, but not its hydrolysis, is essential for assembly and proteolytic activity of HslVU. The ability of ATP and its analogs in supporting the proteolytic activity is closely

correlated with their ability in supporting the oligomerization of HslU and the formation of the HslVU complex [11]; <4> ATP activates hydrolysis of benzyloxycarbonyl-GGL-7-amido-4-methylcoumarin 150fold [18]; <4> no cleavage of SulA in absence of ATP [17]; <4> HslV and HslU can function together as a novel ATP-dependent protease, the HslVU protease. Pure HslV is a weak peptidase degrading certain hydrophobic peptides. HslU dramatically stimulates peptide hydrolysis by HslV when ATP is present. With a 1:4 molar ratio of HslV to HslU, approximately a 200fold increase in peptide hydrolysis is observed. HslV stimulates the ATPase activity of HslU 2-4fold. CTP and dATP are slowly hydrolyzed by HslU and allow some peptide hydrolysis [10]; <4> the enzyme degrades SulA and the fusion protein of SulA and maltose-binding protein in presence of ATP but not with ATPγS [20]; <4> HslV can slowly hydrolyze insulin B-chain, casein or carboxymethylated lactalbumin, but its activity is stimulated 20fold by HslU in presence of ATP [27]; <4> ATP concentrations that activate hydrolysis of benzyloxycarbonyl-GGL-7-amido-4-methylcoumarin are 50-100fold lower than those necessary for degradation of proteins, e.g. casein. ATP binding to a high affinity site triggers the formation of an active state capable of peptide cleavage, although ATP hydrolysis facilitates this process [14]; <4> dependent on, HslU, ATP cleavage involves the pore motif GYVG [33]; <4> required, ATP [36]; <4> ATP binding and hydrolysis are critical for protein degradation by HslUV, an AAA+ machine containing one or two HslU ATPases and the HslV peptidase. Asymmetric mechanism of ATP binding and hydrolysis. Molecular contacts between HslU and HslV vary dynamically throughout the ATPase cycle. Nucleotide binding controls HslUV assembly and activity. Binding of a single ATP allows HslU to bind HslV, whereas additional ATPs must bind HslU to support substrate recognition and to activate ATP hydrolysis, which powers substrate unfolding and translocation [45]) [10,11,14,17,18,20,27,33,34,35,36,37,45,47,48,49]
ATPγS <4> (<4> HslVU degrades insulin B-chain more rapidly in the presence of ATPγS than with ATP [11]) [11]
adenosine 5'-(α,β-methylene)triphosphate <4> (<4> HslVU degrades insulin B-chain more rapidly in the presence of ATPγS than with ATP [11]) [11]
β,γ-Imido-ATP <4> (<4> supports proteolytic activity to an extent less than 10% of that seen with ATP [11]) [11]
Additional information <4> (<4> HslU requires Mg^{2+} together with ATP for activity [36]) [36]

Activating compounds

HslU <2,4,6> (<4> HslV can slowly hydrolyze insulin B-chain, casein or carboxymethylated lactalbumin, but its activity is stimulated 20fold by HslU in presence of ATP [27]; <2> HslV can be activated by binding of a hexameric HslU(ΔI)6 ring lacking the I domain. The activation is effected through a conformational change in hslV rather than through alteration of the size of the entry channel into the protease catalytic cavity. The two HslV6 rings in the protease dodecamer are activated independently rather than cooperatively [29]; <4> the HslU C-terminal tails act as a molecular switch for the assembly of HslVU complex and the activation of HslV peptidase [16]; <2> protease

HslV is activated by the ATPase HslU. Mutations in hslV that disrupt the interaction with the C termini of HslU invariably lead to inactive enzyme [28]; <2,4,6> HslV protomer interfaces perform distinct functions: whereas intraring interface participates in HslV:HslU interaction resulting in allosteric activation of HslV protease by HslU, the interring interfaces uphold the oligomeric form of HslV [40]) [16,27,28,29,40]

Metals, ions

$CaCl_2$ <4> (<4> allows some peptidase and caseinase activity in the absence of any nucleotide, however Ca^{2+} abolishes ATP hydrolysis and prevents further activation by ATP and 5-adenylyl β,γ-imidodiphosphate [14]) [14]
Cs^+ <4> (<4> stimulates 4-6fold the peptidase activity with 5-adenylyl β,γ-imidodiphosphate present and eliminates the time lag for activation, no stimulatory effect with ATP [14]) [14]
KCl <2,4> (<4> stimulates 4-6fold the peptidase activity with 5-adenylyl β,γ-imidodiphosphate present and eliminates the time lag for activation, no stimulatory effect with ATP [14]) [14,34]
Mg^{2+} <2,4> (<4> required [36]) [33,34,36,37]
$MgCl_2$ <4> (<4> allows some peptidase and caseinase activity in the absence of any nucleotide [14]) [14]
$MnCl_2$ <4> (<4> allows some peptidase and caseinase activity in the absence of any nucleotide, however Mn^{2+} abolishes ATP hydrolysis and prevents further activation by ATP and 5-adenylyl β,γ-imidodiphosphate [14]) [14]
NH_4^+ <4> (<4> stimulates 4-6fold the peptidase activity with 5-adenylyl β,γ-imidodiphosphate present and eliminates the time lag for activation, no stimulatory effect with ATP [14]) [14]
Additional information <4> (<4> HslU requires Mg^{2+} together with ATP for activity [36]) [36]

Turnover number (s^{-1})

0.033 <2> (SulA mutant P8L, <2> pH 5.5, 37°C, recombinant enzyme [34]) [34]
0.05 <2> (SulA, <2> pH 5.5, 37°C, wild-type SulA, recombinant enzyme [34]) [34]
0.063 <2> (SulA mutant F10A, <2> pH 5.5, 37°C, recombinant enzyme [34]) [34]
0.068 <2> (SulA mutant I37V, <2> pH 5.5, 37°C, recombinant enzyme [34]) [34]
0.077 <4> (Arc-MYL-st11 plus, <4> pH 7.6, 37°C, HslUV [36]) [36]
0.11 <4> (Arc-MYL-st11, <4> pH 7.6, 37°C, HslUV [36]) [36]
0.11 <4> (Arc1-53-st11-titin-ssrA, <4> pH 7.6, 37°C, HslUV [36]) [36]

K_m-Value (mM)

0.001 <2> (SulA mutant P8L, <2> pH 5.5, 37°C, recombinant enzyme [34]) [34]
0.0023 <2> (SulA, <2> pH 5.5, 37°C, wild-type SulA, recombinant enzyme [34]) [34]
0.0032 <2> (SulA mutant I37V, <2> pH 5.5, 37°C, recombinant enzyme [34]) [34]

0.0034 <2> (SulA mutant F10A, <2> pH 5.5, 37°C, recombinant enzyme [34]) [34]
0.004 <4> (Arc1-53-st11-titin-ssrA, <4> pH 7.6, 37°C, HslUV [36]) [36]
0.0052 <4> (Arc-MYL-st11, <4> pH 7.6, 37°C, HslUV [36]) [36]
0.014 <4> (insulin B-chain, <4> pH 8, 37°C [27]) [27]
0.04 <4> (Arc-MYL-st11 plus, <4> pH 7.6, 37°C, HslUV [36]) [36]
Additional information <4> (<4> Michaelis-Menten kinetics [36]; <4> kinetics, analysis of interaction of free and inhibited HslV with HslU [37]) [36,37]

pH-Optimum

7.5 <4> (<4> assay at [37]) [37]
7.6 <4> (<4> assay at [36]) [36]
7.8 <2> (<2> assay at [34]) [34]
8 <4> (<4> assay at [33,48]) [33,48]

Temperature optimum (°C)

30 <2,4> (<2,4> assay at [34,35]) [34,35]
37 <4> (<4> assay at [33,36,37,48]) [33,36,37,48]

4 Enzyme Structure

Molecular weight

220000 <4> (<4> gel filtration [26]; <4> ClpQ in presence of ATP [26]) [26]
250000 <4> (<4> purified HslV in presence or absence of ATP, gel filtration [10]) [10]

Subunits

? <4,8> (<4> x * 19000, HslV protein, SDS-PAGE [10]; <8> x * 19095, calculation from nucleotide sequence [8]) [8,10]
dimer <4> (<4> wild-type enzyme [36]) [36]
dodecamer <4,6> (<4> HslV, the proteolytic active sites are sequestered in the inner chamber of HslV [33]; <4> HslVU, a two-component proteasome-related prokaryotic system is composed of HslV protease and HslU ATPase. HslV protomers assemble in a dodecamer of two-stacked hexameric rings that form a complex with HslU hexamers. Structural analyses of protomer interfaces in HslV dodecamer suggests that HslV interfaces involve extensive area in which major determinants for function and stability constitute hot spots [40]; <6> HslVU, a two-component proteasome-related prokaryotic system is composed of HslV protease and HslU ATPase. HslV protomers assemble in a dodecamer of two-stacked hexameric rings that form a complex with HslU hexamers. Structural analysis of protomer interfaces in HslV dodecamer suggests that HslV interfaces involve extensive area in which major determinants for function and stability constitute hot spots [40]) [33,40]
hexamer <2,4> (<4> HslU [33]; <4> self-oligomerization of each ClpQ and ClpY, four hexamers constitute a dumb-bell-shaped complex ina Y6Q6Q6Y6 configuration [35]; <2> the HslU12HslV12 protease-chaperone complex [34]) [33,34,35]

monomer <4> (<4> recombinant mutant I37A, predominantly [36]) [36]
oligomer <4> (<4> HslVU is a bacterial ATP-dependent protease consisting of hexameric HslU ATPase and dodecameric HslV protease. HslV has 12 active sites among the 14β-subunits that can potentially contribute to proteolytic activity [48]) [48]
Additional information <4,5> (<4> HslVU protease is a two-component protease in which HslV harbors the peptidase activity, while HslU provides an essential ATPase activity [10]; <4> the crystal strcuture shows that HslU forms a hexamer with a pore at one end and HslV forms a dodecamer with translocation pores at both ends of two back-to-back stacked hexameric rings [22]; <4> HslVU is a ATP-dependent protease composed of two multimeric complexes: the hslU ATPase and the HslV peptitase [14]; <4> ClpYQ is an ATP-dependent protease that consists of an ATPase large subunit, ClpY, and a peptidase small subunit, ClpQ. Six identical subunits of both ClpY and ClpQ self-assemble into an oligomeric ring, and two rings of each subunit, two ClpQ rings surrounded by single ClpY rings, form a dumbbell shape complex [15]; <4> HslVU is an ATP-dependent protease consisting of two multimeric components: the HslU ATPase and the HslV peptidase [11]; <4> the subunits of ClpY and ClpQ are arranged in hexagonal rings. The structure of ClpQ is a double hexameric ring [26]; <4> HslV and HslU form cylindrical four-ring structures in which the HslV dodecamer is flanked at each end by a HslU ring [25]; <4> structure analysis using crystal structure PDB code 1G4A, the GYVG motif is essential for enzyme complex activity, overview [33]; <5> the HslUV complex is an assembly of heat shock locus gene products U and V. The formation of the complete complex is essential for the proteasome to carry out its biochemical and physiological role in the parasite, namely to degrade specific target proteins in an ATP-dependent chaperone assisted manner. Homology modeling, molecular docking and computational alanine scanning to model the complex, are used to predict the binding mode of PfHslU-V interaction and to predict the binding-energy hot-spots in protein-protein interface, respectively [44]; <4> ClpYQ is a two-component ATP-dependent protease in which ClpQ is the peptidase subunit and ClpY is the ATPase and the substrate-binding subunit. ClpY has three domains, N, I, and C, and these domains are discrete and exhibit different binding preferences [47]; <4> mathematical models for stochastically assembled HslV dodecamers, overview [48]) [10,11,14,15,22,25,26,33,44,47,48]

5 Isolation/Preparation/Mutation/Application

Purification

<2> (recombinant His-tagged enzyme from Escherichia coli strain BL21(DE3) by nickel affinity chromatography) [34]
<3> [41]
<4> [10,25,26,42]
<4> (recombinant His-tagged HslU and HslUV from strain BB101 by nickel affinity and ion exchange chromatography, and gel filtration) [36]

<4> (recombinant His-tagged wild-type and mutant enzymes from BW25113 ΔhslVU::kan cells by nickel affinity chromatography) [48]
<8> [6]

Crystallization

<2> [34]
<2> (asymmetric HslU(ΔI)6HslV12 complex.HslV can be activated by binding of a hexameric HslU(ΔI)6 ring lacking the I domain) [29]
<3> (purified recombinant CodX and CodW and hybrid complexes with Escherichia coli enzymes CodW-HslU and HslV-CodX, X-ray diffraction strucure determination and analysis at 3.5-4.6 A resolution, the co-crystals contain lattice-translocation defects, correction, application of the lattice-translocation defect theory to atomic models, overview) [31]
<3> (sitting drop vapor diffusion method) [41]
<4> (hanging-drop vapor diffusion method. 3.0 A resolution crystal structure of hslV with an HslU hexamer bound at one end of an HslV dodecamer. The structure shows that the central pores of the ATPase and peptidase are next to each other and alligned) [23]
<4> (purified recombinant HslU and HslV and hybrid complexes with Bacillus subtilis enzymes CodW-HslU and HslV-CodX, X-ray diffraction strucure determination and analysis at 3.5-4.6 A resolution, the co-crystals contain lattice-translocation defects, correction, application of the lattice-translocation defect theory to atomic models, overview) [31]
<4> (quarternary arrangement of hslU and hslV in a cocrystal) [12]
<4> (the crystal strcuture shows that HslU forms a hexamer with a pore at one end and HslV forms a dodecamer with translocation pores at both ends of two back-to-back stacked hexameric rings) [22]
<8> (crystal structure of an 820000 Da relative molecular mass complex of the ATPase HslU and the protease component HslV, sitting drop vapour diffusion against a reservoir containing 100 mM sodium cacodylate pH 6.5, 15% glycerol, 10.5% polyethylene glycol PEG 8K and 500 mM $(NH_4)_2SO_4$) [7]
<8> (sitting drop vapor difussion against a reservoir containing 100 mM Hepes/NaOH at pH 7.5, 200 mM sodium acetate, 0.02% NaN_3 and between 9% and 14% ethanol) [6]
<9> (wild-type or HslV-HsvU complexed with resorufin casein, hanging-drop vapor diffusion method) [21]

Cloning

<1> (gene clpY and gene clpQ, DNA and amino acid sequence determination and analysis, subcloning and expression in Escherichia coli strain DH5α) [32]
<2> [29,34]
<2> (HslU and HslV are coexpressed in BL21 (DE3) pLysS cells) [43]
<4> [26,42]
<4> (HslU and HslV are coexpressed in BL21 (DE3) pLysS cells) [43]
<4> (expression of His-tagged wild-type and mutant enzymes in BW25113 ΔhslVU::kan cells) [48]

<4> (gene clpQY or hslVU, expression of diverse gene constructs, e.g. as lacZ fusion constructs, and of truncated variants, in AC3112 cells, analysis of regulation of gene expression, overview. The stem-loop secondary structure of 5'-UTR of clpQ+Y+ is responsible for its mRNA stability) [49]
<4> (genes clpQ and clpY, DNA sequence determination, overexpression in a Lon protease-deficient mutant strain suppresses expression of the cps gene and of mucoid phenotype) [35]
<4> (genes clpY, co-expression of ClpQ and ClpY mutants in AC3112 cells. Co-expression of ClpY with HA-tagged SulA and mutant SulA M89I, RcsA, RpoH, and TraJ molecules in the yeast two-hybrid system, expression of recombinant ClpYQ mutants) [47]
<4> (mutant enzymes K80T, E286Q, E312Q, R325E, R393A, Δ137-150, Δ175-209, Δ^{11}1-239, E266Q, Es66Q/E385K, I312W, ins(264,265), Ins(311, 312), Ins(387,388), Ins(435,436), Δ^{4}32-443, E436A/D437A, E436K/D437K, E88Q, E88Q/E266Q, Y91G, V92G, G93A, E95W, Δ^{8}8-92, Δ^{8}9-92) [21]
<4> (overexpression of His-tagged HslU and HslUV in strain BB101) [36]
<8> (the amplified fragment coding for HslV-EFHHHHHH is cloned into pET12b usind restriction sites Nde and SalI, expression in Escherichia coli) [6]

Engineering

A188S <4> (<4> clpY mutant, the mutant shows altered interaction with SulA substrates, wild-type and mutant, and altered induction by arabinose or glutamate compared to the wild-type, overview [47]) [47]
Δ111-239 <4> (<4> 2 Gly linker, amidolytic ativity is 60-80% of the activity of the wild-type enzyme, caseinolytic activity is 60-80% of the activity of the wild-type enzyme, activity with SulA-MBP fusion protein is less than 20% of the activity of the wild-type enzyme, ATPase activity is 60-80% of the activity of the wild-type enzyme [21]) [21]
Δ137-150 <4> (<4> 2 Gly linker, amidolytic ativity, caseinolytic activity, activity with SulA-MBP fusion protein and ATPase activity are unchanged [21]) [21]
Δ175-209 <4> (<4> 2 Gly linker, amidolytic ativity, caseinolytic activity, and ATPase activity are unchanged, activity with the SalU-MBP fusion protein is less than 20% of the activity of the wild-type enzyme [21]) [21]
Δ423-443 <4> (<4> 5 Gly insertion, no amidolytic activity, no activity with casein and SulA-MBP fusion protein, no ATPase activity [21]) [21]
Δ83-92 <2> (<2> hydrolysis of casein, SulA-MBP or benzyloxycarbonyl-GGL-7-amido-4-methylcoumarin is less than 20% of the activity of the wild-type enzyme [28]) [28]
Δ86-91 <2> (<2> hydrolysis of casein, SulA-MBP or benzyloxycarbonyl-GGL-7-amido-4-methylcoumarin is unchanged [28]) [28]
Δ88-92 <4> (<4> 3 Gly linker, amidolytic ativity, caseinolytic activity, activity with SulA-MBP fusion protein and ATPase activity are less than 20% of the activity of the wild-type enzyme [21]) [21]
Δ89-92 <4> (<4> 1 Gly linker, amidolytic ativity is 40-60% of the activity of the wild-type enzyme, caseinolytic activity is 40-60% of the activity of the

wild-type enzyme, activity with SulA-MBP fusion protein is less than 20% of the activity of the wild-type enzyme, ATPase activity is 40-60% of the activity of the wild-type enzyme [21]) [21]
E193L/E194L <4> (<4> clpY mutant, the mutant shows altered interaction with SulA substrates, wild-type and mutant, and altered induction by arabinose or glutamate compared to the wild-type, overview [47]) [47]
E266Q <4> (<4> amidolytic ativity, caseinolytic activity, activity with SulA-MBP fusion protein and ATPase activity are unchanged [21]) [21]
E266Q/E385 <4> (<4> amidolytic ativity, caseinolytic activity, activity with SulA-MBP fusion protein and ATPase activity are unchanged [21]) [21]
E286Q <4> (<4> amidolytic ativity is 40-60% of the activity of the wild-type enzyme, caseinolytic activity is 40-60% of the activity of the wild-type enzyme, activity with SulA-MBP fusion protein is 40-60% of the activity of the wild-type enzyme, ATPase activity is unchanged [21]) [21]
E321Q <4> (<4> amidolytic ativity, caseinolytic activity, activity with SulA-MBP fusion protein and ATPase activity is less than 20% of the activity of the wild-type enzyme [21]) [21]
E325E <4> (<4> amidolytic ativity, caseinolytic activity, activity with SulA-MBP fusion protein and ATPase activity are less than 20% of the activity of the wild-type enzyme. Crystal structure of the mutant complex is nearly identical to then active complex [21]) [21]
E436K/D437K <4> (<4> amidolytic ativity is 60-80% of the activity of the wild-type enzyme, caseinolytic activity is unchanged, activity with SulA-MBP fusion protein is less than 20% of the activity of the wild-type enzyme, ATPase activity is unchanged [21]) [21]
E61C <4> (<4> clpQ mutant [47]) [47]
E88Q <4> (<4> amidolytic ativity is 20-40% of the activity of the wild-type enzyme, caseinolytic activity is less than 20% of the activity of the wild-type enzyme, activity with SulA-MBP fusion protein is less than 20% of the activity of the wild-type enzyme, ATPase activity is unchanged [21]) [21]
E88Q/E266Q <4> (<4> amidolytic ativity is 20-40% of the activity of the wild-type enzyme, caseinolytic activity is less than 20% of the activity of the wild-type enzyme, activity with SulA-MBP fusion protein is less than 20% of the activity of the wild-type enzyme, ATPase activity is unchanged [21]) [21]
E95W <4> (<4> amidolytic activity, activity with casein and ATPase activity are unchanged, activity with SulA-MBP fusion protein is 20-40% of the activity of the wild-type enzyme [21]) [21]
G90P <4> (<4> mutation of the GYVG motif residues affects protein unfolding, ATP hydrolysis, affinity for ADP, and interaction of HslU and HslV, overview, the mutant shows 41% reduced ATP hydrolysis activity compared to wild-type HslU [33]) [33]
G93A <4> (<4> amidolytic ativity is 20-40% of the activity of the wild-type enzyme, caseinolytic activity is 20-40% of the activity of the wild-type enzyme, activity with SulA-MBP fusion protein is less than 20% of the activity of the wild-type enzyme, ATPase activity is 40-60% of the activity of the wild-type enzyme [21]; <4> mutation of the GYVG motif residues affects

protein unfolding, ATP hydrolysis, affinity for ADP, and interaction of HslU and HslV, overview [33]) [21,33]
G93P <4> (<4> mutation of the GYVG motif residues affects protein unfolding, ATP hydrolysis, affinity for ADP, and interaction of HslU and HslV, overview [33]) [33]
I186N <4> (<4> clpY mutant, the mutant does not interact with SulA compared to the wild-type ClpY [47]) [47]
I312W <4> (<4> amidolytic ativity, caseinolytic activity, activity with SulA-MBP fusion protein and ATPase activity are higher than the wild-type activities [21]) [21]
Ins(435,436) <4> (<4> 5 Gly insertion, no amidolytic activity, no activity with casein and SulA-MBP fusion protein, no ATPase activity [21]) [21]
K28A <2> (<2> hydrolysis of casein, SulA-MBP or benzyloxycarbonyl-GGL-7-amido-4-methylcoumarin is less than 20% of the activity of the wild-type enzyme [28]) [28]
K80T <4> (<4> amidolytic ativity is 20-40% of the activity of the wild-type enzyme, caseinolytic activity is 40-60% of the activity of the wild-type enzyme, activity with SulA-MBP fusion protein is unchanged, ATPase activity is unchanged [21]) [21]
L199Q <4> (<4> clpY mutant, the mutant shows altered interaction with SulA substrates, wild-type and mutant, and altered induction by arabinose or glutamate compared to the wild-type, overview. SulA accumulates in the bacterial cells that express ClpY [47]) [47]
M187I <4> (<4> clpY mutant, the mutant shows altered interaction with SulA substrates, wild-type and mutant, and altered induction by arabinose or glutamate compared to the wild-type, overview [47]) [47]
N141L/N142L <4> (<4> the ClpY loop 1 mutant is defective in complete degradation of SulA [47]) [47]
N205K <4> (<4> clpY mutant, the mutant shows altered interaction with SulA substrates, wild-type and mutant, and altered induction by arabinose or glutamate compared to the wild-type, overview [47]) [47]
Q148L/Q149L/Q150L <4> (<4> the ClpY loop 1 mutant shows altered substrate recognition and binding, but shows normal activity similar to that of the wild-type ClpY [47]) [47]
Q198L/Q200L <4> (<4> clpY mutant, the mutant shows altered interaction with SulA substrates, wild-type and mutant, and altered induction by arabinose or glutamate compared to the wild-type, overview [47]) [47]
Q311_I312insGGGGG <4> (<4> 5 Gly insertion, amidolytic ativity, caseinolytic activity and activity with SulA-MBP fusion protein are less than 20% of the activity of the wild-type enzyme, ATPase activity is 20-40% of the activity of the wild-type enzyme [21]) [21]
R35A <2> (<2> hydrolysis of casein, SulA-MBP or benzyloxycarbonyl-GGL-7-amido-4-methylcoumarin is less than 20% of the activity of the wild-type enzyme [28]) [28]
R393A <4> (<4> amidolytic ativity, caseinolytic activity, activity with SulA-MBP fusion protein and ATPase activity is less than 20% of the activity of the wild-type enzyme [21]) [21]

R86D <2> (<2> hydrolysis of casein, SulA-MBP or benzyloxycarbonyl-GGL-7-amido-4-methylcoumarin is less than 20% of the activity of the wild-type enzyme [28]) [28]
R86G <4> (<4> ATP inhibits the degradation of unfolded proteins by HslV. This inhibitory effect of ATP is markedly diminished by substitution of the Arg86 residue located in the apical pore of HslV with Gly [38]) [38]
R89A/K90A <2> (<2> hydrolysis of casein, SulA-MBP or benzyloxycarbonyl-GGL-7-amido-4-methylcoumarin is less than 20% of the activity of the wild-type enzyme [28]) [28]
R89D <2> (<2> hydrolysis of casein, SulA-MBP or benzyloxycarbonyl-GGL-7-amido-4-methylcoumarin is 40-60% of the activity of the wild-type enzyme [28]) [28]
R89D/K90E <2> (<2> hydrolysis of casein and SulA-MBP is less than 20% of the activity of the wild-type enzyme, hydrolysis of benzyloxycarbonyl-GGL-7-amido-4-methylcoumarin is higher than that of the wild-type enzyme [28]) [28]
S103A <8> (<8> 50% of the activity of the wild-type enzyme with benzyloxycarbonyl-GGL-7-amido-4-methylcoumarin in presence of the ATPase component HslU [9]) [9]
S124A <8> (<8> 3% of the activity of the wild-type enzyme with benzyloxycarbonyl-GGL-7-amido-4-methylcoumarin in presence of the ATPase component HslU [9]) [9]
S143A <8> (<8> 95% of the activity of the wild-type enzyme with benzyloxycarbonyl-GGL-7-amido-4-methylcoumarin in presence of the ATPase component HslU [9]) [9]
S172A <8> (<8> 1% of the activity of the wild-type enzyme with benzyloxycarbonyl-GGL-7-amido-4-methylcoumarin in presence of the ATPase component HslU [9]) [9]
S5A <8> (<8> 124% of the activity of the wild-type enzyme with benzyloxycarbonyl-GGL-7-amido-4-methylcoumarin in presence of the ATPase component HslU [9]) [9]
T387_E388insGGGGG <4> (<4> 5 Gly insertion, amidolytic ativity is unchanged, caseinolytic activity is 60-80% of the activity of the wild-type enzyme, ATPase activity is unchanged [21]) [21]
V112A <2> (<2> hydrolysis of casein, SulA-MBP or benzyloxycarbonyl-GGL-7-amido-4-methylcoumarin is less than 20% of the activity of the wild-type enzyme [28]) [28]
V92A <4> (<4> mutation of the GYVG motif residues affects protein unfolding, ATP hydrolysis, affinity for ADP, and interaction of HslU and HslV, overview [33]) [33]
V92G <4> (<4> amidolytic activity, activity with casein and ATPase activity are unchanged, activity with SulA-MBP fusion protein is less than 20% of the activity of the wild-type enzyme [21]) [21]
V92I <4> (<4> mutation of the GYVG motif residues affects protein unfolding, ATP hydrolysis, affinity for ADP, and interaction of HslU and HslV, overview [33]) [33]

V92S <4> (<4> mutation of the GYVG motif residues affects protein unfolding, ATP hydrolysis, affinity for ADP, and interaction of HslU and HslV, overview [33]) [33]
Y91A <4> (<4> mutation of the GYVG motif residues affects protein unfolding, ATP hydrolysis, affinity for ADP, and interaction of HslU and HslV, overview [33]) [33]
Y91F <4> (<4> mutation of the GYVG motif residues affects protein unfolding, ATP hydrolysis, affinity for ADP, and interaction of HslU and HslV, overview [33]) [33]
Y91G <4> (<4> amidolytic ativity is 40-60% of the activity of the wild-type enzyme, caseinolytic activity is 40-60% of the activity of the wild-type enzyme, activity with SulA-MBP fusion protein is less than 20% of the activity of the wild-type enzyme, ATPase activity is unchanged [21]) [21]
Y91S <4> (<4> mutation of the GYVG motif residues affects protein unfolding, ATP hydrolysis, affinity for ADP, and interaction of HslU and HslV, overview [33]) [33]
Additional information <4> (<4> clpQ+Y+ promoter is fused to a lacZ reporter gene. The transcriptional or translational clpQ+::lacZ fusion gene is each crossed into lambda phage. The lambdaclpQ+::lacZ+, a transcriptional fusion gene, is used to form lysogens in the wild-type, rpoH or/and rpoS mutants. Upon shifting the temperature up from 30°C to 42°C, the wild-type transcriptional lambdaclpQ+::lacZ+ demonstrates an increased β-galactosidase activity, overview. RpoH itself regulates clpQ+Y+ gene expression. The clpQ+Y+ message carries a conserved 71 bp at the 5-untranslated region that is predicted to form the stem-loop structure by analysis of its RNA secondary structure [49]; <4> construction of mixed dodecamers having varied numbers of HslV and T1A subunits, and of a series of HslV dodecamers containing different numbers of active sites showing that HslV with only 6 active sites is sufficient to support full catalytic activity, a further reduction of the number of active sites leads to a proportional decrease in activity. Substrate-mediated stabilization of the HslV-HslU interaction remains unchanged until the number of the active sites is decreased to 6 but is gradually compromised upon further reduction. Deletion of Thr1 causes a dramatic increase in affinity between HslV and HslU [48]; <4> construction of truncation mutants lacking the substrate binding residues 137-209 of ClpY [47]) [47,48,49]

6 Stability

General stability information

<4>, rapid freezing and thawing inactivates [10]

Storage stability

<4>, -70°C, stable for at least 1 month in presence of 20% glycerol and 1 mM dithiothreitol [10]
<4>, 4°C rapid inactivation in absence of dithiothreitol [10]

References

[1] Welch, R.A.; Burland, V.; Plunkett, G.III; Redford, P.; Roesch, P.; Rasko, D.; Buckles, E.L.; Liou, S.R.; Boutin, A.; Hackett, J.; Stroud, D.; Mayhew, G.F.; Rose, D.J.; Zhou, S.; Schwartz, D.C.; Perna, N.T.; Mobley, H.L.T.; Donnenberg, M.S.; Blattner, F.R.: Extensive mosaic structure revealed by the complete genome sequence of uropathogenic Escherichia coli. Proc. Natl. Acad. Sci. USA, **99**, 17020-17024 (2002)

[2] Jin, Q.; Yuan, Z.; Xu, J.; Wang, Y.; et al.: Genome sequence of Shigella flexneri 2a: insights into pathogenicity through comparison with genomes of Escherichia coli K12 and O157. Nucleic Acids Res., **30**, 4432-4441 (2002)

[3] Plunkett, G.3rd; Burland, V.; Daniels, D.L.; Blattner, F.R.: Analysis of the Escherichia coli genome. III. DNA sequence of the region from 87.2 to 89.2 minutes. Nucleic Acids Res., **21**, 3391-3398 (1993)

[4] Perna, N.T.; Plunkett, G.; Burland, V.; Mau, B.; Glasner, J.D.; et al.: Genome sequence of enterohaemorrhagic Escherichia coli O157:H7. Nature, **409**, 529-533 (2001)

[5] Hayashi, T.; Makino, K.; Ohnishi, M.; Kurokawa, K.; Ishii, K.; et al.: Complete genome sequence of enterohemorrhagic Escherichia coli O157:H7 and genomic comparison with a laboratory strain K-12. DNA Res., **8**, 11-22 (2001)

[6] Bochtler, M.; Ditzel, L.; Groll, M.; Huber, R.: Crystal structure of heat shock locus V (HslV) from Escherichia coli. Proc. Natl. Acad. Sci. USA, **94**, 6070-6074 (1997)

[7] Bochtler, M.; Hartmann, C.; Song, H.K.; Bourenkov, G.P.; Bartunik, H.D.; Huber R.: The structures of HslU and the ATP-dependent protease HslU-HslV. Nature, **403**, 800-805 (2000)

[8] Chuang, S.E.; Burland, V.; Plunkett, G.III; Daniels, D.L.; Blattner, F.R.: Sequence analysis of four new heat-shock genes constituting the hslTS/ibpAB and hslVU operons in Escherichia coli. Gene, **134**, 1-6 (1993)

[9] Yoo, S.J.; Shim, Y.K.; Seong, I.S.; Seol, J.H.; Kang, M.S.; Chung, C.H.: Mutagenesis of two N-terminal Thr and five Ser residues in HslV, the proteolytic component of the ATP-dependent HslVU protease. FEBS Lett., **412**, 57-60 (1997)

[10] Yoo, S.J.; Seol, J.H.; Shin, D.H.; Rohrwild, M.; Kang, M.S.; Tanaka, K.; Goldberg, A.L.; Chung, C.H.: Purification and characterization of the heat shock proteins HslV and HslU that form a new ATP-dependent protease in Escherichia coli. J. Biol. Chem., **271**, 14035-14040 (1996)

[11] Yoo, S.J.; Seol, J.H.; Seong, I.S.; Kang, M.S.; Chung, C.H.: ATP binding, but not its hydrolysis, is required for assembly and proteolytic activity of the HslVU protease in Escherichia coli. Biochem. Biophys. Res. Commun., **238**, 581-585 (1997)

[12] Bochtler, M.; Song, H.K.; Hartmann, C.; Ramachandran, R.; Huber, R.: The quaternary arrangement of HslU and HslV in a cocrystal: a response to Wang, Yale. J. Struct. Biol., **135**, 281-293 (2001)

[13] Bogyo, M.; McMaster, J.S.; Gaczynska, M.; Tortorella, D.; Goldberg, A.L.; Ploegh, H.: Covalent modification of the active site threonine of proteasomal β subunits and the Escherichia coli homolog HslV by a new class of inhibitors. Proc. Natl. Acad. Sci. USA, **94**, 6629-6634 (1997)
[14] Huang, H.; Goldberg, A.L.: Proteolytic activity of the ATP-dependent protease HslVU can be uncoupled from ATP hydrolysis. J. Biol. Chem., **272**, 21364-21372 (1997)
[15] Lee, Y.Y.; Chang, C.F.; Kuo, C.L.; Chen, M.C.; Yu, C.H.; Lin, P.I.; Wu, W.F.: Subunit oligomerization and substrate recognition of the Escherichia coli ClpYQ (HslUV) protease implicated by in vivo protein-protein interactions in the yeast two-hybrid system. J. Bacteriol., **185**, 2393-2401 (2003)
[16] Seong, I.S.; Kang, M.S.; Choi, M.K.; Lee, J.W.; Koh, O.J.; Wang, J.; Eom, S.H.; Chung, C.H.: The C-terminal tails of HslU ATPase act as a molecular switch for activation of HslV peptidase. J. Biol. Chem., **277**, 25976-25982 (2002)
[17] Nishii, W.; Takahashi, K.: Determination of the cleavage sites in SulA, a cell division inhibitor, by the ATP-dependent HslVU protease from Escherichia coli. FEBS Lett., **553**, 351-354 (2003)
[18] Rohrwild, M.; Coux, O.; Huang, H.C.; Moerschell, R.P.; Yoo, S.J.; Seol, J.H.; Chung, C.H.; Goldberg, A.L.: HslV-HslU: A novel ATP-dependent protease complex in Escherichia coli related to the eukaryotic proteasome. Proc. Natl. Acad. Sci. USA, **93**, 5808-5813 (1996)
[19] Slominska, M.; Wahl, A.; Wegrzyn, G.; Skarstad, K.: Degradation of mutant initiator protein DnaA204 by proteases ClpP, ClpQ and Lon is prevented when DNA is SeqA-free. Biochem. J., **370**, 867-871 (2003)
[20] Seong, I.S.; Oh, J.Y.; Yoo, S.J.; Seol, J.H.; Chung, C.H.: ATP-dependent degradation of SulA, a cell division inhibitor, by the HslVU protease in Escherichia coli. FEBS Lett., **456**, 211-214 (1999)
[21] Song, H.K.; Hartmann, C.; Ramachandran, R.; Bochtler, M.; Behrendt, R.; Moroder, L.; Huber, R.: Mutational studies on HslU and its docking mode with HslV. Proc. Natl. Acad. Sci. USA, **97**, 14103-14108 (2000)
[22] Wang, J.: A corrected quaternary arrangement of the peptidase HslV and atpase HslU in a cocrystal structure. J. Struct. Biol., **134**, 15-24 (2001)
[23] Wang, J.; Song, J.J.; Franklin, M.C.; Kamtekar, S.; Im, Y.J.; Rho, S.H.; Seong, I.S.; Lee, C.S.; Chung, C.H.; Eom, S.H.: Crystal structures of the HslVU peptidase-ATPase complex reveal an ATP-dependent proteolysis mechanism. Structure, **9**, 177-184 (2001)
[24] Missiakas, D.; Schwager, F.; Betton, J.M.; Georgopoulos, C.; Raina, S.: Identification and characterization of HsIV HsIU (ClpQ ClpY) proteins involved in overall proteolysis of misfolded proteins in Escherichia coli. EMBO J., **15**, 6899-6909 (1996)
[25] Rohrwild, M.; Pfeifer, G.; Santarius, U.; Muller, S.A.; Huang, H.C.; Engel, A.; Baumeister, W.; Goldberg, A.L.: The ATP-dependent HslVU protease from Escherichia coli is a four-ring structure resembling the proteasome. Nat. Struct. Biol., **4**, 133-139 (1997)
[26] Kessel, M.; Wu, W.; Gottesman, S.; Kocsis, E.; Steven, A.C.; Maurizi, M.R.: Six-fold rotational symmetry of ClpQ, the E. coli homolog of the 20S pro-

teasome, and its ATP-dependent activator, ClpY. FEBS Lett., **398**, 274-278 (1996)
[27] Seol, J.H.; Yoo, S.J.; Shin, D.H.; Shim, Y.K.; Kang, M.S.; Goldberg, A.L.; Chung, C.H.: The heat-shock protein HslVU from Escherichia coli is a protein-activated ATPase as well as an ATP-dependent proteinase. Eur. J. Biochem., **247**, 1143-1150 (1997)
[28] Ramachandran, R.; Hartmann, C.; Song, H.K.; Huber, R.; Bochtler, M.: Functional interactions of HslV (ClpQ) with the ATPase HslU (ClpY). Proc. Natl. Acad. Sci. USA, **99**, 7396-7401 (2002)
[29] Kwon, A.R.; Kessler, B.M.; Overkleeft, H.S.; McKay, D.B.: Structure and reactivity of an asymmetric complex between HslV and I-domain deleted HslU, a prokaryotic homolog of the eukaryotic proteasome. J. Mol. Biol., **330**, 185-195 (2003)
[30] Wei, J.; Goldberg, M.B.; Burland, V.; et al.: Complete genome sequence and comparative genomics of Shigella flexneri serotype 2a strain 2457T. Infect. Immun., **71**, 2775-2786 (2003)
[31] Wang, J.; Rho, S.H.; Park, H.H.; Eom, S.H.: Correction of X-ray intensities from an HslV-HslU co-crystal containing lattice-translocation defects. Acta Crystallogr. Sect. D, **61**, 932-941 (2005)
[32] Frees, D.; Thomsen, L.E.; Ingmer, H.: Staphylococcus aureus ClpYQ plays a minor role in stress survival. Arch. Microbiol., **183**, 286-291 (2005)
[33] Park, E.; Rho, Y.M.; Koh, O.J.; Ahn, S.W.; Seong, I.S.; Song, J.J.; Bang, O.; Seol, J.H.; Wang, J.; Eom, S.H.; Chung, C.H.: Role of the GYVG pore motif of HslU ATPase in protein unfolding and translocation for degradation by HslV peptidase. J. Biol. Chem., **280**, 22892-22898 (2005)
[34] Kwon, A.R.; Trame, C.B.; McKay, D.B.: Kinetics of protein substrate degradation by HslUV. J. Struct. Biol., **146**, 141-147 (2004)
[35] Kuo, M.S.; Chen, K.P.; Wu, W.F.: Regulation of RcsA by the ClpYQ (HslUV) protease in Escherichia coli. Microbiology, **150**, 437-446 (2004)
[36] Burton, R.E.; Baker, T.A.; Sauer, R.T.: Nucleotide-dependent substrate recognition by the AAA+ HslUV protease. Nat. Struct. Mol. Biol., **12**, 245-251 (2005)
[37] Azim, M.K.; Goehring, W.; Song, H.K.; Ramachandran, R.; Bochtler, M.; Goettig, P.: Characterization of the HslU chaperone affinity for HslV protease. [Erratum to document cited in CA143:073777]. Protein Sci., **14**, 2484 (2005)
[38] Lee, J.W.; Park, E.; Bang, O.; Eom, S.H.; Cheong, G.W.; Chung, C.H.; Seol, J.H.: Nucleotide triphosphates inhibit the degradation of unfolded proteins by HslV peptidase. Mol. Cell., **23**, 252-257 (2007)
[39] Lau-Wong, I.C.; Locke, T.; Ellison, M.J.; Raivio, T.L.; Frost, L.S.: HslVU protease. Mol. Microbiol., **67**, 516-527 (2008)
[40] Azim, M.K.; Noor, S.: Characterization of protomer interfaces in HslV protease, the bacterial homologue of 20S proteasome. Protein J., **26**, 213-219 (2007)
[41] Rho, S.; Park, H.H.; Kang, G.B.; Im, Y.J.; Kang, M.S.; Lim, B.K.; Seong, I.S.; Seol, J.; Chung, C.H.; Wang, J.; Eom, S.H.: Crystal structure of Bacillus sub-

tilis CodW, a noncanonical HslV-like peptidase with an impaired catalytic apparatus. Proteins Struct. Funct. Bioinform., **71**, 1020-1026 (2008)
[42] Park, E.; Lee, J.W.; Eom, S.H.; Seol, J.H.; Chung, C.H.: Binding of MG132 or deletion of the Thr active sites in HslV subunits increases the affinity of HslV protease for HslU ATPase and makes this interaction nucleotide-independent. J. Biol. Chem., **283**, 33258-33266 (2008)
[43] Koodathingal, P.; Jaffe, N.E.; Kraut, D.A.; Prakash, S.; Fishbain, S.; Herman, C.; Matouschek, A.: ATP-dependent proteases differ substantially in their ability to unfold globular proteins.. J. Biol. Chem., **284**, 18674-18684 (2009)
[44] Subramaniam, S.; Mohmmed, A.; Gupta, D.: Molecular modeling studies of the interaction between Plasmodium falciparum HslU and HslV subunits.. J. Biomol. Struct. Dyn., **26**, 473-479 (2009)
[45] Yakamavich, J.A.; Baker, T.A.; Sauer, R.T.: Asymmetric nucleotide transactions of the HslUV protease. J. Mol. Biol., **380**, 946-957 (2008)
[46] Lee, J.W.; Park, E.; Bang, O.; Eom, S.H.; Cheong, G.W.; Chung, C.H.; Seol, J.H.: Nucleotide triphosphates inhibit the degradation of unfolded proteins by HslV peptidase. Mol. Cells, **23**, 252-257 (2007)
[47] Lien, H.Y.; Shy, R.S.; Peng, S.S.; Wu, Y.L.; Weng, Y.T.; Chen, H.H.; Su, P.C.; Ng, W.F.; Chen, Y.C.; Chang, P.Y.; Wu, W.F.: Characterization of the Escherichia coli ClpY (HslU) substrate recognition site in the ClpYQ (HslUV) protease using the yeast two-hybrid system. J. Bacteriol., **191**, 4218-4231 (2009)
[48] Lee, J.W.; Park, E.; Jeong, M.S.; Jeon, Y.J.; Eom, S.H.; Seol, J.H.; Chung, C.H.: HslVU ATP-dependent protease utilizes maximally six among twelve threonine active sites during proteolysis. J. Biol. Chem., **284**, 33475-33484 (2009)
[49] Lien, H.Y.; Yu, C.H.; Liou, C.M.; Wu, W.F.: Regulation of clpQY (hslVU) gene expression in Escherichia coli. Open Microbiol. J., **3**, 29-39 (2009)

fatty acid amide hydrolase 3.5.1.99

1 Nomenclature

EC number
3.5.1.99

Systematic name
fatty acylamide amidohydrolase

Recommended name
fatty acid amide hydrolase

Synonyms
AAH <3> [15]
FAAH <1,2,3,4,5,6,7,8> [1,2,3,5,7,8,9,10,11,12,13,14,16,17,18,19,20,21,22,24,25,26,27,28,29]
FAAH-1 <6,7,8> [6]
FAAH-2 <2,9> (<9> FAAH-2 is an ancient gene present in primates, but not murids [6]) [6,24]
anandamide amidohydrolase <3> [12,15]
endocannabinoid-degrading enzyme <3> [27]
fatty acid amide hydrolase <3,9> [23]
fatty-acid amide hydrolase <3> [17]
oleamide hydrolase <3> [12,17]

CAS registry number
153301-19-0

2 Source Organism

<1> *Mus musculus* [3,5,7,22,25,28,29]
<2> *Homo sapiens* [7,20,24]
<3> *Rattus norvegicus* [1,2,4,7,8,9,10,12,13,14,15,16,17,18,19,20,23,26,27]
<4> *Sus scrofa* [7]
<5> *Oryctolagus cuniculus* [11]
<6> *Mus musculus* (UNIPROT accession number: O08914) [6,19]
<7> *Rattus norvegicus* (UNIPROT accession number: P97612) [6,21]
<8> *Homo sapiens* (UNIPROT accession number: O00519) [6,19]
<9> *Homo sapiens* (UNIPROT accession number: Q6GMR7) [6,23]

D. Schomburg and I. Schomburg (eds.), *Class 3.4–6 Hydrolases, Lyases, Isomerases, Ligases: EC 3.4–6*, Springer Handbook of Enzymes S10, DOI 10.1007/978-3-642-36260-6_10,

3 Reaction and Specificity

Catalyzed reaction

anandamide + H_2O = arachidonic acid + ethanolamine
oleamide + H_2O = oleic acid + NH_3

Natural substrates and products

S 2-arachidonoylglycerol + H_2O <1> (<1> FAAH is responsible for approximately one-half of the 2-arachidonoylglycerol hydrolysis occurring in BV-2 cell homogenate [5]) (Reversibility: ?) [5]
P ?
S anandamide + H_2O <1,2,3> (<1> i.e. N-arachidonoylethanolamine [28]; <2> substrate of FAAH and FAAH-2, the latter shows lower activity than FAAH [24]) (Reversibility: ?) [24,25,26,27,28,29]
P arachidonic acid + ethanolamine
S anandamide + H_2O <1,3,5,8> (<8> FAAH-1 plays a primary role in regulating endocannabinoid signaling [6]; <1> anandamide hydrolysis in BV-2 cells is entirely attributable to FAAH [5]; <3> enzyme is responsible for the catabolism of neuromodulatory fatty acid amides, including anandamide and oleamide [9]; <1> fatty acid amide hydrolase is a modulator of endogenous signaling compounds affecting sleep (oleamide) and analgesia (anandamide) [22]; <5> the enzyme cleaves anandamide and regulates in vivo the magnitude and duration of the signaling induced by this lipid messenger [11]; <3> the enzyme is responsible for the hydrolysis of a number of neuromodulatory fatty acid amides, including the endogenous cannabinoid anandamide and the sleep-inducing lipid oleamide [14]; <3> the serine hydrolase is responsible for the degradation of endogenous oleamide and anandamide, fatty acid amides that function as chemical messengers [12]) (Reversibility: ?) [5,6,9,11,12,14,17,22]
P arachidonic acid + ethanolamine
S oleamide + H_2O <1,3> (<3> enzyme is responsible for the catabolism of neuromodulatory fatty acid amides, including anandamide and oleamide [9]; <1> fatty acid amide hydrolase is a modulator of endogenous signaling compounds affecting sleep (oleamide) and analgesia (anandamide) [22]; <3> role of FAAH in epithelial cells of the choroid plexus may be to control the concentration of oleamide in the cerebrospinal fluid. FAAH may exert an important regulatory role in shaping the duration and magnitude of the sleep-inducing effect of endogenously or exogenously derived oleamide [18]; <3> the enzyme is responsible for the hydrolysis of a number of neuromodulatory fatty acid amides, including the endogenous cannabinoid anandamide and the sleep-inducing lipid oleamide [14]; <3> the serine hydrolase is responsible for the degradation of endogenous oleamide and anandamide, fatty acid amides that function as chemical messengers [12]) (Reversibility: ?) [9,12,14,17,18,22]
P oleic acid + NH_3
S palmitoylethanolamide + H_2O <2> (<2> substrate of FAAH and FAAH-2, the latter shows lower activity than FAAH [24]) (Reversibility: ?) [24]

P palmitic acid + ethanolamine
S Additional information <2> (<2> FAAH inactivates anandamide and other bioactive N-acylethanolamines [24]) (Reversibility: ?) [24]
P ?

Substrates and products

S (11Z)-eicosenamide + H_2O <3> (<3> 105% of the activity with oleamide [12]) (Reversibility: ?) [12]
P (11Z)-eicosenoic acid + NH_3
S (12Z)-octadecenamide + H_2O <3> (<3> 92% of the activity with oleamide [12]) (Reversibility: ?) [12]
P (12Z)-octadecenoic acid + NH_3
S (13Z)-eicosenamide + H_2O <3> (<3> 103% of the activity with oleamide [12]) (Reversibility: ?) [12]
P (13Z)-eicosenoic acid + NH_3
S (13Z)-octadecenamide + H_2O <3> (<3> 82% of the activity with oleamide [12]) (Reversibility: ?) [12]
P (13Z)-octadecenoic acid + NH_3
S (15Z)-octadecenamide + H_2O <3> (<3> 90% of the activity with oleamide [12]) (Reversibility: ?) [12]
P (15Z)-octadecenoic acid + NH_3
S (5Z)-eicosenamide + H_2O <3> (<3> 116% of the activity with oleamide [12]) (Reversibility: ?) [12]
P (5Z)-eicosenoic acid + NH_3
S (5Z,8Z,11Z,14Z)-N-(2-fluoroethyl)icosa-5,8,11,14-tetraenamide + H_2O <3> (<3> hydrolysis rate is 1.3fold higher than the rate of anandamide hydrolysis [15]) (Reversibility: ?) [15]
P ?
S (5Z,8Z,11Z,14Z)-N-(2-hydroxy-1,1-dimethylethyl)icosa-5,8,11,14-tetraenamide + H_2O <3> (<3> hydrolyzed at 4.3% the rate of anandamide [15]) (Reversibility: ?) [15]
P ?
S (5Z,8Z,11Z,14Z)-N-(2-methylpropyl)icosa-5,8,11,14-tetraenamide + H_2O <3> (<3> hydrolyzed at 2% the rate of anandamide [15]) (Reversibility: ?) [15]
P ?
S (5Z,8Z,11Z,14Z)-N-(3-hydroxyphenyl)icosa-5,8,11,14-tetraenamide + H_2O <3> (<3> hydrolysis rate is 1.5fold higher than the rate of anandamide hydrolysis [15]) (Reversibility: ?) [15]
P ?
S (5Z,8Z,11Z,14Z)-N-(4-hydroxyphenyl)icosa-5,8,11,14-tetraenamide + H_2O <3> (<3> hydrolyzed at 16% the rate of anandamide [15]) (Reversibility: ?) [15]
P ?
S (5Z,8Z,11Z,14Z)-N-[(1S)-1-methylpropyl]icosa-5,8,11,14-tetraenamide + H_2O <3> (<3> hydrolyzed at 6.3% the rate of anandamide [15]) (Reversibility: ?) [15]

P ?
S (5Z,8Z,11Z,14Z)-N-[(2R)-2-hydroxypropyl]icosa-5,8,11,14-tetraenamide + H_2O <3> (<3> hydrolysis rate is 1.2fold higher than the rate of anandamide hydrolysis [15]) (Reversibility: ?) [15]
P ?
S (5Z,8Z,11Z,14Z)-N-[(2S)-2-hydroxypropyl]icosa-5,8,11,14-tetraenamide + H_2O <3> (<3> hydrolyzed at 21% the rate of anandamide [15]) (Reversibility: ?) [15]
P ?
S (5Z,8Z,11Z,14Z)-N-tert-butylicosa-5,8,11,14-tetraenamide + H_2O <3> (<3> hydrolyzed at 1.8% the rate of anandamide [15]) (Reversibility: ?) [15]
P ?
S (6Z)-octadecenamide + H_2O <3> (<3> 91% of the activity with oleamide [12]) (Reversibility: ?) [12]
P (6Z)-octadecenoic acid + NH_3
S (7Z)-octadecenamide + H_2O <3> (<3> 109% of the activity with oleamide [12]) (Reversibility: ?) [12]
P (7Z)-octadecenoic acid + NH_3
S (8Z)-eicosenamide + H_2O <3> (<3> 112% of the activity with oleamide [12]) (Reversibility: ?) [12]
P (8Z)-eicosenoic acid + NH_3
S (9E)-octadecenamide + H_2O <3> (<3> 52% of the activity with oleamide [12]) (Reversibility: ?) [12]
P (9E)-octadecenoic acid + NH_3
S (9Z)-N-(2-hydroxyethyl)octadec-9-enamide + H_2O <3> (<3> hydrolyzed at 61% the rate of anandamide [15]) (Reversibility: ?) [15]
P ?
S (9Z,12Z)-N-(2-hydroxyethyl)octadeca-9,12-dienamide + H_2O <3> (<3> hydrolyzed at 75% the rate of anandamide [15]) (Reversibility: ?) [15]
P ?
S (9Z,12Z)-N-[(1R)-2-hydroxy-1-methylethyl]octadeca-9,12-dienamide + H_2O <3> (<3> hydrolyzed at 20.5% the rate of anandamide [15]) (Reversibility: ?) [15]
P ?
S (R)-α-methanandamide + H_2O <3> (<3> 2.4% of the activity with anandamide [15]) (Reversibility: ?) [15]
P ?
S (R)-β-methanandamide + H_2O <3> (<3> 121% of the activity with anandamide [15]) (Reversibility: ?) [15]
P ?
S (S)-α-methanandamide + H_2O <3> (<3> 23% of the activity with anandamide [15]) (Reversibility: ?) [15]
P ?
S (S)-β-methanandamide + H_2O <3> (<3> 21% of the activity with anandamide [15]) (Reversibility: ?) [15]
P ?

S 1-arachidonoylglycerol + H_2O <3> (Reversibility: ?) [15]
P ?
S 11,14,17-eicosatrienamide + H_2O <3> (<3> 140% of the activity with oleamide [12]) (Reversibility: ?) [12]
P 11,14,17-eicosatrienoic acid + NH_3
S 11,14-eicosadienamide + H_2O <3> (<3> 127% of the activity with oleamide [12]) (Reversibility: ?) [12]
P ? + NH_3
S 2,2-dimethyloleamide + H_2O <3> (<3> 3% of the activity with oleamide [12]) (Reversibility: ?) [12]
P 2,2-dimethyloleic acid + NH_3
S 2-arachidonoylglycerol + H_2O <1,3> (<1> FAAH is responsible for approximately one-half of the 2-arachidonoylglycerol hydrolysis occurring in BV-2 cell homogenate [5]) (Reversibility: ?) [5,15]
P ?
S 2-methyloleamide + H_2O <3> (<3> 7% of the activity with oleamide [12]) (Reversibility: ?) [12]
P 2-methyloleic acid + NH_3
S 2-oleoylglycerol + H_2O <3> (Reversibility: ?) [4]
P ?
S 4,7,10,13,16,19-docosohexenamide + H_2O <3> (<3> 82% of the activity with oleamide [12]) (Reversibility: ?) [12]
P 4,7,10,13,16,19-docosohexenamide + NH_3
S 8,11,14-eicosatrienamide + H_2O <3> (<3> 138% of the activity with oleamide [12]) (Reversibility: ?) [12]
P 8,11,14-eicosatrienoic acid + NH_3
S N-(2-hydroxyethyl)linoleoylamide + H_2O <1> (Reversibility: ?) [25]
P ?
S N-(2-hydroxyethyl)octadecanamide + H_2O <3> (<3> hydrolyzed at 15.0% the rate of anandamide [15]) (Reversibility: ?) [15]
P ?
S N-(4-hydroxy-2-methylphenyl) arachidonoyl amide + H_2O <3> (<3> the rate of metabolism of VDM11 is about 15-20% of that for anandamide [2]) (Reversibility: ?) [2]
P 4-amino-*m*-cresol + NH_3
S N-(*o*-hydroxyphenyl)arachidonamide + H_2O <3> (Reversibility: ?) [15]
P ?
S N-oleoylethanolamine + H_2O <8,9> (<9> 23% of the activity with oleamide [6]; <8> 33% of the activity with anandamide [6]) (Reversibility: ?) [6]
P oleic acid + ethanolamine
S N-oleoyltaurine + H_2O <8> (<8> 4% of the activity with anandamide [6]) (Reversibility: ?) [6]
P taurine + oleic acid
S N-palmitoylethanolamine + H_2O <8,9> (<8> 12% of the activity with anandamide [6]; <9> 2.3% of the activity with oleamide [6]) (Reversibility: ?) [6]

P palmitic acid + ethanolamine
S all-trans-anandamide + H_2O <5> (<5> all-trans-anandamide is an equally good substrate for rabbit platelet FAAH compared to anandamide [11]) (Reversibility: ?) [11]
P ethanolamine + arachidonic acid
S α-linolenamide + H_2O <3> (<3> 138% of the activity with oleamide [12]) (Reversibility: ?) [12]
P ? + NH_3
S anadamide + H_2O <1,2,3> (<1> i.e. N-arachidonoylethanolamine [28]; <2> substrate of FAAH and FAAH-2, the latter shows lower activity than FAAH [24]) (Reversibility: ?) [24,25,26,27,28,29]
P arachidonic acid + ethanolamine
S anandamide + H_2O <1,2,3,4,5,8,9> (<8> FAAH-1 plays a primary role in regulating endocannabinoid signaling [6]; <1> anandamide hydrolysis in BV-2 cells is entirely attributable to FAAH [5]; <3> enzyme is responsible for the catabolism of neuromodulatory fatty acid amides, including anandamide and oleamide [9]; <1> fatty acid amide hydrolase is a modulator of endogenous signaling compounds affecting sleep (oleamide) and analgesia (anandamide) [22]; <5> the enzyme cleaves anandamide and regulates in vivo the magnitude and duration of the signaling induced by this lipid messenger [11]; <3> the enzyme is responsible for the hydrolysis of a number of neuromodulatory fatty acid amides, including the endogenous cannabinoid anandamide and the sleep-inducing lipid oleamide [14]; <3> the serine hydrolase is responsible for the degradation of endogenous oleamide and anandamide, fatty acid amides that function as chemical messengers [12]; <3> 168% of the activity with oleamide [12]; <9> 5% of the activity with oleamide [6]) (Reversibility: ?) [2,3,4,5,6,7,9,11,12,14,15,17,19,22]
P ethanolamine + arachidonic acid
S arachidonamide + H_2O <3> (Reversibility: ?) [15]
P arachidonic acid + NH_3
S arachidonamide + H_2O <3> (<3> 311% of the activity with oleamide [12]) (Reversibility: ?) [12]
P arachidonic acod + NH_3
S arachidonoyl ethanolamide + H_2O <3> (Reversibility: ?) [23]
P oleic acid + ethanolamine
S arachidonoyl ethanolamide + H_2O <9> (Reversibility: ?) [23]
P arachidonic acid + ethanolamine
S arachidonoyl *p*-nitroanilide + H_2O <3> (Reversibility: ?) [10]
P arachidonate + *p*-nitroaniline
S β-arachidonoylglycerol + H_2O <3> (<3> hydrolysis is 2.5fold higher than the rate of anandamide hydrolysis [15]) (Reversibility: ?) [15]
P ?
S decanoyl *p*-nitroanilide + H_2O <3> (Reversibility: ?) [10]
P decanoate + *p*-nitroaniline
S dodecanoamide + H_2O <3> (<3> 74% of the activity with oleamide [12]) (Reversibility: ?) [12]

P dodecanoic acid + NH_3
S erucamide + H_2O <3> (<3> 83% of the activity with oleamide [12]) (Reversibility: ?) [12]
P ? + NH_3
S heptanoyl *p*-nitroanilide + H_2O <3> (Reversibility: ?) [10]
P heptanoate + *p*-nitroaniline
S lauroyl *p*-nitroanilide + H_2O <3> (Reversibility: ?) [10]
P laurate + *p*-nitroaniline
S linoelaidamide + H_2O <3> (<3> 54% of the activity with oleamide [12]) (Reversibility: ?) [12]
P ? + NH_3
S linoleic amide + H_2O <3> (<3> 104% of the activity with oleamide [12]) (Reversibility: ?) [12]
P ? + NH_3
S myristic amide + H_2O <3,8> (<3> 24.3% of the activity with oleamide [17]; <3> 24% of the activity with anandamide [19]; <8> 65% of the activity with anandamide [19]) (Reversibility: ?) [17,19]
P myristic acid + NH_3
S myristic amide + H_2O <3> (<3> 83% of the activity with oleamide [12]) (Reversibility: ?) [12]
P myristic acid + NH_3
S myristoleic amide + H_2O <3> (<3> 86% of the activity with oleamide [12]) (Reversibility: ?) [12]
P myristoleic acid + NH_3
S myristoyl *p*-nitroanilide + H_2O <3> (Reversibility: ?) [10]
P myristate + *p*-nitroaniline
S nervonamide + H_2O <3> (<3> 82% of the activity with oleamide [12]) (Reversibility: ?) [12]
P ? + NH_3
S nonanoyl *p*-nitroanilide + H_2O <3> (Reversibility: ?) [10]
P nonanoate + *p*-nitroaniline
S octanoyl *p*-nitroanilide + H_2O <3> (Reversibility: ?) [10]
P octanoate + *p*-nitroaniline
S oleamide + H_2O <1,3,8,9> (<3> enzyme is responsible for the catabolism of neuromodulatory fatty acid amides, including anandamide and oleamide [9]; <1> fatty acid amide hydrolase is a modulator of endogenous signaling compounds affecting sleep (oleamide) and analgesia (anandamide) [22]; <3> role of FAAH in epithelial cells of the choroid plexus may be to control the concentration of oleamide in the cerebrospinal fluid. FAAH may exert an important regulatory role in shaping the duration and magnitude of the sleep-inducing effect of endogenously or exogenously derived oleamide [18]; <3> the enzyme is responsible for the hydrolysis of a number of neuromodulatory fatty acid amides, including the endogenous cannabinoid anandamide and the sleep-inducing lipid oleamide [14]; <3> the serine hydrolase is responsible for the degradation of endogenous oleamide and anandamide, fatty acid amides that function as chemical messengers [12]; <8> 57% of the activity with anandamide [6]; <3>

serine residue 241 acts as the catalytic nucleophile of the enzyme. FAAH does not utilize a histidine base for the activation of its serine nucleophile [9]) (Reversibility: ?) [1,6,8,9,12,14,16,17,18,19,22]
P oleic acid + NH_3
S oleoyl ethanolamide + H_2O <3> (Reversibility: ?) [23]
P arachidonic acid + ethanolamine
S oleoyl ethanolamide + H_2O <9> (Reversibility: ?) [23]
P oleic acid + ethanolamine
S oleoyl methyl amide + H_2O <3> (Reversibility: ?) [8]
P ?
S oleoyl methyl ester + H_2O <3> (Reversibility: ?) [14]
P oleic acid + methanol
S oleoyl methyl ester + H_2O <3> (Reversibility: ?) [8]
P ?
S oleoyl *p*-nitroanilide + H_2O <3> (Reversibility: ?) [10]
P oleate + *p*-nitroaniline
S oleoyl *p*-nitroanilide + H_2O <3> (Reversibility: ?) [8]
P ?
S palmitic amide + H_2O <3> (<3> 9.9% of the activity with oleamide [17]) (Reversibility: ?) [17]
P palmitic acid + NH_3
S palmitic amide + H_2O <3,8> (<3> 10% of the activity with anandamide [19]; <8> 33% of the activity with anandamide [19]) (Reversibility: ?) [19]
P palmitic acid + NH_3
S palmitoamide + H_2O <3> (<3> 72% of the activity with oleamide [12]) (Reversibility: ?) [12]
P palmitoic acid + NH_3
S palmitoleamide + H_2O <3> (<3> 79% of the activity with oleamide [12]) (Reversibility: ?) [12]
P palmitoleic acid + NH_3
S palmitoyl *p*-nitroanilide + H_2O <3> (Reversibility: ?) [10]
P palmitate + *p*-nitroaniline
S palmitoylethanolamide + H_2O <2> (<2> substrate of FAAH and FAAH-2, the latter shows lower activity than FAAH [24]) (Reversibility: ?) [24]
P palmitic acid + ethanolamine
S stearamide + H_2O <3> (<3> 69% of the activity with oleamide [12]) (Reversibility: ?) [12]
P stearic acid + NH_3
S stearic amide + H_2O <3> (<3> 5.8% of the activity with oleamide [17]) (Reversibility: ?) [17]
P stearic acid + NH_3
S stearic amide + H_2O <3,8> (<3,8> 5.8% of the activity with anandamide [19]) (Reversibility: ?) [19]
P stearic + NH_3
S Additional information <2,3,9> (<3> catalytic efficiency (k_{cat}/K_m) of FAAH for nonanoyl *p*-nitroanilide is approximately 50fold higher than for hexanoyl *p*-nitroanilide. NAI491 participates in hydrophobic binding

interactions with medium-chain FAAH substrates. Use of *p*-nitroanilide substrates allows for the precise monitoring of enzymatic hydrolysis rates by following the increase in UV absorbance at 382 nm due to the release of *p*-nitroaniline. *p*-Nitroanilides are slower FAAH substrates than the corresponding primary amides, however, the binding affinities of these two classes of substrates are equivalent. Due to the slower rates of *p*-nitroanilide hydrolysis relative to the corresponding primary amides, it can be assumed that pNA substrates are hydrolyzed by FAAH in an acylation rate-limiting manner, allowing for the direct measurement of substrate binding constants through the determination of K_m values [10]; <3> FAAH is an enzyme of broad substrate specificity and is capable of hydrolyzing a wide array of unsaturated, and to a lesser extent saturated, fatty acid primary amides. However, when substituted adjacent to the amide carbonyl, the substrates can be made sterically or electronically resistant to hydrolysis. Long chain saturated fatty acid amides are hydrolyzed slower than the corresponding Z unsaturated fatty acid amides and the rate of hydrolysis increases incrementally with increases in the degree of unsaturation [12]; <3> hybrid quantum mechanics/molecular mechanics (QM/MM) calculations reveal a new mechanism of nucleophile activation involving a Lys-Ser-Ser catalytic triad. The proposed mechanism, shows that Lys142 and cis-Ser217 have a direct role in the activation of Ser241, in agreement with kinetic labelling experiments employing the highly reactive fluorophosphonatetetramethyl rhodamine. The greater reduction of Ser241 labelling rate in the K142A/S217A double mutant, compared to the K142A and S217A single mutants, suggests that Lys142 and Ser217 cooperate to deprotonate Ser241 [13]; <3> N,N-bis(2-hydroxyethyl)arachidonamide is not hydrolyzed [15]; <9> no activity with N-oleoyltaurine [6]; <2> FAAH inactivates anandamide and other bioactive N-acylethanolamines [24]) (Reversibility: ?) [6,10,12,13,15,24]

P ?

Inhibitors

(10Z)-1,1,1-trifluorononadec-10-en-2-one <2> [20]
(10Z)-1-bromononadec-10-en-2-one <2> [20]
(10Z)-2-oxononadec-10-enamide <2> [20]
(2R)-oxiran-2-ylmethyl (5Z,8Z,11Z,14Z)-icosa-5,8,11,14-tetraenoate <3> [4]
(2S)-oxiran-2-ylmethyl (5Z,8Z,11Z,14Z)-icosa-5,8,11,14-tetraenoate <3> [4]
(5Z,8Z,11Z,14Z)-1-[1,3]oxazolo[4,5-b]pyridin-2-ylicosa-5,8,11,14-tetraen-1-one <2> [20]
(5Z,8Z,11Z,14Z)-1-[1,3]oxazolo[4,5-c]pyridin-2-ylicosa-5,8,11,14-tetraen-1-one <2> [20]
(5Z,8Z,11Z,14Z)-1-[1,3]oxazolo[5,4-c]pyridin-2-ylicosa-5,8,11,14-tetraen-1-one <2> [20]
(5Z,8Z,11Z,14Z)-1-pyridazin-3-ylicosa-5,8,11,14-tetraen-1-one <2> [20]
(5Z,8Z,11Z,14Z)-N-((2,2-dimethyl-1,3-dioxolan-4-yl)methyl)icosa-5,8,11,14-tetraenamide <3> [4]

(5Z,8Z,11Z,14Z)-N-[(2R)-tetrahydrofuran-2-ylmethyl]icosa-5,8,11,14-tetraenamide <3> [4]
(5Z,8Z,11Z,14Z)-N-[(2S)-tetrahydrofuran-2-ylmethyl]icosa-5,8,11,14-tetraenamide <3> [4]
(6aR,10aR)-3-(1,1-dimethylheptyl)-9-(hydroxymethyl)-6,6-dimethyl-6a,7,10,10a-tetrahydro-6H-benzo[c]chromen-1-ol <3> [15]
(9E)-1-[1,3]oxazolo[4,5-b]pyridin-2-yloctadec-9-en-1-one <2> [20]
(9E)-1-pyridazin-3-yloctadec-9-en-1-one <2> [20]
(9Z)-1-(1,3-benzothiazol-2-yl)octadec-9-en-1-one <2> [20]
(9Z)-1-(1,3-benzoxazol-2-yl)octadec-9-en-1-one <2> [20]
(9Z)-1-(1,3-oxazol-2-yl)octadec-9-en-1-one <2> [20]
(9Z)-1-(1,3-thiazol-2-yl)octadec-9-en-1-one <2> [20]
(9Z)-1-(1-methyl-1H-benzimidazol-2-yl)octadec-9-en-1-one <2> [20]
(9Z)-1-(1-methyl-1H-imidazol-2-yl)octadec-9-en-1-one <2> [20]
(9Z)-1-(1-methyl-1H-tetrazol-5-yl)octadec-9-en-1-one <2> [20]
(9Z)-1-(1H-benzimidazol-2-yl)octadec-9-en-1-one <2> [20]
(9Z)-1-(1H-tetrazol-5-yl)octadec-9-en-1-one <2> [20]
(9Z)-1-(2-methyl-2H-tetrazol-5-yl)octadec-9-en-1-one <2> [20]
(9Z)-1-(4,5-dihydro-1,3-oxazol-2-yl)octadec-9-en-1-one <2> [20]
(9Z)-1-(4-methyl-1,3-benzoxazol-2-yl)octadec-9-en-1-one <2> [20]
(9Z)-1-(5-methyl-1,3-benzoxazol-2-yl)octadec-9-en-1-one <2> [20]
(9Z)-1-(6-methyl-1,3-benzoxazol-2-yl)octadec-9-en-1-one <2> [20]
(9Z)-1-(7-methyl-1,3-benzoxazol-2-yl)octadec-9-en-1-one <2> [20]
(9Z)-1-[1,3]oxazolo[4,5-b]pyridin-2-yloctadec-9-en-1-one <2> [20]
(9Z)-1-[1,3]oxazolo[4,5-c]pyridin-2-yloctadec-9-en-1-one <2> [20]
(9Z)-1-[1,3]oxazolo[5,4-b]pyridin-2-yloctadec-9-en-1-one <2> [20]
(9Z)-1-[1,3]oxazolo[5,4-c]pyridin-2-yloctadec-9-en-1-one <2> [20]
(9Z)-1-phenyloctadec-9-en-1-one <2> [20]
(9Z)-1-pyrazin-2-yloctadec-9-en-1-one <2> [20]
(9Z)-1-pyridazin-3-yloctadec-9-en-1-one <2> [20]
(9Z)-1-pyridin-2-yloctadec-9-en-1-one <2> [20]
(9Z)-1-pyrimidin-2-yloctadec-9-en-1-one <2> [20]
(9Z)-1-pyrimidin-4-yloctadec-9-en-1-one <2> [20]
(9Z)-octadec-9-enal <2> [20]
(R,S)-ibuprofen <3> [26]
1,1'-(5,5'-bi-1,3-oxazole-2,2'-diyl)bis(7-phenylheptan-1-one) <3> [16]
1,1-biphenyl-3-yl-carbamic acid cyclohexyl ester <1> (<1> i.e. URB602 [5]) [5]
1,3-benzodioxol-5-ylmethyl (5Z,8Z,11Z,14Z)-icosa-5,8,11,14-tetraenoate <3> [4]
1-(1,3-benzoxazol-2-yl)octadecan-1-one <2> [20]
1-(1,3-oxazol-2-yl)-7-phenylheptan-1-one <3> [16]
1-(5-acetyl-1,3-oxazol-2-yl)-7-phenylheptan-1-one <3> [16]
1-(5-bromo-1,3-oxazol-2-yl)-7-phenylheptan-1-one <3> [16]
1-(5-chloro-1,3-oxazol-2-yl)-7-phenylheptan-1-one <3> [16]
1-(5-fluoro-1,3-oxazol-2-yl)-7-phenylheptan-1-one <3> [16]
1-(5-furan-2-yl-1,3-oxazol-2-yl)-7-phenylheptan-1-one <3> [16]

1-(5-iodo-1,3-oxazol-2-yl)-7-phenylheptan-1-one <3> [16]
1-(5-methyl-1,3-oxazol-2-yl)-7-phenylheptan-1-one <3> [16]
1-[1,3]oxazolo[4,5-b]pyridin-2-yl-4-phenylbutan-1-one <2> [20]
1-[1,3]oxazolo[4,5-b]pyridin-2-yl-5-phenylpentan-1-one <2> [20]
1-[1,3]oxazolo[4,5-b]pyridin-2-yl-6-phenylhexan-1-one <2> [20]
1-[1,3]oxazolo[4,5-b]pyridin-2-yl-7-phenylheptan-1-one <2> [20]
1-[1,3]oxazolo[4,5-b]pyridin-2-yl-8-phenyloctan-1-one <2> [20]
1-[1,3]oxazolo[4,5-b]pyridin-2-yl-9-phenylnonan-1-one <2> [20]
1-[1,3]oxazolo[4,5-b]pyridin-2-yldec-9-en-1-one <2> [20]
1-[1,3]oxazolo[4,5-b]pyridin-2-yldec-9-yn-1-one <2> [20]
1-[1,3]oxazolo[4,5-b]pyridin-2-yldecan-1-one <2> [20]
1-[1,3]oxazolo[4,5-b]pyridin-2-yldodecan-1-one <2> [20]
1-[1,3]oxazolo[4,5-b]pyridin-2-ylethanone <2> [20]
1-[1,3]oxazolo[4,5-b]pyridin-2-ylheptan-1-one <2> [20]
1-[1,3]oxazolo[4,5-b]pyridin-2-ylhexadecan-1-one <2> [20]
1-[1,3]oxazolo[4,5-b]pyridin-2-ylhexan-1-one <2> [20]
1-[1,3]oxazolo[4,5-b]pyridin-2-yloctadec-9-yn-1-one <2> [20]
1-[1,3]oxazolo[4,5-b]pyridin-2-yloctadecan-1-one <2> [20]
1-[1,3]oxazolo[4,5-b]pyridin-2-yloctan-1-one <2> [20]
1-[1,3]oxazolo[4,5-b]pyridin-2-ylpentan-1-one <2> [20]
1-[1,3]oxazolo[4,5-b]pyridin-2-yltetradecan-1-one <2> [20]
1-[5-(2,4-dimethoxypyrimidin-5-yl)-1,3-oxazol-2-yl]-7-phenylheptan-1-one <3> [16]
1-[5-(2,6-dimethoxypyrimidin-4-yl)-1,3-oxazol-2-yl]-7-phenylheptan-1-one <3> [16]
1-[5-(2-aminophenyl)-1,3-oxazol-2-yl]-7-phenylheptan-1-one <3> [16]
1-[5-(2-fluorophenyl)-1,3-oxazol-2-yl]-7-phenylheptan-1-one <3> [16]
1-[5-(2-hydroxyphenyl)-1,3-oxazol-2-yl]-7-phenylheptan-1-one <3> [16]
1-[5-(2-methoxyphenyl)-1,3-oxazol-2-yl]-7-phenylheptan-1-one <3> [16]
1-[5-(2-nitrophenyl)-1,3-oxazol-2-yl]-7-phenylheptan-1-one <3> [16]
1-[5-(3-aminophenyl)-1,3-oxazol-2-yl]-7-phenylheptan-1-one <3> [16]
1-[5-(3-fluorophenyl)-1,3-oxazol-2-yl]-7-phenylheptan-1-one <3> [16]
1-[5-(3-hydroxyphenyl)-1,3-oxazol-2-yl]-7-phenylheptan-1-one <3> [16]
1-[5-(3-methoxyphenyl)-1,3-oxazol-2-yl]-7-phenylheptan-1-one <3> [16]
1-[5-(3-methylpyridin-2-yl)-1,3-oxazol-2-yl]-7-phenylheptan-1-one <3> [16]
1-[5-(3-nitrophenyl)-1,3-oxazol-2-yl]-7-phenylheptan-1-one <3> [16]
1-[5-(4-aminophenyl)-1,3-oxazol-2-yl]-7-phenylheptan-1-one <3> [16]
1-[5-(4-aminopyridin-2-yl)-1,3-oxazol-2-yl]-7-phenylheptan-1-one <3> [16]
1-[5-(4-fluorophenyl)-1,3-oxazol-2-yl]-7-phenylheptan-1-one <3> [16]
1-[5-(4-fluoropyridin-2-yl)-1,3-oxazol-2-yl]-7-phenylheptan-1-one <3> [16]
1-[5-(4-hydroxyphenyl)-1,3-oxazol-2-yl]-7-phenylheptan-1-one <3> [16]
1-[5-(4-methoxyphenyl)-1,3-oxazol-2-yl]-7-phenylheptan-1-one <3> [16]
1-[5-(4-methoxypyridin-2-yl)-1,3-oxazol-2-yl]-7-phenylheptan-1-one <3> [16]
1-[5-(4-methylpyridin-2-yl)-1,3-oxazol-2-yl]-7-phenylheptan-1-one <3> [16]
1-[5-(4-nitrophenyl)-1,3-oxazol-2-yl]-7-phenylheptan-1-one <3> [16]
1-[5-(4-nitropyridin-2-yl)-1,3-oxazol-2-yl]-7-phenylheptan-1-one <3> [16]

1-[5-(5-methylpyridin-2-yl)-1,3-oxazol-2-yl]-7-phenylheptan-1-one <3> [16]
1-[5-(6-methylpyridin-2-yl)-1,3-oxazol-2-yl]-7-phenylheptan-1-one <3> [16]
1-[5-(methylsulfanyl)-1,3-oxazol-2-yl]-7-phenylheptan-1-one <3> [16]
1-[5-(morpholin-4-ylcarbonyl)-1,3-oxazol-2-yl]-7-phenylheptan-1-one <3> [16]
1-[5-[(4-methylpiperazin-1-yl)carbonyl]-1,3-oxazol-2-yl]-7-phenylheptan-1-one <3> [16]
1-oxazolo[4,5-b]pyridin-2-yl-9-octadecyn-1-one <3> [2]
1-pyridazin-3-yloctadecan-1-one <2> [20]
2,2-dimethyl-1,3-dioxolan-4-ylmethyl (5Z,8Z,11Z,14Z)-icosa-5,8,11,14-tetraenoate <3> [4]
2-(5,5-dimethyl-1,3-dioxan-2-yl)ethyl (5Z,8Z,11Z,14Z)-icosa-5,8,11,14-tetraenoate <3> [4]
2-(7-phenylheptanoyl)-1,3-oxazole-5-carbaldehyde <3> [16]
2-(7-phenylheptanoyl)-1,3-oxazole-5-carbonitrile <3> [16]
2-(7-phenylheptanoyl)-1,3-oxazole-5-carboxamide <3> [16]
2-(7-phenylheptanoyl)-1,3-oxazole-5-carboxylic acid <3> [16]
2-[2-(7-phenylheptanoyl)-1,3-oxazol-5-yl]benzamide <3> [16]
2-[2-(7-phenylheptanoyl)-1,3-oxazol-5-yl]benzenesulfonamide <3> [16]
2-[2-(7-phenylheptanoyl)-1,3-oxazol-5-yl]benzoic acid <3> [16]
2-[2-(7-phenylheptanoyl)-1,3-oxazol-5-yl]benzonitrile <3> [16]
2-[2-(7-phenylheptanoyl)-1,3-oxazol-5-yl]pyridine-3-carboxylic acid <3> [16]
2-[2-(7-phenylheptanoyl)-1,3-oxazol-5-yl]pyridine-4-carbonitrile <3> [16]
2-[2-(7-phenylheptanoyl)-1,3-oxazol-5-yl]pyridine-4-carboxylic acid <3> [16]
2-iodobenzylarachidonoylamide <1> [25]
2-iodobenzyllinoleoylamide <1> [25]
2-iodophenethylarachidonoylamide <1> [25]
2-iodophenethyllinoleoylamide <1> [25]
2-methoxyphenethylarachidonoylamide <1> [25]
2-methoxyphenethyllinoleoylamide <1> [25]
3'-carbamoyl-biphenyl-3-yl-cyclohexylcarbamate <3> [2]
3'-carbamoylbiphenyl-3-yl cyclohexylcarbamate <8> [6]
3'-carbamoylbiphenyl-3-yl undec-10-yn-1-ylcarbamate <8> [6]
3-[2-(7-phenylheptanoyl)-1,3-oxazol-5-yl]benzamide <3> [16]
3-[2-(7-phenylheptanoyl)-1,3-oxazol-5-yl]benzenesulfonamide <3> [16]
3-[2-(7-phenylheptanoyl)-1,3-oxazol-5-yl]benzoic acid <3> [16]
3-[2-(7-phenylheptanoyl)-1,3-oxazol-5-yl]benzonitrile <3> [16]
3-iodobenzylarachidonoylamide <1> [25]
3-iodobenzyllinoleoylamide <1> [25]
3-iodophenethylarachidonoylamide <1> [25]
3-iodophenethyllinoleoylamide <1> [25]
3-methoxyphenethylarachidonoylamide <1> [25]
3-methoxyphenethyllinoleoylamide <1> [25]
4-(3-phenyl-[1,2,4]thiadiazol-5-yl)piperazine-1-carboxylic acid phenylamide <3,9> (<3> JNJ-1661010 [23]) [23]
4-(acetylamino)phenyl (4-[[2-(trifluoromethyl)pyridin-4-yl]amino]phenyl) acetate <3> [26]

4-(acetylamino)phenyl 2-(4-[[2-(trifluoromethyl)pyridin-4-yl]amino]phenyl)-propanoate <3> (<3> competitive, also able to inhibit the FAAH activity in rat basophilic leukemia cells as assessed by measuring either the hydrolysis of anandamide, the FAAH-dependent cellular accumulation of anandamide, or the FAAH-dependent recycling of tritium to the cellmembranes [26]) [26]
4-(acetylamino)phenyl 2-[[2-(trifluoromethyl)pyridin-4-yl]amino]pyridine-3-carboxylate <3> [26]
4-(acetylamino)phenyl 2-[[3-(trifluoromethyl)phenyl]amino]benzoate <3> [26]
4-(acetylamino)phenyl 2-[[3-(trifluoromethyl)phenyl]amino]pyridine-3-carboxylate <3> [26]
4-(acetylamino)phenyl 3-(4-[[2-(trifluoromethyl)pyridin-4-yl]amino]phenyl)-propanoate <3> [26]
4-(acetylamino)phenyl 3-[[2-(trifluoromethyl)pyridin-4-yl]amino]benzoate <3> [26]
4-(acetylamino)phenyl 3-methyl-4-[[2-(trifluoromethyl)pyridin-4-yl]amino] benzoate <3> [26]
4-(acetylamino)phenyl 4-([[2-(trifluoromethyl)pyridin-4-yl]amino]methyl) benzoate <3> [26]
4-(acetylamino)phenyl 4-[[2-(trifluoromethyl)pyridin-4-yl]amino]benzoate <3> [26]
4-(acetylamino)phenyl 4-chloro-2-[[2-(trifluoromethyl)pyridin-4-yl]amino]-benzoate <3> [26]
4-(acetylamino)phenyl 5-chloro-2-[[2-(trifluoromethyl)pyridin-4-yl]amino]-benzoate <3> [26]
4-(acetylamino)phenyl 5-methyl-2-[[2-(trifluoromethyl)pyridin-4-yl]amino]-benzoate <3> [26]
4-(acetylamino)phenyl N-(3-methyl-4-[[2-(trifluoromethyl)pyridin-4-yl]amino]benzoyl)glycinate <3> [26]
4-(acetylamino)phenyl N-(4-[[2-(trifluoromethyl)pyridin-4-yl]amino]benzoyl) glycinate <3> [26]
4-(acetylamino)phenyl N-[(4-[[2-(trifluoromethyl)pyridin-4-yl]amino]phenyl) acetyl]glycinate <3> [26]
4-(acetylamino)phenyl N-[2-(4-[[2-(trifluoromethyl)pyridin-4-yl]amino]phenyl)propanoyl]glycinate <3> [26]
4-(benzyloxy)phenyl butylcarbamate <8> [6]
4-[2-(7-phenylheptanoyl)-1,3-oxazol-5-yl]benzamide <3> [16]
4-[2-(7-phenylheptanoyl)-1,3-oxazol-5-yl]benzenesulfonamide <3> [16]
4-[2-(7-phenylheptanoyl)-1,3-oxazol-5-yl]benzoic acid <3> [16]
4-[2-(7-phenylheptanoyl)-1,3-oxazol-5-yl]benzonitrile <3> [16]
4-acetamidophenyl2-(2-(trifluoromethyl)pyridin-4-ylamino)benzoate <3> [26]
4-iodobenzylarachidonoylamide <1> [25]
4-iodobenzyllinoleoylamide <1> [25]
4-iodophenethylarachidonoylamide <1> [25]
4-iodophenethyllinoleoylamide <1> [25]
4-methoxyphenethylarachidonoylamide <1> [25]
4-methoxyphenethyllinoleoylamide <1> [25]

5-(4-chlorophenyl)-1-(2,4-dichlorophenyl)-4-methyl-N-morpholin-4-yl-1H-pyrazole-3-carboxamide <3> [15]
5-[2-(7-phenylheptanoyl)-1,3-oxazol-5-yl]furan-2-carboxylic acid <3> [16]
5-[2-(7-phenylheptanoyl)-1,3-oxazol-5-yl]pyrimidine-2,4(1H,3H)-dione <3> [16]
5-[2-(7-phenylheptanoyl)-1,3-oxazol-5-yl]thiophene-2-carboxylic acid <3> [16]
5-[2-(7-phenylheptanoyl)-1,3-oxazol-5-yl]thiophene-2-sulfonamide <3> [16]
6-[2-(7-phenylheptanoyl)-1,3-oxazol-5-yl]pyridine-2-carboxamide <3> [16]
6-[2-(7-phenylheptanoyl)-1,3-oxazol-5-yl]pyridine-2-carboxylic acid <3> [16]
6-[2-(7-phenylheptanoyl)-1,3-oxazol-5-yl]pyridine-3-carboxamide <3> [16]
6-[2-(7-phenylheptanoyl)-1,3-oxazol-5-yl]pyridine-3-carboxylic acid <3> [16]
6-[2-(7-phenylheptanoyl)-1,3-oxazol-5-yl]pyrimidine-2,4(1H,3H)-dione <3> [16]
7-phenyl-1-(5-phenyl-1,3-oxazol-2-yl)heptan-1-one <3> [16]
7-phenyl-1-(5-pyridin-2-yl-1,3-oxazol-2-yl)heptan-1-one <3,8> [6,16]
7-phenyl-1-(5-pyrimidin-2-yl-1,3-oxazol-2-yl)heptan-1-one <3> [16]
7-phenyl-1-(5-pyrimidin-4-yl-1,3-oxazol-2-yl)heptan-1-one <3> [16]
7-phenyl-1-(5-pyrimidin-5-yl-1,3-oxazol-2-yl)heptan-1-one <3> [16]
7-phenyl-1-(5-thiophen-2-yl-1,3-oxazol-2-yl)heptan-1-one <3> [16]
7-phenyl-1-[5-(1H-tetrazol-5-yl)-1,3-oxazol-2-yl]heptan-1-one <3> [16]
7-phenyl-1-[5-(piperidin-1-ylcarbonyl)-1,3-oxazol-2-yl]heptan-1-one <3> [16]
7-phenyl-1-[5-(thiomorpholin-4-ylcarbonyl)-1,3-oxazol-2-yl]heptan-1-one <3> [16]
7-phenyl-1-[5-(trifluoroacetyl)-1,3-oxazol-2-yl]heptan-1-one <3> [16]
7-phenyl-1-[5-(trifluoromethyl)-1,3-oxazol-2-yl]heptan-1-one <3> [16]
7-phenyl-1-[5-[2-(trifluoroacetyl)phenyl]-1,3-oxazol-2-yl]heptan-1-one <3> [16]
7-phenyl-1-[5-[3-(trifluoroacetyl)phenyl]-1,3-oxazol-2-yl]heptan-1-one <3> [16]
7-phenyl-1-[5-[4-(trifluoroacetyl)phenyl]-1,3-oxazol-2-yl]heptan-1-one <3> [16]
7-phenyl-1-[5-[4-(trifluoromethyl)pyridin-2-yl]-1,3-oxazol-2-yl]heptan-1-one <3> [16]
CF3-OH <3,8> [19]
DFP <1> [22]
JP104 <9> [6]
N,N-dimethyl-2-(7-phenylheptanoyl)-1,3-oxazole-5-carboxamide <3> [16]
N-(2-hydroxyethyl)linoleoylamide <1> (<1> competitive versus anadamide [25]) [25]
N-(3-methylpyridin-2-yl)-2-(4'-isobutylphenyl)propionamide <3> (<3> i.e. Ibu-am5 [26]) [26]
N-(4-hydroxy-2-methylphenyl) arachidonoyl amide <3> (<3> i.e. VDM11, inhibits the metabolism of anandamide by rat brain FAAH. Inhibition may at least in part be a consequence of the compound acting as an alternative substrate [2]) [2]
N-(4-hydroxyphenyl)-5Z,8Z,11Z,14Z-eicosatetraenamide <3> (<3> i.e. AM404, a bioactive N-acylphenolamine, derived from paracetamol, competitve inhibition [26]) [26]
N-(4-hydroxyphenyl)arachidonylamide <3> (<3> i.e. AM404, inhibits the metabolism of anandamide by rat brain FAAH [2]) [2]

N-methyl-2-(7-phenylheptanoyl)-1,3-oxazole-5-carboxamide <3> [16]
N-n-heptyl benzodioxaphosphorin oxide <1> [3]
O-n-octyl benzodioxaphosphorin oxide <1> [3]
O-octyl-benzodioxaphosphorin oxide <1> [22]
OL-135 <9> [6]
S-heptyl benzodioxaphosphorin oxide <1> [3]
S-nonyl benzodioxaphosphorin oxide <1> [3]
S-pentyl benzodioxaphosphorin oxide <1> [3]
URB532 <9> [6]
URB597 <3,9> [6,27]
[(4R)-2,2-dimethyl-1,3-dioxolan-4-yl]methyl (5Z,8Z,11Z,14Z)-icosa-5,8,11,14-tetraenoate <3> [4]
[(4S)-2,2-dimethyl-1,3-dioxolan-4-yl]methyl (5Z,8Z,11Z,14Z)-icosa-5,8,11,14-tetraenoate <3> [4]
anadamide <1> (<1> i.e. (5Z,8Z,11Z,14Z)-N-(2-hydroxyethyl)icosa-5,8,11,14-tetraenamide or N-arachidonoylethanolamine, competitive [25]) [25]
benzol <1> [3]
chlorpyrifos oxon <1> [3,22]
cis-anandamide <5> (<5> inhibits hydrolysis of anandamide [11]) [11]
cyclohexylcarbamic acid 3'-carbamoylbiphenyl-3-yl ester <1> (<1> i.e. URB597, attenuates the development of lipopolysaccharide-induced paw edema and reverses lipopolysaccharide-induced hyperalgesia through the respective CB2 and CB1 mechanisms of action. The inhibition is not affected by capsazepine, a transient receptor potential vanilloid type 1 antagonist [28]) [28]
decyl benzodioxaphosphorin oxide <1> [3]
diazoxon <1> [3]
dichlorvos <1> [3]
diisopropyl fluorophosphate <1> [3]
dodecyl benzodioxaphosphorin oxide <1> [3]
dodecyl sulfonyl fluoride <1> [3]
dodecyl-benzodioxaphosphorin oxide <1> [22]
ethoxy oleoyl fluorophosphonate <3> (<3> irreversible inhibitor, exclusively modifies FAAH at S241 [9]) [9]
ethyl (10Z)-2-oxononadec-10-enoate <2> [20]
ethyl octylphosphonofluoridate <1> [3,22]
heptyl benzodioxaphosphorin oxide <1> [3]
ibuprofen <3> [7]
isopropyl dodecylfluorophosphate <1> [3]
methyl 2-(7-phenylheptanoyl)-1,3-oxazole-5-carboxylate <3> [16]
methyl 2-[2-(7-phenylheptanoyl)-1,3-oxazol-5-yl]benzoate <3> [16]
methyl 2-[2-(7-phenylheptanoyl)-1,3-oxazol-5-yl]pyridine-3-carboxylate <3> [16]
methyl 2-[2-(7-phenylheptanoyl)-1,3-oxazol-5-yl]pyridine-4-carboxylate <3> [16]
methyl 3-[2-(7-phenylheptanoyl)-1,3-oxazol-5-yl]benzoate <3> [16]
methyl 4-[2-(7-phenylheptanoyl)-1,3-oxazol-5-yl]benzoate <3> [16]
methyl 5-[2-(7-phenylheptanoyl)-1,3-oxazol-5-yl]furan-2-carboxylate <3> [16]

methyl 5-[2-(7-phenylheptanoyl)-1,3-oxazol-5-yl]thiophene-2-carboxylate <3> [16]
methyl 6-[2-(7-phenylheptanoyl)-1,3-oxazol-5-yl]pyridine-2-carboxylate <3> [16]
methyl 6-[2-(7-phenylheptanoyl)-1,3-oxazol-5-yl]pyridine-3-carboxylate <3> [16]
methyl arachidonyl fluorophosphonate <1> (<1> MAFP, a potent irreversible FAAH inhibitor [25]) [5,25]
methyl arachidonyl phosphonofluoridate <1> [22]
methyl arachidonylfluoroposphate <1> [3]
methyl octylphosphonofluoridate <1> [3]
octyl sulfonyl fluoride <1> [3]
octyl-benzodioxaphosphorin oxide <1> [22]
oleyl-benzodioxaphosphorin oxide <1> [22]
oxiran-2-ylmethyl (5Z,8Z,11Z,14Z)-icosa-5,8,11,14-tetraenoate <3> [4]
oxiran-2-ylmethyl (9Z)-hexadec-9-enoate <3> [4]
oxiran-2-ylmethyl (9Z)-octadec-9-enoate <3> [4]
oxiran-2-ylmethyl (9Z,12Z)-octadeca-9,12-dienoate <3> [4]
oxiran-2-ylmethyl (9Z,12Z,15Z)-octadeca-9,12,15-trienoate <3> [4]
oxiran-2-ylmethyl 1,1'-biphenyl-2-carboxylate <3> [4]
oxiran-2-ylmethyl 1,1'-biphenyl-3-carboxylate <3> [4]
oxiran-2-ylmethyl 1,1'-biphenyl-4-carboxylate <3> [4]
oxiran-2-ylmethyl benzoate <3> [4]
paraoxon <1> [3,22]
phenyl-benzodioxaphosphorin oxide <1> [22]
profenofos <1> [22]
stearyl benzodioxaphosphorin oxide <1> [3]
tetrahydro-2H-pyran-2-ylmethyl (5Z,8Z,11Z,14Z)-icosa-5,8,11,14-tetraenoate <3> [4]
tetrahydro-2H-pyran-2-ylmethyl (9Z)-hexadec-9-enoate <3> [4]
tetrahydro-2H-pyran-2-ylmethyl (9Z)-octadec-9-enoate <3> [4]
tetrahydro-2H-pyran-2-ylmethyl (9Z,12Z)-octadeca-9,12-dienoate <3> [4]
tetrahydro-2H-pyran-2-ylmethyl (9Z,12Z,15Z)-octadeca-9,12,15-trienoate <3> [4]
tetrahydro-2H-pyran-2-ylmethyl 1,1'-Biphenyl-4-carboxylate <3> [4]
tetrahydro-2H-pyran-2-ylmethyl 1,1'-biphenyl-2-carboxylate <3> [4]
tetrahydro-2H-pyran-2-ylmethyl 1,1'-biphenyl-3-carboxylate <3> [4]
tetrahydro-2H-pyran-2-ylmethyl benzoate <3> [4]
tetrahydro-2H-pyran-4-yl (5Z,8Z,11Z,14Z)-icosa-5,8,11,14-tetraenoate <3> [4]
trans-anandamide <5> (<5> inhibits hydrolysis of anandamide [11]) [11]
Additional information <1,2,3> (<1> the microglial-specific isozyme is not inhibited by URB597, i.e. 3-carbamoyl-biphenyl-3-ylcyclohexylcarbamate, and inhibitors of cyclooxygenases, lipooxygenases, and diacylglycerol lipases, overview [5]; <3> a series of 5-substituted 7-phenyl-1-(oxazol-2-yl)heptan-1-ones are prepared and evaluated for FAAH inhibitory potency as well as FAAH selectivity versus competitive serine proteases [16]; <2> fatty acid-derived FAAH inhibitors [7]; <1> organophosphorus compound-induced FAAH

inhibition and the associated anandamide accumulation may lead to reduced limb mobility as a secondary neurotoxic effect [22]; <2> analysis of the enzyme inhibition by quantum mechanics/molecular mechanics (QM/MM) modelling [24]; <3> paracetamol itself does not inhibit FAAH, but undergoes a FAAH-dependent two-step metabolic transformation in the brain, liver, and spinal cord to form the bioactive N-acylphenolamine AM404. Synthesis and evaluation of paracetamol ester enzyme inhibitors, structure-activity relationship studies, overview [26]; <1> synthesis of 18 aryl analogues of anandamide. In vitro evaluation of inhibitory potency, binding to CB1 and CB2 cannabinoid receptors, and potential as metabolic trapping tracers of 4-methoxyphenethyllinoleoylamide and 4-methoxyphenethylarachidonoylamide, overview [25]) [5,7,16,22,24,25,26]

Turnover number (s^{-1})

0.0001 <3> (oleoyl methyl amide, <3> pH 9.0, mutant enzyme K142A [8]) [8]
0.0002 <3> (oleoyl methyl ester, <3> pH 9.0, mutant enzyme K142E [8]) [8]
0.00026 <3> (oleamide, <3> pH 9.0, mutant enzyme K142A [8]) [8]
0.00031 <3> (oleoyl methyl amide, <3> pH 9.0, mutant enzyme K142E [8]) [8]
0.00052 <3> (oleoyl *p*-nitroanilide, <3> pH 9.0, mutant enzyme K142E [8]) [8]
0.00064 <3> (oleamide, <3> pH 9.0, mutant enzyme K142E [8]) [8]
0.0022 <3> (oleamide, <3> pH 9.0, mutant enzyme S217A, FAAH protein lacking its N-terminal 39 amino acids is used. This modification removes the predicted N-terminal transmembrane domain of FAAH, the deletion of which is previously found to leave catalytic properties of FAAH unaltered, while at the same time facilitating the purification [9]) [9]
0.012 <3> (oleoyl methyl ester, <3> pH 9.0, mutant enzyme K142A [8]) [8]
0.055 <3> (oleamide, <3> pH 9.0, mutant enzyme S218A, FAAH protein lacking its N-terminal 39 amino acids is used. This modification removes the predicted N-terminal transmembrane domain of FAAH, the deletion of which is previously found to leave catalytic properties of FAAH unaltered, while at the same time facilitating the purification [9]) [9]
0.13 <3> (myristoyl *p*-nitroanilide, <3> pH 9.0, mutant enzyme A487V [10]) [10]
0.14 <3> (myristoyl *p*-nitroanilide, <3> pH 9.0, mutant enzyme G489A [10]) [10]
0.15 <3> (oleoyl *p*-nitroanilide, <3> pH 9.0, mutant enzyme K142A [8]) [8]
0.17 <3> (oleoyl methyl ester, <3> pH 9.0, wild-type enzyme [8]) [8]
0.19 <3> (myristoyl *p*-nitroanilide, <3> pH 9.0, mutant enzyme T488A [10]) [10]
0.2 <3> (nonanoyl *p*-nitroanilide, <3> pH 9.0, mutant enzyme G489A [10]) [10]
0.21 <3> (myristoyl *p*-nitroanilide, <3> pH 9.0, mutant enzyme I491A [10]) [10]
0.21 <3> (oleoyl *p*-nitroanilide, <3> pH 9.0, mutant enzyme A487V [10]; <3> pH 9.0, mutant enzyme T488A [10]) [10]

0.22 <3> (oleoyl *p*-nitroanilide, <3> pH 9.0, mutant enzyme I491A [10]) [10]
0.25 <3> (oleoyl *p*-nitroanilide, <3> pH 9.0, mutant enzyme G489A [10]) [10]
0.27 <3> (oleoyl *p*-nitroanilide, <3> pH 9.0, wild-type enzyme [10]) [10]
0.27 <3> (palmitoyl *p*-nitroanilide, <3> pH 9.0, wild-type enzyme [10]) [10]
0.29 <3> (myristoyl *p*-nitroanilide, <3> pH 9.0, wild-type enzyme [10]) [10]
0.46 <3> (heptanoyl *p*-nitroanilide, <3> pH 9.0, wild-type enzyme [10]) [10]
0.46 <3> (lauroyl *p*-nitroanilide, <3> pH 9.0, wild-type enzyme [10]) [10]
0.48 <3> (arachidonoyl *p*-nitroanilide, <3> pH 9.0, wild-type enzyme [10]) [10]
0.51 <3> (nonanoyl *p*-nitroanilide, <3> pH 9.0, mutant enzyme T488A [10]) [10]
0.56 <3> (decanoyl *p*-nitroanilide, <3> pH 9.0, wild-type enzyme [10]) [10]
0.58 <3> (nonanoyl *p*-nitroanilide, <3> pH 9.0, mutant enzyme I491A [10]) [10]
0.6 <3> (nonanoyl *p*-nitroanilide, <3> pH 9.0, mutant enzyme A487V [10]; <3> pH 9.0, wild-type enzyme [10]) [10]
0.73 <3> (octanoyl *p*-nitroanilide, <3> pH 9.0, wild-type enzyme [10]) [10]
1.9 <3> (oleoyl methyl amide, <3> pH 9.0, wild-type enzyme [8]) [8]
2.8 <3> (oleoyl *p*-nitroanilide, <3> pH 9.0, wild-type enzyme [8]) [8]
3.3 <3> (oleamide, <3> pH 9.0, recombinantly expressed FAAH protein lacking the N-terminal transmembrane domain [1]) [1]
4.4 <3> (oleamide, <3> pH 9.0, mutant enzyme H358A, FAAH protein lacking its N-terminal 39 amino acids is used. This modification removes the predicted N-terminal transmembrane domain of FAAH, the deletion of which is previously found to leave catalytic properties of FAAH unaltered, while at the same time facilitating the purification [9]) [9]
5.2 <3> (oleamide, <3> pH 9.0, wild-type enzyme, FAAH protein lacking its N-terminal 39 amino acids is used. This modification removes the predicted N-terminal transmembrane domain of FAAH, the deletion of which is previously found to leave catalytic properties of FAAH unaltered, while at the same time facilitating the purification [9]) [9]
7.1 <3> (oleamide, <3> pH 9.0, recombinantly expressed wild-type enzyme [1]) [1]
7.7 <3> (oleamide, <3> pH 9.0, mutant enzyme H449A, FAAH protein lacking its N-terminal 39 amino acids is used. This modification removes the predicted N-terminal transmembrane domain of FAAH, the deletion of which is previously found to leave catalytic properties of FAAH unaltered, while at the same time facilitating the purification [9]) [9]
9 <3> (oleamide, <3> pH 9.0, wild-type enzyme [8]) [8]
20 <3> (oleamide, <3> pH 9.0, mutant enzyme H184Q, FAAH protein lacking its N-terminal 39 amino acids is used. This modification removes the predicted N-terminal transmembrane domain of FAAH, the deletion of which is previously found to leave catalytic properties of FAAH unaltered, while at the same time facilitating the purification [9]) [9]

K_m-Value (mM)

0.007 <3> (oleamide, <3> pH 9.0, mutant enzyme S218A, FAAH protein lacking its N-terminal 39 amino acids is used. This modification removes the predicted N-terminal transmembrane domain of FAAH, the deletion of which is previously found to leave catalytic properties of FAAH unaltered, while at the same time facilitating the purification [9]) [9]
0.009 <3> (oleoyl methyl amide, <3> pH 9.0, wild-type enzyme [8]) [8]
0.011 <3> (oleamide, <3> pH 9.0, wild-type enzyme, FAAH protein lacking its N-terminal 39 amino acids is used. This modification removes the predicted N-terminal transmembrane domain of FAAH, the deletion of which is previously found to leave catalytic properties of FAAH unaltered, while at the same time facilitating the purification [9]) [9]
0.012 <3> (oleamide, <3> pH 9.0, recombinantly expressed FAAH protein lacking the N-terminal transmembrane domain [1]) [1]
0.012 <3> (oleoyl *p*-nitroanilide, <3> pH 9.0, mutant enzyme K142A [8]) [8]
0.015 <3> (oleamide, <3> pH 9.0, mutant enzyme H358A, FAAH protein lacking its N-terminal 39 amino acids is used. This modification removes the predicted N-terminal transmembrane domain of FAAH, the deletion of which is previously found to leave catalytic properties of FAAH unaltered, while at the same time facilitating the purification [9]; <3> pH 9.0, mutant enzyme S217A, FAAH protein lacking its N-terminal 39 amino acids is used. This modification removes the predicted N-terminal transmembrane domain of FAAH, the deletion of which is previously found to leave catalytic properties of FAAH unaltered, while at the same time facilitating the purification [9]) [9]
0.02 <3> (oleamide, <3> pH 9.0, mutant enzyme K142A [8]) [8]
0.021 <3> (oleoyl *p*-nitroanilide, <3> pH 9.0, wild-type enzyme [8]) [8]
0.022 <3> (oleoyl methyl ester, <3> pH 9.0, wild-type enzyme [8]) [8]
0.023 <3> (oleamide, <3> pH 9.0, recombinantly expressed wild-type enzyme [1]) [1]
0.029 <3> (oleamide, <3> pH 9.0, mutant enzyme H449A, FAAH protein lacking its N-terminal 39 amino acids is used. This modification removes the predicted N-terminal transmembrane domain of FAAH , the deletion of which is previously found to leave catalytic properties of FAAH unaltered, while at the same time facilitating the purification [9]) [9]
0.03 <3> (oleamide, <3> pH 9.0, mutant enzyme H184Q, FAAH protein lacking its N-terminal 39 amino acids is used. This modification removes the predicted N-terminal transmembrane domain of FAAH, the deletion of which is previously found to leave catalytic properties of FAAH unaltered, while at the same time facilitating the purification [9]) [9]
0.031 <3> (oleamide, <3> pH 9.0, rat liver FAAH [1]) [1]
0.032 <3> (oleoyl methyl ester, <3> pH 9.0, mutant enzyme K142E [8]) [8]
0.037 <3> (oleamide, <3> pH 9.0, wild-type enzyme [8]) [8]
0.041 <3> (oleoyl methyl amide, <3> pH 9.0, mutant enzyme K142A [8]) [8]
0.057 <3> (decanoyl *p*-nitroanilide, <3> pH 9.0, wild-type enzyme [10]) [10]

0.057 <3> (nonanoyl *p*-nitroanilide, <3> pH 9.0, mutant enzyme A487V [10]) [10]
0.06 <3> (arachidonoyl *p*-nitroanilide, <3> pH 9.0, wild-type enzyme [10]) [10]
0.063 <3> (oleoyl methyl ester, <3> pH 9.0, mutant enzyme K142A [8]) [8]
0.065 <3> (lauroyl *p*-nitroanilide, <3> pH 9.0, wild-type enzyme [10]) [10]
0.069 <3> (myristoyl *p*-nitroanilide, <3> pH 9.0, mutant enzyme A487V [10]) [10]
0.072 <3> (myristoyl *p*-nitroanilide, <3> pH 9.0, mutant enzyme I491A [10]) [10]
0.073 <3> (nonanoyl *p*-nitroanilide, <3> pH 9.0, mutant enzyme G489A [10]) [10]
0.074 <3> (nonanoyl *p*-nitroanilide, <3> pH 9.0, wild-type enzyme [10]) [10]
0.074 <3> (oleoyl *p*-nitroanilide, <3> pH 9.0, wild-type enzyme [10]) [10]
0.074 <3> (palmitoyl *p*-nitroanilide, <3> pH 9.0, wild-type enzyme [10]) [10]
0.083 <3> (oleoyl *p*-nitroanilide, <3> pH 9.0, mutant enzyme A487V [10]) [10]
0.092 <3> (myristoyl *p*-nitroanilide, <3> pH 9.0, mutant enzyme T488A [10]) [10]
0.094 <3> (myristoyl *p*-nitroanilide, <3> pH 9.0, mutant enzyme G489A [10]) [10]
0.095 <3> (oleoyl *p*-nitroanilide, <3> pH 9.0, mutant enzyme T488A [10]) [10]
0.098 <3> (oleoyl *p*-nitroanilide, <3> pH 9.0, mutant enzyme G489A [10]) [10]
0.099 <3> (myristoyl *p*-nitroanilide, <3> pH 9.0, wild-type enzyme [10]) [10]
0.126 <3> (oleoyl *p*-nitroanilide, <3> pH 9.0, mutant enzyme I491A [10]) [10]
0.179 <3> (nonanoyl *p*-nitroanilide, <3> pH 9.0, mutant enzyme T488A [10]) [10]
0.22 <3> (octanoyl *p*-nitroanilide, <3> pH 9.0, wild-type enzyme [10]) [10]
0.41 <3> (heptanoyl *p*-nitroanilide, <3> pH 9.0, wild-type enzyme [10]) [10]
0.57 <3> (nonanoyl *p*-nitroanilide, <3> pH 9.0, mutant enzyme I491A [10]) [10]
2.34 <3> (arachidonamide, <3> pH 7.4, 37°C [15]) [15]
2.78 <3> (anandamide, <3> pH 7.4, 37°C [15]) [15]
7.31 <3> (N-(*o*-hydroxyphenyl)arachidonamide, <3> pH 7.4, 37°C [15]) [15]
7.94 <3> ((S)-α-methanandamide, <3> pH 7.4, 37°C [15]) [15]
33 <3> ((R)-α-methanandamide, <3> pH 7.4, 37°C [15]) [15]

K_i-Value (mM)

0.00000014 <2> (1-[1,3]oxazolo[4,5-b]pyridin-2-yloctadec-9-yn-1-one) [20]
0.00000015 <2> (1-[1,3]oxazolo[4,5-b]pyridin-2-yldec-9-en-1-one) [20]
0.00000018 <2> (1-[1,3]oxazolo[4,5-b]pyridin-2-yldec-9-yn-1-one) [20]
0.0000002 <2> (1-[1,3]oxazolo[4,5-b]pyridin-2-yl-6-phenylhexan-1-one) [20]
0.00000028 <2> (1-[1,3]oxazolo[4,5-b]pyridin-2-yl-7-phenylheptan-1-one) [20]

0.0000003 <2> (1-[1,3]oxazolo[4,5-b]pyridin-2-yl-5-phenylpentan-1-one) [20]
0.00000039 <2> (1-[1,3]oxazolo[4,5-b]pyridin-2-yl-8-phenyloctan-1-one) [20]
0.0000004 <3> (2-(7-phenylheptanoyl)-1,3-oxazole-5-carbonitrile) [16]
0.00000052 <2> (1-[1,3]oxazolo[4,5-b]pyridin-2-yl-9-phenylnonan-1-one) [20]
0.00000057 <2> (1-[1,3]oxazolo[4,5-b]pyridin-2-yldodecan-1-one) [20]
0.0000006 <3> (1-[5-(4-methylpyridin-2-yl)-1,3-oxazol-2-yl]-7-phenylheptan-1-one) [16]
0.00000069 <2> (1-[1,3]oxazolo[4,5-b]pyridin-2-yloctan-1-one) [20]
0.00000075 <2> (1-[1,3]oxazolo[4,5-b]pyridin-2-yldecan-1-one) [20]
0.0000008 <3> (1-[5-(4-methoxypyridin-2-yl)-1,3-oxazol-2-yl]-7-phenylheptan-1-one) [16]
0.0000008 <3> (7-phenyl-1-[5-(trifluoromethyl)-1,3-oxazol-2-yl]heptan-1-one) [16]
0.0000009 <3> (methyl 2-(7-phenylheptanoyl)-1,3-oxazole-5-carboxylate) [16]
0.000001 <2> ((5Z,8Z,11Z,14Z)-1-[1,3]oxazolo[4,5-b]pyridin-2-ylicosa-5,8,11,14-tetraen-1-one) [20]
0.000001 <3> (6-[2-(7-phenylheptanoyl)-1,3-oxazol-5-yl]pyridine-2-carboxamide) [16]
0.0000011 <3> (2-[2-(7-phenylheptanoyl)-1,3-oxazol-5-yl]pyridine-4-carbonitrile) [16]
0.0000012 <3> (6-[2-(7-phenylheptanoyl)-1,3-oxazol-5-yl]pyridine-3-carboxamide) [16]
0.0000013 <3> (methyl 2-[2-(7-phenylheptanoyl)-1,3-oxazol-5-yl]pyridine-4-carboxylate) [16]
0.0000017 <2> (1-[1,3]oxazolo[4,5-b]pyridin-2-yltetradecan-1-one) [20]
0.0000019 <2> (1-[1,3]oxazolo[4,5-b]pyridin-2-ylhexadecan-1-one) [20]
0.000002 <2> ((5Z,8Z,11Z,14Z)-1-[1,3]oxazolo[4,5-c]pyridin-2-ylicosa-5,8,11,14-tetraen-1-one) [20]
0.000002 <3> (1-(5-acetyl-1,3-oxazol-2-yl)-7-phenylheptan-1-one) [16]
0.000002 <3> (1-[5-(4-fluoropyridin-2-yl)-1,3-oxazol-2-yl]-7-phenylheptan-1-one) [16]
0.000002 <3> (3-[2-(7-phenylheptanoyl)-1,3-oxazol-5-yl]benzenesulfonamide) [16]
0.000002 <3> (N,N-dimethyl-2-(7-phenylheptanoyl)-1,3-oxazole-5-carboxamide) [16]
0.0000021 <2> (1-[1,3]oxazolo[4,5-b]pyridin-2-ylheptan-1-one) [20]
0.0000023 <2> ((9Z)-1-[1,3]oxazolo[4,5-b]pyridin-2-yloctadec-9-en-1-one) [20]
0.0000023 <3> (7-phenyl-1-(5-pyrimidin-4-yl-1,3-oxazol-2-yl)heptan-1-one) [16]
0.0000028 <3> (1-[5-(5-methylpyridin-2-yl)-1,3-oxazol-2-yl]-7-phenylheptan-1-one) [16]
0.000003 <3> (1-(5-bromo-1,3-oxazol-2-yl)-7-phenylheptan-1-one) [16]
0.000003 <3> (1-(5-iodo-1,3-oxazol-2-yl)-7-phenylheptan-1-one) [16]
0.000003 <3> (5-[2-(7-phenylheptanoyl)-1,3-oxazol-5-yl]thiophene-2-sulfonamide) [16]
0.0000032 <2> ((9E)-1-[1,3]oxazolo[4,5-b]pyridin-2-yloctadec-9-en-1-one) [20]

0.0000032 <3> (1-[5-(4-nitropyridin-2-yl)-1,3-oxazol-2-yl]-7-phenylheptan-1-one) [16]
0.0000033 <3> (1-[5-(6-methylpyridin-2-yl)-1,3-oxazol-2-yl]-7-phenylheptan-1-one) [16]
0.00000035 <3> (7-phenyl-1-[5-[4-(trifluoromethyl)pyridin-2-yl]-1,3-oxazol-2-yl]heptan-1-one) [16]
0.0000035 <3> (methyl 6-[2-(7-phenylheptanoyl)-1,3-oxazol-5-yl]pyridine-3-carboxylate) [16]
0.0000037 <2> ((9Z)-1-[1,3]oxazolo[5,4-c]pyridin-2-yloctadec-9-en-1-one) [20]
0.000004 <3> (7-phenyl-1-[5-(trifluoroacetyl)-1,3-oxazol-2-yl]heptan-1-one) [16]
0.0000047 <3> (7-phenyl-1-(5-pyridin-2-yl-1,3-oxazol-2-yl)heptan-1-one) [16]
0.000005 <3> (1-(5-chloro-1,3-oxazol-2-yl)-7-phenylheptan-1-one) [16]
0.000005 <3> (1-[5-(2,6-dimethoxypyrimidin-4-yl)-1,3-oxazol-2-yl]-7-phenylheptan-1-one) [16]
0.000005 <3> (2-(7-phenylheptanoyl)-1,3-oxazole-5-carboxamide) [16]
0.000005 <3> (3-[2-(7-phenylheptanoyl)-1,3-oxazol-5-yl]benzoic acid) [16]
0.0000053 <3> (7-phenyl-1-(5-pyrimidin-2-yl-1,3-oxazol-2-yl)heptan-1-one) [16]
0.0000055 <3> (methyl 5-[2-(7-phenylheptanoyl)-1,3-oxazol-5-yl]furan-2-carboxylate) [16]
0.000006 <3> (2-(7-phenylheptanoyl)-1,3-oxazole-5-carbaldehyde) [16]
0.000006 <3> (3-[2-(7-phenylheptanoyl)-1,3-oxazol-5-yl]benzamide) [16]
0.0000069 <2> (1-[1,3]oxazolo[4,5-b]pyridin-2-yl-4-phenylbutan-1-one) [20]
0.000007 <3> (6-[2-(7-phenylheptanoyl)-1,3-oxazol-5-yl]pyridine-3-carboxylic acid) [16]
0.000007 <3> (N-methyl-2-(7-phenylheptanoyl)-1,3-oxazole-5-carboxamide) [16]
0.000007 <3> (methyl 5-[2-(7-phenylheptanoyl)-1,3-oxazol-5-yl]thiophene-2-carboxylate) [16]
0.0000072 <2> ((9Z)-1-[1,3]oxazolo[4,5-c]pyridin-2-yloctadec-9-en-1-one) [20]
0.000008 <3> (7-phenyl-1-[5-(piperidin-1-ylcarbonyl)-1,3-oxazol-2-yl]heptan-1-one) [16]
0.000008 <3> (methyl 6-[2-(7-phenylheptanoyl)-1,3-oxazol-5-yl]pyridine-2-carboxylate) [16]
0.00001 <3> (4-[2-(7-phenylheptanoyl)-1,3-oxazol-5-yl]benzamide) [16]
0.00001 <3> (4-[2-(7-phenylheptanoyl)-1,3-oxazol-5-yl]benzenesulfonamide) [16]
0.00001 <3> (7-phenyl-1-[5-(thiomorpholin-4-ylcarbonyl)-1,3-oxazol-2-yl]heptan-1-one) [16]
0.000011 <2> ((9Z)-1-[1,3]oxazolo[5,4-b]pyridin-2-yloctadec-9-en-1-one) [20]
0.000011 <2> (1-[1,3]oxazolo[4,5-b]pyridin-2-yloctadecan-1-one) [20]
0.000011 <3> (5-[2-(7-phenylheptanoyl)-1,3-oxazol-5-yl]thiophene-2-carboxylic acid) [16]
0.000012 <3> (1-(5-furan-2-yl-1,3-oxazol-2-yl)-7-phenylheptan-1-one) [16]
0.000012 <3> (6-[2-(7-phenylheptanoyl)-1,3-oxazol-5-yl]pyrimidine-2,4(1H,^{3}H)-dione) [16]

0.000012 <3> (methyl 3-[2-(7-phenylheptanoyl)-1,3-oxazol-5-yl]benzoate) [16]
0.000015 <2> (1-[1,3]oxazolo[4,5-b]pyridin-2-ylhexan-1-one) [20]
0.000015 <3> (1-[5-(3-methylpyridin-2-yl)-1,3-oxazol-2-yl]-7-phenylheptan-1-one) [16]
0.000015 <3> (3-[2-(7-phenylheptanoyl)-1,3-oxazol-5-yl]benzonitrile) [16]
0.000015 <3> (5-[2-(7-phenylheptanoyl)-1,3-oxazol-5-yl]furan-2-carboxylic acid) [16]
0.000016 <3> (7-phenyl-1-[5-[3-(trifluoroacetyl)phenyl]-1,3-oxazol-2-yl]heptan-1-one) [16]
0.000017 <2> ((9Z)-1-(1,3-oxazol-2-yl)octadec-9-en-1-one) [20]
0.000018 <2> ((5Z,8Z,11Z,14Z)-1-[1,3]oxazolo[5,4-c]pyridin-2-ylicosa-5,8,11,14-tetraen-1-one) [20]
0.000019 <3> (1-[5-(3-aminophenyl)-1,3-oxazol-2-yl]-7-phenylheptan-1-one) [16]
0.00002 <3> (6-[2-(7-phenylheptanoyl)-1,3-oxazol-5-yl]pyridine-2-carboxylic acid) [16]
0.000022 <3> (7-phenyl-1-(5-pyrimidin-5-yl-1,3-oxazol-2-yl)heptan-1-one) [16]
0.000024 <3> (1-[5-(morpholin-4-ylcarbonyl)-1,3-oxazol-2-yl]-7-phenylheptan-1-one) [16]
0.000025 <3> (1-[5-(4-aminopyridin-2-yl)-1,3-oxazol-2-yl]-7-phenylheptan-1-one) [16]
0.000025 <3> (1-[5-(methylsulfanyl)-1,3-oxazol-2-yl]-7-phenylheptan-1-one) [16]
0.000026 <3> (1-[5-(2,4-dimethoxypyrimidin-5-yl)-1,3-oxazol-2-yl]-7-phenylheptan-1-one) [16]
0.000028 <3> (1-[5-(3-nitrophenyl)-1,3-oxazol-2-yl]-7-phenylheptan-1-one) [16]
0.00003 <3> (1-(5-fluoro-1,3-oxazol-2-yl)-7-phenylheptan-1-one) [16]
0.00003 <3> (2-(7-phenylheptanoyl)-1,3-oxazole-5-carboxylic acid) [16]
0.00004 <3> (1-[5-(3-methoxyphenyl)-1,3-oxazol-2-yl]-7-phenylheptan-1-one) [16]
0.00004 <3> (4-[2-(7-phenylheptanoyl)-1,3-oxazol-5-yl]benzonitrile) [16]
0.00004 <3> (methyl 4-[2-(7-phenylheptanoyl)-1,3-oxazol-5-yl]benzoate) [16]
0.000047 <2> ((5Z,8Z,11Z,14Z)-1-pyridazin-3-ylicosa-5,8,11,14-tetraen-1-one) [20]
0.000048 <3> (1-(1,3-oxazol-2-yl)-7-phenylheptan-1-one) [16]
0.00005 <2> (1-[1,3]oxazolo[4,5-b]pyridin-2-ylpentan-1-one) [20]
0.00005 <3> (1-[5-(3-fluorophenyl)-1,3-oxazol-2-yl]-7-phenylheptan-1-one) [16]
0.00005 <3> (1-[5-(3-hydroxyphenyl)-1,3-oxazol-2-yl]-7-phenylheptan-1-one) [16]
0.00005 <3> (1-[5-(4-nitrophenyl)-1,3-oxazol-2-yl]-7-phenylheptan-1-one) [16]
0.00005 <3> (2-[2-(7-phenylheptanoyl)-1,3-oxazol-5-yl]pyridine-4-carboxylic acid) [16]
0.000055 <3> (7-phenyl-1-(5-thiophen-2-yl-1,3-oxazol-2-yl)heptan-1-one) [16]
0.00006 <3> (4-[2-(7-phenylheptanoyl)-1,3-oxazol-5-yl]benzoic acid) [16]
0.00006 <3> (methyl 2-[2-(7-phenylheptanoyl)-1,3-oxazol-5-yl]benzoate) [16]

0.000062 <3> (1-[5-(4-fluorophenyl)-1,3-oxazol-2-yl]-7-phenylheptan-1-one) [16]
0.000063 <3> (7-phenyl-1-[5-(1H-tetrazol-5-yl)-1,3-oxazol-2-yl]heptan-1-one) [16]
0.000065 <2> ((9Z)-1-(2-methyl-2H-tetrazol-5-yl)octadec-9-en-1-one) [20]
0.000065 <3> (7-phenyl-1-[5-[4-(trifluoroacetyl)phenyl]-1,3-oxazol-2-yl]heptan-1-one) [16]
0.00008 <3> (1-(5-methyl-1,3-oxazol-2-yl)-7-phenylheptan-1-one) [16]
0.00008 <3> (1-[5-[(4-methylpiperazin-1-yl)carbonyl]-1,3-oxazol-2-yl]-7-phenylheptan-1-one) [16]
0.00008 <3> (7-phenyl-1-(5-phenyl-1,3-oxazol-2-yl)heptan-1-one) [16]
0.000082 <2> ((10Z)-1,1,1-trifluorononadec-10-en-2-one) [20]
0.00009 <3> (1-[5-(4-aminophenyl)-1,3-oxazol-2-yl]-7-phenylheptan-1-one) [16]
0.0001 <3> (1-[5-(4-methoxyphenyl)-1,3-oxazol-2-yl]-7-phenylheptan-1-one) [16]
0.00011 <2> ((9Z)-1-pyrimidin-4-yloctadec-9-en-1-one) [20]
0.00011 <3> (1-[5-(2-fluorophenyl)-1,3-oxazol-2-yl]-7-phenylheptan-1-one) [16]
0.00013 <2> ((9Z)-1-pyridazin-3-yloctadec-9-en-1-one) [20]
0.00013 <3> (1-[5-(2-nitrophenyl)-1,3-oxazol-2-yl]-7-phenylheptan-1-one) [16]
0.00013 <3> (2-[2-(7-phenylheptanoyl)-1,3-oxazol-5-yl]benzonitrile) [16]
0.00013 <3> (methyl 2-[2-(7-phenylheptanoyl)-1,3-oxazol-5-yl]pyridine-3-carboxylate) [16]
0.00014 <3> (1-[5-(4-hydroxyphenyl)-1,3-oxazol-2-yl]-7-phenylheptan-1-one) [16]
0.00015 <2> ((9E)-1-pyridazin-3-yloctadec-9-en-1-one) [20]
0.00016 <3> (4-(acetylamino)phenyl 2-(4-[[2-(trifluoromethyl)pyridin-4-yl]amino]phenyl)propanoate, <3> pH 7.4, 37°C [26]) [26]
0.00017 <3> (1-[5-(2-hydroxyphenyl)-1,3-oxazol-2-yl]-7-phenylheptan-1-one) [16]
0.0003 <3> (2-[2-(7-phenylheptanoyl)-1,3-oxazol-5-yl]benzamide) [16]
0.00035 <3> (5-[2-(7-phenylheptanoyl)-1,3-oxazol-5-yl]pyrimidine-2,4(1H,^{3}H)-dione) [16]
0.00037 <2> ((9Z)-1-(1,3-benzoxazol-2-yl)octadec-9-en-1-one) [20]
0.0004 <3> (1-[5-(2-methoxyphenyl)-1,3-oxazol-2-yl]-7-phenylheptan-1-one) [16]
0.0005 <2> (ethyl (10Z)-2-oxononadec-10-enoate) [20]
0.00054 <2> ((9Z)-1-pyrazin-2-yloctadec-9-en-1-one) [20]
0.0007 <2> (1-pyridazin-3-yloctadecan-1-one) [20]
0.00075 <3> (1-[5-(2-aminophenyl)-1,3-oxazol-2-yl]-7-phenylheptan-1-one) [16]
0.0009 <2> ((10Z)-2-oxononadec-10-enamide) [20]
0.001 <2> ((10Z)-1-bromononadec-10-en-2-one) [20]
0.0015 <3> (2-[2-(7-phenylheptanoyl)-1,3-oxazol-5-yl]benzenesulfonamide) [16]

0.0021 <3> (N-(4-hydroxyphenyl)arachidonylamide, <3> in the presence of fatty acid-free bovine serum albumin (0.125% w/v). In the absence of fatty acid-free bovine serum albumin, the IC50 value is reduced [2]) [2]
0.0024 <2> (1-(1,3-benzoxazol-2-yl)octadecan-1-one) [20]
0.0025 <2> ((9Z)-1-pyrimidin-2-yloctadec-9-en-1-one) [20]
0.0026 <3> (N-(4-hydroxy-2-methylphenyl) arachidonoyl amide, <3> in the presence of fatty acid-free bovine serum albumin (0.125% w/v). In the absence of fatty acid-free bovine serum albumin, the IC50 value is reduced [2]) [2]
0.0035 <3> (1,1'-(5,5'-bi-1,3-oxazole-2,2'-diyl)bis(7-phenylheptan-1-one)) [16]
0.0037 <2> ((9Z)-1-(1-methyl-1H-tetrazol-5-yl)octadec-9-en-1-one) [20]
0.0045 <2> ((9Z)-1-(4,5-dihydro-1,3-oxazol-2-yl)octadec-9-en-1-one) [20]
0.005 <3> (7-phenyl-1-[5-[2-(trifluoroacetyl)phenyl]-1,3-oxazol-2-yl]heptan-1-one) [16]
0.006 <3> (2-[2-(7-phenylheptanoyl)-1,3-oxazol-5-yl]benzoic acid) [16]
0.0085 <2> ((9Z)-octadec-9-enal) [20]
0.0098 <2> ((9Z)-1-(1H-tetrazol-5-yl)octadec-9-en-1-one) [20]
0.013 <2> ((9Z)-1-(7-methyl-1,3-benzoxazol-2-yl)octadec-9-en-1-one) [20]

pH-Optimum

7.4 <3> (<3> assay at [26]) [26]
7.6 <1> (<1> assay at [25,29]) [25,29]
9 <2> (<2> assay at [24]) [24]
9.5 <3> (<3> native and recombinant enzymes [1]) [1]

pH-Range

Additional information <3> (<3> pH rate profiles of FAAH mutants [14]) [14]

Temperature optimum (°C)

37 <1,3> (<1,3> assay at [25,26,29]) [25,26,29]

4 Enzyme Structure

Subunits

oligomer <3> (<3> wild-type FAAH behaves as a larger oligomer than FAAH protein lacking the N-terminal transmembrane domain. Presence of SDS-resistant oligomers for wild-type FAAH, but not for FAAH protein lacking the N-terminal transmembrane domain. Self-association through the transmembrane domain is demonstrated [1]) [1]

Posttranslational modification

glycoprotein <2> (<2> FAAH is N-glycosylated [24]) [24]
no glycoprotein <2> (<2> FAAH-2 does not undergo N-glycosylation [24]) [24]

5 Isolation/Preparation/Mutation/Application

Source/tissue

BV-2 cell <1> [5]
C6 glioma cell <3> [7]
MCF-7 cell <8,9> [6]
N18TG2 cell <1> [7]
OVCAR-3 cell <8,9> [6]
basophilic leukemia cell <3> [7,26]
blood platelet <3,5> (<3> very little expression [7]) [7,11]
brain <1,3,4,8> (<1> temporal changes in mouse brain fatty acid amide hydrolase activity, determination by ex vivo autoradiography, overview [29]) [2,3,6,7,15,19,22,25,26,29]
cerebellum <3> [4]
choroid plexus <3> (<3> role of FAAH in epithelial cells of the choroid plexus may be to control the concentration of oleamide in the cerebrospinal fluid. FAAH may exert an important regulatory role in shaping the duration and magnitude of the sleep-inducing effect of endogenously or exogenously derived oleamide [18]) [18]
dorsal root ganglion <3> (<3> L4 and L5 [27]) [27]
heart <9> (<9> highly expressed [6]) [6]
kidney <8,9> [6,19]
liver <1,3,6,8,9> [1,6,7,17,19,20,22]
lung <8,9> [6]
lymphocyte <2> [7]
macrophage <3> [7]
nerve <3> (<3> peripheral [27]) [27]
neuroblastoma cell <1> [7]
neuron <1,3> (<3> primary sensory, FAAH is localized in the soma, in small dorsal root ganglion neurons [27]) [27,28]
placenta <8> [19]
prostate <8,9> [6]
sciatic nerve <3> [27]
skeletal muscle <8> [19]
small intestine <8> [6]
spinal cord <3> [27]
testis <8> [6]
Additional information <2,3,8,9> (<9> no activity in brain, small intestine and testis [6]; <8> no activity in heart [6]; <2> not in human HeLa epithelioid carcinoma. Human HMC-1 mast cells show FAAH activity only when 5-lipoxygenase activity is inhibited [7]; <3> culturing does not induce major changes in FAAH expression in primary sensory neurons [27]) [6,7,27]

Localization

endoplasmic reticulum <2> (<2> FAAH [24]) [24]
lipid droplet <2> (<2> FAAH-2, localization of FAAH-2 on the cytoplasmic face of lipid droplets, lipid droplet localization is essential for FAAH-2 [24]) [24]

membrane <1,2,3,4,6,7,8,9> (<3,7> integral membrane protein [1,21]; <1,2,3,4> bound to [7,9]; <3> integral membrane enzyme [14]; <9> FAAH-2 is luminally orientated in the membrane [6]; <8> FAAH-1 shows a predominantly cytoplasmic orientation in the membrane [6]) [1,4,6,7,9,14,19,21,26]
microsome <3,4> [7,15]
plasma membrane <2,3> [17,20]
Additional information <2> (<2> FAAH-2 is not translocated into the endoplasmic reticulum lumen [24]) [24]

Purification

<3> (all Escherichia coli expression constructs contained a deletion of the N-terminal transmembrane domain of FAAH. Deletion of this region facilitates its purification from Escherichia coli but had no effect on the enzymatic activity of FAAH) [14]
<3> (partial) [17]
<3> (recombinantly expressed wild-type FAAH and FAAH protein lacking the N-terminal transmembrane domain) [1]

Crystallization

<7> (2.8 A crystal structure) [21]

Cloning

<1> [7]
<2> [7]
<2> (FLAG-tagged FAAH and FAAH-2 expression in HeLa and COS-7 cells, analysis of subcellular localization of full-length and truncated enzymes in transfected cells, overview) [24]
<3> (FAAH is cloned from rat liver plasma membranes and expressed in COS-7 cells) [7]
<3> (FAAH mutants are expressed in the Escherichia coli strain BL21. All Escherichia coli expression constructs contained a deletion of the N-terminal transmembrane domain of FAAH. Deletion of this region facilitates its purification from Escherichia coli but has no effect on the enzymatic activity of FAAH. Some mutants are expressed mainly as inclusion body in Escherichia coli, preventing a detailed analysis of their catalytic function in this system. The expression of FAAH mutants in COS-7 cells provides a system where the majority of these variants can be directly compared) [14]
<3> (expressed in COS-7) [19]
<3> (expression in COS-7 cells) [17]
<3> (wild-type FAAH and FAAH protein lacking the N-terminal transmembrane domain, expression in COS-7 cells and in Escherichia coli) [1]
<4> [7]
<6> [19]
<8> (expressed in COS-7) [19]
<9> [23]

Engineering

A487V <3> (<3> k_{cat}/K_m for nonanoyl *p*-nitroanilide is 1.3fold higher than wild-type value, k_{cat}/K_m for myristoyl *p*-nitroanilide is 1.5fold lower than wild-type value, k_{cat}/K_m for oleoyl *p*-nitroanilide is 1.4fold lower than wild-type value [10]) [10]

D167A <3> (<3> mutant enzyme shows 48% of wild-type activity with oleamide as substrate [14]) [14]

D237E <3> (<3> mutant enzyme shows 12% of wild-type activity with oleamide as substrate [14]) [14]

D237N <3> (<3> mutant enzyme shows 2.3% of wild-type activity with oleamide as substrate [14]) [14]

E143Q <3> (<3> mutant enzyme shows 60% of wild-type activity with oleamide as substrate [14]) [14]

G489A <3> (<3> k_{cat}/K_m for nonanoyl *p*-nitroanilide is 3fold lower than wild-type value, k_{cat}/K_m for myristoyl *p*-nitroanilide is 1.9fold lower than wild-type value, k_{cat}/K_m for oleoyl *p*-nitroanilide is 1.4fold than wild-type value [10]) [10]

H184Q <3> (<3> activity with oleamide is similar to wild-type enzyme [9]) [9]

H358A <3> (<3> activity with oleamide is similar to wild-type enzyme [9]) [9]

H449A <3> (<3> activity with oleamide is similar to wild-type enzyme [9]) [9]

I491A <3> (<3> mutant displays a greatly reduced binding affinity for medium-chain pNA substrates (7-12 carbons), k_{cat}/K_m for nonanoyl *p*-nitroanilide is 8.1fold lower than wild-type value, k_{cat}/K_m for myristoyl *p*-nitroanilide is identical to wild-type value, k_{cat}/K_m for oleoyl *p*-nitroanilide is 2.1fold lower than wild-type value [10]) [10]

K142A <3> (<3> mutation abolishes the property of FAAH to degrade amides and esters with equivalent catalytic efficiencies, generating a catalytically compromised enzyme that hydrolyzes esters more than 500fold faster than amides. Mutant enzyme shows an altered pH-rate profile [8]; <3> mutation decreases the amidase activity of FAAH greater than 100fold without detectably impacting the structural integrity of the enzyme, mutant enzyme shows 3% of the oleoyl ester hydrolysis compared to wild-type enzyme [14]; <3> the greater reduction of Ser241 labelling rate in the K142A/S217A double mutant, compared to the K142A and S217A single mutants, suggests that Lys142 and Ser217 cooperate to deprotonate Ser241 [13]) [8,13,14]

K142A/R243A <3> (<3> no hydrolysis of oleoyl methyl ester [14]) [14]

K142A/S217A <3> (<3> the greater reduction of Ser241 labelling rate in the K142A/S217A double mutant, compared to the K142A and S217A single mutants, suggests that Lys142 and Ser217 cooperate to deprotonate Ser241 [13]) [13]

K142E <3> (<3> mutant enzyme displays severely diminished catalytic activity, but one that now maintains ability of FAAG to react with amides and esters at competitive rates. Mutant enzyme shows an altered pH-rate profile [8]) [8]

K142Q <3> (<3> mutation abolishes the property of FAAH to degrade amides and esters with equivalent catalytic efficiencies, generating a catalytically compromised enzyme that hydrolyzes esters more than 500fold faster than amides. Mutant enzyme shows an altered pH-rate profile [8]) [8]
K255A <3> (<3> mutant enzyme shows 17% of wild-type activity with oleamide as substrate [14]) [14]
N206A <3> (<3> mutant enzyme shows 11% of wild-type activity with oleamide as substrate [14]) [14]
R243A <3> (<3> mutation decreases the amidase activity of FAAH greater than 100fold without detectably impacting the structural integrity of the enzyme, mutant enzyme shows 24% of the oleoyl ester hydrolysis compared to wild-type enzyme [14]) [14]
S217A <3> (<3> mutant shows 2300fold reductions in k_{cat} for oleamide [9]; <3> mutation decreases the amidase activity of FAAH greater than 100fold without detectably impacting the structural integrity of the enzyme, no hydrolysis of oleoyl methyl ester [14]; <3> the greater reduction of Ser241 labelling rate in the K142A/S217A double mutant, compared to the K142A and S217A single mutants, suggests that Lys142 and Ser217 cooperate to deprotonate Ser241 [13]) [9,13,14]
S217A/S218A <3> (<3> mutant displays a 230000fold decrease in k_{cat} for oleamide [9]) [9]
S218A <3> (<3> mutant shows 95fold reductions in k_{cat} for oleamide [9]; <3> mutation decreases the amidase activity of FAAH greater than 100fold without detectably impacting the structural integrity of the enzyme, mutant enzyme shows 3% of the oleoyl ester hydrolysis compared to wild-type enzyme [14]) [9,14]
S241A <3> (<3> mutant exhibits no detectable catalytic activity for oleamide [9]; <3> mutation decreases the amidase activity of FAAH greater than 100fold without detectably impacting the structural integrity of the enzyme, no hydrolysis of oleoyl methyl ester [14]) [9,14]
T257A <3> (<3> mutant enzyme shows 65% of wild-type activity with oleamide as substrate [14]) [14]
T488A <3> (<3> k_{cat}/K_m for nonanoyl *p*-nitroanilide is 2.8fold lower than wild-type value, k_{cat}/K_m for myristoyl *p*-nitroanilide is 1.4fold lower than wild-type value, k_{cat}/K_m for oleoyl *p*-nitroanilide is 1.6fold lower than wild-type value [10]) [10]
Additional information <2> (<2> FAAH-2 chimeras excluded from lipid droplets lack activity and/or are poorly expressed [24]) [24]

Application

drug development <1> (<1> FAAH is an attractive target for treating pain [28]) [28]
medicine <3> (<3> FAAH is a promising target for the treatment of several central and peripheral nervous system disorders, such as anxiety, pain and hypertension [13]) [13]
pharmacology <1> (<1> FAAH is a potential therapeutic target [29]) [29]

6 Stability

pH-Stability

5 <3> (<3> not stable below [14]) [14]

General stability information

<3>, 100 mM Na_2CO_3 incubation (30 min at 4°C and pH 11.0) destroys the catalytic activity of both wild-type FAAH and FAAH protein lacking the N-terminal transmembrane domain derived from transfected COS-7 cells, whereas the native liver-isolated FAAH is stable to this treatment [1]

References

[1] Patricelli, M.P.; Lashuel, H.A.; Giang, D.K.; Kelly, J.W.; Cravatt, B.F.: Comparative characterization of wild type and transmembrane domain-deleted fatty acid amide hydrolase identification of the transmembrane domain as a site for oligomerization. Biochemistry, **37**, 15177-15187 (1998)

[2] Vandevoorde, S.; Fowler, C.J.: Inhibition of fatty acid amide hydrolase and monoacylglycerol lipase by the anandamide uptake inhibitor VDM11: evidence that VDM11 acts as an FAAH substrate. Br. J. Pharmacol., **145**, 885-893 (2005)

[3] Quistad, G.B.; Klintenberg, R.; Caboni, P.; Liang, S.N.; Casida, J.E.: Monoacylglycerol lipase inhibition by organophosphorus compounds leads to elevation of brain 2-arachidonoylglycerol and the associated hypomotility in mice. Toxicol. Appl. Pharmacol., **211**, 78-83 (2006)

[4] Cisneros, J.A.; Vandevoorde, S.; Ortega-Gutierrez, S.; Paris, C.; Fowler, C.J.; Lopez-Rodriguez, M.L.: Structure-activity relationship of a series of inhibitors of monoacylglycerol hydrolysis - comparison with effects upon fatty acid amide hydrolase. J. Med. Chem., **50**, 5012-5023 (2007)

[5] Muccioli, G.G.; Xu, C.; Odah, E.; Cudaback, E.; Cisneros, J.A.; Lambert, D.M.; Lopez Rodriguez, M.L.; Bajjalieh, S.; Stella, N.: Identification of a novel endocannabinoid-hydrolyzing enzyme expressed by microglial cells. J. Neurosci., **27**, 2883-2889 (2007)

[6] Wei, B.Q.; Mikkelsen, T.S.; McKinney, M.K.; Lander, E.S.; Cravatt, B.F.: A second fatty acid amide hydrolase with variable distribution among placental mammals. J. Biol. Chem., **281**, 36569-36578 (2006)

[7] Fowler, C.J.; Jonsson, K.O.; Tiger, G.: Fatty acid amide hydrolase: biochemistry, pharmacology, and therapeutic possibilities for an enzyme hydrolyzing anandamide, 2-arachidonoylglycerol, palmitoylethanolamide, and oleamide. Biochem. Pharmacol., **62**, 517-26 (2001)

[8] Patricelli, M.P.; Cravatt, B.F.: Fatty acid amide hydrolase competitively degrades bioactive amides and esters through a nonconventional catalytic mechanism. Biochemistry, **38**, 14125-14130 (1999)

[9] Patricelli M.P.; Lovato, M.A.; Cravatt, B.F.: Chemical and mutagenic investigations of fatty acid amide hydrolase: evidence for a family of serine hydrolases with distinct catalytic properties. Biochemistry, **38**, 9804-9812 (1999)

[10] Patricelli, M.P.; Cravatt, B.F.: Characterization and manipulation of the acyl chain selectivity of fatty acid amide hydrolase. Biochemistry, **40**, 6107-6115 (2001)
[11] Ferreri, C.; Anagnostopoulos, D.; Lykakis, I.N.; Chatgilialoglu, C.; Siafaka-Kapadai, A.: Synthesis of all-trans anandamide: A substrate for fatty acid amide hydrolase with dual effects on rabbit platelet activation. Bioorg. Med. Chem., **16**, 8359-8365 (2008)
[12] Boger, D.L.; Fecik, R.A.; Patterson, J.E.; Miyauchi, H.; Patricelli, M.P.; Cravatt, B.F.: Fatty acid amide hydrolase substrate specificity. Bioorg. Med. Chem. Lett., **10**, 2613-2616 (2000)
[13] Lodola, A.; Mor, M.; Hermann, J.C.; Tarzia, G.; Piomelli, D.; Mulholland, A.J.: QM/MM modelling of oleamide hydrolysis in fatty acid amide hydrolase (FAAH) reveals a new mechanism of nucleophile activation. Chem. Commun. (Camb.), **35**, 4399-401 (2005)
[14] Patricelli, M.P.; Cravatt, B.F.: Clarifying the catalytic roles of conserved residues in the amidase signature family. J. Biol. Chem., **275**, 19177-19184 (2000)
[15] Lang, W.; Qin, C.; Lin, S.; Khanolkar, A.D.; Goutopoulos, A.; Fan, P.; Abouzid, K.; Meng, Z.; Biegel, D.; Makriyannis, A.: Substrate specificity and stereoselectivity of rat brain microsomal anandamide amidohydrolase. J. Med. Chem., **42**, 898-902 (1999)
[16] Romero, F.A.; Du, W.; Hwang, I.; Rayl, T.J.; Kimball, F.S.; Leung, D.; Hoover, H.S.; Apodaca, R.L.; Breitenbucher, J.G.; Cravatt, B.F.; Boger, D.L.J.: Potent and selective α-ketoheterocycle-based inhibitors of the anandamide and oleamide catabolizing enzyme, fatty acid amide hydrolase. J. Med. Chem., **50**, 1058-68 (2007)
[17] Cravatt, B.F.; Giang, D.K.; Mayfield, S.P.; Boger, D.L.; Lerner, R.A.; Gilula, N.B.: Molecular characterization of an enzyme that degrades neuromodulatory fatty-acid amides. Nature, **384**, 83-87 (1996)
[18] Egertova, M.; Cravatt, B.F.; Elphick, M.R.: Fatty acid amide hydrolase expression in rat choroid plexus: possible role in regulation of the sleep-inducing action of oleamide. Neurosci. Lett., **282**, 13-16 (2000)
[19] Giang, D.K.; Cravatt, B.F.: Molecular characterization of human and mouse fatty acid amide hydrolases. Proc. Natl. Acad. Sci. USA, **94**, 2238-2242 (1997)
[20] Boger, D.L.; Sato, H.; Lerner, A.E.; Hedrick, M.P.; Fecik, R.A.; Miyauchi, H.; Wilkie, G.D.; Austin, B.J.; Patricelli, M.P.; Cravatt, B.F.: Exceptionally potent inhibitors of fatty acid amide hydrolase: the enzyme responsible for degradation of endogenous oleamide and anandamide. Proc. Natl. Acad. Sci. USA, **97**, 5044-5049 (2000)
[21] Bracey, M.H.; Hanson, M.A.; Masuda, K.R.; Stevens, R.C.; Cravatt, B.F.: Structural adaptations in a membrane enzyme that terminates endocannabinoid signaling.. Science, **298**, 1793-1796 (2002)
[22] Quistad, G.B.; Sparks, S.E.; Casida, J.E.: Fatty acid amide hydrolase inhibition by neurotoxic organophosphorus pesticides. Toxicol. Appl. Pharmacol., **173**, 48-55 (2001)

[23] Karbarz, M.J.; Luo, L.; Chang, L.; Tham, C.S.; Palmer, J.A.; Wilson, S.J.; Wennerholm, M.L.; Brown, S.M.; Scott, B.P.; Apodaca, R.L.; Keith, J.M.; Wu, J.; Breitenbucher, J.G.; Chaplan, S.R.; Webb, M.: Biochemical and biological properties of 4-(3-phenyl-[1,2,4] thiadiazol-5-yl)-piperazine-1-carboxylic acid phenylamide, a mechanism-based inhibitor of fatty acid amide hydrolase. Anesth. Analg., **108**, 316-329 (2009)
[24] Kaczocha, M.; Glaser, S.T.; Chae, J.; Brown, D.A.; Deutsch, D.G.: Lipid droplets are novel sites of N-acylethanolamine inactivation by fatty acid amide hydrolase-2. J. Biol. Chem., **285**, 2796-2806 (2010)
[25] Wyffels, L.; Muccioli, G.G.; De Bruyne, S.; Moerman, L.; Sambre, J.; Lambert, D.M.; De Vos, F.: Synthesis, in vitro and in vivo evaluation, and radiolabeling of aryl anandamide analogues as candidate radioligands for in vivo imaging of fatty acid amide hydrolase in the brain. J. Med. Chem., **52**, 4613-4622 (2009)
[26] Onnis, V.; Congiu, C.; Bjoerklund, E.; Hempel, F.; Soederstroem, E.; Fowler, C.J.: Synthesis and evaluation of paracetamol esters as novel fatty acid amide hydrolase inhibitors. J. Med. Chem., **53**, 2286-2298 (2010)
[27] Lever, I.J.; Robinson, M.; Cibelli, M.; Paule, C.; Santha, P.; Yee, L.; Hunt, S.P.; Cravatt, B.F.; Elphick, M.R.; Nagy, I.; Rice, A.S.: Localization of the endocannabinoid-degrading enzyme fatty acid amide hydrolase in rat dorsal root ganglion cells and its regulation after peripheral nerve injury. J. Neurosci., **29**, 3766-3780 (2009)
[28] Naidu, P.S.; Kinsey, S.G.; Guo, T.L.; Cravatt, B.F.; Lichtman, A.H.: Regulation of inflammatory pain by inhibition of fatty acid amide hydrolase. J. Pharmacol. Exp. Ther., **334**, 182-190 (2010)
[29] Glaser, S.T.; Kaczocha, M.: Temporal changes in mouse brain fatty acid amide hydrolase activity. Neuroscience, **163**, 594-600 (2009)

(R)-amidase 3.5.1.100

1 Nomenclature

EC number
3.5.1.100

Systematic name
(R)-piperazine-2-carboxamide amidohydrolase

Recommended name
(R)-amidase

Synonyms
R-amidase <1,2> [1,2]
R-stereoselective amidase <1> [1]
RamA <1> [1]

2 Source Organism

<1> *Pseudomonas sp.* (UNIPROT accession number: Q75SP7) [1]
<2> *Delftia tsuruhatensis* [2]

3 Reaction and Specificity

Catalyzed reaction
(R)-piperazine-2-carboxamide + H_2O = (R)-piperazine-2-carboxylic acid + NH_3
β-alaninamide + H_2O = β-alanine + NH_3

Substrates and products
S (R)-2,2-dimethylcyclopropane carboxamide + H_2O <2> (Reversibility: ?) [2]
P (R)-2,2-dimethylcyclopropane carboxylic acid + NH_3
S (R)-piperazine-2-carboxamide + H_2O <1> (<1> hydrolysis with strict R-stereoselectivity [1]) (Reversibility: ?) [1]
P (R)-piperazine-2-carboxylic acid + NH_3
S (R)-piperazine-2-tert-butylcarboxamide <1> (<1> hydrolysis with strict R-stereoselectivity, 9% of the activity with (R)-piperazine-2-carboxamide [1]) (Reversibility: ?) [1]
P (R)-piperazine-2-tert-butylcarboxylic acid + NH_3
S (R)-piperidine-3-carboxamide + H_2O <1> (<1> 68.9% of the activity with (R)-piperazine-2-carboxamide [1]) (Reversibility: ?) [1]
P (R)-piperidine-3-carboxylic acid + NH_3

D. Schomburg and I. Schomburg (eds.), *Class 3.4–6 Hydrolases, Lyases, Isomerases, Ligases: EC 3.4–6*, Springer Handbook of Enzymes S10, DOI 10.1007/978-3-642-36260-6_11,

S D-glutamine amide + H_2O <1> (<1> no formation of glutamine, 27% of the activity with (R)-piperazine-2-carboxamide [1]) (Reversibility: ?) [1]
P D-glutamic acid + NH_3
S L-glutamine amide + H_2O <1> (<1> no formation of glutamine, 0.35% of the activity with (R)-piperazine-2-carboxamide [1]) (Reversibility: ?) [1]
P L-glutamic acid + NH_3
S β-alaninamide + H_2O <1> (<1> 108% of the activity with (R)-piperazine-2-carboxamide [1]) (Reversibility: ?) [1]
P β-alanine + NH_3
S piperidine-4-carboxamide + H_2O <1> (<1> 0.23% of the activity with (R)-piperazine-2-carboxamide [1]) (Reversibility: ?) [1]
P piperidine-4-carboxylic acid + NH_3
S Additional information <1> (<1> RamA has hydrolyzing activity toward the carboxamide compounds, in which an amino or imino group is connected to β- or γ-carbon, such as β-alanine amide, (R)-piperazine-2-carboxamide (R)-piperidine-3-carboxamide, D-glutamine amide and (R)-piperazine-2-tert-butylcarboxamide. The enzyme does not act on the other amide substrates for the aliphatic amidase: D-alanine amide, D-valine amide, D-leucine amide, D-isoleucine amide, D-proline amide, D-phenylalanine amide, D-tryptophan amide, D-methionine amide, D-serine amide, D-threoninamide, D-tyrosine amide, D-aspartic acid amide, D-glutamic acid amide, D-lysine amide, D-arginine amide, D-histidine amide, L-alanine amide, L-valine amide, L-leucine amide, L-isoleucine amide, L-proline amide, L-phenylalanine amide, L-tryptophanamide, L-methioninamide, L-serine amide, L-threonine amide, L-tyrosine amide, L-asparagine amide, L-aspartic acid amide, L-glutamic acid amide, L-lysine amide, L-arginine amide, L-histidine amide, glycine amide and (R,S)-piperidine-2-carboxamide. Carboxamides of the side chains in D-asparagine, D-glutamine, L-asparagine and L-glutamine are not hydrolyzed by the enzyme. The enzyme does not show peptidase activity toward β-alanyl-L-alanine, β-alanylglycine, β-alanyl-L-histidine, glycylglycine, glycylglycylglycine, L-alanylglycine, D-alanylglycine, D-alanylglycylglycine, DL-alanyl-DL-asparagine, DL-alanyl-DL-isoleucine, DL-alanyl-DL-leucine, DL-alanyl-DL-methionine, DL-alanyl-DL-phenylalanine, DL-alanyl-DL-serine, DL-alanyl-DL-valine and L-aspartyl-D-alanine. The enzyme could not hydrolyze the following aliphatic amides, aromatic amides and nitriles: acetamide, propionamide, n-butyramide, isobutyramide, n-valeramide, n-capronamide, crotonamide, methacrylamide, cyclohexanecarboxamide, benzamide, *o*-aminobenzamide, *m*-aminobenzamide, *p*-aminobenzamide, *p*-toluamide, *p*-chlorobenzamide, *p*-nitrobenzamide, 2-picolinamide, nicotinamide, pyridine-4-carboxamide, pyrazinamide,2-thiophenecarboxamide, phenylacetamide, indole-3-acetamide, acetonitrile, propionitrile, 3-hydroxypropionitrile, n-capronitrile, methacrylonitrile, crotononitrile, glutaronitrile, 2,4-dicyanobut-1-ene, β-phenylpropionitrile, cinnamonitrile, 2-cyanopiperidine, 2-cyanopiperazine, phenylacetonitrile, 4-methoxyphenylacetonitrile, α-methylbenzyl cyanide, 2-pyridineacetonitrile, 3-pyridineacetonitrile, thiophene-2-acetonitrile, β-indoleacetonitrile, diphenylacetonitrile,

4-chlorobenzyl cyanide, benzonitrile, 4-chlorobenzonitrile, 4-nitrobenzonitrile, *p*-tolunitrile, anisonitrile, 2-cyanophenol, 2-cyanopyridine, 3-cyanopyridine, 4-cyanopyridine, pyrazinecarbonitrile, 3-cyanoindole, a-naphthonitrile, 2-thiophenecarbonitrile, terephthalonitrile and isophthalonitrile [1]) (Reversibility: ?) [1]

P ?

Inhibitors

$AgNO_3$ <1> (<1> 1 mM, incubation at 30°C for 10 min, complete inhibition [1]) [1]
$CdCl_2$ <1> (<1> 1 mM, incubation at 30°C for 10 min, complete inhibition [1]) [1]
$CoCl_2$ <1> (<1> 1 mM, incubation at 30°C for 10 min, complete inhibition [1]) [1]
$CuCl_2$ <1> (<1> 1 mM, incubation at 30°C for 10 min, complete inhibition [1]) [1]
$CuSO_4$ <1> (<1> 1 mM, incubation at 30°C for 10 min, complete inhibition [1]) [1]
$Fe(NH_4)_2(SO_4)_2$ <1> (<1> 1 mM, incubation at 30°C for 10 min, 67% inhibition [1]) [1]
$FeCl_3$ <1> (<1> 1 mM, incubation at 30°C for 10 min, 78% inhibition [1]) [1]
$HgCl_2$ <1> (<1> 1 mM, incubation at 30°C for 10 min, complete inhibition [1]) [1]
$MnCl_2$ <1> (<1> 1 mM, incubation at 30°C for 10 min, complete inhibition [1]) [1]
$MnSO_4$ <1> (<1> 1 mM, incubation at 30°C for 10 min, complete inhibition [1]) [1]
N-ethylmaleimide <1> (<1> 1 mM, incubation at 30°C for 10 min, complete inhibition [1]) [1]
$NiCl_2$ <1> (<1> 1 mM, incubation at 30°C for 10 min, complete inhibition [1]) [1]
$PbCl_2$ <1> (<1> 1 mM, incubation at 30°C for 10 min, complete inhibition [1]) [1]
$ZnCl_2$ <1> (<1> 1 mM, incubation at 30°C for 10 min, complete inhibition [1]) [1]
$ZnSO_4$ <1> (<1> 1 mM, incubation at 30°C for 10 min, complete inhibition [1]) [1]
p-chloromercuribenzoate <1> (<1> 1 mM, incubation at 30°C for 10 min, complete inhibition [1]) [1]
Additional information <1> (<1> chelating reagents, e.g. *o*-phenanthroline, 8-hydroxyquinoline, ethylenediaminetetraacetic acid and 2,2-dipyridyl have no significant effect on the enzyme. Carbonyl reagents such as hydroxylamine, phenylhydrazine, hydrazine, DL-penicillamine and D-cycloserine are not inhibitory toward the enzyme [1]) [1]

Specific activity (U/mg)
0.0242 <1> (<1> R-amidase from Pseudomonas sp. MCI3434 [1]) [1]
4.59 <1> (<1> RamA from Escherichia coli JM109 harboring pRTB1EX [1]) [1]

Temperature optimum (°C)
45 <1> [1]

4 Enzyme Structure

Molecular weight
36000 <1> (<1> gel filtration [1]) [1]

Subunits
monomer <1> (<1> 1 * 29500, SDS-PAGE [1]; <1> 1 * 30128, calculated from sequence [1]) [1]

5 Isolation/Preparation/Mutation/Application

Source/tissue
Additional information <2> (<2> optimization of R-amidase production by a newly isolated strain of Delftia tsuruhatensis ZJB-05174. Effect of carbon sources, nitrogen sources, and inducers is analyzed. The maximal R-amidase production is achieved when glucose is tested as carbon source, yeast extract as nitrogen source and (R,S)-2,2-dimethylcyclopropane carboxamide as inducer [2]) [2]

Purification
<1> [1]

Cloning
<1> (expression in Escherichia coli) [1]

Application
synthesis <1> (<1> R-amidase is the first enzyme useful for the enzymatic optical resolution of racemic piperazine-2-tert-butylcarboxamide carried out under mild conditions. Enantiomerically pure piperazine-2-carboxylic acid and its tert-butylcarboxamide derivative are important chiral building blocks for some pharmacologically active compounds such as N-methyl-D-aspartate antagonist for glutamate receptor, cardioprotective nucleoside transport blocker, and HIV protease inhibitor [1]) [1]

6 Stability

pH-Stability

6-9 <1> (<1> 30°C, 10 min, most stable in pH-range 6.0-9.0 [1]) [1]

Temperature stability

35 <1> (<1> 10 min, stable [1]) [1]
40 <1> (<1> 10 min, stable [1]) [1]
45 <1> (<1> 10 min, 13% loss of activity [1]) [1]
50 <1> (<1> 10 min, 97% loss of activity [1]) [1]
55 <1> (<1> 10 min, complete loss of activity [1]) [1]

Storage stability

<1>, -20°C, stable for more than 2 months in the buffer containing 50% glycerol [1]

References

[1] Komeda, H.; Harada, H.; Washika, S.; Sakamoto, T.; Ueda, M.; Asano, Y.: A novel R-stereoselective amidase from Pseudomonas sp. MCI3434 acting on piperazine-2-tert-butylcarboxamide. Eur. J. Biochem., **271**, 1580-1590 (2004)
[2] Wang, Y.S.; Xu, J.M.; Zheng, R.C.; Zheng, Y.G.; Shen, Y.C.: Improvement of amidase production by a newly isolated Delftia tsuruhatensis ZJB-05174 through optimization of culture medium. J. Microbiol. Biotechnol., **18**, 1932-1937 (2008)

L-proline amide hydrolase 3.5.1.101

1 Nomenclature

EC number
3.5.1.101

Systematic name
(S)-piperidine-2-carboxamide amidohydrolase

Recommended name
L-proline amide hydrolase

Synonyms
L-amino acid amidase <1> [1]
LaaA <1> [1]
S-stereoselective piperazine-2-tert-butylcarboxamide hydrolase <1> [1]

CAS registry number
79633-25-3

2 Source Organism

<1> *Pseudomonas azotoformans* (UNIPROT accession number: Q76KX0) [1]

3 Reaction and Specificity

Catalyzed reaction
(S)-piperidine-2-carboxamide + H_2O = (S)-piperidine-2-carboxylic acid + NH_3
L-prolinamide + H_2O = L-proline + NH_3

Substrates and products
S (R,S)-piperazine-2-tert-butylcarboxamide + H_2O <1> (<1> % of the activity with L-proline amide [1]) (Reversibility: ?) [1]
P (S)-piperazine-2-tert-butylcarboxylic acid + NH_3
S (S)-piperazine-2-carboxamide + H_2O <1> (<1> 3.7% of the activity with L-proline amide [1]) (Reversibility: ?) [1]
P (S)-piperazine-2-carboxylic acid + NH_3
S (S)-piperazine-2-tert-butylcarboxamide + H_2O <1> (<1> 0.2% of the activity with L-proline amide [1]) (Reversibility: ?) [1]
P (S)-piperazine-2-carboxylic acid + tert-butylamine
S (S)-piperidine-2-carboxamide + H_2O <1> (<1> 32% of the activity with L-proline amide [1]) (Reversibility: ?) [1]

D. Schomburg and I. Schomburg (eds.), *Class 3.4–6 Hydrolases, Lyases, Isomerases, Ligases: EC 3.4–6*, Springer Handbook of Enzymes S10, DOI 10.1007/978-3-642-36260-6_12,

P (S)-piperidine-2-carboxylic acid + NH_3
S L-alanine amide + H_2O <1> (<1> 10.6% of the activity with L-proline amide [1]) (Reversibility: ?) [1]
P L-alanine + NH_3
S L-isoleucine amide + H_2O <1> (<1> 0.17% of the activity with L-proline amide [1]) (Reversibility: ?) [1]
P L-isoleucine + NH_3
S L-leucine amide + H_2O <1> (<1> 0.46% of the activity with L-proline amide [1]) (Reversibility: ?) [1]
P L-leucine + NH_3
S L-methionine amide + H_2O <1> (<1> 4.2% of the activity with L-proline amide [1]) (Reversibility: ?) [1]
P L-methionine + NH_3
S L-phenylalanine amide amide + H_2O <1> (<1> 0.97% of the activity with L-proline amide [1]) (Reversibility: ?) [1]
P L-phenylalanine + NH_3
S L-proline amide + H_2O <1> (Reversibility: ?) [1]
P L-proline + NH_3
S L-proline-*p*-nitroanilide + H_2O <1> (<1> 40.9% of the activity with L-proline amide [1]) (Reversibility: ?) [1]
P ? + NH_3
S L-serine amide + H_2O <1> (<1> 0.43% of the activity with L-proline amide [1]) (Reversibility: ?) [1]
P L-serine + NH_3
S L-threonine amide + H_2O <1> (<1> 0.12% of the activity with L-proline amide [1]) (Reversibility: ?) [1]
P L-threonine + NH_3
S L-tryptophane amide + H_2O <1> (<1> 0.2% of the activity with L-proline amide [1]) (Reversibility: ?) [1]
P L-tryptophan + NH_3
S L-tyrosine amide + H_2O <1> (<1> 0.086% of the activity with L-proline amide [1]) (Reversibility: ?) [1]
P L-tyrosine + NH_3
S Additional information <1> (<1> the following compounds are not substrates for the amidase: L-arginine amide, L-asparagine amide, L-isoasparagine, L-glutaminamide, L-isoglutamine, glycine amide, L-histidine amide, L-lysine amide, L-valine amide, D-proline amide, L-alanyl-L-alanine, L-alanylglycine, glycylglycine, L-prolyl-L-alanine and L-prolylglycine. LaaA can not act on the peptide substrates such as L-prolyl-L-alanine, L-prolylglycine, L-alanyl-L-alanine, L-alanylglycine and glycylglycine [1]) (Reversibility: ?) [1]
P ?

Inhibitors

Ag^+ <1> (<1> 1 mM, complete inhibition [1]) [1]
Cd^{2+} <1> (<1> 1 mM, complete inhibition [1]) [1]
$CoCl_2$ <1> (<1> 1 mM, 52% inhibition [1]) [1]

Hg^{2+} <1> (<1> 1 mM, complete inhibition [1]) [1]
NEM <1> (<1> 1 mM, 24% inhibition [1]) [1]
$NiCl_2$ <1> (<1> 1 mM, 70% inhibition [1]) [1]
$PbCl_2$ <1> (<1> 1 mM, 73% inhibition [1]) [1]
Zn^{2+} <1> (<1> 1 mM, complete inhibition [1]) [1]
iodoacetate <1> (<1> 1 mM, 40% inhibition [1]) [1]
p-chloromercuribenzoate <1> (<1> 1 mM, 67% inhibition [1]) [1]
phenylhydrazine <1> (<1> 1 mM, complete inhibition [1]) [1]

Specific activity (U/mg)
0.000894 <1> (<1> S-stereoselective amidase from Pseudomonas azotoformans IAM 1603 [1]) [1]
192 <1> (<1> LaaA from Escharichia coli JM109 harboring pSTB20 [1]) [1]

K_m-Value (mM)
0.58 <1> (L-proline-*p*-nitroanilide, <1> 30°C, pH 7.0 [1]) [1]

pH-Optimum
9 <1> [1]

Temperature optimum (°C)
45 <1> [1]

4 Enzyme Structure

Molecular weight
32000 <1> (<1> gel filtration [1]) [1]

Subunits
monomer <1> (<1> 1 * 34000, SDS-PAGE [1]) [1]

5 Isolation/Preparation/Mutation/Application

Purification
<1> [1]

Cloning
<1> (expression in Escherichia coli) [1]

Application
synthesis <1> (<1> Escherichia coli cells overexpressing the laaA gene have been demonstrated to be applicable to the S-stereoselective hydrolysis of (R,S)-piperazine-2-tert-butylcarboxamide to produce (S)-piperazine-2-carboxylic acid with high optical purity. Enantiomerically pure piperazine-2-carboxylic acid and its tert-butylcarboxamide derivative are important chiral building blocks for some pharmacologically active compounds such as N-methyl-D-aspartate antagonist for glutamate receptor, cardioprotective nucleoside transport blocker and HIV protease inhibitor [1]) [1]

6 Stability

Temperature stability
45 <1> (<1> stable up to [1]) [1]

Storage stability
<1>, -20°C, stored without loss of activity for more than six months in the buffer containing 50% glycerol [1]

References

[1] Komeda, H.; Harada, H.; Washika, S.; Sakamoto, T.; Ueda, M.; Asano, Y.: S-stereoselective piperazine-2-tert-butylcarboxamide hydrolase from Pseudomonas azotoformans IAM 1603 is a novel L-amino acid amidase. Eur. J. Biochem., **271**, 1465-1475 (2004)

2-amino-5-formylamino-6-ribosylaminopyrimidin-4(3H)-one 5′-monophosphate deformylase 3.5.1.102

1 Nomenclature

EC number
3.5.1.102

Systematic name
2-amino-5-formylamino-6-(5-phospho-D-ribosylamino)pyrimidin-4(3H)-one amidohydrolase

Recommended name
2-amino-5-formylamino-6-ribosylaminopyrimidin-4(3H)-one 5'-monophosphate deformylase

Synonyms
2-amino-5-formylamino-6-ribosylamino-4(3H)-pyrimidinone 5'-monophosphate deformylase <1> [1]
ArfB <1> [1]
MJ0116 <1> (<1> gene name [1]) [1]

2 Source Organism

<1> *Methanocaldococcus jannaschii* (UNIPROT accession number: Q57580) [1]

3 Reaction and Specificity

Catalyzed reaction
2-amino-5-formylamino-6-(5-phospho-D-ribosylamino)pyrimidin-4(3H)-one + H_2O = 2,5-diamino-6-(5-phospho-D-ribosylamino)pyrimidin-4(3H)-one + formate

Reaction type
hydrolysis

Natural substrates and products
S 2-amino-5-formylamino-6-(D-ribosylamino)pyrimidin-4(3H)-one 5'-phosphate + H_2O <1> (<1> enzyme catalyzes the second step in archaeal riboflavin and 7,8-didemethyl-8-hydroxy-5-deazariboflavin biosynthesis. The archaeal pathway begins with an archaeal-specific GTP cyclohydrolase IIa (EC 3.5.4.29) that hydrolyzes the imidazole ring of GTP. The bacterial enzyme, EC 3.5.4.25 (GTP cyclohydrolase II) catalyzes both reactions [1]) (Reversibility: ?) [1]

D. Schomburg and I. Schomburg (eds.), *Class 3.4–6 Hydrolases, Lyases, Isomerases, Ligases: EC 3.4–6*, Springer Handbook of Enzymes S10, DOI 10.1007/978-3-642-36260-6_13,

P 2,5-diamino-6-(D-ribosylamino)pyrimidin-4(3H)-one 5'-phosphate + formate

Substrates and products

S 2-amino-5-formylamino-6-(D-ribosylamino)pyrimidin-4(3H)-one 5'-phosphate + H_2O <1> (<1> enzyme catalyzes the second step in archaeal riboflavin and 7,8-didemethyl-8-hydroxy-5-deazariboflavin biosynthesis. The archaeal pathway begins with an archaeal-specific GTP cyclohydrolase IIa (EC 3.5.4.29) that hydrolyzes the imidazole ring of GTP. The bacterial enzyme, EC 3.5.4.25 (GTP cyclohydrolase II) catalyzes both reactions [1]) (Reversibility: ?) [1]

P 2,5-diamino-6-(D-ribosylamino)pyrimidin-4(3H)-one 5'-phosphate + formate

Activating compounds

dithiothreitol <1> (<1> ArfB is not active in the absence of 2 mM dithiothreitol [1]) [1]

Metals, ions

Fe^{2+} <1> (<1> addition of more than 1 mM Fe^{2+} increases the rate of 2,5-diamino-6-ribosylamino-4(3H)-pyrimidinone 5-phosphate production by more than 10fold, purified enzyme contains both 1.4 mol iron and 6.2 mol magnesium per mol of protomer, maximum activity of Chelex-treated enzyme with added Fe^{2+} is 30% that of the untreated enzyme indicating that the apoenzyme cannot be fully reconstituted with the addition of just one metal [1]) [1]

Mg^{2+} <1> (<1> enzyme contains both 1.4 mol Fe^{2+} and 6.2 mol Mg^{2+} per mol of protomer [1]) [1]

Mn^{2+} <1> (<1> addition of more than 1 mM Mn^{2+} increases the rate of 2,5-diamino-6-ribosylamino-4(3H)-pyrimidinone 5-phosphate production by more than 10fold, maximum activity of Chelex-treated enzyme with added Mn^{2+} is 30% that of the untreated enzyme indicating that the apoenzyme cannot be fully reconstituted with the addition of just one metal [1]) [1]

Zn^{2+} <1> (<1> zinc is associated with the purified protein, 1.5 mol/protomer, despite the presence of zinc in the protein, addition of Zn(II) to the incubation mixture containing purified enzyme or apo-enzyme does not activate ArfB [1]) [1]

Specific activity (U/mg)

6 <1> (<1> V_{max} at a concentration of 2 mM Fe^{2+}, 5 mM $MgCl_2$, 10 mM dithiothreitol and 25 mM TES, pH 7.2 [1]) [1]

K_m-Value (mM)

1 <1> (2-amino-5-formylamino-6-ribosylamino-4(3H)-pyrimidinone 5'-phosphate, <1> pH 7.2, 70°C, apparent K_m-value is about 1 mM at a concentration of 2 mM Fe^{2+}, type of curve is typically indicative of homomeric cooperativity and suggests that ArfB may exhibit positive cooperative substrate binding [1]) [1]

pH-Optimum
7.2 <1> (<1> assay at [1]) [1]

pH-Range
6.5-8.5 <1> (<1> pH 6.5: about 80% of maximal activity, pH 8.5: about 40% of maximal activity [1]) [1]

Temperature optimum (°C)
70 <1> (<1> assay at [1]) [1]

4 Enzyme Structure

Subunits
dimer <1> (<1> 2 * 25000 [1]) [1]

5 Isolation/Preparation/Mutation/Application

Purification
<1> (purified by anion-exchange chromatography) [1]

Cloning
<1> (in Escherichia coli) [1]

6 Stability

Temperature stability
80 <1> (<1> stable at [1]) [1]

References

[1] Grochowski, L.L.; Xu, H.; White, R.H.: An iron(II) dependent formamide hydrolase catalyzes the second step in the archaeal biosynthetic pathway to riboflavin and 7,8-didemethyl-8-hydroxy-5-deazariboflavin. Biochemistry, **48**, 4181-4188 (2009)

N-acetyl-1-D-myo-inositol-2-amino-2-deoxy-α-D-glucopyranoside deacetylase 3.5.1.103

1 Nomenclature

EC number
3.5.1.103

Systematic name
1-(2-acetamido-2-deoxy-α-D-glucopyranosyl)-1D-myo-inositol acetylhydrolase

Recommended name
N-acetyl-1-D-myo-inositol-2-amino-2-deoxy-α-D-glucopyranoside deacetylase

Synonyms
1-D-myo-inosityl 2-N-acetamido-2-deoxy-α-D-glucopyranoside deacetylase <3> [2]
1-D-myo-inosityl-2-acetamido-2-deoxy-α-D-glucopyranoside deacetylase <3> [6]
1D-myo-inosityl-2-acetamido-2-deoxy-α-D-glucopyranoside deacetylase <3> [9]
AcGI deacetylase <3> [2]
GlcNAc-Ins deacetylase <3> [4,9]
GlcNAc-Ins-deacetylase <2> [3]
MshB <1,2,3,4> (<2,3> gene name [1,3,9]) [1,3,5,6,7,8,9]
N-acetyl-1-D-myo-inosityl-2-amino-2-deoxy-α-D-glucopyranoside deacetylase <3> [5]
N-acetyl-1-D-myo-inosityl-2-deoxy-α-D-glucopyranoside deacetylase <3> [7]
N-acetylglucosaminylinositol-deacetylase <2> [3]
Rv1170 <3> (<3> gene name [1,9]) [1,4,5,7,9]

CAS registry number
340703-87-9

2 Source Organism

<1> *Mycobacterium smegmatis* [8]
<2> *Mycobacterium tuberculosis* [3]
<3> *Mycobacterium tuberculosis* (UNIPROT accession number: O50426) [1,2,4,5,6,7,9]
<4> *Mycobacterium smegmatis* (UNIPROT accession number: O50426) [8]

D. Schomburg and I. Schomburg (eds.), *Class 3.4–6 Hydrolases, Lyases, Isomerases, Ligases: EC 3.4–6*, Springer Handbook of Enzymes S10, DOI 10.1007/978-3-642-36260-6_14,

3 Reaction and Specificity

Catalyzed reaction

1-(2-acetamido-2-deoxy-α-D-glucopyranosyl)-1D-myo-inositol + H_2O = 1-(2-amino-2-deoxy-α-D-glucopyranoside)-1D-myo-inositol + acetate (<3> proposed catalytic mechanism: the substrate binds to MshB so that the carbonyl oxygen of the acetyl group replaces the second water molecule on the Zn^{2+} ion. This leaves the first water molecule in an ideal position for general base-assisted nucleophilic attack of the carbonyl carbon of the acetyl group. The general base is the carboxylate of Asp-15. The tetrahedral transition state would then have a negatively charged oxygen atom that is stabilized by the positively charged Zn^{2+} and by the imidazolium side chain of His-144. Proton transfer to the nitrogen of the leaving group (GlcN-Ins) would be via the general acid function of the carboxyl group of Asp-15 [6])

Natural substrates and products

S 1-(2-acetamido-2-deoxy-a-D-glucopyranosyl)-1D-myo-inositol + H_2O <3> (<3> step in mycothiol biosynthesis [1]) (Reversibility: ?) [1]
P 1-(2-amino-2-deoxy-α-D-glucopyranoside)-1D-myo-inositol + acetate
S 1-(2-acetamido-2-deoxy-α-D-glucopyranosyl)-1D-myo-inositol + H_2O <2,3> (<3> biosynthesis of mycothiol [2]; <2> biosynthesis of mycothiol and detoxification of xenobiotics as their mycothiol-S-conjugates [3]; <3> key enzyme in mycothiol biosynthesis [6]; <3> mycothiol biosynthesis [5,9]) (Reversibility: ?) [2,3,5,6,9]
P 1-(2-amino-2-deoxy-α-D-glucopyranoside)-1D-myo-inositol + acetate
S 1-D-myo-inosityl-2-acetamido-2-deoxy-α-D-glucopyranoside + H_2O <3> (<3> key enzyme in mycothiol biosynthesis. Mycothiol is the major low molecular weight thiol in actinomycetes and is essential for growth of Mycobacterium tuberculosis [9]) (Reversibility: ?) [9]
P 1-(2-amino-2-deoxy-α-D-glucopyranoside)-1D-myo-inositol + acetate
S Additional information <4> (<4> MshB activity as a control point regulating mycothiol production [8]) [8]
P ?

Substrates and products

S 1-(2-acetamido-2-deoxy-a-D-glucopyranosyl)-1D-myo-inositol + H_2O <3> (<3> step in mycothiol biosynthesis [1]) (Reversibility: ?) [1]
P 1-(2-amino-2-deoxy-α-D-glucopyranoside)-1D-myo-inositol + acetate
S 1-(2-acetamido-2-deoxy-α-D-glucopyranosyl)-1D-myo-inositol + H_2O <2,3> (<3> biosynthesis of mycothiol [2]; <2> biosynthesis of mycothiol and detoxification of xenobiotics as their mycothiol-S-conjugates [3]; <3> key enzyme in mycothiol biosynthesis [6]; <3> mycothiol biosynthesis [5,9]; <3> activity with 1-D-myo-inosityl-2-acetamido-2-deoxy-α-D-glucopyranoside as the substrate is over 300fold greater than the deacetylase activity determined with N-acety-D-glucosamine and 23fold greater than the amidase activity measured with MSmB [5]; <3> the enzyme is specific for 1-D-myo-inosityl

2-N-acetamido-2-deoxy-α-D-glucopyranoside [2]) (Reversibility: ?) [1,2,3,5,6,9]

P 1-(2-amino-2-deoxy-α-D-glucopyranoside)-1D-myo-inositol + acetate

S 1-D-myo-inosityl-2-acetamido-2-deoxy-α-D-glucopyranoside + H_2O <3> (<3> key enzyme in mycothiol biosynthesis. Mycothiol is the major low molecular weight thiol in actinomycetes and is essential for growth of Mycobacterium tuberculosis [9]) (Reversibility: ?) [9]

P 1-(2-amino-2-deoxy-α-D-glucopyranoside)-1D-myo-inositol + acetate

S N-acetyl-D-glucosamine + H_2O <3> (<3> activity is 300fold lower than with 1-(2-acetamido-2-deoxy-α-D-glucopyranosyl)-1D-myo-inositol [5]; <3> activity is 73fold lower than with 1-D-myo-inosityl-2-acetamido-2-deoxy-α-D-glucopyranoside [9]) (Reversibility: ?) [5,9]

P D-glucosamine + acetate

S N-deacetyl-N-formylmycothiol-monobromobimane conjugate + H_2O <3> (Reversibility: ?) [9]

P ?

S cyclohexyl-2-acetamido-2-deoxy-1-thio-α-D-glucopyranoside + H_2O <2> (<2> 6% of the activity with 1-(2-acetamido-2-deoxy-α-D-glucopyranosyl)-1D-myo-inositol [3]) (Reversibility: ?) [3]

P cyclohexyl-2-amino-2-deoxy-1-thio-α-D-glucopyranoside + acetate

S cyclohexyl-2-acetamido-2-deoxy-α-D-glucopyranoside + H_2O <2> (<2> 6% of the activity with 1-(2-acetamido-2-deoxy-α-D-glucopyranosyl)-1D-myo-inositol [3]) (Reversibility: ?) [3]

P cyclohexyl-2-amino-2-deoxy-α-D-glucopyranoside + acetate

S phenyl-2-acetamido-2-deoxy-1-thio-α-D-glucopyranoside + H_2O <2> (<2> 25% of the activity with 1-(2-acetamido-2-deoxy-α-D-glucopyranosyl)-1D-myo-inositol [3]) (Reversibility: ?) [3]

P phenyl-2-amino-2-deoxy-1-thio-α-D-glucopyranoside + acetate

S Additional information <3,4> (<4> MshB activity as a control point regulating mycothiol production [8]; <3> MshB shows amidase activity with a wide range of substrates [9]; <3> the enzyme is unable to remove the acetyl residue from the acetylcysteinyl group of mycothiol or S-(2-oxo-2-phenylethyl)mycothiol, and it exhibits barely detectable amidase activity with mycothiol or mycothiol disulfide. It has significant amidase activity with S-(2-oxo-2-phenylethyl)mycothiol and even greater activity with N-deacetyl-N-formylmycothiol-monobromobimane conjugate, N-deacetyl-mycothiol-monobromobimane conjugate, formyl-CySmB-GlcN-Ins, and mycothiol-monobromobimane conjugate [9]) [8,9]

P ?

Inhibitors

1,10-phenanthroline <3> (<3> 0.1 mM, 82% inhibition of the enzyme isolated on the Ni-affinity column. 0.1mM 1,10-phenanthroline produces no signifiant inhibition of the enzyme isolated on the Zn-affinity column and 10% activity remains after treatment with 1 mM 1,10-phenanthroline. MshB activity lost by incubation of the Ni enzyme with 1,10-phenanthroline can be restored following removal of 1,10-phenanthroline by incubation with 0.1 mM

Zn^{2+}, Ni^{2+}, Mn^{2+}, or Co^{2+}, the latter promoting the highest activity, but Ca^{2+} and Mg^{2+} produce no restoration of activity [9]; <3> inhibition of the Zn enzyme by 1,10-phenanthroline is slower or less complete than inhibition of the Ni enzyme. MshB activity lost by incubation of the Ni enzyme with 1,10-phenanthroline can be restored following removal of 1,10-phenanthroline by incubation with 0.1 mM Zn^{2+}, Ni^{2+}, Mn^{2+}, or Co^{2+}, the latter promoting the highest activity. Ca^{2+} and Mg^{2+} produce no restoration of activity [9]) [9]
benzyl 2-deoxy-2-acetamido-1-thio-β-D-glucopyranoside <2> (<2> 0.5 mM, 13% inhibition [3]) [3]
cyclohexyl (2''R),(2''S)-3,3''-anhydro-2-deoxy-2-C-(2'',3''-dihydroxypropyl)-α-D-glucopyranoside <2> (<2> 0.5 mM, 6.6% inhibition [3]) [3]
cyclohexyl 2-deoxy-2-C-(2'',3''-epoxypropyl)-α-D-glucopyranoside <2> (<2> 0.5 mM, 19.7% inhibition [3]) [3]
cyclohexyl 2-deoxy-2-C-(2''-hydroxypropyl)-α-D-glucopyranoside <2> (<2> 0.5 mM, 11.4% inhibition [3]) [3]
cyclohexyl 2-deoxy-2-C-(2''-oxopropyl)-a-D-glucopyranoside <2> (<2> 0.5 mM, 6.7% inhibition [3]) [3]
cyclohexyl-2-chloroacetamido-2-deoxy-1-thio-α-D-glucopyranoside <2> (<2> 0.5 mM, 15% inhibition [3]) [3]
phenyl-2-acetamido-2-deoxy-1-thio-α-D-glucopyranoside <2> (<2> 0.5 mM, 6% inhibition [3]) [3]
phenyl-2-deoxy-2-[3'-(8''-hydroxy-3''-methyl-1'',4''-dioxo-1'',4''-dihydronaphthalen-2''-yl)butanamido]-1-thio-α-D-glucopyranoside <2> (<2> 0.5 mM, 81.6% inhibition [3]) [3]
phenyl-2-deoxy-2-[3'-(8''-hydroxy-3''-methyl-1'',4''-dioxo-1'',4''-dihydronaphthalen-2''-yl)pentanamido]-1-thio-α-D-glucopyranoside <2> (<2> 0.5 mM, 81.4% inhibition [3]) [3]
phenyl-2-deoxy-2-[3'-(8''-hydroxy-3''-methyl-1'',4''-dioxo-1'',4''-dihydronaphthalen-2''-yl)propanamido]-1-thio-α-D-glucopyranoside <2> (<2> 0.5 mM, 57.4% inhibition [3]) [3]
phenyl-2-deoxy-2-acetamido-1-thio-β-D-glucopyranoside <2> (<2> 0.5 mM, 15% inhibition [3]) [3]
Additional information <3> (<3> no inhibition is observed with 0.1 M 1,7-phenanthroline [9]) [9]

Activating compounds

1,7-phenanthroline <3> (<3> 1 mM, slight enhancement of activity [9]) [9]

Metals, ions

Co^{2+} <3> (<3> MshB activity lost by incubation of the Ni enzyme with 1,10-phenanthroline can be restored following removal of 1,10-phenanthroline by incubation with 0.1 mM Zn^{2+}, Ni^{2+}, Mn^{2+}, or Co^{2+}, the latter promoting the highest activity. Ca^{2+} and Mg^{2+} produce no restoration of activity [9]; <3> MshB contains a divalent transition metal ion essential for activity. MshB isolated on the Ni-affinity column contains 0.36 equivalent of Ca and 0.82 equivalent of Ni, and less than 0.08 equivalent of Zn per subunit. MshB isolated on the Zn-affinity column contains less than 0.1 equivalent of Ca and 2.3 equivalents of Zn, and less than 0.08 equivalent of Ni per subunit. MshB ac-

tivity lost by incubation of the Ni enzyme with 1,10-phenanthroline can be restored following removal of 1,10-phenanthroline by incubation with 0.1 mM Zn^{2+}, Ni^{2+}, Mn^{2+}, or Co^{2+}, the latter promoting the highest activity, but Ca^{2+} and Mg^{2+} produce no restoration of activity [9]) [9]
Mn^{2+} <3> (<3> MshB activity lost by incubation of the Ni enzyme with 1,10-phenanthroline can be restored following removal of 1,10-phenanthroline by incubation with 0.1 mM Zn^{2+}, Ni^{2+}, Mn^{2+}, or Co^{2+}, the latter promoting the highest activity. Ca^{2+} and Mg^{2+} produce no restoration of activity [9]; <3> MshB contains a divalent transition metal ion essential for activity. MshB isolated on the Ni-affinity column contains 0.36 equivalent of Ca and 0.82 equivalent of Ni, and less than 0.08 equivalent of Zn per subunit. MshB isolated on the Zn-affinity column contains less than 0.1 equivalent of Ca and 2.3 equivalents of Zn, and less than 0.08 equivalent of Ni per subunit. MshB activity lost by incubation of the Ni enzyme with 1,10-phenanthroline can be restored following removal of 1,10-phenanthroline by incubation with 0.1 mM Zn^{2+}, Ni^{2+}, Mn^{2+}, or Co^{2+}, the latter promoting the highest activity, but Ca^{2+} and Mg^{2+} produce no restoration of activity [9]) [9]
Ni^{2+} <3> (<3> MshB activity lost by incubation of the Ni enzyme with 1,10-phenanthroline can be restored following removal of 1,10-phenanthroline by incubation with 0.1 mM Zn^{2+}, Ni^{2+}, Mn^{2+}, or Co^{2+}, the latter promoting the highest activity. Ca^{2+} and Mg^{2+} produce no restoration of activity [9]; <3> MshB contains a divalent transition metal ion essential for activity. MshB isolated on the Ni-affinity column contains 0.36 equivalent of Ca and 0.82 equivalent of Ni, and less than 0.08 equivalent of Zn per subunit. MshB isolated on the Zn-affinity column contains less than 0.1 equivalent of Ca and 2.3 equivalents of Zn, and less than 0.08 equivalent of Ni per subunit. MshB activity lost by incubation of the Ni enzyme with 1,10-phenanthroline can be restored following removal of 1,10-phenanthroline by incubation with 0.1 mM Zn^{2+}, Ni^{2+}, Mn^{2+}, or Co^{2+}, the latter promoting the highest activity, but Ca^{2+} and Mg^{2+} produce no restoration of activity [9]) [9]
Zn^{2+} <3> (<3> contains an active site divalent transition metal. MshB activity lost by incubation of the Ni enzyme with 1,10-phenanthroline can be restored following removal of 1,10-phenanthroline by incubation with 0.1 mM Zn^{2+}, Ni^{2+}, Mn^{2+}, or Co^{2+}, the latter promoting the highest activity. Ca^{2+} and Mg^{2+} produce no restoration of activity [9]; <3> metalloprotein, the deacetylase activity is completely dependent on the presence of a divalent metal cation. The Zn^{2+} is 5 coordinate with 3 residues from MshB (His-13, Asp-16, His-147) and two water molecules [6]; <3> MshB contains a divalent transition metal ion essential for activity. MshB isolated on the Ni-affinity column contains 0.36 equivalent of Ca and 0.82 equivalent of Ni, and less than 0.08 equivalent of Zn per subunit. MshB isolated on the Zn-affinity column contains less than 0.1 equivalent of Ca and 2.3 equivalents of Zn, and less than 0.08 equivalent of Ni per subunit. MshB activity lost by incubation of the Ni enzyme with 1,10-phenanthroline can be restored following removal of 1,10-phenanthroline by incubation with 0.1 mM Zn^{2+}, Ni^{2+}, Mn^{2+}, or Co^{2+}, the latter promoting the highest activity, but Ca^{2+} and Mg^{2+} produce no restoration of activity [9]; <3> MshB is a Zn^{2+} metalloprotein, the deacetylase activ-

ity is completely dependent on the presence of a divalent metal cation. The Zn^{2+} is 5 coordinate with 3 residues from MshB (His-13, Asp-16, His-147) and two water molecules [6]) [6,9]

Turnover number (s^{-1})

0.12 <2> (phenyl-2-acetamido-2-deoxy-1-thio-α-D-glucopyranoside, <2> pH 7.5, 37°C [3]) [3]
0.24 <2> (1-(2-acetamido-2-deoxy-α-D-glucopyranosyl)-1D-myo-inositol, <2> pH 7.5, 37°C [3]) [3]
0.49 <3> (1-(2-acetamido-2-deoxy-α-D-glucopyranosyl)-1D-myo-inositol, <3> pH 7.5, 37°C [9]) [9]
0.49 <3> (N-deacetyl-N-formylmycothiol-monobromobimane conjugate, <3> pH 7.4, 37°C [9]) [9]

Specific activity (U/mg)

0.19 <3> [9]

K_m-Value (mM)

0.34 <3> (1-(2-acetamido-2-deoxy-α-D-glucopyranosyl)-1D-myo-inositol, <3> pH 7.5, 37°C [9]) [9]
0.34 <3> (N-deacetyl-N-formylmycothiol-monobromobimane conjugate, <3> pH 7.4, 37°C [9]) [9]
0.348 <2> (1-(2-acetamido-2-deoxy-α-D-glucopyranosyl)-1D-myo-inositol, <2> pH 7.5, 37°C [3]) [3]
1.695 <2> (phenyl-2-acetamido-2-deoxy-1-thio-α-D-glucopyranoside) [3]

pH-Optimum

7.4 <3> (<3> assay at [2,9]) [2,9]
7.5 <2> (<2> assay at [3]) [3]

Temperature optimum (°C)

32 <3> (<3> assay at [2]) [2]
37 <2,3> (<2,3> assay at [3,9]) [3,9]

4 Enzyme Structure

Molecular weight

79000 <3> (<3> dimer, gel filtration [9]; <3> dimer, the enzyme behaves as a dimer at normal ionic strength but may associate to a tetramer at low ionic strength, gel filtration [9]) [9]
158000 <3> (<3> tetramer, gel filtration [9]; <3> tetramer, the enzyme behaves as a dimer at normal ionic strength but may associate to a tetramer at low ionic strength, gel filtration [9]) [9]

Subunits

dimer <3> (<3> 2 * 32000, SDS-PAGE [9]; <3> 2 * 32000, the enzyme appears to behave as a dimer at normal ionic strength but may associate to a tetramer at low ionic strength, SDS-PAGE [9]; <3> 2 * 33423, the enzyme

appears to behave as a dimer at normal ionic strength but may associate to a tetramer at low ionic strength, calculated from sequence [9]) [9]
tetramer <3> (<3> 4 * 32000, the enzyme appears to behave as a dimer at normal ionic strength but may associate to a tetramer at low ionic strength, SDS-PAGE [9]; <3> 4 * 33423, the enzyme appears to behave as a dimer at normal ionic strength but may associate to a tetramer at low ionic strength, calculated from sequence [9]) [9]

5 Isolation/Preparation/Mutation/Application

Purification

<3> [1,7,9]

Crystallization

<3> (crystals prepared in the presence of β-octylglucoside as a key additive, are suitable for high-resolution X-ray structural analysis. The crystals are orthorhombic, with unit-cell parameters a = 71.69, b = 83.74, c = 95.65 A, space group P2(1)2(1)2(1) and two molecules in the asymmetric unit. Collection of X-ray diffraction data to 1.9 A resolution) [1]
<3> (hanging-drop vapour-diffusion method, crystallized both in native and SeMet-substituted forms) [7]
<3> (structure, determined at 1.9 A resolution by X-ray crystallography) [7]
<3> (the structure, determined at 1.9 A resolution by X-ray crystallography, reveals an α/β fold in which helices pack against a seven-stranded mostly parallel β-sheet) [7]
<3> (vapor-diffusion method) [6]
<3> (vapor-diffusion method with a mother liquor consisting of 15% polyethylene glycol 4000, 50 mm Tris-HCl (pH 8.0), 0.1 m $Mg(NO_3)2$, 6% 1,6-hexanediol, and 10% ethylene glycol. A 1:2 ratio of protein solution (6 mg/ml) to mother liquor is mixed and left for vapor equilibration. Triclinic crystals form after approximately 1 week at room temperature) [6]

Cloning

<3> [2]
<3> (Rv1170 is cloned to contain a C-terminal His-6 tag to facilitate purifiation, expression in Escherichia coli) [9]
<3> (expression in Escherichia coli) [5,9]
<3> (expression in Escherichia coli both in native and SeMet-substituted forms) [1,7]

Application

medicine <3> (<3> antisense oligonucleotides to GlcNAc-Ins deacetylase (Rv1170) mRNA affect mycobacterial growth. The enzyme is sensitive to free radical generating antituberculosis drugs and may be a useful targets for new drug development [4]) [4]

References

[1] McCarthy, A.A.; Knijff, R.; Peterson, N.A.; Baker, E.N.: Crystallization and preliminary X-ray analysis of N-acetyl-1-D-myo-inosityl-2-deoxy-α-D-glucopyranoside deacetylase (MshB) from Mycobacterium tuberculosis. Acta Crystallogr. Sect. D, **59**, 2316-2318 (2003)
[2] Nicholas, G.M.; Eckman, L.L.; Kovac, P.; Otero-Quintero, S.; Bewley, C.A.: Synthesis of 1-D- and 1-L-myo-inosityl 2-N-acetamido-2-deoxy-α-D-glucopyranoside establishes substrate specificity of the Mycobacterium tuberculosis enzyme AcGI deacetylase. Bioorg. Med. Chem., **11**, 2641-2647 (2003)
[3] Gammon, D.W.; Steenkamp, D.J.; Mavumengwana, V.; Marakalala, M.J.; Mudzunga, T.T.; Hunter, R.; Munyololo, M.: Conjugates of plumbagin and phenyl-2-amino-1-thioglucoside inhibit MshB, a deacetylase involved in the biosynthesis of mycothiol. Bioorg. Med. Chem., **18**, 2501-2514 (2010)
[4] Hayward, D.; Wiid, I.; van Helden, P.: Differential expression of mycothiol pathway genes: are they affected by antituberculosis drugs?. IUBMB Life, **56**, 131-138 (2004)
[5] Newton, G.L.; Av-Gay, Y.; Fahey, R.C.: N-Acetyl-1-D-myo-inosityl-2-amino-2-deoxy-α-D-glucopyranoside deacetylase (MshB) is a key enzyme in mycothiol biosynthesis. J. Bacteriol., **182**, 6958-6963 (2000)
[6] Maynes, J.T.; Garen, C.; Cherney, M.M.; Newton, G.; Arad, D.; Av-Gay, Y.; Fahey, R.C.; James, M.N.: The crystal structure of 1-D-myo-inosityl 2-acetamido-2-deoxy-α-D-glucopyranoside deacetylase (MshB) from Mycobacterium tuberculosis reveals a zinc hydrolase with a lactate dehydrogenase fold. J. Biol. Chem., **278**, 47166-47170 (2003)
[7] McCarthy, A.A.; Peterson, N.A.; Knijff, R.; Baker, E.N.: Crystallization and preliminary X-ray analysis of N-acetyl-1-D-myo-inosityl-2-deoxy-α-D-glucopyranoside deacetylase (MshB) from Mycobacterium tuberculosis. J. Mol. Biol., **335**, 1131-1141 (2004)
[8] Rawat, M.; Kovacevic, S.; Billman-Jacobe, H.; Av-Gay, Y.: Inactivation of mshB, a key gene in the mycothiol biosynthesis pathway in Mycobacterium smegmatis. Microbiology, **149**, 1341-1349 (2003)
[9] Newton, G.L.; Ko, M.; Ta, P.; Av-Gay, Y.; Fahey, R.C.: Purification and characterization of Mycobacterium tuberculosis 1D-myo-inosityl-2-acetamido-2-deoxy-α-D-glucopyranoside deacetylase, MshB, a mycothiol biosynthetic enzyme. Protein Expr. Purif., **47**, 542-550 (2006)

peptidoglycan-N-acetylglucosamine deacetylase 3.5.1.104

1 Nomenclature

EC number
3.5.1.104

Systematic name
peptidoglycan-N-acetylglucosamine amidohydrolase

Recommended name
peptidoglycan-N-acetylglucosamine deacetylase

Synonyms
HP310 <4> [8]
Lmo0415 <5> [9]
N-acetylglucosamine deacetylase <8> [11]
N-acetylglucosamine deacetylase BC1960 <7> [2]
PG N-deacetylase <5> [7]
SpPgdA <2> [6]
enzyme BC1960 <3> [4]
enzyme BC3618 <3> [4]
peptidoglycan GlcNAc deacetylase <2> [6]
peptidoglycan N-acetylglucosamine deacetylase <1,3,5,7> [2,4,5,9]
peptidoglycan N-acetylglucosamine deacetylase BC1960 <7> [2]
peptidoglycan deacetylase <4> [8]
pgdA <1,5,6,8> [5,7,9,10,11]

CAS registry number
75217-01-5

2 Source Organism

<1> *Lactococcus lactis* [5]
<2> *Streptococcus pneumoniae* [6]
<3> *Bacillus cereus* [1,3,4]
<4> *Helicobacter pylori* [8]
<5> *Listeria monocytogenes* [7,9]
<6> *Streptococcus suis* [10]
<7> *Bacillus cereus* (UNIPROT accession number: Q81EK9) [2]
<8> *Streptococcus pneumoniae* (UNIPROT accession number: Q97PW1) [11]

D. Schomburg and I. Schomburg (eds.), *Class 3.4–6 Hydrolases, Lyases, Isomerases, Ligases: EC 3.4–6*, Springer Handbook of Enzymes S10, DOI 10.1007/978-3-642-36260-6_15,

3 Reaction and Specificity

Catalyzed reaction

peptidoglycan-N-acetyl-D-glucosamine + H_2O = peptidoglycan-D-glucosamine + acetate

Natural substrates and products

- **S** acetylated peptidoglycan + H_2O <1,2,3,5,8> (<3> enzymatic deacetylation of chemically acetylated vegetative peptidoglycan from Bacillus cereus by BC1960 and BC3618 results in increased resistance to lysozyme digestion [4]; <1> enzymic N-acetylglucosamine deacetylation protects peptidoglycan from hydrolysis by the major autolysin AcmA in Lactococcus lactis cells, and this leads to decreased cellular autolysis [5]; <5> N-deacetylation is a major modification of Listeria peptidoglycan. PG N-deacetylation could be a general mechanism used by bacteria to evade the host innate immune system [7]; <2> peptidoglycan GlcNAc deacetylase protects the Gram-positive bacterial cell wall from host lysozymes by deacetylating peptidoglycan GlcNAc residues [6]) (Reversibility: ?) [4,5,6,7,11]
- **P** deacetylated peptidoglycan + acetate
- **S** peptidoglycan-N-acetyl-D-glucosamine + H_2O <4,5> (<4> Helicobacter pylori is highly resistant to lysozyme (up to 50 mg/ml), but the HP310 mutant is less resistant compared with the parent strain. The peptidoglycan deacetylation appears to confer lysozyme resistance to escape immunedetection [8]; <5> peptidoglycan N-deacetylation is an important modification of Listeria peptidoglycan, which allows this human pathogen to evade the innate immune system [9]) (Reversibility: ?) [8,9]
- **P** peptidoglycan-D-glucosamine + acetate

Substrates and products

- **S** GlcNAc-β-1,4-GlcNAc + H_2O <3> (<3> no deacetylation of the reducing GlcNAc residue [4]) (Reversibility: ?) [4]
- **P** ?
- **S** GlcNAc-β-1,4-GlcNAc-β-1,4-GlcNAc + H_2O <2> (Reversibility: ?) [6]
- **P** GlcNAc-β-1,4-Glc-β-1,4-GlcNAc + NH_3
- **S** GlcNAc-β-1,4-GlcNAc-β-1,4-GlcNAc + H_2O <3> (<3> deacetylates all GlcNAc residues of the oligomer except the reducing end ones [4]) (Reversibility: ?) [4]
- **P** ?
- **S** GlcNAc-β-1,4-GlcNAc-β-1,4-GlcNAc-β-1,4-GlcNAc + H_2O <3> (<3> GlcNAc-β-1,4-GlcNAc-β-1,4-GlcNAc-β-1,4-GlcNAc is the favorable substrate. Deacetylates all GlcNAc residues of the oligomer except the reducing end ones [4]) (Reversibility: ?) [4]
- **P** ?
- **S** GlcNAc-β-1,4-GlcNAc-β-1,4-GlcNAc-β-1,4-GlcNAc-β-1,4-GlcNAc + H_2O <3> (<3> deacetylates all GlcNAc residues of the oligomer except the reducing end ones [4]) (Reversibility: ?) [4]
- **P** ?

S GlcNAc-β-1,4-GlcNAc-β-1,4-GlcNAc-β-1,4-GlcNAc-β-1,4-GlcNAc-β-1,4-GlcNAc + H_2O <3> (<3> deacetylates all GlcNAc residues of the oligomer except the reducing end ones [4]) (Reversibility: ?) [4]
P ?
S GlcNAcβ(1-4)GlcNAcβ(1-4)GlcNAcβ(1-4)GlcNAcβ(1-4)GlcNAcβ(1-4)GlcNAc + H_2O <7> (Reversibility: ?) [2]
P GlcNβ(1-4)GlcNβ(1-4)GlcNβ(1-4)GlcNβ(1-4)GlcNβ(1-4)GlcNAc
S acetylated peptidoglycan + H_2O <1,2,3,5,8> (<3> enzymatic deacetylation of chemically acetylated vegetative peptidoglycan from Bacillus cereus by BC1960 and BC3618 results in increased resistance to lysozyme digestion [4]; <1> enzymic N-acetylglucosamine deacetylation protects peptidoglycan from hydrolysis by the major autolysin AcmA in Lactococcus lactis cells, and this leads to decreased cellular autolysis [5]; <5> N-deacetylation is a major modification of Listeria peptidoglycan. PG N-deacetylation could be a general mechanism used by bacteria to evade the host innate immune system [7]; <2> peptidoglycan GlcNAc deacetylase protects the Gram-positive bacterial cell wall from host lysozymes by deacetylating peptidoglycan GlcNAc residues [6]; <3> effective in deacetylating cell wall peptidoglycan from the Gram(+) Bacillus cereus and Bacillus subtilis and the Gram(-) Helicobacter pylori [4]; <8> contribution of lysozyme and peptidoglycan modifications during colonization of the upper respiratory tract analyzed [11]) (Reversibility: ?) [3,4,5,6,7,11]
P deacetylated peptidoglycan + acetate
S glycolchitin + H_2O <3> (<3> poor substrate [1]) (Reversibility: ?) [1]
P ?
S peptidoglycan + H_2O <3> (Reversibility: ?) [1]
P ?
S peptidoglycan-N-acetyl-D-glucosamine + H_2O <4,5> (<4> Helicobacter pylori is highly resistant to lysozyme (up to 50 mg/ml), but the HP310 mutant is less resistant compared with the parent strain. The peptidoglycan deacetylation appears to confer lysozyme resistance to escape immunedetection [8]; <5> peptidoglycan N-deacetylation is an important modification of Listeria peptidoglycan, which allows this human pathogen to evade the innate immune system [9]; <5> N-acetylated murein after lysozyme digestion [9]) (Reversibility: ?) [8,9]
P peptidoglycan-D-glucosamine + acetate
S Additional information <3,5> (<3> no activity with N-acetyl-D-glucosamine [4]; <3> reaction of the deacetylase with (GlcNAc-MurNAc)3 is less than 1/100 of that with peptidoglycan, while the enzyme is inactive towards (GlcNAc-MurNAc), GlcNAc-MurNAc, and monomeric N-acetylglucosamine derivatives [3]; <5> N-acetylmuramic acid is not a substrate. With N-acetylglucosamine as substrate D-glucosamine is formed [9]) (Reversibility: ?) [3,4,9]
P ?

Inhibitors

$CuCl_2$ <3> [4]
$ZnCl_2$ <3> [4]

Metals, ions

Co^{2+} <2,3> (<2> 0.05 mM, 30fold increase in activity [6]; <3> 1 mM, 10% increase in activity [4]) [4,6]
Zn^{2+} <2> (<2> 0.05 mM, 5.5fold increase in activity [6]) [6]
Additional information <2> (<2> SpPgdA is a metalloenzyme using a His-His-Asp zinc-binding triad with a nearby aspartic acid and histidine acting as the catalytic base and acid, respectively [6]) [6]

Turnover number (s^{-1})

0.27 <2> (GlcNAc-β-1,4-GlcNAc-β-1,4-GlcNAc, <2> mutant enzyme I419G [6]) [6]
0.55 <2> (GlcNAc-β-1,4-GlcNAc-β-1,4-GlcNAc, <2> wild-type enzyme [6]) [6]
1.5 <2> (GlcNAc-β-1,4-GlcNAc-β-1,4-GlcNAc, <2> mutant enzyme L302A [6]) [6]
1.6 <2> (GlcNAc-β-1,4-GlcNAc-β-1,4-GlcNAc, <2> mutant enzyme K304I [6]) [6]

Specific activity (U/mg)

Additional information <8> (<8> competition experiments with wild-type and mutant strains in lysozyme M-sufficient mice, effect of peptidoglycan modifying enzymes on growth, viability and hydrolysis of pneumococcal cell walls as well as on relative fitness during murine colonization in the presence or absence of lysozyme shown, contribution of lysozyme from neutrophils to survival and colonization of mutants lacking peptidoglycan modifications, effect of peptidoglycan modifying enzymes on expression of capsular polysaccharide (CPS) [11]) [11]

K_m-Value (mM)

0.3 <3> (GlcNAc-β-1,4-GlcNAc-β-1,4-GlcNAc-β-1,4-GlcNAc-β-1,4-GlcNAc-β-1,4-GlcNAc, <3> enzyme BC1960 [4]) [4]
0.37 <3> (GlcNAc-β-1,4-GlcNAc-β-1,4-GlcNAc-β-1,4-GlcNAc-β-1,4-GlcNAc, <3> enzyme BC1960 [4]) [4]
0.45 <3> (GlcNAc-β-1,4-GlcNAc-β-1,4-GlcNAc-β-1,4-GlcNAc-β-1,4-GlcNAc-β-1,4-GlcNAc) [4]
0.5 <3> (GlcNAc-β-1,4-GlcNAc-β-1,4-GlcNAc-β-1,4-GlcNAc-β-1,4-GlcNAc) [4]
1.18 <3> (GlcNAc-β-1,4-GlcNAc-β-1,4-GlcNAc-β-1,4-GlcNAc, <3> enzyme BC1960 [4]) [4]
1.5 <3> (GlcNAc-β-1,4-GlcNAc-β-1,4-GlcNAc-β-1,4-GlcNAc) [4]
2.2 <3> (GlcNAc-β-1,4-GlcNAc-β-1,4-GlcNAc) [4]
2.46 <3> (GlcNAc-β-1,4-GlcNAc-β-1,4-GlcNAc, <3> enzyme BC1960 [4]) [4]
3.8 <2> (GlcNAc-β-1,4-GlcNAc-β-1,4-GlcNAc, <2> wild-type enzyme [6]) [6]
3.9 <3> (GlcNAc-β-1,4-GlcNAc) [4]
4 <2> (GlcNAc-β-1,4-GlcNAc-β-1,4-GlcNAc, <2> mutant enzyme L302A [6]) [6]

4.1 <3> (GlcNAc-β-1,4-GlcNAc, <3> enzyme BC1960 [4]) [4]
6.2 <2> (GlcNAc-β-1,4-GlcNAc-β-1,4-GlcNAc, <2> mutant enzyme K304I [6]) [6]
26 <2> (GlcNAc-β-1,4-GlcNAc-β-1,4-GlcNAc, <2> mutant enzyme I419G [6]) [6]

pH-Optimum
6 <3> (<3> enzyme BC1960 [4]) [4]
7 <3> [1]
8 <3> (<3> enzyme BC3618 [4]) [4]

Temperature optimum (°C)
37 <3> (<3> enzyme BC3618 [4]) [4]
50 <3> (<3> enzyme BC1960 [4]) [4]

5 Isolation/Preparation/Mutation/Application

Source/tissue
nasopharynx <8> (<8> peptidoglycan modifications during colonizing the mucosal surface of the upper respiratory tract, lysozyme M-sufficient mice [11]) [11]

Localization
cell wall <5> [9]

Purification
<3> [4]
<3> (partial AHU 1030) [1]
<5> (hexa-His-tagged form of PgdA) [9]
<7> [2]

Crystallization
<2> (sitting-drop vapor diffusion method, native crystal structure and product complexes of SpPgdA) [6]
<7> (hanging-drop vapour diffusion method) [2]
<7> (hanging-drop vapour diffusion method, enzyme is crystallized in the presence of $(GlcNAc)_6$]) [2]

Cloning
<1> (cloning of pgdA on a multicopy plasmid vector results in an increased degree of peptidoglycan deacetylation) [5]
<3> (the gene bc1960 is cloned and expressed in Escherichia coli) [4]
<3> (the gene bc3618 is cloned and expressed in Escherichia coli) [4]
<7> (expressed in Escherichia coli) [2]
<7> (expression in Escherichia coli) [2]
<8> (generation of mutant (pgdA and pgdAadr) and revertant strains) [11]

Engineering

I419G <2> (<2> k_{cat}/K_m is 15fold lower than wild-type value [6]) [6]
K304I <2> (<2> k_{cat}/K_m is 1.7fold higher than wild-type value [6]) [6]
L302A <2> (<2> k_{cat}/K_m is 2.5fold higher than wild-type value [6]) [6]

Application

pharmacology <8> (<8> studies on peptidoglycan modifications by Streptococcus pneumoniae [11]) [11]

6 Stability

Temperature stability

50 <3> (<3> enzyme BC1960 retains 95% of its activity after 24 h [4]; <3> enzyme BC3618 is inactivated after 1h [4]) [4]

References

[1] Araki, Y.; Fukuoka, S.; Oba, S.; Ito, E.: Enzymatic deacetylation of N-acetylglucosamine residues in peptidoglycan from Bacillus cereus cell walls. Biochem. Biophys. Res. Commun., **45**, 751-758 (1971)
[2] Tsalafouta, A.; Psylinakis, E.; Kapetaniou, E.G.; Kotsifaki, D.; Deli, A.; Roidis, A.; Bouriotis, V.; Kokkinidis, M.: Purification, crystallization and preliminary X-ray analysis of the peptidoglycan N-acetylglucosamine deacetylase BC1960 from Bacillus cereus in the presence of its substrate $(GlcNAc)_6$]. Acta Crystallogr. Sect. F, **64**, 203-205 (2008)
[3] Araki, Y.; Oba, S.; Araki, S.; Ito, E.: Enzymic deacetylation of N-acetylglucosamine residues in cell wall peptidoglycan. J. Biochem., **88**, 469-479 (1980)
[4] Psylinakis, E.; Boneca, I.G.; Mavromatis, K.; Deli, A.; Hayhurst, E.; Foster, S.J.; Varum, K.M.; Bouriotis, V.: Peptidoglycan N-acetylglucosamine deacetylases from Bacillus cereus, highly conserved proteins in Bacillus anthracis. J. Biol. Chem., **280**, 30856-30863 (2005)
[5] Meyrand, M.; Boughammoura, A.; Courtin, P.; Mezange, C.; Guillot, A.; Chapot-Chartier, M.P.: Peptidoglycan N-acetylglucosamine deacetylation decreases autolysis in Lactococcus lactis. Microbiology, **153**, 3275-3285 (2007)
[6] Blair, D.E.; Schuttelkopf, A.W.; MacRae, J.I.; van Aalten, D.M.F.: Structure and metal-dependent mechanism of peptidoglycan deacetylase, a streptococcal virulence factor. Proc. Natl. Acad. Sci. USA, **102**, 15429-15434 (2005)
[7] Boneca, I.G.; Dussurget, O.; Cabanes, D.; Nahori, M.A.; Sousa, S.; Lecuit, M.; Psylinakis, E.; Bouriotis, V.; Hugot, J.P.; Giovannini, M.; Coyle, A.; Bertin, J.; Namane, A.; Rousselle, J.C.; Cayet, N.; Prevost, M.C.; Balloy, V.; Chignard, M.; Philpott, D.J.; Cossart, P.; Girardin, S.E.: A critical role for peptidoglycan N-deacetylation in Listeria evasion from the host innate immune system. Proc. Natl. Acad. Sci. USA, **104**, 997-1002 (2007)

[8] Wang, G.; Olczak, A.; Forsberg, L.S.; Maier, R.J.: Oxidative stress-induced peptidoglycan deacetylase in Helicobacter pylori. J. Biol. Chem., **284**, 6790-6800 (2009)
[9] Popowska, M.; Kusio, M.; Szymanska, P.; Markiewicz, Z.: Inactivation of the wall-associated de-N-acetylase (PgdA) of Listeria monocytogenes results in greater susceptibility of the cells to induced autolysis. J. Microbiol. Biotechnol., **19**, 932-945 (2009)
[10] Fittipaldi, N.; Sekizaki, T.; Takamatsu, D.; Dominguez-Punaro Mde, L.; Harel, J.; Bui, N.K.; Vollmer, W.; Gottschalk M.: Significant contribution of the pgdA gene to the virulence of Streptococcus suis. Mol. Microbiol., **70**, 1120-1135 (2008)
[11] Davis, K.M.; Akinbi, H.T.; Standish, A.J.; Weiser, J.N.: Resistance to mucosal lysozyme compensates for the fitness deficit of peptidoglycan modifications by Streptococcus pneumoniae. PLoS Pathog., **4**, e1000241 (2008)

chitin disaccharide deacetylase 3.5.1.105

1 Nomenclature

EC number
3.5.1.105

Systematic name
2-(acetylamino)-4-O-[2-(acetylamino)-2-deoxy-β-D-glucopyranosyl]-2-deoxy-D-glucopyranose acetylhydrolase

Recommended name
chitin disaccharide deacetylase

Synonyms
CE family 4 COD <1,2,3,4,5,7> [5]
COD <1,2,3,4,5,7> [5]
Pa-COD <1> [1,2,3]
carbohydrate esterase family 4 chitin oligosaccharide deacetylase <1> [5]
chitin oligosaccharide deacetylase <1,2,3,4,5,7> [1,2,3,5]
deacetylase DA1 <6> [4,6]

2 Source Organism

<1> *Vibrio parahaemolyticus* [1,2,3,5]
<2> *Vibrio proteolyticus* [5]
<3> *Vibrio cholerae* [5]
<4> *Vibrio alginolyticus* [5]
<5> *Vibrio campbellii* [5]
<6> *Vibrio alginolyticus* (UNIPROT accession number: Q99PX1) [4,6]
<7> *Vibrio parahaemolyticus* (UNIPROT accession number: A6P4T5) [5]
<8> no activity in *Vibrio orientalis* [5]
<9> no activity in *Vibrio furnissii* [5]
<10> no activity in *Vibrio nereis* [5]

3 Reaction and Specificity

Catalyzed reaction
2-(acetylamino)-4-O-[2-(acetylamino)-2-deoxy-β-D-glucopyranosyl]-2-deoxy-β-D-glucopyranose + H_2O = 2-(acetylamino)-4-O-(2-amino-2-deoxy-β-D-glucopyranosyl)-2-deoxy-β-D-glucopyranose + acetate

D. Schomburg and I. Schomburg (eds.), *Class 3.4–6 Hydrolases, Lyases, Isomerases, Ligases: EC 3.4–6*, Springer Handbook of Enzymes S10, DOI 10.1007/978-3-642-36260-6_16,

Natural substrates and products

- **S** GlcNAc-β-(1,4)-GlcNAc + H_2O <1> (<1> i.e. 2-(acetylamino)-4-O-[2-(acetylamino)-2-deoxy-β-D-glucopyranosyl]-2-deoxy-D-glucopyranose. Besides being a nutrient, the heterodisaccharide product 4-O-(N-acetyl-β-D-glucosaminyl)-D-glucosamine is a unique inducer of chitinase production in Vibrio bacteria that have the chitin oligosaccharide deacetylase producing ability. Chitin oligosaccharide deacetylase involved in the synthesis of this signal compound is one of the key enzymes in the chitin catabolic cascade of chitinolytic Vibrio strains [5]) (Reversibility: ?) [5]
- **P** GlcNAc-β-(1,4)-GlcN + acetate
- **S** GlcNAc-β-1,4-GlcNAc + H_2O <1> (<1> GlcNAc-β-1,4-GlcN is produced from chitin by the cooperative hydrolytic reactions of both chitinase and chitin oligosaccharide deacetylase [1]) (Reversibility: ?) [1]
- **P** GlcNAc-β-1,4-GlcN + acetate

Substrates and products

- **S** GlcNAc-β-(1,4)-GlcNAc + H_2O <1> (<1> i.e. 2-(acetylamino)-4-O-[2-(acetylamino)-2-deoxy-β-D-glucopyranosyl]-2-deoxy-D-glucopyranose. Besides being a nutrient, the heterodisaccharide product 4-O-(N-acetyl-β-D-glucosaminyl)-D-glucosamine is a unique inducer of chitinase production in Vibrio bacteria that have the chitin oligosaccharide deacetylase producing ability. Chitin oligosaccharide deacetylase involved in the synthesis of this signal compound is one of the key enzymes in the chitin catabolic cascade of chitinolytic Vibrio strains [5]; <1> i.e. 2-(acetylamino)-4-O-[2-(acetylamino)-2-deoxy-β-D-glucopyranosyl]-2-deoxy-D-glucopyranose [5]) (Reversibility: ?) [5]
- **P** GlcNAc-β-(1,4)-GlcN + acetate (<1> i.e. 4-O-(N-acetyl-β-D-glucosaminyl)-D-glucosamine [5])
- **S** GlcNAc-β-(1-4)-GlcNAc + H_2O <1,2,3,4,5,6,7> (<6> i.e. 2-(acetylamino)-4-O-[2-(acetylamino)-2-deoxy-β-D-glucopyranosyl]-2-deoxy-D-glucopyranose. No activity with chitotriose, chitotetraose, chitopentaose and chitohexaose. The 2-acetamido group is completely hydrolyzed within 3 h, no hydrolysis of 2-acetamide group occurs [4]) (Reversibility: ?) [4,5]
- **P** GlcNAc-β-(1-4)-GlcN + acetate (<6> i.e. 4-O-(N-acetyl-β-D-glucosaminyl)-D-glucosamine [4])
- **S** GlcNAc-β-1,4-GlcNAc + H_2O <1> (<1> GlcNAc-β-1,4-GlcN is produced from chitin by the cooperative hydrolytic reactions of both chitinase and chitin oligosaccharide deacetylase [1]) (Reversibility: ?) [1,2,3]
- **P** GlcNAc-β-1,4-GlcN + acetate
- **S** GlcNAc-β-1,4-GlcNAc-β-1,4-GlcNAc + H_2O <1> (<1> 20% of the activity with GlcNAc-β-1,4-GlcNAc [1]; <1> 30% of the activity with GlcNAc-β-1,4-GlcNAc [2]) (Reversibility: ?) [1,2]
- **P** ?
- **S** Additional information <1> (<1> no activity with: GlcNAc-β-1,4-GlcNAc-β-1,4-GlcNAc-β-1,4-GlcNAc, GlcNAc-β-1,4-GlcNAc-β-1,4-GlcNAc-β-1,4-

GlcNAc-β-1,4-GlcNAc or GlcNAc-β-1,4-GlcNAc-β-1,4-GlcNAc-β-1,4-GlcNAc-β-1,4-GlcNAc-β-1,4-GlcNAc [1,2]) (Reversibility: ?) [1,2]

P ?

Inhibitors

Ag^{+} <6> (<6> 1 mM $AgNO_3$, complete inhibition [4]) [4]
Al^{3+} <6> (<6> 1 mM $AlCl_3$, 30% inhibition [4]) [4]
Cu^{2+} <6> (<6> 1 mM $CuCl_2$, 53% inhibition [4]) [4]
Fe^{2+} <6> (<6> 1 mM $FeSO_4$, 26% inhibition [4]) [4]
Hg^{2+} <6> (<6> 1 mM $HgCl_2$, complete inhibition [4]) [4]
Sn^{2+} <6> (<6> 1 mM $SnCl_2$, 44% inhibition [4]) [4]

Specific activity (U/mg)

25.2 <1> [2]
31 <1> [1,3]
32.2 <6> [4]

pH-Optimum

8.5-9 <1,6> [1,4]

pH-Range

6.5-11 <6> (<6> pH 6.5: about 45% of maximal activity, pH 11: about 55% of maximal activity [4]) [4]

pi-Value

3.3 <6> (<6> isoelectric focusing [4]) [4]

Temperature optimum (°C)

45 <1,6> [1,4]

Temperature range (°C)

30-50 <6> (<6> about 50% of maximal activity at 30°C and 50°C [4]) [4]

4 Enzyme Structure

Subunits

? <1,6> (<6> x * 48000, SDS-PAGE [4]; <1> x * 45000, SDS-PAGE [2]; <1> x * 46000, SDS-PAGE [1]; <6> x * 44700, calculated from sequence [6]) [1,2,4,6]

5 Isolation/Preparation/Mutation/Application

Source/tissue

cell culture <1> [3]

Localization

extracellular <1> [1,3,5]

Purification

<1> [1,3]
<1> (recombinant) [2]
<6> [4]

Cloning

<1> (expression in Escherichia coli) [3]
<1> (production of a recombinant chitin oligosaccharide deacetylase from Vibrio parahaemolyticus in the culture medium of Escherichia coli cells. The concentration of the recombinant enzyme in the Escherichia coli culture medium is 150times higher than that of wild-type enzyme produced in the culture medium by Vibrio parahaemolyticus KN1699) [2]
<6> [6]

6 Stability

pH-Stability

4 <6> (<6> 37°C, 20 min, about 75% loss of activity [4]) [4]
5 <6> (<6> 37°C, 20 min, about 40% loss of activity [4]) [4]
6-10 <1> (<1> 37°C, 60 min, stable [1]) [1]
7-11 <6> (<6> 37°C, 20 min, stable [4]) [4]

Temperature stability

30 <6> (<6> pH 7.5, 30 min, about 10% loss of activity [4]) [4]
40 <1> (<1> pH 7.0, 30 min, stable [1]) [1]
50 <6> (<6> pH 7.5, 30 min, about 40% loss of activity [4]) [4]
70 <6> (<6> pH 7.5, 30 min, about 80% loss of activity [4]) [4]

References

[1] Kadokura, K.; Rokutani, A.; Yamamoto, M.; Ikegami, T.; Sugita, H.; Itoi, S.; Hakamata, W.; Oku, T.; Nishio, T.: Purification and characterization of Vibrio parahaemolyticus extracellular chitinase and chitin oligosaccharide deacetylase involved in the production of heterodisaccharide from chitin. Appl. Microbiol. Biotechnol., **75**, 357-365 (2007)
[2] Kadokura, K.; Sakamoto, Y.; Saito, K.; Ikegami, T.; Hirano, T.; Hakamata, W.; Oku, T.; Nishio, T.: Production of a recombinant chitin oligosaccharide deacetylase from Vibrio parahaemolyticus in the culture medium of Escherichia coli cells. Biotechnol. Lett., **29**, 1209-1215 (2007)
[3] Kadokura, K.; Sakamoto, Y.; Rokutani, A.; Ikegami, T.; Hirano, T.; Yamamoto, M.; Saito, K.; Hakamata, W.; Itoi, S.; Sugita, H.; Oku, T.; Nishio, T.: Purification, characterization and cloning of Vibrio parahaemolyticus chitinolytic enzymes and application to oligosaccharide production. J. Appl. Glycosci., **55**, 157-164 (2008)

[4] Ohishi, K.; Yamagishi, M.; Ohta, T.; Motosugi, M.; Izumida, H.; Sano, H.; Adachi, K.; Miwa, T.: Purification and properties of two deacetylases produced by Vibrio alginolyticus H-8. Biosci. Biotechnol. Biochem., **61**, 1113-1117 (1997)
[5] Hirano, T.; Kadokura, K.; Ikegami, T.; Shigeta, Y.; Kumaki, Y.; Hakamata, W.; Oku, T.; Nishio, T.: Heterodisaccharide 4-O-(N-acetyl-β-D-glucosaminyl)-D-glucosamine is a specific inducer of chitinolytic enzyme production in Vibrios harboring chitin oligosaccharide deacetylase genes. Glycobiology, **19**, 1046-1053 (2009)
[6] Ohishi, K.; Murase, K.; Ohta, T.; Etoh, H.: Cloning and sequencing of the deacetylase gene from Vibrio alginolyticus H-8. J. Biosci. Bioeng., **90**, 561-563 (2000)

N-formylmaleamate deformylase 3.5.1.106

1 Nomenclature

EC number
3.5.1.106

Systematic name
N-formylmaleamic acid amidohydrolase

Recommended name
N-formylmaleamate deformylase

Synonyms
NicD <1> [1]

2 Source Organism

<1> *Pseudomonas putida* [1]

3 Reaction and Specificity

Catalyzed reaction
N-formylmaleamic acid + H_2O = maleamate + formate

Natural substrates and products
- **S** N-formylmaleamic acid + H_2O <1> (<1> aerobic catabolism of nicotinic acid [1]) (Reversibility: ?) [1]
- **P** maleamate + formate

Substrates and products
- **S** N-formylmaleamic acid + H_2O <1> (<1> aerobic catabolism of nicotinic acid [1]; <1> S101, D125, and H245 are essential for the enzyme activity, constituting the catalytic triad of the NicD deformylase [1]) (Reversibility: ?) [1]
- **P** maleamate + formate

4 Enzyme Structure

Subunits
? <1> (<1> x * 29000, SDS-PAGE [1]; <1> x * 29100, calculated from sequence [1]) [1]

D. Schomburg and I. Schomburg (eds.), *Class 3.4–6 Hydrolases, Lyases, Isomerases, Ligases: EC 3.4–6*, Springer Handbook of Enzymes S10, DOI 10.1007/978-3-642-36260-6_17,

5 Isolation/Preparation/Mutation/Application

Cloning

<1> (expression in Escherichia coli) [1]

Engineering

D125A <1> (<1> mutation leads to a complete loss of the deformylase activity [1]) [1]
E221A <1> (<1> 70% of wild-type deformylase acticity [1]) [1]
H245A <1> (<1> mutation leads to a complete loss of the deformylase activity [1]) [1]
S101A <1> (<1> mutation leads to a complete loss of the deformylase activity [1]) [1]

References

[1] Jimenez, J.; Canales, A.; Jimenez-Barbero, J.; Ginalski, K.; Rychlewski, L.; Garcia, J.; Diaz, E.: Deciphering the genetic determinants for aerobic nicotinic acid degradation: The nic cluster from Pseudomonas putida KT2440. Proc. Natl. Acad. Sci. USA, **105**, 11329-11334 (2008)

maleamate amidohydrolase 3.5.1.107

1 Nomenclature

EC number
3.5.1.107

Systematic name
maleamate amidohydrolase

Recommended name
maleamate amidohydrolase

Synonyms
NicF <1> [1]

2 Source Organism

<1> *Pseudomonas putida* [1]

3 Reaction and Specificity

Catalyzed reaction
maleamate + H_2O = maleate + NH_3

Natural substrates and products
- **S** maleamate + H_2O <1> (<1> aerobic catabolism of nicotinic acid [1]) (Reversibility: ?) [1]
- **P** maleate + NH_3

Substrates and products
- **S** maleamate + H_2O <1> (<1> aerobic catabolism of nicotinic acid [1]) (Reversibility: ?) [1]
- **P** maleate + NH_3

Specific activity (U/mg)
0.0193 <1> [1]

5 Isolation/Preparation/Mutation/Application

Cloning
<1> (overexpression in Escherichia coli BL21 (plasmid pETNicF)) [1]

D. Schomburg and I. Schomburg (eds.), *Class 3.4–6 Hydrolases, Lyases, Isomerases, Ligases: EC 3.4–6*, Springer Handbook of Enzymes S10, DOI 10.1007/978-3-642-36260-6_18,

References

[1] Jimenez, J.; Canales, A.; Jimenez-Barbero, J.; Ginalski, K.; Rychlewski, L.; Garcia, J.; Diaz, E.: Deciphering the genetic determinants for aerobic nicotinic acid degradation: The nic cluster from Pseudomonas putida KT2440. Proc. Natl. Acad. Sci. USA, **105**, 11329-11334 (2008)

UDP-3-O-acyl-N-acetylglucosamine deacetylase 3.5.1.108

1 Nomenclature

EC number
3.5.1.108

Systematic name
UDP-3-O-[(3R)-3-hydroxymyristoyl]-N-acetylglucosamine amidohydrolase

Recommended name
UDP-3-O-acyl-N-acetylglucosamine deacetylase

Synonyms
EnvA protein <1> [23]
LpxC <1,2,3,4,5,6,7,8,9> [6,12,14,15,16,17,19,20,21,24,26,28,29,30,32,33,34]
LpxC deacetylase <6> [11]
LpxC enzyme <1> [5]
LpxC protein <1,5,8> [3,10,22,23]
UDP-(3-O-(R-3-hydroxymyristoyl))-N-acetylglucosamine deacetylase <6> [32]
UDP-(3-O-acyl)-N-acetylglucosamine deacetylase <1,5> [10,29]
UDP-3-O-((R)-3-hydroxymyristoyl)-N-acetylglucosamine deacetylase <1,9> [24]
UDP-3-O-(R-3-hydroxyacyl)-N-acetylglucosamine deacetylase <1,3,4,6,7> [16, 33]
UDP-3-O-(R-3-hydroxymyristoyl)-GlcNAc deacetylase <1,2> [7]
UDP-3-O-(R-3-hydroxymyristoyl)-N-acetylglucosamine deacetylase <1,8> [1,5, 6,9,13,14,34]
UDP-3-O-(R-3-hydroxymyristoyl)-Nacetylglucosamine deacetylase <1> [25]
UDP-3-O-[R-3-hydroxymyristoyl]-GlcNAc deacetylase <1,2> [17,20,29]
UDP-3-O-[R-3-hydroxymyristoyl]-GlcNAc deacetylase enzyme <2> [20]
UDP-3-O-acyl-GlcNAc deacetylase <1,8> [22,23]
UDP-3-O-acyl-N-acetylglucosamine deacetylase <1,6> [4,11,23]
deacetylase <1> [21]
deacetylase LpxC <1,2,6,7> [17,18,20,26,27,28,33]
uridine diphosphate-(3-O-(R-3-hydroxymyristoyl))-N-acetylglucosamine deacetylase <5> [19]
zinc deacetylase LpxC <5> [19]

CAS registry number
157971-99-8

D. Schomburg and I. Schomburg (eds.), *Class 3.4–6 Hydrolases, Lyases, Isomerases, Ligases: EC 3.4–6*, Springer Handbook of Enzymes S10, DOI 10.1007/978-3-642-36260-6_19,

2 Source Organism

<1> *Escherichia coli* [1,2,3,5,6,7,8,9,10,12,13,14,16,21,22,23,24,25,27,29,33]
<2> *Pseudomonas aeruginosa* [7,17,18,20,26,27,28]
<3> *Helicobacter pylori* [16]
<4> *Rhizobium leguminosarum* [16]
<5> *Aquifex aeolicus* [10,12,19,30,31]
<6> *Aquifex aeolicus* (UNIPROT accession number: O67648) [4,11,15,32,33]
<7> *Rhizobium leguminosarum* (UNIPROT accession number: Q1ME43) [33]
<8> *Pseudomonas aeruginosa* (UNIPROT accession number: P47205) [22,34]
<9> *Aquifex aeolicus* (UNIPROT accession number: O67848) [24]

3 Reaction and Specificity

Catalyzed reaction

UDP-3-O-[(3R)-3-hydroxymyristoyl]-N-acetylglucosamine + H_2O = UDP-3-O-[(3R)-3-hydroxymyristoyl]-D-glucosamine + acetate

Natural substrates and products

S UDP-3-O-((R)-3-hydroxymyristoyl)-N-acetylglucosamine + H_2O <1> (<1> natural substrate [6]) (Reversibility: ?) [6]
P UDP-3-O-((R)-3-hydroxymyristoyl)glucosamine + acetate
S UDP-3-O-((R)-3-hydroxymyristoyl)-N-acetylglucosamine + H_2O <1,2,5,6,8> (<8> a committed step of lipopolysaccharide biosynthesis [22]; <1> biosynthesis of lipid A in Gram negarive bacteria [8]; <2> by placing the lpxC gene of Pseudomonas aeruginosa under tight control of an arabinose-inducible promoter, the essentiality of LpxC activity for Pseudomonas aeruginosa is demonstrated [7]; <1> committed step in the biosynthesis of lipid A [13]; <1> committed step of lipopolysaccharide biosynthesis [22]; <1> first committed step of lipid A biosynthesis, regulation of enzyme activity, overview [1]; <1,5> LpxC catalyzes a step in the biosynthesis of lipid A in Gram-negative bacteria [10]; <5,6> LpxC catalyzes the first committed step in the biosynthesis of lipid A, the hydrophobic anchor of lipopolysaccharide (LPS) that constitutes the outermost monolayer of Gram-negative bacteria. As LpxC is crucial for the survival of Gram-negative organisms and has no sequence homology to known mammalian deacetylases or amidases [11,31]; <5> LpxC is a key enzyme in the biochemical synthesis of Lipid A [30]; <1> LpxC is one of the key enzymes of bacterial lipid A biosynthesis, catalyzing the removal of the N-acetyl group of UD-3-O-(R-3-hydroxymyristoyl)-N-acetylglucosamine. The lpxC gene is essential in Gram-negative bacteria but absent from mammalian genomes, making it an attractive target for antibacterial drug discovery [5]; <1> second enzymatic step of lipid A biosynthesis [23]; <1> the enzyme is involved in lipid A biosynthesis [3]; <1> this reaction is essential in the biosynthesis of lipopolysaccharide (LPS) of Gram-negative bacteria and is an attractive target for the development of new antibacterial agents [25]) (Reversibility: ?) [1,3,5,7,8,9,10,11,13,22,23,25,30,31]

P UDP-3-O-((R)-3-hydroxymyristoyl)-D-glucosamine + acetate
S Additional information <1> (<1> catalyses the second step of lipid A biosynthesis in Gram-negative bacteria [21]; <1> catalyzes the second step in the biosynthesis of lipid A [6,14]; <1> catalyzes the second step of lipid A biosynthesis in Gram negative bacteria [29]) [6,14,21,29]
P ?

Substrates and products

S UDP-(2-acetamino)-2-deoxy-3-O-[2-(hexylamino)-1-methyl-2-oxoethyl]-D-glucopyranose + H_2O <1> (<1> a homogenous fluorescence-based assay is developed that uses UDP-3-O-(N-hexyl-propionamide)-N-acetylglucosamine as a surrogate substrate. This surrogate can be prepared from commercially available UDP-GlcNAc by enzymatic conversion to UDP-MurNAc, which is then chemically coupled to n-hexylamine. Following the LpxC reaction, the free amine of the deacetylation product can be derivatized by fluorescamine, thus generating a fluorescent signal [5]) (Reversibility: ?) [5]
P UDP-2-amino-2-deoxy-3-O-[2-(hexylamino)-1-methyl-2-oxoethyl]-D-glucopyranose + acetate
S UDP-3-O-((3R)-3-hydroxydecanoyl)-N-acetylglucosamine + H_2O <2> (Reversibility: ?) [28]
P UDP-3-O-((3R)-3-hydroxydecanoyl)glucosamine + acetate
S UDP-3-O-((R)-3-hydroxymyristoyl)-N-acetylglucosamine + H_2O <1,2,5,9> (<1> natural substrate [6]; <9> LpxC catalyzes deacetylation by using Glu78 and His265 as a general acid-base pair and the zinc-bound water as a nucleophile [24]) (Reversibility: ?) [6,12,14,16,20,21,24,29]
P UDP-3-O-((R)-3-hydroxymyristoyl)glucosamine + acetate
S UDP-3-O-((R)-3-hydroxymyristoyl)-N-acetylglucosamine + H_2O <1,2,5,6,8> (<8> a committed step of lipopolysaccharide biosynthesis [22]; <1> biosynthesis of lipid A in Gram negarive bacteria [8]; <2> by placing the lpxC gene of Pseudomonas aeruginosa under tight control of an arabinose-inducible promoter, the essentiality of LpxC activity for Pseudomonas aeruginosa is demonstrated [7]; <1> committed step in the biosynthesis of lipid A [13]; <1> committed step of lipopolysaccharide biosynthesis [22]; <1> first committed step of lipid A biosynthesis, regulation of enzyme activity, overview [1]; <1,5> LpxC catalyzes a step in the biosynthesis of lipid A in Gram-negative bacteria [10]; <5,6> LpxC catalyzes the first committed step in the biosynthesis of lipid A, the hydrophobic anchor of lipopolysaccharide (LPS) that constitutes the outermost monolayer of Gram-negative bacteria. As LpxC is crucial for the survival of Gram-negative organisms and has no sequence homology to known mammalian deacetylases or amidases [11,31]; <5> LpxC is a key enzyme in the biochemical synthesis of Lipid A [30]; <1> LpxC is one of the key enzymes of bacterial lipid A biosynthesis, catalyzing the removal of the N-acetyl group of UD-3-O-(R-3-hydroxymyristoyl)-N-acetylglucosamine. The lpxC gene is essential in Gram-negative bacteria but absent from mammalian genomes, making it an attractive target for antibacterial drug discovery [5]; <1> second enzymatic step of lipid A biosynthesis

[23]; <1> the enzyme is involved in lipid A biosynthesis [3]; <1> this reaction is essential in the biosynthesis of lipopolysaccharide (LPS) of Gram-negative bacteria and is an attractive target for the development of new antibacterial agents [25]; <1> LpxC catalyzes deacetylation by using Glu78 and His265 as a general acid-base pair and the zinc-bound water as a nucleophile [24]; <5> the mechanism of LpxC proceeds via four steps: (1) initial hydroxylation of the substrates´ carbonyl carbon to give a gem-diolate intermediate, (2) protonation of the amide nitrogen by the histidine His265-H^+, (3) a barrier-less change in the active site-intermediate hydrogen-bond network and finally, (4) C-N bond cleavage. The rate-determining step of the mechanism of LpxC is the initial hydroxylation while the final C-N bond cleavage occurs with an overall barrier of 23.6 kJ/mol. LpxC uses a general acid/base pair mechanism as indicated by the fact that both His265-H^+ and Glu78 are accordingly involved [30]) (Reversibility: ?) [1,3,5,7,8,9,10,11,13,22,23,24,25,30,31]

P UDP-3-O-((R)-3-hydroxymyristoyl)-D-glucosamine + acetate

S UDP-3-O-(N-hexyl-propionamide)-N-acetylglucosamine + H_2O <1> (Reversibility: ?) [5]

P ?

S UDP-N-acetylglucosamine + H_2O <1> (<1> k_{cat}/K_M fo UDP-N-acetylglucosamine is 5000000-fold lower than the k_{cat}/K_m for UDP-3-O-((R)-3-hydroxymyristoyl)-N-acetylglucosamine [9]) (Reversibility: ?) [9]

P UDP-D-glucosamine + acetate

S Additional information <1> (<1> catalyses the second step of lipid A biosynthesis in Gram-negative bacteria [21]; <1> catalyzes the second step in the biosynthesis of lipid A [6,14]; <1> catalyzes the second step of lipid A biosynthesis in Gram negative bacteria [29]) [6,14,21,29]

P ?

Inhibitors

(2R)-N-hydroxy-3-naphthalen-2-yl-2-[(naphthalen-2-ylsulfonyl)amino]propanamide <8> (<8> potent inhibitor, shows antibacterial activity against a wide range of Gram-negative pathogens, binding mode [34]) [34]

(3-(4-methoxyphenyl)-4,5-dihydroisoxazol-5-yl)methanethiol <1> [29]

(3R,5R)-3-hydroxy-5-(2-(hydroxyamino)-2-oxoethyl)-2-(hydroxymethyl)tetrahydro-2H-pyran-4-yl tetradecanoate <1,5> (<1,5> substrate-analog LpxC inhibitor, possesses little or no antibacterial activity, because it probably cannot penetrate the Gram-negative cell envelope [12]) [12]

(4R)-2-(3,4-dimethoxy-5-propylphenyl)-N-hydroxy-4,5-dihydro-1,3-oxazole-4-carboxamide <1> (<1> i.e L-161,240 [5]; <1> the inhibitor is active against a Pseudomonas aeruginosa construct in which the endogenous lpxC gene is inactivated and in which LpxC activity is supplied by the lpxC gene from Escherichia coli. An Escherichia coli construct in which growth is dependent on the Pseudomonas aeruginosa lpxC gene is resistant to the compound [7]) [5,7]

(4R)-N-hydroxy-2-(4-methoxyphenyl)-4,5-dihydro-1,3-oxazole-4-carboxamide <1> (<1> i.e. L-159,692 [5]) [5]

(4R)-N-hydroxy-2-tricyclo[3.3.1.1-3,7]dec-1-yl-4,5-dihydro-1,3-oxazole-4-carboxamide <1> (<1> 1 μg/ml, high inhibitory activity [21]) [21]
(R)-(hydroxyamino)((R)-2-(4-methoxy-3-propyl-5-(trifluoromethoxy)phenyl)-4,5-dihydrothiazol-4-yl)methanol <2> [20]
(R)-2-(1-butyl-1H-indazol-3-yl)-N-hydroxy-4,5-dihydrooxazole-4-carboxamide <2> [20]
(R)-2-(2-bromophenyl)-N-hydroxy-4,5-dihydrooxazole-4-carboxamide <1> (<1> 1 μg/ml, nearly complete loss of activity [21]) [21]
(R)-2-(2-butyl-2H-indazol-3-yl)-N-hydroxy-4,5-dihydrooxazole-4-carboxamide <2> [20]
(R)-2-(3,4-dichlorophenyl)-N-hydroxy-4,5-dihydrooxazole-4-carboxamide <1> (<1> 1 μg/ml, exellet biological activity [21]) [21]
(R)-2-(3,4-difluorophenyl)-N-hydroxy-4,5-dihydrooxazole-4-carboxamide <1> (<1> 1 μg/ml, exellet biological activity [21]) [21]
(R)-2-(3,4-dimethoxy-5-propylphenyl)-N-hydroxy-4,5-dihydrooxazole-4-carboxamide <1> (<1> 1 μg/ml [21]) [21]
(R)-2-(3,5-dichlorophenyl)-N-hydroxy-4,5-dihydrooxazole-4-carboxamide <1> (<1> 1 μg/ml, moderate activity [21]) [21]
(R)-2-(3,5-difluoro-4-methoxyphenyl)-N-hydroxy-4,5-dihydrooxazole-4-carboxamide <1> (<1> 1 μg/ml, good activity [21]) [21]
(R)-2-(3,5-difluorophenyl)-N-hydroxy-4,5-dihydrooxazole-4-carboxamide <1> (<1> 1 μg/ml, moderate activity [21]) [21]
(R)-2-(3,5-dimethoxyphenyl)-N-hydroxy-4,5-dihydrooxazole-4-carboxamide <1> (<1> 1 μg/ml, 67% inhibition [21]) [21]
(R)-2-(3-(dichloromethyl)phenyl)-N-hydroxy-4,5-dihydrooxazole-4-carboxamide <1> (<1> 1 μg/ml [21]) [21]
(R)-2-(3-bromo-4-fluorophenyl)-N-hydroxy-4,5-dihydrooxazole-4-carboxamide <1> (<1> 1 μg/ml, exellet biological activity [21]) [21]
(R)-2-(3-chloro-4-fluorophenyl)-N-hydroxy-4,5-dihydrooxazole-4-carboxamide <1> (<1> 1 μg/ml, exellet biological activity [21]) [21]
(R)-2-(3-cyanophenyl)-N-hydroxy-4,5-dihydrooxazole-4-carboxamide <1> (<1> 1 μg/ml [21]) [21]
(R)-2-(3-ethoxy-4-fluorophenyl)-N-hydroxy-4,5-dihydrooxazole-4-carboxamide <2> [20]
(R)-2-(3-fluoro-4-(trifluoromethyl)phenyl)-N-hydroxy-4,5-dihydrooxazole-4-carboxamide <1> (<1> 1 μg/ml, slight lower inhibitory activity than (R)-2-(4-fluoro-3-(trifluoromethyl)phenyl)-N-hydroxy-4,5-dihydrooxazole-4-carboxamide [21]) [21]
(R)-2-(3-fluoro-5-(trifluoromethyl)phenyl)-N-hydroxy-4,5-dihydrooxazole-4-carboxamide <1> (<1> 1 μg/ml, good activity [21]) [21]
(R)-2-(4-(3-fluorobenzyloxy)-3-(trifluoromethoxy)phenyl)-N-hydroxy-4,5-dihydrooxazole-4-carboxamide <2> [20]
(R)-2-(4-(allyloxy)-3-(trifluoromethyl)phenyl)-N-hydroxy-4,5-dihydrooxazole-4-carboxamide <2> [20]
(R)-2-(4-(dimethylamino)phenyl)-N-hydroxy-4,5-dihydrooxazole-4-carboxamide <2> [20]

(R)-2-(4-(hexyloxy)phenyl)-N-hydroxy-4,5-dihydrooxazole-4-carboxamide <1> (<1> 1 μg/ml, 86% inhibition [21]) [21]
(R)-2-(4-(hydroxycarbamoyl)-4,5-dihydrooxazol-2-yl)benzyl benzoate <1> (<1> 1 μg/ml, nearly complete loss of activity [21]) [21]
(R)-2-(4-bromophenylsulfonamido)-3-(5,8-dihydronaphthalen-2-yl)-N-hydroxypropanamide <1> [6]
(R)-2-(4-chloro-3-nitrophenyl)-N-hydroxy-4,5-dihydrooxazole-4-carboxamide <1> (<1> 1 μg/ml [21]) [21]
(R)-2-(4-fluoro-3-(trifluoromethyl)phenyl)-N-hydroxy-4,5-dihydrooxazole-4-carboxamide <1,2> (<1> 1 μg/ml, most potent compound [21]) [20,21]
(R)-2-(4-fluoro-3-methylphenyl)-N-hydroxy-4,5-dihydrooxazole-4-carboxamide <2> [20]
(R)-2-(4-fluoro-3-nitrophenyl)-N-hydroxy-4,5-dihydrooxazole-4-carboxamide <1> (<1> 1 μg/ml [21]) [21]
(R)-2-(4-tert-butylphenyl)-N-hydroxy-4,5-dihydrooxazole-4-carboxamide <1> (<1> 1 μg/ml, 58% inhibition [21]) [21]
(R)-2-(biphenyl-4-yl)-N-hydroxy-4,5-dihydrooxazole-4-carboxamide <1> (<1> 1 μg/ml, 69% inhibition [21]) [21]
(R)-2-decyl-N-hydroxy-4,5-dihydrooxazole-4-carboxamide <1> (<1> 1 μg/ml, high inhibitory activity [21]) [21]
(R)-3-(5,8-dihydronaphthalen-2-yl)-N-hydroxy-2-(naphthalene-2-sulfonamido)propanamide <1,5,7> [6,12,16,33]
(R)-4-(3-(cyclopentyloxy)-4-methoxyphenyl)-N-hydroxy-2-isopropyl-4-oxobutanamide <2> [26]
(R)-4-(3-(cyclopentyloxy)-4-methoxyphenyl)-N-hydroxy-2-methyl-4-oxobutanamide <2> [26]
(R)-N-(1-(2-(3,4-dimethoxy-5-propylphenyl)-4,5-dihydrooxazol-4-yl)vinyl)hydroxylamine <1> [29]
(R)-N-(3-hydroxy-1-(hydroxyamino)-1-oxopropan-2-yl)-1H-indazole-3-carboxamide <2> [20]
(R)-N-(3-hydroxy-1-(hydroxyamino)-1-oxopropan-2-yl)-4-methoxy-3-propyl-5-(trifluoromethoxy)benzamide <2> [20]
(R)-N-hydroxy-2-(1H-indazol-3-yl)-4,5-dihydrooxazole-4-carboxamide <2> [20]
(R)-N-hydroxy-2-(2,3,5-trifluoro-4-methoxyphenyl)-4,5-dihydrooxazole-4-carboxamide <1> (<1> 1 μg/ml, good activity [21]) [21]
(R)-N-hydroxy-2-(2-methylprop-1-enyl)-4,5-dihydrooxazole-4-carboxamide <1> (<1> 1 μg/ml, moderate activity [21]) [21]
(R)-N-hydroxy-2-(3,4,5-triethoxyphenyl)-4,5-dihydrooxazole-4-carboxamide <1> (<1> 1 μg/ml, 72% inhibition [21]) [21]
(R)-N-hydroxy-2-(3-(trifluoromethoxy)phenyl)-4,5-dihydrooxazole-4-carboxamide <1> (<1> 1 μg/ml, exellet inhibitory activity [21]) [21]
(R)-N-hydroxy-2-(3-methoxyphenyl)-4,5-dihydrooxazole-4-carboxamide <1> (<1> 1 μg/ml, 44% inhibition [21]) [21]
(R)-N-hydroxy-2-(4-((3-nitrophenoxy)methyl)phenyl)-4,5-dihydrooxazole-4-carboxamide <2> [20]
(R)-N-hydroxy-2-(4-(3-nitrobenzyloxy)phenyl)-4,5-dihydrooxazole-4-carboxamide <2> [20]

(R)-N-hydroxy-2-(4-(trifluoromethoxy)phenyl)-4,5-dihydrooxazole-4-carboxamide <1> (<1> 1 μg/ml [21]) [21]
(R)-N-hydroxy-2-(4-hydroxyphenyl)-4,5-dihydrooxazole-4-carboxamide <2> [20]
(R)-N-hydroxy-2-(4-methoxy-3,5-dimethylphenyl)-4,5-dihydrooxazole-4-carboxamide <1> (<1> 1 μg/ml, 71% inhibition [21]) [21]
(R)-N-hydroxy-2-(4-methoxy-3-(trifluoromethoxy)phenyl)-4,5-dihydrooxazole-4-carboxamide <2> [20]
(R)-N-hydroxy-2-(4-methoxy-3-nitrophenyl)-4,5-dihydrooxazole-4-carboxamide <1> (<1> 1 μg/ml [21]) [21]
(R)-N-hydroxy-2-(4-methoxy-3-propyl-5-(trifluoromethoxy)phenyl)-4,5-dihydrooxazole-4-carboxamide <2> [20]
(R)-N-hydroxy-2-(4-methoxyphenyl)-4,5-dihydrooxazole-4-carboxamide <1> (<1> 1 μg/ml [21]) [21]
(R)-N-hydroxy-2-(4-methyl-3-nitrophenyl)-4,5-dihydrooxazole-4-carboxamide <1> (<1> 1 μg/ml [21]) [21]
(R)-N-hydroxy-2-(4-nitrophenyl)-4,5-dihydrooxazole-4-carboxamide <1> (<1> 1 μg/ml [21]) [21]
(R)-N-hydroxy-2-*p*-tolyl-4,5-dihydrothiazole-4-carboxamide <2> [20]
(R,E)-2-(2-chlorostyryl)-N-hydroxy-4,5-dihydrooxazole-4-carboxamide <1> (<1> 1 μg/ml, moderate activity [21]) [21]
(R,E)-N-hydroxy-2-(3-(trifluoromethyl)styryl)-4,5-dihydrooxazole-4-carboxamide <1> (<1> 1 μg/ml, moderate activity [21]) [21]
(R,E)-N-hydroxy-2-(4-nitrostyryl)-4,5-dihydrooxazole-4-carboxamide <1> (<1> 1 μg/ml, moderate activity [21]) [21]
(R,E)-N-hydroxy-2-styryl-4,5-dihydrooxazole-4-carboxamide <1> (<1> 1 μg/ml, moderate activity [21]) [21]
(S)-3-(3-(cyclopentyloxy)-4-methoxyphenyl)-N-hydroxy-4,5-dihydroisoxazole-5-carboxamide <2> [26]
(S)-3-(3-(cyclopentyloxy)-4-methoxyphenyl)-N-hydroxy-5-methyl-4,5-dihydroisoxazole-5-carboxamide <2> [26]
(S)-3-(4-methoxyphenyl)-4,5-dihydro-isoxazole-5-carboxylic acid hydroxyamide <1> [29]
(S)-4-(3-(cyclopentyloxy)-4-methoxyphenyl)-N-hydroxy-2-methyl-4-oxobutanamide <2> [26]
(S)-N-(1-(2-(3,4-dimethoxy-5-propylphenyl)-4,5-dihydrooxazol-4-yl)vinyl)-hydroxylamine <1,7> (<1> phenyloxazoline hydroxamic acid, competitive inhibitor in Escherichia coli, not active as an antibiotic against Aquifex aeolicus, Pseudomonas aeruginosa and other clinically important pathogens [12]) [6,12,16,33]
1,5-anhydro-2-C-(carboxymethyl-N-hydroxamide)-2-deoxy-3-O-myristoyl-D-glucitol <6> (<6> the X-ray crystal structure of LpxC complexed with TU-514 allows for a detailed examination of the coordination geometry of the catalytic zinc ion and other enzyme-inhibitor interactions in the active site. The hydroxamate group of TU-514 forms a bidentate chelate complex with the zinc ion and makes hydrogen bond interactions with conserved active site residues E78, H265, and T191. The inhibitor C-4 hydroxyl group makes direct

hydrogen bond interactions with E197 and H58. Finally, the C-3 myristate moiety of the inhibitor binds in the hydrophobic tunnel of the active site [15]) [15]

1,5-anhydro-2-C-(carboxymethyl-N-hydroxyamide)-2-deoxy-3-O-myristoyl-D-glucitol <5,6> (<6> synthesis of the 13C-labeled substrate-analogue inhibitor, and the subsequent refinement of the solution structure of the LpxC-inhibitor complex using residual dipolar couplings. Structural basis for the design of more potent LpxC inhibitors. The best LpxC inhibitors should contain: (1) a zinc-chelating group situated between two hydrophobic molecular moieties and (2) a negatively charged group or polar group capable of forming salt bridges or hydrogen bonds with the basic patch. For the hydrophobic fragment to fit within the hydrophobic passage, a linear chemical group without branches is preferable and the total length from the hydroxamate group (which presumably binds Zn^{2+}) to the terminal end of the linear fragment should be less than 15 A. Any hydrophobic group with a length beyond 15 A might require flexibility to fit the curved surface extending the hydrophobic passage, where the terminal methyl and the last two methylene groups of the 1,5-anhydro-2-C-(carboxymethyl-N-hydroxyamide)-2-deoxy-3-O-myristoyl-D-glucitol acyl chain are located [11]; <5> the solution structure of LpxC in complex with the substrate-analog inhibitor 1,5-anhydro-2-C-(carboxymethyl-N-hydroxyamide)-2-deoxy-3-O-myristoyl-D-glucitol, reveals a novel α/β fold, a unique zinc-binding motif and a hydrophobic passage that captures the acyl chain of the inhibitor [31]) [11,31]

2,3,4-trihydroxybenzaldehyde O-((2R,3R,4S,5R)-5-(2,4-dioxo-3,4-dihydropyrimidin-1(2H)-yl)-3,4-dihydroxytetrahydrofuran-2-yl)methyl oxime <1,3> (<3> 50 μM, 21% inhibition, pH-dependent, two-step, covalent inhibitor. 2,3,4-trihydroxybenzaldehyde O-((2R,3R,4S,5R)-5-(2,4-dioxo-3,4-dihydropyrimidin-1(2H)-yl)-3,4-dihydroxytetrahydrofuran-2-yl)methyl oxime represents a new class of LpxC inhibitors that exploit the uridine binding site to form a covalent complex. While not antibiotic, it may provide a new scaffold for extension of existing LpxC-inhibiting antibiotics to target the UDP binding pocket [16]; <1> 50 μM, 80% inhibition, pH-dependent, two-step, covalent inhibitor. 2,3,4-trihydroxybenzaldehyde O-((2R,3R,4S,5R)-5-(2,4-dioxo-3,4-dihydropyrimidin-1(2H)-yl)-3,4-dihydroxytetrahydrofuran-2-yl)methyl oxime represents a new class of LpxC inhibitors that exploit the uridine binding site to form a covalent complex. While not antibiotic, it may provide a new scaffold for extension of existing LpxC-inhibiting antibiotics to target the UDP binding pocket [16]) [16]

2,3-dihydroxy-benzaldehyde O-[5-(2,4-dioxo-3,4-dihydro-2H-pyrimidin-1-yl)-3,4-dihydroxy-tetrahydro-furan-2-ylmethyl]-oxime <1> (<1> weak inhibitor [16]) [16]

2-(1-butyl-1H-indazol-3-yl)-N-hydroxy-4,5-dihydrooxazole-4-carboxamide <2> [17,18,26,28]

2-(2-butyl-2H-indazol-3-yl)-N-hydroxy-4,5-dihydrooxazole-4-carboxamide <2> [17,18,26,28]

2-(3,4-bis(trifluoromethoxy)phenyl)-N-hydroxy-4,5-dihydrooxazole-4-carboxamide <2> [26]

2-(3-(3-(cyclopentyloxy)-4-methoxyphenyl)-4,5-dihydroisoxazol-5-yl)-N-hydroxyacetamide <2> [26]
2-(3-allyl-5-fluoro-4-methoxy-2-methylphenyl)-N-hydroxy-4,5-dihydrooxazole-4-carboxamide <2> [17,26,28]
2-(3-bromo-4-fluorophenyl)-N-hydroxy-4,5-dihydrooxazole-4-carboxamide <2> [17,26,28]
2-(3-bromo-5-fluoro-4-methoxyphenyl)-N-hydroxy-4,5-dihydrooxazole-4-carboxamide <2> [17,26,28]
2-(3-chloro-4-(trifluoromethoxy)phenyl)-N-hydroxy-4,5-dihydrooxazole-4-carboxamide <2> [17,26,28]
2-(3-chloro-5-fluoro-1H-indol-2-yl)-N-hydroxy-4,5-dihydrooxazole-4-carboxamide <2> [17,26,28]
2-(3-ethoxy-4-fluorophenyl)-N-hydroxy-4,5-dihydrooxazole-4-carboxamide <2> [17,26,28]
2-(3-fluoro-4-(2-(trifluoromethyl)benzyloxy)phenyl)-N-hydroxy-4,5-dihydrooxazole-4-carboxamide <2> [28]
2-(3-fluoro-4-(3-(trifluoromethyl)benzyloxy)phenyl)-N-hydroxy-4,5-dihydrooxazole-4-carboxamide <2> [17,28]
2-(3-fluoro-4-(3-methylbenzyloxy)phenyl)-N-hydroxy-4,5-dihydrooxazole-4-carboxamide <2> [26]
2-(3-fluoro-5-(trifluoromethyl)phenyl)-N-hydroxy-4,5-dihydrooxazole-4-carboxamide <2> [17,26,28]
2-(4-(3-fluorobenzyloxy)-3-(trifluoromethoxy)phenyl)-N-hydroxy-4,5-dihydrooxazole-4-carboxamide <2> [17,26,28]
2-(4-(allyloxy)-3-(trifluoromethoxy)phenyl)-N-hydroxy-4,5-dihydrooxazole-4-carboxamide <2> [28]
2-(4-(allyloxy)-3-(trifluoromethyl)phenyl)-N-hydroxy-4,5-dihydrooxazole-4-carboxamide <2> [17,26,28]
2-(4-(allyloxy)-3-fluorophenyl)-N-hydroxy-4,5-dihydrooxazole-4-carboxamide <2> [28]
2-(4-(but-3-enyloxy)-3-(trifluoromethoxy)phenyl)-N-hydroxy-4,5-dihydrooxazole-4-carboxamide <2> [17,26,28]
2-(4-(but-3-enyloxy)phenyl)-N-hydroxy-4,5-dihydrooxazole-4-carboxamide <2> [17,18,26,28]
2-(4-(but-3-enyloxy)phenyl)-N-hydroxy-4,5-dihydrothiazole-4-carboxamide <2> [17,18,26,28]
2-(4-(dimethylamino)phenyl)-N-hydroxy-4,5-dihydrooxazole-4-carboxamide <2> [17,18,26,28]
2-(4-(heptyloxy)phenyl)-N-hydroxy-4,5-dihydrooxazole-4-carboxamide <2> [17,28]
2-(4-acetamidophenyl)-N-hydroxy-4,5-dihydrooxazole-4-carboxamide <2> [17,28]
2-(4-acetylphenyl)-N-hydroxy-4,5-dihydrooxazole-4-carboxamide <2> [17,26,28]
2-(4-bromophenyl)-N-hydroxy-4,5-dihydrooxazole-4-carboxamide <2> [28]
2-(4-butylphenyl)-N-hydroxy-4,5-dihydrooxazole-4-carboxamide <2> [17,18,26,28]

2-(4-fluoro-3-(trifluoromethyl)phenyl)-N-hydroxy-4,5-dihydrooxazole-4-carboxamide <2> [17,26,28]
2-(4-fluoro-3-(trifluoromethyl)phenyl)-N-hydroxy-5,6-dihydro-4H-1,3-oxazine-4-carboxamide <2> [28]
2-(4-fluoro-3-methylphenyl)-N-hydroxy-4,5-dihydrooxazole-4-carboxamide <2> [17,26,28]
2-(4-fluoro-3-propylphenyl)-N-hydroxy-4,5-dihydrooxazole-4-carboxamide <2> [17,18,26,28]
2-(4-fluorophenyl)-N-hydroxy-4,5-dihydrooxazole-4-carboxamide <2> [17,18,26,28]
2-(4-fluorophenyl)-N-hydroxy-4,5-dihydrothiazole-4-carboxamide <2> [28]
2-(5-fluoro-1H-indol-2-yl)-N-hydroxy-4,5-dihydrooxazole-4-carboxamide <2> [28]
2-(5-fluoro-1H-indol-2-yl)-N-hydroxy-5,6-dihydro-4H-1,3-oxazine-4-carboxamide <2> [28]
2-mercapto-1-[3-(4-methoxyphenyl)-4,5-dihydro-isoxazol-5-yl]ethanone <1> (<1> racemate [29]) [29]
2-thioacetyl-1-[3-(4-methoxyphenyl)-4,5-dihydro-isoxazol-5-yl]ethanone <1> (<1> racemate [29]) [29]
3,4,5-trihydroxy-benzaldehyde O-[5-(2,4-dioxo-3,4-dihydro-2H-pyrimidin-1-yl)-3,4-dihydroxy-tetrahydro-furan-2-ylmethyl]-oxime <1> (<1> weak inhibitor, contains a 5 position hydroxyl and exhibits greatly reduced inhibitory potency [16]) [16]
3,4-dihydroxy-benzaldehyde O-[5-(2,4-dioxo-3,4-dihydro-2H-pyrimidin-1-yl)-3,4-dihydroxy-tetrahydro-furan-2-ylmethyl]-oxime <4> (<4> 50 μM, 49% inhibition [16]) [16]
3,4-dihydroxybenzaldehyde O-[5-(2,4-dioxo-3,4-dihydro-2H-pyrimidin-1-yl)-3,4-dihydroxy-tetrahydro-furan-2-ylmethyl]-oxime <1,3> (<3> 50 μM, 41% inhibition [16]; <1> 50 microM, 60% inhibition, inhibitor as potent as (E)-2,3,4-trihydroxybenzaldehyde O-((2R,3R,4S,5R)-5-(2,4-dioxo-3,4-dihydropyrimidin-1(2H)-yl)-3,4-dihydroxytetrahydrofuran-2-yl)methyl oxime [16]) [16]
3-(3-(cyclopentyloxy)-4-methoxyphenyl)-4,5-dihydroisoxazole-5-carboxamide <2> [26]
3-(3-(cyclopentyloxy)-4-methoxyphenyl)-4,5-dihydroisoxazole-5-carboxylic acid <2> [26]
3-(3-(cyclopentyloxy)-4-methoxyphenyl)-N-hydroxy-4,5-dihydroisoxazole-5-carboxamide <2> [26]
3-(3-(cyclopentyloxy)-4-methoxyphenyl)-N-hydroxy-5-methyl-4,5-dihydroisoxazole-5-carboxamide <2> [26]
3-(3-(cyclopentyloxy)-4-methoxyphenyl)-N-hydroxy-5-propyl-4,5-dihydroisoxazole-5-carboxamide <2> [26]
3-(3-(cyclopentyloxy)-4-methoxyphenyl)-N-hydroxy-N-methyl-4,5-dihydroisoxazole-5-carboxamide <2> [26]
3-(4-methoxyphenyl)-4,5-dihydroisoxazol-5-yl(methyl)phosphinic acid <1> [29]
3-ethoxy-4-fluoro-N-(3-hydroxy-1-(hydroxyamino)-1-oxopropan-2-yl)benzamide <2> [17,28]

4-(3-(cyclopentyloxy)-4-methoxyphenyl)-4-oxobutanoic acid <2> [26]
4-(3-(cyclopentyloxy)-4-methoxyphenyl)-N-hydroxy-4-oxobutanamide <2> [26]
4-(allyloxy)-N-(3-hydroxy-1-(hydroxyamino)-1-oxopropan-2-yl)-3-(trifluoromethoxy)benzamide <2> [17,26,28]
4-(but-3-enyloxy)-N-(3-hydroxy-1-(hydroxyamino)-1-oxopropan-2-yl)benzamide <2> [17,18,26,28]
4-fluoro-N-(3-hydroxy-1-(hydroxyamino)-1-oxopropan-2-yl)benzamide <2> [17,28]
EDTA <1,8> (<1> 5 mM, complete loss of activity [5]; <8> 0.002 mM, complete inactivation, reactivated by the addition of excess heavy metal [22]; <1> $t_{1/2}$: 4 min at 0.005 mM EDTA at 1°C [9]) [5,9,22]
N'-formyl-3-(4-methoxyphenyl)-4,5-dihydroisoxazole-5-carbohydrazide <1> [29]
N-(((2R,3R,4S,5R)-5-(2,4-dioxo-3,4-dihydropyrimidin-1(2H)-yl)-3,4-dihydroxytetrahydrofuran-2-yl)methyl)-2-((Z)-2,3,4-trihydroxybenzylideneaminooxy)acetamide <1> [16]
N-((2S,3R)-3-hydroxy-1-(hydroxyamino)-1-oxobutan-2-yl)-4-((4-(morpholinomethyl)phenyl)ethynyl)benzamide <1,5,6,7> (<1,6> as effectively as ciprofloxacin or tobramycin [33]; <1,5> N-aroyl-L-threonine hydroxamic acid, antibiotic activity comparable to ciprofloxacin, slow, tight-binding LpxC inhibitor [12]; <7> wild-type is insensitive to N-((2S,3R)-3-hydroxy-1-(hydroxyamino)-1-oxobutan-2-yl)-4-((4-(morpholinomethyl)phenyl)ethynyl)benzamide [33]) [12,16,33]
N-(3-hydroxy-1-(hydroxyamino)-1-oxopropan-2-yl)-1H-indazole-3-carboxamide <2> [17,18,26,28]
N-(3-hydroxy-1-(hydroxyamino)-1-oxopropan-2-yl)-4-(trifluoromethoxy)benzamide <2> [17,28]
N-(3-hydroxy-1-(hydroxyamino)-1-oxopropan-2-yl)-4-methoxy-3-propyl-5-(trifluoromethoxy)benzamide <2> [17,28]
N-(3-hydroxy-1-(hydroxyamino)-1-oxopropan-2-yl)-4-methylbenzamide <2> [17,28]
N-ethylmaleimide <1> (<1> 1 mM, complete inhibition [8]) [8]
N-hydroxy-2-(1-phenyl-5-(trifluoromethyl)-1H-pyrazol-4-yl)-4,5-dihydrooxazole-4-carboxamide <2> [17,28]
N-hydroxy-2-(1H-indazol-3-yl)-4,5-dihydrooxazole-4-carboxamide <2> [17,18,26,28]
N-hydroxy-2-(2-(trifluoromethoxy)phenyl)-4,5-dihydrooxazole-4-carboxamide <2> [17,28]
N-hydroxy-2-(3-(trifluoromethoxy)phenyl)-4,5-dihydrooxazole-4-carboxamide <2> [17,18,26,28]
N-hydroxy-2-(3-(trifluoromethyl)phenyl)-4,5-dihydrooxazole-4-carboxamide <2> [17,18,26,28]
N-hydroxy-2-(3-propyl-4,5-bis(trifluoromethoxy)phenyl)-4,5-dihydrooxazole-4-carboxamide <2> [26]
N-hydroxy-2-(4'-propylbiphenyl-4-yl)-4,5-dihydrooxazole-4-carboxamide <2> [17,18,26,28]
N-hydroxy-2-(4-((3-nitrophenoxy)methyl)phenyl)-4,5-dihydrooxazole-4-carboxamide <2> [17,26,28]

N-hydroxy-2-(4-(3-methylbut-2-enyloxy)-3-(trifluoromethoxy)phenyl)-4,5-dihydrooxazole-4-carboxamide <2> [28]
N-hydroxy-2-(4-(3-nitrobenzyloxy)phenyl)-4,5-dihydrooxazole-4-carboxamide <2> [17,26,28]
N-hydroxy-2-(4-(trifluoromethoxy)phenyl)-4,5-dihydrooxazole-4-carboxamide <2> [17,18,26,28]
N-hydroxy-2-(4-(trifluoromethoxy)phenyl)-4,5-dihydrothiazole-4-carboxamide <2> [28]
N-hydroxy-2-(4-(trifluoromethyl)phenyl)-4,5-dihydrooxazole-4-carboxamide <2> [17,26,28]
N-hydroxy-2-(4-hydroxyphenyl)-4,5-dihydrooxazole-4-carboxamide <2> [17,18,28]
N-hydroxy-2-(4-iodophenyl)-4,5-dihydrooxazole-4-carboxamide <2> [28]
N-hydroxy-2-(4-methoxy-3-(trifluoromethoxy)phenyl)-4,5-dihydrooxazole-4-carboxamide <2> [17,28]
N-hydroxy-2-(4-methoxy-3-propyl-5-(trifluoromethoxy)phenyl)-4,5-dihydrooxazole-4-carboxamide <2> [17,18,28]
N-hydroxy-2-(4-methoxy-3-propyl-5-(trifluoromethoxy)phenyl)-4,5-dihydrothiazole-4-carboxamide <2> [17,18,28]
N-hydroxy-2-(4-nitrophenyl)-4,5-dihydrooxazole-4-carboxamide <2> [28]
N-hydroxy-2-(5-methyl-1-phenyl-1H-pyrazol-4-yl)-4,5-dihydrooxazole-4-carboxamide <2> [17,28]
N-hydroxy-2-(5-methyl-1-phenyl-1H-pyrazol-4-yl)-4,5-dihydrothiazole-4-carboxamide <2> [17,28]
N-hydroxy-2-(6-(trifluoromethyl)pyridin-3-yl)-4,5-dihydrooxazole-4-carboxamide <2> [17,26,28]
N-hydroxy-2-*p*-tolyl-4,5-dihydrooxazole-4-carboxamide <2> [17,18,26,28]
N-hydroxy-2-*p*-tolyl-4,5-dihydrothiazole-4-carboxamide <2> [17,18,26,28]
N-hydroxy-2-*p*-tolyl-5,6-dihydro-4H-1,3-oxazine-4-carboxamide <2> [28]
Zn^{2+} <1,5> (<1> 0.1 mM, about 65% loss of activity [5]) [5,9,10]
[3-(4-methoxyphenyl)-4,5-dihydro-isoxazol-5-yl]phosphonic acid <1> [29]
ciprofloxacin <1,5> [12]
dipicolinic acid <1> (<1> 0.02 mM, complete inhibition [9]) [9]
tobramycin <1,5> [12]
Additional information <1,2,5,6,7> (<2> (4R)-2-(3,4-dimethoxy-5-propylphenyl)-N-hydroxy-4,5-dihydro-1,3-oxazole-4-carboxamide is active against a Pseudomonas aeruginosa construct in which the endogenous lpxC gene is inactivated and in which LpxC activity is supplied by the lpxC gene from Escherichia coli. An Escherichia coli construct in which growth is dependent on the Pseudomonas aeruginosa lpxC gene is resistant to the compound [7]; <1> (R)-2-(4-bromophenylsulfonamido)-3-(5,8-dihydronaphthalen-2-yl)-N-hydroxypropanamide and (R)-3-(5,8-dihydronaphthalen-2-yl)-N-hydroxy-2-(naphthalene-2-sulfonamido)propanamide show predominantly Gram-negative activities, with activities against members of the Enterobacteriaceae, Serratia marcescens, Morganella morganii, Moraxella catarrhalis, Haemophilus influenzae, and Burkholderia cepacia. Neither compound showed activity against Pseudomonas aeruginosa; however, against a 'leaky' Pseudomonas

aeruginosa strain, some activity is seen with (R)-3-(5,8-dihydronaphthalen-2-yl)-N-hydroxy-2-(naphthalene-2-sulfonamido)propanamide. (R)-2-(4-bromophenylsulfonamido)-3-(5,8-dihydronaphthalen-2-yl)-N-hydroxypropanamide and (R)-3-(5,8-dihydronaphthalen-2-yl)-N-hydroxy-2-(naphthalene-2-sulfonamido)propanamide have little or no activity against the gram-positive bacteria tested [6]; <6> (S)-N-(1-(2-(3,4-dimethoxy-5-propylphenyl)-4,5-dihydrooxazol-4-yl)vinyl)hydroxylamine and (R)-3-(5,8-dihydronaphthalen-2-yl)-N-hydroxy-2-(naphthalene-2-sulfonamido)propanamide do not inhibit Aquifex aeolicus LpxC [33]; <5> (S)-N-(1-(2-(3,4-dimethoxy-5-propylphenyl)-4,5-dihydrooxazol-4-yl)vinyl)hydroxylamine, phenyloxazoline hydroxamic acid, competitive inhibitor in Escherichia coli, not active as an antibiotic against Aquifex aeolicus, Pseudomonas aeruginosa and other clinically important pathogens [12]; <1> dithiothreitol, glutathione and the C207A mutant prevent the formation of a covalent complex by (E)-2,3,4-trihydroxybenzaldehyde O-((2R,3R,4S,5R)-5-(2,4-dioxo-3,4-dihydropyrimidin-1(2H)-yl)-3,4-dihydroxytetrahydrofuran-2-yl)methyl oxime [16]; <1> incubation of 10 nM LpxC in buffer without bovine serum albumin for 30 min completely inactivates the enzyme. When this enzyme is diluted further (4fold) into buffer containing 1 mg/ml bovine serum albumin, 100% of the activity is restored when assayed after a 2 h incubation. High concentrations of LpxC in the assays can eliminate the requirement of bovine serum albumin [9]; <1> mass spectrometry-based screening is a valuable high-throughput screening tool for detecting inhibitors of enzymatic targets involving difficult to detect reactions [25]; <7> no evidence of time-dependent inhibition is observed in assays with either the wild-type or mutants [33]; <1> no inhibitory effect by 2,4-dihydroxy-benzaldehyde O-[5-(2,4-dioxo-3,4-dihydro-2H-pyrimidin-1-yl)-3,4-dihydroxy-tetrahydro-furan-2-ylmethyl]-oxime, 3,4-dimethoxy-benzaldehyde O-[5-(2,4-dioxo-3,4-dihydro-2H-pyrimidin-1-yl)-3,4-dihydroxy-tetrahydro-furan-2-ylmethyl]-oxime, and 2,3,4-trimethoxy-benzaldehyde O-[5-(2,4-dioxo-3,4-dihydro-2H-pyrimidin-1-yl)-3,4-dihydroxy-tetrahydro-furan-2-ylmethyl]-oxime [16]; <1,2> study the potentially important structural differences in active sites of both proteins responsible for making the inhibitors selective for Escherichia coli as compared to Pseudomonas aeruginosa LpxC, homology models of the LpxC of both organisms are developed and validated on the basis of a 3D profile and PROCHECK. Subsequently, a molecular electrostatic potential (MEP)-based surface and cavity-depth analysis is performed. Finally, a cross-docking analysis of reported inhibitors is performed to reveal selective binding modes. These studies identify differences between the two active sites and have implications for designing effective strategies to identify LpxC inhibitors that can be developed as novel broad-spectrum antibacterial drugs [27]; <1> the affinity of LpxC for both product and fatty acids is significantly influenced by changes in the number and identity of metal ions bound to the LpxC active site. Therefore, interactions with these metal ions are critical for molecular recognition of ligands by LpxC and may mimic similar contacts with active site inhibitors. These data indicate that the potency of LpxC inhibitors in vitro can be altered by assay conditions used in screening and/or development of LpxC inhibitors and that the metal

ion status of LpxC in vivo will likely influence the effectiveness of LpxC inhibitors as antibiotics [13]) [6,7,9,12,13,16,25,27,33]

Activating compounds

bovine serum albumin <1> (<1> addition of bovine serum albumin slightly increases activity [5]) [5]

Metals, ions

Co^{2+} <1> (<1> 0.1 mM, significantly enhances activity [5]; <1> incubation of apo-LpxC (0.125 mM) with stoichiometric amounts of Mn^{2+}, Co^{2+}, and Ni^{2+} reactivates apo-LpxC to varying degrees (Co^{2+}, Ni^{2+} > Zn^{2+} > Mn^{2+}) [9]) [5,9]

Mn^{2+} <1> (<1> incubation of apo-LpxC (0.125 mM) with stoichiometric amounts of Mn^{2+}, Co^{2+}, and Ni^{2+} reactivates apo-LpxC to varying degrees (Co^{2+}, Ni^{2+} > Zn^{2+} > Mn^{2+}) [9]) [9]

Ni^{2+} <1> (<1> incubation of apo-LpxC (0.125 mM) with stoichiometric amounts of Mn^{2+}, Co^{2+}, and Ni^{2+} reactivates apo-LpxC to varying degrees (Co^{2+}, Ni^{2+} > Zn^{2+} > Mn^{2+}) [9]) [9]

Zn^{2+} <1,5,6,9> (<1,5> dependent [12]; <5> dependent, catalytic zinc ion [19]; <1> incubation of apo-LpxC (0.125 mM) with stoichiometric amounts of Mn^{2+}, Co^{2+}, and Ni^{2+} reactivates apo-LpxC to varying degrees (Co^{2+}, Ni^{2+} > Zn^{2+} > Mn^{2+}) [9]; <1> LpxC is a metalloenzyme that requires bound Zn^{2+} for optimal activity. The actual concentration of bound Zn^{2+} varies with different enzyme preparations from 1.3-3.2 mol of Zn^{2+}/mol of LpxC with an average Zn^{2+} content of about 2 mol of Zn^{2+}/mol of LpxC. No other bound metal ions are detected in purified LpxC. The bound Zn^{2+} can be removed from LpxC by incubation with DPA, and the bound zinc ions can be easily reconstituted by incubation with Zn^{2+}. Reconstitution of LpxC in presence of Cd^{2+}, Ca^{2+}, Cu^{2+}, or Mg^{2+} is equal to or below the activity of apo-LpxC, indicating that these metal ions are ineffective at substituting for Zn^{2+}. Incubation of apo-LpxC (0.125 mM) with stoichiometric amounts of Mn^{2+}, Co^{2+}, and Ni^{2+} reactivates apo-LpxC to varying degrees (Co^{2+}, Ni^{2+} > Zn^{2+} > Mn^{2+}) [9]; <1> metal-dependent deacetylase [14]; <1> the low activity of LpxC variants at positions H79 and H238, coupled with the ability of Zn^{2+} to stimulate the activity of these enzymes and the low Zn^{2+} content of the purified variant enzymes suggests that these residues directly coordinate a catalytic Zn^{2+} in LpxC. The variants with alanine substituted at H265 or D246 also exhibit large decreases in LpxC activity, suggesting that one of these residues may constitute a third protein ligand to the active-site Zn^{2+} [10]; <6> the native state of this metallohydrolase may contain a pentacoordinate zinc ion [15]; <5> the solution structure of LpxC in complex with the substrate-analog inhibitor 1,5-anhydro-2-C-(carboxymethyl-N-hydroxyamide)-2-deoxy-3-O-myristoyl-D-glucitol, reveals a novel α/β fold, a unique zinc-binding motif and a hydrophobic passage that captures the acyl chain of the inhibitor [31]; <5> the substrate preferentially coordinates to the active site Zn^{2+} via its carbonyl oxygen between a Zn^{2+}-bound H_2O and an adjacent threonine. Furthermore, upon substrate binding a nearby Glu78 residue is found to readily deprotonate the remaining Zn^{2+}-bound H_2O [30]; <5>

wild-type enzyme contains 0.98 mg of Zn^{2+} per g of protein. The low activity of LpxC variants at positions H79 and H238, coupled with the ability of Zn^{2+} to stimulate the activity of these enzymes and the low Zn^{2+} content of the purified variant enzymes suggests that these residues directly coordinate a catalytic Zn^{2+} in LpxC. The variants with alanine substituted at H265 or D246 also exhibit large decreases in LpxC activity, suggesting that one of these residues may constitute a third protein ligand to the active-site Zn^{2+} [10]; <1> zinc amidase [21,29]; <6> zinc-binding motif. The catalytic zinc ion resides at the base of an active-site cleft and adjacent to a hydrophobic tunnel occupied by a fatty acid [32]; <1,9> zinc-dependent enzyme. LpxC catalyzes deacetylation by using Glu78 and His265 as a general acid-base pair and the zinc-bound water as a nucleophile [24]) [9,10,12,14,15,19,21,24,29,30,31,32]
Additional information <1,8> (<1,8> metalloenzyme [6,22]) [6,22]

Turnover number (s^{-1})

0.00096 <1> (UDP-3-O-((R)-3-hydroxymyristoyl)-N-acetylglucosamine, <1> pH 7.5, 30°C, mutant enzyme E78A/H265A, steady-state [24]) [24]
0.0016 <1> (UDP-3-O-((R)-3-hydroxymyristoyl)-N-acetylglucosamine, <1> pH 7.5, 30°C, mutant enzyme D246A, steady-state [24]) [24]
0.005 <1> (UDP-3-O-((R)-3-hydroxymyristoyl)-N-acetylglucosamine, <1> pH 7.5, 30°C, mutant enzyme H265A, steady-state [24]) [24]
0.01 <1> (UDP-3-O-((R)-3-hydroxymyristoyl)-N-acetylglucosamine, <1> K239A mutant [14]) [14]
0.017 <1> (UDP-3-O-((R)-3-hydroxymyristoyl)-N-acetylglucosamine, <1> H19A mutant [14]) [14]
0.052 <1> (UDP-3-O-((R)-3-hydroxymyristoyl)-N-acetylglucosamine, <1> F192A mutant [14]) [14]
0.053 <1> (UDP-3-O-((R)-3-hydroxymyristoyl)-N-acetylglucosamine, <1> T191A mutant [14]) [14]
0.083 <1> (UDP-3-O-((R)-3-hydroxymyristoyl)-N-acetylglucosamine, <1> pH 7.5, 30°C, mutant enzyme E78A, steady-state [24]) [24]
0.09 <1> (UDP-3-O-((R)-3-hydroxymyristoyl)-N-acetylglucosamine, <1> pH 5.7, 1°C [9]) [9]
0.13 <1> (UDP-3-O-((R)-3-hydroxymyristoyl)-N-acetylglucosamine, <1> H19Q mutant [14]) [14]
0.25 <1> (UDP-3-O-((R)-3-hydroxymyristoyl)-N-acetylglucosamine, <1> H19Y mutant [14]) [14]
0.283 <1> (UDP-3-O-((R)-3-hydroxymyristoyl)-N-acetylglucosamine, <1> pH 7.3 [25]) [25]
0.36 <1> (UDP-3-O-(N-hexyl-propionamide)-N-acetylglucosamine, <1> pH 6.0, 30°C [5]) [5]
0.45 <1> (UDP-3-O-((R)-3-hydroxymyristoyl)-N-acetylglucosamine, <1> pH 7.5, 30°C, wild-type enzyme substituted with Co^{2+}, steady-state [24]) [24]
1.32 <1> (UDP-3-O-((R)-3-hydroxymyristoyl)-N-acetylglucosamine, <1> D197E mutant [14]) [14]

1.5 <1> (UDP-3-O-((R)-3-hydroxymyristoyl)-N-acetylglucosamine, <1> wild-type [14]; <1> D197A mutant [14]; <1> pH 7.5, 30°C, wild-type Zn^{2+}-containing enzyme, steady-state [24]) [14,24]
3.3 <1> (UDP-3-O-((R)-3-hydroxymyristoyl)-N-acetylglucosamine, <1> pH 5.5, 30°C [9]) [9]

Specific activity (U/mg)

0.84 <1,5> [10]
1.33 <8> [22]
2.96 <1> (<1> overproducing strain [23]) [23]

K_m-Value (mM)

0.00019 <1> (UDP-3-O-((R)-3-hydroxymyristoyl)-N-acetylglucosamine, <1> wild-type [14]; <1> pH 7.5, 30°C, wild-type Zn^{2+}-containing enzyme, steady-state [24]) [14,24]
0.00025 <1> (UDP-3-O-((R)-3-hydroxymyristoyl)-N-acetylglucosamine, <1> pH 7.5, 30°C, mutant enzyme D246A, steady-state [24]) [24]
0.00047 <1> (UDP-3-O-((R)-3-hydroxymyristoyl)-N-acetylglucosamine, <1> pH 7.5, 30°C, wild-type enzyme substituted with Co^{2+}, steady-state [24]) [24]
0.0005 <1> (UDP-3-O-((R)-3-hydroxymyristoyl)-N-acetylglucosamine, <1> F192A mutant [14]) [14]
0.0006 <1> (UDP-3-O-((R)-3-hydroxymyristoyl)-N-acetylglucosamine, <1> pH 5.7, 1°C [9]) [9]
0.0008 <1> (UDP-3-O-((R)-3-hydroxymyristoyl)-N-acetylglucosamine, <1> D197E mutant [14]; <1> K239A mutant [14]) [14]
0.0011 <1> (UDP-3-O-((R)-3-hydroxymyristoyl)-N-acetylglucosamine, <1> D197A mutant [14]) [14]
0.0013 <1> (UDP-3-O-((R)-3-hydroxymyristoyl)-N-acetylglucosamine, <1> H19A mutant [14]) [14]
0.0014 <1> (UDP-3-O-((R)-3-hydroxymyristoyl)-N-acetylglucosamine, <1> pH 7.5, 30°C, mutant enzyme H265A, steady-state [24]) [24]
0.0016 <1> (UDP-3-O-((R)-3-hydroxymyristoyl)-N-acetylglucosamine, <1> T191A mutant [14]) [14]
0.0019 <1> (UDP-3-O-((R)-3-hydroxymyristoyl)-N-acetylglucosamine, <1> pH 7.5, 30°C, mutant enzyme E78A/H265A, steady-state [24]) [24]
0.0021 <1> (UDP-3-O-((R)-3-hydroxymyristoyl)-N-acetylglucosamine, <1> pH 5.5, 30°C [9]) [9]
0.0024 <1> (UDP-3-O-((R)-3-hydroxymyristoyl)-N-acetylglucosamine, <1> H19Q mutant [14]) [14]
0.0043 <1> (UDP-3-O-((R)-3-hydroxymyristoyl)-N-acetylglucosamine, <1> pH 7.5, 30°C, mutant enzyme E78A, steady-state [24]) [24]
0.011 <1> (UDP-3-O-((R)-3-hydroxymyristoyl)-N-acetylglucosamine, <1> H19Y mutant [14]) [14]
0.367 <1> (UDP-(2-acetamino)-2-deoxy-3-O-[2-(hexylamino)-1-methyl-2-oxoethyl]-D-glucopyranose, <1> pH 6.0, 30°C [5]) [5]

K_i-Value (mM)

0.000002 <1,5> (N-((2S,3R)-3-hydroxy-1-(hydroxyamino)-1-oxobutan-2-yl)-4-((4-(morpholinomethyl)phenyl)ethynyl)benzamide) [12]
0.000003 <7> (N-((2S,3R)-3-hydroxy-1-(hydroxyamino)-1-oxobutan-2-yl)-4-((4-(morpholinomethyl)phenyl)ethynyl)benzamide, <7> W206Q/S214G mutant [33]) [33]
0.0000035 <7> (N-((2S,3R)-3-hydroxy-1-(hydroxyamino)-1-oxobutan-2-yl)-4-((4-(morpholinomethyl)phenyl)ethynyl)benzamide, <7> S214G mutant [33]) [33]
0.000004 <1> (N-((2S,3R)-3-hydroxy-1-(hydroxyamino)-1-oxobutan-2-yl)-4-((4-(morpholinomethyl)phenyl)ethynyl)benzamide, <1> wild-type [33]) [33]
0.000005 <1> (N-((2S,3R)-3-hydroxy-1-(hydroxyamino)-1-oxobutan-2-yl)-4-((4-(morpholinomethyl)phenyl)ethynyl)benzamide, <1> Q202W/G210S mutant [33]) [33]
0.00002 <1> ((R)-3-(5,8-dihydronaphthalen-2-yl)-N-hydroxy-2-(naphthalene-2-sulfonamido)propanamide) [12]
0.00005 <1> ((S)-N-(1-(2-(3,4-dimethoxy-5-propylphenyl)-4,5-dihydrooxazol-4-yl)vinyl)hydroxylamine, <1> Escherichia coli [12]) [12]
0.000053 <1> ((S)-N-(1-(2-(3,4-dimethoxy-5-propylphenyl)-4,5-dihydrooxazol-4-yl)vinyl)hydroxylamine, <1> wild-type [33]) [33]
0.000069 <1> ((R)-3-(5,8-dihydronaphthalen-2-yl)-N-hydroxy-2-(naphthalene-2-sulfonamido)propanamide, <1> wild-type [33]) [33]
0.000086 <1> ((R)-3-(5,8-dihydronaphthalen-2-yl)-N-hydroxy-2-(naphthalene-2-sulfonamido)propanamide, <1> Q202W/G210S mutant [33]) [33]
0.00034 <1> ((S)-N-(1-(2-(3,4-dimethoxy-5-propylphenyl)-4,5-dihydrooxazol-4-yl)vinyl)hydroxylamine, <1> Q202W/G210S mutant [33]) [33]
0.00034 <7> (N-((2S,3R)-3-hydroxy-1-(hydroxyamino)-1-oxobutan-2-yl)-4-((4-(morpholinomethyl)phenyl)ethynyl)benzamide, <7> wild-type [33]) [33]
0.00065 <1,5> ((3R,5R)-3-hydroxy-5-(2-(hydroxyamino)-2-oxoethyl)-2-(hydroxymethyl)tetrahydro-2H-pyran-4-yl tetradecanoate, <5> pH 5.5 [12]; <1> Escherichia coli and Aquifex aeolicus, pH 5.5 [12]) [12]
0.0007 <7> ((R)-3-(5,8-dihydronaphthalen-2-yl)-N-hydroxy-2-(naphthalene-2-sulfonamido)propanamide, <7> W206Q/S214G mutant [33]) [33]
0.0058 <7> ((R)-3-(5,8-dihydronaphthalen-2-yl)-N-hydroxy-2-(naphthalene-2-sulfonamido)propanamide, <7> wild-type [33]) [33]
0.054 <1> (2,3,4-trihydroxybenzaldehyde O-((2R,3R,4S,5R)-5-(2,4-dioxo-3,4-dihydropyrimidin-1(2H)-yl)-3,4-dihydroxytetrahydrofuran-2-yl)methyl oxime) [16]
0.11 <7> ((S)-N-(1-(2-(3,4-dimethoxy-5-propylphenyl)-4,5-dihydrooxazol-4-yl)vinyl)hydroxylamine, <7> W206Q/S214G mutant [33]) [33]
0.38 <7> ((S)-N-(1-(2-(3,4-dimethoxy-5-propylphenyl)-4,5-dihydrooxazol-4-yl)vinyl)hydroxylamine, <7> wild-type [33]) [33]
Additional information <5> ((S)-N-(1-(2-(3,4-dimethoxy-5-propylphenyl)-4,5-dihydrooxazol-4-yl)vinyl)hydroxylamine, <5> K_i value is higher than 500 microM [12]) [12]

pH-Optimum

5.5 <5> (<5> assay at [10]) [10]
5.9 <1> (<1> assay at [10]) [10]
6 <1> (<1> assay at [29]) [22,29]
7 <1> (<1> assay at [23]) [23]
7.4 <1,5> (<1,5> assay at [12,16,21]) [12,16,21]
7.5 <1,9> (<1,9> assay at [14,24]) [14,24]
8.5 <8> [22]
Additional information <1> (<1> affinity of EcLpxC for the product (myr-UDP-GlcNH$_2$) is determined as a function of pH to ascertain whether there are ionizations important for binding affinity. For wild-type LpxC, the KD product value increases at both low and high pH in a log-linear fashion, indicating that two ionizations affect binding affinity [14]) [14]

pH-Range

5-7 <1> (<1> pH 5.0: about 45% of maximal activity, pH 7.0: about 60% of maximal activity [22]) [22]
7-9 <8> (<8> pH 7.0: about 55% of maximal activity, pH 9.0: about 75% of maximal activity [22]) [22]

Temperature optimum (°C)

30 <1,5,8,9> (<1,5,8,9> assay at [10,12,14,16,21,22,24,29]) [10,12,14,16,21,22,24,29]
37 <1> (<1> assay at [23]) [23]
60 <5> (<5> assay at [10]) [10]

4 Enzyme Structure

Subunits

? <1,8> (<1> x * 34000, SDS-PAGE [23]; <8> x * 33435, calculated from sequence [22]; <8> x * 38600, SDS-PAGE [22]) [22,23]

5 Isolation/Preparation/Mutation/Application

Localization

cytoplasm <1> [8]

Purification

<1> [5,6,9,12,14,16,22,23,24,25]
<2> [28]
<3> [16]
<4> [16]
<5> [10,12]
<5> (C193A/ΔD284-L294 variant of LpxC) [19]
<6> [32]

<8> [22,34]
<9> [24]

Crystallization

<5> (crystal structure of the LpxC-3-(heptyloxy)benzoate complex) [19]
<6> (2.7 A resolution X-ray crystal structure of LpxC complexed with the substrate analogue inhibitor, 1,5-anhydro-2-C-(carboxymethyl-N-hydroxamide)-2-deoxy-3-O-myristoyl-D-glucitol, and the 2.0 A resolution structure of LpxC complexed with imidazole. The X-ray crystal structure of LpxC complexed with 1,5-anhydro-2-C-(carboxymethyl-N-hydroxamide)-2-deoxy-3-O-myristoyl-D-glucitol allows for a detailed examination of the coordination geometry of the catalytic zinc ion and other enzyme-inhibitor interactions in the active site. The hydroxamate group of 1,5-anhydro-2-C-(carboxymethyl-N-hydroxamide)-2-deoxy-3-O-myristoyl-D-glucitol forms a bidentate chelate complex with the zinc ion and makes hydrogen bond interactions with conserved active site residues E78, H265, and T191. The inhibitor C-4 hydroxyl group makes direct hydrogen bond interactions with E197 and H58. Finally, the C-3 myristate moiety of the inhibitor binds in the hydrophobic tunnel of the active site) [15]
<6> (crystallization at 21°C, a sitting drop containing 0.005 ml of protein solution (2.2 mg/ml LpxC, 25 mM Hepes (pH 7.0), 50 mM NaCl, 10 mM magnesium acetate, and 0.5 mM $ZnSO_4$) is equilibrated against a 0.5 ml reservoir of 0.8 M NaCl/0.1 M Hepes (pH 7.0). Crystals of dimensions 0.3 * 0.1 * 0.05 mm3 appear in 5-7 days, larger crystals of dimensions 0.6 * 0.2 * 0.2 mm^3 are obtained by macroseeding) [32]
<6> (crystals of LpxC are grown by hanging-drop vapour diffusion at 20°C, structure of recombinant UDP-3-O-acyl-N-acetylglucosamine deacetylase in complex with UDP, determined to a resolution of 2.2 A. The uracil-binding site is constructed from amino acids that are highly conserved across species. Hydrophobic associations with the Phe155 and Arg250 side chains in combination with hydrogen-bonding interactions with the main chain of Glu154 and the side chains of Tyr151 and Lys227 position the base. The phosphate and ribose groups are directed away from the active site and interact with Arg137, Lys156, Glu186 and Arg250) [4]
<8> (1.9 A resolution crystal structure of LpxC complexed with (2R)-N-hydroxy-3-naphthalen-2-yl-2-[(naphthalen-2-ylsulfonyl)amino]propanamide) [34]
<9> (equilibrating a hanging drop containing 0.003 ml of protein solution (3 mg/ml LpxC, 100 mM HEPES, pH 7.5, 180 mM NaCl, 9-14% PEG3350, and 0.5 mM $ZnSO_4$) and 0.003 ml of precipitant buffer (100 mM HEPES, pH 7.5, 180 mM NaCl, 9-14% PEG3350, and 0.5 mM $ZnSO_4$) over a reservoir containing about 1 ml of precipitant buffer. Crystals with maximum dimensions of 0.3 * 0.15 * 0.15 mm^3 grow within 3 days and are gradually transferred to a stabilization buffer of 100 mM sodium cacodylate, pH 6.0, 180 mM NaCl, 11-16% PEG 3350, 0.5 mM $ZnSO_4$, and 1% glycerol. Crystals are flash-cooled in liquid nitrogen following cryoprotection with 22% glycerol and diffracted X-rays to 2.1 Å. Crystals are isomorphous with those prepared at pH 7.0 and

belong to space group P6(1) with unit cell dimensions a = b = 101.3 A, c = 122.7 A) [24]

Cloning

<1> [5,25]
<1> (Escherichia coli BL21 is used as host for expression of Strep-tagged LpxC protein) [3]
<1> (envA is cloned into an isopropyl-1-thio-β-D-galactopyranoside-inducible T7-based expression system) [23]
<1> (expression in Pseudomonas aeruginosa) [7]
<1> (overepression of LpxC variants in Escherichia coli) [10]
<2> (expression in Escherichia coli) [7]
<5> (C193A/ΔD284-L294 variant of LpxC overexpressed in Escherichia coli) [19]
<5> (overepression of LpxC variants in Escherichia coli) [10]
<8> (subcloned the Pseudomonas aeruginosa lpxC gene into the T7-based expression vector pET11a) [22]
<8> (the paLpxC (residues 1-299, C40S) is cloned from genomic DNA by polymerase chain reaction and inserted into pPW4 expression vectors. The recombinant paLpxC is overexpressed) [34]

Engineering

C125A <1> (<1> as sensitive to 2,3,4-trihydroxybenzaldehyde O-((2R,3R,4S,5R)-5-(2,4-dioxo-3,4-dihydropyrimidin-1(2H)-yl)-3,4-dihydroxytetrahydrofuran-2-yl)methyl oxime as the wild-type enzyme [16]) [16]
C193A/ΔD284-L294 <5> (<5> variant of LpxC [19]) [19]
C207A <1> (<1> much less sensitive to 2,3,4-trihydroxybenzaldehyde O-((2R,3R,4S,5R)-5-(2,4-dioxo-3,4-dihydropyrimidin-1(2H)-yl)-3,4-dihydroxytetrahydrofuran-2-yl)methyl oxime inhibition, suggesting that Cys-207 is necessary to form the E-I complex [16]) [16]
C214N <1> (<1> as sensitive to 2,3,4-trihydroxybenzaldehyde O-((2R,3R,4S,5R)-5-(2,4-dioxo-3,4-dihydropyrimidin-1(2H)-yl)-3,4-dihydroxytetrahydrofuran-2-yl)methyl oxime as the wild-type enzyme [16]) [16]
C250A <1> (<1> as sensitive to 2,3,4-trihydroxybenzaldehyde O-((2R,3R,4S,5R)-5-(2,4-dioxo-3,4-dihydropyrimidin-1(2H)-yl)-3,4-dihydroxytetrahydrofuran-2-yl)methyl oxime as the wild-type enzyme [16]) [16]
C63S <1> (<1> as sensitive to 2,3,4-trihydroxybenzaldehyde O-((2R,3R,4S,5R)-5-(2,4-dioxo-3,4-dihydropyrimidin-1(2H)-yl)-3,4-dihydroxytetrahydrofuran-2-yl)methyl oxime as the wild-type enzyme [16]) [16]
C65A <1> (<1> as sensitive to 2,3,4-trihydroxybenzaldehyde O-((2R,3R,4S,5R)-5-(2,4-dioxo-3,4-dihydropyrimidin-1(2H)-yl)-3,4-dihydroxytetrahydrofuran-2-yl)methyl oxime as the wild-type enzyme [16]) [16]
D105A <5> (<5> expressed to level comparable to wild-type LpxC. The extract overexpressing LpxC exhibits about 56% of the specific activity of the wild-type extract [10]) [10]
D105N <5> (<5> expressed to level comparable to wild-type LpxC. The extract overexpressing LpxC exhibits about 67% of the specific activity of the wild-type extract [10]) [10]

D105S <5> (<5> expressed to level comparable to wild-type LpxC. The extract overexpressing LpxC exhibits about 78% of the specific activity of the wild-type extract [10]) [10]
D197A <1> (<1> site-directed mutagenesis [14]) [14]
D197E <1> (<1> site-directed mutagenesis [14]) [14]
D242A <1> (<1> expressed to level comparable to wild-type LpxC. The extract overexpressing LpxC exhibits about 9.5% of the specific activity of the wild-type extract [10]) [10]
D242Q <1> (<1> expressed to level comparable to wild-type LpxC. The extract overexpressing LpxC exhibits about 0.04% of the specific activity of the wild-type extract [10]) [10]
D246A <1,5,9> (<1> 1210fold decrease in k_{cat}/K_M compared to wild-type Zn^{2+}-containing enzyme [24]; <9> decrease in k_{cat}/K_M compared to wild-type Zn^{2+}-containing enzyme [24]; <5> expressed to level comparable to wild-type LpxC. The extract overexpressing LpxC exhibits about 0.001% of the specific activity of the wild-type extract. Contains 64% Fe^{2+} compared to wild-type Zn^{2+} content [10]; <1> expressed to level comparable to wild-type LpxC. The extract overexpressing LpxC exhibits about 0.06% of the specific activity of the wild-type extract [10]) [10,24]
D246N <5> (<5> expressed to level comparable to wild-type LpxC. The extract overexpressing LpxC exhibits about 3.5% of the specific activity of the wild-type extract [10]) [10]
D246S <5> (<5> expressed to level comparable to wild-type LpxC. The extract overexpressing LpxC exhibits about less than 0.0005% of the specific activity of the wild-type extract [10]) [10]
E100A <5> (<5> expressed to level comparable to wild-type LpxC. The extract overexpressing LpxC exhibits about 72% of the specific activity of the wild-type extract [10]) [10]
E100N <5> (<5> expressed to level comparable to wild-type LpxC. The extract overexpressing LpxC exhibits about 61% of the specific activity of the wild-type extract [10]) [10]
E100S <5> (<5> expressed to level comparable to wild-type LpxC. The extract overexpressing LpxC exhibits about 83% of the specific activity of the wild-type extract [10]) [10]
E234A <5> (<5> expressed to level comparable to wild-type LpxC. The extract overexpressing LpxC exhibits about 4.8% of the specific activity of the wild-type extract [10]) [10]
E234N <5> (<5> expressed to level comparable to wild-type LpxC. The extract overexpressing LpxC exhibits about less than 0.0005% of the specific activity of the wild-type extract [10]) [10]
E234S <5> (<5> expressed to level comparable to wild-type LpxC. The extract overexpressing LpxC exhibits about 6.7% of the specific activity of the wild-type extract [10]) [10]
E78A <1,5,9> (<1> 400fold decrease in k_{cat}/K_M compared to wild-type Zn^{2+}-containing enzyme [24]; <9> decrease in k_{cat}/K_M compared to wild-type Zn^{2+}-containing enzyme [24]; <1> expressed to level comparable to wild-type LpxC. The extract overexpressing LpxC exhibits about 0.1% of the spe-

cific activity of the wild-type extract [10]; <5> expressed to level comparable to wild-type LpxC. The extract overexpressing LpxC exhibits about 9.8% of the specific activity of the wild-type extract. Contains 28% Fe^{2+} compared to wild-type Zn^{2+} content. The specific activity of the E78A LpxC variant is neither inhibited nor activated by the addition of up to 1 mM Zn^{2+} [10]) [10,24]
E78A/H265A <1,9> (<1> 14800fold decrease in k_{cat}/K_M compared to wild-type Zn^{2+}-containing enzyme [24]; <9> decrease in k_{cat}/K_M compared to wild-type Zn^{2+}-containing enzyme [24]) [24]
E78Q <1,5> (<1> expressed to level comparable to wild-type LpxC. The extract overexpressing LpxC exhibits about 0.03% of the specific activity of the wild-type extract [10]; <5> expressed to level comparable to wild-type LpxC. The extract overexpressing LpxC exhibits about less than 0.0005% of the specific activity of the wild-type extract [10]) [10]
F192A <1> (<1> site-directed mutagenesis [14]) [14]
G17S <1> (<1> hypersensitive strain with point mutation in LpxC [21]; <1> partially-inactivated LpxC mutant G17S [12]) [12,21]
H19A <1,5> (<1> site-directed mutagenesis [14]; <1> expressed to level comparable to wild-type LpxC. The extract overexpressing LpxC exhibits about 0.07% of the specific activity of the wild-type extract. [10]; <5> expressed to level comparable to wild-type LpxC. The extract overexpressing LpxC exhibits about 5% of the specific activity of the wild-type extract. Contains 51% Fe^{2+} compared to wild-type Zn^{2+} content [10]) [10,14]
H19Q <1,5> (<1> site-directed mutagenesis [14]; <1> expressed to level comparable to wild-type LpxC. The extract overexpressing LpxC exhibits about 1.1% of the specific activity of the wild-type extract [10]; <5> expressed to level comparable to wild-type LpxC. The extract overexpressing LpxC exhibits about 45% of the specific activity of the wild-type extract [10]) [10,14]
H19Y <1,5> (<1> site-directed mutagenesis [14]; <1> expressed to level comparable to wild-type LpxC. The extract overexpressing LpxC exhibits about 0.5% of the specific activity of the wild-type extract [10]; <5> expressed to level comparable to wild-type LpxC. The extract overexpressing LpxC exhibits about 4.4% of the specific activity of the wild-type extract [10]) [10,14]
H238A <1,5> (<1> expressed to level comparable to wild-type LpxC. The extract overexpressing LpxC exhibits about 0.09% of the specific activity of the wild-type extract [10]; <5> expressed to level comparable to wild-type LpxC. The extract overexpressing LpxC exhibits about 0.1% of the specific activity of the wild-type extract. Extract overexpressing H238A is stimulated approximately 20fold by the addition of $ZnSO_4$ [10]) [10]
H265A <1,9> (<1> 2190fold decrease in k_{cat}/K_M compared to wild-type Zn^{2+}-containing enzyme [24]; <9> decrease in k_{cat}/K_M compared to wild-type Zn^{2+}-containing enzyme [24]; <1> expressed to level comparable to wild-type LpxC. The extract overexpressing LpxC exhibits about 0.03% of the specific activity of the wild-type extract [10]) [10,24]

H265Q <1,5> (<1> expressed to level comparable to wild-type LpxC. The extract overexpressing LpxC exhibits about 0.02% of the specific activity of the wild-type extract [10]; <5> expressed to level comparable to wild-type LpxC. The extract overexpressing LpxC exhibits about less than 0.0005% of the specific activity of the wild-type extract [10]) [10]
H79A <1,5> (<5> expressed to level comparable to wild-type LpxC. The extract overexpressing LpxC exhibits about 0.006% of the specific activity of the wild-type extract. Contains 10% Fe^{2+} compared to wild-type Zn^{2+} content. Extract overexpressing H79A is stimulated approximately 20fold by the addition of $ZnSO_4$ [10]; <1> expressed to level comparable to wild-type LpxC. The extract overexpressing LpxC exhibits about 0.04% of the specific activity of the wild-type extract [10]) [10]
H79Q <1,5> (<5> expressed to level comparable to wild-type LpxC. The extract overexpressing LpxC exhibits about 0.008% of the specific activity of the wild-type extract [10]; <1> expressed to level comparable to wild-type LpxC. The extract overexpressing LpxC exhibits about 0.08% of the specific activity of the wild-type extract [10]) [10]
I38T <1> (<1> lpxC gene [6]) [6]
K143A <1> (<1> site-directed mutagenesis [14]) [14]
K227E <5> (<5> completely inactive mutant enzyme [31]) [31]
K239A <1> (<1> site-directed mutagenesis [14]) [14]
N162A <1> (<1> site-directed mutagenesis [14]) [14]
Q202W/G210S <1> (<1> less sensitive to N-((2S,3R)-3-hydroxy-1-(hydroxyamino)-1-oxobutan-2-yl)-4-((4-(morpholinomethyl)phenyl)ethynyl)benzamide than wild-type, that is inhibited about 75% by 4 nM N-((2S,3R)-3-hydroxy-1-(hydroxyamino)-1-oxobutan-2-yl)-4-((4-(morpholinomethyl)phenyl)ethynyl)benzamide [33]; <1> mutant loses the time-dependence of N-((2S,3R)-3-hydroxy-1-(hydroxyamino)-1-oxobutan-2-yl)-4-((4-(morpholinomethyl)phenyl)ethynyl)benzamide inhibition. Still sensitive to inhibition by 2,3,4-trihydroxybenzaldehyde O-((2R,3R,4S,5R)-5-(2,4-dioxo-3,4-dihydropyrimidin-1(2H)-yl)-3,4-dihydroxytetrahydrofuran-2-yl)methyl oxime in a time-dependent manner [16]) [16,33]
S214G <7> (<7> completely inhibited by 0.5 microM N-((2S,3R)-3-hydroxy-1-(hydroxyamino)-1-oxobutan-2-yl)-4-((4-(morpholinomethyl)phenyl)ethynyl)benzamide, wild-type under the same conditions 50% inhibited [33]) [33]
T179A <6> (<6> LpxC mutant is less sensitive to N-((2S,3R)-3-hydroxy-1-(hydroxyamino)-1-oxobutan-2-yl)-4-((4-(morpholinomethyl)phenyl)ethynyl)benzamide inhibition [33]) [33]
T191A <1> (<1> site-directed mutagenesis [14]) [14]
W206Q/S214G <7> (<7> completely inhibited by 0.5 microM N-((2S,3R)-3-hydroxy-1-(hydroxyamino)-1-oxobutan-2-yl)-4-((4-(morpholinomethyl)phenyl)ethynyl)benzamide, wild-type under the same conditions 50% inhibited [33]) [33]
Additional information <1> (<1> Escherichia coli mutants with decreased susceptibility to (R)-2-(4-bromophenylsulfonamido)-3-(5,8-dihydronaphthalen-2-yl)-N-hydroxypropanamide are selected [6]) [6]

Application

drug development <1,2,5> (<2> enzyme is an attractive target against Pseudomonas infection [17]; <1,5> lipid A is an essential component of the outer membranes of most Gram-negative bacteria, making LpxC an attractive target for antibiotic design [12]; <1> LpxC is a target for the development of antimicrobial agents in the treatment of Gram negative infections [14]; <2> LpxC represents a highly attractive target for a novel antibacterial drug [28]; <2> target for development of anti-infective drugs against gram-negative bacteria [20]) [12,14,17,20,28]

medicine <1> (<1> LpxC is one of the key enzymes of bacterial lipid A biosynthesis, catalyzing the removal of the N-acetyl group of UDP-3-O-(R-3-hydroxymyristoyl)-N-acetylglucosamine. The lpxC gene is essential in Gram-negative bacteria but absent from mammalian genomes, making it an attractive target for antibacterial drug discovery [5]; <1> this enzyme catalyzes a committed step in the biosynthesis of lipid A, and for this reason, LpxC is a target for the development of antibiotics in the treatment of Gram-negative bacterial infections [13]) [5,13]

6 Stability

Temperature stability

30 <1> (<1> 6 h, stable [10]) [10]

60 <5> (<5> stable for up to 20 min [10]) [10]

General stability information

<1>, purified enzyme is unstable, decay half-life of approximately 40 h [23]

References

[1] Sorensen, P.G.; Lutkenhaus, J.; Young, K.; Eveland, S.S.; Anderson, M.S.; Raetz, C.R.H.: Regulation of UDP-3-O-[R-3-hydroxymyristoyl]-N-acetylglucosamine deacetylase in Escherichia coli. The second enzymic step of lipid A biosynthesis. J. Biol. Chem., **271**, 25898-25905 (1996)

[2] Fuehrer, F.; Mueller, A.; Baumann, H.; Langklotz, S.; Kutscher, B.; Narberhaus, F.: Sequence and length recognition of the C-terminal turnover element of LpxC, a soluble substrate of the membrane-bound FtsH protease. J. Mol. Biol., **372**, 485-496 (2007)

[3] Fuehrer, F.; Langklotz, S.; Narberhaus, F.: The C-terminal end of LpxC is required for degradation by the FtsH protease. Mol. Microbiol., **59**, 1025-1036 (2006)

[4] Buetow, L.; Dawson, A.; Hunter, W.N.: The nucleotide-binding site of Aquifex aeolicus LpxC. Acta Crystallogr. Sect. F, **62**, 1082-1086 (2006)

[5] Wang, W.; Maniar, M.; Jain, R.; Jacobs, J.; Trias, J.; Yuan, Z.: A fluorescence-based homogeneous assay for measuring activity of UDP-3-O-(R-3-hydro-

xymyristoyl)-N-acetylglucosamine deacetylase. Anal. Biochem., **290**, 338-346 (2001)
[6] Clements, J.M.; Coignard, F.; Johnson, I.; Chandler, S.; Palan, S.; Waller, A.; Wijkmans, J.; Hunter, M.G.: Antibacterial activities and characterization of novel inhibitors of LpxC. Antimicrob. Agents Chemother., **46**, 1793-1799 (2002)
[7] Mdluli, K.E.; Witte, P.R.; Kline, T.; Barb, A.W.; Erwin, A.L.; Mansfield, B.E.; McClerren, A.L.; Pirrung, M.C.; Tumey, L.N.; Warrener, P.; Raetz, C.R.; Stover, C.K.: Molecular validation of LpxC as an antibacterial drug target in Pseudomonas aeruginosa. Antimicrob. Agents Chemother., **50**, 2178-2184 (2006)
[8] Anderson, M.S.; Robertson, A.D.; Macher, I.; Raetz, C.R.: Biosynthesis of lipid A in Escherichia coli: identification of UDP-3-O-[(R)-3-hydroxymyristoyl]-α-D-glucosamine as a precursor of UDP-N2,O3-bis[(R)-3-hydroxymyristoyl]-α-D-glucosamine. Biochemistry, **27**, 1908-1917 (1988)
[9] Jackman, J.E.; Raetz, C.R.; Fierke, C.A.: UDP-3-O-(R-3-hydroxymyristoyl)-N-acetylglucosamine deacetylase of Escherichia coli is a zinc metalloenzyme. Biochemistry, **38**, 1902-1911 (1999)
[10] Jackman, J.E.; Raetz, C.R.; Fierke, C.A.: Site-directed mutagenesis of the bacterial metalloamidase UDP-(3-O-acyl)-N-acetylglucosamine deacetylase (LpxC). Identification of the zinc binding site. Biochemistry, **40**, 514-523 (2001)
[11] Coggins, B.E.; McClerren, A.L.; Jiang, L.; Li, X.; Rudolph, J.; Hindsgaul, O.; Raetz, C.R.; Zhou, P.: Refined solution structure of the LpxC-TU-514 complex and pKa analysis of an active site histidine: insights into the mechanism and inhibitor design. Biochemistry, **44**, 1114-1126 (2005)
[12] McClerren, A.L.; Endsley, S.; Bowman, J.L.; Andersen, N.H.; Guan, Z.; Rudolph, J.; Raetz, C.R.: A slow, tight-binding inhibitor of the zinc-dependent deacetylase LpxC of lipid A biosynthesis with antibiotic activity comparable to ciprofloxacin. Biochemistry, **44**, 16574-16583 (2005)
[13] Hernick, M.; Fierke, C.A.: Molecular recognition by Escherichia coli UDP-3-O-(R-3-hydroxymyristoyl)-N-acetylglucosamine deacetylase is modulated by bound metal ions. Biochemistry, **45**, 14573-14581 (2006)
[14] Hernick, M.; Fierke, C.A.: Catalytic mechanism and molecular recognition of E. coli UDP-3-O-(R-3-hydroxymyristoyl)-N-acetylglucosamine deacetylase probed by mutagenesis. Biochemistry, **45**, 15240-15248 (2006)
[15] Gennadios, H.A.; Whittington, D.A.; Li, X.; Fierke, C.A.; Christianson, D.W.: Mechanistic inferences from the binding of ligands to LpxC, a metal-dependent deacetylase. Biochemistry, **45**, 7940-7948 (2006)
[16] Barb, A.W.; Leavy, T.M.; Robins, L.I.; Guan, Z.; Six, D.A.; Zhou, P.; Hangauer, M.J.; Bertozzi, C.R.; Raetz, C.R.: Uridine-based inhibitors as new leads for antibiotics targeting Escherichia coli LpxC. Biochemistry, **48**, 3068-3077 (2009)
[17] Kadam, R.U.; Roy, N.: Cluster analysis and two-dimensional quantitative structure-activity relationship (2D-QSAR) of Pseudomonas aeruginosa deacetylase LpxC inhibitors. Bioorg. Med. Chem. Lett., **16**, 5136-5143 (2006)

[18] Kadam, R.U.; Chavan, A.; Roy, N.: Pharmacophoric features of Pseudomonas aeruginosa deacetylase LpxC inhibitors: an electronic and structural analysis. Bioorg. Med. Chem. Lett., **17**, 861-868 (2007)
[19] Shin, H.; Gennadios, H.A.; Whittington, D.A.; Christianson, D.W.: Amphipathic benzoic acid derivatives: synthesis and binding in the hydrophobic tunnel of the zinc deacetylase LpxC. Bioorg. Med. Chem., **15**, 2617-2623 (2007)
[20] Kadam, R.U.; Garg, D.; Roy, N.: Selective mapping of chemical space for Pseudomonas aeruginosa deacetylase LpxC inhibitory potential. Chem. Biol. Drug Des., **71**, 45-56 (2008)
[21] Pirrung, M.C.; Tumey, L.N.; McClerren, A.L.; Raetz, C.R.: High-throughput catch-and-release synthesis of oxazoline hydroxamates. Structure-activity relationships in novel inhibitors of Escherichia coli LpxC: in vitro enzyme inhibition and antibacterial properties. J. Am. Chem. Soc., **125**, 1575-1586 (2003)
[22] Hyland, S.A.; Eveland, S.S.; Anderson, M.S.: Cloning, expression, and purification of UDP-3-O-acyl-GlcNAc deacetylase from Pseudomonas aeruginosa: a metalloamidase of the lipid A biosynthesis pathway. J. Bacteriol., **179**, 2029-2037 (1997)
[23] Young, K.; Silver, L.L.; Bramhill, D.; Cameron, P.; Eveland, S.S.; Raetz, C.R.; Hyland, S.A.; Anderson, M.S.: The envA permeability/cell division gene of Escherichia coli encodes the second enzyme of lipid A biosynthesis. UDP-3-O-(R-3-hydroxymyristoyl)-N-acetylglucosamine deacetylase. J. Biol. Chem., **270**, 30384-30391 (1995)
[24] Hernick, M.; Gennadios, H.A.; Whittington, D.A.; Rusche, K.M.; Christianson, D.W.; Fierke, C.A.: UDP-3-O-((R)-3-hydroxymyristoyl)-N-acetylglucosamine deacetylase functions through a general acid-base catalyst pair mechanism. J. Biol. Chem., **280**, 16969-16978 (2005)
[25] Langsdorf, E.F.; Malikzay, A.; Lamarr, W.A.; Daubaras, D.; Kravec, C.; Zhang, R.; Hart, R.; Monsma, F.; Black, T.; Ozbal, C.C.; Miesel, L.; Lunn, C.A.: Screening for antibacterial inhibitors of the UDP-3-O-(R-3-hydroxymyristoyl)-N-acetylglucosamine deacetylase (LpxC) using a high-throughput mass spectrometry assay. J. Biomol. Screen., **15**, 52-61 (2009)
[26] Kadam, R.U.; Garg, D.; Chavan, A.; Roy, N.: Evaluation of Pseudomonas aeruginosa deacetylase LpxC inhibitory activity of dual PDE4-TNFr inhibitors: a multiscreening approach. J. Chem. Inf. Model., **47**, 1188-1195 (2007)
[27] Kadam, R.U.; Shivange, A.V.; Roy, N.: Escherichia coli versus Pseudomonas aeruginosa deacetylase LpxC inhibitors selectivity: surface and cavity-depth-based analysis. J. Chem. Inf. Model., **47**, 1215-1224 (2007)
[28] Kline, T.; Andersen, N.H.; Harwood, E.A.; Bowman, J.; Malanda, A.; Endsley, S.; Erwin, A.L.; Doyle, M.; Fong, S.; Harris, A.L.; Mendelsohn, B.; Mdluli, K.; Raetz, C.R.; Stover, C.K.; Witte, P.R.; Yabannavar, A.; Zhu, S.: Potent, novel in vitro inhibitors of the Pseudomonas aeruginosa deacetylase LpxC. J. Med. Chem., **45**, 3112-3129 (2002)
[29] Pirrung, M.C.; Tumey, L.N.; Raetz, C.R.; Jackman, J.E.; Snehalatha, K.; McClerren, A.L.; Fierke, C.A.; Gantt, S.L.; Rusche, K.M.: Inhibition of the antibacterial target UDP-(3-O-acyl)-N-acetylglucosamine deacetylase

(LpxC): isoxazoline zinc amidase inhibitors bearing diverse metal binding groups. J. Med. Chem., **45**, 4359-4370 (2002)
[30] Robinet, J.J.; Gauld, J.W.: DFT investigation on the mechanism of the deacetylation reaction catalyzed by LpxC. J. Phys. Chem. B, **112**, 3462-3469 (2008)
[31] Coggins, B.E.; Li, X.; McClerren, A.L.; Hindsgaul, O.; Raetz, C.R.; Zhou, P.: Structure of the LpxC deacetylase with a bound substrate-analog inhibitor. Nat. Struct. Biol., **10**, 645-651 (2003)
[32] Whittington, D.A.; Rusche, K.M.; Shin, H.; Fierke, C.A.; Christianson, D.W.: Crystal structure of LpxC, a zinc-dependent deacetylase essential for endotoxin biosynthesis. Proc. Natl. Acad. Sci. USA, **100**, 8146-8150 (2003)
[33] Barb, A.W.; Jiang, L.; Raetz, C.R.; Zhou, P.: Structure of the deacetylase LpxC bound to the antibiotic CHIR-090: Time-dependent inhibition and specificity in ligand binding. Proc. Natl. Acad. Sci. USA, **104**, 18433-18438 (2007)
[34] Mochalkin, I.; Knafels, J.D.; Lightle, S.: Crystal structure of LpxC from Pseudomonas aeruginosa complexed with the potent BB-78485 inhibitor.. Protein Sci., **17**, 450-457 (2008)

streptothricin hydrolase 3.5.2.19

1 Nomenclature

EC number
3.5.2.19

Systematic name
streptothricin-F hydrolase

Recommended name
streptothricin hydrolase

Synonyms
sstH <3> (<3> gene name [2]) [2]
sttH <1,2,3> (<1,2,3> gene name [1,3]) [1,3]

2 Source Organism

<1> *Streptomyces albulus* [1]
<2> *Streptomyces noursei* (UNIPROT accession number: C5NU54) [1]
<3> *Streptomyces albulus* (UNIPROT accession number: Q1MW86) [2,3]

3 Reaction and Specificity

Catalyzed reaction
streptothricin-F + H_2O = streptothricin-F acid

Natural substrates and products
S streptothricin-D + H_2O <2> (Reversibility: ?) [1]
P streptothricin-D acid
S streptothricin-F + H_2O <2> (Reversibility: ?) [1]
P streptothricin-F acid
S Additional information <3> (<3> the true role of SttH may not be its involvement in resistance against streptothricins, instead, it may catalyze the hydrolysis of naturally occurring cyclic amide compounds in the metabolism of Streptomyces albulus [3]) (Reversibility: ?) [3]
P ?

Substrates and products
S streptothricin-D + H_2O <1,2,3> (Reversibility: ?) [1,2]
P streptothricin-D acid (<1,2,3> the product is identified by reverse-phase HPLC [1,2])

D. Schomburg and I. Schomburg (eds.), *Class 3.4–6 Hydrolases, Lyases, Isomerases, Ligases: EC 3.4–6*, Springer Handbook of Enzymes S10, DOI 10.1007/978-3-642-36260-6_20,

S streptothricin-F + H_2O <1,2,3> (Reversibility: ?) [1,2]
P streptothricin-F acid (<1,2,3> the product is identified by reverse-phase HPLC [1,2])
S Additional information <3> (<3> the true role of SttH may not be its involvement in resistance against streptothricins, instead, it may catalyze the hydrolysis of naturally occurring cyclic amide compounds in the metabolism of Streptomyces albulus [3]; <3> this enzyme catalyzes the hydrolysis of the amide bond of streptolidine lactam, thereby conferring streptothricin resistance [3]) (Reversibility: ?) [3]
P ?

Metals, ions
Additional information <3> (<3> no metal ions required [2]) [2]

K_m-Value (mM)
0.96 <3> (streptothricin-F, <3> pH 6.5, 30°C [2]) [2]
1.3 <2> (streptothricin-F, <2> pH 6.5, 30°C [1]) [1]
3.1 <1> (streptothricin-F, <1> pH 6.5, 30°C [1]) [1]
3.2 <2> (streptothricin-D, <2> pH 6.5, 30°C [1]) [1]
5.74 <3> (streptothricin-D, <3> pH 6.5, 30°C [2]) [2]
17.2 <1> (streptothricin-D, <1> pH 6.5, 30°C [1]) [1]

pH-Optimum
6.5 <3> [2]
7 <1,2> [1]

Temperature optimum (°C)
45 <3> [2]
55 <1,2> [1]

Temperature range (°C)
45-65 <3> (<3> 45°C: maximal activity, 65°C: about 90% of maximal activity [2]) [2]

4 Enzyme Structure

Molecular weight
50000 <3> (<3> gel filtration [2]) [2]

5 Isolation/Preparation/Mutation/Application

Cloning
<1> (expression in Escherichia coli) [1]
<2> (expression in Escherichia coli) [1]
<3> [2]

Engineering

C158S <2> (<2> no activity detected [1]) [1]
C176S <1> (<1> no activity detected [1]) [1]

References

[1] Maruyama, C.; Hamano, Y.: The biological function of the bacterial isochorismatase-like hydrolase SttH. Biosci. Biotechnol. Biochem., **73**, 2494-2500 (2009)
[2] Hamano, Y.; Matsuura, N.; Kitamura, M.; Takagi, H.: A novel enzyme conferring streptothricin resistance alters the toxicity of streptothricin D from broad-spectrum to bacteria-specific. J. Biol. Chem., **281**, 16842-16848 (2006)
[3] Hamano, Y.; Maruyama, C.; Kimoto, H.: Construction of a knockout mutant of the Streptothricin-resistance gene in Streptomyces albulus by electroporation. Actinomycetologica, **20**, 35-41 (2006)

5-nitroanthranilic acid aminohydrolase 3.5.99.8

1 Nomenclature

EC number
3.5.99.8

Systematic name
5-nitroanthranilate aminohydrolase

Recommended name
5-nitroanthranilic acid aminohydrolase

Synonyms
5NAA deaminase <1> [1]
NAAA <1> [1]

2 Source Organism

<1> *Bradyrhizobium sp.* (UNIPROT accession number: D3WZ85) [1]

3 Reaction and Specificity

Catalyzed reaction
5-nitroanthranilate + H_2O = 5-nitrosalicylate + NH_3

Natural substrates and products
S 5-nitroanthranilate + H_2O <1> (<1> initial step in biodegradation of 5-nitroanthranilic acid as sole carbon, nitrogen and energy source [1]) (Reversibility: ?) [1]
P 5-nitrosalicylate + NH_3

Substrates and products
S 5-nitroanthranilate + H_2O <1> (<1> initial step in biodegradation of 5-nitroanthranilic acid as sole carbon, nitrogen and energy source [1]) (Reversibility: ?) [1]
P 5-nitrosalicylate + NH_3

Cofactors/prosthetic groups
Additional information <1> (<1> no added cofactors are required for the transformation [1]) [1]

D. Schomburg and I. Schomburg (eds.), *Class 3.4–6 Hydrolases, Lyases, Isomerases, Ligases: EC 3.4–6*, Springer Handbook of Enzymes S10, DOI 10.1007/978-3-642-36260-6_21,

5 Isolation/Preparation/Mutation/Application

Cloning

<1> (expression in Escherichia coli) [1]

References

[1] Qu, Y.; Spain, J.C.: Biodegradation of 5-nitroanthranilic acid by Bradyrhizobium sp. strain JS329. Appl. Environ. Microbiol., **76**, 1417-1422 (2010)

Mn^{2+}-dependent ADP-ribose/CDP-alcohol diphosphatase 3.6.1.53

1 Nomenclature

EC number
3.6.1.53

Systematic name
CDP-choline phosphohydrolase

Recommended name
Mn^{2+}-dependent ADP-ribose/CDP-alcohol diphosphatase

Synonyms
ADPRibase-I <2> (<2> isozyme [2]) [2]
ADPRibase-II <2> (<2> isozyme [2]) [2]
ADPRibase-Mn <1,2> [2,3]
Mn^{2+}-dependent ADP-ribose/CDP-alcohol pyrophosphatase <1,2> [2,3]

2 Source Organism

<1> *Rattus norvegicus* [1,3]
<2> *Rattus norvegicus* (UNIPROT accession number: Q5M886) [2]
<3> *Mus musculus* (UNIPROT accession number: Q99KS6) [2]

3 Reaction and Specificity

Catalyzed reaction
CDP-choline + H_2O = CMP + phosphocholine
ADP-ribose + H_2O = AMP + D-ribose 5-phosphate

Natural substrates and products
S ADP-ribose + H_2O <1> (<1> best substrate [3]) (Reversibility: ?) [3]
P AMP + D-ribose 5-phosphate
S cyclic ADP-ribose + H_2O <1> (<1> cADPR is an ADPRibase-Mn ligand and substrate [3]) (Reversibility: ?) [3]
P N^1-(5-phosphoribosyl)-AMP
S Additional information <1> (<1> ADPRibase-Mn hydrolyzes the phosphoanhydride linkages of ADP-ribose, CDP-choline, CDP-glycerol, CDP-ethanolamine, and ADP with decreasing efficiencies, requiring low micromolar Mn^{2+} concentrations not substituted by Mg^{2+}. ADPRibase-Mn hy-

D. Schomburg and I. Schomburg (eds.), *Class 3.4–6 Hydrolases, Lyases, Isomerases, Ligases: EC 3.4–6*, Springer Handbook of Enzymes S10, DOI 10.1007/978-3-642-36260-6_22,

drolyzes ADP-ribose, CDP-choline, CDP-glycerol and CDP-ethanolamine with decreasing catalytic efficiencies [3]) [3]
P ?

Substrates and products

S ADP + H_2O <1,2> (<2> 26% of the activity with ADP-ribose [2]; <1> 27% of the activity with ADP-ribose [1]) (Reversibility: ?) [1,2]
P AMP + phosphate
S ADP + H_2O <2> (<2> 27% activity at 0.5 mM substrate compared to ADP-ribose [2]) (Reversibility: ?) [2]
P ?
S ADP-ribose + H_2O <1,2> (<1> best substrate [3]; <2> 100% activity at 0.5 mM substrate [2]) (Reversibility: ?) [1,2,3]
P AMP + D-ribose 5-phosphate
S CDP-choline + H_2O <1,2> (<1> 140% of the activity with ADP-ribose [1]; <2> 156% of the activity with ADP-ribose [2]; <2> 140% activity at 0.5 mM substrate compared to ADP-ribose [2]) (Reversibility: ?) [1,2]
P CMP + phosphocholine
S CDP-ethanolamine + H_2O <1,2> (<2> 84% of the activity with ADP-ribose [2]; <1> 89% of the activity with ADP-ribose [1]) (Reversibility: ?) [1,2]
P CMP + phosphoethanolamine
S CDP-ethanolamine + H_2O <2> (<2> 89% activity at 0.5 mM substrate compared to ADP-ribose [2]) (Reversibility: ?) [2]
P ?
S CDP-glycerol + H_2O <1,2> (<2> 103% of the activity with ADP-ribose [2]; <1> 89% of the activity with ADP-ribose [1]) (Reversibility: ?) [1,2]
P CMP + phosphoglycerol
S CDP-glycerol + H_2O <2> (<2> 89% activity at 0.5 mM substrate compared to ADP-ribose [2]) (Reversibility: ?) [2]
P ?
S FAD + H_2O <1> (Reversibility: ?) [1]
P ? (<1> 39% of the activity with ADP-ribose [1])
S IDP-ribose + H_2O <1> (Reversibility: ?) [1]
P IMP + D-ribose 5-phosphate (<1> 105% of the activity with ADP-ribose [1])
S NAD^+ + H_2O <1> (Reversibility: ?) [1]
P ? (<1> 23% of the activity with ADP-ribose [1])
S NADH + H^+ + H_2O <1> (Reversibility: ?) [1]
P ? (<1> 25% of the activity with ADP-ribose [1])
S adenosine 5'-diphospho-5'-adenosine + H_2O <1> (Reversibility: ?) [1]
P AMP (<1> 45% of the activity with ADP-ribose [1])
S cyclic ADP-ribose + H_2O <1> (<1> ADPRibase-Mn activity on cyclic ADP-ribose is 65fold less efficient than on ADP-ribose [3]) (Reversibility: ?) [3]
P N^1-(5-phosphoribosyl)-AMP + ?

S cyclic ADP-ribose + H_2O <1> (<1> cADPR is an ADPRibase-Mn ligand and substrate [3]; <1> product determination and analysis, cADPR is an ADPRibase-Mn ligand and substrate. ADPRibase-Mn activity on cADPR is 65fold less efficient than on ADP-ribose, the best substrate. Phosphohydrolytic pattern of the reaction, overview [3]) (Reversibility: ?) [3]
P N^1-(5-phosphoribosyl)-AMP
S Additional information <1,2> (<1> ADPRibase-Mn hydrolyzes the phosphoanhydride linkages of ADP-ribose, CDP-choline, CDP-glycerol, CDP-ethanolamine, and ADP with decreasing efficiencies, requiring low micromolar Mn^{2+} concentrations not substituted by Mg^{2+}. ADPRibase-Mn hydrolyzes ADP-ribose, CDP-choline, CDP-glycerol and CDP-ethanolamine with decreasing catalytic efficiencies [3]; <2> ADP-glucose, UDP-glucose, CDP-glucose, CDP, CMP, and AMP are not hydrolysed [2]) [2,3]
P ?

Inhibitors

o-phenanthroline <2> (<2> 5 mM causes near full inactivation in 1.5 h [2]) [2]
Additional information <2> (<2> not inhibitory: EDTA up to 2.5 mM [2]; <2> incubation with 2.5 mM EDTA does not affect ADPRibase-Mn activity [2]) [2]

Metals, ions

Mn^{2+} <1,2> (<1> required [1,3]; <1> dependent on [3]; <2> required. Concentration of $MnCl_2$ giving the half-maximal rate is 0.001-0.004 mM. Mn^{2+} cannot be replaced by Mg^{2+} [2]; <2> dependent on, ADPRibase-Mn is inactive without added Mn^{2+}, and it shows a high affinity for the cation, since saturation is observed at low-micromolar concentrations of Mn^{2+} well below the substrate concentration (0.5 mM), in no case can Mg^{2+} replace Mn^{2+} [2]) [1,2,3]
Additional information <1,2> (<2> Mg^{2+} cannot replace Mn^{2+} [2]; <1> Mg^{2+} cannot substitute for Mn^{2+} [1]) [1,2]

Turnover number (s^{-1})

0.87 <1> (cyclic ADP-ribose, <1> pH 8.5, 25°C [3]) [3]
4.4 <2> (ADP, <2> pH 7.5, 37°C [2]; <2> recombinant enzyme, in 50 mM Tris-HCl (pH 7.5), 0.1 mM $MnCl_2$, at 37°C [2]) [2]
12.8 <2> (ADP-ribose, <2> pH 7.5, 37°C [2]; <2> recombinant enzyme, in 50 mM Tris-HCl (pH 7.5), 01 mM $MnCl_2$, at 37°C [2]) [2]
28.1 <2> (CDP-glycerol, <2> pH 7.5, 37°C [2]; <2> recombinant enzyme, in 50 mM Tris-HCl (pH 7.5), 0.1 mM $MnCl_2$, at 37°C [2]) [2]
28.5 <2> (CDP-choline, <2> pH 7.5, 37°C [2]; <2> recombinant enzyme, in 50 mM Tris-HCl (pH 7.5), 0.1 mM $MnCl_2$, at 37°C [2]) [2]
41.3 <2> (CDP-ethanolamine, <2> pH 7.5, 37°C [2]; <2> recombinant enzyme, in 50 mM Tris-HCl (pH 7.5), 0.1 mM $MnCl_2$, at 37°C [2]) [2]

Specific activity (U/mg)

18.2 <1> (<1> pH 7.5, 37°C [1]) [1]
Additional information <1> [3]

K_m-Value (mM)
0.015 <1> (ADP-ribose, <1> pH 7.5, 37°C [1]) [1]
0.039 <2> (ADP-ribose, <2> pH 7.5, 37°C [2]; <2> recombinant enzyme, in 50 mM Tris-HCl (pH 7.5), 0.1 mM $MnCl_2$, at 37°C [2]) [2]
0.17 <1> (cyclic ADP-ribose, <1> pH 8.5, 25°C [3]) [3]
0.201 <2> (ADP, <2> pH 7.5, 37°C [2]; <2> recombinant enzyme, in 50 mM Tris-HCl (pH 7.5), 0.1 mM $MnCl_2$, at 37°C [2]) [2]
0.3 <2> (CDP-choline, <2> pH 7.5, 37°C [2]; <2> recombinant, in 50 mM Tris-HCl (pH 7.5), 0.1 mM $MnCl_2$, at 37°C [2]) [2]
0.304 <2> (CDP-glycerol, <2> pH 7.5, 37°C [2]; <2> recombinant enzyme, in 50 mM Tris-HCl (pH 7.5), 0.1 mM $MnCl_2$, at 37°C [2]) [2]
1.422 <2> (CDP-ethanolamine, <2> pH 7.5, 37°C [2]; <2> recombinant enzyme, in 50 mM Tris-HCl (pH 7.5), 0.1 mM $MnCl_2$, at 37°C [2]) [2]

pH-Optimum
6-8 <2> (<2> activity towards ADP- and CDP-alcohols [2]) [2]
7.5-8.5 <1> (<1> assay at [3]) [3]
8-8.5 <2> (<2> ADP-ribose hydrolase activity [2]) [2]
9 <1> [1]

pH-Range
6-10 <2> [2]

pi-Value
4.3 <1> (<1> isoelectric focusing [1]) [1]

Temperature optimum (°C)
25 <1> (<1> assay at [3]) [3]

4 Enzyme Structure

Molecular weight
30000 <2> (<2> gel filtration [2]) [2]
32000 <1> (<1> gel filtration [1]) [1]
38000 <2> (<2> SDS-PAGE [2]) [2]
39360 <2> (<2> calculated from amino acid sequence [2]) [2]

Subunits
monomer <2> (<2> 1 * 39360, calculated, 1 * 40000, SDS-PAGE, enzyme plus N-terminal extension GPLGSPNS left after proteolysis of recombinant fusion protein [2]; <2> 1 * 30000, gel filtration [2]) [2]

5 Isolation/Preparation/Mutation/Application

Source/tissue
liver <1,2> [1,2]
skeletal muscle <2> [2]

spleen <2> (<2> ADPRibase-Mn activity in spleen is 2.5-5fold higher than in liver and muscle [2]) [2]
splenocyte <2> [2]
thymus <2> (<2> ADPRibase-Mn activity in thymus is 2.5-5fold higher than in liver and muscle [2]) [2]
Additional information <3> (<3> preferential expression in immune cells [2]) [2]

Purification

<1> [1]
<2> (glutathione-Sepharose column chromatography) [2]
<2> (recombinant GSt-fusion protein, in-column proteolysis of fusion) [2]

Crystallization

<1> (coordinates of rat ADPRibase-Mn, modelled by homology to the X-ray structure of its zebrafish orthologue, taken from the SWISS-MODEL repository, accession code q5m88. cADPR docking to a model of ADPRibase-Mn and molecular dynamics simulation, ADPRibase-Mn complexes with docked ligands show the active center in a closed conformation, overview) [3]
<2> (homology modeling based on crystal structure of the Danio rerio protein, Protein Data Base entry 2NXF, and docking of ADP-ribose) [2]

Cloning

<2> (expressed in Escherichia coli BL21 cells) [2]
<2> (expression as GST-fusion protein) [2]

6 Stability

pH-Stability

6-8 <2> (<2> the activities towards ADP and CDP-alcohols are highest at pH 6-8 and decrease abruptly at higher pH [2]) [2]

Storage stability

<2>, -20°C, 1 mM EDTA, stable for months [2]

References

[1] Canales, J.; Pinto, R.M.; Costas, M.J.; Hernandez, M.T.; Miro, A.; Bernet, D.; Fernandez, A.; Cameselle, J.C.: Rat liver nucleoside diphosphosugar or diphosphoalcohol pyrophosphatase different from nucleotide pyrophosphatase or phosphodiesterase I: substrate specificities of Mg^{2+}- and/or Mn^{2+}-depenent hydrolases acting on ADP-ribose. Biochim. Biophys. Acta, **1246**, 167-177 (1995)
[2] Canales, J.; Fernandez, A.; Ribeiro, J.M.; Cabezas, A.; Rodrigues, J.R.; Cameselle, J.C.; Costas, M.J.: Mn^{2+}-dependent ADP-ribose/CDP-alcohol pyrophosphatase: a novel metallophosphoesterase family preferentially expressed in rodent immune cells. Biochem. J., **413**, 103-113 (2008)

[3] Canales, J.; Fernandez, A.; Rodrigues, J.R.; Ferreira, R.; Ribeiro, J.M.; Cabezas, A.; Costas, M.J.; Cameselle, J.C.: Hydrolysis of the phosphoanhydride linkage of cyclic ADP-ribose by the Mn^{2+}-dependent ADP-ribose/CDP-alcohol pyrophosphatase. FEBS Lett., **583**, 1593-1598 (2009)

UDP-2,3-diacylglucosamine diphosphatase 3.6.1.54

1 Nomenclature

EC number
3.6.1.54

Systematic name
UDP-2,3-bis[(3R)-3-hydroxymyristoyl]-α-D-glucosamine 2,3-bis[(3R)-3-hydroxymyristoyl]-β-D-glucosaminyl 1-phosphate phosphohydrolase

Recommended name
UDP-2,3-diacylglucosamine diphosphatase

Synonyms
LpxH <1,2> [1,2]
UDP-2,3-diacylglucosamine hydrolase <1> [1]
UDP-2,3-diacylglucosamine pyrophosphatase <1> [1]
YbbF <1> [1]

CAS registry number
469863-59-0

2 Source Organism

<1> *Escherichia coli* [1,2]
<2> *Pseudomonas aeruginosa* [2]

3 Reaction and Specificity

Catalyzed reaction
UDP-2,3-bis[(3R)-3-hydroxymyristoyl]-α-D-glucosamine + H_2O = 2,3-bis[(3R)-3-hydroxymyristoyl]-β-D-glucosaminyl 1-phosphate + UMP

Natural substrates and products
S UDP-2,3-bis((3R)-3-hydroxymyristoyl)α-D-glucosamine + H_2O <1,2> (<1> a step of lipid A biosynthesis. LpxH is essential in Escherichia coli [2]; <1> step of lipid A biosynthesis [1]; <2> step of lipid A biosynthesis. Pseudomonas aeruginosa LpxH catalyzes UDP-2,3-diacylglucosamine hydrolysis in vitro and can substitute for Escherichia coli lpxH in vivo [2]) (Reversibility: ?) [1,2]
P 2,3-bis((3R)-3-hydroxymyristoyl)-β-D-glucosaminyl 1-phosphate + UMP

D. Schomburg and I. Schomburg (eds.), *Class 3.4–6 Hydrolases, Lyases, Isomerases, Ligases: EC 3.4–6*, Springer Handbook of Enzymes S10, DOI 10.1007/978-3-642-36260-6_23,

Substrates and products

- **S** UDP-2,3-bis((3R)-3-hydroxymyristoyl)α-D-glucosamine + H_2O <1,2> (<1> a step of lipid A biosynthesis. LpxH is essential in Escherichia coli [2]; <1> step of lipid A biosynthesis [1]; <2> step of lipid A biosynthesis. Pseudomonas aeruginosa LpxH catalyzes UDP-2,3-diacylglucosamine hydrolysis in vitro and can substitute for Escherichia coli lpxH in vivo [2]; <2> Pseudomonas aeruginosa LpxH catalyzes UDP-2,3-diacylglucosamine hydrolysis in vitro and can substitute for Escherichia coli lpxH in vivo [2]) (Reversibility: ?) [1,2]
- **P** 2,3-bis((3R)-3-hydroxymyristoyl)-β-D-glucosaminyl 1-phosphate + UMP
- **S** UDP-N2,O3-bis((3R)-3-hydroxymyristoyl)-α-D-glucosamine + H_2O <1> (<1> strict requirement for a diacylated substrate. LpxH hydrolysis incorporates H218O into UMP by catalyzing the attack of water on the α-phosphorus atom of UDP-2,3-diacylglucosamine [1]) (Reversibility: ?) [1]
- **P** N^2,O^3-bis((3R)-3-hydroxymyristoyl)-α-D-glucosamine 1-phosphate + UMP
- **S** Additional information <1> (<1> no activity with UDP-N-acetylglucosamine and UDP-3-O-(R)-(3-hydroxymyristoyl)glucosamine, LpxH does not cleave CDP-diacylglycerol [1]) [1]
- **P** ?

Inhibitors

Triton X-100 <1> (<1> 0.01% [1]) [1]

Metals, ions

Mn^{2+} <1> (<1> stimulates [1]) [1]

Specific activity (U/mg)

63.2 <1> [1]

K_m-Value (mM)

0.0617 <1> (UDP-N^2,O^3-bis((3R)-3-hydroxymyristoyl)-α-D-glucosamine, <1> pH 8.0, 30°C [1]) [1]

pH-Optimum

8 <1> [1]

pH-Range

6.5-9.5 <1> (<1> pH 6.5: about 50% of maximal activity, pH 9.5: about 50% of maximal activity [1]) [1]

Temperature optimum (°C)

30 <1> (<1> assay at [1]) [1]

4 Enzyme Structure

Subunits

? <1> (<1> x * 26893, calculated from sequence [1]) [1]

5 Isolation/Preparation/Mutation/Application

Purification

<1> (partial) [1]

Cloning

<1> (lpxH overexpression is toxic to cells) [1]

References

[1] Babinski, K.J.; Ribeiro, A.A.; Raetz, C.R.: The Escherichia coli gene encoding the UDP-2,3-diacylglucosamine pyrophosphatase of lipid A biosynthesis. J. Biol. Chem., **277**, 25937-2546 (2002)

[2] Babinski, K.J.; Kanjilal, S.J.; Raetz, C.R.: Accumulation of the lipid A precursor UDP-2,3-diacylglucosamine in an Escherichia coli mutant lacking the lpxH gene. J. Biol. Chem., **277**, 25947-25956 (2002)

DNA helicase 3.6.4.12

1 Nomenclature

EC number
3.6.4.12

Systematic name
ATP phosphohydrolase (DNA helix unwinding)

Recommended name
DNA helicase

Synonyms
3' to 5' DNA helicase <28> [35]
3'-5' DNA helicase <11> [55]
3'-5' PfDH <11> [55]
5' to 3' DNA helicase <26,27> [19,42]
AvDH1 <47> [37]
BACH1 helicase <19> [34]
BLM <3> [28]
BLM protein <3> [28]
BRCA1-associated C-terminal helicase <19> [34]
BcMCM <8> [52]
CeWRN-1 <43> [9]
DDX25 <3,48> [36]
DNA helicase 120 <7> [15]
DNA helicase A <4> [8]
DNA helicase E <5> [44]
DNA helicase II <9> [7]
DNA helicase III <4> [27]
DNA helicase RECQL5β <44> [17]
DNA helicase VI <3> [45]
Dbp9p <46> (<46> a member of the DEAD box protein family [24]) [24]
DmRECQ5 <1> [50]
DnaB helicase <29> [23]
E1 helicase <17> [58]
GRTH/DDX25 <3,48> [36]
HCoV SF1 helicase <23> [3]
HCoV helicase <23> [3]
HDH IV <3> [45]
Hel E <5> [44]
Hmi1p <40> [60]
MCM helicase <6,35,38> [43,54]

D. Schomburg and I. Schomburg (eds.), *Class 3.4–6 Hydrolases, Lyases, Isomerases, Ligases: EC 3.4–6*, Springer Handbook of Enzymes S10, DOI 10.1007/978-3-642-36260-6_24,

MCM protein <6,35> [43]
MER3 helicase <22> [30]
MER3 protein <22> [30]
MPH1 <28> [35]
NS3 <12,50> (<12,50> ambiguous [38,65,66]) [38,65,66]
NS3 NTPase/helicase <14> (<14> ambiguous [67]) [67]
NS3 protein <12> (<12> ambiguous [63]) [63]
NTPase/helicase <12,16> (<12> ambiguous [61]) [61,64]
PDH120 <7> [15]
PIF1 <33> [51]
PIF1 helicase <33> [51,53]
PcrA <37> [20]
PcrA helicase <37,41,49> [20,21,39]
PcrASpn <41> [21]
PfDH A <11> [55]
Pfh1p <27> [42]
RECQ5 <1> [49,50]
RECQ5 helicase <1> (<1> small isoform [49]) [49]
RECQL5β <44> [17]
REcQ <31> [13]
RSF1010 RepA <30> [5]
RecG <45> [6]
RecQ helicase <32> [56]
RecQsim <32> [56]
Rep52 <24> [40]
Rrm3p <26> [19]
Sgs1 <36> [29]
Sgs1 DNA helicase <36> [29]
TWINKLE <21> [33]
Tth UvrD <20> [16]
UvrD <20,42> [16,22]
UvrD helicase <39> [18]
WRN <18> [31]
WRN RecQ helicase <18> [12]
WRN helicase <18> [12]
WRN protein <18> [12]
WRN-1 RecQ helicase <43> [9]
Werner Syndrome helicase <18> [31]
Werner syndrome RecQ helicase <18> [12]
dheI I <1> [46]
dnaB <29> [23]
hPif1 <33> [53]
helicase DnaB <2> [10]
helicase II <25> [25]
helicase PcrA <49> [39]
helicase UvrD <20> [16]
helicase domain of bacteriophage T7 gene 4 protein <10> [47]

non structural protein 3 <12> (<12> ambiguous [61,62]) [61,62]
nonstructural protein 3 <12,14,50,51> (<12,14,50> ambiguous [38,63,65, 66,67]; <51> ambigous [4]) [4,38,63,65,66,67]
protein NS3 <12> (<12> ambiguous [62]) [62]
scHelI <4> [26]
urvD <25> [25]

2 Source Organism

<1> *Drosophila melanogaster* [46,49,50]
<2> *Escherichia coli* [10]
<3> *Homo sapiens* [28,36,45,48]
<4> *Saccharomyces cerevisiae* [8,26,27]
<5> *Bos taurus* [44]
<6> *Methanothermobacter thermautotrophicus* [43]
<7> *Pisum sativum* [14,15]
<8> *Bacillus cereus* [52]
<9> *Schizosaccharomyces pombe* [7]
<10> *Enterobacteria phage T7* [47]
<11> *Plasmodium falciparum* [55]
<12> *Hepatitis C virus* [1,11,38,61,62,63,65]
<13> *Human herpesvirus 1* [59]
<14> *West Nile virus* [2,67]
<15> *SARS coronavirus* (UNIPROT accession number: P0C6X7) [32]
<16> *SARS coronavirus* [64]
<17> *Human papillomavirus type 11* (UNIPROT accession number: P04014) [58]
<18> *Homo sapiens* (UNIPROT accession number: Q14191) [12,31]
<19> *Homo sapiens* (UNIPROT accession number: O14867) [34]
<20> *Thermus thermophilus HB8* (UNIPROT accession number: O24736) [16]
<21> *Homo sapiens* (UNIPROT accession number: Q96RR1) [33]
<22> *Saccharomyces cerevisiae* (UNIPROT accession number: P51979) [30]
<23> *Human coronavirus 229E* (UNIPROT accession number: P0C6X1) [3]
<24> *Adeno-associated virus - 2* (UNIPROT accession number: Q89270) [40]
<25> *Escherichia coli* (UNIPROT accession number: P03018) [25]
<26> *Saccharomyces cerevisiae* (UNIPROT accession number: P07271) [19]
<27> *Schizosaccharomyces pombe* (UNIPROT accession number: Q9UUA2) [42]
<28> *Saccharomyces cerevisiae* (UNIPROT accession number: P40562) [35]
<29> *Bacillus anthracis* (UNIPROT accession number: Q81JI8) [23]
<30> *Escherichia coli* (UNIPROT accession number: P20356) [5]
<31> *Escherichia coli* (UNIPROT accession number: P15043) [13]
<32> *Arabidopsis thaliana* (UNIPROT accession number: Q6Y5A8) [56]
<33> *Homo sapiens* (UNIPROT accession number: Q9H611) [41,51,53]
<34> *Homo sapiens* (UNIPROT accession number: P46063) [57]
<35> *Sulfolobus solfataricus* (UNIPROT accession number: Q9UXG1) [43]
<36> *Saccharomyces cerevisiae* (UNIPROT accession number: P35187) [29]

<37> *Bacillus anthracis* (UNIPROT accession number: Q6I4A9) [20]
<38> *Halobacterium sp.* NRC-1 [54]
<39> *Plasmodium falciparum* (UNIPROT accession number: Q8I3W6) [18]
<40> *Saccharomyces cerevisiae* (UNIPROT accession number: Q12039) [60]
<41> *Streptococcus pneumoniae* (UNIPROT accession number: Q8DPU8) [21]
<42> *Mycobacterium tuberculosis* (UNIPROT accession number: P64320) [22]
<43> *Caenorhabditis elegans* (UNIPROT accession number: Q19546) [9]
<44> *Mus musculus* (UNIPROT accession number: Q8VID5) [17]
<45> *Thermotoga maritima* (UNIPROT accession number: Q9WY48) [6]
<46> *Saccharomyces cerevisiae* (UNIPROT accession number: Q06218) [24]
<47> *Apocynum venetum* (UNIPROT accession number: A8D930) [37]
<48> *Rattus norvegicus* (UNIPROT accession number: Q9QY16) [36]
<49> *Geobacillus stearothermophilus* (UNIPROT accession number: P56255) [39]
<50> *Hepatitis C virus* (UNIPROT accession number: Q9WPH5) [66]
<51> *Japanese encephalitis virus* (UNIPROT accession number: P27395) [4]

3 Reaction and Specificity

Catalyzed reaction

ATP + H_2O = ADP + phosphate

Natural substrates and products

S ATP + H_2O <3,6,7,12,14,15,16,18,20,21,22,26,27,32,35,39,40,41,43,46,47,48,49,51> (<18> 3-5 helicase activity. WRN helicase is involved in preserving DNA integrity during replication. It is proposed that WRN helicase can function in coordinating replication fork progression with replication stress-induced fork remodeling [12]; <27> 5 to 3 DNA helicase. ATPase/helicase activity of Pfh1p is essential. Maintenance of telomeric DNA is not the sole essential function of Pfh1p. Although mutant spores depleted for Pfh1p proceed through S phase, they arrest with a terminal cellular phenotype consistent with a postinitiation defect in DNA replication. Telomeric DNA is modestly shortened in the absence of Pfh1p [42]; <26> 5 to 3 DNA helicase. The ATPase/helicase activity of Rrm3p is required for its role in telomeric and subtelomeric DNA replication. Because Rrm3p is telomere-associated in vivo, it likely has a direct role in telomere replication [19]; <47> AvDH1 belonging to the DEAD-box helicase family is induced by salinity, functions as a typical helicase to unwind DNA and RNA, and may play an important role in salinity tolerance [37]; <40> DNA helicase Hmi1p is involved in the maintenance of mitochondrial DNA [60]; <6,35> during chromosomal DNA replication, the replicative helicase unwinds the duplex DNA to provide the single-stranded DNA substrate for the polymerase. In archaea, the replicative helicase is the minichromosome maintenance complex. The enzyme utilizes the energy of ATP hydrolysis to translocate along one strand of the duplex and unwind the complementary strand [43]; <3,48> gonadotropin-regulated testicular he-

licase (GRTH/DDX25), a target of gonadotropin and androgen action, is a post-transcriptional regulator of key spermatogenesis genes [36]; <20> helicase UvrD protein plays an important role in nucleotide excision repair, mismatch repair, rolling circular plasmid replication, and in DNA replication [16]; <39> helicases play an essential role in nearly all the nucleic acid metabolic processes, catalyzing the transient opening of the duplex nucleic acids in an ATP-dependent manner [18]; <32> involved in DNA recombination, repair and genome stability maintenance [56]; <22> meiosis-specific MER3 protein is required for crossing over, which ensures faithful segregation of homologous chromosomes at the first meiotic division [30]; <41> PcrA is a chromosomally encoded DNA helicase of gram-positive bacteria involved in replication of rolling circle replicating plasmids [21]; <43> the ability of CeWRN-1 to unwind DNA structures may improve the access for DNA repair and replication proteins that are important for preventing the accumulation of abnormal structures, contributing to genomic stability [9]; <12> the C-terminal portion of hepatitis C virus nonstructural protein 3 (NS3) forms a three domain polypeptide that possesses the ability to travel along RNA or single-stranded DNA (ssDNA) in a 3' to 5' direction. Driven by the energy of ATP hydrolysis, this movement allows the protein to displace complementary strands of DNA or RNA [11]; <18> the DNA-dependent ATPase utilizes the energy from ATP hydrolysis to unwind double-stranded DNA. The enzyme unwinds two important intermediates of replication/repair, a 5-ssDNA flap substrate and a synthetic replication fork. The enzyme is able to translocate on the lagging strand of the synthetic replication fork to unwind duplex ahead of the fork. For the 5-flap structure, the enzyme specifically displaces the 5-flap oligonucleotide, suggesting a role of the enzyme in Okazaki fragment processing. The ability of the enzyme to target DNA replication/repair intermediates may be relevant to its role in genome stability maintenance [31]; <21> TWINKLE is the helicase at the mitochondrial DNA replication fork [33]; <12> catalytic DNA helicase activity is coupled with NTPase and is stimulated by ATP [62]; <16> DNA-unwinding activity [64]; <12> multifunctional enzyme possessing serine protease, NTPase, DNA and RNA unwinding activities [65]) (Reversibility: ?) [4,9,11,12,15,16,18,19,21,24,30,31,32,33,36,37,39,42,43,56,60,61,62,64,65,67]

P ADP + phosphate

S NTP + H_2O <12> (<12> different NTP binding rate and processivity, DNA unwinding of nonstructural protein 3 [38]) (Reversibility: ?) [38]

P NDP + phosphate

S dNTP + H_2O <12> (<12> dNTPs support faster DNA unwinding mediated by nonstructural protein 3 [38]) (Reversibility: ?) [38]

P dNDP + phosphate

Substrates and products

S 2'(3')-O-(N-methylanthraniloyl)ATP + H_2O <49> (<49> the fluorescent ATP analogue is used throughout all experiments to provide a complete ATPase cycle for a single nucleotide species [39]) (Reversibility: ?) [39]

P 2'(3')-O-(N-methylanthraniloyl)ADP + phosphate
S 2',3'-ATP + H_2O <12> (<12> 274% of the ability to support helicase catalyzed DNA unwinding compared to ATP [38]) (Reversibility: ?) [38]
P 2',3'-ADP + phosphate
S 2',3'-dATP + H_2O <12> (<12> 274% relative ability to support DNA unwinding by nonstructural protein 3, reported as percentage relative to ATP [38]) (Reversibility: ?) [38]
P 2',3'-dADP + phosphate
S 2'-O-methyl-ATP + H_2O <12> (<12> 34% of the ability to support helicase catalyzed DNA unwinding compared to ATP [38]; <12> 34% relative ability to support DNA unwinding by nonstructural protein 3, reported as percentage relative to ATP [38]) (Reversibility: ?) [38]
P 2'-O-methyl-ADP + phosphate
S 2'-amino-ATP + H_2O <12> (<12> 28% of the ability to support helicase catalyzed DNA unwinding compared to ATP [38]; <12> 28% relative ability to support DNA unwinding by nonstructural protein 3, reported as percentage relative to ATP [38]) (Reversibility: ?) [38]
P 2'-amino-ADP + phosphate
S 2'-ara-ATP + H_2O <12> (<12> 102% of the ability to support helicase catalyzed DNA unwinding compared to ATP [38]) (Reversibility: ?) [38]
P 2'-ara-ADP + phosphate
S 2'-azido-ATP + H_2O <12> (<12> 61% of the ability to support helicase catalyzed DNA unwinding compared to ATP [38]; <12> 61% relative ability to support DNA unwinding by nonstructural protein 3, reported as percentage relative to ATP [38]) (Reversibility: ?) [38]
P 2'-azido-ADP + phosphate
S 2'-dATP + H_2O <12> (<12> 157% relative ability to support DNA unwinding by nonstructural protein 3, reported as percentage relative to ATP [38]) (Reversibility: ?) [38]
P 2'-dADP + phosphate
S 2'-fluoro-ATP + H_2O <12> (<12> 145% of the ability to support helicase catalyzed DNA unwinding compared to ATP [38]; <12> 145% relative ability to support DNA unwinding by nonstructural protein 3, reported as percentage relative to ATP [38]) (Reversibility: ?) [38]
P 2'-fluoro-ADP + phosphate
S 2-amino-ATP + H_2O <12> (<12> 78% of the ability to support helicase catalyzed DNA unwinding compared to ATP [38]; <12> 78% relative ability to support DNA unwinding by nonstructural protein 3, reported as percentage relative to ATP [38]) (Reversibility: ?) [38]
P 2-amino-ADP + phosphate
S 3'-dATP + H_2O <12> (<12> 307% relative ability to support DNA unwinding by nonstructural protein 3, reported as percentage relative to ATP [38]) (Reversibility: ?) [38]
P 3'-dADP + phosphate
S ATP + H_2O <1,2,3,4,5,6,7,8,9,10,11,12,13,14,15,16,17,18,19,20,21,22,23,24,25,26,27,28,29,30,31,32,33,34,35,36,37,38,39,40,41,42,43,44,45,46,47,48,49,51> (<18> 3-5 helicase activity. WRN helicase is involved in preserving DNA

integrity during replication. It is proposed that WRN helicase can function in coordinating replication fork progression with replication stress-induced fork remodeling [12]; <27> 5 to 3 DNA helicase. ATPase/helicase activity of Pfh1p is essential. Maintenance of telomeric DNA is not the sole essential function of Pfh1p. Although mutant spores depleted for Pfh1p proceed through S phase, they arrest with a terminal cellular phenotype consistent with a postinitiation defect in DNA replication. Telomeric DNA is modestly shortened in the absence of Pfh1p [42]; <26> 5 to 3 DNA helicase. The ATPase/helicase activity of Rrm3p is required for its role in telomeric and subtelomeric DNA replication. Because Rrm3p is telomere-associated in vivo, it likely has a direct role in telomere replication [19]; <47> AvDH1 belonging to the DEAD-box helicase family is induced by salinity, functions as a typical helicase to unwind DNA and RNA, and may play an important role in salinity tolerance [37]; <40> DNA helicase Hmi1p is involved in the maintenance of mitochondrial DNA [60]; <6,35> during chromosomal DNA replication, the replicative helicase unwinds the duplex DNA to provide the single-stranded DNA substrate for the polymerase. In archaea, the replicative helicase is the minichromosome maintenance complex. The enzyme utilizes the energy of ATP hydrolysis to translocate along one strand of the duplex and unwind the complementary strand [43]; <3,48> gonadotropin-regulated testicular helicase (GRTH/DDX25), a target of gonadotropin and androgen action, is a post-transcriptional regulator of key spermatogenesis genes [36]; <20> helicase UvrD protein plays an important role in nucleotide excision repair, mismatch repair, rolling circular plasmid replication, and in DNA replication [16]; <39> helicases play an essential role in nearly all the nucleic acid metabolic processes, catalyzing the transient opening of the duplex nucleic acids in an ATP-dependent manner [18]; <32> involved in DNA recombination, repair and genome stability maintenance [56]; <22> meiosis-specific MER3 protein is required for crossing over, which ensures faithful segregation of homologous chromosomes at the first meiotic division [30]; <41> PcrA is a chromosomally encoded DNA helicase of gram-positive bacteria involved in replication of rolling circle replicating plasmids [21]; <43> the ability of CeWRN-1 to unwind DNA structures may improve the access for DNA repair and replication proteins that are important for preventing the accumulation of abnormal structures, contributing to genomic stability [9]; <12> the C-terminal portion of hepatitis C virus nonstructural protein 3 (NS3) forms a three domain polypeptide that possesses the ability to travel along RNA or single-stranded DNA (ssDNA) in a 3′ to 5′ direction. Driven by the energy of ATP hydrolysis, this movement allows the protein to displace complementary strands of DNA or RNA [11]; <18> the DNA-dependent ATPase utilizes the energy from ATP hydrolysis to unwind double-stranded DNA. The enzyme unwinds two important intermediates of replication/repair, a 5-ssDNA flap substrate and a synthetic replication fork. The enzyme is able to translocate on the lagging strand of the synthetic replication fork to unwind duplex ahead of the fork. For the 5-flap structure, the enzyme specifically displaces the 5-flap oligonucleotide, suggesting a role of the enzyme in Okazaki fragment processing. The ability of

the enzyme to target DNA replication/repair intermediates may be relevant to its role in genome stability maintenance [31]; <21> TWINKLE is the helicase at the mitochondrial DNA replication fork [33]; <18> 3-5 helicase activity [12]; <27> 5 to 3 DNA helicase [42]; <13> 5-3 unwinding activity, enzymatic functions of the two subunit helicase-primase complex (enzyme complex consisting of UL5 and UL52 gene functions): DNA-dependent ATPase, DNA primase, and DNA helicase activities [59]; <25> as a DNA-dependent ATPase, helicase II translocates processively along single-stranded DNA. The translocation of helicase II along single-stranded DNA is unidirectional and in th 3' to 5' direction with respect to the DNA strand on which the enzyme is bound [25]; <4> ATP hydrolysis is required for unwinding of DNA catalyzed by the DNA helicase, the enzyme moves in the 5' to 3' direction on a single-stranded DNA to catalyze unwinding of double-stranded regions of DNA in the 3 to 5 direction [27]; <7> ATP is the most active NTP. DNA helicase unwinds DNA unidirectionally from 3' to 5'. DNA helicase can unwind a 17-bp duplex whether it has unpaired single-stranded tails at both the 5' end and 3' end, at the 5' end or at the 3' end only, or at neither end. However, it fails to act on a blunt-ended 17-bp duplex DNA [14]; <43> ATP-dependent 3 to 5 helicase capable of unwinding a variety of DNA structures such as forked duplexes, Holliday junctions, bubble substrates, D-loops, and flap duplexes, and 3-tailed duplex substrates [9]; <6> ATP-dependent 3-5 helicase activity. During chromosomal DNA replication, the replicative helicase unwinds the duplex DNA to provide the single-stranded DNA substrate for the polymerase. In archaea, the replicative helicase is the minichromosome maintenance complex. The enzyme utilizes the energy of ATP hydrolysis to translocate along one strand of the duplex and unwind the complementary strand. ATP binding enhances DNA binding by the helicase. ATPase activity is substantially enhanced in presence of DNA. MCM protein binds DNA ends better than long circular substrates [43]; <35> ATP-dependent 3-5 helicase activity. During chromosomal DNA replication, the replicative helicase unwinds the duplex DNA to provide the single-stranded DNA substrate for the polymerase. In archaea, the replicative helicase is the minichromosome maintenance complex. The enzyme utilizes the energy of ATP hydrolysis to translocate along one strand of the duplex and unwind the complementary strand. Very limited stimulation of its ATPase activity by DNA [43]; <3> ATP-dependent DNA unwinding enzyme. HDH VI unwinds exclusively DNA duplexes with an annealed portion smaller than32 bp and prefers a replication fork-like structure of the substrate. It cannot unwind blunt-end duplexes and is inactive also on DNA-RNA or RNA-RNA hybrids. HDH VI unwinds DNA unidirectionally by moving in the 3 to 5 direction along the bound strand. ATP and dATP are equally good substrates [45]; <19> BACH1 preferentially binds and unwinds a forked duplex substrate compared with a duplex flanked by only one single-stranded DNA (ssDNA) tail. BACH1 helicase requires a minimal 5 ssDNA tail of 15 nucleotides for unwinding of conventional duplex DNA substrates. However, the enzyme is able to catalytically release the third strand of the homologous recombination intermediate D-loop structure irrespective of DNA tail

status. In contrast, BACH1 completely fails to unwind a synthetic Holliday junction structure. Moreover, BACH1 requires nucleic acid continuity in the 5 ssDNA tail of the forked duplex substrate within six nucleotides of the ssDNA-dsDNA junction to initiate efficiently DNA unwinding [34]; <8> BcMCM displays 3 to 5 helicase and ssDNA-stimulated ATPase activity. BcMCM is an active ATPase, and this activity is restricted to the MCM-AAA module [52]; <46> Dbp9p exhibits DNA-DNA and DNA-RNA helicase activity in the presence of ATP [24]; <1> Dhel I moves 5 to 3 on the DNA strand to which it is bound. Unwinding activity decreases with increasing length of the double-stranded region suggesting a distributive mode of action. ATP and dATP are the only nucleoside-5-triphosphates that support the strand displacement reaction. Both have an optimal concentration range between 1 and 2 mM [46]; <28> DNA helicase activity has a 3 to 5 polarity with respect to the DNA strand on which this protein translocates [35]; <24> DNA helicase with 3-to-5 polarity. No helicase activity in absence of NTP [40]; <3> DNA unwinding in 5 to 3 direction [48]; <36> exhibits an ATPase activity in the presence of single- or double-stranded DNA. Displacement of the DNA strand occurs in the 3 to 5 direction with respect to the single-stranded DNA flanking the duplex. The efficiency of unwinding is found to correlate inversely with the length of the duplex region. The recombinant Sgs1 fragment is found to bind more tightly to a forked DNA substrate than to either single or double-stranded DNA. Like the DNA-DNA helicase activity, unwinding of the DNA-RNA hybrid is driven by the hydrolysis of ATP or dATP [29]; <12> HCV helicase unwinds DNA at different rates depending on the nature and concentration of NTPs in solution. The fastest reactions are observed in the presence of CTP followed by ATP, UTP, and GTP. 3-deoxy-NTPs generally support faster DNA unwinding, with dTTP supporting faster rates than any other canonical (d)NTP. ATP is hydrolyzed far faster than DNA is unwound in the presence of both Mn^{2+} and Mg^{2+} [38]; <33> hPifHD (core helicase domain) only unwinds the substrate with a 5 single-stranded DNA (ssDNA) overhang and is a 5 to 3 helicase. Pif1 specifically recognizes and unwinds DNA structures resembling putative stalled replication forks. Notably, the enzyme requires both arms of the replication fork-like structure to initiate efficient unwinding of the putative leading replication strand of such substrates. This DNA structure-specific mode of initiation of unwinding is intrinsic to the conserved core helicase domain (hPifHD) that also possesses a strand annealing activity [53]; <4> hydrolyzes ATP and dATP with equal efficiency. ATPase activity of the enzyme is absolutely DNA-dependent. DNA sequences containing pyrimidine stretches are more effective activators than those containing purine stretches. poly(dC) appears to be the most effective activator of the ATPase activity. DNA helicase migrates on a DNA template in 5 to 3 direction [8]; <41> hydrolyzes both ATP and dATP at similar levels. The enzyme shows 5 to 3 and 3 to 5 DNA helicase activities and binds efficiently to partially duplex DNA containing a hairpin structure adjacent to a 6-nucleotide 5 or 3 single-stranded tail and one unpaired (flap) nucleotide in the complementary strand [21]; <42> only ATP and dATP support helicase activity. 80% of

the duplex is separated in the presence of 1 mM ATP in a 15 min reaction, 58% is unwound in the presence of 1 mM dATP. ATPase activity is dependent upon the presence of DNA. Oligonucleotides of 4 nucleotides are sufficient to promote the ATPase activity. UvrD preferentially unwinds 3-single-stranded tailed duplex substrates over 5-single-stranded ones, indicating that the protein has a duplex-unwinding activity with 3-to-5 polarity. A 3 single-stranded DNA tail of 18 nucleotides is required for effective unwinding. UvrD has an unwinding preference towards nicked DNA duplexes and stalled replication forks [22]; <37> PcrA shows 3 to 5 as well as 5 to 3 helicase activities, with substrates containing a duplex region and a 3 or 5 ss poly(dT) tail. PcrA also efficiently unwinds oligonucleotides containing a duplex region and a 5 or 3 ss tail with the potential to form a secondary structure [20]; <47> purified recombinant protein contains ATP-dependent DNA helicase activity, ATP-independent RNA helicase activity, and DNA- or RNA-dependent ATPase activity [37]; <1> RECQ5 unwinds duplex DNA with a 3-5 polarity. Unwinding of longer partial duplex DNA substrates requires a higher protein concentration than does unwinding of the 20bp partial duplex substrate. The unwinding reaction catalyzed by RECQ5 requires a nucleoside 5-phosphate. dATP is most effective. RECQ5 hydrolyzes dATP more rapidly than ATP regardless of the presence of ssDNA. Both ssDNA cofactors, M13mp18 ssDNA and poly(dT) strongly stimulate the dATPase activity of the protein [49]; <29> strong 5 to 3 DNA helicase activity. At both 0.1 and 0.5 mM, dATP produces comparable or slightly higher levels of unwinding than ATP [23]; <49> the chemical cleavage step is the rate-limiting step in the ATPase cycle and is essentially irreversible and results in the bound ATP complex being a major component at steady state. This cleavage step is greatly accelerated by bound DNA, producing the high activation of this protein compared to the protein alone. The data suggest the possibility that ADP is released in two steps, which results in bound ADP also being a major intermediate, with bound ADP*phosphate being a very small component. It therefore seems likely that the major transition in structure occurs during the cleavage step, rather than phosphate release [39]; <18> the DNA-dependent ATPase utilizes the energy from ATP hydrolysis to unwind double-stranded DNA. The enzyme unwinds two important intermediates of replication/repair, a 5-ssDNA flap substrate and a synthetic replication fork. The enzyme is able to translocate on the lagging strand of the synthetic replication fork to unwind duplex ahead of the fork. For the 5-flap structure, the enzyme specifically displaces the 5-flap oligonucleotide [31]; <7> the enzyme can unwind 17-bp partial duplex substrates with equal efficiency whether or not they contain a fork. It translocates unidirectionally along the bound strand in the 3 to 5 direction. NTPs can support helicase activity in order of decreasing efficiency: ATP, GTP, dCTP, UTP, dTTP, CTP, dATP, dGTP. The optimum concentration of ATP for DNA helicase activity is 1.0 mM. At 8 mM ATP the DNA unwinding activity of PDH120 is inhibited. No significant difference in the DNA unwinding activity of PDH120 with forked or nonforked substrates. The enzyme fails to unwind synthetic blunt-ended duplex DNA suggesting that PDH120 re-

quires ssDNA adjacent to the duplex as a loading zone [15]; <15> the enzyme exhibited a preference for ATP, dATP, and dCTP over the other NTP/dNTP substrates [32]; <20> the enzyme hydrolyzes nucleoside triphosphates in order of decreasing efficiency: ATP, dATP, dGTP, GTP, CTP, dCTP, UTP. The enzyme is highly active on a double-stranded DNA with 5 recessed ends in comparison with substrates with 3 recessed or blunt ends, and supports enzyme translocation in a 3-5 direction relative to the strand bound by the enzyme [16]; <11> the enzyme moves unidirectionally in the 3 to 5 direction along the bound strand and prefers a fork-like substrate structure and could not unwind blunt-ended duplex DNA [55]; <9> the enzyme translocates in a 5-to-3 direction with respect to the substrate strand to which it is bound. The enzyme favours adenosine nucleotides (ATP and dATP) as its energy source, but utilizes to limited extents GTP, CTP, dGTP and dCTP. ATP and dATP support unwinding activity with equal efficiency. GTP, dGTP, CTP, dCTP support unwinding activity to limited extents (5-12% of that with ATP at 1.5 mM). The ATPase activity of DNA helicase II increases proportionally with increasing lengths of single-stranded DNA cofactor. In the presence of circular DNA, ATP hydrolysis continues to increase up to the longest time tested (3 h), whereas it ceases to increase after 5-10 min in the presence of shorter oligonucleotides. The initial rate of ATP hydrolysis during the first 5 min of incubation time is not affected by DNA species used. The enzyme does not dissociate from the single-stranded DNA once it is bound and is therefore highly processive [7]; <3> the enzyme unwinds DNA in the 3-5 direction with respect to the strand to which the enzyme is bound [28]; <5> the helicase is capable of displacing DNA fragments up to 140 nucleotides in length, but is unable to displace a DNA fragment 322 nucleotides in length. Preference for displacing primers whose 5 terminus is fully annealed as opposed to primers with a 12 nucleotide 5 unannealed tail. The presence of a 12 nucleotide 3 tail has no effect on the rate of displacement. DNA helicase E is capable of displacing a primer downstream of either a four nucleotide gap, a one nucleotide gap or a nick in the DNA substrate. Helicase E is inactive on a fully duplex DNA 30 base pairs in length [44]; <2> the NTP hydrolysis step is significantly faster for the purine NTPs than for the pyrimidine NTPs, both in the absence and in the presence of the DNA. The nature of intermediates of the purine nucleotide, ATP, is different from the nature of the analogous intermediates of the pyrimidine nucleotide CTP [10]; <14> the number of ATP hydrolysis events per unwinding cycle is not a constant value. At optimum Mg^{2+} and saturating ATP concentrations 1 pmol of the enzyme unwinds 5.5 fmol (given as nucleotide bases) of the DNA duplex per s [2]; <12> the protein binds RNA and DNA in a sequence specific manner. ATP hydrolysis is stimulated by some nucleic acid polymers much better than it is stimulated by others. The range is quite dramatic. Poly(G) RNA does not stimulate at any measurable level, and poly(U) RNA (or DNA) stimulates best (up to 50 fold). HCV helicase unwinds a DNA duplex more efficiently than an RNA duplex. ATP binds HCV helicase between two RecA-like domains, causing a conformational change that leads to a decrease in the affinity of the protein for

nucleic acids. One strand of RNA binds in a second cleft formed perpendicular to the ATP-binding cleft and its binding leads to stimulation of ATP hydrolysis. RNA and/or ATP binding likely causes rotation of domain 2 of the enzyme relative to domains 1 and 3, and somehow this conformational change allows the protein to move like a motor [11]; <23> the recombinant protein has both RNA and DNA duplex-unwinding activities with 5-to-3 polarity. The DNA helicase activity of the enzyme preferentially unwinds 5-oligopyrimidine-tailed, partial-duplex substrates and requires a tail length of at least 10 nucleotides for effective unwinding [3]; <21> TWINKLE is a DNA helicase with 5 to 3 directionality. The enzyme needs a stretch of 10 nucleotides of single-stranded DNA on the 5-side of the duplex to unwind duplex DNA. In addition, helicase activity is not observed unless a short single-stranded 3-tail is present. UTP efficiently supports DNA unwinding. ATP, GTP, and dTTP are less effective [33]; <22> unwinds DNA in the 3 to 5 direction relative to single-stranded regions in the DNA substrates [30]; <4> unwinds partial duplex DNA substrates, as long as 343 base pairs in length, in a reaction that is dependent on either ATP or dATP hydrolysis. The direction of the unwinding reaction is 5 to 3 with respect to the strand of DNA on which the enzyme is bound [26]; <12> catalytic DNA helicase activity is coupled with NTPase and is stimulated by ATP [62]; <16> DNA-unwinding activity [64]; <12> multifunctional enzyme possessing serine protease, NTPase, DNA and RNA unwinding activities [65]; <51> genome structure, crystals and three-dimensional structure determined, structure of NTP-binding region, conserved residues within the NTP-binding pocket [4]; <12> modified malachite green assay, DNA unwinding by nonstructural protein 3, pH 6.5, 5 mM $MgCl_2$, 2 mM ATP, and 0.1mg/ml polyU, initiated by adding 5-100 nM enzyme [38]; <12> peptide inhibitors derived from amino acid sequence of motif VI analyzed, binding of the inhibitory peptides does not interfere with the NTPase activity, 4.7 pM DNA substrate used for determination of helicase activity [61]; <14> recombinant protein of C-terminal portion of NS3 protein, ATPase catalytic properties but no DNA helicase activities [67]) (Reversibility: ?) [1,2,3,4,5,6,7,8,9,10,11,12,13,14,15,16,17,18,19,20,21,22,23,24,25,26,27,28,29,30,31,32,33,34,35,36,37,38,39,40,41,42,43,44,45,46,47,48,49,51,52,53,54,55,56,57,58,59,60,61,62,64,65,67]

P ADP + phosphate

S CTP + H_2O <1,2,7,9,12,15,20,24> (<24> DNA helicase with 3-to-5 polarity. No helicase activity in absence of NTP [40]; <12> HCV helicase unwinds DNA at different rates depending on the nature and concentration of NTPs in solution. The fastest reactions are observed in the presence of CTP followed by ATP, UTP, and GTP. 3-deoxy-NTPs generally support faster DNA unwinding, with dTTP supporting faster rates than any other canonical (d)NTP [38]; <7> NTPs can support helicase activity in order of decreasing efficiency: ATP, GTP, dCTP, UTP, dTTP, CTP, dATP, dGTP [15]; <1> RECQ5 unwinds duplex DNA with a 3-5 polarity. The unwinding reaction catalyzed RECQ5 requires a nucleoside 5-phosphate. dATP is most effective. ATP supports helicase reaction with 10% of the efficiency obtained with dATP [49]; <20> the enzyme hydrolyzes nucleoside tripho-

sphates in order of decreasing efficiency: ATP, dATP, dGTP, GTP, CTP, dCTP, UTP. The enzyme is highly active on a double-stranded DNA with 5 recessed ends in comparison with substrates with 3 recessed or blunt ends, and supports enzyme translocation in a 3-5 direction relative to the strand bound by the enzyme [16]; <9> the enzyme translocates in a 5-to-3 direction with respect to the substrate strand to which it is bound. The enzyme favours adenosine nucleotides (ATP and dATP) as its energy source, but utilizes to limited extents GTP, CTP, dGTP and dCTP. ATP and dATP support unwinding activity with equal efficiency. GTP, dGTP, CTP, dCTP support unwinding activity to limited extents (5-12% of that with ATP at 1.5 mM). The ATPase activity of DNA helicase II increases proportionally with increasing lengths of single-stranded DNA cofactor. In the presence of circular DNA, ATP hydrolysis continues to increase up to the longest time tested (3 h), whereas it ceases to increase after 5-10 min in the presence of shorter oligonucleotides. The initial rate of ATP hydrolysis during the first 5 min of incubation time is not affected by DNA species used. The enzyme does not dissociate from the single-stranded DNA once it is bound and is therefore highly processive [7]; <2> the NTP hydrolysis step is significantly faster for the purine NTPs than for the pyrimidine NTPs, both in the absence and in the presence of the DNA. The nature of intermediates of the purine nucleotide, ATP, is different from the nature of the analogous intermediates of the pyrimidine nucleotide, CTP [10]; <12> ability of various NTPs to support HCV helicase-catalyzed DNA unwinding by nonstructural protein 3 using a molecular-beacon-based helicase assay [38]) (Reversibility: ?) [7,10,15,16,32,38,40,49]

P CDP + phosphate

S GTP + H_2O <1,2,7,9,12,15,20,21,24> (<24> DNA helicase with 3-to-5 polarity. No helicase activity in absence of NTP [40]; <12> HCV helicase unwinds DNA at different rates depending on the nature and concentration of NTPs in solution. The fastest reactions are observed in the presence of CTP followed by ATP, UTP, and GTP. 3-deoxy-NTPs generally support faster DNA unwinding, with dTTP supporting faster rates than any other canonical (d)NTP. 21% of the ability to support NS3hb(con1)-catalyzed DNA unwinding compared to ATP [38]; <7> NTPs can support helicase activity in order of decreasing efficiency: ATP, GTP, dCTP, UTP, dTTP, CTP, dATP, dGTP [15]; <1> RECQ5 unwinds duplex DNA with a 3-5 polarity. The unwinding reaction catalyzed by RECQ5 requires a nucleoside 5-phosphate. dATP is most effective. ATP supports helicase reaction with 35% of the efficiency obtained with dATP [49]; <20> the enzyme hydrolyzes nucleoside triphosphates in order of decreasing efficiency: ATP, dATP, dGTP, GTP, CTP, dCTP, UTP. The enzyme is highly active on a double-stranded DNA with 5 recessed ends in comparison with substrates with 3 recessed or blunt ends, and supports enzyme translocation in a 3-5 direction relative to the strand bound by the enzyme [16]; <9> the enzyme translocates in a 5-to-3 direction with respect to the substrate strand to which it is bound. The enzyme favours adenosine nucleotides (ATP and dATP) as its energy source, but utilizes to limited

extents GTP, CTP, dGTP and dCTP. ATP and dATP support unwinding activity with equal efficiency. GTP, dGTP, CTP, dCTP support unwinding activity to limited extents (5-12% of that with ATP at 1.5 mM). The ATPase activity of DNA helicase II increases proportionally with increasing lengths of single-stranded DNA cofactor. In the presence of circular DNA, ATP hydrolysis continues to increase up to the longest time tested (3 h), whereas it ceases to increase after 5-10 min in the presence of shorter oligonucleotides. The initial rate of ATP hydrolysis during the first 5 min of incubation time is not affected by DNA species used. The enzyme does not dissociate from the single-stranded DNA once it is bound and is therefore highly processive [7]; <2> the NTP hydrolysis step is significantly faster for the purine NTPs than for the pyrimidine NTPs, both in the absence and in the presence of the DNA. The nature of intermediates of the purine nucleotide, ATP, is different from the nature of the analogous intermediates of the pyrimidine nucleotide, CTP [10]; <21> TWINKLE is a DNA helicase with 5 to 3 directionality. The enzyme needs a stretch of 10 nucleotides of single-stranded DNA on the 5-side of the duplex to unwind duplex DNA. In addition, helicase activity is not observed unless a short single-stranded 3-tail is present. UTP efficiently supports DNA unwinding. ATP, GTP, and dTTP are less effective [33]; <12> ability of various NTPs to support HCV helicase-catalyzed DNA unwinding by nonstructural protein 3 using a molecular-beacon-based helicase assay, 21% relative ability to support DNA unwinding, reported as percentage relative to ATP [38]) (Reversibility: ?) [7,10,15,16,32,33,38,40,49]

P GDP + phosphate

S N^1-methyl-ATP + H_2O <12> (<12> 47% of the ability to support helicase catalyzed DNA unwinding compared to ATP [38]; <12> 47% relative ability to support DNA unwinding by nonstructural protein 3, reported as percentage relative to ATP [38]) (Reversibility: ?) [38]

P N^1-methyl-ADP + phosphate

S N^6-methyl-ATP + H_2O <12> (<12> 122% of the ability to support helicase catalyzed DNA unwinding compared to ATP [38]; <12> 122% relative ability to support DNA unwinding by nonstructural protein 3, reported as percentage relative to ATP [38]) (Reversibility: ?) [38]

P N^6-methyl-ADP + phosphate

S NTP + H_2O <12> (<12> different NTP binding rate and processivity, DNA unwinding of nonstructural protein 3 [38]; <12> ability of various dNTPs to support HCV helicase-catalyzed DNA unwinding by nonstructural protein 3 using a molecular-beacon-based helicase assay [38]) (Reversibility: ?) [38]

P NDP + phosphate

S TTP + H_2O <12> (<12> ability of various NTPs to support HCV helicase-catalyzed DNA unwinding by nonstructural protein 3 using a molecular-beacon-based helicase assay [38]) (Reversibility: ?) [38]

P TDP + phosphate

S UTP + H_2O <7,12,15,20,21> (<12> HCV helicase unwinds DNA at different rates depending on the nature and concentration of NTPs in solution.

The fastest reactions are observed in the presence of CTP followed by ATP, UTP, and GTP. 3-deoxy-NTPs generally support faster DNA unwinding, with dTTP supporting faster rates than any other canonical (d)NTP [38]; <7> NTPs can support helicase activity in order of decreasing efficiency: ATP, GTP, dCTP, UTP, dTTP, CTP, dATP, dGTP [15]; <20> the enzyme hydrolyzes nucleoside triphosphates in order of decreasing efficiency: ATP, dATP, dGTP, GTP, CTP, dCTP, UTP. The enzyme is highly active on a double-stranded DNA with 5 recessed ends in comparison with substrates with 3 recessed or blunt ends, and supports enzyme translocation in a 3-5 direction relative to the strand bound by the enzyme [16]; <21> TWINKLE is a DNA helicase with 5 to 3 directionality. The enzyme needs a stretch of 10 nucleotides of single-stranded DNA on the 5-side of the duplex to unwind duplex DNA. In addition, helicase activity is not observed unless a short single-stranded 3-tail is present. UTP efficiently supports DNA unwinding. ATP, GTP, and dTTP are less effective [33]) (Reversibility: ?) [15,16,32,33,38]

P UDP + phosphate

S XTP + H_2O <12> (<12> 7% of the ability to support helicase catalyzed DNA unwinding compared to ATP [38]) (Reversibility: ?) [38]

P XDP + phosphate

S dATP + H_2O <1> (<1> RECQ5 unwinds duplex DNA with a 3-5 polarity. Unwinding of longer partial duplex DNA substrates requires a higher protein concentration than does unwinding of the 20bp partial duplex substrate. The unwinding reaction catalyzed by RECQ5 requires a nucleoside 5-phosphate. RECQ5 hydrolyzes dATP more rapidly than ATP regardless of the presence of ssDNA. dATP is most effective. ATP supports helicase reaction with 45% of the efficiency obtained with dATP. Both ssDNA cofactors, M13mp18 ssDNA and poly(dT) strongly stimulate the ATPase activity of the protein [49]) (Reversibility: ?) [49]

P ADP + phosphate

S dATP + H_2O <1,3,4,7,9,11,12,15,20,24,29,36,41,42> (<4> ATP hydrolysis is required for unwinding of DNA catalyzed by the DNA helicase, the enzyme moves in the 5´ to 3‘ direction on a single-stranded DNA to catalyze unwinding of double-stranded regions of DNA in the 3 to 5 direction. dATP shows 95% of the activity with ATP [27]; <3> ATP-dependent DNA unwinding enzyme. HDH VI unwinds exclusively DNA duplexes with an annealed portion smaller than32 bp and prefers a replication fork-like structure of the substrate. It cannot unwind blunt-end duplexes and is inactive also on DNA-RNA or RNA-RNA hybrids. HDH VI unwinds DNA unidirectionally by moving in the 3 to 5 direction along the bound strand. ATP and dATP are equally good substrates [45]; <7> dATP shows 25% of the activity compared to ATP. DNA helicase unwinds DNA unidirectionally from 3‘ to 5‘ [14]; <1> Dhel I moves 5 to 3 on the DNA strand to which it is bound. Unwinding activity decreases with increasing length of the double-stranded region suggesting a distributive mode of action. ATP and dATP are the only nucleoside-5-triphosphates that support the strand displacement reaction. Both have an optimal concentration range

between 1 and 2 mM [46]; <24> DNA helicase with 3-to-5 polarity. No helicase activity in absence of NTP. dATP is as efficient as ATP [40]; <36> exhibits an ATPase activity in the presence of single- or double-stranded DNA. Displacement of the DNA strand occurs in the 3 to 5 direction with respect to the single-stranded DNA flanking the duplex. The efficiency of unwinding is found to correlate inversely with the length of the duplex region. The recombinant Sgs1 fragment is found to bind more tightly to a forked DNA substrate than to either single or double-stranded DNA. Like the DNA-DNA helicase activity, unwinding of the DNA-RNA hybrid is driven by the hydrolysis of ATP or dATP [29]; <12> HCV helicase unwinds DNA at different rates depending on the nature and concentration of NTPs in solution. The fastest reactions are observed in the presence of CTP followed by ATP, UTP, and GTP. 3-deoxy-NTPs generally support faster DNA unwinding, with dTTP supporting faster rates than any other canonical (d)NTP [38]; <4> hydrolyzes ATP and dATP with equal efficiency. ATPase activity of the enzyme is absolutely DNA-dependent [8]; <41> hydrolyzes both ATP and dATP at similar levels. The enzyme shows 5 to 3 and 3 to 5 helicase activities and binds efficiently to partially duplex DNA containing a hairpin structure adjacent to a 6-nucleotide 5 or 3 single-stranded tail and one unpaired (flap) nucleotide in the complementary strand [21]; <7> NTPs can support helicase activity in order of decreasing efficiency: ATP, GTP, dCTP, UTP, dTTP, CTP, dATP, dGTP [15]; <42> only ATP and dATP support helicase activity. 80% of the duplex is separated in the presence of 1 mM ATP in a 15 min reaction, 58% is unwound in the presence of 1 mM dATP. ATPase activity is dependent upon the presence of DNA. Oligonucleotides of 4 nucleotides are sufficient to promote the ATPase activity. UvrD preferentially unwinds 3-single-stranded tailed duplex substrates over 5-single-stranded ones, indicating that the protein has a duplex-unwinding activity with 3-to-5 polarity. A 3 single-stranded DNA tail of 18 nucleotides is required for effective unwinding. UvrD has an unwinding preference towards nicked DNA duplexes and stalled replication forks [22]; <29> strong 5 to 3 DNA helicase activity. At both 0.1 and 0.5 mM, dATP produces comparable or slightly higher levels of unwinding than ATP [23]; <1> structure-specific DNA helicase. DmRECQ5 preferentially unwinds specific DNA structures including a 3flap, a three-strand junction and a three-way junction. Unwinding of a Holliday junction, 5flap and 12 nt bubble structures, which can be unwound by other RecQ proteins (WRN, BLM and/or Escherichia coli RecQ), can not be detected or requires significantly higher protein concentrations [50]; <15> the enzyme exhibited a preference for ATP, dATP, and dCTP over the other NTP/dNTP substrates [32]; <20> the enzyme hydrolyzes nucleoside triphosphates in order of decreasing efficiency: ATP, dATP, dGTP, GTP, CTP, dCTP, UTP. The enzyme is highly active on a double-stranded DNA with 5 recessed ends in comparison with substrates with 3 recessed or blunt ends, and supports enzyme translocation in a 3-5 direction relative to the strand bound by the enzyme [16]; <11> the enzyme moves unidirectionally in the 3 to 5 direction

along the bound strand and prefers a fork-like substrate structure and could not unwind blunt-ended duplex DNA. dATP supports unwinding at 42% of the efficiency of ATP [55]; <9> the enzyme translocates in a 5-to-3 direction with respect to the substrate strand to which it is bound. The enzyme favours adenosine nucleotides (ATP and dATP) as its energy source, but utilizes to limited extents GTP, CTP, dGTP and dCTP. ATP and dATP support unwinding activity with equal efficiency. GTP, dGTP, CTP, dCTP support unwinding activity to limited extents (5-12% of that with ATP at 1.5 mM). The ATPase activity of DNA helicase II increases proportionally with increasing lengths of single-stranded DNA cofactor. In the presence of circular DNA, ATP hydrolysis continues to increase up to the longest time tested (3 h), whereas it ceases to increase after 5-10 min in the presence of shorter oligonucleotides. The initial rate of ATP hydrolysis during the first 5 min of incubation time is not affected by DNA species used. The enzyme does not dissociate from the single-stranded DNA once it is bound and is therefore highly processive [7]; <4> unwinds partial duplex DNA substrates, as long as 343 base pairs in length, in a reaction that is dependent on either ATP or dATP hydrolysis. The direction of the unwinding reaction is 5 to 3 with respect to the strand of DNA on which the enzyme is bound [26]; <12> helicase-catalyzed DNA unwinding by nonstructural protein 3 analyzed by molecular beacon-based helicase assay (MBHA), NTP binding occurs with similar affinities, dNTPs support faster DNA unwinding [38]) (Reversibility: ?) [7,8,14,15,16,21,22,23,26,27,29,32,38,40,45,46,50,55]

P dADP + phosphate

S dCTP + H_2O <7,12,15,20> (<12> HCV helicase unwinds DNA at different rates depending on the nature and concentration of NTPs in solution. The fastest reactions are observed in the presence of CTP followed by ATP, UTP, and GTP. 3-deoxy-NTPs generally support faster DNA unwinding, with dTTP supporting faster rates than any other canonical (d)NTP [38]; <7> NTPs can support helicase activity in order of decreasing efficiency: ATP, GTP, dCTP, UTP, dTTP, CTP, dATP, dGTP [15]; <15> the enzyme exhibited a preference for ATP, dATP, and dCTP over the other NTP/dNTP substrates [32]; <20> the enzyme hydrolyzes nucleoside triphosphates in order of decreasing efficiency: ATP, dATP, dGTP, GTP, CTP, dCTP, UTP. The enzyme is highly active on a double-stranded DNA with 5 recessed ends in comparison with substrates with 3 recessed or blunt ends, and supports enzyme translocation in a 3-5 direction relative to the strand bound by the enzyme [16]; <12> helicase-catalyzed DNA unwinding by nonstructural protein 3 analyzed by molecular beacon-based helicase assay (MBHA), NTP binding occurs with similar affinities, dNTPs support faster DNA unwinding [38]) (Reversibility: ?) [15,16,32,38]

P dCDP + phosphate

S dCTP + H_2O <9> (<9> the enzyme translocates in a 5-to-3 direction with respect to the substrate strand to which it is bound. The enzyme favours adenosine nucleotides (ATP and dATP) as its energy source, but utilizes to limited extents GTP, CTP, dGTP and dCTP. ATP and dATP support un-

winding activity with equal efficiency. GTP, dGTP, CTP, dCTP support unwinding activity to limited extents (5-12% of that with ATP at 1.5 mM). The ATPase activity of DNA helicase II increases proportionally with increasing lengths of single-stranded DNA cofactor. In the presence of circular DNA, ATP hydrolysis continues to increase up to the longest time tested (3 h), whereas it ceases to increase after 5-10 min in the presence of shorter oligonucleotides. The initial rate of ATP hydrolysis during the first 5 min of incubation time is not affected by DNA species used. The enzyme does not dissociate from the single-stranded DNA once it is bound and is therefore highly processive [7]) (Reversibility: ?) [7]

P dCTP + phosphate

S dGTP + H_2O <1,7,9,12,15,20> (<12> HCV helicase unwinds DNA at different rates depending on the nature and concentration of NTPs in solution. The fastest reactions are observed in the presence of CTP followed by ATP, UTP, and GTP. 3-deoxy-NTPs generally support faster DNA unwinding, with dTTP supporting faster rates than any other canonical (d)NTP [38]; <7> NTPs can support helicase activity in order of decreasing efficiency: ATP, GTP, dCTP, UTP, dTTP, CTP, dATP, dGTP [15]; <1> RECQ5 unwinds duplex DNA with a 3-5 polarity. The unwinding reaction catalyzed by RECQ5 requires a nucleoside 5-phosphate. dATP is most effective. ATP supports helicase reaction with 30% of the efficiency obtained with dATP [49]; <20> the enzyme hydrolyzes nucleoside triphosphates in order of decreasing efficiency: ATP, dATP, dGTP, GTP, CTP, dCTP, UTP. The enzyme is highly active on a double-stranded DNA with 5 recessed ends in comparison with substrates with 3 recessed or blunt ends, and supports enzyme translocation in a 3-5 direction relative to the strand bound by the enzyme [16]; <9> the enzyme translocates in a 5-to-3 direction with respect to the substrate strand to which it is bound. The enzyme favours adenosine nucleotides (ATP and dATP) as its energy source, but utilizes to limited extents GTP, CTP, dGTP and dCTP. ATP and dATP support unwinding activity with equal efficiency. GTP, dGTP, CTP, dCTP support unwinding activity to limited extents (5-12% of that with ATP at 1.5 mM). The ATPase activity of DNA helicase II increases proportionally with increasing lengths of single-stranded DNA cofactor. In the presence of circular DNA, ATP hydrolysis continues to increase up to the longest time tested (3 h), whereas it ceases to increase after 5-10 min in the presence of shorter oligonucleotides. The initial rate of ATP hydrolysis during the first 5 min of incubation time is not affected by DNA species used. The enzyme does not dissociate from the single-stranded DNA once it is bound and is therefore highly processive [7]; <12> helicase-catalyzed DNA unwinding by nonstructural protein 3 analyzed by molecular beacon-based helicase assay (MBHA), NTP binding occurs with similar affinities, dNTPs support faster DNA unwinding [38]) (Reversibility: ?) [7,15,16,32,38,49]

P dGDP + phosphate

S dNTP + H_2O <12> (<12> dNTPs support faster DNA unwinding mediated by nonstructural protein 3 [38]; <12> ability of various NTPs

to support HCV helicase-catalyzed DNA unwinding by nonstructural protein 3 using a molecular-beacon-based helicase assay [38]) (Reversibility: ?) [38]

P dNDP + phosphate

S dTTP + H_2O <7,12,21> (<12> HCV helicase unwinds DNA at different rates depending on the nature and concentration of NTPs in solution. The fastest reactions are observed in the presence of CTP followed by ATP, UTP, and GTP. 3-deoxy-NTPs generally support faster DNA unwinding, with dTTP supporting faster rates than any other canonical (d)NTP [38]; <7> NTPs can support helicase activity in order of decreasing efficiency: ATP, GTP, dCTP, UTP, dTTP, CTP, dATP, dGTP [15]; <21> TWINKLE is a DNA helicase with 5 to 3 directionality. The enzyme needs a stretch of 10 nucleotides of single-stranded DNA on the 5-side of the duplex to unwind duplex DNA. In addition, helicase activity is not observed unless a short single-stranded 3-tail is present. UTP efficiently supports DNA unwinding. ATP, GTP, and dTTP are less effective [33]) (Reversibility: ?) [15,33,38]

P dTDP + phosphate

S dTTP + H_2O <12> (<12> helicase-catalyzed DNA unwinding by nonstructural protein 3 analyzed by molecular beacon-based helicase assay (MBHA), NTP binding occurs with similar affinities, dNTPs support faster DNA unwinding, dTTP supporting faster rates than any other canonical dNTP [38]) (Reversibility: ?) [38]

P TDP + phosphate

S dUTP + H_2O <15> (Reversibility: ?) [32]

P dUDP + phosphate

S xanthosine-5'-triphophate + H_2O <12> (<12> 7% relative ability to support DNA unwinding by nonstructural protein 3, reported as percentage relative to ATP [38]) (Reversibility: ?) [38]

P xanthosine-5'-diphophate + phosphate

S Additional information <6,9,12,24,41,46> (<46> exhibits RNA unwinding and binding activity in the absence of NTP, and this activity is abolished by a mutation in the RNA-binding domain [24]; <24> no helicase activity is observed with UTP, dCTP or dTTP, low levels of helicase activity is observed with dGTP [40]; <9> non-hydrolysable ATP analogues do not support helicase activity. DNA helicase II lacks any detectable RNA-unwinding activity [7]; <41> the enzyme is inefficient in in vitro replication of pT181, and perhaps as a consequence, this plasmid can not be established in Streptococcus pneumoniae [21]; <6> the helicase is capable of unwinding DNA substrates coated with various proteins, including histones, transcription inhibitors, and the transcription initiation complex. Thus, the helicase can displace at least some of the proteins associated with chromatin [43]; <12> the mature NS3 protein comprises 5 domains: the N-terminal 2 domains form the serine protease along with the NS4A cofactor, and the C-terminal 3 domains form the helicase. The helicase portion of NS3 can be separated form the protease portion by cleaving a linker. Since the protease portion is more hydrophobic, removing it allows

the NS3 helicase fragment to be expressed as a more soluble protein at higher levels in Escherichia coli. The fragment of NS3 possessing helicase activity is referred to as HCV helicase [11]) (Reversibility: ?) [7,11,21,24,40,43]

P ?

Inhibitors

(2Z)-4-[2-(benzyloxy)phenyl]-2-hydroxy-4-oxobut-2-enoic acid <16> (<16> low inhibitory activities [64]) [64]

(2Z)-4-[2-[(4-chlorobenzyl)oxy]phenyl]-2-hydroxy-4-oxobut-2-enoic acid <16> (<16> no or marginal inhibition activities towards ATPase activity or duplex DNA-unwinding activity [64]) [64]

(2Z)-4-[3-(benzylamino)phenyl]-2-hydroxy-4-oxobut-2-enoic acid <16> (<16> inhibition of duplex DNA-unwinding activity [64]) [64]

(2Z)-4-[3-(benzyloxy)phenyl]-2-hydroxy-4-oxobut-2-enoic acid <16> (<16> low inhibitory activities [64]) [64]

(2Z)-4-[3-[(4-chlorobenzyl)amino]phenyl]-2-hydroxy-4-oxobut-2-enoic acid <16> (<16> inhibition of duplex DNA-unwinding activity [64]) [64]

(2Z)-4-[3-[(4-chlorobenzyl)oxy]phenyl]-2-hydroxy-4-oxobut-2-enoic acid <16> (<16> inhibition of duplex DNA-unwinding activity [64]) [64]

(2Z)-4-[4-(benzyloxy)phenyl]-2-hydroxy-4-oxobut-2-enoic acid <16> (<16> low inhibitory activities, *para*-relationship between the diketoacid moiety and the OCH_2Ar group do not show antiviral activities [64]) [64]

(2Z)-4-[4-[(4-chlorobenzyl)oxy]phenyl]-2-hydroxy-4-oxobut-2-enoic acid <16> (<16> low inhibitory activities, *para*-relationship between the diketoacid moiety and the OCH_2Ar group do not show antiviral activities [64]) [64]

$(NH_4)_2SO_4$ <7> (<7> 45 mM [14]) [14]

2',3'-ddATP <12> (<12> inhibition of NTPase activity of NS3 protein by NTP derivatives [62]) [62]

2',3'-ddGTP <12> (<12> inhibition of NTPase activity of NS3 protein by NTP derivatives [62]) [62]

2',3'-ddTTP <12> (<12> inhibition of NTPase activity of NS3 protein by NTP derivatives [62]) [62]

2'-dATP <12> (<12> inhibition of NTPase activity of NS3 protein by NTP derivatives [62]) [62]

2'-dGTP <12> (<12> inhibition of NTPase activity of NS3 protein by NTP derivatives [62]) [62]

2'-dTTP <12> (<12> inhibition of NTPase activity of NS3 protein by NTP derivatives [62]) [62]

2'-deoxythymidine 5'-phosphoryl-β,γ-hypophosphate <12> (<12> i.e. ppopT, dTTP analogue, most efficient inhibitor of NTPase activity among nucleotide derivaties, inhibits the ATP-dependent helicase reaction and also the ATP-independent duplex unwinding, structure of nucleic base and ribose fragment of NTP molecule have a slight effects on inhibitory properties [62]) [62]

3'-dATP <12> (<12> inhibition of NTPase activity of NS3 protein by NTP derivatives [62]) [62]

3'-dGTP <12> (<12> inhibition of NTPase activity of NS3 protein by NTP derivatives [62]) [62]
3'-dUTP <12> (<12> inhibition of NTPase activity of NS3 protein by NTP derivatives [62]) [62]
5-fluoro-2-selenocytosine <14> (<14> reduces ATPase activity, no effect on helicase activity [2]) [2]
ADP <12> (<12> inhibition of NTPase activity of NS3 protein by NTP derivatives [62]) [62]
AMP <12> (<12> inhibition of NTPase activity of NS3 protein by NTP derivatives [62]) [62]
ATP <1,7,47> (<47> above 8 mM [37]; <7> 10 mM [14]; <1> substrate with optimal concentration range between 1 and 2 mM. At high concentrations inhibition of activity can be observed [46]; <7> the optimum concentration of ATP for DNA helicase activity is 1.0 mM. At 8 mM ATP the DNA unwinding activity of PDH120 is inhibited [15]) [14,15,37,46]
ATPγS <1,21> [33,49]
EDTA <3,4,7,11,15> (<7,11> 5 mM [14,55]; <3,7> 5 mM, complete inhibition [15,45]) [14,15,26,32,45,55]
GTP <12> (<12> inhibition of NTPase activity of NS3 protein by NTP derivatives [62]) [62]
K^+ <14> (<14> activation at 100-300 mM, inhibition above 500 mM [2]) [2]
KCl <3,7,11,12,28,47> (<11> 200 mM, inhibits [55]; <28> 30% inhibition occurs when KCl concentration is increased from 15 to 200 mM [35]; <7> 400 mM [14]; <47> helicase activity is inhibited at 200 mM [37]; <3> optimal concentration: 100 mM. Inhibition at 200 mM [45]; <7> optimum concentration: 250 mM. Completely inhibited at 400 mM [15]; <12> slight decrease of activity in presence of [62]) [14,15,35,37,45,55,62]
M13 dsDNA <7> (<7> 0.03 mM, complete inhibition [15]) [15]
M13 ssDNA <7> (<7> 0.03 mM, complete inhibition [15]) [15]
M13mp19 ssDNA <29> (<29> ATPase activity is slightly stimulated by ssDNA, and only M13mp19 ssDNA stimulates it significantly (increase in V_{max}) [23]) [23]
Mg^{2+} <3,7> (<7> absolute requirement for divalent cations. Mg^{2+} at 2.0 mM concentration optimally fulfills this requirement. At 8.0 mM $MgCl_2$ the activity is totally inhibited [15]; <3> required, optimal concentration: 0.8 mM. Inhibition at 4 mM [45]) [15,45]
N^1-hydroxyinosine 5'-triphosphate <12> (<12> inhibition of NTPase activity of NS3 protein by NTP derivatives [62]) [62]
N^1-oxoadenosine 5'-triphosphate <12> (<12> inhibition of NTPase activity of NS3 protein by NTP derivatives [62]) [62]
Na^+ <14> (<14> activation at 100-300 mM, inhibition above 500 mM [2]) [2]
NaCl <1,4,9,11,24> (<1> above 10 mM [46]; <11> 200 mM, inhibits [55]; <9> 57% inhibition at 0.2 M, 81% inhibition at 0.4 M [7]; <4> ATPase activity is inhibited by salt (NaCl) above 50 mM with a half-maximal inhibition at about 110 mM [8]; <24> optimal concentration is 50-100 mM, higher concentrations inhibit helicase activity [40]) [7,8,40,46,55]

O^6-benzyl-N^7-chloroethylguanine <14> (<14> weak inhibitor of the ATPase and helicase activity [2]) [2]
O^6-benzylguanine <14> (<14> weak inhibitor of the ATPase and helicase activity [2]) [2]
poly(C) <46> (<46> moderately inhibits ATPase activity [24]) [24]
poly(U) <46> (<46> moderately inhibits ATPase activity [24]) [24]
RNA <7> (<7> 0.01 mM [14]) [14]
UTP <12> (<12> inhibition of NTPase activity of NS3 protein by NTP derivatives [62]) [62]
aclarubicin <11> [55]
actinomycin C_1 <7> [15]
ammonium sulfate <7> (<7> 45 mM, complete inhibition [15]) [15]
β,γ-methylene-ATP <12> (<12> efficient inhibitor, like the N^1-oxides N^1-oxoadenosine 5-triphosphate and N^1-hydroxyinosine 5-triphosphate [62]) [62]
dATP <1,12> (<12> inhibits unwinding [11]; <1> substrate with optimal concentration range between 1 and 2 mM. At high concentrations inhibition of activity can be observed [46]) [11,46]
daunorubicin <7,11> (<7> 0.01 mM, completely inhibits DNA helicase reaction [14]) [14,15,55]
doxorubicin <11> [55]
dsDNA <7> (<7> 0.01 mM [14]) [14]
ethidium bromide <7> [15]
histone H1 <7> (<7> 0.001 mg/ml, inhibits of the DNA helicase activity [14]) [14]
imidodiphosphate <12> (<12> maximal inhibitory activity among diphosphate analogues, non-catalytic and catalytic conditions, inhibits the ATP-dependent helicase reaction but no effect on the ATP-independent duplex unwinding, structure of nucleic base and ribose fragment of NTP molecule have a slight effects on inhibitory properties [62]) [62]
nogalamycin <7,11> (<7> 0.01 mM, completely inhibits DNA helicase reaction [14]) [14,15,55]
poly(A) <46> (<46> moderately inhibits ATPase activity [24]) [24]
potassium phosphate <7> (<7> 100 mM, complete inhibition [15]) [14,15]
replication protein A <33> (<33> inhibits unwinding and annealing activities [51]) [51]
ribavirin 5'-triphosphate <14> (<14> competitive inhibitor with regard to ATP [2]) [2]
single-stranded DNA <20> [16]
single-stranded DNA-binding proteins <22> [30]
ssDNA <7,29> (<7> 0.01 mM [14]; <29> ATPase activity is slightly stimulated by ssDNA, and only M13mp19 ssDNA stimulats it significantly [23]) [14,23]
streptavidin <18> (<18> the enzyme is completely blocked by streptavidin bound to the 3-ssDNA tail 6 nucleotides upstream of the single-stranded/double-stranded DNA junction. The enzyme efficiently unwinds the forked duplex with streptavidin bound just upstream of the junction, suggesting that

the enzyme recognizes elements of the fork structure to initiate unwinding [31]) [31]
tetrabromobenzotriazole <12> (<12> inhibits unwinding, no inhibition of ATP hydrolysis [11]) [11]
trypsin <7> [15]
yeast total RNA <46> (<46> severly inhibits ATPase activity [24]) [24]
Additional information <5,12> (<5> Hel E is inhibited by replication fork structures [44]; <12> domain 2 of wild-type NS3 protein and domain 2 devoid of the loop structure used for inhibition studies on functions of protein kinase C (PKC), inhibitory potential towards the majority of protein kinase C isoforms shown [63]; <12> inhibitory potential of peptides deduced from amino acid sequence of motif VI tested, NTP-binding and hydrolyzing site not involved, 4.7 pM DNA substrate used for determination of helicase activity [61]) [44,61,63]

Activating compounds

ATP <12> (<12> catalytic DNA helicase activity coupled with NTPase stimulated by [62]) [62]
DNA <46> (<46> ATPase activity is stimulated by yeast genomic DNA and salmon sperm DNA [24]) [24]
N^7-chloroethylguanine <14> (<14> 2.2fold activation at 200-250 mM [2]) [2]
N^9-chloroethylguanine <14> (<14> 8.5fold activation at 200-250 mM [2]) [2]
O^6-benzyl-N^9-chloroethylguanine <14> (<14> stimulator of NTPase activity, with a maximum effect of 350% of control at 650 mM [2]) [2]
double-stranded DNA <3,22> (<22> MER3 ATPase activity is stimulated by either single- or double-stranded DNA [30]; <3> the enzyme is strongly stimulated by either single- or double-stranded DNA [28]) [28,30]
heterotrimeric single-stranded DNA binding protein <28> (<28> enhances DNA helicase activity of Mph1 [35]) [35]
homopolynucleotides <15> (<15> significantly stimulate the ATPase activity (15-25fold) with the exception of poly(G) and poly(dG), which are non-stimulatory. dT24 binds over 10 times more strongly than dA24 [32]) [32]
mitochondrial single-stranded DNA-binding protein <21> (<21> stimultes the enzyme [33]) [33]
poly(U) <23> (<23> strong stimulation [3]) [3]
poly(dA) <14,23> (<23> strong stimulation [3]; <14> 170-180% activation at 1.7-3.3 mM, no activation by other polynucleotides [2]) [2,3]
poly(dI*C) <9> (<9> weakly supports ATPase activity [7]) [7]
poly(dT) <9,23> (<23> strong stimulation [3]; <9> weakly supports ATPase activity [7]) [3,7]
polyadenylate <12> (<12> doubling of ATPase activity in the presence of [62]) [62]
polyuridylate <12> (<12> doubling of ATPase activity in the presence of, lowers K_m for the ATP substrate [62]) [62]
poly* <23> (<23> strong stimulation [3]) [3]

replication protein A <3,5,18,43> (<5> stimulates activity [44]; <43> from Caenorhabditis elegans, stimulates helicase activity [9]; <3> from yeast or human [48]; <18> stimulates helicase activity [12]) [9,12,44,48]
ribavirin <14> (<14> activates ATPase activity, no effect on helicase activity [2]) [2]
single-stranded DANN <3,4,7,8,22,26,28,33,37,47> (<26,37> stimulates [19,20]; <7> required [15]; <4,8> stimulates activity [8,52]; <22> MER3 ATPase activity is stimulated by either single- or double-stranded DNA [30]; <3> more than 5fold stimulation of ATPase activity [48]; <33> nonstructural single-stranded DNA greatly stimulates ATPase activity due to a high affinity for PIF1, even though PIF1 preferentially unwinds forked substrates. The N-terminal portion oF PIF1 helicase, named the PIF1 N-terminal (PINT) domain, contributes to enhancing the interaction with single-stranded DNA through intrinsic binding activity [51]; <47> the ATPase activity of AvDH1 is stimulated more by single-stranded DNA than by double-stranded DNA or RNA. Significantly stimulated by the presence of M13 ssDNA [37]; <3> the enzyme is strongly stimulated by either single- or double-stranded DNA [28]; <28> the enzyme requires single-stranded DNA for activation [35]) [8,15,19,20,28,30,35,37,48,51,52]
single-stranded DNA binding protein <4> (<4> of Escherichia coli (SSB), stimulates to a lower extent [8]) [8]
single-stranded DNA binding protein dRP-A <1> (<1> stimulates the activity on substrates with more than 300 nucleotides double-stranded region [46]) [46]
single-stranded DNA-binding protein <4,22,36> (<4> from Escherichia coli, strongly stimulates when long partial duplex substrates are used [26]; <36> of Escherichia coli, stimulates activity [29]; <22> single-stranded DNA-binding proteins stimulate [30]) [26,29,30]
ssDNA <2,41> (<41> stimulates ATPase activity [21]; <2> the effect of single-stranded DNA on the kinetics of NTP hydrolysis depends on the type of nucleotide cofactor and the base composition of the DNA and is centered at the hydrolysis step. Homoadenosine ssDNA oligomers are particularly effective in increasing the hydrolysis rate [10]) [10,21]
yeast replication protein A <4> (<4> stimulates significantly [8]) [8]
Additional information <3,9,23> (<3> no significant stimulation by Escherichia coli ssDNA-binding protein [48]; <23> no stimulation by poly(G) [3]; <9> synthetic RNA poly(U) does not support ATP hydrolysis at all. Unlike DNA helicase I, DNA helicase II is not stimulated by SpRPA or Escherichia coli SSB at low ATP concentrations [7]) [3,7,48]

Metals, ions

Ca^{2+} <22,40> (<40> ATP hydrolysis in the presence of $MgCl_2$ is 2fold higher than in the presence of either $MnCl_2$ or $CaCl_2$ [60]; <22> MER3 ATPase activity requires a divalent cation. Maximal activity can be observed in the presence of either Ca^{2+}, Mg^{2+}, or Mn^{2+}, whereas Zn^{2+} does not support the ATPase activity [30]) [30,60]

Co^{2+} <12,42> (<42> supports activity similar to that with Mg^{2+} [22]; <12> activity 3-5-fold lower when magnesium ions are replaced by [62]) [22,62]
K^+ <14> (<14> activation at 100-300 mM, inhibition above 500 mM [2]) [2]
KCl <3,7,47> (<47> optimal concentration for ATPase activity: 200 mM. Optimal concentration for helicase activity: 60 mM [37]; <3> optimal concentration: 100 mM. Inhibition at 200 mM [45]; <7> optimum concentration: 250 mM. Completely inhibited at 400 mM [15]) [15,37,45]
Mg^{2+} <1,3,4,7,9,11,12,14,15,20,22,24,26,28,40,43,47,51> (<3,4,26> required [19,26,28]; <15> activity is dependent on [32]; <7> absolute requirement for divalent cations. Mg^{2+} at 2.0 mM concentration optimally fulfills this requirement. At 8.0 mM $MgCl_2$ the activity is totally inhibited [15]; <40> ATP hydrolysis in the presence of $MgCl_2$ is 2fold higher than in the presence of either $MnCl_2$ or $CaCl_2$ [60]; <1> divalent cation required, optimum concentration: 0.5 mM [46]; <12> divalent metal cations are absolutely required for HCV helicase-catalyzed DNA unwinding. When compared with unwinding in the presence of Mg^{2+}, Mn^{2+} supports 10 times faster rates than Mg^{2+} regardless of the concentration of metal in solution. All NTPs support faster unwinding when 2 mM Mn^{2+} is used instead of 2 mM Mg^{2+}. The specificity profile remains mostly unchanged in the presence of Mn^{2+}, while the absolute magnitude of the rates increases [38]; <43> little or no unwinding is observed when Mg^{2+} was replaced with Zn^{2+} [9]; <28> maximal activity is obtained with Mg^{2+}, whereas Co^{2+} and Ca^{2+} are much less effective in this regard. No activity is observed with Mn^{2+} or Zn^{2+} [35]; <22> MER3 ATPase activity requires a divalent cation. Maximal activity can be observed in the presence of either Ca^{2+}, Mg^{2+}, or Mn^{2+}, whereas Zn^{2+} does not support the ATPase activity [30]; <24> Mg^{2+} or Mn^{2+} required, optimal activity at 4 mM $MgCl_2$ [40]; <7> Mg^{2+} or Mn^{2+} required, optimum concentration of $MgCl_2$ is 1 mM [14]; <47> required for ATPase and DNA-unwinding activity, optimal concentration for DNA unwinding reaction: 2.0 mM, optimal concentration for ATP-independent RNA unwinding reaction: 2 mM [37]; <3> required for maximal activity, optimal concentration: 0.8 mM. Inhibition at 4 mM [45]; <14> required, optimum concentration for ATPase reaction is 1-3 mM, optimum concentration for helicase reaction is 0.3-5 mM [2]; <20> requirement for divalent metal ions. Helicase activity is stimulated most by $MgCl_2$ at a concentration of 1.5 mM [16]; <4> requires divent cation, Mg^{2+} or Mn^{2+} [27]; <9> the enzyme requires $MgCl_2$ for its activity. It is not active in the presence of $MnCl_2$ or $CaCl_2$ (1 mM) [7]; <11> unwinding activity requires Mg^{2+} [55]; <12> influences DNA unwinding rates of recombinant nonstructural protein 3, metal ion specificity suggests that NTPs bind two different enzyme conformations [38]; <12> maximal NTPase activity achieved in the presence of 1.5-2 mM $MgCl_2$ [62]; <51> no ATPase activity of the wild-type in the absence of [4]) [2,4,7,9,14,15,16,19,26,27,28,30,32,35,37,38,40,45,46,55,60,62,65]
$MgCl_2$ <42> (<42> required, optimal concentration: 5 mM [22]) [22]
Mn^{2+} <4,7,12,15,20,22,24,40,42> (<7,24> Mg^{2+} or Mn^{2+} required [14,40]; <7> 2.0 mM, supports 80% of the activity compared to Mg^{2+} [15]; <40> ATP hydrolysis in the presence of $MgCl_2$ is 2fold higher than in the presence of either $MnCl_2$ or $CaCl_2$ [60]; <15> can substitute for Mg^{2+}, 40% of the efficiency

with Mg^{2+} at 2.5 mM [32]; <4> can substitute for Mg^{2+}, less effective [26]; <12> divalent metal cations are absolutely required for HCV helicase-catalyzed DNA unwinding. When compared with unwinding in the presence of Mg^{2+}, Mn^{2+} supports 10 times faster rates than Mg^{2+} regardless of the concentration of metal in solution. All NTPs support faster unwinding when 2 mM Mn^{2+} is used instead of 2 mM Mg^{2+}. The specificity profile remains mostly unchanged in the presence of Mn^{2+}, while the absolute magnitude of the rates increases [38]; <22> MER3 ATPase activity requires a divalent cation. Maximal activity can be observed in the presence of either Ca^{2+}, Mg^{2+}, or Mn^{2+}, whereas Zn^{2+} does not support the ATPase activity [30]; <20> $MnCl_2$ stimulates activity, though not as well as the $MgCl_2$ [16]; <4> requires divent cation, Mg^{2+} or Mn^{2+} [27]; <42> supports ATPase activity with 2fold lower efficiency compared to Mg^{2+} [22]; <12> activity 3-5-fold lower when magnesium ions are replaced by [62]; <12> influences DNA unwinding rates of recombinant nonstructural protein 3, supports about 10 times faster unwinding than Mg^{2+}, unlike Mg^{2+}, Mn^{2+} does not support helicase-catalyzed ATP hydrolysis in the absence of stimulating nucleic acids, metal ion specificity suggests that NTPs bind two different enzyme conformations [38]) [14,15,16,22,26,27,30,32,38,40,60,62]

Na^+ <14> (<14> activation at 100-300 mM, inhibition above 500 mM [2]) [2]

NaCl <24,42> (<42> optimal concentration: 50 mM [22]; <24> optimal concentration is 50-100 mM, higher concentrations inhibit helicase activity [40]) [22,40]

Ni^{2+} <12,42> (<42> supports ATPase activity with 3fold lower efficiency compared to Mg^{2+} [22]; <12> activity 3-5-fold lower when magnesium ions are replaced by [62]) [22,62]

Zn^{2+} <8,12> (<8> BcMCM amino-terminus can bind single-stranded DNA and harbors a zinc atom, BcMCM contains 0.11 zinc atoms per mole [52]; <12> activity 3-5-fold lower when magnesium ions are replaced by [62]) [52,62]

Additional information <7> (<7> Ca^{2+}, Zn^{2+}, Cd^{2+}, Cu^{2+}, Ni^{2+}, Ag^{2+} and Co^{2+} are unable to support the activity [15]) [15]

Turnover number (s^{-1})

0.043 <1> (ATP, <1> pH 8.0, 30°C, without ssDNA [49]) [49]

0.1 <49> (2'(3')-O-(N-methylanthraniloyl)ATP, <49> pH 7.5, 20°C, without DNA [39]) [39]

0.25 <1> (dATP, <1> pH 8.0, 30°C, without ssDNA [49]) [49]

0.3 <49> (ATP, <49> pH 7.5, 20°C, without DNA [39]) [39]

1.2 <40> (ATP, <40> pH 7.5, 30°C [60]) [60]

1.5 <34> (ATP, <34> full-length RECQ1 helicase [57]) [57]

5.4 <15> (GTP, <15> pH 6.6, 25°C [32]) [32]

7.41 <34> (ATP, <34> mutant (RECQ1(T1))Y564A, a construct encompassing amino acids 49-616 (of 649) of RECQ1, followed by a C-terminal tag of 22 aa [57]) [57]

7.5 <15> (dGTP, <15> pH 6.6, 25°C [32]) [32]

8.8 <22> (ATP, <22> pH 7.6, 30°C, in presence of M13mp18 single-stranded circular DNA [30]) [30]
9.2 <22> (ATP, <22> pH 7.6, 30°C, in presence of poly(dA) [30]) [30]
10.5 <15> (UTP, <15> pH 6.6, 25°C [32]) [32]
11.25 <34> (ATP, <34> (RECQ1(T1)), a construct encompassing amino acids 49-616 (of 649) of RECQ1, followed by a C-terminal tag of 22 aa [57]) [57]
13.1 <42> (ATP, <42> pH 7.5, in presence of 1 mM Ni^{2+} [22]) [22]
13.9 <15> (CTP, <15> pH 6.6, 25°C [32]) [32]
14.3 <15> (dCTP, <15> pH 6.6, 25°C [32]) [32]
14.8 <15> (dATP, <15> pH 6.6, 25°C [32]) [32]
14.8 <15> (dUTP, <15> pH 6.6, 25°C [32]) [32]
15 <1> (ATP, <1> pH 8.0, 30°C, in presence of ssDNA [49]) [49]
16.9 <49> (ATP, <49> pH 7.5, 20°C, in presence of DNA [39]) [39]
17.2 <49> (2'(3')-O-(N-methylanthraniloyl)ATP, <49> pH 7.5, 20°C, in presence of DNA [39]) [39]
19.1 <15> (ATP, <15> pH 6.6, 25°C [32]) [32]
19.8 <42> (ATP, <42> pH 7.5, in presence of 1 mM Mn^{2+} [22]) [22]
22.2 <42> (ATP, <42> pH 7.5, in presence of 1 mM Co^{2+} [22]) [22]
23 <1> (dATP, <1> pH 8.0, 30°C, in presence of ssDNA [49]) [49]
29.8 <42> (ATP, <42> pH 7.5, in presence of 1 mM Mg^{2+} [22]) [22]
7980 <14> (ATP, <14> pH 7.5, 30°C, in presence of 2 mM Mg^{2+} [2]) [2]
Additional information <49> (<49> turnover numbers for cleavage of dTn DNA (dT10, dT20, dT30, dT40) [39]) [39]

Specific activity (U/mg)

160.8 <14> [2]
Additional information <7,12,14,16,50,51> (<7> highest specific activity among plant helicases [15]; <50> ambiguous helicase activity, also DNA unwinding [66]; <12> DNA helicase reaction can proceed in two modes depending on the ratio between enzyme and substrate concentration, non-catalytic in the case of enzyme excess and catalytic in the case of tenfold substrate excess, structure of nucleic base and ribose fragment of NTP molecule has a slight effect on inhibitory properties, duplex DNA oligonucleotides used for determination of DNA helicase activity [62]; <16> eight analogues of anti-HCV aryl diketoacide (ADK) investigated for inhibitory capacity, phosphate release assay and FRET-based assay [64]; <12> molecular beacon-based helicase assay (MBHA) developed, unwinding of DNA mediated by recombinant nonstructural protein 3 occurs at different rates depending on the nature and concentration of NTPs in solution, presence of an intact NS3 protease domain makes HCV helicase somewhat less specific than truncated NS3 bearing only its helicase region specificity determined by the nature of the Watson-Crick base-pairing region of the NTP base and the nature of the functional groups attached to the 2 and 3 carbons of the NTP sugar [38]; <12> overview of sequences of NTPase/helicase motifs VI derived peptides and their deleted derivatives, kinetic analyses reveals that binding of the peptides do not interfere with the NTPase activity of the enzymes, peptides do not interact with the ATP binding site [61]; <51> structural characterization of catalytic do-

main, mutation analysis of residue substitution in the Walker A motif (Gly199, Lys200 and Thr201), within the NTP-binding pocket (Gln457, Arg461 and Arg464) and of Arg458 in the outside of the pocket in the motif IV, residues crucial for ATPase and DNA helicase activities and virus replication, Lys200 cannot be substituted by other residues to establish sufficient activities, structure of the NTP-binding pocket well conserved among the viruses of the Flaviviridae [4]; <14> structural characterization of the C-terminal portion containing the ATPase/helicase domain, encompasses residues 181-619, monomer structure determined by analytical centrifugation and gel filtration, SDS-PAGE and immunoblotting, structure determined by circular dichroism and fluorescence spectroscopy, ATPase activity stimulated by RNA and ssDNA, DNA helicase activity assayed with different salt concentrations from 5 to 150 mM and ATP concentrations at 40, 80, 100, 250 and 500 microM, respectively, no DNA helicase activity at protein concentrations up to 500 nM, linker region between the protease and the helicase domains predicted as a prerequisite for protein-protein interactions leading to the formation of the active oligomer [67]; <12> surface of domain 2 of the NS3 NTPase/helicase in direct vicinity to a flexible loop that is localized between Val1458 and Thr1476, accessibility of the Arg-rich amino acid motif by this loop for protein kinase C inhibition analyzed, two variants of domain 2 generated, in vitro protein kinase C (PKC) phosphorylation studies, binding and competition assays, modelling of ribbon diagrams, presence of the intact loop abolishes the binding of domain 2 to a tailed duplex RNA, binding of dsDNA not affected, loop structure reduces the extent of inhibition of protein kinase C (PKC) by domain 2 and regulates the binding of dsRNA, various mechanisms by which the NS3 protein perturb signal transduction in infected cells [63]) [4,15,38,61,62,63,64,66,67]

K_m-Value (mM)

0.0026 <49> (2'(3')-O-(N-methylanthraniloyl)ATP, <49> pH 7.5, 20°C, in presence of DNA [39]) [39]
0.0035 <49> (ATP, <49> pH 7.5, 20°C, in presence of DNA [39]) [39]
0.0038 <33> (ATP, <33> pH 8.0, 30°C, with saturating concentration of M13 mp18 ssDNA [51]) [51]
0.005 <49> (ATP, <49> pH 7.5, 20°C, without DNA [39]) [39]
0.006 <49> (2'(3')-O-(N-methylanthraniloyl)ATP, <49> pH 7.5, 20°C, without DNA [39]) [39]
0.0095 <14> (ATP, <14> pH 7.5, 30°C, in presence of 2 mM Mg^{2+} [2]) [2]
0.013 <14> (ATP, <14> recombinant protein including C-terminal portion the ATPase/helicase domain encompassing residues 181-619, ATP concentration 1 mM ATP, ATPase but not DNA helicase activity [67]) [67]
0.0553 <42> (ATP, <42> pH 7.5, in presence of 1 mM Co^{2+} [22]) [22]
0.061 <3> (ATP) [48]
0.07 <12> (ATP, <12> helicase-catalyzed DNA unwinding activity mediated by recombinant nonstructural protein 3, reactions with 1 mM ATP contain 1.25 mM total $MgCl_2$, data are globally fit to a model for substrate inhibition [38]) [38]

0.08 <42> (ATP, <42> pH 7.5, in presence of 1 mM Mg^{2+} [22]) [22]
0.086 <42> (ATP, <42> pH 7.5, in presence of 1 mM Mn^{2+} [22]) [22]
0.09 <4> (ATP, <4> pH 7.5, 30°C [8]) [8]
0.1 <34> (ATP, <34> mutant (RECQ1(T1))Y564A, a construct encompassing amino acids 49-616 (of 649) of RECQ1, followed by a C-terminal tag of 22 aa [57]) [57]
0.115 <34> (ATP, <34> full-length RECQ1 helicase [57]) [57]
0.128 <42> (ATP, <42> pH 7.5, in presence of 1 mM Ni^{2+} [22]) [22]
0.135 <34> (ATP, <34> (RECQ1(T1)), a construct encompassing amino acids 49-616 (of 649) of RECQ1, followed by a C-terminal tag of 22 aa [57]) [57]
0.15 <1,40> (ATP, <40> pH 7.5, 30°C [60]; <1> pH 8.0, 30°C, in presence of ssDNA [49]) [49,60]
0.152 <29> (ATP, <29> pH 7.5, 37°C, addition of 60-mer oligonucleotide [23]) [23]
0.163 <12> (ATP, <12> addition of polyuridylate lowers K_m for the ATP substrate [62]) [62]
0.2 <4> (ATP, <4> pH 7.8, 30°C [27]) [27]
0.2 <15> (GTP, <15> pH 6.6, 25°C [32]) [32]
0.2 <15> (dATP, <15> pH 6.6, 25°C [32]) [32]
0.22 <29> (ATP, <29> pH 7.5, 37°C, addition of M13mp19 ssDNA [23]) [23]
0.22 <15> (dCTP, <15> pH 6.6, 25°C [32]) [32]
0.25 <1,4> (dATP, <4> pH 7.8, 30°C [27]; <1> pH 8.0, 30°C, in presence of ssDNA [49]) [27,49]
0.256 <12> (ATP, <12> wild-type [62]) [62]
0.3 <12> (dTTP, <12> helicase-catalyzed DNA unwinding activity mediated by recombinant nonstructural protein 3, reactions with 0.2 mM ATP contain 0.45 mM total $MgCl_2$, data are globally fit to a model for substrate inhibition [38]) [38]
0.33 <15> (ATP, <15> pH 6.6, 25°C [32]) [32]
0.35 <15> (dGTP, <15> pH 6.6, 25°C [32]) [32]
0.41 <12> (GTP, <12> helicase-catalyzed DNA unwinding activity mediated by recombinant nonstructural protein 3, data for reactions performed at or below 1 mM NTP, data are globally fit to a model for substrate inhibition [38]) [38]
0.47 <22> (ATP, <22> pH 7.6, 30°C, in presence of poly(dA) [30]) [30]
0.47 <15> (CTP, <15> pH 6.6, 25°C [32]) [32]
0.55 <15> (UTP, <15> pH 6.6, 25°C [32]) [32]
0.58 <22> (ATP, <22> pH 7.6, 30°C, in presence of M13mp18 single-stranded circular DNA [30]) [30]
0.65 <9> (ATP, <9> pH 7.8, 37°C [7]) [7]
0.93 <15> (dUTP, <15> pH 6.6, 25°C [32]) [32]
Additional information <49> (<49> K_M-values for cleavage of dTn DNA (dT10, dT20, dT30, dT40) [39]) [39]

K_i-Value (mM)

0.00071 <7> (nogalamycin, <7> pH 8.0, 37°C [15]) [15]
0.004 <7> (daunorubicin, <7> pH 8.0, 37°C [15]) [15]

0.0052 <7> (ethidium bromide, <7> pH 8.0, 37°C [15]) [15]
0.0056 <7> (actinomycin C1, <7> pH 8.0, 37°C [15]) [15]
0.09 <12> (GTP, <12> recombinant nonstructural protein 3 analyzed for DNA unwinding rates, acts as a noncompetitive inhibitor, 22°C, 2 mM $MgCl_2$, 25 nM enzyme, and 5 nM substrate, pH 6.5, initiation by adding each NTP to 0.5 mM [38]) [38]
0.09 <12> (NTP, <12> recombinant nonstructural protein 3 analyzed for DNA unwinding rates, data globally fit to a model for substrate inhibition, 22°C, 2 mM $MgCl_2$, 25 nM enzyme, and 5 nM substrate, pH 6.5, initiation by adding each NTP to 0.5 mM [38]) [38]
0.097 <12> (2'-deoxythymidine 5'-phosphoryl-β,γ-hypophosphate, <12> i.e. ppopT, dTTP analogue, inhibition of NTPase activity of NS3 protein by NTP derivatives [62]) [62]
0.109 <12> (N^1-OH^-ITP, <12> inhibition of NTPase activity of NS3 protein by NTP derivatives [62]) [62]
0.116 <12> (2',3'-ddATP, <12> inhibition of NTPase activity of NS3 protein by NTP derivatives [62]) [62]
0.116 <12> (2'-dTTP, <12> inhibition of NTPase activity of NS3 protein by NTP derivatives [62]) [62]
0.141 <12> (3'-dATP, <12> inhibition of NTPase activity of NS3 protein by NTP derivatives [62]) [62]
0.145 <12> (β,γ-methylene-ATP, <12> efficient inhibitor, like the N^1-oxides N^1-oxoadenosine 5-triphosphate and N^1-hydroxyinosine 5-triphosphate [62]) [62]
0.205 <12> (N^1-O-ATP, <12> inhibition of NTPase activity of NS3 protein by NTP derivatives [62]) [62]
0.26 <12> (3'-dUTP, <12> inhibition of NTPase activity of NS3 protein by NTP derivatives [62]) [62]
0.277 <12> (2'-dGTP, <12> inhibition of NTPase activity of NS3 protein by NTP derivatives [62]) [62]
0.291 <12> (2'-dATP, <12> inhibition of NTPase activity of NS3 protein by NTP derivatives [62]) [62]
0.298 <12> (2',3'-ddTTP, <12> inhibition of NTPase activity of NS3 protein by NTP derivatives [62]) [62]
0.443 <12> (3'-dGTP, <12> inhibition of NTPase activity of NS3 protein by NTP derivatives [62]) [62]
0.576 <12> (GTP, <12> inhibition of NTPase activity of NS3 protein by NTP derivatives [62]) [62]
0.69 <12> (ATP, <12> recombinant nonstructural protein 3 analyzed for DNA unwinding rates, 22°C, 2 mM Mg^{2+}, 25 nM enzyme, and 5 nM substrate, pH 6.5, initiation by adding each NTP to 0.5 mM [38]) [38]
0.721 <12> (2',3'-ddGTP, <12> inhibition of NTPase activity of NS3 protein by NTP derivatives [62]) [62]
1.3 <12> (ADP, <12> inhibition of NTPase activity of NS3 protein by NTP derivatives [62]) [62]
1.46 <12> (UTP, <12> inhibition of NTPase activity of NS3 protein by NTP derivatives [62]) [62]

5 <12> (AMP, <12> inhibition of NTPase activity of NS3 protein by NTP derivatives [62]) [62]

pH-Optimum

6.5 <12> (<12> assay at [38]; <12> helicase-catalyzed DNA unwinding activity at [38]) [38]
6.6 <15,16> (<15,16> assay at [32,64]) [32,64]
6.6-8.4 <28> [35]
7 <5> (<5> assay at [44]) [44]
7.4 <12> (<12> activity assay at [62]) [62]
7.5 <3,4,12,13,14,36,40,49> (<3,12,13,14,36,40,49> assay at [2,28,29,39,59,60,61,67]; <4> unwinding reaction [26]) [2,26,27,28,29,39,59,60,61,67]
7.6 <18,19,22,26,27> (<18,19,22,26,27> assay at [19,30,31,34,42]) [19,30,31,34,42]
7.8 <9,21> (<9,21> assay at [7,33]) [7,33]
8 <1,7,43,47> (<1,43> assay at [9,49,50]; <47> ATPase activity, DNA-unwinding activity [37]) [9,15,37,49,50]
8.9 <20> (<20> assay at [16]) [16]

pH-Range

6-9 <4> (<4> pH 6.0: about 35% of maximal activity, pH 9.0: about 65% of maximal activity [26]) [26]
6.5-8.5 <47> (<47> pH 6.5: about 60% of maximal activity, pH 8.5: about 60% of maximal activity, ATPase activity [37]) [37]
6.5-8.9 <9> (<9> the enzyme functions efficiently over wide ranges of pH from 6.5 to 8.9 [7]) [7]
7.5-9 <7> (<7> significant unwinding activity is observed in the broad pH range (pH 7.5-9.0) [15]) [15]

pi-Value

7.6 <47> (<47> calculated from sequence [37]) [37]
8 <39> (<39> calculated from sequence [18]) [18]

Temperature optimum (°C)

20 <49> (<49> assay at [39]) [39]
22 <12> (<12> helicase-catalyzed DNA unwinding activity at [38]) [38]
25 <15> (<15> assay at [32]) [32]
29 <47> (<47> ATPase activity [37]) [37]
30 <1,12,14,19,22,40> (<1,12,14,19,22,40> assay at [2,30,34,49,50,60,61]) [2,30,34,49,50,60,61]
37 <3,5,9,12,13,14,16,18,21,26,27,36,42,43,51> (<3,5,9,12,13,14,16,18,21,26,27,36,42,43,51> assay at [4,7,9,19,22,28,29,31,33,38,42,44,59,64,67]; <12> activity assay at [62]) [4,7,9,19,22,28,29,31,33,38,42,44,59,62,64,67]
50 <20> [16]

Temperature range (°C)

20-37 <43> (<43> similar active at 20°C, 30°C and 37°C [9]) [9]
25-34 <47> (<47> 25°C: about 55% of maximal activity, 34°C: about 40% of maximal activity, ATPase activity [37]) [37]

30-60 <20> (<20> 30°C: about 65% of maximal activity, 60°C: about 75% of maximal activity [16]) [16]

4 Enzyme Structure

Molecular weight

50480 <47> (<47> calculated from sequence [37]) [37]
54000 <51> (<51> molecular mass of the helicase/NTPase domain, SDS-PAGE [4]) [4]
65000 <9> (<9> gel filtration, glycerol gradient analysis [7]) [7]
66000 <14> (<14> recombinant protein of C-terminal portion the ATPase/helicase domain, residues 181-619, SDS-PAGE, gel filtration [67]) [67]
85000 <42> (<42> sedimentation equilibrium ultracentrifugation [22]) [22]
120000 <7> (<7> gel filtration, glycerol gradient centrifugation [15]) [15]
128000 <3> (<3> gel filtration [45]) [45]
136000 <7> (<7> gel filtration [14]) [14]
170000 <39> (<39> calculated from sequence [18]) [18]
200000 <1> (<1> gel filtration, glycerol gradient centrifugation [46]) [46]
500000 <4> (<4> gel filtration [8]) [8]
600000 <3> (<3> gel filtration [48]) [48]

Subunits

? <1,3,4,11,12,14,15,21,29,47> (<47> x * 54000, SDS-PAGE [37]; <11> x * 90000, SDS-PAGE [55]; <14> x * 60000, SDS-PAGE [2]; <12,15,21> x * 70000, SDS-PAGE [1,32,33]; <29> x * 50000, SDS-PAGE [23]; <3> x * 180000, SDS-PAGE [28]; <4> x * 12000, SDS-PAGE [27]; <47> x * 50478, calculated from sequence [37]; <1> x * 54000, small isoform of RECQ5 helicase, SDS-PAGE [49]) [1,2,23,27,28,32,33,37,49,55]
dimer <7> (<7> 2 * 68000, SDS-PAGE [14]) [14]
heptamer <6> (<6> structural polymorphism: in addition to helical filaments and heptameric rings the protein also forms double heptamers, hexamers and double hexamers, octamers and open rings [43]) [43]
heterodimer <7> (<7> 1 * 54000 + 1 * 66000, SDS-PAGE [15]) [15]
hexamer <3,4,6,35> (<4> 6 * 90000, SDS-PAGE [8]; <3> 6 * 116000, SDS-PAGE [48]; <6> structural polymorphism: in addition to helical filaments and heptameric rings the protein also forms double heptamers, hexamers and double hexamers, octamers and open rings [43]) [8,43,48]
homohexamer <30> (<30> 6 * 30000 [5]) [5]
monomer <3,4,8,9,14,33,42> (<3> 1 * 128000, SDS-PAGE [45]; <9> 1 * 63000, SDS-PAGE [7]; <33> 1 * 71000, SDS-PAGE [51]; <4> 1 * 135000, SDS-PAGE [26]; <42> 1 * 85000, the lack of cooperativity observed for both the ATPase and helicase activities lends support to the view that UvrD monomers are the functional unit [22]; <8> BcMCM is a monomer in solution but likely forms the functional oligomer in vivo [52]; <14> $\alpha\beta$, 29% α-helix, 15% β-sheet, and 56% non-regular structures, globular monomer accounts for 90%, a small

percentage (7%) of dimers or trimers, higher oligomers almost absent (3%), analytical centrifugation and gel filtration [67]) [7,22,26,45,51,52,67]
octamer <6> (<6> structural polymorphism: in addition to helical filaments and heptameric rings the protein also forms double heptamers, hexamers and double hexamers, octamers and open rings [43]) [43]
Additional information <24> (<24> posttranslational modifications lacking in in vitro- or bacterially synthesized Rep52 may be required for efficient Rep52 multimerization [40]) [40]

5 Isolation/Preparation/Mutation/Application

Source/tissue

B-cell <3> [28]
HeLa cell <3> (<3> maximal level of expression is observed in late G1/early S phase [48]) [45,48]
culture medium <14> [2]
embryo <1> [46]
leaf <7,32> [14,15,56]
testis <3,48> (<3,48> GRTH is a negative regulator of apoptosis in spermatocytes and promotes the progress of spermatogenesis [36]) [36]
thymus <5> (<5> calf [44]) [44]

Localization

chloroplast <7> [14]
membrane <12> [61]
mitochondrion <40> (<40> mitochondrial localization of Hmi1p is essential for its role in mtDNA metabolism [60]) [60]
nucleus <7> [15]

Purification

<1> [46]
<1> (enzyme recombinantly expressed in Escherichia coli) [49]
<3> [45,48]
<3> (recombinant) [28]
<4> [8,26,27]
<7> [14,15]
<9> [7]
<10> [47]
<11> [55]
<12> [1,11]
<12> (gel filtration, SDS-PAGE) [61,63]
<12> (gel filtration, recombinant nonstructural protein 3) [38]
<12> (gel filtration, recombinant protein) [62]
<12> (truncated and full-length complexes between nonstructural protein 3 (NS3) and nonstructural protein 4A (NS4), NS3-4A complex purifies as two separable proteins, gel filtration, SDS-PAGE) [65]

<13> (one-step column purification of helicase-primase subcomplex (helicase-primase enzyme complex consisting of UL5 and UL52 gene functions) using C-terminally His-tagged UL5 subunit) [59]
<14> [2]
<14> (gel filtration, recombinant protein, soluble form) [67]
<15> [32]
<20> [16]
<21> (generation of recombinant baculovirus encoding the human TWINKLE gene, expression in insect cells) [33]
<22> [30]
<23> [3]
<26> [19]
<27> [42]
<28> [35]
<29> [23]
<30> [5]
<31> [13]
<33> [53]
<33> (full-length PIF1 with a 6* histidine tag at the N-terminus, a C-terminal truncated form (PIF1N) and a N-terminal truncated form (PIF1C)) [51]
<33> (streamlined purification for the production of near-homogeneous and high yield recombinant forms of the human mitochondrial DNA helicase, minimizing the number of steps and the time elapsed for purification) [41]
<34> (a construct (RECQ1(T1)) encompassing amino acids 49-616 (of 649) of RECQ1, followed by a C-terminal tag of 22 aa is produced in Escherichia coli and purified to more than 95% homogeneity) [57]
<36> (recombinant Sgs1 fragment (amino acids 400-1268 of the 1447-amino acid full-length protein)) [29]
<37> [20]
<38> [54]
<40> (recombinant) [60]
<42> (recombinant histidine-tagged form of the protein) [22]
<43> [9]
<46> (recombinant enzyme) [24]
<47> [37]
<50> (gel filtration) [66]
<51> (gel filtration, recombinant protein) [4]

Crystallization

<10> (crystallization of the helicase domain of bacteriophage T7 gene 4 protein) [47]
<12> [11]
<30> (hanging-drop vapour-diffusion method with polyethyleneglycol monomethyl ether as precipitating agent) [5]
<31> (1.8 A resolution crystal structure of the catalytic core of Escherichia coli RecQ in its unbound form and a 2.5 A resolution structure of the core bound to ATPγS) [13]

<34> (purified RECQ1T1 protein is crystallized in the presence of ATP-γS and oligonucleotides by vapor diffusion from sitting drops equilibrated against 0.2 M sodium bromide, 20% PEG 3350, 10% ethylene glycol, 0.1 M bis-Tris propane (pH 7.5). Crystal structure of a truncated form (RECQ1(T1)) of the human RECQ1 protein with $MgADP^{2-}$) [57]
<45> (hanging-drop vapour diffusion at room temperature) [6]
<51> (enzymatically active fragment of the JEV NTPase/helicase catalytic domain, recombinant protein, crystal structure determined at 1.8 A resolution, data collection and refinement statistics) [4]

Cloning

<3> [36]
<3> (expression in Escherichia coli) [48]
<3> (overexpression of an oligohistidine-tagged version of the BLM gene product in Saccharomyces cerevisiae) [28]
<4> (expression in Escherichia coli) [8]
<10> [47]
<12> [1]
<12> (NS3-plus and NS3/4a-plus genes expressed in Escherichia coli, generation of NS3-4A expression product, pET15b and pet-SUMO vector) [65]
<12> (expressed in Escherichia coli) [61]
<12> (expressed in Escherichia coli BL21(DE3), recombinant protein, NS3d2wt variant corresponding to wild-type domain 2, NS3d2D construct comprises the complete domain, HCV(1361-1503) without loop, pET21b andpET16b vectors) [63]
<12> (expressed in Escherichia coli, strain Rosetta (DE3), recombinant nonstructural protein 3) [38]
<12> (expressed in Escherichia coli, strains XL-1 Blue, Rosetta (DE3), M15 (pREP4), vector pET-21-2c, kinetics of NS3 protein accumulation upon its expression in Escherichia coli at 25°C for 1-5 h shown) [62]
<13> (His6-tagged DNA helicase expressed via recombinant baculovirus) [59]
<14> (expressed in Escherichia coli, C-terminal portion with the ATPase/helicase domain, plasmid pET-30a) [67]
<15> [32]
<20> [16]
<23> (baculovirus expression system) [3]
<26> (expression of a truncated version of Rrm3p as a GST fusion protein in Saccharomyces cerevisiae. This polypeptide (Rrm3pΔN), contains amino acids 194 to 723 of the 723-amino-acid protein, including all seven helicase motifs as well as 56 amino acids amino-terminal of the first helicase motif. Rrm3pΔN is expressed under the control of a galactose-inducible promoter) [19]
<28> (the carboxyl-terminal His6 epitope is attached to the MPH1-coding sequence and the tagged gene is placed under the galactose inducible GAL1 promoter in the vector pYES) [35]
<29> [23]

<32> [56]
<33> (human hPif1 (nuclear form amino acids 1-641) and the hPif helicase domain (hPifHD, amino acid residues 206-620) are cloned as a fusion protein with glutathione S-transferase in pET11c. GST-hPifHD is expressed in Escherichia coli BL21(DE3) cells) [53]
<34> (a construct (RECQ1(T1)) encompassing amino acids 49-616 (of 649) of RECQ1, followed by a C-terminal tag of 22 aa is produced in Escherichia coli) [57]
<36> (a recombinant Sgs1 fragment (amino acids 400-1268 of the 1447-amino acid full-length protein) is overexpressed in yeast) [29]
<37> (PcrA protein is overexpressed with a His6 fusion at its amino-terminal end) [20]
<38> [54]
<40> [60]
<42> (histidine-tagged form of the protein is expressed) [22]
<43> [9]
<44> [17]
<46> (expression of a recombinant Dbp9p in Escherichia coli) [24]
<47> (expression in Escherichia coli) [37]
<48> [36]
<50> (NS3-plus and NS3/4a-plus genes expressed in Escherichia coli, composition of NS3-4A expression product using the pet-SUMO vector) [66]
<51> (expressed in Escherichia coli BL21 (DE3), recombinant protein, pET21b vector) [4]

Engineering

C261A <8> (<8> mutant with a disrupted zinc-binding site. One mol of the C261A mutant contains 0.03 atoms [52]) [52]
D523N <17> (<17> DNA binding and ATPase activity is comparable to wild-type enzyme, no in vitro replication activity [58]) [58]
D542N <17> (<17> DNA binding and ATPase activity is comparable to wild-type enzyme, no in vitro replication activity [58]) [58]
H293A <12> (<12> mutation results in a protein with a significantly higher level of ATPase in the absence of RNA. The mutant protein still unwinds RNA. In the presence of RNA, the H293A mutant hydrolyzes ATP slower than wild-type [11]) [11]
K116H <24> (<24> an MBP-Rep52 chimera bearing K116H mutation within a consensus helicase- and ATPase-associated motif (motif I or Walker A site) is deficient for both DNA helicase and ATPase activities [40]) [40]
K337A <27> (<27> K337A and the K337R alleles are unable to supply the essential function of Pfh1p [42]) [42]
K337R <27> (<27> K337A and the K337R alleles are unable to supply the essential function of Pfh1p [42]) [42]
K340H <24> (<24> in a Rep78 A-site mutant protein bearing mutation K340H, the MBP-Rep52 A-site mutant protein fails to exhibit a trans-dominant negative effect when it is mixed with wild-type MBP-Rep52 or MBP-Rep78 in vitro [40]) [40]

K484E <17> (<17> mutant enzyme binds the immunoaffinity column poorly, the heparin purified E1/K484E is tested for the above activities. The protein that is recovered shows no activity [58]) [58]
K653A <8> (<8> mutation of the ATP-binding site reduces activity to about 30% of wild-type. This drop in ATPase activity corresponds to an abrogation of helicase activity observed in the same mutant [52]) [52]
P479S <17> (<17> DNA binding and ATPase activity is comparable to wild-type enzyme, 50% of in vitro replication activity compared to wild-type enzyme [58]) [58]
Additional information <6,35> (<35> a mutation of the MCM N-terminal β-hairpin reduces but does not abolish DNA binding and helicase activity [43]; <6> a mutation of the zinc finger motif of the MCM protein reduces single-stranded and double-stranded DNA binding and abolishes helicase activity. Removal of the HTH domain from the MCM protein results in an enzyme with increased ATPase and helicase activity. A mutation of the MCM N-terminal β-hairpin completely abolishes DNA binding and helicase activity [43]) [43]

Application

medicine <39> (<39> UvrD helicase is a potential drug targets for chemotherapy of malaria. As Plasmodium falciparum contains only one homologue of UvrD helicase and human lacks this helicase, detailed studies including cloning and characterization of UvrD helicase of malaria parasite may be helpful in identifying a compound that has no effect on the cellular machinery of the host and consequently could be used as the potential drug for the treatment of malaria [18]) [18]
pharmacology <12,51> (<51> conservation of the NTP-binding pocket among viruses of the family Flaviviridae as potential for development of therapeutics [4]; <12> peptide inhibitors reproducing the structure of the autoregulatory motif as possibility to develop effective antivirals [61]) [4,61]

6 Stability

Temperature stability

56 <7> (<7> 1 min, inactivated [14]; <7> 1 min, loss of activity [15]) [14,15]
60 <47> (<47> enzyme is heat labile and loses its activity upon heating at 60°C for 1 min [37]) [37]

General stability information

<3>, enzyme activity is destroyed if trypsin is included in the reaction [45]
<7>, trypsin destroys activity [14]

Storage stability

<3>, 4°C, DNA helicase VI loses 90% of its activity in 24 h [45]
<7>, 4°C, inactivation after prolonged storage [14]
<11>, -70°C, loses 25% of its activity following storage for 6 months [55]

References

[1] Poliakov, A.; Hubatsch, I.; Shuman, C.F.; Stenberg, G.; Danielson, U.H.: Expression and purification of recombinant full-length NS3 protease-helicase from a new variant of hepatitis C virus. Protein Expr. Purif., **25**, 363-371 (2002)
[2] Borowski, P.; Niebuhr, A.; Mueller, O.; Bretner, M.; Felczak, K.; Kulikowski, T.; Schmitz, H.: Purification and characterization of West Nile virus nucleoside triphosphatase (NTPase)/helicase: evidence for dissociation of the NTPase and helicase activities of the enzyme. J. Virol., **75**, 3220-3229 (2001)
[3] Ivanov, K.A.; Ziebuhr, J.: Human coronavirus 229E nonstructural protein 13: characterization of duplex-unwinding, nucleoside triphosphatase, and RNA 5-triphosphatase activities. J. Virol., **78**, 7833-7838 (2004)
[4] Yamashita, T.; Unno, H.; Mori, Y.; Tani, H.; Moriishi, K.; Takamizawa, A.; Agoh, M.; Tsukihara, T.; Matsuura, Y.: Crystal structure of the catalytic domain of Japanese encephalitis virus NS3 helicase/nucleoside triphosphatase at a resolution of 1.8 A. Virology, **373**, 426-436 (2008)
[5] Röleke, D.; Hoier, H.; Bartsch, C.; Umbach, P.; Scherzinger, E.; Lurz, R.; Saenger, W.: Crystallization and preliminary X-ray crystallographic and electron microscopic study of a bacterial DNA helicase (RSF1010 RepA). Acta Crystallogr. Sect. D, **53**, 213-216 (1997)
[6] Singleton, M.R.; Scaife, S.; Raven, N.D.; Wigley, D.B.: Crystallization and preliminary X-ray analysis of RecG, a replication-fork reversal helicase from Thermotoga maritima complexed with a three-way DNA junction. Acta Crystallogr. Sect. D, **57**, 1695-1696 (2001)
[7] Lee, C.; Seo, Y.S.: Isolation and characterization of a processive DNA helicase from the fission yeast Schizosaccharomyces pombe that translocates in a 5'-to-3' direction. Biochem. J., **334**, 377-386 (1998)
[8] Biswas, E.E.; Fricke W.M.; Chen, P.H.; Biswas, S.B.: Yeast DNA helicase A: cloning, expression, purification, and enzymatic characterization. Biochemistry, **36**, 13277-13284 (1997)
[9] Hyun, M.; Bohr, V.A.; Ahn B.: Biochemical characterization of the WRN-1 RecQ helicase of Caenorhabditis elegans. Biochemistry, **47**, 7583-7593 (2008)
[10] Roychowdhury, A.; Szymanski, M.R.; Jezewska, M.J.; Bujalowski, W.: Mechanism of NTP hydrolysis by the Escherichia coli primary replicative helicase DnaB protein. 2. Nucleotide and nucleic acid specificities. Biochemistry, **48**, 6730-6746 (2009)
[11] Frick, D.N.: The hepatitis C virus NS3 protein: a model RNA helicase and potential drug target. Curr. Issues Mol. Biol., **9**, 1-20 (2007)
[12] Sidorova, J.M.: Roles of the Werner syndrome RecQ helicase in DNA replication. DNA Repair, **7**, 1776-1786 (2008)
[13] Bernstein, D.A.; Zittel, M.C.; Keck, J.L.: High-resolution structure of the E.coli RecQ helicase catalytic core. EMBO J., **22**, 4910-4921 (2003)

[14] Tuteja, N.; Phan, T.N.; Tewari, K.K.: Purification and characterization of a DNA helicase from pea chloroplast that translocates in the 3'-to-5' direction. Eur. J. Biochem., **238**, 54-63 (1996)
[15] Phan, T.N.; Ehtesham, N.Z.; Tuteja, R.; Tuteja, N.: A novel nuclear DNA helicase with high specific activity from Pisum sativum catalytically translocates in the 3'→5' direction. Eur. J. Biochem., **270**, 1735-1745 (2003)
[16] Collins, R.; McCarthy, T.V.: Purification and characterization of Thermus thermophilus UvrD. Extremophiles, **7**, 35-41 (2003)
[17] Ohhata, T.; Araki, R.; Fukumura, R.; Kuroiwa, A.; Matsuda, Y.; Abe, M.: Cloning, genomic structure and chromosomal localization of the gene encoding mouse DNA helicase RECQL5β. Gene, **280**, 59-66 (2001)
[18] Shankar, J.; Tuteja, R.: UvrD helicase of Plasmodium falciparum. Gene, **410**, 223-233 (2007)
[19] Ivessa, A.S.; Zhou, J.Q.; Schulz, V.P.; Monson, E.K.; Zakian, V.A.: Saccharomyces Rrm3p, a 5' to 3' DNA helicase that promotes replication fork progression through telomeric and subtelomeric DNA. Genes Dev., **16**, 1383-1396 (2002)
[20] Naqvi, A.; Tinsley, E.; Khan, S.A.: Purification and characterization of the PcrA helicase of Bacillus anthracis. J. Bacteriol., **185**, 6633-6639 (2003)
[21] Ruiz-Maso, J.A.; Anand, S.P.; Espinosa, M.; Khan, S.A.; del Solar, G.: Genetic and biochemical characterization of the Streptococcus pneumoniae PcrA helicase and its role in plasmid rolling circle replication. J. Bacteriol., **188**, 7416-7425 (2006)
[22] Curti, E.; Smerdon, S.J.; Davis, E.O.: Characterization of the helicase activity and substrate specificity of Mycobacterium tuberculosis UvrD. J. Bacteriol., **189**, 1542-1555 (2006)
[23] Biswas, E.E.; Barnes, M.H.; Moir, D.T.; Biswas, S.B.: An essential DnaB helicase of Bacillus anthracis: identification, characterization, and mechanism of action. J. Bacteriol., **191**, 249-260 (2009)
[24] Kikuma, T.; Ohtsu, M.; Utsugi, T.; Koga, S.; Okuhara, K.; Eki, T.; Fujimori, F.; Murakami, Y.: Dbp9p, a member of the DEAD box protein family, exhibits DNA helicase activity. J. Biol. Chem., **14; 279**, 20692-20698 (2004)
[25] Matson, S.W.: Escherichia coli helicase II (urvD gene product) translocates unidirectionally in a 3' to 5' direction. J. Biol. Chem., **261**, 10169-10175 (1986)
[26] Bean, D.W.; Kallam, W.E. Jr.; Matson, S.W.: Purification and characterization of a DNA helicase from Saccharomyces cerevisiae. J. Biol. Chem., **268**, 21783-21790 (1993)
[27] Shimizu, K.; Sugino, A.: Purification and characterization of DNA helicase III from the yeast Saccharomyces cerevisiae. J. Biol. Chem., **268**, 9578-9584 (1993)
[28] Karow, J.K.; Chakraverty, R.K.: Hickson, I.D.: The Bloom's syndrome gene product is a 3'-5' DNA helicase. J. Biol. Chem., **272**, 30611-30604 (1997)
[29] Bennett, R.J.; Sharp, J.A.; Wang, J.C.: Purification and characterization of the Sgs1 DNA helicase activity of Saccharomyces cerevisiae. J. Biol. Chem., **273**, 9644-9650 (1998)

[30] Nakagawa, T.; Flores-Rozas, H.; Kolodner, R.D.: The MER3 helicase involved in meiotic crossing over is stimulated by single-stranded DNA-binding proteins and unwinds DNA in the 3' to 5' direction.. J. Biol. Chem., **276**, 31487-31493 (2001)
[31] Brosh, R.M. Jr.; Waheed, J.; Sommers, J.A.: Biochemical characterization of the DNA substrate specificity of Werner syndrome helicase. J. Biol. Chem., **277**, 23236-23245 (2002)
[32] Tanner, J.A.; Watt, R.M.; Chai, Y.B.; Lu, L.Y.; Lin, M.C.; Peiris, J.S.; Poon. L.L.; Kung, H.F.; Huang, J.D.: The severe acute respiratory syndrome (SARS) coronavirus NTPase/helicase belongs to a distinct class of 5' to 3' viral helicases. J. Biol. Chem., **278**, 39578-3982 (2003)
[33] Korhonen, J.A.; Gaspari, M.; Falkenberg M.: TWINKLE has 5'→3' DNA helicase activity and is specifically stimulated by mitochondrial single-stranded DNA-binding protein. J. Biol. Chem., **278**, 48627-48632 (2003)
[34] Gupta, R.; Sharma, S.; Sommers, J.A.; Jin, Z.; Cantor, S.B.; Brosh, R.M.Jr.: Analysis of the DNA substrate specificity of the human BACH1 helicase associated with breast cancer. J. Biol. Chem., **280**, 25450-25460 (2005)
[35] Prakash, R.; Krejci, L.; van Komen, S.; Schürer, A.K.; Kramer, W.; Sung, P.: Saccharomyces cerevisiae MPH1 gene, required for homologous recombination-mediated mutation avoidance, encodes a 3' to 5' DNA helicase. J. Biol. Chem., **280**, 7854-7860 (2005)
[36] Gutti, R.K.; Tsai-Morris, C.H.; Dufau, M.L.: Gonadotropin-regulated testicular helicase (DDX25), an essential regulator of spermatogenesis, prevents testicular germ cell apoptosis. J. Biol. Chem., **283**, 17055-17064 (2008)
[37] Liu, H.H.; Liu, J.; Fan, S.L.; Song, M.Z.: Han, X.L.; Liu, F.; Shen, F.F.: Molecular cloning and characterization of a salinity stress-induced gene encoding DEAD-box helicase from the halophyte Apocynum venetum. J. Exp. Bot., **59**, 633-644 (2008)
[38] Belon, C.A.; Frick, D.N.: Fuel specificity of the hepatitis C virus NS3 helicase. J. Mol. Biol., **388**, 851-864 (2009)
[39] Toseland, C.P.; Martinez-Senac, M.M.; Slatter, A.F.; Webb, M.R.: The ATPase cycle of PcrA helicase and its coupling to translocation on DNA. J. Mol. Biol., **392**, 1020-1032 (2009)
[40] Smith, R.H.; Kotin, R.M.: The Rep52 gene product of adeno-associated virus is a DNA helicase with 3'-to-5' polarity. J. Virol., **72**, 4874-4881 (1998)
[41] Ziebarth, T.D.; Kaguni, L.S.: Purification strategy for recombinant forms of the human mitochondrial DNA helicase. Methods Mol. Biol., **554**, 121-126 (2009)
[42] Zhou, J.Q.; Qi, H.; Schulz, V.P.; Mateyak, M.K.; Monson, E.K.; Zakian, V.A.: Schizosaccharomyces pombe pfh1+ encodes an essential 5' to 3' DNA helicase that is a member of the PIF1 subfamily of DNA helicases. Mol. Biol. Cell, **13**, 2180-2191 (2002)
[43] Sakakibara, N.; Kelman, L.M.; Kelman, Z.: Unwinding the structure and function of the archaeal MCM helicase. Mol. Microbiol., **72**, 286-296 (2009)
[44] Turchi, J.J.; Murante, R.S.; Bambara, R.A.: DNA substrate specificity of DNA helicase E from calf thymus. Nucleic Acids Res., **20**, 6075-6080 (1992)

[45] Tuteja, N.; Ochem, A.; Taneja, P.; Tuteja, R.; Skopac, D.; Falaschi, A.: Purification and properties of human DNA helicase VI. Nucleic Acids Res., **23**, 2457-2463 (1995)
[46] Thömmes, P.; Marton, R.F.; Cotterill, S.: Purification and characterisation of a DNA helicase, dheI I, from Drosophila melanogaster embryos. Nucleic Acids Res., **23**, 4443-4450 (1995)
[47] Bird, L.E.; Hakansson, K.; Pan, H.; Wigley, D.B.: Characterization and crystallization of the helicase domain of bacteriophage T7 gene 4 protein. Nucleic Acids Res., **25**, 2620-2626 (1997)
[48] Biswas, E.E; Nagele, R.G.; Biswas, S.: A novel human hexameric DNA helicase: expression, purification and characterization.. Nucleic Acids Res., **29**, 1733-1740 (2001)
[49] Ozsoy, A.Z.; Sekelsky, J.J.; Matson, S.W.: Biochemical characterization of the small isoform of Drosophila melanogaster RECQ5 helicase. Nucleic Acids Res., **29**, 2986-2993 (2001)
[50] Ozsoy, A.Z.; Ragonese, H.M.; Matson. S.W.: Analysis of helicase activity and substrate specificity of Drosophila RECQ5. Nucleic Acids Res., **31**, 1554-1564 (2003)
[51] Gu, Y.; Masuda, Y.; Kamiya, K.: Biochemical analysis of human PIF1 helicase and functions of its N-terminal domain. Nucleic Acids Res., **36**, 6295-6308 (2008)
[52] Samuels, M.; Gulati, G.; Shin, J.H.; Opara, R.; McSweeney, E.; Sekedat, M.; Long, S.; Kelman, Z.; Jeruzalmi, D.: A biochemically active MCM-like helicase in Bacillus cereus. Nucleic Acids Res., **37**, 4441-4452 (2009)
[53] George, T.; Wen, Q.; Griffiths, R.; Ganesh, A.; Meuth, M.; Sanders, C.M.: Human Pif1 helicase unwinds synthetic DNA structures resembling stalled DNA replication forks. Nucleic Acids Res., **37**, 6491-6502 (2009)
[54] Sakakibara, N.; Han, M.; Rollor, C.R.; Gilson, R.C.; Busch, C.; Heo, G.; Kelman, Z.: Cloning, purification, and partial characterization of the Halobacterium sp. NRC-1 minichromosome maintenance (MCM) helicase. Open Microbiol. J., **2**, 13-17 (2008)
[55] Suntornthiticharoen, P.; Petmitr, S.; Chavalitshewinkoon-Petmitr, P.: Purification and characterization of a novel 3'-5' DNA helicase from Plasmodium falciparum and its sensitivity to anthracycline antibiotics. Parasitology, **133**, 389-398 (2006)
[56] Bagherieh-Najjar, M.B.; de Vries, O.M.; Kroon, J.T.; Wright, E.L.; Elborough, K.M.; Hille, J.; Dijkwel, P.P.: Arabidopsis RecQsim, a plant-specific member of the RecQ helicase family, can suppress the MMS hypersensitivity of the yeast sgs1 mutant. Plant Mol. Biol., **52**, 273-284 (2003)
[57] Pike, A.C.; Shrestha, B.; Popuri, V.; Burgess-Brown, N.; Muzzolini, L.M.; Costantini, S.; Vindigni, A.; Gileadi, O.: Structure of the human RECQ1 helicase reveals a putative strand-separation pin. Proc. Natl. Acad. Sci. USA, **106**, 1039-1044 (2009)
[58] Dixon, E.P.; Pahel, G.L.; Rocque, W.J.; Barnes, J.A.; Lobe, D.C.; Hanlon, M.H.; Alexander, K.A.; Chao, S.F.; Lindley, K.; Phelps, W.C.: The E1 helicase of human papillomavirus type 11 binds to the origin of replication with low sequence specificity. Virology, **270**, 345-357 (2000)

[59] Schreiner, U.; Theune, M.; Althof, F.; Kehm, E.; Knopf, C.W.: One-step column purification of herpes simplex virus 1 helicase-primase subcomplex using C-terminally his-tagged UL5 subunit. Virus Genes, **39**, 19-29 (2009)
[60] Monroe, D.S. Jr.; Leitzel, A.K.; Klein, H.L.; Matson, S.W.: Biochemical and genetic characterization of Hmi1p, a yeast DNA helicase involved in the maintenance of mitochondrial DNA. Yeast, **22**, 1269-1286 (2005)
[61] Borowski, P.; Heising, M.V.; Miranda, I.B.; Liao, C.L.; Choe, J.; Baier, A.: Viral NS3 helicase activity is inhibited by peptides reproducing the Arg-rich conserved motif of the enzyme (motif VI). Biochem. Pharmacol., **76**, 28-38 (2008)
[62] Mukovnya, A.V.; Tunitskaya, V.L.; Khandazhinskaya, A.L.; Golubeva, N.A.; Zakirova, N.F.; Ivanov, A.V.; Kukhanova, M.K.; Kochetkov, S.N.: Hepatitis C virus helicase/NTPase: an efficient expression system and new inhibitors. Biochemistry (Moscow), **73**, 660-668 (2008)
[63] Hartjen, P.; Medom, B.K.; Reinholz, M.; Borowski, P.; Baier, A.: Regulation of the biochemical function of motif VI of HCV NTPase/helicase by the conserved Phe-loop. Biochimie, **91**, 252-260 (2009)
[64] Lee, C.; Lee, J.M.; Lee, N.R.; Jin, B.S.; Jang, K.J.; Kim, D.E.; Jeong, Y.J.; Chong, Y.: Aryl diketoacids (ADK) selectively inhibit duplex DNA-unwinding activity of SARS coronavirus NTPase/helicase. Bioorg. Med. Chem. Lett., **19**, 1636-1638 (2009)
[65] Beran, R.K.; Pyle, A.M.: Hepatitis C viral NS3-4A protease activity is enhanced by the NS3 helicase. J. Biol. Chem., **283**, 29929-29937 (2008)
[66] Beran, R.K.; Lindenbach, B.D.; Pyle, A.M.: The NS4A protein of hepatitis C virus promotes RNA-coupled ATP hydrolysis by the NS3 helicase. J. Virol., **83**, 3268-3275 (2009)
[67] Feito, M.J.; Gomez-Gutierrez, J.; Ayora, S.; Alonso, J.C.; Peterson, D.; Gavilanes, F.: Insights into the oligomerization state-helicase activity relationship of West Nile virus NS3 NTPase/helicase. Virus Res., **135**, 166-174 (2008)

RNA helicase 3.6.4.13

1 Nomenclature

EC number
3.6.4.13

Systematic name
ATP phosphohydrolase (RNA helix unwinding)

Recommended name
RNA helicase

Synonyms
1a NTPase/helicase <16> [5]
ATP/dATP-dependent RNA helicase <1,42> [32]
ATPase <10,12> [1,36]
ATPase/RNA helicase <1,42> [32]
ATPase/helicase <10> [36,41]
BMV 1a protein <16> [5]
BmL3-helicase <1,42> [32]
Brr2p <6> [50]
DBP2 <24> [30]
DDX17 <33> [12]
DDX19 <43> [56]
DDX25 <23,34,35> [12,21]
DDX3 <25> [8]
DDX3X <25> (<25> the gene is localized to the X chromosome [12]) [12]
DDX3Y <29> (<29> the gene is localized to the Y chromosome [12]) [12]
DDX4 <30> [12]
DDX5 <32> [12]
DEAD box RNA helicase <1,2,3> [32,45,52]
DEAD box helicase <2> [45]
DEAD-box RNA helicase <4,5,7,38,47,48> [9,14,16,25,53,55]
DEAD-box protein DED1 <38> [11]
DEAD-box rRNA helicase <5> [26]
DEAH-box RNA helicase <24> [30]
DEAH-box protein 2 <24> [30]
DED1 <38> [11,14]
DENV NS^3H <10> [41]
DEXD/H-box RNA helicase <43> [56]
DEx(H/D)RNA helicase <12> [23]
DHX9 <44> [58]
DbpA <5> [10,25,26]

D. Schomburg and I. Schomburg (eds.), *Class 3.4–6 Hydrolases, Lyases, Isomerases, Ligases: EC 3.4–6*, Springer Handbook of Enzymes S10, DOI 10.1007/978-3-642-36260-6_25,

Dhx9/RNA helicase A <13> [61]
EhDEAD1 <7> [16]
EhDEAD1 RNA helicase <7> [16]
FRH <9> [54]
FRQ-interacting RNA helicase <9> [54]
GRTH <3> [57]
GRTH/DDX25 <3,35> [21,51]
HCV NS3 helicase <12> [48]
KOKV helicase <27> [7]
Mtr4p <31> [22]
NPH-II <8> [18,28]
NS3 <10,12,17,20,39,41> (<12,39> ambiguous [27,42,44]) [1,2,4,27,35,36,39, 42,44,46]
NS3 ATPase/helicase <10> [41]
NS3 NTPase/helicase <17> (<17> ambiguous [46]) [46]
NS3 helicase <10,12,17> [15,44,46]
NS3 protein <10,12,17,18> (<12> ambiguous [39]) [15,39,40,41,62]
NTPase/helicase <12> (<12> ambiguous [37]) [37,39]
RHA <6> [31,49]
RNA helicase <2> [45]
RNA helicase A <6,44> [31,49,58]
RNA helicase CrhR <14> [59]
RNA helicase DDX3 <25> [8]
RNA helicase Ddx39 <47> [53]
RNA helicase Hera <4> [9]
RNA-dependent ATPase <37> [34]
RNA-dependent NTPase/helicase <12> [1]
RTPase <10> [36]
RhlB <5> [43]
SpolvlgA <48> [55]
Supv3L1 <46> [64]
TGBp1 NTPase/helicase domain <22,28> [24]
Tk-DeaD <15> [47]
VRH1 <26> [33]
YxiN <2> [45]
eIF4A <36> [20]
eIF4A helicase <36> [20]
eIF4AIII <37> [34]
eukaryotic initiation factor eIF 4A <36> [20]
gonadotropin-regulated testicular RNA helicase <3> [51,57]
helicase <10> [41]
helicase B <5> [43]
helicase/nucleoside triphosphatase <10> [4]
non structural protein 3 <12> (<12> ambiguous [37,38]) [37,38]
non-structural 3 <10> [36]
non-structural protein 3 <17> [46]
non-structural protein 3 protein <18> [40]

nonstructural protein 3 <12,17,20,39,40,41> (<12,17,39,40> ambiguous [6,27,39,42,44,46]) [1,2,6,27,35,39,42,44,46]
nucleoside 5'-triphosphatase <10> [4]
nucleoside triphosphatase/RNA helicase and 5'-RNA triphosphatase <20> [2]
nucleoside triphosphatase/helicase <16> [5]
p54 RNA helicase <45> [60]
p68 RNA helicase <3,6> [52,63]
protein NS3 <12> (<12> ambiguous [38]) [38]

2 Source Organism

<1> *Brugia malayi* [32]
<2> *Bacillus subtilis* [45]
<3> *Mus musculus* [51,52,57]
<4> *Thermus thermophilus* [9]
<5> *Escherichia coli* [10,25,26,43]
<6> *Homo sapiens* [17,19,31,49,50,63]
<7> *Entamoeba histolytica* [16]
<8> *Vaccinia virus* [18,28]
<9> *Neurospora sp.* [54]
<10> *Dengue virus* [4,15,36,41]
<11> *Yellow fever virus* [29]
<12> *Hepatitis C virus* [1,13,23,27,37,38,39,42,44,48]
<13> *Human immunodeficiency virus 1* [61]
<14> *Synechocystis sp. PCC 6803* [59]
<15> *Thermococcus kodakarensis* [47]
<16> *Brome mosaic virus* [5]
<17> *West Nile virus* [46,62]
<18> *Rice hoja blanca virus* [40]
<19> *Classical swine fever virus* [35]
<20> *Dengue virus 2* (NPP6 [2]) [2]
<21> *unidentified human coronavirus* (UNIPROT accession number: P0C6X1) [3]
<22> *Potato virus X* [24]
<23> *Rattus norvegicus* (UNIPROT accession number: Q9QY16) [12]
<24> *Homo sapiens* (UNIPROT accession number: O60231) [30]
<25> *Homo sapiens* (UNIPROT accession number: O00571) [8,12]
<26> *Vigna radiata var. radiata* (UNIPROT accession number: Q9M6R6) [33]
<27> *Kokobera virus* [7]
<28> *Poa semilatent virus* [24]
<29> *Homo sapiens* (UNIPROT accession number: O15523) [12]
<30> *Homo sapiens* (UNIPROT accession number: Q9NQI0) [12]
<31> *Saccharomyces cerevisiae* (UNIPROT accession number: P47047) [22]
<32> *Mus musculus* (UNIPROT accession number: Q61656) [12]
<33> *Mus musculus* (UNIPROT accession number: Q501J6) [12]
<34> *Mus musculus* (UNIPROT accession number: Q9QY15) [12]

<35> *Homo sapiens* (UNIPROT accession number: Q9UHL0) [12,21]
<36> *Oryctolagus cuniculus* (UNIPROT accession number: P29562) [20]
<37> *Homo sapiens* (UNIPROT accession number: P38919) [34]
<38> *Saccharomyces cerevisiae* (UNIPROT accession number: P06634) [11,14]
<39> *Hepatitis C virus* (UNIPROT accession number: Q9WPH5) [44]
<40> *Japanese encephalitis virus* (UNIPROT accession number: P27395) [6]
<41> *Classical swine fever virus* (UNIPROT accession number: Q9YS30) [35]
<42> *Brugia malayi (GenBank accession number: EF409381)* [32]
<43> *Homo sapiens* (UNIPROT accession number: Q9UMR2) [56]
<44> *Homo sapiens* (UNIPROT accession number: Q08211) [58]
<45> *Homo sapiens* (UNIPROT accession number: P26196) [60]
<46> *Mus musculus* (UNIPROT accession number: Q80YD1) [64]
<47> *Xenopus laevis* (UNIPROT accession number: Q7ZX48) [53]
<48> *Schmidtea polychroa* (UNIPROT accession number: B9VSG1) [55]

3 Reaction and Specificity

Catalyzed reaction

ATP + H_2O = ADP + phosphate (<5> models: DbpA functions as an active monomer that possesses two distinct RNA binding sites, one in the helicase core domain and the other in the carboxyl-terminal domain that recognizes 23 S rRNA and interacts specifically with hairpin 92 of the peptidyl transferase center [25]; <5> quantitative kinetic and equilibrium characterization of the rRNA-activated ATPase cycle mechanism of DbpA [26])

NTP + H_2O = NDP + phosphate (<10> catalytic mechanism involving a bound sulfate ion, NTPase active site structure, nucleic acid binding site [4])

Natural substrates and products

S ATP + H_2O <2,5,6,8,10,12,13,16,17,20,23,24,25,29,30,31,32,33,34,35,38,39,40,42> (<16> NTPase activity [5]; <35> gonadotropin-regulated testicular helicase (GRTH/DDX25), a target of gonadotropin and androgen action, is a post-transcriptional regulator of key spermatogenesis genes. GRTH has a negative role on its mRNA stability [21]; <31> Mtr4p can unwind duplex RNA in the presence of ATP and a single-stranded RNA tail in the 3 to 5 direction [22]; <8> phosphohydrolase and helicase activities of NPH-II are essential for virus replication [28]; <6> RHA is a coactivator in STAT6-mediated transcription, and this function is dependent on its helicase activity [31]; <25,29,30,32> the ability of RNA helicases to modulate the structure and thus availability of critical RNA molecules for processing leading to protein expression is the likely mechanism by which RNA helicases contribute to differentiation [12]; <23,33,34,35> the ability of RNA helicases to modulate the structure and thus availability of critical RNA molecules for processing leading to protein expression is the likely mechanism by which RNA helicases contribute to differentiation. DDX17 is involved in mRNA splicing [12]; <12> the C-terminal portion of hepatitis C virus nonstructural protein 3 (NS3) forms a three domain polypep-

tide that possesses the ability to travel along RNA or single-stranded DNA (ssDNA) in a 3' to 5' direction. Driven by the energy of ATP hydrolysis, this movement allows the protein to displace complementary strands of DNA or RNA [13]; <38> the DEAD-box protein DED1 has the ability to balance RNA unwinding with a profound strand annealing activity in a highly dynamic fashion [11]; <10,20> RNA helicase activity [2,4]; <12> multifunctional enzyme possessing serine protease, NTPase, and RNA unwinding activities [42]; <12> NTPase activity analyzed, ambiguous helicase activity, enzyme capable for unwinding RNA and DNA [38]; <39> RNA-stimulated ATPase activities determined, interaction between the replicative component nonstructural protein 3 (NS3) with the nonstructural protein 4A (NS4A) [44]; <12> the Arg-rich amino acid motif HCV1487-1500, a fragment of domain 2 NS3 of Hepatitis C virus, as well as the complete domain 2, and domain 2 lacking the flexible loop localized between Val1458 and Thr1476, mediate competitive inhibition of diverse protein kinase C functions, inhibition of rat brain PKC, overview [39]; <17> the West Nile virus RNA helicase uses the energy derived from the hydrolysis of nucleotides to separate complementary strands of RNA [62]; <13> translation of HIV-1 gag mRNA is reliant on the ATP-dependent helicase activity of RNA helicase A [61]) (Reversibility: ?) [2,4,5,6,11,12, 13,21,22,28,30,31,32,37,38,39,41,42,43,44,45,46,61,62]

P ADP + phosphate

S RNA + H_2O <2,5,10,42> (<5> helicase/unwinding activity [43]; <42> helicase/unwinding activity, either ATP or dATP is required for the unwinding activity [32]; <2> RNA unwinding activity, the enzyme contains two RecA-like domains, opening and closing of the interdomain cleft during RNA unwinding [45]) (Reversibility: ?) [32,41,43,45]

P ?

S Additional information <5,10,12,16,17,18,20,41,42> (<16> BMV 1a protein accumulates on endoplasmic reticulum membranes of the host cell, recruits the other RNA replication factor 2apol and induces 50- to 70-nm membrane invaginations serving as RNA replication compartments, BMV 1a protein also recruits viral replication templates such as genomic RNA3 depending on the BMV 1a protein helicase motif, in absence of 2apol, BMV 1a protein highly stabilizes RNA3 by transferring it to a membrane-associated, nuclease-resistant state, overview [5]; <20> nonstructural proteins NS3 and NS5 form complexes in infected mammalian cells [2]; <12> the enzyme is involved in viral replication [1]; <10> the enzyme plays an important role in viral replication [4]; <42> DEAD box proteins are putative RNA unwinding proteins, BmL3-helicase also is a DEAD box RNA helicase [32]; <5> helicase B, RhlB, is one of the five DEAD box RNA-dependent ATPases in Escherichia coli. ATPases found in Escherichia coli. RhlB requires an interaction with the partner protein RNase E for appreciable ATPase and RNA unwinding activities [43]; <17> NS3 possess both protease and helicase activities, the C-terminal portion of the NS3 contains the ATPase/helicase domain presumably involved in viral replication [46]; <41> NS3 possesses three enzyme activities that are

likely to be essential for virus replication: a serine protease located in the N-terminus and NTPase as well as helicase activities located in the C-terminus. Functions of NS3 and NS5B during positive-strand RNA virus replication, the NS3 protein is be involved in the unwinding of the viral RNA template while NS5B protein may be involved in catalyzing the synthesis of new RNA molecules [35]; <12> the C-terminal region of NS3 exhibits RNA-stimulated NTPase, e.g. ATPase, and helicase activity, while the N-terminal serine protease domain of NS3 enhances RNA binding and unwinding by the C-terminal region, NS4A mutants that are defective in ATP-coupled RNA binding are lethal in vivo [44]; <18> the NS3 protein of Rice hoja blanca virus is an RNA silencing suppressor, RSS, that exclusively binds to small dsRNA molecules. This plant viral RSS lacks interferon antagonistic activity, yet it is able to substitute the RSS function of the Tat protein of Human immunodeficiency virus type 1 based on the sequestration of small dsRNA. NS3 is able to inhibit endogenous miRNA action in mammalian cells [40]; <10> The NS3 protein physically associates with the NS5 polymerase, NS3 andNS5 carry out all the enzymatic activities needed for polyprotein processing and genome replication. NS3 possesses an ATPase/helicase and RNA triphosphatase at its C-terminal end that are essential for RNA replication. In addition to its known enzymatic functions, the NS3 protein appears to be involved in the assembly of an infectious flaviviral particle, through its interactions with NS2A and presumably host cell proteins [36]) (Reversibility: ?) [1,2,4,5,32,35,36,40, 4344,46]

P ?

Substrates and products

- **S** 2',3'-dideoxy-ATP + H_2O <17> (<17> 53% of the phosphohydrolase activity with ATP [62]) (Reversibility: ?) [62]
- **P** 2',3'-dideoxy-ADP + phosphate
- **S** 2',3'-dideoxy-GTP + H_2O <17> (<17> 28% of the phosphohydrolase activity with ATP [62]) (Reversibility: ?) [62]
- **P** 2',3'-dideoxy-GDP + phosphate
- **S** 2'-O-methyl-GTP + H_2O <17> (<17> 24% of the phosphohydrolase activity with ATP [62]) (Reversibility: ?) [62]
- **P** 2'-O-methyl-GDP + phosphate
- **S** 2'-deoxy-ATP + H_2O <17> (<17> 62% of the phosphohydrolase activity with ATP [62]) (Reversibility: ?) [62]
- **P** 2'-deoxy-ADP + phosphate
- **S** 2'-deoxy-GTP + H_2O <17> (<17> 39% of the phosphohydrolase activity with ATP [62]) (Reversibility: ?) [62]
- **P** 2'-deoxy-GDP + phosphate
- **S** 2'-deoxy-L-GTP + H_2O <17> (<17> 11% of the phosphohydrolase activity with ATP [62]) (Reversibility: ?) [62]
- **P** 2'-deoxy-L-GDP + phosphate
- **S** 2'-fluoro-2'-deoxy-GTP + H_2O <17> (<17> 22% of the phosphohydrolase activity with ATP [62]) (Reversibility: ?) [62]

P 2'-fluoro-2'-deoxy-GDP + phosphate
S 2'-fluoro-2'-deoxy-ATP + H_2O <17> (<17> 63% of the phosphohydrolase activity with ATP [62]) (Reversibility: ?) [62]
P 2'-fluoro-2'-deoxy-ADP + phosphate
S 2-amino-ATP + H_2O <17> (<17> 103% of the phosphohydrolase activity with ATP [62]) (Reversibility: ?) [62]
P 2-amino-ADP + phosphate
S 2-hydroxy-ATP + H_2O <17> (<17> 40% of the phosphohydrolase activity with ATP [62]) (Reversibility: ?) [62]
P 2-hydroxy-ADP + phosphate
S 3'-O-methyl-GTP + H_2O <17> (<17> 35% of the phosphohydrolase activity with ATP [62]) (Reversibility: ?) [62]
P 3'-O-methyl-GDP + phosphate
S 3'-deoxy-ATP + H_2O <17> (<17> 60% of the phosphohydrolase activity with ATP [62]) (Reversibility: ?) [62]
P 3'-deoxy-ADP + phosphate
S 3'-deoxy-GTP + H_2O <17> (<17> 12% of the phosphohydrolase activity with ATP [62]) (Reversibility: ?) [62]
P 3'-deoxy-GDP + phosphate
S 6-methyl-thio-GTP + H_2O <17> (<17> 40% of the phosphohydrolase activity with ATP [62]) (Reversibility: ?) [62]
P 6-methyl-thio-GDP + phosphate
S 6-methyl-thio-ITP + H_2O <17> (<17> 16% of the phosphohydrolase activity with ATP [62]) (Reversibility: ?) [62]
P 6-methyl-thio-IDP + phosphate
S 6-thio-GTP + H_2O <17> (<17> 93% of the phosphohydrolase activity with ATP [62]) (Reversibility: ?) [62]
P 6-thio-GDP + phosphate
S 7-methyl-GTP + H_2O <17> (<17> 14% of the phosphohydrolase activity with ATP [62]) (Reversibility: ?) [62]
P 7-methyl-GDP + phosphate
S 8-bromo-ATP + H_2O <17> (<17> 124% of the phosphohydrolase activity with ATP [62]) (Reversibility: ?) [62]
P 8-bromo-ADP + phosphate
S 8-bromo-GTP + H_2O <17> (<17> 19% of the phosphohydrolase activity with ATP [62]) (Reversibility: ?) [62]
P 8-bromo-GDP + phosphate
S 8-iodo-GTP + H_2O <17> (<17> 54% of the phosphohydrolase activity with ATP [62]) (Reversibility: ?) [62]
P 8-iodo-GDP + phosphate
S ATP + H_2O <1,2,4,5,6,7,8,10,12,13,15,16,17,19,20,21,22,23,24,25,26,28,29,30,31,32,33,34,35,36,37,38,39,40,41,42,43,44> (<16,20> NTPase activity [2,5]; <12> preferred substrate for NTPase activity [1]; <35> gonadotropin-regulated testicular helicase (GRTH/DDX25), a target of gonadotropin and androgen action, is a post-transcriptional regulator of key spermatogenesis genes. GRTH has a negative role on its mRNA stability [21]; <31> Mtr4p can unwind duplex RNA in the presence of ATP and a single-

stranded RNA tail in the 3 to 5 direction [22]; <8> phosphohydrolase and helicase activities of NPH-II are essential for virus replication [28]; <6> RHA is a coactivator in STAT6-mediated transcription, and this function is dependent on its helicase activity [31]; <25,29,30,32> the ability of RNA helicases to modulate the structure and thus availability of critical RNA molecules for processing leading to protein expression is the likely mechanism by which RNA helicases contribute to differentiation [12]; <23,33,34,35> the ability of RNA helicases to modulate the structure and thus availability of critical RNA molecules for processing leading to protein expression is the likely mechanism by which RNA helicases contribute to differentiation. DDX17 is involved in mRNA splicing [12]; <12> the C-terminal portion of hepatitis C virus nonstructural protein 3 (NS3) forms a three domain polypeptide that possesses the ability to travel along RNA or single-stranded DNA (ssDNA) in a 3' to 5' direction. Driven by the energy of ATP hydrolysis, this movement allows the protein to displace complementary strands of DNA or RNA [13]; <38> the DEAD-box protein DED1 has the ability to balance RNA unwinding with a profound strand annealing activity in a highly dynamic fashion [11]; <31> ATP and dATP are the preferred nucleotide substrates. In the presence of ATP or dATP Mtr4p unwinds the duplex region of a partial duplex RNA substrate in the 3 to 5 direction. Mtr4p displays a marked preference for binding to poly(A) RNA relative to an oligoribonucleotide of the same length and a random sequence [22]; <36> eIF4A may interact directly with double-stranded RNA, and recognition of helicase substrates occurs via chemical and/or structural features of the duplex. The initial rate and amplitude of duplex unwinding by eIF4A is dependent on the overall stability, rather than the length or sequence, of the duplex substrate. eIF4A helicase activity is minimally dependent on the length of the single-stranded region adjacent to the double-stranded region of the substrate. Interestingly, eIF4A is able to unwind blunt-ended duplexes. eIF4A helicase activity is also affected by substitution of 2-OH (RNA) groups with 2-H (DNA) or 2-methoxyethyl groups [20]; <1> either ATP or dATP is required for the unwinding activity [32]; <26> either ATP or dATP is required for the unwinding activity, VrRH1 catalyzes unwinding of a double-stranded RNA [33]; <19> helicase activity requires the substrates possessing a 3 un-base-paired region on the RNA template strand. The NS3h helicase activity is proportional to increasing lengths of the 3 un-base-paired regions up to 16 nucleotides of the RNA substrates. CSFV NS3 helicase activity requires a longer 3-end single-stranded overhang for efficient duplex unwinding and the directionality of NS3 helicase unwinding is 3 to 5 with respect to the template strand [35]; <38> promotes RNA unwinding. The enzyme also catalyzes strand annealing. The balance between unwinding and annealing activities of DED1 depends on the RNA substrate. ADP also modulates the balance between RNA unwinding and strand annealing [11]; <7> recombinant EhDEAD1 protein presents ATPase activity and is able to bind and unwind RNA in an ATPase-dependent manner [16]; <6> RNA helicase A utilizes all hydrolyzable NTPs without preference. RNA

helicase A unwinds dsRNA only in a 3 to 5 direction. The enzyme can only translocate on RNA possessing 3' single-stranded regions [17]; <37> RNA-dependent ATPase, helicase activity [34]; <5> the 3 to 5 helicase activity of DbpA can use a 3 single-stranded loading site on either strand of the substrate helix [10]; <6> the enzyme displaces partial duplex RNA exclusively in a 5 to 3 direction. This reaction is supported by ATP and dATP at relatively high concentrations. The enzyme displays only ATPase and dATPase activity. RNA helicase catalyzes the unwinding of duplex RNA and RNA*DNA hybrids provided that single-stranded RNA is available for the helicase to bind [19]; <21> the enzyme has both RNA and DNA duplex-unwinding activities with 5-to-3 polarity [3]; <22,28> the N-terminal part of the TGBp1 NTPase/helicase domain comprising conserved motifs I, Ia and II is sufficient for ATP hydrolysis, RNA binding and homologous protein-protein interactions [24]; <12> the protein binds RNA and DNA in a sequence specific manner. ATP hydrolysis is stimulated by some nucleic acid polymers much better than it is stimulated by others. The range is quite dramatic. Poly(G) RNA does not stimulate at any measurable level, and poly(U) RNA (or DNA) stimulates best (up to 50 fold). HCV helicase unwinds a DNA duplex more efficiently than an RNA duplex. ATP binds HCV helicase between two RecA-like domains, causing a conformational change that leads to a decrease in the affinity of the protein for nucleic acids. One strand of RNA binds in a second cleft formed perpendicular to the ATP-binding cleft and its binding leads to stimulation of ATP hydrolysis. RNA and/or ATP binding likely causes rotation of domain 2 of the enzyme relative to domains 1 and 3, and somehow this conformational change allows the protein to move like a motor [13]; <38> the Q motif regulates ATP binding and hydrolysis, the affinity of the protein for RNA substrates and the helicase activity. At least three different protein conformations that are associated with free, ADP-bound and ATP-bound forms of the protein [14]; <8> unwinds duplex RNA exclusively in a 3 to 5 direction with respect to the strand to which the enzyme is bound and along which it is presumed to translocate. NTP hydrolysis by RNA bound NPH-II1 drives processive translocation of the protein in a 3' to 5' direction along the RNA strand [18]; <12> unwinds RNA in a discontinuous manner, pausing after long apparent steps of unwinding. It is proposed that the large kinetic step size of NS3 unwinding reflects a delayed, periodic release of the separated RNA product strand from a secondary binding site that is located in the NTPase domain (domain II) of NS3 [23]; <10,20> RNA helicase activity [2,4]; <12> multifunctional enzyme possessing serine protease, NTPase, and RNA unwinding activities [42]; <12> NTPase activity analyzed, ambiguous helicase activity, enzyme capable for unwinding RNA and DNA [38]; <39> RNA-stimulated ATPase activities determined, interaction between the replicative component nonstructural protein 3 (NS3) with the nonstructural protein 4A (NS4A) [44]; <12> the Arg-rich amino acid motif HCV1487-1500, a fragment of domain 2 NS3 of Hepatitis C virus, as well as the complete domain 2, and domain 2 lacking the flexible loop localized between

Val1458 and Thr1476, mediate competitive inhibition of diverse protein kinase C functions, inhibition of rat brain PKC, overview [39]; <10> ATPase activity, ATP binding mode, the ATP binding site is housed between these two subdomains. In the ATP binding pocket, a Mg ion is coordinated in a octahedral manner by the β- and γ-phosphate oxygen atoms from ATP, two equatorial water molecules and oxygen atoms from residues Glu285 in motif II, and Thr200 in motif I, overview [36]; <2> cooperative binding of ATP and RNA leads to a compact helicase structure [45]; <40> genome structure, crystals and three-dimensional structure determined, structure of NTP-binding region, conserved residues within the NTP-binding pocket, ATPase and RNA helicase activities determined [6]; <10> NS3 C-terminal domain catalyzes ATP hydrolysis in the presence of $MgCl_2$ or $MnCl_2$. $MgCl_2$ is more effective than $MnCl_2$ at inducing ATPase activity at concentrations ranging from 0.1 mM to 5 mM. ATP hydrolysis is required for the unwinding activity of DENV NS3H [41]; <12> peptide inhibitors derived from amino acid sequence of motif VI analyzed, binding of the inhibitory peptides does not interfere with the NTPase activity [37]; <17> recombinant protein of C-terminal portion of NS3 protein, ATPase catalytic properties but no RNA helicase activities [46]; <10> wild-type and mutant, NTPase activity analyzed, functional binding of RNA analyzed [41]; <17> the West Nile virus RNA helicase uses the energy derived from the hydrolysis of nucleotides to separate complementary strands of RNA [62]; <13> translation of HIV-1 gag mRNA is reliant on the ATP-dependent helicase activity of RNA helicase A [61]; <17> the amino acids Arg185, Arg202 and Asn417 are critical for phosphohydrolysis [62]; <15> unwinding activity specific for single-strand paired RNA, does not unwind dsRNAs [47]; <12> unwinding of dsRNA [48]) (Reversibility: ?) [1,2,3,4,5,6,8,9,10,11,12,13,14,15,16,17,18,19,20,21,22,23,24,25,26,28,30,31,32,33,34,35,36,37,38,39,41,42,43,44,45,46,47,48,56,58,61,62]

P ADP + phosphate

S Ara-ATP + H_2O <17> (<17> 18% of the phosphohydrolase activity with ATP [62]) (Reversibility: ?) [62]

P Ara-ADP + phosphate

S CTP + H_2O <12,19,44> (<12> NTPase activity [1]; <19> helicase activity is about 85% of the activity with ATP [35]) (Reversibility: ?) [1,35,58]

P CDP + phosphate

S GTP + H_2O <12,17,19,44> (<12> NTPase activity [1]; <19> helicase activity is about 55% of the activity with ATP [35]; <17> 49% of the phosphohydrolase activity with ATP [62]) (Reversibility: ?) [1,35,58,62]

P GDP + phosphate

S ITP + H_2O <17> (<17> 49% of the phosphohydrolase activity with ATP [62]) (Reversibility: ?) [62]

P IDP + phosphate

S N^1-methyl-ATP + H_2O <17> (<17> 66% of the phosphohydrolase activity with ATP [62]) (Reversibility: ?) [62]

P N^1-methyl-ADP + phosphate

S N^1-methyl-GTP + H_2O <17> (<17> 49% of the phosphohydrolase activity with ATP [62]) (Reversibility: ?) [62]
P N^1-methyl-GDP + phosphate
S N^6-methyl-ATP + H_2O <17> (<17> 43% of the phosphohydrolase activity with ATP [62]) (Reversibility: ?) [62]
P N^6-methyl-ADP + phosphate
S O6-methyl-GTP + H_2O <17> (<17> 17% of the phosphohydrolase activity with ATP [62]) (Reversibility: ?) [62]
P O6-methyl-GDP + phosphate
S RNA + H_2O <2,5,10,12,41,42> (<5> helicase/unwinding activity [43]; <42> helicase/unwinding activity, either ATP or dATP is required for the unwinding activity [32]; <2> RNA unwinding activity, the enzyme contains two RecA-like domains, opening and closing of the interdomain cleft during RNA unwinding [45]; <10> helicase/unwinding activity, ATP hydrolysis is required for the unwinding activity of DENV NS3H [41]; <41> NS3 helicase domain helicase activity is dependent on the presence of NTP and divalent cations, with a preference for ATP and Mn^{2+}, and requires a substrates possessing a 3 un-base-paired region on the RNA template strand. The helicase activity is proportional to increasing lengths of the 3 un-base-paired regions up to 16 nucleotides of theRNA substrates, overview [35]; <10> RNA helicase actiivty [36]; <2> RNA unwinding activity, substrate is a 154mer of 23S rRNA generated by T7 polymerase from in vitro transcription [45]; <12> unwinding helicase activity, NS3 is ahighly basic protein with multiple RNA binding sites [44]) (Reversibility: ?) [32,35,36,41,43,44,45]
P ?
S UTP + H_2O <12,19,44> (<12> NTPase activity [1]; <19> helicase activity is about 55% of the activity with ATP [35]) (Reversibility: ?) [1,35,58]
P UDP + phosphate
S XTP + H_2O <17> (<17> 40% of the phosphohydrolase activity with ATP [62]) (Reversibility: ?) [62]
P XDP + phosphate
S dATP + H_2O <1,6,19,26,31> (<31> ATP and dATP are the preferred nucleotide substrates. In the presence of ATP or dATP Mtr4p unwinds the duplex region of a partial duplex RNA substrate in the 3 to 5 direction. Mtr4p displays a marked preference for binding to poly(A) RNA relative to an oligoribonucleotide of the same length and a random sequence [22]; <1> either ATP or dATP is required for the unwinding activity [32]; <26> either ATP or dATP is required for the unwinding activity, VrRH1 catalyzes unwinding of a double-stranded RNA [33]; <19> helicase activity is about 10% of the activity with ATP [35]; <6> the enzyme displaces partial duplex RNA exclusively in a 5 to 3 direction. This reaction is supported by ATP and dATP at relatively high concentrations. The enzyme displays only ATPase and dATPase activity. RNA helicase catalyzes the unwinding of duplex RNA and RNA*DNA hybrids provided that single-stranded RNA is available for the helicase to bind [19]) (Reversibility: ?) [19,22,32,33,35]
P dADP + phosphate

S dCTP + H_2O <19> (<19> helicase activity is about 25% of the activity with ATP [35]) (Reversibility: ?) [35]
P dCDP + phosphate
S dGTP + H_2O <19> (<19> helicase activity is about 10% of the activity with ATP [35]) (Reversibility: ?) [35]
P dGDP + phosphate
S dTTP + H_2O <19> (<19> helicase activity is about 55% of the activity with ATP [35]) (Reversibility: ?) [35]
P dTDP + phosphate
S ribavirin triphosphate + H_2O <17> (<17> 36% of the phosphohydrolase activity with ATP [62]) (Reversibility: ?) [62]
P ribavirin diphosphate + phosphate
S Additional information <2,5,8,10,11,12,16,17,18,19,20,41,42> (<16> BMV 1a protein accumulates on endoplasmic reticulum membranes of the host cell, recruits the other RNA replication factor 2apol and induces 50- to 70-nm membrane invaginations serving as RNA replication compartments, BMV 1a protein also recruits viral replication templates such as genomic RNA3 depending on the BMV 1a protein helicase motif, in absence of 2apol, BMV 1a protein highly stabilizes RNA3 by transferring it to a membrane-associated, nuclease-resistant state, overview [5]; <20> nonstructural proteins NS3 and NS5 form complexes in infected mammalian cells [2]; <12> the enzyme is involved in viral replication [1]; <10> the enzyme plays an important role in viral replication [4]; <10> multifunctional enzyme showing protease, helicase, and NTPase activities [4]; <16> multifunctional enzyme showing protease, helicase, and NTPase activities, the enzyme has a function in RNA replication complex assembly besides its function in RNA synthesis/capping, the enzyme activity is located in the C-terminal nucleoside triphosphatase/helicase domain of the BMV 1a protein RNA replication factor [5]; <20> substrate specificity, bifunctional enzyme, NS3 is an RNA-stimulated nucleoside triphosphatase NTPase/RNA helicase and a 5-RNA triphosphatase RTPase, overview, the full-length NS3 with or without NS2B cofactor domain exhibits a catalytically more efficient RNA helicase activity than the N-terminally-truncated NS3 helicase domain, suggesting that the protease domain enhances RNA helicase activity [2]; <12> the multifunctional enzyme shows RNA-dependent NTPase and helicase activities, no activity with ADP and AMP [1]; <19> nonstructural protein 3 (NS3) possesses three enzyme activities that are likely to be essential for virus replication: a serine protease located in the N-terminus and NTPase as well as helicase activities located in the C-terminus [35]; <11> NS3 includes a protease and a helicase that are essential to virus replication and to RNA capping [29]; <8> the enzyme is unable to unwind duplex DNA [18]; <12> the mature NS3 protein comprises 5 domains: the N-terminal 2 domains form the serine protease along with the NS4A cofactor, and the C-terminal 3 domains form the helicase. The helicase portion of NS3 can be separated form the protease portion by cleaving a linker. Since the protease portion is more hydrophobic, removing it allows the NS3 helicase fragment to be expressed as a

more soluble protein at higher levels in Escherichia coli. The fragment of NS3 possessing helicase activity is referred to as HCV helicase [13]; <42> DEAD box proteins are putative RNA unwinding proteins, BmL3-helicase also is a DEAD box RNA helicase [32]; <5> helicase B, RhlB, is one of the five DEAD box RNA-dependent ATPases in Escherichia coli. ATPases found in Escherichia coli. RhlB requires an interaction with the partner protein RNase E for appreciable ATPase and RNA unwinding activities [43]; <17> NS3 possess both protease and helicase activities, the C-terminal portion of the NS3 contains the ATPase/helicase domain presumably involved in viral replication [46]; <41> NS3 possesses three enzyme activities that are likely to be essential for virus replication: a serine protease located in the N-terminus and NTPase as well as helicase activities located in the C-terminus. Functions of NS3 and NS5B during positive-strand RNA virus replication, the NS3 protein is be involved in the unwinding of the viral RNA template while NS5B protein may be involved in catalyzing the synthesis of new RNA molecules [35]; <12> the C-terminal region of NS3 exhibits RNA-stimulated NTPase, e.g. ATPase, and helicase activity, while the N-terminal serine protease domain of NS3 enhances RNA binding and unwinding by the C-terminal region, NS4A mutants that are defective in ATP-coupled RNA binding are lethal in vivo [44]; <18> the NS3 protein of Rice hoja blanca virus is an RNA silencing suppressor, RSS, that exclusively binds to small dsRNA molecules. This plant viral RSS lacks interferon antagonistic activity, yet it is able to substitute the RSS function of the Tat protein of Human immunodeficiency virus type 1 based on the sequestration of small dsRNA. NS3 is able to inhibit endogenous miRNA action in mammalian cells [40]; <10> The NS3 protein physically associates with the NS5 polymerase, NS3 andNS5 carry out all the enzymatic activities needed for polyprotein processing and genome replication. NS3 possesses an ATPase/helicase and RNA triphosphatase at its C-terminal end that are essential for RNA replication. In addition to its known enzymatic functions, the NS3 protein appears to be involved in the assembly of an infectious flaviviral particle, through its interactions with NS2A and presumably host cell proteins [36]; <10> conformational changes during ATP hydrolysis and RNA unwinding: on ssRNA binding, the NS3 enzyme switches to a catalytic competent state imparted by an inward movement of the P-loop, interdomain closure and a change in the divalent metal coordination shell, providing a structural basis for RNA-stimulated ATP hydrolysis. Determination of enzyme structure-function relationship of enzyme bound to single-stranded RNA, to an ATP analogue, to a transition-state analogue and to ATP hydrolysis products. RNA recognition appears largely sequence independent, reaction mechanism and RNA recognition, overview. RNA-unwinding mechanism, overview [15]; <17> NS3 possess both protease and helicase activities, the C-terminal portion of the NS3 contains the ATPase/helicase domain [46]; <2> open helicase conformation in the absence of nucleotides, or in the presence of ATP, or ADP, or RNA. In the presence of ADP and RNA, the open conformation is retained. By contrast, cooperative binding of ATP and

RNA leads to a compact helicase structure, direct transitions between open and closed conformations, overview [45]; <5> RhlB is the only Escherichia coli DEAD box protein that requires a protein partner to stimulate its ATPase activity [43]; <10> the C-terminal region of NS3 forms the RNA helicase domain, an ATP-driven molecular motor [36]; <10> the helicase domain of Dengue virus NS3 protein, i.e. DENV NS3H, contains RNA-stimulated nucleoside triphosphatase, NTPase, ATPase/helicase, and RNA 5-triphosphatase, RTPase, activities that are essential for viral RNA replication and capping. A 5-tailed RNA is a better RTPase substrate than an RNA containing no 5-dangling nucleotide [41]) (Reversibility: ?) [1,2,4,5,13,15,18,29,32,35,36,40,41,43,44,45,46]

P ?

Inhibitors

2',3'-ddATP <12> (<12> inhibition of NTPase activity of NS3 protein by NTP derivatives [38]) [38]
2',3'-ddGTP <12> (<12> inhibition of NTPase activity of NS3 protein by NTP derivatives [38]) [38]
2',3'-ddTTP <12> (<12> inhibition of NTPase activity of NS3 protein by NTP derivatives [38]) [38]
2',3'-dideoxy-ATP <17> [62]
2',3'-dideoxy-GTP <17> [62]
2'-deoxy-ATP <17> [62]
2'-dATP <12> (<12> inhibition of NTPase activity of NS3 protein by NTP derivatives [38]) [38]
2'-dGTP <12> (<12> inhibition of NTPase activity of NS3 protein by NTP derivatives [38]) [38]
2'-dTTP <12> (<12> inhibition of NTPase activity of NS3 protein by NTP derivatives [38]) [38]
2'-deoxy-GTP <17> [62]
2'-deoxy-L-GTP <17> [62]
2'-deoxythymidine 5'-phosphoryl-β,γ-hypophosphate <12> (<12> i.e. ppopT, dTTP analogue, most efficient inhibitor of NTPase activity among nucleotide derivaties, inhibits the ATP-dependent helicase reaction and also the ATP-independent duplex unwinding, structure of nucleic base and ribose fragment of NTP molecule have a slight effects on inhibitory properties [38]) [38]
2'-fluoro-2'-deoxy-ATP <17> [62]
2-amino-ATP <17> [62]
2-hydroxy-ATP <17> [62]
3'-dATP <12> (<12> inhibition of NTPase activity of NS3 protein by NTP derivatives [38]) [38]
3'-dGTP <12> (<12> inhibition of NTPase activity of NS3 protein by NTP derivatives [38]) [38]
3'-dUTP <12> (<12> inhibition of NTPase activity of NS3 protein by NTP derivatives [38]) [38]
3'-deoxy-ATP <17> [62]
6-methyl-thio-ITP <17> [62]

6-thio-GTP <17> [62]
7-methyl-GTP <17> [62]
8-bromo-ATP <17> [62]
ADP <12,38> (<38> competitive [14]; <12> inhibition of NTPase activity of NS3 protein by NTP derivatives [38]) [14,38]
AMP <12> (<12> inhibition of NTPase activity of NS3 protein by NTP derivatives [38]) [38]
ATP <17> [62]
ATP-γ-S <12> (<12> 5.4 mM, about 50% of the original helicase activity is inhibited, competitive inhibitor [48]) [48]
Ara-ATP <17> [62]
Cu^{2+} <12> (<12> inhibits ATPase activity, IC50: 0.13 mM [1]) [1]
EDTA <6> [17]
Fe^{2+} <12> (<12> inhibits ATPase activity, IC50: 0.75 mM [1]) [1]
GTP <12,17> (<12> inhibition of NTPase activity of NS3 protein by NTP derivatives [38]) [38,62]
Hg^{2+} <12> (<12> inhibits ATPase activity, IC50: 49 nM, targets the cysteine residue in the DECH box, competitive, cysteine or DTT protect at large concentrations [1]) [1]
ITP <17> [62]
KCl <6,10,12> (<6> RNA-dependent ATPase activity is sensitive to high salt concentrations. Maximal activity is obtained in the absence of KCl, and it is inhibited 50% at 0.1 M KC1, completely inhibited at 0.3 M KCl [19]; <6> slight stimulation at 0.05-0.1 M, inhibition at 0.2 M [17]; <12> slight decrease of activity in presence of [38]) [17,19,38,41]
N^1-O-ATP <12> (<12> inhibition of NTPase activity of NS3 protein by NTP derivatives [38]) [38]
N^1-OH-ITP <12> (<12> inhibition of NTPase activity of NS3 protein by NTP derivatives [38]) [38]
N^1-methyl-ATP <17> [62]
N^1-methyl-GTP <17> [62]
N^6-methyl-ATP <17> [62]
NEM <6> (<6> 5 mM, ATPase activity is blocked [19]) [17,19]
PCMB <12> (<12> inhibits ATPase activity, IC50: 88 nM [1]) [1]
UTP <12> (<12> inhibition of NTPase activity of NS3 protein by NTP derivatives [38]) [38]
benzoyl-Nle-Lys-Arg-Arg <10> (<10> competitive inhibition, structure-activity relationship [36]) [36]
β,γ-methylene-ATP <12> (<12> efficient inhibitor, like the N^1-oxides N^1-O-ATP and N^1-OH-ITP [38]) [38]
dATP <12> (<12> inhibits unwinding [13]) [13]
imidodiphosphate <12> (<12> maximal inhibitory activity among diphosphate analogues, non-catalytic and catalytic conditions, inhibits the ATP-dependent helicase reaction but no effect on the ATP-independent duplex unwinding, structure of nucleic base and ribose fragment of NTP molecule have a slight effects on inhibitory properties [38]) [38]
ribavirin triphosphate <17> [62]

tetrabromobenzotriazole <12> (<12> inhibits unwinding, no inhibition of ATP hydrolysis [13]) [13]
Additional information <12> (<12> no or poor inhibition by Mn^{2+}, Zn^{2+}, Co^{2+}, Ca^{2+}, and Ni^{2+} [1]; <12> domain 2 of wild-type NS3 protein and domain 2 devoid of the loop structure used for inhibition studies on functions of protein kinase C (PKC), inhibitory potential towards the majority of protein kinase C isoforms shown [39]; <12> inhibitory potential of sequences of NTPase/helicase motifs VI derived peptides and their deleted derivatives analyzed, NTP-binding and hydrolyzing site not involved [37]; <12> several extracts of marine organisms exhibit different inhibitory effects on the RNA and DNA helicase activities of HCV NS3 [48]) [1,37,39,48]

Activating compounds

MLN51 <37> (<37> stimulates the RNA-helicase activity of eIF4AIII [34]) [34]
RNA <17,20> (<20> RNA-stimulated enzyme [2]; <17> the ATPase activity is stimulated by the presence of RNA and single-stranded DNA molecules [46]) [2,46]
RNase E <5> (<5> is required for ATPase and RNA unwinding activities of the enzyme, forms a complex with the enzyme, interaction analysis, overview. Avid, enthalpy-favored interaction between the helicase and RNase E 696-762 with an equilibrium binding constant Kaof at least 1 x 108 M-1 determined by isothermal titration calorimetry. Protein-protein and RNA-binding surfaces both communicate allosterically with the ATPase catalytic center [43]) [43]
deoxyribonucleotides <42> (<42> ATPase activity of the bacterially expressed BmL3-helicase is triggered by both the ssRNA and the dsRNA and, to a much lesser extent, by the ssDNA and dsDNA [32]) [32]
double-stranded DNA <1> (<1> weak stimulation [32]) [32]
double-stranded RNA <1> (<1> ATPase activity of the recombinant BmL3-helicase is strongly stimulated by dsRNA [32]) [32]
nonstructural protein 4A <12,39> (<39> i.e. NS4A, enhances the coupling between RNA binding and ATPase activity of nonstructural protein 3 (NS3), does not influence the kinetic parameters for RNA unwinding by NS3 [44]; <12> i.e. NS4A, stimulates serine protease activity of NS3 protein, helicase domain enhances serine protease activity and vice versa [42]; <12> NS4A binds to the NS3 protease domain and serves as an obligate cofactor for NS3 serine protease activity, thus NS4A enhances the ability of the C-terminal helicase to bind RNA in presence of ATP acting as a cofactor for helicase activity, 100fold lower K_m of NS3 with RNA in presence of NS4A. NS4A mutants that are defective in ATP-coupled RNA binding sre lethal in vivo [44]) [42,44]
nonstructural protein 5 <20> (<20> interaction with NS5, the viral RNA-dependent RNA polymerase, stimulates NS3 NTPAse and RTPase activities as well as thr RNA helicase activity [2]) [2]
poly(U) <21> (<21> strong stimulation of ATPase activity [3]) [3]
poly(dA) <21> (<21> strong stimulation of ATPase activity [3]) [3]
poly(dT) <21> (<21> strong stimulation of ATPase activity [3]) [3]

poly(rU) <10> (<10> stimulates the ATPase activity of NS3 [41]) [41]
polyU <10> (<10> stimulatory effect of polyU on ATP hydrolysis is significantly attenuated when NaCl concentration is 50 mM or higher, functional binding of polyU mainly through electrostatic interaction, binding triggers a conformational rearrangement that activates the catalytic core of the enzyme for ATP hydrolysis [41]) [41]
poly* <6,21> (<6> stimulates ATPase and dATPase activity [19]; <21> strong stimulation of ATPase activity [3]) [3,19]
rRNA <5> (<5> activates the ATPase activity of DbpA by promoting a conformational change after ATP binding that is associated with hydrolysis [26]) [26]
ribonucleotides <42> (<42> ATPase activity of the bacterially expressed BmL3-helicase is triggered by both the ssRNA and the dsRNA and, to a much lesser extent, by the ssDNA and dsDNA, recombinant BmL3-helicase is strongly stimulated by dsRNA [32]) [32]
single-stranded DANN <1,10,17> (<1> weak stimulation [32]; <10> on single-stranded RNA binding, the NS3 enzyme switches to a catalytic competent state imparted by an inward movement of the P-loop, interdomain closure and a change in the divalent metal coordination shell, providing a structural basis for RNA-stimulated ATP hydrolysis [15]; <17> the ATPase activity is stimulated by the presence of RNA and single-stranded DNA molecules [46]) [15,32,46]
single-stranded RNA <1,6,31> (<1,31> stimulates [22,32]; <6> RNA helicase catalyzes the unwinding of duplex RNA and RNA*DNA hybrids provided that single-stranded RNA is available for the helicase to bind [19]) [19,22,32]
single-strandede DNA <8> (<8> stimulates [18]) [18]
tRNA <31> (<31> stimulates [22]) [22]
Additional information <12,20,21,31,41> (<20> NS3 requires the hydrophilic domain of NS2B for activation [2]; <31> a 20-bp duplex RNA is ineffective in stimulating the (d)ATPase activity of Mtr4p [22]; <12> low salt conditions enhance unwinding by monomeric NS3 [23]; <21> no stimulation by poly(G) of ATPase activity [3]; <41> the NS3 protease domain enhances the helicase activity of NS3 but has no effect on its NTPase activity. For the truncated NS3 helicase domain both NTPase and helicase activities are up-regulated by NS5B, for the full-length NS3, the NTPase activity, but not the helicase activity, is stimulated by NS5B, specific interaction between NS3 and NS5B [35]) [2,3,22,23,35]

Metals, ions

Co^{2+} <12> (<12> activity 3-5-fold lower when magnesium ions are replaced by [38]) [38]
KCl <6> (<6> slight stimulation at 0.05-0.1 M, inhibition at 0.2 M [17]) [17]
Mg^{2+} <2,5,6,10,12,16,17,19,20,40,41,42> (<2,5,17,41,42> activates [32,35,43,45,46]; <16> required for ATPase activity [5]; <10> metal-dependent NTPase activity, mechanism involves a bound sulfate ion [4]; <12> preferred metal ion, ATPase activity [1]; <6> divalent cation required, Ca^{2+} or Mn^{2+} do not substitute for Mg^{2+} [17]; <6> requirement for divalent ions for ATP hydroly-

sis is specific for Mg^{2+} and is not supported by Mn^{2+} and Ca^{2+}. Half-maximum activity is achieved with concentrations of Mg^{2+} of 0.120 mM [19]; <19> the helicase activity requires divalent ions. Mn^{2+} is preferred over Mg^{2+} [35]; <10> activates, binding complexes, overview [15]; <10> activates, preferred metal ion [41]; <10> activity depends on divalent cations, assay concentration 1.5 mM, rate of ATP hydrolysis 10 times enhanced with Mg^{2+} as divalent cation cofactor, rate of ATP hydrolysis increases slightly when the NaCl concentration is elevated in the range of 10 mM and 200 mM [41]; <10> can be substituted by a Mn^{2+} ion for the enzymatic reaction [36]; <12> maximal NTPase activity achieved in the presence of 1.5-2 mM $MgCl_2$ [38]; <40> no ATPase activity of the wild-type in the absence of [6]) [1,2,4,5,6,15,17,19,32,35,36,38,41,42,43,45,46]

Mn^{2+} <10,12,19> (<10> activates [41]; <12> can substitute partially for Mg^{2+}, ATPase activity [1]; <19> the helicase activity requires divalent ions. Mn^{2+} is preferred over Mg^{2+} [35]; <12> activity 3-5-fold lower when magnesium ions are replaced by [38]; <10> activity depends on divalent cations, assay concentration 1.5 mM, rate of ATP hydrolysis more than 100 times over basal levels with Mn^{2+} as divalent cation cofactor [41]; <10> can substitute for a Mg^{2+} ion in the enzymatic reaction [36]) [1,35,36,38,41]

NaCl <8,10> (<8> stimulates at 300-500 mM [18]; <10> slightly activating ATPase activity at 10-200 mM, and RTPase at 15-50 mM [41]) [18,41]

Ni^{2+} <12> (<12> activity 3-5-fold lower when magnesium ions are replaced by [38]) [38]

Zn^{2+} <12> (<12> activity 3-5-fold lower when magnesium ions are replaced by [38]) [38]

sulfate <10> (<10> bound, required for the metal-dependent NTPase reaction mechanism [4]) [4]

Additional information <10,12> (<12> no or poor effect by Mn^{2+}, Zn^{2+}, Co^{2+}, Ca^{2+}, and Ni^{2+} [1]; <10> the ATPase activity requires a divalent cation cofactor to function but is not sensitive to high ionic strength [41]) [1,41]

Turnover number (s^{-1})

0.043 <38> (ATP, <38> pH 7.5, 30°C, mutant enzyme Q169E [14]) [14]

0.3 <38> (ATP, <38> pH 7.5, 30°C, mutant enzyme F162A [14]) [14]

0.58 <17> (ATP, <17> pH 7.5, 37°C, mutant enzyme D172A [62]) [62]

0.64 <2> (RNA, <2> pH 7.5, 37°C, recombinant YxiN mutant S108C/S229C [45]) [45]

0.85 <2> (RNA, <2> pH 7.5, 37°C, recombinant YxiN mutant S108C/E224C [45]) [45]

0.92 <17> (ATP, <17> pH 7.5, 37°C, mutant enzyme E173A [62]) [62]

0.92 <17> (GTP, <17> pH 7.5, 37°C, mutant enzyme D172A [62]) [62]

0.98 <2> (RNA, <2> pH 7.5, 37°C, recombinant wild-type YxiN [45]) [45]

1 <17,38> (ATP, <38> pH 7.5, 30°C, mutant enzyme Q169A [14]; <17> pH 7.5, 37°C, mutant enzyme R170A [62]) [14,62]

1 <17> (GTP, <17> pH 7.5, 37°C, mutant enzyme K187A [62]) [62]

1.1 <17> (ATP, <17> pH 7.5, 37°C, mutant enzyme E180A [62]) [62]

1.1 <17> (GTP, <17> pH 7.5, 37°C, mutant enzyme E173A [62]; <17> pH 7.5, 37°C, mutant enzyme F179A [62]) [62]
1.2 <17> (ATP, <17> pH 7.5, 37°C, mutant enzyme F179A [62]) [62]
1.25 <17> (ATP, <17> pH 7.5, 37°C, mutant enzyme E169A [62]) [62]
1.3 <17> (GTP, <17> pH 7.5, 37°C, mutant enzyme E180A [62]) [62]
1.3 <2> (RNA, <2> pH 7.5, 37°C, recombinant YxiN mutantA115C/S229C [45]) [45]
1.4 <2> (RNA, <2> pH 7.5, 37°C, recombinant YxiN mutantA115C/E224C [45]) [45]
1.41 <2> (RNA, <2> pH 7.5, 37°C, recombinant YxiN mutantA115C/D262C [45]) [45]
1.48 <2> (RNA, <2> pH 7.5, 37°C, native wild-type enzyme [45]) [45]
1.7 <17> (GTP, <17> pH 7.5, 37°C, mutant enzyme K186A [62]; <17> pH 7.5, 37°C, mutant enzyme Q188A [62]; <17> pH 7.5, 37°C, mutant enzyme R170A [62]) [62]
1.8 <38> (ATP, <38> pH 7.5, 30°C, mutant enzyme T166S [14]) [14]
1.83 <17> (GTP, <17> pH 7.5, 37°C, mutant enzyme E169A [62]) [62]
2 <38> (ATP, <38> pH 7.5, 30°C, mutant enzyme F162L [14]; <38> pH 7.5, 30°C, mutant enzyme T166A [14]) [14]
2.2 <17> (ATP, <17> pH 7.5, 37°C, mutant enzyme K187A [62]) [62]
2.7 <17> (ATP, <17> pH 7.5, 37°C, mutant enzyme K186A [62]) [62]
2.75 <17> (GTP, <17> pH 7.5, 37°C, wild-type enzyme [62]) [62]
3 <17> (ATP, <17> pH 7.5, 37°C, wild-type enzyme [62]) [62]
3.3 <17> (ATP, <17> pH 7.5, 37°C, mutant enzyme E182A [62]; <17> pH 7.5, 37°C, mutant enzyme Q188A [62]) [62]
3.5 <38> (ATP, <38> pH 7.5, 30°C, wild-type enzyme [14]) [14]
3.6 <17> (GTP, <17> pH 7.5, 37°C, mutant enzyme E182A [62]) [62]
22.2 <31> (ATP, <31> pH 7.5, 37°C [22]) [22]

Specific activity (U/mg)

0.00000001 <5> (<5> about, wild-type enzyme, RNA helicase activity [43]) [43]
Additional information <10,12,16,17,20,39,40> (<16> RNA replication, RNA protection, spherule formation size, relative ATPase activity, RNA accumulation and stabilization, of wild-type and mutant enzymes, overview [5]; <20> specificities and activities of wild-type and mutant enzymes [2]; <10> biochemical properties and enzymatic activity of the RNA-helicase domain, functional characterization to get information about the flavivirus replication mechanism, NTPase-deficient mutant generated, RNA binding features, electrostatic interaction with RNA, basal ATPase activity insensitive to high ionic strength [41]; <12> helicase capable of unwinding duplex RNA or DNA, ambiguous [27]; <12> overview of sequences of NTPase/helicase motifs VI derived peptides and their deleted derivatives, kinetic analyses reveals that binding of the peptides do not interfere with the NTPase activity, peptides do not interact with the ATP binding site [37]; <40> structural characterization of catalytic domain, mutation analysis of residue substitution in the Walker A motif (Gly199, Lys200 and Thr201), within the NTP-binding pocket (Gln457, Arg461 and Arg464) and of Arg458 in the outside of the pocket in

the motif IV, residues crucial for ATPase and RNA helicase activities and virus replication, Lys200 cannot be substituted by other residues to establish sufficient activities, structure of the NTP-binding pocket well conserved among the viruses of the Flaviviridae [6]; <17> structural characterization of the C-terminal portion containing the ATPase/helicase domain, encompasses residues 181-619, monomer structure determined by analytical centrifugation and gel filtration, SDS-PAGE and immunoblotting, structure determined by circular dichroism and fluorescence spectroscopy, ATPase activity stimulated by RNA and ssDNA, no RNA helicase activity at protein concentrations up to 500 nM, linker region between the protease and the helicase domains predicted as a prerequisite for protein-protein interactions leading to the formation of the active oligomer [46]; <12> structure of nucleic base and ribose fragment of NTP molecule has a slight effect on inhibitory properties [38]; <12> surface of domain 2 of the NS3 NTPase/helicase in direct vicinity to a flexible loop that is localized between Val1458 and Thr1476, accessibility of the Arg-rich amino acid motif by this loop for protein kinase C inhibition analyzed, two variants of domain 2 generated, in vitro protein kinase C (PKC) phosphorylation studies, binding and competition assays, modelling of ribbon diagrams, presence of the intact loop abolishes the binding of domain 2 to a tailed duplex RNA, binding of dsDNA not affected, loop structure reduces the extent of inhibition of protein kinase C (PKC) by domain 2 and regulates the binding of dsRNA, various mechanisms by which the NS3 protein perturb signal transduction in infected cells [39]; <39> the nonstructural protein 4A (NS4A) enhances the ability of the N-terminal domain of NS3 protein to bind RNA in the presence of ATP, stimulates helicase activity, interaction between nonstructural protein 3 (NS3) and nonstructural protein 4A (NS4) mediated by amino acids of the C-terminus of NS4, mutation of the C-terminus of NS4 reduces ATP-coupled RNA binding, RNA binding studies, RNA-stimulated ATPase activity of N3-4a variants [44]; <12> the nonstructural protein 4A (NS4A) stimulates NS3 serine protease activity, truncated and full-length complexes between nonstructural protein 3 (NS3) and nonstructural protein 4A (NS4) purified, serine protease activities analyzed, NS3 protease domain enhances the RNA binding, ATPase, and RNA unwinding activities of the C-terminal NS3 helicase domain, isolated protease domain is much less reactive than full-length NS3, NS3 protease activity is enhanced by the presence of the NS3 helicase domain, indicating that the two domains have evolved to become completely interdependent [42]; <12> development of continuous fluorescence assay based on fluorescence resonance energy transfer for the monitoring of RNA helicase activity in vitro. This assay will be useful for monitoring the detailed kinetics of RNA unwinding mechanisms and screening RNA helicase inhibitors at high throughput [48]) [2,5,6,27,37,38,39,41,42,44,46,48]

K_m-Value (mM)

0.000001 <12> (ATP, <12> pH 6.5, 37°C, RNA-stimulated ATPase activity of mutant NS3-4A [44]) [44]

0.000002 <12> (ATP, <12> pH 6.5, 37°C, RNA-stimulated ATPase activity of mutant S1369R/M1708A [44]) [44]
0.0001 <12> (ATP, <12> pH 6.5, 37°C, RNA-stimulated ATPase activity of wild-type NS3 [44]) [44]
0.000114 <2> (RNA, <2> pH 7.5, 37°C, recombinant YxiN mutant S108C/S229C [45]) [45]
0.000156 <2> (RNA, <2> pH 7.5, 37°C, native wild-type enzyme [45]) [45]
0.00017 <2> (RNA, <2> pH 7.5, 37°C, recombinant wild-type YxiN [45]) [45]
0.000324 <2> (RNA, <2> pH 7.5, 37°C, recombinant YxiN mutantA115C/S229C [45]) [45]
0.000422 <2> (RNA, <2> pH 7.5, 37°C, recombinant YxiN mutantA115C/D262C [45]) [45]
0.000458 <2> (RNA, <2> pH 7.5, 37°C, recombinant YxiN mutant S108C/E224C [45]) [45]
0.000496 <2> (RNA, <2> pH 7.5, 37°C, recombinant YxiN mutantA115C/E224C [45]) [45]
0.0005 <12> (ATP, <12> pH 6.5, 37°C, RNA-stimulated ATPase activity of mutant M1708A [44]; <12> pH 6.5, 37°C, RNA-stimulated ATPase activity of mutant Y1702A [44]) [44]
0.001 <39> (ATP, <39> RNA-stimulated ATPase activity, recombinant protein, NS3-4A construct [44]; <39> RNA-stimulated ATPase activity, recombinant protein, NS3-4A S1369R mutant [44]) [44]
0.002 <39> (ATP, <39> RNA-stimulated ATPase activity, recombinant protein, NS3-4A S1369R/M1708A mutant [44]) [44]
0.0095 <17> (ATP, <17> pH 7.5, 37°C, native WNV NS3 protein purified from infected cells [46]) [46]
0.013 <17> (ATP, <17> recombinant protein including C-terminal portion the ATPase/helicase domain encompassing residues 181-619, ATP concentration 1mM ATP, ATPase but not RNA helicase activity [46]) [46]
0.0157 <6> (ATP, <6> pH 7.6, 37°C [17]) [17]
0.03 <39> (ATP, <39> RNA-stimulated ATPase activity, recombinant protein, NS3-4A S1369R/Y1702A mutant [44]) [44]
0.05 <39> (ATP, <39> RNA-stimulated ATPase activity, recombinant protein, NS3-4A M1708A mutant [44]; <39> RNA-stimulated ATPase activity, recombinant protein, NS3-4A Y1702A mutant [44]) [44]
0.09 <17> (GTP, <17> pH 7.5, 37°C, mutant enzyme F179A [62]; <17> pH 7.5, 37°C, mutant enzyme K187A [62]) [62]
0.1 <39> (ATP, <39> RNA-stimulated ATPase activity, NS3, recombinant protein [44]) [44]
0.1 <17> (GTP, <17> pH 7.5, 37°C, mutant enzyme K186A [62]) [62]
0.11 <17> (GTP, <17> pH 7.5, 37°C, mutant enzyme E173A [62]) [62]
0.13 <17> (ATP, <17> pH 7.5, 37°C, recombinant C-terminal portion of the NS3 [46]) [46]
0.14 <17> (ATP, <17> pH 7.5, 37°C, wild-type enzyme [62]) [62]
0.163 <12> (ATP, <12> addition of polyuridylate lowers K_m for the ATP substrate [38]) [38]

0.18 <17> (ATP, <17> pH 7.5, 37°C, mutant enzyme D172A [62]; <17> pH 7.5, 37°C, mutant enzyme F179A [62]) [62]
0.2 <17> (ATP, <17> pH 7.5, 37°C, mutant enzyme E173A [62]; <17> pH 7.5, 37°C, mutant enzyme R170A [62]) [62]
0.22 <17> (ATP, <17> pH 7.5, 37°C, mutant enzyme E169A [62]) [62]
0.23 <17> (GTP, <17> pH 7.5, 37°C, mutant enzyme E182A [62]) [62]
0.24 <17,37> (ATP, <37> pH 7.5, 25°C, in absence of MLN51 [34]; <17> pH 7.5, 37°C, mutant enzyme E180A [62]) [34,62]
0.256 <12> (ATP, <12> wild-type [38]) [38]
0.27 <17> (ATP, <17> pH 7.5, 37°C, mutant enzyme E182A [62]) [62]
0.27 <17> (GTP, <17> pH 7.5, 37°C, mutant enzyme E180A [62]; <17> pH 7.5, 37°C, mutant enzyme R170A [62]) [62]
0.29 <17> (GTP, <17> pH 7.5, 37°C, mutant enzyme Q188A [62]) [62]
0.33 <17> (GTP, <17> pH 7.5, 37°C, mutant enzyme D172A [62]) [62]
0.34 <38> (ATP, <38> pH 7.5, 30°C, wild-type enzyme [14]) [14]
0.34 <17> (GTP, <17> pH 7.5, 37°C, mutant enzyme E169A [62]) [62]
0.35 <17> (GTP, <17> pH 7.5, 37°C, wild-type enzyme [62]) [62]
0.39 <17,31> (ATP, <31> pH 7.5, 37°C [22]; <17> pH 7.5, 37°C, mutant enzyme K186A [62]) [22,62]
0.51 <38> (ATP, <38> pH 7.5, 30°C, mutant enzyme T166A [14]) [14]
0.64 <17> (ATP, <17> pH 7.5, 37°C, mutant enzyme Q188A [62]) [62]
0.66 <38> (ATP, <38> pH 7.5, 30°C, mutant enzyme T166S [14]) [14]
0.78 <38> (ATP, <38> pH 7.5, 30°C, mutant enzyme F162L [14]) [14]
0.94 <17> (ATP, <17> pH 7.5, 37°C, mutant enzyme K187A [62]) [62]
1.1 <38> (ATP, <38> pH 7.5, 30°C, mutant enzyme Q169E [14]) [14]
3.5 <38> (ATP, <38> pH 7.5, 30°C, mutant enzyme F162A [14]) [14]
33 <38> (ATP, <38> pH 7.5, 30°C, mutant enzyme Q169A [14]) [14]
Additional information <12,20,39> (<20> kinetic study [2]; <12> kinetics of wild-type and mutant enzymes, overview [44]; <12> protease activities of NS3-4A variants analyzed, uncleaved NS3/4A polyprotein lacks protease and helicase activities [42]; <39> RNA-stimulated ATPase activities of NS3-4A variants analyzed, functionally important ATP-bound state of NS3 binds RNA much more tightly in the presence of NS4A, effectively coupling RNA binding to ATPase activity [44]) [2,42,44]

K_i-Value (mM)

0.007 <10> (benzoyl-Nle-Lys-Arg-Arg, <10> full-length enzyme in presence of cofactor CF40-Gly4-Ser-Gly4-NS3FL [36]) [36]
0.097 <12> (2'-deoxythymidine 5'-phosphoryl-β,γ-hypophosphate, <12> i.e. ppopT, dTTP analogue, inhibition of NTPase activity of NS3 protein by NTP derivatives [38]) [38]
0.109 <12> (N^1-OH-ITP, <12> inhibition of NTPase activity of NS3 protein by NTP derivatives [38]) [38]
0.116 <12> (2',3'-ddATP, <12> inhibition of NTPase activity of NS3 protein by NTP derivatives [38]) [38]
0.116 <12> (2'-dTTP, <12> inhibition of NTPase activity of NS3 protein by NTP derivatives [38]) [38]

0.141 <12> (3'-dATP, <12> inhibition of NTPase activity of NS3 protein by NTP derivatives [38]) [38]
0.145 <12> (β,γ-methylene-ATP, <12> efficient inhibitor, like the N^1-oxides N^1-O-ATP and N^1-OH-ITP [38]) [38]
0.2 <17> (2-amino-ATP, <17> pH 7.5, 37°C, wild-type enzyme, inhibition of the ATPase reaction [62]) [62]
0.205 <12> (N^1-O-ATP, <12> inhibition of NTPase activity of NS3 protein by NTP derivatives [38]) [38]
0.26 <12> (3'-dUTP, <12> inhibition of NTPase activity of NS3 protein by NTP derivatives [38]) [38]
0.277 <12> (2'-dGTP, <12> inhibition of NTPase activity of NS3 protein by NTP derivatives [38]) [38]
0.291 <12> (2'-dATP, <12> inhibition of NTPase activity of NS3 protein by NTP derivatives [38]) [38]
0.298 <12> (2',3'-ddTTP, <12> inhibition of NTPase activity of NS3 protein by NTP derivatives [38]) [38]
0.3 <17> (2',3'-dideoxy-GTP, <17> pH 7.5, 37°C, wild-type enzyme, inhibition of the ATPase reaction [62]) [62]
0.3 <17> (ATP, <17> pH 7.5, 37°C, wild-type enzyme [62]) [62]
0.34 <38> (ADP, <38> pH 7.5, 30°C, mutant enzyme T166S [14]) [14]
0.36 <38> (ADP, <38> pH 7.5, 30°C, wild-type enzyme [14]; <38> pH 7.5, 30°C, mutant enzyme T166A [14]) [14]
0.4 <17> (2'-fluoro-2'-deoxy-ATP, <17> pH 7.5, 37°C, wild-type enzyme, inhibition of the ATPase reaction [62]) [62]
0.443 <12> (3'-dGTP, <12> inhibition of NTPase activity of NS3 protein by NTP derivatives [38]) [38]
0.5 <17> (3'-deoxy-ATP, <17> pH 7.5, 37°C, wild-type enzyme, inhibition of the ATPase reaction [62]) [62]
0.5 <17> (Ara-ATP, <17> pH 7.5, 37°C, wild-type enzyme, inhibition of the ATPase reaction [62]) [62]
0.5 <17> (N^6-methyl-ATP, <17> pH 7.5, 37°C, wild-type enzyme, inhibition of the ATPase reaction [62]) [62]
0.576 <12> (GTP, <12> inhibition of NTPase activity of NS3 protein by NTP derivatives [38]) [38]
0.6 <17> (2',3'-dideoxy-ATP, <17> pH 7.5, 37°C, wild-type enzyme, inhibition of the ATPase reaction [62]) [62]
0.6 <17> (2'-deoxy-ATP, <17> pH 7.5, 37°C, wild-type enzyme, inhibition of the ATPase reaction [62]) [62]
0.6 <17> (6-methyl-thio-ITP, <17> pH 7.5, 37°C, wild-type enzyme, inhibition of the ATPase reaction [62]) [62]
0.7 <17> (8-bromo-ATP, <17> pH 7.5, 37°C, wild-type enzyme, inhibition of the ATPase reaction [62]) [62]
0.721 <12> (2',3'-ddGTP, <12> inhibition of NTPase activity of NS3 protein by NTP derivatives [38]) [38]
0.9 <17> (ITP, <17> pH 7.5, 37°C, wild-type enzyme, inhibition of the ATPase reaction [62]) [62]

1 <17> (7-methyl-GTP, <17> pH 7.5, 37°C, wild-type enzyme, inhibition of the ATPase reaction [62]) [62]
1.3 <17> (2'-deoxy-L-GTP, <17> pH 7.5, 37°C, wild-type enzyme, inhibition of the ATPase reaction [62]) [62]
1.3 <12> (ADP, <12> inhibition of NTPase activity of NS3 protein by NTP derivatives [38]) [38]
1.46 <12> (UTP, <12> inhibition of NTPase activity of NS3 protein by NTP derivatives [38]) [38]
1.5 <17> (N^1-methyl-ATP, <17> pH 7.5, 37°C, wild-type enzyme, inhibition of the ATPase reaction [62]) [62]
2.3 <17> (ribavirin triphosphate, <17> pH 7.5, 37°C, wild-type enzyme, inhibition of the ATPase reaction [62]) [62]
2.4 <17> (2-hydroxy-ATP, <17> pH 7.5, 37°C, wild-type enzyme, inhibition of the ATPase reaction [62]) [62]
2.6 <17> (N^1-methyl-GTP, <17> pH 7.5, 37°C, wild-type enzyme, inhibition of the ATPase reaction [62]) [62]
3 <38> (ADP, <38> pH 7.5, 30°C, mutant enzyme F162L [14]) [14]
3.4 <17> (2'-deoxy-GTP, <17> pH 7.5, 37°C, wild-type enzyme, inhibition of the ATPase reaction [62]) [62]
5 <12> (AMP, <12> inhibition of NTPase activity of NS3 protein by NTP derivatives [38]) [38]
8.1 <17> (GTP, <17> pH 7.5, 37°C, wild-type enzyme, inhibition of the ATPase reaction [62]) [62]

pH-Optimum

6.5 <12,39,41> (<41> ATPase assay at [35]; <12> helicase assay at [44]; <39> ATPase and RNA binding assay at [44]) [35,44]
7 <12> (<12> ATPase activity [1]) [1]
7.2 <36> (<36> assay at [20]) [20]
7.4 <16> (<16> ATPase assay at [5]) [5]
7.5 <2,5,10,17,19,20,26,31,37,38,41,42> (<2,5,10,17,20,26,31,37,38,42> assay at [2,4,14,22,32,33,34,41,43,45,46,62]; <41> RNA helicase assay at [35]) [2,4,14,22,32,33,34,35,41,43,45,46,62]

pH-Range

6-9 <12> (<12> activity range, ATPase activity [1]) [1]
6.5 <19> (<19> pH 6.5: about 50% of maximal activity, pH 8: about 80% of maximal activity [35]) [35]

Temperature optimum (°C)

25 <37> (<37> assay at [34]) [34]
30 <38> (<38> assay at [14]) [14]
37 <2,10,12,16,17,20,26,31,36,39,40,41,42> (<2,10,17,20,26,31,36,40,41,42> assay at [2,4,6,20,22,32,33,35,41,45,46,62]; <16> ATPase assay at [5]; <12> helicase assay at [44]; <39> ATPase and RNA binding assay at [44]) [2,4,5,6,20,22,32,33,35,41,44,45,46,62]
50 <15> (<15> maximal ATPase activity and unwinding activity specific for single-strand paired RNA [47]) [47]

Temperature range (°C)

40-50 <15> (<15> 40°C: about 40% of maximal activity, 50°C: optimum, 60°C: less than 10% of maximal activity [47]) [47]

4 Enzyme Structure

Molecular weight

54000 <40> (<40> molecular mass of the helicase/NTPase domain, SDS-PAGE [6]) [6]

66000 <17> (<17> recombinant protein of C-terminal portion the ATPase/helicase domain, residues 181-619, SDS-PAGE, gel filtration [46]) [46]

130000 <6> (<6> glycerol gradient centrifugation [17]) [17]

140000 <6> (<6> MALDI-TOF mass spectrometry [31]) [31]

246000 <6> (<6> calculated from sequence. Apart from an N-terminal domain of unknown function, Brr2p consists of two putative helicase domains, each connected at its C-terminus to a Sec63-like domain [50]) [50]

Subunits

? <6,8,18,24,27> (<6> x * 100000, gel filtration [19]; <24> x * 119037, calculated from sequence [30]; <27> x * 49800, recombinant C-terminal helicase domain (amino-acid sequence corresponding to that between residues 189 and 620 of the predicted NS3 polypeptide), SDS-PAGE [7]; <8> x * 70000, His-tagged enzyme, SDS-PAGE [28]; <18> x * 66000, recombinant NS3, SDS-PAGE, x * 109000, recombinant MBP-fusion NS3 protein, SDS-PAGE [40]) [7,19,28,30,40]

dimer <10> (<10> crystal structure, three-domain structure with asymmetric distribution of charges on the surface and a tunnel structure for RNA substrate access, overview [4]) [4]

monomer <5,6,17> (<6> 1 * 130000, SDS-PAGE [17]; <5> DbpA is monomeric in solution up to a concentration of 25 mM and over the temperature range of 4°C to 22°C [25]; <17> $\alpha\beta$, 29% α-helix, 15% β-sheet, and 56% nonregular structures, globular monomer accounts for 90%, a small percentage (7%) of dimers or trimers, higher oligomers almost absent (3%), analytical centrifugation and gel filtration [46]; <17> in solution, x * 66000, about, recombinant soluble His6-tagged C-terminal portion of NS3, SDS-PAGE [46]) [17,25,46]

Additional information <5,10,16,17,20> (<20> DEN2 nonstructural protein 3, NS3, has a serine protease domain and requires the hydrophilic domain of NS2B for activation [2]; <16> the enzyme activity is located in the C-terminal nucleoside triphosphatase/helicase domain of the BMV 1a protein RNA replication factor, BMV 1a protein contains an N-terminal capping domain with m^7G-methyltransferase and m^7GMP binding activities, and a C-terminal NTPase/helicase-like domain, comprising residues 562-961, containing 7 conserved helicase motifs, the two domains are separated by a proline-rich region, overview [5]; <5> location of the nine conserved sequence motifs in the DEAD box helicase RhlB, structure modelling, overview [43]; <10> the C-

terminal domain of the enzyme contains the Walker A and Walker B motifs, i.e. motif I, GK(S/T) and motif II, DExD/H [41]; <10> the C-terminal region of NS3 forms the RNA helicase domain. The ATP binding site is housed between these two subdomains, structure modelling, overview [36]; <17> the linker region plays a critical role in determining the protein-protein interactions that leads to the formation of the active oligomer [46]) [2,5,36,41,43,46]

Posttranslational modification

phosphoprotein <6,23,32,33,34,35> (<23,32,33,34,35> helicase activity of DDX5 is regulated by phosphorylation and calmodulin binding [12]; <6> phosphorylation of p68 RNA helicase at Y593 upregulates transcription of the Snail1 gene [63]) [12,63]

5 Isolation/Preparation/Mutation/Application

Source/tissue

HEK-293T cell <6> [49]
HeLa cell <6> [17,19,49]
Leydig cell <3,23,34,35> (<3> the 1 kb fragment (5 to the ATG codon) of GRTH gene contains sequences for androgen regulation of its expression in Leydig cells [57]) [12,57]
NIH-3T3 cell <3> [52]
SW-480 cell <6> [63]
SW-620 cell <6> [63]
blastomere <48> [55]
brain <33,46> (<33> DDX17 transcripts are abundant in rat brains in early embryonic stages and are downregulated in late post-natal and adults, suggesting involvement during neuronal differentiation during development of the central nervous system [12]) [12,64]
branchial arch <47> [53]
central nervous system <47> [53]
embryo <47,48> (<48> expressed in blastomeres and embryonic cells in planarian embryonic development [55]) [53,55]
eye <47> (<47> in the ciliary marginal zone adjacent to the neural retina and within the lens epithelium, present in the anterior eye during fibroblast growth factor 2 (FGF2)-mediated retinal regeneration. Ddx39 message is restricted to a subpopulation of proliferating cells in the developing and regenerating optic cup [53]) [53]
germ cell <32> (<32> high level of expression in male germ cells [12]) [12]
larva <42> [32]
limb <47> (<47> developing limb buds at stages 48-55 [53]) [53]
liver <46> (<46> low expression level [64]) [64]
mesenchyme <47> (<47> facial mesenchyme [53]) [53]
muscle <46> [64]
neural tube <47> (<47> Ddx39 is present in the ventricular region of the developing neural tube up to and including stage 48 [53]) [53]

otic vesicle <47> (<47> Ddx39 message is restricted to a subpopulation of proliferating cells in the developing and regenerating optic cup [53]) [53]
reticulocyte <36> [20]
seedling <26> (<26> VrRH1 may play a role in the viability of mung bean seeds [33]) [33]
spermatid <3,23,34,35,48> (<3> GRTH resides in the nucleus, cytoplasm and chromatoid body of round spermatids [51]) [12,51,55]
spermatocyte <23,34,35,48> [12,55]
spermatogonium <48> [55]
spleen <46> [64]
testis <3,23,29,34,35,46> (<23,34,35> highly expressed in [12]; <46> high expression level [64]; <29> expression is restricted to the male germ cell line [12]; <35> GRTH is a negative regulator of apoptosis in spermatocytes and promotes the progress of spermatogenesis [21]; <3> the expression of GRTH in testicular cells is differentially regulated by its 5 flanking sequence [57]) [12,21,57,64]
thymus <46> [64]
trophozoite <7> [16]
Additional information <16,25,30,42> (<16> the virus is propagated in yeast cells [5]; <25> the protein is expressed in all tissues [12]; <30> vasa (DDX4) mRNA and protein are abundantly and specifically expressed in germ cells in both sexes throughout development [12]; <42> presence of BmL3-helicase in various life stages of Brugia malayi [32]) [5,12,32]

Localization

chromatoid body <3> [51]
cytoplasm <3,7> (<3> p68 shuttles between the nucleus and the cytoplasm. The nucleocytoplasmic shuttling of p68 is mediated by two nuclear localization signal and two nuclear exporting signal sequence elements. p68 shuttles via a classical RanGTPase dependent pathway [52]) [16,51,52]
membrane <12> [37]
mitochondrion <46> [64]
nucleus <3,6,7,24> (<24> the GFP-DBP2 gene product, transiently expressed in HeLa cells, is localized in the nucleus [30]; <3> p68 predominately localizes in the cell nucleus [52]) [16,19,30,51,52]
Additional information <16> (<16> BMV 1a protein accumulates on endoplasmic reticulum membranes of the host cell [5]) [5]

Purification

<4> [9]
<5> [25]
<5> (recombinant His-tagged wild-type and mutant RhlB and RNaseE from Escherichia coli strain BL21(DE3) by nickel affinity chromatography and gel filtration) [43]
<6> [17,19,49]
<7> [16]
<8> [28]
<10> [15]

<10> (recombinant His-tag C-terminal domain of NS3 protein from Escherichia coli by nickel affinity chromatography) [41]
<10> (recombinant His-tagged catalytic domain of the NS3 helicase domain from dengue virus serotype 4 from Escherichia coli strain BL21 by nickel affinity chromatography and gel filtration) [15]
<10> (recombinant protein, gel filtration, SDS-PAGE) [41]
<11> [29]
<12> [13]
<12> (gel filtration, SDS-PAGE) [37,39]
<12> (gel filtration, recombinant nonstructural protein 3) [27]
<12> (gel filtration, recombinant protein) [38]
<12> (recombinant C-terminally His-tagged truncated NS3 NTPase/helicase domain from Escherichia coli by nickel affinity chromatography) [1]
<12> (recombinant His10-tagged Arg-rich amino acid motif HCV1487-1500, complete domain 2, and domain 2 lacking the flexible loop from Escherichia coli strain BL21(DE3)) [39]
<12> (recombinant enzyme) [48]
<12> (truncated and full-length complexes between nonstructural protein 3 (NS3) and nonstructural protein 4A (NS4), NS3-4A complex purifies as two separable proteins, gel filtration, SDS-PAGE) [42]
<15> (recombinant enzyme) [47]
<16> (recombinant GST-fusion wild-type and mutant enzymes from Escherichia coli strain C41(DE3) by glutathione affinity chromatography) [5]
<17> [62]
<17> (gel filtration, recombinant protein, soluble form) [46]
<17> (recombinant soluble His6-tagged C-terminal portion of NS3 in Escherichia coli by nickel affinity chromatography and gel filtration) [46]
<20> (recombinant wild-type and N-terminally truncated enzyme from Escherichia coli) [2]
<21> [3]
<26> [33]
<27> [7]
<37> [34]
<38> [14]
<39> (gel filtration) [44]
<40> (gel filtration, recombinant protein) [6]
<42> (recombinant N-terminally His-tagged enzyme from Escherichia coli strain BL21(DE3) by nickel affinity chromatography) [32]
<44> [58]

Crystallization

<4> (RNA helicase Hera C-terminal domain, vapour diffusion, microbatch under oil) [9]
<10> (hanging drop vapour diffusion method, crystallization of native enzyme, enzyme in complex with adenylyl imidodiphosphate, enzyme in complex with ADP, enzyme in complex with single-stranded RNA and enzyme in complex with single-stranded RNA and ADP) [15]

<10> (purified catalytic domain fragment, hanging drop vapour diffusion method, 0.002 ml of 10 mg/ml protein in 0.1 M MES, pH 6.5, 0.2 M ammonium sulfate, 14% PEG 8000, mixed with an equal volume of precipitation solution, 18°C, macroseeding, cryoprotection by 25% glycerol, X-ray diffraction structure determination and analysis at 2.4 A resolution, modeling) [4]
<10> (purified recombinant His-tagged catalytic domain of the NS3, hanging drop vapour diffusion method, at 13°C over a well solution containing 0.1M MES, pH 6.5, and 20% PEG 3350, X-ray diffraction structure determination and analysis. Crystals for the AMPPNP complex are obtained by cocrystallization of NS3h at 5 mg/ml with 5 mM $MnCl_2$ and 5 mM AMPPNP using a precipitating solution containing 0.1M MES, pH 6.5, and 10% PEG 3350, at 13°C. Crystals with ADP are obtained by cocrystallization at a concentration of 2.5 mg/ml with 5 mM $MnCl_2$ and 5 mM ADP in 0.1 M Tris-HCl, pH 7.0, and 7.5% PEG 3350 at 23°C, further preparation of ternary complexes,overview) [15]
<11> (hanging-drop vapor diffusion method, the 1.8 A crystal structure of the helicase region of the YFV NS3 protein (includes residues 187 to 623) and the 2.5 A structure of its complex with ADP) [29]
<12> [13]
<25> (hanging-drop method, crystallization of recombinant DDX3 RNA helicase domain) [8]
<27> (crystals of the recombinant C-terminal helicase domain are obtained by the hanging-drop vapour-diffusion method) [7]
<40> (enzymatically active fragment of the JEV NTPase/helicase catalytic domain, recombinant protein, crystal structure determined at 1.8 A resolution, data collection and refinement statistics) [6]
<43> (crystals of DDX1954-475 in complex with RNA and Mg/adenosine 5'-(β,γ-imido)triphosphate are obtained by vapor diffusion in sitting drops incubated at 4°C by mixing 0.0001 ml of protein solution (20 mg/ml) including 10-molar excess of decauracil ssRNA, adenosine 5'-(β,γ-imido)triphosphate, and $MgCl_2$ and 0.0002 ml of reservoir solution containing 14% polyethylene glycol monomethyl ether 2000, 0.25 M trimethylamine n-oxide, 0.1 M Tris, pH 8. The crystal structures of DDX19, in its RNA-bound prehydrolysis and free posthydrolysis state, reveal an α-helix that inserts between the conserved domains of the free protein to negatively regulate ATPase activity) [56]
<44> (sitting-drop vapor diffusion method at 4 °C. Crystal structures of the conserved domain 1 of the DEIH-motif-containing helicase DHX9 and of the DEAD-box helicase DDX20. Both contain a RecA-like core, but DHX9 differs from DEAD-box proteins in the arrangement of secondary structural elements and is more similar to viral helicases such as NS3. The N-terminus of the DHX9 core contains two long α-helices that reside on the surface of the core without contributing to nucleotide binding) [58]

Cloning

<1> (overexpressed as His-tag fusion protein in Escherichia coli) [32]
<4> (C-terminal domain of Hera is overproduced in Escherichia coli) [9]

<5> (construction of a di-cistronic vector that overexpresses a complex comprising RhlB and its recognition site within RNase E, corresponding to residues 696-762, the expression construct is termed pRneRhlBΔ1-397. Expression of His-tagged wild-type and mutant RhlB and RNaseE in Escherichia coli strain BL21(DE3)) [43]
<6> (expression in Escherichia coli) [49]
<7> [16]
<8> [28]
<10> (expressed in Escherichia coli, recombinant protein) [41]
<10> (expression in Escherichia coli) [15]
<10> (expression of NS3 ATPase/helicase in Escherichia coli, expression of the His-tag C-terminal domain) [41]
<10> (expression of the His-tagged catalytic domain of the NS3 helicase domain from dengue virus serotype 4 in Escherichia coli strain BL21) [15]
<11> [29]
<12> (NS3-plus and NS3/4a-plus genes expressed in Escherichia coli, generation of NS3-4A expression product, pET15b and pet-SUMO vector) [42]
<12> (expressed in Escherichia coli) [37]
<12> (expressed in Escherichia coli BL21(DE3), recombinant protein, NS3d2wt variant corresponding to wild-type domain 2, NS3d2D construct comprises the complete domain, HCV(1361-1503) without loop, pET21b andpET16b vectors) [39]
<12> (expressed in Escherichia coli, strain Rosetta (DE3), recombinant nonstructural protein 3) [27]
<12> (expressed in Escherichia coli, strains XL-1 Blue, Rosetta (DE3), M15 (pREP4), vector pET-21-2c, kinetics of NS3 protein accumulation upon its expression in Escherichia coli at 25°C for 1-5 h shown) [38]
<12> (expression of C-terminally His-tagged truncated NS3 NTPase/helicase domain in Escherichia coli) [1]
<12> (expression of the Arg-rich amino acid motif HCV1487-1500, of the complete domain 2, and of domain 2 lacking the flexible loop localized between Val1458 and Thr1476 as His10-tagged proteins in Escherichia coli strain BL21(DE3)) [39]
<12> (expression of wild-type and mutant NS3, cloning of a His6-tag to the N-terminus of NS3 greatly increases its affinity for RNA) [44]
<15> (expression in Escherichia coli) [47]
<16> (expression of GST-fusion wild-type and mutant enzymes in Escherichia coli strain C41(DE3)) [5]
<17> (expressed in Escherichia coli, C-terminal portion with the ATPase/helicase domain, plasmid pET-30a) [46]
<17> (expression of the soluble His6-tagged C-terminal portion of NS3 in Escherichia coli C41 cells) [46]
<18> (expression of NS3 as maltose-binding protein furion protein using the constitutive elongation factor-1α promoter in HEK-293T cells. Plant viral RSS protein NS3 complements HIV-1 Tat based on the sequestration of small dsRNA) [40]

<20> (expression of wild-type and N-terminally truncated enzyme in Escherichia coli) [2]
<21> (baculovirus expression system) [3]
<24> [30]
<25> (overexpression in Escherichia coli) [8]
<26> (overexpression in Escherichia coli) [33]
<27> (expression of the C-terminal helicase domain (amino-acid sequence corresponding to that between residues 189 and 620 of the predicted NS3 polypeptide) in Escherichia coli) [7]
<35> [21]
<37> [34]
<38> [14]
<39> (NS3-plus and NS3/4a-plus genes expressed in Escherichia coli, composition of NS3-4A expression product using the pet-SUMO vector) [44]
<40> (expressed in Escherichia coli BL21 (DE3), recombinant protein, pET21b vector) [6]
<41> (expression of wild-type and mutant His-tagged NS3 helicase domain in Escherichia coli) [35]
<42> (expression of the N-terminally His-tagged enzyme as soluble protein in Escherichia coli strain BL21(DE3)) [32]
<44> (expression in Escherichia coli) [58]

Engineering

A115C/D262C <2> (<2> site-directed mutagenesis, the mutant shows activity, structure and substrate specificity similar to the wild-type [45]) [45]
A115C/E224C <2> (<2> site-directed mutagenesis, the mutant shows activity, structure and substrate specificity similar to the wild-type [45]) [45]
A115C/S229C <2> (<2> site-directed mutagenesis, the mutant shows activity, structure and substrate specificity similar to the wild-type [45]) [45]
D172A <17> (<17> the ration of (k_{cat}/K_m)ATP/(k_{cat}/K_m)GTP is 41% of the ratio determined for the wild-type enzyme [62]) [62]
D310H <5> (<5> site-directed mutagenesis of the V motif, leads to altered enzyme activity, overview [43]) [43]
D31^{3}H <5> (<5> site-directed mutagenesis of the V motif, leads to altered enzyme activity, overview [43]) [43]
D755A <16> (<16> site-directed mutagenesis, mutation in the conserved BMV 1a protein helicase motif, the mutant shows abolished RNA recruitment and RNA stabilization, and thus RNA replication function, but normal accumulation, localization, and 2apol recruitment, the mutant shows 90% reduced ATPase activity compared to the wild-type enzyme [5]) [5]
E169A <17> (<17> the ration of (k_{cat}/K_m)ATP/(k_{cat}/K_m)GTP is 38% of the ratio determined for the wild-type enzyme [62]) [62]
E173A <17> (<17> the ration of (k_{cat}/K_m)ATP/(k_{cat}/K_m)GTP is 17% of the ratio determined for the wild-type enzyme [62]) [62]
E180A <17> (<17> the ration of (k_{cat}/K_m)ATP/(k_{cat}/K_m)GTP is 35% of the ratio determined for the wild-type enzyme [62]) [62]

E182A <17> (<17> the ration of (k_{cat}/K_m)ATP/(k_{cat}/K_m)GTP is 29% of the ratio determined for the wild-type enzyme [62]) [62]
E300A <8> (<8> mutation causes severe defect in RNA unwinding that correlates with reduced rate of ATP hydrolysis [28]) [28]
F162A <38> (<38> k_{cat}/K_M for ATP is 1% of wild-type value [14]) [14]
F162L <38> (<38> k_{cat}/K_M for ATP is 25% of wild-type value [14]) [14]
F179A <17> (<17> the ration of (k_{cat}/K_m)ATP/(k_{cat}/K_m)GTP is 19% of the ratio determined for the wild-type enzyme [62]) [62]
F788A <16> (<16> site-directed mutagenesis, mutation in the conserved BMV 1a protein helicase motif, the mutant shows abolished RNA recruitment and RNA stabilization, and thus RNA replication function, but normal accumulation, localization, and 2apol recruitment, the mutant shows 30% reduced ATPase activity compared to the wild-type enzyme [5]) [5]
G199A <40> (<40> mutation in WALKER A motif, PCR-based mutagenesis, ATPase and RNA helicase activity lost [6]) [6]
G460A <40> (<40> mutation of residues of the arginine finger within the active sites of ATP hydrolysis, no effect on either ATPase or RNA-unwinding activities [6]) [6]
G463A <40> (<40> mutation of residues of the arginine finger within the active sites of ATP hydrolysis, no effect on either ATPase or RNA-unwinding activities [6]) [6]
G781S <16> (<16> site-directed mutagenesis, mutation in the conserved BMV 1a protein helicase motif, the mutant shows abolished RNA recruitment and RNA stabilization, and thus RNA replication function, but normal accumulation, localization, and 2apol recruitment, the mutant shows 75% reduced ATPase activity compared to the wild-type enzyme [5]) [5]
H293A <12> (<12> mutation results in a protein with a significantly higher level of ATPase in the absence of RNA. The mutant protein still unwinds RNA. In the presence of RNA, the H293A mutant hydrolyzes ATP slower than wild-type [13]) [13]
H299A <8> (<8> mutation elicits defects in RNA unwinding but spares the ATPase activity [28]) [28]
H320D <5> (<5> site-directed mutagenesis of the V motif, leads to altered enzyme activity, overview [43]) [43]
H51A <20> (<20> site-directed mutagenesis, the mutant has an inactivated protease domain showing enhanced RNA helicase compared to wild-type full-length enzyme [2]) [2]
H903A <16> (<16> site-directed mutagenesis, mutation in the conserved BMV 1a protein helicase motif, the mutant shows abolished RNA recruitment and RNA stabilization, and thus RNA replication function, but normal accumulation, localization, and 2apol recruitment, the mutant shows 45% reduced ATPase activity compared to the wild-type enzyme [5]) [5]
K177A <31> (<31> mutant enzyme shows no stimulation of ATPase activity by single-stranded RNA [22]) [22]
K186A <17> (<17> the ration of (k_{cat}/K_m)ATP/(k_{cat}/K_m)GTP is 15% of the ratio determined for the wild-type enzyme [62]) [62]

K187A <17> (<17> the ration of (k_{cat}/K_m)ATP/(k_{cat}/K_m)GTP is 8% of the ratio determined for the wild-type enzyme [62]) [62]
K191A <8> (<8> mutation causes severe defect in RNA unwinding that correlates with reduced rate of ATP hydrolysis [28]) [28]
K199A/T200A <10> (<10> site-directed mutagenesis, mutant avoid of basal and of RNA-stimulated NTPase activity [41]; <10> site-directed mutagenesis, the mutation in the C-terminal domain of NS3 eliminates both the basal and the RNA-stimulated NTPase activity [41]) [41]
K200A <40> (<40> mutation in WALKER A motif, PCR-based mutagenesis, ATPase and RNA helicase activity lost [6]) [6]
K200D <40> (<40> PCR-based mutagenesis, ATPase and RNA helicase activity lost [6]) [6]
K200E <40> (<40> PCR-based mutagenesis, ATPase and RNA helicase activity lost [6]) [6]
K200H <40> (<40> PCR-based mutagenesis, ATPase and RNA helicase activity lost [6]) [6]
K200N <40> (<40> PCR-based mutagenesis, ATPase and RNA helicase activity lost [6]) [6]
K200Q <40> (<40> PCR-based mutagenesis, ATPase and RNA helicase activity lost [6]) [6]
K200R <40> (<40> PCR-based mutagenesis, ATPase and RNA helicase activity lost [6]) [6]
K232A <41> (<41> site-directed mutagenesis in the helicase domain of NS3 [35]) [35]
K691A <16> (<16> site-directed mutagenesis, mutation in the conserved BMV 1a protein helicase motif, the mutant shows abolished RNA recruitment and RNA stabilization, and thus RNA replication function, but normal accumulation, localization, and 2apol recruitment, the mutant shows 80% reduced ATPase activity compared to the wild-type enzyme [5]) [5]
M1708A <12,39> (<39> NS3-4A construct, ability to bind and unwind RNA in vitro, mutation reduces functional NS3-4A binding affinity for RNA by 500-fold relative to the wild-type [44]; <12> site-directed mutagenesis, the NS3-4A mutant shows decreased ATPase activity and reduced RNA stimulation activity compared to wild-type NS3 [44]) [44]
Q169A <38> (<38> k_{cat}/K_M for ATP is 0.3% of wild-type value [14]) [14]
Q169E <38> (<38> k_{cat}/K_M for ATP is 0.4% of wild-type value [14]) [14]
Q188A <17> (<17> the ration of (k_{cat}/K_m)ATP/(k_{cat}/K_m)GTP is 33% of the ratio determined for the wild-type enzyme [62]) [62]
Q457A <40> (<40> mutation of residues of the arginine finger within the active sites of ATP hydrolysis, 80% reduction of ATPase activity, no RNA helicase activity [6]) [6]
Q785A <16> (<16> site-directed mutagenesis, mutation in the conserved BMV 1a protein helicase motif, the mutant shows abolished RNA recruitment and RNA stabilization, and thus RNA replication function, but normal accumulation, localization, and 2apol recruitment, the mutant shows 65% reduced ATPase activity compared to the wild-type enzyme [5]) [5]

Q785E <16> (<16> site-directed mutagenesis, mutation in the conserved BMV 1a protein helicase motif, the mutant shows abolished RNA recruitment and RNA stabilization, and thus RNA replication function, but normal accumulation, localization, and 2apol recruitment, the mutant shows 75% reduced ATPase activity compared to the wild-type enzyme [5]) [5]
R170A <17> (<17> the ration of (k_{cat}/K_m)ATP/(k_{cat}/K_m)GTP is 31% of the ratio determined for the wild-type enzyme [62]) [62]
R184Q/K185N/R186G/K187N <20> (<20> construction of the N-terminally truncated mutant NS3Δ180 containing a mutated RNA substrate biding motif, the mutant shows reduced RTPase activity [2]) [2]
R185A <17> (<17> inactive mutant enzyme [62]) [62]
R229A <8> (<8> mutation causes severe defect in RNA unwinding that correlates with reduced rate of ATP hydrolysis [28]) [28]
R458A <40> (<40> mutation of residues of the arginine finger within the active sites of ATP hydrolysis, 90% reduction of ATPase activity, no RNA helicase activity [6]) [6]
R459A <40> (<40> mutation of residues of the arginine finger within the active sites of ATP hydrolysis, no effect on either ATPase or RNA-unwinding activities [6]) [6]
R461A <40> (<40> mutation of residues of the arginine finger within the active sites of ATP hydrolysis, no ATPase activity, no RNA helicase activity [6]) [6]
R464A <40> (<40> mutation of residues of the arginine finger within the active sites of ATP hydrolysis, no ATPase activity, no RNA helicase activity [6]) [6]
R791A <16> (<16> site-directed mutagenesis, mutation in the conserved BMV 1a protein helicase motif, the mutant shows abolished RNA recruitment and RNA stabilization, and thus RNA replication function, but normal accumulation, localization, and 2apol recruitment, the mutant shows 10% increased ATPase activity compared to the wild-type enzyme [5]) [5]
R806H <9> (<9> interacts with the circadian oscillator component FREQUENCY (FRQ), but interaction between the FRQ-FRHR806H complex (FFC) and White Collar Complex is severely affected [54]) [54]
R815L <16> (<16> site-directed mutagenesis, mutation in the conserved BMV 1a protein helicase motif, the mutant shows abolished RNA recruitment and RNA stabilization, and thus RNA replication function, but normal accumulation, localization, and 2apol recruitment, the mutant shows 60% increased ATPase activity compared to the wild-type enzyme [5]) [5]
R938A <16> (<16> site-directed mutagenesis, mutation in the conserved BMV 1a protein helicase motif, the mutant shows abolished RNA recruitment and RNA stabilization, and thus RNA replication function, but normal accumulation, localization, and 2apol recruitment, the mutant shows 45% reduced ATPase activity compared to the wild-type enzyme [5]) [5]
S108C/E224C <2> (<2> site-directed mutagenesis, the mutant shows activity, structure and substrate specificity similar to the wild-type [45]) [45]
S108C/S229C <2> (<2> site-directed mutagenesis, the mutant shows activity, structure and substrate specificity similar to the wild-type [45]) [45]

S1369R <12,39> (<39> NS3-4A construct, suppressor mutant, ATP-coupled RNA affinity identical to that of wild-type NS3-4A [44]; <12> site-directed mutagenesis, the NS3-4A mutant shows increased ATPase activity and RNA stimulation activity compared to wild-type NS3 [44]) [44]
S1369R/M1708A <12,39> (<39> NS3-4A construct, reduced ATP-coupled RNA affinity of the single mutant suppressed by the addition of the S1369R mutation [44]; <12> site-directed mutagenesis, the NS3-4A mutant shows increased ATPase activity and reduced RNA stimulation activity compared to wild-type NS3 [44]) [44]
S1369R/Y1702A <12,39> (<39> NS3-4A construct, reduced ATP-coupled RNA affinity of the single mutant suppressed by the addition of the S1369R mutation [44]; <12> site-directed mutagenesis, the NS3-4A mutant shows decreased ATPase activity and reduced RNA stimulation activity compared to wild-type NS3 [44]) [44]
S790A <16> (<16> site-directed mutagenesis, mutation in the conserved BMV 1a protein helicase motif, the mutant shows abolished RNA recruitment and RNA stabilization, and thus RNA replication function, but normal accumulation, localization, and 2apol recruitment, the mutant shows 60% reduced ATPase activity compared to the wild-type enzyme [5]) [5]
S790W <16> (<16> site-directed mutagenesis, mutation in the conserved BMV 1a protein helicase motif, the mutant shows abolished RNA recruitment and RNA stabilization, and thus RNA replication function, but normal accumulation, localization, and 2apol recruitment, the mutant shows 70% reduced ATPase activity compared to the wild-type enzyme [5]) [5]
T166A <38> (<38> k_{cat}/K_M for ATP is 37% of wild-type value [14]) [14]
T166S <38> (<38> k_{cat}/K_M for ATP is 26% of wild-type value [14]) [14]
T192A <8> (<8> mutation causes severe defect in RNA unwinding that correlates with reduced rate of ATP hydrolysis [28]) [28]
T201A <40> (<40> mutation in WALKER A motif, PCR-based mutagenesis, ATPase and RNA helicase activity lost [6]) [6]
T326A <8> (<8> mutation elicits defects in RNA unwinding but spares the ATPase activity [28]) [28]
T328A <8> (<8> mutation elicits defects in RNA unwinding but spares the ATPase activity [28]) [28]
T812A/Y813A <16> (<16> site-directed mutagenesis, mutation in the conserved BMV 1a protein helicase motif, the mutant shows abolished RNA recruitment and RNA stabilization, and thus RNA replication function, but normal accumulation, localization, and 2apol recruitment, the mutant shows unaltered ATPase activity compared to the wild-type enzyme [5]) [5]
V462A <40> (<40> mutation of residues of the arginine finger within the active sites of ATP hydrolysis, no effect on either ATPase or RNA-unwinding activities [6]) [6]
Y1702A <12,39> (<39> NS3-4A construct, ability to bind and unwind RNA in vitro, mutation reduces functional NS3-4A binding affinity for RNA by 500-fold relative to the wild-type [44]; <12> site-directed mutagenesis, the NS3-4A mutant shows decreased ATPase activity and reduced RNA stimulation activity compared to wild-type NS3 [44]) [44]

Y383A <5> (<5> site-directed mutagenesis, the mutation causes the formation of a higher order molecular weight species in binding of RNaseE by RhlB [43]) [43]
Y593F <6> (<6> expression of the mutant enzyme in SW620 cells leads to Snail repression, E-cadherin upregulation and vimentin repression [63]) [63]
Additional information <12,16,18,22,28,41,45> (<16> trans interference by BMV 1a protein helicase mutants with BMV 1a protein-stimulated RNA3 accumulation, overview [5]; <22,28> the N-terminal part of the TGBp1 NTPase/helicase domain comprising conserved motifs I, Ia and II is sufficient for ATP hydrolysis, RNA binding and homologous protein-protein interactions. Point mutations in a single conserved basic amino acid residue upstream of motif I have little effect on the activities of C-terminally truncated mutants of both TGBp1 proteins. When introduced into the full-length NTPase/helicase domains, these mutations cause a substantial decrease in the ATPase activity of the protein, suggesting that the conserved basic amino acid residue upstream of motif I is required to maintain a reaction-competent conformation of the TGBp1 ATPase active site [24]; <18> an NS3 mutant, that is deficient in RNA binding and its associated RSS activity, is inactive in complementing the RNA silencing suppressor function of the Tat protein of Human immunodeficiency virus type 1 [40]; <12> construction of the NS3-4A mutant affected in its acidic domain, the mutant shows altered RNA binding and increased ATPase activity, kinetics, overview [44]; <41> for the truncated NS3 helicase domain both NTPase and helicase activities are up-regulated by NS5B, for the full-length NS3, the NTPase activity, but not the helicase activity, is stimulated by NS5B, specific interaction between NS3 and NS5B [35]; <45> mutagenesis of conserved p54 helicase motifs activates translation in the tethered function assay, reduces accumulation of p54 in P-bodies in HeLa cells, and inhibits its capacity to assemble P-bodies in p54-depleted cells [60]) [5,24,35,40,44,60]

Application

drug development <10,12> (<12> the enzyme is a target for anti-HCV drug development [1]; <10> the enzyme is a target for development of specific antiviral inhibitors [4]; <10> the multifunctional NS3 protein from Dengue virus is a target for the design of antiviral inhibitors [36]) [1,4,36]
medicine <6,23,30,32,33,34,35> (<23,30,32,33,34,35> DDX4 can serve as a useful and highly specific biomarker for the diagnosis of germ cell tumors [12]; <6> mutation within hBrr2p can be linked to autosomal dominant retinitis pigmentosa [50]) [12,50]
pharmacology <12,40> (<40> conservation of the NTP-binding pocket among viruses of the family Flaviviridae as potential for development of therapeutics [6]; <12> peptide inhibitors reproducing the structure of the autoregulatory motif as possibility to develop effective antivirals [37]) [6,37]

6 Stability

Temperature stability

20-70 <15> (<15> the enzyme starts to unfold at 20°C and fully unfolds at 70°C [47]) [47]

References

[1] Kyono, K.; Miyashiro, M.; Taguchi, I.: Characterization of ATPase activity of a hepatitis C virus NS3 helicase domain, and analysis involving mercuric reagents. J. Biochem., **134**, 505-511 (2003)
[2] Yon, C.; Teramoto, T.; Mueller, N.; Phelan, J.; Ganesh, V.K.; Murthy, K.H.; Padmanabhan, R.: Modulation of the nucleoside triphosphatase/RNA helicase and 5'-RNA triphosphatase activities of Dengue virus type 2 nonstructural protein 3 (NS3) by interaction with NS5, the RNA-dependent RNA polymerase. J. Biol. Chem., **280**, 27412-27419 (2005)
[3] Ivanov, K.A.; Ziebuhr, J.: Human coronavirus 229E nonstructural protein 13: characterization of duplex-unwinding, nucleoside triphosphatase, and RNA 5-triphosphatase activities. J. Virol., **78**, 7833-7838 (2004)
[4] Xu, T.; Sampath, A.; Chao, A.; Wen, D.; Nanao, M.; Chene, P.; Vasudevan Subhash, G.; Lescar, J.: Structure of the Dengue virus helicase/nucleoside triphosphatase catalytic domain at a resolution of 2.4 A. J. Virol., **79**, 10278-10288 (2005)
[5] Wang, X.; Lee, W.M.; Watanabe, T.; Schwartz, M.; Janda, M.; Ahlquist, P.: Brome mosaic virus 1a nucleoside triphosphatase/helicase domain plays crucial roles in recruiting RNA replication templates. J. Virol., **79**, 13747-13758 (2005)
[6] Yamashita, T.; Unno, H.; Mori, Y.; Tani, H.; Moriishi, K.; Takamizawa, A.; Agoh, M.; Tsukihara, T.; Matsuura, Y.: Crystal structure of the catalytic domain of Japanese encephalitis virus NS3 helicase/nucleoside triphosphatase at a resolution of 1.8 A. Virology, **373**, 426-436 (2008)
[7] De Colibus, L.; Speroni, S.; Coutard, B.; Forrester, N.L.; Gould, E.; Canard, B.; Mattevi, A.: Purification and crystallization of Kokobera virus helicase.. Acta Crystallogr. Sect. F, **63**, 193-195 (2007)
[8] Rodamilans, B.; Montoya, G.: Expression, purification, crystallization and preliminary X-ray diffraction analysis of the DDX3 RNA helicase domain. Acta Crystallogr. Sect. F, **63**, 283-286 (2007)
[9] Rudolph, M.G.; Wittmann, J.G.; Klostermeier, D.: Crystallization and preliminary characterization of the Thermus thermophilus RNA helicase Hera C-terminal domain. Acta Crystallogr. Sect. F, **65**, 248-252 (2009)
[10] Diges, C.M.; Uhlenbeck, O.C.: Escherichia coli DbpA is a 3' -] 5' RNA helicase. Biochemistry, **31; 44**, 7903-7911 (2005)
[11] Yang, Q.; Jankowsky, E.: ATP- and ADP-dependent modulation of RNA unwinding and strand annealing activities by the DEAD-box protein DED1. Biochemistry, **44**, 13591-13601 (2005)

[12] Abdelhaleem, M.: RNA helicases: regulators of differentiation. Clin. Biochem., **38**, 499-503 (2005)
[13] Frick, D.N.: The hepatitis C virus NS3 protein: a model RNA helicase and potential drug target. Curr. Issues Mol. Biol., **9**, 1-20 (2007)
[14] Cordin, O.; Tanner, N.K.; Doere, M.; Linder, P.; Banroques, J.: The newly discovered Q motif of DEAD-box RNA helicases regulates RNA-binding and helicase activity. EMBO J., **23**, 2478-2487 (2004)
[15] Luo, D.; Xu, T.; Watson, R.P.; Scherer-Becker, D.; Sampath, A.; Jahnke, W.; Yeong, S.S.; Wang, C.H.; Lim, S.P.; Strongin, A.; Vasudevan, S.G.; Lescar, J.: Insights into RNA unwinding and ATP hydrolysis by the flavivirus NS3 protein. EMBO J., **27**, 3209-3219 (2008)
[16] Lopez-Camarillo, C.; de la Luz García-Hernandez, M.; Marchat, L.A.; Luna-Arias, J.P.; Hernandez de la Cruz, O.; Mendoza, L.; Orozco, E.: Entamoeba histolytica EhDEAD1 is a conserved DEAD-box RNA helicase with ATPase and ATP-dependent RNA unwinding activities. Gene, **15**, 19-31 (2008)
[17] Lee, C.G.; Hurwitz, J.: A new RNA helicase isolated from HeLa cells that catalytically translocates in the 3' to 5' direction.. J. Biol. Chem., **267**, 4398-4407 (1992)
[18] Shuman S.: Vaccinia virus RNA helicase. Directionality and substrate specificity. J. Biol. Chem., **268**, 11798-11802 (1993)
[19] Flores-Rozas, H.; Hurwitz, J.: Characterization of a new RNA helicase from nuclear extracts of HeLa cells which translocates in the 5' to 3' direction.. J. Biol. Chem., **268**, 21372-21383 (1993)
[20] Rogers, G.W.Jr.; Lima, W.F.; Merrick, W.C.: Further characterization of the helicase activity of eIF4A. Substrate specificity. J. Biol. Chem., **276**, 12598-12608 (2001)
[21] Gutti, R.K.; Tsai-Morris, C.H.; Dufau, M.L.: Gonadotropin-regulated testicular helicase (DDX25), an essential regulator of spermatogenesis, prevents testicular germ cell apoptosis. J. Biol. Chem., **283**, 17055-17064 (2008)
[22] Bernstein, J.; Patterson, D.N.; Wilson, G.M.; Toth, E.A.: Characterization of the essential activities of Saccharomyces cerevisiae Mtr4p, a 3'-]5' helicase partner of the nuclear exosome. J. Biol. Chem., **283**, 4930-4942 (2008)
[23] Serebrov, V.; Beran, R.K.; Pyle, A.M.: Establishing a mechanistic basis for the large kinetic steps of the NS3 helicase.. J. Biol. Chem., **284**, 2512-2521 (2009)
[24] Leshchiner, A.D.; Solovyev, A.G.; Morozov, S.Y.; Kalinina, N.O.: A minimal region in the NTPase/helicase domain of the TGBp1 plant virus movement protein is responsible for ATPase activity and cooperative RNA binding. J. Gen. Virol., **87**, 3087-3095 (2006)
[25] Talavera, M.A.; Matthews, E.E.; Eliason, W.K.; Sagi, I.; Wang, J.; Henn, A.; De La Cruz, E.M.: Hydrodynamic characterization of the DEAD-box RNA helicase DbpA. J. Mol. Biol., **355**, 697-707 (2005)
[26] Henn, A.; Cao, W.; Hackney, D.D.; De La Cruz, E.M.: The ATPase cycle mechanism of the DEAD-box rRNA helicase, DbpA. J. Mol. Biol., **377**, 193-205 (2008)
[27] Belon, C.A.; Frick, D.N.: Fuel specificity of the hepatitis C virus NS3 helicase. J. Mol. Biol., **388**, 851-864 (2009)

[28] Gross, C.H.; Shuman, S.: The nucleoside triphosphatase and helicase activities of vaccinia virus NPH-II are essential for virus replication. J. Virol., **72**, 4729-4736 (1998)
[29] Wu, J.; Bera, A.K.; Kuhn, R.J.; Smith, J.L.: Structure of the Flavivirus helicase: implications for catalytic activity, protein interactions, and proteolytic processing. J. Virol., **79**, 10268-10277 (2005)
[30] Imamura, O.; Saiki, K.; Tani, T.; Ohshima, Y.; Sugawara, M.; Furuichi. Y.: Cloning and characterization of a human DEAH-box RNA helicase, a functional homolog of fission yeast Cdc28/Prp8. Nucleic Acids Res., **26**, 2063-2068 (1998)
[31] Välineva, T.; Yang, J.; Silvennoinen, O.: Characterization of RNA helicase A as component of STAT6-dependent enhanceosome. Nucleic Acids Res., **34**, 3938-3946 (2006)
[32] Singh, M.; Srivastava, K.K.; Bhattacharya, S.M.: Molecular cloning and characterization of a novel immunoreactive ATPase/RNA helicase in human filarial parasite Brugia malayi. Parasitol. Res., **104**, 753-761 (2009)
[33] Li, S.C.; Chung, M.C.; Chen, C.S.: Cloning and characterization of a DEAD box RNA helicase from the viable seedlings of aged mung bean. Plant Mol. Biol., **47**, 761-770 (2001)
[34] Noble, C.G.; Song, H.: MLN51 stimulates the RNA-helicase activity of eIF4AIII. PLoS One, **21**, e303 (2007)
[35] Wen, G.; Xue, J.; Shen, Y.; Zhang, C.; Pan, Z.: Characterization of classical swine fever virus (CSFV) nonstructural protein 3 (NS3) helicase activity and its modulation by CSFV RNA-dependent RNA polymerase. Virus Res., **141**, 63-70 (2009)
[36] Lescar, J.; Luo, D.; Xu, T.; Sampath, A.; Lim, S.P.; Canard, B.; Vasudevan, S.G.: Towards the design of antiviral inhibitors against flaviviruses: the case for the multifunctional NS3 protein from Dengue virus as a target. Antiviral Res., **80**, 94-101 (2008)
[37] Borowski, P.; Heising, M.V.; Miranda, I.B.; Liao, C.L.; Choe, J.; Baier, A.: Viral NS3 helicase activity is inhibited by peptides reproducing the Arg-rich conserved motif of the enzyme (motif VI). Biochem. Pharmacol., **76**, 28-38 (2008)
[38] Mukovnya, A.V.; Tunitskaya, V.L.; Khandazhinskaya, A.L.; Golubeva, N.A.; Zakirova, N.F.; Ivanov, A.V.; Kukhanova, M.K.; Kochetkov, S.N.: Hepatitis C virus helicase/NTPase: an efficient expression system and new inhibitors. Biochemistry (Moscow), **73**, 660-668 (2008)
[39] Hartjen, P.; Medom, B.K.; Reinholz, M.; Borowski, P.; Baier, A.: Regulation of the biochemical function of motif VI of HCV NTPase/helicase by the conserved Phe-loop. Biochimie, **91**, 252-260 (2009)
[40] Schnettler, E.; de Vries, W.; Hemmes, H.; Haasnoot, J.; Kormelink, R.; Goldbach, R.; Berkhout, B.: The NS3 protein of rice hoja blanca virus complements the RNAi suppressor function of HIV-1 Tat. EMBO Rep., **10**, 258-263 (2009)
[41] Wang, C.C.; Huang, Z.S.; Chiang, P.L.; Chen, C.T.; Wu, H.N.: Analysis of the nucleoside triphosphatase, RNA triphosphatase, and unwinding activities

of the helicase domain of dengue virus NS3 protein. FEBS Lett., **583**, 691-696 (2009)
[42] Beran, R.K.; Pyle, A.M.: Hepatitis C viral NS3-4A protease activity is enhanced by the NS3 helicase. J. Biol. Chem., **283**, 29929-29937 (2008)
[43] Worrall, J.A.; Howe, F.S.; McKay, A.R.; Robinson, C.V.; Luisi, B.F.: Allosteric activation of the ATPase activity of the Escherichia coli RhlB RNA helicase. J. Biol. Chem., **283**, 5567-5576 (2008)
[44] Beran, R.K.; Lindenbach, B.D.; Pyle, A.M.: The NS4A protein of hepatitis C virus promotes RNA-coupled ATP hydrolysis by the NS3 helicase. J. Virol., **83**, 3268-3275 (2009)
[45] Theissen, B.; Karow, A.R.; Koehler, J.; Gubaev, A.; Klostermeier, D.: Cooperative binding of ATP and RNA induces a closed conformation in a DEAD box RNA helicase. Proc. Natl. Acad. Sci. USA, **105**, 548-553 (2008)
[46] Feito, M.J.; Gomez-Gutierrez, J.; Ayora, S.; Alonso, J.C.; Peterson, D.; Gavilanes, F.: Insights into the oligomerization state-helicase activity relationship of West Nile virus NS3 NTPase/helicase. Virus Res., **135**, 166-174 (2008)
[47] Shimada, Y.; Fukuda, W.; Akada, Y.; Ishida, M.; Nakayama, J.; Imanaka, T.; Fujiwara, S.: Property of cold inducible DEAD-box RNA helicase in hyperthermophilic archaea. Biochem. Biophys. Res. Commun., **389**, 622-627 (2009)
[48] Tani, H.; Fujita, O.; Furuta, A.; Matsuda, Y.; Miyata, R.; Akimitsu, N.; Tanaka, J.; Tsuneda, S.; Sekiguchi, Y.; Noda, N.: Real-time monitoring of RNA helicase activity using fluorescence resonance energy transfer in vitro. Biochem. Biophys. Res. Commun., **393**, 131-136 (2010)
[49] Tang, W.; You, W.; Shi, F.; Qi, T.; Wang, L.; Djouder, Z.; Liu, W.; Zeng, X.: RNA helicase A acts as a bridging factor linking nuclear β-actin with RNA polymerase II. Biochem. J., **420**, 421-428 (2009)
[50] Hahn, D.; Beggs, J.D.: Brr2p RNA helicase with a split personality: insights into structure and function. Biochem. Soc. Trans., **38**, 1105-1109 (2010)
[51] Sato, H.; Tsai-Morris, C.H.; Dufau, M.L.: Relevance of gonadotropin-regulated testicular RNA helicase (GRTH/DDX25) in the structural integrity of the chromatoid body during spermatogenesis. Biochim. Biophys. Acta, **1803**, 534-543 (2010)
[52] Wang, H.; Gao, X.; Huang, Y.; Yang, J.; Liu, Z.R.: P68 RNA helicase is a nucleocytoplasmic shuttling protein. Cell Res., **19**, 1388-1400 (2009)
[53] Wilson, J.M.; Martinez-De Luna, R.I.; El Hodiri, H.M.; Smith, R.; King, M.W.; Mescher, A.L.; Neff, A.W.; Belecky-Adams, T.L.: RNA helicase Ddx39 is expressed in the developing central nervous system, limb, otic vesicle, branchial arches and facial mesenchyme of Xenopus laevis. Gene Expr. Patterns, **10**, 44-52 (2010)
[54] Shi, M.; Collett, M.; Loros, J.J.; Dunlap, J.C.: FRQ-interacting RNA helicase mediates negative and positive feedback in the Neurospora circadian clock. Genetics, **184**, 351-361 (2010)
[55] Solana, J.; Romero, R.: SpolvlgA is a DDX3/PL10-related DEAD-box RNA helicase expressed in blastomeres and embryonic cells in planarian embryonic development. Int. J. Biol. Sci., **5**, 64-73 (2009)

[56] Collins, R.; Karlberg, T.; Lehtioe, L.; Schuetz, P.; van den Berg, S.; Dahlgren, L.G.; Hammarstroem, M.; Weigelt, J.; Schueler, H.: The DEXD/H-box RNA helicase DDX19 is regulated by an α-helical switch. J. Biol. Chem., **284**, 10296-10300 (2009)
[57] Tsai-Morris, C.H.; Sheng, Y.; Gutti, R.; Li, J.; Pickel, J.; Dufau, M.L.: Gonadotropin-regulated testicular RNA helicase (GRTH/DDX25) gene: cell-specific expression and transcriptional regulation by androgen in transgenic mouse testis. J. Cell. Biochem., **109**, 1142-1147 (2010)
[58] Schuetz, P.; Wahlberg, E.; Karlberg, T.; Hammarstroem, M.; Collins, R.; Flores, A.; Schueler, H.: Crystal structure of human RNA helicase A (DHX9): structural basis for unselective nucleotide base binding in a DEAD-box variant protein. J. Mol. Biol., **400**, 768-782 (2010)
[59] Prakash, J.S.; Krishna, P.S.; Sirisha, K.; Kanesaki, Y.; Suzuki, I.; Shivaji, S.; Murata, N.: An RNA helicase, CrhR, regulates the low-temperature-inducible expression of heat-shock genes groES, groEL1 and $groEL_2$ in Synechocystis sp. PCC 6803. Microbiology, **156**, 442-451 (2010)
[60] Minshall, N.; Kress, M.; Weil, D.; Standart, N.: Role of p54 RNA helicase activity and its C-terminal domain in translational repression, P-body localization and assembly. Mol. Biol. Cell, **20**, 2464-2472 (2009)
[61] Bolinger, C.; Sharma, A.; Singh, D.; Yu, L.; Boris-Lawrie, K.: RNA helicase A modulates translation of HIV-1 and infectivity of progeny virions. Nucleic Acids Res., **38**, 1686-1696 (2010)
[62] Despins, S.; Issur, M.; Bougie, I.; Bisaillon, M.: Deciphering the molecular basis for nucleotide selection by the West Nile virus RNA helicase. Nucleic Acids Res., **38**, 5493-5506 (2010)
[63] Carter, C.L.; Lin, C.; Liu, C.Y.; Yang, L.; Liu, Z.R.: Phosphorylated p68 RNA helicase activates Snail1 transcription by promoting HDAC1 dissociation from the Snail1 promoter. Oncogene, **29**, 5427-5436 (2010)
[64] Paul, E.; Kielbasinski, M.; Sedivy, J.M.; Murga-Zamalloa, C.; Khanna, H.; Klysik, J.E.: Widespread expression of the Supv3L1 mitochondrial RNA helicase in the mouse. Transgenic Res., **19**, 691-701 (2010)

cyclohexane-1,2-dione hydrolase 3.7.1.11

1 Nomenclature

EC number
3.7.1.11

Systematic name
cyclohexane-1,2-dione acylhydrolase (decyclizing)

Recommended name
cyclohexane-1,2-dione hydrolase

2 Source Organism

<1> *Azoarcus sp.* [1,2]

3 Reaction and Specificity

Catalyzed reaction
cyclohexane-1,2-dione + H_2O = 6-oxohexanoate (<1> reaction starts with the monohydrated ketone of cyclohexane-1,2-dione and the thiamine diphosphate-ylide which undergoes a nucleophilic attack on the carbonyl group of cyclohexane-1,2-dione. The subsequent cleavage of the C-C bond yields an α-carbanion, which is in equilibrium with its corresponding enamine. In the following step, the carbonic acid protonates the α-carbanion yielding 6-hydroxyhexanoate-thiamine diphosphate. Finally, the product 6-oxohexanoate is released [2])

Substrates and products
- **S** cyclohexane-1,2-dione + H_2O <1> (<1> conversion of the monohydrated ketone form of cyclohexane-1,2-dione, rather than the monoenol form [2]) (Reversibility: ?) [1,2]
- **P** 6-oxohexanoate (<1> enzyme additionally catalyzes NAD^+-dependent oxidation of 6-oxohexanoate to adipate [2])
- **S** Additional information <1> (<1> no substrate: cyclohexanone, cyclohexane-1,3-dione [1]) [1]
- **P** ?

Inhibitors
NaCl <1> (<1> inhibitory above 50 mM due to binding of the chloride anion in close neighborhood to the thiamine diphosphate cofactor [2]) [2]

D. Schomburg and I. Schomburg (eds.), *Class 3.4–6 Hydrolases, Lyases, Isomerases, Ligases: EC 3.4–6*, Springer Handbook of Enzymes S10, DOI 10.1007/978-3-642-36260-6_26,

Cofactors/prosthetic groups
FAD <1> [2]
NAD^+ <1> [1]
thiamine diphosphate <1> [2]
Additional information <1> (<1> no cofactor: 2,6-dichlorophenol-indophenol [1]) [1]

Metals, ions
Mg^{2+} <1> [2]

pH-Optimum
8 <1> [2]

4 Enzyme Structure

Molecular weight
120000 <1> (<1> gel filtration [2]) [2]

Subunits
dimer <1> (<1> 2 * 59000, SDS-PAGE, 2 * 64500, calculated including FAD, thiamine diphosphate and Mg^{2+} [2]) [2]

References

[1] Harder, J.: Anaerobic degradation of cyclohexane-1,2-diol by a new Azoarcus species. Arch. Microbiol., **168**, 199-204 (1997)
[2] Fraas, S.; Steinbach, A.; Tabbert, A.; Harder, J.; Ermler, U.; Tittmann, K.; Meyer, A.; Kroneck, P.: Cyclohexane-1,2-dione hydrolase: A new tool to degrade alicyclic compounds. J. Mol. Catal. B, **61**, 47-49 (2009)

cobalt-precorrin 5A hydrolase 3.7.1.12

1 Nomenclature

EC number
3.7.1.12

Systematic name
cobalt-precorrin 5A acylhydrolase

Recommended name
cobalt-precorrin 5A hydrolase

Synonyms
CbiG <1> (<1> gene name [3]) [3]

2 Source Organism

<1> *Salmonella enterica* [2,3]
<2> *Bacillus megaterium* (UNIPROT accession number: O87697) [1]

3 Reaction and Specificity

Catalyzed reaction
cobalt-precorrin-5A + H_2O = cobalt-precorrin-5B + acetaldehyde + 2 H^+

5 Isolation/Preparation/Mutation/Application

Application
synthesis <1> (<1> co-expression of the cobA gene from Propionibacterium freudenreichii and the cbiA, -C, -D, -E, -T, -F, -G, -H, -J, -K, -L, and -P genes from Salmonella enterica serovar typhimurium in Escherichia coli result in the production of cobyrinic acid a,c-diamide [3]; <1> synthesis of cobalt corrinoid intermediates cobalt-precorrin 5A and cobalt-precorrin 5B, with the aid of overexpressed enzymes of the vitamin B_{12} pathway of Salmonella enterica serovar typhimurium [2]) [2,3]

D. Schomburg and I. Schomburg (eds.), *Class 3.4–6 Hydrolases, Lyases, Isomerases, Ligases: EC 3.4–6*, Springer Handbook of Enzymes S10, DOI 10.1007/978-3-642-36260-6_27,

References

[1] Raux, E.; Lanois, A.; Warren, M.J.; Rambach, A.; Thermes, C.: Cobalamin (vitamin B_{12}) biosynthesis: identification and characterization of a Bacillus megaterium cobI operon. Biochem. J., **335 (Pt 1)**, 159-166 (1998)

[2] Kajiwara, Y.; Santander, P.J.; Roessner, C.A.; Perez, L.M.; Scott, A.I.: Genetically engineered synthesis and structural characterization of cobalt-precorrin 5A and -5B, two new intermediates on the anaerobic pathway to vitamin B_{12}: definition of the roles of the CbiF and CbiG enzymes. J. Am. Chem. Soc., **128**, 9971-9978 (2006)

[3] Roessner, C.A.; Williams, H.J.; Scott, A.I.: Genetically engineered production of 1-desmethylcobyrinic acid, 1-desmethylcobyrinic acid a,c-diamide, and cobyrinic acid a,c-diamide in Escherichia coli implies a role for CbiD in C-1 methylation in the anaerobic pathway to cobalamin. J. Biol. Chem., **280**, 16748-16753 (2005)

2-hydroxy-6-oxo-6-(2-aminophenyl)hexa-2,4-dienoate hydrolase 3.7.1.13

1 Nomenclature

EC number
3.7.1.13

Systematic name
(2E,4E)-6-(2-aminophenyl)-2-hydroxy-6-oxohexa-2,4-dienoate acylhydrolase

Recommended name
2-hydroxy-6-oxo-6-(2-aminophenyl)hexa-2,4-dienoate hydrolase

Synonyms
CarC <2,3> [2]
HOPDA hydrolase <1> [1]

2 Source Organism

<1> *Pseudomonas sp.* [1]
<2> *Pseudomonas resinovorans* [2]
<3> *Janthinobacterium sp.* J3 (UNIPROT accession number: Q84II3) [2]
<4> *Pseudomonas resinovorans* (UNIPROT accession number: Q9AQM4) [3]

3 Reaction and Specificity

Catalyzed reaction
(2E,4E)-6-(2-aminophenyl)-2-hydroxy-6-oxohexa-2,4-dienoate + H_2O = anthranilate + (2E)-2-hydroxypenta-2,4-dienoate

Substrates and products
S 2-hydroxy-6-oxo-6-(2'-aminophenyl)hexa-2,4-dienoic acid + H_2O <1> (Reversibility: ?) [1]
P benzoic acid + 2-hydroxypenta-2,4-dienoic acid
S 2-hydroxy-6-oxo-6-(2'-hydroxyphenyl)hexa-2,4-dienoate + H_2O <4> (Reversibility: ?) [3]
P ?
S 2-hydroxy-6-oxo-6-(2-aminophenyl)hexa-2,4-dienoate + H_2O <4> (Reversibility: ?) [3]
P anthranilate + 2-hydroxypenta-2,4-dienoate
S 2-hydroxy-6-oxo-6-phenylhexa-2,4-dienoate + H_2O <2,3,4> (Reversibility: ?) [2,3]

D. Schomburg and I. Schomburg (eds.), *Class 3.4–6 Hydrolases, Lyases, Isomerases, Ligases: EC 3.4–6*, Springer Handbook of Enzymes S10, DOI 10.1007/978-3-642-36260-6_28,

P ?
S 2-hydroxy-6-oxohepta-2,4-dienoic acid + H_2O <2,3> (<2> 0.38% of the activity with 2-hydroxy-6-oxo-6-phenylhexa-2,4-dienoate [2]; <3> 0.56% of the activity with 2-hydroxy-6-oxo-6-phenylhexa-2,4-dienoate [2]) (Reversibility: ?) [2]
P ?
S 2-hydroxymuconic semialdehyde + H_2O <2,3> (<3> 0.49% of the activity with 2-hydroxy-6-oxo-6-phenylhexa-2,4-dienoate [2]; <2> 0.54% of the activity with 2-hydroxy-6-oxo-6-phenylhexa-2,4-dienoate [2]) (Reversibility: ?) [2]
P ?
S Additional information <4> (<4> hydrolytic activity decreases in the substrate order of 2-hydroxy-6-oxo-6-(2-aminophenyl)hexa-2,4-dienoate, 2-hydroxy-6-oxo-6-phenylhexa-2,4-dienoate, 2-hydroxy-6-oxo-6-(2-hydroxyphenyl)hexa-2,4-dienoate. Poor substrates: 2-hydroxy-6-oxohepta-2,4-dienoic acid, 2-hydroxymuconic semialdehyde [3]) (Reversibility: ?) [3]
P ?

Cofactors/prosthetic groups

Additional information <1> (<1> no cofactor requirement [1]) [1]

Turnover number (s^{-1})

1.99 <3> (2-hydroxy-6-oxo-6-phenylhexa-2,4-dienoate, <3> pH 7.5, 25°C [2]) [2]
2.1 <4> (2-hydroxy-6-oxo-6-phenylhexa-2,4-dienoate, <4> pH 7.5, 25°C [3]) [3]
2.14 <2> (2-hydroxy-6-oxo-6-phenylhexa-2,4-dienoate, <2> pH 7.5, 25°C [2]) [2]
1300 <1> (2-hydroxy-6-oxo-6-(2'-aminophenyl)hexa-2,4-dienoic acid, <1> pH 7.5, 25°C [1]) [1]

Specific activity (U/mg)

3.84 <4> (<4> pH 7.5, 25°C [3]) [3]
2600 <1> (<1> pH 7.5, 25°C [1]) [1]

K_m-Value (mM)

0.00251 <2,4> (2-hydroxy-6-oxo-6-phenylhexa-2,4-dienoate, <2,4> pH 7.5, 25°C [2,3]) [2,3]
0.00273 <3> (2-hydroxy-6-oxo-6-phenylhexa-2,4-dienoate, <3> pH 7.5, 25°C [2]) [2]
0.0046 <1> (2-hydroxy-6-oxo-6-(2'-aminophenyl)hexa-2,4-dienoic acid, <1> pH 7.5, 25°C [1]) [1]

pH-Optimum

7 <1> [1]
7-7.5 <4> [3]

pH-Range

6.5 <1> (<1> no activity [1]) [1]
9 <1> (<1> about 50% of maximal activity [1]) [1]
10.5 <1> (<1> no activity [1]) [1]

Temperature optimum (°C)
58 <1> [1]

4 Enzyme Structure

Molecular weight
70000 <2,3,4> (<2,3,4> gel filtration [2,3]) [2,3]

Subunits
? <1> (<1> x * 32231, calculated, x * 33000, SDS-PAGE [1]) [1]
dimer <2,3,4> (<2,3> 2 * 33000, SDS-PAGE [2]; <4> 2 * 31000, SDS-PAGE, 2 * 31300, calculated [3]) [2,3]

5 Isolation/Preparation/Mutation/Application

Purification
<1> (recombinant enzyme) [1]
<2> (recombinantv enzyme) [2]
<3> (recombinant enzyme) [2]
<4> (recombinant enzyme) [3]

Crystallization
<3> (to 1.86 A resolution, space group I422. The subunit of ht-CarCJ3 is divided into two domains, i.e., the core domain with residues 15-144 and 209-282, and the lid domain with residues 145-208. The invisible 10 amino acid residues Ile146-Asn155 correspond to the helix α_4, which is the putative first α-helix in the lid domain. Sidechains of the active-site residues, Ser114 and His261, are clearly shown in the electron density map) [2]

Cloning
<1> (expression in Escherichia coli) [1]
<2> (expression in Escherichia coli) [2]
<3> (expression in Escherichia coli) [2]
<4> (expression in Escherichia coli) [3]

Engineering
S114A <1> (<1> mutation in active-site serine. Approximately 40fold reduction in activity for the His-tagged mutant hydrolase relative to similar lysates of His-tagged native CarC [1]) [1]

6 Stability

Temperature stability
55 <4> (<4> 10 min, 75% residual activity [3]) [3]
65 <4> (<4> 10 min, inactivation [3]) [3]

References

[1] Riddle, R.R.; Gibbs, P.R.; Willson, R.C.; Benedik, M.J.: Purification and properties of 2-hydroxy-6-oxo-6-(2-aminophenyl)hexa-2,4-dienoic acid hydrolase involved in microbial degradation of carbazole. Protein Expr. Purif., **28**, 182-189 (2003)

[2] Habe, H.; Morii, K.; Fushinobu, S.; Nam, J.W.; Ayabe, Y.; Yoshida, T.; Wakagi, T.; Yamane, H.; Nojiri, H.; Omori, T.: Crystal structure of a histidine-tagged serine hydrolase involved in the carbazole degradation (CarC enzyme). Biochem. Biophys. Res. Commun., **303**, 631-639 (2003)

[3] Nojiri, H.; Taira, H.; Iwata, K.; Morii, K.; Nam, J.W.; Yoshida, T.; Habe, H.; Nakamura, S.; Shimizu, K.; Yamane, H.; Omori, T.: Purification and characterization of *meta*-cleavage compound hydrolase from a carbazole degrader Pseudomonas resinovorans strain CA10. Biosci. Biotechnol. Biochem., **67**, 36-45 (2003)

malonyl-S-ACP decarboxylase 4.1.1.87

1 Nomenclature

EC number
4.1.1.87

Systematic name
malonyl-[acyl-carrier-protein] carboxy-lyase

Recommended name
malonyl-S-ACP decarboxylase

Synonyms
MdcD,E
MdcD/MdcE
malonyl-S-acyl-carrier protein decarboxylase

CAS registry number
80700-20-5 (multienzyme complex malonate decarboxylase)

2 Source Organism

<1> *Klebsiella pneumoniae* [1]
<2> *Acinetobacter calcoaceticus* (UNIPROT accession number: O54416) [2]

3 Reaction and Specificity

Catalyzed reaction
a malonyl-[acyl-carrier protein] + H^+ = an acetyl-[acyl-carrier protein] + CO_2 (<1> malonate decarboxylation proceeds in two steps: the acetyl residue on the acyl carrier protein is first replaced by a malonyl residue which subsequently undergoes decarboxylation thereby regenerating the acetyl-S-acyl carrier protein [1])

Substrates and products
S malonyl-CoA + H^+ <2> (Reversibility: ?) [2]
P acetyl-CoA + CO_2

Inhibitors
dithioerythritol <1> (<1> formation of a catalytically inactive SH-enzyme from the catalytically active acetyl-S-enzyme [1]) [1]

D. Schomburg and I. Schomburg (eds.), *Class 3.4–6 Hydrolases, Lyases, Isomerases, Ligases: EC 3.4–6*, Springer Handbook of Enzymes S10, DOI 10.1007/978-3-642-36260-6_29,

hydroxylamine <1> (<1> formation of a catalytically inactive SH-enzyme from the catalytically active acetyl-S-enzyme [1]) [1]

Cofactors/prosthetic groups

Additional information <1> (<1> the binding site for the acyl residues on the acyl carrier protein is 2-(5-phosphoribosyl)-3-dephospho-CoA [1]) [1]

Specific activity (U/mg)

0.19 <2> (<2> isolated β subunit of malonate decarboxylase complex [2]) [2]

K_m-Value (mM)

1.2 <2> (malonyl-CoA) [2]

4 Enzyme Structure

Molecular weight

66000 <2> (<2> PAGE [2]) [2]
142000 <1> (<1> gel filtration [1]) [1]

Subunits

dimer <2> (<2> 2 * 33000, SDS-PAGE, isolated β subunit of malonate decarboxylase complex [2]) [2]
tetramer <1> (<1> 1 * 65000, α subunit, 1* 34000, β-subunit, 1 * 30000, γ subunit, 1 * 12000, δ subunit, SDS-PAGE [1]) [1]
Additional information <1,2> (<2> mdcD gene product is the β subunit of malonate decarboxylase carrying the malonyl-CoA decarboxylase activity [2]; <1> presence of two forms of the enzyme: a catalytically inactive SH-enzyme and the catalytically active acetyl-S-enzyme which is formed by post-translational acetylation of the SH-enzyme with ATP, acetate and a specific ligase. the δ subunit is the acyl carrier protein of the enzyme complex [1]) [1,2]

5 Isolation/Preparation/Mutation/Application

Purification

<1> [1]

Renaturation

<1> (reacylation of the catalytically inactive SH-enzyme to form the catalytically active acetyl-S-enzyme can be achieved with acetic anhydride or more efficiently with malonyl-CoA) [1]

Cloning

<2> (expression in Escherichia coli) [2]

References

[1] Schmid, M.; Berg, M.; Hilbi, H.; Dimroth, P.: Malonate decarboxylase of Klebsiella pneumoniae catalyses the turnover of acetyl and malonyl thioester residues on a coenzyme-A-like prosthetic group. Eur. J. Biochem., **237**, 221-228 (1996)

[2] Koo, J.H.; Kim, Y.S.: Functional evaluation of the genes involved in malonate decarboxylation by Acinetobacter calcoaceticus. Eur. J. Biochem., **266**, 683-690 (1999)

biotin-independent malonate decarboxylase 4.1.1.88

1 Nomenclature

EC number
4.1.1.88

Systematic name
malonate carboxy-lyase (biotin-independent)

Recommended name
biotin-independent malonate decarboxylase

Synonyms
malonate decarboxylase
malonate decarboxylase (without biotin)

CAS registry number
80700-20-5 (multienzyme complex malonate decarboxylase)

2 Source Organism

<1> *Pseudomonas fluorescens* [1,7]
<2> *Acinetobacter calcoaceticus* [1,6,7,8]
<3> *Klebsiella pneumoniae* [2,4,5]
<4> *Acinetobacter calcoaceticus* (UNIPROT accession number: O54414 and O54416 and O54417 and O54415) [3]

3 Reaction and Specificity

Catalyzed reaction
malonate + H^+ = acetate + CO_2 (<2> malonate decarboxylation proceeds by a catalytic cycle in which the acetyl group on the active enzyme is displaced by malonate, which binds covalently to a thiol group on the enzyme and is subsequently decarboxylated [8]; <3> malonate decarboxylation proceeds in two steps: the acetyl residue on the acyl carrier protein is first replaced by a malonyl residue which subsequently undergoes decarboxylation thereby re-generating the acetyl-S-acyl carrier protein [4]; <1,2> reaction proceeds with retention of configuration [1])

Substrates and products
S 2-ethylmalonate + H^+ <2> (<2> 0.8% of the activity with malonate [8]) (Reversibility: ?) [8]

D. Schomburg and I. Schomburg (eds.), *Class 3.4–6 Hydrolases, Lyases, Isomerases, Ligases: EC 3.4–6*, Springer Handbook of Enzymes S10, DOI 10.1007/978-3-642-36260-6_30,

P butanoate + CO_2
S 2-methylmalonate + H^+ <2> (<2> 24% of the activity with malonate [8]) (Reversibility: ?) [8]
P propionate + CO_2
S glutarate + H^+ <2> (<2> 1.1% of the activity with malonate [8]) (Reversibility: ?) [8]
P butanoate + CO_2
S malonate + H^+ <1,2> (<2> enzyme is highly specific for malonate [8]) (Reversibility: ?) [6,7,8]
P acetate + CO_2
S oxalate + H^+ <2> (<2> 1.1% of the activity with malonate [8]) (Reversibility: ?) [8]
P CO_2

Inhibitors

2-nitro-5-thiocyanobenzoic acid <2> (<2> 0.64 mM, 2.1% residual activity [8]) [8]
5,5'-dithio-bis(2-nitrobenzoic acid) <2> (<2> 0.5 mM, 1.5% residual activity [7]; <2> 0.5 mM, 14.5% residual activity [8]) [7,8]
N-acetylimidazole <1,2> (<1,2> 1 mM, 95% residual activity [7]) [7]
N-ethylmaleimide <1,2> (<2> 0.5 mM, 0.1% residual activity [7]; <1> 0.5 mM, 0.2% residual activity [7]; <2> 1 mM, 1% residual activity [8]) [7,8]
bromoacetate <1,2> (<1> 0.5 mM, 0.1% residual activity [7]; <1> 0.5 mM, 0.4% residual activity [7]; <2> 0.5 mM, 0.9% residual activity [7]) [7]
diethyldicarbonate <1,2> (<1> 1 mM, 88% residual activity [7]; <2> 1 mM, 91% residual activity [7]) [7]
dithioerythritol <3> (<3> formation of a catalytically inactive SH-enzyme from the catalytically active acetyl-S-enzyme [4]) [4]
hydroxylamine <3> (<3> formation of a catalytically inactive SH-enzyme from the catalytically active acetyl-S-enzyme [4]) [4]
iodoacetamide <2> (<2> 1 mM, 58% residual activity [8]; <2> 0.5 mM, 58% residual activity [7]) [7,8]
pyridoxal 5'phosphate <1,2> (<2> 1 mM, 82% residual activity [7]; <1> 1 mM, 92% residual activity [7]) [7]
sodium borohydride <2> (<2> inactivation [8]) [8]

Cofactors/prosthetic groups

Additional information <2,3> (<3> subunit acyl carrier protein contains a 2-(5-phosphoribosyl)-3-dephospho-CoA prosthetic group attached via a phosphodiester to residue S25. Formation of this phosphodiester bond is catalyzed by a phosphoribosyl-dephospho-coenzyme A transferase MdcG. Site-directed mutagenesis of D134 and/or D136 of MdcG to alanine abolishes the transfer of the prosthetic group to apo acyl carrier protein [2]; <2> the α subunit contains a biotin prosthetic group which does not seem to be directly related to malonate decarboxylation [8]; <2> the prosthetic group of the acyl carrier protein is carboxymethylated 2-(5-phosphoribosyl)-3-dephospho-CoA [6]) [2,6,8]

Activating compounds

N-Acetylimidazole <1> (<1> 1 mM, 117% of initial activity [7]) [7]
diethyldicarbonate <1> (<1> 1 mM, 114% of initial activity [7]) [7]
pyridoxal 5'phosphate <1> (<1> 1 mM, 112% of initial activity [7]) [7]

Specific activity (U/mg)

4.48 <1> (<1> 30°C [7]) [7]
10.02 <2> (<2> 30°C [7]) [7]
Additional information <2> (<2> the α subunit shows CoA-transferase activity with specific activity of 39.03 U/mg [6]) [6]

K_m-Value (mM)

0.11 <2> (malonate, <2> apo-enzyme in presence of acetyl-CoA [6]) [6]
0.16 <2> (malonate, <2> subunit β in presence of acetyl-CoA [6]; <2> subunits β/γ in presence of acetyl-CoA [6]) [6]
1.4 <2> (malonate, <2> pH 6.8, 30°C [8]) [8]
3.23 <2> (malonate, <2> apo-enzyme in presence of acetyl-CoA [6]) [6]

pH-Optimum

6.8 <2> [8]

pi-Value

6.4 <2> (<2> isoelectric focusing [8]) [8]

4 Enzyme Structure

Molecular weight

142000 <3> (<3> gel filtration [4]) [4]
180000 <2> (<2> PAGE [8]) [8]
185000 <1,2> (<1,2> gel filtration [7,8]) [7,8]

Subunits

multimer <1,2> (<2> 2 * 65000, α subunit, 1 * 32000, β subunit, 1 * 25000, γ subunit [8]; <2> 2 * 65000, α subunit, 1 * 32000, β subunit, 1 * 25000, γ subunit, 1 * 11000, δ subunit [7]; <1> 2 * 65000, α subunit, 1 * 33000, β subunit, 1 * 30000, γ subunit, 1 * 11000, δ subunit [7]) [7,8]
tetramer <3> (<3> 1 * 65000, α subunit, 1* 34000, β-subunit, 1 * 30000, γ subunit, 1 * 12000, δ subunit, SDS-PAGE [4]) [4]
Additional information <2,3,4> (<2> enzyme complex is formed by subunits α, β, γ, δ. The mdcA gene product, the α subunit, is malonate/acetyl-CoA transferase and the mdcD gene product, the β subunit, is malonyl-CoA decarboxylase. The mdcE gene product, the γ subunit, may play a role in subunit interaction to form a stable complex or as a codecarboxylase. The mdcC gene product, the δ subunit, is an acyl-carrier protein [6]; <3> enzyme is encoded by a gene cluster consisting of the eight consecutive genes mdcABCDEFCH and the divergently oriented mdcR gene. The mdcA, C, D and E genes encode subunits α, β, γ and δ of malonate decarboxylase. MdcA represents the ACP-transferase and that MdcD and E together probably function as malonyl-S-

acyl carrier protein decarboxylase. MdcC is the (apo) acyl carrier protein subunit. MdcB and MdcG are involved in the synthesis and attachment of the prosthetic group. MdcH is probably involved in the initial activation of the enzyme by malonylation. MdcF is a membrane protein that could function as a malonate carrier [5]; <4> mdcA gene encodes the α subunit carrying acyl carrier protein transferase activity. The mdcD gene encodes the δ subunit, the acyl carrier protein. mdcB encodes the β subunit, the catalytic subunit of decarboxylation of malonate. The mdcC gene encodes the γ subunit involved in decarboxylation of the malonyl-S-acyl carrier protein [3]; <3> presence of two forms of the enzyme: a catalytically inactive SH-enzyme and the catalytically active acetyl-S-enzyme which is formed by post-translational acetylation of the SH-enzyme with ATP, acetate and a specific ligase. the δ subunit is the acyl carrier protein of the enzyme complex [4]; <3> subunit acyl carrier protein contains a 2-(5-phosphoribosyl)-3-dephospho-CoA prosthetic group attached via a phosphodiester to residue S25. Formation of this phosphodiester bond is catalyzed by a phosphoribosyl-dephospho-coenzyme A transferase MdcG. Site-directed mutagenesis of D134 and/or D136 of MdcG to alanine abolishes the transfer of the prosthetic group to apo acyl carrier protein [2]) [2,3,4,5,6]

Posttranslational modification

Additional information <1,2> (<1,2> the δ subunit of the active form of enzyme is acetylated, the acetyl group may form a thioester bond with the thiol group of the prosthetic group [7]) [7]

5 Isolation/Preparation/Mutation/Application

Localization

periplasm <2> [8]

Purification

<1> [7]
<2> [7,8]
<3> [4]

Renaturation

<1> (reactivation of deacetyl malonate decarboxylase with malonyl-CoA to 100%, with acetyl-CoA or methylmalonyl-CoA to about 50% of initial activity, respectively) [7]
<1> (reactivation of deacetyl malonate decarboxylase with malonyl-CoA, acetyl-CoA or methylmalonyl-CoA to more than 80% of initial activity) [7]
<2> (reactivation of deacetyl malonate decarboxylase with malonyl-CoA, acetyl-CoA or methylmalonyl-CoA to more than 80% of initial activity) [7]
<2> (reactivation of deacetylated enzyme by incubation with acetic anhydride or malonyl-CoA) [8]

<3> (reacylation of the catalytically inactive SH-enzyme to form the catalytically active acetyl-S-enzyme can be achieved with acetic anhydride or more efficiently with malonyl-CoA) [4]

Cloning

<2> (expression in Escherichia coli) [6]
<3> (expression in Escherichia coli) [5]
<4> (expression of gene cluster in Escherichia coli, no enzymatic activity) [3]

Engineering

Additional information <4> (<4> expression of gene cluster containing subunits α, β, γ, δ in Escherichia coli, no enzymatic activity [3]) [3]

6 Stability

General stability information

<2>, enzyme is sensitive to repeated freezing and thawing [8]

Storage stability

<2>, -20°C, stable for several months [8]
<2>, 4°C, deacetylated enzyme, full reactivation by addition of malonyl-CoA during 2 months storage [8]

References

[1] Handa, S.; Koo, J.H.; Kim, Y.S.; Floss, H.G.: Stereochemical course of biotin-independent malonate decarboxylase catalysis. Arch. Biochem. Biophys., **370**, 93-96 (1999)
[2] Hoenke, S.; Schmid, M.; Dimroth, P.: Identification of the active site of phosphoribosyl-dephospho-coenzyme A transferase and relationship of the enzyme to an ancient class of nucleotidyltransferases. Biochemistry, **39**, 13233-13240 (2000)
[3] Koo, J.H.; Jung, S.B.; Byun, H.S.; Kim, Y.S.: Cloning and sequencing of genes encoding malonate decarboxylase in Acinetobacter calcoaceticus. Biochim. Biophys. Acta, **1354**, 49-54 (1997)
[4] Schmid, M.; Berg, M.; Hilbi, H.; Dimroth, P.: Malonate decarboxylase of Klebsiella pneumoniae catalyses the turnover of acetyl and malonyl thioester residues on a coenzyme-A-like prosthetic group. Eur. J. Biochem., **237**, 221-228 (1996)
[5] Hoenke, S.; Schmid, M.; Dimroth, P.: Sequence of a gene cluster from Klebsiella pneumoniae encoding malonate decarboxylase and expression of the enzyme in Escherichia coli. Eur. J. Biochem., **246**, 530-538 (1997)
[6] Koo, J.H.; Kim, Y.S.: Functional evaluation of the genes involved in malonate decarboxylation by Acinetobacter calcoaceticus. Eur. J. Biochem., **266**, 683-690 (1999)

[7] Byun, H.S.; Kim, Y.S.: Subunit organization of bacterial malonate decarboxylases: The smallest δ subunit as an acyl-carrier protein. J. Biochem. Mol. Biol., **30**, 132-137 (1997)
[8] Kim, Y.S.; Byun, H.S.: Purification and properties of a novel type of malonate decarboxylase from Acinetobacter calcoaceticus. J. Biol. Chem., **269**, 29636-29641 (1994)

biotin-dependent malonate decarboxylase 4.1.1.89

1 Nomenclature

EC number
4.1.1.89

Systematic name
malonate carboxy-lyase (biotin-dependent)

Recommended name
biotin-dependent malonate decarboxylase

Synonyms
Na^+ pumping malonate decarboxylase <2> [3]
Na^+-activated malonate decarboxylase <2> [2]
malonate decarboxylase

CAS registry number
80700-20-5 (multienzyme complex malonate decarboxylase)

2 Source Organism

<1> *Propionigenium modestum* [1]
<2> *Malonomonas rubra* [1,2,3,4,5,6,7]

3 Reaction and Specificity

Catalyzed reaction
malonate + H^+ = acetate + CO_2 (<2> reaction does not involve intermediate formation of malonyl-CoA but proceeds directly with free malonate. Catalytic mechanism involves exchange of the enzyme-bound acetyl residues by malonyl residues and subsequent decarboxylation releasing CO_2 and regenerating the acetyl-enzyme. Biotin is involved in catalysis [5]; <2> reaction takes place with retention of configuration [7])

Natural substrates and products
S Additional information <2> (<2> subunit acetyl-S-acyl carrier protein: malonate acyl carrier protein-SH transferase catalyzes the transfer of acyl carrier protein from acetyl acyl carrier protein and malonate to yield malonyl acyl carrier protein and acetate. Malonate is thus activated on the enzyme by exchange for the catalytically important enzyme-bound acetyl thioester residues [2]) (Reversibility: ?) [2]

D. Schomburg and I. Schomburg (eds.), *Class 3.4–6 Hydrolases, Lyases, Isomerases, Ligases: EC 3.4–6*, Springer Handbook of Enzymes S10, DOI 10.1007/978-3-642-36260-6_31,

P ?

Substrates and products

S malonate + H^+ <2> (Reversibility: ?) [2,5]
P acetate + CO_2
S Additional information <2> (<2> subunit acetyl-S-acyl carrier protein: malonate acyl carrier protein-SH transferase catalyzes the transfer of acyl carrier protein from acetyl acyl carrier protein and malonate to yield malonyl acyl carrier protein and acetate. Malonate is thus activated on the enzyme by exchange for the catalytically important enzyme-bound acetyl thioester residues [2]) (Reversibility: ?) [2]
P ?

Inhibitors

avidin <2> (<2> inhibition can be partially reversed with an excess of biotin [1]) [1]
hydroxylamine <2> (<2> complete inhibition [5]) [5]
iodoacetate <2> (<2> specific reaction with subunit acyl carrier protein [4]) [4]
thiocyanate <2> (<2> complete inhibition [5]) [5]

Cofactors/prosthetic groups

biotin <1,2> (<1> enzyme complex contains a single biotinyl protein of 120000 Dalton in the cell membrane [1]; <2> enzyme complex contains a single biotinyl protein of 120000 Dalton in the cytoplasm [1]) [1]
Additional information <2> (<2> the acyl carrier protein subunit contains 2-(5“-phosphoribosyl)-3-dephosphocoenzyme A as a prosthetic group [4]) [4]

Specific activity (U/mg)

2.67 <2> (<2> pH 7.5, 30°C [5]) [5]
42 <2> (<2> pH 6.0 [2]) [2]

4 Enzyme Structure

Subunits

? <2> (<2> x * 14000, SDS-PAGE of subunit acyl carrier protein [4]; <2> x * 67000, SDS-PAGE, subunit acetyl-S-acyl carrier protein: malonate acyl carrier protein-SH transferase [2]) [2,4]
Additional information <2> (<2> the genes encoding components of the malonate decarboxylase enzyme system are located within a gene cluster of about 11 kb comprizing 14 genes that have been termed madYZG-BAECDHKFLMN. MadA represents the acyl-carrier-protein-transferase component, MadB is the integral membrane-bound carboxybiotin protein decarboxylase, MadC and MadD are the two subunits of the carboxyltransferase, MadE is the acyl carrier protein and MadF is the biotin protein [6]) [6]

5 Isolation/Preparation/Mutation/Application

Localization

cytoplasm <1,2> (<1,2> enzyme system involving cytoplasmic and membrane components [1]; <2> subunit acyl-carrier protein [4]) [1,4]
membrane <1,2> (<1,2> enzyme system involving cytoplasmic and membrane components [1]) [1]

Purification

<2> (isolation of the biotinyl protein from the complex in catalytically inactive form in presence of detergent) [1]
<2> (purification of subunit acetyl-S-acyl carrier protein: malonate acyl carrier protein-SH transferase and of whole enzyme complex) [2]
<2> (recombinant subunit biotinyl protein MadF. Despite coexpression of biotin ligase birA, MadF is poorly biotinylated) [3]

Renaturation

<2> (enzyme inhibited by thiocyanate or hydroxylamine, 50-65% of the original decarboxylase activity is restored by incubation of the extract with ATP in the presence of acetate, and the extent of reactivation increases after incubation with dithioerythritol. Reactivation is also obtained by chemical acetylation with acetic anhydride) [5]
<2> (inhibition of malonate decarboxylase complex by avidin can be partially reversed with an excess of biotin) [1]

Cloning

<2> (expression of subunit biotinyl protein MadF and biotin ligase birA in Escherichia coli) [3]

References

[1] Hilbi, H.; Hermann, R.; Dimroth, P.: The malonate decarboxylase enzyme system of Malonomonas rubra: evidence for the cytoplasmic location of the biotin-containing component. Arch. Microbiol., **160**, 126-131 (1993)
[2] Hilbi, H.; Dimroth, P.: Purification and characterization of a cytoplasmic enzyme component of the Na^+-activated malonate decarboxylase system of Malonomonas rubra: acetyl-S-acyl carrier protein: malonate acyl carrier protein-SH transferase. Arch. Microbiol., **162**, 48-56 (1994)
[3] Berg, M.; Dimroth, P.: The biotin protein MadF of the malonate decarboxylase from Malonomonas rubra. Arch. Microbiol., **170**, 464-468 (1998)
[4] Berg, M.; Hilbi, H.; Dimroth, P.: The acyl carrier protein of malonate decarboxylase of Malonomonas rubra contains 2-(5"-phosphoribosyl)-3-dephosphocoenzyme A as a prosthetic group. Biochemistry, **35**, 4689-4696 (1996)
[5] Hilbi, H.; Dehning, I.; Schink, B.; Dimroth, P.: Malonate decarboxylase of Malonomonas rubra, a novel type of biotin-containing acetyl enzyme. Eur. J. Biochem., **207**, 117-123 (1992)

[6] Berg, M.; Hilbi, H.; Dimroth, P.: Sequence of a gene cluster from Malonomonas rubra encoding components of the malonate decarboxylase Na^+ pump and evidence for their function. Eur. J. Biochem., **245**, 103-115 (1997)
[7] Micklefield, J.; Harris, K.J.; Groeger, S.; Mocek, U.; Hilbi, H.; Dimroth, P.; Floss, H.G.: Stereochemical course of malonate decarboxylation in Malonomonas rubra. J. Am. Chem. Soc., **117**, 1153-1154 (1995)

peptidyl-glutamate 4-carboxylase 4.1.1.90

1 Nomenclature

EC number
4.1.1.90

Systematic name
peptidyl-glutamate 4-carboxylase (2-methyl-3-phytyl-1,4-naphthoquinone-epoxidizing)

Recommended name
peptidyl-glutamate 4-carboxylase

Synonyms
Ci-GGC <8> [24]
GGCX <1,2,4> [21,22,23,29,30,31,32,33,34]
VKD carboxylase <2> [3,5]
carboxylase <4> [20]
γ glutamyl carboxylase <2> [23]
γ-carboxylase <1> [11]
γ-glutamyl carboxylase <1,2,4,5,6,7,8,9> (<4> polytopic membrane protein [12]) [2,7,9,11,12,13,14,15,16,17,18,19,20,21,22,24,26,27,29,30,32,33,34]
glutamate carboxylase <2,4,5,6,7,9> [1,2,5,6,7,8,9,10,13,14,15,17,18,19,20,23,25,26,27,28]
matrix Gla protein <4,5> [26]
matrix γ-carboxyglutamate protein <4,5> [26]
peptidyl-glutamate 4-carboxylase <3> [4]
peptidyl-glutamate 4-carboxylase (2-methyl-3-phytyl-1,4-naphthoquinone-epoxidizing) <3> [4]
two-chain carboxylase <2> (<2> carboxylase and epoxidase activities similar to those of one-chain carboxylase [9]) [9]
vitamin K-dependent carboxylase <2,5> [3,25]
vitamin K-dependent γ-glutamyl carboxylase <2> [31]

CAS registry number
81181-72-8

2 Source Organism

<1> *Mus musculus* [11,32]
<2> *Homo sapiens* [3,5,9,22,23,29,30,31,33,34]
<3> *Rattus norvegicus* [4]

D. Schomburg and I. Schomburg (eds.), *Class 3.4–6 Hydrolases, Lyases, Isomerases, Ligases: EC 3.4–6*, Springer Handbook of Enzymes S10, DOI 10.1007/978-3-642-36260-6_32,

<4> *Homo sapiens* (UNIPROT accession number: P38435) [12,20,21,26,27]
<5> *Bos taurus* (UNIPROT accession number: Q07175) [1,2,8,15,16,17,18,25,26,28]
<6> *Rattus norvegicus* (UNIPROT accession number: O88496) (CTPZ [7,14]) [6,7,10,14]
<7> *Drosophila melanogaster* (UNIPROT accession number: Q9W0C4) [19]
<8> *Ciona intestinalis* (UNIPROT accession number: Q008V9) [24]
<9> *Conus textile* (UNIPROT accession number: Q8IA33) [13]

3 Reaction and Specificity

Catalyzed reaction

peptidyl-4-carboxyglutamate + 2,3-epoxyphylloquinone + H_2O = peptidyl-glutamate + CO_2 + O_2 + phylloquinone (<3> in the physiological process reaction runs in reversed direction [4])

Reaction type

carboxylation
γ-carboxylation

Natural substrates and products

S L-glutamate + CO_2 + O_2 + vitamin K hydroquinone <5,6> (Reversibility: ?) [1,2,14,28]
P γ-carboxy L-glutamate + vitamin K epoxide + H_2O
S L-glutamate + CO_2 + O_2 + vitamin K hydroquinone <5> (Reversibility: ?) [17]
P γ-carboxy-L-glutamate + vitamin K epoxide + H_2O
S peptidyl-L-glutamate + CO_2 + O_2 + menaquinone <3> (Reversibility: ?) [4]
P ?
S peptidyl-L-glutamate + CO_2 + O_2 + phylloquinone <3> (Reversibility: ?) [4]
P peptidyl-4-carboxy L-glutamate + 2,3-epoxyphylloquinone + H_2O
S Additional information <1,2,3,4,5,7> (<1> an essential posttranslational modification required for the biological activity of a number of proteins, including proteins involved in blood coagulation and its regulation [11]; <3> cis-isomer of vitamin K_1, the 2-desmethyl derivative of phylloquinone, MK-1, or menadione (2 -methyl-1,4-naphthoquinone) have little or no activity [4]; <4> enzyme accomplishes the post-translational modification required for the activity of all of the vitamin K-dependent proteins [27]; <5> enzyme catalyzes the posttranslational modification of specific glutamic acid residues to form γ-carboxygutamic acid residues within the vitamin K-dependent proteins [1]; <4> enzyme important for γ-carboxylation of gla-proteins [21]; <5> enzyme required for the posttranslational modification of vitamin K-dependent proteins [18]; <7> one of the most distinctive of the extracellular post-translational modifications is the vitamin K-dependent γ-carboxylation of glutamate residues to give γ-carboxyglutamate [19]; <2> uses the oxygenation of vitamin K to convert glutamyl residues to γ-carboxylated glutamyl residues in vitamin K-dependent

proteins [5]; <4,5> vitamin K-dependent carboxylation of glutamate to form γ-carboxyglutamate (Gla) is unusual among known posttranslational modifications in that substrate recognition does not require a specific sequence around the glutamate residues to be modified [26]; <2> vitamin K-dependent proteins require carboxylation for activity [23]) [1,4,5,11,18,19,21,23,26,27]

P ?

Substrates and products

S CDADWVEGYSMEYLSR + CO_2 + O_2 + vitamin K hydroquinone <5> (<5> CDADWVEGYSMEYLSR [18]) (Reversibility: ?) [18]

P ? + vitamin K epoxide + H_2O

S CGRPSLEQLAQEVTYA + CO_2 + O_2 + vitamin K hydroquinone <5> (<5> CGRPSLEQLAQEVTYA [18]) (Reversibility: ?) [18]

P ? + vitamin K epoxide + H_2O

S FLEEL + CO_2 + O_2 + ammonium sulfate <4> (<4> carboxylase activity is measured by $^{14}CO_2$ incorporation into the synthetic peptide substrate FLEEL [27]) (Reversibility: ?) [27]

P ? + vitamin K epoxide + H_2O

S FLEEL + CO_2 + O_2 + phylloquinone <5> (Reversibility: ?) [16]

P ? + 2,3-epoxyphylloquinone + H_2O

S FLEEL + CO_2 + O_2 + proFIX 19 <4> (<4> carboxylase activity is measured by $^{14}CO_2$ incorporation into the synthetic peptide substrate FLEEL [27]) (Reversibility: ?) [27]

P ? + vitamin K epoxide + H_2O

S FLEEL + CO_2 + O_2 + vitamin K hydroquinone <2,4,5,7> (<2> pentapeptide substrate FLEEL: Phe-Leu-Glu-Glu-Leu, used for carboxylation activity [9]) (Reversibility: ?) [1,9,19,20]

P ? + vitamin K epoxide + H_2O

S FLEEL + CO_2 + O_2 + vitamin K_1 hydroquinone <1> (<1> a synthetic peptide substrate, assay for vitamin K-dependent carboxylase activity [11]) (Reversibility: ?) [11]

P ? + vitamin K_1 epoxide + H_2O

S FLEEL + CO_2 + O_2 + vitamin KH_2 <4,5,9> (<4> carboxylase activity is measured by $^{14}CO_2$ incorporation into the synthetic peptide substrate FLEEL [27]; <5> Phe-Leu-Glu-Glu-Leu [25]) (Reversibility: ?) [2,8,13,17,25,27]

P ? + vitamin K epoxide + H_2O

S FLEEV + CO_2 + O_2 + vitamin K hydroquinone <5> (Reversibility: ?) [15]

P ? + vitamin K epoxide + H_2O

S GKDRLTQMKRILKQRGNKARGEEELY + CO_2 + O_2 + vitamin K hydroquinone <7> (Reversibility: ?) [19]

P ? + vitamin K epoxide + H_2O

S L-glutamate + CO_2 + O_2 + vitamin K hydroquinone <2,4,5> (<5> catalyzes modification of specific glutamic acids to γ-carboxyglutamic acid in several blood-coagulation proteins [25]; <4> reaction is essential for the

activity of all of the vitamin K-dependent proteins [27]) (Reversibility: ?) [17,23,25,27]
P γ-carboxy-L-glutamate + vitamin K epoxide + H_2O
S L-glutamate + CO_2 + O_2 + vitamin K hydroquinone <1,2,4,5,6,7,9> (<5> vitamin K epoxide must be recycled to vitamin K hydroquinone by the enzyme epoxide reductase for the reaction to continue [18]) (Reversibility: ?) [1,2,3,7,11,12,13,14,18,19,20,26,28]
P γ-carboxy L-glutamate + vitamin K epoxide + H_2O
S N-(bromoacetyl)-FLEELY + CO_2 + O_2 + vitamin KH_2 <5> (Reversibility: ?) [8]
P ? + vitamin K epoxide + H_2O
S ProFIX 19-6BPA + CO_2 + O_2 + FLEEL + vitamin KH_2 <5> (<5> TVFLDHENANKIBNRPKR [8]) (Reversibility: ?) [8]
P ? + vitamin K epoxide + H_2O
S ProFIX 19-7BPA + CO_2 + O_2 + FLEEL + vitamin KH_2 <5> (<5> TVFLDHENfiNKBLNRPKR [8]) (Reversibility: ?) [8]
P ? + vitamin K epoxide + H_2O
S ProFIX19-13BPA + CO_2 + O_2 + FLEEL + vitamin KH_2 <5> (<5> TVFLDBENWKILNRPKRY [8]) (Reversibility: ?) [8]
P ? + vitamin K epoxide + H_2O
S ProFIX19-16BPA + CO_2 + O_2 + FLEEL + vitamin KH_2 <5> (<5> TVBLDHENANKILNRPKRY [8]) (Reversibility: ?) [8]
P ? + vitamin K epoxide + H_2O
S TVFLDHENANKILNRPKRANTBLEEVRK + CO_2 + O_2 + vitamin K hydroquinone <5> (<5> carboxylase probe1, TVFLDHENANKILNRPKRANTBLEEVRK as a substrate [15]) (Reversibility: ?) [15]
P ? + vitamin K epoxide + H_2O
S TVFLDHENANKILNRPKRYNTBLEEVRK + CO_2 + O_2 + vitamin K hydroquinone <5> (Reversibility: ?) [15]
P ? + vitamin K epoxide + H_2O
S YVFLDHQDADANLILNRPKR + CO_2 + O_2 + vitamin KH_2 <5> (Reversibility: ?) [2]
P ? + vitamin K epoxide + H_2O
S conantokin G + CO_2 + O_2 + vitamin K hydroquinone <7> (<7> poorly carboxylated [19]) (Reversibility: ?) [19]
P ? + vitamin K epoxide + H_2O
S conotoxin ε-TxIX + CO_2 + O_2 + vitamin KH_2 <9> (Reversibility: ?) [13]
P ?
S e-TxIX12 + CO_2 + O_2 + vitamin KH_2 <9> (<9> residues 1-12 of e-TxIX [13]) (Reversibility: ?) [13]
P ?
S γ-carboxylated glutamyl containing vitamin K-dependent protein + vitamin K epoxide + H_2O <2> (Reversibility: ?) [5]
P ?
S glutamyl containing vitamin K-dependent protein + CO_2 + vitamin K hydroquinone + O_2 <2> (<2> propeptide binding increases carboxylase affinity for the Glu substrate, and the coordinated binding of the vitamin K-

dependent propeptide and Glu substrate increase carboxylase affinity for vitamin K and activity, possibly through a mechanism of substrate-assisted catalysis. The propeptide adjacent to the Gla domain is cleaved subsequently to carboxylation. The carboxylase uses the energy of vitamin K hydroquinone oxygenation to convert glutamyl residues to γ-carboxylated glutamyl residues in vitamin K-dependent proteins. During carboxylation, the vitamin K hydroquinone cofactor is oxidized to a vitamin K epoxide product. The carboxylase itself is also a vitamin K-dependent protein and carboxylase carboxylation may be important in regulating the overall process of vitamin K-dependent protein carboxylation. All vitamin K-dependent proteins contain multiple glutamyl residues that undergo carboxylation, which is accomplished by a processive mechanism. A single binding event between carboxylase and vitamin K-dependent protein can give rise to all of the glutamyl to gamm-carboxylated glutamyl conversions in the vitamin K-dependent protein. Carboxylation is limited to the glutamyl residue residing within the Gla domain substrate [5]) (Reversibility: ?) [5]

P ?

S osteocalcin + reduced vitamin K + CO_2 + O_2 <6> (Reversibility: ?) [7]

P ? + vitamin K epoxide + H_2O

S *p*-benzoylphenylalanine + CO_2 + O_2 + vitamin K hydroquinone <5> (<5> BPA [18]) (Reversibility: ?) [18]

P ? + vitamin K epoxide + H_2O

S peptidyl-L-glutamate + CO_2 + O_2 + menaquinone <3> (Reversibility: ?) [4]

P ?

S peptidyl-L-glutamate + CO_2 + O_2 + phylloquinone <3> (Reversibility: ?) [4]

P peptidyl-4-carboxy L-glutamate + 2,3-epoxyphylloquinone + H_2O

S pro-FIX19 + CO_2 + O_2 + vitamin K hydroquinone <5> (<5> pro-FIX19: peptide comprising residues of human factor IX AVFLDHENANKILNRPKRY [18]) (Reversibility: ?) [18]

P ? + vitamin K epoxide + H_2O

S pro-FIX19-16BPA + CO_2 + O_2 + vitamin K hydroquinone <5> (<5> pro-FIX19-16BPA: peptide comprising residues TVBLDHENANKILNRPKRY [18]) (Reversibility: ?) [18]

P ? + vitamin K epoxide + H_2O

S pro-e-TxIX/12 + CO_2 + O_2 + vitamin KH_2 <9> (<9> residues -12 to -1 of e-TxIX precursor [13]) (Reversibility: ?) [13]

P ?

S pro-e-TxIX/24 + CO_2 + O_2 + vitamin KH_2 <9> (<9> residues -12 to +12 of e-TxIX precursor [13]) (Reversibility: ?) [13]

P ?

S pro-e-TxIX/41 + CO_2 + O_2 + vitamin KH_2 <9> (<9> residues -29 to +12 of e-TxIX precursor [13]) (Reversibility: ?) [13]

P ?

S proFIX 19 + CO_2 + O_2 + vitamin K hydroquinone <5> (<5> proFIX 19, peptide sequence: TVFLDHENANKILNRPKRY [15]) [15]

P ? + vitamin K epoxide + H_2O
S proFIX/PT28 + CO_2 + O_2 + vitamin K hydroquinone <5> (<5> proFIX/PT28, peptide sequence: TVFLDHENANKILNRPKRANTFLEEVRK [15]) (Reversibility: ?) [15]
P ? + vitamin K epoxide + H_2O
S proFIX18 + CO_2 + O_2 + vitamin KH_2 <9> (<9> residues -18 to -1 of proFactor IX [13]) (Reversibility: ?) [13]
P ?
S proFIX19 + CO_2 + O_2 + FLEEL + vitamin KH_2 <5> (<5> TVFLDHENANKILNRPKRY [8]) (Reversibility: ?) [8]
P ? + vitamin K epoxide + H_2O
S proFIX28 + CO_2 + O_2 + vitamin KH_2 <9> (<9> residues -18 to +10 of proFactor IX [13]) (Reversibility: ?) [13]
P ?
S proFIXl9 + CO_2 + O_2 + vitamin KH_2 <5> (<5> AVFLDHENANKILNRPKRY [25]) (Reversibility: ?) [25]
P ? + vitamin K epoxide + H_2O
S proPT18 + CO_2 + O_2 + vitamin KH_2 <9> (<9> residues -18 to -1 of prothrombin. 28-residue peptides based on residues -18 to +10 of human proprothrombin and proFactor IX with K_m values of 420 lM, 1.7 μM and 6ÎmicroM [13]) (Reversibility: ?) [13]
P ?
S proPT28 + CO_2 + O_2 + FLEEL + vitamin KH_2 <5> (<5> HVFLAPQQARSLLQRVRRANTFLEEVRK [8]) (Reversibility: ?) [8]
P ? + vitamin K epoxide + H_2O
S proPT28 + CO_2 + O_2 + vitamin K hydroquinone <5> (<5> proPT28: synthetic peptide is designated by the following nomenclature: pro indicates the presence of the propeptide sequence, PT indicates prothrombin, the protein on which the peptide sequence is based, and 28 indicates the number of amino acid residues in the peptide [1]) (Reversibility: ?) [1]
P ? + vitamin K epoxide + H_2O
S proPT28 + CO_2 + O_2 + vitamin KH_2 <9> (<9> residues -18 to +10 of proprothrombin [13]) (Reversibility: ?) [13]
P ?
S proPTl8 + CO_2 + O_2 + FLEEL + vitamin KH_2 <5> (<5> HVFLAPQQARSLLQRVRR [8]) (Reversibility: ?) [8]
P ? + vitamin K epoxide + H_2O
S Additional information <1,2,3,4,5,6,7,9> (<1> an essential posttranslational modification required for the biological activity of a number of proteins, including proteins involved in blood coagulation and its regulation [11]; <3> cis-isomer of vitamin K_1, the 2-desmethyl derivative of phylloquinone, MK-1, or menadione (2 -methyl-1,4-naphthoquinone) have little or no activity [4]; <4> enzyme accomplishes the post-translational modification required for the activity of all of the vitamin K-dependent proteins [27]; <5> enzyme catalyzes the posttranslational modification of specific glutamic acid residues to form γ-carboxygutamic acid residues within the vitamin K-dependent proteins [1]; <4> enzyme important for γ-car-

boxylation of gla-proteins [21]; <5> enzyme required for the posttranslational modification of vitamin K-dependent proteins [18]; <7> one of the most distinctive of the extracellular post-translational modifications is the vitamin K-dependent γ-carboxylation of glutamate residues to give γ-carboxyglutamate [19]; <2> uses the oxygenation of vitamin K to convert glutamyl residues to γ-carboxylated glutamyl residues in vitamin K-dependent proteins [5]; <4,5> vitamin K-dependent carboxylation of glutamate to form γ-carboxyglutamate (Gla) is unusual among known posttranslational modifications in that substrate recognition does not require a specific sequence around the glutamate residues to be modified [26]; <2> vitamin K-dependent proteins require carboxylation for activity [23]; <9> amino-acid sequences of the synthetic substrates and propeptides are shown [13]; <4,5> identification of a striking homology between exon 3 in all known matrix Gla proteins and a 24-residue sequence in the bovine and human γ-glutamyl carboxylases. Alignment of exon 3 of matrix Gla protein with the homologous region of the γ-glutamyl carboxylase shown [26]; <5> photolabeling of Q-glutamyl carboxylase with Bpa peptides [15]; <6> separate active sites are required to support vitamin K-dependent epoxide formation and carboxylation. The binding site for vitamin K oxygenase contains an active thiol group [6]; <5> vitamin K carboxylase specifically interacts with the propeptide region of the precursor forms of vitamin K dependent proteins [8]) [1,4,5,6,8,11,13,15,18,19,21,23,26,27]

P ?

Inhibitors

2,3,5,6-tetrachloro-4-pyridinol <3> (<3> TCP, anticoagulant action, effective in vitro inhibitor of the carboxylase [4]) [4]

2-chloro-3-phytyl-1,4-naphthoquinone <3,5> (<3> chloro-K, effective in vivo antagonist of vitamin K, inhibits the enzyme in an competitive fashion [4]) [4,28]

Boc-(2S,4S)-4-methylglutamic acid-Glu-Val <4> (<4> competitive inhibitor, FLEEL as substrate [20]) [20]

Boc-Ser(OPO_4)-Ser(OPO_4)-Leu-OMe <3> (<3> inhibits the enzyme apparently competitively with regard to other peptide substrate [4]) [4]

CN^- <3> (<3> enzyme is blocked by mM concentrations of CN^- [4]) [4]

CsCl <6> [10]

Cu^{2+} <3> (<3> free Cu^{2+} and Cu^{2+}-complexes inhibit the reaction [4]) [4]

FFRCK <5> (<5> peptide, protease inhibitor [25]) [25]

FPRCK <5> (<5> peptide, protease inhibitor [25]) [25]

N-ethylmaleimide <5,6> (<6> preincubation with vitamin K hydroquinone prevents NEM inhibition of epoxide formation but not of carboxylation [6]) [6,16]

TVFLDHENANKILNRPKRANTBLEEVRK <5> (<5> the enzyme is photoirradiated on ice at 365 nm with TVFLDHENANKILNRPKRANTBLEEVRK, TVFLDHENANKILNRPKRYNTBLEEVRK and mono [127I]TVFLDHENANKILNRPKRYNTBLEEVRK for various times [15]) [15]

TVFLDHENANKILNRPKRYNTBLEEVRK <5> (<5> the enzyme is photoirradiated on ice at 365 nm with TVFLDHENANKILNRPKRANTBLEEVRK, TVFLDHENANKILNRPKRYNTBLEEVRK and mono [127I]TVFLDHENAN KILNRPKRYNTBLEEVRK for various times. Presence of TVFLDHENAN KILNRPKRYNTBLEEVRK or its iodinated derivative 80% inactivation is observed [15]) [15]
anti-carboxylase antiserum <5> (<5> effect of anti-carboxylase antiserum on carboxylase activity: under the conditions employed the carboxylation is inhibited by 80%, with parallel inhibition of CO_2 incorporation into FLEEL and proPT28 (synthetic peptide) [1]) [1]
bromoacetyl-FLEEL peptide <5> (<5> the His6-carboxylase is irreversibly inactivated. Up to 85% of the carboxylase activity is lost over a period of 120 min [17]) [17]
deoxycholate <6> [10]
ethanol <3> (<3> high concentrations [4]) [4]
hematin <3> [4]
iodoacetic acid <6> (<6> poor inhibitor [6]) [6]
methemoglobin <3> [4]
p-chloromercuribenzoate <6> (<6> 97% inhibition with 1.25 mM and at 5 mM the reaction is completely inhibited [10]) [10]
p-hydroxymercuribenzoate <3,6> (<6> 1 mM, more than 90% inhibition, inhibition is reversed by dithiothreitol [6]) [4,6]
proFIX/PT28 (Bpa +4) <5> (<5> presence of proFIX/PT28 (Bpa +4) or its iodinated derivative 56% inactivation is observed [15]) [15]
proFIX19-16BPA propeptide <5> [8]
protease inhibitor mixture <5> (<5> PIC, freshly prepared as a 10x PIC stock containing 20 mM dithiothreitol, 20 mM EDTA, FFRCK (1.25 μg/ml), FPRCK (1.25 μg/ml), leupeptin (5 μg/ml), pepstatin A (7 μg/ml), phenylmethylsulfonyl fluoride (340 μg/ml), aprotinin (20 μg/ml) [25]) [25]
sucrose <6> [10]
tetrachloropyridin <5> [28]
trypsin <6> [10]
vitamin K <5> (<5> carboxylation of FLEEL by bovine liver carboxylase is inhibited by high concentrations of vitamin KH_2. vitamin K (up to 400 mM) and vitamin K epoxide (up to 1 mM) are not inhibitory. R234A/H235A mutant, R406A/H408A mutant, and R513A/K515A mutant are more susceptible to inhibition by vitamin KH_2 than wild type enzyme. R234A/H235A mutant and R406A/H408A mutant exhibit maximal activity at 111 mM vitamin KH_2 and R513A/K515A mutant at 56 mM vitamin KH_2 [2]) [2]
warfarin <2,5,6> [10,16,23]
Additional information <2,5,6> (<5> 15 min irradiation in the absence of peptide resulted in a 10% inactivation of the carboxylase [15]; <5> in the presence of high concentrations of propeptide, only minimal carboxylase activity is measurable. Antibodies to the protein inhibit the carboxylase activity in crude preparations [1]; <6> NADH, dithiothreitol, and ATP deficiency decrease enzyme activity [10]; <2> the carboxylase reaction is inhibited by sulfhydryl-specific reagents [23]) [1,10,15,23]

Cofactors/prosthetic groups

phylloquinone <5> [16]

vitamin K <2,3,4,5,6,7,8> (<6> aquamephyton [10]; <4> carboxylase and soybean seed lipoxygenase share 19.3% identity over a span of 198 amino acids, from residues 468 to 666 of carboxylase. This is interesting because the carboxylase acts as an oxygenase on the cofactor vitamin K-hydroquinone, and the similarity occurs in that region of the carboxylase likely to have enzymatic function [27]; <4> conversion of glutamic acid to γ-carboxyglutamic acid is coupled with the oxygenation of KH_2 to vitamin K 2,3-epoxide and has been referred to as vitamin K epoxidase activity [20]; <7> phytonadione [19]; <2> the carboxylase uses the energy of vitamin K hydroquinone oxygenation to convert glutamyl residues to γ-carboxylated glutamyl residues in vitamin K-dependent proteins. During carboxylation, the vitamin K hydroquinone cofactor is oxidized to a vitamin K epoxide product [5]) [1,2,3,4,5,6,7,8,9,10,12,14,15,17,18,19,20,21,23,24,25,26,27,28]

vitamin K_1 <1,9> [11,13]

Activating compounds

ammonium sulfate <4> [27]

benzoylphenylalanine <5> (<5> Bpa, the four Bpa peptides enhance γ-carboxylation by 1.5-2.3fold, and the rate enhancement profiles are very similar to that of proFIX19, showing that these propeptides are recognized by the carboxylase [8]) [8]

decarboxylated plasma prothrombin <3> (<3> activates the enzyme [4]) [4]

endogenous precursor <3> (<3> activates the enzyme [4]) [4]

proFIX 19 <4> [27]

proFIX19 <5> (<5> enhances γ-carboxylation of the synthetic FLEEL peptide by 2.2-2.3fold [8]) [8]

proPT18 <5> (<5> enhances γ-carboxylation of the synthetic FLEEL peptide by 2.2-2.3fold [8]) [8]

Additional information <3> (<3> enzyme activity increases 2-3fold by a vitamin K deficiency or Warfarin treatment [4]) [4]

Metals, ions

Additional information <3,5> (<5> calcium-binding protein [1]; <3> Mn^{2+}, high concentrations significantly decrease or have no effect on K_m of a peptide substrate for the enzyme [4]) [1,4]

Turnover number (s^{-1})

0.0019 <4> (FLEEL, <4> Y395A, pH 7.4, 20°C [20]) [20]

0.002 <5> (YVFLDHQDADANLILNRPKR, <5> R359A/H360A/K361A mutant [2]) [2]

0.0033 <4> (FLEEL, <4> W399A, pH 7.4, 20°C [20]) [20]

0.01 <5> (YVFLDHQDADANLILNRPKR, <5> R234A/H235A mutant, peptides comprising residue YVFLDHQDADANLILNRPKR concentration 0 μM [2]) [2]

0.015 <5> (YVFLDHQDADANLILNRPKR, <5> R406A/H408A mutant, peptides comprising residue YVFLDHQDADANLILNRPKR concentration 0 μM [2]) [2]

0.018 <5> (vitamin KH_2, <5> proPT28, R513A/K515A mutant [2]) [2]

0.02 <5> (YVFLDHQDADANLILNRPKR, <5> FLAG-vitamin K-dependent γ-glutamyl carboxylase [2]) [2]
0.02 <5> (vitamin KH_2, <5> proPT28, FLAG-vitamin K-dependent γ-glutamyl carboxylase [2]) [2]
0.025 <5> (vitamin KH_2, <5> proPT28, R406A/H408A mutant [2]) [2]
0.033 <5> (vitamin KH_2, <5> proPT28, R234A/H235A mutant [2]) [2]
0.042 <5> (YVFLDHQDADANLILNRPKR, <5> R406A/H408A mutant [2]) [2]
0.056 <5> (YVFLDHQDADANLILNRPKR, <5> R513A/K515A mutant [2]) [2]
0.059 <5> (YVFLDHQDADANLILNRPKR, <5> FLAG-vitamin K-dependent γ-glutamyl carboxylase, peptides comprising residue YVFLDHQDADAN LILNRPKR concentration 0 μM [2]) [2]
0.06 <5> (YVFLDHQDADANLILNRPKR, <5> R234A/H235A mutant [2]) [2]
0.07 <5> (FLEEL, <5> R513A/K515A mutant [2]) [2]
0.1 <5> (vitamin KH_2, <5> FLEEL, R513A/K515A mutant [2]) [2]
0.11 <4> (FLEEL, <4> L394R, pH 7.4, 20°C [20]) [20]
0.11 <5> (vitamin KH_2, <5> FLEEL, R359A/H360A/K361A mutant [2]) [2]
0.153 <5> (YVFLDHQDADANLILNRPKR, <5> R406A/H408A mutant, peptides comprising residue YVFLDHQDADANLILNRPKR concentration 0.16 μM [2]) [2]
0.175 <5> (YVFLDHQDADANLILNRPKR, <5> R234A/H235A mutant, peptides comprising residue YVFLDHQDADANLILNRPKR concentration 0.16 μM [2]) [2]
0.19 <5> (FLEEL, <5> R359A/H360A/K361A mutant [2]) [2]
0.21 <4> (FLEEL, <4> wild type, pH 7.4, 20°C [20]) [20]
0.324 <5> (YVFLDHQDADANLILNRPKR, <5> FLAG-vitamin K-dependent γ-glutamyl carboxylase, peptides comprising residue YVFLDHQDADAN LILNRPKR concentration 0.16 μM [2]) [2]
0.347 <5> (YVFLDHQDADANLILNRPKR, <5> R406A/H408A mutant, peptides comprising residue YVFLDHQDADANLILNRPKR concentration 1.6 μM [2]) [2]
0.391 <5> (YVFLDHQDADANLILNRPKR, <5> R234A/H235A mutant, peptides comprising residue YVFLDHQDADANLILNRPKR concentration 1.6 μM [2]) [2]
0.465 <5> (YVFLDHQDADANLILNRPKR, <5> FLAG-vitamin K-dependent γ-glutamyl carboxylase, peptides comprising residue YVFLDHQDADAN LILNRPKR concentration 1.6 μM [2]) [2]
0.488 <5> (YVFLDHQDADANLILNRPKR, <5> FLAG-vitamin K-dependent γ-glutamyl carboxylase, peptides comprising residue YVFLDHQDADAN LILNRPKR concentration 160 μM [2]) [2]
0.56 <5> (YVFLDHQDADANLILNRPKR, <5> R406A/H408A mutant, peptides comprising residue YVFLDHQDADANLILNRPKR concentration 160 μM [2]) [2]
0.56 <5> (vitamin KH_2, <5> FLEEL, R406A/H408A mutant [2]) [2]
0.6 <5> (FLEEL, <5> for wild type FLAG-vitamin K-dependent γ-glutamyl carboxylase [2]) [2]
0.6 <5> (vitamin KH_2, <5> FLEEL, R234A/H235A mutant [2]) [2]
0.64 <5> (FLEEL, <5> R234A/H235A mutant [2]) [2]

0.645 <5> (YVFLDHQDADANLILNRPKR, <5> R234A/H235A mutant, peptides comprising residue YVFLDHQDADANLILNRPKR concentration 160 microM [2]) [2]
0.66 <5> (vitamin KH_2, <5> FLEEL, FLAG-vitamin K-dependent γ-glutamyl carboxylase [2]) [2]
0.7 <5> (FLEEL, <5> wild type [2]; <5> FLAG-vitamin K-dependent γ-glutamyl carboxylase [2]) [2]
0.72 <5> (FLEEL, <5> R406A/H408A mutant [2]) [2]
1 <5> (CO_2, <5> pH 7.4 [16]) [16]
1 <5> (FLEEL, <5> wild-type carboxylase in bovine liver microsomes [17]) [17]
1.7 <5> (FLEEL, <5> recombinant His6-carboxylase present in Sf9 cell microsomes [17]) [17]
Additional information <4> (<4> k_{cat} values relative to wild type are 51% (L394R), 1% (Y395A), and 2% (W399A), pH 7.4, 20°C [20]) [20]

Specific activity (U/mg)

0.0000026 <2> (<2> H160A mutant [3]) [3]
0.0000027 <2> (<2> wild type [3]) [3]
0.0000045 <2> (<2> H381A mutant [3]) [3]
Additional information <5> (<5> propeptide eluate of gel: 608 U/mg, carboxylase units are expressed as 100000 dpm of $^{14}CO_2$ fixed in the standard assay [28]; <5> specific activities of the partially purified microsomes and the homogeneous vitamin K-dependent carboxylase are 2.77 and 279.6 nmol of vitamin K epoxide per h per mg of protein, a 101fold purification of the vitamin K epoxidase activity from partially purified microsomes [1]) [1,28]

K_m-Value (mM)

0.0017 <9> (28-residue peptides based on residues -18 to +10 of human proprothrombin, <9> pH 7.0 [13]) [13]
0.0023 <5> (YVFLDHQDADANLILNRPKR, <5> FLAG-vitamin K-dependent γ-glutamyl carboxylase [2]) [2]
0.0038 <5> (vitamin KH_2, <5> proPT28, R406A/H408A mutant [2]) [2]
0.004 <5> (vitamin KH_2, <5> proPT28, FLAG-vitamin K-dependent γ-glutamyl carboxylase [2]) [2]
0.0041 <5> (YVFLDHQDADANLILNRPKR, <5> R359A/H360A/K361A mutant [2]) [2]
0.0052 <5> (YVFLDHQDADANLILNRPKR, <5> R406A/H408A mutant [2]) [2]
0.006 <9> (proFactor IX, <9> pH 7.0 [13]) [13]
0.0068 <5> (TVFLDHENANKILNRPKRANTBLEEVRK, <5> carboxylase probe1, TVFLDHENANKILNRPKRANTBLEEVRK as a substrate [15]) [15]
0.007 <5> (vitamin KH_2, <5> proPT28, R234A/H235A mutant [2]) [2]
0.0081 <5> (YVFLDHQDADANLILNRPKR, <5> R234A/H235A mutant [2]) [2]
0.0123 <5> (vitamin KH_2, <5> proPT28, R513A/K515A mutant [2]) [2]
0.0144 <5> (YVFLDHQDADANLILNRPKR, <5> R513A/K515A mutant [2]) [2]

0.032 <5> (vitamin KH_2, <5> FLEEL, R513A/K515A mutant [2]) [2]
0.043 <5> (vitamin KH_2, <5> FLEEL, R359A/H360A/K361A mutant [2]) [2]
0.052 <9> (vitamin K_1, <9> pH 7.0 [13]) [13]
0.053 <5> (vitamin KH_2, <5> FLEEL, R406A/H408A mutant [2]) [2]
0.074 <9> (precursor analog containing 29 amino acids of the propeptide region, <9> pH 7.0 [13]) [13]
0.074 <5> (vitamin KH_2, <5> FLEEL, FLAG-vitamin K-dependent γ-glutamyl carboxylase [2]) [2]
0.075 <9> (precursor analog containing 12 of the propeptide region, <9> pH 7.0 [13]) [13]
0.097 <5> (vitamin KH_2, <5> FLEEL, R234A/H235A mutant [2]) [2]
0.3 <5> (CO_2, <5> pH 7.4 [16]) [16]
0.42 <9> (FLEEL, <9> pH 7.0 [13]) [13]
0.54 <4> (FLEEL, <4> wild type, pH 7.4, 20°C [20]) [20]
0.565 <9> (conotoxin ε-TxIX, <9> pH 7.0 [13]) [13]
0.78 <5> (YVFLDHQDADANLILNRPKR, <5> FLAG-vitamin K-dependent γ-glutamyl carboxylase, peptides comprising residue YVFLDHQDADAN LILNRPKR concentration 1.6 μM [2]; <5> FLAG-vitamin K-dependent γ-glutamyl carboxylase, peptides comprising residue YVFLDHQDADAN LILNRPKR concentration 160 μM [2]) [2]
0.91 <5> (YVFLDHQDADANLILNRPKR, <5> FLAG-vitamin K-dependent γ-glutamyl carboxylase, peptides comprising residue YVFLDHQDADAN LILNRPKR concentration 0.16 μM [2]) [2]
0.92 <5> (YVFLDHQDADANLILNRPKR, <5> R234A/H235A mutant, peptides comprising residue YVFLDHQDADANLILNRPKR concentration 160 μM [2]) [2]
1 <5> (FLEEL, <5> wild type [2]) [2]
1.01 <5> (YVFLDHQDADANLILNRPKR, <5> R406A/H408A mutant, proIX18 concentration 160 μM [2]) [2]
1.1 <5> (FLEEL, <5> FLAG-vitamin K-dependent γ-glutamyl carboxylase [2]) [2]
1.23 <5> (YVFLDHQDADANLILNRPKR, <5> R406A/H408A mutant, peptides comprising residue YVFLDHQDADANLILNRPKR concentration 1.6 μM [2]) [2]
1.25 <5> (YVFLDHQDADANLILNRPKR, <5> R234A/H235A mutant, peptides comprising residue YVFLDHQDADANLILNRPKR concentration 1.6 μM [2]) [2]
1.3 <5> (FLEEL, <5> R234A/H235A mutant [2]) [2]
1.5 <5> (FLEEL, <5> for wild type FLAG-vitamin K-dependent γ-glutamyl carboxylase [2]; <5> proPTl8 propeptide [8]; <5> R359A/H360A/K361A mutant [2]; <5> wild-type carboxylase in bovine liver microsomes [17]) [2,8,17]
1.54 <5> (YVFLDHQDADANLILNRPKR, <5> R234A/H235A mutant, peptides comprising residue YVFLDHQDADANLILNRPKR concentration 0.16 μM [2]) [2]
1.6 <5> (FLEEL, <5> pH 7.4 [16]; <5> proFIX19 propeptide [8]; <5> R406A/H408A mutant [2]; <5> recombinant His6-carboxylase present in Sf9 cell microsomes [17]) [2,8,16,17]

1.78 <5> (YVFLDHQDADANLILNRPKR, <5> R406A/H408A mutant, peptides comprising residue YVFLDHQDADANLILNRPKR concentration 0.16 μM [2]) [2]
1.8 <5> (FLEEL, <5> proFIX 19-6BPA propeptide [8]) [8]
1.9 <5> (FLEEL, <5> proFIX19-16BPA propeptide [8]; <5> R513A/K515A mutant [2]) [2,8]
2 <5> (FLEEL, <5> proFIX19-13BPA propeptide [8]; <5> proFIX19-7BPA-propeptide [8]) [8]
2.01 <5> (YVFLDHQDADANLILNRPKR, <5> FLAG-vitamin K-dependent γ-glutamyl carboxylase, peptides comprising residue YVFLDHQDADANLILNRPKR concentration 0 μM [2]) [2]
2.03 <5> (YVFLDHQDADANLILNRPKR, <5> R234A/H235A mutant, peptides comprising residue YVFLDHQDADANLILNRPKR concentration 0 microM [2]) [2]
2.06 <5> (YVFLDHQDADANLILNRPKR, <5> R406A/H408A mutant, peptides comprising residue YVFLDHQDADANLILNRPKR concentration 0 μM [2]) [2]
6.49 <4> (FLEEL, <4> L394R, pH 7.4, 20°C [20]) [20]
9 <5> (FLEEL, <5> none propeptide [8]) [8]
14.8 <4> (FLEEL, <4> Y395A, pH 7.4, 20°C [20]) [20]
24.3 <4> (FLEEL, <4> W399A, pH 7.4, 20°C [20]) [20]
Additional information <5> (<5> K_m-values measured by hyperbolic weighted least-squares analysis [8]) [8]

K_i-Value (mM)

0.013 <4> (Boc-(2S,4S)-4-methylglutamic acid-Glu-Val, <4> wild type, pH 7.4, 20°C [20]) [20]
0.0174 <5> (proFIX19-16BPA propeptide, <5> competitive inhibition experiments using prom28 substrate [8]) [8]
1.4 <4> (Boc-(2S,4S)-4-methylglutamic acid-Glu-Val, <4> L394R, pH 7.4, 20°C [20]) [20]
2.1 <4> (Boc-(2S,4S)-4-methylglutamic acid-Glu-Val, <4> Y395A, pH 7.4, 20°C [20]) [20]
Additional information <4> (<4> K_i value for Boc-(2S,4S)-4-methylglutamic acid-Glu-Val is above 5 mM for W399A, pH 7.4, 20°C [20]) [20]

pH-Optimum

7.2-7.4 <3> (<3> assay at. The activity falls off sharply above pH 8 or below pH 7 [4]) [4]
7.5 <2> [3]
8.5 <2> (<2> assay at [3]) [3]

pH-Range

5.5-8.5 <2> [3]

4 Enzyme Structure

Molecular weight

33000 <9> (<9> cells transfected with the CAT-V5/His plasmid, Western Blot [13]) [13]
60000 <4> (<4> proteinase K digestion of the hGC-FLAG reveals a 60 kDa fragment, indicating the lumenal location of the FLAG tag and therefore the carboxyl-terminus of the carboxylase. In contrast, FLAG-hGC does not show a proteinase K-resistant fragment except for the residual undigested full-length carboxylase, which indicates the cytoplasmic location of the FLAG tag and therefore the amino-terminus of the carboxylase [12]) [12]
77000 <5> (<5> single major band on SDS gel electrophoresis. The eluted protein contains both stable vitamin K-dependent carboxylase and vitamin K epoxidase activity [1]) [1]
85700 <6> (<6> calculated from sequence [14]) [14]
87540 <4> (<4> calculated from sequence [27]) [27]
94000 <4,5> (<4,5> SDS-PAGE [8,18,25,27]; <5> SDS-PAGE and Western Blot, His6-carboxylase-Ac-FLEEL confirming affinity-purified carboxylase [17]) [8,17,18,25,27]
95000 <4> (<4> full-length carboxylase [12]) [12]
99000 <5> (<5> SDS-PAGE, Western Blot. CHO cells transfected with the cDNA for wild type FLAG-vitamin K-dependent γ-glutamyl carboxylase [2]) [2]
130000 <9> (<9> SDS-PAGE, Sf21 cells transfected with the carboxylase cDNA-containing plasmid, Western Blot [13]) [13]
Additional information <2> (<2> determination of disulfide bond formation in purified two-chain carboxylase and P80L and P378L two-chain carboxylases by SDS-PAGE and Western Blot analyses [9]) [9]

Subunits

? <4,5> (<4,5> x * 94000, SDS-PAGE [8,18,25,27]; <5> x * 99000, SDS-PAGE [2]) [2,8,18,25,27]
monomer <5> (<5> 1 * 77000, SDS-PAGE [1]) [1,17]
Additional information <2,5> (<5> binding site in the carboxyl half of the γ-glutamyl carboxylase. Carboxylase may be cleaved by trypsin into an amino-terminal 30 kDa and a carboxyl-terminal 60 kDa fragment joined by disulfide bond(s), and the propeptide binds to the 60 kDa fragment [18]; <2> disulfide bond between cysteines 99 and 450, five transmembrane domains [23]; <2> five transmembrane domains. Transmembrane domain interactions and residue proline 378 are essential for proper structure, especially disulfide bond formation [9]; <5> limited tryptic digestion of the carboxylase yields two disulfide-linked fragments with molecular masses of 30 and 60 kDa, corresponding to the amino and carboxy-terminal part of the γ-glutamyl carboxylase [15]) [9,15,18,23]

Posttranslational modification

glycoprotein <2> [9]
Additional information <4> (<4> enzyme catalyzes vitamin K-dependent posttranslational modification of glutamate to γ-carboxyl glutamate [12]) [12]

5 Isolation/Preparation/Mutation/Application

Source/tissue

CJ7 cell <1> (<1> γ-carboxylase gene targeting [11]) [11]
H4-II$^-$E-C_3 cell <6> (<6> rat hepatoma cell line [14]) [14]
HEK-293 cell <2,4> [23,27]
R1 cell <1> (<1> γ-carboxylase gene targeting [11]) [11]
S2 cell <7> [19]
blood plasma <1> (<1> coagulation assays [11]) [11]
bone <3> [4]
cartilage <3> [4]
embryo <6> (<6> vitamin K-dependent carboxylase mRNA expression in early rat embryonic development [14]) [14]
epithelial cell <2> [34]
fat <6> (<6> expression of rat vitamin K-dependent carboxylase in adult and embryonic tissues [14]) [14]
fibroblast <3> [4]
heart <6> (<6> expression of rat vitamin K-dependent carboxylase in adult and embryonic tissues [14]) [14]
kidney <3,6> (<6> adult Sprague-Dawley rat [14]) [4,14]
kidney cell line <3> [4]
liver <1,3,5,6> (<6> expression of rat vitamin K-dependent carboxylase in adult and embryonic tissues [14]; <1> preparation of solubilized γ-carboxylase [11]) [1,2,4,6,7,8,10,11,14,15,16,17,25,28]
lung <3,6> (<6> expression of rat vitamin K-dependent carboxylase in adult and embryonic tissues [14]) [4,14]
muscle <6> (<6> expression of rat vitamin K-dependent carboxylase in adult and embryonic tissues [14]) [14]
ovary <6> (<6> expression of rat vitamin K-dependent carboxylase in adult and embryonic tissues [14]) [14]
pancreas <3,6> (<6> expression of rat vitamin K-dependent carboxylase in adult and embryonic tissues [14]) [4,14]
placenta <3> [4]
renal tubule <2> [34]
spleen <3,6> (<6> expression of rat vitamin K-dependent carboxylase in adult and embryonic tissues [14]) [4,14]
stomach <6> (<6> expression of rat vitamin K-dependent carboxylase in adult and embryonic tissues [14]) [14]
tendon <3> [4]

testis <3,6> (<6> expression of rat vitamin K-dependent carboxylase in adult and embryonic tissues [14]) [4,14]
thymus <3> [4]
thyroid <3> [4]
uterus <3> [4]
Additional information <2> (<2> 6-year-old Mexican American male [33]) [33]

Localization

cytoplasm <2,4> (<4> human glutamyl carboxylase spans the membrane at least 5times, with its N-terminus in the cytoplasm and its C-terminus in the lumen of the endoplasmic reticulum [12]) [12,34]
endoplasmic reticulum <1,2,4,5,6> (<4> rough [20]; <1> transmembrane protein [11]; <2> potential impact of quality control components on carboxylation, which occurs in the endoplasmic reticulum during the secretion of vitamin K-dependent proteins [5]) [5,7,9,11,18,20,23]
endoplasmic reticulum membrane <4,5> (<4> amino-terminus of the γ-glutamyl carboxylase is on the cytoplasmic side of the endoplasmic reticulum, while the carboxylterminus is on the lumenal side [12]) [2,12]
membrane <4,5> (<5> integral membrane protein [18]; <4> 758 residue integral membrane protein [27]) [1,18,27]
microsome <2,3,4,5,6> (<5> from a dicoumarol-treated cow [28]; <4> microsomal carboxylase activity is compared from cells transfected with pCMV5 [27]) [1,2,4,6,8,9,10,16,17,25,27,28]
rough endoplasmic reticulum <3> [4]

Purification

<2> [9]
<2> (affinity chromatography) [3]
<3> (difficult, different methods shown) [4]
<4> [20]
<5> [8,16]
<5> (affinity chromatography) [1]
<5> (degree of purification is about 7000fold with reference to ammonium sulfate-fractionated microsomal protein from liver. Purification of carboxylase, solubilized microsomes: 281000 cpm/mg/h, flow-through of Affi-FIXQ/S: 200000 cpm/mg/h, bound to Affi-FIXQ/S: 140000000 cpm/mg/h, affinity-purified carboxylase: 1930000000 cpm/mg/h) [25]
<5> (inactivated His6-carboxylase-Ac-FLEEL purified under denaturing conditions by Ni-chelation chromatography followed by preparative polyacrylamide gel electrophoresis) [17]
<5> (partial purification of the enzyme by antibody affinity techniques. Purified 500fold by adsorption to an antiprothrombin column and elution with a dodeca peptide which competes with a prothrombin precursor enzyme recognition site. The purified enzyme is devoid of bound precursors, and has the same ratio of vitamin K epoxidase activity to carboxylase activity as the crude microsomal preparation) [28]
<6> [6]

Cloning

<2> [23]
<2> (expressed in Sf9 cells) [9]
<2> (mutational analysis is performed using an expression system lacking endogenous carboxylase. Construction of baculo viruses containing FLAG-tagged carboxylase mutants and expression in infected SF21 cells. Expresses the 758 amino acid human VKD carboxylase bearing a C-terminal extension of AAADYKDDDDK, where the last eight amino acids are the FLAG epitope) [3]
<4> (expressed in 293 cells) [12]
<4> (expression of the cloned cDNA results in an increase in carboxylase activity in microsomes of transfected cells compared to mock-transfected cells) [27]
<5> (His6-tagged bovine liver carboxylase (His6-carboxylase) is produced in insect cells using a baculovirus expression system) [8]
<5> (expressed in Chinese hamster ovary cells with an immunodetectable octapeptide inserted at the amino-terminal ends) [2]
<5> (expressed in baculovirus-infected insect cell. Produced His6-tagged carboxylase as a recombinant protein using a baculovirus expression system) [17]
<6> [7,14]
<9> (expression in COS cells or expressed in Sf21 insect cells) [13]

Engineering

E373L/Q374L <2> (<2> transmembrane domain residues in the C-terminal peptide to test for polar/charge residues [9]) [9]
E567A/K569A <5> (<5> CBX567/568 [2]) [2]
E612A/D614A <5> (<5> CBX612/614 [2]) [2]
G125L <2> (<2> two-chain carboxylase [9]) [9]
G128L <2> (<2> two-chain carboxylase [9]) [9]
G132L <2> (<2> two-chain carboxylase [9]) [9]
G363L/T367L <2> (<2> transmembrane domain residues in the C-terminal peptide to test for polar/charge residues [9]) [9]
H160A <2> (<2> His to Ala mutants all show full epoxidase activity [3]) [3]
H177A/H178A <5> (<5> CBX177/178 [2]) [2]
H287A <2> (<2> His to Ala mutants all show full epoxidase activity [3]) [3]
H381A <2> (<2> His to Ala mutants all show full epoxidase activity [3]) [3]
H404A <4> (<4> carboxylases W390A, S398A, and H404A have activities similar to that of wild type [20]) [20]
H678A/E679A/R680A <5> (<5> CBX678/679/680 [2]) [2]
K217A/K218A <5> (<5> inactive, CBX217/218 [2]) [2]
K218A <2> (<2> K218A activity is not detectable. The addition of exogenous amines restores K218A activity while having little effect on wild type carboxylase [3]) [3]
K346A/R347A <5> (<5> CBX346/347 [2]) [2]
K438A/D439A/H440A <5> (<5> CBX438/439/440 [2]) [2]
K622A/E623A/K624A <5> (<5> CBX622/623/624 [2]) [2]

L128R <2> (<2> warfarin resistent mutant [23]) [23]
L368/372P <2> (<2> mutation to disrupt the transmembrane helix [9]) [9]
L394R <4> (<4> natural mutant, certain individuals with combined deficiencies of vitamin K-dependent proteins have a mutation, L394R, in their γ-glutamyl carboxylase causing impaired glutamate binding [20]) [20]
P378L <2> (<2> significantly decreases the disulfide formation in carboxylase [9]) [9]
P80L <2> (<2> mutation of residue P80, which has activity similar to that of wild-type carboxylase, has a minor effect on disulfide formation [9]) [9]
R189A/K190A/R191A <5> (<5> CBX189/190/191 [2]) [2]
R234A/H235A <5> (<5> vitamin K epoxidase activities are reduced in parallel with the carboxylase activities. Showed defects in the propeptide binding site. Slightly faster mobility than wild-type FLAG-CBX. CBX234/235 [2]) [2]
R359A/H360A/K361A <5> (<5> vitamin K epoxidase activities are reduced in parallel with the carboxylase activities. Showed defects in the propeptide binding site. CBX359/360/361 [2]) [2]
R406A/H408A <5> (<5> vitamin K epoxidase activities are reduced in parallel with the carboxylase activities. Showed defects in the propeptide binding site. CBX406/408 [2]) [2]
R416A/D417A <5> (<5> CBX416/417 [2]) [2]
R513A/K515A <5> (<5> vitamin K epoxidase activities are reduced in parallel with the carboxylase activities. They show normal affinity for the propeptide, FLEEL, proPT28, and vitamin K hydroquinone but exhibited a low catalytic rate for carboxylation. CBX513/515 [2]) [2]
R58G <2> (<2> warfarin resistent mutant [23]) [23]
R661A/R662A <5> (<5> CBX622/623/624 [2]) [2]
R671A/R672A/R673A <5> (<5> CBX671/672/673 [2]) [2]
R687A/K688A <5> (<5> CBX687/688 [2]) [2]
S398A <4> (<4> carboxylases W390A, S398A, and H404A have activities similar to that of wild type [20]) [20]
V29L <2> (<2> warfarin resistent mutant [23]) [23]
V45A <2> (<2> warfarin resistent mutant [23]) [23]
W390A <4> (<4> carboxylases W390A, S398A, and H404A have activities similar to that of wild type [20]) [20]
W399A <4> (<4> lower activity than wild type [20]) [20]
Y395A <4> (<4> lower activity than wild type [20]) [20]
Additional information <1,2,4,5> (<4> 38-BamHI site introduces 2 amino acid residues (glycine and serine) between the hGC fragment and the Lep tag. A 10-amino acid peptide (MDYKDDDDKG), including the FLAG epitope, is introduced to the amino-terminus of the full length of hGC to make FLAG-hGC and a 8-amino acid peptide (DYKDDDDK) is attached to the carboxyl-terminus of the full length of hGC to make hGC-FLAG. The FLAG-tagged hGC cDNA is subcloned into the EcoRI (Escherichia coli RY13) site of the expression vector pCl-neo under control of the cytωlovirus (CMV) promoter [12]; <1> analysis of a Ggcx+/- intercross reveals a partial developmental block with only 50% of expected Ggcx-/- offspring surviving to term, with the latter animals dying uniformly at birth of massive intra-abdominal he-

morrhage. This phenotype closely resembles the partial midembryonic loss and postnatal hemorrhage previously reported for both prothrombin and factor V (F5)-deficient mice. Ggcx-/-, dying uniformly at birth of massive intra-abdominal hemorrhage. Heterozygous mice carrying a null mutation at the γ-carboxylase (Ggcx) gene exhibit normal development and survival with no evidence of hemorrhage and normal functional activity of the vitamin K-dependent clotting factors IX, X, and prothrombin [11]; <2> N-terminal carboxylase peptide (residues 1-345) and the C-terminal peptide (345-758) two-chain form (residues 1-345 and residues 346-758) of the vitamin K-dependent γ-glutamyl carboxylase expressed in Sf9 insect cells. The carboxylase and epoxidase activities similar to those of one-chain carboxylase. The two-chain carboxylase is joined by a disulfide bond [9]; <5> R234A/H235A mutant, R406A/H408A mutant, and R513A/K515A mutant are more susceptible to inhibition by vitamin KH_2 than wild type enzyme. R234A/H235A mutant and R406A/H408A mutant exhibit maximal activity at 111 mM vitamin KH_2 and R513A/K515A mutant at 56 mM vitamin KH_2 [2]; <4> six out of seven patients with Pseudoxanthoma Elasticum habor mutations in the GGCX gene (γ-glutamyl carboxylase) [21]; <4> Y395A propeptide affinity is similar to that of wild type, but those of L394R and W399A are 16-22fold less than that of wild type. Results of kinetic studies with a propeptide-containing substrate are consistent with results of propeptide binding and FLEEL kinetics. Although propeptide and vitamin K binding in some mutants are affected, our data provide compelling evidence that glutamate recognition is the primary function of the conserved region around Leu394 [20]) [2,9,11,12,20,21]

Application

medicine <2,4> (<4> six out of seven patients with Pseudoxanthoma Elasticum habor mutations in the GGCX gene (γ-glutamyl carboxylase) [21]; <2> warfarin therapy [23]; <2> multiplexed single nucleotide polymorphism panel (interrogation of the CYP2C9 *2, *3, VKORC1 (-1639G3A), and GGCX (1181T3G) alleles simultaneously) can be successfully used in genotyping of patient blood samples, whereby results can be combined with other clinical parameters in an algorithm for warfarin dosing [30]) [21,23,30]

6 Stability

Temperature stability

37 <3> (<3> enzyme is not very stable at 37°C and lower temperatures are more desirable. At temperatures below 20°C, extended linear rates of incorporation of $^{14}CO_2$ into exogenous peptide substrates can be observed [4]) [4]

General stability information

<5>, freeze-thawing, three times, stable [16]

Storage stability

<5>, -70°C, 6 months, stable [16]

References

[1] Hubbard, B.R.; Ulrich, M.M.W.; Jacobs, M.; Vermeer, C.; Walsh, C.; Furie, B.; Furie, B.C.: Vitamin K-dependent carboxylase: affinity purification from bovine liver by using a synthetic propeptide containing the γ-carboxylation recognition site. Proc. Natl. Acad. Sci. USA, **86**, 6893-6897 (1989)

[2] Sugiura, I.; Furie, B.; Walsh, C.T.; Furie, B.C.: Profactor IX propeptide and glutamate substrate binding sites on the vitamin K-dependent carboxylase identified by site-directed mutagenesis. J. Biol. Chem., **271**, 17837-17844 (1996)

[3] Rishavy, M.A.; Hallgren, K.W.; Yakubenko, A.V.; Shtofman, R.L.; Runge, K.W.; Berkner, K.L.: Bronsted analysis reveals Lys218 as the carboxylase active site base that deprotonates vitamin K hydroquinone to initiate vitamin K-dependent protein carboxylation. Biochemistry, **45**, 13239-13248 (2006)

[4] Suttie, J.W.: Vitamin K-dependent carboxylase. Annu. Rev. Biochem., **54**, 459-477 (1985)

[5] Berkner, K.L.: The vitamin K-dependent carboxylase. Annu. Rev. Nutr., **25**, 127-149 (2005)

[6] Canfield, L.M.: Vitamin K-dependent oxygenase/carboxylase; differential inactivation by sulfhydryl reagents. Biochem. Biophys. Res. Commun., **148**, 184-191 (1987)

[7] Romero, E.E.; Deo, R.; Velazquez-Estades, L.J.; Roth, D.A.: Cloning, structural organization, and transcriptional activity of the rat vitamin K-dependent γ-glutamyl carboxylase gene. Biochem. Biophys. Res. Commun., **248**, 783-788 (1998)

[8] Yamada, M.; Kuliopulos, A.; Nelson, N.P.; Roth, D.A.; Furie, B.; Furie, B.C.; Walsh, C.T.: Localization of the factor IX propeptide binding site on recombinant vitamin K dependent carboxylase using benzoylphenylalanine photoaffinity peptide inactivators: carboxylase using benzoylphenylalanine photoaffinity peptide inactivators. Biochemistry, **34**, 481-489 (1995)

[9] Tie, J.K.; Zheng, M.Y.; Hsiao, K.L.; Perera, L.; Stafford, D.W.; Straight, D.L.: Transmembrane domain interactions and residue proline 378 are essential for proper structure, especially disulfide bond formation, in the human vitamin K-dependent γ-glutamyl carboxylase. Biochemistry, **47**, 6301-6310 (2008)

[10] Helgeland, L.: The submicrosomal site for the conversion of prothrombin precursor to biologically active prothrombin in rat liver. Biochim. Biophys. Acta, **499**, 181-193 (1977)

[11] Zhu, A.; Sun, H.; Raymond, R.M. Jr.; Furie, B.C.; Furie, B.; Bronstein, M.; Kaufman, R.J.; Westrick, R.; Ginsburg, D.: Fatal hemorrhage in mice lacking (γ)-glutamyl carboxylase. Blood, **109**, 5270-5275 (2007)

[12] Tie, J.; Wu, S.; Jin, D.; Nicchitta, C.V.; Stafford, D.W.: A topological study of the human γ-glutamyl carboxylase. Blood, **96**, 973-978 (2000)

[13] Czerwiec, E.; Begley, G.S.; Bronstein, M.; Stenflo, J.; Taylor, K.; Furie, B.C.; Furie, B.: Expression and characterization of recombinant vitamin K-de-

pendent γ-glutamyl carboxylase from an invertebrate, Conus textile. Eur. J. Biochem., **269**, 6162-6172 (2002)
[14] Romero, E.E.; Velazquez-Estades, L.J.; Deo, R.; Schapiro, B.; Roth, D.A.: Cloning of rat vitamin K-dependent γ-glutamyl carboxylase and developmentally regulated gene expression in postimplantation embryos. Exp. Cell Res., **243**, 334-346 (1998)
[15] Maillet, M.; Morris, D.; Gaudry, M.; Marquet, A.: The active site region of the vitamin K-dependent carboxylase includes both the amino-terminal hydrophobic and carboxy-terminal hydrophilic domains of the protein. FEBS Lett., **413**, 1-6 (1997)
[16] Morris, D.P.; Soute, B.A.; Vermeer, C.; Stafford, D.W.: Characterization of the purified vitamin K-dependent γ-glutamyl carboxylase. J. Biol. Chem., **268**, 8735-8742 (1993)
[17] Kuliopulos, A.; Nelson, N.P.; Yamada, M.; Walsh, C.T.; Furie, B.; Furie, B.C.; Roth, D.A.: Localization of the affinity peptide-substrate inactivator site on recombinant vitamin K-dependent carboxylase. J. Biol. Chem., **269**, 21364-21370 (1994)
[18] Wu, S.M.; Mutucumarana. V.P.; Geromanos, S.; Stafford, D.W.: The propeptide binding site of the bovine γ-glutamyl carboxylase. J. Biol. Chem., **272**, 11718-11722 (1997)
[19] Walker, C.S.; Shetty, R.P.; Clark, K.; Kazuko, S.G.; Letsou, A.; Olivera, B.M.; Bandyopadhyay, P.K.: On a potential global role for vitamin K-dependent γ-carboxylation in animal systems. Evidence for a γ-glutamyl carboxylase in Drosophila. J. Biol. Chem., **276**, 7769-7774 (2001)
[20] Mutucumarana, V.P.; Acher, F.; Straight, D.L.; Jin, D.Y.; Stafford, D.W.: A conserved region of human vitamin K-dependent carboxylase between residues 393 and 404 is important for its interaction with the glutamate substrate. J. Biol. Chem., **278**, 46488-46493 (2003)
[21] Vanakker, O.M.; Martin, L.; Gheduzzi, D.; Leroy, B.P.; Loeys, B.L.; Guerci, V.I.; Matthys, D; Terry, S.F.; Coucke, P.J.; Pasquali-Ronchetti, I.; De Paepe, A.: Pseudoxanthoma elasticum-like phenotype with cutis laxa and multiple coagulation factor deficiency represents a separate genetic entity. J. Invest. Dermatol., **127**, 581-587 (2007)
[22] Crosier, M.D.; Peter, I.; Booth, S.L.; Bennett, G.; Dawson-Hughes, B.; Ordovas, J.M.: Association of sequence variations in vitamin K epoxide reductase and γ-glutamyl carboxylase genes with biochemical measures of vitamin K status. J. Nutr. Sci. Vitaminol., **55**, 112-119 (2009)
[23] Stafford, D.W.: The vitamin K cycle. J. Thromb. Haemost., **3**, 1873-1878 (2005)
[24] Kulman, J.D.; Harris, J.E.; Nakazawa, N.; Ogasawara, M.; Satake, M.; Davie, E.W.: Vitamin K-dependent proteins in Ciona intestinalis, a basal chordate lacking a blood coagulation cascade. Proc. Natl. Acad. Sci. USA, **103**, 15794-15799 (2006)
[25] Wu, S.M.; Morris, D.P.; Stafford, D.W.: Identification and purification to near homogeneity of the vitamin K-dependent carboxylase. Proc. Natl. Acad. Sci. USA, **88**, 2236-2240 (1991)

[26] Price, P.A.; Williamson, M.K.: Substrate recognition by the vitamin K-dependent γ-glutamyl carboxylase: Identification of a sequence homology between the carboxylase and the carboxylase recognition site in the substrate. Protein Sci., **2**, 1987-1988 (1993)
[27] Wu, S.M.; Cheung, W.F.; Frazier, D.; Stafford, D.W.: Cloning and expression of the cDNA for human γ-glutamyl carboxylase. Science, **13**, 1634-1636 (1991)
[28] Harbeck, M.C.; Cheung, A.Y.; Suttie, J.W.: Vitamin K-dependent carboxylase: partial purification of the enzyme by antibody affinity techniques. Thromb. Res., **56**, 317-323 (1989)
[29] Li, Q.; Schurgers, L.J.; Smith, A.C.; Tsokos, M.; Uitto, J.; Cowen, E.W.: Coexistent pseudoxanthoma elasticum and vitamin K-dependent coagulation factor deficiency: compound heterozygosity for mutations in the GGCX gene. Am. J. Pathol., **174**, 534-540 (2009)
[30] Rai, A.J.; Udar, N.; Saad, R.; Fleisher, M.: A multiplex assay for detecting genetic variations in CYP2C9, VKORC1, and GGCX involved in warfarin metabolism. Clin. Chem., **55**, 823-826 (2009)
[31] Qiao, J.; Wang, T.; Yang, J.; Liu, J.; Gong, X.; Guo, X.; Wang, S.; Ye, Z.: Genetic mutation of vitamin K-dependent γ-glutamyl carboxylase domain in patients with calcium oxalate urolithiasis. J. Huazhong Univ. Sci. Technol. Med. Sci., **29**, 604-608 (2009)
[32] Li, Q.; Uitto, J.: The mineralization phenotype in Abcc6 (-/-) mice is affected by Ggcx gene deficiency and genetic background–a model for pseudoxanthoma elasticum. J. Mol. Med., **88**, 173-181 (2010)
[33] Titapiwatanakun, R.; Rodriguez, V.; Middha, S.; Dukek, B.A.; Pruthi, R.K.: Novel splice site mutations in the γ glutamyl carboxylase gene in a child with congenital combined deficiency of the vitamin K-dependent coagulation factors (VKCFD). Pediatr. Blood Cancer, **53**, 92-95 (2009)
[34] Wang, T.; Yang, J.; Qiao, J.; Liu, J.; Guo, X.; Ye, Z.: Activity and expression of vitamin K-dependent γ-glutamyl carboxylase in patients with calcium oxalate urolithiasis. Urol. Int., **85**, 94-99 (2010)

3-hexulose-6-phosphate synthase 4.1.2.43

1 Nomenclature

EC number
4.1.2.43

Systematic name
D-arabino-hex-3-ulose-6-phosphate formaldehyde-lyase (D-ribulose-5-phosphate-forming)

Recommended name
3-hexulose-6-phosphate synthase

Synonyms
3-hexulose phosphate synthase <8,15,23> [2,7,9]
3-hexulose-6-phosphate formaldehyde lyase <24> [8]
3-hexulose-6-phosphate synthase <1,2,3,5,7,8,10,11,12,14,15,17,19,20,21,22,23,24,25,26,27,28> (<12> 3-hexulose-6-phosphate synthase and 6-phospho-3-hexuloisomerase activities are expressed constitutively in archea [13]) [1,3,4,8,13,14,22]
3-hexulose-phosphate synthase <15> [18]
3-hexulosephosphate synthase <4,6,8,9,13,15,16,22> [5,6,12,20,21]
D-arabino-3-hexulose 6-phosphate formaldehyde lyase <8,22> [2,12]
D-arabino-3-hexulose 6-phosphate formaldehyde-lyase
Fae-Hps <1> (<1> protein with hexulose-6-phosphate synthase and formaldehyde activating enzyme activities [10]) [10]
HPS <1,2,3,4,5,6,7,8,9,10,11,12,13,14,15,16,17,18,19,20,21,22,23,24,25,26,27,28> (<1,5,7,8,15,19,22,23> 3-hexulose-6-phosphate synthase and 6-phospho-3-hexuloisomerase activities are expressed constitutively in archea [13]) [1,2,3,5,6,7,8,13,16,17,18,19,20,21,22]
HPS-PHI <12> (<12> bifunctional enzyme with 3-hexulose-6-phosphate synthase and 6-phospho-3-hexuloisomerase activities [3]) [3]
HPS-aldolase <15> [9]
HPS/PHI <17> (<17> bifunctional fusion enzyme [4]) [4]
hexose phosphate synthase <8> [11]
hexulose-6-phosphate synthase <1> [10]

CAS registry number
55576-36-8

D. Schomburg and I. Schomburg (eds.), *Class 3.4–6 Hydrolases, Lyases, Isomerases, Ligases: EC 3.4–6*, Springer Handbook of Enzymes S10, DOI 10.1007/978-3-642-36260-6_33,

2 Source Organism

<1> *Methanosarcina barkeri* [10,13]
<2> *Brevibacillus brevis* (ARA2 [22]) [22]
<3> *Bacillus subtilis* [19,22]
<4> *Pseudomonas sp.* [21]
<5> *Bacillus sp.* [13,14,22]
<6> *Arthrobacter globiformis* [21]
<7> *Methylophilus methylotrophus* [13]
<8> *Methylococcus capsulatus* [2,11,13,17,21,22]
<9> *Acetobacter sp.* [5,6]
<10> *Bacillus methanolicus* [22]
<11> *Methanocaldococcus jannaschii* [22]
<12> *Pyrococcus horikoshii* [3,13,22]
<13> *Pseudomonas oleovorans* [20,21]
<14> *Methylobacillus flagellatus* [22]
<15> *Methylomonas sp.* [9,13,18,21]
<16> *Methylomonas methylovora* [21]
<17> *Thermococcus kodakarensis* [4,22]
<18> *Acidomonas methanolica* [16]
<19> *Methanosarcina mazei* [13]
<20> *Pyrococcus sp.* [22]
<21> *Methanosarcina sp.* [22]
<22> *Methylomonas aminofaciens* [12,13,21,22]
<23> *Mycobacterium gastri* [1,7,13,15,22]
<24> *Aminomonas aminovorus* (UNIPROT accession number: Q9F6B7) [8]
<25> *Salmonella sp.* [22]
<26> *Thermococcus sp.* [22]
<27> *Methanococcus sp.* [22]
<28> *Staphylococcus sp.* [22]

3 Reaction and Specificity

Catalyzed reaction

D-arabino-hex-3-ulose 6-phosphate = D-ribulose 5-phosphate + formaldehyde

Natural substrates and products

S D-ribulose 5-phosphate + formaldehyde <15> (Reversibility: ?) [9]
P D-arabino-hex-3-ulose 6-phosphate
S D-ribulose 5-phosphate + formaldehyde <2,3,5,8,10,11,12,14,17,20,21,22, 23,25,26,27,28> (<12> the apparent specific activity of the reverse reaction is approximately one-seventh of that of the forward reaction [22]) (Reversibility: r) [22]
P D-arabino-3-hexulose 6-phosphate

S Additional information <12> (<12> key enzyme of the ribulose monophosphate pathway [3]) (Reversibility: ?) [3]
P ?

Substrates and products

S D-ribulose 5-phosphate + DL-glyceraldehyde <15> (Reversibility: ?) [9]
P ?
S D-ribulose 5-phosphate + acetaldehyde <15> (Reversibility: ?) [9]
P ?
S D-ribulose 5-phosphate + benzaldehyde <15> (Reversibility: ?) [9]
P ?
S D-ribulose 5-phosphate + bromoacetaldehyde <15> (Reversibility: ?) [9]
P ?
S D-ribulose 5-phosphate + butyraldehyde <15> (Reversibility: ?) [9]
P ?
S D-ribulose 5-phosphate + chloral <15> (Reversibility: ?) [9]
P ?
S D-ribulose 5-phosphate + chloroacetaldehyde <15> (Reversibility: ?) [9]
P ?
S D-ribulose 5-phosphate + chloropropionaldehyde <15> (Reversibility: ?) [9]
P ?
S D-ribulose 5-phosphate + dichloroacetaldehyde <15> (Reversibility: ?) [9]
P ?
S D-ribulose 5-phosphate + formaldehyde <2,3,5,8,10,11,12,14,17,20,21,22,23,25,26,27,28> (<12> the apparent specific activity of the reverse reaction is approximately one-seventh of that of the forward reaction [22]) (Reversibility: r) [22]
P D-arabino-3-hexulose 6-phosphate
S D-ribulose 5-phosphate + formaldehyde <1,3,4,5,6,7,8,12,13,15,16,17,18,19,22,23,24> (<23> the enzyme is highly specific for D-ribulose 5-phosphate as an acceptor of aldehydes [15]; <22> the enzyme is specific for formaldehyde and D-ribulose 5-phosphate [12]) (Reversibility: ?) [1,2,3,4,7,8,9,10,11,12,13,14,15,16,17,18,19,20,21]
P D-arabino-hex-3-ulose 6-phosphate
S D-ribulose 5-phosphate + glutaraldehyde <15> (Reversibility: ?) [9]
P ?
S D-ribulose 5-phosphate + glycolaldehyde <23> (Reversibility: ?) [7]
P 4-heptulose 7-phosphate
S D-ribulose 5-phosphate + glycolaldehyde <15,23> (Reversibility: ?) [9,15]
P ?
S D-ribulose 5-phosphate + glyoxal <15> (Reversibility: ?) [9]
P ?
S D-ribulose 5-phosphate + isobutyraldehyde <15> (Reversibility: ?) [9]
P ?
S D-ribulose 5-phosphate + isovaleraldehyde <15> (Reversibility: ?) [9]
P ?

S D-ribulose 5-phosphate + methylglyoxal <15,23> (Reversibility: ?) [7,9,15]
P ?
S D-ribulose 5-phosphate + methylmercaptopropionaldehyde <15> (Reversibility: ?) [9]
P ?
S D-ribulose 5-phosphate + propionaldehyde <15> (Reversibility: ?) [9]
P ?
S D-ribulose 5-phosphate + pyridine-2-carboxaldehyde <15> (Reversibility: ?) [9]
P ?
S D-ribulose 5-phosphate + pyridine-3-carboxaldehyde <15> (Reversibility: ?) [9]
P ?
S D-ribulose 5-phosphate + pyridine-4-carboxaldehyde <15> (Reversibility: ?) [9]
P ?
S D-ribulose 5-phosphate + valeraldehyde <15> (Reversibility: ?) [9]
P ?
S Additional information <12,15,23> (<12> key enzyme of the ribulose monophosphate pathway [3]; <15> does not accept D-ribose 5-phosphate, D-ribulose, D-xylose, D-xylulose 5-phosphate, D-fructose 6-phosphate, D-fructose 1-phosphate, D-fructose 1,6-bisphosphate, D-glucose 6-phosphate, D-glucose 1-phosphate, D-fructose, D-glucose, DL-glyceraldehyde 3-phosphate, dihydroxyacetone phosphate, hydroxypyruvate, dihydroxyacetone, D-erythrose 4-phospate, pivalaldehyde, acrolein, crotonaldehyde, glyoxalic acid, malonaldehyde, furfural as substrates [9]; <15> no detectable activity with D-fructose 6-phosphate, D-fructose 1,6-bisphosphate, D-glucose 1-phosphate, D-glucose 6-phosphate, lithium hydroxypyruvate, glyceraldehyde 3-phosphate, dihydroxyacetone phosphate, D-ribose 5-phosphate, and D-xylose 5-phosphate [18]; <23> no detectable activity with D-ribulose 1,5-bisphosphate, D-ribose 5-phosphate, D-erythrose 4-phosphate, D-fructose 6-phosphate, D-fructose 1,6-bisphosphate, D-glucose 6-phosphate, D-glucose 1-phosphate, and D-xyluloSe 5-phosphate [15]) (Reversibility: ?) [3,9,15,18]
P ?

Inhibitors

Ca^{2+} <8> (<8> 49% inhibition at 1 mM [2]) [2]
Cu^{2+} <8,18,22> (<8> 24% inhibition at 1 mM [2]; <18> 1 mM Cu^{2+} is inhibitory, and the effect is partly abolished by Mg^{2+} [16]; <22> 45% inhibition with 1 mM Cu^{2+} [12]) [2,12,16]
D-ribulose 5-phosphate <5> (<5> commercial D-ribulose 5-phosphate inhibits the enzyme [14]) [14]
EDTA <5,15,22,23> (<15> complete inhibition at 10 mM [9]; <23> the enzyme is completely inhibited by the presence of 2 mM EDTA [15]; <22> the enzyme is completely inhibited in the presence of EDTA, but the activity is restored depending on the amount of $MgCl_2$ supplemented [12]) [9,12,14,15]

Hg^{2+} <22> (<22> 81% inhibition with 1 mM Hg^{2+} [12]) [12]
Methylglyoxal <22> (<22> 26% inhibition at 4 mM [12]) [12]
Ni^{2+} <8> (<8> 64% inhibition at 1 mM [2]) [2]
Pb^{2+} <22> (<22> 48% inhibition with 1 mM Pb^{2+} [12]) [12]
Tiron <23> (<23> the enzyme is completely inhibited by the presence of 2 mM tiron [15]) [15]
glutaraldehyde <22> (<22> 22% inhibition at 4 mM [12]) [12]
glyceraldehyde <22> (<22> 13% inhibition at 4 mM [12]) [12]
glycolaldehyde <22> (<22> 49% inhibition at 4 mM [12]) [12]
glycolic acid <23> (<23> glycolic acid inhibits the enzyme competitively with respect to formaldehyde [7]) [7]
glyoxylate <22> (<22> 12% inhibition at 4 mM [12]) [12]
o-phenanthroline <23> (<23> the enzyme is completely inhibited by the presence of 2 mM *o*-phenanthroline [15]) [15]
Additional information <8,15,23> (<15> not influenced by $NaBH_4$ [9]; <8> not inhibited by ATP, ADP, AMP, NADH, D-fructose 6-phosphate, and phosphoenolpyruvate [2]; <23> the enzyme is inactivated irreversibly on dialysis against buffer without Mg^{2+} [15]) [2,9,15]

Activating compounds

HxlR <3> (<3> necessary for formaldehyde-induced expression of the HPS coding hxlAB operon [19]) [19]
formaldehyde <3> (<3> expression of the HPS coding hxlAB operon is induced by the presence of formaldehyde [19]) [19]

Metals, ions

Ca^{2+} <5,18> (<18> 1 mM Ca^{2+} is less than 50% less effective in activity stimulation than 1 mM Mg^{2+} [16]; <5> 28% stimulation of activity at 1 mM [14]) [14,16]
Cd^{2+} <22> (<22> the enzyme activity is also promoted with 1 mM Cd^{2+} [12]) [12]
Co^{2+} <5,8,18,22> (<18> 1 mM Co^{2+} is less than 50% less effective in activity stimulation than 1 mM Mg^{2+} [16]; <5> 100% stimulation of activity at 1 mM [14]; <8> 17% as effective as Mg^{2+} or Mn^{2+} in promoting synthase activity [2]; <22> the enzyme activity is also promoted with 5 mM Co^{2+} [12]) [2,12,14,16]
Cu^{2+} <5> (<5> 33% stimulation of activity at 1 mM [14]) [14]
Fe^{2+} <18,22> (<18> 1 mM Fe^{2+} is less than 50% less effective in activity stimulation than 1 mM Mg^{2+} [16]; <22> the enzyme activity is also promoted with 1 mM Fe^{2+} [12]) [12,16]
Mg^{2+} <1,2,3,5,7,8,10,11,12,14,15,17,18,19,20,21,22,23,25,26,27,28> (<1,5,7,8,12,15,19,22,23> dependent on [13]; <15> required for activity [9]; <23> 1 mM Mg^{2+} is absolutely required for the enzyme activity and stability [7]; <8> 5 mM, essential for activity and stability, 3-hexulose phosphate synthase is rapidly and apparently irreversibly denatured by storage in the absence of one of Mg^{2+} [2]; <5> 98% stimulation of activity at 1 mM [14]; <18> bivalent cations are essential for activity, most effective is Mg^{2+} [16]; <23> essential

requirement for Mg^{2+} [15]; <22> essential requirement for Mg^{2+} (5 mM) [12]) [2,7,9,12,13,14,15,16,22]
Mn^{2+} <1,2,3,5,7,8,10,11,12,14,15,17,18,19,20,21,22,23,25,26,27,28> (<1,5,7,8,12,15,19,22,23> dependent on [13]; <15> required for activity [9]; <18> 1 mM Mn^{2+} is 20% less effective in activity stimulation than 1 mM Mg^{2+} [16]; <5> 100% stimulation of activity at 1 mM [14]; <8> essential for activity and stability [2]; <23> essential requirement for Mn^{2+} [15]; <22> essential requirement for Mn^{2+} (5 mM) [12]; <23> Mg^{2+} can be replaced by Mn^{2+} (1 mM) [7]) [2,7,9,12,13,14,15,16,22]
Ni^{2+} <5> (<5> 97% stimulation of activity at 1 mM [14]) [14]
Zn^{2+} <5,8,22> (<8> 10% as effective as Mg^{2+} or Mn^{2+} in promoting synthase activity [2]; <5> 39% stimulation of activity at 1 mM [14]; <22> the enzyme activity is also promoted with 5 mM Zn^{2+} [12]) [2,12,14]

Turnover number (s^{-1})

62.2 <12> (formaldehyde, <12> recombinant HPS, at 80°C [3]) [3]
159 <12> (formaldehyde, <12> recombinant HPS, at 60°C [3]) [3]

Specific activity (U/mg)

1.4 <18> (<18> cell free extract, at 30°C [16]) [16]
1.71 <8> (<8> cell free extract, at 30°C [2]) [2]
3.2 <23> (<23> cell free extract, at 30°C [7,15]) [7,15]
3.3 <22> (<22> cell free extract [12]) [12]
3.5 <5> (<5> cell free extract, at 50°C [14]) [14]
4.4 <1> (<1> hexulose-6-phosphate synthase activity of the gene product Fae-Hps, at 30°C, pH 7.0 [10]) [10]
4.5 <15> (<15> crude extract, at 30°C [18]) [18]
9.8 <17> (<17> cell free extract [4]) [4]
20 <24> (<24> purified enzyme [8]) [8]
26 <15> (<15> crude extract [9]) [9]
41.1 <23> (<23> cell free extract, recombinant HPS [1]) [1]
52 <22> (<22> after 16fold purification [12]) [12]
56.7 <12> (<12> crude cell extract [3]) [3]
64 <5,18> (<5> after 18fold purification, at 50°C [14]; <18> after 46fold purification, at 30°C [16]) [14,16]
66.5 <15> (<15> after 14.8fold purification, at 30°C [18]) [18]
69 <8> (<8> after 41fold purification, at 30°C [2]) [2]
70.9 <23> (<23> after 1.73fold purification, recombinant HPS [1]) [1]
74.2 <23> (<23> after 23fold purification, at 30°C [7,15]) [7,15]
148 <17> (<17> after 15.1fold purification [4]) [4]
235 <12> (<12> after 4.14fold purification [3]) [3]
4100 <15> (<15> after 161fold purification [9]) [9]

K_m-Value (mM)

0.00147 <5> (formaldehyde, <5> at 50°C [14]) [14]
0.0045 <5> (D-ribulose 5-phosphate, <5> D-ribulose 5-phosphate generated from ribose 5-phosphate, at 50°C [14]) [14]

0.007 <5> (D-ribulose 5-phosphate, <5> commercial D-ribulose 5-phosphate, at 50°C [14]) [14]
0.059 <22> (D-ribulose 5-phosphate, <22> in 50 mM potassium phosphate buffer (pH 7.4), 5 mM $MgCl_2$ [12]) [12,13,21]
0.075 <8> (D-arabino-hex-3-ulose 6-phosphate, <8> in 50 mM sodium potassium phosphate buffer, 5 mM $MgCl_2$, at pH 7.0, at 30°C [2]) [2]
0.081 <22> (D-ribulose 5-phosphate) [21]
0.083 <8> (D-ribulose 5-phosphate, <8> in 50 mM sodium potassium phosphate buffer, 5 mM $MgCl_2$, at pH 7.0, at 37°C [2]) [2,13,21]
0.11 <4> (D-ribulose 5-phosphate, <4> crude extract [21]) [21]
0.136 <7> (D-ribulose 5-phosphate) [13]
0.15 <5> (formaldehyde) [13]
0.29 <22> (formaldehyde, <22> in 50 mM potassium phosphate buffer (pH 7.4), 5 mM $MgCl_2$ [12]) [12,13,21]
0.45 <5> (D-ribulose 5-phosphate) [13]
0.49 <8> (formaldehyde, <8> in 50 mM sodium potassium phosphate buffer, 5 mM $MgCl_2$, at pH 7.0, at 37°C [2]) [2,13,21]
0.53 <7> (formaldehyde) [13]
0.74 <22> (formaldehyde) [21]
1.1 <15> (formaldehyde, <15> in 300 mM Tris-HCI buffer (pH 7.5), at 30°C [18]) [13,18,21]
1.14 <4> (formaldehyde, <4> crude extract [21]) [21]
1.4 <23> (formaldehyde, <23> apparent value, in 50 mM potassium phosphate, pH 7.5, with 5 mM $MgCl_2$, at 30°C [7]; <23> in 500 mM potassium phosphate buffer, at pH 7.5, at 30°C [15]) [7,15]
1.5 <23> (formaldehyde) [13]
1.6 <15> (D-ribulose 5-phosphate, <15> in 300 mM Tris-HCI buffer (pH 7.5), at 30°C [18]) [13,18,21]
1.95 <12> (formaldehyde, <12> recombinant HPS, at 80°C [3]) [3]
2.31 <12> (formaldehyde, <12> recombinant HPS, at 60°C [3]) [3]
2.96 <23> (formaldehyde, <23> purified recombinant enzyme, at 30°C [1]) [1]
4.3 <23> (glycolaldehyde, <23> apparent value, in 50 mM potassium phosphate, pH 7.5, with 5 mM $MgCl_2$, at 30°C [7]; <23> in 500 mM potassium phosphate buffer, at pH 7.5, at 30°C [15]) [7,15]
5.7 <23> (methylglyoxal, <23> apparent value, in 50 mM potassium phosphate, pH 7.5, with 5 mM $MgCl_2$, at 30°C [7]; <23> in 500 mM potassium phosphate buffer, at pH 7.5, at 30°C [15]) [7,15]

pH-Optimum

7 <5,8> [2,14]
7-8 <18> [16]
7.5-8 <15,23> (<23> in potassium phosphate buffer [15]) [7,15,18]
8 <22> [12]

pi-Value

5.1 <22> (<22> isoelectric focusing [12]) [12]

Temperature optimum (°C)
30 <23> [7]
40 <23> (<23> purified recombinant enzyme [1]) [1]
45 <22> [12]
60 <18> [16]

4 Enzyme Structure

Molecular weight
22000 <15> (<15> SDS-PAGE [9]) [9]
24000 <23> (<23> SDS-PAGE [7]) [7]
25000 <12> (<12> recombinant HPS, gel filtration [3]) [3]
27000 <5,12> (<5> SDS-PAGE [14]; <12> recombinant HPS, SDS-PAGE [3]) [3,14]
32000 <5> (<5> gel filtration [14]; <5> holenzyme [13]) [13,14]
40000 <7,15> (<15> gel filtration [18]; <7> holenzyme [13]) [13,18]
42000 <1> (<1> SDS-PAGE [10]) [10]
43000 <15,23> (<15> sedimentation equilibrium method [18]; <23> native enzyme, gel filtration [7]; <23> holenzyme [13]; <23> TSK gel G-3000SW chromatography [15]) [7,13,15,18]
44000 <15,17> (<15> holenzyme [13]; <17> recombinant fusion enzyme HPS-PHI, SDS-PAGE [4]) [4,13]
45000 <22,23> (<23> gel filtration [1]; <22> native enzyme, gel filtration [12]) [1,12]
46000 <22> (<22> holoenzyme [13]) [13]
47000 <22> (<22> sedimentation velocity [12]) [12]
80000 <18> (<18> gel filtration [16]) [16]
162000 <12> (<12> EDTA-solubilized HPS-PHI fusion enzyme, gel filtration [3]) [3]
310000 <8> (<8> gel filtration, under conditions of low pH or low ionic strength [2]; <8> holoenzyme [13]) [2,13]

Subunits
homodimer <1,5,7,12,15,19,22,23> (<23> 2 * 48000, SDS-PAGE [15]; <22> 2 * 23000, SDS-PAGE [12]; <15,23> 2 * 22000, SDS-PAGE [1,18]; <15> 2 * 22000 [13]; <5> 2 * 27000 [13]; <22> 2 * 23000 [13]; <7> 2 * 22500 [13]; <23> 2 * 24000 [13]) [1,12,13,15,18]
homohexamer <8> (<8> 6 * 49000 [13]; <8> 6 * 49000, gel filtration, at pH 4.6 [2]) [2,13]
homotetramer <12,18> (<18> 4 * 20400, SDS-PAGE [16]; <12> 4 * 47000, HPS-PHI fusion enzyme, SDS-PAGE [3]) [3,16]
monomer <5,12> (<5> 1 * 27000, SDS-PAGE [14]; <12> 1 * 27000, recombinant HPS, SDS-PAGE [3]) [3,14]
Additional information <13> (<13> multiple forms of the enzyme may be responsible for the generation of the complex shape, and thus, the kinetic characteristic should he the sum of differing characteristics [20]) [20]

5 Isolation/Preparation/Mutation/Application

Purification

<1> (DEAE-Sephacel column chromatography, Q-Sepharose column chromatography, and hydroxyapatite column chromatography) [10]
<5> (Q-Sepharose column chromatography, phenyl-Superose column chromatography, Superose 12 chromatography, and Sephadex G-25 gel filtration) [14]
<8> (ammonium sulfate precipitation, DEAE-cellulose column chromatography) [2]
<9> [6]
<12> (DEAE-Toyopearl column chromatography, butyl-Toyopearl column chromatography, and ammonium sulfate precipitation) [3]
<13> [20]
<15> (DEAE-cellulose column chromatography, DEAE-Sephadex A-50 gel filtration, and Sephadex G-75 gel filtration) [18]
<15> (polyethylene imine precipitation, S-Sepharose column chromatography, Q-Sepharose column chromatography, and Sephadex G-75 gel filtration) [9]
<17> (ultracentrifugation) [4]
<18> (ammonium sulfate fractionation, DEAE-cellulose column chromatography, and Sephadex G-100 gel filtration) [16]
<22> (DEAE-cellulose column chromatography, hydroxylapatite column chromatography, Sephadex G-150 gel filtration, Sephadex G-100 gel filtration, and DEAE-Sephadex A-50 gel filtration) [12]
<23> (DEAE-Toyopearl column chromatography butyl-Toyopearl column chromatography) [1]
<23> (phenyl-Sepharose column chromatography and DEAE-Sephacel column chromatography) [7]
<23> (phenyl-Sepharose column chromatography, and DEAE-Sephacel column chromatography) [15]
<24> (Ni-chelating Sepharose column chromatography) [8]

Cloning

<1> (expressed in Escherichia coli BL21 (DE3) pLysS cells) [10]
<12> (expressed in Escherichia coli) [13]
<12> (expressed in Escherichia coli Rosetta(DE3) cells) [3]
<17> (expressed in Escherichia coli Rosetta(DE3) cells) [4]
<20> (expression in Escherichia coli) [22]
<21> (expression in Escherichia coli) [22]
<23> (expressed in Escherichia coli Rosetta (DE3) cells, HPS only, or as fusion enzyme with 6-phospho-3-hexuloisomerase) [1]
<24> (expressed in Escherichia coli BL21 (DE3) cells) [8]
<26> (expression in Escherichia coli) [22]

Engineering

Additional information <2,22,23> (<22> in order to improve the rate of vanillin degradation by Burkholderia cepacia TM1, the hps and φ genes from Methylomonas aminofaciens 77a are heterologously expressed in strain TM1, the transformant strain constitutively produces active 3-hexulose-6-phosphate synthase and 6-phospho-3-hexuloisomerase enzymes and the degradation of vanillic acid and the growth yield are significantly improved [22]; <23> the hps and phi genes from the methylotrophic bacterium Mycobacterium gastri MB19 are introduced into tobacco. Both genes are expressed under the control of the tomato rbcS-3C promoter, and the gene products are targeted to the chloroplasts by artificially added transit peptide sequence, the expression of both genes in plants enhances the tolerance of the transgenic plant to formaldehyde and capability of eliminating environmental formaldehyde [22]; <2> the solvent-tolerant bacterium, Pseudomonas putida S12, is engineered to efficiently utilize methanol and formaldehyde as auxiliary substrates by introducing the hps and φ genes from the thermotolerant methylotrophic bacterium Bacillus brevis, by chemostat culture experiments using glucose and formaldehyde, the hps and φ-expressing strain shows both significantly improved cell mass and growth at higher formaldehyde concentrations than the control strain [22]) [22]

Application

environmental protection <23> (<23> formaldehyde is thought to be the cause of sick house syndrome, transgenic plants harboring the ribulose monophosphate pathway could be useful to improve air pollution in the indoor environment [22]) [22]

synthesis <22> (<22> enzymatic preparation is suitable for the synthesis of sugars labeled with 13C at specific positions, enzymatic preparation of [1-^{13}C]D-fructose-6-phosphate by using D-ribose-5 phosphate and [1-^{13}C]-formaldehyde as substrates [22]) [22]

6 Stability

pH-Stability

6-8 <15> (<15> remains stable at pH 6.0-8.0 at 30°C for 1 h, enzyme stability decreases at pH values below 6.0 [18]) [18]

7-8 <22> (<22> stable in neutral to slightly alkaline solutions [12]) [12]

Temperature stability

6.5-7.5 <23> (<23> remains stable in the pH range of 6.5-7.5 at 30°C for 6 h [15]) [15]

40-60 <18> (<18> no decrease in activity is observed within 6 h at 40°C in the presence of 5 mM $MgCl_2$, at 50°C and 60°C the enzyme is stable for 2.5 and 0.5 h, respectively, one-half the initial activities are found after 6 and 1.5 h respectively [16]) [16]

40-80 <22> (<22> almost full activity is retained after incubation at 40°C for 30 min, whereas at 80°C for 10 min the enzyme is completely inactivated [12]) [12]
55-65 <5> (<5> the enzyme retains more than 50% of its activity at 55°C after 1 h, the enzyme retains more than 50% of its activity at 65°C after 30 min [14]) [14]
60 <8> (<8> 3-hexulose phosphate synthase is rapidly inactivated at elevated temperatures, activity is totally lost within 5 min at 60°C [2]) [2]
90 <1,5,7,8,12,15,19,22,23> (<1,5,7,8,12,15,19,22,23> the recombinant enzyme is stable at 90°C [13]) [13]

Storage stability

<5>, -80°C, purified enzyme, in the presence of 5 mM $MgSO_4$, 5 mM D-ribose 5-phosphate, and 1.75 units/ml phosphoriboisomerase, at least 5 months, no loss of activity [14]
<8>, -15°C, in the presence of 2.5 mM $MgCl_2$, 6 months, remains stable unless repeatedly frozen and thawed [2]
<18>, -20°C, purified enzyme, at least 1 year, no loss of activity [16]
<18>, 0°C to -4°C, purified enzyme in the presence of 3.2 M ammonium sulfate, at least 1 year, no loss of activity [16]

References

[1] Orita, I.; Sakamoto, N.; Kato, N.; Yurimoto, H.; Sakai, Y.: Bifunctional enzyme fusion of 3-hexulose-6-phosphate synthase and 6-phospho-3-hexuloisomerase. Appl. Microbiol. Biotechnol., **76**, 439-445 (2007)
[2] Ferenci, T.; Stroem, T.; Quayle, J.R.: Purification and properties of 3-hexulose phosphate synthase and phospho-3-hexuloisomerase from Methylococcus capsulatus. Biochem. J., **144**, 477-486 (1974)
[3] Orita, I.; Yurimoto, H.; Hirai, R.; Kawarabayasi, Y.; Sakai, Y.; Kato, N.: The archaeon Pyrococcus horikoshii possesses a bifunctional enzyme for formaldehyde fixation via the ribulose monophosphate pathway. J. Bacteriol., **187**, 3636-3642 (2005)
[4] Orita, I.; Sato, T.; Yurimoto, H.; Kato, N.; Atomi, H.; Imanaka, T.; Sakai, Y.: The ribulose monophosphate pathway substitutes for the missing pentose phosphate pathway in the archaeon Thermococcus kodakaraensis. J. Bacteriol., **188**, 4698-4704 (2006)
[5] Mueller, R.; Babel, W.: Multiplicity of 3-hexulosephosphate synthase from bacterium MB 58. 1. Product-induced transition in velocity. Acta Biol. Med. Ger., **40**, 123-135 (1981)
[6] Mueller, R.; Babel, W.: Multiplicity of 3-hexulosephosphate synthase from bacterium MB 58. 2. Generation of complex kinetic characteristics. Acta Biol. Med. Ger., **40**, 137-146 (1981)
[7] Kato, N.; Miyamoto, N.; Shimao, M.; Sakazawa, C.: 3-Hexulose phosphate synthase from a new facultative methylotroph, Mycobacterium gastri MB19. Agric. Biol. Chem., **52**, 2659-2661 (1988)

[8] Taylor, E.J.; Smith, N.L.; Colby, J.; Charnock, S.J.; Black, G.W.: The gene encoding the ribulose monophosphate pathway enzyme, 3-hexulose-6-phosphate synthase, from Aminomonas aminovorus C2A1 is adjacent to coding sequences that exhibit similarity to histidine biosynthesis enzymes. Antonie van Leeuwenhoek, **86**, 167-172 (2004)
[9] Beisswenger, R.; Kula, M.R.: Catalytic properties and substrate specificity of 3-hexulose phosphate synthase from Methylomonas M15. Appl. Microbiol. Biotechnol., **34**, 604-607 (1991)
[10] Goenrich, M.; Thauer, R.K.; Yurimoto, H.; Kato, N.: Formaldehyde activating enzyme (Fae) and hexulose-6-phosphate synthase (Hps) in Methanosarcina barkeri: a possible function in ribose-5-phosphate biosynthesis. Arch. Microbiol., **184**, 41-48 (2005)
[11] Kemp, M.B.: Hexose phosphate synthase from Methylcoccus capsulatus makes D-arabino-3-hexulose phosphate. Biochem. J., **139**, 129-134 (1974)
[12] Kato, N.; Ohashi, H.; Tani, Y.; Ogata, K.: 3-Hexulosephosphate synthase from Methylomonas aminofaciens 77a. Purification, properties and kinetics. Biochim. Biophys. Acta, **523**, 236-244 (1978)
[13] Kato, N.; Yurimoto, H.; Thauer, R.K.: The physiological role of the ribulose monophosphate pathway in bacteria and archaea. Biosci. Biotechnol. Biochem., **70**, 10-21 (2006)
[14] Arfman, N.; Bystrykh, L.V.; Govorukhina, N.I.; Dijkhuizen, L.: 3-Hexulose-6-phosphate synthase from thermotolerant methylotroph Bacillus C1. Methods Enzymol., **188**, 391-397 (1990)
[15] Kato, N.: 3-Hexulose-6-phosphate synthase from Mycobacterium gastri MB19. Methods Enzymol., **188**, 397-401 (1990)
[16] Mueller, R.H.; Babel, W.: 3-Hexulose-6-phosphate synthase from Acetobacter methanolicus MB58. Methods Enzymol., **188**, 401-405 (1990)
[17] Quayle, J.R.: 3-Hexulose-6-phosphate synthase from Methylomonas (Methylococcus) capsulatus. Methods Enzymol., **90**, 314-319 (1982)
[18] Sahm, H.; Schuette, H.; Kula, M.R.: 3-Hexulose-phosphate synthase from Methylomonas M15. Methods Enzymol., **90**, 319-323 (1982)
[19] Yurimoto, H.; Hirai, R.; Matsuno, N.; Yasueda, H.; Kato, N.; Sakai, Y.: HxlR, a member of the DUF24 protein family, is a DNA-binding protein that acts as a positive regulator of the formaldehyde-inducible hxlAB operon in Bacillus subtilis. Mol. Microbiol., **57**, 511-519 (2005)
[20] Mueller, R.; Sokolov, A.P.: Kinetic properties of the purified 3-hexulosephosphate synthase from Pseudomonas oleovorans. Z. Allg. Mikrobiol., **19**, 261-267 (1979)
[21] Mueller, R.; Babel, W.: A critical analysis of kinetic data of 3-hexulosephosphate synthases. Michaelis-Menten or complex characteristics. Z. Allg. Mikrobiol., **20**, 325-333 (1980)
[22] Yurimoto, H.; Kato, N.; Sakai, Y.: Genomic organization and biochemistry of the ribulose monophosphate pathway and its application in biotechnology. Appl. Microbiol. Biotechnol., **84**, 407-416 (2009)

benzoyl-CoA-dihydrodiol lyase 4.1.2.44

1 Nomenclature

EC number
4.1.2.44

Systematic name
2,3-dihydro-2,3-dihydroxybenzoyl-CoA 3,4-didehydroadipyl-CoA semialdehyde-lyase (formate-forming)

Recommended name
benzoyl-CoA-dihydrodiol lyase

Synonyms
BoxC <1> [2]
benzoyl-CoA oxidation component C <1> [2]
dihydrodiol transforming enzyme <1> [2]

2 Source Organism

<1> *Azoarcus evansii* (UNIPROT accession number: Q84HH6) [1,2]

3 Reaction and Specificity

Catalyzed reaction
2,3-dihydro-2,3-dihydroxybenzoyl-CoA + H_2O = 3,4-didehydroadipyl-CoA semialdehyde + formate

Natural substrates and products
S 2,3-dihydro-2,3-dihydroxybenzoyl-CoA + H_2O <1> (<1> the enzyme is involved in the aerobic benzoyl-CoA catabolic pathway. Benzoyl-CoA is oxidized to 2,3-dihydro-2,3-dihydroxybenzoyl-CoA (benzoyl-CoA dihydrodiol) by benzoyl-CoA oxygenase/reductase BoxBA in the presence of molecular oxygen. The next, ring cleaving step is catalysed by BoxC [2]) (Reversibility: ?) [2]
P 3,4-dehydroadipyl-CoA semialdehyde + formate

Substrates and products
S 2,3-dihydro-2,3-dihydroxybenzoyl-CoA + H_2O <1> (<1> the enzyme is involved in the aerobic benzoyl-CoA catabolic pathway. Benzoyl-CoA is oxidized to 2,3-dihydro-2,3-dihydroxybenzoyl-CoA (benzoyl-CoA dihydrodiol) by benzoyl-CoA oxygenase/reductase BoxBA in the presence of

D. Schomburg and I. Schomburg (eds.), *Class 3.4–6 Hydrolases, Lyases, Isomerases, Ligases: EC 3.4–6*, Springer Handbook of Enzymes S10, DOI 10.1007/978-3-642-36260-6_34,

molecular oxygen. The next, ring cleaving step is catalysed by BoxC [2]; <1> NADPH and semicarbazide are analysed directly by NMR spectroscopy and mass spectrometry. The purified protein does not require molecular oxygen for activity [2]) (Reversibility: ?) [2]

P 3,4-dehydroadipyl-CoA semialdehyde + formate
S Additional information <1> (<1> no activity with crotonyl-CoA [2]) [2]
P ?

Inhibitors

Additional information <1> (<1> acetoacetyl-CoA (0.2 mM), a potential inhibitor of enoyl-CoA hydratase, has no impact on enzyme activity of BoxC-mal. Crotonyl-CoA (0.2 mM), a potential substrate of enoyl-CoA hydratase (crotonase), is neither converted to 3-hydroxybutyryl-CoA nor does it inhibit the standard assay [2]) [2]

Cofactors/prosthetic groups

Additional information <1> (<1> the purified protein does not require divalent metals or any cosubstrates or coenzymes for activity [2]) [2]

Activating compounds

Additional information <1> (<1> addition of 1 mM thiamine diphosphate to the standard assay causes only a minimal stimulation (8%) [2]) [2]

Metals, ions

Additional information <1> (<1> the purified protein does not require divalent metals or any cosubstrates or coenzymes for activity [2]) [2]

Turnover number (s^{-1})

20 <1> (2,3-dihydro-2,3-dihydroxybenzoyl-CoA) [2]

Specific activity (U/mg)

4.9 <1> [2]

K_m-Value (mM)

0.017 <1> (2,3-dihydro-2,3-dihydroxybenzoyl-CoA) [2]

pH-Optimum

9 <1> [2]

pH-Range

7-11 <1> (<1> half maximal activity at pH 7 and pH 11 [2]) [2]

pi-Value

5.44 <1> (<1> calculated from sequence [1]) [1]
5.6 <1> [2]

4 Enzyme Structure

Molecular weight

120000 <1> (<1> gel filtration [2]) [2]

Subunits
? <1> (<1> x * 61000, calculated from sequence [1]) [1]
homodimer <1> (<1> 2 * 60000, SDS-PAGE [2]) [2]

5 Isolation/Preparation/Mutation/Application

Source/tissue
culture condition:benzoate-grown cell <1> [2]

Localization
cytosol <1> [1]

Purification
<1> (wild type and recombinant proteins) [2]

Cloning
<1> [1]
<1> (the boxC gene is expressed in a recombinant Escherichia coli strain as a fusion protein with maltose binding protein (BoxCmal)) [2]

6 Stability

Storage stability
<1>, -20°C, the protein can be stored without appreciable loss of activity for months in the presence of 10% (v/v) glycerol [2]

References

[1] Gescher, J.; Zaar, A.; Mohamed, M.; Schägger, H.; Fuchs, G.: Genes coding for a new pathway of aerobic benzoate metabolism in Azoarcus evansii. J. Bacteriol., **184**, 6301-6315 (2002)
[2] Gescher, J.; Eisenreich, W.; Wörth, J.; Bacher, A.; Fuchs, G.: Aerobic benzoyl-CoA catabolic pathway in Azoarcus evansii: studies on the non-oxygenolytic ring cleavage enzyme. Mol. Microbiol., **56**, 1586-1600 (2005)

trans-*o*-hydroxybenzylidenepyruvate hydratase-aldolase 4.1.2.45

1 Nomenclature

EC number
4.1.2.45

Systematic name
(3E)-4-(2-hydroxyphenyl)-2-oxobut-3-enoate hydro-lyase

Recommended name
trans-*o*-hydroxybenzylidenepyruvate hydratase-aldolase

Synonyms
2'-hydroxybenzalpyruvate aldolase <1,3,4> [3,6,8]
fHBP HA A <2> [5]
fHBP HA B <2> [5]
nsaE <4> [8]
o-tHBPA hydratase-aldolase <5> [2]
tHBPA hydratase-aldolase <5> [1,2]
trans-*o*-hydroxybenzylidenepyruvate hydratase-aldolase <5> [4]

2 Source Organism

<1> *Pseudomonas sp.* [3]
<2> *Sphingomonas paucimobilis* [5]
<3> *Sphingobium xenophagum* [6,7]
<4> *Sphingobium xenophagum* (UNIPROT accession number: Q9X9Q6) [8]
<5> *Pseudomonas putida* (UNIPROT accession number: Q51947) [1,2,4]

3 Reaction and Specificity

Catalyzed reaction
(3E)-4-(2-hydroxyphenyl)-2-oxobut-3-enoate + H_2O = salicylaldehyde + pyruvate

Natural substrates and products
S (3E)-4-(2-hydroxyphenyl)-2-oxobut-3-enoate + H_2O <3> (<3> this reaction is part of the degradative pathways for naphthalene and naphthalenesulfonates by bacteria [6]) (Reversibility: ?) [6]
P salicylaldehyde + pyruvate

D. Schomburg and I. Schomburg (eds.), *Class 3.4–6 Hydrolases, Lyases, Isomerases, Ligases: EC 3.4–6*, Springer Handbook of Enzymes S10, DOI 10.1007/978-3-642-36260-6_35,

S (E)-2'-hydroxybenzylidenepyruvate + H_2O <3> (<3> involved in metabolism of naphthalene to salicylate [7]) (Reversibility: ?) [7]
P salicylaldehyde + pyruvate
S (E)-2'-hydroxybenzylidenepyruvate + O_2 <1> (<1> naphthalene metabolism [3]) (Reversibility: ?) [3]
P salicylaldehyde + pyruvate

Substrates and products

S (3E)-4-(2,4-dihydroxyphenyl)-2-oxobut-3-enoate + H_2O <3> (Reversibility: ?) [6]
P 2,4-dihydroxybenzaldehyde + pyruvate
S (3E)-4-(2,6-dihydroxyphenyl)-2-oxobut-3-enoate + H_2O <3> (Reversibility: ?) [6]
P 2,6-dihydroxybenzaldehyde + pyruvate
S (3E)-4-(2-hydroxyphenyl)-2-oxobut-3-enoate + H_2O <2,3,5> (<3> this reaction is part of the degradative pathways for naphthalene and naphthalenesulfonates by bacteria [6]; <2> i.e. 2-hydroxybenzylidinepyruvate, i.e. 2-hydroxybenzalpyruvate [5]; <5> i.e. 2-hydroxybenzylidinepyruvate, i.e. 2-hydroxybenzalpyruvate, i.e. trans-O-hydroxybenzylidenepyruvate [2]; <3> i.e. 2-hydroxybenzylidinepyruvate, i.e. 2-hydroxybenzalpyruvate, i.e. trans-O-hydroxybenzylidenepyruvate, intermediate formation of a stable Schiff base between enzyme and substrate [6]) (Reversibility: ?) [2,5,6]
P salicylaldehyde + pyruvate (<3> salicylaldehyde i.e. 2-hydroxybenzaldehyde [6])
S (E)-2'-hydroxybenzylidenepyruvate + H_2O <3> (<3> involved in metabolism of naphthalene to salicylate [7]) (Reversibility: ?) [7]
P salicylaldehyde + pyruvate
S (E)-2'-hydroxybenzylidenepyruvate + O_2 <1,5> (<1> naphthalene metabolism [3]; <5> the equilibrium in this reaction favors cleavage [1]) (Reversibility: ?) [1,3]
P salicylaldehyde + pyruvate
S 1-hydroxy-2-naphthaldehyde + pyruvate <5> (Reversibility: ?) [2]
P (3E)-4-(1-hydroxynaphthalen-2-yl)-2-oxobut-3-enoate + H_2O
S 1-methylindole-3-carboxaldehyde + pyruvate <5> (Reversibility: ?) [2]
P (3E)-4-(1-methyl-1H-indol-3-yl)-2-oxobut-3-enoate + H_2O
S 1-naphthaldehyde + pyruvate <5> (Reversibility: ?) [2]
P (3E)-4-naphthalen-1-yl-2-oxobut-3-enoate + H_2O
S 2,3-dihydroxybenzaldehyde + pyruvate <5> (Reversibility: ?) [2]
P (3E)-4-(2,3-dihydroxyphenyl)-2-oxobut-3-enoate + H_2O
S 2-carboxybenzaldehyde + pyruvate <5> (Reversibility: ?) [2]
P (3E)-4-(2-carboxyphenyl)-2-oxobut-3-enoate + H_2O
S 2-chlorobenzaldehyde + pyruvate <5> (<5> in the reverse reaction (3E)-4-(2-chlorophenyl)-2-oxobut-3-enoate is cleaved at 1.6% the rate of (3E)-4-(2-hydroxyphenyl)-2-oxobut-3-enoate [2]) (Reversibility: ?) [2]
P (3E)-4-(2-chlorophenyl)-2-oxobut-3-enoate + H_2O
S 2-formylbenzenesulfonate + pyruvate <5> (Reversibility: ?) [2]
P (3E)-2-oxo-4-(2-sulfophenyl)but-3-enoate + H_2O

S 2-furaldehyde + pyruvate <5> (Reversibility: ?) [2]
P (3E)-4-furan-2-yl-2-oxobut-3-enoate + H_2O
S 2-hydroxy-1-naphthaldehyde + pyruvate <5> (Reversibility: ?) [2]
P (3E)-4-(2-hydroxynaphthalen-1-yl)-2-oxobut-3-enoate + H_2O
S 2-hydroxy-5-nitrobenzaldehyde + pyruvate <5> (Reversibility: ?) [2]
P (3E)-4-(2-hydroxy-5-nitrophenyl)-2-oxobut-3-enoate + H_2O
S 2-methoxybenzaldehyde + pyruvate <5> (<5> i.e. *o*-anisaldehyde [2]) [2]
P (3E)-4-(2-methoxyphenyl)-2-oxobut-3-enoate + H_2O
S 2-naphthaldehyde + pyruvate <5> (Reversibility: ?) [2]
P (3E)-4-naphthalen-2-yl-2-oxobut-3-enoate + H_2O
S 2-nitrobenzaldehyde + pyruvate <5> (Reversibility: ?) [2]
P (3E)-4-(2-nitrophenyl)-2-oxobut-3-enoate + H_2O
S 2-pyridinecarboxaldehyde + pyruvate <5> (Reversibility: ?) [2]
P (3E)-2-oxo-4-pyridin-2-ylbut-3-enoate + H_2O
S 2-quinolinecarboxaldehyde + pyruvate <5> (Reversibility: ?) [2]
P (3E)-2-oxo-4-quinolin-2-ylbut-3-enoate + H_2O
S 2-thiophenecarboxaldehyde + pyruvate <5> (Reversibility: ?) [2]
P (3E)-2-oxo-4-thiophen-2-ylbut-3-enoate + H_2O
S 3-furaldehyde + pyruvate <5> (Reversibility: ?) [2]
P (3E)-4-furan-3-yl-2-oxobut-3-enoate + H_2O
S 3-hydroxybenzaldehyde + pyruvate <5> (<5> in the reverse reaction (3E)-4-(3-hydroxyphenyl)-2-oxobut-3-enoate is cleaved at 75% the rate of (3E)-4-(2-hydroxyphenyl)-2-oxobut-3-enoate [2]) (Reversibility: r) [2]
P (3E)-4-(3-hydroxyphenyl)-2-oxobut-3-enoate + H_2O
S 3-methoxysalicylaldehyde + pyruvate <5> (<5> i.e *o*-vanillin [2]) (Reversibility: ?) [2]
P (3E)-4-(2-hydroxy-3-methoxyphenyl)-2-oxobut-3-enoate + H_2O
S 3-pyridinecarboxaldehyde + pyruvate <5> (Reversibility: ?) [2]
P (3E)-2-oxo-4-pyridin-3-ylbut-3-enoate + H_2O
S 3-quinolinecarboxaldehyde + pyruvate <5> (Reversibility: ?) [2]
P (3E)-2-oxo-4-quinolin-3-ylbut-3-enoate + H_2O
S 3-thiophenecarboxaldehyde + pyruvate <5> (Reversibility: ?) [2]
P (3E)-2-oxo-4-thiophen-3-ylbut-3-enoate + H_2O
S 4-biphenylcarboxaldehyde + pyruvate <5> (Reversibility: ?) [2]
P (3E)-4-biphenyl-4-yl-2-oxobut-3-enoate + H_2O
S 4-hydroxybenzaldehyde + pyruvate <5> (<5> in the reverse reaction (3E)-4-(4-hydroxyphenyl)-2-oxobut-3-enoate is cleaved at less than 1% the rate of (3E)-4-(2-hydroxyphenyl)-2-oxobut-3-enoate [2]) (Reversibility: ?) [2]
P (3E)-4-(4-hydroxyphenyl)-2-oxobut-3-enoate + H_2O
S 4-isopropylbenzaldehyde + pyruvate <5> (Reversibility: ?) [2]
P (3E)-4-[4-(1-methylethyl)phenyl]-2-oxobut-3-enoate + H_2O
S 4-quinolinecarboxaldehyde + pyruvate <5> (Reversibility: ?) [2]
P (3E)-2-oxo-4-quinolin-4-ylbut-3-enoate + H_2O
S benzaldehyde + pyruvate <5> (<5> the product benzylidenepyruvate is not a substrate in the reverse direction [2]) (Reversibility: ir) [2]
P benzylidenepyruvate + H_2O

S benzylidenepyruvate + H_2O <3> (<3> with 1% of the activity found with (E)-2-hydroxybenzylidinepyruvate [6]) (Reversibility: ?) [6]
P benzaldehyde + pyruvate
S crotonaldehyde + pyruvate <5> (Reversibility: ?) [2]
P (3E,5E)-2-oxohepta-3,5-dienoate + H_2O
S cyclohexanecarboxaldehyde + pyruvate <5> (Reversibility: ?) [2]
P (3E)-4-cyclohexyl-2-oxobut-3-enoate + H_2O
S indole-3-carboxaldehyde + pyruvate <5> (Reversibility: ?) [2]
P (3E)-4-(1H-indol-3-yl)-2-oxobut-3-enoate + H_2O
S *o*-tolualdehyde + pyruvate <5> (Reversibility: ?) [2]
P (3E)-4-(2-methylphenyl)-2-oxobut-3-enoate + H_2O
S *p*-tolualdehyde + pyruvate <5> (<5> in the reverse reaction (3E)-4-(4-methylphenyl)-2-oxobut-3-enoate is cleaved at less than 1% the rate of (3E)-4-(2-hydroxyphenyl)-2-oxobut-3-enoate [2]) (Reversibility: ?) [2]
P (3E)-4-(4-methylphenyl)-2-oxobut-3-enoate + H_2O
S phenanthrene-9-carboxaldehyde + pyruvate <5> (Reversibility: ?) [2]
P (3E)-2-oxo-4-phenanthren-9-ylbut-3-enoate + H_2O
S phthalaldehyde + pyruvate <5> (Reversibility: ?) [2]
P (3E)-4-(2-formylphenyl)-2-oxobut-3-enoate + H_2O
S Additional information <3,5> (<5> no activity with trans-benzylidenepyruvate, trans-*o*-methoxybenzylidenepyruvate or trans-*o*-hydroxycinnamate. The hydratase-aldolase catalyzes the condensation of pyruvate with several other aromatic aldehydes, including benzaldehyde, to give trans-benzylidenepyruvate. Since benzylidenepyruvate is not a substrate for the enzyme, the reaction is irreversible and can be carried out to completion by using relatively low concentrations of the substrates, benzaldehyde and pyruvate [1]; <3> no activity with: benzylideneacetone and cinnamic acid [6]; <5> the enzyme catalyzes a reversible reaction in vitro (the reverse reaction being an aldol-condensation). It accepts a broad range of aldehydes and 4-substituted 2-keto-but-3-enoates as substrates. Acetophenone, 2-hydroxyacetophenone, phenylacetaldehyde, and trans-cinnamaldehyde are not substrates [2]) [1,2,6]
P ?

Inhibitors

2-hydroxy-6-oxo-6-phenylhexa-2,4-dienoate <3> [6]
Hg^{2+} <2> (<2> 1 mM, 40% inhibition of fHBP HA B [5]) [5]
NEM <2> (<2> 1 mM, 30 min, 25°C, 35% inhibition of fHBP HA B, more than 85% of the initial activity of fHBP HA A remains [5]) [5]
PCMB <2> (<2> 1 mM, 30 min, 25°C, complete inhibition of fHBP HA B, more than 85% of the initial activity of fHBP HA A remains [5]) [5]
p-chloromercuribenzoate <3> (<3> enzyme is partially reactivated by addition of dithiothreitol [6]) [6]
salicylaldehyde <3> [6]
sodium borhydride <3> [6]
Additional information <2,3,5> (<3> no inhibition: benzylideneacetone, cinnamic acid [6]; <2> no inhibition: monoiodoacetic acid, N-ethylmaleimide,

PCMB, diisopropyl fluorophosphate, phenylmethanesulfonyl fluoride, EDTA, NaN_3, KCN, *o*-phenanthroline, 2,2-bipyridine, Fe^{2+}, Fe^{3+}, Mg^{2+}, Mn^{2+}, Co^{2+}, Ca^{2+}, Zn^{2+}, Cd^{2+}, Cu^{2+}, Ni^{2+}, EDTA, *o*-phenanthroline, 2-bipyridine, KCN [5]; <5> not sensitive to 5 mM EDTA [1]) [1,5,6]

Cofactors/prosthetic groups

Additional information <5> (<5> no cofactor required [1]) [1]

Specific activity (U/mg)

1.55 <5> (<5> recombinant enzyme [1]) [1]
7.7 <2> (<2> enzyme form fHBP HA B [5]) [5]
11 <2> (<2> enzyme form fHBP HA A [5]) [5]
23.67 <3> [6]

K_m-Value (mM)

0.003 <2> ((3E)-4-(2-hydroxyphenyl)-2-oxobut-3-enoate, <2> 30°C, pH 8.1, enzyme form fHBP HA A [5]) [5]
0.006 <3> ((3E)-4-(2,6-dihydroxyphenyl)-2-oxobut-3-enoate, <3> pH 7.0 [6]) [6]
0.009 <2> ((3E)-4-(2-hydroxyphenyl)-2-oxobut-3-enoate, <2> 30°C, pH 8.1, enzyme form fHBP HA B [5]) [5]
0.015 <3> ((3E)-4-(2,4-dihydroxyphenyl)-2-oxobut-3-enoate, <3> pH 7.0 [6]) [6]
0.017 <3> ((3E)-4-(2-hydroxyphenyl)-2-oxobut-3-enoate, <3> pH 7.0 [6]) [6]
0.4 <3> (benzylidenepyruvate, <3> pH 7.0 [6]) [6]

K_i-Value (mM)

0.013 <3> (2-hydroxy-6-oxo-6-phenylhexa-2,4-dienoate, <3> pH 7.0 [6]) [6]

pH-Optimum

8 <3> (<3> in Tris/HCl or Na/K-phosphate buffer [6]) [6]
9 <2> (<2> enzyme form fHBP HA A and enzyme form fHBP HA B [5]) [5]

pH-Range

5-8 <1> (<1> the activity is independent of pH between pH 5.5 and 8.0, but above pH 8.0 activity declines rapidly [3]) [3]
6-9 <3> (<3> more than 80% of the maximal activity at pH 6.0 and pH 9.0, pH 5.0: 18% of maximal activity, pH 10.0: 14% of maximal activity [6]) [6]
6-9.5 <2> (<2> pH 6: about 60% of maximal activity, pH 9.5: about 80% of maximal activity, enzyme form fHBP HA A and enzyme form fHBP HA B [5]) [5]

pi-Value

4.3 <2> (<2> enzyme form fHBP HA B, isoelectric focusing [5]) [5]
4.8 <2> (<2> enzyme form fHBP HA A, isoelectric focusing [5]) [5]
5.4 <5> (<5> calculated from sequence [4]) [4]

4 Enzyme Structure

Molecular weight

104000 <2> (<2> enzyme form fHBP HA B, ultracentrifugation [5]) [5]
116000 <2> (<2> enzyme form fHBP HA A, ultracentrifugation [5]) [5]
120000 <3> (<3> gel filtration [6]) [6]

Subunits

? <5> (<5> x * 36640, calculated from sequence [4]) [4]
trimer <2,3> (<2> 3 * 37200, enzyme form fHBP HA B, SDS-PAGE [5]; <2> 3 * 37600, enzyme form fHBP HA A, SDS-PAGE [5]; <3> 3 * 38500, SDS-PAGE [6]) [5,6]

5 Isolation/Preparation/Mutation/Application

Purification

<1> (partial) [3]
<2> (presence of at least three trans-*o*-hydroxybenzylidenepyruvate hydratase-aldolases, purification of two typical trans-*o*-hydroxybenzylidenepyruvate hydratase-aldolases (fHBP HA A and fHBP HA B)) [5]
<3> [6]

Cloning

<4> (a gene cluster is identified on the plasmid pBN6 which codes for several enzymes participating in the degradative pathway for naphthalenesulfonates. A DNA fragment of 16915 bp is sequenced which contains 17 ORFs. The genes encoding the 1,2-dihydroxynaphthalene dioxygenase, 2-hydroxychromene-2-carboxylate isomerase, and 2'-hydroxybenzalpyruvate aldolase of the naphthalenesulfonate pathway are identified on the DNA fragment and the encoded proteins are heterologously expressed in Escherichia coli) [8]
<5> (expression in Escherichia coli) [1]

6 Stability

pH-Stability

6-9.3 <2> (<2> 4°C, 20 h, enzyme form fHBP HA A is stable [5]) [5]
7 <1> (<1> the enzyme was very stable in buffer at pH 7, stored either at 0°C or frozen [3]) [3]
7.1-10.7 <2> (<2> 4°C, 20 h, enzyme form fHBP HA B is stable [5]) [5]

Temperature stability

50 <2> (<2> pH 7.3, 20 mM Tris-HCl buffer, 5 min, enzyme form fHBP HA A and enzyme form fHBP HA B, stable up to [5]) [5]
65 <2> (<2> pH 7.3, 20 mM Tris-HCl buffer, 5 min, enzyme form fHBP HA A and enzyme form fHBP HA B, 80% loss of activity [5]) [5]

General stability information

<3>, -16°C, 4°C or 20°C, the enzyme is very stable in cell free extracts, after a 1-week incubation (protein concentration: 2.6 mg/ml) in Na/K-phosphate buffer (pH 7.3, 50 mM) the initial enzyme activity is completely recovered [6]

References

[1] Eaton, R.W.; Chapman, P.J.: Bacterial metabolism of naphthalene: Construction and use of recombinant bacteria to study ring cleavage of 1,2-dihydroxynaphthalene and subsequent reactions. J. Bacteriol., **174**, 7542-7554 (1992)
[2] Eaton, R.W.: trans-*o*-Hydroxybenzylidenepyruvate hydratase-aldolase as a biocatalyst. Appl. Environ. Microbiol., **66**, 2668-2672 (2000)
[3] E.A. Barnsley: Naphthalene metabolism by pseudomonads: The oxidation of 1,2-dihydroxynaphthalene to 2-hydroxychromene-2-carboxylic acid and the formation of 2'-hydroxybenzalpyruvate. Biochem. Biophys. Res. Commun., **72**, 1116-1121 (1976)
[4] R. W., Eaton: Organization and evolution of naphthalene catabolic pathways: sequence of the DNA encoding 2-hydroxychromene-2-carboxylate isomerase and trans-*o*-hydroxybenzylidenepyruvate hydratase-aldolase from the NAH7 plasmid. J. Bacteriol., **176**, 7757-7762 (1994)
[5] Ohmoto, T.; Moriyoshi, K.; Sakai, K.; Hamada, N.; Ohe, T.: Presence of two trans-*o*-hydroxybenzylidenepyruvate hydratase-aldolases in naphthalenesulfonate-assimilating Sphingomonas paucimobilis TA-2: comparison of some properties. J. Biochem., **127**, 43-49 (2000)
[6] Kuhm, A.E.; Knackmuss, H.J.; Stolz, A.: Purification and properties of 2'-hydroxybenzalpyruvate aldolase from a bacterium that degrades naphthalenesulfonates. J. Biol. Chem., **268**, 9484-9489 (1993)
[7] Stolz, A.: Degradation of substituted naphthalenesulfonic acids by Sphingomonas xenophaga BN6. J. Ind. Microbiol. Biotechnol., **23**, 391-399 (1999)
[8] Keck, A.; Conradt, D.; Mahler, A.; Stolz, A.; Mattes, R.; Klein, J.: Identification and functional analysis of the genes for naphthalenesulfonate catabolism by Sphingomonas xenophaga BN6. Microbiology, **152**, 1929-1940 (2006)

aliphatic (R)-hydroxynitrile lyase 4.1.2.46

1 Nomenclature

EC number
4.1.2.46

Systematic name
(2R)-2-hydroxy-2-methylbutanenitrile butan-2-one lyase (cyanide forming)

Recommended name
aliphatic (R)-hydroxynitrile lyase

Synonyms
(R)-HNL <3> [7]
(R)-oxynitrilase <1,2> [2,3]
(R)-hydroxynitrile lyase <3> [7]
acetone cyanohydrin lyase <1,3> [1,6]
hydroxynitrile lyase <1,2,3> [5,6]
LuHNL <1,2,3> [4,5,6,9,10]

2 Source Organism

<1> *Linum usitatissimum* [1,3,4,5,10]
<2> *Linum usitatissimum* (UNIPROT accession number: O22574) [2,5]
<3> *Linum usitatissimum* (UNIPROT accession number: P93243) [6,7,8,9]

3 Reaction and Specificity

Catalyzed reaction
(2R)-2-hydroxy-2-methylbutanenitrile = cyanide + butan-2-one

Natural substrates and products
S 2-hydroxy-2-methylpropanenitrile <1,3> (<1> i.e. acetone cyanohydrin [1]; <3> the enzyme is involved in the catabolism of cyanogenic glycosides in young seedlings of Linum usitatissimum [6]) (Reversibility: ?) [1,6]
P cyanide + acetone
S cyanide + acetone <2> (<2> natural substrates for the (R)-oxynitrilase from Linum usitatissimum are acetone and butan-2-one, which are the building blocks of the cyanogenic glycosides in Linum, linamarin and lotaustralin, or linustatin and neolinustatin, respectively [2]) (Reversibility: ?) [2]

D. Schomburg and I. Schomburg (eds.), *Class 3.4–6 Hydrolases, Lyases, Isomerases, Ligases: EC 3.4–6*, Springer Handbook of Enzymes S10, DOI 10.1007/978-3-642-36260-6_36,

P 2-hydroxy-2-methylpropanenitrile
S cyanide + butan-2-one <2> (<2> natural substrates for the (R)-oxynitrilase from Linum usitatissimum are acetone and butan-2-one, which are the building blocks of the cyanogen glycosides in Linum, linamarin and lotaustralin, or linustatin and neolinustatin, respectively [2]) (Reversibility: ?) [2]
P (2R)-butan-2-one cyanohydrin

Substrates and products

S (2R)-2-hydroxy-2-methylbutanenitrile <1> (Reversibility: ?) [1]
P cyanide + 2-butanone
S (R)-2-butanone-cyanhydrin <1> (Reversibility: ?) [4]
P HCN + butanone
S 2-hydroxy-2-methylpropanenitrile <1,3> (<1> i.e. acetone cyanohydrin [1]; <3> the enzyme is involved in the catabolism of cyanogenic glycosides in young seedlings of Linum usitatissimum [6]) (Reversibility: ?) [1,6]
P cyanide + acetone
S HCN + 4-hydroxybutanal <1> (Reversibility: ?) [3]
P 2,5-dihydroxypentanenitrile <1> [3]
S HCN + benzaldehyde <1> (Reversibility: ?) [3]
P (R)-mandelonitrile <1> [3]
S HCN + butanone <2> (Reversibility: ?) [5]
P (R)-2-butanone cyanhydrin
S cyanide + 2-methylcyclopentanone <2> (Reversibility: ?) [2]
P ?
S cyanide + 2-pentanone <3> (<3> 93% enantiomeric excess [9]) (Reversibility: ?) [9]
P (2R)-2-hydroxy-2-methylpentanenitrile
S cyanide + acetone <2> (<2> natural substrates for the (R)-oxynitrilase from Linum usitatissimum are acetone and butan-2-one, which are the building blocks of the cyanogenic glycosides in Linum, linamarin and lotaustralin, or linustatin and neolinustatin, respectively [2]) (Reversibility: ?) [2]
P 2-hydroxy-2-methylpropanenitrile
S cyanide + acetylcyclopropane <2> (Reversibility: ?) [2]
P ?
S cyanide + acrolein <3> (<3> 74% enantiomeric excess [9]) (Reversibility: ?) [9]
P (2R)-2-hydroxybut-3-enenitrile
S cyanide + butan-2-one <2> (<2> natural substrates for the (R)-oxynitrilase from Linum usitatissimum are acetone and butan-2-one, which are the building blocks of the cyanogen glycosides in Linum, linamarin and lotaustralin, or linustatin and neolinustatin, respectively [2]) (Reversibility: ?) [2]
P (2R)-butan-2-one cyanohydrin

S cyanide + butan-2-one <1,2,3> (<3> 95% enantiomeric excess [9]; <1> reaction with an immobilized form of the hydroxynitrile lyase as cross-linked enzyme aggregate with high specific activity and recovery on a preparative scale [5]) (Reversibility: ?) [2,5,9]
P (2R)-2-hydroxy-2-methylbutanenitrile (<2> 77.2% enantiomeric excess [2])
S cyanide + butyraldehyde <2,3> (<3> 98% enantiomeric excess [9]) (Reversibility: ?) [2,9]
P (2R)-2-hydroxypentanenitrile
S cyanide + chloroacetone <2> (Reversibility: ?) [2]
P (2R)-3-chloro-2-hydroxy-2-methylpropionitrile
S cyanide + crotonaldehyde <2,3> (<3> 99% enantiomeric excess [9]) (Reversibility: ?) [2,9]
P (2R)-2-hydroxy-3-pentenenitrile
S cyanide + hexan-2-one <2> (Reversibility: ?) [2]
P (2R)-2-hydroxy-2-methylhexanenitrile
S cyanide + hydroxyacetone <2> (Reversibility: ?) [2]
P (2R)-1,2-dihydroxy-2-methyl-propane-3-nitrile
S cyanide + hydroxypivaldehyde <3> (<3> 73% enantiomeric excess [9]) (Reversibility: ?) [9]
P (2R)-2,4-dihydroxy-3,3-dimethylbutanenitrile
S cyanide + isobutyraldehyde <3> (<3> 93% enantiomeric excess [9]) (Reversibility: ?) [9]
P (2R)-2-hydroxy-4-methylpentanenitrile
S cyanide + methacrolein <3> (<3> 98% enantiomeric excess [9]) (Reversibility: ?) [9]
P (2R)-2-hydroxy-3-methylbut-3-enenitrile
S cyanide + methyl vinyl ketone <2> (Reversibility: ?) [2]
P (2R)-2-hydroxy-2-methyl-3-butenenitrile
S cyanide + methyl vinyl ketone <3> (Reversibility: ?) [9]
P (2R)-2-hydroxy-2-methylbut-3-enenitrile (<3> despite a short reaction time of 0.8 h, the conversion of methyl vinyl ketone results in a poor (38%) enantiomeric excess value. As in the same time there is almost no conversion without enzyme. This compound is one of the rare examples, where the enzyme exerts only a partial stereoselectivity for a defined substrate [9])
S cyanide + pentan-2,4-dione <2> (Reversibility: ?) [2]
P ?
S cyanide + pentan-2-one <2> (Reversibility: ?) [2]
P (2R)-2-hydroxy-2-methylpentanenitrile
S cyanide + pinacolone <2> (Reversibility: ?) [2]
P (2R)-2-hydroxy-2,3,3-trimethylbutyronitrile
S cyanide + pivalaldehyde <2> (Reversibility: ?) [2]
P (2R)-3,3-dimethyl-2-hydroxybutyronitrile
S cyanide + propionaldehyde <2,3> (<3> 97% enantiomeric excess [9]) (Reversibility: ?) [2,9]
P (2R)-2-hydroxybutyronitrile

S cyanide + pyruvic acid ethyl ester <2> (Reversibility: ?) [2]
P ?
S Additional information <1,3> (<1> no activity with aromatic substrates [4]; <1> no activity towards mandelonitrile and *p*-hydroxymandelonitrile [1]; <1> synthesis of aromatic (S)-cyanohydrins. Most active towards derivatives of phenylacetone, converting 30-65% of the starting material to (S)-cyanohydrin with 55-95% enantiomeric excess in less than 1 day [10]; <3> the enzyme catalyzes the stereoselective synthesis of aliphatic (R)-cyanohydrins. Conversion of aromatic aldehydes (3-phenylpropionaldehyde or cinnamic aldehyde) and the aliphatic ketones is incomplete and gives poor enantiomeric excess-values, caused by the long reaction time [9]) (Reversibility: ?) [1,4,9,10]
P ?

Inhibitors

benzaldehyde <2> (<2> leads to a complete and irreversible deactivation of the enzyme within 2 h incubation [2]) [2]
diisopropyl fluorophosphate <3> (<3> 10 mM, 25% inhibition [6]) [6]
Additional information <1> (<1> no inhibition by 10 mM 2-mercaptoethanol, 1 mM iodoacetamide or iodoacetic acid, 10 mM isobutyronitrile or isopropanol [1]) [1]

Cofactors/prosthetic groups

Additional information <1> (<1> not a flavoprotein [1]) [1]

Activating compounds

Additional information <1> (<1> molecular imprinting using 2-butanone as additive in the immobilization process improves the synthetic activity of the biocatalyst [5]) [5]

Metals, ions

Zn^{2+} <3> (<3> LuHNL has significant homologies to members of the Zn^{2+}-containing alcohol dehydrogenases. In particular, residues responsible for coordination of Zn^{2+} ions or fulfilling structural or functional tasks in Zn^{2+}-alcohol dehydrogenases are conserved. Contains about 2-4 mol zinc per mol of recombinant enzyme. Hydroxynitrile lyase from Linum usitatissimum and Zn^{2+}-alcohol dehydrogenases have similar structural requirements with respect to maintaining a catalytically active structure. Residues essentially involved in catalysis of Zn^{2+}-ADHs are also of functional importance in hydroxynitrile lyase from Linum usitatissimum [9]) [9]

Specific activity (U/mg)

34.1 <1> [1]
52.9 <2> [2]
Additional information <1,2> (<2> development of an immobilized form of the hydroxynitrile lyase as crosslinked enzyme aggregate (CLEA) with high specific activity (303.5 U/g) and recovery (33%), 180.5 U/g LuCLEA (crosslinked enzyme aggregate) (using sat. $(NH_4)_2SO_4$), 9.9 U/g LuEA (Enzyme aggregate of LuHNL) (using sat. $(NH_4)_2SO_4$), 110.9 U/g LuCLEA (using tert-

butanol), 221.9 U/g LuEA (using tert-butanol) [5]; <1> development of an immobilized form of the hydroxynitrile lyase as crosslinked enzyme aggregate with high specific activity (303.5 U/g) and recovery [5]) [5]

K_m-Value (mM)
1.25 <1> ((2R)-2-hydroxy-2-methylbutanenitrile, <1> pH 5.5, 25°C [1]) [1]
2.5 <1> (2-hydroxy-2-methylpropanenitrile, <1> pH 5.5, 25°C [1]) [1]

pH-Optimum
5.5 <1,2> [1,2]

pH-Range
4.1-5.5 <2> (<2> pH 4.1: about 70% of maximal activity, pH 5.5: maximal activity [2]) [2]

pi-Value
4.5-4.8 <1> (<1> chromatofocusing [1]) [1]

Temperature optimum (°C)
25 <2> (<2> assay at [2]) [2]

4 Enzyme Structure

Molecular weight
80000 <3> (<3> gel filtration [9]) [9]
82000 <1> (<1> gel filtration [1]) [1]
87000 <2> (<2> gel filtration [2]) [2]

Subunits
? <3> (<3> x * 45780, calculated from sequence [6]) [6]
dimer <1,2,3> (<3> 2 * 40000, SDS-PAGE [9]; <1> 2 * 42000, SDS-PAGE [1]; <2> 2 * 43000, SDS-PAGE [2]) [1,2,9]

5 Isolation/Preparation/Mutation/Application

Source/tissue
cotyledon <3> [8]
seedling <2> [2]
shoot <1> [1]

Localization
cytoplasm <3> (<3> highest detection level in cytoplasm, with lower levels in organelles, not detected in cell wall or vacuole [8]) [8]

Purification
<1> [1,3]
<2> [2]
<3> [7]

Cloning

<1> (cloned into Pichia pastoris, expressed in Escherichia coli as an N-terminal hexa-histidine fusion protein) [4]
<3> (cloning of a myc-His-tagged LuHNL-cDNA under control of the methanol-inducible AOX1 (alcohol oxidase) promotor of Pichia pastoris and introduction in the SMD1168 strain. Recombinant LuHNL is kinetically indistinguishable from the authentic flax enzyme) [9]
<3> (expressed in Escherichia coli as N-terminal hexa-histidine fusion protein) [7]
<3> (expression in Escherichia coli) [6]

Engineering

G104A <3> (<3> 5-10% of wild-type activity [9]) [9]
G95A <3> (<3> complete destruction of enzymatic activity [9]) [9]

Application

synthesis <1> (<1> optically active aliphatic ω-hydroxycyanohydrins are valued materials in organic synthesis [3]) [3]

6 Stability

pH-Stability

4 <2> (<2> half-life: 1 h [2]) [2]
5 <2> (<2> immobilization on Eupergit (carrier consisting of macroporous beads) improves the stability considerably in the pH range below pH 5 [2]) [2]
6-11 <2> (<2> stable [2]) [2]

General stability information

<2>, immobilization on Eupergit (carrier consisting of macroporous beads) improves the stability considerably in the pH range below pH 5 [2]

Storage stability

<1>, 4°C, stable for at least 45 d [1]

References

[1] Xu, L.L.; Singh, B.K.; Conn, E.E.: Purification and characterization of acetone cyanohydrin lyase from Linum usitatissimum. Arch. Biochem. Biophys., **263**, 256-263 (1988)
[2] Albrecht, J.; Jansen, I.; Kula, M.R.: Improved purification of an (R)-oxynitrilase from Linum usitatissimum (flax) and investigation of the substrate range. Biotechnol. Appl. Biochem., **17**, 191-203 (1993)
[3] de Gonzalo, G.; Brieva, R.; Gotor, V.: (R)-Oxynitrilase-catalyzed transformation of ω-hydroxyalkanals. J. Mol. Catal. B, **19-20**, 223-230 (2002)
[4] Fechter, M.H.; Griengl, H.: Hydroxynitrile lyases: biological sources and application as biocatalysts. Food Technol. Biotechnol., **42**, 287-294 (2004)

[5] Cabirol, F.L.; Tan, P.L.; Tay, B.; Cheng, S.; Hanefeld, U.; Sheldon, R.A.: Linum usitatissimum hydroxynitrile lyase cross-linked enzyme aggregates: a recyclable enantioselective catalyst. Adv. Synth. Catal., **350**, 2329-2338 (2008)
[6] Trummler, K.; Wajant, H.: Molecular cloning of acetone cyanohydrin lyase from flax (Linum usitatissimum). Definition of a novel class of hydroxynitrile lyases. J. Biol. Chem., **272**, 4770-4774 (1997)
[7] Breithaupt, H.; Pohl, M.; Bönigk, W.; Heim, P.; Schimz, K.-L.; Kula, M.-R.: Cloning and expression of (R)-hydroxynitrile lyase from Linum usitatissimum (flax). J. Mol. Catal. B, **6**, 315-332 (1999)
[8] Wajant, H.; Riedel, D.; Benz, S.; Mundry, K.-W.: Immunocytological localization of hydroxynitrile lyases from Sorghum bicolor L. and Linum usitatissimum L.. Plant Sci., **103**, 145-154 (1994)
[9] Trummler, K.; Roos, J.; Schwaneberg, U.; Effenberger, F.; Förster, S.; Pfizenmaier, K.; Wajant, H.: Expression of the Zn^{2+}-containing hydroxynitrile lyase from flax (Linum usitatissimum) in Pichia pastoris - utilization of the recombinant enzyme for enzymatic analysis and site-directed mutagenesis. Plant Sci., **139**, 19-27 (1998)
[10] Roberge, D.; Fleitz, F.; Pollard, D.; Devine, P.: Synthesis of optically active cyanohydrins from aromatic ketones: evidence of an increased substrate range and inverted stereoselectivity for the hydroxynitrile lyase from Linum usitatissimum. Tetrahedron Asymmetry, **18**, 208-214 (2007)

3-hydroxy-D-aspartate aldolase 4.1.3.41

1 Nomenclature

EC number
4.1.3.41

Systematic name
3-hydroxy-D-aspartate glyoxylate-lyase (glycine-forming)

Recommended name
3-hydroxy-D-aspartate aldolase

Synonyms
D-3-hydroxyaspartate aldolase <1> [1]
D-HAA <1> [1]

2 Source Organism

<1> *Paracoccus denitrificans* (UNIPROT accession number: Q8GRC8) [1]

3 Reaction and Specificity

Catalyzed reaction
D-erythro-3-hydroxyaspartate = glycine + glyoxylate
threo-3-hydroxy-D-aspartate = glycine + glyoxylate

Substrates and products
S 2-amino-3-hydroxybutanedioic acid <1> (Reversibility: r) [1]
P aminoacetic acid + oxoacetic acid
S D-3-3,4-dihydroxyphenylserine <1> (Reversibility: ?) [1]
P ?
S D-erythro-3-3,4-methylenedioxyphenylserine <1> (Reversibility: ?) [1]
P ?
S D-erythro-3-hydroxyaspartate <1> (<1> the enzyme is strictly D-specific as to the α-position, whereas it does not distinguish between threo and erythro forms at the β-position [1]) (Reversibility: ?) [1]
P glycine + glyoxylate
S D-erythro-3-phenylserine <1> (Reversibility: ?) [1]
P ?
S D-threo-3-3,4-methylenedioxyphenylserine <1> (Reversibility: ?) [1]
P ?

D. Schomburg and I. Schomburg (eds.), *Class 3.4–6 Hydrolases, Lyases, Isomerases, Ligases: EC 3.4–6*, Springer Handbook of Enzymes S10, DOI 10.1007/978-3-642-36260-6_37,

S D-threo-3-phenylserine <1> (Reversibility: ?) [1]
P ?
S allo-threonine <1> (Reversibility: ?) [1]
P ?
S Additional information <1> (<1> the enzyme shows no activity towards L-erythro-3-hydroxyaspartate, L-threo-3-hydroxyaspartate, L-threonine, L-allo-threonine, L-erythro-3-phenylserine, L-threo-3-phenylserine, L-erythro-3-3,4-methylenedioxyphenylserine, and L-threo-3-3,4-methylenedioxyphenylserine [1]) (Reversibility: ?) [1]
P ?

Inhibitors

EDTA <1> (<1> 82% inhibition at 1 mM [1]) [1]

Cofactors/prosthetic groups

pyridoxal 5'-phosphate <1> [1]

Metals, ions

Co^{2+} <1> (<1> 2.0fold increase of specific activity in the presence of 1 mM Co^{2+} [1]) [1]
Mg^{2+} <1> (<1> 5.4fold increase of specific activity in the presence of 1 mM Mg^{2+} [1]) [1]
Mn^{2+} <1> (<1> 8.1fold increase of specific activity in the presence of 1 mM Mn^{2+} [1]) [1]
Additional information <1> (<1> K^+ and Na^+ do not have an effect on the enzymatic activity [1]) [1]

Specific activity (U/mg)

0.36 <1> (<1> after 50fold purification, using DL-threo-3-hydroxyaspartate as substrate, in 0.02 mM HEPES buffer, pH 8.0, at 30°C [1]) [1]
0.6 <1> (<1> crude extract, in 0.02 mM HEPES buffer, pH 8.0, at 30°C [1]) [1]
14.6 <1> (<1> after 50fold purification, using D-threo-3-3,4-methylenedioxyphenylserine as substrate, in 0.02 mM HEPES buffer, pH 8.0, at 30°C [1]) [1]
17.5 <1> (<1> after 50fold purification, using D-erythro-3-3,4-methylenedioxyphenylserine as substrate, in 0.02 mM HEPES buffer, pH 8.0, at 30°C [1]) [1]
20 <1> (<1> after 50fold purification, using D-threonine as substrate, in 0.02 mM HEPES buffer, pH 8.0, at 30°C [1]) [1]
25 <1> (<1> after 50fold purification, using D-allo-threonine as substrate, in 0.02 mM HEPES buffer, pH 8.0, at 30°C [1]) [1]
30 <1> (<1> after 50fold purification, using D-erythro-3-hydroxyaspartate as substrate, in 0.02 mM HEPES buffer, pH 8.0, at 30°C [1]) [1]
95 <1> (<1> after 50fold purification, using D-threo-3-phenylserine as substrate, in 0.02 mM HEPES buffer, pH 8.0, at 30°C [1]) [1]
99 <1> (<1> after 50fold purification, using D-erythro-3-phenylserine as substrate, in 0.02 mM HEPES buffer, pH 8.0, at 30°C [1]) [1]

K_m-Value (mM)

0.4 <1> (D-erythro-3-hydroxyaspartate, <1> in 0.02 mM HEPES buffer, pH 8.0, at 30°C [1]) [1]

pH-Optimum
9 <1> [1]

pH-Range
7.5-10 <1> [1]

Temperature optimum (°C)
35 <1> [1]

4 Enzyme Structure

Molecular weight
80000 <1> (<1> gel filtration [1]) [1]

Subunits
homodimer <1> (<1> 2 * 43000, SDS-PAGE [1]; <1> 2 * 41633, calculated from amino acid sequence [1]) [1]

5 Isolation/Preparation/Mutation/Application

Purification
<1> (ammonium sulfate fractionation, hydroxyapatite column chromatography, DEAE-Toyopearl column chromatography, phenyl-Toyopearl column chromatography, Superdex 200 gel filtration, and Mono Q column chromatography) [1]

Cloning
<1> (expressed in Escherichia coli XL1-Blue MRF' cells) [1]

6 Stability

pH-Stability
6.5-8.5 <1> (<1> the enzyme is stable between pH 6.5 and 8.5 for 30 min at 30°C [1]) [1]

Temperature stability
45 <1> (<1> the enzyme retains 50% activity upon heating at 45°C for 30 min [1]) [1]

References

[1] Liu, J.Q.; Dairi, T.; Itoh, N.; Kataoka, M.; Shimizu, S.: A novel enzyme, D-3-hydroxyaspartate aldolase from Paracoccus denitrificans IFO 13301: purification, characterization, and gene cloning. Appl. Microbiol. Biotechnol., **62**, 53-60 (2003)

(6-4)DNA photolyase 4.1.99.13

1 Nomenclature

EC number
4.1.99.13

Systematic name
(6-4) photoproduct pyrimidine-lyase

Recommended name
(6-4)DNA photolyase

Synonyms
(6-4) DNA photolyase <1> [26]
(6-4) PHR <3> [24]
(6-4) photolyase <1,2,3,4,5,6> [2,3,5,6,7,8,9,10,11,12,13,14,15,16,17,18,19,20,25,27,28]
(6-4)-Phr <1,3> [27]
(6-4)photolyase <8> [4]
6-4PP-photolyase <2> [22]
At64PHR <3> [24]
DNA photolyase <8> [4]
H64PRH <2> [11]
NF-10 <2> [14]
OtCPF1 <9> [23]
PL-(6-4) <1> [6]
human (6-4) photolyase homologous protein <2> [20]
phr (6-4) <1> [10]

CAS registry number
37290-70-3 (not distinguished from DNA photolyase, spore photoproduct lyase)

2 Source Organism

<1> *Drosophila melanogaster* [6,10,12,13,20,26,27]
<2> *Homo sapiens* [11,14,20,22]
<3> *Arabidopsis thaliana* [9,19,24,27]
<4> *Xenopus laevis* [2,3,7,8,15,16,17,18,21,25,28]
<5> *Crotalus atrox* [18]
<6> *Dunaliella salina* [5]
<7> *Aphrocallistes vastus* (UNIPROT accession number: Q86RA1) [1]

D. Schomburg and I. Schomburg (eds.), *Class 3.4–6 Hydrolases, Lyases, Isomerases, Ligases: EC 3.4–6*, Springer Handbook of Enzymes S10, DOI 10.1007/978-3-642-36260-6_38,

<8> *Dunaliella salina* (UNIPROT accession number: Q52Z99) [4]
<9> *Ostreococcus tauri* (UNIPROT accession number: Q5IFN1) [23]

3 Reaction and Specificity

Catalyzed reaction

(6-4) photoproduct (in DNA) = 2 pyrimidine residues (in DNA) (<4> A mechanism is proposed in which the histidines residues His354 and His358 catalyze the formation of the four-membered ring intermediate in the repair process of this enzyme. When deuterium oxide is used as a solvent, the repair activity is decreased. The proton transfer shown by this isotope effect supports the proposed mechanism [2]; <1,2,3,4,5,6> The overall repair reaction consists of two distinct steps, one of which is light-independent and the other one light-dependent. In the initial light-independent step, a 6-iminium ion is thought to be generated via proton transfer induced by two histidines highly conserved among the (6-4) photolyases.This intermediate spontaneously rearranges to form an oxetane intermediate by intramolecular nucleophilic attack. In the subsequent light-driven reaction, one electron is believed to be transferred from the fully reduced FAD cofactor (FADH-) to the oxetane intermediate thus forming a neutral FADH radical and an anionic oxetane radical, which spontaneously fractures. The excess electron is then back-transferred to the flavin radical restoring the fully reduced flavin cofactor and a pair of pyrimidine bases [5,6,7,8,11,12,13,14,15,16,17,18,19,20])

Natural substrates and products

- **S** T[6-4]T (in DNA) <4> (Reversibility: ?) [7]
- **P** 2 thymine residues (in DNA)
- **S** cyclobutadipyrimidine in DNA <7> (Reversibility: ?) [1]
- **P** 2 pyrimidine residues in DNA <7> [1]
- **S** Additional information <2> (<2> cyclobutane pyrimidine dimer-photolyase (EC 4.1.99.3) or 6-4PP-photolyase are able to prevent UV-induced apoptosis in cells deficient for nucleotide excision repair to a similar extent, while in nucleotide excision repair-proficient cells UV-induced apoptosis is prevented only by cyclobutane pyrimidine dimer-photolyase, with no effects observed when pyrimidine-(6-4)-pyrimidone photoproducts are removed by the specific photolyase. Both cyclobutane pyrimidine dimers and pyrimidine-(6-4)-pyrimidone photoproducts contribute to UV-induced apoptosis in nucleotide excision repair-deficient cells, while in nucleotide excision repair-proficient cells, cyclobutane pyrimidine dimers are the only lesions responsible for UV-killing, probably due to the rapid repair of pyrimidine-(6-4)-pyrimidone photoproducts by nucleotide excision repair [22]) (Reversibility: ?) [22]
- **P** ?

Substrates and products

- **S** (6-4) photoproduct (in DNA) <1,2,3,4> (Reversibility: ?) [14,16,19,20]
- **P** 2 pyrimidine residues (in DNA)

S (6-4) photoproduct (in DNA) <6> (Reversibility: ?) [5]
P pyrimidine residues (in DNA)
S C(6-4)C (in DNA) <1> (Reversibility: ?) [12]
P 2 cytosine residues (in DNA)
S Dewar photoproduct <4> (<4> although the affinity of the enzyme for the Dewar photoproduct-containing duplex is similar to that for the (6-4) photoproduct containing substrate a repair rate could not be shown. These results indicate that the (6-4) photolyase binds the DNA containing the Dewar photoproduct and induces a structural change in DNA to some extent, suggesting a difference in the binding mode compared to the (6-4) photoproduct [16]) (Reversibility: ?) [16]
P ?
S T(6-4)C <1> (Reversibility: ?) [12]
P 2 thymidine + cytosine (in DNA)
S T(6-4)C photoproduct (in DNA) <4> (<4> A T(6-4)C photoproduct is synthesized. Differences from T(6-4)T is formation of cytosine hydrates by UV irradiation, and acylation of the amino function with the capping reagent. The capping step is omitted to improve the yield of the desired oligonucleotides. (6-4) photolyase restores the pyrimidines in T(6-4)C to their original structures [17]) (Reversibility: ?) [17]
P thymine-cytosine
S T(6-4)T <1> (Reversibility: ?) [12]
P 2 thymidine resdiues (in DNA)
S T(6-4)T (in DNA) <4> (Reversibility: ?) [15]
P thymidine residues (in DNA)
S T(6-4)T photoproduct (in DNA) <1,4> (Reversibility: ?) [2,27,28]
P 2 thymidine residues (in DNA)
S T[6-4]T (in DNA) <4> (Reversibility: ?) [7]
P 2 thymine residues (in DNA)
S cyclobutadipyrimidine in DNA <7> (Reversibility: ?) [1]
P 2 pyrimidine residues in DNA <7> [1]
S cyclobutadipyrimidine in herring sperm DNA <7> (Reversibility: ?) [1]
P 2 pyrimidine residues in herring sperm DNA <7> [1]
S deoxyoligonucleotide containing (6-4) photoproduct + H_2O <3> (Reversibility: ?) [24]
P deoxyoligonucleotide containing 2 pyrimidine residues
S Additional information <1,2,4> (<4> (6-4) photolyase is examined by optical spectroscopy, electron paramagnetic resonance, and pulsed electron nuclear double resonance spectroscopy. It is suggested that His354 and His358 catalyze the formation of the oxetane intermediate that precedes light-initiated DNA repair. At pH 9.5 where the enzyme repair activity is highest His358 is deprotonated, whereas His354 is protonated, acting as the proton donor that initiates oxetane formation from the (6-4) photoproduct [8]; <1> binding and catalytic properties of the enzyme are investigated using natural substrates, T[6-4]T and T[6-4]C, and the Dewar isomer of (6-4) photoproduct and substrate analogs s5T[6-4]T/thietane, mes5T[6-4]T, and the N-methyl-3'T thietane analog of the oxetane inter-

mediate. The enzyme binds to the natural substrates and to mes5T[6-4]T with high affinity and produces a DNase I footprint of about 20 base pairs around the photolesion. Of the four substrates that bind with high affinity to the enzyme, T[6-4]T and T[6-4]C are repaired with relatively high quantum yields compared with the Dewar isomer and the mes5T[6-4]T which are repaired with 300-400-fold lower quantum yield [6]; <2> by electrophoretic mobility shift assay it is demonstrated that NF-10 binds to UV-irradiated double-stranded DNA but not to unirradiated DNA [14]; <1> enzyme catalyzes the light-dependent repair of (6-4) photoproducts in Drosophilia melanogaster [13]; <2> cyclobutane pyrimidine dimer-photolyase (EC 4.1.99.3) or 6-4PP-photolyase are able to prevent UV-induced apoptosis in cells deficient for nucleotide excision repair to a similar extent, while in nucleotide excision repair-proficient cells UV-induced apoptosis is prevented only by cyclobutane pyrimidine dimer-photolyase, with no effects observed when pyrimidine-(6-4)-pyrimidone photoproducts are removed by the specific photolyase. Both cyclobutane pyrimidine dimers and pyrimidine-(6-4)-pyrimidone photoproducts contribute to UV-induced apoptosis in nucleotide excision repair-deficient cells, while in nucleotide excision repair-proficient cells, cyclobutane pyrimidine dimers are the only lesions responsible for UV-killing, probably due to the rapid repair of pyrimidine-(6-4)-pyrimidone photoproducts by nucleotide excision repair [22]; <4> 2-thio analog of the the (6-4) photoproduct, in which the carbonyl group at the C_2 of the 3-pyrimidone is replaced with a thiocarbonyl group, is not repaired by the (6-4) photolyase. Cationic imine analogue of the (6-4) photoproduct, in which the carbonyl group at the C_2 of the 3-pyrimidone is replaced with an imine (T(6-4)TNH_2), is not repaired by the (6-4) photolyase, even in the presence of a 10 molar excess of the enzyme. 3carbonyl group of the (6-4) photoproduct is involved in the recognition and reaction of the (6-4) photolyse [28]; <1> can not repair T(Dew)T lesion, direct electron injection into the lesion may be the first step of the repair reaction performed by (6-4) DNA photolyase [26]; <4> imine analogue of the (6-4) photoproduct (T(6-4)TNH_2), in which the carbonyl group is replaced with an iminium cation, is not repaired by the (6-4) photolyase, even in the presence of a 10fold molar excess of the enzyme, although the enzyme binds to the oligonucleotide with considerable affinity. Carbonyl group of the 3 pyrimidone ring plays an important role in the (6-4) photolyase reaction [25]) (Reversibility: ?) [6,8,13,14,22,25,26,28]

P ?

Cofactors/prosthetic groups

8-hydroxy-5-deazariboflavin <1> [27]

FAD <1,2,3,4,5,6,9> (<3> Resonance Raman spectra of (6-4) photolyase having neutral semiquinoid and oxidized forms of FAD. Density functional theory (DFT) calculations are carried out on the neutral semiquinone. The marker band of a neutral semiquinone at 1606 cm-1 in H_2O, splits into two comparable bands at 1594 and 1608 cm-1 in D_2O, and similarly, that at 1522 cm-1

in H_2O does into three bands at 1456, 1508, and 1536 cm-1 in D_2O. This D_2O effect is recognized only after being oxidized once and photoreduced to form a semiquinone again, but not by simple H/D exchange of solvent. Some Raman bands of the oxidized form are observed at significantly low frequencies (1621, 1576 cm-1) and with band splittings (1508/1493, 1346/1320 cm-1). These Raman spectral characteristics indicate strong H-bonding interactions, a fairly hydrophobic environment, and an electron-lacking feature in benzene ring of the FAD cofactor, which seems to specifically control the reactivity of (6-4) photolyase [9]; <4> FAD cofactor photoactivation in (6-4) photolyase occurs via two sequential single-electron reduction steps with a tyrosine residue acting as final electron donor [3]; <9> non-covalently bound to the enzyme. Flavin to apoprotein molecular ratio of 64%. FAD is present in three different redox states: the fully oxidized form (FADox, 82%), the neutral semiquinone (14%) and the fully reduced anion (4%) [23]; <3> in the structure of (6-4) photolyase, there is a phosphate anion bound to Glu-243 and Trp-238, close to FAD [27]) [2,3,5,6,7,8,9,11,12,13,14,15,16,17,18,19,20,23,24,27]
Additional information <9> (<9> lacks a light-harvesting chromophore [23]) [23]

Activating compounds

DTT <4,5> [7,18]
dithionite <1> (<1> reduction of the FAD cofactor with dithionite increases the quantum yield of repair [6]) [6]

Metals, ions

Na^+ <4,5,6> [5,7,18]
Additional information <6> (<6> enzyme is also active under high salinity [5]; <6> NH_4Cl or NaH_2PO_4 increase activity of the enzyme. CH_3COONa or Na_2CO_3 strongly decrease the enzyme's activity. Maximum activity occurs in the presence of NaH_2PO_4, which is increased eight times than that in the presence of Na_2CO_3. When the ions that possess stronger ability to donate a proton are added to enzyme reaction buffer, the rate of photoreactivation increases [5]) [5]

Specific activity (U/mg)

Additional information <2,4,5,6> (<4> (6-4) photolyase binds to T[6-4]T in double stranded DNA with high affinity (K_D= 10*exp-9) and to T[6-4]T in single-stranded DNA with slightly lower-affinity (KD= 2*10 exp-8). Majority of the T[6-4]T-(6-4) photolyase complex dissociates very slowly (K_{off}= 2.9* 10exp-5/sec). Its absolute action spectrum without a second chromophore in the 350-600 nm region closely matches the absorption spectrum of the enzyme [7]; <5> activity is unstable [18]; <2> enzyme does not show any detectable photolyase activity [11]; <6> enzyme shows activity with the GST tag [5]; <4> the recombinant protein repairs (6-4)photoproducts [15]) [5,7,11, 15,18]

pH-Optimum

7.4 <4,5> (<4,5> assay at [7,18]) [7,18]
8 <4> (<4> assay at [16]) [16]

8.5 <4,6> (<6> maximum activity occurs at pH 8.5 and is 2.4fold higher than that at pH 7.0 [5]) [2,5]
9.5 <4> [8]

pH-Range

6-9.5 <4> [8]
8.5-9 <4,6> (<6> highest activity at [5]) [2,5]

4 Enzyme Structure

Molecular weight

40000 <2> (<2> SDS-PAGE [14]) [14]
62000 <1> (<1> SDS-PAGE [12]; <1> deduced from cDNA [20]) [12,20]
63000 <2> (<2> SDS-PAGE [11]) [11]
63920 <7> (<7> calculated from amino acid sequence [1]) [1]
65000 <7> (<7> SDS-PAGE [1]) [1]
67000 <8> (<8> deduced from cDNA [4]) [4]
110000 <1> (<1> molecular weight of fusion protein, determined by SDS-PAGE [10]) [10]

5 Isolation/Preparation/Mutation/Application

Source/tissue

HeLa cell <2> [14]
Xenopus A6 cell <4> (<4> exposure of the cells to blue light, but not red light, for 12 h results in more than 20fold increase of the (6-4) photolyase mRNA [21]) [21]
fibroblast <2,5> [18,22]
ovary <1> (<1> by Northern blot analysis it is demonstrated that the transcript is expressed at highest level only in adult ovary [20]) [20]
seedling <3> [19]
Additional information <2,3,6,7> (<7> gene is strongly expressed in the upper part of the animal and not in the middle part or the base [1]; <2> by Northern blot analysis an ubiquitous expression pattern is demonstrated [11]; <2> by Northern blot analysis it is demonstrated that the transcript is expressed in multiple tissues [20]; <6> expression levels of (6-4) photolyase in 24 h dark-maintained algae increase rapidly after 8-h exposure to white light, and also increase after being treated with NaCl for 8 h [5]; <2> immunoblot analysis using a monoclonal antibody reveals that the NF-10 protein is expressed in cell lines from all complementation groups of xeroderma pigmentosum [14]; <3> it is found that the 6-4 photoreactivating activity is constitutively expressed prior to as well as during the period of repair [19]) [1,5,11,14,19,20]

Purification

<1> [26]
<1> (by fractionation of crude cell extracts with Heparin agarose and UV DNA affinity column chromatography) [13]
<1> (by using affinity chromatography and UV-irradiated DNA attached beads) [20]
<1> (fusion protein is applied to amylose column. At this point the protein is above 90% pure. Further purification can be obtained by applying the eluted material to a 10 ml heparin-agarose column. Maltose-binding protein is removed by treatment with factor Xa protease) [10]
<1> (fusion protein is purified through a 20-ml amylose column and through heparin-agarose column) [6]
<1> (purified to near homogeneity from Drosophila embryonic cells by using NH_4SO_4 precipitation, SP sepharose column, UV DNA affinity beads, heparin sepharose column and Mono S column) [12]
<2> (NF^-1 is isolated from nuclear extracts prepared from HeLa cell culture using a heparin column, an anion exchange Fractogel EMD TMAE-650 (S) column and a FPLC MonoS HR5/5 column) [14]
<2> (by using a glutathione sepharose column and a Hi Trap Q column. Concentrated fusion protein is cleaved with thrombin from bovine plasma by incubation overnight at 4°C. For chromophore determination, the eluate from the glutathione sepharose column is purified through a Q sepharose column, omitting gel filtration procedure, and concentrated by ultrafiltration) [11]
<4> (by using a glutathione-Sepharose column and UV-irradiated DNA affinity column, fusion protein is cleaved with thrombin) [15]
<4> (by using glutathione-sepharose columns) [7]
<4> (protein is isolated from whole cell extracts from Xenopus laevis, purified by using a sepharose column and a UV-damaged DNA affinity column) [18]
<5> ((6-4) photoproduct DNA photolyase activity is detected in Crotalus atrox fibroblast. Activity is considerably enhanced when a UV-damaged DNA affinity column is used for purification. However, the activity is unstable and it is lost during purification or upon storage at -20° or -70°C for 2-3 months) [18]
<6> (by using glutathione-sepharose columns) [5]
<9> [23]

Crystallization

<1> (T(6-4)C lesion containing DNA duplex in complex with the (6-4) photolyase, by the hanging-drop vapour diffusion method, at 18°C, to 2.95 A resolution. Lesion is flipped out of the opened DNA duplex into the active site of the enzyme) [26]
<1> (two crystal structures of the (6-4) photolyase bound to lesion containing DNA before and after repair, repair does not involve oxetane formation before light-induced electron transfer. The histidine 369, supposed to activate the acylimine, is in a position that does not allow efficient proton donation and hence activation of this substructure) [27]
<3> (hanging drop vapor diffusion at 4°C) [24]

Cloning

<1> (due to insolubility problems (6-4) photolyases is overexpressed as a fusion protein in Escherichia coli. Plasmid pXZ1997, a derivative of pMal-c2 containing the Drosophila melanogaster phr(6-4) cDNA fused in frame to the malE gene encoding maltose-binding protein (MBP), is propagated in Escherichia coli strain UNC523 (phr::kan uvrA::Tn10) selecting for ampicillin resistance. Cells are cultured in 2 liter of LB to A600: 0.6-0.8. IPTG is added to 0.3 mM, and incubation continued for 6 h prior to harvesting the cells by centrifugation.) [10]
<1> (expressed in Escherichia coli as a MBP-PL-(6-4) fusion protein) [6]
<1> (overexpressed in Escherichia coli) [26]
<1> (recombinant protein expressed in Escherichia coli) [20]
<2> (expressed as a GSTtagged fusion protein in Escherichia coli) [11]
<3> (expressed in Escherichia coli) [9]
<3> (expression in Escherichia coli) [24]
<4> (cloned and overexpressed in Escherichia coli) [8]
<4> (expressed as a GST-fusion protein in Escherichia coli) [7]
<4> (expressed in Escherichia coli) [2]
<4> (expressed in Escherichia coli as a GST-fusion protein) [15]
<6> (expressed as a GST-tagged fusion protein in Escherichia coli) [5]
<7> (expressed in Escherichia coli, fusion protein with glutathione S-transferase) [1]
<8> (a cDNA of (6-4)photolyase from Dunaliella salina is cloned, sequenced and its amino acid sequence is deduced) [4]
<9> [23]

Engineering

H354A <4> (<4> almost complete loss of repair activity [2]; <4> mutation of a conserved His residue: mutant is inactive in photorepair [8]) [2,8]
H358A <4> (<4> almost complete loss of repair activity, suggesting that His354 and His358 are essential for catalytic activity [2]; <4> mutation of a conserved His residue: mutant is inactive in photorepair [8]) [2,8]
L355A <4> (<4> large decrease in the affinity to the (6-4) photoproduct substrate, suggesting a hydrophobic interaction with the (6-4)photoproduct [2]) [2]
Q288A <4> (<4> repair activity is not reduced [2]) [2]
W291A <4> (<4> some enzymatic activity is retained [2]) [2]
W398A <4> (<4> some enzymatic activity is retained [2]) [2]
Additional information <2,3,4,8> (<8> construction of a theoretical 3D model shows that the protein has a FAD-binding domain. Although the amino acids identity between Dunaliella salina (6-4)photolyase and Escherichia coli CPD photolyase is just 23%, the backbone structure shows a high similarity in overall folding, suggesting a parallel photoreversal mechanism in the two enzymes [4]; <2> expression of H64PRH does not show any photoreactivating effects on the survival of UV-irradiated Escherichia coli. Using a gel shift assay with with un-irradiated and UV-irradiated DNA probes it is shown that H64PRH protein does not possess any binding activity to either DNA probe

[11]; <3> light-dependent repair of UV-induced (6-4) photoproducts is investigated in an excision repair-deficient Arabidopsis mutant. It is demonstrated that (6-4) photoproducts are efficiently eliminated in a light-dependent manner which occurs in the presence of blue light (435 nm) but not upon exposure to light of longer wavelengths [19]; <4> sequencing of the cDNA clone reveals an open reading frame of encoding a protein of 526 amino acids (60600 Da) cDNA shows 58-54% amino acid identity to Drosophila (6-4)photolyase and its human homologue and 20-24% identity to the class I CPD photolyase [15]; <2> the predicted amino acid sequence of the human protein has 48% identity with the Drosophila (6-4)photolyase over the entire protein [20]) [4,11,15,19,20]

6 Stability

Storage stability

<1>, glycerol to a final concentration of 50% (v/v) is added to the photolyase, storage at -70°C [10]

<2>, protein is stored in aliquots at -80 °C after addition of glycerol to 20% [14]

<4>, protein in aliquots is kept at -20°C until further use or stored at -80°C. The protein sample remained active after 6 months storage [18]

<5>, activity is unstable and it is lost upon storage at -20° or -70°C for 2-3 months [18]

References

[1] Schroder, H.C.; Krasko, A.; Gundacker, D.; Leys, S.P.; Muller, I.M.; Muller, W.E.: Molecular and functional analysis of the (6-4) photolyase from the hexactinellid Aphrocallistes vastus. Biochim. Biophys. Acta, **1651**, 41-49 (2003)

[2] Hitomi, K.; Nakamura, H.; Kim, S.T.; Mizukoshi, T.; Ishikawa, T.; Iwai, S.; Todo, T.: Role of two histidines in the (6-4) photolyase reaction. J. Biol. Chem., **276**, 10103-10109 (2001)

[3] Weber, S.; Kay, C.W.; Mogling, H.; Mobius, K.; Hitomi, K.; Todo, T.: Photoactivation of the flavin cofactor in Xenopus laevis (6 - 4) photolyase: observation of a transient tyrosyl radical by time-resolved electron paramagnetic resonance. Proc. Natl. Acad. Sci. USA, **99**, 1319-1322 (2002)

[4] Yi, Y.; Yi, C.; Qian, L.; Min, L.; Long, C.; Linhan, B.; Zhirong, Y.; Dairong, Q.: Cloning and sequence analysis of the gene encoding (6-4) photolyase from Dunaliella salina. Biotechnol. Lett., **28**, 309-314 (2006)

[5] Yan Lv, X.; Rong Qiao, D.; Xiong, Y.; Xu, H.; You, F.F.; Cao, Y.; He, X.: Photoreactivation of (6-4) photolyase in Dunaliella salina. FEMS Microbiol. Lett., **283**, 42-46 (2008)

[6] Zhao, X.; Liu, J.; Hsu, D.S.; Zhao, S.; Taylor, J.S.; Sancar, A.: Reaction mechanism of (6-4) photolyase. J. Biol. Chem., **272**, 32580-32590 (1997)

[7] Hitomi, K.; Kim, S.T.; Iwai, S.; Harima, N.; Otoshi, E.; Ikenaga, M.; Todo, T.: Binding and catalytic properties of Xenopus (6-4) photolyase. J. Biol. Chem., **272**, 32591-32598 (1997)
[8] Schleicher, E.; Hitomi, K.; Kay, C.W.; Getzoff, E.D.; Todo, T.; Weber, S.: Electron nuclear double resonance differentiates complementary roles for active site histidines in (6-4) photolyase. J. Biol. Chem., **282**, 4738-4747 (2007)
[9] Li, J.; Uchida, T.; Ohta, T.; Todo, T.; Kitagawa, T.: Characteristic structure and environment in FAD cofactor of (6-4) photolyase along function revealed by resonance Raman spectroscopy. J. Phys. Chem. B, **110**, 16724-16732 (2006)
[10] Sancar, G.B.; Sancar, A.: Purification and characterization of DNA photolyases. Methods Enzymol., **408**, 121-156 (2006)
[11] Todo, T.; Tsuji, H.; Otoshi, E.; Hitomi, K.; Kim, S.T.; Ikenaga, M.: Characterization of a human homolog of (6-4) photolyase. Mutat. Res., **384**, 195-204 (1997)
[12] Todo, T.; Ryo, H.; Borden, A.; Lawrence, C.; Sakaguchi, K.; Hirata, H.; Nomura, T.: Non-mutagenic repair of (6-4)photoproducts by (6-4)photolyase purified from Drosophila melanogaster. Mutat. Res., **385**, 83-93 (1997)
[13] Todo, T.; Takemori, H.; Ryo, H.; Ihara, M.; Matsunaga, T.; Nikaido, O.; Sato, K.; Nomura, T.: A new photoreactivating enzyme that specifically repairs ultraviolet light-induced (6-4)photoproducts. Nature, **361**, 371-374 (1993)
[14] Wakasugi, M.; Abe, Y.; Yoshida, Y.; Matsunaga, T.; Nikaido, O.: Purification of a novel UV-damaged-DNA binding protein highly specific for (6-4) photoproduct. Nucleic Acids Res., **24**, 1099-1004 (1996)
[15] Todo, T.; Kim, S.T.; Hitomi, K.; Otoshi, E.; Inui, T.; Morioka, H.; Kobayashi, H.; Ohtsuka, E.; Toh, H.; Ikenaga, M.: Flavin adenine dinucleotide as a chromophore of the Xenopus (6-4)photolyase. Nucleic Acids Res., **25**, 764-768 (1997)
[16] Yamamoto, J.; Hitomi, K.; Todo, T.; Iwai, S.: Synthesis of oligonucleotides containing the Dewar valence isomer of the (6-4) photoproduct and their application to (6-4) photolyase studies. Nucleic Acids Symp. Ser., **50**, 61-62 (2006)
[17] Iwai, S.; Mizukoshi, T.; Hitomi, K.; Todo, T.: Chemical synthesis of oligonucleotides containing the (6-4) photoproduct at the thymine-cytosine site and its repair by (6-4) photolyase. Nucleosides Nucleotides, **18**, 1325-1327 (1999)
[18] Kim, S.T.; Malhotra, K.; Taylor, J.S.; Sancar, A.: Purification and partial characterization of (6-4) photoproduct DNA photolyase from Xenopus laevis. Photochem. Photobiol., **63**, 292-295 (1996)
[19] Chen, J.J.; Mitchell, D.L.; Britt, A.B.: A light-dependent pathway for the elimination of UV-induced pyrimidine (6-4) pyrimidinone photoproducts in Arabidopsis. Plant Cell, **6**, 1311-1317 (1994)
[20] Todo, T.; Ryo, H.; Yamamoto, K.; Toh, H.; Inui, T.; Ayaki, H.; Nomura, T.; Ikenaga, M.: Similarity among the Drosophila (6-4)photolyase, a human photolyase homolog, and the DNA photolyase-blue-light photoreceptor family. Science, **272**, 109-112 (1996)

[21] Fukushima, N.; Naito, Y.; Ryoji, M.: Induction of (6-4) photolyase gene transcription by blue light in Xenopus A6 cells. Biochem. Biophys. Res. Commun., **383**, 231-234 (2009)
[22] de Lima-Bessa, K.M.; Armelini, M.G.; Chigancas, V.; Jacysyn, J.F.; Amarante-Mendes, G.P.; Sarasin, A.; Menck, C.F.: CPDs and 6-4PPs play different roles in UV-induced cell death in normal and NER-deficient human cells. DNA Repair, **7**, 303-312 (2008)
[23] Usman, A.; Brazard, J.; Martin, M.M.; Plaza, P.; Heijde, M.; Zabulon, G.; Bowler, C.: Spectroscopic characterization of a (6-4) photolyase from the green alga Ostreococcus tauri. J. Photochem. Photobiol. B Biol., **96**, 38-48 (2009)
[24] Hitomi, K.; DiTacchio, L.; Arvai, A.S.; Yamamoto, J.; Kim, S.T.; Todo, T.; Tainer, J.A.; Iwai, S.; Panda, S.; Getzoff, E.D.: Functional motifs in the (6-4) photolyase crystal structure make a comparative framework for DNA repair photolyases and clock cryptochromes. Proc. Natl. Acad. Sci. USA, **106**, 6962-6967 (2009)
[25] Yamamoto, J.; Hitomi, K.; Hayashi, R.; Getzoff, E.D.; Iwai, S.: Role of the carbonyl group of the (6-4) photoproduct in the (6-4) photolyase reaction. Biochemistry, **48**, 9306-9312 (2009)
[26] Glas, A.F.; Schneider, S.; Maul, M.J.; Hennecke, U.; Carell, T.: Crystal structure of the T(6-4)C lesion in complex with a (6-4) DNA photolyase and repair of UV-induced (6-4) and Dewar photolesions. Chemistry, **15**, 10387-10396 (2009)
[27] Mueller, M.; Carell, T.: Structural biology of DNA photolyases and cryptochromes. Curr. Opin. Struct. Biol., **19**, 277-285 (2009)
[28] Yamamoto, J.; Hitomi, K.; Hayashi, R.; Getzoff, E.D.; Iwai, S.: Recognition and reaction mechanisms of the (6-4) photolyase as determined by using a (6-4) photoproduct analog. Nucleic Acids Symp. Ser., **53**, 221-222 (2009)

spore photoproduct lyase 4.1.99.14

1 Nomenclature

EC number
4.1.99.14

Systematic name
spore photoproduct pyrimidine-lyase

Recommended name
spore photoproduct lyase

Synonyms
SAM <2> [1]
SP lyase <1,2> [1,2]
SPL <2> [1,2]
spore photoproduct lyase <1,2> [1]

2 Source Organism

<1> *Bacillus subtilis* [1]
<2> *Clostridium acetobutylicum* [2]

3 Reaction and Specificity

Catalyzed reaction
(5R)-5,6-dihydro-5-(thymidin-7-yl)thymidine (in double-helical DNA) = thymidylyl-(3'→5')-thymidylate (in double-helical DNA)

Natural substrates and products
S (5''R)-α-5''(6''H)-bithymine + S-adenosyl-L-methionine <2> (<2> SPL repairs specifically the 5R isomer. (5R)-α-5(6H)-bithymine is the diastereomer produced upon UV irradiation of a TpT dinucleotide [2]) (Reversibility: ?) [2]
P thymidylyl-(3'-5')-thymidylate + 5'-deoxyadenosine + L-methionine

Substrates and products
S (5''-R)-α-5''(6''-H)-bithymine + S-adenosyl-L-methionine <2> (<2> SPL repairs specifically the 5R isomer. (5R)-α-5(6H)-bithymine is the diastereomer produced upon UV irradiation of a TpT dinucleotide [2]; <2> SPL repairs specifically the 5R isomer [2]) (Reversibility: ?) [2]
P thymidylyl-(3'-5')-thymidylate + 5'-deoxyadenosine + L-methionine

D. Schomburg and I. Schomburg (eds.), *Class 3.4–6 Hydrolases, Lyases, Isomerases, Ligases: EC 3.4–6*, Springer Handbook of Enzymes S10, DOI 10.1007/978-3-642-36260-6_39,

S 5-thyminyl-5,6 dihydrothymine + S-adenosyl-L-methionine <1> (Reversibility: ?) [1]
P thymidylyl-(3'-5')-thymidylate + 5'-deoxyadenosine + L-methionine

Cofactors/prosthetic groups
S-adenosyl-L-methionine <1> [1]

Metals, ions
Fe <2> (<2> iron-sulfur enzyme, 2.9 Fe per enzyme [2]) [2]

5 Isolation/Preparation/Mutation/Application

Cloning
<2> (overexpression in Escherichia coli) [2]

Application
analysis <1> (<1> a rapid separation technique for detecting and quantitating SP by chromatography : tritiated thymine-containing photoproducts from trifluoroacetic acid-hydrolyzed DNA purified from UV-irradiated cells or spores of Bacillus subtilis are identified and isolated from paper chromatograms, subjected to HPLC on a Microsorb phenyl 5-micrometer column using 100% water as the mobile phase, and detected by scintillation counting of collected fractions [1]) [1]

References

[1] Sun, Y.; Palasingam, K.; Nicholson, W.L.: High-pressure liquid chromatography assay for quantitatively monitoring spore photoproduct repair mediated by spore photoproduct lyase during germination of uv-irradiated Bacillus subtilis spores. Anal. Biochem., **221**, 61-65 (1994)
[2] Chandra, T.; Silver, S.C.; Zilinskas, E.; Shepard, E.M.; Broderick, W.E.; Broderick, J.B.: Spore photoproduct lyase catalyzes specific repair of the 5R but not the 5S spore photoproduct. J. Am. Chem. Soc., **131**, 2420-2421 (2009)

S-specific spore photoproduct lyase 4.1.99.15

1 Nomenclature

EC number
4.1.99.15 (deleted)

Recommended name
S-specific spore photoproduct lyase

This enzyme was classified on the basis of an incorrect reaction. The activity is covered by EC 4.1.99.14, spore photoproduct lyase.

D. Schomburg and I. Schomburg (eds.), *Class 3.4–6 Hydrolases, Lyases, Isomerases, Ligases: EC 3.4–6*, Springer Handbook of Enzymes S10, DOI 10.1007/978-3-642-36260-6_40,

methanogen homoaconitase 4.2.1.114

1 Nomenclature

EC number
4.2.1.114

Systematic name
(R)-2-hydroxybutane-1,2,4-tricarboxylate hydro-lyase [(1R,2S)-1-hydroxybutane-1,2,4-tricarboxylate-forming]

Recommended name
methanogen homoaconitase

Synonyms
HACN <1,2> [1,2]
Homoaconitase <2> [1]
MJ1003 <1> (<1> large subunit protein of HACN [2]) [2]
MJ1271 <1> (<1> small subunit protein of HACN [2]) [2]
methanogen HACN
Additional information <2> (<2> the enzyme belongs to the aconitase superfamily [1]) [1]

2 Source Organism

<1> *Methanocaldococcus jannaschii* [2]
<2> *Methanocaldococcus jannaschii* (UNIPROT accession number: Q58991, the sequence contains the alteration $C_{22}9A$ resulting in Q77K amino acid exchange compared to the MJ1596 sequence reported by the genome sequencing project, cf. EC 1.1.1.87 [1]) [1]

3 Reaction and Specificity

Catalyzed reaction
(R)-2-hydroxybutane-1,2,4-tricarboxylate = (1R,2S)-1-hydroxybutane-1,2,4-tricarboxylate (overall reaction)
(1a) (R)-2-hydroxybutane-1,2,4-tricarboxylate = (Z)-but-1-ene-1,2,4-tricarboxylate + H_2O
(1b) (Z)-but-1-ene-1,2,4-tricarboxylate + H_2O = (1R,2S)-1-hydroxybutane-1,2,4-tricarboxylate

D. Schomburg and I. Schomburg (eds.), *Class 3.4–6 Hydrolases, Lyases, Isomerases, Ligases: EC 3.4–6*, Springer Handbook of Enzymes S10, DOI 10.1007/978-3-642-36260-6_41,

Natural substrates and products

- **S** Additional information <2> (<2> homoaconitase enzymes catalyze hydrolyase reactions in the α-aminoadipate pathway for lysine biosynthesis or the 2-oxosuberate pathway for methanogenic coenzyme B biosynthesis [1]) (Reversibility: ?) [1]
- **P** ?

Substrates and products

- **S** (1E)-hex-1-ene-1,2,6-tricarboxylic acid + H_2O <1> (Reversibility: ?) [2]
- **P** (2R)-hexane-1,2,6-tricarboxyclic acid
- **S** (1E)-pent-1-ene-1,2,5-tricarboxylic acid + H_2O <1> (Reversibility: ?) [2]
- **P** (2R)-pentane-1,2,5-tricarboxylic acid
- **S** (2R)-butane-1,2,4-tricarboxylic acid <1> (Reversibility: ?) [2]
- **P** but-1-ene-1,2,4-tricarboxylic acid + H_2O
- **S** (R)-2-hydroxybutane-1,2,4-tricarboxylate <2> (<2> i.e. (R)-homocitrate, first half-reaction [1]) (Reversibility: r) [1]
- **P** (Z)-but-1-ene-1,2,4-tricarboxylate + H_2O (<2> i.e. cis-homoaconitate, the activity in the reverse direction is similar as with (R)-homocitrate [1])
- **S** (R)-2-hydroxybutane-1,2,4-tricarboxylate <2> (<2> i.e. (R)-homocitrate, overall reaction, the enzyme catalyzes both the dehydration of (R)-homocitrate to form cis-homoaconitate, and hydration producing homoisocitrate [1]) (Reversibility: r) [1]
- **P** (1R,2S)-1-hydroxybutane-1,2,4-tricarboxylate (<2> i.e. homoisocitrate [1])
- **S** (Z)-but-1-ene-1,2,4-tricarboxylate + H_2O <2> (<2> second half-reaction [1]) (Reversibility: r) [1]
- **P** (1R,2S)-1-hydroxybutane-1,2,4-tricarboxylate (<2> i.e. homoisocitrate [1])
- **S** but-1-ene-1,2,4-tricarboxylic acid + H_2O <1> (Reversibility: ?) [2]
- **P** (2R)-butane-1,2,4-tricarboxylic acid
- **S** cis-$(homo)_2$aconitate + H_2O <2> (<2> the activity is similar as with (R)-homocitrate [1]) (Reversibility: ?) [1]
- **P** ?
- **S** cis-$(homo)_3$aconitate + H_2O <2> (<2> the activity is similar as with (R)-homocitrate [1]) (Reversibility: ?) [1]
- **P** ?
- **S** cis-$(homo)_4$aconitate + H_2O <2> (<2> the activity is similar as with (R)-homocitrate [1]) (Reversibility: ?) [1]
- **P** ?
- **S** maleate + H_2O <2> (Reversibility: ?) [1]
- **P** ?
- **S** Additional information <1,2> (<2> homoaconitase enzymes catalyze hydrolyase reactions in the α-aminoadipate pathway for lysine biosynthesis or the 2-oxosuberate pathway for methanogenic coenzyme B biosynthesis [1]; <2> homoaconitase together with the endogenous homoisocitrate dehydrogenase, EC 1.1.1.87, catalyze all of the isomerization and oxidative decarboxylation reactions required to form 2-oxoadipate, 2-oxopimelate,

and 2-oxosuberate, completing three iterations of the 2-oxoacid elongation pathway. Methanogenic archaeal homoaconitases and fungal homoaconitases evolved in parallel in the aconitase superfamily, LC-MS analysis of enzyme reaction products, overview [1]; <1> HACN has no detectable activity with citraconate or isopropylmalate [2]) (Reversibility: ?) [1,2]

P ?

Inhibitors

(S)-homocitrate <2> (<2> complete inhibition at 0.1 mM [1]) [1]
cis-aconitate <2> (<2> 50% inhibition of the hydrolase activity at 0.025 mM [1]) [1]
cis-homoaconitate/(R)-homocitrate <2> (<2> mixtures of 0.1 mM cis-homoaconitate and 0.05 mM (R)-homocitrate reduce the HACN hydrolyase activity by 50% [1]) [1]
trans-(homo)3aconitate <2> (<2> 50% inhibition of the hydrolase activity at 0.4 mM [1]) [1]
trans-aconitate <2> (<2> 50% inhibition of the hydrolase activity at 0.1 mM [1]) [1]
Additional information <2> (<2> no inhibition by citraconate up to 0.2 mM [1]) [1]

Metals, ions

Fe^{2+} <2> (<2> the enzyme contains an iron-sulfur center, reconstitution of the purified recombinant apoenzyme with iron-sulfur, overview [1]) [1]
Mg^{2+} <2> (<2> required for the hydratase reaction, not for the hydrolase reaction [1]) [1]

Turnover number (s^{-1})

0.37 <2> ((R)-homocitrate, <2> pH 8.5, 60°C, recombinant enzyme, dehydratase reaction [1]) [1]
0.48 <1> (but-1-ene-1,2,4-tricarboxylic acid, <1> mutant enzyme R26V [2]) [2]
0.66 <1> ((1E)-pent-1-ene-1,2,5-tricarboxylic acid, <1> wild type enzyme [2]) [2]
0.66 <2> (cis-homo2aconitate, <2> pH 9.0, 60°C, recombinant enzyme, hydrolase reaction [1]) [1]
0.75 <1> (but-1-ene-1,2,4-tricarboxylic acid, <1> wild type enzyme [2]) [2]
0.75 <2> (cis-homoaconitate, <2> pH 9.0, 60°C, recombinant enzyme, hydrolase reaction [1]) [1]
1.43 <1> (but-1-ene-1,2,4-tricarboxylic acid, <1> mutant enzyme R26K [2]) [2]
1.7 <1> (but-1-ene-1,2,4-tricarboxylic acid, <1> mutant enzyme R26V/T27Y [2]) [2]
1.9 <1> ((1E)-hex-1-ene-1,2,6-tricarboxylic acid, <1> mutant enzyme R26V/T27Y [2]) [2]
2.2 <1> ((1E)-pent-1-ene-1,2,5-tricarboxylic acid, <1> mutant enzyme T27A [2]) [2]

2.5 <1> ((1E)-hex-1-ene-1,2,6-tricarboxylic acid, <1> wild type enzyme [2]) [2]
2.5 <1> (but-1-ene-1,2,4-tricarboxylic acid, <1> mutant enzyme T27A [2]) [2]
2.5 <2> (cis-homo3aconitate, <2> pH 9.0, 60°C, recombinant enzyme, hydrolase reaction [1]) [1]
2.8 <1> ((1E)-hex-1-ene-1,2,6-tricarboxylic acid, <1> mutant enzyme R26V [2]) [2]
4.1 <1> ((1E)-hex-1-ene-1,2,6-tricarboxylic acid, <1> mutant enzyme T27A [2]) [2]
5.6 <2> (cis-homo4aconitate, <2> pH 9.0, 60°C, recombinant enzyme, hydrolase reaction [1]) [1]
5.8 <1> ((1E)-pent-1-ene-1,2,5-tricarboxylic acid, <1> mutant enzyme R26V [2]) [2]
6 <2> (maleate, <2> pH 9.0, 60°C, recombinant enzyme, hydrolase reaction [1]) [1]
6.6 <1> ((1E)-pent-1-ene-1,2,5-tricarboxylic acid, <1> mutant enzyme R26V/T27Y [2]) [2]

K_m-Value (mM)

0.022 <1> (but-1-ene-1,2,4-tricarboxylic acid, <1> wild type enzyme [2]) [2]
0.022 <2> (cis-homoaconitate, <2> pH 9.0, 60°C, recombinant enzyme, hydrolase reaction [1]) [1]
0.03 <1> ((1E)-pent-1-ene-1,2,5-tricarboxylic acid, <1> wild type enzyme [2]) [2]
0.03 <2> (cis-homo2aconitate, <2> pH 9.0, 60°C, recombinant enzyme, hydrolase reaction [1]) [1]
0.036 <1> ((1E)-hex-1-ene-1,2,6-tricarboxylic acid, <1> wild type enzyme [2]) [2]
0.036 <2> (cis-homo3aconitate, <2> pH 9.0, 60°C, recombinant enzyme, hydrolase reaction [1]) [1]
0.135 <1> (but-1-ene-1,2,4-tricarboxylic acid, <1> mutant enzyme R26K [2]) [2]
0.175 <2> (cis-homo4aconitate, <2> pH 9.0, 60°C, recombinant enzyme, hydrolase reaction [1]) [1]
0.22 <1> (but-1-ene-1,2,4-tricarboxylic acid, <1> mutant enzyme R26V [2]; <1> mutant enzyme T27A [2]) [2]
0.269 <1> ((1E)-pent-1-ene-1,2,5-tricarboxylic acid, <1> mutant enzyme T27A [2]) [2]
0.33 <2> (maleate, <2> pH 9.0, 60°C, recombinant enzyme, hydrolase reaction [1]) [1]
0.46 <1> (but-1-ene-1,2,4-tricarboxylic acid, <1> mutant enzyme R26V/T27Y [2]) [2]
0.64 <1> ((1E)-hex-1-ene-1,2,6-tricarboxylic acid, <1> mutant enzyme R26V/T27Y [2]) [2]
0.65 <1> ((1E)-hex-1-ene-1,2,6-tricarboxylic acid, <1> mutant enzyme T27A [2]) [2]

0.66 <1> ((1E)-hex-1-ene-1,2,6-tricarboxylic acid, <1> mutant enzyme R26V [2]) [2]
0.87 <1> ((1E)-pent-1-ene-1,2,5-tricarboxylic acid, <1> mutant enzyme R26V [2]) [2]
1.5 <2> ((R)-homocitrate, <2> pH 8.5, 60°C, recombinant enzyme, dehydratase reaction [1]) [1]
1.6 <1> ((1E)-pent-1-ene-1,2,5-tricarboxylic acid, <1> mutant enzyme R26V/T27Y [2]) [2]
Additional information <2> (<2> steady-state kinetics [1]) [1]

pH-Optimum
8.5 <2> (<2> hydratase assay at [1]) [1]
9 <2> (<2> hydrolase assay at [1]) [1]

Temperature optimum (°C)
60 <2> (<2> hydrolase and hydratase assay at [1]) [1]

4 Enzyme Structure

Subunits
tetramer <2> (<2> heterotetramer, MJ1003 and MJ1271 proteins form an active homoaconitase enzyme [1]) [1]

5 Isolation/Preparation/Mutation/Application

Purification
<1> (Toyopearl SuperQ-650 M column chromatography, Resource S column chromatography, and Superdex 200 gel filtration) [2]
<2> (recombinant MJ1003 and MJ1271 proteins from Escherichia coli strain BL21(DE3) by heat treatment of the cell lysate, followed by anion exchange chromatography, dialysis, and ultrafiltration) [1]

Crystallization
<1> (small-subunit HACN protein (MJ1271), micro batch method, using 50% (w/v) polyethylene glycol 200 and 0.1 M Tris-HCl, pH 4.6, at 20°C) [2]

Cloning
<1> (small-subunit HACN protein MJ1271 is expressed in Escherichia coli BL21 CodonPlus (DE3)-RIL cells) [2]
<2> (DNA and amino acid sequence determination and analysis, coexpression of MJ1003 and MJ1271 proteins in Escherichia coli strain BL21(DE3)) [1]

Engineering
R26K <1> (<1> the variant forms an relatively efficient isopropylmalate isomerase enzyme [2]) [2]
R26V <1> (<1> the variant forms an relatively efficient isopropylmalate isomerase enzyme [2]) [2]

R26V/T27Y <1> (<1> the variant resembles the MJ1277 isopropylmalate isomerase small subunit in its flexible loop sequence but demonstrates the broad substrate specificity of the R26V variant [2]) [2]
T27A t <1> (<1> the variant has uniformly lower specificity constants for both isopropylmalate isomerase and methanogen homoaconitase substrates [2]) [2]

References

[1] Drevland, R.M.; Jia, Y.; Palmer, D.R.; Graham, D.E.: Methanogen homoaconitase catalyzes both hydrolyase reactions in coenzyme B biosynthesis. J. Biol. Chem., **283**, 28888-28896 (2008)
[2] Jeyakanthan, J.; Drevland, R.M.; Gayathri, D.R.; Velmurugan, D.; Shinkai, A.; Kuramitsu, S.; Yokoyama, S.; Graham, D.E.: Substrate specificity determinants of the methanogen homoaconitase enzyme: structure and function of the small subunit. Biochemistry, **49**, 2687-2696 (2010)

UDP-N-acetylglucosamine 4,6-dehydratase (inverting) 4.2.1.115

1 Nomenclature

EC number
4.2.1.115

Systematic name
UDP-N-acetylglucosamine hydro-lyase (inverting; UDP-2-acetamido-2,6-dideoxy-β-L-arabino-hex-4-ulose-forming)

Recommended name
UDP-N-acetylglucosamine 4,6-dehydratase (inverting)

Synonyms
4,6-dehydratase/5-epimerase <1> [2]
Cj1293 <2> [9]
FlaA1 <1,3,5,6> [4,5,6,7,8,9]
HP0840 <1> [9]
$NAD(P)^+$-dependent dehydratase/epimerase <1> [3]
PseB <1,2> [1,2,3,9]
UDP-GlcNAc 5-inverting 4,6-dehydratase <2> [1]
UDP-GlcNAc C6 dehydratase <1,4> [7,10]
UDP-GlcNAc C6 dehydratase/C4 reductase <1> [7]
UDP-N-acetylglucosamine 5-inverting 4,6-dehydratase <2> [1]
UDP-α-D-GlcNAc modifying dehydratase <1,2> [9]
WbpM <4> [10]
inverting 4,6-dehydratase <1> [8]
Additional information <1,2> (<1> the enzyme belongs to the SDR superfamily [8]; <2> the enzyme is a member of the short chain dehydrogenase/reductase, SDR, family [1]) [1,8]

CAS registry number
9076-60-2

2 Source Organism

<1> *Helicobacter pylori* [2,3,6,7,8,9]
<2> *Campylobacter jejuni* [1,9]
<3> *Brachyspira hyodysenteriae* [4]
<4> *Pseudomonas aeruginosa* (UNIPROT accession number: P72145) [10]
<5> *Helicobacter pylori* (UNIPROT accession number: Q6VYQ6) (strain NCTC 11637 [5]) [5]

D. Schomburg and I. Schomburg (eds.), *Class 3.4–6 Hydrolases, Lyases, Isomerases, Ligases: EC 3.4–6*, Springer Handbook of Enzymes S10, DOI 10.1007/978-3-642-36260-6_42,

<6> *Helicobacter pylori* (UNIPROT accession number: Q6VYQ5) (strain SS1 [5]) [5]

3 Reaction and Specificity

Catalyzed reaction

UDP-N-acetylglucosamine = UDP-2-acetamido-2,6-dideoxy-β-L-arabino-hex-4-ulose + H_2O (<2> Asp126, Lys127, and Tyr135 are the active site residues [1]; <4> reaction mechanism of WbpM [10]; <1> reaction mechanism, FlaA1 is a UDP-GlcNAc 4,6-dehydratase that additionally inverts the chirality at the C-5 position [8])

Natural substrates and products

- **S** UDP-GlcNAc <2> (<2> the enzyme is involved in the pseudaminic acid biosynthesis, it is responsible for the biosynthesis of 6-deoxyhexose [1]) (Reversibility: ?) [1]
- **P** UDP-2-acetamido-2,6-dideoxy-β-L-arabino-hexos-4-ulose + H_2O
- **S** UDP-N-acetylglucosamine <1,4> (<1> production of a precursor of pseudaminic acid, i.e. 5,7-diacetamido-3,5,7,9-tetradeoxy-L-glycero-α-L-manno-nonulosonic acid, required for flagellin glycosylation in Helicobacter pylori, analysis of all reaction steps in the pathway and related enzymes, overview [3]; <1> the enzyme catalyzes the first step in the biosynthetic pathway of a pseudaminic acid derivative, which is implicated in protein glycosylation [8]; <1> the enzyme is required for pseudaminic acid biosynthesis, which is required for O-linked flagellin glycosylation [2]; <4> WbpM is specific for UDP-GlcNAc [10]) (Reversibility: ?) [2,3,6,7,8,10]
- **P** UDP-2-acetamido-2,6-dideoxy-β-L-arabino-hex-4-ulose + H_2O
- **S** UDP-N-acetylglucosamine <1,2> (<2> the Cj1293 enzyme exhibits C6 dehydratase as well as C5 epimerase activity resulting in the production of both UDP-2-acetamido-2,6-dideoxy-β-L-arabino-4-hexulose and UDP-2-acetamido-2,6-dideoxy-α-D-xylo-4-hexulose. The enzyme is involved in biosynthesis of pseudaminic acid for glycomodification of the bacterial falgellins, overview [9]; <1> the HP0840 enzyme exhibits C6 dehydratase as well as C5 epimerase activity resulting in the production of both UDP-2-acetamido-2,6-dideoxy-β-L-arabino-4-hexulose and UDP-2-acetamido-2,6-dideoxy-α-D-xylo-4-hexulose. The enzyme is involved in biosynthesis of pseudaminic acid for glycomodification of the bacterial falgellins, overview [9]) (Reversibility: ?) [9]
- **P** UDP-2-acetamido-2,6-dideoxy-β-L-arabino-4-hexulose + UDP-2-acetamido-2,6-dideoxy-α-D-xylo-4-hexulose + H_2O
- **S** Additional information <1,2,4,5,6> (<1> dependence of O-linked flagellin glycosylation on PseB, cross-talk between the Pse and α-D-QuiNAc4NAc, i.e. 2,4-diacetamido-2,4,6-trideoxy-a-d-Glc, pathways via PseB [2]; <5> the enzyme is involved in lipopolysaccharide biosynthesis, flagellum assembly, or protein glycosylation, and might play an important role in the pathogenesis of Helicobacter pylori. It is at the interface between several

pathways that govern the expression of different virulence factors synthesizing sugar derivatives dedicated to the glycosylation of proteins which are involved in lipopolysaccharide and flagellum production with glycosylation regulating the activity of these proteins [5]; <6> the enzyme is involved in lipopolysaccharide biosynthesis, flagellum assembly, or protein glycosylation, and might play an important role in the pathogenesis of Helicobacter pylori. It is at the interface between several pathways that govern the expression of different virulence factors synthesizing sugar derivatives dedicated to the glycosylation of proteins which are involved in LPS and flagellum production with glycosylation regulating the activity of these proteins [5]; <2> the flagellar aminotransferases Cj1294 utilize only UDP-2-acetamido-2,6-dideoxy-β-L-arabino-4-hexulose as substrate producing UDP-4-amino-4,6-dideoxy-β-L-AltNAc, a precursor in the Pse biosynthetic pathway [9]; <1> the flagellar aminotransferases HP0366 utilize only UDP-2-acetamido-2,6-dideoxy-β-L-arabino-4-hexulose as substrate producing UDP-4-amino-4,6-dideoxy-β-L-AltNAc, a precursor in the Pse biosynthetic pathway [9]; <4> WbpM is essential for the biosynthesis of B-band lipopolysaccharide in many serotypes of Pseudomonas aeruginosa [10]) (Reversibility: ?) [2,5,9,10]

P ?

Substrates and products

S UDP-6-deoxy-6-fluoro-GlcNAc <2> (<2> elimination of fluoride from the substrate by the wild-type PseB, no activity by mutant enzymes K127A, D126N, and Y135F [1]) (Reversibility: ?) [1]

P UDP-GlcNAc + HF

S UDP-GlcNAc <2> (<2> the enzyme is involved in the pseudaminic acid biosynthesis, it is responsible for the biosynthesis of 6-deoxyhexose [1]; <2> the C-5 epimerization of UDP-4-keto-6-deoxy-L-IdoNAc to UDP-4-keto-6-deoxy-GlcNAc is PseB-catalyzed, and is about 50fold lower than the dehydratase activity [1]) (Reversibility: ?) [1]

P UDP-2-acetamido-2,6-dideoxy-β-L-arabino-hexos-4-ulose + H_2O

S UDP-N-acetylglucosamine <1,4> (<1> production of a precursor of pseudaminic acid, i.e. 5,7-diacetamido-3,5,7,9-tetradeoxy-L-glycero-α-L-manno-nonulosonic acid, required for flagellin glycosylation in Helicobacter pylori, analysis of all reaction steps in the pathway and related enzymes, overview [3]; <1> the enzyme catalyzes the first step in the biosynthetic pathway of a pseudaminic acid derivative, which is implicated in protein glycosylation [8]; <1> the enzyme is required for pseudaminic acid biosynthesis, which is required for O-linked flagellin glycosylation [2]; <4> WbpM is specific for UDP-GlcNAc [10]; <1> NMR reaction analysis, a possible three-step reaction mechanism that involves Lys133 functioning as both a catalytic acid and base [8]; <1> NMR reaction analysis, substrate binding at the active site, mapping of dynamic interactions of the enzyme with its ligand, molecular docking, overview [2]; <1> the enzyme catalyzes the stereospecific conversion of UDP-GlcNAc to Qui2NAc, i.e. 2-acetamido-2,6-dideoxy-D-glucose or N-acetylquinovosamine, via the for-

mation of a 4-keto, 6-deoxy intermediate [7]; <4> WbpM is specific for UDP-GlcNAc. Although WbpM possesses an altered catalytic triad composed of SMK as opposed to SYK commonly found in other dehydratases, its catalysis is very efficient [10]) (Reversibility: ?) [2,3,6,7,8,10]

P UDP-2-acetamido-2,6-dideoxy-β-L-arabino-hex-4-ulose + H_2O

S UDP-N-acetylglucosamine <1,2> (<2> the Cj1293 enzyme exhibits C6 dehydratase as well as C5 epimerase activity resulting in the production of both UDP-2-acetamido-2,6-dideoxy-β-L-arabino-4-hexulose and UDP-2-acetamido-2,6-dideoxy-α-D-xylo-4-hexulose. The enzyme is involved in biosynthesis of pseudaminic acid for glycomodification of the bacterial falgellins, overview [9]; <1> the HP0840 enzyme exhibits C6 dehydratase as well as C5 epimerase activity resulting in the production of both UDP-2-acetamido-2,6-dideoxy-β-L-arabino-4-hexulose and UDP-2-acetamido-2,6-dideoxy-α-D-xylo-4-hexulose. The enzyme is involved in biosynthesis of pseudaminic acid for glycomodification of the bacterial falgellins, overview [9]) (Reversibility: ?) [9]

P UDP-2-acetamido-2,6-dideoxy-β-L-arabino-4-hexulose + UDP-2-acetamido-2,6-dideoxy-α-D-xylo-4-hexulose + H_2O (<1,2> NMR analysis of reaction products, overview [9])

S Additional information <1,2,4,5,6> (<1> dependence of O-linked flagellin glycosylation on PseB, cross-talk between the Pse and α-D-QuiNAc4NAc, i.e. 2,4-diacetamido-2,4,6-trideoxy-a-d-Glc, pathways via PseB [2]; <5> the enzyme is involved in lipopolysaccharide biosynthesis, flagellum assembly, or protein glycosylation, and might play an important role in the pathogenesis of Helicobacter pylori. It is at the interface between several pathways that govern the expression of different virulence factors synthesizing sugar derivatives dedicated to the glycosylation of proteins which are involved in lipopolysaccharide and flagellum production with glycosylation regulating the activity of these proteins [5]; <6> the enzyme is involved in lipopolysaccharide biosynthesis, flagellum assembly, or protein glycosylation, and might play an important role in the pathogenesis of Helicobacter pylori. It is at the interface between several pathways that govern the expression of different virulence factors synthesizing sugar derivatives dedicated to the glycosylation of proteins which are involved in LPS and flagellum production with glycosylation regulating the activity of these proteins [5]; <2> the flagellar aminotransferases Cj1294 utilize only UDP-2-acetamido-2,6-dideoxy-β-L-arabino-4-hexulose as substrate producing UDP-4-amino-4,6-dideoxy-β-L-AltNAc, a precursor in the Pse biosynthetic pathway [9]; <1> the flagellar aminotransferases HP0366 utilize only UDP-2-acetamido-2,6-dideoxy-β-L-arabino-4-hexulose as substrate producing UDP-4-amino-4,6-dideoxy-β-L-AltNAc, a precursor in the Pse biosynthetic pathway [9]; <4> WbpM is essential for the biosynthesis of B-band lipopolysaccharide in many serotypes of Pseudomonas aeruginosa [10]; <1> FlaA1 is a bifunctional C6 dehydratase/C4 reductase specific for UDPGlcNAc. It converts UDP-GlcNAc into a UDP-4-keto-6-methyl-GlcNAc intermediate, which is stereospecifically reduced into UDP-QuiNAc [6]; <1> no activity with UDP-Glc, UDP-Gal, or UDP-GalNAc or

with substrates of other known C6 dehydratases, i.e. GDP-mannose or dTDP-glucose, structure-function analysis, overview [7]; <4> no activity with UDP-Glc, UDP-GalNAc or UDP-Gal, and with substrates of other known C6 dehydratases such as GDP-mannose, dTDP-Glc and CDP-Glc. Structure-function analysis, although the membrane domains do not have any catalytic activity, they are important for the polymerization of high-molecular weight B-band lipopolysaccharide, overview [10]; <1> PseB catalyzes an additional C_5 epimerization forming UDP-2-acetamido-2,6-dideoxy-α-D-xylo-hexos-4-ulose [2]) (Reversibility: ?) [2,5,6,7,9,10]

P ?

Inhibitors

CMP-pseudaminic acid <1> (<1> mapping of the dynamic interactions of the enzyme with the inhibitor, overview [2]) [2]

Cofactors/prosthetic groups

$NAD(P)^+$ <2> (<2> dependent on, tightly bound [1]) [1]
NAD^+ <1,4> [6,10]
$NADP^+$ <1> (<1> $NADP^+$/NADPH is tightly bound to FlaA1 [8]) [8]
Additional information <1,2> (<1,2> the dehydratase does not require the addition of exogenous cofactor $NAD(P)^+$ [9]) [9]

Turnover number (s^{-1})

0.028 <1> (UDP-N-acetylglucosamine, <1> pH 7.0, 37°C, mutant Y141M [7]) [7]
0.065 <1> (UDP-N-acetylglucosamine, <1> pH 10.0, 37°C, mutant Y141M [7]) [7]
0.077 <1> (UDP-N-acetylglucosamine, <1> pH 7.0, 37°C, mutant H86A [7]) [7]
0.095 <1> (UDP-N-acetylglucosamine, <1> pH 7.0, 37°C, wild-type enzyme [7]) [7]
0.16 <1> (UDP-N-acetylglucosamine, <1> pH 7.0, 37°C, mutant V266E [7]) [7]
2.8 <4> (UDP-N-acetylglucosamine, <4> pH 10.0, 30°C, recombinant soluble truncated WbpM mutant His-S262 [10]) [10]

Specific activity (U/mg)

0.000037 <2> (<2> wild-type enzyme activity with UDP-6-deoxy-6-fluoro-GlcNAc for elimination of fluoride [1]) [1]
0.23 <2> (<2> wild-type enzyme activity with UDP-GlcNAc conversion to UDP-4-keto-6-deoxy-L-IdoNAc [1]) [1]
Additional information <1,2> [1,7]

K_m-Value (mM)

0.151 <1> (UDP-N-acetylglucosamine, <1> pH 7.0, 37°C, mutant V266E [7]) [7]
0.159 <1> (UDP-N-acetylglucosamine, <1> pH 7.0, 37°C, wild-type enzyme [7]) [7]
0.251 <1> (UDP-N-acetylglucosamine, <1> pH 10.0, 37°C, mutant Y141M [7]) [7]

0.494 <1> (UDP-N-acetylglucosamine, <1> pH 7.0, 37°C, mutant H86A [7]) [7]
0.565 <1> (UDP-N-acetylglucosamine, <1> pH 7.0, 37°C, mutant Y141M [7]) [7]
2.77 <4> (UDP-N-acetylglucosamine, <4> pH 10.0, 30°C, recombinant soluble truncated WbpM mutant His-S262 [10]) [10]

pH-Optimum

7 <1> (<1> assay at [6]) [6]
7.2 <1,2> (<1,2> assay at [8,9]) [8,9]
7.3 <1> (<1> assay at [2,3]) [2,3]
7.4 <2> (<2> assay at [1]) [1]
10 <4> [10]

pi-Value

8.65 <1> (<1> sequence calculation [6]) [6]

Temperature optimum (°C)

23-30 <2> (<2> assay at [1]) [1]
25 <1> (<1> assay at [3,8]) [3,8]
25-30 <4> [10]
37 <1,2> (<1,2> assay at [6,9]) [6,9]

Temperature range (°C)

15-65 <1> [6]

4 Enzyme Structure

Molecular weight

75000 <1> (<1> about, recombinant His-tagged enzyme, gel filtration [6]) [6]

Subunits

? <4> (<4> x * 63000, recombinant N-terminally His-tagged WbpM, SDS-PAGE, x * 64000, recombinant C-terminally His-tagged WbpM, SDS-PAGE, x * 60000, recombinant His-tagged truncated WbpM, SDS-PAGE [10]) [10]
dimer <1> (<1> 2 * 37400, recombinant His-tagged enzyme, SDS-PAGE [6]) [6]
hexamer <1> (<1> the enzyme possesses a hexameric doughnut-shaped quaternary structure, crystal stucture analysis [8]) [8]
Additional information <1,4> (<1> FlaA1 is a short soluble protein that exhibits a typical SYK catalytic triad, structure-function analysis, overview [7]; <4> WbpM is anchored to the inner membrane via four N-terminal transmembrane domains, whereas the C-terminal catalytic domain resided in the cytoplasm, topological model of WbpM, overview [10]) [7,10]

5 Isolation/Preparation/Mutation/Application

Localization

flagellum <3> [4]
inner membrane <4> [10]
periplasm <3> [4]
soluble <1> [6,7]

Purification

<1> (recombinant His-tagged FlaA1 9.9fold from Escherichia coli strain BL21(DE3) to homogeneity by nickel chelation and cation exchange chromatography) [6]
<2> (recombinant His-tagged wild-type and mutant enzymes from Escherichia coli strain BL21(DE3)) [1]
<4> (recombinant N-terminally His-tagged and C-terminally His-tagged WbpMs from Escherichia coli by selective solubilization from the inner membrane by lauryl sarcosine and nickel chelation chromatography) [10]

Crystallization

<1> (FlaA1-$NADP^+$-UDP-GlcNAc and FlaA1-$NADP^+$-UDPGlc ternary complexes, at room temperature by hanging-drop vapor diffusion in presence of NAD^+, using as reservoir solution 10% v/v polyethylene glycol-200, 100 mM MES, pH 6.0, 5% v/w PEG 3000, and 4% acetone, and providing 10 mM excess of substrate, X-ray diffraction structure determination and analysis) [8]

Cloning

<1> (gene flaA1, expression of the N-terminally His-tagged enzyme in Escherichia coli strain BL21(DE3), complementation of a Pseudomonas aeruginosa WbpM knockout by expression of His-tagged FlaA1) [6]
<2> (gene pseB, expression of His-tagged wild-type and mutant enzymes in Escherichia coli strain BL21(DE3)) [1]
<3> (gene flaA1, DNA and amino acid sequence determination and analysis) [4]
<4> (overexpression of wild-type N-terminally His-tagged and C-terminally His-tagged WbpMs, and mutant truncated WbpM in membranes of Escherichia coli, reaction yields are lower with C-terminally His-tagged than with N-terminally His-tagged recombinant enzyme) [10]
<5> (gene flaA1, DNA and amino acid sequence determination, expression analysis) [5]
<6> (gene flaA1, DNA and amino acid sequence determination, expression analysis) [5]

Engineering

C_{10}3M <1> (<1> site-directed mutagenesis, the mutant is inactive, dimerization is prevented but the secondary structure is not significantly affected [7]) [7]
C_{11}8M <1> (<1> site-directed mutagenesis, not recombinantly expressable mutant [7]) [7]
D126N <2> (<2> site-directed mutagenesis, the mutant shows about 100fold lower activity with UDP-GlcNAc and with UDP-6-deoxy-6-fluoro-GlcNAc for

HF elimination compared to the wild-type enzyme. Upon addition of UDP-4-keto-6-deoxy-GlcNAc to D126N the tightly bound NADPH is immediately oxidized [1]) [1]
D149K/K150A <1> (<1> site-directed mutagenesis, the mutant is inactive [7]) [7]
D149K/K150D <1> (<1> site-directed mutagenesis, the mutant is inactive [7]) [7]
D70A <1> (<1> site-directed mutagenesis, the mutant is inactive [7]) [7]
D70N <1> (<1> site-directed mutagenesis, not recombinantly expressable mutant [7]) [7]
G20A <1> (<1> site-directed mutagenesis, the mutant is inactive [7]) [7]
H86A <1> (<1> site-directed mutagenesis, insoluble protein, the mutant shows reduced activity compared to the wild-type enzyme [7]) [7]
H86F <1> (<1> site-directed mutagenesis, insoluble protein, the mutant is inactive [7]) [7]
K127A <2> (<2> site-directed mutagenesis, the mutant shows about 100fold lower activity with UDP-GlcNAc and with UDP-6-deoxy-6-fluoro-GlcNAc for HF elimination compared to the wild-type enzyme. Upon addition of UDP-4-keto-6-deoxy-GlcNAc to K127A the tightly bound NADPH is immediately oxidized [1]) [1]
K133E <1> (<1> site-directed mutagenesis, inactive mutant [8]) [8]
K133M <1> (<1> site-directed mutagenesis, inactive mutant [8]) [8]
V266E <1> (<1> site-directed mutagenesis, the mutant shows increased activity compared to the wild-type enzyme [7]) [7]
Y135F <2> (<2> site-directed mutagenesis, the mutant shows about 100fold lower activity with UDP-GlcNAc and with UDP-6-deoxy-6-fluoro-GlcNAc for HF elimination compared to the wild-type enzyme, slow oxidation of NADPH upon addition of UDP-4-keto-6-deoxy-GlcNAc to Y135F [1]) [1]
Y141F <1> (<1> site-directed mutagenesis, the mutant is inactive [7]) [7]
Y141M <1> (<1> site-directed mutagenesis of a FlaA1 catalytic triad mutant, the mutant shows slightly reduced activity compared to the wild-type enzyme [7]) [7]
Additional information <3,4,5> (<4> construction of a soluble truncated form of WbpM, His-S262 [10]; <5> construction of flaA1 knockout mutant by gene disruption in strain NCTC 11637, the nonmotile mutant exhibits altered lipopolysaccharides, with loss of most O-antigen and core modification, and increased sensitivity to sodium dodecyl sulfate compared to wild-type bacteria. The flaA1 mutant produces flagellins but no flagellum. Phynotype, detailed overview [5]; <3> disruption of flaA1 and flaB1 genes by replacement of internal fragments with chloramphenicol and/or kanamycin gene cassettes. Both mutations selectively abolish expression of the targeted gene without affecting synthesis of the other flagellar polypeptide. flaA1 and flaB1 mutant strains exhibit altered motility in vitro and are less efficient in movement through a liquid medium. Paradoxically, isogenic strains containing specifically disrupted flaA1 or flaB1 alleles are capable of assembling periplasmic flagella that are morphologically wild-type, phenotype, detailed overview [4]) [4,5,10]

Application

drug development <2> (<2> PseB is a potential target for the development of antibiotics [1]) [1]

References

[1] Morrison, J.P.; Schoenhofen, I.C.; Tanner, M.E.: Mechanistic studies on PseB of pseudaminic acid biosynthesis: a UDP-N-acetylglucosamine 5-inverting 4,6-dehydratase. Bioorg. Chem., **36**, 312-320 (2008)

[2] McNally, D.J.; Schoenhofen, I.C.; Houliston, R.S.; Khieu, N.H.; Whitfield, D.M.; Logan, S.M.; Jarrell, H.C.; Brisson, J.: CMP-pseudaminic acid is a natural potent inhibitor of PseB, the first enzyme of the pseudaminic acid pathway in Campylobacter jejuni and Helicobacter pylori. ChemMedChem, **3**, 55-59 (2008)

[3] Schoenhofen, I.C.; McNally, D.J.; Brisson, J.; Logan, S.M.: Elucidation of the CMP-pseudaminic acid pathway in Helicobacter pylori: synthesis from UDP-N-acetylglucosamine by a single enzymatic reaction. Glycobiology, **16**, 8C-^{14}C (2006)

[4] Rosey, E.L.; Kennedy, M.J.; Petrella, D.K.; Ulrich, R.G.; Yancey, R.J.: Inactivation of Serpulina hyodysenteriae flaA1 and flaB1 periplasmic flagellar genes by electroporation-mediated allelic exchange. J. Bacteriol., **177**, 5959-5970 (1995)

[5] Merkx-Jacques, A.; Obhi, R.K.; Bethune, G.; Creuzenet, C.: The Helicobacter pylori flaA1 and wbpB genes control lipopolysaccharide and flagellum synthesis and function. J. Bacteriol., **186**, 2253-2265 (2004)

[6] Creuzenet, C.; Schur, M.J.; Li, J.; Wakarchuk, W.W.; Lam, J.S.: FlaA1, a new bifunctional UDP-GlcNAc C6 Dehydratase/C4 reductase from Helicobacter pylori. J. Biol. Chem., **275**, 34873-34880 (2000)

[7] Creuzenet, C.; Urbanic, R.V.; Lam, J.S.: Structure-function studies of two novel UDP-GlcNAc C6 dehydratases/C4 reductases. Variation from the SYK dogma. J. Biol. Chem., **277**, 26769-26778 (2002)

[8] Ishiyama, N.; Creuzenet, C.; Miller, W.L.; Demendi, M.; Anderson, E.M.; Harauz, G.; Lam, J.S.; Berghuis, A.M.: Structural studies of FlaA1 from Helicobacter pylori reveal the mechanism for inverting 4,6-dehydratase activity. J. Biol. Chem., **281**, 24489-24495 (2006)

[9] Schoenhofen, I.C.; McNally, D.J.; Vinogradov, E.; Whitfield, D.; Young, N.M.; Dick, S.; Wakarchuk, W.W.; Brisson, J.R.; Logan, S.M.: Functional characterization of dehydratase/aminotransferase pairs from Helicobacter and Campylobacter: enzymes distinguishing the pseudaminic acid and bacillosamine biosynthetic pathways. J. Biol. Chem., **281**, 723-732 (2006)

[10] Creuzenet, C.; Lam, J.S.: Topological and functional characterization of WbpM, an inner membrane UDP-GlcNAc C6 dehydratase essential for lipopolysaccharide biosynthesis in Pseudomonas aeruginosa. Mol. Microbiol., **41**, 1295-1310 (2001)

3-hydroxypropionyl-CoA dehydratase 4.2.1.116

1 Nomenclature

EC number
4.2.1.116

Systematic name
3-hydroxypropionyl-CoA hydro-lyase

Recommended name
3-hydroxypropionyl-CoA dehydratase

2 Source Organism

<1> *Metallosphaera sedula* (UNIPROT accession number: A4YI89) [1]

3 Reaction and Specificity

Catalyzed reaction
3-hydroxypropanoyl-CoA = acrylyl-CoA + H_2O

Substrates and products
- **S** (S)-3-hydroxybutyryl-CoA <1> (<1> no substrate: (R)-3-hydroxybutyryl-CoA [1]) (Reversibility: ?) [1]
- **P** crotonyl-CoA + H_2O
- **S** 3-hydroxypropionyl-CoA <1> (Reversibility: ?) [1]
- **P** acryloyl-CoA + H_2O

Turnover number (s^{-1})
96 <1> (3-hydroxypropionyl-CoA, <1> pH 8.6, 65°C [1]) [1]

Specific activity (U/mg)
2.4 <1> (<1> extract of autotrophically grown cells, pH 8.6 [1]) [1]
3.1 <1> (<1> extract of heterotrophically grown cells, pH 8.6 [1]) [1]
151 <1> (<1> purified, recombinant protein, pH 8.6 [1]) [1]

K_m-Value (mM)
0.06 <1> (3-hydroxypropionyl-CoA, <1> pH 8.6, 65°C [1]) [1]
0.075 <1> ((S)-3-hydroxybutyryl-CoA, <1> pH 8.6, 65°C [1]) [1]

pH-Optimum
8.1 <1> [1]

D. Schomburg and I. Schomburg (eds.), *Class 3.4–6 Hydrolases, Lyases, Isomerases, Ligases: EC 3.4–6*, Springer Handbook of Enzymes S10, DOI 10.1007/978-3-642-36260-6_43,

pH-Range
6.5 <1> (<1> half-maximal activity [1]) [1]
9.5 <1> (<1> half-maximal activity [1]) [1]

4 Enzyme Structure

Molecular weight
23000 <1> (<1> gel filtration [1]) [1]

Subunits
monomer <1> (<1> 1 * 29000, SDS-PAGE, 1 * 28300, calculated [1]) [1]

References

[1] Teufel, R.; Kung, J.; Kockelkorn, D.; Alber, B.; Fuchs, G.: 3-Hydroxypropionyl-coenzyme A dehydratase and acryloyl-coenzyme A reductase, enzymes of the autotrophic 3-hydroxypropionate/4-hydroxybutyrate cycle in the Sulfolobales. J. Bacteriol., **191**, 4572-4581 (2009)

2-methylcitrate dehydratase (2-methyl-trans-aconitate forming) 4.2.1.117

1 Nomenclature

EC number
4.2.1.117

Systematic name
(2S,3S)-2-hydroxybutane-1,2,3-tricarboxylate hydro-lyase (2-methyl-trans-aconitate forming)

Recommended name
2-methylcitrate dehydratase (2-methyl-trans-aconitate forming)

Synonyms
AcnD <1> [1]

2 Source Organism

<1> *Shewanella oneidensis* [1]

3 Reaction and Specificity

Catalyzed reaction
(2S,3S)-2-methylcitrate = 2-methyl-trans-aconitate + H_2O

Substrates and products
S 2-methylcitrate <1> (Reversibility: ?) [1]
P 2-methyl-cis-aconitate + H_2O
S cis-aconitate + H_2O <1> (Reversibility: ?) [1]
P citrate
S citrate <1> (Reversibility: r) [1]
P cis-aconitate + H_2O
S Additional information <1> (<1> no substrate: 2-methylisocitrate, isocitrate. Enzyme only catalyzes the first half of the aconitase-like reaction [1]) [1]
P ?

Inhibitors
EDTA <1> (<1> complete loss of activity [1]) [1]
ferricyanide <1> (<1> complete loss of activity [1]) [1]

D. Schomburg and I. Schomburg (eds.), *Class 3.4–6 Hydrolases, Lyases, Isomerases, Ligases: EC 3.4–6*, Springer Handbook of Enzymes S10, DOI 10.1007/978-3-642-36260-6_44,

Cofactors/prosthetic groups

4Fe-4S-center <1> (<1> enzyme requires an intact Fe/S cluster for activity [1]) [1]

Metals, ions

iron <1> (<1> enzyme requires an intact Fe/S cluster for activity [1]) [1]

Specific activity (U/mg)

2.9 <1> (<1> pH 8.0, 37°C, substrate citrate [1]) [1]
5 <1> (<1> pH 8.0, 37°C, substrate cis-aconitate [1]) [1]
7.8 <1> (<1> pH 8.0, 37°C, substrate 2-methylcitrate [1]) [1]

4 Enzyme Structure

Subunits

? <1> (<1> x * 94000, SDS-PAGE and calculated [1]) [1]

5 Isolation/Preparation/Mutation/Application

Cloning

<1> [1]

6 Stability

Oxidation stability

<1>, in presence of air, activity is lost over time [1]

References

[1] Grimek, T.L.; Escalante-Semerena, J.C.: The acnD genes of Shewenella oneidensis and Vibrio cholerae encode a new Fe/S-dependent 2-methylcitrate dehydratase enzyme that requires prpF function in vivo. J. Bacteriol., **186**, 454-462 (2004)

3-dehydroshikimate dehydratase 4.2.1.118

1 Nomenclature

EC number
4.2.1.118

Systematic name
3-dehydroshikimate hydro-lyase

Recommended name
3-dehydroshikimate dehydratase

Synonyms
(-)-3-dehydroshikimate dehydratase <5> [3]
AroZ <3> [5]
Qa-1 <2> [4]
QutC <1> [2]

CAS registry number
9044-87-5

2 Source Organism

<1> *Emericella nidulans* [2]
<2> *Neurospora crassa* [4,6]
<3> *Klebsiella pneumoniae* [5]
<4> *Vigna mungo* [7]
<5> *Bacillus thuringiensis* [3]
<6> *Podospora pauciseta* [1]

3 Reaction and Specificity

Catalyzed reaction
3-dehydro-shikimate = protocatechuate + H_2O

Substrates and products
S (-)-3-dehydroshikimate <5> (Reversibility: ?) [3]
P 3,4-dihydroxybenzoate + H_2O
S 3-dehydroshikimate <2> (Reversibility: ?) [6]
P protocatechuate + H_2O
S Additional information <5> (<5> enzyme displays to ionizable groups with pK_{a1} 7.9, and pK_{a2} 9.3 [3]) [3]

D. Schomburg and I. Schomburg (eds.), *Class 3.4–6 Hydrolases, Lyases, Isomerases, Ligases: EC 3.4–6*, Springer Handbook of Enzymes S10, DOI 10.1007/978-3-642-36260-6_45,

P ?

Inhibitors

EDTA <2,4,5> (<4> weak [7]; <5> 1 mM, complete loss of activity. More than 95% of activity can be restored in presence of Mg^{2+} [3]; <2> presence of Mg^{2+} reactivates [6]) [3,6,7]
K^+ <2> (<2> weak [6]) [6]
NH_4^+ <2> (<2> weak [6]) [6]
Na^+ <2> (<2> weak [6]) [6]

Metals, ions

Ba^{2+} <2> (<2> activation [6]) [6]
Co^{2+} <2,5> (<2> activation [6]) [3,6]
Mg^{2+} <2,4,5> (<4> stabilization [7]; <5> presence of Mg^{2+} restores activity after incubation with EDTA [3]; <2> up to 35fold activation. Presence at 25 mM protects from thermal inactivation [6]) [3,6,7]
Mn^{2+} <2,5> (<2> activation [6]) [3,6]
Mo^{2+} <2> (<2> activation [6]) [6]
Additional information <5> (<5> a divalent metal ion is absolutely required [3]) [3]

Turnover number (s^{-1})

3.8 <5> ((-)-3-dehydroshikimate, <5> 37°C [3]) [3]

Specific activity (U/mg)

257 <2> (<2> pH 7.5, 37°C [6]) [6]

K_m-Value (mM)

0.00059 <2> (3-dehydroshikimate, <2> pH 7.5, 37°C [6]) [6]
0.125 <5> ((-)-3-dehydroshikimate, <5> 37°C [3]) [3]

pH-Optimum

7.4 <4> [7]
8.4-8.8 <5> [3]

pH-Range

7.4 <5> (<5> less than 15% residual activity [3]) [3]

pi-Value

4.8 <2> (<2> minor component, and 5.0, minor component [6]) [6]
5 <2> (<2> major component, and 4.8, minor component [6]) [6]

4 Enzyme Structure

Molecular weight

36500 <2> (<2> gel filtration [6]) [6]
37000 <2> (<2> SDS-PAGE [6]) [6]

Subunits

? <2> (<2> x * 40367, calculated [4]) [4]

5 Isolation/Preparation/Mutation/Application

Source/tissue
cell culture <4> (<4> cultured in presence of shikimate [7]) [7]

Purification
<2> [6]
<4> (partial) [7]

Renaturation
<5> (complete loss of activity in presence of EDTA. More than 95% of activity can be restored in presence of Mg^{2+}) [3]

Cloning
<1> (overexpression in Aspergillus nidulans) [2]
<2> [4]
<3> (expression in Escherichia coli) [5]
<5> (expression in Escherichia coli) [3]

Application
synthesis <3,6> (<3> introduction of both 3-dehydroshikimate dehydratase and protocatechuic acid decarboxylase into an Escherichia coli construct synthesizing elevated levles of 3-dehydroshikimic acid leads to production of up to 18.5 mM catechol from 56 mM D-glucose on 1 l-scale [5]; <6> production of vanillin by engineered pathway in Schizosaccharomyces pombe or Saccharomyces cerevisiae. Pathway involves incorporation of 3-dehydroshikimate dehydratase, an aromatic carboxylic acid reductase from a bacterium of the Nocardia genus, and an O-ethyltransferase from Homo sapiens. In Saccharomyces cerevisiae, the aromatic carboxylic acid reductase enzyme requires activation by phosphopantetheinylation, achieved by coexpression of a Corynebacterium glutamicum phosphopantetheinyl transferase. Prevention of reduction of vanillin to vanillyl alcohol is achieved by knockout of the host alcohol dehydrogenase ADH6. In Schizosaccharomyces pombe, the biosynthesis is further improved by introduction of an Arabidopsis thaliana family 1 UDPglycosyltransferase, converting vanillin into vanillin β-D-glucoside, which is not toxic to the yeast cells and thus may be accumulated in larger amounts [1]) [1,5]

6 Stability

Temperature stability
46 <5> (<5> half-life 10 min [3]) [3]
47 <2> (<2> half-life below 12 min, presence of 25 mM Mg^{2+} extends the half-life to 220 min [6]) [6]
Additional information <4> (<4> enzyme is sensitive to thermal denaturation [7]) [7]

Storage stability

<2>, -20°C, loss of 50% of activity within 3 days [6]

<2>, 0-2°C, presence of 25 mM Mg^{2+}, one week, less than 50% loss of activity [6]

References

[1] Hansen, E.H.; Moeller, B.L.; Kock, G.R.; Bunner, C.M.; Kristensen, C.; Jensen, O.R.; Okkels, F.T.; Olsen, C.E.; Motawia, M.S.; Hansen, J.: De novo biosynthesis of vanillin in fission yeast (Schizosaccharomyces pombe) and baker's yeast (Saccharomyces cerevisiae). Appl. Environ. Microbiol., **75**, 2765-2774 (2009)

[2] Lamb, H.K.; Van den Hombergh, J.P.T.W.; Newton, G.H.; Moore, J.D.; Roberts, C.F.; Hawkins, A.R.: Differential flux through the quinate and shikimate pathways. Implications for the channeling hypothesis. Biochem. J., **284**, 181-187 (1992)

[3] Fox, D.T.; Hotta, K.; Kim, C.Y.; Koppisch, A.T.: The missing link in petrobactin biosynthesis: asbF encodes a (-)-3-dehydroshikimate dehydratase. Biochemistry, **47**, 12251-12253 (2008)

[4] Rutledge, B.: Molecular characterization of the qa-4 gene of Neurospora crassa. Gene, **32**, 275-287 (1984)

[5] Draths, K.; Frost, J.: Environmentally compatible synthesis of catechol from D-glucose. J. Am. Chem. Soc., **117**, 2395-2400 (1995)

[6] Stroeman, P.; Reinert, W.R.; Giles, N.H.: Purification and characterization of 3-dehydroshikimate dehydratase, an enzyme in the inducible quinic acid catabolic pathway of Neurospora crassa. J. Biol. Chem., **253**, 4593-4598 (1978)

[7] Tateoka, T.; Yasuda, I.: 3-Dehydroshikimate dehydratase in mung bean cultured cells. Plant Cell Rep., **15**, 212-217 (1995)

enoyl-CoA hydratase 2 4.2.1.119

1 Nomenclature

EC number
4.2.1.119

Systematic name
(3R)-3-hydroxyacyl-CoA hydro-lyase

Recommended name
enoyl-CoA hydratase 2

Synonyms
(3R)-hydroxyacyl-CoA dehydrogenase/2-enoyl-CoA hydratase 2 <8> [16]
(R)-specific enoyl coenzyme A hydratase <6> [2]
(R)-specific enoyl-CoA hydratase <6> [4]
2-enoyl-CoA hydratase <3> (<3> monofunctional, has not been observed as a wild-type protein. Part of perMFE-2 (2-enoyl-CoA hydratase 2/(R)-3-hydroxyacyl-CoA dehydrogenase) [13]) [13,14]
2-enoyl-CoA hydratase 2 <2,3,4,8,9,10> (<2> domain in human MFE-2 [8]; <2,8> domain of multifunctional enzyme type 2 (MFE-2), (3R)-hydroxyacyl-CoA dehydrogenase/2-enoyl-CoA hydratase 2 [16]; <3> has also D-3-hydroxyacyl-CoA dehydrogenase activity [12]; <4> part of the multifunctional enzyme (MHE) [12]; <4> part of the multifunctional protein (MFP) containing crotonase, L-3-hydroxyacyl-CoA dehydrogenase, D-3-hydroxyacyl-CoA dehydrogenase, and 3-hydroxyacyl-CoA epimerase [15]; <9> is a part of multifunctional enzyme type 2 [10]; <10> the enzyme is the middle part of the mammalian peroxisomal multifunctional enzyme type 2 (MFE-2) [9]; <3> is part of peroxisomal multifunctional enzyme perMFE-II together with D-specific 3-hydroxyacyl-CoA dehydrogenase (EC 1.1.1.36) [18]) [5,8,9,10,12,14,15,16,18]
2-enoyl-hydratase 2 <3> [14]
AtECH2 <5> (<5> gene name. Alignment of AtECH2 with homologous proteins is shown [11]; <5> monofunctional enzyme in Arabidopsis thaliana [11]) [11]
D-(-)-3-hydroxyacyl-CoA hydro-lyase <7> [19]
D-3-hydroxyacyl-CoA dehydratase <2> [3]
D-3-hydroxyacyl-CoA hydro-lyase <7> [19]
D-specific 2-trans-enoyl-CoA hydratase <7> [19]
ECH2 <3> [17]
MFE-2 <2,8> (<8> multifunctional enzyme [5]; <8> (3R)-hydroxyacyl-CoA dehydrogenase/2-enoyl-CoA hydratase 2 [16]; <8> multifunctional enzyme with 2-enoyl-CoA hydratase 2 activity and 2/(3R)-hydroxyacyl-CoA dehydrogenase (EC 1.1.1.36) activity [5]; <2> peroxisomal hydratase 2 together with

D. Schomburg and I. Schomburg (eds.), *Class 3.4–6 Hydrolases, Lyases, Isomerases, Ligases: EC 3.4–6*, Springer Handbook of Enzymes S10, DOI 10.1007/978-3-642-36260-6_46,

(3R)-hydroxyacyl-CoA dehydrogenase is present as multifunctional enzyme [8]) [5,8,16]
MaoC <1> (<1> the classification is ambiguous because the stereochemistry of the reaction product is not exactly determined [7]) [7]
Mfe2p [CtMfe2p(dha+bδ)] <8> (<8> 2-enoyl-CoA hydratase 2 domain of Candida tropicalis [5]) [5]
PhaJAc <6> [2,6]
enoyl-CoA hydratase 2 <3,5> (<5> monofunctional enzyme in Arabidopsis thaliana [11]) [11,17]
hydratase 2 <3>
multifunctional enzyme type 2 <8> (<8> (3R)-hydroxyacyl-CoA dehydrogenase/2-enoyl-CoA hydratase 2 [16]) [16]
perMFE-II <3> (<3> peroxisomal multifunctional enzyme perMFE-II has 2-enoyl-CoA hydratase 2 (D-specific) activity and D-specific 3-hydroxyacyl-CoA dehydrogenase (EC 1.1.1.36) activity. Peroxisomal multifunctional enzyme perMFE-I has 2-enoyl-CoA hydratase 1 activity (L-specific, EC 4.2.1.17) and L-specific 3-hydroxyacyl-CoA dehydrogenase (EC 1.1.1.35) activity [18]) [18]
phaJ <6> [2]

CAS registry number
9027-13-8 (cf. EC 4.2.1.17)

2 Source Organism

<1> *Escherichia coli* [7]
<2> *Homo sapiens* [3,8]
<3> *Rattus norvegicus* [1,12,13,14,17,18]
<4> *Saccharomyces cerevisiae* [15]
<5> *Arabidopsis thaliana* [11]
<6> *Aeromonas caviae* [2,4,6]
<7> *Cucumis sativus* [19]
<8> *Candida tropicalis* [5,16]
<9> *Candida tropicalis* (UNIPROT accession number: P22414) (2-enoyl-CoA hydratase 2 is a part of multifunctional enzyme type 2 [10]) [10]
<10> *Homo sapiens* (UNIPROT accession number: P51659) (2-enoyl-CoA hydratase 2 is the middle part of the mammalian peroxisomal multifunctional enzyme type 2 (MFE-2) [9]) [9]

3 Reaction and Specificity

Catalyzed reaction
(3R)-3-hydroxyacyl-CoA = (2E)-2-enoyl-CoA + H_2O

Reaction type
hydration

Natural substrates and products

S (2E)-2-enoyl-CoA + H_2O <3,4,9,10> (<9> 2-enoyl-CoA hydratase 2 is a part of multifunctional enzyme type 2, hydrates trans-2-enoyl-CoA to 3-hydroxyacyl-CoA as a key enzyme in the (3R)-hydroxy-dependent route of peroxisomal β-oxidation of fatty acids [10]; <10> peroxisomal multifunctional enzyme type 2 (MFE-2) is a 79000 Da enzyme composed of three functional units: (3R)-hydroxyacyl-CoA dehydrogenase, 2-enoyl-CoA hydratase 2 and sterol carrier protein 2-like units. It catalyzes the second and third steps of peroxisomal β-oxidation, and its importance in human lipid metabolism is shown by the severe clinical symptoms (dysmorphic features, such as macrocephaly and large fontanelles, hypotonia, seizures, etc.) in patients having defects in the gene encoding MFE-2. Typical biochemical observations include a high ratio of C26:0 to C22:0 fatty acids and elevated levels of pristanic acid (2,6,10,14-tetramethylpentadecanoic acid) in the patients´ plasma and fibroblasts, indicating the significance of MFE-2 in the breakdown of very-long-chain and α-methylbranched-chain fatty acids. The patients also have high levels of di- and trihydroxycholestanoic acids, which are precursors of bile acids, showing that MFE-2 also participates in bile acid synthesis [9]) (Reversibility: r) [9,10,15]

P (3R)-3-hydroxyacyl-CoA

S (3R)-3-hydroxyacyl-CoA <5> (<5> AtECH2 participates in vivo in the conversion of the intermediate (3R)-hydroxyacyl-CoA, generated by the metabolism of fatty acids with a cis (Z)-unsaturated bond on an even-numbered carbon, to the (2E)-enoyl-CoA for further degradation through the core β-oxidation cycle. AtECH2 is a monofunctional enzyme in Arabidopsis thaliana that is devoid of 3-hydroxyacyl-CoA dehydrogenase activity [11]) (Reversibility: ?) [11]

P (2E)-2-enoyl-CoA + H_2O

S Additional information <1,2,3,6,8> (<6> channelling pathway for supplying (R)-3-hydroxyacyl-CoA monomer units from fatty acid β-oxidation to poly(3-hydroxybutyrate-co-3-hydroxyhexanoate) biosynthesis [2]; <8> domains A and B have different enzymatic properties and both domains play a functional role in the β-oxidation of fatty acids in yeast peroxisomes [16]; <8> in yeast, the second and the third reaction of the fatty-acid β-oxidation spiral are catalysed by peroxisomal multifunctional enzyme type 2 (Mfe2p/Fox2p). This protein has two (3R)-hydroxyacyl-CoA dehydrogenase domains and a C-terminal 2-enoyl-CoA hydratase 2 domain [5]; <1> MaoC is an enoyl-CoA hydratase which is involved in converting enoyl-CoAs to (R)-3-hydroxyacyl coenzyme A in fadB mutant Escherichia coli. Metabolic link between fatty acid metabolism and polyhydroxyalkanoate biosynthesis [7]; <2> peroxisomal hydratase 2 together with (3R)-hydroxyacyl-CoA dehydrogenase, and peroxisomal hydratase 1 together with (3S)-hydroxyacyl-CoA dehydrogenase, are present as multifunctional enzymes. When present simultaneously in peroxisomes, β-oxidation has two stereochemical possibilities [8]; <3> the β-oxidation in mitochondria involves a (3S)-hydroxyacyl-CoA intermediate, while the β-oxidation in peroxisomes has a (3R)-hydroxyacyl-CoA intermediate. The

enzymes responsible for the formation of these two different intermediates are enoyl-CoA hydratase 1 (ECH1) in mitochondria and enoyl-CoA hydratase 2 (ECH2) in peroxisomes [17]; <6> the enzyme is essential for polyhydroxyalkanoate biosynthesis [4]) [2,4,5,7,8,16,17]

P ?

Substrates and products

S (24E)-3α,7α,12α-trihydroxy-5β-cholest-24-enoyl-CoA + H_2O <3> (<3> reaction of the recombinant enzyme, protein converted rapidly [13]) (Reversibility: ?) [13]

P (24R,25R)-3α,7α,12α,24-tetrahydroxy-5β-cholestanoyl-CoA (<3> a physiological intermediate in bile acid synthesis [13])

S (2E)-2-decenoyl-CoA + H_2O <8> (<8> activity measurements are based on the formation of the magnesium complex of 3-ketoacyl-CoA from (2E)-2-decenoyl-CoA [5]) (Reversibility: ?) [5]

P (3R)-3-hydroxydecanoyl-CoA

S (2E)-2-enoyl-CoA + H_2O <3,4,9,10> (<9> 2-enoyl-CoA hydratase 2 is a part of multifunctional enzyme type 2, hydrates trans-2-enoyl-CoA to 3-hydroxyacyl-CoA as a key enzyme in the (3R)-hydroxy-dependent route of peroxisomal β-oxidation of fatty acids [10]; <10> peroxisomal multifunctional enzyme type 2 (MFE-2) is a 79000 Da enzyme composed of three functional units: (3R)-hydroxyacyl-CoA dehydrogenase, 2-enoyl-CoA hydratase 2 and sterol carrier protein 2-like units. It catalyzes the second and third steps of peroxisomal β-oxidation, and its importance in human lipid metabolism is shown by the severe clinical symptoms (dysmorphic features, such as macrocephaly and large fontanelles, hypotonia, seizures, etc.) in patients having defects in the gene encoding MFE-2. Typical biochemical observations include a high ratio of C26:0 to C22:0 fatty acids and elevated levels of pristanic acid (2,6,10,14-tetramethylpentadecanoic acid) in the patients´ plasma and fibroblasts, indicating the significance of MFE-2 in the breakdown of very-long-chain and α-methylbranched-chain fatty acids. The patients also have high levels of di- and trihydroxycholestanoic acids, which are precursors of bile acids, showing that MFE-2 also participates in bile acid synthesis [9]) (Reversibility: r) [9,10,15]

P (3R)-3-hydroxyacyl-CoA

S (2E)-decenoyl-CoA + H_2O <3,5> (Reversibility: ?) [11,13]

P (3R)-3-hydroxydecanoyl-CoA

S (2E)-enoyl-CoA + H_2O <3> (<3> straight-chain [13]) (Reversibility: ?) [13]

P (3R)-hydroxyacyl-CoA

S (2E)-hexadecenoyl-CoA + H_2O <5> (Reversibility: ?) [11]

P (3R)-3-hydroxyhexadecanoyl-CoA

S (2E)-hexenoyl-CoA + H_2O <3,5> (Reversibility: ?) [11,13]

P (3R)-3-hydroxyhexanoyl-CoA

S (3R)-3-hydroxyacyl-CoA <5> (<5> $AtECH_2$ participates in vivo in the conversion of the intermediate (3R)-hydroxyacyl-CoA, generated by the metabolism of fatty acids with a cis (Z)-unsaturated bond on an even-

numbered carbon, to the (2E)-enoyl-CoA for further degradation through the core β-oxidation cycle. AtECH2 is a monofunctional enzyme in Arabidopsis thaliana that is devoid of 3-hydroxyacyl-CoA dehydrogenase activity [11]) (Reversibility: ?) [11]
P (2E)-2-enoyl-CoA + H_2O
S (R)-3-hydroxydecanoyl-CoA <3> (Reversibility: r) [1]
P trans-2-decenoyl-CoA + H_2O
S (R)-3-hydroxyoctanoyl-CoA <2> (<2> no activity with (S)-3-hydroxyoctanoyl-CoA [3]) (Reversibility: r) [3]
P octenoyl-CoA + H_2O
S 2-trans-butenoyl-CoA + H_2O <7> (Reversibility: ?) [19]
P (3R)-hydroxybutenoyl-CoA
S 2-trans-decenoyl-CoA + H_2O <7> (Reversibility: ?) [19]
P (3R)-hydroxydecenoyl-CoA
S Crotonyl-CoA + H_2O <3> (<3> ratio of hydration rates trans-2-decenoyl-CoA/crotonyl-CoA is 14.4 [14]) (Reversibility: ?) [13,14]
P (3R)-3-Hydroxybutanoyl-CoA
S crotonyl-CoA + H_2O <6> (Reversibility: ?) [6]
P 3-hydroxybutanoyl-CoA <6> [6]
S crotonyl-CoA + H_2O <2,6> (<2> very low activity with crotonyl-CoA [3]) (Reversibility: ?) [2,3]
P (R)-3-hydroxybutanoyl-CoA
S crotonyl-CoA + H_2O <1,3> (<3> activity is 7fold higher than activity with trans-decenoyl-CoA [18]; <1> the classification is ambiguous because the stereochemistry of the reaction product is not exactly determined [7]) (Reversibility: ?) [7,18]
P ?
S dec-2-enoyl-CoA + H_2O <2> (<2> 9-12% of the activity with hexenoyl-CoA, depending on preparation [3]) (Reversibility: ?) [3]
P (R)-3-hydroxydecenoyl-CoA
S dec-2-enoyl-CoA + H_2O <6> (Reversibility: ?) [6]
P 3-hydroxydecanoyl-CoA <6> [6]
S dodec-2-enoyl-CoA + H_2O <2> (<2> 4-5% of the activity with hexenoyl-CoA, depending on preparation [3]) (Reversibility: ?) [3]
P (R)-3-hydroxydodecenoyl-CoA
S dodec-2-enoyl-CoA + H_2O <6> (Reversibility: ?) [6]
P 3-hydroxydodecanoyl-CoA <6> [6]
S hex-2-enoyl-CoA + H_2O <2,6> (Reversibility: r) [2,3]
P (R)-3-hydroxyhexanoyl-CoA
S hex-2-enoyl-CoA + H_2O <6> (Reversibility: ?) [6]
P 3-hydroxyhexanoyl-CoA <6> [6]
S oct-2-enoyl-CoA + H_2O <2,6> (<2> 30-40% of the activity with hexenoyl-CoA, depending on preparation [3]) (Reversibility: ?) [2,3]
P (R)-3-hydroxyoctanoyl-CoA
S oct-2-enoyl-CoA + H_2O <6> (Reversibility: ?) [6]
P 3-hydroxyoctanoyl-CoA <6> [6]
S pent-2-enoyl-CoA + H_2O <6> (Reversibility: ?) [2]

P (R)-3-hydroxypentanoyl-CoA
S tetradec-2-enoyl-CoA + H_2O <2> (Reversibility: ?) [3]
P ?
S trans-2-decenoyl-CoA <8> (Reversibility: ?) [16]
P (3R)-hydroxydecanoyl-CoA + H_2O
S trans-2-decenoyl-CoA + H_2O <2> (Reversibility: r) [8]
P (3R)-3-hydroxydecanoyl-CoA
S trans-2-decenoyl-CoA + H_2O <3> (<3> ratio of hydration rates trans-2-decenoyl-CoA/crotonyl-CoA is 14.4 [14]) (Reversibility: r) [14]
P (3R)-hydroxydecanoyl-CoA
S trans-2-hexadecenoyl-CoA <8> (Reversibility: ?) [16]
P (3R)-hydroxyhexadecanoyl-CoA + H_2O
S trans-2-octenoyl-CoA + H_2O <6> (Reversibility: ?) [6]
P 3-hydroxyoctanoyl-CoA <6> [6]
S trans-dec-2-enoyl-CoA <3> (<3> activity is 7fold lower than activity with crotonyl-CoA [18]) (Reversibility: ?) [18]
P ?
S Additional information <1,2,3,6,8> (<6> channelling pathway for supplying (R)-3-hydroxyacyl-CoA monomer units from fatty acid β-oxidation to poly(3-hydroxybutyrate-co-3-hydroxyhexanoate) biosynthesis [2]; <8> domains A and B have different enzymatic properties and both domains play a functional role in the β-oxidation of fatty acids in yeast peroxisomes [16]; <8> in yeast, the second and the third reaction of the fatty-acid β-oxidation spiral are catalysed by peroxisomal multifunctional enzyme type 2 (Mfe2p/Fox2p). This protein has two (3R)-hydroxyacyl-CoA dehydrogenase domains and a C-terminal 2-enoyl-CoA hydratase 2 domain [5]; <1> MaoC is an enoyl-CoA hydratase which is involved in converting enoyl-CoAs to (R)-3-hydroxyacyl coenzyme A in fadB mutant Escherichia coli. Metabolic link between fatty acid metabolism and polyhydroxyalkanoate biosynthesis [7]; <2> peroxisomal hydratase 2 together with (3R)-hydroxyacyl-CoA dehydrogenase, and peroxisomal hydratase 1 together with (3S)-hydroxyacyl-CoA dehydrogenase, are present as multifunctional enzymes. When present simultaneously in peroxisomes, β-oxidation has two stereochemical possibilities [8]; <3> the β-oxidation in mitochondria involves a (3S)-hydroxyacyl-CoA intermediate, while the β-oxidation in peroxisomes has a (3R)-hydroxyacyl-CoA intermediate. The enzymes responsible for the formation of these two different intermediates are enoyl-CoA hydratase 1 (ECH1) in mitochondria and enoyl-CoA hydratase 2 (ECH2) in peroxisomes [17]; <6> the enzyme is essential for polyhydroxyalkanoate biosynthesis [4]; <8> MFE-2 is a multifunctional enzyme with 2-enoyl-CoA hydratase 2 activity and 2/(3R)-hydroxyacyl-CoA dehydrogenase (EC 1.1.1.36) activity [5]; <2> no activity with (S)-3-hydroxyoctanoyl-CoA [3]; <3> the (S)-3-hydroxy-CoA is not dehydrated [1]) [1,2,3,4,5,7,8,16,17]
P ?

Inhibitors

(R)-methylenecyclopropylformyl-CoA <3> (<3> methylenecyclopropylformyl-CoA is a better inhibitor for enoyl-CoA hydratase 2 than for enoyl-CoA hydratase 1 [17]) [17]
(S)-methylenecyclopropylformyl-CoA <3> (<3> methylenecyclopropylformyl-CoA is a better inhibitor for enoyl-CoA hydratase 2 than for enoyl-CoA hydratase 1 [17]) [17]
3-octynoyl-CoA <3> (<3> irreversible inhibitor of enoyl-CoA hydratase 2 [17]) [17]
NEM <3> (<3> 60% inhibition by 5 mM, 96% inhibition by 10 mM NEM [14]) [14]

Turnover number (s^{-1})

1.3 <2> ((2E)-2-decenoyl-CoA, <2> mutant enzyme E366A, pH 5 [8]) [8]
2.3 <3> (crotonyl-CoA) [13]
17.9 <2> ((2E)-2-decenoyl-CoA, <2> mutant enzyme E366A, pH 8 [8]) [8]
22.8 <3> ((2E)-hexenoyl-CoA) [13]
26 <3> ((2E)-decenoyl-CoA) [13]
105 <2> ((2E)-2-decenoyl-CoA, <2> wild type enzyme, pH 5 [8]) [8]
196 <2> ((2E)-2-decenoyl-CoA, <2> wild type enzyme, pH 8 [8]) [8]
388 <8> ((2E)-2-decenoyl-CoA, <8> recombinant enzyme CtMfe2p(dha+bδ) [5]) [5]
Additional information <3,7> (<3> kinetic parameters of the enzyme are measured with concentrations of substrates from 5 to 200 microM [13]; <7> k_{cat}/K_m for 2-trans-decenoyl-CoA is 24 microM/s, k_{cat}/K_m for 2-trans-butenoyl-CoA is 0.44 microM/s [19]) [13,19]

Specific activity (U/mg)

0.05 <6> (<6> L654G/V130G mutant with crotonyl-CoA as substrate, cell extract [6]) [6]
0.08 <6> (<6> L65A/V130G mutant with crotonyl-CoA as substrate, cell extract [6]) [6]
0.12 <2> (<2> strain HsMFE-2(D490A) [8]) [8]
0.16 <2> (<2> strain HsMFE-2(G16S) [8]) [8]
0.2 <2> (<2> strain HsMFE-2(H532A) [8]) [8]
0.21 <2> (<2> strain HsMFE-2(D370A), strain HsMFE-2(H406A) [8]) [8]
0.24 <2> (<2> strain HsMFE-2(Y410A) [8]) [8]
0.26 <2> (<2> strain HsMFE-2(D517A), strain HsMFE-2(E408A) [8]) [8]
0.4 <2> (<2> strain UTL-7A [8]) [8]
0.54 <2> (<2> strain HsMFE-2 [8]) [8]
0.55 <6> (<6> S62A mutant with octenoyl-CoA as substrate, cell extract [6]) [6]
0.86 <6> (<6> wild-type with octenoyl-CoA as substrate, cell extract [6]) [6]
1.2 <5> (<5> 0.03 mM (2E)-hexadecenoyl-CoA as a substrate [11]) [11]
1.98 <6> (<6> L65G mutant with octenoyl-CoA as substrate, cell extract [6]) [6]
2.25 <6> (<6> L65I mutant with octenoyl-CoA as substrate, cell extract [6]) [6]

3.5 <5> (<5> 0.03 m (2E)-hexenoyl-CoA as a substrate [11]) [11]
6.59 <6> (<6> V130A mutant with octenoyl-CoA as substrate, cell extract [6]) [6]
7.92 <6> (<6> L65V mutant with octenoyl-CoA as substrate, cell extract [6]) [6]
12.4 <5> (<5> 0.1 mM, 3-hydroxydecanoyl-CoA as a substrate [11]) [11]
15.8 <6> (<6> L65G mutant with crotonyl-CoA as substrate, cell extract [6]) [6]
21.2 <6> (<6> V130G mutant with octenoyl-CoA as substrate, cell extract [6]) [6]
30 <5> (<5> 0.05 mM (2E)-decenoyl-CoA as a substrate [11]) [11]
33.4 <3> (<3> pET-Hydr2 expressed in Escherichia coli, soluble extract of the cells [13]) [13]
37.5 <3> (<3> purified enzyme [1]) [1]
48 <3> (<3> recombinant 46 kDa hydratase 2, last purification step: size exclusion [13]) [13]
67 <6> (<6> S62A mutant with crotonyl-CoA as substrate, cell extract [6]) [6]
68.5 <6> (<6> V130G mutant with crotonyl-CoA as substrate, cell extract [6]) [6]
69.8 <6> (<6> L65A mutant with octenoyl-CoA as substrate, cell extract [6]) [6]
259 <7> [19]
883 <6> (<6> V130G mutant with crotonyl-CoA as substrate, purified enzyme [6]) [6]
1256 <6> (<6> L65A mutant with crotonyl-CoA as substrate, cell extract [6]) [6]
1288 <6> (<6> V130A mutant with crotonyl-CoA as substrate, cell extract [6]) [6]
1538 <6> (<6> L65V mutant with crotonyl-CoA as substrate, cell extract [6]) [6]
1594 <6> (<6> wild-type with crotonyl-CoA as substrate, cell extract [6]) [6]
1880 <6> (<6> L65I mutant with crotonyl-CoA as substrate, cell extract [6]) [6]
Additional information <3> (<3> activity is below the detection limit of the assay system when using extracts from non-transformed cells or cells transformed with the vector only [13]) [13]

K_m-Value (mM)

0.005 <2> (dodec-2-enoyl-CoA) [3]
0.005 <6> (dodec-2-enoyl-CoA, <6> pH 8, 30°C, V130G mutant [6]) [6]
0.005 <2> (tetradec-2-enoyl-CoA) [3]
0.007 <2> (dec-2-enoyl-CoA) [3]
0.0081 <2> ((2E)-2-decenoyl-CoA, <2> wild type, pH 8 [8]) [8]
0.0089 <2> ((2E)-2-decenoyl-CoA, <2> wild type, pH 5 [8]) [8]
0.009 <2> (oct-2-enoyl-CoA) [3]
0.0092 <2> ((2E)-2-decenoyl-CoA, <2> mutant enzyme E366A, pH 5 [8]) [8]

0.0095 <7> (2-trans-decenoyl-CoA, <7> pH 8.0, 25°C [19]) [19]
0.013 <6> (decenoyl-CoA, <6> pH 8, 30°C, V130G mutant [6]) [6]
0.0131 <2> ((2E)-2-decenoyl-CoA, <2> mutant enzyme E366A, pH 8 [8]) [8]
0.015 <2> (hex-2-enoyl-CoA) [3]
0.018 <6> (hex-2-enoyl-CoA, <6> pH 8, 30°C, L65A mutant [6]) [6]
0.021 <6> (oct-2-enoyl-CoA, <6> pH 8, 30°C, L65A mutant [6]) [6]
0.024 <6> (crotonyl-CoA, <6> pH 8, 30°C, wild-type [6]) [6]
0.027 <6> (dec-2-enoyl-CoA, <6> pH 8, 30°C, L65A mutant [6]) [6]
0.029 <6> (crotonyl-CoA, <6> pH 8.0, 30°C [2]) [2]
0.03 <2> (crotonyl-CoA) [3]
0.033 <6> (crotonyl-CoA, <6> pH 8, 30°C, L65A mutant [6]) [6]
0.034 <6> (dodec-2-enoyl-CoA, <6> pH 8, 30°C, L65A mutant [6]) [6]
0.034 <6> (hex-2-enoyl-CoA, <6> pH 8.0, 30°C [2]) [2]
0.036 <6> (pent-2-enoyl-CoA, <6> pH 8.0, 30°C [2]) [2]
0.04 <6> (hex-2-enoyl-CoA, <6> pH 8, 30°C, wild-type [6]) [6]
0.042 <6> (dec-2-enoyl-CoA, <6> pH 8, 30°C, wild-type [6]) [6]
0.042 <6> (oct-2-enoyl-CoA, <6> pH 8, 30°C, wild-type [6]) [6]
0.043 <6> (dodec-2-enoyl-CoA, <6> pH 8, 30°C, wild-type [6]) [6]
0.05 <6> (oct-2-enoyl-CoA, <6> pH 8.0, 30°C [2]) [2]
0.076 <6> (oct-2-enoyl-CoA, <6> pH 8, 30°C, V130G mutant [6]) [6]
0.102 <6> (hex-2-enoyl-CoA, <6> pH 8, 30°C, V130G mutant [6]) [6]
0.11 <7> (2-trans-butenoyl-CoA, <7> pH 8.0, 25°C [19]) [19]
0.154 <6> (crotonyl-CoA, <6> pH 8, 30°C, V130G mutant [6]) [6]
4.6 <3> ((2E)-decenoyl-CoA) [13]
8.7 <3> ((2E)-hexenoyl-CoA) [13]
60 <3> (crotonyl-CoA) [13]
Additional information <3> (<3> kinetic parameters of the enzyme are measured with concentrations of substrates from 5 to 200 microM [13]) [13]

K_i-Value (mM)

0.041 <3> ((R)-methylenecyclopropylformyl-CoA, <3> 25°C [17]) [17]
0.053 <3> ((S)-methylenecyclopropylformyl-CoA, <3> 25°C [17]) [17]
0.065 <3> (3-octynoyl-CoA, <3> 25°C [17]) [17]

pH-Optimum

7.5-8 <7> [19]
8 <1,6> (<1,6> assay at [2,7]) [2,7]
9 <3> (<3> assay at [1]) [1]

pH-Range

5-10 <2> (<2> pH dependence experiment is performed in 200 mM potassium phosphate buffer at pH values varying from 5 to 10 [8]) [8]

pi-Value

7.6 <5> (<5> calculated from sequence [11]) [11]
9 <7> (<7> around, estimated by comparing the elution of cationic enzymes on carboxymethyl-cellulose [19]) [19]

Temperature optimum (°C)
22 <2> (<2> assay at [8]) [8]
25 <3> (<3> assay at [1]) [1]
30 <6> (<6> assay at [2]) [2]

Temperature range (°C)
22 <8> (<8> assay at [16]) [16]

4 Enzyme Structure

Molecular weight
30000 <6> (<6> gel filtration [2]) [2]
46000 <3> (<3> recombinant hydratase 2, SDS-PAGE [13]) [13]
60000 <3> (<3> microsomal isoform, gel filtration [1]) [1]
60000-88000 <3> [12]
62000 <3> (<3> peroxisomal isoform, gel filtration [1]) [1]
63000 <8> (<8> both recombinant CtMfe2p(dha+bδ) and its SeMet analogue, SDS-PAGE [5]) [5]
65000 <7> (<7> gel filtration [19]) [19]

Subunits
? <2,3,5,8> (<3> x * 31500-44000 [12]; <5> x * 34000, calculated from sequence [11]; <2> x * 45000, HsMFE-2(dhδ), HsMFE-2(dhδ, E366A), HsMFE-2(dhδ, D510A), SDS-PAGE [8]; <8> x * 63000, both recombinant CtMfe2p(dha+bδ) and its SeMet analogue, SDS-PAGE [5]) [5,8,11,12]
dimer <6> (<6> 2 * 13954, calculated from sequence [2]) [2]
homodimer <3,7> (<7> 2 * 33000, SDS-PAGE [19]; <3> 2 * 31500, microsomal isoform, SDS-PAGE [1]; <3> 2 * 33500, peroxisomal isoform, SDS-PAGE [1]) [1,19]
monomer <3> (<3> size-exclusion chromatography on a Superdex 200 HR column gives a native molecular mass of 59 kDa, suggesting that the recombinant protein is monomeric [13]) [13]

5 Isolation/Preparation/Mutation/Application

Source/tissue
cotyledon <7> (<7> fat-degrading [19]) [19]
flower bud <5> [11]
leaf <5> (<5> AtECH2 gene expression is strongest in tissues with high β-oxidation activity, such as germinating seedlings and senescing leaves [11]) [11]
liver <3> [1,12,14,18]
root <5> [11]
seedling <5,7> (<5> AtECH2 gene expression is strongest in tissues with high β-oxidation activity, such as germinating seedlings and senescing leaves [11]) [11,19]

skin fibroblast <2> [3]
stem <5> [11]

Localization

microsome <3> (<3> enzyme different from peroxisomal hydratase 2 though their kinetic properties are similar. They differ in immunological data, subunit size, and chromatographic behaviour, the peroxisomal isoform is not recognized by the antibody to its microsomal counterpart [1]) [1,12]
peroxisome <2,3,5,7,8> (<7> D-specific 2-trans-enoyl-CoA hydratase is exclusively located in [19]; <2> peroxisomal hydratase 2 together with (3R)-hydroxyacyl-CoA dehydrogenase, and hydratase 1 together with (3S)-hydroxyacyl-CoA dehydrogenase, are present as multifunctional enzymes. When present simultaneously in peroxisomes, β-oxidation has two stereochemical possibilities [8]; <3> enzyme different from microsomal hydratase 2 though their kinetic properties are similar. They differ in immunological data, subunit size, and chromatographic behaviour, the peroxisomal isoform is not recognized by the antibody to its microsomal counterpart [1]) [1,3,8,11,12,13,16,17,18,19]

Purification

<2> [3,8]
<3> (0.2% yield,the microsomal isoform elutes at 0.4-0.7 MKCl, at low salt concentrations, whereas the peroxisomal isoform elutes at high salt concentrations) [1]
<3> (recombinant protein purified from the cell extract to apparent homogeneity by three chromatographic steps on anion-exchange, cation-exchange and size-exclusion columns) [13]
<4> (the FOX2 gene is overexpressed from a multicopy vector (YEp352) in Saccharomyces cerevisiae and the gene product purified to apparent homogenity. A truncated version of MFP lacking 271 carboxyl-terminal amino acids is also overexpressed and purified) [15]
<6> [4]
<7> [19]
<8> [5]
<10> [9]

Crystallization

<6> (sitting drop vapour diffusion against a reservoir solution containing 20% polyethylene glycol 4000, 5% 2-propanol and 20 mM HEPES pH 7.0 at 25°C. Crystals belong to the monoclinic space group C2, with unit-cell parameters a = 111.54 A, b = 59.29 A, c = 47.27 A, β = 113.04° and contain a dimeric molecule in the asymmetric unit) [4]
<8> (hanging-drop vapour-diffusion method. Crystals of native and SeMet CtMfe2p(dha+bδ)) [5]
<9> (structure determination. The eukaryotic hydratase 2 has a complete hot dog fold only in its C-domain, whereas the N-domain lacks a long central α-helix, thus creating space for bulkier substrates in the binding pocket. The hydrogen bonding network of the active site of 2-enoyl-CoA hydratase 2 re-

sembles the active site geometry of mitochondrial (S)-specific 2-enoyl-CoA hydratase 1, although in a mirror image fashion) [10]
<10> (hanging-drop vapor diffusion method, crystal structure to 3 A resolution. MFE-2 has a two-domain subunit structure with a C-domain complete hot-dog fold housing the active site, and an N-domain incomplete hot-dog fold housing the cavity for the aliphatic acyl part of the substrate molecule. The ability of human hydratase 2 to utilize such bulky compounds which are not physiological substrates for the fungal ortholog, e.g. CoA esters of C26 fatty acids, pristanic acid and di/trihydroxycholestanoic acids, is explained by a large hydrophobic cavity formed upon the movements of the extremely mobile loops I-III in the N-domain. In the unliganded form of human hydratase 2, however, the loop I blocks the entrance of fatty enoyl-CoAs with chain-length above C8) [9]

Cloning

<1> [7]
<2> (wild type (HsMFE-2) and its variants are expressed in Saccharomyces cerevisiae, the recombinant HsMFE-2(dhδ) and its variants are expressed in Escherichia coli BL21(DE3)pLysS) [8]
<3> (a truncated version (amino acid residues 318-735) of perMFE-2 is expressed in Escherichia coli BL21(DE3) plysS cells as a recombinant protein) [13]
<3> (expression in Pichia pastoris) [18]
<5> (AtECH2 contains a peroxisome targeting signal at the C-terminal end, is addressed to the peroxisome in Saccharomyces cerevisiae, and a fusion protein between AtECH2 and a fluorescent protein is targeted to peroxisomes in onion cells. To assess the peroxisomal addressing of AtECH2, a fusion protein between an EYFP at the N terminus and AtECH2 at the C terminus is constructed and expressed under the control of a double cauliflower mosaic virus (CaMV) 35 S viral promoter to allow transient expression of the fusion protein in onion cells following biolistic bombardment. The fluorescence is examined by confocal microscopy after 12 h) [11]
<6> [4,6]
<6> (expression in Escherichia coli BL21 (DE3)) [2]
<8> (expressed in Escherichia coli BL21(DE3)) [5]
<10> (expression in Escherichia coli BL21(DE3)) [9]

Engineering

D370A <2> (<2> reduced specific acitivity of 2-enoyl-CoA hydratase 2 when expressed in Saccharomyces cerevisiae [8]) [8]
D490A <2> (<2> reduced specific acitivity of 2-enoyl-CoA hydratase 2 when expressed in Saccharomyces cerevisiae [8]) [8]
D510A <2> (<2> inactive mutant enzyme [8]) [8]
D517A <2> (<2> reduced specific acitivity of 2-enoyl-CoA hydratase 2 when expressed in Saccharomyces cerevisiae [8]) [8]
Δ629-990 <4> (<4> truncated version (lacking the carboxyl-terminal 271 amino acids). The truncated form contains only the D-3-hydroxyacyl-CoA dehydrogenase activity [15]) [15]

E366A <2> (<2> k_{cat}/K_m 100times lower than that of the wild type [8]) [8]
E408A <2> (<2> reduced specific acitivity of 2-enoyl-CoA hydratase 2 when expressed in Saccharomyces cerevisiae [8]) [8]
G16S <2> (<2> reduced specific acitivity of 2-enoyl-CoA hydratase 2 when expressed in Saccharomyces cerevisiae [8]) [8]
H406A <2> (<2> reduced specific acitivity of 2-enoyl-CoA hydratase 2 when expressed in Saccharomyces cerevisiae [8]) [8]
H515A <2> (<2> inactive mutant enzyme [8]) [8]
H532A <2> (<2> reduced specific acitivity of 2-enoyl-CoA hydratase 2 when expressed in Saccharomyces cerevisiae [8]) [8]
L654G/V130G <6> (<6> decreased specific activity for crotonyl-CoA [6]) [6]
L65A <6> (<6> enzyme activity similar to wild-type enzyme [6]) [6]
L65A/V130G <6> (<6> decreased specific activity for crotonyl-CoA [6]) [6]
L65G <6> (<6> enzyme activity similar to wild-type enzyme [6]) [6]
L65I <6> (<6> specific activity with crotonyl-CoA similar to wild-type enzyme [6]) [6]
L65V <6> (<6> specific activity with crotonyl-CoA similar to wild-type enzyme [6]) [6]
S62A <6> (<6> decreased specific activity for crotonyl-CoA [6]) [6]
V130A <6> (<6> specific activity with crotonyl-CoA similar to wild-type enzyme [6]) [6]
V130G <6> (<6> enzyme activity similar to wild-type enzyme, lower structural stability than wild-type enzyme [6]) [6]
Y347A <2> (<2> inactive mutant enzyme [8]) [8]
Y410A <2> (<2> reduced specific acitivity of 2-enoyl-CoA hydratase 2 when expressed in Saccharomyces cerevisiae [8]) [8]
Y505A <2> (<2> inactive mutant enzyme [8]) [8]
Additional information <2,8> (<8> CtMfe2p(dha+bδ) labelled with selenomethionine (SeMet), the plasmid pET3a::CtMfe2p(dha+bδ) is transformed to the methionine-auxotrophic Escherichia coli strain B834(DE3). The incorporation of SeMet into the structure does not affect the hydratase 2 activity [5]; <2> mutant constructs are tested for complementation in Saccharomyces cerevisiae [8]) [5,8]

Application

biotechnology <3> (<3> recombinant 46 kDa hydratase 2 survives in a purified form under storage, thus being the first protein of this type amenable to application as a tool in metabolic studies [13]) [13]

6 Stability

Storage stability

<2>, -20°C, stable for several months [3]
<3>, The purified enzyme can be stored as an active enzyme for at least half a year at -4°C or frozen at -20°C. [13]

References

[1] Malila, L.H.; Siivari, K.M.; Mäkelä, M.J.; Jalonen, J.E.; Latipää, P.M.; Kunau, W.H.; Hiltunen, J.K.: Enzymes converting D-3-hydroxyacyl-CoA to trans-2-enoyl-CoA. Microsomal and peroxisomal isoenzymes in rat liver. J. Biol. Chem., **268**, 21578-21585 (1993)

[2] Fukui, T.; Shiomi, N.; Doi, Y.: Expression and characterization of (R)-specific enoyl coenzyme A hydratase involved in polyhydroxyalkanoate biosynthesis by Aeromonas caviae. J. Bacteriol., **180**, 667-673 (1998)

[3] Jiang, L.L.; Kobayashi, A.; Matsuura, H.; Fukushima, H.; Hashimoto, T.: Purification and properties of human D-3-hydroxyacyl-CoA dehydratase: medium-chain enoyl-CoA hydratase is D-3-hydroxyacyl-CoA dehydratase. J. Biochem., **120**, 624-632 (1996)

[4] Hisano, T.; Fukui, T.; Iwata, T.; Doi, Y.: Crystallization and preliminary X-ray analysis of (R)-specific enoyl-CoA hydratase from Aeromonas caviae involved in polyhydroxyalkanoate biosynthesis. Acta Crystallogr. Sect. D, **57**, 145-147 (2001)

[5] Koski, M.K.; Haapalainen, A.M.; Hiltunen, J.K.; Glumoff, T.: Crystallization and preliminary crystallographic data of 2-enoyl-CoA hydratase 2 domain of Candida tropicalis peroxisomal multifunctional enzyme type 2. Acta Crystallogr. Sect. D, **59**, 1302-1305 (2003)

[6] Tsuge, T.; Hisano, T.; Taguchi, S.; Doi, Y.: Alteration of chain length substrate specificity of Aeromonas caviae R-enantiomer-specific enoyl-coenzyme A hydratase through site-directed mutagenesis. Appl. Environ. Microbiol., **69**, 4830-4836 (2003)

[7] Park, S.J.; Lee, S.Y.: Identification and characterization of a new enoyl coenzyme A hydratase involved in biosynthesis of medium-chain-length polyhydroxyalkanoates in recombinant Escherichia coli. J. Bacteriol., **185**, 5391-5397 (2003)

[8] Qin, Y.M.; Haapalainen, A.M.; Kilpelainen, S.H.; Marttila, M.S.; Koski, M.K.; Glumoff, T.; Novikov, D.K.; Hiltunen, J.K.: Human peroxisomal multifunctional enzyme type 2: site-directed mutagenesis studies show the importance of two protic residues for 2-enoyl-CoA hydratase 2 activity. J. Biol. Chem., **275**, 4965-4972 (2000)

[9] Kristian Koski, M.; Haapalainen, A.M.; Hiltunen, J.K.; Glumoff, T.: Crystal structure of 2-enoyl-CoA hydratase 2 from human peroxisomal multifunctional enzyme type 2. J. Mol. Biol., **345**, 1157-1169 (2005)

[10] Koski, M.K.; Haapalainen, A.M.; Hiltunen, J.K.; Glumoff, T.: A two-domain structure of one subunit explains unique features of eukaryotic hydratase 2. J. Biol. Chem., **279**, 24666-24672 (2004)

[11] Goepfert, S.; Hiltunen, J.K.; Poirier, Y.: Identification and functional characterization of a monofunctional peroxisomal enoyl-CoA hydratase 2 that participates in the degradation of even cis-unsaturated fatty acids in Arabidopsis thaliana. J. Biol. Chem., **281**, 35894-35903 (2006)

[12] Hiltunen, J.K.; Filppula, S.A.; Koivuranta, K.T.; Siivari, K.; Qin, Y.M.; Haeyrinen, H.M.: Peroxisomal β-oxidation and polyunsaturated fatty acids. Ann. N. Y. Acad. Sci., **804**, 116-128 (1996)
[13] Qin, Y.; Haapalainen, A.M.; Conry, D.; Cuebas, D.A.; Hiltunen, J.K.; Novikov, D.K.: Recombinant 2-enoyl-CoA hydratase derived from rat peroxisomal multifunctional enzyme 2: role of the hydratase reaction in bile acid synthesis. Biochem. J., **328**, 377-382 (1997)
[14] Hiltunen, J.K.; Palosaari, P.M.; Kunau, W.H.: Epimerization of 3-hydroxyacyl-CoA esters in rat liver. Involvement of two 2-enoyl-CoA hydratases. J. Biol. Chem., **264**, 13536-13540 (1989)
[15] Hiltunen, J.K.; Wenzel, B.; Beyer, A.; Erdmann, R.; Fossa, A.; Kunau, W.H.: Peroxisomal multifunctional β-oxidation protein of Saccharomyces cerevisiae. Molecular analysis of the fox2 gene and gene product. J. Biol. Chem., **267**, 6646-6653 (1992)
[16] Qin, Y.M.; Marttila, M.S.; Haapalainen, A.M.; Siivari, K.M.; Glumoff, T.; Hiltunen, J.K.: Yeast peroxisomal multifunctional enzyme: (3R)-hydroxyacyl-CoA dehydrogenase domains A and B are required for optimal growth on oleic acid. J. Biol. Chem., **274**, 28619-28625 (1999)
[17] Wu, L.; Lin, S.; Li, D.: Comparative inhibition studies of enoyl-CoA hydratase 1 and enoyl-CoA hydratase 2 in long-chain fatty acid oxidation. Org. Lett., **10**, 3355-3358 (2008)
[18] Qin, Y.M.; Poutanen, M.H.; Helander, H.M.; Kvist, A.P.; Siivari, K.M.; Schmitz, W.; Conzelmann, E.; Hellman, U.; Hiltunen, J.K.: Peroxisomal multifunctional enzyme of β-oxidation metabolizing D-3-hydroxyacyl-CoA esters in rat liver: molecular cloning, expression and characterization. Biochem. J., **321**, 21-28 (1997)
[19] Engeland K, Kindl H.: Evidence for a peroxisomal fatty acid β-oxidation involving D-3-hydroxyacyl-CoAs. Characterization of two forms of hydrolyase that convert D-(-)-3-hydroxyacyl-CoA into 2-trans-enoyl-CoA. Eur. J. Biochem., **200**, 171-178 (1991)

4-hydroxybutanoyl-CoA dehydratase 4.2.1.120

1 Nomenclature

EC number
4.2.1.120

Systematic name
4-hydroxybutanoyl-CoA hydro-lyase

Recommended name
4-hydroxybutanoyl-CoA dehydratase

Synonyms
AbfD <2> [4]

CAS registry number
129430-44-0

2 Source Organism

<1> *Clostridium kluyveri* [1]
<2> *Clostridium aminobutyricum* [2,3,4,5,6,7,8,9,10]
<3> *Metallosphaera sedula* [11]

3 Reaction and Specificity

Catalyzed reaction
4-hydroxybutanoyl-CoA = but-3-enoyl-CoA + H_2O (<2> cleavage is achieved by a FAD-dependent oxidation of 4-hydroxybutanoyl-CoA to 4-hydroxycrotonyl-CoA. In a second step, the hydroxyl group is substituted by a hydride derived from the now reduced FAD in an S_N2 reaction leading to vinylacetyl-CoA. Isomerization yields crotonyl-CoA [2]; <2> mechanism includes a direct dehydration of of 4-hydroxybutanoyl-CoA to vinylacetyl-CoA [9]; <2> mechanism involves transient one-electron oxidation of the substrate to activate the β-C-H-bond. the 4Fe-4S-center could serve a structural role and/or as Lewis acid facilitating the leaving of the hydroxyl group [5]; <2> the pro-(S) hydrogen atom is stereospecifically abstracted from C-3 of 4-hydroxybutanoyl-CoA, and this atom is not returned to C-4 [7])

Substrates and products
S 4-hydroxybutanoyl-CoA <2> (Reversibility: r) [2]
P vinylacetyl-CoA + H_2O

D. Schomburg and I. Schomburg (eds.), *Class 3.4–6 Hydrolases, Lyases, Isomerases, Ligases: EC 3.4–6*, Springer Handbook of Enzymes S10, DOI 10.1007/978-3-642-36260-6_47,

S 4-hydroxybutanoyl-CoA <1,2,3> (<2> reaction involves cleavage of an unactivated C-H bond at the β-carbon [6]; <2> selective removal of the (2Re)-hydrogen atom. The stereochemical course at C_2 and C_3 can be described as anti elimination of the two hydrogen atoms, which is identical to that of acyl-CoA dehydrogenases. The formation of the methyl group of crotonyl-CoA from the hydroxymethyl group of 4-hydroxybutanoyl-CoA occurs with retention of configuration [3]) (Reversibility: ?) [1,3,6,11]
P but-3-enoyl-CoA + H_2O
S Additional information <1,2> (<1> enzyme has an intrinsic vinylacetyl-CoA isomerase activity [1]; <2> no substrate: cyclopropylcarboxyl-CoA [2]) [1,2]
P ?

Inhibitors

dithionite <1> (<1> inactivation, oxidation with potassium hexacyanoferrate(III) results in up to 84% reactivation [1]) [1]
Additional information <2> (<2> enzyme is not inactivated by 5 mM 4-nitrophenol, 5 mM chloramphenicol, and 5 mM hydroxylamine [2]) [2]

Cofactors/prosthetic groups

4Fe-4S-center <2> (<2> a [4Fe-4S]2+ cluster, coordinated by three cysteine and one histidine residues, is located 7 A from the Re-side of a flavin adenine dinucleotide moiety [10]; <2> enzyme shows [4Fe-4S]2+ clusters, two clusters/homotetramer. The four iron atoms in each cluster are coordinated in an identical fashion, and there is no direct interaction with substrates. The Fe-S clusters serve a structural rather than a catalytic role in 4-hydroxybutyryl-CoA dehydratase [8]; <2> Fe-S-cluster is difficult to reduce. No equilibration of electrons between the flavin and the Fe-S-center [5]; <2> one 4Fe-4S-center per subunit [4]) [4,5,6,8,10]
FAD <1,2> (<2> 2 mol per mol of enzyme [2]; <1> 2 mol FAD per mol of enzyme [1]; <2> a [4Fe-4S]2+cluster, coordinated by three cysteine and one histidine residues, is located 7 A from the Re-side of a flavin adenine dinucleotide moiety [10]; <2> protein-bound FAD, is easily reduced to the semiquinone and only slowly to the hydroquinone. No equilibration of electrons between the flavin and the Fe-S-center [5]; <2> substrate interacts with the flavin. Partial reduction of the enzyme using dithionite results in formation of a neutral flavin semiquinone, which may interact with the 4Fe-4S-center [6]) [1,2,5,6,10]

Activating compounds

Additional information <2> (<2> enzyme does not require ATP, $MgCl_2$, and Ti(III)citrate [2]) [2]

Metals, ions

iron <1,2> (<1> 13.6 mol iron per mol of enzyme [1]; <2> 16 mol per mol of enzyme, plus 14 mol sulfur per mol of enzyme [2]; <2> enzyme shows [4Fe-4S]$^{2+}$ clusters, two clusters/homotetramer. The four iron atoms in each cluster are coordinated in an identical fashion, and there is no direct interaction

with substrates. The Fe-S clusters serve a structural rather than a catalytic role in 4-hydroxybutyryl-CoA dehydratase [8]) [1,2,8]

Specific activity (U/mg)
0.04 <3> (<3> 65°C [11]) [11]
7.38 <1> [1]
12.5 <2> (<2> pH 9.0, 25°C [2]) [2]

K_m-Value (mM)
0.05 <2> (4-hydroxybutanoyl-CoA, <2> pH 9.0, 25°C [2]) [2]

4 Enzyme Structure

Molecular weight
232000 <2> (<2> gel filtration [2]) [2]
237000 <1> (<1> gel filtration [1]) [1]

Subunits
tetramer <1,2> (<1> 4 * 59000, SDS-PAGE [1]; <2> 4 * 56000, SDS-PAGE [2]) [1,2]

5 Isolation/Preparation/Mutation/Application

Localization
membrane <2> (<2> enzyme is largely membrane- or particle-bound and may be solubilized by detergent [9]) [9]
soluble <1> (<1> high enzymic activity in anaerobically grown cell extract grown on succinate plus ethanol [1]) [1]

Purification
<1> (purification under strictly anaerobic conditions) [1]
<2> (using anaerobic conditions) [2]

Renaturation
<1> (enzyme is inactivated by dithionite, oxidation with potassium hexacyanoferrate(III) results in up to 84% reactivation) [1]

Crystallization
<2> (to 1.6 A resolution. A $[4Fe\text{-}4S]^{2+}$ cluster, coordinated by three cysteine and one histidine residues, is located 7 A from the Re-side of a flavin adenine dinucleotide moiety. The substrate can be bound between the $[4Fe\text{-}4S]^{2+}$ cluster and the FAD with both cofactors contributing to its radical activation and catalytic conversio) [10]

Cloning
<2> (expression in Escherichia coli) [4]

6 Stability

Oxidation stability

<1>, exposure to air leads to irreversible inactivation [1]
<2>, exposure to air results in initial activation followed by irreversible inactivation [2]
<2>, inactivation by oxygen [9]
<2>, upon exposure to air at 0°C, complete loss of dehydration activity within 40 min [5]

General stability information

<2>, stable under anaerobic conditions [9]

References

[1] Scherf, U.; Söhling, B.; Gottschalk, G.; Linder, D.; Buckel, W.: Succinate-ethanol fermentation in Clostridium kluyveri: purification, characterisation of 4-hydroxybutyryl-CoA dehydratase/vinylacetyl-CoA Δ^3-Δ^2-isomerase. Arch. Microbiol., **161**, 239-245 (1994)
[2] Scherf, U.; Buckel, W.: Purification and properties of an iron-sulfur and FAD-containing 4-hydroxybutyryl-CoA dehydratase/vinylacetyl-CoA Δ^3-Δ^2-isomerase from Clostridium aminobutyricum. Eur. J. Biochem., **215**, 421-429 (1993)
[3] Friedrich, P.; Darley, D.J.; Golding, B.T.; Buckel, W.: The complete stereochemistry of the enzymatic dehydration of 4-hydroxybutyryl coenzyme A to crotonyl coenzyme A. Angew. Chem., **47**, 3254-3257 (2008)
[4] Gerhardt, A.; Cinkaya, I.; Linder, D.; Huisman, G.; Buckel, W.: Fermentation of 4-aminobutyrate by Clostridium aminobutyricum: cloning of two genes involved in the formation and dehydration of 4-hydroxybutyryl-CoA. Arch. Microbiol., **174**, 189-199 (2000)
[5] Mueh, U.; Cinkaya, I.; Albracht, S.P.J.; Buckel, W.: 4-Hydroxybutyryl-CoA dehydratase from Clostridium aminobutyricum: Characterization of FAD and iron-sulfur clusters involved in an overall non-redox reaction. Biochemistry, **35**, 11710-11718 (1996)
[6] Cinkaya, I.; Buckel, W.; Medina, M.; Gomez-Moreno, C.; Cammack, R.: Electron-nuclear double resonance spectroscopy investigation of 4-hydroxybutyryl-CoA dehydratase from Clostridium aminobutyricum: Comparison with other flavin radical enzymes. Biol. Chem., **378**, 843-849 (1997)
[7] Scott, R.; Naeser, U.; Friedrich, P.; Selmer, T.; Buckel, W.; Golding, B.T.: Stereochemistry of hydrogen removal from the 'unactivated' C-3 position of 4-hydroxybutyryl-CoA catalysed by 4-hydroxybutyryl-CoA dehydratase. Chem. Commun. (Camb.), **0000**, 1210-1211 (2004)
[8] Muh, U.; Buckel, W.; Bill, E.: Moessbauer study of 4-hydroxybutyryl-CoA dehydratase. Probing the role of an iron-sulfur cluster in an overall non-redox reaction. Eur. J. Biochem., **248**, 380-384 (1997)

[9] Willadsen, P.; Buckel, W.: Assay of 4-hydroxybutyryl-CoA dehydratase from Clostridium aminobutyricum. FEMS Microbiol. Lett., **70**, 187-191 (1990)
[10] Martins, B.M.; Dobbek, H.; Cinkaya, I.; Buckel, W.; Messerschmidt, A.: Crystal structure of 4-hydroxybutyryl-CoA dehydratase: Radical catalysis involving a [4Fe-4S] cluster and flavin. Proc. Natl. Acad. Sci. USA, **101**, 15645-15649 (2004)
[11] Berg, I.A.; Kockelkorn, D.; Buckel, W.; Fuchs, G.: A 3-hydroxypropionate/4-hydroxybutyrate autotrophic carbon dioxide assimilation pathway in Archaea. Science, **318**, 1782-1786 (2007)

colneleate synthase 4.2.1.121

1 Nomenclature

EC number
4.2.1.121

Systematic name
(8E)-9-[(1E,3E)-nona-1,3-dien-1-yloxy]non-8-enoate synthase

Recommended name
colneleate synthase

Synonyms
9-DES <1,4> [2,10]
9-divinyl ether synthase <1,2,4> [2,10,11]
CYP74 cytochrome P-450 <5> [3]
CYP74D <1,3,4> [2,12]
CYP74D1 <5> [3]
DES <1,3,4> [9,12]
DES1 <2> [11]
DVE synthase <2> [11]
LeDES <5> [3]
NtDES1 <6> [8]
divinyl ether synthase <1,3,4> [9,12]

2 Source Organism

<1> *Solanum tuberosum* [1,4,5,6,7,10,12]
<2> *Nicotiana tabacum* [11]
<3> *Solanum lycopersicum* [12]
<4> *Solanum tuberosum* (UNIPROT accession number: Q9AVQ1) [2,9]
<5> *Solanum lycopersicum* (UNIPROT accession number: Q9FPM6) [3]
<6> *Nicotiana tabacum* (UNIPROT accession number: Q8W2N5) [8]

3 Reaction and Specificity

Catalyzed reaction
(9S,10E,12Z)-9-hydroperoxyoctadeca-10,12-dienoate = (8E)-9-[(1E,3Z)-nona-1,3-dien-1-yloxy]non-8-enoate + H_2O (<1> intervention of an epoxycarbonium ion intermediate. A mechanism is proposed [6]; <1> selective removal of the pro-R hydrogen at C-8 in the biosynthesis of colneleic acid [1,7]; <1>

D. Schomburg and I. Schomburg (eds.), *Class 3.4–6 Hydrolases, Lyases, Isomerases, Ligases: EC 3.4–6*, Springer Handbook of Enzymes S10, DOI 10.1007/978-3-642-36260-6_48,

the oxygen inserted enzymically between carbons 9- and 10- of the C-18 chain in forming colneleic acid originates from $^{18}O_2$ gas via the hydroperoxide group of linoleic acid. A mechanism is proposed [5])

Natural substrates and products

- **S** (9S,10E,12Z)-9-hydroperoxy-10,12-octadecadienoate <1,4> (Reversibility: ?) [2,7]
- **P** (8E)-9-[(1E,3Z)-nona-1,3-dien-1-yloxy]non-8-enoic acid + H_2O (<1> i.e. colneleate [7]; <4> i.e. colneleate, the fatty acid derivative colneleate functions as a plant antimicrobial compound [2])

Substrates and products

- **S** (9S)-hydroperoxy linoleic acid + H_2O <4> (Reversibility: ?) [9]
- **P** colneleic acid
- **S** (9S)-hydroperoxylinoleic acid + H_2O <1> (<1> potato divinyl ether synthase stereospecifically utilizes (9S)-hydroperoxylinoleic acid [12]) (Reversibility: ?) [12]
- **P** ?
- **S** (9S,10E,12Z)-9-hydroperoxy-10,12-octadecadienoate <1,4,5,6> (<1> intervention of an epoxycarbonium ion intermediate. A mechanism is proposed [6]; <5> poorly active against the the corresponding 13-hydroperoxide [3]; <1> selective removal of the pro-R hydrogen at C-8 in the biosynthesis of colneleic acid [7]; <1> selective removal of the pro-R hydrogen at C-8 in the biosynthesis of colneleic acid. Generation of colneleic acid from the (8R)-deuterated (9S)-hydroperoxide is accompanied by loss of most of the deuterium label (retention, 8%) [1]; <6> the corresponding 13-hydroperoxide is a poor substrate [8]; <4> the corresponding 13-hydroperoxide is not accepted as substrate [2]) (Reversibility: ?) [1,2,3,5,6,7,8]
- **P** (8E)-9-[(1E,3Z)-nona-1,3-dien-1-yloxy]non-8-enoic acid + H_2O (<1> i.e. colneleate [1,5,6,7]; <4> i.e. colneleate, the fatty acid derivative colneleate functions as a plant antimicrobial compound [2]; <4,5,6> i.e. colneleate, characterization of the product [2,3,8])
- **S** (9S,10E,12Z)-9-hydroperoxy-10,12-octadecadienoic acid + H_2O <1> (Reversibility: ?) [10]
- **P** colneleic acid (<1> i.e. 9-[1E,3Z-nonadienyloxy]-8E-nonenoic acid [10])
- **S** (9S,10E,12Z)-9-hydroperoxyoctadeca-10,12-dienoate + H_2O <1,3> (Reversibility: ?) [12]
- **P** 9-[1'(E),3'(Z)-nonadienyloxy]-8(E)-nonenoic acid (<1,3> i.e. colneleic acid [12])
- **S** (9S,10E,12Z,15Z)-9-hydroperoxy-10,12,15-octadecatrienoate <4,5,6> (<5> poorly active against the the corresponding 13-hydroperoxide [3]; <6> the corresponding 13-hydroperoxide is a poor substrate [8]; <4> the corresponding 13-hydroperoxide is not accepted as substrate [2]) (Reversibility: ?) [2,3,8]
- **P** (8E)-9-[(1E,3Z,6Z)-nona-1,3,6-trien-1-yloxy]non-8-enoic acid + H_2O (<5,6> i.e. colnelenate [3,8]; <4> i.e. colnelenic acid [2])

S (9S,10E,12Z,15Z)-9-hydroperoxy-10,12,15-octadecatrienoic acid + H_2O <1> (Reversibility: ?) [10]
P colnelenic acid (<1> i.e 9-[1E,3Z,6Z-nonatrienyloxy]-8E-nonenoic acid [10])
S (9S,10E,12Z,15Z)-9-hydroperoxy-10,12,15-octadecatrienoic acid + H_2O <1,3> (Reversibility: ?) [12]
P 9-[1'(E),3'(Z),6'(Z)-nonatrienyloxy]-8(E)-nonenoic acid (<1,3> i.e. colnelenic acid [12])
S Additional information <1,3,4> (<1> irrespective of which hydroperoxide regioisomer serves as the substrate, divinyl ether synthases abstracting the pro-R hydrogen generate divinyl ethers having an (E)-vinyl ether double bond, whereas enzymes abstracting the pro-S hydrogen produce divinyl ethers having a (Z)-vinyl ether double bond [1]; <4> 13-hydroperoxides are only poor substrates [9]; <1,3> the enzyme utilizes linoleic and α-linolenic acid 9-hydroperoxides as substrates, but is inactive towards 13-hydroperoxides [12]) (Reversibility: ?) [1,9,12]
P ?

Cofactors/prosthetic groups

cytochrome P-450 <5> (<5> the enzyme has spectral properties of cytochrome P-450 [3]) [3]
heme <1> [10]

Turnover number (s^{-1})

500 <5> ((9S,10E,12Z,15Z)-9-hydroperoxy-10,12,15-octadecatrienoate, <5> pH 7.0, 25°C [3]) [3]
890 <5> ((9S,10E,12Z)-9-hydroperoxy-10,12-octadecadienoate, <5> pH 7.0, 25°C [3]) [3]

K_m-Value (mM)

0.0174 <4> ((9S,10E,12Z)-9-hydroperoxy-10,12-octadecadienoate, <4> pH 6.5 [2]) [2]
0.0261 <4> ((9S,10E,12Z,15Z)-9-hydroperoxy-10,12,15-octadecatrienoate, <4> pH 6.5 [2]) [2]
0.048 <5> ((9S,10E,12Z,15Z)-9-hydroperoxy-10,12,15-octadecatrienoate, <5> pH 7.0, 25°C [3]) [3]
0.067 <5> ((9S,10E,12Z)-9-hydroperoxy-10,12-octadecadienoate, <5> pH 7.0, 25°C [3]) [3]

pH-Optimum

5.5-7.5 <4> [2]
9 <1> [6]

4 Enzyme Structure

Subunits

? <5> (<5> x * 55254, calculated from sequence [3]) [3]

5 Isolation/Preparation/Mutation/Application

Source/tissue

cell culture <1> (<1> preferential stimulation of the 9-lipoxygenase pathway in elicitor-treated potato cells [4]) [4]
leaf <4> (<4> accumulation of divinyl ether synthase transcripts both upon infiltration of potato leaves with Pseudomonas syringae and after infection with Phytophthora infestans [2]) [2]
plant <1> [10]
root <3,4,5,6> (<5> LeDES transcripts are most abundant in roots. A low level of LeDES mRNA is observed in stem tissue, but no accumulation is detected in flower buds, petioles, cotyledons, or leaves. Extracts from roots of young plants, but not extracts from stem or leaf tissue, catalyze efficient formation of colneleate from the hydroperoxide precursor [3]; <4> present in roots of green-house-grown potato plants [2]) [2,3,8,12]
seedling <2> [11]
stem <5> (<5> LeDES transcripts are most abundant in roots. A low level of LeDES mRNA is observed in stem tissue, but no accumulation is detected in flower buds, petioles, cotyledons, or leaves. Extracts from roots of young plants, but not extracts from stem or leaf tissue, catalyze efficient formation of colneleate from the hydroperoxide precursor [3]) [3]
tuber <1> [1,5,6]

Localization

cytoplasm <6> [8]
microsome <1,3> [12]

Purification

<1> (partial) [6]
<4> (recombinant enzyme) [2]
<5> [3]
<6> (recombinant glutathione S-transferase fusion protein) [8]

Cloning

<4> (expression in Escherichia coli) [2]
<5> (expression in Escherichia coli) [3]
<6> (expression in Escherichia coli as a glutathione S-transferase fusion protein) [8]

References

[1] Hamberg, M.: Hidden stereospecificity in the biosynthesis of divinyl ether fatty acids. FEBS J., **272**, 736-743 (2005)
[2] Stumpe, M.; Kandzia, R.; Gobel, C.; Rosahl, S.; Feussner, I.: A pathogen-inducible divinyl ether synthase (CYP74D) from elicitor-treated potato suspension cells. FEBS Lett., **507**, 371-376 (2001)

[3] Itoh, A.; Howe, G.A.: Molecular cloning of a divinyl ether synthase. Identification as a CYP74 cytochrome P-450. J. Biol. Chem., **276**, 3620-3627 (2001)
[4] Göbel, C.; Feussner, I.; Schmidt, A.; Scheel, D.; Sanchez-Serrano, J.; Hamberg, M.; Rosahl, S.: Oxylipin profiling reveals the preferential stimulation of the 9-lipoxygenase pathway in elicitor-treated potato cells. J. Biol. Chem., **276**, 6267-6273 (2001)
[5] Crombie, L.; Morgan, D.O.; Smith, E.H.: The enzymic formation of colneleic acid, a divinyl ether fatty acid: experiments with [(9S)-$^{18}O_2$]hydroperoxyoctadeca-(10E),(12Z)-dienoic acid. J. Chem. Soc. Chem. Commun., **1987**, 502-503 (1987)
[6] Crombie, L.; Morgan, D.O.; Smith, E.H.: An isotopic study (^{2}H and ^{18}O) of the enzymic conversion of linoleic acid into colneleic acid with carbon chain fracture: the origin of shorter chain aldehydes. J. Chem. Soc. Perkin Trans. I, **1991**, 567-575 (1991)
[7] Fahlstadius, P.; Hamberg, M.: Stereospecific removal of the pro-R hydrogen at C-8 of (9S)-hydroperoxyoctadecadienoic acid in the biosynthesis of colneleic acid. J. Chem. Soc. Perkin Trans., **1990**, 2027-2030 (1990)
[8] Fammartino, A.; Cardinale, F.; Göbel, C.; Mene-Saffrane, L.; Fournier, J.; Feussner, I.; Esquerre-Tugaye, M.T.: Characterization of a divinyl ether biosynthetic pathway specifically associated with pathogenesis in tobacco. Plant Physiol., **143**, 378-388 (2007)
[9] Stumpe, M.; Feussner, I.: Formation of oxylipins by CYP74 enzymes. Phytochem. Rev., **5**, 347-357 (2006)
[10] Eschen-Lippold, L.; Rothe, G.; Stumpe, M.; Goebel, C.; Feussner, I.; Rosahl, S.: Reduction of divinyl ether-containing polyunsaturated fatty acids in transgenic potato plants. Phytochemistry, **68**, 797-801 (2007)
[11] Fammartino, A.; Verdaguer, B.; Fournier, J.; Tamietti, G.; Carbonne, F.; Esquerre-Tugaye, M.T.; Cardinale, F.: Coordinated transcriptional regulation of the divinyl ether biosynthetic genes in tobacco by signal molecules related to defense. Plant Physiol. Biochem., **48**, 225-231 (2010)
[12] Grechkin, A.N.: Hydroperoxide lyase and divinyl ether synthase. Prostaglandins Other Lipid Mediat., **68-69**, 457-470 (2002)

ent-cassa-12,15-diene synthase 4.2.3.28

1 Nomenclature

EC number
4.2.3.28

Systematic name
ent-copalyl-diphosphate diphosphate-lyase (ent-cassa-12,15-diene-forming)

Recommended name
ent-cassa-12,15-diene synthase

Synonyms
OsDTC1 <1,2> [1,2]
OsKSL7 <1,2> [1,2]

2 Source Organism

<1> *Oryza sativa* [2]
<2> *Oryza sativa* (UNIPROT accession number: Q0E088) [1]

3 Reaction and Specificity

Catalyzed reaction
ent-copalyl diphosphate = ent-cassa-12,15-diene + diphosphate

Natural substrates and products
S ent-copalyl diphosphate <2> (<2> the enzyme produces ent-cassa-12,15-diene, a precursor of the rice phytoalexins (-)-phytocassanes A-E. Cholic acid induces transcription of the AsKSL7 gene [1]) (Reversibility: ?) [1]
P ent-cassa-12,15-diene + diphosphate

Substrates and products
S ent-copalyl diphosphate <1,2> (<2> the enzyme produces ent-cassa-12,15-diene, a precursor of the rice phytoalexins (-)-phytocassanes A-E. Cholic acid induces transcription of the AsKSL7 gene [1]) (Reversibility: ?) [1,2]
P ent-cassa-12,15-diene + diphosphate

D. Schomburg and I. Schomburg (eds.), *Class 3.4–6 Hydrolases, Lyases, Isomerases, Ligases: EC 3.4–6*, Springer Handbook of Enzymes S10, DOI 10.1007/978-3-642-36260-6_49,

5 Isolation/Preparation/Mutation/Application

Cloning

<2> [1]

References

[1] Sassa, T.; Yajima, A.; Yabuta, G.; Mori, K.; Oikawa, H.; Toshima, H.; Shibuya, N.; Nojiri, H.; Omori, T.; Nishiyama, M.; Yamane, H.: Molecular cloning and characterization of a cDNA encoding ent-cassa-12,15-diene synthase, a putative diterpenoid phytoalexin biosynthetic enzyme, from suspension-cultured rice cells treated with a chitin elicitor. Plant J., **37**, 1-8 (2004)

[2] Okada, A.; Okada, K.; Miyamoto, K.; Koga, J.; Shibuya, N.; Nojiri, H.; Yamane, H.: OsTGAP1, a bZIP transcription factor, coordinately regulates the inductive production of diterpenoid phytoalexins in rice. J. Biol. Chem., **284**, 26510-26518 (2009)

ent-sandaracopimaradiene synthase 4.2.3.29

1 Nomenclature

EC number
4.2.3.29

Systematic name
ent-copalyl-diphosphate diphosphate-lyase [ent-sandaracopimara-8(14),15-diene-forming]

Recommended name
ent-sandaracopimaradiene synthase

Synonyms
OsKS10 <2> [1,2]
OsKSL10 <1> [3]
ent-(sandaraco)pimar-8(14),15-diene synthase <1> [3]

CAS registry number
160047-79-0

2 Source Organism

<1> *Oryza sativa* [3]
<2> *Oryza sativa* (UNIPROT accession number: Q2QQJ5) [1,2]

3 Reaction and Specificity

Catalyzed reaction
ent-copalyl diphosphate = ent-sandaracopimara-8(14),15-diene + diphosphate

Natural substrates and products
S ent-copalyl diphosphate <2> (<2> the enzyme is involved in the biosynthesis of oryzalexins A-F, phytoalexin biosynthesis [1]) (Reversibility: ?) [1]
P ent-pimara-8(14),15-diene + diphosphate
S Additional information <1> (<1> OsKSL10, is induced by either fungal elicitor or UV-irradiation [3]) (Reversibility: ?) [3]
P ?

D. Schomburg and I. Schomburg (eds.), *Class 3.4–6 Hydrolases, Lyases, Isomerases, Ligases: EC 3.4–6*, Springer Handbook of Enzymes S10, DOI 10.1007/978-3-642-36260-6_50,

Substrates and products

- **S** ent-copalyl diphosphate <2> (Reversibility: ?) [1,2]
- **P** ent-sandaracopimara-8(14),15-diene + diphosphate
- **S** ent-copalyl diphosphate <2> (<2> the enzyme is involved in the biosynthesis of oryzalexins A-F, phytoalexin biosynthesis [1]) (Reversibility: ?) [1]
- **P** ent-pimara-8(14),15-diene + diphosphate
- **S** Additional information <1> (<1> OsKSL10, is induced by either fungal elicitor or UV-irradiation [3]) (Reversibility: ?) [3]
- **P** ?

5 Isolation/Preparation/Mutation/Application

Source/tissue

leaf <2> (<2> the transcript of OsKS10 increases strongly after UV irradiation [2]) [2]

Cloning

<1> [3]
<2> [1]

References

[1] Otomo, K.; Kanno, Y.; Motegi, A.; Kenmoku, H.; Yamane, H.; Mitsuhashi, W.; Oikawa, H.; Toshima, H.; Itoh, H.; Matsuoka, M.; Sassa, T.; Toyomasu, T.: Diterpene cyclases responsible for the biosynthesis of phytoalexins, momilactones A, B, and oryzalexins A-F in rice. Biosci. Biotechnol. Biochem., **68**, 2001-2006 (2004)

[2] Kanno, Y.; Otomo, K.; Kenmoku, H.; Mitsuhashi, W.; Yamane, H.; Oikawa, H.; Toshima, H.; Matsuoka, M.; Sassa, T.; Toyomasu, T.: Characterization of a rice gene family encoding type-A diterpene cyclases. Biosci. Biotechnol. Biochem., **70**, 1702-1710 (2006)

[3] Xu, M.; Wilderman, P.R.; Morrone, D.; Xu, J.; Roy, A.; Margis-Pinheiro, M.; Upadhyaya, N.M.; Coates, R.M.; Peters, R.J.: Functional characterization of the rice kaurene synthase-like gene family. Phytochemistry, **68**, 312-326 (2007)

ent-pimara-8(14),15-diene synthase 4.2.3.30

1 Nomenclature

EC number
4.2.3.30

Systematic name
ent-copalyl-diphosphate diphosphate-lyase [ent-pimara-8(14),15-diene-forming]

Recommended name
ent-pimara-8(14),15-diene synthase

Synonyms
OsKS5 <1> [1]

2 Source Organism

<1> *Oryza sativa* (UNIPROT accession number: Q6Z5J6) [1]

3 Reaction and Specificity

Catalyzed reaction
ent-copalyl diphosphate = ent-pimara-8(14),15-diene + diphosphate

Substrates and products
S ent-copalyl diphosphate <1> (Reversibility: ?) [1]
P ent-pimara-8(14),15-diene + diphosphate

5 Isolation/Preparation/Mutation/Application

Source/tissue
leaf <1> (<1> no change in transcript level of OsKS5 after UV irradiation [1]) [1]

Purification
<1> (recombinant enzyme) [1]

Cloning
<1> (truncated coding region of OsKS5 is subcloned into the pGEX4T-3-bacterial expression vector, expression in Escherichia coli) [1]

D. Schomburg and I. Schomburg (eds.), *Class 3.4–6 Hydrolases, Lyases, Isomerases, Ligases: EC 3.4–6*, Springer Handbook of Enzymes S10, DOI 10.1007/978-3-642-36260-6_51,

References

[1] Kanno, Y.; Otomo, K.; Kenmoku, H.; Mitsuhashi, W.; Yamane, H.; Oikawa, H.; Toshima, H.; Matsuoka, M.; Sassa, T.; Toyomasu, T.: Characterization of a rice gene family encoding type-A diterpene cyclases. Biosci. Biotechnol. Biochem., **70**, 1702-1710 (2006)

ent-pimara-9(11),15-diene synthase 4.2.3.31

1 Nomenclature

EC number
4.2.3.31

Systematic name
ent-copalyl-diphosphate diphosphate-lyase [ent-pimara-9(11),15-diene-forming]

Recommended name
ent-pimara-9(11),15-diene synthase

2 Source Organism

<1> *Streptomyces sp.* [1]

3 Reaction and Specificity

Catalyzed reaction
ent-copalyl diphosphate = ent-pimara-9(11),15-diene + diphosphate

Substrates and products
S ent-copalyl diphosphate <1> (Reversibility: ?) [1]
P pimara-9(11),15-diene + diphosphate
S Additional information <1> (<1> no substrates: farnesyl diphosphate, geranylgeranyl diphosphate, terpentecin diphosphate [1]) (Reversibility: ?) [1]
P ?

Activating compounds
2-mercaptoethanol <1> (<1> 5 mM, required for full activity [1]) [1]
Tween-80 <1> (<1> 0.1%, required for full activity [1]) [1]

Metals, ions
Co^{2+} <1> (<1> 1 mM, 100% of the activity with Mg^{2+} [1]) [1]
Mg^{2+} <1> (<1> absolutely required, optimal concentraion 1 mM [1]) [1]
Ni^{2+} <1> (<1> 1 mM, 57% of the activity with Mg^{2+} [1]) [1]
Zn^{2+} <1> (<1> 1 mM, 59% of the activity with Mg^{2+} [1]) [1]
Additional information <1> (<1> no or very weak activity in presence of Mn^{2+}, Ca^{2+}, Cu^{2+} and Fe^{2+} [1]) [1]

D. Schomburg and I. Schomburg (eds.), *Class 3.4–6 Hydrolases, Lyases, Isomerases, Ligases: EC 3.4–6*, Springer Handbook of Enzymes S10, DOI 10.1007/978-3-642-36260-6_52,

Turnover number (s^{-1})
0.0014 <1> (ent-copalyl diphosphate, <1> 30°C, pH 7.0 [1]) [1]

K_m-Value (mM)
0.00026 <1> (ent-copalyl diphosphate, <1> 30°C, pH 7.0 [1]) [1]

pH-Optimum
7 <1> [1]

pH-Range
6-8 <1> [1]

Temperature optimum (°C)
30 <1> (<1> 0.05 M Tris, pH 7.0 [1]) [1]

4 Enzyme Structure

Molecular weight
35000 <1> (<1> gel filtration [1]) [1]

Subunits
monomer <1> (<1> x * 35000, SDS-PAGE [1]) [1]

6 Stability

Temperature stability
35 <1> (<1> pH 5.5, stable for at least 1 h [1]) [1]

References

[1] Ikeda, C.; Hayashi, Y.; Itoh, N.; Seto, H.; Dairi, T.: Functional analysis of eubacterial ent-copalyl diphosphate synthase and pimara-9(11),15-diene synthase with unique primary sequences. J. Biochem., **141**, 37-45 (2007)

levopimaradiene synthase 4.2.3.32

1 Nomenclature

EC number
4.2.3.32

Systematic name
ent-copalyl-diphosphate diphosphate-lyase [ent-abieta-8(14),12-diene-forming]

Recommended name
levopimaradiene synthase

Synonyms
TPS-LAS <2> [1]

CAS registry number
369596-13-4

2 Source Organism

<1> *Picea abies* (UNIPROT accession number: Q675L4) [3]
<2> *Pinus taeda* (UNIPROT accession number: Q50EK2) [1]
<3> *Ginkgo biloba* (UNIPROT accession number: Q947C4) [2]

3 Reaction and Specificity

Catalyzed reaction
copalyl diphosphate = abieta-8(14),12-diene + diphosphate

Reaction type
cyclization
elimination of diphosphate

Natural substrates and products
S Additional information <3> (<3> catalyzes an intermediate step in synthesis of ginkgolide A [2]) (Reversibility: ?) [2]
P ?

Substrates and products
S (+)-copalyl-diphosphate <1,2> (<1,2> reaction intermediate is C8-sandaracopimaradienyl cation [1,3]) (Reversibility: ?) [1,3]

D. Schomburg and I. Schomburg (eds.), *Class 3.4–6 Hydrolases, Lyases, Isomerases, Ligases: EC 3.4–6*, Springer Handbook of Enzymes S10, DOI 10.1007/978-3-642-36260-6_53,

P (-)-abietadiene + levopimaradiene + neoabietadiene + palustradiene + diphosphate (<1> bifunctional levopimaradiene/abietadiene synthase produces a mixture of diterpenes [3]; <2> bifunctional levopimaradiene/abietadiene synthase, about 47% levopimaradiene, 27% abietadiene, 22% neoabietadiene, 3% palustradiene [1])
S (+)-copalyl-diphosphate <3> (<3> reaction intermediate is labdadienyl diphosphate [2]) (Reversibility: ?) [2]
P levopimaradiene + diphosphate
S Additional information <3> (<3> catalyzes an intermediate step in synthesis of ginkgolide A [2]) (Reversibility: ?) [2]
P ?

Activating compounds

dithiothreitol <3> (<3> optimal activity in the presence of 5 mM DTT and 5% glycerol [2]) [2]

Metals, ions

Mn^{2+} <3> (<3> required [2]) [2]
Additional information <3> (<3> enzyme is not dependent on Mg^{2+} [2]) [2]

pH-Optimum

7.2 <3> [2]

4 Enzyme Structure

Subunits

? <3> (<3> x * 100289, calculated [2]) [2]

Posttranslational modification

Additional information <3> (<3> sequence includes a putative N-terminal plastid transit peptide and three aspartate-rich regions [2]) [2]

5 Isolation/Preparation/Mutation/Application

Source/tissue

root <3> (<3> root of seedling [2]) [2]
seedling <3> (<3> root of seedling [2]) [2]

Localization

endoplasmic reticulum <2> [1]
plastid <2,3> (<3> sequence includes a putative N-terminal plastid transit peptide [2]) [1,2]

Crystallization

<1> (homology model of the second active site of enzyme based on the structure of 5-epiaristolochene synthase from Nicotiana tabacum, Protein Data Bank ID code 5EAT) [3]

Cloning

<2> (expression of green fluorescent fusion protein in tobacco cells) [1]
<3> (expression in Escherichia coli) [2]

Engineering

A713S <1> (<1> products are isopimaradiene and sandaracopimaradiene [3]) [3]
G651V <1> (<1> no change in product [3]) [3]
V717L <1> (<1> no change in product [3]) [3]
W679L/Y686H/A713S/V717L <1> (<1> products are isopimaradiene and sandaracopimaradiene [3]) [3]
Y686H <1> (<1> no change in product [3]) [3]
Y686H/A713S <1> (<1> main products are isopimaradiene and sandaracopimaradiene [3]) [3]
Y686H/A713S A713S <1> (<1> main products are isopimaradiene and sandaracopimaradiene [3]) [3]
Y686H/A713S/V717L <1> (<1> products are isopimaradiene and sandaracopimaradiene [3]) [3]
Additional information <1,3> (<3> removal of 60 or 79 N-terminal residues increases levopimaradiene production, deletion of 128 N-terminal residues results in loss of catalytic activity [2]; <1> swapping of residues 568-640 of isopimaradiene synhase to corresponding residues 560-632 of levopimaradiene/abietadiene synthase results in complete reversion of the product profiles of the two enzymes [3]) [2,3]

References

[1] Ro, D.K.; Bohlmann, J.: Diterpene resin acid biosynthesis in loblolly pine (Pinus taeda): Functional characterization of abietadiene/levopimaradiene synthase (PtTPS-LAS) cDNA and subcellular targeting of PtTPS-LAS and abietadienol/abietadienal oxidase (PtAO, CYP720B1). Phytochemistry, **67**, 1572-1578 (2006)
[2] Schepmann, H.G.; Pang, J.; Matsuda, S.P.T.: Cloning and characterization of Ginkgo biloba levopimaradiene synthase, which catalyzes the first committed step in ginkgolide biosynthesis. Arch. Biochem. Biophys., **392**, 263-269 (2001)
[3] Keeling, C.I.; Weisshaar, S.; Lin, r.P.C.; Bohlmann, J.: Functional plasticity of paralogous diterpene synthases involved in conifer defense. Proc. Natl. Acad. Sci. USA, **105**, 1085-1090 (2008)

stemar-13-ene synthase 4.2.3.33

1 Nomenclature

EC number
4.2.3.33

Systematic name
9α-copalyl-diphosphate diphosphate-lyase (stemar-13-ene-forming)

Recommended name
stemar-13-ene synthase

Synonyms
OsDTC2 <1,2> [2,3]
stemar-13-ene synthase <1> [2]

2 Source Organism

<1> *Oryza sativa* [1,2]
<2> *Oryza sativa* (UNIPROT accession number: Q6BDZ9) [3]

3 Reaction and Specificity

Catalyzed reaction
9α-copalyl diphosphate = stemar-13-ene + diphosphate

Natural substrates and products
S 9α-copalyl diphosphate <1,2> (<1> the enzyme converts syn-copalyl diphosphate into stemar-13-ene, a putative diterpene hydrocarbon precursor of the phytoalexin oryzalexin S. The transcriptional expression of $OsDTC_2$ is induced by treatment of suspension-cultured rice cells with a chitin oligosaccharide elicitor [2]; <2> the enzyme converts syn-copalyl diphosphate to stemar-13-ene, a putative diterpene hydrocarbon precursor of the phytoalexin oryzalexin S [3]) (Reversibility: ?) [2,3]
P stemar-13-ene + diphosphate

Substrates and products
S 9α-copalyl diphosphate <1,2> (<1> the enzyme converts syn-copalyl diphosphate into stemar-13-ene, a putative diterpene hydrocarbon precursor of the phytoalexin oryzalexin S. The transcriptional expression of $OsDTC_2$ is induced by treatment of suspension-cultured rice cells with a chitin oligosaccharide elicitor [2]; <2> the enzyme converts syn-copalyl

D. Schomburg and I. Schomburg (eds.), *Class 3.4–6 Hydrolases, Lyases, Isomerases, Ligases: EC 3.4–6*, Springer Handbook of Enzymes S10, DOI 10.1007/978-3-642-36260-6_54,

diphosphate to stemar-13-ene, a putative diterpene hydrocarbon precursor of the phytoalexin oryzalexin S [3]) (Reversibility: ?) [1,2,3]
P stemar-13-ene + diphosphate

5 Isolation/Preparation/Mutation/Application

Source/tissue

cell suspension culture <1,2> (<2> the level of OsDTC2 mRNA in suspension-cultured rice cells began to increase 3 h after addition of the elicitor and reached the maximum after 8 h [3]) [1,2,3]
leaf <2> (<2> expression of OsDTC2 is induced in UV-irradiated rice leaves [3]) [3]

Cloning

<2> ($OsDTC_2$ cDNA is overexpressed in Escherichia coli as a fusion protein with glutathione S-transferase) [3]

References

[1] Mohan, R.S.; Yee, N.K.; Coates, R.M.; Ren, Y.Y.; Stamenkovic, P.; Mendez, I.; West, C.A.: Biosynthesis of cyclic diterpene hydrocarbons in rice cell suspensions: conversion of 9,10-syn-labda-8(17),13-dienyl diphosphate to 9β-pimara-7,15-diene and stemar-13-ene. Arch. Biochem. Biophys., **330**, 33-47 (1996)
[2] Nemoto, T.; Okada, A.; Okada, K.; Shibuya, N.; Toyomasu, T.; Nojiri, H.; Yamane, H.: Promoter analysis of the rice stemar-13-ene synthase gene OsDTC2, which is involved in the biosynthesis of the phytoalexin oryzalexin S. Biochim. Biophys. Acta, **1769**, 678-683 (2007)
[3] Nemoto, T.; Cho, E.M.; Okada, A.; Okada, K.; Otomo, K.; Kanno, Y.; Toyomasu, T.; Mitsuhashi, W.; Sassa, T.; Minami, E.; Shibuya, N.; Nishiyama, M.; Nojiri, H.; Yamane, H.: Stemar-13-ene synthase, a diterpene cyclase involved in the biosynthesis of the phytoalexin oryzalexin S in rice. FEBS Lett., **571**, 182-186 (2004)

stemod-13(17)-ene synthase 4.2.3.34

1 Nomenclature

EC number
4.2.3.34

Systematic name
9α-copalyl-diphosphate diphosphate-lyase [stemod-13(17)-ene-forming]

Recommended name
stemod-13(17)-ene synthase

Synonyms
OsKSL11 <1> [1]

2 Source Organism

<1> *Oryza sativa* (UNIPROT accession number: Q1AHB2) [1]

3 Reaction and Specificity

Catalyzed reaction
9α-copalyl diphosphate = stemod-13(17)-ene + diphosphate

Natural substrates and products
- **S** 9α-copalyl diphosphate <1> (<1> the enzyme catalyzes the committed step in biosynthesis of the stemodane family of diterpenoid natural products, some of which possess antiviral activity [1]) (Reversibility: ?) [1]
- **P** stemod-13(17)-ene + diphosphate

Substrates and products
- **S** 9α-copalyl diphosphate <1> (<1> the enzyme catalyzes the committed step in biosynthesis of the stemodane family of diterpenoid natural products, some of which possess antiviral activity [1]) (Reversibility: ?) [1]
- **P** stemod-13(17)-ene + diphosphate

5 Isolation/Preparation/Mutation/Application

Cloning
<1> [1]

D. Schomburg and I. Schomburg (eds.), *Class 3.4–6 Hydrolases, Lyases, Isomerases, Ligases: EC 3.4–6*, Springer Handbook of Enzymes S10, DOI 10.1007/978-3-642-36260-6_55,

References

[1] Morrone, D.; Jin, Y.; Xu, M.; Choi, S.Y.; Coates, R.M.; Peters, R.J.: An unexpected diterpene cyclase from rice: functional identification of a stemodene synthase. Arch. Biochem. Biophys., **448**, 133-140 (2006)

syn-pimara-7,15-diene synthase 4.2.3.35

1 Nomenclature

EC number
4.2.3.35

Systematic name
9α-copalyl-diphosphate diphosphate-lyase (9β-pimara-7,15-diene-forming)

Recommended name
syn-pimara-7,15-diene synthase

Synonyms
9β-pimara-7,15-diene synthase <1> [3]
OsDTS2 <1> [3]
OsKS4 <2> [2]

2 Source Organism

<1> *Oryza sativa* [1,3]
<2> *Oryza sativa* (UNIPROT accession number: Q0JEZ8) [2]
<3> *Picea abies* (UNIPROT accession number: Q675L5) [4]

3 Reaction and Specificity

Catalyzed reaction
9α-copalyl diphosphate = 9β-pimara-7,15-diene + diphosphate

Reaction type
cyclization
elimination of diphosphate

Natural substrates and products
S 9,10-syn-copalyl diphosphate <1> (Reversibility: ?) [1]
P 9β-pimara-7,15-diene + diphosphate (<1> product identification via radio TLC, GC and GC/MS [1])
S 9α-copalyl diphosphate <2> (<2> the enzyme is involved in the biosynthesis of oryzalexins A-F, phytoalexin biosynthesis [2]) (Reversibility: ?) [2]
P 9β-pimara-7,15-diene + diphosphate

D. Schomburg and I. Schomburg (eds.), *Class 3.4–6 Hydrolases, Lyases, Isomerases, Ligases: EC 3.4–6*, Springer Handbook of Enzymes S10, DOI 10.1007/978-3-642-36260-6_56,

Substrates and products

- **S** (+)-copalyl-diphosphate <3> (<3> reaction intermediate is C8-sandaracopimaradienyl cation [4]) (Reversibility: ?) [4]
- **P** 9β-isopimara-7,15-diene + diphosphate
- **S** 9,10-syn-copalyl diphosphate <1> (Reversibility: ?) [1]
- **P** 9β-pimara-7,15-diene + diphosphate (<1> product identification via radio TLC, GC and GC/MS [1])
- **S** 9α-copalyl diphosphate <1,2> (<2> the enzyme is involved in the biosynthesis of oryzalexins A-F, phytoalexin biosynthesis [2]) (Reversibility: ?) [2,3]
- **P** 9β-pimara-7,15-diene + diphosphate

5 Isolation/Preparation/Mutation/Application

Source/tissue

callus <1> (<1> cell culture [1]) [1]
leaf <1> (<1> OsDTS2 mRNA in leaves is up-regulated by conditions that stimulate phytoalexin biosynthesis [3]) [3]
root <1> (<1> OsDTS2 mRNA is constitutively expressed [3]) [3]

Crystallization

<3> (homology model of the second active site of enzyme based on the structure of 5-epiaristolochene synthase from Nicotiana tabacum, Protein Data Bank ID code 5EAT) [4]

Cloning

<1> [3]
<2> [2]

Engineering

A713S <3> (<3> products are isopimaradiene and sandaracopimaradiene [4]) [4]
G651V <3> (<3> no change in product [4]) [4]
V717L <3> (<3> no change in product [4]) [4]
W679L/Y686H/A713S/V717L <3> (<3> products are isopimaradiene and sandaracopimaradiene [4]) [4]
Y686H <3> (<3> no change in product [4]) [4]
Y686H/A713S <3> (<3> main products are isopimaradiene and sandaracopimaradiene [4]) [4]
Y686H/A713S A713S <3> (<3> main products are isopimaradiene and sandaracopimaradiene [4]) [4]
Y686H/A713S/V717L <3> (<3> products are isopimaradiene and sandaracopimaradiene [4]) [4]
Additional information <3> (<3> swapping of residues 568-640 of isopimaradiene synhase to corresponding residues 560-632 of levopimaradiene/abietadiene synthase results in complete reversion of the product profiles of the two enzymes [4]) [4]

References

[1] Mohan, R.S.; Yee, N.K.; Coates, R.M.; Ren, Y.Y.; Stamenkovic, P.; Mendez, I.; West, C.A.: Biosynthesis of cyclic diterpene hydrocarbons in rice cell suspensions: conversion of 9,10-syn-labda-8(17),13-dienyl diphosphate to 9β-pimara-7,15-diene and stemar-13-ene. Arch. Biochem. Biophys., **330**, 33-47 (1996)

[2] Otomo, K.; Kanno, Y.; Motegi, A.; Kenmoku, H.; Yamane, H.; Mitsuhashi, W.; Oikawa, H.; Toshima, H.; Itoh, H.; Matsuoka, M.; Sassa, T.; Toyomasu, T.: Diterpene cyclases responsible for the biosynthesis of phytoalexins, momilactones A, B, and oryzalexins A-F in rice. Biosci. Biotechnol. Biochem., **68**, 2001-2006 (2004)

[3] Wilderman, P.R.; Xu, M.; Jin, Y.; Coates, R.M.; Peters, R.J.: Identification of syn-pimara-7,15-diene synthase reveals functional clustering of terpene synthases involved in rice phytoalexin/allelochemical biosynthesis. Plant Physiol., **135**, 2098-2105 (2004)

[4] Keeling, C.I.; Weisshaar, S.; Lin, r.P.C.; Bohlmann, J.: Functional plasticity of paralogous diterpene synthases involved in conifer defense. Proc. Natl. Acad. Sci. USA, **105**, 1085-1090 (2008)

terpentetriene synthase 4.2.3.36

1 Nomenclature

EC number
4.2.3.36

Systematic name
terpentedienyl-diphosphate diphosphate-lyase (terpentetriene-forming)

Recommended name
terpentetriene synthase

Synonyms
Cyc2 <1> [2]

CAS registry number
429681-55-0

2 Source Organism

<1> *Kitasatospora griseola* [1,2,3]

3 Reaction and Specificity

Catalyzed reaction
terpentedienyl diphosphate = terpentetriene + diphosphate

Substrates and products
S terpentedienyl diphosphate <1> (Reversibility: ?) [1,2,3]
P terpentetriene + diphosphate

Activating compounds
Additional information <1> (<1> 20% glycerol, 5 mM 2-mercaptoethanol, and 0.1% Tween 80 are required for the full activity of the Cy2c2 [2]) [2]

Metals, ions
Co^{2+} <1> (<1> 1 mM, 3% of the activity with Mg^{2+}, substrate: terpentedienyl diphosphate [2]) [2]
Fe^{2+} <1> (<1> 1 mM, 5% of the activity with Mg^{2+}, substrate: terpentedienyl diphosphate [2]) [2]
Mg^{2+} <1> (<1> required, substrate: terpentedienyl diphosphate [2]) [2]
Mn^{2+} <1> (<1> 1 mM, 37% of the activity with Mg^{2+}, substrate: terpentedienyl diphosphate [2]) [2]

D. Schomburg and I. Schomburg (eds.), *Class 3.4–6 Hydrolases, Lyases, Isomerases, Ligases: EC 3.4–6*, Springer Handbook of Enzymes S10, DOI 10.1007/978-3-642-36260-6_57,

K_m-Value (mM)
0.0076 <1> (terpentedienyl diphosphate) [2]

pH-Optimum
6.8 <1> (<1> Tris-HCl buffer, substrate: terpentedienyl diphosphate [2]) [2]

pH-Range
6.8-7.5 <1> [2]

Temperature optimum (°C)
50 <1> (<1> 0.05 M Tris-HCl buffer [2]) [2]

4 Enzyme Structure

Molecular weight
70000 <1> (<1> gel filtration [2]) [2]

Subunits
dimer <1> (<1> 2 * 37000, calculated from sequence [2]) [2]

5 Isolation/Preparation/Mutation/Application

Purification
<1> [1]

Cloning
<1> [2]
<1> (heterologous expression of the cyclase genes in Streptomyces lividans and Escherichia coli) [1]

6 Stability

Temperature stability
30 <1> (<1> stable after incubation at 30°C in 0.05 M Tris-HCl buffer (pH 6.8) for 1 h [2]) [2]

References

[1] Dairi, T.; Hamano, Y.; Kuzuyama, T.; Itoh, N.; Furihata, K.; Seto, H.: Eubacterial diterpene cyclase genes essential for production of the isoprenoid antibiotic terpentecin. J. Bacteriol., **183**, 6085-6094 (2001)
[2] Hamano, Y.; Kuzuyama, T.; Itoh, N.; Furihata, K.; Seto, H.; Dairi, T.: Functional analysis of eubacterial diterpene cyclases responsible for biosynthesis of a diterpene antibiotic, terpentecin. J. Biol. Chem., **277**, 37098-37104 (2002)

[3] Eguchi, T.; Dekishima, Y.; Hamano, Y.; Dairi, T.; Seto, H.; Kakinuma, K.: A new approach for the investigation of isoprenoid biosynthesis featuring pathway switching, deuterium hyperlabeling, and 1H NMR spectroscopy. The reaction mechanism of a novel streptomyces diterpene cyclase. J. Org. Chem., **68**, 5433-5438 (2003)

epi-isozizaene synthase 4.2.3.37

1 Nomenclature

EC number
4.2.3.37

Systematic name
(2E,6E)-farnesyl-diphosphate diphosphate-lyase [(+)-epi-isozizaene-forming]

Recommended name
epi-isozizaene synthase

Synonyms
SCO5222 protein <3> [3]
epi-isozizaene synthase <1,3> [2,3]

2 Source Organism

<1> *Streptomyces coelicolor A3(2)* [2]
<2> *Streptomyces coelicolor* (UNIPROT accession number: Q9K499) (testis-specific serine/threonine protein kinase 5 variant α [1]) [1]
<3> *Streptomyces coelicolor A3(2)* (UNIPROT accession number: Q9K499) [3]

3 Reaction and Specificity

Catalyzed reaction
(2E,6E)-farnesyl diphosphate = (+)-epi-isozizaene + diphosphate (<2> ionization and isomerization of farnesyl diphosphate will give (3R)-nerolidyl diphosphate. Rotation about the newly generated C-2/C-3 bond generates the corresponding cisoid nerolidyl diphosphate conformer which can undergo ionization and cyclization to form a bisabolyl cation. Following 1,2-hydride shift and spirocyclization, the resultant acorenyl cation can undergo further cyclization, ring contraction, methyl migration, and deprotonation to yield (+)-epi-isozizaene [1])

Substrates and products
S (2E,6E)-farnesyl diphosphate <1,3> (Reversibility: ?) [2,3]
P (+)-epi-isozizaene + diphosphate (<3> major product [3]; <1> major product (79%) [2])
S (3R)-(Z)-nerolidyl diphosphate <3> (<3> 93:7 preference for (3R)-nerolidyl diphosphate over (3S)-nerolidyl diphosphate [3]) (Reversibility: ?) [3]

D. Schomburg and I. Schomburg (eds.), *Class 3.4–6 Hydrolases, Lyases, Isomerases, Ligases: EC 3.4–6*, Springer Handbook of Enzymes S10, DOI 10.1007/978-3-642-36260-6_58,

P (+)-epi-isozizaene + diphosphate
S (2E,6E)-farnesyl diphosphate <2> (Reversibility: ?) [1]
P (+)-epi-isozizaene + diphosphate

Metals, ions
Mg^{2+} <1,3> [2,3]

Turnover number (s^{-1})
0.00024 <1> ((2E,6E)-farnesyl diphosphate, <1> F96A mutant protein [2]) [2]
0.0003 <1> ((2E,6E)-farnesyl diphosphate, <1> F198A mutant protein [2]) [2]
0.00034 <1> ((2E,6E)-farnesyl diphosphate, <1> F203F mutant protein [2]) [2]
0.045 <1> ((2E,6E)-farnesyl diphosphate, <1> wild-type protein [2]) [2]
0.049 <2> ((2E,6E)-farnesyl diphosphate, <2> pH 6.5, 30°C [1]) [1]

K_m-Value (mM)
0.000147 <2> ((2E,6E)-farnesyl diphosphate, <2> pH 6.5, 30°C [1]) [1]
0.00071 <1> ((2E,6E)-farnesyl diphosphate, <1> wild-type protein [2]) [2]
0.00077 <1> ((2E,6E)-farnesyl diphosphate, <1> F96A mutant protein [2]) [2]
0.0012 <1> ((2E,6E)-farnesyl diphosphate, <1> F198A mutant protein [2]) [2]
0.00145 <1> ((2E,6E)-farnesyl diphosphate, <1> F203F mutant protein [2]) [2]

pH-Optimum
6.5 <2> (<2> assay at [1]) [1]

5 Isolation/Preparation/Mutation/Application

Purification
<1> (immobilized metal ion affinity chromatography (Co^{2+})) [2]
<3> [3]

Crystallization
<1> (sitting drop vapor diffusion method) [2]

Cloning
<1> (His-tagged version expressed in Escherichia coli BL21(DE3)) [2]
<3> [3]

Engineering
D100N <3> (<3> below 5% of wild-type activity [3]) [3]
D99E <3> (<3> below 5% of wild-type activity [3]) [3]
D99N <1,3> (<3> completely inactive [3]; <1> coordinates to Mg^{2+} [2]) [2,3]
E248D <3> (<3> below 5% of wild-type activity [3]) [3]
F198A <1> (<1> major products: Z-γ-bisabolene (24%), sesqusabine (20%) [2]) [2]
F96A <1> (<1> major product: β-farnesene (70%) [2]) [2]
N240D <3> (<3> below 5% of wild-type activity [3]) [3]
S244A <3> (<3> below 5% of wild-type activity [3]) [3]
W203F <1> (<1> major product: Z-γ-bisabolene (47%) [2]) [2]

References

[1] Lin, X.; Hopson, R.; Cane, D.E.: Genome mining in Streptomyces coelicolor: molecular cloning and characterization of a new sesquiterpene synthase. J. Am. Chem. Soc., **128**, 6022-6023 (2006)
[2] Aaron, J.A.; Lin, X.; Cane, D.E.; Christianson, D.W.: Structure of epi-isozizaene synthase from Streptomyces coelicolor A3(2), a platform for new terpenoid cyclization templates. Biochemistry, **49**, 1787-1797 (2010)
[3] Lin, X.; Cane, D.E.: Biosynthesis of the sesquiterpene antibiotic albaflavenone in Streptomyces coelicolor. Mechanism and stereochemistry of the enzymatic formation of epi-isozizaene. J. Am. Chem. Soc., **131**, 6332-6333 (2009)

α-bisabolene synthase 4.2.3.38

1 Nomenclature

EC number
4.2.3.38

Systematic name
(2E,6E)-farnesyl-diphosphate diphosphate-lyase [(E)-α-bisabolene-forming]

Recommended name
α-bisabolene synthase

Synonyms
(E)-α-bisabolene synthase <1,2,4> [2,3,4]
E-α-bisabolene synthase <3> [1]
TPS3 <1> [2]
bisabolene synthase
Additional information <3,4> (<3> the enzyme belongs to the sesquiterpene synthase family of enzymes, TPS-d subfamily [1]; <4> the enzyme belongs to the terpenoid synthases, subgroup sesquiterpene synthases [4]) [1,4]

CAS registry number
211049-94-4

2 Source Organism

<1> *Pseudotsuga menziesii* [2]
<2> *Picea glauca* [3]
<3> *Picea abies* (UNIPROT accession number: Q675L6) [1]
<4> *Abies grandis* (UNIPROT accession number: O81086) [4]

3 Reaction and Specificity

Catalyzed reaction
(2E,6E)-farnesyl diphosphate = (E)-α-bisabolene + diphosphate (<4> electrophilic reaction mechanism [4])

Natural substrates and products
S (2E,6E)-farnesyl diphosphate <3,4> (<3> a step in the terpene synthesis pathway, overview [1]) (Reversibility: ?) [1,4]

D. Schomburg and I. Schomburg (eds.), *Class 3.4–6 Hydrolases, Lyases, Isomerases, Ligases: EC 3.4–6*, Springer Handbook of Enzymes S10, DOI 10.1007/978-3-642-36260-6_59,

P (E)-α-bisabolene + diphosphate (<4> (E)-α-bisabolene is the precursor in Abies species of todomatuic acid, juvabione, and related insect juvenile hormone mimics, overview [4])
S Additional information <4> (<4> induced (E)-α-bisabolene biosynthesis constitutes part of a defense response targeted to insect herbivores, and possibly fungal pathogens, that is distinct from induced oleoresin monoterpene production [4]) (Reversibility: ?) [4]
P ?

Substrates and products

S (2E,6E)-farnesyl diphosphate <1> (<1> product identification by GC-MS, overview [2]) (Reversibility: ?) [2]
P (E)-γ-bisabolene + diphosphate
S (2E,6E)-farnesyl diphosphate <3,4> (<3> a step in the terpene synthesis pathway, overview [1]; <4> the recombinant enzymes is substrate-specific and produces (E)-α-bisabolene as sole product [4]) (Reversibility: ?) [1,4]
P (E)-α-bisabolene + diphosphate (<3> product identification by GC-MS [1]; <4> (E)-α-bisabolene is the precursor in Abies species of todomatuic acid, juvabione, and related insect juvenile hormone mimics, overview [4])
S Additional information <4> (<4> induced (E)-α-bisabolene biosynthesis constitutes part of a defense response targeted to insect herbivores, and possibly fungal pathogens, that is distinct from induced oleoresin monoterpene production [4]) (Reversibility: ?) [4]
P ?

Inhibitors

Mn^{2+} <4> (<4> activates, but Mn^{2+} at concentrations higher than 1 mM results in a decline of activity with either substrate [4]) [4]

Activating compounds

Additional information <4> (<4> the enzyme is wound-inducible [4]) [4]

Metals, ions

KCl <4> (<4> only weakly influences GDP conversion with the ag1 enzyme causing a 2fold activation at 100 mM KCl, but the monovalent cation has no effect with FDP as substrate [4]) [4]
Mg^{2+} <4> (<4> activates, saturation with Mg^{2+} is reached at 5 mM, and no apparent inhibition of catalysis occurs up to 100 mM [4]) [4]
Mn^{2+} <4> (<4> activates, but Mn^{2+} at concentrations higher than 1 mM results in a decline of activity with either substrate [4]) [4]
Additional information <4> (<4> the activity of recombinant ag1 requires a divalent cation cofactor, Mg^{2+} or Mn^{2+}, which is employed to neutralize the negative charge of the diphosphate leaving group in the substrate ionization step of the reaction sequence. Mg^{2+} is more efficient in catalysis than is Mn^{2+}. With GDP as substrate, however, Mn^{2+} at 0.5 mM yields a 4fold higher rate of monoterpene synthase activity compared to Mg^{2+} at concentrations up to 50 mM [4]) [4]

pi-Value
5.03 <4> (<4> sequence calculation [4]) [4]

Temperature optimum (°C)
25 <4> (<4> assay at [4]) [4]
30 <1> (<1> assay at [2]) [2]

4 Enzyme Structure

Subunits
? <4> (<4> x * 93776, sequence calculation [4]) [4]

5 Isolation/Preparation/Mutation/Application

Source/tissue
bark <1> (<1> from 1-year-old rooted saplings [2]) [2]
seedling <2> (<2> determination of enzyme expression [3]) [3]
shoot <1> (<1> fresh, green, with needles, from 1-year-old rooted saplings [2]) [2]

Cloning
<1> (cloning from a cDNA library, DNA and amino acid sequence determination and analysis, sequence comparisons, functional expression in Escherichia coli strain BL21) [2]
<2> (expression of the enzyme under control of the potato proteinase inhibitor II pinII-promoter in Picea glauca seedlings, as well as in Arabidopsis thaliana and Nicotiana tabacum in a cell-specific manner in trichomes, expression analysis of theGUS-(E)-α-bisabolene synthase construct, overview) [3]
<3> (gene PaTPS-Bis, DNA and amino acid sequence determination and analysis, expression and phylogenetic analysis, sequence comparison with other enzymes of the terpene synthase family, functional expression in Escherichia coli) [1]
<4> (gene ag1, cloning from a wound-induced stem-cDNA library, DNA and amino acid sequence determination and analysis, sequence comparisons, phylogenetic tree, functional expression in Escherichia coli strain XL1-Blue) [4]

References

[1] Martin, D.M.; Faeldt, J.; Bohlmann, J.: Functional characterization of nine Norway spruce TPS genes and evolution of gymnosperm terpene synthases of the TPS-d subfamily. Plant Physiol., **135**, 1908-1927 (2004)
[2] Huber, D.P.; Philippe, R.N.; Godard, K.A.; Sturrock, R.N.; Bohlmann, J.: Characterization of four terpene synthase cDNAs from methyl jasmonate-in-

duced Douglas-fir, Pseudotsuga menziesii. Phytochemistry, **66**, 1427-1439 (2005)
[3] Godard, K.A.; Byun-McKay, A.; Levasseur, C.; Plant, A.; Seguin, A.; Bohlmann, J.: Testing of a heterologous, wound- and insect-inducible promoter for functional genomics studies in conifer defense. Plant Cell Rep., **26**, 2083-2090 (2007)
[4] Bohlmann, J.; Crock, J.; Jetter, R.; Croteau, R.: Terpenoid-based defenses in conifers: cDNA cloning, characterization, and functional expression of wound-inducible (E)-α-bisabolene synthase from grand fir (Abies grandis). Proc. Natl. Acad. Sci. USA, **95**, 6756-6761 (1998)

epi-cedrol synthase 4.2.3.39

1 Nomenclature

EC number
4.2.3.39

Systematic name
(2E,6E)-farnesyl-diphosphate diphosphate-lyase (8-epi-cedrol-forming)

Recommended name
epi-cedrol synthase

Synonyms
8-epicedrol synthase <2> [1,4]
epicedrol synthase
sesquiterpene cyclase <1> [2]

CAS registry number
251113-52-7

2 Source Organism

<1> *Artemisia annua* [2,3]
<2> *Artemisia annua* (UNIPROT accession number: Q9LLR9) (gene ecs1 [1]) [1,4]

3 Reaction and Specificity

Catalyzed reaction
(2E,6E)-farnesyl diphosphate + H_2O = 8-epi-cedrol + diphosphate (<1> reaction mechanism, overview [2]; <2> reaction mechanism and cyclization of 8-epi-cedrol. Allylic carbocation formation, isomerization to nerolidyl diphosphate, and cyclization generate the monocyclic bisabolyl cation, a hydride shift is followed by two cyclizations to yield the cedryl cation, and the reaction is terminated by quenching the tricyclic cation with a hydroxide equivalent to form 8-epicedrol, overview [1])

Natural substrates and products
S (2E,6E)-farnesyl diphosphate + H_2O <1,2> (<1,2> the enzyme is involved in the artemisinin biosynthesis pathway, overview [1,2]) (Reversibility: ?) [1,2,3]
P 8-epi-cedrol + diphosphate

D. Schomburg and I. Schomburg (eds.), *Class 3.4–6 Hydrolases, Lyases, Isomerases, Ligases: EC 3.4–6*, Springer Handbook of Enzymes S10, DOI 10.1007/978-3-642-36260-6_60,

S Additional information <1> (<1> Sesquiterpene cyclases or synthases catalyze the conversion of the isoprenoid intermediate farnesyl diphosphate to various sesquiterpene structural types [2]) (Reversibility: ?) [2]
P ?

Substrates and products

S (2E,6E)-farnesyl diphosphate + H_2O <1,2> (<1,2> the enzyme is involved in the artemisinin biosynthesis pathway, overview [1,2]; <1> the native enzyme is specific for farnesyl diphosphate as substrate [2]; <2> the native enzyme is specifically producing 8-epi-cedrol, but the enzyme recombinantly expressed in Escherichia coli also produces cedrol, with 8-epi-cedrol and cedrol in a 96:4 ratio, GC-MS product analysis, overview [1]) (Reversibility: ?) [1,2,3]
P 8-epi-cedrol + diphosphate
S geranyl diphosphate + H_2O <1> (<1> geranyl diphosphate is converted to monoterpenes by the recombinant enzyme at a rate of about 15% of that observed with farnesyl diphosphate as substrate [2]) (Reversibility: ?) [2]
P ? + diphosphate
S Additional information <1> (<1> Sesquiterpene cyclases or synthases catalyze the conversion of the isoprenoid intermediate farnesyl diphosphate to various sesquiterpene structural types [2]; <1> product formation specificity, overview. Native epi-cedrol synthase is not active with geranylgeranyl diphosphate as substrate. The recombinant enzyme catalyzes the formation of both olefinic sesquiterpene, i.e. 57% α-cedrene, 13% β-cedrene, 5% (E)-β-farnesene , 1% α-acoradiene, 8% (E)-α-bisabolene, and 16% of three unknown olefins, but mainly oxygenates sesquiterpenes, 97% of total sesquiterpene generated, composed of 96% epi-cedrol and 4% cedrol, from farnesyl diphosphate, GC-MS product analysis, overview [2]) (Reversibility: ?) [2]
P ?

Inhibitors

Mn^{2+} <1> (<1> highly activating at 0.060 mM, inhibiting at 0.12 mM [2]) [2]

Metals, ions

Mg^{2+} <1> (<1> activates at 2 mM [2]) [2]
Mn^{2+} <1> (<1> highly activating at 0.060 mM, inhibiting at 0.12 mM [2]) [2]

K_m-Value (mM)

0.0004 <1> ((2E,6E)-farnesyl diphosphate, <1> pH 7.0, 25°C, recombinant enzyme [2]) [2]
0.0013 <1> ((2E,6E)-farnesyl diphosphate, <1> pH 9.0, 25°C, recombinant enzyme [2]) [2]

pH-Optimum

8 <2> (<2> assay at [1]) [1]
8.5-9 <1> (<1> alcohol product formation [2]) [2]

pH-Range

6.3-9 <1> [2]

pi-Value
4.94 <1> (<1> sequence calculation [2]) [2]

Temperature optimum (°C)
22 <2> (<2> assay at room temperature [1]) [1]
25 <1> (<1> assay at [2]) [2]

4 Enzyme Structure

Subunits
? <1> (<1> x * 63500, about, sequence calculation [2]) [2]

5 Isolation/Preparation/Mutation/Application

Source/tissue
leaf <1> [2]

Cloning
<1> (cloning from a cDNA library, DNA and amino acid sequence determination and analysis, expression in Escherichia coli strain XL1-Blue) [2]
<1> (functional expression in Saccharomyces cerevisiae, native mating type α yeast strain JBY574 and constructed strain EHY42, leading to production of sesquiterpenes in yeast. Expressing epi-cedrol synthase in the upc2-1 mutant CJ-2A actually decreases foreign sesquiterpene yields relative to wild-type strain. FPP is apparently less accessible to the epi-cedrol synthase in the upc2-1 mutant, overview. Mating type influences foreign sesquiterpene production, overview) [3]
<2> (homology-based cloning from a cDNA library, DNA and amino acid sequence determination and analysis, cloning and expression in Escherichia coli strains DH5α and BL21(DE3), respectively) [1]

References

[1] Hua, L.; Matsuda, S.P.: The molecular cloning of 8-epicedrol synthase from Artemisia annua. Arch. Biochem. Biophys., **369**, 208-212 (1999)
[2] Mercke, P.; Crock, J.; Croteau, R.; Brodelius, P.E.: Cloning, expression, and characterization of epi-cedrol synthase, a sesquiterpene cyclase from Artemisia annua L. Arch. Biochem. Biophys., **369**, 213-222 (1999)
[3] Jackson, B.E.; Hart-Wells, E.A.; Matsuda, S.P.: Metabolic engineering to produce sesquiterpenes in yeast. Org. Lett., **5**, 1629-1632 (2003)
[4] Feng, L.; Yang, R.; Yang, X.; Zeng, X.; Lu, W.; Zeng, Q.: Synergistic re-channeling of mevalonate pathway for enhanced artemisinin production in transgenic Artemisia annua. Plant Sci., **177**, 57-67 (2009)

(Z)-γ-bisabolene synthase 4.2.3.40

1 Nomenclature

EC number
4.2.3.40

Systematic name
(2E,6E)-farnesyl-diphosphate diphosphate-lyase [(Z)-γ-bisabolene-forming]

Recommended name
(Z)-γ-bisabolene synthase

Synonyms
TPS12 <1> [1]
TPS13 <1> [1]

2 Source Organism

<1> *Arabidopsis thaliana* [1]

3 Reaction and Specificity

Catalyzed reaction
(2E,6E)-farnesyl diphosphate = (Z)-γ-bisabolene + diphosphate

Natural substrates and products
S (2E,6E)-farnesyl diphosphate <1> (Reversibility: ?) [1]
P (Z)-γ-bisabolene + diphosphate

Substrates and products
S (2E,6E)-farnesyl diphosphate <1> (<1> product identification by GC-MS, additional minor products are E-nerolidol and α-bisabolol, overview [1]) (Reversibility: ?) [1]
P (Z)-γ-bisabolene + diphosphate

Activating compounds
Additional information <1> (<1> wound-inducible (Z)-γ-bisabolene synthase, mechanical wounding of leaves induces local expression of At4g13280 and At4g13300 [1]) [1]

Metals, ions
Mg^{2+} <1> [1]

D. Schomburg and I. Schomburg (eds.), *Class 3.4–6 Hydrolases, Lyases, Isomerases, Ligases: EC 3.4–6*, Springer Handbook of Enzymes S10, DOI 10.1007/978-3-642-36260-6_61,

pH-Optimum

7.3 <1> (<1> assay at [1]) [1]

Temperature optimum (°C)

30 <1> (<1> assay at [1]) [1]

5 Isolation/Preparation/Mutation/Application

Source/tissue

leaf <1> (<1> young rosette leaves, enzyme induction by mechanical wounding [1]) [1]

root <1> (<1> root-specific (Z)-γ-bisabolene synthase, in cortex and sub-epidermal layers [1]) [1]

Additional information <1> (<1> enzyme tissue localization study [1]) [1]

Cloning

<1> (root-specific genes At4g13280 and At4g13300 show constitutive promoter activities in the cortex and sub-epidermal layers of Arabidopsis thaliana roots, hierarchical cluster analysis of terpene synthases TPS gene expression, expression analysis, microarray profiling, overview. Expression in Escherichia coli strain BL21) [1]

References

[1] Ro, D.K.; Ehlting, J.; Keeling, C.I.; Lin, R.; Mattheus, N.; Bohlmann, J.: Microarray expression profiling and functional characterization of AtTPS genes: duplicated Arabidopsis thaliana sesquiterpene synthase genes At4g13280 and At4g13300 encode root-specific and wound-inducible (Z)-γ-bisabolene synthases. Arch. Biochem. Biophys., **448**, 104-116 (2006)

elisabethatriene synthase 4.2.3.41

1 Nomenclature

EC number
4.2.3.41

Systematic name
geranylgeranyl-diphosphate diphosphate-lyase (elisabethatriene-forming)

Recommended name
elisabethatriene synthase

Synonyms
elisabethatriene cyclase

CAS registry number
334022-59-2

2 Source Organism

<1> *Pseudopterogorgia elisabethae* [1,2]

3 Reaction and Specificity

Catalyzed reaction
geranylgeranyl diphosphate = elisabethatriene + diphosphate

Natural substrates and products
- **S** geranylgeranyl diphosphate <1> (Reversibility: ?) [2]
- **P** elisabethatriene + diphosphate

Substrates and products
- **S** farnesyl diphosphate <1> (<1> formation of 28% γ-humulene, 43% β-ylangene, 17% α-patchoulene and two minor products [2]) (Reversibility: ?) [2]
- **P** γ-humulene + β-ylangene + α-patchoulene + diphosphate
- **S** geranyl diphosphate <1> (<1> formation of eleven terpene reaction products [2]) (Reversibility: ?) [2]
- **P** ? + diphosphate
- **S** geranylgeranyl diphosphate <1> (Reversibility: ?) [1,2]
- **P** elisabethatriene + diphosphate

D. Schomburg and I. Schomburg (eds.), *Class 3.4–6 Hydrolases, Lyases, Isomerases, Ligases: EC 3.4–6*, Springer Handbook of Enzymes S10, DOI 10.1007/978-3-642-36260-6_62,

Inhibitors
diethyl diphosphate <1> [1]
phenyl glyoxal <1> [1]
Additional information <1> (<1> no inhibition by 0.05 mM N-ethylmaleimide [1]) [1]

Metals, ions
Mg^{2+} <1> (<1> the enzyme can not catalyze the cyclization reaction in the absence of Mg^{2+}, saturating concentration is 1.5 mM, K_m-value: 0.78 mM. At a concentration of 2 mM, Mg^{2+} supports the cyclization reaction most efficiently. When substituting Mn^{2+} for Mg^{2+}, approximately one-third of the elisabethatriene synthase activity is observed [1]) [1]
Mn^{2+} <1> (<1> at a concentration of 2 mM, Mg^{2+} supports the cyclization reaction most efficiently. When substituting Mn^{2+} for Mg^{2+}, approximately one-third of the elisabethatriene synthase activity is observed [1]) [1]

Turnover number (s^{-1})
1300 <1> (geranyl diphosphate, <1> pH 7.1, 29°C [2]) [2]
3400 <1> (farnesyl diphosphate, <1> pH 7.1, 29°C [2]) [2]
41000 <1> (geranylgeranyl diphosphate, <1> pH 7.1, 29°C [2]) [2]

K_m-Value (mM)
0.0023 <1> (geranylgeranyl diphosphate, <1> pH 7.1, 29°C [2]) [2]
0.0035 <1> (farnesyl diphosphate, <1> pH 7.1, 29°C [2]) [2]
0.007 <1> (geranylgeranyl diphosphate, <1> 29°C [1]) [1]
0.0285 <1> (geranyl diphosphate, <1> pH 7.1, 29°C [2]) [2]

pH-Optimum
7.1 <1> (<1> assay at [2]; <1> highest activity in phosphate buffer [1]) [1,2]

pi-Value
5.1 <1> (<1> isoelectric focusing, pH-range 5-8 [1]) [1]

Temperature optimum (°C)
29 <1> (<1> assay at [2]) [2]

4 Enzyme Structure

Molecular weight
47000 <1> (<1> gel filtration [1]) [1]

Subunits
monomer <1> (<1> 1 * 47000, SDS-PAGE [1]) [1]

5 Isolation/Preparation/Mutation/Application

Purification

<1> [2]
<1> (partial) [1]

References

[1] Kohl, A.C.; Kerr, R.G.: Identification and characterization of the pseudopterosin diterpene cyclase, elisabethatriene synthase, from the marine gorgonian, Pseudopterogorgia elisabethae. Arch. Biochem. Biophys., **424**, 97-104 (2004)
[2] Brueck, T.B.; Kerr, R.G.: Purification and kinetic properties of elisabethatriene synthase from the coral Pseudopterogorgia elisabethae. Comp. Biochem. Physiol. B, **143**, 269-278 (2006)

aphidicolan-16β-ol synthase 4.2.3.42

1 Nomenclature

EC number
4.2.3.42

Systematic name
9α-copalyl-diphosphate diphosphate-lyase (aphidicolan-16β-ol-forming)

Recommended name
aphidicolan-16β-ol synthase

Synonyms
PbACS <1> (<1> bifunctional enzyme which also has EC 5.5.1.14 syn-copalyl diphosphate synthase activity [2]; <1> bifunctional enzyme which also has EC 5.5.1.14, syn-copalyl diphosphate synthase activity [1]) [1,2]

CAS registry number
348150-23-2

2 Source Organism

<1> *Phoma βe* (UNIPROT accession number: Q96WT2) (bifunctional enzyme which also has EC 5.5.1.14 syn-copalyl diphosphate synthase activity [2]; <1> bifunctional enzyme which also has EC 5.5.1.14, syn-copalyl diphosphate synthase activity [1]) [1,2]

3 Reaction and Specificity

Catalyzed reaction
9α-copalyl diphosphate + H_2O = aphidicolan-16β-ol + diphosphate

Natural substrates and products
- **S** 9α-copalyl diphosphate + H_2O <1> (<1> bifunctional enzyme which also has EC 5.5.1.14, syn-copalyl diphosphate synthase activity [2]) (Reversibility: ?) [2]
- **P** aphidicolan-16β-ol + diphosphate

Substrates and products
- **S** 9α-copalyl diphosphate + H_2O <1> (<1> bifunctional enzyme which also has EC 5.5.1.14, syn-copalyl diphosphate synthase activity [2]; <1> bi-

D. Schomburg and I. Schomburg (eds.), *Class 3.4–6 Hydrolases, Lyases, Isomerases, Ligases: EC 3.4–6*, Springer Handbook of Enzymes S10, DOI 10.1007/978-3-642-36260-6_63,

functional enzyme which also has EC 5.5.1.14 syn-copalyl diphosphate synthase activity [1]) (Reversibility: ?) [1,2]

P aphidicolan-16β-ol + diphosphate

5 Isolation/Preparation/Mutation/Application

Cloning

<1> [1]

<1> (bifunctional enzyme which also has EC 5.5.1.14, syn-copalyl diphosphate synthase activity) [2]

References

[1] Toyomasu, T.; Nakaminami, K.; Toshima, H.; Mie, T.; Watanabe, K.; Ito, H.; Matsui, H.; Mitsuhashi, W.; Sassa, T.; Oikawa, H.: Cloning of a gene cluster responsible for the biosynthesis of diterpene aphidicolin, a specific inhibitor of DNA polymerase α. Biosci. Biotechnol. Biochem., **68**, 146-152 (2004)

[2] Oikawa, H.; Toyomasu, T.; Toshima, H.; Ohashi, S.; Kawaide, H.; Kamiya, Y.; Ohtsuka, M.; Shinoda, S.; Mitsuhashi, W.; Sassa, T.: Cloning and functional expression of cDNA encoding aphidicolan-16 β-ol synthase: A key enzyme responsible for formation of an unusual diterpene skeleton in biosynthesis of aphidicolin. J. Am. Chem. Soc., **123**, 5154-5155 (2001)

fusicocca-2,10(14)-diene synthase 4.2.3.43

1 Nomenclature

EC number
4.2.3.43

Systematic name
geranylgeranyl diphosphate-lyase (fusicocca-2,10(14)-diene-forming)

Recommended name
fusicocca-2,10(14)-diene synthase

Synonyms
PaDC4
PaFS <2> [1]
fusicoccadiene synthase <1,2,3> [1,2,3]
usicoccadiene synthase

2 Source Organism

<1> *Alternaria brassicicola* [2]
<2> *Phomopsis amygdali* (UNIPROT accession number: A2PZA5) [1]
<3> *Alternaria brassicicola* (UNIPROT accession number: C9K2Q3) [3]

3 Reaction and Specificity

Catalyzed reaction
geranylgeranyl diphosphate = fusicocca-2,10(14)-diene + diphosphate

Natural substrates and products
S geranylgeranyl diphosphate <2> (<2> the enzyme contains two domains, an N-terminal terpene cyclase domain and a C-terminal prenyltransferase domain, and converts isoprene units sequentially into geranylgeranyl diphosphate and then into fusicocca-2,10 (14)-diene [1]) (Reversibility: ?) [1]
P fusicocca-2,10(14)-diene + diphosphate

Substrates and products
S geranylgeranyl diphosphate <2> (<2> the enzyme contains two domains, an N-terminal terpene cyclase domain and a C-terminal prenyltransferase domain, and converts isoprene units sequentially into geranylgeranyl diphosphate and then into fusicocca-2,10 (14)-diene [1]) (Reversibility: ?) [1]
P fusicocca-2,10(14)-diene + diphosphate

D. Schomburg and I. Schomburg (eds.), *Class 3.4–6 Hydrolases, Lyases, Isomerases, Ligases: EC 3.4–6*, Springer Handbook of Enzymes S10, DOI 10.1007/978-3-642-36260-6_64,

S geranylgeranyl diphosphate <3> (<3> multifunctional enzyme: geranylgeranyl diphosphate formation from isopentenyl diphosphate and dimethylallyl diphosphate [3]) (Reversibility: ?) [3]
P fusicocca-2,10(14-diene) + diphosphate

5 Isolation/Preparation/Mutation/Application

Source/tissue
mycelium <2> [1]

Cloning
<1> (expressed in Saccharomyces cerevisiae) [2]
<2> (heterologous expression of PaFS alone results in the accumulation of fusicocca-2,10 (14)-diene in Escherichia coli cells) [1]
<3> (expressed in Escherichia coli) [3]

References

[1] Toyomasu, T.; Tsukahara, M.; Kaneko, A.; Niida, R.; Mitsuhashi, W.; Dairi, T.; Kato, N.; Sassa, T.: Fusicoccins are biosynthesized by an unusual chimera diterpene synthase in fungi. Proc. Natl. Acad. Sci. USA, **104**, 3084-3088 (2007)
[2] Hashimoto, M.; Higuchi, Y.; Takahashi, S.; Osada, H.; Sakaki, T.; Toyomasu, T.; Sassa, T.; Kato, N.; Dairi, T.: Functional analyses of cytochrome P450 genes responsible for the early steps of brassicicene C biosynthesis. Bioorg. Med. Chem. Lett., **19**, 5640-5643 (2009)
[3] Minami, A.; Tajima, N.; Higuchi, Y.; Toyomasu, T.; Sassa, T.; Kato, N.; Dairi, T.: Identification and functional analysis of brassicicene C biosynthetic gene cluster in Alternaria brassicicola. Bioorg. Med. Chem. Lett., **19**, 870-874 (2009)

isopimara-7,15-diene synthase 4.2.3.44

1 Nomenclature

EC number
4.2.3.44

Systematic name
copalyl diphosphate-lyase (isopimara-7,15-diene-forming)

Recommended name
isopimara-7,15-diene synthase

Synonyms
PaTPS-Iso <1> [1]

2 Source Organism

<1> *Picea abies* (UNIPROT accession number: Q675L5) [1]

3 Reaction and Specificity

Catalyzed reaction
copalyl diphosphate = isopimara-7,15-diene + diphosphate (<1> proposed reaction scheme [1])

Substrates and products
S copalyl diphosphate <1> (<1> proposed reaction scheme [1]) (Reversibility: ?) [1]
P isopimara-7,15-diene + diphosphate

pi-Value
5.8 <1> (<1> calculated from sequence [1]) [1]

5 Isolation/Preparation/Mutation/Application

Cloning
<1> (expression in Escherichia coli) [1]

D. Schomburg and I. Schomburg (eds.), *Class 3.4–6 Hydrolases, Lyases, Isomerases, Ligases: EC 3.4–6*, Springer Handbook of Enzymes S10, DOI 10.1007/978-3-642-36260-6_65,

References

[1] Martin, D.M.; Faeldt, J.; Bohlmann, J.: Functional characterization of nine Norway spruce TPS genes and evolution of gymnosperm terpene synthases of the TPS-d subfamily. Plant Physiol., **135**, 1908-1927 (2004)

phyllocladan-16α-ol synthase 4.2.3.45

1 Nomenclature

EC number
4.2.3.45

Systematic name
(+)-copalyl-diphosphate diphosphate-lyase (phyllocladan-16α-ol-forming)

Recommended name
phyllocladan-16α-ol synthase

Synonyms
DC1 <1> [1]

2 Source Organism

<1> *Phomopsis amygdali* (UNIPROT accession number: B2DBF0) [1]

3 Reaction and Specificity

Catalyzed reaction
(+)-copalyl diphosphate + H_2O = phyllocladan-16α-ol + diphosphate

Substrates and products
- **S** (+)-copalyl diphosphate + H_2O <1> (Reversibility: ?) [1]
- **P** phyllocladan-16α-ol + phosphate (<1> plus trace amounts of labdane-related hydrocarbons [1])
- **S** geranylgeranyl diphosphate + H_2O <1> (<1> reaction proceeds via (+)-copalyl diphosphate [1]) (Reversibility: ?) [1]
- **P** phyllocladan-16α-ol + phosphate (<1> plus trace amounts of labdane-related hydrocarbons [1])

4 Enzyme Structure

Subunits
? <1> (<1> x * 113000, SDS-PAGE [1]) [1]

D. Schomburg and I. Schomburg (eds.), *Class 3.4–6 Hydrolases, Lyases, Isomerases, Ligases: EC 3.4–6*, Springer Handbook of Enzymes S10, DOI 10.1007/978-3-642-36260-6_66,

References

[1] Toyomasu, T.; Niida, R.; Kenmoku, H.; Kanno, Y.; Miura, S.; Nakano, C.; Shiono, Y.; Mitsuhashi, W.; Toshima, H.; Oikawa, H.; Hoshino, T.; Dairi, T.; Kato, N.; Sassa, T.: Identification of diterpene biosynthetic gene clusters and functional analysis of labdane-related diterpene cyclases in Phomopsis amygdali. Biosci. Biotechnol. Biochem., **72**, 1038-1047 (2008)

α-farnesene synthase 4.2.3.46

1 Nomenclature

EC number
4.2.3.46

Systematic name
(2E,6E)-farnesyl-diphosphate lyase [(3E,6E)-α-farnesene-forming]

Recommended name
α-farnesene synthase

Synonyms
(E,E)-α-farnesene synthase <1,2> [2,3]
AFS-1 <1> [5]
AFS1 <1> [2]
AdAFS1 <3> [7]
E,E-α-farnesene synthase <1,4,5> [4]
MdAFS1 <1,2> [1,3,6]
α farnesene synthase 1 <3> [7]
α-farnesene synthase <1,7> [1,8]
α-farnesene synthase-1 <1> [5]
sesquiterpene synthase <1> [2]

2 Source Organism

<1> *Malus x domestica* (UNIPROT accession number: Q84LB2) [1,2,4,5]
<2> *Malus x domestica* (UNIPROT accession number: B2ZZ11) [1,3,6]
<3> *Actinidia deliciosa* (UNIPROT accession number: C7SHN9) [7]
<4> *Malus x domestica* (UNIPROT accession number: Q6Q2J2) [4]
<5> *Malus x domestica* (UNIPROT accession number: Q6QWJ1) [4]
<6> *Cucumis melo* (UNIPROT accession number: B2KSJ5) [9]
<7> *Malus x domestica* (UNIPROT accession number: Q32WI2) [8]

3 Reaction and Specificity

Catalyzed reaction
(2E,6E)-farnesyl diphosphate = (3E,6E)-α-farnesene + diphosphate

D. Schomburg and I. Schomburg (eds.), *Class 3.4–6 Hydrolases, Lyases, Isomerases, Ligases: EC 3.4–6*, Springer Handbook of Enzymes S10, DOI 10.1007/978-3-642-36260-6_67,

Natural substrates and products

- **S** (2E,6E)-farnesyl diphosphate <1,4,5,7> (<1> commentary [1]; <4> α-farnesene synthase is a key enzyme in the pathway of α-farnesene synthesis [4]; <1,5> apha-farnesene synthase is a key enzyme in the pathway of α-farnesene synthesis [4]) (Reversibility: ?) [1,4,8]
- **P** (3E,6E)-α-farnesene + diphosphate
- **S** (2E,6E)-farnesyl diphosphate <1> (<1> isomers of farnesene produced in apple fruit are (E,E)-α and (Z,E)-α are in a ratio of 300:1 [2]) (Reversibility: ?) [2]
- **P** (Z,E)-α-farnesene (<1> trace amounts [2])
- **S** (2E,6E)-farnesyl diphosphate <1> (<1> sesquiterpene synthase activity [2]) (Reversibility: ?) [2]
- **P** (E,E)-α-farnesene + diphosphate
- **S** geranyl diphosphate <1> (<1> in monoterpene synthase assays, only (E)-β-ocimene is produced at much reduced levels [2]) (Reversibility: ?) [2]
- **P** (E)-β-ocimene + diphosphate
- **S** geranyl diphosphate <1> (<1> monoterpene synthase activity [2]) (Reversibility: ?) [2]
- **P** (Z)-β-ocimene + diphosphate
- **S** Additional information <1> (<1> other sesquiterpenes identified in trace amounts are (E)-nerolidol and β-farnesene [2]; <1> the monoterpene synthase ((E)-β-ocimene and β-myrcene) and sesquiterpene synthase (α-farnesene) products produced by the mutated and wild-type enzymes are identical, there are no significant alterations in the ratios of the α-farnesene isomers produced [1]) (Reversibility: ?) [1,2]
- **P** ?

Substrates and products

- **S** (2E,6E)-farnesyl diphosphate <6> (Reversibility: ?) [9]
- **P** α-farnesene + diphosphate
- **S** (2E,6E)-farnesyl diphosphate <1,2,3,4,5,7> (<1> commentary [1]; <4> α-farnesene synthase is a key enzyme in the pathway of α-farnesene synthesis [4]; <1,5> apha-farnesene synthase is a key enzyme in the pathway of α-farnesene synthesis [4]; <3> the product consists primarily of (E,E)-α-farnesene (more than 95%) with trace amounts of (Z,E)-α-farnesene [7]) (Reversibility: ?) [1,4,7,8]
- **P** (3E,6E)-α-farnesene + diphosphate
- **S** (2E,6E)-farnesyl diphosphate <7> (<7> when farnesyl diphosphate, synthesised from 96% (E,E)-farnesol, is incubated with recombinant protein, (E,E)- and (Z,E)-α-farnesene are produced in a ratio of 96:4, respectively [8]) (Reversibility: ?) [8]
- **P** (3E,6E)-α-farnesene + β-farnesene + diphosphate
- **S** farnesyl diphosphate <1> (<1> isomers of farnesene produced in apple fruit are (E,E)-α and (Z,E)-α are in a ratio of 300:1 [2]) (Reversibility: ?) [2]
- **P** (Z,E)-α-farnesene (<1> trace amounts [2])
- **S** farnesyl diphosphate <1> (<1> sesquiterpene synthase activity [2]) (Reversibility: ?) [2]

P (E,E)-α-farnesene + diphosphate
S geranyl diphosphate <1,3> (<1> in monoterpene synthase assays, only (E)-β-ocimene is produced at much reduced levels [2]; <3> AdAFS1 can function as a bifunctional enzyme possessing both sesquiterpene and monoterpene synthase activities. Exhibits significant monoterpene synthase activity, producing exclusively (E)-β-ocimene. k_{cat}/K_m is about 5fold lower than k_{cat}/K_m for farnesyl diphosphate [7]) (Reversibility: ?) [2,7]
P (E)-β-ocimene + diphosphate
S geranyl diphosphate <1> (<1> monoterpene synthase activity [2]) (Reversibility: ?) [2]
P (Z)-β-ocimene + diphosphate
S geranyl diphosphate <2> (<2> poor substrate [1]) (Reversibility: ?) [1]
P (E)-β-ocimene + β-myrcene
S geranyl diphosphate <7> (<7> at 18% of the optimised rate for α-farnesene synthesis from farnesyl diphosphate [8]) (Reversibility: ?) [8]
P linalool + (Z)-β-ocimene + (E)-β-ocimene + β-myrcene
S Additional information <1,7> (<1> other sesquiterpenes identified in trace amounts are (E)-nerolidol and β-farnesene [2]; <1> the monoterpene synthase ((E)-β-ocimene and β-myrcene) and sesquiterpene synthase (α-farnesene) products produced by the mutated and wild-type enzymes are identical, there are no significant alterations in the ratios of the α-farnesene isomers produced [1]; <7> although (E,E)-farnesyl diphosphate is the preferred substrate, the enzyme accepts all four isomeric forms of the farnesyl diphosphate precursor. Both isomers of β-farnesene are also synthesised by the enzyme presumably from a specific farnesene isomer. The enzyme also produces α-farnesene by a reaction involving coupling of geranyl diphosphate and isoprenyl diphosphate but at less than 1% of the rate with farnesyl diphosphate [8]) (Reversibility: ?) [1,2,8]
P ?

Inhibitors

1-methylcyclopropene <1> (<1> after treatment of fruits at harvest with a blocker of ethylene action, AFS1 mRNA declines sharply over the initial 4 weeks of cold storage, and falls to nearly undetectable levels by 8 weeks [2]) [2]
Mn^{2+} <3> (<3> above 0.03 mM [7]) [7]
Na_2MoO_4 <7> (<7> 10 mM, 96% inhibition [8]) [8]

Metals, ions

K^+ <1,2,7> (<1> 500 mM are included in monoterpene synthase assay [2]; <1> MdAFS1 retains up to 12% of its activity in the absence of K^+, enzyme contains K^+ binding region, $MdAFS_1$ exhibits a type II K^+ response, $MdAFS_1$ is not absolutely dependent upon M+ its unequivocal classification as type I or type II K^+ activated, or that of any other terpene synthases, will not be possibl, then type I enzymes can exhibit type II kinetics and vice versa. [1]; <7> 30-50 mM, enhances activity 5fold. K_m: 3 mM. Addition of K^+ reduces monoterpene synthase activity [8]; <2> activity is dependent on K^+, the potassium binding region is defined [1]) [1,2,8]

Mg^{2+} <1,3,7> (<7> K_m: 0.7 mM [8]; <1> 10 mM are included in farnesyl diphosphate activity assay [1]; <1> 10 mM are included in sesquiterpene synthase assay [2]; <3> K_m: 0.248 mM, divalent cation required, preference for Mg^{2+}. Maximal velocities with Mn^{2+} is about 50% of that with Mg^{2+} [7]) [1,2,7,8]
Mn^{2+} <1,3,7> (<1> 1 mM is included in monoterpene synthase assay [2]; <7> K_m: 0.015 mM [8]; <3> K_M: about 0.02 mM, divalent cation required, preference for Mg^{2+}. Maximal velocities with Mn^{2+} is about 50% of that with Mg^{2+} [7]) [2,7,8]

Turnover number (s^{-1})

0.000005 <1,2> (geranyl diphosphate, <1> mutant S487A [1]; <2> pH 7.5, 30°C, mutant enzyme S487A [1]) [1]
0.000034 <1,2> (geranyl diphosphate, <1> mutant D484A [1]; <2> pH 7.5, 30°C, mutant enzyme D484A [1]) [1]
0.000052 <1,2> (geranyl diphosphate, <1> mutant S488A [1]; <2> pH 7.5, 30°C, mutant enzyme S488A [1]) [1]
0.000281 <1,2> (geranyl diphosphate, <1> wild-type [1]; <2> pH 7.5, 30°C, wild-type enzyme [1]) [1]
0.000588 <1,2> (geranyl diphosphate, <1> mutant S485A [1]; <2> pH 7.5, 30°C, mutant enzyme S485A [1]) [1]
0.0026 <2> ((2E,6E)-farnesyl diphosphate, <2> pH 7.5, 30°C, mutant enzyme S487A [1]) [1]
0.0026 <1> (farnesyl diphosphate, <1> mutant S487A, 50 mM KCl, 10 mM $MgCl_2$ [1]) [1]
0.0062 <1> (farnesyl diphosphate, <1> without K^+ [1]) [1]
0.0086 <2> ((2E,6E)-farnesyl diphosphate, <2> pH 7.5, 30°C, mutant enzyme D484A [1]) [1]
0.0086 <1> (farnesyl diphosphate, <1> mutant D484A, 50 mM KCl, 10 mM $MgCl_2$ [1]) [1]
0.022 <1> (farnesyl diphosphate, <1> without K^+, sesquiterpene synthase activity in mutant S487K is independent of K^+ [1]) [1]
0.03 <3> (geranyl diphosphate, <3> pH 7.5 [7]) [7]
0.039 <2> ((2E,6E)-farnesyl diphosphate, <2> pH 7.5, 30°C, mutant enzyme S488A [1]) [1]
0.039 <1> (farnesyl diphosphate, <1> mutant S488A, 50 mM KCl, 10 mM $MgCl_2$ [1]) [1]
0.0533 <1> (farnesyl diphosphate, <1> wild-type MdAFS, 50 mM KCl, 10 mM $MgCl_2$ [1]) [1]
0.0553 <2> ((2E,6E)-farnesyl diphosphate, <2> pH 7.5, 30°C, wild-type enzyme [1]) [1]
0.0613 <2> ((2E,6E)-farnesyl diphosphate, <2> pH 7.5, 30°C, mutant enzyme S485A [1]) [1]
0.0613 <1> (farnesyl diphosphate, <1> mutant S485A, 50 mM KCl, 10 mM $MgCl_2$ [1]) [1]
0.44 <3> ((2E,6E)-farnesyl diphosphate, <3> pH 7.5 [7]) [7]

Specific activity (U/mg)
0.027 <7> [8]
Additional information <1> (<1> S487K mutant has 35-45% of the wild-type activity with farnesyl diphosphate with no significant alterations in the α-farnesene isomer ratios produced and a small decrease in catalytic efficiency (wild-type and S487K respective k_{cat}/K_m values of 17.5 and 13.3 mM/s) [1]) [1]

K_m-Value (mM)
0.0028 <3> (geranyl diphosphate, <3> pH 7.5 [7]) [7]
0.003 <7> ((2E,6E)-farnesyl diphosphate, <7> pH 7.5, 30°C [8]) [8]
0.0095 <3> ((2E,6E)-farnesyl diphosphate, <3> pH 7.5 [7]) [7]

pH-Optimum
7-8.5 <7> [8]
7.3 <1> (<1> sesquiterpene synthase assay [2]) [2]
7.5 <1> (<1> farnesyl diphosphate activity assay [1]; <1> monoterpene synthase assay [2]) [1,2]

pH-Range
7-8 <1> (<1> maximal sesquiterpene synthase activity is observed [2]) [2]

pi-Value
5.93 <3> (<3> calculated from sequence [7]) [7]

Temperature optimum (°C)
30 <1> (<1> assay at [2]; <1> farnesyl diphosphate and geranyl diphosphate activity assay [1]) [1,2]

4 Enzyme Structure

Molecular weight
66000 <1> (<1> without myc-epitope tag, determined by PAGE analysis [2]) [2]
68000 <1> (<1> with myc-epitope tag, determined by PAGE analysis [2]) [2]

Subunits
? <3> (<3> x * 88100, calculated from sequence [7]) [7]
monomer <7> [8]

5 Isolation/Preparation/Mutation/Application

Source/tissue
epidermal cell <1> (<1> production of (E,E)-α-farnesene occurs in the epidermal (peel tissue) or adjacent hypodermal cell layers and the sesquiterpene can accumulate to high levels in the natural epicuticular coating of scald-susceptible apples during the first weeks of storage [2]) [2]
flower <3> (<3> expression of AdAFS1 is significantly higher in flowers than in leaf tissue. Within floral tissues, expression is highest in petals and sta-

mens. AdAFS1 expression is low in sepals in both sexes and also in 'Hayward' pistils. AdAFS1 expression in 'Hayward' is co-ordinated with anthesis, with low levels of expression in unopened flower buds and high levels detected in open flowers. The temporal accumulation patterns of AdAFS1 mRNA is constitutive. No difference in expression between male and female flowers [7]) [7]
fruit <2,6> (<6> CmTpsDul expression is specific to 'Dulce' rind. CmTpsDul is not expressed in either the rind or flesh of 'Noy Yizre'el' melons at any developmental stage [9]) [6,9]
fruit skin <7> [8]
hypodermis <1> [2]
leaf <3,4> (<3> expression of AdAFS1 is significantly higher in flowers than in leaf tissue. AdAFS1 expression is similar in leaves of both cultivars 'Chieftain' and 'Hayward' [7]) [4,7]
petal <3> (<3> within floral tissues, expression is highest in petals and stamens [7]) [7]
skin <2> [3]
stamen <3> (<3> within floral tissues, expression is highest in petals and stamens [7]) [7]

Localization

cytosol <1,3> (<1> The encoded protein appears to lack approximately 20 amino acids that are present in the N-terminal chloroplast-targeting region of monoterpene synthases. Thus, the product of this TS gene is most likely localized in the cytosol. [2]) [2,7]
Additional information <3> (<3> AdAFS1 protein sequences lacks predicted N-terminal transit peptide-like sequences for chloroplast targeting [7]) [7]

Purification

<1> (recombinant MdAFS1protein is extracted and purified) [1]
<3> [7]
<7> [8]

Renaturation

<1> (myc-tagged and untagged AFS1 expressed protein in bacterial inclusion-body fractions is urea-denatured, purified and renatured prior to assay of enzymatic activity.) [2]

Cloning

<1> [5]
<1> (After screening a cDNA library generated from the peel tissue mRNA, a full-length terpene synthase cDNA 1931 nucleotides long is isolated (hot phenol RNA extraction protocol is used). The 1728-bp open reading frame encodes the 576 amino acid protein. Expression of the apple gene in Escherichia coli.) [2]
<1> (mutated enzymes are generated using the QuickChange II site-directed mutagenesis kit. The PCR-based mutagenesis protocol is performed using pET-30a harbouring the MdAFS1 cDNAs as template. The single-site mutant enzymes overexpressed in Escherichia coli.) [1]

<3> (heterologously expressed in Escherichia coli) [7]
<6> (expression in Escherichia coli) [9]
<7> (expressed in Escherichia coli) [8]

Engineering

D326A <7> (<7> α-farnesene synthase, monoterpene synthase and prenyltransferase activities are lost in the mutant [8]) [8]
D326A/D330A <7> (<7> α-farnesene synthase, monoterpene synthase and prenyltransferase activities are lost in the mutant [8]) [8]
D484A <1,2> (<1> 85% loss of sesquiterpene synthase activity compared with wild-type enzyme when K^+ is present [1]; <2> 85% loss of sesquiterpene synthase activity compared with wild-type enzyme. Little change in K^+-independent activity [1]) [1]
S485A <1,2> (<1> exhibits marginally increased sesquiterpene synthase activities, and an approximate 2fold increase in monoterpene synthase activity compared with the wild-type enzyme [1]; <2> mutant exhibits marginally increased sesquiterpene synthase activities, and an approximate 2fold increase in monoterpene synthase activity compared with the wild-type enzyme [1]) [1]
S487A <1,2> (<1> 95% decrease in sesquiterpene synthase activity compared with wild-type enzyme when K^+ is present [1]; <2> 95% decrease in sesquiterpene synthase activity compared with wild-type enzyme. Little change in K^+-independent activity [1]) [1]
S487K <1,2> (<1> The S487K mutant has 35-45% of the wild-type activity with farnesyl diphosphate, with no significant alterations in the α-farnesene isomer ratios produced and a small decrease in catalytic efficiency [1]; <2> mutant has 35-45% of the wild-type activity with farnesyl diphosphate, with no significant alterations in the α-farnesene isomer ratios produced and a small decrease in catalytic efficiency [1]) [1]
S488A <1,2> (<1> mutant shows decreases in both sesqui- and monoterpene synthase activities compared with the WT enzyme, with mono-TPS activity being reduced more than sesquiterpene synthase activity. Sesquiterpene synthase (α-farnesene) products produced by the mutated and wild-type enzymes are identical, there are no significant alterations in the ratios of the α-farnesene isomers produced. [1]; <2> mutant shows decreases in both sesqui- and mono-terpene synthases activities, compared with the wild-type enzyme, with mono-terpene synthases activity being reduced more than sesqui-terpene synthases activity [1]) [1]

Application

agriculture <1> (<1> Because diphenylamine treatment leaves unwanted chemical residues on the fruit, restricts export markets, and creates environmental concerns, a long-range molecular genetic strategy for control of scald by reduction of (E,E)-α-farnesene synthesis in scald-susceptible apples is searched. The success of this strategy will rely on our ability to identify, clone, and characterize key genes involved in α-farnesene biosynthesis and its regulation by ethylene. [2]) [2]

6 Stability

pH-Stability

Additional information <1> (<1> sesquiterpene synthase activity declined below pH 7.0 and at pH 5.0-5.5, it is reduced more than 50% [2]) [2]

Temperature stability

Additional information <1> (<1> AFS1 transcript increases about 4fold in peel tissue of apple fruit during the first 4 weeks of storage at 0.5°C [2]) [2]

References

[1] Green, S.; Squire, C.J.; Nieuwenhuizen, N.J.; Baker, E.N.; Laing, W.: Defining the potassium binding region in an apple terpene synthase. J. Biol. Chem., **284**, 8661-8669 (2009)
[2] Pechous S.W.; Whitaker, B.D.: Cloning and functional expression of an (E,E)-α-farnesene synthase cDNA from peel tissue of apple fruit. Planta, **219**, 84-94 (2004)
[3] Ban, Y.; Oyama-Okubo, N.; Honda, C.; Nakayama, M.; Moriguchi, T.: Emitted and endogenous volatiles in 'Tsugaru' apple: The mechanism of ester and (E,E)-a-farnesene accumulation. Food Chem., **118**, 272-277 (2010)
[4] Yuan, K.; Liu, Q.; Li, B.; Zhang, L.: Genomic structure and sequence polymorphism of E,E-α-farnesene synthase gene in apples (Malus domestica Borkh.). Front. Agric. China, **2**, 190-193 (2008)
[5] Beuning, L.; Green, S.; Yauk, Y.-K.: The genomic sequence of AFS-1 - an α-farnesene synthase from the apple cultivar Royal Gala. Front. Agric. China, **4**, 74-78 (2010)
[6] Tsantili, E.; Gapper, N.E.; Arquiza, J.M.; Whitaker, B.D.; Watkins, C.B.: Ethylene and α-farnesene metabolism in green and red skin of three apple cultivars in response to 1-methylcyclopropene (1-MCP) treatment. J. Agric. Food Chem., **55**, 5267-5276 (2007)
[7] Nieuwenhuizen, N.J.; Wang, M.Y.; Matich, A.J.; Green, S.A.; Chen, X.; Yauk, Y.-K.; Beuning, L.L.; Atkinson, R.G.: Two terpene synthases are responsible for the major sesquiterpenes emitted from the flowers of kiwifruit (Actinidia deliciosa). J. Exp. Bot., **60**, 3203-3219 (2009)
[8] Green, S.; Friel, E.N.; Matich, A.; Beuning, L.L.; Cooney, J.M.; Rowan, D.D.; MacRae, E.: Unusual features of a recombinant apple α-farnesene synthase. Phytochemistry, **68**, 176-188 (2006)
[9] Portnoy, V.; Benyamini, Y.; Bar, E.; Harel-Beja, R.; Gepstein, S.; Giovannoni, J.J.; Schaffer, A.A.; Burger, J.; Tadmor, Y.; Lewinsohn, E.; Katzir, N.: The molecular and biochemical basis for varietal variation in sesquiterpene content in melon (Cucumis melo L.) rinds. Plant Mol. Biol., **66**, 647-661 (2008)

β-farnesene synthase 4.2.3.47

1 Nomenclature

EC number
4.2.3.47

Systematic name
(2E,6E)-farnesyl-diphosphate diphosphate-lyase [(E)-β-farnesene-forming]

Recommended name
β-farnesene synthase

Synonyms
(E)-β-farnesene synthase <2,3> [1,3]
CJFS <3> [1]
TPS10 <4,5,6,7,8> [4]
TPS10-dip <7> [4]
acyclic sesquiterpene synthase <3> [1]
farnesene synthase <1> [2]
sesquiterpene synthase <1> [2]
terpene synthase <1> [2]
terpene synthase 10 <4,5,6,7,8> [4]
terpene synthase 10-B73 <4> [4]
terpene synthase 10-per <8> [4]
terpene synthase T0 <4> [5]
terpene synthase TPS10 <4> [5]

2 Source Organism

<1> *Streptomyces coelicolor* (testis-specific serine/threonine protein kinase 5 variant α [2]) [2]
<2> *Artemisia annua* (UNIPROT accession number: Q4VM12) [3]
<3> *Citrus junos* (UNIPROT accession number: Q94JS8) [1]
<4> *Zea mays* (UNIPROT accession number: Q2NM15) [4,5]
<5> *Zea mays* (UNIPROT accession number: C7E5V7) [4]
<6> *Zea mays* (UNIPROT accession number: C7E5V8) [4]
<7> *Zea diploperennis* (UNIPROT accession number: C7E5V9) [4]
<8> *Zea perennis* (UNIPROT accession number: C7E5W0) [4]

D. Schomburg and I. Schomburg (eds.), *Class 3.4–6 Hydrolases, Lyases, Isomerases, Ligases: EC 3.4–6*, Springer Handbook of Enzymes S10, DOI 10.1007/978-3-642-36260-6_68,

3 Reaction and Specificity

Catalyzed reaction

(2E,6E)-farnesyl diphosphate = (E)-β-farnesene + diphosphate

Natural substrates and products

- **S** (2E,6E)-farnesyl diphosphate <4,5,6,7> (<4,5,6,7> maize plants attacked by lepidopteran larvae emit a volatile mixture that consists mostly of the sesquiterpene olefins, (E)-α-bergamotene and (E)-β-farnesene. These volatiles are produced by the herbivore-induced terpene synthase TPS10 and attract natural enemies to the damaged plants. The TPS10 products (E)-α-bergamotene and (E)-β-farnesene are consistently induced by herbivory, indicating that release of TPS10 volatiles is a defense trait conserved among maize and its wild relatives [4]) (Reversibility: ?) [4,5]
- **P** (E)-β-farnesene + diphosphate
- **S** (2E,E)-farnesyl diphosphate <8> (<8> maize plants attacked by lepidopteran larvae emit a volatile mixture that consists mostly of the sesquiterpene olefins, (E)-α-bergamotene and (E)-β-farnesene. These volatiles are produced by the herbivore-induced terpene synthase TPS10 and attract natural enemies to the damaged plants. The TPS10 products (E)-α-bergamotene and (E)-β-farnesene are consistently induced by herbivory, indicating that release of TPS10 volatiles is a defense trait conserved among maize and its wild relatives [4]) (Reversibility: ?) [4]
- **P** (E)-β-farnesene + diphosphate

Substrates and products

- **S** (2E,6E)-farnesyl diphosphate <2,3,4,5,6,7,8> (<4,5,6,7> maize plants attacked by lepidopteran larvae emit a volatile mixture that consists mostly of the sesquiterpene olefins, (E)-α-bergamotene and (E)-β-farnesene. These volatiles are produced by the herbivore-induced terpene synthase TPS10 and attract natural enemies to the damaged plants. The TPS10 products (E)-α-bergamotene and (E)-β-farnesene are consistently induced by herbivory, indicating that release of TPS10 volatiles is a defense trait conserved among maize and its wild relatives [4]) (Reversibility: ?) [1,3,4,5]
- **P** (E)-β-farnesene + diphosphate
- **S** (2E,E)-farnesyl diphosphate <8> (<8> maize plants attacked by lepidopteran larvae emit a volatile mixture that consists mostly of the sesquiterpene olefins, (E)-α-bergamotene and (E)-β-farnesene. These volatiles are produced by the herbivore-induced terpene synthase TPS10 and attract natural enemies to the damaged plants. The TPS10 products (E)-α-bergamotene and (E)-β-farnesene are consistently induced by herbivory, indicating that release of TPS10 volatiles is a defense trait conserved among maize and its wild relatives [4]) (Reversibility: ?) [4]
- **P** (E)-β-farnesene + diphosphate
- **S** farnesyl diphosphate <1> (Reversibility: ?) [2]

P (E)-β-farnesene + diphosphate (<1> 61% (E)-β-farnesene, by-products: (3E,6E)-α-farnesene (26%), (3Z,6E)-α-farnesene (6.8%), neroliol (4.9%), and farnesol (1.8%) [2])
S Additional information <1,2> (<1> CYP170A1 posseses two distinct active sites that catalyze two very different and probably unrelated biochemical activities: β-farnesene synthase and albaflavenone synthase (monooxygenase activity) [2]; <2> geranyl diphosphate is not a substrate for the recombinant enzyme [3]) [2,3]
P ?

Inhibitors

Cu^{2+} <2> (<2> no activity when Zn^{2+}, Ni^{2+} or Cu^{2+} is used as divalent metal ion [3]) [3]
Mn^{2+} <2> (<2> above 0.02 mM [3]) [3]
Ni^{2+} <2> (<2> no activity when Zn^{2+}, Ni^{2+} or Cu^{2+} is used as divalent metal ion [3]) [3]
Zn^{2+} <2> (<2> no activity when Zn^{2+}, Ni^{2+} or Cu^{2+} is used as divalent metal ion [3]) [3]
epi-isozizaene <1> (<1> about 3-fold decreases in k_{cat} for both farnesene synthase activity and P_{450} monooxygenase activity when the two substrates are present at the same time [2]) [2]

Metals, ions

Ca^{2+} <1> (<1> strict requirement for a divalent cation cofactor, highest activity being observed in the presence of Mg^{2+} or Ca^{2+}. Mn^{2+} shows relatively high activity at lower concentration, reaching 50% of the maximum synthase activity observed with Mg^{2+} as cofactor [2]) [2]
Co^{2+} <2> (<2> the enzyme exhibits substantial activity in the presence of Mg^{2+}, Mn^{2+} or Co^{2+}. Maximal activity with Mg^{2+} below 0.01 mM [3]) [3]
Mg^{2+} <1,2> (<1> strict requirement for a divalent cation cofactor, highest activity being observed in the presence of Mg^{2+} or Ca^{2+}. Mn^{2+} shows relatively high activity at lower concentration, reaching 50% of the maximum synthase activity observed with Mg^{2+} as cofactor [2]; <2> the enzyme exhibits substantial activity in the presence of Mg^{2+}, Mn^{2+} or Co^{2+}. Maximal activity with Mg^{2+} at 5 mM [3]) [2,3]
Mn^{2+} <1,2> (<1> strict requirement for a divalent cation cofactor, highest activity being observed in the presence of Mg^{2+} or Ca^{2+}. Mn^{2+} shows relatively high activity at lower concentration, reaching 50% of the maximum synthase activity observed with Mg^{2+} as cofactor [2]; <2> the enzyme exhibits substantial activity in the presence of Mg^{2+}, Mn^{2+} or Co^{2+}. Maximal activity with Mg^{2+} at 0.5 mM [3]) [2,3]
Additional information <2> (<2> no activity when Zn^{2+}, Ni^{2+} or Cu^{2+} is used as divalent metal ion [3]) [3]

Turnover number (s^{-1})

0.0095 <2> ((2E,6E)-farnesyl diphosphate) [3]
0.019 <1> ((2E,6E)-farnesyl diphosphate, <1> pH 5.5, in the presence of Mg^{2+} [2]) [2]

K_m-Value (mM)
0.0021 <2> ((2E,6E)-farnesyl diphosphate) [3]
0.0168 <1> ((2E,6E)-farnesyl diphosphate, <1> pH 5.5, in the presence of Mg^{2+} [2]) [2]

pH-Optimum
5.5 <1> (<1> maximum between pH 5.5 and 6.5 (farnesene synthase activity) [2]) [2]
6.5-7 <2> [3]

pH-Range
4-7 <1> (<1> pH 4.0: about 25% of maximal activity, pH 7.0: about 40% of maximal activity [2]) [2]

pi-Value
5.03 <2> (<2> calculated from sequence [3]) [3]

4 Enzyme Structure

Subunits
? <2,3> (<3> x * 62000, SDS-PAGE [1]; <3> x * 63800, calculated from sequence [1]; <2> x * 66900, calculated from sequence [3]) [1,3]

5 Isolation/Preparation/Mutation/Application

Source/tissue
leaf <2,3> [1,3]

Purification
<1> [2]
<2> [3]
<4> [4]
<5> [4]
<6> [4]
<7> [4]
<8> [4]

Crystallization
<1> [2]

Cloning
<1> [2]
<2> (expression in Escherichia coli) [3]
<3> [1]
<4> (expressed in Escherichia coli) [4]
<4> (expression in Arabidopsis thaliana) [5]
<5> (expressed in Escherichia coli) [4]
<6> (expressed in Escherichia coli) [4]

<7> (expressed in Escherichia coli) [4]
<8> (expressed in Escherichia coli) [4]

Engineering

Additional information <4,7,8> (<4,7,8> generation the two cross-convergent mutants, TPS10-B73 L356F and TPS10-dip F356L, by site-directed mutagenesis. The mutated enzymes are heterologously expressed, purified and assayed with the substrate (E,E)-farnesyl diphosphate. The mutant enzyme TPS10-B73 L356F produces less cyclic compounds than the wild type TPS10-B73 and has a product spectrum nearly identical to that of the wild type allele TPS10-dip which contains a phenylalanine at position 356. Conversely, the mutation of phenylalanine 356 to leucine in TPS10-dip results in a product profile dominated by (E)-α-bergamotene that is very similar to that of TPS10-B73. These results demonstrate that phenylalanine at position 356 is responsible for the decreased production of cyclic compounds in TPS10-dip and TPS10-per [4]) [4]

6 Stability

pH-Stability

6.5-9 <1> (<1> partially denatured below pH 6.5 and above pH 9.0. At pH 5.5, all of the P450 form of CYP170A1 is converted to the P420 form, which is consistent with the absence of residual monooxygenase activity at this pH. Monooxygenase activity declines at the lower pH, which favors sesquiterpene synthase activity [2]) [2]

References

[1] Maruyama, T.; Ito, M.; Honda, G.: Molecular cloning, functional expression and characterization of (E)-β farnesene synthase from Citrus junos. Biol. Pharm. Bull., **24**, 1171-1175 (2001)
[2] Zhao, B.; Lei, L.; Vassylyev, D.G.; Lin, X.; Cane, D.E.; Kelly, S.L.; Yuan, H.; Lamb, D.C.; Waterman, M.R.: Crystal structure of albaflavenone monooxygenase containing a moonlighting terpene synthase active site. J. Biol. Chem., **284**, 36711-36719 (2009)
[3] Picaud, S.; Brodelius, M.; Brodelius, P.E.: Expression, purification and characterization of recombinant (E)-β-farnesene synthase from Artemisia annua. Phytochemistry, **66**, 961-967 (2005)
[4] Köllner, T.G.; Gershenzon, J.; Degenhardt, J.: Molecular and biochemical evolution of maize terpene synthase 10, an enzyme of indirect defense. Phytochemistry, **70**, 1139-1145 (2009)
[5] Schnee, C.; Köllner, T.G.; Held, M.; Turlings, T.C.; Gershenzon, J.; Degenhardt, J.: The products of a single maize sesquiterpene synthase form a volatile defense signal that attracts natural enemies of maize herbivores. Proc. Natl. Acad. Sci. USA, **103**, 1129-1134 (2006)

(3S,6E)-nerolidol synthase 4.2.3.48

1 Nomenclature

EC number
4.2.3.48

Systematic name
(2E,6E)-farnesyl-diphosphate diphosphate-lyase [(3S,6E)-nerolidol-forming]

Recommended name
(3S,6E)-nerolidol synthase

Synonyms
(3S)-(E)-nerolidol synthase <2,4> [4]
FaNES <3> [1]
FaNES1 <3> (<3> gene name [3]) [3]
MtTPS3 <5> (<5> gene name [6]) [6]
linalool/nerolidol synthase <3> [1]
nerolidol/geranyl linalool synthase <5> [6]

2 Source Organism

<1> *Zea mays* [5]
<2> *Cucumis sativus* [4]
<3> *Fragaria x ananassa* [1,3]
<4> *Phaseolus lunatus* [2,4]
<5> *Medicago truncatula* (UNIPROT accession number: Q5UB06) [6]
<6> *Spathiphyllum wallisii* [2]

3 Reaction and Specificity

Catalyzed reaction
(2E,6E)-farnesyl diphosphate + H_2O = (3S,6E)-nerolidol + diphosphate

Natural substrates and products
S (2E,6E)-farnesyl diphosphate + H_2O <1,2,3,4> (<2,4> (3S)-(E)-nerolidol synthase plays an important role in regulating the formation of 4,8-dimethyl-1,3(E),7-nonatriene, a key signal molecule in induced plant defense mediated by the attraction of enemies of herbivores [4]; <1> biosynthesis of the C11 homoterpene (3E)-4,8-dimethyl-1,3,7-nonatriene [5]) (Reversibility: ?) [3,4,5]

D. Schomburg and I. Schomburg (eds.), *Class 3.4–6 Hydrolases, Lyases, Isomerases, Ligases: EC 3.4–6*, Springer Handbook of Enzymes S10, DOI 10.1007/978-3-642-36260-6_69,

P (3S,6E)-nerolidol + diphosphate

Substrates and products

S (2E,6E)-farnesyl diphosphate + H_2O <1,2,3,4,5,6> (<2,4> (3S)-(E)-nerolidol synthase plays an important role in regulating the formation of 4,8-dimethyl-1,3(E),7-nonatriene, a key signal molecule in induced plant defense mediated by the attraction of enemies of herbivores [4]; <1> biosynthesis of the C11 homoterpene (3E)-4,8-dimethyl-1,3,7-nonatriene [5]; <5> MtTPS3 produces linalool at 5% of the rate of (E)-nerolidol. Using geranylgeranyl diphosphate the enzyme fails to produce diterpenoids. The recombinant MtTPS3 generates the diterpene geranyllinalool when supplied with geranylgeranyl diphosphate (65% of the rate of (E)-nerolidol) [6]; <3> the enzyme also converts geranyl diphosphate to (3S)-linalool, EC 4.2.3.25 (S-linalool synthase) [3]; <1> the enzymer does not form linalool or other metabolites from geranyl diphosphate [5]) (Reversibility: ?) [2,3,4,5,6]

P (3S,6E)-nerolidol + diphosphate

Inhibitors

EDTA <1> (<1> 1 mM, activity is fully restored by the addition of Mg^{2+} to a saturating concentration of 1 mM. Mn^{2+} is about half as effective as Mg^{2+} at 1 mM [5]) [5]

Mn^{2+} <1> (<1> activates at 1 mM, inhibits at higher concentrations [5]) [5]

Metals, ions

Co^{2+} <1> (<1> nerolidol synthase is completely inactive in the absence of added divalent metal ion. Mg^{2+} is most effective. Co^{2+} shows 11% of the activity compared to Mg^{2+} [5]) [5]

Cu^{2+} <1> (<1> nerolidol synthase is completely inactive in the absence of added divalent metal ion. Mg^{2+} is most effective. Cu^{2+} shows 12% of the activity compared to Mg^{2+} [5]) [5]

Mg^{2+} <1> (<1> nerolidol synthase is completely inactive in the absence of added divalent metal ion. Mg^{2+} is most effective. Other divalent cations are less effective in supporting catalysis. Metal ions in order of edcreasing efficiency: Mg^{2+}, Mn^{2+}, Co^{2+}, Cu^{2+}, Ni^{2+}, Zn^{2+}. K_M-value for Mg^{2+} is 0.125 mM [5]) [5]

Mn^{2+} <1> (<1> nerolidol synthase is completely inactive in the absence of added divalent metal ion. Mn^{2+} is half as effective as Mg^{2+} at 1 mM, inhibits at higher concentrations [5]) [5]

Ni^{2+} <1> (<1> nerolidol synthase is completely inactive in the absence of added divalent metal ion. Mg^{2+} is most effective. Ni^{2+} shows 17% of the activity compared to Mg^{2+} [5]) [5]

K_m-Value (mM)

0.0038 <1> ((2E,6E)-farnesyl diphosphate) [5]

0.0081 <3> ((2E,6E)-farnesyl diphosphate) [3]

pH-Optimum

6.8 <1> [5]

pH-Range

6.4-7.2 <1> (<1> 50% of maximal activity at pH 6.4 and pH 7.2 [5]) [5]

4 Enzyme Structure

Molecular weight

50000 <1> (<1> gel filtration [5]) [5]

5 Isolation/Preparation/Mutation/Application

Source/tissue

fruit <3> (<3> FaNES1 is strongly expressed in cultivated strawberry (octaploid) varieties but hardly expressed at all in wild strawberry species. Increase in FaNES1 transcript levels during fruit ripening [3]) [3]
leaf <1,2,4,6> (<1> leaves fed upon by Spodoptera littoralis [5]; <4> slightly active in uninfested lima bean leaves, and strongly induced by feeding of the two-spotted spider mite (Tetranychus urticae Koch) on both plant species, but not by mechanical wounding [4]; <2> the enzyme is inactives in uninfested lima bean leaves, and strongly induced by feeding of the two-spotted spider mite (Tetranychus urticae Koch) on both plant species, but not by mechanical wounding [4]) [2,4,5]
Additional information <3> (<3> no expression detected in leaf tissue [3]) [3]

Cloning

<3> (expression in Lactococcus lactis and actively expressed using the nisin-induced expression system) [1]
<3> (recombinant FaNES1 enzyme produced in Escherichia coli cells is capable of generating both linalool and nerolidol when supplied with geranyl diphosphate or farnesyl diphosphate, respectively) [3]
<5> (subcloned into the pHis8-3 expression vector and transformed into Escherichia coli BL21-CodonPlus(DE3)) [6]

6 Stability

Storage stability

<1>, -80°C, stable for 1 week [5]

References

[1] Hernandez, I.; Molenaar, D.; Beekwilder, J.; Bouwmeester, H.; van Hylckama Vlieg, J.E.: Expression of plant flavor genes in Lactococcus lactis. Appl. Environ. Microbiol., **73**, 1544-1552 (2007)

[2] Donath, J.; Boland, W.: Biosynthesis of acyclic homoterpenes: enzyme selectivity and absolute configuration of the nerolidol precursor. Phytochemistry, **39**, 785-790 (1995)
[3] Aharoni, A.; Giri, A.P.; Verstappen, F.W.; Bertea, C.M.; Sevenier, R.; Sun, Z.; Jongsma, M.A.: Schwab, W.; Bouwmeester, H.J.: Gain and loss of fruit flavor compounds produced by wild and cultivated strawberry species. Plant Cell, **16**, 3110-3131 (2004)
[4] Bouwmeester, H.J.; Verstappen, F.W.; Posthumus, M.A.; Dicke, M.: Spider mite-induced (3S)-(E)-nerolidol synthase activity in cucumber and lima bean. The first dedicated step in acyclic C_{11}-homoterpene biosynthesis. Plant Physiol., **121**, 173-180 (1999)
[5] Degenhardt, J.; Gershenzon, J.: Demonstration and characterization of (E)-nerolidol synthase from maize: a herbivore-inducible terpene synthase participating in (3E)-4,8-dimethyl-1,3,7-nonatriene biosynthesis. Planta, **210**, 815-822 (2000)
[6] Arimura, G.; Garms, S.; Maffei, M.; Bossi, S.; Schulze, B.; Leitner, M.; Mithöfer, A.; Boland, W.: Herbivore-induced terpenoid emission in Medicago truncatula: concerted action of jasmonate, ethylene and calcium signaling. Planta, **227**, 453-464 (2008)

(3R,6E)-nerolidol synthase 4.2.3.49

1 Nomenclature

EC number
4.2.3.49

Systematic name
(2E,6E)-farnesyl-diphosphate diphosphate-lyase [(3R,6E)-nerolidol-forming]

Recommended name
(3R,6E)-nerolidol synthase

Synonyms
TPS1 <1> (<1> gene name [1]) [1]
terpene synthase 1 <1> [1]

2 Source Organism

<1> *Zea mays* (UNIPROT accession number: Q84ZW8) [1]

3 Reaction and Specificity

Catalyzed reaction
(2E,6E)-farnesyl diphosphate + H_2O = (3R,6E)-nerolidol + diphosphate

Natural substrates and products
S (2E,6E)-farnesyl diphosphate + H_2O <1> (<1> herbivore-induced production of (3R,6E)-nerolidol, an intermediate in the formation of 4,8-dimethyl-1,3(E),7-nonatriene [1]) (Reversibility: ?) [1]
P (3R,6E)-nerolidol + diphosphate

Substrates and products
S (2E,6E)-farnesyl diphosphate + H_2O <1> (<1> herbivore-induced production of (3R,6E)-nerolidol, an intermediate in the formation of 4,8-dimethyl-1,3(E),7-nonatriene [1]; <1> in the presence of geranyl diphosphate the enzyme catalyzes the formation of (3R)-linalool and geraniol [1]) (Reversibility: ?) [1]
P (3R,6E)-nerolidol + diphosphate

Metals, ions
Mg^{2+} <1> (<1> divalent metal ion cofactor is required for enzyme activity, K_M-value for Mg^{2+}: 0.47 mM. Mg^{2+} and Mn^{2+} give substantial activity, with

D. Schomburg and I. Schomburg (eds.), *Class 3.4–6 Hydrolases, Lyases, Isomerases, Ligases: EC 3.4–6*, Springer Handbook of Enzymes S10, DOI 10.1007/978-3-642-36260-6_70,

Mg^{2+} at 5 mM giving the highest activity [1]; <1> divalent metal ion cofactor is required for enzyme activity, K_M-value for Mn^{2+}: 0.026 mM. Mg^{2+} and Mn^{2+} give substantial activity, with Mg^{2+} at 5 mM giving the highest activity [1]) [1]

K_m-Value (mM)
0.001 <1> ((2E,6E)-farnesyl diphosphate, <1> 30°C [1]) [1]

pH-Optimum
7 <1> [1]

pH-Range
6-7.7 <1> (<1> half-maximal activity at pH 6.0 and pH 7.7 [1]) [1]

Temperature optimum (°C)
30-37 <1> [1]

4 Enzyme Structure

Molecular weight
71000 <1> (<1> monomer, gel filtration [1]) [1]
140000 <1> (<1> dimer, recombinant enzyme, gel filtration [1]) [1]

Subunits
dimer <1> (<1> 2 * 67400, calculated from sequence [1]) [1]
monomer <1> (<1> 1 * 67400, calculated from sequence [1]) [1]

5 Isolation/Preparation/Mutation/Application

Source/tissue
leaf <1> (<1> transcripts are detected in the leaf and sheath tissue of 2-week-old uninjured maize plants, but none is found in the roots. After 16 h of herbivory by Egyptian cotton leafworm larvae, transcript levels in the leaves of maize cv B73 are induced about 8-fold. The tps1 transcript levels in the maize cv Delprim are high even in uninjured plants and are only marginally elevated by herbivory. In older plants (3 months), moderate levels of transcript are present in leaves of both herbivore-treated and untreated plants of both cultivars. 16 hours after the initiation of herbivore damage, there is a significant elevation in transcript level [1]) [1]

Cloning
<1> (overexpression in Escherichia coli) [1]

6 Stability

Storage stability
<1>, -80°C, stable for at least 1 week [1]

References

[1] Schnee, C.; Köllner, T.G.; Gershenzon, J.; Degenhardt, J.: The maize gene terpene synthase 1 encodes a sesquiterpene synthase catalyzing the formation of (E)-β-farnesene, (E)-nerolidol, and (E,E)-farnesol after herbivore damage. Plant Physiol., **130**, 2049-2060 (2002)

2-succinyl-6-hydroxy-2,4-cyclohexadiene-1-carboxylate synthase 4.2.99.20

1 Nomenclature

EC number
4.2.99.20 (formerly a partial reaction of EC 2.5.1.64)

Systematic name
5-enolpyruvoyl-6-hydroxy-2-succinylcyclohex-3-ene-1-carboxylate pyruvate-lyase [(1R,6R)-6-hydroxy-2-succinylcyclohexa-2,4-diene-1-carboxylate-forming]

Recommended name
2-succinyl-6-hydroxy-2,4-cyclohexadiene-1-carboxylate synthase

Synonyms
(1R,6R)-2-succinyl-6-hydroxy-2,4-cyclohexadiene-1-carboxylate synthase <1> [2,3]
MenH <1> [2,3]
SHCHC <1> [3]
SHCHC synthase <1,2> [1,2]
YfbB <1> [2]

CAS registry number
122007-88-9

2 Source Organism

<1> *Escherichia coli* [2,3]
<2> *Escherichia coli K-12* [1]

3 Reaction and Specificity

Catalyzed reaction
5-enolpyruvoyl-6-hydroxy-2-succinylcyclohex-3-ene-1-carboxylate = (1R,6R)-6-hydroxy-2-succinylcyclohexa-2,4-diene-1-carboxylate + pyruvate

Reaction type
elimination

Natural substrates and products
S 5-enolpyruvoyl-6-hydroxy-2-succinyl-cyclohex-3-ene-1-carboxylate <1,2> (<1> step in menaquinone biosynthesis [2]; <2> the enzyme is involved

D. Schomburg and I. Schomburg (eds.), *Class 3.4–6 Hydrolases, Lyases, Isomerases, Ligases: EC 3.4–6*, Springer Handbook of Enzymes S10, DOI 10.1007/978-3-642-36260-6_71,

in biosynthesis of vitamin K_2 (manoquinone). Under basic conditions, the product can spontaneously lose pyruvate to form (1R,6R)-6-hydroxy-2-succinylcyclohexa-2,4-diene-1-carboxylate [1]) (Reversibility: ?) [1,2]

P (1R,6R)-6-hydroxy-2-succinylcyclohexa-2,4-diene-1-carboxylate + pyruvate

Substrates and products

S (1R,2S,5S,6S)-2-succinyl-5-enolpyruvyl-6-hydroxy-3-cyclohexene-1-carboxylate <1> (Reversibility: ?) [3]

P (1R,6R)-2-succinyl-6-hydroxy-2,4-cyclohexadiene-1-carboxylate + pyruvate

S 2-succinyl-5-enolpyruvyl-6-hydroxy-3-cyclohexene-1-carboxylate <1> (<1> assay at 37°C, pH 7.0 [2]) (Reversibility: ?) [2]

P (1R,6R)-2-succinyl-6-hydroxy-2,4-cyclohexadiene-1-carboxylate + pyruvate

S 5-enolpyruvoyl-6-hydroxy-2-succinyl-cyclohex-3-ene-1-carboxylate <1,2> (<1> step in menaquinone biosynthesis [2]; <2> the enzyme is involved in biosynthesis of vitamin K2 (manoquinone). Under basic conditions, the product can spontaneously lose pyruvate to form (1R,6R)-6-hydroxy-2-succinylcyclohexa-2,4-diene-1-carboxylate [1]) (Reversibility: ?) [1,2]

P (1R,6R)-6-hydroxy-2-succinylcyclohexa-2,4-diene-1-carboxylate + pyruvate

Metals, ions

Additional information <1> (<1> SHCHC synthase activity of MenH is not affected by the addition of a divalent ion (1 mM of Mg^{2+}, Ba^{2+}, Mn^{2+}, Ca^{2+}, Co^{2+}, or Ni^{2+}) [2]) [2]

Turnover number (s^{-1})

0.00058 <1> ((1R,2S,5S,6S)-2-succinyl-5-enolpyruvyl-6-hydroxy-3-cyclohexene-1-carboxylate, <1> H232A mutant protein [3]) [3]

0.021 <1> ((1R,2S,5S,6S)-2-succinyl-5-enolpyruvyl-6-hydroxy-3-cyclohexene-1-carboxylate, <1> H232K mutant protein [3]) [3]

0.047 <1> ((1R,2S,5S,6S)-2-succinyl-5-enolpyruvyl-6-hydroxy-3-cyclohexene-1-carboxylate, <1> R90A mutant protein [3]) [3]

0.056 <1> ((1R,2S,5S,6S)-2-succinyl-5-enolpyruvyl-6-hydroxy-3-cyclohexene-1-carboxylate, <1> W147A mutant protein [3]) [3]

0.18 <1> ((1R,2S,5S,6S)-2-succinyl-5-enolpyruvyl-6-hydroxy-3-cyclohexene-1-carboxylate, <1> D210A mutant protein [3]) [3]

0.18 <1> (5-enolpyruvoyl-6-hydroxy-2-succinyl-cyclohex-3-ene-1-carboxylate, <1> 25°C, mutant enzyme D210A [2]) [2]

0.29 <1> ((1R,2S,5S,6S)-2-succinyl-5-enolpyruvyl-6-hydroxy-3-cyclohexene-1-carboxylate, <1> S86A mutant protein [3]) [3]

0.29 <1> (5-enolpyruvoyl-6-hydroxy-2-succinyl-cyclohex-3-ene-1-carboxylate, <1> 25°C, mutant enzyme S86A [2]) [2]

0.51 <1> ((1R,2S,5S,6S)-2-succinyl-5-enolpyruvyl-6-hydroxy-3-cyclohexene-1-carboxylate, <1> R124A mutant protein [3]) [3]

2.58 <1> ((1R,2S,5S,6S)-2-succinyl-5-enolpyruvyl-6-hydroxy-3-cyclohexene-1-carboxylate, <1> Y85F mutant protein [3]) [3]

2.9 <1> ((1R,2S,5S,6S)-2-succinyl-5-enolpyruvyl-6-hydroxy-3-cyclohexene-1-carboxylate, <1> R168A mutant protein [3]) [3]
5.8 <1> (5-enolpyruvoyl-6-hydroxy-2-succinyl-cyclohex-3-ene-1-carboxylate, <1> 25°C, mutant enzyme H232A [2]) [2]
15.4 <1> ((1R,2S,5S,6S)-2-succinyl-5-enolpyruvyl-6-hydroxy-3-cyclohexene-1-carboxylate, <1> W147F mutant protein [3]) [3]
41.5 <1> ((1R,2S,5S,6S)-2-succinyl-5-enolpyruvyl-6-hydroxy-3-cyclohexene-1-carboxylate, <1> K212A mutant protein [3]) [3]
115 <1> ((1R,2S,5S,6S)-2-succinyl-5-enolpyruvyl-6-hydroxy-3-cyclohexene-1-carboxylate, <1> D128A mutant protein [3]) [3]
147 <1> ((1R,2S,5S,6S)-2-succinyl-5-enolpyruvyl-6-hydroxy-3-cyclohexene-1-carboxylate, <1> wild-type protein [3]) [3]
147 <1> (5-enolpyruvoyl-6-hydroxy-2-succinyl-cyclohex-3-ene-1-carboxylate, <1> 25°C, wild-type enzyme [2]) [2]
167 <1> (5-enolpyruvoyl-6-hydroxy-2-succinyl-cyclohex-3-ene-1-carboxylate, <1> pH 7.0, 37°C [2]) [2]

K_m-Value (mM)

0.0083 <1> (2-succinyl-5-enolpyruvyl-6-hydroxy-3-cyclohexene-1-carboxylate, <1> wild-type at 37°C [2]) [2]
0.0083 <1> (5-enolpyruvoyl-6-hydroxy-2-succinyl-cyclohex-3-ene-1-carboxylate, <1> pH 7.0, 37°C [2]) [2]
0.0086 <1> ((1R,2S,5S,6S)-2-succinyl-5-enolpyruvyl-6-hydroxy-3-cyclohexene-1-carboxylate, <1> H232A mutant protein [3]) [3]
0.0086 <1> (2-succinyl-5-enolpyruvyl-6-hydroxy-3-cyclohexene-1-carboxylate, <1> mutant H232A [2]) [2]
0.0086 <1> (5-enolpyruvoyl-6-hydroxy-2-succinyl-cyclohex-3-ene-1-carboxylate, <1> 25°C, mutant enzyme H232A [2]) [2]
0.01 <1> ((1R,2S,5S,6S)-2-succinyl-5-enolpyruvyl-6-hydroxy-3-cyclohexene-1-carboxylate, <1> wild-type protein [3]) [3]
0.0101 <1> (2-succinyl-5-enolpyruvyl-6-hydroxy-3-cyclohexene-1-carboxylate, <1> wild-type at 25°C [2]) [2]
0.014 <1> ((1R,2S,5S,6S)-2-succinyl-5-enolpyruvyl-6-hydroxy-3-cyclohexene-1-carboxylate, <1> Y85F mutant protein [3]) [3]
0.0191 <1> (5-enolpyruvoyl-6-hydroxy-2-succinyl-cyclohex-3-ene-1-carboxylate, <1> 25°C, wild-type enzyme [2]) [2]
0.0194 <1> ((1R,2S,5S,6S)-2-succinyl-5-enolpyruvyl-6-hydroxy-3-cyclohexene-1-carboxylate, <1> K212A mutant protein [3]) [3]
0.0237 <1> ((1R,2S,5S,6S)-2-succinyl-5-enolpyruvyl-6-hydroxy-3-cyclohexene-1-carboxylate, <1> W147A mutant protein [3]) [3]
0.028 <1> ((1R,2S,5S,6S)-2-succinyl-5-enolpyruvyl-6-hydroxy-3-cyclohexene-1-carboxylate, <1> S86A mutant protein [3]) [3]
0.028 <1> (2-succinyl-5-enolpyruvyl-6-hydroxy-3-cyclohexene-1-carboxylate, <1> mutant S86A at 25°C [2]) [2]
0.028 <1> (5-enolpyruvoyl-6-hydroxy-2-succinyl-cyclohex-3-ene-1-carboxylate, <1> 25°C, mutant enzyme S86A [2]) [2]

0.074 <1> ((1R,2S,5S,6S)-2-succinyl-5-enolpyruvyl-6-hydroxy-3-cyclohexene-1-carboxylate, <1> W147F mutant protein [3]) [3]
0.084 <1> ((1R,2S,5S,6S)-2-succinyl-5-enolpyruvyl-6-hydroxy-3-cyclohexene-1-carboxylate, <1> R124A mutant protein [3]) [3]
0.085 <1> ((1R,2S,5S,6S)-2-succinyl-5-enolpyruvyl-6-hydroxy-3-cyclohexene-1-carboxylate, <1> D128A mutant protein [3]) [3]
0.118 <1> ((1R,2S,5S,6S)-2-succinyl-5-enolpyruvyl-6-hydroxy-3-cyclohexene-1-carboxylate, <1> D210A mutant protein [3]) [3]
0.118 <1> (2-succinyl-5-enolpyruvyl-6-hydroxy-3-cyclohexene-1-carboxylate, <1> mutant D210A at 25°C [2]) [2]
0.118 <1> (5-enolpyruvoyl-6-hydroxy-2-succinyl-cyclohex-3-ene-1-carboxylate, <1> 25°C, mutant enzyme D210A [2]) [2]
0.134 <1> ((1R,2S,5S,6S)-2-succinyl-5-enolpyruvyl-6-hydroxy-3-cyclohexene-1-carboxylate, <1> R168A mutant protein [3]) [3]
0.159 <1> ((1R,2S,5S,6S)-2-succinyl-5-enolpyruvyl-6-hydroxy-3-cyclohexene-1-carboxylate, <1> R90A mutant protein [3]) [3]
0.532 <1> ((1R,2S,5S,6S)-2-succinyl-5-enolpyruvyl-6-hydroxy-3-cyclohexene-1-carboxylate, <1> H232K mutant protein [3]) [3]

pH-Optimum
7 <1> (<1> assay at [2]) [2]

Temperature optimum (°C)
37 <1> (<1> assay at [2]) [2]

4 Enzyme Structure

Molecular weight
25400 <1> (<1> gel filtration [2]) [2]

Subunits
monomer <1> (<1> 1 * 25400 [2]) [2]

5 Isolation/Preparation/Mutation/Application

Purification
<1> [2]
<1> (combination of Ni^{2+}-affinity chromatography and size-exclusion chromatography) [2]
<1> (immobilized metal ion affinity chromatography, gel filtration) [3]

Cloning
<1> (expressed in Escherichia coli BL21(DE3)) [3]

Engineering
D128A <1> (<1> conserved among MenH proteins [3]) [3]

D210A <1> (<1> decreased activity [2]; <1> k_{cat}/K_m is 9091fold lower than wild-type value [2]; <1> part of the catalytically essential triad [3]) [2,3]
H232A <1> (<1> decreased activity [2]; <1> k_{cat}/K_m is 208333fold lower than wild-type value [2]; <1> part of the catalytically essential triad [3]) [2,3]
H232K <1> (<1> part of the catalytically essential triad [3]) [3]
K212A <1> (<1> conserved among MenH proteins [3]) [3]
R124A <1> (<1> conserved among MenH proteins [3]) [3]
R168A <1> (<1> conserved among MenH proteins [3]) [3]
R90A <1> (<1> conserved among MenH proteins [3]) [3]
S86A <1> (<1> decreased activity [2]; <1> k_{cat}/K_m is 1498fold lower than wild-type value [2]; <1> part of the catalytically essential triad [3]) [2,3]
W147A <1> (<1> conserved among MenH proteins [3]) [3]
W147F <1> (<1> conserved among MenH proteins [3]) [3]
Y85F <1> (<1> conserved among MenH proteins [3]) [3]

References

[1] Jiang, M.; Cao, Y.; Guo, Z.F.; Chen, M.; Chen, X.; Guo, Z.: Menaquinone biosynthesis in Escherichia coli: identification of 2-succinyl-5-enolpyruvyl-6-hydroxy-3-cyclohexene-1-carboxylate as a novel intermediate and re-evaluation of MenD activity. Biochemistry, **46**, 10979-10989 (2007)
[2] Jiang, M.; Chen, X.; Guo, Z.F.; Cao, Y.; Chen, M.; Guo, Z.: Identification and characterization of (1R,6R)-2-succinyl-6-hydroxy-2,4-cyclohexadiene-1-carboxylate synthase in the menaquinone biosynthesis of Escherichia coli. Biochemistry, **47**, 3426-3434 (2008)
[3] Jiang, M.; Chen, X.; Wu, X.H.; Chen, M.; Wu, Y.D.; Guo, Z.: Catalytic mechanism of SHCHC synthase in the menaquinone biosynthesis of Escherichia coli: identification and mutational analysis of the active site residues. Biochemistry, **48**, 6921-6931 (2009)

isochorismate lyase 4.2.99.21

1 Nomenclature

EC number
4.2.99.21

Systematic name
isochorismate pyruvate-lyase (salicylate-forming)

Recommended name
isochorismate lyase

Synonyms
IPL <2,3> [9,18]
Irp9 <6> [14]
MbtI <4> [4]
PchB <3> [13]
isochorismate pyruvate lyase <3> [9]
pyochelin biosynthetic protein PchB
salicylate biosynthesis protein pchB
salicylate synthase <4> [6]

CAS registry number
383896-77-3

2 Source Organism

<1> *Escherichia coli* [2,3]
<2> *Nicotiana tabacum* [18]
<3> *Pseudomonas aeruginosa* [1,5,7,8,9,12,13,17]
<4> *Mycobacterium tuberculosis* [4,6]
<5> *Yersinia enterocolitica* [10,16]
<6> *Yersinia enterocolitica* (UNIPROT accession number: Q9X9I8) [11,14]
<7> *Pseudomonas aeruginosa* (UNIPROT accession number: Q51507) [15]

3 Reaction and Specificity

Catalyzed reaction
isochorismate = salicylate + pyruvate (<3> [1,5]-sigmatropic reaction mechanism that invokes electrostatic catalysis in analogy to the [3,3]-pericyclic rearrangement of chorismate in chorismate mutase [1])

D. Schomburg and I. Schomburg (eds.), *Class 3.4–6 Hydrolases, Lyases, Isomerases, Ligases: EC 3.4–6*, Springer Handbook of Enzymes S10, DOI 10.1007/978-3-642-36260-6_72,

Substrates and products

- **S** isochorismate <3,4> (Reversibility: ?) [1,4,5,6,7,12]
- **P** salicylate + pyruvate
- **S** Additional information <1,3,4,5,6> (<3> enzyme additionally catalyzes the rearrangement of chorismate into prephenate and shows chorismate mutase activity. Both transformation of isochorismate into pyruvate and salicylate and the rearrangement of chorismate into prephenate proceed via a pericyclic reaction mechanism [9]; <6> enzyme converts chorismate to salicylate. The reaction proceeds through the intermediate isochorismate [11]; <5> enzyme directly converts chorismat into salicylate [10]; <4> isochorismate is a kinetically competent intermediate in the synthesis of salicylate from chorismate. At pH values below 7.5 isochorismate is the dominant product while above this pH value the enzyme converts chorismate to salicylate without the accumulation of isochorismate in solution. MbtI may exploit a sigmatropic pyruvate elimination mechanism [4]; <1> nucleophilic substitution reaction, enzyme is able to use H_2O as a nucleophile. Catalytic base K147 is not solely responsible for activation of H_2O as a nucleophile [2]; <3> the 2H kinetic isotope effects on k_{cat} and the ratio k_{cat}/K_m are 2.34 and 1.75, respectively. Chemistry is significantly rate-determining for the enzyme. The magnitude of the isotope effect is consistent with considerable C-H bond cleavage in the transition state. The significant 2H kinetic isotope effect and quantitative transfer of the label to pyruvate are both consistent with a pericyclic reaction mechanism [7]) (Reversibility: ?) [2,4,7,9,10,11]
- **P** ?

Inhibitors

(E)-3-(1-carboxyprop-1-enyloxy)-2-hydroxybenzoic acid <4> (<4> low micromolar inhibition of both isochorismate lyase and anthranilate synthase [6]) [6]
2-amino-3-(1-carboxyethoxy)benzoic acid <5> [16]
3-(1-carboxy-2-phenylvinyloxy)-2-hydroxybenzoic acid <4> (<4> low micromolar inhibition of both isochorismate lyase and anthranilate synthase [6]) [6]
3-(1-carboxy-3-methylbut-1-enyloxy)-2-hydroxybenzoic acid <4> (<4> low micromolar inhibition of both isochorismate lyase and anthranilate synthase [6]) [6]
3-(1-carboxybut-1-enyloxy)-2-hydroxybenzoic acid <4> (<4> low micromolar inhibition of both isochorismate lyase and anthranilate synthase [6]) [6]
3-(1-carboxyethoxy)-2-hydroxybenzoic acid <5> [16]
4-amino-3-(1-carboxyethoxy)benzoic acid <5> [16]
Additional information <3> (<3> not inhibitory at 1 mM: EDTA, EGTA, or *o*-phenanthroline. No substrate inhibition up to 1.2 mM [12]) [12]

Cofactors/prosthetic groups

Additional information <3> (<3> no cofactor required [12]) [12]

Metals, ions

Mg^{2+} <4> (<4> the salicylate and isochorismate synthase activities of MbtI are Mg^{2+}-dependent, and in the absence of Mg^{2+}, MbtI has a promiscuous chorismate mutase activity similar to that of the isochorismate pyruvate lyase, PchB, from Pseudomonas aeruginosa [4]) [4]
Additional information <3> (<3> no metal cofactor requirement [12]) [12]

Turnover number (s^{-1})

0.0142 <3> (isochorismate, <3> mutant I87T, pH 7.5, 25°C [5]) [5]
0.0245 <3> (isochorismate, <3> mutant K42A, pH 7.5, 25°C [5]) [5]
0.035 <4> (isochorismate, <4> pH 7.0, 37°C [4]) [4]
0.037 <3> (isochorismate, <3> mutant K42H, pH 7.5, 25°C [5]) [5]
0.0468 <3> (isochorismate, <3> mutant K42E, pH 7.5, 25°C [5]) [5]
0.1 <3> (isochorismate, <3> mutant R54K, pH 7.5, 30°C [1]) [1]
0.118 <3> (isochorismate, <3> mutant K42H, pH 5.0, 25°C [5]) [5]
0.177 <3> (isochorismate, <3> wild-type, pH 7.5, 25°C [5]) [5]
0.188 <3> (isochorismate, <3> mutant A43P, pH 7.5, 25°C [5]) [5]
0.27 <3> (isochorismate, <3> mutant Q91N, pH 7.5, 30°C [1]) [1]
0.43 <3> (isochorismate, <3> substrate 2-2H-isochorismate, pH 7.5, 30°C [7]) [7]
0.8 <4> (isochorismate, <4> pH 8.0, 25°C [6]) [6]
1 <3> (isochorismate, <3> pH 7.5, 30°C [7]) [7]
1.06 <3> (isochorismate, <3> wild-type, pH 7.5, 30°C [1]) [1]
1.76 <3> (isochorismate, <3> pH 7.0, 37°C [12]) [12]

Specific activity (U/mg)

12.89 <3> (<3> pH 7.0, 37°C [12]) [12]

K_m-Value (mM)

0.00079 <3> (isochorismate, <3> substrate 2-2H-isochorismate, pH 7.5, 30°C [7]) [7]
0.00105 <3> (isochorismate, <3> pH 7.5, 30°C [7]) [7]
0.0011 <3> (isochorismate, <3> mutant I87T, pH 7.5, 25°C [5]) [5]
0.0021 <4> (isochorismate, <4> pH 8.0, 25°C [6]) [6]
0.0026 <4> (isochorismate, <4> pH 7.0, 37°C [4]) [4]
0.0043 <3> (isochorismate, <3> wild-type, pH 7.5, 25°C [5]) [5]
0.0053 <3> (isochorismate, <3> mutant A43P, pH 7.5, 25°C [5]) [5]
0.0125 <3> (isochorismate, <3> pH 7.0, 37°C [12]) [12]
0.051 <3> (isochorismate, <3> mutant K42A, pH 7.5, 25°C [5]) [5]
0.057 <3> (isochorismate, <3> mutant K42H, pH 7.5, 25°C [5]) [5]
0.066 <3> (isochorismate, <3> mutant K42E, pH 7.5, 25°C [5]; <3> mutant K42H, pH 5.0, 25°C [5]) [5]

K_i-Value (mM)

0.012 <4> (3-(1-carboxybut-1-enyloxy)-2-hydroxybenzoic acid, <4> pH 8.0, 25°C [6]) [6]
0.013 <4> ((E)-3-(1-carboxyprop-1-enyloxy)-2-hydroxybenzoic acid, <4> pH 8.0, 25°C [6]) [6]

0.014 <4> (3-(1-carboxy-3-methylbut-1-enyloxy)-2-hydroxybenzoic acid, <4> pH 8.0, 25°C [6]) [6]
0.019 <5> (3-(1-carboxyethoxy)-2-hydroxybenzoic acid, <5> pH not specified in the publication, temperature not specified in the publication [16]) [16]
0.021 <4> (3-(1-carboxy-2-phenylvinyloxy)-2-hydroxybenzoic acid, <4> pH 8.0, 25°C [6]) [6]
0.024 <5> (2-amino-3-(1-carboxyethoxy)benzoic acid, <5> pH not specified in the publication, temperature not specified in the publication [16]) [16]
0.043 <5> (4-amino-3-(1-carboxyethoxy)benzoic acid, <5> pH not specified in the publication, temperature not specified in the publication [16]) [16]

pH-Optimum

6.8 <3> [12]

pH-Range

Additional information <4> (<4> at pH values below 7.5 isochorismate is the dominant product while above this pH value the enzyme converts chorismate to salicylate without the accumulation of isochorismate in solution [4]) [4]

pi-Value

5.3 <7> (<7> calculated [15]) [15]

4 Enzyme Structure

Molecular weight

30000 <3> (<3> PAGE [12]) [12]
31000-34000 <3> (<3> gel filtration [12]) [12]
88500 <1> (<1> laser light scattering experiments [3]) [3]
100000 <6> (<6> gel filtration [11]) [11]

Subunits

? <7> (<7> x * 11563, calculated [15]) [15]
dimer <1,3,6> (<6> 2 * 50000, SDS-PAGE [11]; <3> 2 * 14000, SDS-PAGE, 2 * 11500, calculated [12]; <1> 2 * 48500, calculated [3]) [3,11,12]
Additional information <3> (<3> enzyme is an intertwined dimer of three helices with connecting loops, and amino acids from each monomer participate in each of two active sites, crystallization data [13]) [13]

5 Isolation/Preparation/Mutation/Application

Source/tissue

leaf <2> (<2> highest production of isochorismate and salicylic acid in vitro by protein extracts of the young leaves of constitutively salicylic acid producing tobacco plants. Synthesis varies among the tested lines and within one line [18]) [18]

Purification

<3> [12]
<6> (recombinant enzyme) [11]

Crystallization

<1> (to 2.5 A resolution, space group P21) [3]
<3> (X-ray crystallographic structures for mutant K42A with salicylate and pyruvate bound, to 2.5 A resolution, and for apo-I87T, to 2.15 A resolution. Circular dichroism studies of mutants K42A, K42Q, K42E, and K42H, A43P and I87T) [5]
<3> (apo-structure, to 2.35 A resolution, has one dimer per asymmetric unit with nitrate bound in an open active site. The loop between the first and second helices is disordered, providing a gateway for substrate entry and product exit. The pyruvate-bound structure, to 1.95 A resolution, has two dimers per asymmetric unit. One has two open active sites like the apo structure, and the other has two closed active sites with the loop between the first and second helices ordered for catalysis) [13]
<3> (molecular dynamics simulations and averaged intermolecular substrate-protein distances, active-site volumes for reactants and transition state) [9]
<4> (docking studies of inhibitors (E)-3-(1-carboxyprop-1-enyloxy)-2-hydroxybenzoic acid, 3-(1-carboxy-3-methylbut-1-enyloxy)-2-hydroxybenzoic acid, 3-(1-carboxybut-1-enyloxy)-2-hydroxybenzoic acid, and 3-(1-carboxy-2-phenylvinyloxy)-2-hydroxybenzoic acid) [6]
<4> (native protein and selenomethionine-derivative, to 2.5-3.2 A resolution) [4]
<6> (crystal structure of Irp9 and of its complex with the reaction products salicylate and pyruvate at 1.85 A and 2.1 A resolution, respectively. Irp9 has a complex α/β fold. The crystal structure of Irp9 contains one molecule each of phosphate and acetate derived from the crystallization buffer. The enzyme is still catalytically active in the crystal. Both structures contain Mg^{2+} in the active site. There is no evidence of an allosteric tryptophan binding site) [14]

Cloning

<3> (expression in Escherichia coli) [9,13]
<3> (expression of a fusion of genes pchA and pchB from Pseudomonas aeruginosa, which encode isochorismate synthase and isochorismate pyruvate-lyase, in Arabidopsis thaliana) [17]
<6> (expression in Escherichia coli) [11]
<7> [15]

Engineering

A37I <3> (<3> mutation increases the rate constant for the chorismate mutase activity by a factor of 1000, and also increases the isochorismate pyruvate lyase catalytic efficiency, by a factor of 6 [9]) [9]
A43P <3> (<3> about 25% decrease in both chorismate mutase and isochorismate pyruvate lyase activity [5]) [5]
E240A <6> (<6> complete loss of activity [14]) [14]
H321M <6> (<6> complete loss of activity [14]) [14]

I87T <3> (<3> structure demonstrates considerable mobility, decrease in both chorismate mutase and isochorismate pyruvate lyase activity [5]) [5]
I88T <3> (<3> no isochorismate pyruvate lyase activity, retains chorismate mutase activity [12]) [12]
K147Q <1> (<1> mutation in proposed catalytic base, about 50fold decrease in activity [2]) [2]
K42A <3> (<3> residue presumably involved in electrostatic transition state stabilization. Active site architecture is maintained in mutant K42A [5]) [5]
K42E <3> (<3> almost complete loss of activity [5]) [5]
K42H <3> (<3> strong decrease in activity [5]) [5]
K42Q <3> (<3> almost complete loss of activity [5]) [5]
Q91N <3> (<3> 20fold decrease in both isochorismate pyruvate lyase and chorismate mutase activity [1]) [1]
R54K <3> (<3> 100fold decrease in both isochorismate pyruvate lyase and chorismate mutase activity [1]) [1]
Y372F <6> (<6> about 20% residual activity [14]) [14]
Y372W <6> (<6> strong decrease in activity [14]) [14]
Additional information <3,5> (<3> a CM-deficient Escherichia coli mutant, which is auxotrophic for phenylalanine and tyrosine, is functionally complemented by the cloned pchB gene for growth in minimal medium [12]; <5> enzyme is not able to complement Escherichia coli entC for the production of enterobactin. Expression of Irp9 in Escherichia coli entC mutant leads to salicylate synthesis [10]) [10,12]

Application

agriculture <3> (<3> expression of a fusion of genes pchA and pchB from Pseudomonas aeruginosa, which encode isochorismate synthase and isochorismate pyruvate-lyase, in Arabidopsis thaliana, with targeting of the gene product either to the cytosol, c-SAS plants, or to the chloroplast, *p*-SAS plants. In *p*-SAS plants, the amount of free and conjugated SA is increased more than 20fold above wild type level. P-SAS plants show a strongly dwarfed phenotype and produce very few seeds. Targeting of SAS to the cytosol causes a slight increase in free salicylic acid and a significant threefold increase in conjugated salicylic acid. The modest increase in total salicylic content does not strongly induce the resistance marker PR-1, but results in enhanced disease resistance towards a virulent isolate of Peronospora parasitica. Increased resistance of c-SAS lines is paralleled with reduced seed production [17]) [17]
biotechnology <3> (<3> alternative computational rational approach to improve the secondary catalytic activity of enzymes, taking as a test case the IPL enzyme. The approach is based on the use of molecular dynamic simulations employing hybrid quantum mechanics/molecular mechanics methods that allow describing breaking and forming bonds [8]) [8]
synthesis <3> (<3> alternative computational rational approach to improve the secondary catalytic activity of enzymes, taking as a test case the IPL enzyme. The approach is based on the use of molecular dynamic simulations employing hybrid quantum mechanics/molecular mechanics methods that allow describing breaking and forming bonds [8]) [8]

References

[1] Kunzler, D.E.; Sasso, S.; Gamper, M.; Hilvert, D.; Kast, P.: Mechanistic insights into the isochorismate pyruvate lyase activity of the catalytically promiscuous PchB from combinatorial mutagenesis and selection. J. Biol. Chem., **280**, 32827-32834 (2005)

[2] Ziebart, K.T.; Toney, M.D.: Nucleophile specificity in anthranilate synthase, aminodeoxychorismate synthase, isochorismate synthase, and salicylate synthase. Biochemistry, **49**, 2851-2859 (2010)

[3] Parsons, J.F.; Shi, K.; Calabrese, K.; Ladner, J.E.: Crystallization and X-ray diffraction analysis of salicylate synthase, a chorismate-utilizing enyzme involved in siderophore biosynthesis. Acta Crystallogr. Sect. F, **F62**, 271-274 (2006)

[4] Zwahlen, J.; Kolappan, S.; Zhou, R.; Kisker, C.; Tonge, P.J.: Structure and mechanism of MbtI, the salicylate synthase from Mycobacterium tuberculosis. Biochemistry, **46**, 954-964 (2007)

[5] Luo, Q.; Olucha, J.; Lamb, A.L.: Structure-function analyses of isochorismate-pyruvate lyase from Pseudomonas aeruginosa suggest differing catalytic mechanisms for the two pericyclic reactions of this bifunctional enzyme. Biochemistry, **48**, 5239-5245 (2009)

[6] Manos-Turvey, A.; Bulloch, E.M.M.; Rutledge, P.J.; Baker, E.N.; Lott, J.S.; Payne, R.J.: Inhibition studies of Mycobacterium tuberculosis salicylate synthase (MbtI). ChemMedChem, **5**, 1067-1079 (2010)

[7] DeClue, M.S.; Baldridge, K.K.; Kunzler, D.E.; Kast, P.; Hilvert, D.: Isochorismate pyruvate lyase: a pericyclic reaction mechanism?. J. Am. Chem. Soc., **127**, 15002-15003 (2005)

[8] Marti, S.; Andres, J.; Moliner, V.; Silla, E.; Tunon, I.; Bertran, J.: Predicting an improvement of secondary catalytic activity of promiscuous isochorismate pyruvate lyase by computational design. J. Am. Chem. Soc., **130**, 2894-2895 (2008)

[9] Marti, S.; Andres, J.; Moliner, V.; Silla, E.; Tunon, I.; Bertran, J.: Mechanism and plasticity of isochorismate pyruvate lyase: a computational study. J. Am. Chem. Soc., **131**, 16156-16161 (2009)

[10] Pelludat, C.; Brem, D.; Heesemann, J.: Irp9, encoded by the high-pathogenicity island of Yersinia enterocolitica, is able to convert chorismate into salicylate, the precursor of the siderophore yersiniabactin. J. Bacteriol., **185**, 5648-5653 (2003)

[11] Kerbarh, O.; Ciulli, A.; Howard, N.I.; Abell, C.: Salicylate biosynthesis: overexpression, purification, and characterization of Irp9, a bifunctional salicylate synthase from Yersinia enterocolitica. J. Bacteriol., **187**, 5061-5066 (2005)

[12] Gaille, C.; Kast, P.; Haas, D.: Salicylate biosynthesis in Pseudomonas aeruginosa. Purification and characterization of PchB, a novel bifunctional enzyme displaying isochorismate pyruvate-lyase and chorismate mutase activities. J. Biol. Chem., **277**, 21768-21775 (2002)

[13] Zaitseva, J.; Lu, J.; Olechoski, K.L.; Lamb, A.L.: Two crystal structures of the isochorismate pyruvate lyase from Pseudomonas aeruginosa. J. Biol. Chem., **281**, 33441-33449 (2006)
[14] Kerbarh, O.; Chirgadze, D.Y.; Blundell, T.L.; Abell, C.: Crystal structures of Yersinia enterocolitica salicylate synthase and its complex with the reaction products salicylate and pyruvate. J. Mol. Biol., **357**, 524-534 (2006)
[15] Serino, L.; Reimmann, C.; Baur, H.; Beyeler, M.; Visca, P.; Haas, D.: Structural genes for salicylate biosynthesis from chorismate in Pseudomonas aeruginosa. Mol. Gen. Genet., **249**, 217-228 (1995)
[16] Payne, R.J.; Kerbarh, O.; Miguel, R.N.; Abell, A.D.; Abell, C.: Inhibition studies on salicylate synthase. Org. Biomol. Chem., **3**, 1825-1827 (2005)
[17] Mauch, F.; Mauch-Mani, B.; Gaille, C.; Kull, B.; Haas, D.; Reimmann, C.: Manipulation of salicylate content in Arabidopsis thaliana by the expression of an engineered bacterial salicylate synthase. Plant J., **25**, 67-77 (2001)
[18] Nugroho, L.H.; Verberne, M.C.; Verpoorte, R.: Salicylic acid produced by isochorismate synthase and isochorismate pyruvate lyase in various parts of constitutive salicylic acid producing tobacco plants. Plant Sci., **161**, 911-915 (2001)

chromopyrrolate synthase 4.3.1.26

1 Nomenclature

EC number
4.3.1.26

Systematic name
2-imino-3-(7-chloroindol-3-yl)propanoate ammonia-lyase (dichlorochromopyrrolate-forming)

Recommended name
chromopyrrolate synthase

Synonyms
RebD <1> [1,2]

2 Source Organism

<1> *Lechevalieria aerocolonigenes* (UNIPROT accession number: Q8KHV6) [1,2]

3 Reaction and Specificity

Catalyzed reaction
2 2-imino-3-(7-chloroindol-3-yl)propanoate = dichlorochromopyrrolate + NH_3

Natural substrates and products
S 2 2-imino-3-(7-chloroindol-3-yl)propanoate <1> (<1> rebeccamycin biosynthetic pathway [1,2]) (Reversibility: ?) [1,2]
P dichlorochromopyrrolate + NH_3

Substrates and products
S 2 2-imino-3-(7-chloroindol-3-yl)propanoate <1> (<1> rebeccamycin biosynthetic pathway [1,2]) (Reversibility: ?) [1,2]
P dichlorochromopyrrolate + NH_3
S Additional information <1> (<1> RebD acts as an efficient catalase, effecting the disproportionation of hydrogen peroxide to give oxygen and water [1]) [1]
P ?

D. Schomburg and I. Schomburg (eds.), *Class 3.4–6 Hydrolases, Lyases, Isomerases, Ligases: EC 3.4–6*, Springer Handbook of Enzymes S10, DOI 10.1007/978-3-642-36260-6_73,

Cofactors/prosthetic groups

heme <1> (<1> contains one molecule of heme b per monomer [1]; <1> the cytochrome cofactor is noncovalently bound to the enzyme [2]) [1,2]

Metals, ions

Fe <1> (<1> contains non-heme iron that is not part of an iron-sulfur center [1]) [1]

4 Enzyme Structure

Molecular weight

113000 <1> (<1> gel filtration, MALDI-TOF mass spectrometry [1]) [1]

Subunits

dimer <1> (<1> 2 * 56000, SDS-PAGE [1]) [1]

5 Isolation/Preparation/Mutation/Application

Purification

<1> (purified as a C-terminally His6-tagged protein) [1]

Cloning

<1> (overproduced as a C-terminally His6-tagged protein, expression in Escherichia coli) [1]

References

[1] Howard-Jones, A.R.; Walsh, C.T.: Enzymatic generation of the chromopyrrolic acid scaffold of rebeccamycin by the tandem action of RebO and RebD. Biochemistry, **44**, 15652-15663 (2005)

[2] Nishizawa, T.; Grüschow, S.; Jayamaha, D.H.; Nishizawa-Harada, C.; Sherman, D.H.: Enzymatic assembly of the bis-indole core of rebeccamycin. J. Am. Chem. Soc., **128**, 724-725 (2006)

threo-3-hydroxy-D-aspartate ammonia-lyase 4.3.1.27

1 Nomenclature

EC number
4.3.1.27

Systematic name
threo-3-hydroxy-D-aspartate ammonia-lyase (oxaloacetate-forming)

Recommended name
threo-3-hydroxy-D-aspartate ammonia-lyase

Synonyms
D-THA DH <1> [1]
D-threo-3-hydroxyaspartate ammonia-lyase <1> [1]
D-threo-3-hydroxyaspartate dehydratase <1> [1]

2 Source Organism

<1> *Delftia sp.* HT23 (UNIPROT accession number: B2DFG5) [1]

3 Reaction and Specificity

Catalyzed reaction
threo-3-hydroxy-D-aspartate = oxaloacetate + NH_3

Substrates and products
S D-serine <1> (<1> poor substrate [1]) (Reversibility: ?) [1]
P ?
S D-threo-3-hydroxyaspartate <1> (Reversibility: ?) [1]
P oxaloacetate + NH_3
S L-erythro-3-hydroxyaspartate <1> (Reversibility: ?) [1]
P ?
S L-serine <1> (<1> poor substrate [1]) (Reversibility: ?) [1]
P ?
S L-threo-3-hydroxyaspartate <1> (Reversibility: ?) [1]
P ?
S L-threo-3-hydroxyaspartate <1> (Reversibility: ?) [1]
P oxaloacetate + NH_3

D. Schomburg and I. Schomburg (eds.), *Class 3.4–6 Hydrolases, Lyases, Isomerases, Ligases: EC 3.4–6*, Springer Handbook of Enzymes S10, DOI 10.1007/978-3-642-36260-6_74,

S Additional information <1> (<1> D-erythro-3-hydroxyaspartate is not a substrate [1]; <1> the purified enzyme shows no alanine racemase activity [1]) (Reversibility: ?) [1]
P ?

Inhibitors
EDTA <1> (<1> the enzyme is modestly inhibited by EDTA (27% inhibition at 1 mM) [1]) [1]
hydroxylamine <1> (<1> the enzyme is strongly inhibited by hydroxylamine (91.2% inhibition at 1 mM) [1]) [1]

Cofactors/prosthetic groups
pyridoxal 5'-phosphate <1> [1]

Metals, ions
Ca^{2+} <1> (<1> activator [1]) [1]
Co^{2+} <1> (<1> the recombinant enzyme is highly activated by Co^{2+} [1]) [1]
Fe^{2+} <1> (<1> activator [1]) [1]
Mn^{2+} <1> (<1> the recombinant enzyme is highly activated by Mn^{2+} [1]) [1]
Ni^{2+} <1> (<1> the recombinant enzyme is highly activated by Ni^{2+} [1]) [1]
Zn^{2+} <1> (<1> activator [1]) [1]
Additional information <1> (<1> no activity is detected when Sn^{2+} or Cu^{2+} is added [1]) [1]

Turnover number (s^{-1})
0.18 <1> (L-serine, <1> at pH 8.5 and 50°C [1]) [1]
3.03 <1> (L-threo-3-hydroxyaspartate, <1> at pH 8.5 and 50°C [1]) [1]
8.68 <1> (D-serine, <1> at pH 8.5 and 50°C [1]) [1]
8.68 <1> (L-erythro-3-hydroxyaspartate, <1> at pH 8.5 and 50°C [1]) [1]
10.93 <1> (D-threo-3-hydroxyaspartate, <1> at pH 8.5 and 50°C [1]) [1]

Specific activity (U/mg)
0.18 <1> (<1> cell extract, at 50°C, pH 8.5 [1]) [1]
21.3 <1> (<1> after 115.8fold purification, at 50°C, pH 8.5 [1]) [1]

K_m-Value (mM)
0.15 <1> (D-serine, <1> at pH 8.5 and 50°C [1]) [1]
0.16 <1> (L-erythro-3-hydroxyaspartate, <1> at pH 8.5 and 50°C [1]) [1]
0.42 <1> (D-threo-3-hydroxyaspartate, <1> at pH 8.5 and 50°C [1]) [1]
6.16 <1> (L-threo-3-hydroxyaspartate, <1> at pH 8.5 and 50°C [1]) [1]
38.7 <1> (L-serine, <1> at pH 8.5 and 50°C [1]) [1]

pH-Optimum
8.5 <1> [1]

Temperature optimum (°C)
50 <1> [1]

4 Enzyme Structure

Molecular weight

36000 <1> (<1> gel filtration [1]) [1]
40300 <1> (<1> calculated from amino acid sequence [1]) [1]
40900 <1> (<1> calculated from the deduced amino acid sequence of the recombinant enzyme [1]) [1]
41600 <1> (<1> MALDI-TOF mass spectrometry [1]) [1]

Subunits

monomer <1> (<1> 1 * 41000, SDS-PAGE [1]) [1]

5 Isolation/Preparation/Mutation/Application

Purification

<1> (ammonium sulfate precipitation, HiPrep Q column chromatography, HiTrap phenyl column chromatography, Superdex-200 gel filtration, Resource Q column chromatography, and HiTrap butyl column chromatography) [1]

Cloning

<1> (expressed in Escherichia coli JM109 cells) [1]

Engineering

K43A <1> (<1> the mutant enzyme shows no detectable activity [1]) [1]

References

[1] Maeda, T.; Takeda, Y.; Murakami, T.; Yokota, A.; Wada, M.: Purification, characterization and amino acid sequence of a novel enzyme, D-threo-3-hydroxyaspartate dehydratase, from Delftia sp. HT23. J. Biochem., **148**, 705-712 (2010)

carboxybiotin decarboxylase 4.3.99.2

1 Nomenclature

EC number
4.3.99.2

Systematic name
carboxybiotinyl-[protein] carboxy-lyase

Recommended name
carboxybiotin decarboxylase

Synonyms
MadB <3> [4]
MmdB <2> [1]
Na^+ pumping malonate decarboxylase <3> [2]
carboxybiotin protein decarboxylase

2 Source Organism

<1> *Klebsiella pneumoniae* [3]
<2> *Propionigenium modestum* [1]
<3> *Malonomonas rubra* [2,4]

3 Reaction and Specificity

Catalyzed reaction
a carboxybiotinyl-[protein] + n Na^+_{in} + H^+_{out} = CO_2 + a biotinyl-[protein] + n Na^+_{out} (n = 1-2) (<1> residue Asp2O3 in its dissociated form binds Na^+ and promotes its translocation, while the protonated residue transfers the proton to the acid-labile carboxybiotin which initiates its decarboxylation. Na^+ transport by oxaloacetate decarboxylation is accompanied by H^+ transport in the opposite direction [3])

Natural substrates and products
S Additional information <3> (<3> carboxybiotin is cleaved at the membrane-bound subunit MadB of malonate decarboxylase Na^+ pump with concomitant generation of a transmembrane Na^+ gradient [4]) (Reversibility: ?) [4]
P ?

D. Schomburg and I. Schomburg (eds.), *Class 3.4–6 Hydrolases, Lyases, Isomerases, Ligases: EC 3.4–6*, Springer Handbook of Enzymes S10, DOI 10.1007/978-3-642-36260-6_75,

Substrates and products

S Additional information <3> (<3> carboxybiotin is cleaved at the membrane-bound subunit MadB of malonate decarboxylase Na^+ pump with concomitant generation of a transmembrane Na^+ gradient [4]) (Reversibility: ?) [4]

P ?

4 Enzyme Structure

Subunits

? <2,3> (<2> x * 41200, calculated [1]; <3> x * 43023, calculated [4]) [1,4]

5 Isolation/Preparation/Mutation/Application

Localization

membrane <1,3> (<1> membrane-bound β-subunit of the oxaloacetate decarboxylase Na^+ pump is responsible for the decarboxylation of carboxybiotin and the coupled translocation of Na^+ ions across the membrane [3]) [3,4]

Purification

<2> (methymalonyl-CoA decarboxylase complex) [1]

<3> (recombinant isoform MadF. Despite coexpression of biotin ligase birA, MadF is poorly biotinylated. Existence of a biotin ligase in Malonomonas rubra with an altered substrate specificity different from that of BirA) [2]

Cloning

<3> (coexpression with biotin ligase birA in Escherichia coli) [2]

Engineering

D149E <1> (<1> mutation within putative membrane-spanning domains of the β-subunit. Mutant retains oxaloacetate decarboxylase and Na^+ transport activities [3]) [3]

D149Q <1> (<1> mutation within putative membrane-spanning domains of the β-subunit. Mutant retains oxaloacetate decarboxylase and Na^+ transport activities [3]) [3]

D203E <1> (<1> loss of oxaloacetate decarboxylase and Na^+ transport activities, mutant retains the ability to form the carboxybiotin enzyme [3]) [3]

D203N <1> (<1> loss of oxaloacetate decarboxylase and Na^+ transport activities, mutant retains the ability to form the carboxybiotin enzyme [3]) [3]

References

[1] Bott, M.; Pfister, K.; Burda, P.; Kalbermatter, O.; Woehlke, G.; Dimroth, P.: Methylmalonyl-CoA decarboxylase from Propionibacterium modestum.

Cloning and sequencing of the structural genes and purification of the enzyme complex. Eur. J. Biochem., **250**, 590-599 (1997)
[2] Berg, M.; Dimroth, P.: The biotin protein MadF of the malonate decarboxylase from Malonomonas rubra. Arch. Microbiol., **170**, 464-468 (1998)
[3] Di Berardino, M.; Dimroth, P.: Aspartate 203 of the oxaloacetate decarboxylase β-subunit catalyses both the chemical and vectorial reaction of the Na^+ pump. EMBO J., **15**, 1842-1849 (1996)
[4] Berg, M.; Hilbi, H.; Dimroth, P.: Sequence of a gene cluster from Malonomonas rubra encoding components of the malonate decarboxylase Na^+ pump and evidence for their function. Eur. J. Biochem., **245**, 103-115 (1997)

heme ligase 4.99.1.8

1 Nomenclature

EC number
4.99.1.8

Systematic name
Fe^{3+}:ferriprotoporphyrin IX ligase (β-hematin-forming)

Recommended name
heme ligase

Synonyms
HDP <1,2> [1,2]
heme detoxification protein <1,2> [1,2]

2 Source Organism

<1> *Plasmodium falciparum* [1,2,3]
<2> *Plasmodium yoelii* [2]

3 Reaction and Specificity

Catalyzed reaction
2 ferriprotoporphyrin IX = β-hematin

Natural substrates and products
S ferriprotoporphyrin IX <1> (<1> hemozoin consists of an unusual polymer of hemes linked between the central ferric ion of one heme and a carboxylate side-group oxygen of another. The hemes are sequestered via this linkage into an insoluble product, providing a unique way for the malaria parasite to avoid the toxicity associated with soluble heme [3]) (Reversibility: ?) [3]
P β-hematin

Substrates and products
S ferriprotoporphyrin IX <1,2> (<1> hemozoin consists of an unusual polymer of hemes linked between the central ferric ion of one heme and a carboxylate side-group oxygen of another. The hemes are sequestered via this linkage into an insoluble product, providing a unique way for the malaria parasite to avoid the toxicity associated with soluble heme [3]; <2> HDP possesses 2.7 heme binding sites [2]; <1> hemozoin con-

D. Schomburg and I. Schomburg (eds.), *Class 3.4–6 Hydrolases, Lyases, Isomerases, Ligases: EC 3.4–6*, Springer Handbook of Enzymes S10, DOI 10.1007/978-3-642-36260-6_76,

sists of an unusual polymer of hemes linked between the central ferric ion of one heme and a carboxylate side-group oxygen of another [3]) (Reversibility: ?) [2,3]
P β-hematin

pH-Optimum
3-4.4 <1> [2]

pH-Range
3.3-5.2 <1> (<1> pH 3.3-4.4: optimum, pH 5.2: about 75% of maximal activity, no activity above pH 5.6 [2]) [2]

5 Isolation/Preparation/Mutation/Application

Localization
extracellular <1> (<1> the parasite utilizes a circuitous outbound-inbound trafficking route by initially secreting HDP into the cytosol of infected red blood cells [2]) [2]
food vacuole <1> [2]

Purification
<1> (native enzyme, full-length recombinant enzyme and truncated enzymes) [2]
<2> (recombinant enzyme) [2]

Cloning
<1> (expression of full length enzyme in Escherichia coli, expression of two truncated enzyme proteins (HDP3 encoded by amino acids 88-205 of the full-length protein, representing the fasciclin domain and HDP2 encoded by amino acids 1-87 and lacking the fasciclin domain)) [2]
<2> (expression in Escherichia coli) [2]

Engineering
Additional information <1> (<1> the truncated enzyme proteins HDP3 (encoded by amino acids 88-205 of the full-length protein, representing the fasciclin domain) and HDP2 (encoded by amino acids 1-87 and lacking the fasciclin domain) are unable to produce hemozoin. The full-length enzyme is required for heme binding and hemozoin production activities of the protein [2]) [2]

Application
medicine <1,2> (<1> HDP is a conserved target for future antimalarial development [1]; <1,2> involvement of heme detoxification protein in the process of formation of hemozoin suggests that it could be a malaria drug target [2]) [1,2]

6 Stability

Temperature stability
94 <1> (<1> 10 min, stable [2]) [2]

References

[1] Vinayak, S.; Rathore, D.; Kariuki, S.; Slutsker, L.; Shi, Y.P.; Villegas, L.; Escalante, A.A.; Udhayakumar, V.: Limited genetic variation in the Plasmodium falciparum heme detoxification protein (HDP). Infect. Genet. Evol., **9**, 286-289 (2009)
[2] Jani, D.; Nagakatti, R.; Beatty, W.; Angel, R.; Slebodnick, C.; Andersen, J.; Kumar, S.; Rathore, D.: HDP - a novel heme detoxification protein from the malaria parasite. PLos Pathog., **25**, 0000 (2008)
[3] Slater, A.F.G.; Swiggard, W.J.; Orton, B.R.; Flitter, W.D.; Goldberg, D.E.; Cerami, A.; Henderson, G.B.: An iron-carboxylate bond links the heme units of malaria pigment. Proc. Natl. Acad. Sci. USA, **88**, 325-329 (1991)

hydantoin racemase 5.1.99.5

1 Nomenclature

EC number
5.1.99.5

Systematic name
D-5-monosubstituted-hydantoin racemase

Recommended name
hydantoin racemase

Synonyms
5'-monosubstituted-hydantoin racemase
HyuA
HyuE
hydantoin racemase

CAS registry number
111310-51-1

2 Source Organism

<1> *Sinorhizobium meliloti* [3,5,7,12]
<2> *Pseudomonas sp.* [1]
<3> *Arthrobacter sp.* [4]
<4> *Agrobacterium tumefaciens* [6,8,10]
<5> *Microbacterium liquefaciens* [2,9]
<6> *Pseudomonas sp.* (UNIPROT accession number: Q00924) [11]

3 Reaction and Specificity

Catalyzed reaction
D-5-monosubstituted hydantoin = L-5-monosubstituted hydantoin (<3> keto-enol automerism of 5-monosubstituted hydantoins is responsible for racemization [4]; <1> two-base mechanism for the racemization of 5-monosubstituted hydantoins [12])

Substrates and products
S (5R)-5-(1H-indol-2-ylmethyl)-3-methylimidazolidine-2,4-dione <3> (<3> 20.2% of the activity with (5S)-5-(1H-indol-2-ylmethyl)imidazolidine-2,4-dione [4]) (Reversibility: r) [4]

D. Schomburg and I. Schomburg (eds.), *Class 3.4–6 Hydrolases, Lyases, Isomerases, Ligases: EC 3.4–6*, Springer Handbook of Enzymes S10, DOI 10.1007/978-3-642-36260-6_77,

P (5S)-5-(1H-indol-2-ylmethyl)-3-methylimidazolidine-2,4-dione
S (5S)-5-(1H-indol-2-ylmethyl)imidazolidine-2,4-dione <3> (Reversibility: r) [4]
P (5R)-5-(1H-indol-2-ylmethyl)imidazolidine-2,4-dione
S (5S)-5-(2-methylpropyl)imidazolidine-2,4-dione <3> (<3> 9.8% of the activity with (5S)-5-(1H-indol-2-ylmethyl)imidazolidine-2,4-dione [4]) (Reversibility: r) [4]
P (5S)-5-(2-methylpropyl)imidazolidine-2,4-dione
S (5S)-5-(4-hydroxybenzyl)imidazolidine-2,4-dione <3> (<3> 76.7% of the activity with (5S)-5-(1H-indol-2-ylmethyl)imidazolidine-2,4-dione [4]) (Reversibility: r) [4]
P (5R)-5-(4-hydroxybenzyl)imidazolidine-2,4-dione
S (5S)-5-[2-(methylsulfanyl)ethyl]imidazolidine-2,4-dione <3> (<3> 20.4% of the activity with (5S)-5-(1H-indol-2-ylmethyl)imidazolidine-2,4-dione [4]) (Reversibility: r) [4]
P (5R)-5-[2-(methylsulfanyl)ethyl]imidazolidine-2,4-dione
S (5S)-5-benzylimidazolidine-2,4-dione <3> (<3> 62.7% of the activity with (5S)-5-(1H-indol-2-ylmethyl)imidazolidine-2,4-dione [4]) (Reversibility: r) [4]
P (5R)-5-benzylimidazolidine-2,4-dione
S D-5-isobutylhydantoin <6> (<6> complete racemization [11]) (Reversibility: r) [11]
P L-5-isobutylhydantoin
S D-5-methylhydantoin <6> (<6> complete racemization [11]) (Reversibility: r) [11]
P L-5-methylhydantoin
S D-benzylhydantoin <1> (Reversibility: r) [5]
P L-benzylhydantoin
S D-benzylhydantoin <5> (<5> final molecular ratio between the isomers is 1:1. Initial specific acitivity with D-benzylhydantoin is 79 U/mg, with L-benzymhydantoin is 100 U/mg [9]) (Reversibility: r) [9]
P R-benzylhydantoin
S D-isobutylhydantoin <1> (Reversibility: r) [5]
P L-isbutylhydantoin
S L-5-(2-methylthioethyl)hydantoin <6> (<6> complete racemization [11]) (Reversibility: r) [11]
P D-5-(2-methylthioethyl)hydantoin
S L-5-methylhydantoin <6> (<6> about 50% racemization [11]) (Reversibility: r) [11]
P D-5-methylhydantoin
S L-5-methylthioethylhydantoin <1,4> (Reversibility: r) [6,8,12]
P D-5-methylthioethylhydantoin
S L-benzylhydantoin <1,4,5> (<5> final molecular ratio between the isomers is 1:1. Initial specific acitivity with D-benzylhydantoin is 79 U/mg, with L-benzymhydantoin is 100 U/mg [9]; <4> slow racemization [6,8]) (Reversibility: r) [5,6,8,9]
P D-benzylhydantoin

S L-ethylhydantoin <1,4> (Reversibility: r) [5,6,8,12]
P D-ethylhydantoin
S L-isobutylhydantoin <1> (Reversibility: r) [5]
P D-isbutylhydantoin
S L-isobutylhydantoin <4> (Reversibility: r) [6,8]
P D-isobutylhydantoin
S L-isopropylhydantoin <1> (Reversibility: r) [12]
P D-isopropylhydantoin
S Additional information <4,6> (<6> no substrate: DL-5-isopropylhydantoin [11]; <4> preference for hydantoins with short rather than long aliphatic side chains or hydantoins with aromatic rings [6,8]) (Reversibility: ?) [6,8,11]
P ?

Inhibitors

Co^{2+} <4> (<4> slight inhibition [6]) [6]
Cu^{2+} <3,4,5,6> (<4,6> strong inhibition [6,8,11]; <3> 80% loss of activity [4]) [4,6,8,9,11]
D-5-methylthioethyl-hydantoin <1> (<1> determination of thermodynamic binding parameters. Binding of the inhibitor is entropically and thermodynamically favoured [7]) [7]
DL-5-isopropylhydantoin <6> (<6> complete inhbition, pre-incubation with DL-5-(2-methylthioethyl)hydantoin protects [11]) [11]
Hg^{2+} <3,4> (<4> strong inhibition [6,8]; <3> complete loss of activity [4]) [4,6,8]
L-5-methylthioethylhydantoin <1> (<1> determination of thermodynamic binding parameters. Binding of the inhibitor is entropically and thermodynamically favoured [7]) [7]
N-ethylmaleimide <5> [9]
Ni^{2+} <4> (<4> slight inhibition [6]) [6]
Zn^{2+} <6> (<6> strong inhibition [11]) [11]
iodoacetamide <3,5> (<3> complete loss of activity [4]) [4,9]
p-mercuribenzoate <3> (<3> complete loss of activity [4]) [4]
Additional information <4> (<4> not inhibitory: EDTA, dithiothreitol [8]; <4> not inhibtory: EDTA, Mn^{2+}, dithiothreitol [6]) [6,8]

Activating compounds

EDTA <3> (<3> slight stimulation [4]) [4]
Sodium dodecyl sulfate <3> (<3> slight stimulation [4]) [4]
cysteine <3> (<3> slight stimulation [4]) [4]
dithiothreitol <3> (<3> up to 50% stimulation [4]) [4]

Metals, ions

Co^{2+} <6> (<6> slight stimulation [11]) [11]
Mn^{2+} <6> (<6> slight stimulation [11]) [11]

Turnover number (s^{-1})

0.18 <4> (L-benzylhydantoin, <4> pH 7.5, 40°C [8]) [8]
0.46 <4> (D-benzylhydantoin, <4> pH 7.5, 40°C [8]) [8]

0.48 <4> (L-isobutylhydantoin, <4> pH 7.5, 40°C [8]) [8]
0.5 <4> (D-5-methylthioethylhydantoin, <4> pH 7.5, 40°C [8]) [8]
0.78 <4> (L-5-methylthioethylhydantoin, <4> pH 7.5, 40°C [8]) [8]
0.83 <4> (D-isobutylhydantoin, <4> pH 7.5, 40°C [8]) [8]
1.8 <4> (D-ethylhydantoin, <4> pH 7.5, 40°C [8]) [8]
1.81 <4> (L-ethylhydantoin, <4> pH 7.5, 40°C [8]) [8]
1.94 <1> (L-benzylhydantoin, <1> pH 8.5 [5]) [5]
2.12 <1> (L-isobutylhydantoin, <1> pH 8.5 [5]) [5]
2.29 <1> (D-benzylhydantoin, <1> pH 8.5 [5]) [5]
3.24 <1> (D-isobutylhydantoin, <1> pH 8.5 [5]) [5]
6.42 <1> (L-ethylhydantoin, <1> pH 8.5 [5]) [5]

Specific activity (U/mg)

20.8 <6> (<6> pH 7.5, 30°C [11]) [11]
79 <5> (<5> pH 8.0, 37°C, substrate D-benzylhydantoin [9]) [9]
100 <5> (<5> pH 8.0, 37°C, substrate L-benzylhydantoin [9]) [9]

K_m-Value (mM)

1.23 <4> (L-isobutylhydantoin, <4> pH 7.5, 40°C [6]) [6]
3.02 <4> (L-isobutylhydantoin, <4> pH 7.5, 40°C [8]) [8]
3.76 <1> (D-isobutylhydantoin, <1> pH 8.5 [5]) [5]
4.26 <4> (D-ethylhydantoin, <4> pH 7.5, 40°C [6]) [6]
4.45 <4> (L-ethylhydantoin, <4> pH 7.5, 40°C [6]) [6]
4.47 <4> (D-5-methylthioethylhydantoin, <4> pH 7.5, 40°C [6]) [6]
4.58 <4> (D-isobutylhydantoin, <4> pH 7.5, 40°C [6]) [6]
4.71 <4> (D-benzylhydantoin, <4> pH 7.5, 40°C [6]) [6]
5.41 <4> (L-5-methylthioethylhydantoin, <4> pH 7.5, 40°C [6]) [6]
5.56 <4> (L-benzylhydantoin, <4> pH 7.5, 40°C [6]) [6]
6.3 <4> (D-5-methylthioethylhydantoin, <4> pH 7.5, 40°C [8]) [8]
6.41 <1> (L-isobutylhydantoin, <1> pH 8.5 [5]) [5]
6.79 <4> (D-isobutylhydantoin, <4> pH 7.5, 40°C [8]) [8]
8.3 <1> (L-benzylhydantoin, <1> pH 8.5 [5]) [5]
10.9 <4> (L-5-methylthioethylhydantoin, <4> pH 7.5, 40°C [8]) [8]
12.54 <4> (D-ethylhydantoin, <4> pH 7.5, 40°C [8]) [8]
13.89 <1> (D-benzylhydantoin, <1> pH 8.5 [5]) [5]
17.32 <1> (L-ethylhydantoin, <1> pH 8.5 [5]) [5]
18.4 <4> (L-benzylhydantoin, <4> pH 7.5, 40°C [8]) [8]
19.42 <4> (L-ethylhydantoin, <4> pH 7.5, 40°C [8]) [8]
20.8 <4> (D-benzylhydantoin, <4> pH 7.5, 40°C [8]) [8]
29.8 <6> (D-5-(2-methylthioethyl)hydantoin, <6> pH 7.5, 30°C [11]) [11]
79.7 <6> (L-5-(2-methylthioethyl)hydantoin, <6> pH 7.5, 30°C [11]) [11]

pH-Optimum

7.5 <4> [6]
8.2 <5> [9]
8.5 <1,3> [4,5]
9.5 <6> [11]

pH-Range
7.5 <4> [8]
11 <6> (<6> 95% of maximum activity [11]) [11]

pi-Value
4.5 <3> (<3> isoelectric focusing [4]) [4]

Temperature optimum (°C)
37 <3> [4]
40 <1> [5]
45 <6> [11]
55 <4,5> [6,8,9]

4 Enzyme Structure

Molecular weight
84000 <3> (<3> gel filtration [4]) [4]
100000 <1,4> (<1,4> gel filtration [5,6,8]) [5,6,8]
117000 <5> (<5> gel filtration [9]) [9]
190000 <6> (<6> gel filtration [11]) [11]

Subunits
? <4> (<4> x * 25412, calculated [10]) [10]
hexamer <6> (<6> x * 32000, SDS-PAGE [11]) [11]
tetramer <1,3,4,5> (<1> 4 * 31000, SDS-PAGE [5]; <4,5> 4 * 27000, SDS-PAGE [8,9]; <4> 4 * 32000, SDS-PAGE [6]; <3> 4 * 21000, SDS-PAGE [4]) [4,5,6,8,9]

5 Isolation/Preparation/Mutation/Application

Purification
<3> [4]
<4> (recombinant protein) [6,8]
<5> [9]

Renaturation
<1> (thermodynamic parameters of the guanidinium hydrochloride-induced denaturation of wild-type and mutants C76A, C181A) [12]

Crystallization
<1> (active-site mutant C76A, in presence and absence of substrate DL-5-isopropyl hydantoin, diffraction to 2.17 and 1.85 A, respectively. both crystals belong to space group R3) [3]

Cloning

<1> (expression in Escherichia coli) [5,7]
<1> (expression with His-tag) [3]
<4> (concomitant expression of D-hydantoinase, D-carbamoylase, and hydantoin recemase in Escherichia coli) [10]
<4> (expression in Escherichia coli) [6,8]
<5> (expression in Escherichia coli, together with D-specific hydantoinase, and N-carbamoyl-D-amino acid amidohydrolase) [2]
<6> (expression in Escherichia coli) [11]

Engineering

C181A <1> (<1> no residual activity [7]; <1> no residual activity. The secondary and the tertiary structure of the mutant is not significantly affected. Residue Cys181 is responsible for L-isomer recognition and racemization. Binding thermodynamic parameters of different substrates, thermodynamic parameters of the guanidinium hydrochloride-induced denaturation [12]) [7,12]
C181S <1> (<1> less than 1% of wild-type activity [7]) [7]
C76A <1> (<1> no residual activity [7]; <1> active site mutant, crystallization data [3]; <1> no residual activity. The secondary and the tertiary structure of the mutant is not significantly affected. Residue Cys76 is responsible for recognition and proton retrieval of D-isomers. Binding thermodynamic parameters of different substrates, thermodynamic parameters of the guanidinium hydrochloride-induced denaturation [12]) [3,7,12]
C76S <1> (<1> less than 0.5% of wild-type activity [7]) [7]

Application

synthesis <2,4,5> (<5> enzymatic production of D-amino acids via a combination of hydantoin hydrolysis and hydantoin racemization. The D-forms of amino acids D-phenylalanine, D-tyrosine, D-tryptophan, O-benzyl-D-serine, D-valine, D-norvaline, D-leucine and D-norleucine can efficiently be converted from the corresponding DL-5-monosubtituted hydantoin compounds [2]; <4> reaction system for the production of D-amino acids from DL-5-monosubstituted hydantoins based on recombinant Escherichia coli whole cell biocatalysts containing separately expressed D-hydantoinase, D-carbamoylase, and hydantoin recemase. The system shows high substrate specificity and is effective toward both aliphatic and aromatic DL-5-monosubstituted hydantoins. At pH 8 and 50°C, 100% conversion of DL-5-(2-methylthioethyl)-hydantoin (15 mM) into D-methionine is obtained in 30 min [10]; <2> stereospecific production of L-amino acids from the corresponding DL-5-substituted hydantoins. DL-5-substituted hydantoins are converted exclusively to the L-forms of the corresponding N-carbamyl-amino acids by hydantoinase in combination with hydantoin racemase. The N-carbamyl-l-amino acids are then converted to L-amino acids by N-carbamyl-L-amino acid amidohydrolase [1]) [1,2,10]

6 Stability

pH-Stability
6-9 <5> [9]

Temperature stability
37 <5> (<5> stable at temperatures below [9]) [9]
45 <6> (<6> in presence of substrate, stable [11]) [11]

General stability information
<1>, the enzyme remains active after 10 freeze-thawing cycles [5]
<4>, enzyme is active after 10 freeze-thawing cycles [6]

Storage stability
<1>, -20°C, 0.1 M Tris, 20% glycerol, pH 8.5, stable for at least 3 months [5]
<1>, 4°C, 0.1 M Tris, pH 8.5, stable for 10 weeks [5]
<4>, -20°C, pH 8.0, 20% glycerol, stable for at least 6 months [6]
<4>, 4°C, pH 8.0, stable for 8 weeks [6]
<6>, 4°C, ammonium sulfate at 90% saturation, stable for 6 months [11]

References

[1] Ishikawa, T.; Watabe, K.; Mukohara, Y.; Nakamura, H.: Mechanism of stereospecific conversion of DL-5-substituted hydantoins to the corresponding L-amino acids by Pseudomonas sp. strain NS671. Biosci. Biotechnol. Biochem., **61**, 185-187 (1997)
[2] Nozaki, H.; Takenaka, Y.; Kira, I.; Watanabe, K.; Yokozeki, K.: D-Amino acid production by E. coli co-expressed three genes encoding hydantoin racemase, D-hydantoinase and N-carbamoyl-D-amino acid amidohydrolase. J. Mol. Catal. B, **32**, 213-218 (2005)
[3] Martinez-Rodriguez, S.; Gonzalez-Ramirez, L.A.; Clemente-Jimenez, J.M.; Rodriguez-Vico, F.; Las Heras-Vazquez, F.J.; Gavira, J.A.; Garcia-Ruiz, J.M.: Crystallization and preliminary crystallographic studies of an active-site mutant hydantoin racemase from Sinorhizobium meliloti CECT 4114. Acta Crystallogr. Sect. F, **F64**, 50-53 (2008)
[4] Pietzsch, M.; Syldatk, C.; Wagner, F.: A new racemase for 5-monosubstituted hydantoins. Ann. N.Y. Acad. Sci., **672**, 478-483 (1992)
[5] Martinez-Rodriguez, S.; Las Heras-Vazquez, F.J.; Mingorance-Cazorla, L.; Clemente-Jimenez, J.M.; Rodriguez-Vico, F.: Molecular cloning, purification, and biochemical characterization of hydantoin racemase from the legume symbiont Sinorhizobium meliloti CECT 4114. Appl. Environ. Microbiol., **70**, 625-630 (2004)
[6] Las Heras-Vazquez, F.J.; Martinez-Rodriguez, S.; Mingorance-Cazorla, L.; Clemente-Jimenez, J.M.; Rodriguez-Vico, F.: Overexpression and characterization of hydantoin racemase from Agrobacterium tumefaciens C58. Biochem. Biophys. Res. Commun., **303**, 541-547 (2003)

[7] Andujar-Sanchez, M.; Martinez-Rodriguez, S.; Heras-Vazquez, F.J.; Clemente-Jimenez, J.M.; Rodriguez-Vico, F.; Jara-Perez, V.: Binding studies of hydantoin racemase from Sinorhizobium meliloti by calorimetric and fluorescence analysis. Biochim. Biophys. Acta, **1764**, 292-298 (2006)
[8] Martinez-Rodriguez, S.; Las Heras-Vazquez, F.J.; Clemente-Jimenez, J.M.; Rodriguez-Vico, F.: Biochemical characterization of a novel hydantoin racemase from Agrobacterium tumefaciens C58. Biochimie, **86**, 77-81 (2004)
[9] Suzuki, S.; Onishi, N.; Yokozeki, K.: Purification and characterization of hydantoin racemase from Microbacterium liquefaciens AJ 3912. Biosci. Biotechnol. Biochem., **69**, 530-536 (2005)
[10] Martinez-Rodriguez, S.; Las Heras-Vazquez, F.J.; Clemente-Jimenez, J.M.; Mingorance-Cazorla, L.; Rodriguez-Vico, F.: Complete conversion of DL-5-monosubstituted hydantoins with a low velocity of chemical racemization into D-amino acids using whole cells of recombinant Escherichia coli. Biotechnol. Prog., **18**, 1201-1206 (2002)
[11] Watabe, K.; Ishikawa, T.; Mukohara, Y.; Nakamura, H.: Purification and characterization of the hydantoin racemase of Pseudomonas sp. strain NS671 expressed in Escherichia coli. J. Bacteriol., **174**, 7989-7995 (1992)
[12] Martinez-Rodriguez, S.; Andujar-Sanchez, M.; Neira, J.L.; Clemente-Jimenez, J.M.; Jara-Perez, V.; Rodriguez-Vico, F.; Las Heras-Vazquez, F.J.: Site-directed mutagenesis indicates an important role of cysteines 76 and 181 in the catalysis of hydantoin racemase from Sinorhizobium meliloti. Protein Sci., **15**, 2729-2738 (2006)

6-phospho-3-hexuloisomerase 5.3.1.27

1 Nomenclature

EC number
5.3.1.27

Systematic name
D-arabino-hex-3-ulose-6-phosphate isomerase

Recommended name
6-phospho-3-hexuloisomerase

Synonyms
3-hexulose-6-phosphate isomerase
6-phospho-3-hexuloisomerase <1,2,3,4,5,6,7,9,10,11,12,20,21> [10]
PHI <1,2,3,4,5,6,7,9,10,11,12,20,21> [10]
YckF <15> [1]
[acyl-carrier protein]:acetate ligase
phospho-3-hexuloisomerase

2 Source Organism

<1> *Pyrococcus sp.* [10]
<2> *Brevibacillus brevis* [10]
<3> *Bacillus subtilis* [6,10]
<4> *Methylococcus capsulatus* [4,10]
<5> *Bacillus methanolicus* [10]
<6> *Thermococcus sp.* [10]
<7> *Pyrococcus horikoshii* [10]
<8> *uncultured bacterium* [2]
<9> *Thermococcus kodakarensis* [8,10]
<10> *Methanosarcina sp.* [10]
<11> *Methylobacillus flagellatus KT* [10]
<12> *Methylomonas aminofaciens* [10]
<13> no activity in *Hansenula polymorpha* [2]
<14> *Methanocaldococcus jannaschii* (UNIPROT accession number: Q58644) [9]
<15> *Bacillus subtilis* (UNIPROT accession number: P42404) [1]
<16> no activity in *Kloeckera sp.* [2]
<17> *Mycobacterium gastri* (UNIPROT accession number: Q9LBW5) [3]
<18> *Methylomonas aminofaciens* (UNIPROT accession number: Q950X3) [5]
<19> *Pyrococcus horikoshii* (UNIPROT accession number: O59601) [7]

D. Schomburg and I. Schomburg (eds.), *Class 3.4–6 Hydrolases, Lyases, Isomerases, Ligases: EC 3.4–6*, Springer Handbook of Enzymes S10, DOI 10.1007/978-3-642-36260-6_78,

<20> *Mycobacterium gastri* [10]
<21> *Aminomonas aminovorus* [10]

3 Reaction and Specificity

Catalyzed reaction
D-arabino-hex-3-ulose 6-phosphate = D-fructose 6-phosphate

Reaction type
isomerization

Natural substrates and products
S D-arabino-hex-3-ulose 6-phosphate <1,2,3,4,5,6,7,9,10,11,12,20,21> (Reversibility: ?) [10]
P D-fructose 6-phosphate
S Additional information <9> (<9> bifunctional 3-hexulose-6-phosphate synthase/6-phospho-3-hexuloisomerase is essential for the biosynthesis of ribulose 5-phosphate. The ribulose monophosphate pathway substitutes for the classical pentose phosphate pathway in Thermococcus kodakarensis [8]) (Reversibility: ?) [8]
P ?

Substrates and products
S D-arabino-3-hexulose 6-phosphate <4,17> (Reversibility: r) [3,4]
P D-fructose 6-phosphate
S D-arabino-hex-3-ulose 6-phosphate <1,2,3,4,5,6,7,8,9,10,11,12,15,20,21> (Reversibility: ?) [1,2,10]
P D-fructose 6-phosphate
S D-fructose 6-phosphate <8> (Reversibility: r) [2]
P D-arabino-hex-3-ulose 6-phosphate
S D-fructose 6-phosphate <4> (Reversibility: r) [4]
P D-arabino-3-hexulose 6-phosphate
S Additional information <4,9> (<9> bifunctional 3-hexulose-6-phosphate synthase/6-phospho-3-hexuloisomerase is essential for the biosynthesis of ribulose 5-phosphate. The ribulose monophosphate pathway substitutes for the classical pentose phosphate pathway in Thermococcus kodakarensis [8]; <4> enzyme is specific for substrates D-arabino-3-hexulose 6-phosphate and D-fructose 6-phosphate [4]; <4> no substrate: D-ribulose 5-phosphate, D-xylulose 5-phosphate or D-allulose 6-phosphate [4]) (Reversibility: ?) [4,8]
P ?

Inhibitors
Co^{2+} <4> (<4> 1 mM, 35% residual activity [4]) [4]
Cu^{2+} <4> (<4> 1 mM, 8% residual activity [4]) [4]
Mg^{2+} <4> (<4> 5 mM, 30% loss of activity [4]) [4]
Ni^{2+} <4> (<4> 1 mM, 14% residual activity [4]) [4]
Zn^{2+} <4> (<4> 1 mM, 40% residual activity [4]) [4]

Additional information <4> (<4> at 1 mM sugar phosphate concentration, D-allulose 6-phosphate, D-fructose 6-phosphate, 6-phospho-D-gluconate, D-ribulose 5-phosphate, D-xylulose 5-phosphate, D-erythrose 4-phosphate and glyceraldehyde 3-phosphate do not affect the isomerase activity [4]) [4]

Activating compounds

formaldehyde <3> (<3> concomitant induction of 3-hexulose 6-phosphate synthase and 6-phospho-3-hexuloisomerase by formaldehyde [6]) [6]
Additional information <3> (<3> no induction by by methanol, formate, or methylamine [6]) [6]

Metals, ions

Additional information <4> (<4> no requirement for divalent cations [4]) [4]

Specific activity (U/mg)

20 <8> (<8> pH 7.0, 30°C [2]) [2]
154 <17> (<17> 3-hexulose-6-phosphate synthase/6-phospho-3-hexuloisomerasefusion enzyme, 30°C [3]) [3]
563 <17> (<17> 6-phospho-3-hexuloisomerase, 30°C [3]) [3]
1560 <4> (<4> 30°C, pH 7.0 [4]) [4]

K_m-Value (mM)

0.029 <8> (D-arabino-hex-3-ulose 6-phosphate, <8> pH 7.0, 30°C [2]) [2]
0.1 <4> (D-arabino-3-hexulose 6-phosphate, <4> 30°C, pH 7.0 [4]) [4]
0.67 <8> (D-fructose 6-phosphate, <8> pH 7.0, 30°C [2]) [2]
1.1 <4> (D-fructose 6-phosphate, <4> 30°C, pH 7.0 [4]) [4]

pH-Optimum

7.5 <8> [2]
8.3 <4> [4]

Temperature optimum (°C)

30 <8,17> (<17> both recombinant 6-phospho-3-hexuloisomerase and 3-hexulose-6-phosphate synthase /6-phospho-3-hexuloisomerase fusion enzyme [3]) [2,3]
60 <19> (<19> separately expressed 6-phospho-3-hexuloisomerase domain [7]) [7]
80-85 <19> (<19> bifunctional enzyme [7]) [7]

4 Enzyme Structure

Molecular weight

67000 <4> (<4> gel filtration [4]) [4]
75000 <19> (<19> separately expressed 6-phospho-3-hexuloisomerase domain [7]) [7]
94000 <17> (<17> gel filtration, recombinant 6-phospho-3-hexuloisomerase [3]) [3]
162000 <19> (<19> gel filtration, bifunctional enzyme [7]) [7]

Subunits

? <17> (<17> x * 42000, recombinant 3-hexulose-6-phosphate synthase /6-phospho-3-hexuloisomerasefusion enzyme [3]) [3]
tetramer <17,19> (<17> 4 * 21000, SDS-PAGE, recombinant 6-phospho-3-hexuloisomerase [3]; <19> 4 * 47000, SDS-PAGE, bifunctional enzyme, 4 * 21000, SDS-PAGE, and 4 * 21475, calculated, separately expressed 6-phospho-3-hexuloisomerase domain [7]) [3,7]

5 Isolation/Preparation/Mutation/Application

Purification

<4> [4]

Crystallization

<14> (diffraction to 2.0 A resolution. MJ1247 is an α/β structure consisting of a five-stranded parallel β-sheet flanked on both sides by α-helices, forming a three-layered α-β-α sandwich. The fold represents the nucleotide binding motif of a flavodoxin type. Protein forms a tetramer in the crystal an in solution and each monomer has a folding similar to the isomerase domain of glucosamine 6-phosphate synthase) [9]
<15> (diffraction to 1.7 A, space group P6522 or P6122) [1]

Cloning

<9> [8]
<14> (expression in Escherichia coli) [9]
<15> (expression in Escherichia coli) [1]
<19> (expression in Escherichia coli) [7]

Engineering

Additional information <3,9,17,19> (<9> deletion of bifunctional 3-hexulose-6-phosphate synthase /6-phospho-3-hexuloisomerase results in loss of growth in minimal medium, which can be recovered by addition of nucleosides to the medium [8]; <19> expression of the full-length gene encoding the hybrid enzyme 3-hexulose 6-phosphate synthase/6-phospho-3-hexuloisomerase, the sequence corresponding to the 3-hexulose 6-phosphate synthase region, and the sequence corresponding to the 6-phospho-3-hexuloisomerase region produces active enzymes in Escherichia coli. The bifunctional enzyme catalyzes the sequential reaction much more efficiently than a mixture of the isolated domains [7]; <17> fusion gene construct of 3-hexulose-6-phosphate synthase and 6-phospho-3-hexuloisomerase. The gene product of 3-hexulose-6-phosphate synthase /6-phospho-3-hexuloisomerase exhibits both activities at room temperature and catalyzes the sequential reactions more efficiently than a simple mixture of the individual enzymes. The gene product of 6-phospho-3-hexuloisomerase /3-hexulose-6-phosphate synthase fails to display any enzyme activity. Escherichia coli strains harboring the 3-hexulose-6-phosphate synthase /6-phospho-3-hexuloisomerase gene consume formaldehyde more efficiently and exhibited better growth in

a formaldehyde containing medium than the host strain [3]; <3> gene disruption causes moderate sensitivity to formaldehyde [6]) [3,6,7,8]

Application

synthesis <18> (<18> production of D-[1-^{13}C]fructose 6-phosphate from ^{13}C-enriched formaldehyde and D-ribose 5-phosphate using 3-hexulose 6-phosphate synthase and 6-phospho-3-hexuloisomerase from Methylomonas aminofaciens and spinach ribose 5-phosphate isomerase [5]) [5]

6 Stability

Temperature stability

60 <4> (<4> 10 min, complete loss of activity [4]) [4]

90 <19> (<19> half-life above 90 min, bifunctional enzyme. Half-life below 5 min, separately expressed 6-phospho-3-hexuloisomerase domain [7]) [7]

Storage stability

<4>, -15°C, l0 mM-Tris-HCI, 1 mM-EDTA buffer, pH 7.5, stable for 4 months [4]

<4>, 0-4°C, l0 mM-Tris-HCI, 1 mM-EDTA buffer, pH 7.5, stable for 4 months [4]

References

[1] Taylor, E.J.; Charnock, S.J.; Colby, J.; Davies, G.J.; Black, G.W.: Cloning, purification and characterization of the 6-phospho-3-hexulose isomerase YckF from Bacillus subtilis. Acta Crystallogr. Sect. D, **D57**, 1138-1140 (2001)

[2] Kato, N.; Ohashi, H.; Hori, T.; Tani, Y.; Ogata, K.: Properties of 3-hexulose phosphate synthase and phospho-3-hexuloisomerase of a methanol-utilizing bacterium, 77a. Agric. Biol. Chem., **41**, 1133-1140 (1977)

[3] Orita, I.; Sakamoto, N.; Kato, N.; Yurimoto, H.; Sakai, Y.: Bifunctional enzyme fusion of 3-hexulose-6-phosphate synthase and 6-phospho-3-hexuloisomerase. Appl. Microbiol. Biotechnol., **76**, 439-445 (2007)

[4] Ferenci, T.; Stroem, T.; Quayle, J.R.: Purification and properties of 3-hexulose phosphate synthase and phospho-3-hexuloisomerase from Methylococcus capsulatus. Biochem. J., **144**, 477-486 (1974)

[5] Yanase, H.; Koike, Y.; Matsuzaki, K.; Kita, K.; Sato, Y.; Kato, N.: Production of D-[1-^{13}C]fructose 6-phosphate by a formaldehyde-fixing system in Methylomonas aminofaciens 77a. Biosci. Biotechnol. Biochem., **56**, 541-542 (1992)

[6] Yasueda, H.; Kawahara, Y.; Sugimoto, S.: Bacillus subtilis yckG and yckF encode two key enzymes of the ribulose monophosphate pathway used by methylotrophs, and yckH is required for their expression. J. Bacteriol., **181**, 7154-7160 (1999)

[7] Orita, I.; Yurimoto, H.; Hirai, R.; Kawarabayasi, Y.; Sakai, Y.; Kato, N.: The archaeon Pyrococcus horikoshii possesses a bifunctional enzyme for for-

maldehyde fixation via the ribulose monophosphate pathway. J. Bacteriol., **187**, 3636-3642 (2005)
[8] Orita, I.; Sato, T.; Yurimoto, H.; Kato, N.; Atomi, H.; Imanaka, T.; Sakai, Y.: The ribulose monophosphate pathway substitutes for the missing pentose phosphate pathway in the archaeon Thermococcus kodakaraensis. J. Bacteriol., **188**, 4698-4704 (2006)
[9] Martinez-Cruz, L.A.; Dreyer, M.K.; Boisvert, D.C.; Yokota, H.; Martinez-Chantar, M.L.; Kim, R.; Kim, S.: Crystal structure of MJ1247 protein from M. jannaschii at 2.0 A resolution infers a molecular function of 3-hexulose-6-phosphate isomerase. Structure, **10**, 195-204 (2002)
[10] Yurimoto, H.; Kato, N.; Sakai, Y.: Genomic organization and biochemistry of the ribulose monophosphate pathway and its application in biotechnology. Appl. Microbiol. Biotechnol., **84**, 407-416 (2009)

D-sedoheptulose 7-phosphate isomerase 5.3.1.28

1 Nomenclature

EC number
5.3.1.28

Systematic name
D-glycero-D-manno-heptose 7-phosphate aldose-ketose-isomerase

Recommended name
D-sedoheptulose 7-phosphate isomerase

Synonyms
phosphoheptose isomerase <5,6,7,8,9,10,11,12,13,14,15,17,18,19,20,21> [4,6,9]
sedoheptulose 7-phosphate isomerase <17> [5,7]
sedoheptulose-7-phosphate isomerase <1,2,4> [1,8]

2 Source Organism

<1> *Escherichia coli* [8]
<2> *Pseudomonas aeruginosa* [8]
<3> *Yersinia pestis* [3]
<4> *Burkholderia pseudomallei* [1]
<5> *Clostridium acetobutylicum* (UNIPROT accession number: Q97EQ4) [9]
<6> *Haemophilus influenzae* (UNIPROT accession number: P45093) [4,9]
<7> *Helicobacter pylori* J99 (UNIPROT accession number: Q9ZKZ1) [9]
<8> *Mycobacterium tuberculosis* (UNIPROT accession number: P0A604) [9]
<9> *Neisseria meningitidis* (UNIPROT accession number: P0A0Y5) [9]
<10> *Neisseria meningitidis* (UNIPROT accession number: P0A0Y6) [9]
<11> *Pseudomonas aeruginosa* (UNIPROT accession number: Q9HVZ0) [9]
<12> *Salmonella enterica subsp. enterica serovar Typhimurium* (UNIPROT accession number: P63223) [9]
<13> *Vibrio cholerae* (UNIPROT accession number: Q9KPY2) [9]
<14> *Yersinia pestis* (UNIPROT accession number: Q8ZBY7) [9]
<15> *Escherichia coli* (UNIPROT accession number: P63224) (α-subunit of Fdh3 [6]) [5,6,9]
<16> *Haemophilus ducreyi* (UNIPROT accession number: O87340) [2]
<17> *Aneurinibacillus thermoaerophilus* (UNIPROT accession number: Q9AGY7) [5,7,9]
<18> *Campylobacter jejuni* (UNIPROT accession number: Q9PNE6) [9]
<19> *Campylobacter jejuni* (UNIPROT accession number: Q9PMN3) [9]
<20> *Burkholderia mallei* (UNIPROT accession number: Q9AI36) [9]

D. Schomburg and I. Schomburg (eds.), *Class 3.4–6 Hydrolases, Lyases, Isomerases, Ligases: EC 3.4–6*, Springer Handbook of Enzymes S10, DOI 10.1007/978-3-642-36260-6_79,

<21> *Burkholderia pseudomallei* (UNIPROT accession number: Q93UJ2) [9]

3 Reaction and Specificity

Catalyzed reaction

D-sedoheptulose 7-phosphate = D-glycero-D-manno-heptose 7-phosphate

Natural substrates and products

- **S** D-sedoheptulose 7-phosphate <1,2,5,6,7,8,9,10,11,12,13,14,15,17,18,19,20,21> (<1,2> first committed step in the formation of ADP-heptose [8]; <17> the enzyme is involved in the biosynthesis of nucleotide-activated heptose [7]) (Reversibility: ?) [5,7,8,9]
- **P** D-glycero-D-manno-heptose 7-phosphate
- **S** D-sedoheptulose 7-phosphate <15> (<15> first step of the biosynthesis of the inner core lipopolysaccharide precursor, ADP-L-glycero-D-manno-heptose [6]; <15> synthesis of ADP-D-β-D-heptose in Escherichia coli requires three proteins, GmhA (sedoheptulose 7-phosphate isomerase), HldE (bifunctional D-β-D-heptose 7-phosphate kinase/D-β-D-heptose 1-phosphate adenylyltransferase), and GmhB (DD-heptose 1,7-bisphosphate phosphatase) [5]) (Reversibility: ?) [5,6]
- **P** D-glycero-α,β-D-manno-heptose 7-phosphate
- **S** Additional information <16> (<16> the gmhA gene product is essential for the expression of wild-type lipooligosaccharide by this pathogen [2]) [2]
- **P** ?

Substrates and products

- **S** D-sedoheptulose 7-phosphate <1,2,5,6,7,8,9,10,11,12,13,14,15,17,18,19,20,21> (<1,2> first committed step in the formation of ADP-heptose [8]; <17> the enzyme is involved in the biosynthesis of nucleotide-activated heptose [7]; <1,2> it is postulated that GmhA acts through an enediol-intermediate isomerase mechanism [8]) (Reversibility: ?) [5,7,8,9]
- **P** D-glycero-D-manno-heptose 7-phosphate
- **S** D-sedoheptulose 7-phosphate <15> (<15> first step of the biosynthesis of the inner core lipopolysaccharide precursor, ADP-L-glycero-D-manno-heptose [6]; <15> synthesis of ADP-D-β-D-heptose in Escherichia coli requires three proteins, GmhA (sedoheptulose 7-phosphate isomerase), HldE (bifunctional D-β-D-heptose 7-phosphate kinase/D-β-D-heptose 1-phosphate adenylyltransferase), and GmhB (DD-heptose 1,7-bisphosphate phosphatase) [5]) (Reversibility: ?) [5,6]
- **P** D-glycero-α,β-D-manno-heptose 7-phosphate
- **S** Additional information <16> (<16> the gmhA gene product is essential for the expression of wild-type lipooligosaccharide by this pathogen [2]) [2]
- **P** ?

Turnover number (s^{-1})
0.23 <1> (D-sedoheptulose 7-phosphate, <1> pH 8.0, mutant enzyme H61Q [8]) [8]
0.44 <1> (D-sedoheptulose 7-phosphate, <1> pH 8.0, wild-type enzyme [8]) [8]
0.45 <1> (D-sedoheptulose 7-phosphate, <1> pH 8.0, mutant enzyme R69Q [8]) [8]

K_m-Value (mM)
0.5 <1> (D-sedoheptulose 7-phosphate, <1> pH 8.0, mutant enzyme R69Q [8]) [8]
0.9 <1> (D-sedoheptulose 7-phosphate, <1> pH 8.0, wild-type enzyme [8]) [8]
1.2 <1> (D-sedoheptulose 7-phosphate, <1> pH 8.0, mutant enzyme H61Q [8]) [8]

pH-Optimum
8 <1> (<1> assay at [8]) [8]

4 Enzyme Structure

Molecular weight
60000-80000 <15> (<15> gel filtration [9]) [9]

Subunits
? <4,15,17> (<17> x * 25000, SDS-PAGE [7]; <4> x * 22000, SDS-PAGE [1]; <15> x * 20600, calculated from sequence [6]; <17> x * 21495, calculated from sequence [7]) [1,6,7]
dimer <15> (<15> 2 * 29000, SDS-PAGE [9]) [9]

5 Isolation/Preparation/Mutation/Application

Localization
cytosol <15> [6]

Purification
<1> [8]
<2> [8]
<4> [1]
<17> [7]

Crystallization
<1> (hanging drop vapor diffusion method, crystal structures of GmhA in apo, substrate, and product-bound forms) [8]
<2> (hanging drop vapor diffusion method, crystal structures of GmhA in apo, substrate, and product-bound forms) [8]

<4> (sitting-drop vapour-diffusion method at room temperature, the crystal belong to the primitive orthorhombic space group $P2_12_12_1$, with unit-cell parameters a = 61.3, b = 84.2, c = 142.3 A) [1]

Cloning

<2> (expression in Escherichia coli) [8]
<3> [3]
<4> (expression in Escherichia coli) [1]
<6> [4]
<16> (cloned into the pLS88 vector) [2]
<17> (overexpressed in Escherichia coli) [7]

Engineering

D169N <1> (<1> inactive [8]) [8]
D94N <1> (<1> k_{cat}/K_m for D-sedoheptulose 7-phosphate is 1.8fold higher than wild-type value [8]) [8]
E65N <1> (<1> inactive [8]) [8]
H180Q <1> (<1> inactive [8]) [8]
H61Q <1> (<1> k_{cat}/K_m for D-sedoheptulose 7-phosphate is 2.5fold lower than wild-type value [8]) [8]
Q172E <1> (<1> inactive [8]) [8]
R69Q <1> (<1> inactive [8]) [8]
T120A <1> (<1> inactive [8]) [8]

Application

medicine <4> (<4> determination of the three-dimensional structure of GmhA from Burkholderia pseudomallei to provide a structural template for the development of antibiotic adjuvants as antimelioidosis agents [1]) [1]

References

[1] Kim, M.S.; Shin, D.H.: A preliminary X-ray study of sedoheptulose-7-phosphate isomerase from Burkholderia pseudomallei. Acta Crystallogr. Sect. F, **65**, 1110-1112 (2009)
[2] Bauer, B.A.; Stevens, M.K.; Hansen, E.J.: Involvement of the Haemophilus ducreyi gmhA gene product in lipooligosaccharide expression and virulence. Infect. Immun., **66**, 4290-4298 (1998)
[3] Darby, C.; Ananth, S.L.; Tan, L.; Hinnebusch, B.J.: Identification of gmhA, a Yersinia pestis gene required for flea blockage, by using a Caenorhabditis elegans biofilm system. Infect. Immun., **73**, 7236-7242 (2005)
[4] Brooke, J.S.; Valvano, M.A.: Molecular cloning of the Haemophilus influenzae gmhA (lpcA) gene encoding a phosphoheptose isomerase required for lipooligosaccharide biosynthesis. J. Bacteriol., **178**, 3339-3341 (1996)
[5] Kneidinger, B.; Marolda, C.; Graninger, M.; Zamyatina, A.; McArthur, F.; Kosma, P.; Valvano, M.A.; Messner, P.: Biosynthesis pathway of ADP-L-glycero-β-D-manno-heptose in Escherichia coli. J. Bacteriol., **184**, 363-369 (2002)

[6] Brooke, J.S.; Valvano, M.A.: Biosynthesis of inner core lipopolysaccharide in enteric bacteria identification and characterization of a conserved phosphoheptose isomerase. J. Biol. Chem., **271**, 3608-3614 (1996)
[7] Kneidinger, B.; Graninger, M.; Puchberger, M.; Kosma, P.; Messner, P.: Biosynthesis of nucleotide-activated D-glycero-D-manno-heptose. J. Biol. Chem., **276**, 20935-20944 (2001)
[8] Taylor, P.L.; Blakely, K.M.; de Leon, G.P.; Walker, J.R.; McArthur, F.; Evdokimova, E.; Zhang, K.; Valvano, M.A.; Wright, G.D.; Junop, M.S.: Structure and function of sedoheptulose-7-phosphate isomerase, a critical enzyme for lipopolysaccharide biosynthesis and a target for antibiotic adjuvants. J. Biol. Chem., **283**, 2835-2845 (2008)
[9] Valvano, M.A.; Messner, P.; Kosma, P.: Novel pathways for biosynthesis of nucleotide-activated glycero-manno-heptose precursors of bacterial glycoproteins and cell surface polysaccharides. Microbiology, **148**, 1979-1989 (2002)

syn-copalyl-diphosphate synthase 5.5.1.14

1 Nomenclature

EC number
5.5.1.14

Systematic name
9α-copalyl-diphosphate lyase (decyclizing)

Recommended name
syn-copalyl-diphosphate synthase

Synonyms
OsCPSsyn <1> [2]
OsCyc1 <2> [1]
syn-CDP synthase <2> [1]
syn-copalyl diphosphate lyase (decyclizing)
syn-copalyl diphosphate synthase <1,2> [1,2]

CAS registry number
173585-12-1

2 Source Organism

<1> *Oryza sativa* (UNIPROT accession number: Q6E7D7) [2]
<2> *Oryza sativa* (UNIPROT accession number: Q0JF02) [1]

3 Reaction and Specificity

Catalyzed reaction
geranylgeranyl diphosphate = 9α-copalyl diphosphate (<1,2> in contrast to EC 5.5.1.12 and EC 5.5.1.13, this enzyme produces copalyl diphosphate having the syn conformation [1,2])

Reaction type
intramolecular lyase

Natural substrates and products
S geranylgeranyl diphosphate <1,2> (Reversibility: ?) [1,2]
P syn-copalyl diphosphate (<1> precursor of the phytoalexins oryzalexin S, momilactone A, and momilactone B [2])

D. Schomburg and I. Schomburg (eds.), *Class 3.4–6 Hydrolases, Lyases, Isomerases, Ligases: EC 3.4–6*, Springer Handbook of Enzymes S10, DOI 10.1007/978-3-642-36260-6_80,

Substrates and products

S geranylgeranyl diphosphate <1,2> (Reversibility: ?) [1,2]
P syn-copalyl diphosphate (<1> precursor of the phytoalexins oryzalexin S, momilactone A, and momilactone B [2])

5 Isolation/Preparation/Mutation/Application

Source/tissue

leaf <1,2> [1,2]

Localization

plastid <1,2> (<1,2> deduced from the existence of a transit peptide sequence [1,2]) [1,2]

Purification

<1> (hydroxyapatite chromatography, partially purified) [2]
<2> (affinity chromatography using Glutathione Sepharose B) [1]

Cloning

<1> (expression of the full-length preprotein including the transit peptid in Escherichia coli, protein alone and as a C-terminal fusion to glutathione-S-transferase. Additionally, a partial cDNA sequence resembling the mature native protein was expressed alone as a potential pseudomature protein) [2]
<2> (expression of the full-length protein as a fusion protein with glutathione-S-transferase at the N-terminus in Escherichia coli XL1-Blue) [1]

References

[1] Otomo, K.; Kenmoku, H.; Oikawa, H.; Konig, W.A.; Toshima, H.; Mitsuhashi, W.; Yamane, H.; Sassa, T.; Toyomasu, T.: Biological functions of ent- and syn-copalyl diphosphate synthases in rice: key enzymes for the branch point of gibberellin and phytoalexin biosynthesis. Plant J., **39**, 886-893 (2004)
[2] Xu, M.; Hillwig, M.L.; Prisic, S.; Coates, R.M.; Peters, R.J.: Functional identification of rice syn-copalyl diphosphate synthase and its role in initiating biosynthesis of diterpenoid phytoalexin/allelopathic natural products. Plant J., **39**, 309-318 (2004)

terpentedienyl-diphosphate synthase 5.5.1.15

1 Nomenclature

EC number
5.5.1.15

Systematic name
terpentedienyl-diphosphate lyase (decyclizing)

Recommended name
terpentedienyl-diphosphate synthase

Synonyms
Cyc1 <2> [2]

CAS registry number
429681-55-0

2 Source Organism

<1> *Streptomyces lividans* [3]
<2> *Kitasatospora griseola* [1,2]

3 Reaction and Specificity

Catalyzed reaction
geranylgeranyl diphosphate = terpentedienyl diphosphate

Substrates and products
S geranylgeranyl diphosphate <1,2> (<1> the triggering proton is lost at the end of the cyclization reaction [3]) (Reversibility: ?) [1,2,3]
P terpentedienyl diphosphate

Inhibitors
EDTA <2> [2]
geranylgeranyl diphosphate <2> (<2> above 0.05 mM [2]) [2]

Activating compounds
Additional information <2> (<2> 20% glycerol, 5 mM 2-mercaptoethanol, and 0.1% Tween 80 are required for the full activity of the Cyc1 [2]) [2]

D. Schomburg and I. Schomburg (eds.), *Class 3.4–6 Hydrolases, Lyases, Isomerases, Ligases: EC 3.4–6*, Springer Handbook of Enzymes S10, DOI 10.1007/978-3-642-36260-6_81,

Metals, ions
Mg^{2+} <2> (<2> the enzyme activity of the Cyc1 is highest at a concentration of 1 mM but slightly inhibited at a concentration of 10 mM (decreased 40%) [2]) [2]
Additional information <2> (<2> no activity is detected with other divalent metal ions such as Ca^{2+}, Co^{2+}, Cu^{2+}, Fe^{2+}, Mn^{2+}, and Zn^{2+} at both 1 and 10 mM [2]) [2]

K_m-Value (mM)
0.0642 <2> (geranylgeranyl diphosphate) [2]

pH-Optimum
6.8 <2> (<2> Tris-HCl buffer [2]) [2]

Temperature optimum (°C)
25-30 <2> [2]

Temperature range (°C)
25-50 <2> (<2> 25-30: optimum, 50°C, no activity detected above [2]) [2]

4 Enzyme Structure

Molecular weight
50000 <2> (<2> gel filtration [2]) [2]

5 Isolation/Preparation/Mutation/Application

Purification
<2> [1]

Cloning
<2> [2]
<2> (heterologous expression of the cyclase genes in Streptomyces lividans and Escherichia coli) [1]

6 Stability

Temperature stability
30 <2> (<2> full activity after incubation at 30°C in 0.05 M Tris-HCl buffer for 1 h [2]) [2]

References

[1] Dairi, T.; Hamano, Y.; Kuzuyama, T.; Itoh, N.; Furihata, K.; Seto, H.: Eubacterial diterpene cyclase genes essential for production of the isoprenoid antibiotic terpentecin. J. Bacteriol., **183**, 6085-6094 (2001)
[2] Hamano, Y.; Kuzuyama, T.; Itoh, N.; Furihata, K.; Seto, H.; Dairi, T.: Functional analysis of eubacterial diterpene cyclases responsible for biosynthesis of a diterpene antibiotic, terpentecin. J. Biol. Chem., **277**, 37098-37104 (2002)
[3] Eguchi, T.; Dekishima, Y.; Hamano, Y.; Dairi, T.; Seto, H.; Kakinuma, K.: A new approach for the investigation of isoprenoid biosynthesis featuring pathway switching, deuterium hyperlabeling, and 1H NMR spectroscopy. The reaction mechanism of a novel streptomyces diterpene cyclase. J. Org. Chem., **68**, 5433-5438 (2003)

halimadienyl-diphosphate synthase 5.5.1.16

1 Nomenclature

EC number
5.5.1.16

Systematic name
halima-5,13-dien-15-yl-diphosphate lyase (decyclizing)

Recommended name
halimadienyl-diphosphate synthase

Synonyms
HPS <1> [2]

2 Source Organism

<1> *Mycobacterium tuberculosis* [1,2]

3 Reaction and Specificity

Catalyzed reaction
geranylgeranyl diphosphate = tuberculosinyl diphosphate

Substrates and products
S geranylgeranyl diphosphate <1> (Reversibility: ?) [2]
P halimadienyl diphosphate
S geranylgeranyl diphosphate <1> (Reversibility: ?) [1]
P halima-5,13-dien-15-yl diphosphate

Inhibitors
(E,E,E)-geranylgeranyl diphosphate <1> (<1> substrate inhibition [2]) [2]
15-aza-14,15-dihydrogeranylgeranyl diphosphate <1> [2]
15-aza-14,15-dihydrogeranylgeranyl thiolodiphosphate <1> [2]
Mg^{2+} <1> (<1> the enzyme displays a rapid loss of activity as the Mg^{2+} concentration is raised above 0.1 mM [2]) [2]

Metals, ions
Mg^{2+} <1> (<1> Mg^{2+} is essential to the cyclization reaction [1]; <1> the enzyme requires Mg^{2+} and reacts most efficiently in the presence of low levels (0.1 mM) of Mg^{2+} [2]) [1,2]

D. Schomburg and I. Schomburg (eds.), *Class 3.4–6 Hydrolases, Lyases, Isomerases, Ligases: EC 3.4–6*, Springer Handbook of Enzymes S10, DOI 10.1007/978-3-642-36260-6_82,

Turnover number (s^{-1})
0.12 <1> (geranylgeranyl diphosphate) [2]

K_m-Value (mM)
0.0016 <1> (geranylgeranyl diphosphate) [2]

K_i-Value (mM)
0.018 <1> (geranylgeranyl diphosphate) [2]

5 Isolation/Preparation/Mutation/Application

Purification
<1> (amylose resin column chromatography) [2]

Cloning
<1> (expressed in Escherichia coli strain C41) [2]
<1> (expression in Escherichia coli) [1]

6 Stability

Temperature stability
-4 <1> (<1> freezing leads to loss of about 10% activity over the course of 1 week [2]) [2]

Storage stability
<1>, 4°C, less than 24 h, the enzyme retains essentially full activity [2]

References

[1] Nakano, C.; Okamura, T.; Sato, T.; Dairi, T.; Hoshino, T.: Mycobacterium tuberculosis H37Rv3377c encodes the diterpene cyclase for producing the halimane skeleton. Chem. Commun. (Camb.), **28**, 1016-1018 (2005)
[2] Mann, F.M.; Prisic, S.; Hu, H.; Xu, M.; Coates, R.M.; Peters, R.J.: Characterization and inhibition of a class II diterpene cyclase from Mycobacterium tuberculosis: Implications for tuberculosis. J. Biol. Chem., **284**, 23574-23579 (2009)

2-hydroxychromene-2-carboxylate isomerase 5.99.1.4

1 Nomenclature

EC number
5.99.1.4

Systematic name
2-hydroxy-2H-chromene-2-carboxylate-(3E)-4-(2-hydroxyphenyl)-2-oxobut-3-enoate isomerase

Recommended name
2-hydroxychromene-2-carboxylate isomerase

Synonyms
2-hydroxychromene-2-carboxylate isomerase <2,3,5> [1,3,6]
2-hydroxychromene-2-carboxylic acid isomerase <5> [2]
2HC2CA isomerase <1> [4]
2HCCAI <2,3> [6]
HCCA isomerase <5> [1,2]
nsaD <4> [5]

2 Source Organism

<1> *Pseudomonas sp.* [4]
<2> *Comamonas testosteroni* [6]
<3> *Brevundimonas vesicularis* [6]
<4> *Sphingobium xenophagum* (UNIPROT accession number: Q9X9Q7) [5]
<5> *Pseudomonas putida* (UNIPROT accession number: Q51948) [1,2,3]

3 Reaction and Specificity

Catalyzed reaction
2-hydroxy-2H-chromene-2-carboxylate = (3E)-4-(2-hydroxyphenyl)-2-oxobut-3-enoate

Natural substrates and products
S Additional information <2,3> (<2,3> enzyme degrades naphthalenesulfonates [6]) (Reversibility: ?) [6]
P ?

Substrates and products
S 2-hydroxy-2H-chromene-2-carboxylate <2,3> (Reversibility: ?) [6]

D. Schomburg and I. Schomburg (eds.), *Class 3.4–6 Hydrolases, Lyases, Isomerases, Ligases: EC 3.4–6*, Springer Handbook of Enzymes S10, DOI 10.1007/978-3-642-36260-6_83,

P (3E)-4-(2-hydroxyphenyl)-2-oxobut-3-enoate
S 2-hydroxy-2H-chromene-2-carboxylate <1,5> (<5> extracts of Escherichia coli JM109 carrying pRE718 catalyze the conversion of trans-*o*-hydroxybenzylidenepyruvate or 2-hydroxychromene-2-carboxylate to an equilibrium mixture that contained 55% 2-hydroxychromene-2-carboxylate and 45% trans-*o*-hydroxybenzylidenepyruvate at pH 7. At pH 10 the reaction occus entirely in on direction, the conversion of 2-hydroxychromene-2-carboxylate to trans-*o*-hydroxybenzylidenepyruvate. The product is identified by nuclear magnetic resonance spectroscopy. This isomerization occurs spontaneously, although at a slower rate than the enzyme-catalyzed reaction [1]; <5> glutathione (GSH)-dependent interconversion. The isomerization reaction involves a short-lived covalent adduct between the sulfur of GSH and C_7 of the substrate [2]; <1> the product trans-*o*-hydroxybenzylidenepyruvate is analyzed by 1H NMR spectrum [4]) (Reversibility: r) [1,2,4]
P (3E)-4-(2-hydroxyphenyl)-2-oxobut-3-enoate (<1,5> i.e. (E)-2-hydroxybenzylidenepyruvate, i.e. trans-*o*-hydroxybenzylidenepyruvate [1,2,4])
S 2-hydroxybenzo[g]chromene-2-carboxylate <2,3> (<2,3> more unstable than 2-hydroxychromene-2-carboxylate [6]) (Reversibility: ?) [6]
P ?
S Additional information <2,3> (<2,3> enzyme degrades naphthalenesulfonates [6]; <2,3> 2,5-dihydroxychromene-2-carboxylate is no substrate [6]) (Reversibility: ?) [6]
P ?

Inhibitors

(3E)-4-(2-hydroxyphenyl)-2-oxobut-3-enoate <5> (<5> i.e. (E)-2-hydroxybenzylidenepyruvate [2]) [2]
Cu^{2+} <1> [4]
Hg^{2+} <1> [4]
iodoacetic acid <1> [4]
monoiodoacetate <1> [4]
Additional information <2,3> (<2,3> no significant inhibition is observed after one day incubation with 50 mM EDTA [6]) [6]

Cofactors/prosthetic groups

glutathione <5> (<5> the dimeric protein binds one molecule of GSH very tightly and a second molecule of GSH with much lower affinity. The enzyme is unstable in the absence of GSH. The turnover number in the forward direction greatly exceeds off rates for GSH, suggesting that GSH acts as a tightly bound cofactor in the reaction. K_m: 0.017 mM [2]) [2]

Activating compounds

2-mercaptoethanol <2> [6]
dithiothreitol <2> [6]
glutathione <1,2,3> (<1> activates above 0.15 mM [4]; <2> highest enzyme activity is found after preincubation of the enzyme with glutathione at alkaline pH-values. To determine enzyme activities during the purification pro-

cedure, it is necessary to reactivate the enzyme with glutathione [6]; <3> no enzyme activity is found when the enzyme preparations have been preincubated without or with only 10 mM glutathione [6]) [4,6]

Metals, ions

Additional information <2,3> (<2,3> no increase of enzyme activity is found after (pre)incubation of the enzyme with $ZnSO_4$, $COCl_2$, $FeCl_2$ or $MnCl_2$ (each 2 mM) [6]) [6]

Turnover number (s^{-1})

19 <5> ((3E)-4-(2-hydroxyphenyl)-2-oxobut-3-enoate, <5> pH 7.0, 25°C [2]) [2]
47 <5> (2-hydroxy-2H-chromene-2-carboxylate, <5> pH 7.0, 25°C [2]) [2]

Specific activity (U/mg)

0.005 <2,3> (<2,3> spectrophotometrically [6]) [6]
0.14 <3> (<3> for 2-hydroxychromene-2-carboxylate as substrate [6]) [6]
0.2 <2,3> (<2,3> enzyme activity increases when the cell extract is incubated for 15 min with glutathione (5 mM) prior to the assay. The addition of glutathione (0.2 mM) directly to the assay does not increase enzyme activity [6]) [6]
0.27 <2> (<2> for 2-hydroxychromene-2-carboxylate as substrate [6]) [6]
55.4 <2> (<2> last purification step [6]) [6]
62 <1> [4]

K_m-Value (mM)

0.053 <1> (2-hydroxy-2H-chromene-2-carboxylate, <1> pH 7.4, 30°C [4]) [4]
0.084 <5> (2-hydroxychromene-2-carboxylate, <5> pH 7.0, 25°C [2]) [2]
0.138 <5> ((E)-2'-hydroxybenzylidenepyruvate, <5> pH 7.0, 25°C [2]) [2]
0.23 <2> (2-hydroxychromene-2-carboxylate) [6]
0.27 <3> (2-hydroxy-2H-chromene-2-carboxylate) [6]

K_i-Value (mM)

0.136 <5> ((3E)-4-(2-hydroxyphenyl)-2-oxobut-3-enoate, <5> pH 7.0, 25°C [2]) [2]

pH-Optimum

9 <2> (<2> in glycine-$NaOH^-$buffer, highest enzyme activity is found after preincubation of the enzyme with glutathione at alkaline pH-values [6]) [6]
9.5 <3> (<3> in glycine-$NaOH^-$buffer [6]) [6]
10 <2> (<2> assay at [6]) [6]

pH-Range

8-9.3 <2> (<2> effect of glutathione is optimal between pH 8 and pH 9.3. In contrast, no activation is observed when the enzyme is incubated with glutathione at pH 5.0. Activities higher than 70% of this optimal activity are found at pH-values in the range 8.0-9.5 in glycine-$NaOH^-$ or Tris/HC1-buffer. At pH 7 about 50% and at pH 5.5 10% of the optimal activity is observed [6]) [6]

8-9.5 <3> (<3> at pH 9.0 50% and at pH 8.0 only 5% of the maximal activity is found, respectively [6]) [6]

pi-Value

5 <1> (<1> isoelectric focusing [4]) [4]
5.4 <5> (<5> calculated from sequence [3]) [3]

Temperature optimum (°C)

8 <1> [4]

Temperature range (°C)

6.8-9.5 <1> (<1> pH 6.8: about 35% of maximal activity, pH 9.5: about 40% of maximal activity [4]) [4]

4 Enzyme Structure

Molecular weight

24700 <2,3> (<2,3> SDS-PAGE [6]) [6]
27000 <1> (<1> gel filtration [4]) [4]

Subunits

? <5> (<5> x * 23031, calculated from sequence [3]) [3]
dimer <5> [2]
monomer <1,2,3> (<1> 1 * 25000, SDS-PAGE [4]; <2,3> 1 * 24700, SDS-PAGE [6]) [4,6]

5 Isolation/Preparation/Mutation/Application

Purification

<1> [4]
<2> (at room temperature by use of a fast-protein liquid chromatography system) [6]
<3> (partially purified by anion-exchange chromatography) [6]

Crystallization

<5> (crystal structure of the enzyme at 1.7 A resolution) [2]

Cloning

<4> (a gene cluster is identified on the plasmid pBN6 which codes for several enzymes participating in the degradative pathway for naphthalenesulfonates. A DNA fragment of 16915 bp is sequenced which contains 17 ORFs. The genes encoding the 1,2-dihydroxynaphthalene dioxygenase, 2-hydroxychromene-2-carboxylate isomerase, and 29-hydroxybenzalpyruvate aldolase of the naphthalenesulfonate pathway are identified on the DNA fragment and the encoded proteins are heterologously expressed in Escherichia coli) [5]
<5> (expression in Escherichia coli) [1]

6 Stability

pH-Stability

1.5-10 <1> (<1> 4°C, 40 h, stable in the range of pH 1.5 to 10.0 [4]) [4]

Temperature stability

45 <1> (<1> 10 min, stable at temperature up to [4]) [4]

50 <1> (<1> 10 min, in presence of glutathione at 2.5 mM, the enzyme is stable up to [4]) [4]

55 <1> (<1> 10 min, 13% of the original activity remains. In presence of glutathione at 2.5 mM, 68% of the original activity remains after 10 min [4]) [4]

General stability information

<5>, unstable in absence of GSH [2]

Storage stability

<2,3>, 4°C, purifed enzyme, Tris HCl, pH 7.5, 100 mM NaCl, 1 month 52% loss of activity [6]

References

[1] Eaton, R.W.; Chapman, P.J.: Bacterial metabolism of naphthalene: Construction and use of recombinant bacteria to study ring cleavage of 1,2-dihydroxynaphthalene and subsequent reactions. J. Bacteriol., **174**, 7542-7554 (1992)

[2] Thompson, L.C.; Ladner, J.E.; Codreanu, S.G.; Harp, J.; Gilliland, G.L.; Armstrong, R.N.: 2-Hydroxychromene-2-carboxylic acid isomerase: a kappa class glutathione transferase from Pseudomonas putida. Biochemistry, **46**, 6710-6722 (2007)

[3] R. W., Eaton: Organization and evolution of naphthalene catabolic pathways: sequence of the DNA encoding 2-hydroxychromene-2-carboxylate isomerase and trans-*o*-hydroxybenzylidenepyruvate hydratase-aldolase from the NAH7 plasmid. J. Bacteriol., **176**, 7757-7762 (1994)

[4] Ohmoto, T.; Kinoshita, T.; Moriyoshi, K.; Sakai, K.; Hamada, N.; Ohe, T.: Purification and some properties of 2-hydroxychromene-2-carboxylate isomerase from naphthalenesulfonate-assimilating Pseudomonas sp. TA-2. J. Biochem., **124**, 591-597 (1998)

[5] Keck, A.; Conradt, D.; Mahler, A.; Stolz, A.; Mattes, R.; Klein, J.: Identification and functional analysis of the genes for naphthalenesulfonate catabolism by Sphingomonas xenophaga BN6. Microbiology, **152**, 1929-1940 (2006)

[6] Kuhm, A.E.; Knackmuss, H.-J.; Stolz, A.: 2-Hydroxychromene-2-carboxylate isomerase from bacteria that degrade naphthalenesulfonates. Biodegradation, **4**, 155-162 (1993)

O-phospho-L-serine-tRNA ligase 6.1.1.27

1 Nomenclature

EC number
6.1.1.27

Systematic name
O-phospho-L-serine:tRNA^{Cys} ligase (AMP-forming)

Recommended name
O-phospho-L-serine-tRNA ligase

Synonyms
CysRS <1,7> [1]
SepRS <1,2,3,5> (<1> SepRS-SepCysS binary complex [4]) [2,3,4,5,6,7]
phosphoseryl-tRNA synthetase <2,3,5> [3,5,6,7]
Additional information <5> (<5> the enzyme is a class II tRNA synthetase [6]; <5> the enzyme is a class II tRNA synthetase and belongs to the PLP-dependent superfamily of enzymes [3]) [3,6]

2 Source Organism

<1> *Methanocaldococcus jannaschii* [1,4]
<2> *Archaeoglobus fulgidus* [5]
<3> *Methanococcus maripaludis* [2,7]
<4> no activity in *Methanobrevibacter smithii* [2]
<5> *Methanosarcina mazei* [3,6]
<6> no activity in *Methanosphaera stadtmanae* [2]
<7> *Archaeoglobus fulgidus* (UNIPROT accession number: O30126) [1]

3 Reaction and Specificity

Catalyzed reaction
ATP + O-phospho-L-serine + tRNA^{Cys} = AMP + diphosphate + O-phospho-L-seryl-tRNA^{Cys} (<7> anticodon recognition mechanism [1])

Natural substrates and products
S ATP + O-phospho-L-serine + tRNA^{Cys} <1,7> (Reversibility: ?) [1]
P AMP + diphosphate + O-phospho-L-serine-tRNA^{Cys}
S ATP + O-phospho-L-serine + tRNA^{Cys} <1,2,3,5> (<5> half-of-the-sites activity: the tetrameric enzyme binds two tRNAs. Only two of the four che-

D. Schomburg and I. Schomburg (eds.), *Class 3.4–6 Hydrolases, Lyases, Isomerases, Ligases: EC 3.4–6*, Springer Handbook of Enzymes S10, DOI 10.1007/978-3-642-36260-6_84,

mically equivalent subunits catalyze formation of phosphoseryl adenylate [6]; <1> Methanocaldococcus jannaschii synthesizes Cys-tRNA^{Cys} by an indirect pathway, whereby O-phosphoseryl-tRNA synthetase (SepRS) acylates tRNA^{Cys} with phosphoserine (Sep), and Sep-tRNA-Cys-tRNA synthase (SepCysS) converts the tRNA-bound phosphoserine to cysteine [4]; <3> Methanococcus maripaludis encodes both the direct and indirect paths for Cys-tRNA^{Cys} synthesis. SepS (encoding SepRS) can be deleted when the organism is grown in the presence of Cys [2]; <2> phosphoseryl-tRNA synthetase is a natural non-standard aminoacyl-tRNA synthetase, which charges a non-standard amino acid, phosphoserine, to tRNA^{Cys} containing a GCA anticodon for tRNA-dependent cysteine biosynthesis in some archaea [5]; <5> some methanogenic archaea synthesize Cys-tRNA^{Cys} needed for protein synthesis using both a canonical cysteinyl-tRNA synthetase as well as a set of two enzymes that operate via a separate indirect pathway. In the indirect route, Sep-tRNA^{Cys} is first synthesized by SepRS, and this misacylated intermediate is then converted to Cys-tRNA^{Cys} by Sep-tRNA:Cys-tRNA synthase via a pyridoxal phosphate-dependent mechanism, structural basis for the tRNA^{Cys} isoacceptor preferences of SepRS and CysRS, detailed overview [3]) (Reversibility: ?) [2,3,4,5,6]

P AMP + diphosphate + O-phospho-L-seryl-tRNA^{Cys}

S Additional information <1,7> (<7> two-step Cys-tRNA^{Cys} formation: in organisms like Archaeoglobus fulgidus lacking a canonical cysteinyl-tRNA synthetase for the direct Cys-tRNA^{Cys} formation, Cys-tRNA^{Cys} is produced by the indirect pathway, in which the noncanonical O-phosphoseryl-tRNA synthetase, SepRS, ligates the noncanonical amino acid O-phosphoserine, Sep, to tRNA^{Cys}, and the Sep-tRNA:Cys-tRNA synthase converts the produced Sep-tRNA^{Cys} to Cys-tRNA^{Cys}, overview, the SepRS/SepCysS pathway is the sole route for cysteine biosynthesis in the organism [1]; <1> two-step Cys-tRNA^{Cys} formation: in organisms like Methanococcus jannaschii lacking a canonical cysteinyl-tRNA synthetase for the direct Cys-tRNA^{Cys} formation, Cys-tRNA^{Cys} is produced by the indirect pathway, in which the noncanonical O-phosphoseryl-tRNA synthetase, SepRS, ligates the noncanonical amino acid O-phosphoserine, Sep, to tRNA^{Cys}, and the Sep-tRNA:Cys-tRNA synthase converts the produced Sep-tRNA^{Cys} to Cys-tRNA^{Cys}, overview, the SepRS/SepCysS pathway is the sole route for cysteine biosynthesis in the organism [1]; <1> Methanocaldococcus jannaschii synthesizes Cys-tRNA^{Cys} by an indirect pathway, whereby O-phosphoseryl-tRNA synthetase acylates tRNA^{Cys} with phosphoserine, and Sep-tRNA-Cys-tRNA synthase converts the tRNA-bound phosphoserine to cysteine. Methanocaldococcus jannaschii SepRS differs from CysRS by recruiting the m1G37 modification as a determinant for aminoacylation [4]) (Reversibility: ?) [1,4]

P ?

Substrates and products

- **S** ATP + O-phospho-L-serine + tRNAAmber <2> (<2> mutant D418N/D420N/T423V [5]) (Reversibility: ?) [5]
- **P** AMP + diphosphate + O-phospho-L-seryl-tRNAAmber
- **S** ATP + O-phospho-L-serine + tRNAAmber <7> (<7> recognition of U34 and C35 of tRNAAmber by mutant E418N/E420N, no activity with wild-type SepRS, overview [1]) (Reversibility: ?) [1]
- **P** AMP + diphosphate + O-phospho-L-serine-tRNAAmber
- **S** ATP + O-phospho-L-serine + $tRNA^{Cys}$ <1,7> (Reversibility: ?) [1]
- **P** AMP + diphosphate + O-phospho-L-serine-$tRNA^{Cys}$
- **S** ATP + O-phospho-L-serine + $tRNA^{Cys}$ <1,2,3,5> (<5> half-of-the-sites activity: the tetrameric enzyme binds two tRNAs. Only two of the four chemically equivalent subunits catalyze formation of phosphoseryl adenylate [6]; <1> Methanocaldococcus jannaschii synthesizes Cys-$tRNA^{Cys}$ by an indirect pathway, whereby O-phosphoseryl-tRNA synthetase (SepRS) acylates $tRNA^{Cys}$ with phosphoserine (Sep), and Sep-tRNA-Cys-tRNA synthase (SepCysS) converts the tRNA-bound phosphoserine to cysteine [4]; <3> Methanococcus maripaludis encodes both the direct and indirect paths for Cys-$tRNA^{Cys}$ synthesis. SepS (encoding SepRS) can be deleted when the organism is grown in the presence of Cys [2]; <2> phosphoseryl-tRNA synthetase is a natural non-standard aminoacyl-tRNA synthetase, which charges a non-standard amino acid, phosphoserine, to $tRNA^{Cys}$ containing a GCA anticodon for tRNA-dependent cysteine biosynthesis in some archaea [5]; <5> some methanogenic archaea synthesize Cys-$tRNA^{Cys}$ needed for protein synthesis using both a canonical cysteinyl-tRNA synthetase as well as a set of two enzymes that operate via a separate indirect pathway. In the indirect route, Sep-$tRNA^{Cys}$ is first synthesized by SepRS, and this misacylated intermediate is then converted to Cys-$tRNA^{Cys}$ by Sep-tRNA:Cys-tRNA synthase via a pyridoxal phosphate-dependent mechanism, structural basis for the $tRNA^{Cys}$ isoacceptor preferences of SepRS and CysRS, detailed overview [3]; <2> cognate substrate is $tRNA^{Cys}$ with the GCA anticodon, $tRNA^{Cys}$ containing the (pyrrole-2-carbaldehyde)UA anticodon [5]; <5> efficient phosphoserylation by SepRS requires methylation of $tRNA^{Cys}$ at the N^1 position of G37 in the anticodon loop. Comparative aminoacylation kinetics by CysRS (EC 6.1.1.16) and SepRS reveals that each enzyme prefers a distinct $tRNA^{Cys}$ isoacceptor or pair of isoacceptors [3]; <5> half-of-the-sites activity: the tetrameric enzyme binds two tRNAs. Only two of the four chemically equivalent subunits catalyze formation of phosphoseryl adenylate. Efficient phosphoserylation by SepRS requires methylation of $tRNA^{Cys}$ at the N^1 position of G37 in the anticodon loop [6]; <5> recognition determinants distinguishing the tRNAs reside in the globular core of the molecule. The enzyme also requires the S-adenosylmethione-dependent formation of m1G37 in the anticodon loop for efficient aminoacylation [3]; <1> SepRS differs from CysRS (EC 6.1.1.16) by recruiting the m1G37 modification as a determinant for aminoacylation, and in showing limited discrimination against mutations of conserved nucleotides. O-Phosphoseryl-

tRNA synthetase and Sep-tRNA-Cys-tRNA synthase bind the reaction intermediate O-phospho-L-serine-$tRNA^{Cys}$ tightly, and these two enzymes form a stable binary complex that promotes conversion of the intermediate to the product and sequesters the intermediate from binding to elongation factor $EF^{-}1a$ or infiltrating into the ribosome [4]; <1> SepRS differs from CysRS by recruiting the m1G37 modification as a determinant for aminoacylation, and in showing limited discrimination against mutations of conserved nucleotides. The enzyme requires the S-adenosylmethione-dependent formation of m1G37 in the anticodon loop for efficient aminoacylation [4]; <5> the tetrameric enzyme binds two tRNAs and only two of the four chemically equivalent subunits catalyze formation of phosphoseryl adenylate. $tRNA^{Cys}$ binding to SepRS also enhances the capacity of the enzyme to discriminate among amino acids, indicating the existence of functional connectivity between the tRNA and amino acid binding sites of the enzyme [6]) (Reversibility: ?) [2,3,4,5,6]

P AMP + diphosphate + O-phospho-L-seryl-$tRNA^{Cys}$

S ATP + O-phospho-L-serine + $tRNA^{Cys}$ <1,7> (<7> tRNA substrate from Escherichia coli, wheat germ and Saccharomyces cerevisiae in a mixture, the catalytic domain of SepRS recognizes the negatively charged side chain of O-phosphoserine at a noncanonical site, using the dipole moment of a conserved α-helix, the unique C-terminal domain specifically recognizes the anticodon GCA of $tRNA^{Cys}$, overview [1]) (Reversibility: ?) [1]

P AMP + diphosphate + O-phospho-L-serine-$tRNA^{Cys}$?

S ATP + O-phospho-L-serine + tRNAOpal <2> (<2> mutant D418N/D420N/T423V [5]) (Reversibility: ?) [5]

P AMP + diphosphate + O-phospho-L-seryl-tRNAOpal

S ATP + O-phospho-L-serine + tRNAOpal <7> (<7> recognition of U34 and C35 of tRNAOpal by mutant E418N/E420N, no activity with wild-type SepRS, overview [1]) (Reversibility: ?) [1]

P AMP + diphosphate + O-phospho-L-serine-tRNAOpal

S ATP + O-phospho-L-threonine + $tRNA^{Cys}$ <5> (<5> low activity [6]; <5> about 35% of the plateau aminoacylation observed with O-phospho-L-serine [6]) (Reversibility: ?) [6]

P AMP + diphosphate + O-phospho-L-threonyl-$tRNA^{Cys}$

S Additional information <1,2,5,7> (<7> two-step Cys-$tRNA^{Cys}$ formation: in organisms like Archaeoglobus fulgidus lacking a canonical cysteinyl-tRNA synthetase for the direct Cys-$tRNA^{Cys}$ formation, Cys-$tRNA^{Cys}$ is produced by the indirect pathway, in which the noncanonical O-phosphoseryl-tRNA synthetase, SepRS, ligates the noncanonical amino acid O-phosphoserine, Sep, to $tRNA^{Cys}$, and the Sep-tRNA:Cys-tRNA synthase converts the produced Sep-$tRNA^{Cys}$ to Cys-$tRNA^{Cys}$, overview, the SepRS/SepCysS pathway is the sole route for cysteine biosynthesis in the organism [1]; <1> two-step Cys-$tRNA^{Cys}$ formation: in organisms like Methanococcus jannaschii lacking a canonical cysteinyl-tRNA synthetase for the direct Cys-$tRNA^{Cys}$ formation, Cys-$tRNA^{Cys}$ is produced by the indirect pathway, in which the noncanonical O-phosphoseryl-tRNA synthetase,

SepRS, ligates the noncanonical amino acid O-phosphoserine, Sep, to $tRNA^{Cys}$, and the Sep-tRNA:Cys-tRNA synthase converts the produced Sep-$tRNA^{Cys}$ to Cys-$tRNA^{Cys}$, overview, the SepRS/SepCysS pathway is the sole route for cysteine biosynthesis in the organism [1]; <1> Methanocaldococcus jannaschii synthesizes Cys-$tRNA^{Cys}$ by an indirect pathway, whereby O-phosphoseryl-tRNA synthetase acylates $tRNA^{Cys}$ with phosphoserine, and Sep-tRNA-Cys-tRNA synthase converts the tRNA-bound phosphoserine to cysteine. Methanocaldococcus jannaschii SepRS differs from CysRS by recruiting the m1G37 modification as a determinant for aminoacylation [4]; <1> kinetic and binding measurements show that both SepRS and Sep-tRNA-Cys-tRNA synthase, SepCysS, bind the reaction intermediate Sep-$tRNA^{Cys}$ tightly, and these two enzymes form a stable binary complex that promotes conversion of the intermediate to the product and sequesters the intermediate from binding to elongation factor EF-1α or infiltrating into the ribosome, mechanism of the binary complex, detailed overview [4]; <5> SepRS is able to discriminate against the noncognate amino acids glutamate, serine, and phosphothreonine without the need for a separate hydrolytic editing site [6]; <5> SepRS is able to discriminate against the noncognate amino acids glutamate, serine, and phosphothreonine without the need for a separate hydrolytic editing site. Determination of the ATP-diphosphate exchange activity. Serine and glutamate are poor substrates, overview [6]; <2> substrate specificity, site-specific incorporation of phosphoserine into proteins by mutant D418N/D420N/T423V in response to the 7-(2-thienyl)-imidazo[4,5-b]pyridineUA or C7-(2-thienyl)-imidazo[4,5-b]pyridineA codons within mRNA, substrate binding structures and structural models for tRNA anticodon recognition, overview [5]; <7> two-step Cys-$tRNA^{Cys}$ formation: in organisms like Archaeoglobus fulgidus lacking a canonical cysteinyl-tRNA synthetase for the direct Cys-$tRNA^{Cys}$ formation, Cys-$tRNA^{Cys}$ is produced by the indirect pathway, in which the noncanonical O-phosphoseryl-tRNA synthetase, SepRS, ligates the noncanonical amino acid O-phosphoserine, Sep, to $tRNA^{Cys}$, and the Sep-tRNA:Cys-tRNA synthase converts the produced Sep-$tRNA^{Cys}$ to Cys-$tRNA^{Cys}$, overview, the SepRS/SepCysS pathway is the sole route for cysteine biosynthesis in the organism. RNA substrate specificity of wild-type and mutant enzymes, overview, structural insights into the first step of RNA-dependent cysteine biosynthesis, a two-step mechanism, in archaea [1]) (Reversibility: ?) [1,4,5,6]

P ?

Cofactors/prosthetic groups

ATP <1,2,5> [3,4,5,6]

Metals, ions

Mg^{2+} <1,2,5> [3,4,5,6]

Turnover number (s^{-1})

0.0054 <5> (O-phospho-L-threonine, <5> wild-type enzyme [6]) [6]
0.008 <2> ($tRNA^{Cys}$, <2> pH 7.6, 50°C, mutant D418N/D420N/T423V [5]) [5]
0.014 <5> (O-phospho-L-threonine, <5> pH 7.5, 37°C, recombinant enzyme [6]) [6]
0.021 <5> (O-phospho-L-threonine, <5> pH 7.5, 37°C, recombinant mutant T307S [6]) [6]
0.0471 <2> ($tRNA^{Cys}$, <2> 50°C, pH 7.6, $tRNA^{Cys}$ containing the (pyrrole-2-carbaldehyde)UA anticodon, mutant enzyme D418N D420N T423V [5]) [5]
0.048 <2> ($tRNA^{Cys}$, <2> 50°C, pH 7.6, $tRNA^{Cys}$ containing the C(pyrrole-2-carbaldehyde)A anticodon, mutant enzyme D418N D420N T423V [5]) [5]
0.07 <1> ($tRNA^{Cys}$, <1> 60°C, pH 6.0, steady-state kinetics [4]) [4]
0.115 <2> ($tRNA^{Cys}$, <2> 50°C, pH 7.6, $tRNA^{Cys}$ with the GCA anticodon, wild-type enzyme [5]; <2> pH 7.6, 50°C, wild-type enzyme [5]) [5]
0.12 <5> ($tRNA^{Cys}$, <5> pH 7.5, 37°C, recombinant enzyme [3]) [3]
0.24 <1> (m^1G37-$tRNA^{Cys}$, <1> 60°C, pH 6.0, steady-state kinetics [4]) [4]
0.24 <1> ($tRNA^{Cys}$, <1> pH 7.5, 37°C, recombinant enzyme, m1G37 $tRNA^{Cys}$ [4]) [4]
0.45 <5> (O-phospho-L-serine, <5> wild-type enzyme [6]) [6]
1 <1> ($tRNA^{Cys}$, <1> pH 7.5, 37°C, recombinant enzyme, native $tRNA^{Cys}$ [4]) [4]
10.6 <5> (O-phospho-L-serine, <5> pH 7.5, 37°C, recombinant enzyme [6]) [6]
11.2 <5> (O-phospho-L-serine, <5> pH 7.5, 37°C, recombinant mutant T307S [6]) [6]
Additional information <5> (<5> turnover number for $tRNA^{Cys}$ isoacceptor [3]) [3]

Specific activity (U/mg)

Additional information <5> (<5> recombinant enzyme, ATP-diphosphate exchange activity [6]) [6]

K_m-Value (mM)

0.00097 <1> (m1G37-$tRNA^{Cys}$, <1> 60°C, pH 6.0, steady-state kinetics [4]) [4]
0.0011 <1> ($tRNA^{Cys}$, <1> 60°C, pH 6.0, steady-state kinetics [4]) [4]
0.0064 <5> ($tRNA^{Cys}$, <5> pH 7.5, 37°C, recombinant enzyme [3]) [3]
0.007 <1> ($tRNA^{Cys}$, <1> pH 7.5, 37°C, recombinant enzyme, native $tRNA^{Cys}$ [4]) [4]
0.0097 <1> ($tRNA^{Cys}$, <1> pH 7.5, 37°C, recombinant enzyme, m1G37 $tRNA^{Cys}$ [4]) [4]
0.0269 <2> ($tRNA^{Cys}$, <2> pH 7.6, 50°C, wild-type enzyme [5]) [5]
0.0372 <2> ($tRNA^{Cys}$, <2> pH 7.6, 50°C, mutant D418N/D420N/T423V [5]) [5]
0.04 <5> (O-phospho-L-serine, <5> wild-type enzyme [6]) [6]
0.15 <5> (O-phospho-L-serine, <5> pH 7.5, 37°C, recombinant mutant T307S [6]) [6]

0.151 <2> ($tRNA^{Cys}$, <2> 50°C, pH 7.6, $tRNA^{Cys}$ containing the (pyrrole-2-carbaldehyde)UA anticodon, mutant enzyme D418N D420N T423V [5]; <2> 50°C, pH 7.6, $tRNA^{Cys}$ containing the C(pyrrole-2-carbaldehyde)A anticodon, mutant enzyme D418N D420N T423V [5]) [5]
0.269 <2> ($tRNA^{Cys}$, <2> 50°C, pH 7.6, $tRNA^{Cys}$ with the GCA anticodon, wild-type enzyme [5]) [5]
0.27 <5> (O-phospho-L-serine, <5> pH 7.5, 37°C, recombinant enzyme [6]) [6]
0.93 <5> (O-phospho-L-threonine, <5> pH 7.5, 37°C, recombinant mutant T307S [6]) [6]
2.2 <5> (O-phospho-L-threonine, <5> pH 7.5, 37°C, recombinant enzyme [6]) [6]
8.4 <5> (O-phospho-L-threonine, <5> wild-type enzyme [6]) [6]
Additional information <1,2,5> (<2> kinetic analysis of Sep-tRNA formation, overview [5]; <5> K_m-values for $tRNA^{Cys}$ isoacceptor [3]; <5> recombinant enzyme, ATP/diphosphate and aminoacylation kinetics, Michaelis-Menten kinetics [6]; <5> steady-state aminoacylation kinetics [3]; <1> steady-state and single-turnover kinetics, kinetic analysis, overview [4]) [3,4,5,6]

pH-Optimum

7.5 <2,5> (<2,5> assay at [3,5,6]) [3,5,6]
7.6 <7> (<7> assay at [1]) [1]

Temperature optimum (°C)

37 <5> (<5> assay at [3,6]) [3,6]
50 <2,7> (<2,7> assay at [1,5]) [1,5]

4 Enzyme Structure

Molecular weight

250000 <5> (<5> gel filtration [6]; <5> recombinant enzyme,native PAGE, and gel filtration [6]) [6]
255400 <5> (<5> recombinant enzyme, mass spectrometry [6]) [6]

Subunits

tetramer <1,3,5,7> (<3> homotetramer [7]; <5> 4 * 60909, calculated from sequence [6]; <5> 4 * 60909, sequence calculation, 4 * 68992, homotetramer α_4, mass spectrometry [6]; <1> SepRS contains two $tRNA^{Cys}$ molecules per tetramer indicating an asymmetry of the four identical subunits [4]) [1,4,6,7]
Additional information <1,5> (<1> both SepRS and SepCysS are active as a monomer in theSepRS-SepCysS binary complex [4]; <5> the tetrameric enzyme binds two tRNAs and only two of the four chemically equivalent subunits catalyze formation of phosphoseryl adenylate, active site titrations reveal calculation of 2.3 active sites per tetramer, overview [6]) [4,6]

5 Isolation/Preparation/Mutation/Application

Purification

<1> (recombinant) [1]
<5> (recombinant) [6]
<5> (recombinant His-tagged enzyme from Escherichia coli by anion exchange chromatography, gel filtration, and nickel affinity chromatography) [3]
<5> (recombinant His-tagged wild-type and mutant enzymes from Escherichia coli to homogeneity by nickel affinity chromatography, the His-tag is cleaved off) [6]
<5> (recombinant enzyme) [3]
<7> (recombinant) [1]

Crystallization

<1> (tRNA-free SepRS, hanging drop vapor diffusion method, 0.001 ml of protein solution mixed with 0.001 ml reservoir solution containing 11.25% w/v PEG 4,000, 75 mM sodium citrate, 75 mM N-(2-acetamido)iminodiacetic acid-NaOH buffer, pH 6.7, versus 1 ml reservoir solution, 20°C, cryoprotection by 22% v/v glycerol, X-ray diffraction structure determination and analysis at 3.6 A resolution, modeling) [1]
<3> (hanging-drop vapor diffusion, 3.2 A resolution) [7]
<7> (SepRS tetramer in complex with $tRNA^{Cys}$ and O-phosphoserine, selenomethionine SAD method, and SepRS-$tRNA^{Cys}$ binary complex, 0.001 ml of 6-8 mg/ml protein in 10 mM Tris-HCl buffer, pH 8.0, 5 mM $MgCl_2$, 150 mM NaCl and 5 mM 2-mercaptoethanol, and 2 mM O-phospho-L-serine, mixed with 0.001 ml reservoir solution containing 8% w/v PEG 6000 and 1.2 M NaCl, 20°C, cryoprotection by 22% v/v glycerol, X-ray diffraction structure determination and analysis at 2.6 A and 2.8 A resolution, respectively, modeling, determination of crystal structures of SepRS(E418N/E420N)-tRNAOpal-O-phosphoserine and SepRS(E418N/E420N)-tRNAAmber-O-phosphoserine at 3.2 and 3.3 resolutions, respectively) [1]

Cloning

<5> (expression in Escherichia coli) [3]
<5> (expression of His-tagged enzyme in Escherichia coli) [3]
<5> (expression of His-tagged wild-type and mutant enzymes in Escherichia coli) [6]
<7> (overexpression of wild-type and mutant enzymes in Escherichia coli strain BL21(DE3), overexpression of SeMet-labeled SepRS in Escherichia coli strain B834(DE3)) [1]

Engineering

D418N/D420N/T423V <2> (<2> site-directed mutagenesis, the mutant shows reduced activity and altered substrate specificity compared to the wild-type enzyme, it is active with tRNA substrate containing unusual residues 7-(2-thienyl)-imidazo[4,5-b]pyridine and pyrrole-2-carbaldehyde in the anticodon, overview [5]) [5]

E418D <7> (<7> site-directed mutagenesis, the mutant shows reduced activity and altered tRNA substrate specificity, compared to the wild-type enzyme [1]) [1]
E418D/E420D <7> (<7> site-directed mutagenesis, the mutant shows reduced activity and altered tRNA substrate specificity, compared to the wild-type enzyme [1]) [1]
E418D/E420Q <7> (<7> site-directed mutagenesis, the mutant shows reduced activity and altered tRNA substrate specificity, compared to the wild-type enzyme [1]) [1]
E418N <7> (<7> site-directed mutagenesis, the mutant shows reduced activity and altered tRNA substrate specificity, compared to the wild-type enzyme [1]) [1]
E418N/E420D <7> (<7> site-directed mutagenesis, the mutant shows reduced activity and altered tRNA substrate specificity, compared to the wild-type enzyme [1]) [1]
E418N/E420N <7> (<7> site-directed mutagenesis, the mutant shows reduced activity and altered tRNA substrate specificity, compared to the wild-type enzyme [1]) [1]
E418N/E420N/T423V <2,7> (<7> site-directed mutagenesis, the mutant shows reduced activity and altered tRNA substrate specificity, compared to the wild-type enzyme [1]; <2> efficiently charged phosphoserine to tRNA containing the (pyrrole-2-carbaldehyde)UA anticodon [5]) [1,5]
E418N/E420Q <7> (<7> site-directed mutagenesis, the mutant shows reduced activity and altered tRNA substrate specificity, compared to the wild-type enzyme [1]) [1]
E418Q <7> (<7> site-directed mutagenesis, the mutant shows reduced activity and altered tRNA substrate specificity, compared to the wild-type enzyme [1]) [1]
E418Q/E420D <7> (<7> site-directed mutagenesis, the mutant shows reduced activity and altered tRNA substrate specificity, compared to the wild-type enzyme [1]) [1]
E418Q/E420N <7> (<7> site-directed mutagenesis, the mutant shows reduced activity and altered tRNA substrate specificity, compared to the wild-type enzyme [1]) [1]
E418Q/E420Q <7> (<7> site-directed mutagenesis, the mutant shows reduced activity and altered tRNA substrate specificity, compared to the wild-type enzyme [1]) [1]
E420D <7> (<7> site-directed mutagenesis, the mutant shows reduced activity and altered tRNA substrate specificity, compared to the wild-type enzyme [1]) [1]
E420K <7> (<7> site-directed mutagenesis, the mutant shows reduced activity and altered tRNA substrate specificity, compared to the wild-type enzyme [1]) [1]
E420N <7> (<7> site-directed mutagenesis, the mutant shows reduced activity and altered tRNA substrate specificity, compared to the wild-type enzyme [1]) [1]

E420Q <7> (<7> site-directed mutagenesis, the mutant shows reduced activity and altered tRNA substrate specificity, compared to the wild-type enzyme [1]) [1]
E420R <7> (<7> site-directed mutagenesis, the mutant shows reduced activity and altered tRNA substrate specificity, compared to the wild-type enzyme [1]) [1]
T307S <5> (<5> mutant reveals a 3.2fold improvement in k_{cat}/K_m for phosphothreonyl adenylate synthesis, as compared with wild-type SepRS. The mutant is unable to transfer phosphothreonine to $tRNA^{Cys}$ at greater than 10% plateau levels [6]; <5> site-directed mutagenesis, the mutant shows increased activity with phosphothreonine, thus reduced substrate specificity [6]) [6]
Additional information <1,7> (<7> engineering of SepRS to recognize $tRNA^{Cys}$ mutants with the anticodons UCA and CUA on the basis of the structure, phosphoserine ligation activity of the wild-type and mutant SepRSs for $tRNA^{Cys}$, overview [1]; <1> mutation of the three anticodon nucleotides, G34, C35 and A36, as well as the next residue, G37, reduces the phosphoserylation activity [1]) [1]

Application

biotechnology <7> (<7> the mutant SepRS-tRNA pairs may be useful for translational incorporation of O-phosphoserine into proteins in response to the stop codons UGA and UAG, so that it could ligate O-phosphoserine to a suppressor tRNA for genetic-code expansion [1]) [1]

References

[1] Fukunaga, R.; Yokoyama, S.: Structural insights into the first step of RNA-dependent cysteine biosynthesis in archaea. Nat. Struct. Mol. Biol., **14**, 272-279 (2007)
[2] Yuan, J.; Sheppard, K.; Soell, D.: Amino acid modifications on tRNA. Acta Biochim. Biophys. Sin. (Shanghai), **40**, 539-553 (2008)
[3] Hauenstein, S.I.; Perona, J.J.: Redundant synthesis of cysteinyl-$tRNA^{Cys}$ in Methanosarcina mazei. J. Biol. Chem., **283**, 22007-22017 (2008)
[4] Zhang, C.M.; Liu, C.; Slater, S.; Hou, Y.M.: Aminoacylation of tRNA with phosphoserine for synthesis of cysteinyl-$tRNA^{Cys}$. Nat. Struct. Mol. Biol., **15**, 507-514 (2008)
[5] Fukunaga, R.; Harada, Y.; Hirao, I.; Yokoyama, S.: Phosphoserine aminoacylation of tRNA bearing an unnatural base anticodon. Biochem. Biophys. Res. Commun., **372**, 480-485 (2008)
[6] Hauenstein, S.I.; Hou, Y.M.; Perona, J.J.: The homotetrameric phosphoseryl-tRNA synthetase from Methanosarcina mazei exhibits half-of-the-sites activity. J. Biol. Chem., **283**, 21997-22006 (2008)
[7] Kamtekar, S.; Hohn, M.J.; Park, H.S.; Schnitzbauer, M.; Sauerwald, A.; Söll, D.; Steitz, T.A.: Toward understanding phosphoseryl-$tRNA^{Cys}$ formation: the crystal structure of Methanococcus maripaludis phosphoseryl-tRNA synthetase. Proc. Natl. Acad. Sci. USA, **104**, 2620-2625 (2007)

ACP-SH:acetate ligase 6.2.1.35

1 Nomenclature

EC number
6.2.1.35

Systematic name
acetate:[acyl-carrier-protein] ligase (AMP-forming)

Recommended name
ACP-SH:acetate ligase

Synonyms
ACP-SH:acetate ligase
HS-acyl-carrier protein:acetate ligase
S01.274 (Merops-ID)
[acyl-carrier protein]:acetate ligase

CAS registry number
80700-20-5 (multienzyme complex malonate decarboxylase)

2 Source Organism

<1> *Klebsiella pneumoniae* [2]
<2> *Malonomonas rubra* [1]

3 Reaction and Specificity

Catalyzed reaction
ATP + acetate + an [acyl-carrier protein] = AMP + diphosphate + an acetyl-[acyl-carrier protein]

Substrates and products
S acyl-carrier protein + acetate + ATP <2> (Reversibility: ?) [1]
P acetyl-acyl carrier protein + AMP + diphosphate (<2> acyl carrier protein contains 2-(5-phosphoribosyl)-3-dephosphocoenzyme A as a prosthetic group [1])
S Additional information <1> (<1> catalytic mechanism of malonate decarboxylase and involvement of ACP-SH acetate:ligase [2]) [2]
P ?

D. Schomburg and I. Schomburg (eds.), *Class 3.4–6 Hydrolases, Lyases, Isomerases, Ligases: EC 3.4–6*, Springer Handbook of Enzymes S10, DOI 10.1007/978-3-642-36260-6_85,

Inhibitors

Additional information <2> (<2> not inhibitory: dithioerythritol, iodoacetate [1]) [1]

5 Isolation/Preparation/Mutation/Application

Purification

<1> (during purification of the malonate decarboxylase complex, the ligase is separated from the decarboxylase by treatment with 1.5 M ammonium sulfate after the TSK-DEAE column) [2]

References

[1] Berg, M.; Hilbi, H.; Dimroth, P.: The acyl carrier protein of malonate decarboxylase of Malonomonas rubra contains 2-(5"-phosphoribosyl)-3-dephosphocoenzyme A as a prosthetic group. Biochemistry, **35**, 4689-4696 (1996)

[2] Schmid, M.; Berg, M.; Hilbi, H.; Dimroth, P.: Malonate decarboxylase of Klebsiella pneumoniae catalyses the turnover of acetyl and malonyl thioester residues on a coenzyme-A-like prosthetic group. Eur. J. Biochem., **237**, 221-228 (1996)

3-hydroxypropionyl-CoA synthase 6.2.1.36

1 Nomenclature

EC number
6.2.1.36

Systematic name
hydroxypropionate:CoA ligase (AMP-forming)

Recommended name
3-hydroxypropionyl-CoA synthase

Synonyms
3-hydroxypropionyl-CoA synthetase (AMP-forming) <1> [2]

2 Source Organism

<1> *Metallosphaera sedula* (UNIPROT accession number: A4YGR1) [1,2]
<2> *Sulfolobus tokodaii* (UNIPROT accession number: Q973W5) [1]

3 Reaction and Specificity

Catalyzed reaction
3-hydroxypropionate + ATP + coenzyme A = 3-hydroxypropionyl-CoA + AMP + diphosphate

Natural substrates and products
- **S** 3-hydroxypropionate + ATP + coenzyme A <1,2> (<1,2> the enzyme is involved in autotrophic CO_2 fixation [1]; <1> the enzyme is involved in the autotrophic 3-hydroxypropionate/4-hydroxybutyrate cycle (autotrophic carbon dioxide assimilation pathway in archaea) [2]) (Reversibility: ?) [1,2]
- **P** 3-hydroxypropionyl-CoA + AMP + diphosphate

Substrates and products
- **S** 3-chloropropionate + ATP + coenzyme A <2> (<2> 64% of the activity with 3-hydroxypropionate [1]) (Reversibility: ?) [1]
- **P** 3-chloropropionyl-CoA + AMP + diphosphate
- **S** 3-hydroxypropionate + ATP + coenzyme A <1,2> (<1,2> the enzyme is involved in autotrophic CO_2 fixation [1]; <1> the enzyme is involved in the autotrophic 3-hydroxypropionate/4-hydroxybutyrate cycle (autotrophic carbon dioxide assimilation pathway in archaea) [2]; <1> the en-

D. Schomburg and I. Schomburg (eds.), *Class 3.4–6 Hydrolases, Lyases, Isomerases, Ligases: EC 3.4–6*, Springer Handbook of Enzymes S10, DOI 10.1007/978-3-642-36260-6_86,

zyme is specific for 3-hydroxypropionate and propionate [1]) (Reversibility: ?) [1,2]
P 3-hydroxypropionyl-CoA + AMP + diphosphate
S 3-hydroxypropionate + CTP + coenzyme A <1> (<1> 13% of the activity with ATP [1]) (Reversibility: ?) [1]
P 3-hydroxypropionyl-CoA + CMP + diphosphate
S 3-hydroxypropionate + UTP + coenzyme A <1> (<1> 32% of the activity with ATP [1]) (Reversibility: ?) [1]
P 3-hydroxypropionyl-CoA + UMP + diphosphate
S 3-mercaptopropionate + ATP + coenzyme A <2> (<2> 36% of the activity with 3-hydroxypropionate [1]) (Reversibility: ?) [1]
P 3-mercaptopropionyl-CoA + AMP + diphosphate
S acetate + ATP + coenzyme A <1,2> (<1> 42% of the activity with 3-hydroxypropionate [1]; <2> 65% of the activity with 3-hydroxypropionate [1]) (Reversibility: ?) [1]
P acetyl-CoA + AMP + diphosphate
S acrylate + ATP + coenzyme A <1,2> (<1> 77% of the activity with 3-hydroxypropionate [1]; <2> 96% of the activity with 3-hydroxypropionate [1]) (Reversibility: ?) [1]
P acryloyl-CoA + AMP + diphosphate
S butyrate + ATP + coenzyme A <1,2> (<1> 20% of the activity with 3-hydroxypropionate [1]; <2> 27% of the activity with 3-hydroxypropionate [1]) (Reversibility: ?) [1]
P butyryl-CoA + AMP + diphosphate
S propionate + ATP + coenzyme A <1,2> (<2> 98% of the activity with 3-hydroxypropionate [1]; <1> the enzyme is specific for 3-hydroxypropionate and propionate [1]) (Reversibility: ?) [1]
P propionyl-CoA + AMP + diphosphate
S Additional information <1,2> (<1,2> less than 1% of the activity with 3-hydroxypropionate: 3-hydroxybutyrate, crotonate, glycerate, malonate [1]) (Reversibility: ?) [1]
P ?

Turnover number (s^{-1})

5.4 <1> (acrylate, <1> pH 8.5, 45°C [1]) [1]
5.6 <1> (aropionate, <1> pH 8.5, 45°C [1]) [1]
5.7 <1> (3-hydroxypropionate, <1> pH 8.5, 45°C [1]) [1]

Specific activity (U/mg)

6.7 <2> (<2> pH 8,5, 65°C [1]) [1]
18 <1> (<1> pH 8,5, 45°C, autotrophically grown cells [1]) [1]

K_m-Value (mM)

0.045 <1> (ATP, <1> pH 8.5, 45°C [1]) [1]
0.12 <1> (propionate, <1> pH 8.5, 45°C [1]) [1]
0.18 <1> (3-hydroxypropionate, <1> pH 8.5, 45°C [1]) [1]
1.42 <1> (acrylate, <1> pH 8.5, 45°C [1]) [1]

pH-Optimum

8.5 <1,2> (<1,2> assay at [1]) [1]

Temperature optimum (°C)

45 <1> (<1> assay at [1]) [1]
55 <1> (<1> assay at [2]) [2]
65 <2> (<2> assay at [1]) [1]

4 Enzyme Structure

Molecular weight

140000 <2> (<2> gel filtration [1]) [1]
340000 <1> (<1> gel filtration [1]) [1]

Subunits

dimer <2> (<2> 2 * 74000, SDS-PAGE [1]) [1]
homotetramer <1> (<1> 4 * 78000, SDS-PAGE [1]) [1]

5 Isolation/Preparation/Mutation/Application

Purification

<1> [1]
<2> (recombinant enzyme) [1]

Cloning

<2> (expression in Escherichia coli) [1]

6 Stability

Temperature stability

80 <1> (<1> 15 min, stable up to 80°C [1]) [1]
100 <1> (<1> 15 min, 50% loss of activity [1]) [1]

References

[1] Alber, B.E.; Kung, J.W.; Fuchs, G.: 3-Hydroxypropionyl-coenzyme A synthetase from Metallosphaera sedula, an enzyme involved in autotrophic CO_2 fixation. J. Bacteriol., **190**, 1383-1389 (2008)
[2] Berg, I.A.; Kockelkorn, D.; Buckel, W.; Fuchs, G.: A 3-hydroxypropionate/4-hydroxybutyrate autotrophic carbon dioxide assimilation pathway in Archaea. Science, **318**, 1782-1786 (2007)

L-cysteine:1D-myo-inositol 2-amino-2-deoxy-α-D-glucopyranoside ligase 6.3.1.13

1 Nomenclature

EC number
6.3.1.13

Systematic name
L-cysteine:1-O-(2-amino-2-deoxy-α-D-glucopyranosyl)-1D-myo-inositol ligase (AMP-forming)

Recommended name
L-cysteine:1D-myo-inositol 2-amino-2-deoxy-α-D-glucopyranoside ligase

Synonyms
Cys:GlcN-Ins ligase <1,2> [1]
L-cysteine:1-D-myo-inosityl 2-amino-2-deoxy-α-D-glucopyranoside ligase <2> [2]
MshC <1,2,3> [2,3,4,5,6,7]
MshC ligase <1,2> [1]
cysteine ligase <1> [3]
mycothiol ligase <1> [4]
Additional information <1,2> (<1,2> enzyme is related to class I cysteinyl-tRNA synthetase [1]) [1]

CAS registry number
442171-76-8

2 Source Organism

<1> *Mycobacterium smegmatis* [1,3,4,5,6]
<2> *Mycobacterium tuberculosis* [1,2,8]
<3> *Rhodococcus jostii* [7]

3 Reaction and Specificity

Catalyzed reaction
1-O-(2-amino-2-deoxy-α-D-glucopyranosyl)-1D-myo-inositol + L-cysteine + ATP = 1D-myo-inositol + 1-O-[2-(L-cysteinamido)-2-deoxy-α-D-glucopyranosyl]-1D-myo-inositol + AMP + diphosphate (<1> bi uni uni bi ping pong reaction mechanism [3])

D. Schomburg and I. Schomburg (eds.), *Class 3.4–6 Hydrolases, Lyases, Isomerases, Ligases: EC 3.4–6*, Springer Handbook of Enzymes S10, DOI 10.1007/978-3-642-36260-6_87,

Natural substrates and products

- **S** 1D-myo-inositol 2-amino-2-deoxy-α-D-glucopyranoside + L-cysteine + ATP <1,2> (<1,2> enzyme is important in the biosynthesis of mycothiol, which plays a role in protecting bacteria against oxidative stress [1]) (Reversibility: ?) [1]
- **P** 1D-myo-inositol 2(L-cysteinyl)amido-2-deoxy-α-D-glucopyranoside + AMP + diphosphate <1,2> [1]
- **S** 1D-myo-inositol 2-amino-2-deoxy-α-D-glucopyranoside + L-cysteine + ATP <1,3> (<3> inactivation of the mshC gene in RHA1 results in the accumulation of the MSH pathway intermediate, 1D-myo-inositol 2-amino-2-deoxy-α-D-glucopyranoside. The mutant is deficient in the biochemical degradation of a number of xenobiotics metabolized by the parent strain, it shows increased susceptibility to a number of antibiotics and it shows unusual growth characteristics, exhibiting a long lag phase before normal exponential growth [7]; <1> the product 1D-myo-inositol 2-(L-cysteinyl)amido-2-deoxy-α-D-glucopyranoside is an intermediate in the biosynthetic pathway of mycothiol. Mycothiol is produced by Mycobacterium tuberculosis to maintain an intracellular reducing environment and protect against oxidative and antibiotic induced stress. The biosynthesis of mycothiol is essential for cell growth [6]) (Reversibility: ?) [6,7]
- **P** 1D-myo-inositol 2-(L-cysteinyl)amido-2-deoxy-α-D-glucopyranoside + AMP + diphosphate
- **S** 1D-myo-inositol 2-amino-2-deoxy-α-D-glycopyranoside + L-cysteine + ATP <1,2> (<1> a key step in mycothiol, i.e. 1-D-myo-inosityl-2-(N-acetyl-L-cysteinyl)amido-2-deoxy-R-D-glucopyranoside or MSH or AcCys-GlcN-Ins, biosynthesis, mycothiol is produced to act against oxidative and antibiotic stress and is essential for cell growth, biosynthetic pathway, overview [3]; <1> key enzyme in the biosynthesis of mycothiol, pathway overview [4]; <2> the ATP-dependent ligation of Cys to GlcNIns is a key step in mycothiol biosynthesis, catalyzed by MshC, which is essential for growth of Mycobacterium tuberculosis [2]) (Reversibility: ?) [2,3,4]
- **P** 1D-myo-inositol 2-(cysteinyl)amido-2-deoxy-α-D-glycopyranoside + AMP + diphosphate
- **S** Additional information <1> (<1> penultimate enzyme in the mycothiol biosynthetic pathway [5]) (Reversibility: ?) [5]
- **P** ?

Substrates and products

- **S** 1D-myo-inositol 2-amino-2-deoxy-α-D-glucopyranoside + L-cysteine + ATP <1,2> (<1,2> enzyme is important in the biosynthesis of mycothiol, which plays a role in protecting bacteria against oxidative stress [1]) (Reversibility: ?) [1]
- **P** 1D-myo-inositol 2(L-cysteinyl)amido-2-deoxy-α-D-glucopyranoside + AMP + diphosphate <1,2> [1]
- **S** 1D-myo-inositol 2-amino-2-deoxy-α-D-glucopyranoside + L-cysteine + ATP <1,3> (<3> inactivation of the mshC gene in RHA1 results in the accumulation of the MSH pathway intermediate, 1D-myo-inositol 2-ami-

no-2-deoxy-α-D-glucopyranoside. The mutant is deficient in the biochemical degradation of a number of xenobiotics metabolized by the parent strain, it shows increased susceptibility to a number of antibiotics and it shows unusual growth characteristics, exhibiting a long lag phase before normal exponential growth [7]; <1> the product 1D-myo-inositol 2-(L-cysteinyl)amido-2-deoxy-α-D-glucopyranoside is an intermediate in the biosynthetic pathway of mycothiol. Mycothiol is produced by Mycobacterium tuberculosis to maintain an intracellular reducing environment and protect against oxidative and antibiotic induced stress. The biosynthesis of mycothiol is essential for cell growth [6]; <1> positional isotope exchange analysis confirms that MshC catalyzes the formation of a kinetically competent cysteinyl-adenylate intermediate after the addition of ATP and cysteine [6]) (Reversibility: ?) [6,7]

P 1D-myo-inositol 2-(L-cysteinyl)amido-2-deoxy-α-D-glucopyranoside + AMP + diphosphate

S 1D-myo-inositol 2-amino-2-deoxy-α-D-glycopyranoside + L-cysteine + ATP <1,2> (<1> a key step in mycothiol, i.e. 1-D-myo-inosityl-2-(N-acetyl-L-cysteinyl)amido-2-deoxy-R-D-glucopyranoside or MSH or AcCys-GlcN-Ins, biosynthesis, mycothiol is produced to act against oxidative and antibiotic stress and is essential for cell growth, biosynthetic pathway, overview [3]; <1> key enzyme in the biosynthesis of mycothiol, pathway overview [4]; <2> the ATP-dependent ligation of Cys to GlcNIns is a key step in mycothiol biosynthesis, catalyzed by MshC, which is essential for growth of Mycobacterium tuberculosis [2]) (Reversibility: ?) [2,3,4]

P 1D-myo-inositol 2-(cysteinyl)amido-2-deoxy-α-D-glycopyranoside + AMP + diphosphate

S Additional information <1> (<1> penultimate enzyme in the mycothiol biosynthetic pathway [5]) (Reversibility: ?) [5]

P ?

Inhibitors

5'-O-[N-(L-cysteinyl)sulfamonyl]adenosine <1> (<1> competitive inhibition [5]; <1> a stable bisubstrate analogue, exhibits competitive inhibition versus ATP and noncompetitive inhibition versus cysteine [3]) [3,5]

dequalinium chloride <2> (<2> ATP-competitive inhibitor of MshC, binds MshC with a K_D of 0.22 microM, and inhibits the growth of Mycobacterium tuberculosis under aerobic and anaerobic conditions with minimum inhibitory and anaerobic bactericidal concentrations of 1.2 and 0.3 μg/ml, respectively [8]) [8]

Additional information <2> (<2> screening for inhibitor molecules [2]) [2]

Cofactors/prosthetic groups

ATP <1,2> (<1,2> dependent on [1]) [1,2,3]

Metals, ions

Mg^{2+} <1,2> [2,3]

Turnover number (s^{-1})

3.15 <1> (1D-myo-inositol 2-amino-2-deoxy-α-D-glycopyranoside, <1> pH 7.8, 25°C, recombinant enzyme [3]) [3]

Specific activity (U/mg)

0.009 <1> (<1> purified recombinant GST-tagged MshC [4]) [4]
0.025 <1> (<1> purified recombinant maltose binding protein-MshC [4]) [4]
0.054 <1> (<1> purified enzyme [1]) [1]
0.15 <2> (<2> purified recombinant enzyme [2]) [2]
Additional information <1,2> (<2> spectrophotometric assay method development with coupling of diphosphatase to convert diphosphate to phosphate and spectrophotometric detection of the latter via the phosphomolybdate complex with malachite green, overview [2]) [2,4]

K_m-Value (mM)

0.04 <1> (L-cysteine, <1> pH 7.5, 37°C [1]) [1]
0.072 <1> (1D-myo-inositol 2-amino-2-deoxy-α-D-glucopyranoside, <1> pH 7.5, 37°C [1]) [1]
0.1 <1> (L-cysteine, <1> pH 7.8, 25°C, recombinant enzyme [3]) [3]
0.16 <1> (1D-myo-inositol 2-amino-2-deoxy-α-D-glycopyranoside, <1> pH 7.8, 25°C, recombinant enzyme [3]) [3]
1.8 <1> (ATP, <1> pH 7.8, 25°C, recombinant enzyme [3]) [3]
Additional information <1> (<1> steady-state and pre-steady-state kinetic analysis, single-turnover reactions of the first and second half reactions [3]) [3]

K_i-Value (mM)

0.00031 <1> (5'-O-[N-(L-cysteinyl)sulfamonyl]adenosine, <1> versus ATP [3]) [3]

pH-Optimum

7.5 <1> (<1> assay at [1]) [1]
7.8 <1> (<1> assay at [3]) [3]
8.5 <2> [2]

Temperature optimum (°C)

23 <2> (<2> assay at [2]) [2]
25 <1> (<1> assay at [3]) [3]

4 Enzyme Structure

Molecular weight

40700 <1> (<1> recombinant His-tagged enzyme, gel filtration [3]) [3]

Subunits

monomer <1> (<1> 1 * 47000, recombinant His-tagged enzyme, 1 * 47562, amino acid sequence calculation [3]) [3]

5 Isolation/Preparation/Mutation/Application

Purification

<1> (2400fold, 2 peaks) [1]
<1> (recombinant GST-tagged MshC and recombinant maltose binding protein-MshC by affinity chromatography on glutathione and amylose resins, respectively) [4]
<1> (recombinant His-tagged enzyme from Escherichia coli strain BL21 by nickel affinity chromatography and gel filtration to about 95% purity) [3]
<2> (recombinant enzyme from mshC-deficient mutant strain I64 of Mycobacterium smegmatis by ammonium sulfate fractionation, anion exchange chromatography, hydroxyapatite chromatography, and gel filtration) [2]

Crystallization

<1> (incubation of the enzyme with the cysteinyl adenylate analogue, 5'-O-[N-(L-cysteinyl)-sulfamonyl]adenosine, followed by a 24 h limited trypsin proteolysis yields an enzyme preparation that readily crystallizes, 1.6 A crystal structure) [5]

Cloning

<1> (DNA and amino acid sequence determination and analysis, expression in Escherichia coli BL21(DE3) as N-terminally His-tagged enzyme) [1]
<1> (expression of His-tagged enzyme in Escherichia coli strain BL21) [3]
<1> (gene mshC, construction of three N-terminal-MshC fusion proteins where N-terminal tags include the B1 domain of 1. streptococcal protein G to give GB1-MshC, 2. glutathione-S-transferase to give GST-MshC, and 3. maltose binding protein to give MBP-MshC, for expression in M. smegmatis, expression in enzyme-deficient mutant strain mc2155, i.e. I64 L205P, optimization of recombinant enzyme expression, overview) [4]
<2> (DNA and amino acid sequence determination and analysis, expression in Escherichia coli BL21(DE3) as His-tagged enzyme) [1]
<2> (gene mshC, expression in the mshC-deficient mutant strain I64 of Mycobacterium smegmatis, expression as insoluble protein in Escherichia coli) [2]

Application

drug development <1,2> (<1> MshC may represent a novel target for new classes of antituberculars [4]; <2> the enzyme is a potential target for drugs directed against tuberculosis [2]) [2,4]
pharmacology <1,2> (<1,2> enzyme is a traget for drug development against actinomycetes [1]) [1]

References

[1] Sareen, D.; Steffek, M.; Newton, G.L.; Fahey, R.C.: ATP-dependent L-cysteine:1D-myo-inosityl 2-amino-2-deoxy-α-D-glucopyranoside ligase, mycothiol biosynthesis enzyme MshC, is related to class I cysteinyl-tRNA synthetases. Biochemistry, **41**, 6885-6890 (2002)

[2] Newton, G.L.; Ta, P.; Sareen, D.; Fahey, R.C.: A coupled spectrophotometric assay for l-cysteine:1-D-myo-inosityl 2-amino-2-deoxy-α-D-glucopyranoside ligase and its application for inhibitor screening. Anal. Biochem., **353**, 167-173 (2006)
[3] Fan, F.; Luxenburger, A.; Painter, G.F.; Blanchard, J.S.: Steady-state and pre-steady-state kinetic analysis of Mycobacterium smegmatis cysteine ligase (MshC). Biochemistry, **46**, 11421-11429 (2007)
[4] Gutierrez-Lugo, M.T.; Newton, G.L.; Fahey, R.C.; Bewley, C.A.: Cloning, expression and rapid purification of active recombinant mycothiol ligase as B1 immunoglobulin binding domain of streptococcal protein G, glutathione-S-transferase and maltose binding protein fusion proteins in Mycobacterium smegmatis. Protein Expr. Purif., **50**, 128-136 (2006)
[5] Tremblay, L.W.; Fan, F.; Vetting, M.W.; Blanchard, J.S.: The 1.6 A crystal structure of Mycobacterium smegmatis MshC: the penultimate enzyme in the mycothiol biosynthetic pathway. Biochemistry, **47**, 13326-13335 (2008)
[6] Williams, L.; Fan, F.; Blanchard, J.S.; Raushel, F.M.: Positional isotope exchange analysis of the Mycobacterium smegmatis cysteine ligase (MshC). Biochemistry, **47**, 4843-4850 (2008)
[7] Dosanjh, M.; Newton, G.L.; Davies, J.: Characterization of a mycothiol ligase mutant of Rhodococcus jostii RHA1. Res. Microbiol., **159**, 643-650 (2008)
[8] Gutierrez-Lugo, M.T.; Baker, H.; Shiloach, J.; Boshoff, H.; Bewley, C.A.: Dequalinium, a new inhibitor of Mycobacterium tuberculosis mycothiol ligase identified by high-throughput screening. J. Biomol. Screen., **14**, 643-652 (2009)

diphthine-ammonia ligase 6.3.1.14

1 Nomenclature

EC number
6.3.1.14

Systematic name
diphthine:ammonia ligase (ADP-forming)

Recommended name
diphthine-ammonia ligase

Synonyms
Diphthamide synthase
Synthetase, diphthamide

CAS registry number
114514-33-9

2 Source Organism

<1> *Cricetulus griseus* (isozyme UGT1A3 [1,2]) [1,2]

3 Reaction and Specificity

Catalyzed reaction
ATP + diphthine + NH_3 = ADP + phosphate + diphthamide

Reaction type
peptide synthase reaction

Substrates and products
S ATP + diphthine + ammonia <1> (Reversibility: ?) [1,2]
P ADP + phosphate + diphthamide <1> [1,2]
S CTP + diphthine + ammonia <1> (<1> 11% of activity compared to ATP [2]) (Reversibility: ?) [2]
P CDP + phosphate + diphthamide
S GTP + diphthine + ammonia <1> (<1> 14% of activity compared to ATP [2]) (Reversibility: ?) [2]
P GDP + phosphate + diphthamide

Temperature optimum (°C)
30 <1> (<1> assay at [2]) [2]

D. Schomburg and I. Schomburg (eds.), *Class 3.4–6 Hydrolases, Lyases, Isomerases, Ligases: EC 3.4–6*, Springer Handbook of Enzymes S10, DOI 10.1007/978-3-642-36260-6_88,

5 Isolation/Preparation/Mutation/Application

Source/tissue
ovary <1> [1,2]

Purification
<1> (partial) [1,2]

References

[1] Moehring, J.M.; Moehring, T.J.: The post-translational trimethylation of diphthamide studied in vitro. J. Biol. Chem., **263**, 3840-3844 (1988)
[2] Moehring, T.J.; Danley, D.E.; Moehring, J.M.: In vitro biosynthesis of diphthamide, studied with mutant chinese hamster ovary cells resistant to diphtheria toxin. Mol. Cell. Biol., **4**, 642-650 (1984)

coenzyme F_{420}-0:L-glutamate ligase 6.3.2.31

1 Nomenclature

EC number
6.3.2.31

Systematic name
L-glutamate:coenzyme F_{420}-0 ligase (GDP-forming)

Recommended name
coenzyme F_{420}-0:L-glutamate ligase

Synonyms
CofE <1> [1]
CofE-AF <2> [2]
F_{420}-0:γ-glutamyl ligase <1> [1]
MJ0768 <1> [1]

2 Source Organism

<1> *Methanocaldococcus jannaschii* (UNIPROT accession number: Q58178) [1]
<2> *Archaeoglobus fulgidus* DSM 4304 (UNIPROT accession number: O28028) [2]

3 Reaction and Specificity

Catalyzed reaction
GTP + coenzyme F_{420}-0 + L-glutamate = GDP + phosphate + coenzyme F_{420}-1

Natural substrates and products
S L-glutamate + GTP + coenzyme F_{420}-0 <1,2> (<1> step in the biosynthesis of coenzyme F_{420} [1]; <2> the enzyme protein catalyzes two distinct and independent reactions, firstly attaching a glutamte via its α-NH_2 to F_{420}-0. The second reaction (cf. coenzyme F_{420}-1:γ-glutamyl ligase) is a γ ligation, taking place when a certain amount of monoglutamylated F_{420}-1 has accumulated [2]) (Reversibility: ?) [1,2]
P GDP + phosphate + coenzyme γ-F_{420}-1

Substrates and products
S L-glutamate + ATP + coenzyme F_{420}-0 <1> (Reversibility: ?) [1]
P ADP + phosphate + coenzyme F_{420}-1

D. Schomburg and I. Schomburg (eds.), *Class 3.4–6 Hydrolases, Lyases, Isomerases, Ligases: EC 3.4–6*, Springer Handbook of Enzymes S10, DOI 10.1007/978-3-642-36260-6_89,

S L-glutamate + GTP + coenzyme F_{420}-0 <1> (<1> coenzyme F_{420}-1 is coenzyme F_{420} with one glutamic acid residue attached via its α-NH_2 to F_{420}-0 [1]) (Reversibility: ?) [1]
P GDP + phosphate + coenzyme F_{420}-1
S L-glutamate + GTP + coenzyme F_{420}-0 <1,2> (<1> step in the biosynthesis of coenzyme F_{420} [1]; <2> the enzyme protein catalyzes two distinct and independent reactions, firstly attaching a glutamte via its α-NH_2 to F_{420}-0. The second reaction (cf. coenzyme F_{420}-1:γ-glutamyl ligase) is a γ ligation, taking place when a certain amount of monoglutamylated F_{420}-1 has accumulated [2]) (Reversibility: ?) [1,2]
P GDP + phosphate + coenzyme γ-F_{420}-1
S L-glutamate + UTP + coenzyme F_{420}-0 <1> (<1> coenzyme F_{420}-1 is coenzyme F_{420} with one glutamic acid residue attached via its α-NH_2 to F_{420}-0 [1]) (Reversibility: ?) [1]
P UDP + phosphate + coenzyme F_{420}-1
S L-glutamate + dGTP + coenzyme F_{420}-0 <1> (<1> coenzyme F_{420}-1 is coenzyme F_{420} with one glutamic acid residue attached via its α-NH_2 to F_{420}-0 [1]) (Reversibility: ?) [1]
P UDP + phosphate + coenzyme F_{420}-1
S Additional information <1> (<1> CofE incubated with 10 mM β-glutamate, D-glutamate, γ-glutamylglutamate, DL-2-amino-3-phosphonopropionic acid, 2-carboxyethylphosphonic acid, or L-R-aminoadipic acid produces no F_{420}-1 [1]) [1]
P ?

Inhibitors

Ca^{2+} <1> (<1> 10 mM, only 26% F_{420}-0 is converted to F_{420}-1 [1]) [1]
Cs^{2+} <1> (<1> in the presence of either Rb^+ or Cs^+ at 0.2 M concentration, the only product of reaction is F_{420}-1 [1]) [1]
GDP <1> (<1> 5 mM, 67% inhibition [1]) [1]
Rb^{2+} <1> (<1> in the presence of either Rb^+ or Cs^+ at 0.2 M concentration, the only product of reaction is F_{420}-1 [1]) [1]
Zn^{2+} <1> (<1> 10 mM, only 26% F_{420}-0 is converted to F_{420}-1 [1]) [1]
β,γ-CH_2-GTP <1> (<1> 5 mM, 56% inhibition [1]) [1]
Additional information <1> (<1> no significant inhibition when CofE is incubated with the following compound (10 mM): L-aspartate, L-glutamine, L-homocysteic acid, or DL-amino-4-phosphono-butyric acid [1]) [1]

Activating compounds

Additional information <1> (<1> no change of CofE activity is observed when the enzyme is assayed with the addition of 10 mM dithiothreitol to the reaction mixture [1]) [1]

Metals, ions

Co^{2+} <1> (<1> divalent cation requirement, maximum CofE activity is observed with the addition of 10 mM $MnCl_2$ [1]) [1]
K^+ <1> (<1> CofE absolutely requires a monovalent cation for activity, the greatest extent of activation is achieved by K^+, with maximum stimulation

occurring at 0.2 M KCl, NH_4^+ stimulates activity to a lesser extent, extent, whereas Na^+ and Li^+ have no effect on CofE activity. A mixture of Mn^{2+}, Mg^{2+}, and K^+ is the most effective [1]) [1]
Mg^{2+} <1> (<1> divalent cation requirement, maximum CofE activity is observed with the addition of 10 mM $MnCl_2$. The combination of 5 mM $MgCl_2$ and 2-5 mM of $MnCl_2$ supports the highest activity [1]) [1]
Mn^{2+} <1,2> (<1> divalent cation requirement, maximum CofE activity is observed with the addition of 10 mM $MnCl_2$. The combination of 5 mM $MgCl_2$ and 2-5 mM of $MnCl_2$ supports the highest activity [1]; <2> there are two Mn^{2+}-binding sites per monomer within close proximity of the GDP α and β-phosphate groups [2]) [1,2]
NH_4^+ <1> (<1> CofE absolutely requires a monovalent cation for activity, the greatest extent of activation is achieved by K^+, NH_4^+ stimulates activity to a lesser extent, whereas Na^+ and Li^+ have no effect on CofE activity. A mixture of Mn^{2+}, Mg^{2+}, and K^+ is the most effective [1]) [1]

K_m-Value (mM)
0.001 <1> (coenzyme γ-F_{420}-0, <1> pH 8.5, 50°C [1]) [1]

pH-Optimum
8.5 <1,2> (<2> assay at [2]; <1> with 50 mM CHES/Na^+ buffer [1]) [1,2]

Temperature optimum (°C)
50 <2> (<2> assay at [2]) [2]
60 <1> [1]

Temperature range (°C)
35-80 <1> (<1> 35°C: about 30% of maximal activity, 80°C: about 55% of maximal activity [1]) [1]

4 Enzyme Structure

Molecular weight
52100 <1> (<1> gel filtration [1]) [1]

Subunits
homodimer <1> (<1> 2 * 27150, calculated from sequence [1]) [1]

5 Isolation/Preparation/Mutation/Application

Purification
<1> (recombinant enzyme) [1]
<2> [2]

Crystallization
<2> (crystal structure of the enzyme from Archaeoglobus fulgidus and its complex with GDP at 2.5 A and 1.35 A resolution, respectively. CofE-AF crys-

tallization is performed by the sitting-drop and hanging-drop methods using vapor diffusion at 18°C) [2]

Cloning

<1> (expressed in Escherichia coli) [1]
<2> [2]

6 Stability

Temperature stability

80 <1> (<1> 15 min, 30% loss of activity [1]) [1]

References

[1] Li, H.; Graupner, M.; Xu, H.; White, R.H.: CofE catalyzes the addition of two glutamates to F_{420}-0 in F_{420} coenzyme biosynthesis in Methanococcus jannaschii. Biochemistry, **42**, 9771-9778 (2003)
[2] Nocek, B.; Evdokimova, E.; Proudfoot, M.; Kudritska, M.; Grochowski, L.L.; White, R.H.; Savchenko, A.; Yakunin, A.F.; Edwards, A.; Joachimiak, A.: Structure of an amide bond forming F_{420}:γ-glutamyl ligase from Archaeoglobus fulgidus - a member of a new family of non-ribosomal peptide synthases. J. Mol. Biol., **372**, 456-469 (2007)

coenzyme γ-F_{420}-2:α-L-glutamate ligase 6.3.2.32

1 Nomenclature

EC number
6.3.2.32

Systematic name
L-glutamate:coenzyme γ-F_{420}-2 (ADP-forming)

Recommended name
coenzyme γ-F_{420}-2:α-L-glutamate ligase

Synonyms
CofF <1> [1]
CofF protein <1> [1]
MJ1001 <1> [1]
γ-F_{420}-2:α-L-glutamate ligase <1> [1]

2 Source Organism

<1> *Methanocaldococcus jannaschii* (UNIPROT accession number: Q58407) [1]

3 Reaction and Specificity

Catalyzed reaction
ATP + coenzyme γ-F_{420}-2 + L-glutamate = ADP + phosphate + coenzyme α-F_{420}-3

Natural substrates and products
S ATP + coenzyme γ-F_{420}-2 + L-glutamate <1> (<1> the enzyme caps the γ-glutamyl tail of the hydride carrier coenzyme F_{420}. CofF specifically adds an α-linked glutamate to γ-F_{420}-2 produced by the Methanococcus jannaschii CofE protein. Coenzyme F_{420}-2 is coenzyme F_{420} with two glutamic acid residue, coenzyme F_{420}-3 is coenzyme F_{420} with three glutamic acid residues [1]) (Reversibility: ?) [1]
P ADP + phosphate + coenzyme α-F_{420}-3

Substrates and products
S ATP + coenzyme γ-F_{420}-2 + L-glutamate <1> (<1> the enzyme caps the γ-glutamyl tail of the hydride carrier coenzyme F_{420}. CofF specifically adds an α-linked glutamate to γ-F_{420}-2 produced by the Methanococcus jannaschii CofE protein. Coenzyme F_{420}-2 is coenzyme F_{420} with two gluta-

D. Schomburg and I. Schomburg (eds.), *Class 3.4–6 Hydrolases, Lyases, Isomerases, Ligases: EC 3.4–6*, Springer Handbook of Enzymes S10, DOI 10.1007/978-3-642-36260-6_90,

mic acid residue, coenzyme F_{420}-3 is coenzyme F_{420} with three glutamic acid residues [1]; <1> CofF specifically adds an α-linked glutamate to γ-F_{420}-2 produced by the Methanococcus jannaschii CofE protein. Coenzyme F_{420}-2 is coenzyme F_{420} with two glutamic acid residue, coenzyme F_{420}-3 is coenzyme F_{420} with three glutamic acid residues [1]) (Reversibility: ?) [1]

P ADP + phosphate + coenzyme α-F_{420}-3

S GTP + coenzyme γ-F_{420}-2 + L-glutamate <1> (<1> activity with GTP is 25% of the activity with ATP at 5 mM. CofF specifically adds an α-linked glutamate to γ-F_{420}-2 produced by the Methanococcus jannaschii CofE protein. Coenzyme F_{420}-2 is coenzyme F_{420} with two glutamic acid residue, coenzyme F_{420}-3 is coenzyme F_{420} with three glutamic acid residues [1]) (Reversibility: ?) [1]

P GDP + phosphate + coenzyme α-F_{420}-3

S Additional information <1> (<1> the phosphonate nucleotide analogs α,β-CH_2-ATP and β,γ-CH_2-ATP support no ligase activity at concentrations of 5 mM. None of the following amino acids or analogs support ligase activity at 10-mM concentrations: D-glutamate, β-glutamate, L-aspartate, L-glutamine, L-α-aminoadipate, or DL-2-amino-4-phosphono-butyrate [1]) [1]

P ?

Inhibitors

KCl <1> (<1> in the presence of 0.1 M or 0.2 M KCl, activities are 40% and 15% relative to reactions without KCl [1]) [1]

α,β-CH_2-ATP <1> (<1> when added to a reaction mixture containing an equal amount of ATP, α,β-CH_2-ATP inhibits 30% of the activity [1]) [1]

Additional information <1> (<1> no inhibition by β,γ-CH_2-ATP [1]) [1]

Activating compounds

2-mercaptoethanol <1> (<1> without 2 mM dithiothreirol or 2-mercaptoethanol in the reaction mixture, CofF activity is up to 5fold lower [1]) [1]

dithiothreirol <1> (<1> without 2 mM dithiothreirol or 2-mercaptoethanol in the reaction mixture, CofF activity is up to 5fold lower [1]) [1]

Metals, ions

Mg^{2+} <1> (<1> the CofF protein strictly requires a divalent metal ion for ligase activity. CofF enzyme incubated with 10 mM $MgCl_2$ has about 33% of the activity supported by 10 mM $MnCl_2$ [1]) [1]

Mn^{2+} <1> (<1> the CofF protein strictly requires a divalent metal ion for ligase activity. CofF enzyme incubated with 10 mM $MgCl_2$ has about 33% of the activity supported by 10 mM $MnCl_2$ [1]) [1]

K_m-Value (mM)

0.0012 <1> (coenzyme γ-F_{420}-2, <1> pH 8.5, 50°C [1]) [1]

pH-Optimum

8.5 <1> (<1> assay at [1]) [1]

Temperature optimum (°C)
50 <1> (<1> assay at [1]) [1]

4 Enzyme Structure

Molecular weight
37000 <1> (<1> gel filtration [1]) [1]

Subunits
monomer <1> (<1> 1 * 35000, SDS-PAGE [1]; <1> 1 * 33278, calculated from sequence [1]) [1]

5 Isolation/Preparation/Mutation/Application

Purification
<1> (recombinant enzyme) [1]

Cloning
<1> (expression in Escherichia coli) [1]

6 Stability

Temperature stability
Additional information <1> (<1> the heterologously expressed protein is thermostable [1]) [1]

References

[1] Li, H.; Xu, H.; Graham, D.E.; White, R.H.: Glutathione synthetase homologs encode α-L-glutamate ligases for methanogenic coenzyme F420 and tetrahydrosarcinapterin biosyntheses. Proc. Natl. Acad. Sci. USA, **100**, 9785-9790 (2003)

tetrahydrosarcinapterin synthase 6.3.2.33

1 Nomenclature

EC number
6.3.2.33

Systematic name
tetrahydromethanopterin:α-L-glutamate ligase (ADP-forming)

Recommended name
tetrahydrosarcinapterin synthase

Synonyms
H4MPT:α-L-glutamate ligase <1> [1]
MJ0620 <1> [1]
MptN protein <1> [1]
tetrahydromethanopterin:α-L-glutamate ligase <1> [1]

2 Source Organism

<1> *Methanocaldococcus jannaschii* (UNIPROT accession number: Q58037) [1]

3 Reaction and Specificity

Catalyzed reaction
ATP + tetrahydromethanopterin + L-glutamate = ADP + phosphate + 5,6,7,8-tetrahydrosarcinapterin

Natural substrates and products
- **S** ATP + tetrahydromethanopterin + L-glutamate <1> (<1> biosynthesis of the cofactor 5,6,7,8-tetrahydrosarcinapterin, the enzyme does not discriminate between ATP and GTP [1]) (Reversibility: ?) [1]
- **P** ADP + phosphate + 5,6,7,8-tetrahydrosarcinapterin
- **S** GTP + tetrahydromethanopterin + L-glutamate <1> (<1> biosynthesis of the cofactor 5,6,7,8-tetrahydrosarcinapterin, the enzyme does not discriminate between ATP and GTP [1]) (Reversibility: ?) [1]
- **P** GDP + phosphate + 5,6,7,8-tetrahydrosarcinapterin

Substrates and products
- **S** ATP + tetrahydromethanopterin + L-glutamate <1> (<1> biosynthesis of the cofactor 5,6,7,8-tetrahydrosarcinapterin, the enzyme does not discri-

D. Schomburg and I. Schomburg (eds.), *Class 3.4–6 Hydrolases, Lyases, Isomerases, Ligases: EC 3.4–6*, Springer Handbook of Enzymes S10, DOI 10.1007/978-3-642-36260-6_91,

minate between ATP and GTP [1]; <1> the enzyme does not discriminate between ATP and GTP [1]) (Reversibility: ?) [1]
P ADP + phosphate + 5,6,7,8-tetrahydrosarcinapterin
S GTP + tetrahydromethanopterin + L-glutamate <1> (<1> biosynthesis of the cofactor 5,6,7,8-tetrahydrosarcinapterin, the enzyme does not discriminate between ATP and GTP [1]; <1> the enzyme does not discriminate between ATP and GTP [1]) (Reversibility: ?) [1]
P GDP + phosphate + 5,6,7,8-tetrahydrosarcinapterin

Metals, ions
Mg^{2+} <1> (<1> conserved Mg-ATP-binding domain [1]) [1]
Additional information <1> (<1> does not require K^+ for activity [1]) [1]

Specific activity (U/mg)
12 <1> (<1> under rate-limiting assay conditions, MptN produces 12.7 nmol of sarcinapterin per min per mg of protein in the presence of ATP and K^+ [1]) [1]
12.7 <1> (<1> under rate-limiting assay conditions, MptN produces 12.7 nmol of sarcinapterin per min per mg of protein in the presence of GTP and K^+ [1]) [1]

pH-Optimum
7 <1> (<1> assay at [1]) [1]

Temperature optimum (°C)
60 <1> (<1> assay at [1]) [1]

4 Enzyme Structure

Molecular weight
72000 <1> (<1> gel filtration [1]) [1]

Subunits
homodimer <1> (<1> 2 * 35000, SDS-PAGE [1]; <1> 2 * 33278, calculated from sequence [1]) [1]

5 Isolation/Preparation/Mutation/Application

Purification
<1> [1]

Cloning
<1> (expression in Escherichia coli) [1]

References

[1] Li, H.; Xu, H.; Graham, D.E.; White, R.H.: Glutathione synthetase homologs encode α-L-glutamate ligases for methanogenic coenzyme F_{420} and tetrahydrosarcinapterin biosyntheses. Proc. Natl. Acad. Sci. USA, **100**, 9785-9790 (2003)

coenzyme F_{420}-1:γ-L-glutamate ligase 6.3.2.34

1 Nomenclature

EC number
6.3.2.34

Systematic name
L-glutamate:coenzyme F_{420}-1 ligase (GDP-forming)

Recommended name
coenzyme F_{420}-1:γ-L-glutamate ligase

Synonyms
CofE <1> [1]
CofE-AF <2> [2]
F_{420}-0:γ-glutamyl ligase <1> [1]
F_{420}:γ-glutamyl ligase <2> (<2> family of non-ribosomal peptide synthases [2]) [2]
MJ0768 <1> [1]

2 Source Organism

<1> *Methanocaldococcus jannaschii* (UNIPROT accession number: Q58178) [1]
<2> *Archaeoglobus fulgidus* DSM 4304 (UNIPROT accession number: O28028) [2]

3 Reaction and Specificity

Catalyzed reaction
GTP + coenzyme F_{420}-1 + L-glutamate = GDP + phosphate + coenzyme γ-F_{420}-2

Natural substrates and products
- **S** L-glutamate + GTP + coenzyme F_{420}-1 <2> (<2> the enzyme protein catalyzes two distinct and independent reactions, firstly attaching a glutamte via its α-NH_2 to F_{420}-0 (cf. coenzyme F_{420}-0:glutamyl ligase). The second reaction is a γ ligation, taking place when a certain amount of monoglutamylated F_{420}-1 has accumulated [2]) (Reversibility: ?) [2]
- **P** GDP + phosphate + coenzyme γ-F_{420}-2
- **S** L-glutamate + GTP + coenzyme γ-F_{420}-1 <1> (<1> step in the biosynthesis of coenzyme F_{420} [1]) (Reversibility: ?) [1]
- **P** GDP + phosphate + coenzyme γ-F_{420}-2

D. Schomburg and I. Schomburg (eds.), *Class 3.4–6 Hydrolases, Lyases, Isomerases, Ligases: EC 3.4–6*, Springer Handbook of Enzymes S10, DOI 10.1007/978-3-642-36260-6_92,

Substrates and products

- **S** L-glutamate + GTP + coenzyme F_{420}-1 <2> (<2> the enzyme protein catalyzes two distinct and independent reactions, firstly attaching a glutamte via its α-NH_2 to F_{420}-0 (cf. coenzyme F_{420}-0:glutamyl ligase). The second reaction is a γ ligation, taking place when a certain amount of monoglutamylated F_{420}-1 has accumulated [2]) (Reversibility: ?) [2]
- **P** GDP + phosphate + coenzyme γ-F_{420}-2
- **S** L-glutamate + GTP + coenzyme γ-F_{420}-1 <1> (<1> step in the biosynthesis of coenzyme F_{420} [1]; <1> coenzyme F_{420}-1 is coenzyme F_{420} with one glutamic acid residue (attached via its α-NH_2 to F_{420}-0), the second glutamate in bound via a γ ligation [1]) (Reversibility: ?) [1]
- **P** GDP + phosphate + coenzyme γ-F_{420}-2
- **S** L-glutamate + UTP + coenzyme γ-F_{420}-1 <1> (<1> maximum activity for coenzyme F_{420}-2 formation is 66% of the maximum activity with GTP. Coenzyme F_{420}-1 is coenzyme F_{420} with one glutamic acid residue (attached via its α-NH_2 to F_{420}-0), the second glutamate in bound via a γ ligation [1]) (Reversibility: ?) [1]
- **P** UDP + phosphate + coenzyme γ-F_{420}-2
- **S** L-glutamate + dGTP + coenzyme F_{420}-0 <1> (<1> maximum activity for coenzyme F_{420}-2 formation is 25% of the maximum activity with GTP. Coenzyme F_{420}-1 is coenzyme F_{420} with one glutamic acid residue (attached via its α-NH_2 to F_{420}-0), the second glutamate in bound via a γ ligation [1]) (Reversibility: ?) [1]
- **P** UDP + phosphate + coenzyme γ-F_{420}-1
- **S** L-glutamate + dGTP + coenzyme γ-F_{420}-1 <1> (<1> maximum activity for coenzyme F_{420}-2 formation is 25% of the maximum activity with GTP. Coenzyme F_{420}-1 is coenzyme F_{420} with one glutamic acid residue (attached via its α-NH_2 to F_{420}-0), the second glutamate in bound via a γ ligation [1]) (Reversibility: ?) [1]
- **P** dGDP + phosphate + coenzyme γ-F_{420}-2
- **S** Additional information <1> (<1> CofE incubated with 10 mM β-glutamate, D-glutamate, γ-glutamylglutamate, DL-2-amino-3-phosphonopropionic acid, 2-carboxyethylphosphonic acid, or L-R-aminoadipic acid produces no F_{420}-2 or other F_{420} analogues. CofE cannot use F_{420}-2 as substrate to add more glutamate residues [1]) [1]
- **P** ?

Inhibitors

Ca^{2+} <1> (<1> 10 mM [1]) [1]
Cs^{2+} <1> (<1> in the presence of either Rb^+ or Cs^+ at 0.2 M concentration no γ-F_{420}-2 is formed [1]) [1]
GDP <1> (<1> 5 mM, 67% inhibition [1]) [1]
Ni^{2+} <1> (<1> in the presence of $NiCl_2$ no γ-F_{420}-2 is formed [1]) [1]
Rb2+ <1> (<1> in the presence of either Rb^+ or Cs^+ at 0.2 M concentration no γ-F_{420}-2 is formed [1]) [1]
Zn^{2+} <1> (<1> 10 mM [1]) [1]
β,γ-CH_2-GTP <1> (<1> 5 mM, 56% inhibition [1]) [1]

Additional information <1> (<1> no significant inhibition when CofE is incubated with the following compound (10 mM): L-aspartate, L-glutamine, L-homocysteic acid, or DL-amino-4-phosphono-butyric acid [1]) [1]

Activating compounds

Additional information <1> (<1> no change of CofE activity is observed when the enzyme is assayed with the addition of 10 mM dithiothreitol to the reaction mixture [1]) [1]

Metals, ions

Co^{2+} <1> (<1> divalent cation requirement, maximum CofE activity is observed with the addition of 10 mM $MnCl_2$. Reactions containing 10 mM either $MgCl_2$ or $CoCl_2$ produce 40% of the F_{420}-2 of that is produced with $MnCl_2$ [1]) [1]

K^+ <1> (<1> CofE absolutely requires a monovalent cation for activity, the greatest extent of activation is achieved by K^+, with maximum stimulation occurring at 0.2 M KCl, NH_4^+ stimulates activity to a lesser extent, extent, whereas Na^+ and Li^+ have no effect on CofE activity. A mixture of Mn^{2+}, Mg^{2+}, and K^+ is the most effective [1]) [1]

Mg^{2+} <1> (<1> divalent cation requirement, maximum CofE activity is observed with the addition of 10 mM $MnCl_2$. Reactions containing 10 mM either $MgCl_2$ or $CoCl_2$ produce 40% of the F_{420}-2 of that is produced with $MnCl_2$. The combination of 5 mM $MgCl_2$ and 2-5 mM of $MnCl_2$ supports the highest activity [1]) [1]

Mn^{2+} <1,2> (<1> divalent cation requirement, maximum CofE activity is observed with the addition of 10 mM $MnCl_2$. Reactions containing 10 mM either $MgCl_2$ or $CoCl_2$ produce 40% of the F_{420}-2 of that is produced with $MnCl_2$. The combination of 5 mM $MgCl_2$ and 2-5 mM of $MnCl_2$ supports the highest activity [1]; <2> there are two Mn^{2+}-binding sites per monomer within close proximity of the GDP α and β-phosphate groups [2]) [1,2]

NH_4^+ <1> (<1> CofE absolutely requires a monovalent cation for activity, the greatest extent of activation is achieved by K^+, NH_4^+ stimulates activity to a lesser extent, whereas Na^+ and Li^+ have no effect on CofE activity. A mixture of Mn^{2+}, Mg^{2+}, and K^+ is the most effective [1]) [1]

K_m-Value (mM)

0.00021 <1> (coenzyme γ-F_{420}-1, <1> pH 8.5, 50°C [1]) [1]

pH-Optimum

8.5 <1,2> (<2> assay at [2]; <1> with 50 mM CHES/Na^+ buffer [1]) [1,2]

Temperature optimum (°C)

50 <2> (<2> assay at [2]) [2]

60 <1> [1]

Temperature range (°C)

35-80 <1> (<1> 35°C: about 30% of maximal activity, 80°C: about 55% of maximal activity [1]) [1]

4 Enzyme Structure

Molecular weight
52100 <1> (<1> gel filtration [1]) [1]

Subunits
homodimer <1> (<1> 2 * 27150, calculated from sequence [1]) [1]

5 Isolation/Preparation/Mutation/Application

Purification
<1> (recombinant enzyme) [1]
<2> [2]

Crystallization
<2> (crystal structure of the enzyme from Archaeoglobus fulgidus and its complex with GDP at 2.5 A and 1.35 A resolution, respectively. CofE-AF crystallization is performed by the sitting-drop and hanging-drop methods using vapor diffusion at 18°C) [2]

Cloning
<1> (expressed in Escherichia coli) [1]
<2> [2]

6 Stability

Temperature stability
80 <1> (<1> 15 min, 30% loss of activity [1]) [1]

References

[1] Li, H.; Graupner, M.; Xu, H.; White, R.H.: CofE catalyzes the addition of two glutamates to F_{420}-0 in F_{420} coenzyme biosynthesis in Methanococcus jannaschii. Biochemistry, **42**, 9771-9778 (2003)
[2] Nocek, B.; Evdokimova, E.; Proudfoot, M.; Kudritska, M.; Grochowski, L.L.; White, R.H.; Savchenko, A.; Yakunin, A.F.; Edwards, A.; Joachimiak, A.: Structure of an amide bond forming F_{420}:γ-glutamyl ligase from Archaeoglobus fulgidus - a member of a new family of non-ribosomal peptide synthases. J. Mol. Biol., **372**, 456-469 (2007)

D-alanine-D-serine ligase 6.3.2.35

1 Nomenclature

EC number
6.3.2.35

Systematic name
D-alanine:D-serine ligase (ADP-forming)

Recommended name
D-alanine-D-serine ligase

Synonyms
VanC2 <2> [4]
VanE <3> [3]
VanG <1> [2]

2 Source Organism

<1> *Enterococcus faecalis* [1,2]
<2> *Enterococcus casseliflavus* [4]
<3> *Enterococcus faecalis* (UNIPROT accession number: Q9S4K1) [3]

3 Reaction and Specificity

Catalyzed reaction
D-alanine + D-serine + ATP = D-alanyl-D-serine + ADP + phosphate

Substrates and products
S D-alanine + D-alanine + ATP <2> (<2> formation of D-alanyl-D-serine is 400fold prefered over formation of D-alanyl-D-alanine [4]) (Reversibility: ?) [4]
P D-alanyl-D-alanine + ADP + phosphate
S D-alanine + D-allo-threonine + ATP <2> (Reversibility: ?) [4]
P D-alanyl-D-allo-threonine + ADP + phosphate
S D-alanine + D-2-aminobutanoate + ATP <2> (Reversibility: ?) [4]
P D-alanyl-D-2-aminobutanoate + ADP + phosphate
S D-alanine + D-asparagine + ATP <2> (Reversibility: ?) [4]
P D-alanyl-D-asparagine + ADP + phosphate
S D-alanine + D-glutamine + ATP <2> (Reversibility: ?) [4]
P D-alanyl-D-glutamine + ADP + phosphate

D. Schomburg and I. Schomburg (eds.), *Class 3.4–6 Hydrolases, Lyases, Isomerases, Ligases: EC 3.4–6*, Springer Handbook of Enzymes S10, DOI 10.1007/978-3-642-36260-6_93,

S D-alanine + D-homoserine + ATP <2> (Reversibility: ?) [4]
P D-alanyl-D-homoserine + ADP + phosphate
S D-alanine + D-serine + ATP <1,2> (<2> formation of D-alanyl-D-serine is 400fold prefered over formation of D-alanyl-D-alanine [4]) (Reversibility: ?) [1,4]
P D-alanyl-D-serine + ADP + phosphate
S D-alanine + D-threonine + ATP <2> (Reversibility: ?) [4]
P D-alanyl-D-threonine + ADP + phosphate
S Additional information <2> (<2> amino acid preference in decreasing order: D-Ser, D-Asn, D-Thr, D-Gln, D-homoserine, D-aminobutanoate, D-allo-Thr [4]) (Reversibility: ?) [4]
P ?

Turnover number (s^{-1})
8.17 <2> (D-serine, <2> pH 7.5 [4]) [4]
8.87 <2> (D-asparagine, <2> pH 7.5 [4]) [4]

Specific activity (U/mg)
8.2 <1> [1]

K_m-Value (mM)
1.8 <2> (D-serine, <2> pH 7.5 [4]) [4]
1.9 <2> (ATP, <2> pH 7.5 [4]) [4]
7.2 <2> (D-asparagine, <2> pH 7.5 [4]) [4]

pH-Optimum
8-9.5 <2> (<2> broad [4]) [4]

4 Enzyme Structure

Subunits
? <1> (<1> x * 39947, MALDI-TOF, x * 39932, calculated for His-tagged protein [1]) [1]

5 Isolation/Preparation/Mutation/Application

Localization
cytoplasm <1> [2]

Purification
<1> (recombinant protein) [1]
<2> (recombinant protein) [4]

Crystallization
<1> (to 2.35 A resolution, P3121 or P3221, with unit-cell parameters a and b 116.1, c 177.2 A) [1]

Cloning

<1> (expression in Escherichia coli) [1]
<2> (expression in Escherichia coli) [4]

References

[1] Weber, P.; Meziane-Cherif, D.; Haouz, A.; Saul, F.A.; Courvalin, P.: Crystallization and preliminary X-ray analysis of a D-Ala:D-Ser ligase associated with VanG-type vancomycin resistance. Acta Crystallogr. Sect. F, **65**, 1024-1026 (2009)
[2] Fines, M.; Perichon, B.; Reynolds, P.; Sahm, D.F.; Courvalin, P.: VanE, a new type of acquired glycopeptide resistance in Enterococcus faecalis BM4405. Antimicrob. Agents Chemother., **43**, 2161-2164 (1999)
[3] Abadia Patino, L.; Courvalin, P.; Perichon, B.: vanE gene cluster of vancomycin-resistant Enterococcus faecalis BM4405. J. Bacteriol., **184**, 6457-6464 (2002)
[4] Park, I.S.; Lin, C.H.; Walsh, C.T.: Bacterial resistance to vancomycin: overproduction, purification, and characterization of VanC2 from Enterococcus casseliflavus as a D-Ala-D-Ser ligase. Proc. Natl. Acad. Sci. USA, **94**, 10040-10044 (1997)

4-phosphopantoate-β-alanine ligase 6.3.2.36

1 Nomenclature

EC number
6.3.2.36

Systematic name
(R)-4-phosphopantoate:β-alanine ligase (AMP-forming)

Recommended name
4-phosphopantoate-β-alanine ligase

Synonyms
Pps <1> [1]
TK1686 protein <1> [1]
phosphopantothenate synthetase <1> [1]

2 Source Organism

<1> *Thermococcus kodakarensis* (UNIPROT accession number: Q5JIZ8) [1]

3 Reaction and Specificity

Catalyzed reaction
ATP + (R)-4-phosphopantoate + β-alanine = AMP + diphosphate + (R)-4'-phosphopantothenate

Natural substrates and products
S ATP + 4-phosphopantoate + β-alanine <1> (<1> the pantoate kinase/phosphopantothenate synthetase system represents the pathway for 4-phosphopantothenate biosynthesis in Thermococcus kodakaraensis. The enzymes are necessary for CoA biosynthesis in this organism [1]) (Reversibility: ?) [1]
P AMP + diphosphate + 4'-phosphopantothenate

Substrates and products
S ATP + 4-phosphopantoate + β-alanine <1> (<1> the pantoate kinase/phosphopantothenate synthetase system represents the pathway for 4-phosphopantothenate biosynthesis in Thermococcus kodakaraensis. The enzymes are necessary for CoA biosynthesis in this organism [1]) (Reversibility: ?) [1]
P AMP + diphosphate + 4'-phosphopantothenate

D. Schomburg and I. Schomburg (eds.), *Class 3.4–6 Hydrolases, Lyases, Isomerases, Ligases: EC 3.4–6*, Springer Handbook of Enzymes S10, DOI 10.1007/978-3-642-36260-6_94,

pH-Optimum

8 <1> (<1> assay at [1]) [1]

4 Enzyme Structure

Subunits

dimer <1> (<1> 2 * 29843, calculated from sequence [1]) [1]

5 Isolation/Preparation/Mutation/Application

Purification

<1> (recombinant enzyme) [1]

Cloning

<1> (expression in Escherichia coli) [1]

References

[1] Yokooji, Y.; Tomita, H.; Atomi, H.; Imanaka, T.: Pantoate kinase and phosphopantothenate synthetase, two novel enzymes necessary for CoA biosynthesis in the archaea. J. Biol. Chem., **284**, 28137-28145 (2009)